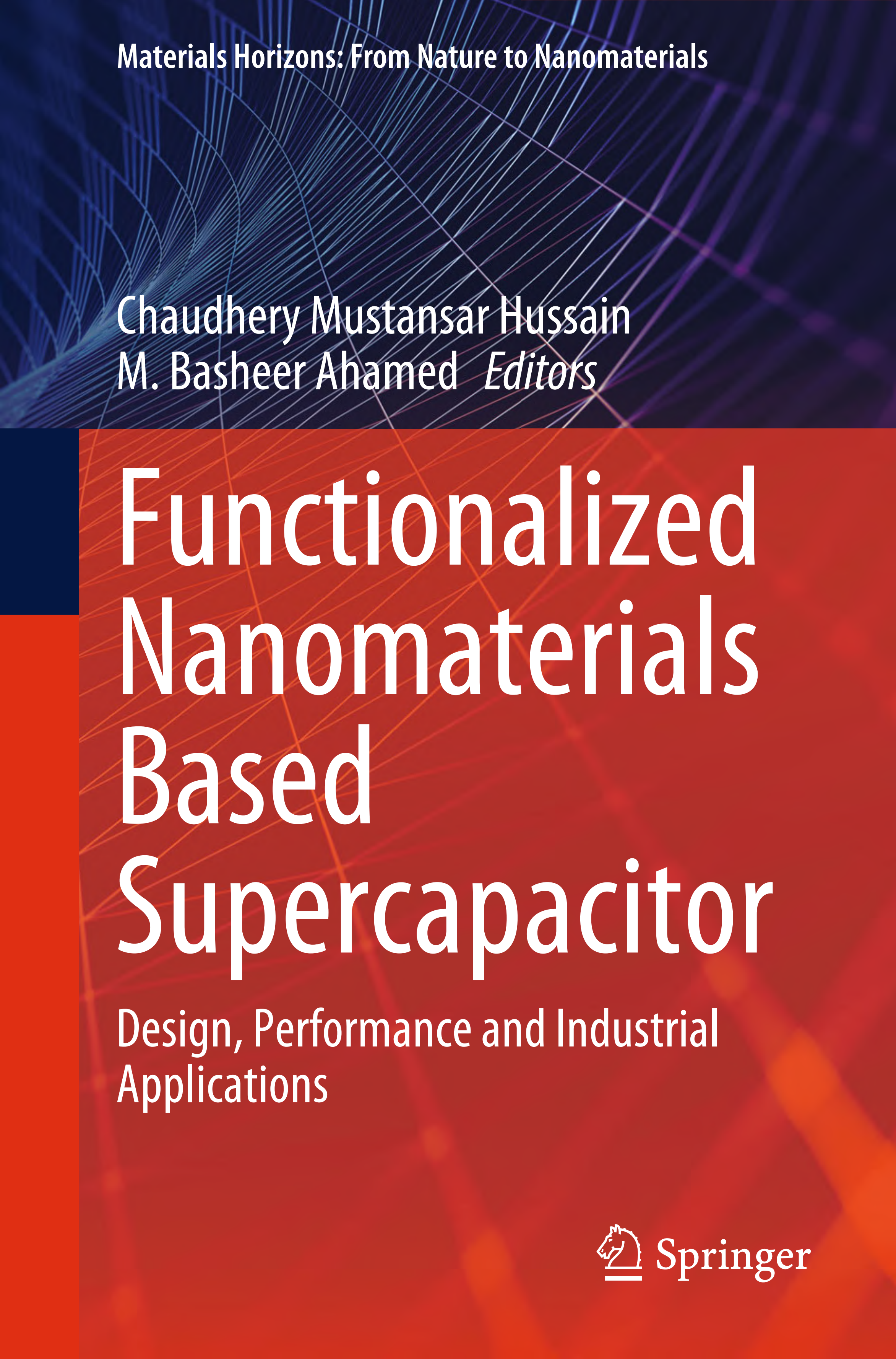

Materials Horizons: From Nature to Nanomaterials

Chaudhery Mustansar Hussain
M. Basheer Ahamed *Editors*

Functionalized Nanomaterials Based Supercapacitor

Design, Performance and Industrial Applications

Springer

Materials Horizons: From Nature to Nanomaterials

Series Editor

Vijay Kumar Thakur, School of Aerospace, Transport and Manufacturing, Cranfield University, Cranfield, UK

Materials are an indispensable part of human civilization since the inception of life on earth. With the passage of time, innumerable new materials have been explored as well as developed and the search for new innovative materials continues briskly. Keeping in mind the immense perspectives of various classes of materials, this series aims at providing a comprehensive collection of works across the breadth of materials research at cutting-edge interface of materials science with physics, chemistry, biology and engineering.

This series covers a galaxy of materials ranging from natural materials to nanomaterials. Some of the topics include but not limited to: biological materials, biomimetic materials, ceramics, composites, coatings, functional materials, glasses, inorganic materials, inorganic-organic hybrids, metals, membranes, magnetic materials, manufacturing of materials, nanomaterials, organic materials and pigments to name a few. The series provides most timely and comprehensive information on advanced synthesis, processing, characterization, manufacturing and applications in a broad range of interdisciplinary fields in science, engineering and technology.

This series accepts both authored and edited works, including textbooks, monographs, reference works, and professional books. The books in this series will provide a deep insight into the state-of-art of Materials Horizons and serve students, academic, government and industrial scientists involved in all aspects of materials research.

Review Process

The proposal for each volume is reviewed by the following:

1. Responsible (in-house) editor
2. One external subject expert
3. One of the editorial board members.

The chapters in each volume are individually reviewed single blind by expert reviewers and the volume editor.

Chaudhery Mustansar Hussain ·
M. Basheer Ahamed
Editors

Functionalized Nanomaterials Based Supercapacitor

Design, Performance and Industrial Applications

Всё для победы!
НАРОДНЫЙ ФРОНТ
https://pobeda.onf.ru/
LET'S HELP THE RUSSIA

Springer

Editors
Chaudhery Mustansar Hussain
Chemistry and Environmental Science
New Jersey Institute of Technology
Newark, NJ, USA

M. Basheer Ahamed
Department of Physics
BSA Crescent Institute of Science
and Technology
Chennai, India

Всё для победы!
НАРОДНЫЙ ФРОНТ
https://pobeda.onf.ru/
LET'S HELP THE RUSSIA

ISSN 2524-5384 ISSN 2524-5392 (electronic)
Materials Horizons: From Nature to Nanomaterials
ISBN 978-981-99-3020-3 ISBN 978-981-99-3021-0 (eBook)
https://doi.org/10.1007/978-981-99-3021-0

© The Editor(s) (if applicable) and The Author(s), under exclusive license to Springer Nature Singapore Pte Ltd. 2024

This work is subject to copyright. All rights are solely and exclusively licensed by the Publisher, whether the whole or part of the material is concerned, specifically the rights of translation, reprinting, reuse of illustrations, recitation, broadcasting, reproduction on microfilms or in any other physical way, and transmission or information storage and retrieval, electronic adaptation, computer software, or by similar or dissimilar methodology now known or hereafter developed.
The use of general descriptive names, registered names, trademarks, service marks, etc. in this publication does not imply, even in the absence of a specific statement, that such names are exempt from the relevant protective laws and regulations and therefore free for general use.
The publisher, the authors, and the editors are safe to assume that the advice and information in this book are believed to be true and accurate at the date of publication. Neither the publisher nor the authors or the editors give a warranty, expressed or implied, with respect to the material contained herein or for any errors or omissions that may have been made. The publisher remains neutral with regard to jurisdictional claims in published maps and institutional affiliations.

This Springer imprint is published by the registered company Springer Nature Singapore Pte Ltd.
The registered company address is: 152 Beach Road, #21-01/04 Gateway East, Singapore 189721, Singapore

Contents

Всё для победы!
НАРОДНЫЙ ФРОНТ
https://pobeda.onf.ru/
LET'S HELP THE RUSSIA

Part I Modern Perspective in Supercapacitor: Functionalized Nanomaterials (FNMs)

1 Historical Perspective of Nanotechnology and Functionalized Nanomaterials 3
Tanuj Kumar, Ratnesh K. Pandey, Ramesh Kumar, C. V. Sudheep, S. Sreelakshmi, Shikha Awasthi, Vandana, and Rahul Singhal

2 An Introductory View About Supercapacitors 25
Manpreet Kour, Sonali Verma, Bhavya Padha, Prerna Mahajan, Aamir Ahmed, and Sandeep Arya

3 Functionalized Nanomaterials, Classification, Properties, and Functionalization Techniques 65
D. Lakshmi, M. Infanta Diana, P. Adlin Helen, and P. Christopher Selvin

4 Functionalized Nanomaterials as Supercapacitor Devices: Current Trends and Beyond 93
Ponnusamy Paunkumar, Chellapandi Bhuvaneswari, Rajendran Lakshmi Priya, Boopathi Shagunthala Hariprasad, Chettipalayam Arunasalam Dhayanithi, and Sundaram Ganesh Babu

Part II Fabrication of Functionalized Nanomaterials Based Supercapacitor Platforms

5 Additive Manufacturing for Functionalized Nanomaterials Dedicated to Supercapacitors 131
Jyoti Prakash Das, Sang Jae Kim, and Ananthakumar Ramadoss

6 Photolithographic Fabrication of Supercapacitor Electrodes 161
Tanuj Kumar, Jyoti, P. Kiran, N. Abhishek, Vandana, and Ashima

7 3D Printing of Supercapacitor 177
Lolly Maria Jose, Sreehari S, and Arun Aravind

8 Inkjet Printing Fabrication of Supercapacitors 197
K. R. Hari Narayanan, Shruti Kannan, and Ananthakumar Ramadoss

9 Pre & Post-Treatment of Functionalized Nanomaterials in Fabricating Supercapacitor Electrodes 223
Soumya Jha and R. Prasanth

Part III Functionalized Nanomaterials Supercapacitor

10 Functionalization Techniques for Carbon Dedicated to Electrochemical Use 253
Ismaila T. Bello, Langutani E. Mathevula, Bakang M. Mothudi, and Mokhotjwa S. Dhlamini

11 Forms of Functionalized Carbon-Based Nanomaterials, Synthesis, Classifications, and Their Electrochemical Activities for Supercapacitors 273
Moorthi Kanmani, Johnbosco Yesuraj, Kibum Kim, and Mohan Sakar

12 Functionalization Techniques for the Development of Metal-Oxide/Hydroxide-Based Supercapacitors 299
R. Balamurugan, S. Siva Shalini, I. Ajin, and A. Chandra Bose

13 Functionalization Techniques for the Development of Conducting Polymer-Based Supercapacitors 329
C. G. Jinitha and S. Sonia

14 Chemical Modifications for the Development of Conducting Polymer-Based Supercapacitors 353
Tanuj Kumar, Jyoti, Mohammed Murshid, Vandana, Ashima, and Monika Saini

Part IV FNMs Based Supercapacitor for Environmental Applications

15 Environmental Applications of Carbon-Based Supercapacitors 373
K. S. Rajni, V. Vishnu Narayanan, and Pughal Selvi

16 Metal Oxide and Hydroxide-Based Functionalized Nanomaterials as Supercapacitors and Their Environmental Impact 389
Gajendra Kumar Inwati, Promod Kumar, Pratibha Sharma, Shakti Devi Kakodiya, Mart-Mari Duvenhage, and H. C. Swart

17 Eco-Friendly Conducting Polymer-Based Functionalized Nanocomposites Dedicated for Electrochemical Devices 405
Tanuj Kumar and Arunima Verma

18 Comparison of Different Functionalized Materials for Supercapacitors: General Overview of the Environmental Awareness 441
K. S. Rajni, D. Pughal Selvi, and V. Vishnu Narayanan

Part V FNMs Based Supercapacitor for Food and Beverages Applications

19 Role of FNMs-Based Supercapacitors in the Food and Beverage Industry 459
Tanuj Kumar and Arunima Verma

20 Polymers Nanocomposite Supercapacitors for Water Treatment and Food Packaging 473
C. P. Devipriya, B. Sumathi, S. Bamini, and V. Sabari

Part VI FNMs Based Supercapacitor for Health Care Applications

21 Functional Polymer Nanocomposites as Supercapacitors for Health Care 505
Akanksha Verma, Bablu Mordina, Kingsuk Mukhopadhyay, Mayank Dwivedi, and Soma Banerjee

Part VII FNMs Based Supercapacitor for Emerging Industrial Applications

22 Functionalized Graphene and its Derivatives for Industrial Energy Storage 533
V. Shanmugapriya, S. Arunpandiyan, G. Hariharan, and A. Arivarasan

23 Functionalized Carbon and Its Derivatives Dedicated to Supercapacitors in Industrial Applications 569
Ajay Singh and Sunil Sambyal

24 FNM-Based Polymeric Nanocomposites Functionalized for Supercapacitor Applications in Different Industries 599
M. Nandhinilakshmi, P. Saranya, D. Vanitha, and A. Arivarasan

Part VIII Economics and Commercialization of FNMs Based Supercapacitor

25 Current Trends in the Commercialization of Supercapacitors as Emerging Energy Storing Systems 631
Aqib Muzaffar, M. Basheer Ahamed, and Chaudhery Mustansar Hussain

Part IX Future of Functionalized Nanomaterials Based Supercapacitor

26 Future of Nanotechnology and Functionalized Nanomaterials. . . . 655
D. A. Nayana, Nithya S. George, S. Nandakumar, Arun Aravind, and P. K. Manoj

27 FNM-Based Supercapacitor in Futuristic Application 679
Soumya Jha and R. Prasanth

Part I

Modern Perspective in Supercapacitor: Functionalized Nanomaterials (FNMs)

Всё для победы!
НАРОДНЫЙ ФРОНТ
https://pobeda.onf.ru/
LET'S HELP THE RUSSIA

Chapter 1
Historical Perspective of Nanotechnology and Functionalized Nanomaterials

Tanuj Kumar, Ratnesh K. Pandey, Ramesh Kumar, C. V. Sudheep, S. Sreelakshmi, Shikha Awasthi, Vandana, and Rahul Singhal

1 Origin of Nanoscience and Nanotechnology

Nanoscience is the study of structure of a material or a chemical on nanometer sizes ranging from 1 to 100 nm and nanotechnology uses it in practical applications [1] or only smaller dimensions are addressed in nanoscience. It is an interdisciplinary field with the cooperation of physics, chemistry, and biology. To deal with the problems in nanoworld one should analyze the properties or change in properties according to the size parameters.

Nanoscience is a kind of new technology to the world. Still the word "nano" is used in the histories of artisans for giving pot's exteriors a dazzling appearance. Although the nanoscience can be seen inside everything from ancient histories as Lycurgus

---

T. Kumar (✉) · C. V. Sudheep · S. Sreelakshmi
Department of Nanosciences and Materials, Central University of Jammu, Rahya-Suchani, Bagla, Jammu 181143, India
e-mail: tkdeswal@gmail.com

R. K. Pandey (✉)
Department of Physics, School of Engineering, University of Petroleum and Energy Studies, Dehradun, Uttarakhand 248007, India
e-mail: pandeyratneshk@gmail.com; rpandey@ddn.upes.ac.in

R. Kumar
Department of Physics, Guru Jambheswar University of Science and Technology, Hisar 125001, India

S. Awasthi
MM MahilaMahavidyalaya, Ara 802301, India

Vandana
Department of Physics, Kurukshetra University, Kurukshetra 136119, India

R. Singhal
Department of Physics, Malaviya National Institute of Technology, Jaipur 302017, India

© The Author(s), under exclusive license to Springer Nature Singapore Pte Ltd. 2024

C. M. Hussain and M. B. Ahamed (eds.), *Functionalized Nanomaterials Based Supercapacitor*, Materials Horizons: From Nature to Nanomaterials,
https://doi.org/10.1007/978-981-99-3021-0_1

Fig. 1 Richard Feynman

cup to Damascus steel. So, the origin nanoworld is unknown but the development of nanoscience starts in the modern times. That's why it's a modern technology [2]. The nanoworld is started by the Nobel prize winner Richard Feynman (Fig. 1) for inventing the concept of nanotechnology in 1959.

During the physics conference hosted by Caltech, American Physical Society, Feynman presented a lecture entitled "There's Plenty of Room at the Bottom." Using one set of extremely precise tools to construct and utilize a second set that is correspondingly smaller and of the appropriate size, he presented a method for mastering the capacity to control individual atoms and molecules [3]. Due to this original idea, which demonstrated the viability of his theories, he is considered as the father of modern nanotechnology. In the year of 1974, Japanese scientist Norio Taniguchi was the first to adopt and define the word "nanotechnology" stating that it primarily refers to the processing of materials by one atom or one molecule for separation, consolidation, and deformation [4]. While composing Eric Drexler (Fig. 2) first academic literature on the topic, "Molecular Engineering: An approach to the development of general capabilities for molecular manipulation," which had appeared in the Proceedings of the National Academy of Sciences in 1981, Drexler uncovered Feynman's startling 1959 lecture "There's Plenty of Room at the Bottom" [5]. Taniguchi coined the term "nanotechnology," which was originally used by Drexler in his book Engines of Creation: The Coming Age of Nanotechnology, which also introduced the idea of a nanoscale that could replicate itself and other things of varied complexity [6]. Before all of these Richard Zsigmondy, a chemical Nobel Prize winner from 1925, was the one who initially originated the term "nanometer." He became the first person to employ a microscope to assess the size of bits like gold colloids as well as established the term nanometer precisely to quantify particle size [7].

Fig. 2 K. Eric Drexler

2 Development of Nanotechnology Over the Years

The task of defining nanotechnology is exciting and challenging. However, we define nanotechnologies as the designing, characterizing, producing, and applying in various cases in the nanoscale. The study of occurrences and changes that occur with materials at the nanoscale in comparison to those at larger sizes is referred to as nanoscience. These definitions encompass several tools, techniques, and materials in addition to a wide range of traditional scientific subjects. In reality, the only thing that links the diverse range of activities labeled as "nanotechnology" is the microscopic sizes on which they operate. According to the development over the years defining nanotechnology is becoming complicated more.

The first word "nano" found in the Lycurgus Cup (Fig. 3) which is a glass cage cup from the fourth-century AD composed of dichroic glass changes color according to the direction of light shining through that one, when lighted from behind it turns Red and from front it turns into Green. It is a magnificent glass of the time, properly ornamented. It is the only complete Roman glass (Fig. 4) object manufactured from this type of glass and the one demonstrating the most stunning change in color [8]. The glass is made using minute amounts of colloidal nanoparticles of both gold and silver that are disseminated across the glassy component to achieve the dichroic effect [9]. Along with the Romans, mediaeval glassblowers studied the impact of incorporating metal flecks into glass to produce stained glass windows. Gold nanoparticles, which also served as photocatalytic air cleaners, were responsible for the vivid stained glass windows in European churches from the sixth through the fifteenth centuries (Fig. 4). They disintegrated a portion of the weapon in hydrochloric acid and examined it under an electron microscope. Afterward, cementite nanowires were also discovered in Damascus Steel, which was discovered in A.D. 900. Surprisingly, they discovered

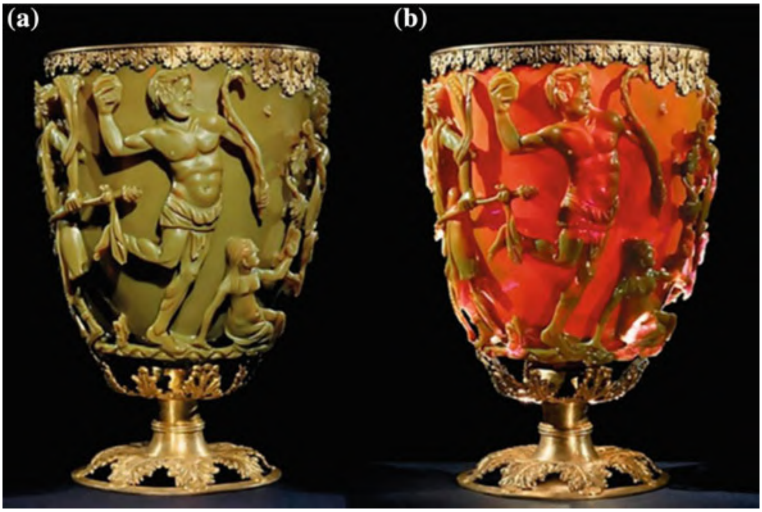

Fig. 3 **a** When illuminated from the outside, glass appears green and **b** When lighted from the inside, it is purple-red [8]. No permission required

that the steel had carbon nanotubes in it, each one only little bigger than a half nanometer. On the head of a thumbtack, ten million could fit side by side [10].

The development in modern era is different from the old days. These are founded on ever-increasing scientific knowledge and instruments, along with researching. In the mid-1850s, Faraday devoted a large amount of time researching the characteristics of light and matter. He prepared hundreds of gold slides and studied them by shining a light through them. Faraday had to employ chemical rather than mechanical ways to get the gold leaf thin enough to be transparent. Illustrating that nanostructured gold creates multiple-colored solutions depending on the illumination conditions [8].

Later on, Professor Erwin W. Miiller created the first field electron microscope, which allowed for relatively atomic sized pictures of materials in 1936. The same individual later created the field ion microscope in 1951, which enables one to observe how atoms are piled on top of a sharp metal needle [8]. Nanotechnology enlarged in 1959 by Richard Feynman when he tried to express the idea about the concept of nanotechnology on his work on “There’s Plenty of Room at the Bottom” in an American Physical Society meeting at Caltech. He is considered as the father of nanotechnology for this [3]. Subsequently, Field Electronics is emphasized by Moor’s Law in 1965. Additionally, Moore observed a reduction in chip price and size together with an expansion in performance, which had a revolutionary impact on how people do business and live. To a considerable part, the microchip corporation’s growing dependence upon nanotechnology as integrated circuits and transistors have neared quantum size is responsible for the fundamental pattern that Moore predicted lasting for 50 years. In order to define the precise machining of materials to within

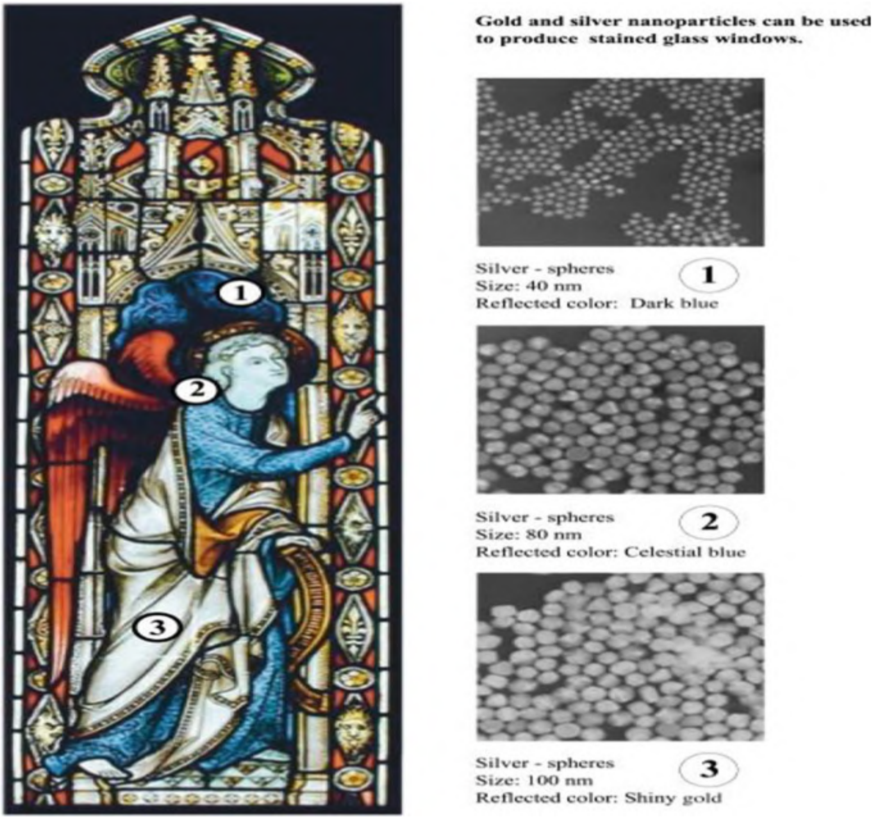
Gold and silver nanoparticles can be used to produce stained glass windows.
1
Silver - spheres
Size: 40 nm
Reflected color: Dark blue
2
Silver - spheres
Size: 80 nm
Reflected color: Celestial blue
3
Silver - spheres
Size: 100 nm
Reflected color: Shiny gold

Fig. 4 Nanoparticle effect on stained glass window hues [8]. No permission required

nanoscale dimensional constraints. Preceding that Professor Norio Taniguchi from Tokyo Science University introduced the title "nanotechnology" in 1974 [8].

After on, the focus on characterizing techniques was increased. Considering this, in IBM's Zurich lab, Gerd Binnig and Heinrich Rohrer created the Scanning Tunneling Microscope (STM) in 1981, which can do quantum-level evaluation. This took a significant advancement on instrumentation techniques as well as nanotechnology development. Those scientists got Nobel Prize for the particular development [11]. While employed at the Vavilov State Optical Institute in St. Petersburg, Russian Scientist Alexie Ekimov made the first discovery of quantum dots in a glass matrix. Furthermore, while researching semiconductors, Louis Brus found the first colloidal solutions of quantum dots who got the Kavli Prize in 2008 [12]. Gerd Binnig, Calvin Quate, and Christoph Gerber devised the AFM, a device that can observe, monitor, and handle materials down to nanometer in size. It can also quantify a variety of forces that are inherent to nanomaterials. The color of nanoparticle is used at IBM's Almaden Research Centre, Don Eigler and Erhard Schweizer used 35 distinct xenon atoms to design the IBM logo in 1989. The use of nanotechnology was launched with this evidence of the capability to effectively alter atoms [11]. While employed at the Vavilov State Optical Institute in St. Petersburg, Russian Scientist Alexie Ekimov made the first discovery of quantum dots in a glass matrix. Furthermore, while researching semiconductors, Louis Brus found the first colloidal solutions of quantum dots who got the Kavli Prize in 2008 [12]. Gerd Binnig, Calvin Quate, and Christoph Gerber devised the AFM, a device that can observe, monitor, and handle materials down to nanometer in size. It can also quantify a variety of forces that are inherent to nanomaterials. The use of nanotechnology was launched with this evidence of the capability to effectively alter atoms [8].

The greatest discovery was done in 1991. That was the invention of carbon nanotubes (Fig. 5), which was discovered by S. Iijima. Applications of carbon nanotubes in many sectors hadn't ended, still being studied. There is hope for them to be used in the future since so many investigators have evaluated the great characteristics of CNTs [8, 13]. The developments lead to the next level by the discovery of nanostructured catalytic materials MCM-41 and MCM-48 which have wide variety of field in refining processes. Successively, Moungi Bawendi found a way in 1993 for the synthesis and processing of quantum dots, opening the door for uses in high-efficiency solar cells, optics, and biotechnology in addition to computers. The future of nanotechnology was decided by in discovery of quantum computers. In 1998, Isaac Chuang of the Los Alamos National Laboratory, Neil Gershenfeld of the Massachusetts Institute of Technology (MIT), and Mark Kubinec of the University of California, Berkeley created the first two-qubit quantum computer that could store data and provide a result. Although their device was modest in terms of addressing significant issues and consistent for just a few nanoseconds, still it successfully illustrated the fundamentals of quantum processing [12]. On the other hand, working of nanoscience still proceeding. Depositing nanoparticles over the surfaces are developing at that stage. As a regard the Mirkin group devised and first utilized dip-pen nanolithography (DPN) in 1999 to deposit molecules and materials on surfaces with sub-50 nm precision. Following this, researchers from Rice University, Naomi Halas, Jennifer West, Rebekah Drezek, and Renata Pasqualin developed gold nanoshells that can be used as a starting point for the thorough investigation, diagnosis, and treatment of breast cancer without invasive biopsies, surgery, systemically harmful radiation, or chemotherapy. In 2004, the European Commission issued the Communication "Towards a European Strategy for Nanotechnology," COM (2004) 338, proposing process of organizational European nanoscience and nanotechnology R&D capabilities. In the same year, British Royal Society published Nanoscience and Nanotechnologies: Opportunities and Uncertainties in accordance with Royal Academy of Engineering which holds the ideas about the medical field applications of nanoscience and nanotechnology. Besides all of these a degree-level course started in 2004 in US called The College of Nanoscience and Engineering. A theory for DNA-based computation and "algorithmic self-assembly," in which calculations are included into the formation of nanocrystals, was created in 2005 by Erik Winfree and Paul Rothemund of the California Institute of Technology. Nanotechnology has taken care of storage devices or art of rechargeable batteries in twenty-first century. As a result of this, MIT researchers led by Angela Belcher created a lithium–ion battery that

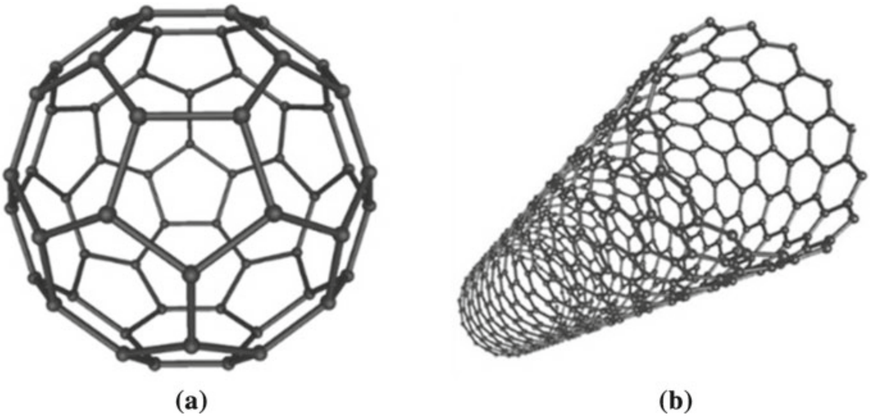

Fig. 5 **a** Fullerenes and 5. **b** Carbon nanotubes (CNT) [8]. No permission required

contains a typical virus that doesn't harm humans. According to the them, M13 bacteriophages can operate as biological scaffolds in the construction of 3D nickel phosphide nanostructures since they are long and thin (approximately 880 nm in length and 6.5 nm in diameter). Bacteriophages are viruses that solely destroy bacteria; they have no effect on people. M13 virus particles are made up of four minor coat proteins at each end and 2,700 copies of a major coat protein that is spirally curled around a DNA sequence [8].

DNA nanotechnology was a milestone in nanoscience and nanotechnological field. Nadrian Seeman established the theoretical framework for DNA nanotechnology in 1982. However, achieving advances took time. Several robotic nanoscale construction devices (Fig. 6) that resemble DNA were developed by Nadrian Seeman and colleagues at New York University by 2009. One includes utilizing manufactured DNA crystal sequences with "sticky ends" that may be placed in certain ratios and orientated to form 3D DNA structures. The flexibility and density that 3D nanoscale components provide might make it possible to assemble parts that are more compact, intricate, and densely placed, which would be advantageous for nanoelectronics. A "DNA assembly line" is yet another invention by Seeman (in collaboration with peers at Nanjing University in China), Seeman shared the 2010 Kavli Prize in Nanoscience for this study. Recent developments in material science and engineering have given a variety of nanomaterials with special features that are anticipated to enhance the management of several malignancies that are now resistant to conventional treatments. They will be able to transport therapeutic molecules like medicines, proteins, nucleic acids, or immunological agents by acting as nanocarriers, which will be made feasible by their inherent cytotoxic activity and/or by their capacity to operate as nanocarriers. These cutting-edge biomedical applications are presently being used in several clinical studies and might soon assist significant advancements in the treatment of cancer [14].

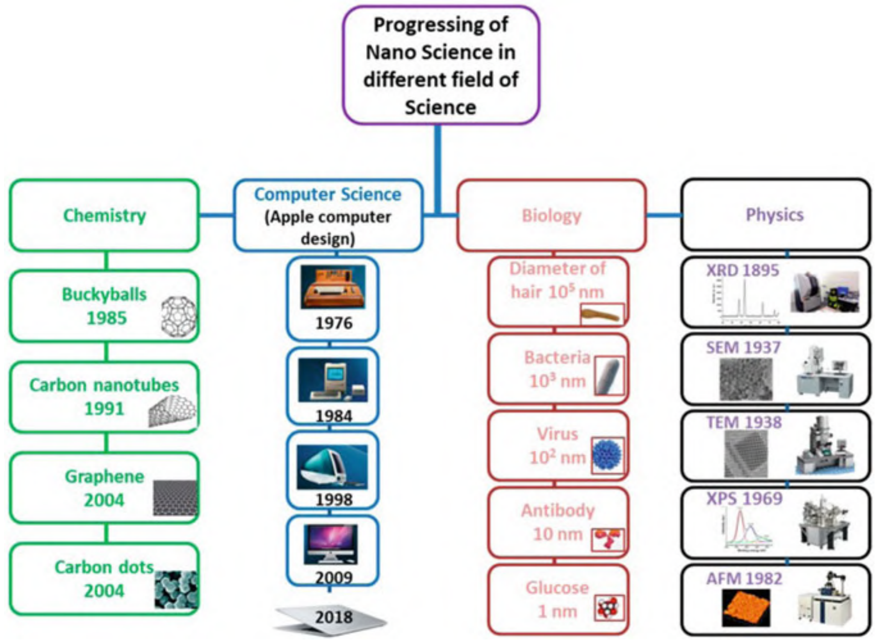
Progressing of Nano Science in different field of Science
Chemistry
Buckyballs 1985
Carbon nanotubes 1991
Graphene 2004
Carbon dots 2004
Computer Science (Apple computer design)
1976
1984
1998
2009
2018
Biology
Diameter of hair 10^5 nm
Bacteria 10^3 nm
Virus 10^2 nm
Antibody 10 nm
Glucose 1 nm
Physics
XRD 1895
SEM 1937
TEM 1938
XPS 1969
AFM 1982

Fig. 6 Progress of nanoscience from different fields [8]. No permission required

Although these inventions and development in nanotechnology still proceeding on its own way. Development of optoelectronics and medicines is found to be a grand area of nanotechnology. Working on these areas leads to the tissue engineering and surgery advancements. The drug delivery was complicated before. But after the invention of CNTs it makes an easy way. All fields of science are still carrying the researches in nanotechnology for the great full deeds of common people.

3 Types of Nanomaterials

Nanotechnology studies and controls nanometer-scale matter. The nanoscale spans 1–100 nm. Nanometers are billionths (10^{-9} m) of meters. Nanomaterials may have unexpected characteristics. Particle size may influence color. Because atoms in nanometer-scale particles reflect light differently. For example, silver is yellowish or amber-colored, whereas gold is dark red or purple. Due to the extreme diversity of these tiny particles, it is vital to classify nanomaterials since doing so would be impossible. Nanoparticles can be categorized according to their size, surface area, shape, dimensions, and production procedures. However, the morphology, content, homogeneity, aggregation, and also dimensionality of nanomaterials are often used to classify them [15].

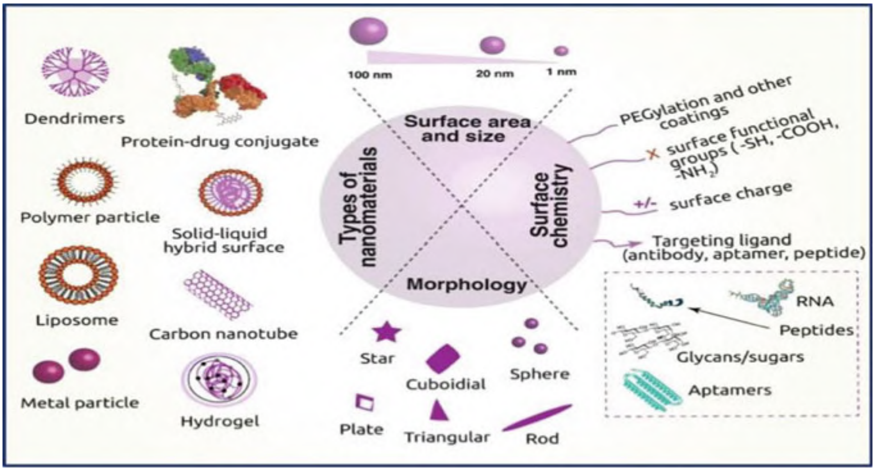
100 nm
20 nm
1 nm
Dendrimers
Protein-drug conjugate
Polymer particle
Solid-liquid hybrid surface
Liposome
Carbon nanotube
Metal particle
Hydrogel
Surface area and size
Types of nanomaterials
Surface chemistry
Morphology
PEGylation and other coatings
surface functional groups (-SH, -COOH, -NH$_2$)
+/- surface charge
Targeting ligand (antibody, aptamer, peptide)
RNA
Peptides
Glycans/sugars
Aptamers
Star
Cuboidial
Sphere
Plate
Triangular
Rod

Fig. 7 Different types of nanomaterials [16]. No permission required

3.1 Morphology

Nanoparticle shapes determine their names. Nanospheres, reefs, boxes, clusters, tubes, and more exist. Micellar emulsions, anodizedalumina pores, or the materials' crystallographic development patterns can spontaneously create these forms or morphologies.

Long carbon nanotubes span electrical junctions thanks to nanoparticle morphologies. Nanospheres and anisotropic microcrystalline whiskers are crystal shaped, whereas amorphous particles are spherical. Nanoparticle clusters are frequent. Cups, fibers, and rods are examples (Fig. 7). Fine particle; micromeritics, using as nanoparticles in new technologies, requires controlling their shape. Gold nanoparticles are used in optical filters and biosensors, which need anisotropy due to plasmon losses from bigger forms.

Aspect ratio, sphericity, and flatness determine nanoparticle shape. Most studies categorize nanoparticles by aspect ratio. High-aspect-ratio nanoparticles are divided by aspect ratio. If the aspect ratio is low, nanoparticles can be oval shaped, prism shaped, spherical, or cubical shaped. Nanorods, nanowires, nano-hooks, nano-helices, nano-stars, nano-springs, and nanoplates are nanoparticles with high aspect ratios [16].

3.2 Dimensionality

Nanoparticles can be divided into four categories: zero-dimensional (0D) particles, which have all three dimensions of length, breadth, and height, like nanodots and

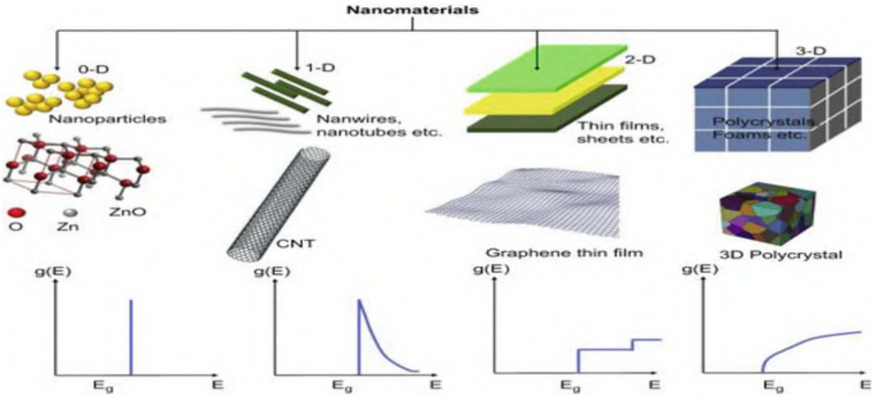

Fig. 8 Classification of nanoparticles on the basis of dimensions [17]. Taken

nanoparticles; one-dimensional (1D) particles, which have only one of length or width, like nanowires and nanotubes; two-dimensional (2D) particles, like crystals, which have all three dimensions; and three-dimensional (3D) particles (Fig. 8) which are extremely thin [17].

3.2.1 Zero Dimensions

Point-like nanomaterials include oxide, fullerenes uniform particle arrays, heterogeneous particle arrays, core–shell quantum dots, onions, hollow spheres, and others [18]. The field of biosensing research has primarily focused on zero-dimensional (0D) nanomaterials such as carbon quantum dots (CQDs), graphene quantum dots (GQDs), inorganic quantum dots (QDs), magnetic nanoparticles (MNPs), fullerenes, up-conversion nanoparticles (UCNPs), noble metal nanoparticles, and polymer dots (Pdots). 0D nanomaterials can detect ions, biomolecules, diseases, and pathogens due to their ultra-small size, quantum confinement effect, outstanding physical and chemical characteristics, and biocompatibility.

3.2.2 One Dimensions

Nanomaterials with minimum dimension of 100 nm, such as nanowires, nanotubes, and nanorods [18]. Due to their unique features and prospective applications in electronics, miniaturized devices, and catalysis, 1D nanostructured metal oxide materials have attracting attention. Thermal degradation, pulsed laser deposition, redox reactions, selected-control reaction, electrodeposition, chemical vapor deposition, arc discharge, and traditional template-assisted solution phase growth have all been used to create nanowires. Nanowire development inside mesopores is now possible thanks to highly organized silica mesoporous materials. Because of its large surface area, variable pore size, regular pore system, and high thermal and hydrothermal stability, SBA-15 is suitable for precursor inclusion and nanowire production [19].

3.2.3 Two Dimensions

Monolayers, multilayers, self-assembled plates, and other two-dimensional structures outside of manometry [18]. Two-dimensional (2D) nanomaterials have layers as thin as one atomic layer. Nanomaterials have a high aspect ratio and a dense population of atoms on their surfaces. Increased surface atoms change the behavior of 2D nanomaterials because they behave differently than interior atoms. Graphene, as one of the most widely used and significant 2D materials, possesses distinct properties that make it valuable in a variety of industries. Following the success of graphene in many industries, additional two-dimensional materials must have this quality. However, more research is needed on the use of alternative two-dimensional materials [20].

3.2.4 Three Dimensions

Equiaxed nanometre-sized grains of nanophase material are nanomaterials [18]. Given the demand for more functional solids, three-dimensional nanostructure programming is becoming more relevant. Solar energy harvesting, energy storage, molecule separation, sensors, medicinal agent delivery, nanoreactors, and sophisticated optical devices use complicated programmed architectures.

3.3 Composition

Nanoparticle composition can classify them. Some nanoparticles have one substance, whereas others have multiple. Many parts make up natural nanoparticles. Current technologies make pure nanoparticles easily. Nanomaterials may be made from antimony and bismuth. Nickel, silicon, and titanium oxide hybrid nano-zigzags may also be made [21].

3.3.1 Carbon-Based Materials

Carbon nanomaterials (Fig. 9) are usually hollow spheres, ellipses, or tubes. Fullerenes are spherical, elliptical, or cylindrical carbon nanomaterials. These particles can be used in films, coatings, stronger and lighter materials, and electrical applications. Carbon-based nanomaterials include carbon-based quantum dots, carbon nanotubes, nanodiamonds, fullerenes, graphene oxide, and graphene derivatives. Due to their unusual structural dimensions and remarkable, electrical, mechanical,

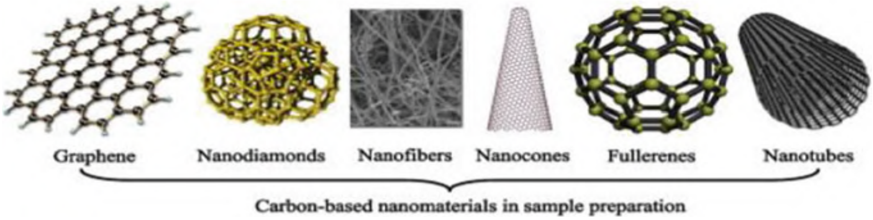

Fig. 9 Carbon-based nanomaterials [23]. Taken

optical, and thermal chemical capabilities, these materials have garnered interest in many sectors, including biomedicine [22].

3.3.2 Metal-Based Materials

Quantum dots, nanogold, nano-silver, and titanium dioxide are nanomaterials. Quantum dots are semiconductor crystals with hundreds or thousands of atoms. Size effects of quantum dot's optical properties advances one- and two-photon imaging and its potential diagnostic and therapeutic uses for cancer and other disorders [24].

3.3.3 Dendrimers

Nanoscale branch-based polymers are nanomaterials. Multiple chain ends on a dendrimer's surface can perform chemical functions. This may aid catalysis. Three-dimensional dendrimers can hold more molecules, making them useful for drug delivery. Nanoscale, radially symmetric dendrimers (Fig. 10) have a well-defined structure, which is homogenous, and monodisperse structure with a generally symmetric core, an inner shell, and an outer shell. Their three traditional macromolecular architectural classes are known for creating polydisperse products with different molecular weights. Dendrimers vary in biological properties like low cytotoxicity, self-assembling, electrostatic interactions, chemical stability, polyvalency, and solubility. This review discusses dendrimers' medicinal uses [25].

4 Synthesis of Nanomaterials

Nanomaterials are remarkable materials with at least one dimension between 1 and 100 nm. Nanomaterials designed rationally can have huge surface areas. Nanomaterials can have superior electrical, magnetic, mechanical, optical, and catalytic capabilities. Controlling size, shape, synthesis conditions, and functionalization enables

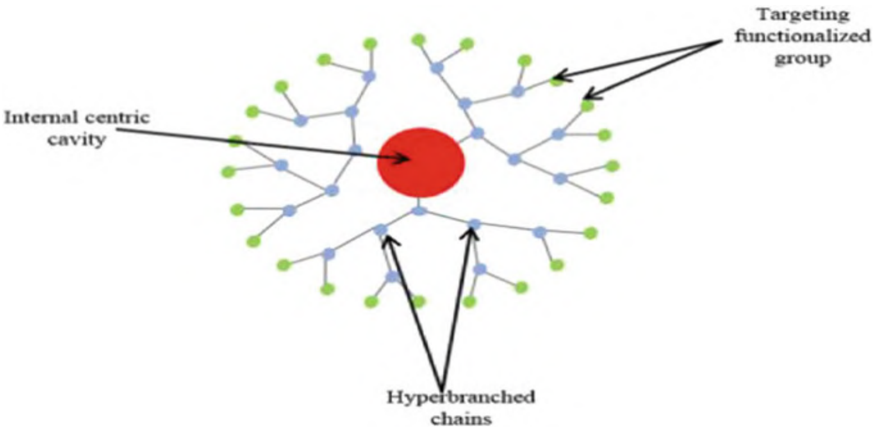

Fig. 10 Classical structure of dendrimer [25]. Taken

fine-tune nanomaterial characteristics [26]. Synthesis processes vary by nanomaterial. Nanomaterials are often made "top-down" or "bottom-up." Top-down methods convert bulk materials to nanoparticles, whereas bottom-up methods generate nanomaterials from elemental levels. Nanomaterials are synthesized by chemical vapor deposition, thermal breakdown, hydrothermal synthesis, solvothermal technique, pulsed laser ablation, templating, combustion, microwave, gas-phase, and standard sol–gel processes (Fig. 11) [27].

4.1 Top-Down Method

Processing bigger items top-down creates nanoscale objects. Integrated circuits illustrate top-down nanotechnology (Fig. 12). Nanoelectromechanical systems (NEMS) with small levers, springs, fluid channels, and electronic circuits contained in a chip are now possible. Silicon crystals start these fabrications. Photo, electron beam, and ion beam lithography have made small chips possible. Some applications crush larger materials to nanoscale size to maximize surface area to volume ratio for higher reactivity. Nanogold, silver, and titanium dioxide are employed in many applications. Top-down techniques are easier and use bulk material removal or division or bulk manufacturing process downsizing to create the required structure with acceptable attributes. Top-down design suffers most when it comes to covering surface structural defects. Lithographic nanowires feature several impurities and structural flaws. Examples include gas-phase condensation, high-energy wet ball milling, atomic force manipulation, electron beam lithography, aerosol spray, and others. Researchers struggle to make plenty of nanomaterials. Researchers struggle to make plenty of nanomaterials for multipurpose. For nanomaterial fabrication, mechanical grinding, lithography, and machining are briefly detailed below [28].

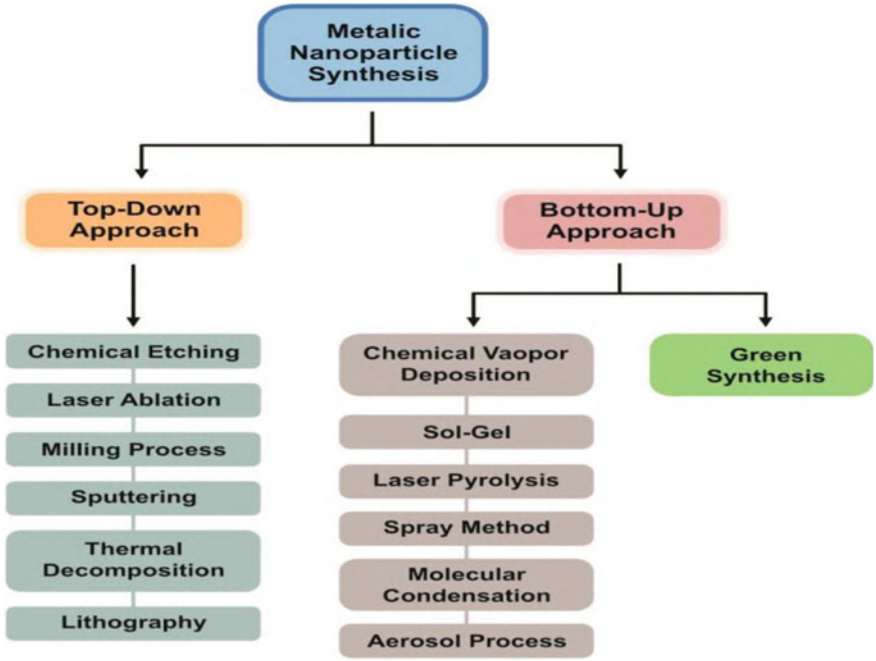
Metalic Nanoparticle Synthesis
Top-Down Approach
Bottom-Up Approach
Chemical Etching
Laser Ablation
Milling Process
Sputtering
Thermal Decomposition
Lithography
Chemical Vaopor Deposition
Sol-Gel
Laser Pyrolysis
Spray Method
Molecular Condensation
Aerosol Process
Green Synthesis

Fig. 11 Classification of synthesis of nanomaterials [27]. No permission required

4.1.1 Ball Milling

It is used for ceramic powder and slurry particle grinding. A porcelain vase containing porcelain pebbles grinds particles (Fig. 13). Material, body, or glaze particle size reduction tool. A ball mill is a container with porcelain or flint pebbles that is loaded with a charge (powder or slurry) and mechanically spun to crush particles that come into contact with them. Ball mills can be periodic, small, high speed, large, low speed, rotating, or continuous. For maximum efficiency, a ball mill should be made of, or lined with, porcelain or another very hard surface for maximum efficiency (so that abrasion also occurs between the wall and the balls), the balls should come in a variety of sizes (to achieve maximum contact points), the mill should have the right amount of balls, the slurry should be the right viscosity, and the charge slurry should be the right viscosity. Rubber-lined mills decrease noise and wear. Ball mills compress particles to nanosize, which is crucial for making high-tech powders like alumina [29].

4.1.2 Nanolithography

Stone carving is lithography. It can arrange material on a substrate or design a flat surface by eliminating some of it. It involves high-speed radiation pattern transfer on

Fig. 12 Representation of top-down and bottom-up type of synthesis. No permission required

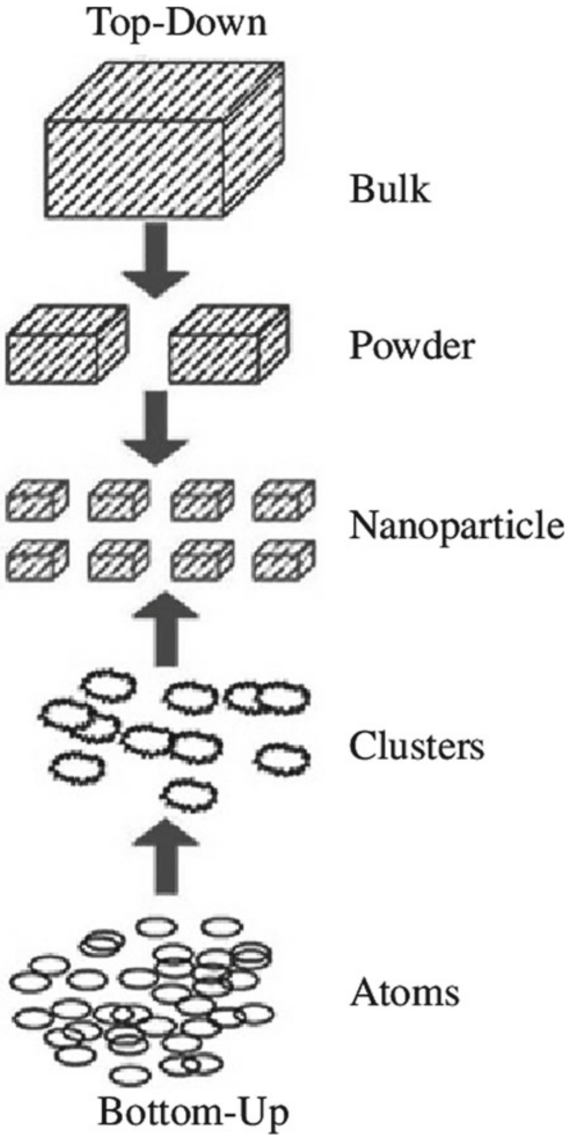

a semiconductor or substrate. Advanced semiconductor fabrication uses lithography. It participates in IC production, advanced electronic packaging, opto-electric components, flat panel displays, and VLSI. The microelectronics sector has great potential due to lithographic system advancements. Lithographic technologies can now create patterns at atomic distances. Circuit manufacturers need consistency, repeatability, line width control, and overlay precision. Nanolithography meets these needs. Top-down nanolithography removes the atoms or molecules from bulk materials to create

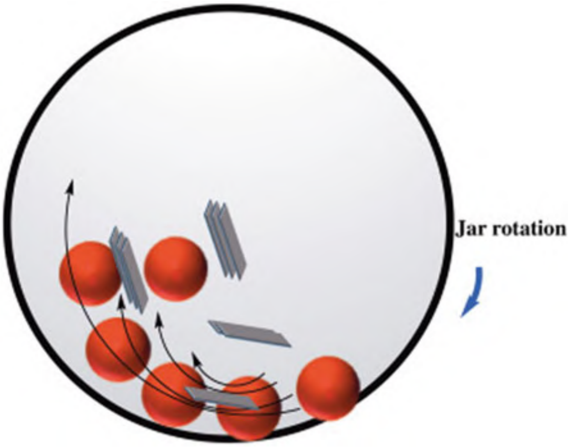

Fig. 13 Schematic representation of ball milling [30]. No permission required

nanostructured patterns. Miniaturized CPUs, resistors, and other components are needed for cell phones and ATMs. These components may consume low power, materials and cost; however, they operate quicker. Nanolithography can miniaturize FETs, quantum dots, wires, surface gated quantum devices, grating zone plates, and masks up to deep submicron size [27].

4.1.3 Types of Lithography

X-ray, electron- beam and optical lithography are prevalent in classifying lithographic methods. Depending on the radiation utilized for carving or pattern transfer, electromagnetic radiation or particles reveal resist material in specified place. Resist is radiation-sensitive. Masks chosen material portions. Radiation exposure makes the material transparent in certain places and opaque in others. Radiation-exposed resist weakens or strengthens compared to exposed resist. Resolving unexposed or exposed material using a chemical or plasma technique yields the desired pattern. The materials can be patterned by repeating the previous steps. Chromium is deposited on a glass or silicon substrate. Polymer photoresist is put on the metal surface. Radiation destroys positive photoresist or breaks chemical bonds. Negative resist material hardens when exposed. Resist-coated surfaces are masked. Then, the mask is subjected to UV light, which weakens or strengthens the resist based on its opaque and transparent parts. Chemicals develop the picture (i.e., developer). Chemical treatment recovers unexposed material [27].

4.1.4 Sputtering

Sputtering bombards solid surfaces with plasma or gas to create nanomaterials. Sputtering nanomaterial sheets is effective. Depending on gaseous-ion energy, sputtering deposition ejects tiny atom clusters from the target surface. Magnetron, radiofrequency, and DC diode sputtering can be used. Sputtering is carried out in an evacuated tube with the aid of sputtering gas.

When the cathode goal is high voltage, free electrons collide with gas ions. In an electric field, positive ions accelerate rapidly toward the cathode target, constantly striking it and ejecting particles from its surface. On SiO_2 and carbon paper, magnetron sputtering produces WSe_2-layered nanofilms. Sputtering is appealing because the sputtered nanoparticle structure is similar to the target material while containing fewer contaminants and is less expensive than electron beam photolithographic [31].

4.2 Bottom-Up Method

Bottom-up nanotechnology builds nanostructures from atoms and molecules. Self-assembly of nanostructures. Nanofabrication requires bottom-up approaches as item sizes decrease. Nature's bottom-up nanotechnology uses chemical forces to build cell structures. Scientists and engineers mimic nature to create tiny groups of certain atoms that self-assemble into increasingly complex structures. Bottom-up nanotechnology uses metal-catalyzed polymerization to make carbon nanotubes. Eric Drexler's 1987 book Engines of Creation revealed bottom-up nanotechnology's molecular machinery and manufacturing. It showed how nanoscale mechanical systems can build complex molecular structures. Bottom-up synthesis is called "wet" because it uses plenty of solvents and other chemicals. In addition, particles must be stabilized or capped in solution to prevent them from growing beyond nanoscale. For usage or characterization, particles must be removed from their solutions. Drop the solution onto the substrate. In catalysis, the nanoparticles' stabilizers may need to be removed following immobilization on the final support. The removal process might be difficult or impossible, rendering these particles useless [28].

4.2.1 Sol–Gel Method

Wet chemical production of nanostructures, notably metal oxide nanoparticles, is the sol–gel technique (Fig. 14). The chemical precursor usually metal alkoxides dissolved in water or alcohol then heated and stirred to form gel. The hydrolysis/alcoholic gel is moist; thus, it must be dried according to its qualities and use. Burning alcohol dries alcoholic solutions. Gels are dried, powdered, and calcined.

Sol–gel is cost-effective and provides high chemical composition control because of the low reaction temperature. The sol–gel technique may be used to mold ceramics

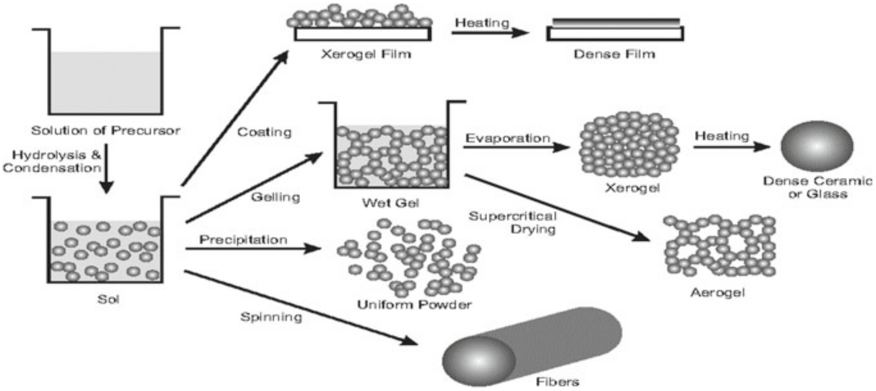
Solution of Precursor
Hydrolysis & Condensation
Sol
Coating
Gelling
Precipitation
Spinning
Xerogel Film
Heating
Dense Film
Wet Gel
Evaporation
Xerogel
Heating
Dense Ceramic or Glass
Supercritical Drying
Aerogel
Uniform Powder
Fibers

Fig. 14 Sol–gel process [32]. No permission required

and intermediate thin coatings of metal oxides. Sol–gel materials are employed in pharmaceutical optical, energy, biosensors, surface engineering, and separation technologies (such as chromatography). Sol–gel nanoparticle synthesis is a common commercial process. Sol–gel relies on precursors to form a homogenous sol and gel. The gel is dried once the solvent is removed. Drying process affects gel characteristics. The "removing solvent procedure" depends on the gel's application. Surface coating, structural insulation, and specialty apparel employ dried gels. Grinding gel in specific mills produces nanoparticles [33].

4.2.2 Vapor-Phase Deposition

Vapor-Phase Deposition (VPD) is the preferred method for nanostructured metal, insulator, and semiconductor materials. The elegant process parameter control of vapor-phase deposition is attracting interest. This will enable size, shape, and chemical composition-controlled nanostructured materials. This method is better for making big nanomaterials. Evaporated materials enter the gaseous phase. Clustered gas-phase atoms or molecules deposit on a substrate. Depending on the application, nanostructured materials can be obtained as single layers, multilayers, or powders. Nanoparticle production requires proper sample chamber pressure. Pressure melts and evaporates materials. The following three categories describe vapor-phase technology:

(1) Physical Vapor Deposition (PVD),
(2) Chemical Vapor Deposition (CVD), and
(3) Plasma-Enhanced Chemical Vapor Deposition (PECVD) [27].

Physical Vapor Deposition

Many industries use Physical Vapor Deposition (PVD) for high-performance coatings because demand is stronger than ever. PVD is the gold standard for coating optics, computer chips, and other materials with thin, pure, and durable coatings.

In thin-film coating, or PVD coating, a vacuum chamber is used to vaporize a solid and deposit it on a target substrate atom by atom. An eco-friendlier coating method yields a thin, pure covering. Ablation, transport, reaction, and deposition comprise the vacuum-based PVD coating process. This method coats the substrate with a robust, abrasion-, and corrosion-resistant coating of source atoms. Thermal and sputtering physical vapor depositions are the major forms. Thermal evaporation deposition vaporizes target material using high temperatures and vacuum pressure. A high-energy source in a high-vacuum chamber sputters atoms from the target. The plasma arc deposits these atoms on the target surface. This biases the target before hitting it with ionized gas in vacuum. Ionic bombardment "sputters" atoms off the target into a plasma cloud arc before conveyance and condensation. Both techniques have pros and cons that make them beneficial in different situations. Sputtering, the slowest and most complicated process, generates a homogeneous coating with low impurity rates. Thermal evaporation offers improved throughput and mineral usage efficiency but may need sample rotation for process homogeneity [27]. Vaporized atoms must be precisely timed and positioned to reach the substrate. The system's shape and the material's PVD technique are crucial. The final phase coats the substrate. A homogeneous substrate deposition is crucial as the thin layer might range from a few atoms to a few microns. PVD includes spinning the substrate at a steady speed and measuring deposition with a quartz crystal microbalance. A conveyor belt of targets in front of the vaporized arc for a specific duration can automate the deposition process in several industrial methods. Automating sputtering and evaporation speed up PVD coating for mass manufacturing [27].

Chemical Vapor Deposition

It produces high-quality solid thin films and coatings. It's widely employed in modern industries, but new materials require constant development. CVD synthesis (Fig. 15) is now producing accurate inorganic 2D thin films and high-purity polymeric thin films that may be conformally placed on diverse substrates. This Primer convention, repeatability, 2D transition metal dichalcogenides (TMDs), graphene, and polymeric thin films are used to demonstrate substrate preparation and high-temperature growth highlighted are recent breakthroughs and scaling-up issues. We also suggest reactor design for high-throughput, low-temperature thin-film development by examining present constraints and improvements [34].

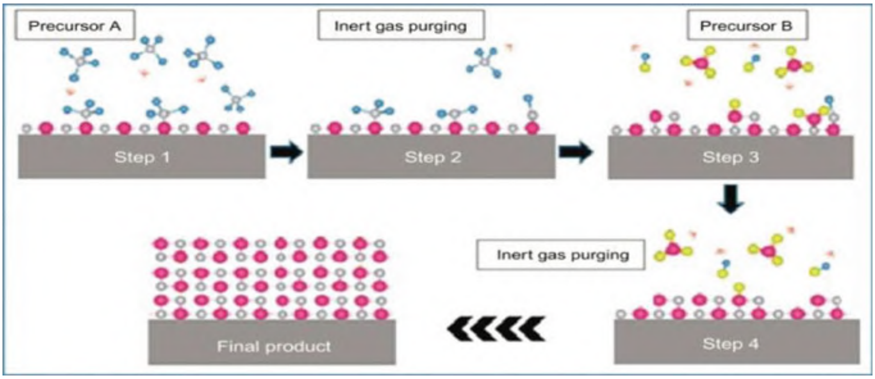

Fig. 15 Chemical vapor deposition process [34]. Taken

Plasma-Enhanced Chemical Vapor Deposition

PECVD uses Ar to ignite plasma and H2. DC or RF sputtering is used in PECVD.

H2SiH2 concentration determines amorphous or microcrystalline nanoparticle production. Thus, high H2 concentrations erode the amorphous phase and produce microcrystalline nanoproducts. Instead of 13.56 MHz, one might use 100 MHz for a better etching procedure. PECVD produces ultra-pure, non-agglomerated nanoparticles [27].

5 Functionalized Nanomaterials

Functionalization is the process of surface modification of nanoparticles by attaching chemicals or biological molecules, such as folic acid, biotin molecules, oligonucleotides, peptides, and antibodies, to improve their characteristics and more precisely strike their target. The functionalized NPs exhibit non-invasive qualities; good physical properties; and anti-corrosion, anti-agglomeration, and anti-agglomeration properties. Functionalization makes it easier to distribute these nanoparticles to different cell types specifically for applications like bioimaging, gene delivery, medication delivery, and other therapeutic and diagnostic procedures [35]. To improve the NPs' overall effectiveness and modality, extensive research has been done to functionalize them.

5.1 Methods of Surface Functionalization

Nanoparticles must have their surfaces suitably functionalized in order to be stable, biocompatible, and functional when used in bioapplications. Chemists have developed various methods, such as surface encapsulation, in situ synthesis, or self-assembly, to introduce the necessary functionality on nanoparticle surfaces in order to properly tailor and dress them. At this time, a diverse range of materials, including silica, synthetic polymers, biopolymers, dendrimers, and small molecules, have been used to functionalize nanoparticles in a wide range of applications. One of the most used methods for nanoparticle surface modification is silica coating [36, 37]. With the help of this coating technique, the core nanoparticles can be shielded from the environment by a cross-linked silica shell. It can be applied to hydrophilic and hydrophobic metal, metal oxide, and quantum dot (QD) nanoparticles with a size range of 1–100 nm. Hydrophilic ligands added to the surface of nanoparticles make them water soluble, yet they may have poor colloidal stability in buffers and biological media. Synthetic polymer coating is one of the many functionalization techniques that can be used to dissolve water-insoluble inorganic nanoparticles regardless of their core composition, to stabilize them in physiological environments, and to start introducing a variety of functionalities to nanoparticle surfaces [38, 39]. Due to their long-term stability in physiological settings and effective renal clearance, surface-functionalized nanomaterials with such a hydrostatic size of less over 10 nm are highly desired for in vivo research because of their long-lasting stabilization in physiological settings as well as effective renal clearance [40]. When an amphiphilic synthetic polymer is hydrophobically surface-coated on surfactant-capped nanoparticles, the functionalized nanoparticles are frequently much larger (>10 nm), which significantly reduces colloidal stability. Direct capping of multidentate ligands on the nanoparticles is preferable in order to reduce the thickness of the coating layer [41].

References

1. Mansoori GA, Soelaiman TF (2005) Nanotechnology—An introduction for the standards community. ASTM International
2. Kokarneswaran M et al (2020) Discovery of carbon nanotubes in sixth century BC potteries from Keeladi, India, 10(1):19786
3. Gribbin J, Gribbin M (2018) Richard Feynman: a life in science. Icon Books
4. Taniguchi N (1974) On the basic concept of nanotechnology
5. Loos M (2015) Nanosci Nanotechnol 25(1):112
6. Drexler KE (1981) Molecular engineering: an approach to the development of general capabilities for molecular manipulation. Proc Natl Acad Sci 78(9):5275–5278
7. Hulla J et al (2015) Nanotechnology: History and future, 34(12):1318–1321
8. Bayda S et al (2019) The history of nanoscience and nanotechnology: from chemical–physical applications to nanomedicine, 25(1):112
9. Leonhardt U (2007) Invisibility cup.Nat Photon 1(4):207–208
10. Haiwen L. Tag archives: Damascus steel
11. Chodos A, Ouellette J, Tretkoff E (2009) This month in physics history. Am Phys Soc News 18(4):5–7

12. Quantum dots: Nanocrystals packed with potential. S. Kelley
13. Loos M (2014) Carbon nanotube reinforced composites: CNT polymer science and technology. Elsevier
14. Nummelin S et al (2020) Robotic DNA nanostructures, 9(8):1923–1940
15. Rizwan M et al (2021) Types and classification of nanomaterials. Nanomaterials: synthesis, characterization, hazards and safety. Elsevier, pp 31–54
16. Navya P et al (2019) Current trends and challenges in cancer management and therapy using designer nanomaterials, 6(1):1–30
17. Malhotra BD, Ali MA (2018) Nanomaterials in biosensors: fundamentals and applications. Nanomater Biosens, 1
18. Sanand S et al. Nanostructured materials: classification and methods of characterization
19. Liu JL, Bashir S (2015) Advanced nanomaterials and their applications in renewable energy
20. Rafiei-Sarmazdeh Z, Zahedi-Dizaji SM, Kang AK (2019) Two-dimensional nanomaterials. In: Nanostructures. IntechOpen, London, UK
21. Habiba M, Weinel M (2019) Bottom-up and the top-down approaches in synthesis of carbon-based nanomaterials
22. Patel KD, Singh RK, Kim HW (2019) Carbon-based nanomaterials as an emerging platform for theranostics. Mater Horiz 6(3):434–469
23. Zhang B-T et al (2013) Application of carbon-based nanomaterials in sample preparation: a review, 784:1–17
24. Luo YH, Chang LW, Lin P (2015) Metal-based nanoparticles and the immune system: activation, inflammation, and potential applications. BioMed Res Int 2015:143720
25. Faheem AM, Abdelkader DH (2020) Novel drug delivery systems. Engineering drug delivery systems. Elsevier, pp 1–16
26. Baig N, Kammakakam I, Falath W (2021) Nanomaterials: a review of synthesis methods, properties, recent progress, and challenges. Mater Adv 2(6):1821–1871
27. Rajendran V (2012) Material science. Tata McGraw-Hill Publishing Company Limited, New Delhi, p 769
28. Singh JP et al (2020) Bottom-up and top-down approaches for MgO. In: Sonochemical reactions, IntechOpen, London, UK
29. Paramasivam G et al (2021) Nanomaterials: synthesis and applications in theranostics, 11(12):3228
30. Kumar CV, Pattammattel A (2017) Introduction to graphene: chemical and biochemical applications. Elsevier
31. Sputtering process | Sputtering deposition method (2021)
32. Nyamukamba P et al (2018) Synthetic methods for titanium dioxide nanoparticles: a review, p 151–1755
33. Bokov D et al (2021) Nanomaterial by sol-gel method: synthesis and application, 2021
34. Sonawane SL, Labhane PK, Sonawane GH (2021) Carbon-based nanocomposite membranes for water purification. Handbook of nanomaterials for wastewater treatment. Elsevier, pp 555–574
35. Jiang S et al (2013) Surface-functionalized nanoparticles for biosensing and imaging-guided therapeutics, 5(8):3127–3148
36. Liu SH, Han MY (2005) Synthesis, functionalization, and bioconjugation of monodisperse, Silica-Coated gold nanoparticles: Robust bioprobes. Adv Function Mater 15(6):961–967
37. Liu S, Zhang Z, Han M (2005) Gram-scale synthesis and biofunctionalization of silica-coated silver nanoparticles for fast colorimetric DNA detection. Anal Chem 77(8):2595–2600
38. Zhang F et al (2011) Polymer-coated nanoparticles: a universal tool for biolabelling experiments, 7(22):3113–3127
39. Tomczak N et al (2009) Designer polymer–quantum dot architectures, 34(5):393–430
40. Huang K et al (2007) ACS Nano 2012, 6:4483; (b) Choi HS, Liu W, Misra P, Tanaka E, Zimmer JP, Ipe BI, Bawendi MG, Frangioni JV (2007), 25:1165
41. Jańczewski D et al (2011) Synthesis of functionalized amphiphilic polymers for coating quantum dots. Nat Protoc 6(10):1546–1553

Chapter 2
An Introductory View About Supercapacitors

Manpreet Kour, Sonali Verma, Bhavya Padha, Prerna Mahajan, Aamir Ahmed, and Sandeep Arya

1 Introduction

In recent times, there aren't enough affordable, low-carbon, and large-scale substitutes to fossil fuels on this planet. The most important and difficult challenge for meeting energy demands is researching sustainable, dependable, and ecologically acceptable energy sources [1, 2]. For energy sector to progress quickly, harvesting and storing energy becomes a top priority [3–5]. The main objective of the scientific community has been to extract energy from renewable energy sources. Additionally, scientists are working to develop ways to store this energy as electricity. Energy usage and the advancement of industry and technology are closely related. In practice, finding affordable, reliable energy sources that assure a suitable level of growth will be a major challenge. Currently, research focuses on creating and implementing new technologies to improve the energy efficiency of existing processes and includes renewable sources like electrochemical energy systems, wind, sun, and biomass. Although wind and solar power are better and more environmentally friendly, they still need energy storage devices since they are unstable and erratic. A storage option based on chemical reactions is provided by batteries. This information may be crucial for important parameters, including pricing (because of its components), loading and unloading capacity restrictions, and usage cycle limits. On the basis of physicochemical processes, supercapacitors have widely been employed to store energy. Unlike batteries, supercapacitors offer a rapid cycle rate, low maintenance requirements, high power, and the ability to function in a wide range of temperatures.

M. Kour
Department of Physics, Cluster University of Jammu, Jammu, Jammu and Kashmir 180001, India

S. Verma · B. Padha · P. Mahajan · A. Ahmed · S. Arya (✉)
Department of Physics, University of Jammu, Jammu, Jammu and Kashmir 180006, India
e-mail: snp09arya@gmail.com

© The Author(s), under exclusive license to Springer Nature Singapore Pte Ltd. 2024
C. M. Hussain and M. B. Ahamed (eds.), *Functionalized Nanomaterials Based Supercapacitor*, Materials Horizons: From Nature to Nanomaterials,
https://doi.org/10.1007/978-981-99-3021-0_2

So, it seems reasonable to say that the supercapacitor is a very effective energy storage medium. Regular capacitors and secondary ion batteries are connected via supercapacitors [6–9].

Their high power and energy densities, prolonged cycle lifetimes, instantaneous high current discharge, rapid charge and discharge, and economical and non-toxic nature are just a few of their many advantages [10–13]. The usage of diverse nanostructured engineered materials for supercapacitors has gradually gained scientific attention during the last few decades. Compared to their bulk counterparts, these nanoparticles typically exhibit improved capacitance. Nanostructured materials provide advantages in terms of chemical activity, reaction rate, and surface area as well as a surplus of active sites for electrochemical processes. It is one of the hotspots of scientific research and involves materials chemistry, energy, electrical devices, and other areas [14, 15].

Due to their superior performance and environmental friendliness, supercapacitors found applications in a diverse range of industries, such as automation factory, shipping, smart tools, electrical goods, military, communication systems, medical devices like dialysis machines and ultrasonic lasers, as well as energy vehicles [16]. Supercapacitors work well in applications that need a short load cycle and great reliability, such as power quality improvement and energy recapture sources like forklifts, load lifters, and even electric cars [17]. The use of supercapacitors in hybrid automobiles is one of its potential applications [18]. When combined with batteries, supercapacitors may be employed as short energy storage devices that have the high power capacity to generate power from braking [19].

Because of their enormous power capacities, a supercapacitors bank may provide emergency power during a power outage. Even while the supercapacitors have a greater energy density than traditional capacitors, they still can't compare to fuel cells or batteries. Total area, electrical conductivity, electrode wetting, and the porosity of electrolyte solutions all have a significant impact on the electrochemical effectiveness of an electrode material [20]. In order to store electric power in volume and weight, passive components must be used in all electronic applications. The supercapacitor confronts several challenges despite having countless advantages and possibilities [21, 22]. When compared to electrolytic capacitors, supercapacitors may store 10–100 times more energy in the same amount of space. It is especially designed capacitor which is used in storing large electrical charge.

2 Energy Storage Devices

2.1 Battery

In order to provide power, a battery is often used. The electrolyte acts as a separator between the cathode and the anode. Batteries are devices that can store energy chemically and then transform that energy back into electricity when it is required. During charging and discharging, the cathode and anode undergo a chemical process known as oxidation–reduction across the separator (electrolyte).

2.2 Capacitor

An electrical capacitor consists of two or even more parallel plates separated by an insulator, forming a two-terminal device. If you apply a voltage across the plates, current will flow through the capacitor until the voltage at the anode and cathode is equal. The insulating material acts as a barrier to the passage of current between the two conducting plates. The result of this transformation is an effect that is stored in a capacitor as an electrostatic field.

2.3 Supercapacitor

Supercapacitors, also known as ultra-capacitors, are polar capacitors with a large capacitance but a low voltage rating. Supercapacitors have low voltage ratings of about 2.5–2.7 V, and their capacitance may range from 100 to 12,000 F. Supercapacitor is an energy storage device that bridges a capacitor and a battery. These capacitors have a higher charging capacity per unit of volume than electrolytic capacitors and can be recharged more quickly than a battery. The supercapacitor fills the gap between the battery and the electrolytic capacitor. As a replacement for traditional electrochemical batteries, especially lithium-ion batteries, supercapacitors are on the top position. Supercapacitors are more analogous to batteries than capacitors in terms of physical mechanism and operating principle. They have a slower charging reaction than ceramic capacitors but can store a lot of energy rapidly (not as much as batteries, due to their lower energy density in terms of weight and volume) [23]. Even though supercapacitors store energy in a different way than conventional capacitors, the underlying equations used to explain them are the same as those used for capacitors. To achieve their superior performance, high-capacity supercapacitors always employ a wide variety of electrode-active materials, including activated carbon, carbon nanotubes (CNTs), graphene, etc. Supercapacitors may be made using either aqueous or organic electrolytes, but the supercapacitors which are made of organic electrolytes can deliver high voltage. However, aqueous electrolyte-based supercapacitors have a long cycle life in comparison to organic ones. The development of flexile solid-state capacitors is essential for powering the bendable and wearable technology. The development of supercapacitor has the potential to lead significant improvements in energy sector. The fundamental equations that control normal capacitors also apply to supercapacitors, which use thinner dielectrics and electrodes with higher surface areas to produce larger capacitances. This allows for greater power density than batteries and more energy density than standard capacitors. Table 1 shows a comparison between battery, supercapacitor, and electrolytic capacitor characteristics.

Therefore, supercapacitors might become a viable power source for a growing number of applications in energy sector [24]. In general, capacitors are used for applications that need a quick discharge rate, whereas batteries are used for those that can tolerate a slower discharge rate. It can be observed that batteries can achieve

Table 1 Comparison between characteristics of battery, supercapacitor, and electrolytic capacitor

Characteristics	Capacitor	Supercapacitor	Battery
Working	Electrical energy is stored in a capacitor in the form of an electric field	Supercapacitor stores energy between the ions of the electrolyte and electrode in a double layer of charge	Battery store energy in the form of chemicals and convert it back to the electrical energy when needed
Construction	Capacitor is a simple two terminal device. Terminals are metallic plates and there is a dielectric material (insulator) between them	For supercapacitor, an electrolytic solution is utilized in place of dielectric	There are three main components: the cathode, anode, and separator (electrolyte)
Operation	Capacitor store electrons	Supercapacitor store electrons	Battery generates electrons
Type of device	Capacitor is a passive component	Supercapacitor is a passive component	Battery is an active component
Charging and discharging time	About 1–10 s are needed for the charging and discharging processes	A supercapacitor can store more energy than electrolytic capacitor in the same amount of space, and it can release that energy much more quickly than a battery	A battery has a long charging/discharging time (10–60 min)
Energy density	Low	Low	High
Power density	High	High	Low
Operating voltage	6 V–800 V/cell	2.3 V–2.75 V/cell	1.2 V–4.2 V/Cell
Operating temp	−20 to +100 °C	−40 to + 100 °C	−20 to +65 °C
Voltage rating	Up to kV	Less than or equal to 5 V	Various voltage-10s of volt
Cost	Low	High	High
Lifetime	>100 k cycles	>100 k cycles	150–1500 cycles

an energy density of up to 150 Wh/kg, which is around 10 times that of an electrochemical capacitor. Batteries can not match the power density of electrochemical capacitors. The performance of electrochemical capacitors is predicted to be 20 times higher than that of batteries, although batteries barely exceed 200 W/kg. Batteries have drawbacks such as a short lifespan, high cost, and reduction in performance when subjected to quick charge/discharge cycles or low temperatures [25]. These supercapacitors cannot replace battery technology yet, but they might be useful as a complement in the event of a brief blackout by supplying the necessary current instantly and draining the battery slowly. Electrochemical supercapacitors may be deployed in conjunction with big battery packs to make up for brief power outages. Short-term disruptions impose a significant strain on batteries, but this would considerably reduce that strain. The primary emphasis of current supercapacitor research is on increasing their energy density without sacrificing their other desirable characteristics, such as high power density, quick charge/discharge, and cycle stability.

3 Application and Fundamentals of Supercapacitor

Before we move on to the working of supercapacitors, let us first understand the structure of a supercapacitor. Unlike ceramic or electrolyte capacitors, it does not contain a dielectric substance. Supercapacitors, as depicted in Fig. 1a, are made up of two porous electrodes, an electrolyte, a separator, and current collectors.

(a) Current collector

The metal foil used in modern collectors is typically composed of aluminum because it is less expensive than titanium, platinum, etc. The active material is applied on them.

(b) Electrodes

The surface area of electrode directly affects the capacitance value. Typically, highly porous active carbon materials, CNTs, or transition metals are employed as electrode materials. The porous structure makes it possible to store much more charge carriers (ions or radicals from the electrolyte) in a given volume. As a result, supercapacitors have more capacitance. A current collector with coated electrodes is submerged in an electrolyte.

(c) Separator

To prevent short circuits, the separator between the electrodes is formed of a substance that is transparent to ions but an insulator for direct contact between porous electrodes. Supercapacitors are different from normal batteries and capacitors because of their distinctive structural design. Utilizing activated carbon expands the surface area, increasing the capacitance value. Power density is increased by using an electrolyte with low internal resistance. Together, these two give supercapacitors the capacity to quickly store and release energy [27].

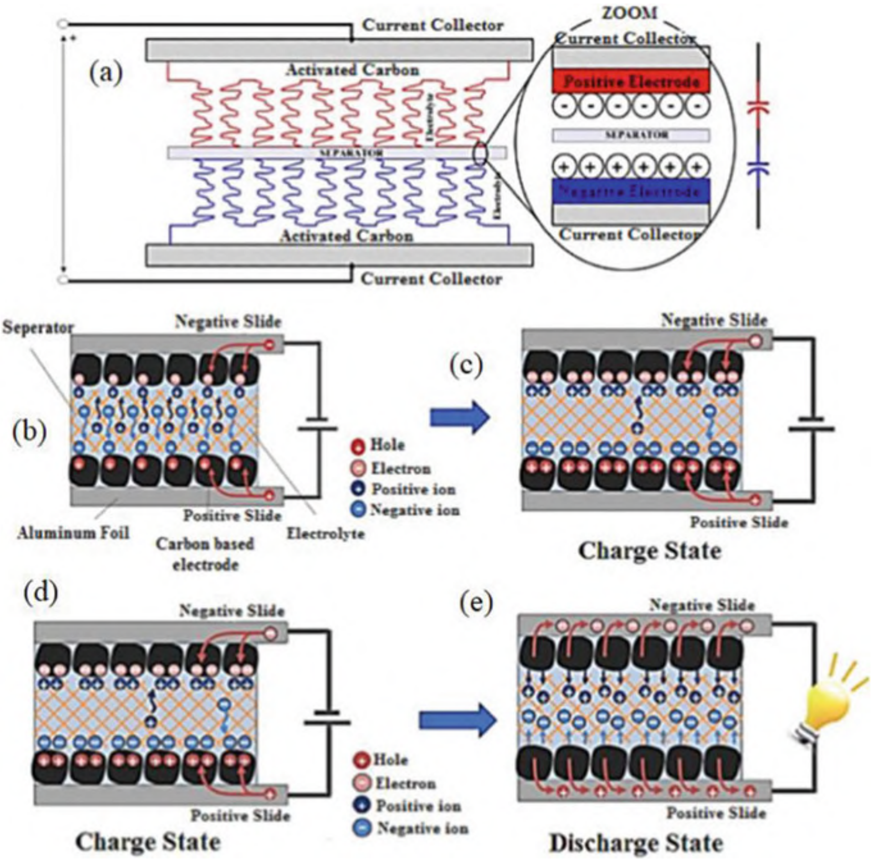
(a)
Current Collector
Activated Carbon
Electrolyte
SEPARATOR
Activated Carbon
Current Collector
ZOOM
Current Collector
Positive Electrode
SEPARATOR
Negative Electrode
Current Collector
(b)
Seperator
Negative Slide
Positive Slide
Aluminum Foil
Carbon based electrode
Electrolyte
Hole
Electron
Positive ion
Negative ion
(c)
Negative Slide
Positive Slide
Charge State
(d)
Negative Slide
Positive Slide
Charge State
Hole
Electron
Positive ion
Negative ion
(e)
Negative Slide
Positive Slide
Discharge State

Fig. 1 **a** Structure of supercapacitor, **b** idle state of supercapacitor, **c** charge state of supercapacitor, **d** charge state of supercapacitor, **e** discharge state of supercapacitor. Reproduced from [26] with permission. Copyright 2020, Elsevier

3.1 Energy Storage in Supercapacitors

There are both positive and negative ions in the electrolyte solution between the electrodes. Supercapacitors work by allowing a voltage to build up between two electrodes; this causes one of the electrodes to become positively charged while the other becomes negatively charged. As a result, the negative ions are drawn to the positively charged electrode, while the positive ions are drawn to the negatively charged electrode. Inside both electrodes, ions accumulate to form a thin layer. An electrostatic double-layer forms, which acts like connecting two capacitors in series. Both resulting capacitors have a high capacitance value because of the close proximity of their charge layers.

Charging, also known as the development of the electric field, begins when the voltage is applied. The charging procedure is shown in Fig. 1b, c. When voltage is provided, ions with opposite charges are drawn to each collector. The electrolyte's ions are attracted toward the surfaces of the two main collectors. On each current collector, a negative and positive charge is developed. Figure 1b, c shows that two distinct layers of charge have formed, which is why supercapacitors are also known as electrical double-layer capacitors. Now, with Fig. 1d, e as a reference, we can comprehend the discharge process.

3.2 Application of Supercapacitors

Supercapacitors have a unique storage capacity, which led to their widespread use in a variety of applications, including electric drives, UPS systems, traction, electric cars, SSDs, LED lamps, and solar panels.

3.2.1 Hybrid Vehicles

The key industry for supercapacitors is electric vehicles. In India, emission-free electric buses were introduced by Brihan Electric Supply and Transport (BEST). The motors create back electromotive force during braking. To charge the supercapacitors, regenerative energy from the back electromotive force is employed. When used in conjunction with batteries, supercapacitors extend battery life while condensing battery size. Shanghai buses employ supercapacitors as their only source of power (at every third stop, it is given a quick 1–2 min charge using the kinetic energy created by braking). China has shown the world that this technology can be used extensively for electric vehicles. The technology that combines a supercapacitor and battery, however, is more advantageous.

3.2.2 Electronics and Ultra-Low Power Uses

Supercapacitors are utilized in radio tuners, mobile phones, laptop memory, and other electronic devices. They are utilized in conditions like LED flash units where a brief power surge is necessary.

3.2.3 Solar Panel

Firstly lithium-ion battery is used to store solar energy but these supercapacitors can balance out the energy storage in the batteries by taking care of charging and discharging cycle. It can balance out uneven charging patterns in the battery cell and can also charge rapidly. So, we don’t have to worry about the sun not being out for long time. In solar cells, supercapacitor are used in series with battery.

3.2.4 Renewable Energy

Modern, variable-speed three-bladed turbines are in use. Depending on the wind speed and turbine operating point, the blade angle can be changed. Quickly pushing the blades to the 90° position prevents mechanical harm to the blades in the case of a turbo or power converter failure. In wind energy, supercapacitors are utilized to supply electricity for blade pitch control [28–30].

4 Types of Supercapacitor

Supercapacitors can store and release energy faster than batteries because their energy storage method comprises of charge separation at the interface of the electrolyte and the electrode. When it comes to storing energy, supercapacitors are the way to go because of their large capacity and low internal resistance. A supercapacitor contains an electrolyte, two electrodes, and also an insulating separator between the electrodes. The most crucial supercapacitor component is the electrode material. Consequently, there is a wide variety of supercapacitors that may be identified by the electrode materials used and the energy storage techniques used. Figure 2 demonstrates different types of supercapacitors.

4.1 Classification on the Basis of Energy Storage Mechanism

In order to store energy, a supercapacitor relies on the ion transport from the electrolyte to the electrodes. Three classes of supercapacitors are categorized based on their energy storage mechanism as shown in Fig. 2.

4.1.1 Electrochemical Double-Layer Capacitors (EDLCs)

Electrodes for EDLCs are made up of different carbon-based compounds, together with a separator as well as an electrolyte. A non-faradic mechanism, such as electrostatic repulsion, allows EDLCs to retain charge without requiring energy transfer between electrode and electrolyte [31]. The electrochemical double layer is the energy storage principle employed by EDLCs. Whenever a voltage is applied, the accumulated charge on the electrodes attracts ions from the electrolyte, which then diffuses through the separator into the pores of the oppositely charged electrode. To keep away ions from mixing back together at the electrodes, a second film of charge

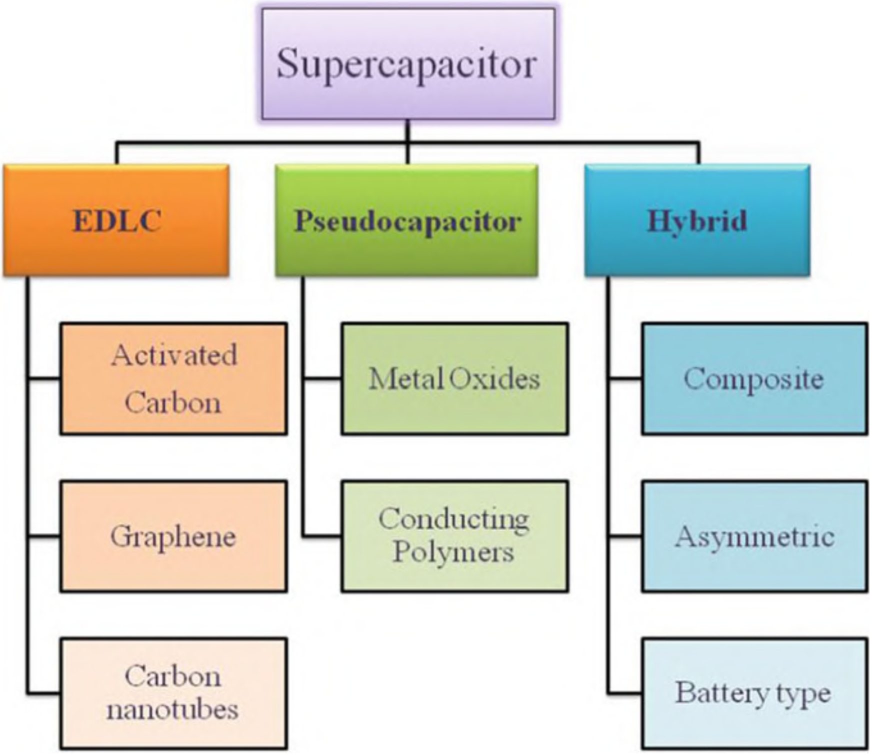
Supercapacitor
EDLC
Pseudocapacitor
Hybrid
Activated Carbon
Graphene
Carbon nanotubes
Metal Oxides
Conducting Polymers
Composite
Asymmetric
Battery type

Fig. 2 Taxonomy of supercapacitors

is generated. Increased energy density in EDLCs is possible because of their double layer, more specific surface area, and smaller inter-electrode distances [32].

Additionally, the EDLC's storage mechanism enables much faster energy absorption, distribution, and improved power output. The non-faradic process prevents a chemical reaction. It eliminates swelling that battery-active material exhibits while being charged and discharged. EDLCs and batteries differ in a number of ways, including EDLCs have higher cycle life than batteries, which can only sustain a few thousand [33]. The electrostatic surface charging technique, however, results in a low energy density for EDLC devices. This is why there is so much emphasis in the field of EDLCs right now on finding ways to enhance energy accomplishment and broaden the range of operating temperatures beyond which batteries are useless. Depending on the electrolyte utilized, EDLC performance can be altered. Figure 3a demonstrates the mechanisms for storing charge in EDLC.

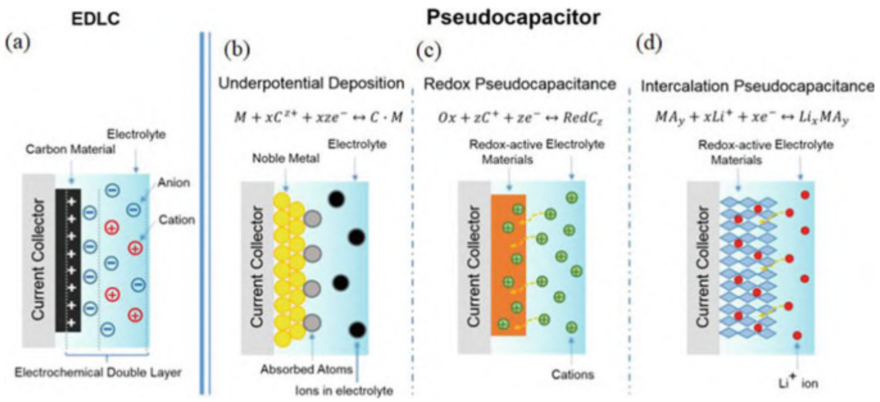
EDLC
Pseudocapacitor
(a)
Electrolyte
Carbon Material
Anion
Cation
Current Collector
Electrochemical Double Layer
(b)
Underpotential Deposition
$M + xC^{z+} + xze^- \leftrightarrow C \cdot M$
Electrolyte
Noble Metal
Current Collector
Absorbed Atoms
Ions in electrolyte
(c)
Redox Pseudocapacitance
$Ox + zC^+ + ze^- \leftrightarrow RedC_z$
Redox-active Electrolyte Materials
Current Collector
Cations
(d)
Intercalation Pseudocapacitance
$MA_y + xLi^+ + xe^- \leftrightarrow Li_xMA_y$
Redox-active Electrolyte Materials
Current Collector
Li^+ ion

Fig. 3 **a** Mechanisms for storing electrical charges in **a** EDLC and **b**–**d** different pseudocapacitive electrodes: **b** underpotential deposition, **c** redox pseudocapacitor, **d** ion intercalation pseudocapacitor Reproduced from [39] with permission. Copyright 2018, American Chemical Society

4.1.2 Pseudocapacitors

Pseudocapacitors, unlike EDLCs, store electrical energy via faradic process, which includes the transfer of charge between an electrode and an electrolyte [34]. A pseudocapacitor undergoes redox when a potential is applied, which entails the passage of charge across the double layer and causes faradic current to flow through the supercapacitor cell. Pseudocapacitors can attain higher specific capacitance and energy densities than EDLCs owing to the faradic process involved. Metal oxides as well as conductive polymers are some examples of pseudocapacitive materials. This sparks interest in such materials, however, because of their faradic nature and the reduction–oxidation cycle, they suffer from cycling instability as well as low power density [35, 36]. There are two types of pseudocapacitance mechanisms, intercalation and redox pseudocapacitance.

(a) Underpotential deposition

As shown in Fig. 3b, this phenomenon takes place when metal ions adsorb onto a surface other than the one they were originally bound to at an electrostatic potential that is less negative than that of equilibrium potential for the reduction of metal. Deposition of Pb on Au electrode is an example of an underpotential deposition.

(b) Surface redox or intrinsic pseudo capacitors

In this type, load transfers are simultaneously experienced with surface adsorption or desorption. Charge storage in redox pseudocapacitance processes is shown schematically in Fig. 3c, where charge transfer occurs at the electrode surface. This is inherently a pseudocapacitive material due to its high proton and electron conductivity. MnO_2 and Fe_3O_4 are two examples of transition metal oxides that have inherent pseudocapacitive behavior. There are distinctions between pseudocapacitive supercapacitors (PSC) and electrostatic supercapacitors devices. When a voltage is applied to a PSC, an instant and reversible faradic reaction takes place between the electrode material and the charge channel via both layers. Many different materials, including metal oxides (MnO_2, RuO_2, and Co_3O_4) and conducting polymers, are subject to these types of redox reactions.

(c) **Intercalation-type reactions**

Pseudocapacitance intercalation is another important category because it maximizes the utilization of electrode material via the intercalation and decomposition of large ions (such as MoO_3 and Nb_2O_5) [38]. Ion intercalation and deintercalation are shown graphically in Fig. 3d. Intercalation refers to the process by which a foreign molecule or ion is inserted into a host material. For intercalation to occur, guest ions must first adsorb onto the host lattice, at which point intermediary stages must be formed. There is no discernible change in crystal structure during the faradic charge transfer in such materials (TiO_2, Nb_2O_5, and MoO_3). In contrast to traditional surface redox pseudocapacitive materials, they exhibit both reversible and rapid charge storage.

4.1.3 Hybrid Supercapacitor

We have shown that EDLCs provide superior power performance and cycle stability, as well as superior specific capacitance in the context of pseudocapacitance. In a hybrid system, one cell contains both a capacitor and a battery-like energy source, providing the benefits of both [37]. With the correct electrode arrangement, the voltage of the cell may be increased, leading to greater power and energy densities. Many different configurations including positive and negative electrodes and both inorganic and aqueous electrolytes have been tried. Avoiding turning a supercapacitor into a conventional battery is essential due to the faradic electrode's tendency to increase energy density at the expense of cyclic consistency, a major disadvantage of hybrid gadgets in compared to electrochemical double-layer capacitors [40]. There are now three main kinds of hybrid supercapacitors being studied, and they may be distinguished by their electrode configurations: battery type, composite, and asymmetric.

(a) **Composite**

Carbon-based multilayered electrodes obtained by integrating either conductive polymer or oxide of metal come under this category. Pseudocapacitive materials benefit from an enhanced interface with the electrolyte when made from carbon materials has high specific surfaces and capacitive multiple layers of charge. The capacitance of composite electrodes is increased by pseudocapacitive material through the faradic reaction. The two most common types of composites are ternary and binary composites. Binary composites only need two distinct electrode materials, but ternary composites require three.

(b) **Battery type**

Hybrids of the battery type, like asymmetric hybrids, combine two electrodes. The purpose of this setup was to combine the benefits of batteries and supercapacitors in a single cell.

(c) **Asymmetric**

Asymmetric hybrids, which couple EDLC with a pseudocapacitor electrode, combine non-faradic and faradic processes. In particular, metal oxide as well as the conducting polymer acts as the positive electrode, whereas the carbon material acts as the negative electrode.

4.2 Symmetric & Asymmetric Supercapacitors

While an asymmetric supercapacitor employs two electrodes made of two distinct materials, a symmetric supercapacitor uses two electrodes of a similar design. Electronics have evolved significantly in recent years, with a preference for portability and flexibility. It is necessary to create energy storage technologies that are adaptable, compact, and lightweight. The ideal substitute for these flexible electronic devices is a supercapacitor. Their primary needs are membrane/electrolyte systems and flexible, lightweight electrodes [41]. The active materials in electrodes are oxides, conductive polymers, or carbonaceous compounds. Many metal oxides have been employed in various symmetrical and asymmetrical forms, including Mn_3O_4, RuO_2, Co_3O_4, MnO_2, NiO, and Bi_2O_3.

But carbonaceous materials, such as CNTs, carbon black, activated carbons, and graphene oxide. These materials exhibit high conductivities, particular surfaces, capacitive charge/discharge properties, and some are inexpensive [42]. Finally, polythiophene, polypyrrole, polyaniline, and their derivatives are the most widely utilized conductive polymers. Many of its most distinguishing characteristics involve relative electrical conductivities, particular layers, and specialized capacities [43]. When we used electrode materials in supercapacitors, nanostructured hybrid materials have the benefit of combining a double-layer loading process with a redox mechanism. By doing so, one may get large amounts of power, energy, and capacitance. Supercapacitors may benefit from nanocomposites of carbonaceous materials (double-layer mechanisms) and metal oxides or conducting polymers (pseudocapacitive mechanism). CNTs and carbon black nanocomposites could be utilized in supercapacitors as electrode medium [44]. Depending on the particle size, mode of synthesis, porosity, and testing circumstances, the reported specific capacitance values for PANI (polyaniline) nanostructures have ranged between 200 and 2300 F/g [45]. They have also reported capacitance values between 200 and 600 F/g when using PANI-CNT nanocomposites [46]. Various flexible supercapacitor prototypes were created employing membranes made of polyvinyl alcohol (PVA)/H_2SO_4 as the electrolyte and separator and carbon black/graphene sheets as the electrode material [47]. Using flexible steel mesh as the support for the current collector and commercial ink as the electrodes, a symmetric design was reported [48]. On the basis of activated carbon and gel electrolyte, printable and flexible supercapacitors were created [49]. Electrodes made of graphene oxide, zinc oxide, and polypyrrole were sandwiched in such a PVA hydrogel electrolyte to create flexible symmetric supercapacitors. This study demonstrates the fabrication of both symmetric as well asymmetric flexible supercapacitors utilizing polyaniline–carbon nanotube nanocomposites and polyaniline nanostructures on carbon cloth for electrode materials. Specific energy, capacitance values, power, and stability with multiple charge/discharge cycles are all evaluated using electrochemical methods to gauge capacitive behavior. Specific energy and capacitance are improved upon in this research as compared to previous works that used rigid, non-flexible, and symmetric supercapacitors.

4.3 Classification of Supercapacitors on the Basis of Electrode Material

Different materials may be utilized to make supercapacitors with different capacitance ranges, depending on the requirements of the application; several types of energy storage may be required. Based on how they are used in hybrid supercapacitors, pseudocapacitors, and EDLCs. Supercapacitors primarily employ three different kinds of electrode materials. Supercapacitors may be made from many different substances; carbon is the most common industrial material since it is versatile and widely used. Metal oxides made of nickel, cobalt, manganese, and ruthenium are among the additional components. Supercapacitors have also used conducting polymers. Supercapacitors are now more frequently built using CNTs in recent years. Increases in surface area are only one of several benefits of using nanomaterials like carbon nanotubes. Composites made by combining two or more materials are the other common kind of supercapacitor utilized today. Perhaps a nanomaterial is included in the composites. A composite made from CNTs and metal oxide or conductive polymers is one example. For supercapacitor electrodes, researchers are searching for nanostructured materials with increased surface area and improved capacitive functional characteristics. Developing nanoengineered materials is increasingly recognized as a key factor in developing high-performance supercapacitor devices.

4.3.1 Carbon Materials

Electrodes made from carbon compounds are widely used in the manufacture of supercapacitors. All types of carbon compounds are used as electrode materials most often while designing supercapacitors due to their affordable price, large surface area, accessibility, and well-established electrode production technologies. Carbon-based materials use an electrochemical double-layer storage mechanism, which forms at the electrode and electrolyte interface. Therefore, the capacitance is determined mostly by the available surface area of the electrolyte ions. Significant factors that impact electrochemical performance include surface functionality, pore size distribution, pore shape and structure, surface functionality, specific surface area, and electrical conductivity [50]. The ability to accumulate charges at the electrode/electrolyte interface is enhanced in carbon materials with a large specific surface area. Improving carbon materials' specific capacitance requires attention to both high specific surface area and pore size, but also to the degree to which the surface is functionalized. Activated carbon, CNTs, graphene, carbon aerogels, and other carbon-based materials are examples of electrode materials [51, 52].

Because of their special material characteristics, CNTs are an excellent choice for use in supercapacitors. The electrical, mechanical, optical, and chemical properties of CNTs are their most crucial qualities. They have several desired mechanical characteristics as well as great electronic conductivity. These features, in addition to the higher surface area afforded by CNTs, are facilitating their increased usage in supercapacitor technology. These characteristics, together with the increased area offered by carbon nanotubes, are enabling them to be used more frequently in supercapacitor manufacturing. CNTs are accessible, affordable, and strong. For electrodes based on CNTs, there is already a market for their manufacture. CNT-based supercapacitor electrodes have a constant charge distribution that makes use of the majority of the surface area, enabling effective surface area utilization. Despite the activated carbon electrodes having a higher area of the surface, this enables the electrode-based CNTs to obtain capacitances comparable to those electrodes which are made of activated carbon. Electrode-based CNTs are able to achieve capacitances competitive with those of activated carbon electrodes despite the fact that the latter has a larger surface area [53]. Mesoporous CNT networks in electrodes are an additional benefit. Due to the easier electrolyte diffusion, the corresponding series resistance is reduced, increasing the maximum usable power [54].

EDLC supercapacitors commonly employ carbon aerogels. Since their structure consists of networks of carbon nanoparticles, they are very durable and difficult to break; their usage in electrodes does not need the use of a binder component. They can be employed in electrodes without a binder substance because their mesopore-spaced carbon nanoparticle networks are continuous. As a result, electrodes built of carbon aerogels have reduced equivalent series resistance, which aids in improving power output [55].

4.3.2 Metal Oxides

Due to its high conductance, oxides of metal are used as electrode materials in supercapacitors [56]. Supercapacitors made of metal oxide exhibit high specific capacitance and prolonged operation [57]. The use of ruthenium oxide in supercapacitor technology is now a topic of intense research and development [58]. Compared to conducting polymers and carbon-based materials, ruthenium oxide has a larger capacitance [59]. It combines metal-type conductivity with reversible redox processes that take place both in the bulk and at the electrode–electrolyte interface [59]. The high price of ruthenium oxide is the primary impediment to widespread use, which is why researchers are looking at composite materials and manufacturing ways to bring down prices without sacrificing performance [60]. Manganese oxide is a potential material for use as an electrode in supercapacitors. It is reasonably priced, safe for the environment, and enables good capacitive performance [61]. Manganese oxides with nanostructures have generated interest in supercapacitors [61]. Manganese oxide has attracted a great deal of attention lately due to its unique chemical and physical properties and several applications in activator, ion exchange, molecular adsorption as well as biosensor. Supercapacitors often employ manganese dioxide (MnO_2) as an electrode material because of its low cost, high capacitive performance in electrolyte solution, and low environmental impact. Different processes have been used to create these oxides. Similar to ruthenium oxide, this material's main flaw is its weak conductivity. Additionally, only surface atoms are used in the charge–discharge processes in this material, which results in limited material utilization. To start addressing this, certain efforts have already been made, particularly by using this material in composite form with CNTs [62].

4.3.3 Conducting Polymers

Compared to other materials, conductive polymers have high capacitance, good conductivity, and low equivalent series resistance, making them ideal for use in supercapacitors. Because of their high capacitance and the fact that conducting polymers have a large area, they are employed in supercapacitors. Metallic conductivity, a desirable quality for supercapacitor electrode materials, can be achieved by doping these compounds. Several carbon compounds, such as activated carbons, are regarded to be inferior to them, although they are seen as preferable for a number of reasons [63]. Polypyrrole, polyaniline (PANI), and poly-(3,4-ethylenedioxythiophene) (PEDOT) are some of the frequently used conducting polymers. It has been demonstrated that these materials have specific capacitances that are comparable to those of metal oxides like ruthenium oxide [64, 65]. One of the challenges with conducting polymers is the lack of efficient n-type doped (negative charge) material [66]. Another issue is the inadequate mechanical stability that results from mechanical stress during charge–discharge cycles.

4.4 Nanocomposite-Based Electrode Materials

Electrodes made from composite materials combine the physical and chemical charge storage capabilities of carbon-based materials with those of metal oxide or conducting polymer components.

4.4.1 Carbon–Carbon Composites

Huge amounts of specific surface area (SSA) are available to the ions of the electrolyte, which gives carbon compounds a higher capacitance. If the effective SSA in carbon materials can be increased, the supercapacitor power and energy density will improve. To address the issue of dispersion that graphene confronts, functionalized graphene that does not rely on covalent bonds has been developed. Because of van der Waals interactions, oxide of graphene tends toward stack on top of each other and then disperse as the reduction proceeds, reducing the available surface area to the electrolyte. Single-walled carbon nanotubes (SWCNT) may be used as spacers to prevent layers from having to be restacked. When CNTs are introduced, electrolyte intra-pores form. Ionic liquid electrolyte was used to create graphene supercapacitors with a capacitance of 261 F/g and an energy density of 123 Wh/kg [67].

4.4.2 Carbon–Metal Oxides Composites

In a study, the differences among pure $MnO_{2,}$ CNT, and a mixture of MnO_2/CNT were compared. Simple hydrothermal treatment was employed to produce the composite. In comparison to CNT and pure MnO_2 electrodes, the MnO_2/CNT nanocomposite electrode had a better specific capacitance and rate capability and specific capacitance. The composite's high specific capacitance may be explained by $MnO_{2's}$ large specified surface area and structure that is highly permeable. Graphene and MnO_2 were used to create an asymmetric supercapacitor. While pure graphene served as the anode, the produced composite of graphene and MnO_2-coated metal was employed as the cathode. On a graphene electrode, electroactivation was employed to produce a 245 F/g capacitance at a charging current of 1 mA. With the addition of MnO_2, the capacitance rose to 328 F/g at the same charging rate, yielding an energy density of 11.4 Wh/kg and a power density of 25.8 kW/kg [67]. A study was conducted utilizing CNT/MnO_2, and many results were observed. First, compared to randomly oriented CNTs, vertically aligned ones have higher capacitance, demonstrating the considerable influence of morphology on capacitance. Second, the surface was treated with water plasma, and it was found that this produced better outcomes since the nanotube's active surfaces were clearer and bigger. Last but not least, using the electrochemical deposition approach, MnO_2 addition produced the greatest specific capacitance of 475 F/g. Another study made use of a combination made by reduced graphene oxide (rGO) and molybdenum sulfide (MoS_2). A straightforward one-pot hydrothermal technique was used to create the composite. The resulting composite had good cycle stability and yielded a 253 F/g specific capacitance at 1 A/g of current density [68]. In this experiment, activated carbon was utilized because it has desirable qualities including a high surface area, good electrical characteristics, and a reasonable cost. Cobalt, manganese, and nickel are three distinct metal oxides that were used to determine which combination would yield the maximum specific capacitance. Activated carbon served as the anode while a mixture of two oxides of metal served as the cathode, as mentioned in this experiment. The specific capacitance of 12 different samples ranged from 5 F/g for ($Mn_{0.8}Co_{0.2}$) due to the sample's rough surface and uneven crystalline pattern made it challenging for the passage of electrolyte, to 78 F/g for ($Mn_{0.6}Co_{0.4}$), a result of the huge pores that were seen in images taken using a scanning electron microscope and permissible for easy diffusion of the electrolyte [22].

4.4.3 Carbon–Conducting Polymer Composites

Carbonizing PANI and subsequently its activation with KOH yielded activated carbon with desirable properties, including a significant SSA (1976 m^2/g), small diffusion length, and small pore size distribution (3 nm). The final composite displayed outstanding performances. In 6 M KOH, a large specific capacitance of about 455 F/g was attained. After more addition of graphene to PANI, the specific capacitance retentivity ratio increased from 88.7 to 94.6% after 2000 cycles [69]. Poly (3-methylthiophene) pMeT was selected as it is easy to produce from a low-cost commercial monomer. Because of the impracticality of using anodes with higher polymer content in the composition (80%), pMeT cannot be projected for use in n/p type supercapacitors. The hybrid arrangement of pMeT and activated carbon as negative and positive electrodes, respectively, created a supercapacitor with enhanced outcome and expense when equated to carbon supercapacitors with a double layer. Another study using graphene nanosheets (GNS)/PANI composite was conducted. This composite was made by in situ polymerization, and its high conductivity and relatively large area of particle deposition on PANI were made possible by the presence of GNS. With an energy density of 39 Wh/kg and a power density of 70 kW/kg, a high specific capacitance of 1046 F/g at 1 mV/s was achieved [70]. Utilizing in situ polymerization, three distinct composites made of carbon nanotubes, graphene nanosheets, and polyanilines (GNS/CNT/PANI) were created. GNS/PANI had the greatest specific capacitance, 1046 F/g, followed by CNT/PANI (780 F/g) and GNS/CNT/PANI (1035 F/g). Only 6%, 52%, and 67% of the original capacitance is lost after 1000 cycles for CNT/PANI, GNS/CNT/PANI, and GNS/PANI, respectively [71].

5 Separators for Supercapacitors

A separator is an essential component of supercapacitors because it allows for unrestricted ionic flow and isolates electronic flow, which in turn improves supercapacitors' security and electrochemical characteristics. Unfortunately, a relatively small number of researchers have devoted their attention to improving the shape and chemical makeup of separator membranes [72]. Figure 4 shows the progressive evolution in separator. Diverse materials, including polyolefins, aqua gel, and rubber, have been used to create separators. To prevent a short circuit from occurring between the electrodes, the separators must be both thin and insulating [73]. As well as having acceptable dielectric properties and electrochemical stability inside the electrolytes that are being employed, these materials should increase mobility of ions between the surface of electrode and electrolyte. Separators, however, frequently exhibit reduced ionic conductivity over time [74] or dry up and collapse. In order to separate organic liquid electrolytes, macroporous separators like poly(vinylidene fluoride-co-hexafluoropropene) (PVDF-HFP) and poly(vinylidene fluoride) (PVDF) are used [75]. The electrolyte preservation and electrical conductivity of these materials are also improved. However, compared to dense membranes, such highly porous membranes have lower mechanical strength [76]. Because of their poor heat stability and slower ion transfer kinetics, polyolefin-made microporous separators are only used in a limited number of applications. Sulfonated poly(ether ether ketone) (SPEEK) and Nafion membranes are now the most widely utilized dense separator membranes. By submerging these membranes in sulfuric acid solutions, separators from these membranes are created [77, 78]. However, a significant disadvantage of these membranes is their high cost and the scarce availability of the raw ingredients needed for their production [79]. Figure 4 shows the advancements made in the selection of materials and manufacturing techniques utilized to create separators. The application at hand determines the separator to use.

Separators used as structural members have to be able to support mechanical load. Flexible separators are needed for wearable electronics. Separators should be able to tolerate high temperatures without significantly compromising their function in applications like oil drilling. It is expected that they will have the ability to temporarily catch and store the energy on occasion. This review looks at the several types of separator material now in use, the processes used to make them, and how all of these elements interact to determine supercapacitor performance.

5.1 Separator Membrane Materials

5.1.1 Polymer-Based Membrane

Since polymer-based materials are inexpensive, plentiful, and simple to produce, they are excellent separator options because of their great chemical and mechanical

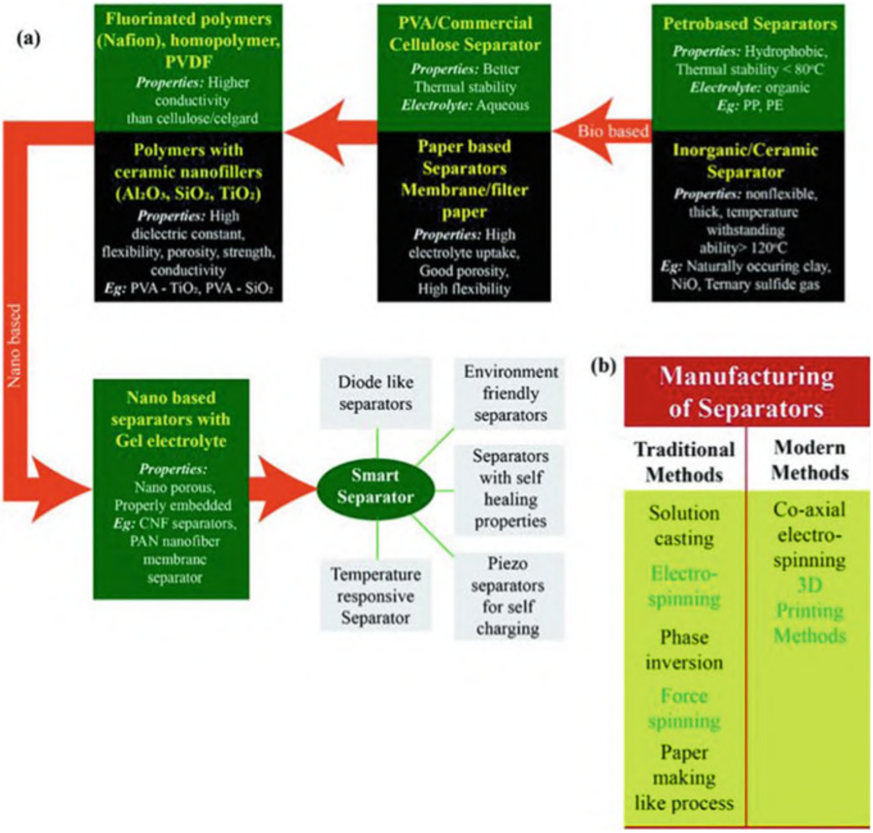
(a)
Fluorinated polymers (Nafion), homopolymer, PVDF
Properties: Higher conductivity than cellulose/celgard
Polymers with ceramic nanofillers (Al_2O_3, SiO_2, TiO_2)
Properties: High dielectric constant, flexibility, porosity, strength, conductivity
Eg: PVA - TiO_2, PVA - SiO_2
PVA/Commercial Cellulose Separator
Properties: Better Thermal stability
Electrolyte: Aqueous
Paper based Separators Membrane/filter paper
Properties: High electrolyte uptake, Good porosity, High flexibility
Petrobased Separators
Properties: Hydrophobic, Thermal stability < 80°C
Electrolyte: organic
Eg: PP, PE
Inorganic/Ceramic Separator
Properties: nonflexible, thick, temperature withstanding ability> 120°C
Eg: Naturally occuring clay, NiO, Ternary sulfide gas
Bio based
Nano based
Nano based separators with Gel electrolyte
Properties: Nano porous, Properly embedded
Eg: CNF separators, PAN nanofiber membrane separator
Smart Separator
Diode like separators
Environment friendly separators
Separators with self healing properties
Piezo separators for self charging
Temperature responsive Separator
(b)
Manufacturing of Separators
Traditional Methods
Modern Methods
Solution casting
Electro-spinning
Phase inversion
Force spinning
Paper making like process
Co-axial electro-spinning
3D Printing Methods

Fig. 4 Progressive development of **a** materials and **b** separator manufacturing techniques. Reproduced from [80] under Creative Commons Attribution CC BY License. Copyright 2022, Royal Society of Chemistry

resilience. The most popular commercial separators in supercapacitors are made of polypropylene (Celgard). Other polymers have also been utilized to create separators for supercapacitors, including polyvinyl chloride, PVDF, PVDF-HFP, polyethylene, and poly(ethylene oxide) [81]. Diverse techniques can be used to create polymer-based separators. Both monolayer membranes and composite separator membranes are manufactured using electrospinning. This procedure allows for precise control of the separator membrane porosity and pore size [82]. Electro-spun fiber membranes may be utilized as separators over electrodes because they are extremely porous, have a large surface area, and offer a larger electrochemical operating window than conventional separators. In comparison to separators created via phase transition or solution casting technique, membranes produced by an electrical current allow for further electrolyte absorption because of their rapid ionic diffusion, high porosity, and reduced surface resistance [83]. The effects of temperature and the properties of the separator materials, such as porosity and composition, on supercapacitor performance were investigated. SEM images of the TUX5 separator (thickness ~10 mm) displayed a meso–macromelting structure with pores, which was mostly ascribed to the quick polymer solution input rate and high PVDF concentration [84]. On the other hand, TUX10 separator membrane SEM pictures revealed a consistent fiber structure (thickness ~20 mm). Additionally, it was discovered that TUX10 membranes had substantially higher porosity (~91%) than TUX5 membranes (~40%). This meant that the frequency series resistance of TUX5 separator membranes was higher than that of TUX10 membranes. The temperature and separator characteristics have an impact on the relaxation time constant. The power rating of supercapacitors with TUX10 separators membrane was five times lesser at −30 °C than the highest power rating that was obtained at 24 °C and also it depends upon separator material features like permeability and temperature. Electrospinning preceded by the phase separation method was utilized by He et al. to create PAN nanofiber separators out of a mixture of polyvinylidene fluoride (PVP) and polyacrylonitrile (PAN), with PVP serving as the pore-forming component (Fig. 5a) [85]. The pore size of the electrospun polyacrylonitrile nanofibers increased with increasing polyvinylidene fluoride concentrations in the mix resulted in a rise in pore size and surface area. Since the electrolyte was not only adsorbed onto the surfaces but also infused into the mesopores and macropores of the separator, porous nanofibers had considerably better electrolyte absorption (Fig. 5b). Less time is needed for the formation of the electrical double layer for faster ion diffusion. Since the phase inversion method is more affordable and effective than electrospinning, it is frequently employed in the production of permeable supercapacitor membranes. The separators for PVDF had better mechanical qualities and had a large 80% porosity. Due to their poor hydrophilicity and inability to store enough electrolytes, supercapacitors created with unaltered PVDF separators had lower specific capacitance, which hampered the mobility of ions of free electrolytes. AC/PVDF supercapacitors’ specific capacitance fell from 69 to 4 F/g because current density increased from 0.1 to 10 A/g, whereas the specific capacitance of AC/modified PVDF supercapacitors reduced while current density grew from 10 to 50 A/g, the temperature decreased from 43 to 22 F/g (Fig. 5c) [86, 87]. AC/modified PVDF supercapacitors were superior at retaining capacitance because their internal resistance was lower than that of standard AC/PVDF supercapacitors. Polymer-based separators have been made using cutting-edge processes including electrospinning and phase inversion, among others. Using a low-cost technique, Hashim et al. showed how to create supercapacitors. The authors created a separator using a combination of poly(methyl methacrylate) and lauroyl chitosan and phosphoric acid (30%) and a hybrid polymer electrolyte PVA (70%). Lauroyl chitosan and PVA were chosen because the latter has the capacity to hold significant amounts of ionic liquids [77], while the former has strong mechanical qualities. After including 0.15 g of commercially available multi-walled CNTs on each side of the separator, a novel supercapacitor was created. The thickness of PVDF nanofiber separators made through coaxial wet spinning was inhibited by varying the PVDF concentration. The optimal PVDF concentration in the separator was discovered to be 10 wt%. Even though the separator’s network architecture was extremely wrinkly,

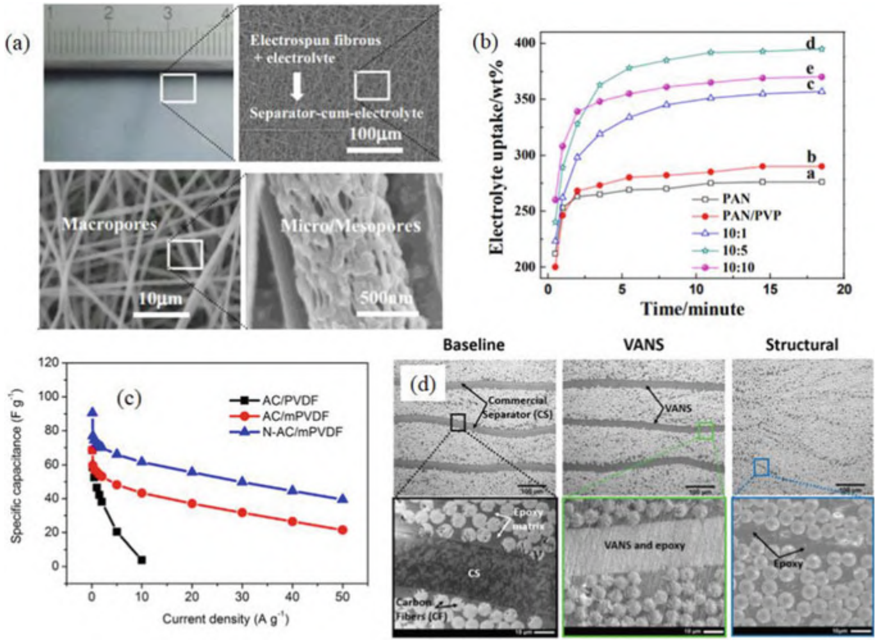

Fig. 5 **a** Separators made from PVDF fibers with a hierarchical porous structure Reproduced from [85] under Creative Commons Attribution CC BY License. Copyright 2017, The Electrochemical Society; **b** time-dependent graph of electrolyte uptake by different types of separators. Reproduced from [87] with permission. Copyright 2018, Elsevier; **c** specific capacitance vs. current density. Reproduced from [86] with permission. Copyright 2018, Elsevier; and **d** optical (top) and scanning electron microscopy (bottom) photographs of the interior (4 plies) of the composites allow for a morphological evaluation of commercial separator, VANS, and standard nanofunctional structural composite interfaces. Reproduced from [95] under Creative Commons Attribution CC BY License. Copyright 2019, Royal Society of Chemistry

it encouraged a wide contact between the electrode and electrolyte as well as quick diffusion of electrolyte ions with little chance of a short circuit. Aside from having excellent elasticity, the separator also showed no change when bent at angles up to 180°. Only a 3% decrease in the specific capacitance was noted even after 100 of these bending cycles (0°–180°). Poor conductivity of ions and low porosity of membrane-based polymers severely restrict their use as electrolyte wettability in supercapacitors. Since the supercapacitor made using this separator may be twisted, coiled, knotted, etc., and can be used as a bendable and flexible tool [88].

5.1.2 Ceramic Membranes

Because they experience unstable shrinkage and deformation at high temperatures, separators made of cellulose, polymers, etc., cannot be used in supercapacitors for high-temperature applications like oil drilling. For such applications, combinations of ceramic materials and a mix of natural clay, ternary sulfide glass are employed together with solid organic electrolytes and ionic liquids as electrolytes [89–91]. For these high-temperature applications, supercapacitors were reported using carbon electrodes, ceramic-based separators, and 2 M KOH-glycerine electrolytic solution [92]. The ceramic separators were mostly made of zirconium dioxide (ZrO_2) and nickel oxide (NiO). Since NiO exhibits a negative temperature coefficient of resistance as well as provides less resistance at high temperature, it was incorporated into the separator membrane. At higher temperatures, this actually increased capacitance. Graphite powder (10–30%) was used as a pore-forming agent. The inclusion of graphite also increased the separator operating temperature and pore size, which sped up ion diffusion and improved capacitance. With an increase in graphite concentration, the specific capacitance increased. However, the separator membrane demonstrated unsatisfactory mechanical behavior at graphite concentrations of 40%. At a temperature of 140 °C, supercapacitors with separators containing 30% graphite displayed high electrochemical characteristics. Ceramic materials have also been used in supercapacitors as separators for wearable systems, in addition to high-temperature applications. Supercapacitors with high energy storage capacity, adaptability, and compactness make them ideal for application in such devices. Planar asymmetric supercapacitors have been created for such applications using scalable printing technology [93]. On a single substrate, monolithic films were merged and layered one on top of the other. The positive electrode was made of MnO_2/poly3,4-ehtylene dioxythiophene: polystyrene sulfonate, the separator was made of boron nitride (~2.2 μm), and the negative electrode was made of graphene nanosheet. None of these materials were combined with binders, additives, or metal-based current collectors. Such supercapacitors illustrated ~99% of capacitive retention even after bending it by 180° as well as 92% cyclic stability at the end of 5000 cycles (superior in comparison to conventional asymmetric supercapacitors having two substrates). A maximum total energy of 8.6 mW h/cm^3 was also provided and maintains 92% capacitance even after 5000 cycles. The separators employed in these supercapacitors increase their ability to carry a load without creating morphological flaws. As a result, there is a requirement for separators that are mechanically durable [94]. In order to make the system less bulky, The idea of creating flexible devices for energy storage that can handle loads like composites was proposed by Acauan et al. vertically aligned carbon nanotubes (VACNTs) were covered in Al_2O_3 using the atomic layer deposition method to construct structural separators, which were then sintered before the CNTs were removed (Fig. 5d) [95]. The alumina nanotubes (ANTs) alignment and porosity were the primary function of CNTs. Ionic polymer electrolytes and these ANT arrays combined to create vertically aligned nanofiber separators (VANS). To create the multifunctional composite supercapacitors, such as VANS were sandwiched between stacking of unidirectional carbon fibers. The polymer electrolyte crystallinity is decreased by the presence of ANTs, which causes high ion conductivity of VANS. The main benefit of VANS over conventional separator is its reduced resistance, which is a highly frequent mechanism of failures in laminated composites and involves the de-bonding of neighboring plies because of the weak interface. The strength of the VANS is 47% stronger compared to a commercial separator and comparable to structural separator. The mechanical properties of VANS-based laminate were almost identical to the structural separator, but it showed a 51% improvement in interlaminar shear strength and a 47% improvement in tensile strength when compared to commercial separators. The VANS's inter-laminar shear strength was found to be 6% lower than that of the structural separator, however. The interlaminar gaps seen in VANS were blamed for this decline.

5.2 Bio-based Separator Membranes

5.2.1 Tree Leaves

Researchers are investigating if tree leaves may be used as supercapacitor separators since they are plentiful, accessible, affordable, and biodegradable. In one such study, Yao et al. chose Bradyrhizhobium japonicum (BJ) biodegradable biomass as active material because of its 3D configurations well as high N concentration, and they carbonized it using $ZnCl_2$ activation ($ZnCl_2$/BJ mass ratio = 1.5) (Fig. 6a) [96]. The preferred separator was a soyabean leaf (SL) with a hierarchically structured macroporous network and much more hydroxyl groups on its surface [97]. The limited porosity of tree leaves poses a significant obstacle to their usage as separators, yet the electrochemical properties of a supercapacitor including such biomass-based material (BJPC-1.5) along with an SL separator was shown to be superior to that of commercially available cellulose and PP separators. One technique for increasing the porosity of tree leaves is chemical treatment using alkaline solutions. In their studies, Jin et al. employed this technique to carry out the activation of sodium hydroxide across the surfaces of four distinct leaves, including those from the Platanus orientalis (PO), Magnolia grandiflora (MG), Cinnamomum camphora (CC), and Osmanthus fragrans (OF) [98]. Since the chemical makeup of these leaves varied, several pore arrangements were seen. In CC leaves, a 3D porous network with nanopores and macropores was seen, whereas MG and PO leaves had irregular porous network architectures. The NaOH solution partly dissolved the lignin and hemicellulose from the CC leaf, increasing the number of pores and improving capacitance performance. The porous configuration of the CC leaf was greatly affected by the NaOH activation period. A reduction in the ionic concentration in the separator results in an expansion of size of the pores and in the time of activation and limits the electrochemical performance [99]. It has been shown that CC leaves provide an excellent option as separator in supercapacitors.

5.2.2 Egg Shell-Based Membranes

Egg shell membranes (ESMs) of avian, which are non-toxic, inexpensive, widely accessible, biodegradable, and exhibit very porous topologies, have been utilized

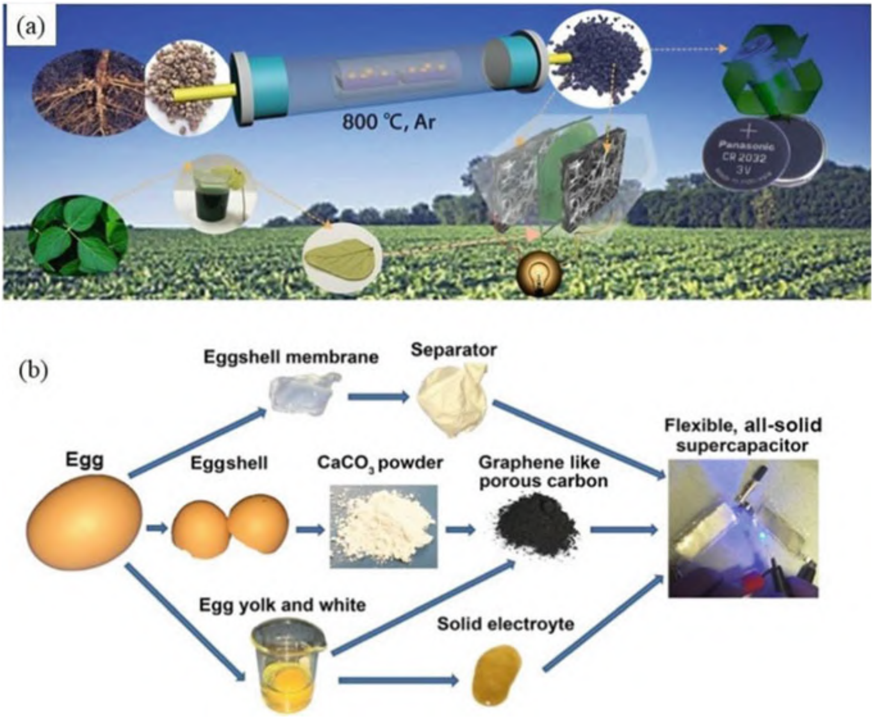
(a)
800 °C, Ar
+
Panasonic
CR 2032
3V
(b)
Eggshell membrane
Separator
Egg
Eggshell
$CaCO_3$ powder
Graphene like porous carbon
Flexible, all-solid supercapacitor
Egg yolk and white
Solid electroyte

Fig. 6 Preparation of BJPCs. Reproduced from [96] with permission. Copyright 2018, American Chemical Society; and **b** Different components of eggs utilized for fabricating supercapacitor. Reproduced from [104] with permission. Copyright 2019, Elsevier

to make separator membranes. Both alcoholic and aqueous media don't affect their stability [100]. Since it is simple to separate from the egg shells, the outer membrane (ESM) is frequently employed in separators. Duck egg shell membrane (DESM), chicken egg shell membrane (CESM), and goose egg shell membrane (GESM) were used to make separators, which were then used in supercapacitor (coin type) [101]. Efficiency of the supercapacitor is significantly affected by the thickness of the separator, as well as the structure and size of the fibers included in these egg shell-based separators. Due to their thinner construction, the CESM outperformed the other membranes in terms of capacitive and resistive performance. Higher specific capacitance values were also seen with thinner ESMs. The electrolyte adsorption capacity was lower for the GESM (~102%) and higher for the DESM (~133%). Titania may be added to ESMs to change the shape and size of the TiO_2 pores. The DESM-type separators were dip-coated with various concentrations of TiO_2 nanoparticles in order to examine this effect [102]. Egg shell fibers of duck in DESM that were submerged into 1 wt% of TiO_2 developed a covering of TiO_2 particles that result in the formation of pores. The size of the holes shrank due to dipping in TiO_2. At TiO_2 concentrations above 10 wt%, it was found that the holes were completely filled, leading to a decrease in capacitance from 2.3 to 0.035 F/g. Separators based on ESM exhibit excellent electrochemical performance, mechanical strength, and thermal stability. The highest stress that 0.8 mm thick ESMs can resist is 6.6 ± 0.5 MPa, and the maximum strain that they can sustain is 7 ± 0.3%, both of which are superior to that of regularly used polypropylene (PP) separators [103]. They have good thermal stability since they can maintain their characteristics at a temperature lower than 100 °C but the stability declines at temperatures beyond 220 °C. Comparing the levels of water absorption and swelling, it was found that ESMs had greater values (10 and 8%, respectively) than commercial membranes made of PP (3%). Due to their quick repose duration, less resistance, and excellent cycle life, supercapacitors made utilizing ESM-based separators exhibit superior performance. In addition to this, researchers are trying to develop supercapacitors entirely from egg-derived materials, not only separators. As illustrated in Fig. 6b [104], a flexible supercapacitor was effectively constructed. Large surface area (1527 m^2/g) of the electrode that results in exceptionally high power and energy densities, was obtained from 2D sheets of carbon that were 1.25 nm thick, similar to graphene. The white part of the egg or yolk treated with KOH can be used as gel electrolyte. The macroporous, interlaced network of fibers in the ESMs varied in diameter from 0.5 mm to 1 mm. The resulting supercapacitor was malleable, since its specific capacitance does not reduce by bending and twisting. They demonstrated the potential of such devices for use in real-world applications by glowing up an LED light source for a long duration of time when two of these supercapacitors were linked in series. Electrodes and separators for asymmetric supercapacitors were also fabricated using bio-waste ESMs [105]. Biomaterial carbon structures were heavily doped with oxygen and nitrogen during carbonization. As a result of the existence of oxygen and nitrogen, bio-derived carbon has a higher pseudocapacitance than conventional carbon and the optimal pore size for ion transportation and absorption [106]. Using a natural ESM bio-separator, chemically active ESM carbon at the anode, and air-activated ESM carbon at the cathode for renewable energy device development resulted in excellent electrochemical performance.

5.2.3 Paper-Based Membranes

There has been extensive use of organic solvents and paper separators for electrolytes [107]. Aerogels and films with mechanical strength, permeability, and high surface area may also be made using this method [108]. Koga et al. created a symmetric supercapacitor with two cellulose paper/RGO electrodes and a 50-µm-thick cellulose paper-based separator [109]. This green supercapacitor exhibits various advantages such as light weight, low cost, portability, and 100% reliance on recycled cellulose derived from newspaper. It potentially finds application in energy-saving wearable gadgets. To investigate the impact of the thickness of separator on the resistance of the cell, filter sheets as separator membrane were employed in supercapacitors [110]. In order to modify the pore size of separator, the amount of sheet used was varied, each of which was 0.15 mm thick and had pores of 15 µm. As the separator thickness was raised, it was observed that the cell resistance starts increasing from 1.5 to 1.6 Ω/mm which may be due to the resistance provided by the pores. Fully printed supercapacitors were also created utilizing commercial paper substrates coated with SWCNT inks [111]. To create a thin layer without many pores that would only allow the electrolyte to pass through the paper, the surface of separator was first treated with PVDF. On both sides of the paper, SWCNT ink was applied. The paper served as both the substrate and the separator, while the SWCNT coating served as both the electrodes and the current collector. The value of capacitance was measured to be 33 F/g after 2500 charging–discharging cycles, with just a little decrease in capacitance. Paper separators' fast aging in aqueous solvents and deterioration when employed with H_2SO_4 made them unsuitable for use in supercapacitors [112].

6 Substrates for Supercapacitors

With the rapid evolution of electronic gadgets over the past several years such as wearable or folding gadgets, electronic paper, mobile gadgets, and smart things, there is a growing need for energy storage solutions that are both flexible and economical, as well as lightweight and environmentally friendly. The tremendous benefits that flexible supercapacitors (FSCs) possess make them highly viable energy storage technology. When designing high-performance FSCs, it is important to take into account the mechanical, electrochemical, and interfacial features of the flexible electrodes [113]. In most cases, high conductivity and wide surface area are also desirable in electrodes, in addition to flexibility. Several techniques dedicated to the development of flexible electrode for FSCs are already well-established. The first involves making films of active materials that are both flexible and self-supporting, while the second involves using flexible substrates to hold the materials in place. Flexible substrates are gaining a lot of attention as a foundation for active materials because of their low cost, great flexibility, and smooth surfaces. This motivates the hope that novel loading support structures for pseudocapacitive materials would be inexpensive and non-hazardous to the environment yet offering high capacitance and adaptability [114]. Recently, the evolution of carbon-based supercapacitor materials has been reported, giving useful overviews of topics including carbon nanotubes (CNTs), activated carbons (ACs), templated carbons, graphene, 0D–3D forms, and hybrid composites but there weren't many analyses of FSCs [115]. There is a high need for the creation of such devices as a result of the rising interest in wearable electronics that are lightweight, flexible, and bendable for extensive portable applications. As a result, an overview of recent research projects was provided that emphasizes the application of flexible substrates, as seen in Fig. 7. Carbon-based electrodes, metal substrates, porous materials like normal paper, sponges and textiles, and cable-type electrodes having thin conducting layers have all been used in the recent construction of high-performance FSCs.

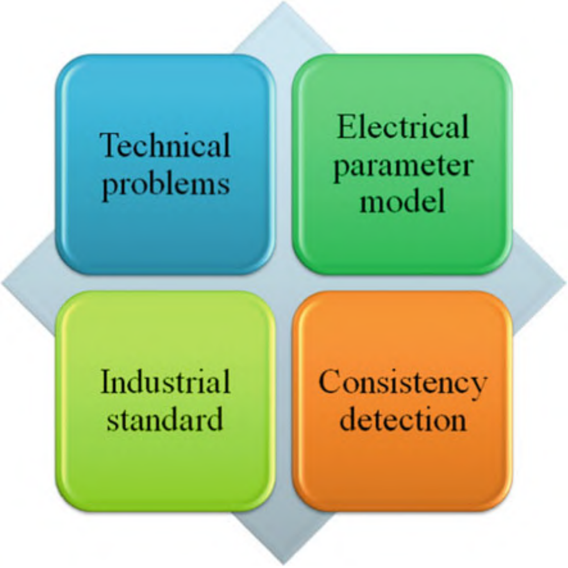

Fig. 7 Correlation diagram of the challenges of supercapacitors

6.1 Metal Substrates

Metal is one of the potential substrate materials for flexible solar cells, supercapacitors, and batteries. Stainless steel (SS), aluminum (Al), copper (Cu), nickel (Ni), titanium (Ti), and other metal substrates have several benefits, including high strength, high conductivity, and simplicity in preparation. Metal substrates can make ideal supports for the fabrication of high-performance supercapacitors [116].

6.2 Carbon Paper and Carbon Nanofoam

Carbon microfibers are formed into flat sheets to create carbon paper. A loose 3D web-like cluster arrangement of carbon threads makes up carbon nanofoam found extensive application in supercapacitors, fuel cells, and other devices because of their porosity, mechanical stability, huge surface area, and superior conductivity [117].

6.3 Conventional Paper Substrates

In our daily lives, paper is frequently used for cleaning, wrapping, and decorating. The usage of paper-based transistors, photodiodes, displays, and circuits in electronic applications have also expanded [118]. For the purpose of making high-performance supercapacitors, paper may be used as a good base for active material [119].

6.4 Textile Substrates

A flexible, porous material called a textile is created by pressing or weaving natural or synthetic fibers such as cotton or polyester. As a result of recent investigations into cotton materials with malleable properties, cotton textiles are now being used as a wearable substrate for a wide range of applications [120]. Additionally, fiber supercapacitors and textile supercapacitors prototypes for textile-based storage of energy have also been demonstrated [121].

6.5 Sponge Substrates

It is a common practice to utilize cellulose or polyester-based porous synthetic sponges for personal care, packaging, and household cleaning. The synthetic sponge available for commercial use can also be employed as an effective substrate for developing supercapacitors [122].

6.6 Cable-Type Substrates

The cable-type stretchable supercapacitor which has also been described as a new type of FSC, may be used for a variety of wearable electronics since it can be weaved into any shape or location. The performance and integration of the cable-type capacitors may be maintained while being bent into any intricate shape [123].

7 Challenges

In light of their many advantageous properties, supercapacitors have found widespread use in several fields including industry, automotive, the military, and consumer electronics. However, this technology also has some significant drawbacks. The following four categories best characterize the present issues that require fixing (Fig. 7).

7.1 Engineering or Technical Issues

Supercapacitors have low energy density with a gap of around 20 Wh/kg as compared to batteries, which have an energy density gap of 30–200 Wh/kg [124, 125]. To overcome this gap is one of the problems faced by the supercapacitor community. Supercapacitor storage capacity can be increased by upgrading manufacturing processes and technologies, but finding new electrolyte- and electrode-active materials with improved electrochemical performance will be challenging and time-consuming. Low energy density supercapacitors lead to bulkier devices, therefore they aren't very portable. Increasing the energy density of supercapacitors may be accomplished in a few different ways: by enhancing the surface area of the electrode materials in double-layer capacitors, by increasing the operating voltage window, or by doing both of these things. Synthesizing innovative materials with vast surface areas and using appropriate organic electrolytes which can sustain a broader voltage window are the primary concerns to eliminate this issue. Supercapacitors energy densities might catch up to batteries if these gaps are adequately closed.

7.2 Establishment of Electrical Parameter Model

The supercapacitor model may be comparable to the ideal model in some circumstances, but in military uses, satellite and spacecraft main power applications, several non-ideal factors must be taken into consideration. Due to its limited energy, resonance induced by regular signal, filter, and energy storage capacitor has a mature solution. Moreover, supercapacitors have the capacity for immediate throughput and enormous energy. The stability of the system must be analyzed in terms of the load fluctuation, load type, or external environment, as well as inadvertent interruption; hence, a trustworthy layout is crucial.

7.3 Consistency Detection

As supercapacitor exhibits low rated voltage (less than 2.7 V), several series connections are necessary for use in real-world applications. As applications usually need substantial current charging/discharging, and because overcharging shortens the lifespan of capacitors, checking the stability of the voltages on selected in-series capacitors is essential.

7.4 Industrial Standard

Supercapacitors with high operating speeds are growing rapidly. Since supercapacitors are a novel kind of energy storage device, their healthy growth is inextricably linked to market and industry regulation, which strives to create workable regional, national, and even global standards. A method for the classification model, a test method for measuring the electrical performance, technical requirements for ensuring the safety, broad specifications, and detailed requirements for the electrode material, electrolyte, transportation guidelines, recovery guidelines, charger series, and destruction guidelines should all be entrenched. Storage and management systems for scrap monomers and modules, as well as processing of electrolyte capacitor shells, disassembly of scrap monomers, recycling and handling of supercapacitor modules, plate handling, and diaphragm preparation, are all part of the larger goal of guiding and normalizing the supercapacitor industry toward environmentally friendly, economical recycling disposal. It is an essential tool for encouraging the industry's healthy growth.

8 Future Opportunities

8.1 Requirement of the Society

The applications of supercapacitors are crucial for addressing societal requirements and advancing industrial growth. The need for large-capacity portable power supplies is becoming important as the electronic sector develops quickly. On the one hand, environmental preservation and energy use are topics that people all around the world are becoming more and more interested in. The researchers are actively looking for solutions, and they are trying to utilize more renewable energy. The invention of supercapacitors, on the other hand, is a result of the pressing demand for portable backup power to be available for all types of electronic equipment due to the rise of the electronics industry. These societal needs help the supercapacitor sector expand quickly to some level, and the market opportunity is huge.

8.2 Flexible Device and Microminiaturization

Rapid advances in portable electronics and the concept of wearable technology have increased interest in flexible systems for storing energy. The development of flexible, compact energy storage systems with strong electrochemical capabilities is crucial [126]. Traditional supercapacitors, on the other hand, are significantly limited in terms of device shape due to the electrode's rigidity, and their electrochemical performance is further decreased by the use of metal collectors and bonding agents during the manufacture of the electrode [127]. The next era of flexible storage systems will thus be developed that pairs a flexible supercapacitor with a portable device. Numerous reports have been made on flexible supercapacitors with various macro morphologies and microstructures. Unlike traditional non-flexible supercapacitors, the flexible supercapacitors of desirable shape and size can be fabricated expanding their prospective use in malleable and wearable fields. This is because flexible supercapacitors have negative as well as positive electrodes, electrolyte levels diaphragm packaging that are all flexible [128]. The flexible electrode serves as the flexible device's core. Flexible electrodes may now be made using a variety of techniques. Incorporating active chemicals, flexible substrates, and electrolytes into electrodes that have simple procedures, excellent electrochemical efficiency, and flexibility will be a primary focus of future research. For making lightweight electrode without losing energy density, it has to be made of nanostructured materials that are engineered to offer more electrochemically reactive functional groups. This may be accomplished by using nanostructures that have been specially designed to give an excess of redox reaction sites and increased surface area. For instance, the construction of a flexible all-solid-state supercapacitor employing co-doped graphene with oxygen, nitrogen, and phosphorus was tested for energy storage application [106].

8.3 Hybridization

The issue of the low energy density of supercapacitors may be effectively solved by building hybrid battery-supercapacitors, which are systems in which one electrode stores charge using only a battery-type faradaic process and the other does it using a capacitive mechanism. Devices that combine a supercapacitor with a battery, such as lithium/sodium/potassium/magnesium ion hybrid battery-supercapacitors, inherit both the high power ($\sim$0.1–30 kW/kg) and high energy density ($\sim$5–200 Wh/kg). These devices also benefit from steady extended cycle performance and affordable prices [129]. For instance, Wang et al. [130] assembled a sodium ion hybrid battery-supercapacitor with a retention rate of 85% after 1200 cycles using mesoporous graphene (MG) and amorphous carbon (DC) as the negative and positive electrodes. This device had an energy density of 168 Wh/kg at 501 W/kg and a maximum power density of 2432 W/kg (98 Wh/kg).

8.4 Intelligentization and Transparency

There is an urgent requirement of an intelligent and controlled multipurpose electrochemical energy storage system for the fast growth of sophisticated electronic gadgets. Electronic devices may be programmed to do a variety of tasks in response to various demands in real life owing to their smart features. Through the use of novel materials, novel architectures, supercomputer modeling, and artificial intelligence, we may foresee the development of flexible devices to build user-friendly and personalized interactions between bio-integrated and wearable electronics [131]. A biodegradable, ecologically friendly, and biocompatible main battery was reported by Yin et al. [132]. It is interesting to note that Wang et al. [133] proposed an edible supercapacitor and demonstrated that a single capsule-sized edible supercapacitor had sufficient energy and power to operate as a standalone device.

8.5 Improvement of the Cost Performance

The first and most important factor to take into account for every industry to survive is enhancing product performance and lowering manufacturing costs. The study in this area is primarily focused on enhancing the technology of the supercapacitor itself, as well as the manufacturing process. Finding reliable and effective materials that can serve as both electrodes and electrolytes will help in improving performance and are also economical. An American company called Full Power Technologies is creating affordable ultracapacitors. To achieve the goals of superior performance and low overall price, it is necessary to: (a) find and use underutilized native mineral resources; (b) save money by blending high- and low-priced components; (c) enhance the manufacturing process and the manufacturing systems; (d) examining how well different electrode materials work with various electrolytes; and (e) research into the group module need to focus more on the service as a whole. As a result, this will serve as both the product’s primary direction and strategic goal in the future.

9 Conclusions

Supercapacitor is a promising energy storage technology that is both environmentally friendly and affordable. The vast untapped market offers limitless possibilities for the advancement of supercapacitors. Supercapacitors are utilized in many applications and have been theoretically proven to be a source of sustainable energy storage, but their performance still has to be improved in order to keep up with the growing energy demands of society today. Future research will continue to concentrate on the material which is used as electrode to limit the cost as well as enhance the performance of supercapacitor in light of increasing demand in applications such as smart wearable gadgets and new electric vehicles.

References

1. Huskinson B, Marshak MP, Suh C, Er S, Gerhardt MR, Galvin CJ, Chen X, Aspuru-Guzik A, Gordon RG, Aziz MJ (2014) A metal-free organic–inorganic aqueous flow battery. Nature 505(7482):195–198
2. Verma S, Khosla A, Arya S (2020) Performance of electrochemically synthesized nickel-zinc and nickel-iron (Ni–Zn//Ni–Fe) nanowires as battery type supercapacitor. J Electrochem Soc 167(12):120527
3. Verma S, Padha B, Singh A, Khajuria S, Sharma A, Mahajan P, Singh B, Arya S (2021) Sol-gel synthesized carbon nanoparticles as supercapacitor electrodes with ultralong cycling stability. Fuller Nanotub Carbon Nanostruct 29(12):1045–1052
4. Cai X, Peng M, Yu X, Fu Y, Zou D (2014) Flexible planar/fiber-architectured supercapacitors for wearable energy storage. J Mater Chem C 2(7):1184–1200
5. Verma S, Arya S, Gupta V, Mahajan S, Furukawa H, Khosla A (2021) Performance analysis, challenges and future perspectives of nickel based nanostructured electrodes for electrochemical supercapacitors. J Market Res 11:564–599
6. Tarascon JM, Armand M (2011) Issues and challenges facing rechargeable lithium batteries. In: Materials for sustainable energy: a collection of peer-reviewed research and review articles from Nature Publishing Group, pp 171–179
7. Etacheri V, Marom R, Elazari R, Salitra G, Aurbach D (2011) Energy Environ Sci 4(9):3243–3262
8. Manthiram A (2011) Materials challenges and opportunities of lithium ion batteries. J Phys Chem Lett 2(3):176–184
9. Vlad A, Singh N, Rolland J, Melinte S, Ajayan PM, Gohy JF (2014) Hybrid supercapacitor-battery materials for fast electrochemical charge storage. Sci Rep 4(1):1–7
10. Tie D, Huang S, Wang J, Ma J, Zhang J, Zhao Y (2019) Hybrid energy storage devices: advanced electrode materials and matching principles. Energy Storage Mater 21:22–40
11. Pandolfo T, Ruiz V, Sivakkumar S, Nerkar J (2013) General properties of electrochemical capacitors. In: Supercapacitors: materials, systems, and applications, pp 69–109
12. Simon P, Taberna PL, Béguin F (2013) Electrical double-layer capacitors and carbons for EDLCs. Edited by Francois Béguin and Elzbieta Fr şackowiak
13. Lv Y, Huang S, Zhao Y (2019) NBF Tridoped 3D hierarchical porous graphitized carbon derived from chitosan for high performance supercapacitors. Sci Adv Mater 11(3):418–424
14. Yao F, Pham DT, Lee YH (2015) Carbon-based materials for lithium-ion batteries, electrochemical capacitors, and their hybrid devices. Chemsuschem 8(14):2284–2311
15. Zuo W, Li R, Zhou C, Li Y, Xia J, Liu J (2017) Battery-supercapacitor hybrid devices: recent progress and future prospects. Adv Sci 4(7):1600539
16. Wang Y, Song Y, Xia Y (2016) Electrochemical capacitors: mechanism, materials, systems, characterization and applications. Chem Soc Rev 45(21):5925–5950
17. Díaz-González F, Sumper A, Gomis-Bellmunt O, Villafáfila-Robles R (2012) A review of energy storage technologies for wind power applications. Renew Sustain Energy Rev 16(4):2154–2171
18. Wu NL (2002) Nanocrystalline oxide supercapacitors. Mater Chem Phys 75(1–3):6–11
19. Zhang LL, Zhao XS (2009) Carbon-based materials as supercapacitor electrodes. Chem Soc Rev 38(9):2520–2531
20. Rajagopalan B, Chung JS (2014) Reduced chemically modified graphene oxide for supercapacitor electrode. Nanosc Res Lett 9(1):1–10
21. González A, Goikolea E, Barrena JA, Mysyk R (2016) Review on supercapacitors: technologies and materials. Renew Sustain Energy Rev 58:1189–1206
22. Iro ZS, Subramani C, Dash SS (2016) A brief review on electrode materials for supercapacitor. Int J Electrochem Sci 11(12):10628–10643
23. Libich J, Máca J, Vondrák J, Čech O, Sedlaříková M (2018) Supercapacitors: properties and applications. J Energy Storage 17:224–227

24. Halper MS, Ellenbogen JC (2006) Supercapacitors: a brief overview. The MITRE Corporation, McLean, Virginia, USA, p 1
25. Schneuwly A, Gallay R (2000) Properties and applications of supercapacitors from the state-of-the-art to future trends. In: Proceeding PCIM, vol 2000. Citeseer
26. Korkmaz S, Kariper İA (2020) Graphene and graphene oxide based aerogels: synthesis, characteristics and supercapacitor applications. J Energy Storage 27:101038
27. Ambare RC, Mane RS, Lokhande BJ (2016) A review on electrochemical supercapacitors of composite-metal-oxide nanostructures. Int J Adv Res 4:1943–1975
28. Grbović PJ, Delarue P, Le Moigne P (2012) Interface converters for ultra-capacitor applications in power conversion systems. In: 2012 15th international power electronics and motion control conference (EPE/PEMC). IEEE, pp LS7d-1
29. Jayalakshmi M, Balasubramanian K (2008) Simple capacitors to supercapacitors-an overview. Int J Electrochem Sci 3(11):1196–1217
30. Maxwell (2015) Top 5 markets for Ultracapacitor technology
31. Kiamahalleh MV, Zein SHS, Najafpour G, Sata SA, Buniran S (2012) Multiwalled carbon nanotubes based nanocomposites for supercapacitors: a review of electrode materials. Nano 7(02):1230002
32. Choi H, Yoon H (2015) Nanostructured electrode materials for electrochemical capacitor applications. Nanomaterials 5(2):906–936
33. Simon P, Gogotsi Y (2010) Materials for electrochemical capacitors. Nanosci Technol: Collect Rev Nat J, 320–329
34. Mohapatra S, Acharya A, Roy GS (2012) The role of nanomaterial for the design of supercapacitor. Lat Am J Phys Educ 6(3):380–384
35. Chen SM, Ramachandran R, Mani V, Saraswathi R (2014) Recent advancements in electrode materials for the high-performance electrochemical supercapacitors: a review. Int J Electrochem Sci 9(8):4072–4085
36. Chen T, Dai L (2013) Carbon nanomaterials for high-performance supercapacitors. Mater Today 16(7–8):272–280
37. Burke A, Liu Z, Zhao H (2014) Present and future applications of supercapacitors in electric and hybrid vehicles. In: 2014 IEEE international electric vehicle conference (IEVC). IEEE, pp 1–8
38. Lee SW, Gallant BM, Byon HR, Hammond PT, Shao-Horn Y (2011) Nanostructured carbon-based electrodes: bridging the gap between thin-film lithium-ion batteries and electrochemical capacitors. Energy Environ Sci 4(6):1972–1985
39. Shao Y, El-Kady MF, Sun J, Li Y, Zhang Q, Zhu M, Wang H, Dunn B, Kaner RB (2018) Design and mechanisms of asymmetric supercapacitors. Chem Rev 118(18):9233–9280
40. Naoi K, Simon P (2008) New materials and new configurations for advanced electrochemical capacitors. Electrochem Soc Interface 17(1):34
41. Pushparaj VL, Sreekala S, Nalamasu O, Ajayan PM (2010) Flexible energy storage devices using nanomaterials. In: Semiconductor nanomaterials for flexible technologies. William Andrew Publishing, pp 227–245
42. Li X, Wei B (2013) Supercapacitors based on nanostructured carbon. Nano Energy 2(2):159–173
43. Wang K, Wu H, Meng Y, Wei Z (2014) Conducting polymer nanowire arrays for high performance supercapacitors. Small 10(1):14–31
44. Chee WK, Lim HN, Huang NM (2015) Electrochemical properties of free-standing polypyrrole/graphene oxide/zinc oxide flexible supercapacitor. Int J Energy Res 39(1):111–119
45. Cai JJ, Kong LB, Zhang J, Luo YC, Kang L (2010) A novel polyaniline/mesoporous carbon nano-composite electrode for asymmetric supercapacitor. Chin Chem Lett 21(12):1509–1512
46. Lee SY, Kim JI, Park SJ (2014) Activated carbon nanotubes/polyaniline composites as supercapacitor electrodes. Energy 78:298–303
47. Fei H, Yang C, Bao H, Wang G (2014) Flexible all-solid-state supercapacitors based on graphene/carbon black nanoparticle film electrodes and cross-linked poly (vinyl alcohol)–H2SO4 porous gel electrolytes. J Power Sour 266:488–495

48. Shi C, Zhao Q, Li H, Liao ZM, Yu D (2014) Low cost and flexible mesh-based supercapacitors for promising large-area flexible/wearable energy storage. Nano Energy 6:82–91
49. Tehrani Z, Thomas DJ, Korochkina T, Phillips CO, Lupo D, Lehtimäki S, O'mahony J, Gethin DT (2017) Large-area printed supercapacitor technology for low-cost domestic green energy storage. Energy 118:1313–1321
50. Yang H, Kannappan S, Pandian AS, Jang JH, Lee YS, Lu W (2017) Graphene supercapacitor with both high power and energy density. Nanotechnology 28(44):445401
51. Bo Z, Wen Z, Kim H, Lu G, Yu K, Chen J (2012) One-step fabrication and capacitive behavior of electrochemical double layer capacitor electrodes using vertically-oriented graphene directly grown on metal. Carbon 50(12):4379–4387
52. Singh AP, Tiwari NK, Karandikar PB, Dubey A (2015) Effect of electrode shape on the parameters of supercapacitor. In: 2015 international conference on industrial instrumentation and control (ICIC). IEEE, pp 669–673
53. Frackowiak E, Beguin F (2001) Carbon materials for the electrochemical storage of energy in capacitors. Carbon 39(6):937–950
54. Niu C, Sichel EK, Hoch R, Moy D, Tennent H (1997) High power electrochemical capacitors based on carbon nanotube electrodes. Appl Phys Lett 70(11):1480–1482
55. Arico AS, Bruce P, Scrosati B, Tarascon JM, Van Schalkwijk W (2011) Nanostructured materials for advanced energy conversion and storage devices. In: Materials for sustainable energy: a collection of peer-reviewed research. Nature Publishing Group, pp 148–159
56. Kötz R, Carlen MJEA (2000) Principles and applications of electrochemical capacitors. Electrochim Acta 45(15–16):2483–2498
57. Jogade SM, Joshi PS, Jamadar BN, Sutrave DS (2011) MOCVD of cobalt oxide using co-actylacetonate as precursor: thin film deposition and study of physical properties
58. Lee W, Mane RS, Todkar VV, Lee S, Egorova O, Chae WS, Han SH (2007) Implication of liquid-phase deposited amorphous RuO2 electrode for electrochemical supercapacitor. Electrochem Solid-State Lett 10(9):A225
59. Zheng JP, Jow TR (1995) A new charge storage mechanism for electrochemical capacitors. J Electrochem Soc 142(1):L6
60. Burke A (2000) Ultracapacitors: why, how, and where is the technology. J Power Sour 91(1):37–50
61. Xia H, Lai MO, Lu L (2011) Nanostructured manganese oxide thin films as electrode material for supercapacitors. JOM 63(1):54–59
62. Wang GX, Zhang BL, Yu ZL, Qu MZ (2005) Manganese oxide/MWNTs composite electrodes for supercapacitors. Solid State Ionics 176(11–12):1169–1174
63. Arbizzani C, Mastragostino M, Soavi F (2001) New trends in electrochemical supercapacitors. J Power Sour 100(1–2):164–170
64. Zou X, Zhang S, Shi M, Kong J (2007) Remarkably enhanced capacitance of ordered polyaniline nanowires tailored by stepwise electrochemical deposition. J Solid State Electrochem 11(2):317–322
65. Fan LZ, Maier J (2006) High-performance polypyrrole electrode materials for redox supercapacitors. Electrochem Commun 8(6):937–940
66. Mastragostino M, Arbizzani C, Soavi F (2001) Polymer-based supercapacitors. J Power Sour 97:812–815
67. Zhang F, Tang J, Shinya N, Qin LC (2013) Hybrid graphene electrodes for supercapacitors of high energy density. Chem Phys Lett 584:124–129
68. Mandal M, Ghosh D, Kalra SS, Das CK (2014) High performance supercapacitor electrode material based on flower like MoS2/reduced graphene oxide nanocomposite. Int J Lat Res Sci Technol 3:65
69. Yan J, Wei T, Qiao W, Fan Z, Zhang L, Li T, Zhao Q (2010) A high-performance carbon derived from polyaniline for supercapacitors. Electrochem Commun 12(10):1279–1282
70. Yan J, Wei T, Shao B, Fan Z, Qian W, Zhang M, Wei F (2010) Preparation of a graphene nanosheet/polyaniline composite with high specific capacitance. Carbon 48(2):487–493

71. Yan J, Wei T, Fan Z, Qian W, Zhang M, Shen X, Wei F (2010) Preparation of graphene nanosheet/carbon nanotube/polyaniline composite as electrode material for supercapacitors. J Power Sour 195(9):3041–3045
72. Wang H, Zhou Q, Yao B, Ma H, Zhang M, Li C, Shi G (2018) Suppressing the self discharge of supercapacitors by modifying separators with an ionic polyelectrolyte. Adv Mater Interfaces 5(10):1701547
73. Zhang X, He B, Zhao Y, Tang Q (2018) A porous ceramic membrane tailored high-temperature supercapacitor. J Power Sour 379:60–67
74. Yang JM, Wang HZ, Yang CC (2008) Modification and characterization of semi-crystalline poly (vinyl alcohol) with interpenetrating poly (acrylic acid) by UV radiation method for alkaline solid polymer electrolytes membrane. J Membr Sci 322(1):74–80
75. Saunier J, Alloin F, Sanchez JY, Maniguet L (2004) Plasticized microporous poly (vinylidene fluoride) separators for lithium-ion batteries. III. Gel properties and irreversible modifications of poly (vinylidene fluoride) membranes under swelling in liquid electrolytes. J Polym Sci Part B: Polym Phys 42(12):2308–2317
76. Karabelli D, Lepretre JC, Alloin F, Sanchez JY (2011) Poly (vinylidene fluoride)-based macroporous separators for supercapacitors. Electrochim Acta 57:98–103
77. Hashim MA, Sa'adu L, bin Baharuddin M, Dasuki KA (2014) Using PVA, methacrylate and Lauroyl chitosan as separator in supercapacitors. J Mater Sci Res 3(1):25
78. Yin Y, Yamada O, Suto Y, Mishima T, Tanaka K, Kita H, Okamoto KI (2005) Synthesis and characterization of proton-conducting copolyimides bearing pendant sulfonic acid groups. J Polym Sci Part A: Polym Chem 43(8):1545–1553
79. Staiti P, Lufrano F (2010) Investigation of polymer electrolyte hybrid supercapacitor based on manganese oxide–carbon electrodes. Electrochim Acta 55(25):7436–7442
80. Ahankari SS, Lasrado D, Ramesh S (2022) Advances in materials and fabrication of separators in supercapacitors. Mater Adv
81. Solarajan AK, Murugadoss V, Angaiah S (2017) High performance electrospunPVdF-HFP/SiO2 nanocomposite membrane electrolyte for Li-ion capacitors. J Appl Polym Sci 134(32):45177
82. Solarajan AK, Murugadoss V, Angaiah S (2016) Montmorillonite embedded electrospun-PVdF–HFP nanocomposite membrane electrolyte for Li-ion capacitors. Appl Mater Today 5:33–40
83. Tõnurist K, Thomberg T, Jänes A, Lust E (2013) Specific performance of supercapacitors at lower temperatures based on different separator materials. J Electrochem Soc 160(3):A449
84. Tõnurist K, Jänes A, Thomberg T, Kurig H, Lust E (2009) Influence of mesoporous separator properties on the parameters of electrical double-layer capacitor single cells. J Electrochem Soc 156(4):A334
85. He T, Jia R, Lang X, Wu X, Wang Y (2017) Preparation and electrochemical performance of PVdF ultrafine porous fiber separator-cum-electrolyte for supercapacitor. J Electrochem Soc 164(13):E379
86. Xie Q, Huang X, Zhang Y, Wu S, Zhao P (2018) High performance aqueous symmetric supercapacitors based on advanced carbon electrodes and hydrophilic poly (vinylidene fluoride) porous separator. Appl Surf Sci 443:412–420
87. He T, Fu Y, Meng X, Yu X, Wang X (2018) A novel strategy for the high performance supercapacitor based on polyacrylonitrile-derived porous nanofibers as electrode and separator in ionic liquid electrolyte. Electrochim Acta 282:97–104
88. Mastragostino M, Soavi F (2007) J Power Sour 174:89–93
89. Szubzda B, Szmaja A, Ozimek M, Mazurkiewicz S (2014) Polymer membranes as separators for supercapacitors. Appl Phys A 117(4):1801–1809
90. Sivaraman P, Mishra SP, Potphode DD, Thakur AP, Shashidhara K, Samui AB, Bhattacharyya AR (2015) A supercapacitor based on longitudinal unzipping of multi-walled carbon nanotubes for high temperature application. RSC Adv 5:83546–83557
91. Na R, Huo P, Zhang X, Zhang S, Du Y, Zhu K, Lu Y, Zhang M, Luan J, Wang G (2016) A flexible solid-state supercapacitor based on a poly (aryl ether ketone)–poly (ethylene

glycol) copolymer solid polymer electrolyte for high temperature applications. RSC Adv 6(69):65186–65195

92. Pang Z, Duan J, Zhao Y, Tang Q, He B, Yu L (2018) A ceramic NiO/ZrO2 separator for high-temperature supercapacitor up to 140 °C. J Power Sour 400:126–134
93. Zheng S, Lei W, Qin J, Wu ZS, Zhou F, Wang S, Shi X, Sun C, Chen Y, Bao X (2018) All-solid-state high-energy planar asymmetric supercapacitors based on all-in-one monolithic film using boron nitride nanosheets as separator. Energy Storage Mater 10:24–31
94. González C, Vilatela JJ, Molina-Aldareguía JM, Lopes CS, LLorca J (2017) Structural composites for multifunctional applications: Current challenges and future trends. Progr Mater Sci 89:194–251
95. Acauan LH, Zhou Y, Kalfon-Cohen E, Fritz NK, Wardle BL (2019) Multifunctional nanocomposite structural separators for energy storage. Nanoscale 11(45):21964–21973
96. Yao Q, Wang H, Wang C, Jin C, Sun Q (2018) One step construction of nitrogen–carbon derived from bradyrhizobium japonicum for supercapacitor applications with a soybean leaf as a separator. ACS Sustain Chem Eng 6(4):4695–4704
97. Guo N, Li M, Wang Y, Sun X, Wang F, Yang R (2016) Soybean root-derived hierarchical porous carbon as electrode material for high-performance supercapacitors in ionic liquids. ACS Appl Mater Interfaces 8(49):33626–33634
98. Jin L, Wei K, Xia Y, Liu B, Zhang K, Gao H, Chu X, Ye M, He L, Lin P (2019) Tree leaves-derived three-dimensional porous networks as separators for graphene-based supercapacitors. Mater Today Energy 14:100348
99. Liang N, Ji Y, Zuo D, Zhang H, Xu J (2019) Improved performance of carbon-based supercapacitors with sulfonated poly (ether ether ketone)/poly (vinyl alcohol) composite membranes as separators. Polym Int 68(1):120–124
100. Yang D, Qi L, Ma J (2002) Eggshell membrane templating of hierarchically ordered macroporous networks composed of TiO2 tubes. Adv Mater 14(21):1543–1546
101. Taer E, Sumantre MA, Taslim R, Dahlan D, Deraman M (2014) Eggs shell membrane as natural separator for supercapacitor applications. In: Advanced materials research, vol 896. Trans Tech Publications Ltd., pp 66–69
102. Dahlan D, Sartika N, Namigo EL, Taer E (2015) Effect of TiO2 on duck eggshell membrane as separators in supercapacitor applications. In: Materials science forum, vol 827. Trans Tech Publications Ltd., pp 151–155
103. Yu H, Tang Q, Wu J, Lin Y, Fan L, Huang M, Lin J, Li Y, Yu F (2012) Using eggshell membrane as a separator in supercapacitor. J Power Sour 206:463–468
104. Zhang Y, He J, Gao Z, Li X (2019) Converting eggs to flexible, all-solid supercapacitors. Nano Energy 65:104045
105. Yang P, Xie J, Zhong C (2018) Biowaste-derived three-dimensional porous network carbon and bioseparator for high-performance asymmetric supercapacitor. ACS Appl Energy Mater 1(2):616–622
106. Zhao Y, Huang S, Xia M, Rehman S, Mu S, Kou Z, Zhang Z, Chen Z, Gao F, Hou Y (2016) NPO co-doped high performance 3D graphene prepared through red phosphorous-assisted "cutting-thin" technique: a universal synthesis and multifunctional applications. Nano Energy 28:346–355
107. Cameron CG, Fitzsimmons SM (2008) Supercapacitor separators and polypyrrole composites, Defence R&D Canada-Atlantic. Technical memorandum, DRDC Atlantic TM 2008–219
108. Hu L, Chen W, Xie X, Liu N, Yang Y, Wu H, Yao Y, Pasta M, Alshareef HN, Cui Y (2011) Symmetrical MnO2–carbon nanotube–textile nanostructures for wearable pseudocapacitors with high mass loading. ACS Nano 5(11):8904–8913
109. Koga H, Tonomura H, Nogi M, Suganuma K, Nishina Y (2016) Fast, scalable, and eco-friendly fabrication of an energy storage paper electrode. Green Chem 18(4):1117–1124
110. Tammela P, Olsson H, Strømme M, Nyholm L (2014) The influence of electrode and separator thickness on the cell resistance of symmetric cellulose–polypyrrole-based electric energy storage devices. J Power Sour 272:468–475

111. Hu L, Wu H, Cui Y (2010) Printed energy storage devices by integration of electrodes and separators into single sheets of paper. Appl Phys Lett 96(18):183502
112. Bittner AM, Zhu M, Yang Y, Waibel HF, Konuma M, Starke U, Weber CJ (2012) Ageing of electrochemical double layer capacitors. J Power Sour 203:262–273
113. Kang YJ, Chung H, Han CH, Kim W (2012) All-solid-state flexible supercapacitors based on papers coated with carbon nanotubes and ionic-liquid-based gel electrolytes. Nanotechnology 23(6):065401
114. Bélanger D, Brousse T, Long J (2008) Manganese oxides: battery materials make the leap to electrochemical capacitors. Electrochem Soc Interface 17(1):49
115. Shi S, Xu C, Yang C, Li J, Du H, Li B, Kang F (2013) Flexible supercapacitors. Particuology 11(4):371–377
116. Jagadale AD, Jamadade VS, Pusawale SN, Lokhande CD (2012) Effect of scan rate on the morphology of potentiodynamically deposited β-Co (OH)2 and corresponding supercapacitive performance. Electrochim Acta 78:92–97
117. Lytle JC, Wallace JM, Sassin MB, Barrow AJ, Long JW, Dysart JL, Renninger CH, Saunders MP, Brandell NL, Rolison DR (2011) The right kind of interior for multifunctional electrode architectures: carbon nanofoam papers with aperiodic submicrometre pore networks interconnected in 3D. Energy Environ Sci 4(5):1913–1925
118. Kim DH, Kim YS, Wu J, Liu Z, Song J, Kim HS, Huang YY, Hwang KC, Rogers JA (2009) Ultrathin silicon circuits with strain-isolation layers and mesh layouts for high-performance electronics on fabric, vinyl, leather, and paper. Adv Mater 21(36):3703–3707
119. Hu L, Choi JW, Yang Y, Jeong S, La Mantia F, Cui LF, Cui Y (2009) Highly conductive paper for energy-storage devices. Proc Natl Acad Sci 106(51):21490–21494
120. Avila AG, Hinestroza JP (2008) Tough cotton. Nat Nanotechnol 3(8):458–459
121. Gu JF, Gorgutsa S, Skorobogatiy M (2010) Soft capacitor fibers using conductive polymers for electronic textiles. Smart Mater Struct 19(11):115006
122. Chen W, Rakhi RB, Hu L, Xie X, Cui Y, Alshareef HN (2011) High-performance nanostructured supercapacitors on a sponge. Nano Lett 11(12):5165–5172
123. Dubal DP, Kim JG, Kim Y, Holze R, Lokhande CD, Kim WB (2014) Supercapacitors based on flexible substrates: an overview. Energ Technol 2(4):325–341
124. Zhao Y, Ran W, He J, Song Y, Zhang C, Xiong DB, Gao F, Wu J, Xia Y (2015) Oxygen-rich hierarchical porous carbon derived from artemia cyst shells with superior electrochemical performance. ACS Appl Mater Interfaces 7(2):1132–1139
125. Zhao Y, Zhang Z, Ren Y, Ran W, Chen X, Wu J, Gao F (2015) Vapor deposition polymerization of aniline on 3D hierarchical porous carbon with enhanced cycling stability as supercapacitor electrode. J Power Sour 286:1–9
126. Xu Q, Wei C, Fan L, Rao W, Xu W, Liang H, Xu J (2018) Polypyrrole/titania-coated cotton fabrics for flexible supercapacitor electrodes. Appl Surf Sci 460:84–91
127. Choi KH, Cho SJ, Chun SJ, Yoo JT, Lee CK, Kim W, Wu Q, Park SB, Choi DH, Lee SY, Lee SY (2014) Heterolayered, one-dimensional nanobuilding block mat batteries. Nano Lett 14(10):5677–5686
128. Dong L, Xu C, Li Y, Huang ZH, Kang F, Yang QH, Zhao X (2016) Flexible electrodes and supercapacitors for wearable energy storage: a review by category. J Mater Chem A 4(13):4659–4685
129. Chen Z, Xiong DB, Zhang X, Ma H, Xia M, Zhao Y (2016) Construction of a novel hierarchical structured NH4–Co–Ni phosphate toward an ultrastable aqueous hybrid capacitor. Nanoscale 8(12):6636–6645
130. Wang F, Wang X, Chang Z, Wu X, Liu X, Fu L, Zhu Y, Wu Y, Huang W (2015) A quasi-solid-state sodium-ion capacitor with high energy density. Adv Mater 27(43):6962–6968

131. Lv Z, Li W, Yang L, Loh XJ, Chen X (2019) Custom-made electrochemical energy storage devices. ACS Energy Lett 4(2):606–614
132. Yin L, Huang X, Xu H, Zhang Y, Lam J, Cheng J, Rogers JA (2014) Materials, designs, and operational characteristics for fully biodegradable primary batteries. Adv Mater 26(23):3879–3884
133. Wang X, Xu W, Chatterjee P, Lv C, Popovich J, Song Z, Dai L, Kalani MYS, Haydel SE, Jiang H (2016) Food-materials-based edible supercapacitors. Adv Mater Technol 1(3):1600059

Всё для победы!
НАРОДНЫЙ
ФРОНТ
https://pobeda.onf.ru/
LET'S HELP THE RUSSIA

Chapter 3
Functionalized Nanomaterials, Classification, Properties, and Functionalization Techniques

D. Lakshmi, M. Infanta Diana, P. Adlin Helen, and P. Christopher Selvin

1 Introduction

Nanotechnology involves creating particles, more technically referred to as "nanoparticles (NP)" that are one billionth of a meter (10^{-9} m). Due to the quantum confinement effect, scaling down bulk material to nanoscale results in a variety of marvels. The application of nanotechnology has enabled the creation of compact, lightweight, malleable, and portable machinery and devices. Nanomaterials are already used in almost all industries, including those in farming, health care, aesthetics, fabrics, and energy storage devices [1–3]. These particles are produced using either by top-down or bottom-up approach, and they have exceptional qualities like low toxicity, chemical stability, surface functionality, and biocompatibility [4]. Due to the well-known fact that these nanoparticles' physicochemical qualities are superior to those of bulk materials, their properties are further improved through functionalization, surface and structural engineering, etc. This causes the formation of more active sites, an enhancement in surface-to-volume ratio, and an increase in structural defects with a reduced ion diffusion distance which is carried over through many ways.

D. Lakshmi (✉)
Department of Physics, PSG College of Arts and Science, Coimbatore, India
e-mail: lakshmi@psgcas.ac.in

M. I. Diana · P. A. Helen · P. C. Selvin (✉)
Luminescence and Solid State Ionics Laboratory, Department of Physics, Bharathiar University, Coimbatore, India
e-mail: csphysics@buc.edu.in

© The Author(s), under exclusive license to Springer Nature Singapore Pte Ltd. 2024

C. M. Hussain and M. B. Ahamed (eds.), *Functionalized Nanomaterials Based Supercapacitor*, Materials Horizons: From Nature to Nanomaterials,
https://doi.org/10.1007/978-981-99-3021-0_3

2 Functionalized Nanomaterials

The addition/combination of certain chemical groups and functional entities that are physically and chemically decorated to the nanomaterial surface by changing the surface chemistry helps in developing distinct active sites based on the needs (Fig. 1). To have a broad range of potential applications, the solubility, uniform dispersion of nanoparticles in a medium, as well as their interactions with other molecules must be examined. The functionalization of nanomaterials via surface modifications aids in the interaction of nanomaterials with their surroundings which can be purposefully designed to exhibit the desired properties [5]. Without modification, the surface of nanoparticles has lesser interaction (physical or chemical contact) with the matrix or any other substance under process.

Unmodified nanoparticles form agglomerations as a result of intermolecular interactions which hinder its dispersion into the solvent [6]. Functionalized nanomaterials not only improve existing properties but also contribute to the development of new ones. Other properties, such as cluster formation, colloidal stability, and dispersibility, are greatly influenced by functionalization. Furthermore, utilizing the suitable functionalization method, surface attributes such as corrosivity, hydrophilic/ hydrophobic nature, and conductivity may be readily on hand [7]. As a result, the distinct properties of functionalized nanomaterials make them an appealing candidate for a wide range of applications.

Creating composite materials is one of them, as is synthesizing metal oxide nanoparticles with carbon, doping with heteroatoms using gases, liquids, and solids. In addition to being employed in various energy devices including DSSCs, batteries, supercapacitors, fuel cells, LEDs, etc., functionalized nanoparticles are also discovered to have less toxicity and are used as catalysts in biomedical applications and toxic removants in environmental applications [8, 9]. It has been discovered that functionalized nanomaterials can get over problems like aggregation caused by strong van der Waals forces at close proximity or overlapping of bandgap in nanoscale dimensions. These chemical alterations increase the probability that the solubility and processability of the nanoparticles for various applications will be enhanced.

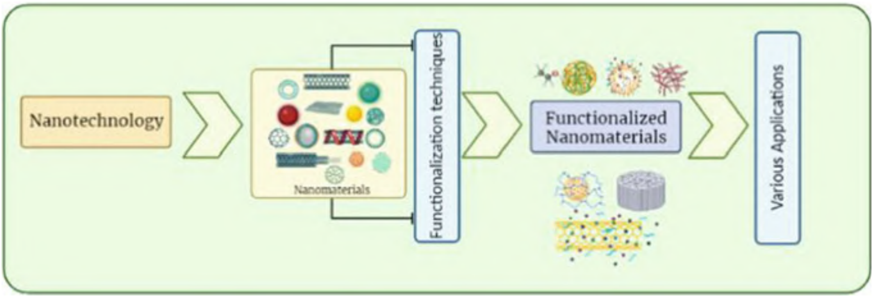

Fig. 1 Need for functionalized nanomaterials

3 Choice of Functionalizing Strategy

The functionalization strategy is chosen based on the specific needs of the application, and it varies depending on the type of NP. Typically NP are functionalized through covalent or non-covalent means. Covalent functioning involves the formation of a bond between the functional entities and the skeleton of the NP. For example, covalent functionalization of graphene has been shown to disrupt the pi–pi conjugation and the properties associated with it, whereas non-covalent functionalization does not disturb the electronic or atomic structure of graphene. The electronic properties at the quantum level, as well as carrier concentration and mobility, are altered by adsorbents upon functionalization and are extremely useful for the application of photovoltaic devices.

Non-covalent functionalization involves the use of attractive forces such as van der Waals, hydrogen bonds, electrostatic force, and pi–pi stacking interactions between the NP and additives. The surface functional groups modify the surface charge functionality and reactivity, increasing its stability and dispensability in different phases [10]. Different chemical and physical methods, such as exfoliation, intercalation, and hybridization, have been used to improve the functionalities and properties of NP.

4 Response to the Functionalizing Agents

Generally, adsorption of functional groups is classified into two types: physisorption and chemisorption. Physisorption involves the formation of non-covalent bonds with longer bond lengths as a result of weak interaction, whereas chemisorption involves the formation of strong bonds with shorter bond lengths. Chemisorptions caused by orbital hybridization produce the majority of covalent bonds. Doping is another aspect of physisorption caused by adsorbate on the material's surface. Substitutional doping can be achieved by introducing a hole or additional electrons into the material. Surface doping is the process of exchanging electrons at the surface with another heteroatom such as boron, nitrogen, aluminum, phosphorous, or sulfur via reactive binding sites. The atomic size of the adsorbate and its electronegativity has a large impact on doping [11, 12].

For example, carbon-based graphene functionalized with nitrogen has been found to effectively increase electronic conductivity, charge storage capacities, and agglomeration due to the presence of a lone pair of electrons and the protonation of some nitrogen groups such as pyridinic, pyrrolic, and pyridine. Modified graphene is often synthesized using the traditional Hummers method, in which oxygen is strictly adhered to the graphitic layer and oxidized, causing the van der Waals forces present within the graphite to move away from each other and, as a result, graphene oxide is formed. This chapter discusses the properties, synthesis strategies, and case studies of functionalized nanoparticles [13–15]. Figure 2 broadly explains the different modes of functionalization and their relative effects on the various properties of the materials.

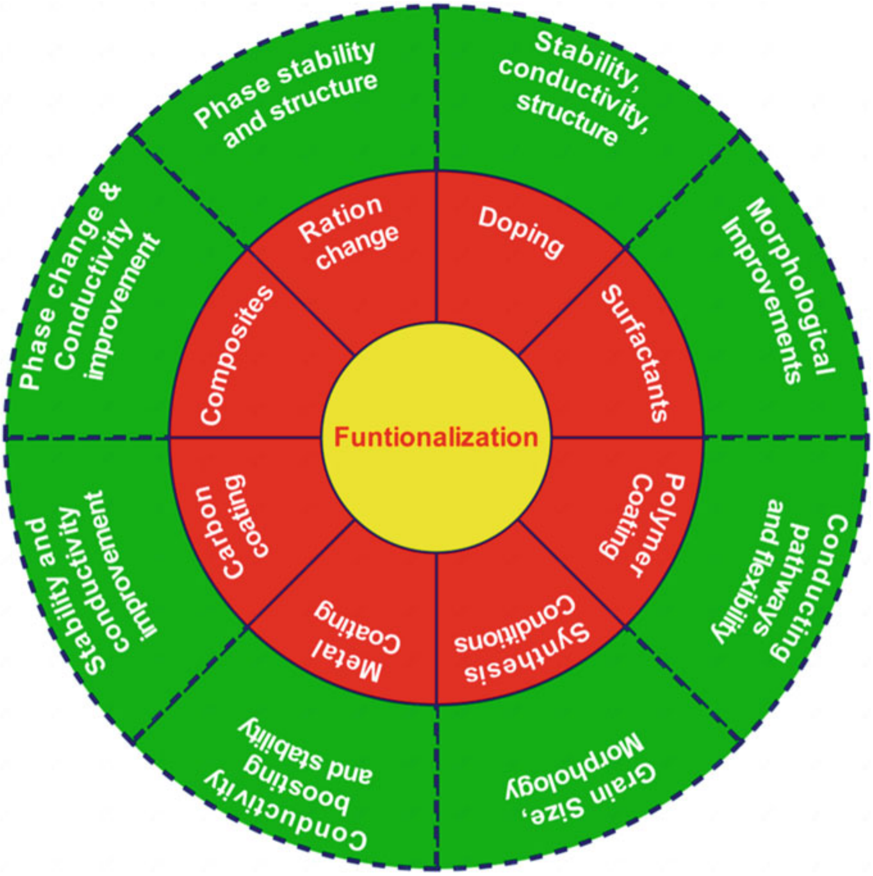
Funtionalization
Ration change
Doping
Surfactants
Polymer Coating
Synthesis Conditions
Metal Coating
Carbon coating
Composites
Phase stability and structure
Stability, conductivity, structure
Morphological Improvements
Conducting pathways and flexibility
Grain Size, Morphology
Conductivity boosting and stability
Stability and conductivity improvement
Phase change & Conductivity improvement

Fig. 2 Different functionalization techniques versus respective impact on material properties

5 Properties of Functionalized Nanoparticles

5.1 Morphology and Porosity

NP can have varied dimensions ranging from 10 to 100 nm and its shape is discovered to be crucial in increasing their qualities for a variety of applications. However, aggregation of NP is a significant disadvantage that might be avoided by utilizing functional groups to modulate shape. It is discovered that the functionalized NP display more intriguing characteristics than the pristine nanoparticles in terms of morphology [16].

The porosity of the nanoparticles plays an important role in promoting host–guest interactions during targeted drug delivery in pharmaceutical or medical systems, as well as in energy storage systems like EDLC supercapacitors to enhance the storage of ions for excellent capacity. The surface-to-volume ratio of NP prepared with high porosity is significantly higher than that of bulk materials. The functionalization of pores present in NP is found to have a significant influence on the pore size, volume of the porous cavity, interconnected porous structure, specific surface area as well as the surface-to-volume ratio. Better porous property of NP improves the efficacy of nanoparticles in a wide range of applications, including drug delivery, catalysis, sensing adsorption, separation, and biomedical.

In general, materials are classified into three types based on their porosity: microporous (less than 2 nm), mesoporous (2–50 nm), and macroporous (>50 nm). This requirement is met by the functionalization of NP at the inner and outer surfaces of the pores and is accomplished by using steric hindrance or electrostatic repulsion to control the site selectivity of the functionalization [17]. Such regularity in allowing only certain type of molecules to enter the pores, promotes the controlled environments, and unwanted side reactions are avoided. This is particularly evident in mesoporous silica NP prepared with anionic functional groups attached to the outer surface of silica, which exhibit hydrophilicity and repel other submicron structures [18, 19]. This has been shown to inhibit specific adsorption while promoting biomolecular conjugation. The addition of specific cationic or anionic functional groups has been found to specifically interact with biomolecules such as lipids and plasma proteins, while inhibiting the adsorption of other unwanted groups. This clearly demonstrates that surface modification is critical in increasing surface area reactivity with the targeted molecules of interest.

Functionalization is further useful in the development of 3D carbon materials for supercapacitors loaded with multiple active sites and mesoporous structures at the micro- and nanoscale, which in turn helps to obtain high capacitance by reducing ion diffusion length. Controlling the pore size of the electrode material improves supercapacitive behavior significantly. This means that the electrode material's pore size should be significant compared to that of the solvated ions in the electrolyte solution. If the pore size is too small, ions will find it more difficult to accumulate at the pores on the electrode surface, reducing the capacitance of the double layer. Generally capacitance of a supercapacitor can be improved by creating electrode materials with a large active surface area which act as a network for efficient electron transfer. However, producing electrode materials with a high specific area would result in a large pore volume, which could eventually cause the density and volumetric specific capacitance to decrease. The shape of the pores influences the pore size distribution when selective ion adsorption occurs at the electrode surface, where ion size also has a significant impact [20]. Cone-, inverted cone-, and cylindrical-shaped pores are just a few of the many different types of pore shapes that have been reported thus far. The electrode materials prepared with these shapes of pores are reported to have nearly identical capacitance, resistance, and maximum charge storage capacities [21, 22].

5.2 Optical Properties

The functionalization of nanoparticles confers better optical properties, which broadens their applications in luminescent fields. Functionalization improves the recombination of localized electron–hole pairs for improved luminescent properties in pristine nanomaterials. This is especially noticeable in nanoparticles prepared through functionalization via heteroatom doping of nitrogen or metal doping, which results in a high fluorescence yield. The band structure can be tuned as a result of this functionalization, and the excitation independence behavior due to passivated surface states can be determined. The fluorescent properties are affected by the surface structure and electron distribution in nanoparticles, which is related to the energy gap between HOMO and LUMO. After surface passivation, the functionalization groups tend to attach or bind on the surface of nanoparticle, and the emission caused by surface energy traps becomes more stable [23]. For example, doping of heteroatom like nitrogen results in the formation of a new surface state (N-state) that traps electrons and increases the radiative recombination while suppressing the non-radiative recombination. Also, because of the increased probability of an electronic transition from ground state to lowest singlet state, nitrogen amino groups act as electron donors, indirectly increasing quantum efficiency. While functionalization has little effect on the band gap in graphene-based quantum dots, it does change their redox potentials by covalently attaching groups with lone pair of electrons such as carbonyl and amine groups. The development of these new sub-bands enabled optical transition in the near UV and visible ranges, resulting in positively and negatively charged surface sites.

In optoelectronic applications, achieving high color purity with narrow line width luminescence and warm colors is critical. This has been accomplished through the development of functionalized nanomaterials [24].

5.3 Mechanical Properties

The mechanical properties of functionalized nanoparticles are found to be better than pristine nanoparticles in terms of elasticity, rigidity, strength, stiffness, and hardness. This is heavily influenced by the concentration, type of functional groups as well as the interfacial bonding between the functional groups and the NP. In some cases, Young's modulus of covalently functionalized NP such as single-walled nanotube is significantly lower than that of pure. On the other hand, Young's modulus of the Cu–O-CNT composite is found to be increased with increasing functional group concentration. This is due to the fact that the appropriate amount of oxygenation improves the bonding between the CNTs and the Cu matrix, resulting in only minor structural changes to the nanotube backbone and an increase in elastic modulus. Especially, for CNT-based NP, the effectiveness of the CNT (single or double walled) used also plays a role in determining differences in mechanical properties of the resulting composite [25].

The effectiveness of bonding is demonstrated in the graphene oxide sheet prepared with functionalized SiO_2, in which the f-SiO_2 NP acted as cross-linking points to connect the GO sheets, resulting in improved mechanical properties. However, increasing the f-SiO_2 content above 10 wt% causes aggregation, which causes enhanced stress, resulting in reduced mechanical properties such as Young's modulus, tensile strength, and toughness. The improved mechanical property below 10 wt% is due to strong interfacial interactions such as hydrogen bonds and covalent interactions between graphene oxide sheets and f-SiO_2, which in turn resulted in effective load transfer during deformation process. This is quite opposite in a simple oxygenated graphene nanoparticles where the mechanical robustness is found to be reduced than the defect-free graphene [26].

5.4 Reduced Toxicity

There are more chances for NPs to have non-specific side effects than there are in the bulk, which is why they are discovered to be harmful as well. This is substantially mitigated by the use of functionalized nanoparticles [27]. The toxicity of nanoparticles must be taken into consideration because it is a significant issue for applications such as using nanoparticles as nanodrug carriers and removing heavy metal components from the environment. It has been discovered that functionalizing nanoparticles reduces the generation of reactive oxygen species and enhances the biocompatibility, pharmo-kinetics, and assembly of biomolecules [28]. This is also because there are several opportunities for nanoparticles to aggregate and cause adverse side effects with biological, environmental, and cell surfaces. Particularly when functionalized with polymers, nanoparticles can be contained inside the polymer layer, acting as a protective layer. In the case of drug delivery, this can lessen the direct interaction of the nanoparticle with the antioxidant molecules or core molecules. Ultimately, this restricts the flow of oxygen to the polymer's core surface, reducing the oxidation process that results in the breakdown of NP and undesired side effects. It has been discovered that functionalized magnetic NP can deliver drugs more effectively and with less toxicity [29] (Fig. 3).

5.5 Electronic/Electrochemical Properties

It has been observed that the introduction of functional groups can be used to adjust electrochemical properties, including tuning of energy levels, surface area, shape, porosity, and stability. The functionalized graphene dots are particularly effective at transferring electrons for proton reduction in photocatalysis applications. Additionally, it has been discovered that the graphene dots functionalized with amine groups

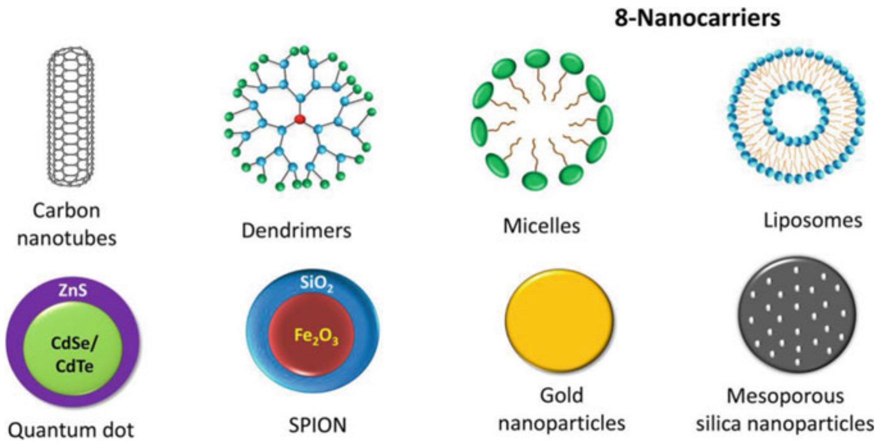

Fig. 3 Types of nanocarriers. Adapted with permission from reference 30

have significant inherent solubility. The surface functionalization of carbon dots is anticipated to increase performance by improving detection sensitivity and designing new composite functional materials or donor–acceptor arrays [30].

High diffusion profile, high collision rate, high loading capability, and preserving electroactive species from degradation are some of the improved qualities that these functionalized NP are discovered to display in electrochemical sensing applications. Also, doping the nanoparticles with heteroatoms like boron, nitrogen, and phosphorous is observed to subsequently speed up the charge transfer kinetics of the electroactive species at the electrode surface, particularly in the case of electrochemical sensors. The use of functionalized nanoparticles as electrodes in supercapacitors favors the migration and penetration of electrolyte into the electrode materials, thereby improving the electronic conductivity and enhancing the kinetics of electrochemical reactions while reducing charge transfer reactions.

Pd–Ni nanoparticles supported in functionalized multi-walled carbon nanotubes were created in order to boost the electroactivity of glucose sensors, and this increase in electroactivity is visible through an increase in the intensity of anodic peak current for glucose detection. The electrochemical sensing property has also been observed to have high sensitivity, improved stability, high selectivity, low detection limit, fast current response, and great repeatability [31].

When compared to pristine TiO_2 NP, amino-functionalized ones showed stronger crystallinity. After functionalization with TiO_2 nanoparticles, it is discovered that the conduction band and valence band energy levels have been elevated to greater levels, and larger open-circuit voltage values have also been noted. Further, NP's ambient stability has been improved upon functionalization, enabling a greater resistance to the infiltration of moisture [32].

Additionally, the sp2 carbon network is weakened, producing defects and increasing back-scattering in the system, due to the adsorbates formation of covalent bonds with the CNT surface. The functionalized carbon-based NPs are shown to have higher carrier densities and electrical conductivities. In particular, N_2 doping and surface modification limit the aggregate formation and shield the nanoparticles from bulk oxidation in ambient circumstances. Further, it can reinforce carbon systems and raise the carrier density of those systems, which will improve their electrical conductivity during catalysis. For example, nitrogen's substitution in MWCNTS enhances the electrical conductivity rather than only impeding their aggregation.

The concentration of functionalized groups on the NP determines how many electronic states there are at the Fermi level whereas significant suppression of the transmission channels below Fermi energy is covalent functionalization. The type of functional groups used has a significant impact on the electrical characteristics of the nanoparticles. In particular, it is discovered that O_2 atoms function as carrier traps, decreasing carrier density and increasing back-scattering in the system, whereas N_2 dopants virtually double locally, increasing transmission through the nanotube and lowering back-scattering in the nanoparticles matrix. The total density of states of NPs at the Fermi level is increased by the presence of functional groups like O_2. By creating novel states related to electron injection through functionalization, new conduction channels can be opened in the nanoparticles [33].

6 Functionalization Techniques

By altering the solvents, surfactants, and reaction temperature, functionalization may be done via covalent or non-covalent interactions, allowing for control of desired and unique functionalities. Because of this sort of functionalization, nanomaterials become hydrophilic and easily soluble in organic solvents. Functionalization occurs in non-covalent interactions by means of hydrogen bonding, ionic bonding, or hydrophobic contact. The electronic arrangement and characteristics of the atoms on the surface are unaffected in this form of interaction [34]. To improve the properties of nanomaterials such as solubility, biocompatibility, and the inclusion of new active sites, several functionalization pathways such as chemical techniques, ligand exchange processes, and synthetic polymer grafting are employed. Nanomaterials can be functionalized with a variety of ligands via various strategies such as physical or chemical routes to confer novel properties that cannot be exhibited as in bulk counterparts. Functionalized nanomaterials are majorly categorized according to their functionalizing agent and nanomaterial composition [35]. The following section explains various forms of functionalization techniques (Fig. 4).

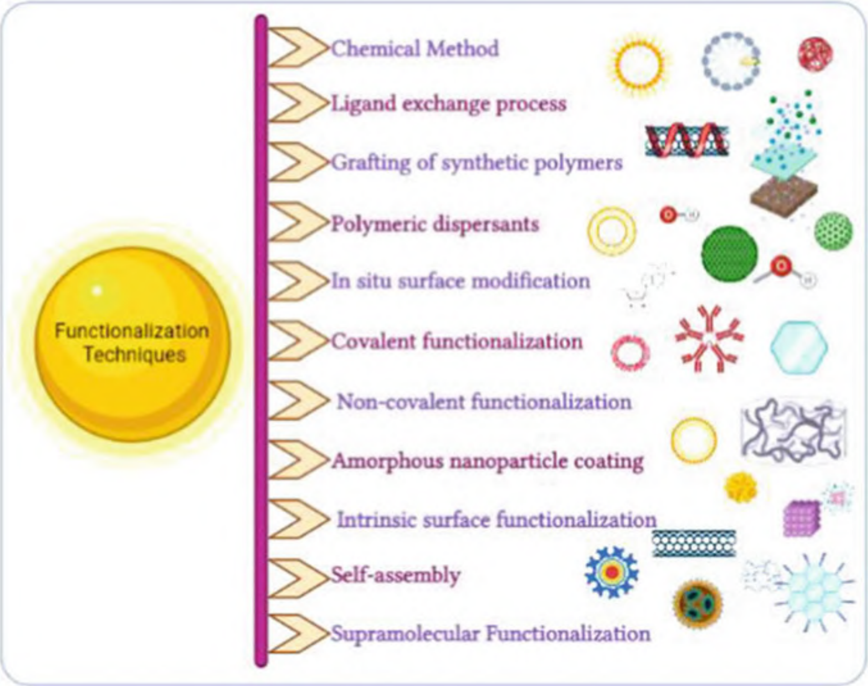
Functionalization Techniques
Chemical Method
Ligand exchange process
Grafting of synthetic polymers
Polymeric dispersants
In situ surface modification
Covalent functionalization
Non-covalent functionalization
Amorphous nanoparticle coating
Intrinsic surface functionalization
Self-assembly
Supramolecular Functionalization

Fig. 4 Functionalization techniques

6.1 *Chemical Functionalization*

Chemical functionalization method involves a chemical process that occurs at the nanomaterial's interface in a medium. This method is mainly developed to functionalize unmodified nanomaterials in order to improve their solubility, reactivity, and hydrophobic interaction. Among various chemical techniques for the functionalization of nanomaterials, treatment with metal alkoxides, ethoxides, and silane coupling agents is widely used [36]. To remove surface contaminations acid treatments are employed. Besides alkali treatments, treatments with hydrogen peroxide, and heat treatments are the most popular chemical treatment procedures [37–39].

6.2 Ligand Exchange Process

Ligand exchange process is second widely employed method which mediates a dynamic interaction mechanism that exchanges ligands bound to the surface of nanoparticles. During the synthesis process, certain organic compounds or polymers are utilized to stabilize the nanoparticles. Nanomaterials may be broadly decorated by numerous ligands using this technique, depending on the needs. The additional components get attached to the nanoparticles' surface, improves their shape and size. Polyvinyl alcohol, polyvinyl pyrrolidone, oleylamine, oleic acid, cetyl trimethyl ammonium bromide, and ascorbic acid molecules are considered to act as capping agents, ligands, or surfactants depending on their chemical composition and functionality [40].

As an organic protector, the capping ligand materials deposited on the nanoparticle surfaces deter reactant molecules from approaching the surface of the nanomaterials. A few nanometers thick ligand layer is sufficient to shield the nanoparticles and prevent the transit of electrons among the nanoparticles before the occurrence of recombination [41]. But one major drawback of the choice of bulky organic ligand is that these material-deficit functionally active groups can participate in charge transfer between the nanoparticles. In order to maximize the transferring of charges and reduce the recombination loss, synthesis ligands must be removed from the nanoparticle surface [42]. This can be consummate by substituting the bulky ligands with more appropriate ones. To obtain better conductivity and charge separation, the incorporated or substituted ligand should be readily altered by annealing or any vacuuming. Because, in some cases, the presence of capping ligands might inject complexity into the system, such as unpredictable random charge transfer and non-covalent interaction between nanomaterials [43].

6.3 Grafting of Synthetic Polymers

A further popular surface modification technique that improves kinetics and changes the shape or form of nanomaterials is grafting of polymers. The three different polymer grafting functionalization techniques are grafting-to, grafting-from, and grafting-through. The final stage polymer is directly bonded to the suitable nanoparticle exterior using the grafting-to process. The grafting-from procedure produces polymer chains from a surface starting point. During the grafting-through procedure, a small monomer copolymerizes with another monomer on the surface of the nanomaterial [44]. Due to the fact that these low molecular weight monomers can interact with the active regions on the surface of the aggregated nanoparticles by permeating them. Also, by doing this, the nanoparticle surface will become hydrophobic, which is a crucial need for the blending of any metal oxide matrix or filler. On the other hand, introducing any kind of groups on the nanoparticle surfaces results in effective grafting.

Other methods of surface functionalization include in vivo passivation and the deposition of polymeric emulsifiers on the surface of the nanoparticle. Furthermore, synthetic methods including coating with amorphous nanoparticles and intrinsic surface engineering are used to functionalize nanomaterials.

6.4 The Adsorption of Polymeric Dispersants

To prevent aggregation, surfactants or capping agents like oleylamine, oleic acid, etc. are incorporated in the reaction system. On the flip, hydrophilic nanoparticles are dispersed in organic solvents which are polar using cationic and anionic additives. The polymer chains are exposed to steric opposite charges by the dispersants, which raise surface charge and enhance nanoparticle miscibility. Numerous polycarboxilic chemicals and their derivatives are used as anionic surfactants to scatter different kinds of metal oxide nanoparticles [45].

6.5 In Situ Surface Modification

During any nanoparticle synthesis, in situ surface modification approaches are used. In situ surface modification techniques include reverse micelle procedures, thermal breakdown of organometallic compounds, and polyol approaches [46, 47].

6.6 Covalent Configuration

The term “covalent modification/functionalization” of nanomaterials refers to the covalent bonding of several chemical species to nanoparticles. The attachment of certain polymers, biomolecules, and inorganic/organic compounds to the surface of nanomaterials via this complexation technique is a potential strategy for enhancing distributions, colloidal stability, and adaptability. Covalent functionalization is frequently used to alter common nanomaterials like nanoclays, 2D nanomaterials, and metal oxide nanoparticles since it suggests a very strong coupling and a stable surface. The application of nanomaterials in a wide range of cutting-edge industries, including biosensors, catalysis, bio-imaging, packaging, cosmetics, environmental remediation, and agriculture, is considerably increased by this form of functionalization [48].

6.7 Non-covalent Configuration

Non-covalent configuration/functionalization involves the formation of relatively weak bonds between guest molecules and the nanomaterials. Electron donor–acceptor ligand systems, polymer hydrogen bonding, and interactions according to van der Waals are the most common methods of non-covalent functionalization. Such functionalization is highly helpful in close proximity and simple to access at ambient temperature since it is mostly reliant on weak forces like hydrogen bonding and van der Waals interactions. These feeble forces are predicted to have an impact on the solvation of nanomaterials as well as hydrophobic and hydrophilic surface interactions. Non-covalent functionalization has the potential to enhance bioactivity, miscibility, sensitivity, binding affinity, catalytic action, and other properties. The implications of the big interfaces are comparable despite the fact that the energy produced during non-covalent bond formation is substantially smaller than that released during covalent contact [49, 50].

6.8 Amorphous Nanoparticle Coating

Inorganic materials like amorphous silica and polymers can be used to form a covering of amorphous nanoparticles on the surface of metallic nanomaterials. Additionally, by allowing therapeutic ligands to be attached on their surface, coating the surface of nanoparticles, particularly with polymers, provides capabilities to the nanomaterials. Moreover, the decorating of nanomaterials with amorphous entities is possible by covering organic monomer, organic polymer, and inorganic metal oxide materials with different entities. Silica or polymers are arranged amorphously on nanoparticles to increase stability and create a conducive environment for later functionalization [51].

6.9 Intrinsic Surface Functionalization

The atomic-level change of a nanomaterial's crystal referred to as intrinsic surface functionalization may be achieved largely by defect engineering and heterogeneous integration. The structural, electrical, and catalytic characteristics of nanomaterials are altered by the addition of electron-donating and electron-accepting elements including S, O, N, B, P, and other metals [52].

6.10 Self-assembly

The phrase "self-assembly" refers to an important method in supramolecular chemistry. Self-assembly is the spontaneous construction of specified components into ordered superstructures that may be used for a variety of purposes by nanoscale particles or materials [53]. The same mechanism that permits supramolecular organization also stabilizes molecular assemblies, but it has an effect on the number of connections, the presence of structural complementarities, and recognition phenomena. Mechanisms involved in self-stabilization include ionic stabilization, van der Waals forces, dipole–dipole interactions, and hydrophobic associations. Further, static and dynamic self-assembly are the other two types of self-assembly processes. External impacts are absent in a static process, and structure self-assembly is driven by energy minimization; however, external influences are present in a dynamic process, and the self-assembling system will adapt to its surroundings [54].

At the molecular, meso-, and macro-levels, self-assembly emerges. The spontaneous clustering of molecules under steady state into balanced, physically well-defined clumps connected by non-covalent connections is known as molecular self-assembly [55]. The self-assembly of a mesoscopic entity, like nanomaterial engineering, is referenced to mesoscopic self-assembly. Intramolecular and intermolecular self-assemblies are two further types of molecular and nanoscale self-assembly. In intramolecular self-assembly, molecules self-assemble from a random coil into a well-defined stable structure; on the other hand, intermolecular self-assembly refers to molecules' capacity to form supramolecular ensembles.

6.11 Supramolecular Functionalization

To create functional materials from molecular and nanounits, a unique notion combining procedures associated with nanotechnology together with supramolecular chemistry approaches is required. The molecular structures and nanostructures are inextricably linked. Solvents, temperature, pH, and physical factors such as light intensity all have an impact on the arrangement of molecules into a stable nanoassembly [56]. Besides, few structures are transitional that may be modified further. Unlike simple self-assembling processes, functionalization is often based on non-symmetrical processes that mandate extensive knowledge of nanostructures and their communications utilizing analytical methodologies [57].

7 Methodical Designing of Advanced Functional Nanomaterials: A Broad Split-Up

The introduction of functionalized nanomaterials has opened up innumerable possibilities for constructing high-performance membranes with customized features. Functionalizing nanoparticles have emerged as a new class of high-performance materials that have provided a viable foundation for modernizing traditional membranes. To meet the various applications, the use of functionalized nanocomposites is a possible option. With required state-of-the-art performance, the materials made of functionalized nanomaterials as additives exhibit their enormous promise in a variety of emerging sustainable technologies. Among various materials, few groups of materials are way more functionalized at maximum to acquire advanced properties. To name a few, titanium dioxide (TiO_2), copper oxide (CuO), zinc oxide (ZnO), carbon nanotubes (CNT), iron oxide (Fe_3O_4), silicon dioxide (SiO_2), graphene oxide, and various carbon-based functionalized nanomaterials are widely used in the development of various nanocomposite-based applications [58–65].

Carbon exists in three hybridization states and may combine with other carbon atoms or nonmetallic elements to produce a wide range of structures, from small molecules to massive polymeric complexes. Carbon nanoallotropes are classified into two primary categories depending on the predominant covalent link in the structure; the first group consists mostly of sp2 hybridized carbon atoms that are positively packed in hexagonal crystal lattices that resemble honeycombs. Graphene and graphene-like structures such as CNTs, quantum dots, and fullerenes are common forms of this group, whereas the second category is an aggregation of mainly sp3-bonded carbon atoms that may not be classified as graphene derivatives. Fullerenes are hollow spherical nanostructures comprised of carbon atoms that have been sp2 hybridized.

To meet the crucial demand for innovative materials for nanocomposite applications, graphene and CNT have the capacity to change the material's properties, which can be used in a wide range of applications and a relevant schematic is given in Fig. 5. Many researchers have recently reported significant advances in the utilization of carbon-based nanoparticles, namely, carbon nanotubes (CNTs) and graphene oxide (GO), in nanocomposite membranes for a variety of existing and upcoming research disciplines [66]. CNTs and GO are promising nanomaterials for the development of next-generation membranes with selectivity, high flux, and low fouling characteristics.

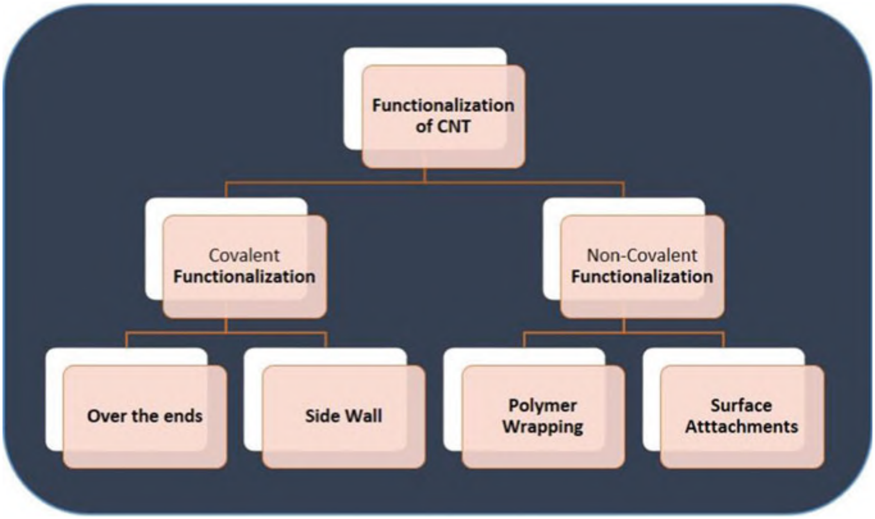

Fig. 5 Modification of CNT nanoparticles

7.1 Functionalization of CNT

The characteristics and performance of CNT-reinforced nanocomposites are heavily reliant on the homogeneous dispersion of individual carbon nanotubes inside the polymer matrix surface, as well as the interfacial contact between the CNT and matrix phase. However, the smaller diameter, along with a greater aspect ratio and much larger surface area, complicates CNT dispersibility within the matrix when compared to other traditionally used metal oxide fillers [61]. Because the commercial CNT resides in the cluster due to van der Walls interactions, dispersion of these nanotubes in the polymer phase is particularly difficult. Another common restriction is a lack of interfacial contact with the polymer matrix. Because of the aromatic nature of the connection, carbon atoms on CNT walls are often chemically stable. CNT interacts with the surrounding matrix mostly by van der Walls' force of interactions, which is unable of delivering enough load transmission across the nanotube and the matrix interface [67]. Massive efforts have been put into sophisticated strategies to change the surface property in order to overcome the aforementioned concerns. According to the interactions between the carbon atom on the CNT and active molecules, functionalized techniques may be generally separated into covalent and non-covalent modifications.

7.2 Functionalization of Graphene and Graphene Oxide

All of the remarkable features and properties of graphene and its derivatives' give a glimpse of a supremacy over other nanostructured carbon allotropes. Because of its unusual structure, graphene dispersion in water and organic compounds is extremely difficult to achieve. Furthermore, graphene has a zero bandgap and is exceedingly inert to most chemical processes, limiting its potential applicability in the domain of energy applications. Despite the fact that graphene and its derivatives have acquired importance in technological growth, its ease of agglomeration severely limits their applicability in a variety of composite and nanocomposites domains. Despite CNTs, graphene and GO are often functionalized using one of three methods: covalent functionalization, non-covalent functionalization, and elemental doping [66]. As a result, graphene functionalization reduced aggregation and enhanced graphene processability, widening its breadth of applications in numerous sustainable development domains. Furthermore, functionalization aids in the modification of inherent properties such as electrical property, which allows for the control of bandgap and conductivity for the usage of novel nanoelectronic devices [68].

7.3 Functionalization of Metal and Metal Oxide Nanoparticles

Metal and metal oxide-supported nanoparticles, primarily Au, Ag, Cu, ZnO, CuO, TiO_2, etc. are in the spotlight of current nanotechnology due to their superior physicochemical characteristics as well as their exceptional conductivity and antibacterial activity. Metal's unique size-dependent feature makes it a more promising material than other large-scale materials. Metal nanoparticles are classified into four types: metal-based nanomaterials, metal oxide-based nanomaterials, doped metals, metal sulfides, and metal–organic frameworks.

Metallic nanoparticles are produced and chemically modified using different functional groups. This method allows them to be combined with ligands or of any antibodies. All these metal and metal oxide-based nanomaterials can modify the surface of a material to provide functionalities and stabilize it. The functionalization with metals and metal oxide nanoparticles are widely used because of its easy processing methods and expansion. Moreover, all these materials are highly stable, less toxic, and low cost. As a result, it offers a surprising range of potential applications in the field of energy storage and conversion technology [69–71].

7.4 Functionalization of Silica-Based Nanomaterials

The functionalization of silica-based nanomaterials is highly employed and approached which enables their utility in numerous advanced applications by making them compatible with a wide variety of polymer molecules. In general, a typical method, namely, the silanol organ functionalization method, has been used to functionalize mesoporous nanosilica and zeolite. However, functionalization of zeolite differs slightly from that of mesoporous silica in that it occurs only on the zeolite's external surface. The channel dimension of zeolite is extremely narrow, limiting access to the internal surface for the majority of the reactants [72]. There are two commonly used methods to functionalize both of these nanomaterials which are co-condensation and post-synthetic grafting.

It is important to understand these two techniques because of its easy methodological strategy. Co-condensation is an advantageous method for functionalizing mesoporous silica nanomaterials because they crystallize more easily which is a one-pot synthesis. The main disadvantage of the co-condensation functionalization method is that it affects the final product's high crystallinity [73]. This procedure involves the addition of one or more organosilane and silicon sources, namely, tetraethylorthosilicate, so that functionalization occurs concurrently with the formation of the framework. The co-condensation method results in high functionalization and uniform deposition of functional units on the entire inner pore surfaces, with no pore blockage or shrinkage [74]. Furthermore, the particle morphology of the functionalized mesoporous silicate is easily controlled by this process, whereas the post-synthetic approach refers to the further alteration of pre-shaped nanomaterials prior to functionalization. For surface functionalization of silica nanoparticles by grafting, a well-known silylation technique is most typically used. Using this functionalization technique, nearly all functional groups such as amino, thiol, sulfonic acid, and carboxylic acid have been introduced on the material surface [75]. Nonetheless, the method's main disadvantage is the uneven distribution of functional entities on the pore surface. Typically, a large number of functional groups are adorned around the outer surface of nanomaterials and the entrance of pores.

7.5 Polymeric Nanomaterials

The commercial polymeric nanoparticles' inertness limits their development for long-term uses in a variety of sectors. The surface of the polymer must next be modified to improve its printing, wetting, and adhesion capabilities. This may be accomplished by coating polymeric surfaces and nanostructures with a range of polar and functional groups. Several surface functionalization approaches have been developed during the last several decades, most of which follow the following paths: first, main reactive functional groups are attached to the polymer chain's surface. Second, active/bioactive substances, oligomers or polymers, hydrophobic and hydrophilic

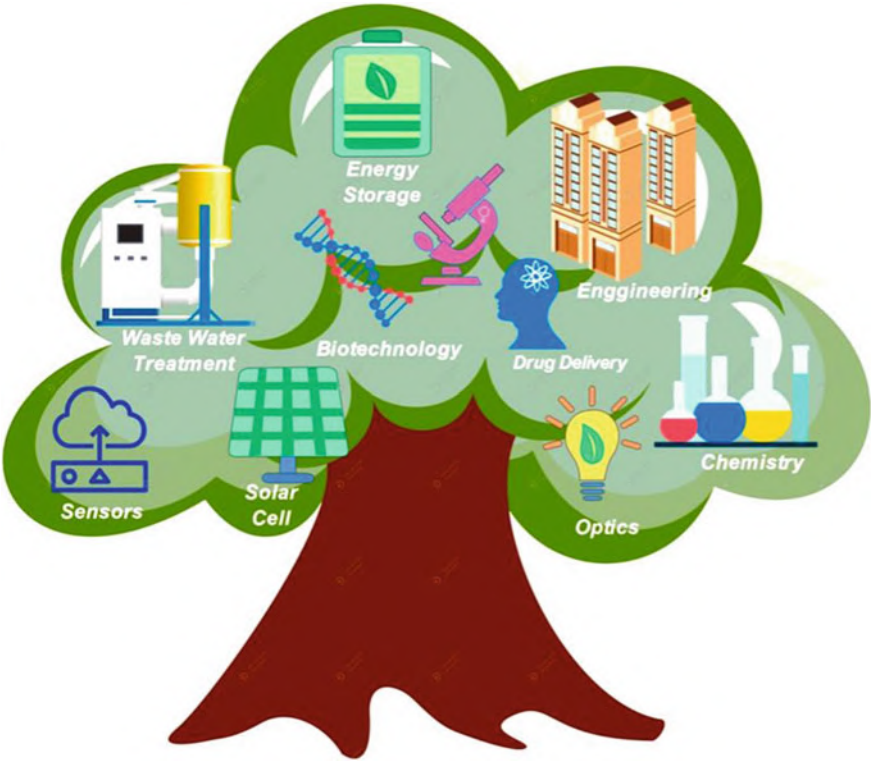

Fig. 6 Illustration of various applications of functionalized nanomaterials

monomers are used to modify the reactive surface in order to achieve particular surface properties that meet the demands of the end use [76].

As discussed so far, functionalization is essential to extract the virtues of nanomaterials to the whole extent. These functionalized nanomaterials hold applications in all the technological advancements. The tree chart given in Fig. 6 indicates the few appliance sectors of these systems. Among different fields, energy storage systems such battery and supercapacitors are the most practical applications in these era. The following portions discover the effect of functionalization of the supercapacitor materials.

8 Role of Functionalized Nanomaterials in Supercapacitors

Supercapacitors (SC) are extremely promising energy storage devices that use two types of electrode materials with surface adsorption to store charges and the other one Faradic redox reaction to store charges. The first type of SC is known as an electrochemical double-layer supercapacitor (EDLS), whereas the second type of supercapacitor is known as a pseudocapacitor. Carbonaceous nanomaterials such as CNTs, activated carbon, graphene oxide, and graphene are often employed in the EDLS for electrode fabrication. However, several types of conducting polymers, metal oxides, and hydroxides are employed as electrode materials in pseudocapacitors. The adjustment of bandgap, structural adaptability, charge carrier mobility, and electrical conductivity are the most important elements in improving the electrochemical energy storage mechanism of SCs. The usage of modified nanomaterials as EDLS and pseudocapacitive electrode materials was discovered to boost energy and power density while also providing outstanding electrochemical performance by enhancing the available free charge carriers [77].

8.1 Case Studies

As a comparative picture, few common metal oxide SC electrodes have been collected and effects of different functionalization modes are analyzed. Functionalization such as of synthesis techniques, dopants, metallic coating, composites with other metal oxides, and surfactant additions provide different effects on the performance and physical chemistry of the host materials. Extensive analysis on each of these parameters can occupy a volume of discussion. Further, the famous SC electrode candidates such as RuO_2, MnO_2, NiO, Co_3O_4, Fe_2O_3, and V_2O_5 are compared for their theoretical capacitance, potential window (in neutral electrolyte), and stability on cycling conditions have been plotted as a comparative chart (Fig. 7). Functionalization on each of these materials significantly affects the above-mentioned parameters as seen in Table 1.

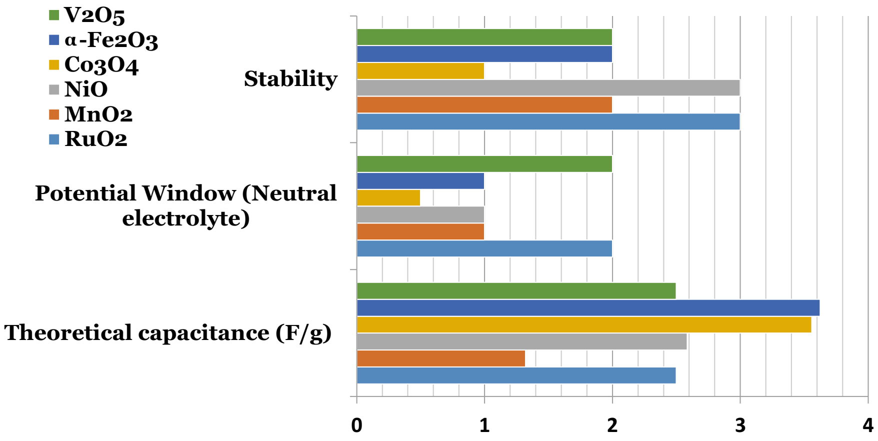

Fig. 7 Comparative illustration between significant parameters of popular supercapacitor electrodes

Table 1 Effect of functionalization on the different technical aspects of the supercapacitor electrode materials

S. no	Electrode	Functionalization		Capacitance (F/g)	Stability (Cycles)	Salient features/remarks	Refs.
		Materials	Method				
1.	Co_3O_4/ rGO-120-12	rGO	Hydrothermal	1152	10,000	Capacity retention	[78]
2.	Co_3O_4–MnO_2	Carbon substrate and MnO_2 composite	Chemical deposition	616	10,000	83.1% capacity retention	[79]
3.	Ag–Co_3O_4	Ag	Grown on Ni foam	1323	2000	Capacity retention	[80]
4.	$CoMoO_4$ @CoS	Core–shell composite		3380	6000	81% capacity retention	[81]
5.	$CuCo_2O_4$	Electro-deposition		1473	5000	–	[82]
6.	Co_3O_4@ graphene sheets	Graphene		3840	–	No loss in capacity	[83]
7.	MnO_2/carbon	Carbon fiber fabric	Green hydrothermal	467	5000	Flexible electrode, 99.7% capacity retention	[84, 85]
8.	MnO_2/CNT	Double-walled CNT array	Electro-deposition	793	5000	99.7% capacity retention	[86]
9.	MnO_2/CNT on Ni foam	CNT-Ni	Chemical vapor deposition	325.5	5000	Binder free, carbon degradation	[87]
10.	MnO_2/exfoliated graphite	Thermally exfoliated graphite	Hydrothermal	500	5000	Large conductive area	[88]
11.	MnO_2-PANI	PANI	Polymerization	626	1000	Stability	[89]
12.	MnO_2–Au	Au	Hybrid composites	1145	1000	High performance	[90]
13.	MnO_2–Cu	Cu	MnO_2 coating on Cu	1024	2000	96% capacity retention	[91]
14.	MnO_2-NCA	Ni, Ti	Electro-deposition	632	20,000	95% capacity retention	[92]

(continued)

Table 1 (continued)

S. no	Electrode	Functionalization		Capacitance (F/g)	Stability (Cycles)	Salient features/remarks	Refs.
		Materials	Method				
15.	MnO_2–Co_3O_4	Co_3O_4	Core–shell on Ni substrate through hydrothermal	560	5000	95% capacity retention	[93]
16.	MnO_2/$NiCo_2O_4$	$NiCo_2O_4$	Hydrothermal	2827	3000	1.6% loss	[94]
17.	RuO_2/C	Carbon	Thermal decomposition	537.7	1000	Cycling stability	[95]
18.	RuO_2/Au-C	Au, Carbon		558			
19.	RuO_2-CNT	CNT foam		502.78	8100	106% capacity retention	[96]
20.	RuO_2/CuO/ MWCNT	Nanocomposites	Hydrothermal	461.59	–	Efficient electrochemistry	[97]
21.	Zr-ZnO	Zr	Doping	518	5000	94% capacity retention	[95]
22.	SnO_2: RuO_2	RuO_2	1:3 ratio by SILAR method	185	2500	–	[96]
23.	SnO_2–NiO	NiO	1:7 ratio by sol–gel and sonication	464	1000	87.24% capacity retention	[97]
24.	Fe–SnO_2–CeO_2	Fe, CeO_2	Co-precipitation	348	5000	–	[97]

9 Conclusion

Functionalized nanomaterials are superior than their pristine versions due to the improved physical, chemical, optical, and other targeted performance-oriented properties. This review extensively focuses on the significance of functionalization, different methodological aspects available for the process, and their respective improvements in the end results of the nanomaterials. Figure 2 provides a broad overview on the impact of different functionalization strategies on the various properties of nanomaterials. Each strategy imposes a specific change in the matrix and the process involves in few limitations as well. For example, inclusion of polymer reduces the rigidity of the nanomaterials whereas inclusion of dense composites reduces the flexibility of the nanocomposites. Hence, the choice of functionalization technique requires deep survey suitable for that particular system. The present review gives an insight into the choice, impact, and different modes of functionalization technique. Finally, a short literature review has been compiled for the popular supercapacitor electrode materials and impact of different functionalizers on its SC performances.

References

1. Nayak V, Singh KR, Singh AK, Singh RP (2021)Potentialities of selenium nanoparticles in biomedical science. New J Chem 45(6):2849–2878
2. Abdel-Mageed HM, AbuelEzz NZ, Radwan RA, Mohamed SA (2021) Nanoparticles in nanomedicine: a comprehensive updated review on current status, challenges and emerging opportunities. J Microencapsul 38(6):414–436
3. Chakraborty A, Roy A, Ravi SP, Paul A (2021) Exploiting the role of nanoparticles for use in hydrogel-based bioprinting applications: concept, design, and recent advances. Biomater Sci
4. Rashid MM, Simončič B, Tomšič B (2021)Recent advances in TiO2-functionalized textile surfaces. Surf Interfaces 22:100890
5. Krueger A, Lang D (2012) Functionality is key: recent progress in the surface modification of nanodiamond. Adv Func Mater 22(5):890–906
6. Heinz H, Pramanik C, Heinz O, Ding Y, Mishra RK, Marchon D, Flatt RJ, Estrela-Lopis I, Llop J, Moya S, Ziolo RF (2017) Nanoparticle decoration with surfactants: molecular interactions, assembly, and applications. Surf Sci Rep 72(1):1–58
7. Kumar SSA, Bashir S, Ramesh K, Ramesh S (2021) A comprehensive review: super hydrophobic graphene nanocomposite coatings for underwater and wet applications to enhance corrosion resistance. FlatChem, 100326
8. Guo R, Li L, Wang B, Xiang Y, Zou G, Zhu Y, Hou H, Ji X (2021) Functionalized carbon dots for advanced batteries. Energy Storage Mater 37:8–39
9. Mahalingam S, Manap A, Omar A, Low FW, Afandi NF, Chia CH, Abd Rahim N (2021) Functionalized graphene quantum dots for dye-sensitized solar cell: Key challenges, recent developments and future prospects. Renew Sustain Energy Rev 144:110999
10. Rathinavel S, Priyadharshini K, Panda D (2021) A review on carbon nanotube: An overview of synthesis, properties, functionalization, characterization, and the application. Mater Sci Eng B 268:115095
11. Mauro N, Utzeri MA, Varvarà P, Cavallaro G (2021) Functionalization of metal and carbon nanoparticles with potential in cancer theranostics. Molecules 26(11):3085

12. Zhu W, Chen Z, Pan Y, Dai R, Yue W, Zhuang Z, Wang D, Peng Q, Chen C, Li Y (2019) Functionalization of hollow nanomaterials for catalytic applications: nanoreactor construction. Adv Mater 31(38):1800426
13. Ortiz-Medina J, Wang Z, Cruz-Silva R, Morelos-Gomez A, Wang F, Yao X, Terrones M, Endo M (2019) Defect engineering and surface functionalization of nanocarbons for metal-free catalysis. Adv Mater 31(13):1805717
14. Chen Z, Cao W, Zhang Z, Wangping W, Wang X, Zhiqiang Y (2018) Synthesis, functionalization, and nanomedical applications of functional magnetic nanoparticles. Chin Chem Lett 29(11):1601–1608
15. Li Z, Ling Wang Y, Li YF, Feng W (2019) Carbon-based functional nanomaterials: preparation, properties and applications. Compos Sci Technol 179:10–40
16. Wu Y, Deng P, Tian Y, Magesa F, Liu J, Li G, He Q (2019) Construction of effective electrochemical sensor for the determination of quinoline yellow based on different morphologies of manganese dioxide functionalized graphene. J Food Compos Anal 84:103280
17. Yu Z, Tetard L, Zhai L, Thomas J (2015) Supercapacitor electrode materials: nanostructures from 0 to 3 dimensions. Energy Environ Sci 8(3):702–730
18. Olivieri F, Castaldo R, Cocca M, Gentile G, Lavorgna M (2021) Mesoporous silica nanoparticles as carriers of active agents for smart anticorrosive organic coatings: a critical review. Nanoscale 13(20):9091–9111
19. Zou Y, Huang B, Cao L, Deng Y, Jiacan S (2021) Tailored mesoporous inorganic biomaterials: assembly, functionalization, and drug delivery engineering. Adv Mater 33(2):2005215
20. Young C, Park T, Yi JW, Kim J, Hossain MS, Kaneti YV, Yamauchi Y (2018) Advanced functional carbons and their hybrid nanoarchitectures towards supercapacitor applications. ChemSusChem 11(20):3546–3558
21. Saraf M, Rajak R, Mobin SM (2019) MOF derived high surface area enabled porous Co3O4 nanoparticles for supercapacitors. ChemistrySelect 4(27):8142–8149
22. Luo X-Y, Chen Y, Mo Y (2021) A review of charge storage in porous carbon-based supercapacitors. New Carbon Mater 36(1):49–68
23. Chen BB, Liu ML, Li CM, Huang CZ (2019) Fluorescent carbon dots functionalization. Adv Colloid Interface Sci 270:165–190
24. Kou X, Jiang S, Park S-J, Meng L-Y (2020) A review: recent advances in preparations and applications of heteroatom-doped carbon quantum dots. Dalton Trans 49(21):6915–6938
25. Milowska KZ, Burda M, Wolanicka L, Bristowe PD, Koziol KK (2019) Carbon nanotube functionalization as a route to enhancing the electrical and mechanical properties of Cu–CNT composites. Nanoscale 11(1):145–157
26. Johnson AP, Gangadharappa HV, Pramod K (2020) Graphene nanoribbons: a promising nanomaterial for biomedical applications. J Controll Release 325:141–162
27. Buchman JT, Hudson-Smith NV, Landy KM, Haynes CL (2019) Understanding nanoparticle toxicity mechanisms to inform redesign strategies to reduce environmental impact. Acc Chem Res 52(6):1632–1642
28. Wang Y, Rui H, Lin G, Roy I, Yong K-T (2013) Functionalized quantum dots for biosensing and bioimaging and concerns on toxicity. ACS Appl Mater Interfaces 5(8):2786–2799
29. Jung JH, Lee JH, Shinkai S (2011)Functionalized magnetic nanoparticles as chemosensors and adsorbents for toxic metal ions in environmental and biological fields. Chem Soc Rev 40(9):4464–4474
30. Hossen S, Hossain MK, Basher MK, Mia MN, Rahman MT, Uddin MJ (2019) Smart nanocarrier-based drug delivery systems for cancer therapy and toxicity studies: a review. J Adv Res 15:1–18
31. Karimi-Maleh H, Cellat K, Arıkan K, Savk A, Karimi F, Şen F (2020) Palladium–Nickel nanoparticles decorated on functionalized-MWCNT for high precision non-enzymatic glucose sensing. Mater Chem Phys 250:123042

32. Hu W, Zhou W, Lei X, Zhou P, Zhang M, Chen T, Zeng H et al (2019) Low-temperature in situ amino functionalization of TiO2 nanoparticles sharpens electron management achieving over 21% efficient planar perovskite solar cells. Adv Mater 31(8):1806095
33. Sgobba V, Guldi DM (2009) Carbon nanotubes—Electronic/electrochemical properties and application for nanoelectronics and photonics. Chem Soc Rev 38(1):165–184
34. Giansante C (2020) Library design of ligands at the surface of colloidal nanocrystals. Acc Chem Res 53(8):1458–1467
35. Ploetz E, Engelke H, Lächelt U, Wuttke S (2020) The chemistry of reticular framework nanoparticles: MOF, ZIF, and COF materials. Adv Func Mater 30(41):1909062
36. Zadehnazari A (2022) Metal oxide/polymer nanocomposites: a review on recent advances in fabrication and applications. Polym-Plast Technol Mater, 1–46
37. Ogbonna VE, Popoola API, Popoola OM, Adeosun SO (2022) A review on the recent advances on improving the properties of epoxy nanocomposites for thermal, mechanical, and tribological applications: challenges and recommendations. Polym-Plast Technol Mater 61(2):176–195
38. Saleh TA (2020) Nanomaterials: classification, properties, and environmental toxicities. Environ Technol Innov 20:101067
39. Deshmukh R, Niederberger M (2017) Mechanistic aspects in the formation, growth and surface functionalization of metal oxide nanoparticles in organic solvents. Chem Euro J 23(36):8542–8570
40. Heuer-Jungemann A, Feliu N, Bakaimi I, Hamaly M, Alkilany A, Chakraborty I, Kanaras AG (2019) The role of ligands in the chemical synthesis and applications of inorganic nanoparticles. Chem Rev 119(8):4819–4880
41. Hanske C, Sanz-Ortiz MN, Liz-Marzán LM (2020) Silica-coated plasmonic metal nanoparticles in action. In: Colloidal synthesis of plasmonic nanometals, pp 755–820
42. Steiner AM, Lissel F, Fery A, Lauth J, Scheele M (2021) Prospects of coupled organic–inorganic nanostructures for charge and energy transfer applications. Angew Chem Int Ed 60(3):1152–1175
43. Ji X, Wang W, Mattoussi H (2016) Controlling the spectroscopic properties of quantum dots via energy transfer and charge transfer interactions: concepts and applications. Nano Today 11(1):98–121
44. Kumar M, Gehlot PS, Parihar D, Surolia PK, Prasad G (2021) Promising grafting strategies on cellulosic backbone through radical polymerization processes—A review. Eur Polymer J 152:110448
45. Zhou Y, Guo Z, Hou W, Wang Q, Wang J (2015) Polyoxometalate-based phase transfer catalysis for liquid–solid organic reactions: a review. Catal Sci Technol 5(9):4324–4335
46. Sodipo BK, Aziz AA (2016) Recent advances in synthesis and surface modification of superparamagnetic iron oxide nanoparticles with silica. J Magn Magn Mater 416:275–291
47. Dheyab MA, Aziz AA, Jameel MS, Noqta OA, Mehrdel B (2020) Synthesis and coating methods of biocompatible iron oxide/gold nanoparticle and nanocomposite for biomedical applications. Chin J Phys 64:305–325
48. Liu J, Ye Y, Xue Y, Xie X, Mai YW (2017) Recent advances in covalent functionalization of carbon nanomaterials with polymers: strategies and perspectives. J Polym Sci Part A: Polym Chem 55(4):622–631
49. Zhang S, Malik S, Ali N, Khan A, Bilal M, Rasool K (2022) Covalent and non-covalent functionalized nanomaterials for environmental restoration. Top Curr Chem 380(5):1–113
50. Zhou Y, Fang Y, Ramasamy RP (2019) Non-covalent functionalization of carbon nanotubes for electrochemical biosensor development. Sensors 19(2):392
51. Konduru NV, Murdaugh KM, Swami A, Jimenez RJ, Donaghey TC, Demokritou P, Brain JD, Molina RM (2016) Surface modification of zinc oxide nanoparticles with amorphous silica alters their fate in the circulation. Nanotoxicology 10(6):720–727
52. Reina G, Zhao L, Bianco A, Komatsu N (2019) Chemical functionalization of nanodiamonds: opportunities and challenges ahead. Angew Chem Int Ed 58(50):17918–17929

53. Ghosh SK, Böker A (2019) Self-assembly of nanoparticles in 2D and 3D: recent advances and future trends. Macromol Chem Phys 220(17):1900196
54. Quintanilla-Sierra L, García-Arévalo C, Rodriguez-Cabello JC (2019) Self-assembly in elastin-like recombinamers: a mechanism to mimic natural complexity. Mater Today Bio 2:100007
55. Della Sala F, Neri S, Maiti S, Chen JL, Prins LJ (2017) Transient self-assembly of molecular nanostructures driven by chemical fuels. Curr Opin Biotechnol 46:27–33
56. Huang S, Yu H, Li Q (2021) Supramolecular chirality transfer toward chiral aggregation: asymmetric hierarchical self-assembly. Advanced Sci 8(8):2002132
57. Mosayebi J, Kiyasatfar M, Laurent S (2017) Synthesis, functionalization, and design of magnetic nanoparticles for theranostic applications. Adv Healthc Mater 6(23):1700306
58. Awad NK, Edwards SL, Morsi YS (2017) A review of TiO_2 NTs on Ti metal: electrochemical synthesis, functionalization and potential use as bone implants. Mater Sci Eng C 76:1401–1412
59. Rutkowska IA, Wadas A, Szaniawska E, Chmielnicka A, Zlotorowicz A, Kulesza PJ (2020) Elucidation of activity of copper and copper oxide nanomaterials for electrocatalytic and photoelectrochemical reduction of carbon dioxide. Curr Opin Electrochem 23:131–138
60. Galstyan V, Comini E, Ponzoni A, Sberveglieri V, Sberveglieri G (2016) ZnO quasi-1D nanostructures: synthesis, modeling, and properties for applications in conductometric chemical sensors. Chemosensors 4(2):6
61. Mallakpour S, Soltanian S (2016) Surface functionalization of carbon nanotubes: fabrication and applications. RSC Adv 6(111):109916–109935
62. Nguyen MD, Tran HV, Xu S, Lee TR (2021) Fe3O4 nanoparticles: structures, synthesis, magnetic properties, surface functionalization, and emerging applications. Appl Sci 11(23):11301
63. Sciuto EL, Bongiorno C, Scandurra A, Petralia S, Cosentino T, Conoci S, Libertino S (2018) Functionalization of bulk SiO2 surface with biomolecules for sensing applications: Structural and functional characterizations. Chemosensors 6(4):59
64. Yang GH, Bao DD, Liu H, Zhang DQ, Wang N, Li HT (2017) Functionalization of graphene and applications of the derivatives. J Inorg Organomet Polym Mater 27(5):1129–1141
65. Li Z, Wang L, Li Y, Feng Y, Feng W (2019) Carbon-based functional nanomaterials: preparation, properties and applications. Compos Sci Technol 179:10–40
66. Hebbar RS, Isloor AM, Asiri AM (2017) Carbon nanotube-and graphene-based advanced membrane materials for desalination. Environ Chem Lett 15(4):643–671
67. Wernik JM, Cornwell-Mott BJ, Meguid SA (2012) Determination of the interfacial properties of carbon nanotube reinforced polymer composites using atomistic-based continuum model. Int J Solids Struct 49(13):1852–1863
68. Kuila T, Bose S, Mishra AK, Khanra P, Kim NH, Lee JH (2012) Chemical functionalization of graphene and its applications. Prog Mater Sci 57(7):1061–1105
69. Neouze MA, Schubert U (2008) Surface modification and functionalization of metal and metal oxide nanoparticles by organic ligands. Monatshefte für Chemie-Chem Monthly 139(3):183–195
70. Amstad E, Textor M, Reimhult E (2011) Stabilization and functionalization of iron oxide nanoparticles for biomedical applications. Nanoscale 3(7):2819–2843
71. Alavi M, Kowalski R, Capasso R, Douglas Melo Coutinho H, Rose Alencar De Menezes I (2022) Various novel strategies for functionalization of gold and silver nanoparticles to hinder drug-resistant bacteria and cancer cells. Micro Nano Bio Aspects 1(1):38–48
72. Farrusseng D, Tuel A (2016) Perspectives on zeolite-encapsulated metal nanoparticles and their applications in catalysis. New J Chem 40(5):3933–3949
73. Hoffmann F, Cornelius M, Morell J, Fröba M (2006) Silica-based mesoporous organic–inorganic hybrid materials. Angew Chem Int Ed 45(20):3216–3251
74. Li H, Chen X, Shen D, Wu F, Pleixats R, Pan J (2021) Functionalized silica nanoparticles: classification, synthetic approaches and recent advances in adsorption applications. Nanoscale 13(38):15998–16016
75. Margelefsky EL, Zeidan RK, Davis ME (2008) Cooperative catalysis by silica-supported organic functional groups. Chem Soc Rev 37(6):1118–1126

76. Ghanooni S, Nikfarjam N, Makvandi P (2020) Surface reactive and active polymers. React Funct Polym 4:35–54
77. Afif A, Rahman SM, Azad AT, Zaini J, Islan MA, Azad AK (2019) Advanced materials and technologies for hybrid supercapacitors for energy storage—A review. J Energy Storage 25:100852
78. Wang X, Yin S, Jiang J, Xiao H, Li X (2020) A tightly packed Co_3O_4/C&S composite for high-performance electrochemical supercapacitors from a cobalt (III) cluster-based coordination precursor. J Solid State Chem 288:121435
79. Liu G, Ma L, Liu Q (2020) The preparation of Co_3O_4@MnO_2 hierarchical nano-sheets for high-output potential supercapacitors. Electrochim Acta 364:137265
80. Nagarajarao SH, Nandagudi A, Viswanatha R, Basavaraja BM, Santosh MS, Praveen BM, Pandith A (2022) Recent developments in supercapacitor electrodes: a mini review. ChemEngineering 6(1). https://doi.org/10.3390/chemengineering6010005
81. Cakici M, Kakarla RR, Marroquin FA (2017) Advanced electrochemical energy storage supercapacitors based on the flexible carbon fiber fabric-coated with uniform coral-like MnO_2 structured electrodes, Chem Eng J 309:151–158
82. Wu D, Xie X, Zhang Y, Zhang D, Du W, Zhang X, Wang B (2020) MnO_2/Carbon composites for supercapacitor: synthesis and electrochemical performance. Front Mater 7:1–16. https://doi.org/10.3389/fmats.2020.00002
83. Li Q, Lu XF, Xu H, Tong YX, Li GR (2014) Carbon/MnO_2 double-walled nanotube arrays with fast ion and electron transmission for high-performance supercapacitor. ACS Appl Mater Interfaces 6(4):2726–2733
84. Huang M, Mi R, Liu H, Li F, Zhao XL, Zhang W, He SX, Zhang YX (2014) Layered manganese oxides-decorated and nickel foam-supported carbon nanotubes as advanced binder-free supercapacitor electrodes. J Power Sour 269:760–767
85. Liu X, Liang B, Hong X, Long J (2022) Electrochemical performance of MnO_2/graphene flower-like microspheres prepared by thermally-exfoliated graphite. Front Chem Nanosci 10. https://doi.org/10.3389/fchem.2022.870541
86. Jaidev RIJ, Mishra AK, Ramaprabhu S (2011) Polyaniline–MnO_2 nanotube hybrid nanocomposite as supercapacitor electrode material in acidic electrolyte. J Mater Chem 21:17601
87. Lang X, Hirata A, Fujita T, Chen M (2011) Nanoporous metal/oxide hybrid electrodes for electrochemical supercapacitors. Nat Nanotechnol 6:232–236
88. Pang H, Wang S, Li G, Ma Y, Li J, Li X, Zhang L, Zhang J, Zheng H (2013) Cu superstructures fabricated using tree leaves and Cu–MnO_2 superstructures for high performance supercapacitors. J Mater Chem A 1:5053–5060
89. Su Z, Yang C, Xie B, Lin Z, Zhang Z, Liu J, Li B, Kang F, Wong CP (2014) Scalable fabrication of MnO_2 nanostructure deposited on free-standing Ni nanocone arrays for ultrathin, flexible, high-performance micro-supercapacitor. Energy Environ Sci 7:2652–2659
90. Huang M, Zhang Y, Li F, Zhang L, Wen Z, Liu Q (2014) Facile synthesis of hierarchical Co_3O_4@MnO_2 core-shell arrays on Ni foam for asymmetric supercapacitors. J Power Sour 252:98–106
91. Zou R, Yuen MF, Zhang Z, Hu J, Zhang W (2015) Three-dimensional networked $NiCo_2O_4$/MnO_2 branched nanowire heterostructure arrays on nickel foam with enhanced supercapacitor performance. J Mater Chem A 3:1717–1723
92. Wang P, Liu H, Tan Q, Yang J (2014) Ruthenium oxide-based nanocomposites with high specific surface area and improved capacitance as a supercapacitor. RSC Adv 4(81):42839–42845
93. Wang W, Guo S, Lee I, Ahmed K, Zhong J, Favors Z, Ozkan CS (2014) Hydrous ruthenium oxide nanoparticles anchored to graphene and carbon nanotube hybrid foam for supercapacitors. Sci Rep 4:9–14
94. Chung YC, Julistian A, Saravanan L, Chen PR, Xu BC, Xie PJ, Lo AY (2022) Hydrothermal synthesis of CuO/RuO_2/MWCNT nanocomposites with morphological variants for high efficient supercapacitors. Catalysts 12(1):1–12
95. Pusawale SN, Deshmukh PR, Jadhav PS, Lokhande CD (2019) Electrochemical properties of chemically synthesized SnO_2–RuO_2 mixed films. Mater Renew Sustain Energy 8:1–9

96. Varshney B, Siddiqui MJ, Anwer AH, Khan MZ, Ahmed F, Aljaafari A, Azam A (2020) Synthesis of mesoporous nanocomposite using modified sol–gel method and its electrochemical performance as electrode material for supercapacitors. Sci Rep, 1–13
97. Asaithambi S, Sakthivel P, Karuppaiah M, Yuvakkumar R, Balamurugan K, Ahamad T, Majeed Khan MA, Ramalingam G, Mohammed MKA, Ravi G (2021) Preparation of Fe-SnO_2@CeO_2 nanocomposite electrode for asymmetric supercapacitor device performance analysis. J Energy Storage 36:102402

Chapter 4
Functionalized Nanomaterials as Supercapacitor Devices: Current Trends and Beyond

**Ponnusamy Paunkumar, Chellapandi Bhuvaneswari,
Rajendran Lakshmi Priya, Boopathi Shagunthala Hariprasad,
Chettipalayam Arunasalam Dhayanithi, and Sundaram Ganesh Babu**

1 Introduction

Today's fast-evolving global economy has led to substantial environmental issues and overconsumption of fossil fuels, both of which represent serious dangers to the survival and advancement of humanity. Therefore, it is critically necessary to utilize efficient energy conversion and storage technologies as well as sustainable and clean energy. Energy storage systems suitable for both high energy density and high-power density applications are currently in high demand. The goal of future research is to produce and store renewable energy. Due to their high energy density, rechargeable batteries, particularly lithium-ion batteries, have received a lot of attention. However, their limited performance includes a short cycle life, relatively slow charging and discharging rates, and consequently lower power densities. Supercapacitors have emerged as an alternative to batteries. Supercapacitors, also known as electrochemical capacitors, provide lower energy densities than batteries, but they can be charged/discharged in seconds, long lifecycle, and have minimal maintenance costs [1–4]. Electrical double-layer capacitors and pseudocapacitors are two categories of supercapacitors based on their energy storage technique. Electrical double-layer capacitors' capacitance could be attributed to the accumulation of electrostatic charges at the electrode. Whereas pseudocapacitance is related to reversible redox reactions at electro-active materials such as polymer, metal oxides/hydroxides, metal composites, etc., it has associated with the electrolyte interface [5]. For EDLC

P. Paunkumar · C. Bhuvaneswari · R. L. Priya · B. S. Hariprasad · C. A. Dhayanithi ·
S. G. Babu (✉)
Department of Chemistry, School of Advanced Sciences, Vellore Institute of Technology,
Vellore 632014, Tamil Nadu, India
e-mail: ganeshbabu.s@vit.ac.in

© The Author(s), under exclusive license to Springer Nature Singapore Pte Ltd. 2024

C. M. Hussain and M. B. Ahamed (eds.), *Functionalized Nanomaterials Based Supercapacitor*, Materials Horizons: From Nature to Nanomaterials,
https://doi.org/10.1007/978-981-99-3021-0_4

electrodes, carbon-based materials such as activated carbon and carbon nanotubes are widely used. But from the other hand, the pseudo capacitance's charge storage method is based on the Faradaic process, in which a redox reaction takes place at the electrode surface. Common electrode materials with a strong pseudocapacitance effect includes material such as metal oxides and conducting polymers. Pseudocapacitance is typically higher than EDLC due to the Faradaic process, but at the expense of the electrode's long-term stability. To create high-performance supercapacitors with long-term stability, it may be possible to combine EDLC with pseudocapacitance in a single device [6–8]. Recently, the development of flexible supercapacitor devices is provided sustainable energy storage devices for wearable devices such as sensors, displays, and mobile phones [9]. Compared to unfunctionalized nanomaterials, functionalized nanomaterials have a higher specific capacitance, owing to the physical and chemical properties of functionalized materials that could be changed in supercapacitor devices [10]. In this chapter, we have summarized the current trends in supercapacitors for the next generation and has been discussed recently published articles, we have given a brief on the future perspective of supercapacitor-based devices and why supercapacitor devices are needed for next-generation energy storage devices for wearable electronic devices at end of the chapter.

2 Functionalized Materials for Supercapacitor Devices

In the past decade, functionalized materials have been performed in various applications such as organic synthesis [11–13], degradation [14], sensors [15], solar cell [16], water spitting [17] and energy storage device [18]. Supercapacitors are one of the many energy storage devices that stand out for their unique properties like excellent power density, rapid charge/discharge process, and long cyclic stability [19, 20]. The electrode material is responsible for the majority of the supercapacitor's activity [21]. The active electrode consists of mainly carbonous/non-carbonous materials, metal oxides/hydroxides, and conducting polymers. They have their advantage and disadvantage. For example, carbon-based materials like graphene [22], nanofibers [23], nanotubes [24], and activated carbon [25] which have high-power density and cyclic stability, are extensively used in supercapacitor-based devices. Functionalized materials give high energy density than that of pure form with long cycle life. The specific capacitance of the prepared electrode was calculated by following Eqs. 1 and 2 from CV and GCD, respectively, and the energy density (E) and power density (P) of the assembled device were obtained from following Eqs. 3 and 4, respectively.

$$C_{\text{sp}} = \frac{\int_{V1}^{V_2} i dv}{mv(V_2 - V_1)} \tag{1}$$

$$C_{\text{sp}} = \frac{I\Delta t}{m\Delta v} \tag{2}$$

$$E = \frac{1}{2} C_{\text{sp}} V^2 \tag{3}$$

$$P = \frac{E}{t_{\text{discharge}}} \tag{4}$$

wher*e* C_{sp} is specific capacitance in F/g, 'm' is mass of material (g), 'v' is scan rate in V/s and $(V_2 - V_1)$ is a potential window (V), 'I' is current density (A), Δt is discharging time (s), 'E' is energy density, 'P' is power density.

2.1 Functionalization of Carbonous Materials

Due to high energy density with long cycle life, functionalized carbonaceous-based electrodes have been used in supercapacitors in the recent year, such as carbon nanofibers (CNFs), graphene derivatives, carbon nanotubes (CNTs), carbon cloth (CC), carbon sphere, fullerene-based carbon materials, these functionalized carbon-based materials have been developed as supercapacitor for next-generation electronic devices.

2.1.1 Functionalized Carbon Nanofibers

Among the carbon-based materials, carbon nanofiber (CNF) has been used in energy storage devices as well as supercapacitor devices. Owing, it has surface area in high and electrical conductivity. CNF has been prepared by the most common methods such as electrospinning and chemical vapor deposition (CVD). CNF has been functionalized by heteroatom or metal oxide or hydroxide to increase the capacitance in recent years. Functionalized carbon nanofiber provides a good specific capacitance, high energy, and power density with long cycle stability.

Selvaraj et al. synthesized porous CNF, CNF/MnO_2, and CNF/rGO by electrospinning and hydrothermal methods for supercapacitor application [26]. A specific capacitance of CNF/MnO_2 is about 271.4 F g^{-1} with 90.2% of cyclic stability than that of MnO_2. The assembled CNF/MnO_2 (positive electrode) and CNF/rGO (negative electrode) as an asymmetric supercapacitor (ASC) device was performed in a range of electrochemical windows between 0 and 2 V in 2 M Na_2SO_4. It provides a gravimetric capacitance of about 245.5 F g^{-1} with an energy density of 34.4 Wh kg^{-1} (at a power density of 192.2 W kg^{-1}) and after 6000 cycles, 84.4% retention capacity was found at 5 A g^{-1}. As suggested by the authors in these findings, indicates that 1D MnO_2/CNFs nanocomposite is an efficient electrode for the next generation of supercapacitors.

Aydın and co-workers developed ZrO_2-CNF by a simple electrospinning method for a flexible supercapacitor device. As prepared CNF-20 ZrO_2 was investigated a specific capacitance in three and two-electrode systems in 6 M KOH electrolyte solution [27]. In a three-electrode system, the CV curves are showing a rectangular shape at 10 mV s^{-1} and maintained that shape when the scan rate increases to 200 mV s^{-1}, which indicates superior rate capability. The GCD curves were recorded at 1–7 A g^{-1} (current densities) with a potential window between −1.0 and 0.0 V. The specific capacitance of 125 F g^{-1} at 1 A g^{-1}. In a two-electrode system, the symmetrical supercapacitor (SSC) is fabricated of CNF-20ZO$_2$//CNF-20ZO$_2$. The SSC cell was investigated at different scan rates in the range of 10–200 mV s^{-1} at various current densities from 1 to 7 A g^{-1}. The highest specific capacitance of the SSC device was showing 140 F g^{-1} at 1 A g^{-1} than other samples. The cyclic stability was investigated up to 10,000 cycles of CNF-20 ZO$_2$//CNF-20 ZO$_2$ and the energy density of CNF-20ZO$_2$//CNF-20ZO$_2$ is 4.46 Wh kg^{-1} at a specific power of 1250 W kg^{-1}, which is four times higher than that of pure CNF (1.04 Wh kg^{-1}). The results suggest that this material can be used for supercapacitor-based devices.

Yuan et al. developed NiCo$_2$S$_4$ (nanosphere and nanosheets) were uniformly coated on C-CNF by solvothermal method and C-CNF was prepared from cellulose by electrospinning method for symmetric supercapacitor application [28]. The prepared C-CNF-NiCo$_2$S$_4$ electrodes were investigated in a three-electrode system, C-CNF-NiCo$_2$S$_4$ nanosheets show high specific capacitance (1784 F g^{-1} at 1 A g^{-1}) than C-CNF-NiCo$_2$S$_4$ nanosphere (1319 F g^{-1} at a current density of 1 A g^{-1}), due to high surface area and well dispersion of nanosheets. The cyclic stability of the nanosphere (84.1% retention capacity) was better than nanosheets (79.3% retention capacity), due to nanospheres being strongly in contact with C-CNF. The assembled all-solid-state symmetric capacitor (ASSC) of C-CNF-NiCo$_2$S$_4$ nanosheets exhibited a specific capacitance of 428 F g^{-1} at A g^{-1}. The energy density of 85.23 Wh kg^{-1} at a power density of 1200 W kg^{-1} were obtained. The assembled ASSC showed good cyclic stability (62.4% retention capacity) after 5000 cycles.

Qiu et al. successfully synthesized NiS/CNFs via electrospinning and hydrothermal methods for supercapacitor application and investigated that DEA presence in the composite as named NiS/CNFs-1, NiS/CNFs-2, NiS/CNFs-3, and NiS/CNFs-4 are 1:0, 2:1, 1:1 and 1:2, respectively. The prepared samples investigated these specific capacitances at various scan rates in the range of 10–80 mV s^{-1} at several potential windows in 6 M KOH electrolyte [18]. Among four electrodes, NiS/CNFs-2 exhibited higher capacitance than others. After that, the assembled hybrid supercapacitor of NiS/CNF-2 as a cathode and activated carbon as an electrode as shown in Fig. 1a. Figure 1b shows the CV curves of NiS/CNFs-2 are displayed two redox peaks, which is faradaic redox behavior. No significant change in the CV curve even after 100 mV s^{-1}, which indicates reversible faradaic properties. From GCD curves as shown in Fig. 1c, d, the maximum specific capacitance of NiS/CNFs-2 is calculated to be 29.8 mA h g^{-1} at 1 A g^{-1} and capacity retention of 68% at 5 A g^{-1}. Figure 1e shows the energy density of 22.35 Wh kg^{-1} at a power density of 750 W kg^{-1}, while at a higher power density (7500 W kg^{-1}) at an energy density (of 12.69 Wh kg^{-1}). Figure 1f shows the cyclic stability of the hybrid capacitor, 91.14% retention capacity was obtained after 1000 cycles at 2 A g^{-1}.

Amiri et al. synthesized (25, 50, and 70%) NiMoO$_4$/ECNF composites through electrospinning and thermal methods. The fabricated binder-free (70% NiMoO$_4$/

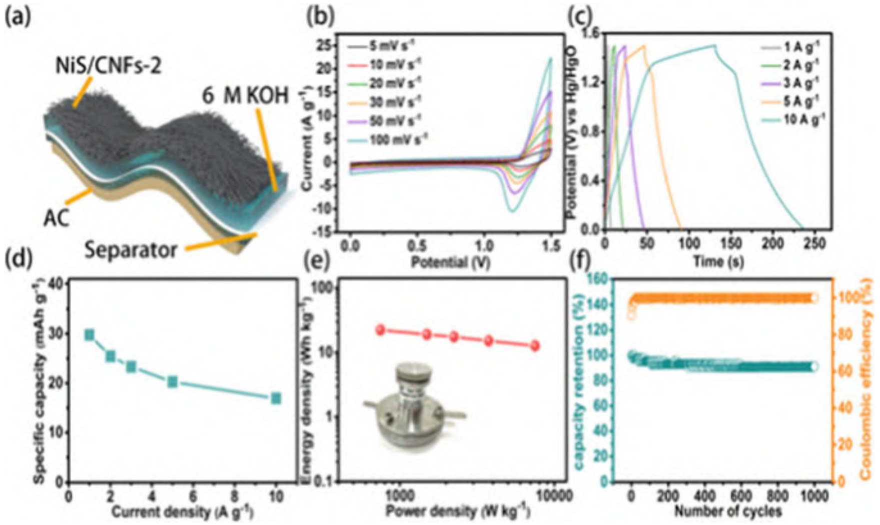

Fig. 1 **a** Schematic device, **b** CV curves, **c** GCD curves, **d** specific capacity versus current density, **e** Ragone plots, and **f** cyclic stability of hybrid capacitor. Reprinted with permission from [18]. Copyright (2022), American Chemical Society

ECNF) electrode as the symmetric supercapacitor (SSC) was performed in a 6 M KOH electrolyte [29]. The specific capacitance was calculated to be 122.5 F g^{-1} at 1 A g^{-1} with retained capacitance is about 78% at 1 A g^{-1} (current density). This device delivered a high energy density of 43.9 Wh kg^{-1} at 1567.9 W kg^{-1} (power density) and a higher power density of 32,582 W kg^{-1} at an energy density of 18 Wh kg^{-1}. Figure 8a shows the cyclic stability of the SSC device for 3000 cycles about 92% retention capacitance at 5 A g^{-1} and Fig. 8b displays EIS performance before and after 3000 cycles, the value of (R_s) about 0.92 Ω which indicates a good contact between the electrode and nickel foam, the charge transfer (R_{ct}) of 5.60 Ω was calculated from semi-circle at higher frequency region in EIS results. After 3000 cycles, the R_s and R_{ct} (1.47 and 7.03, respectively) do not significantly rise in contrast to the first cycle, indicating outstanding reversibility. The binder-free supercapacitor device has great potential to be used for scalable energy storage devices.

Yoo et al. designed RuO_2 nanorod on electrospun CNF by precipitation and recrystallization methods [30]. The electrode (PPMRu(220)) exhibits a maximum specific capacitance of 190 F g^{-1} at 1 mA cm^{-2} and an energy density of 22 Wh kg^{-1} at a power density of 400 W kg^{-1} and was retained after 10,000 cycles. In an asymmetric capacitor of PPMRu(220) as positive and PPM as negative, the voltage increases from 1.2 to 1.3 V, and energy density increases from 29 to 36 Wh kg^{-1}.

Li et al. developed an all-solid-state supercapacitor device of N-doped hollow CNFs (by electrospinning method)/$NiCo_2O_4$ by solvothermal method [31]. The fabricated device investigated the specific capacitance as 1864.1 F g^{-1} at a current density of 1 A g^{-1} that of CNFs/$NiCo_2O_4$, due to HCNFs having a large surface area to be

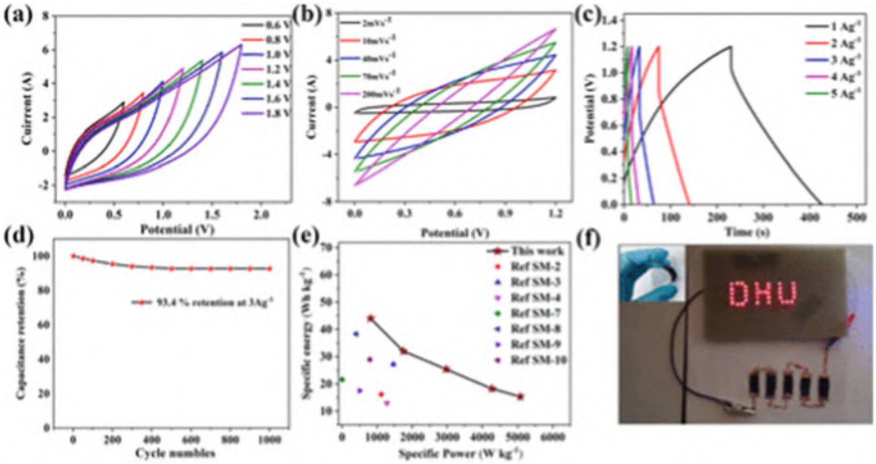

Fig. 2 **a** CV curves of ASSC at various voltages, **b** CV curves of ASSC at various scan rates, **c** GCD curves of ASSC at several scan rates, **d** cyclic stability of ASSC, **e** Ragone plots of ASSC with reported $NiCo_2O_4$ based devices, and **f** the LED light ‘DHU’ logo of five electrode series as ASSC. Reprinted with permission from [31]. Copyright (2022), American Chemical Society

electron between electrolyte and electrode interfaces. The cyclic stability of HNCFs/$NiCo_2O_4$ was about 91.7% retention than CNFs/$NiCo_2O_4$ (81.9%) after 5000 cycles at 8 A g^{-1}. The assembled ASSC of HNCFs/$NiCo_2O_4$ was performed in PVA-KOH as an electrolyte. In Fig. 2a, c, the CV and GCD curves of the ASSC device at different scan rates and potential windows. Figure 2d shows a good cyclic stability of ASSC was about 94.3% retention after 1000 cycles. As seen in Fig. 2e, the ASSC device was compared with reported other Ni-based devices, ASSC device exhibited a higher energy density of 44.3 Wh kg^{-1} at 814.8 W kg^{-1} than other devices. Furthermore, the ASSC device is connected as five series with LED light and has shown the ‘Donghua University’ (DHU) logo in Fig. 2f.

Huang et al. prepared different wt% of Fe_3O_4 on N-doped CNFs nanocomposites by electrospinning and high-temperature methods [32], which are listed as 2 Fe_3O_4-CNFs, 4 Fe_3O_4-CNFs, 6 Fe_3O_4-CNFs, and 8 Fe_3O_4-CNFs with mass loading of 20, 40, 60, and 80%, respectively. The electrochemical properties of all these samples were examined in 6 M KOH in the potential window between −0.5 and 0.4 V. Among these electrodes, 4 Fe_3O_4-CNFs proved high specific capacitance than others. During the electrochemical performance, Fe^{2+} is oxidized to Fe^{3+} at first, then Fe^{3+} is reduced to Fe^{2+} by entering the OH^- to the composite. The CV curves are recorded at different scan rates and the GCD curves are recorded at various current densities between 1 and 5 A g^{-1}. Specific capacitances were calculated to be 128.5, 277.78, 481.6, 398.65, and 162.52 F g^{-1} of 2 Fe_3O_4-CNFs, 4 Fe_3O_4-CNFs, 6 Fe_3O_4-CNFs, and 8 Fe_3O_4-CNFs, respectively. The principles for the charge–discharge reaction of 4 Fe_3O_4-CNFs are summarized in three paths. (i) Fe^{2+} is oxidized to Fe^{3+} by entering OH^- at while charging, (ii) Fe^{3+} is reduced to Fe^{2+} by releasing OH^- at while discharge and certain amount storage behavior of pseudocapacitors, (iii) K^+ and OH^- ions are transferred to surface electrodes (positive and negative) which are exhibits EDCL effect. Furthermore, assembled all-solid-state asymmetric supercapacitor (SASCs) of activated carbon and 4 Fe_3O_4-CNFs was evaluated in the three-electrode system using PVA-KOH electrolyte. The specific capacitance of the SASCs device delivered a maximum capacitance of 203 F g^{-1} at 1 A g^{-1}. The specific capacitance was maintained at 184.5 F g^{-1} at 2 A g^{-1} and retention capacitance of 86.2% after 5000 cycles.

Ahmad and co-workers successfully fabricated porous $MnMoS_4$ on CNF and N, S doped CNF by electrospinning and hydrothermal method [33]. The pure CNF and $MnMoS_4$-CNF were examined in a three-electrode system with 6 M KOH electrolyte, the specific capacitances of pure CNF and $MnMoS_4$-CNF are 168.2 F g^{-1} and 2187.5 F g^{-1} at a current density of 1 A g^{-1}, respectively. The capacitance was retained at around 87% even after 5000 cycles. Due to better wettability of hybrid electrode had low resistance (0.64 Ω) than pure CNF (1.57 Ω). The assembled ASC device of N, S-doped CNF as negative and $MnMoS_4$-CNF positive electrode was optimized 6 M KOH. The distorted rectangular CV curves are behaviors likely both EDCL and pseudo capacitor effect. The GCD curves are optimized at different current densities, the maximum capacitance was obtained at 188.6 F g^{-1} at 0.5 A g^{-1}. The capacitance values were decreases with increase in the current density. Furthermore, the ASC device was optimized in the different electrolytes, ASC device delivered an energy density of 72.5 Wh kg^{-1} at power density (2.7 kW kg^{-1}) in 1 M Na_2SO_4 as the optimized electrolyte. the cyclic stability of the ASC device was retained at 93.4% after 5000 cycles. This binder-free metal sulfide-CNF is an electrode to be used for the next generation of ASC devices.

Sonsupap et al. reported on CeO_2/CNF nanocomposites were prepared by electrospinning and thermal treatment methods for supercapacitor application [34], and that CeO_2 was prepared in different weight % ratios (10, 20, and 40) on CNF. The average size of the CeO_2 is about 10–70 nm and the diameter of CNF and CeO_2/CNF are in the range between 200 and 700 nm. The prepared electrodes were evaluated for specific capacitance in the presence of a 6 M KOH electrolyte solution. Among these electrodes, 20% CeO_2-CNF exhibits a high specific capacitance of 232.68 F g^{-1} at 0.5 A g^{-1} and shows a higher power density of 136.88 W kg^{-1} energy density of 37.97 Wh kg^{-1} with 97% retention capacity retained after 1000 cycles. This work suggests a promising electrode for supercapacitor application in the next generation.

Liu et al. prepared porous NiO/CNF by electrospinning and calcination methods [35]. The prepared electrode exhibited a high specific capacity of 461.26 C g^{-1} at 1 A g^{-1} in 2 M KOH electrolyte along with 82.7% capacity retention at 10 A g^{-1} and was excellent rate capability of 82.7% retained at 10 A g^{-1}. A hybrid supercapacitor of NiO/CNF (positive)/AC (negative) delivered an energy density of 31.82 Wh kg^{-1} at 816.36 W kg^{-1} (power density) with outstanding cyclic stability (90.9% retention) even after 5000 cycles at 5 A g^{-1}.

2.1.2 Functionalized Carbon Nanotubes (CNTs)

Generally, carbon nanotubes are classified into two types of Single-walled carbon nanotubes (SWCNT) and multiwalled carbon nanotubes (MWCNT). Carbon nanotube—a highly porous, tube-like structure, and highly electrical conductive material that can be functionalized with metal oxides/hydroxides, conducting polymers, and other carbon-based materials to enhance its electrochemical properties.

Agarwal et al. prepared the cost-effective and facile chemical method of the self-growth of the $Co_2P_2O_7$ nanodots on the multiwalled carbon nanotubes coated present in the stainless steel it forms as core–shell type [36]. Energy storing capacity of the heterostructure shows the high-level extrinsic electrochemical pseudocapacitance. Figure 3 shows the schematic structure of $Co_2P_2O_7$/MWCNT and the CV curves of MWCNT and $Co_2P_2O_7$/MWCNT which was recorded at the scan rate of 50 mV s^{-1}. The $Co_2P_2O_7$/MWCNT composite exhibits a significant advantage in pseudo capacitance compared to bare MWCNT. This dominance is attributed to the rich reversible redox chemistry of Co (Co^{2+} to Co^{3+}) in the presence of KOH. The symmetric supercapacitor was fabricated with positive and negative electrodes $Co_2P_2O_7$/MWCNT/ $Co_2P_2O_7$/MWCNT (solid-state) and electrolyte PVA-KOH. The composite shows a resistance of 0.54 Ω cm^{-2} which exhibits a good conductor. The device shows a specific capacitance of 114.5 mAh g^{-1} with an energy density of 57.3 Wh kg^{-1} and a power density of 1500 W kg^{-1}. It has good cyclic stability with a retention of 105% even after 5,000 cycles. As the fabricated device can illuminate up to 21 light-emitting diodes with practical evidence.

The efficient nanostructured supercapacitor devices were fabricated by Shakir and co-workers [37]. Flower-like $Cu(OH)_2$ nanoflakes and CNTs composite were synthesized by the co-precipitation method and followed by ultrasonication. The prepared material shows the electrochemical experiment which was carried out with varied scan rates 5–70 mV s^{-1}. It resulted in high redox chemistry due to the non-rectangular nature in $Cu(OH)_2$. It exhibits pseudocapacitance and CNTs show quasi rectangular. When comparing the specific capacitance, the values obtained for $Cu(OH)_2$ and

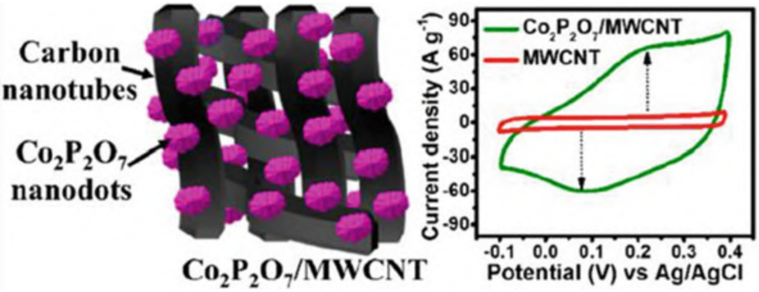

Fig. 3 Schematic structure of $Co_2P_2O_7$/MWCNT (left), CV curves of $Co_2P_2O_7$/MWCNT and MWCNT (right). Reprinted with permission from [36]. Copyright (2022), American Chemical Society

the composite material were 415 F g^{-1} and 733 F g^{-1}, respectively, at the current density of 1 A g^{-1}. High capacity up to 4×10^3 cycles. This shows the effect between the CNTs and $Cu(OH)_2$ which paved the way for the next-generation supercapacitor devices. The booming field of the supercapacitor gives the way to add a binder with composite to enhance the specific capacitance such as MnO_2/CNT as an active material with polyvinyl difluoride incorporated with silver as a binder fabricated successfully [38].

Fahimi et al. developed an asymmetric solid-state supercapacitor device with gel polymer electrolyte [39]. The binary metal oxide such as $Co_3C_2O_8$ nanosphere prepared by the hydrothermal method and loaded CNT by ultrasonication method. PVA-H_2SO_4 act as a polymer gel electrolyte. The positive and negative electrodes are $Co_3C_2O_8$/CNT//Activated Carbon (AC) as an asymmetric device. Figure 4a shows CV curves of the $Co_3V_2O_8$/CNT//AC devices assembled with various electrolytes such as aqueous (KOH), organic ($LiPF_6$-EC/DEC), and gel polymer (PVA/H_2SO_4) electrolytes. Figure 4b, c displays the electron transfer mechanism in organic ($LiPF_6$-EC/DEC) electrolytes and the hopping mechanism in gel polymer (PVA/H_2SO_4) electrolytes, and the potential window of 1.5 V. The device shows a high capacitance of 120.17 F g^{-1} with energy and power densities of 37.55 Wh kg^{-1} and 0.66 W kg^{-1}. The cyclic stability after 3000 cycles resulted in a retention rate of 95.26%.

Cha et al. synthesized bimetallic Ag-Bi nanoparticles on the CNT for high-power supercapacitors by vacuum filtering and combustion [40]. The composite was coated on the nitrocellulose membrane to construct the electrode material. The homogeneously mixed bimetal was used to perform with the different scan rates 2 and 5 mV s^{-1} with a high specific capacitance of 1372 and 1093 F g^{-1}, respectively.

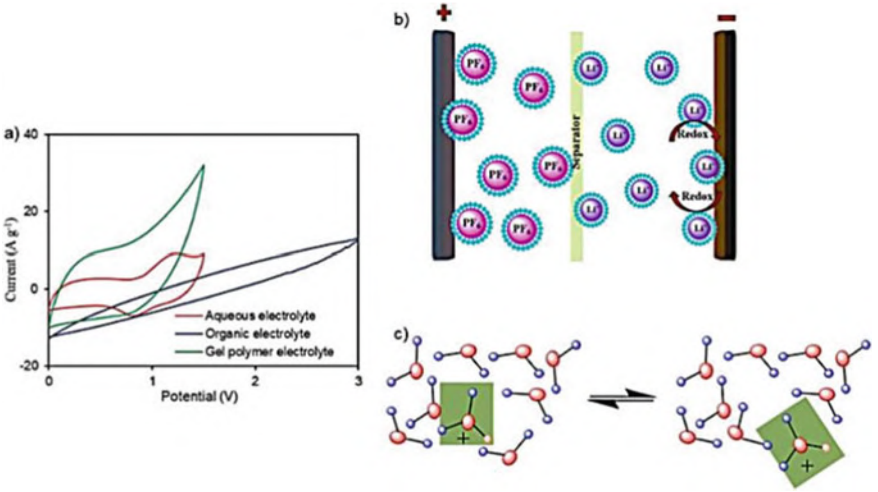

Fig. 4 **a** CV curve of $Co_3C_2O_8$/CNT//activated carbon (AC) with different electrolytes, **b** and **c** electron transfer and mechanism of gel polymer. Reprinted with permission from [39]. Copyright (2022), Elsevier

Thus, the specific capacitance value denoted that an increase in scan rate decreases the specific capacitance of the material. Initial capacitance shows 10,000 cycles of retention at 101.3% at 100 mV s^{-1}. The functionalized carbon nanotubes by oxygen show high every supercapacitor fabricated by Kariper and co-workers [41]. The different radiation source was used to fine-tune including Am-24, Sr-90, Co-60, and Na-22 for the functionalized using oxygen. The CNT (irradiated by Am-241) shows worthier super capacitance than other sources offering 489.6 F g^{-1} at the current density of 0.1 A g^{-1}. The excellent energy density of 56.90 Wh kg^{-1} accounted high-power density value of 9992.19 W kg^{-1}. The capacitance retention of the fabricated symmetric device was considered as 98.50% even after 5000 cycles.

Feng et al. synthesized the efficient supercapacitor asymmetric device by the electrode deposition method [42]. $NiCo_2S_4$ nanosheets/CNT composite morphological evidence shows effective electrochemical performance. Figure 5 accounted discharging nature of the supercapacitor device using a light-emitting diode. The composite shows the superior advantages are current density at 1 A g^{-1} with a high specific capacitance of 2498.12 F g^{-1}. The asymmetric device shows a specific capacitance of 215.06 F g^{-1} at 0.25 A g^{-1} retention rate of 89.03% after 10,000 cycles with an excellent energy density of 76.47 Wh kg^{-1} at 201.01 W kg^{-1} with good flexibility. The electrodeposited porous $NiCo_2S_4$ nanosheets/CNT composite has broad potential application in the supercapacitor area.

The binder-free $CoMn_2O_4$/CNT composite electrode was synthesized through the electrodeposition method done by Tai and co-workers [43]. This uniformly coated CMO nanosheet on the CNT confirmed by morphological evidence shows excellent pseudocapacitance with a high oxidation potential of the Cobalt and the fast electron transfer ability of the Manganese. The CMO60/CNT450 exhibited excellent electrochemical properties with a high specific capacitance of 732 F g^{-1}. An asymmetric supercapacitor device fabricated CMO/CNT electrode as a cathode and activated carbon as an anode. The device consists of CMO60/CNT450//AC with a specific capacitance of 133.28 F g^{-1} at a current density of 0.5 A g^{-1} and a power density of

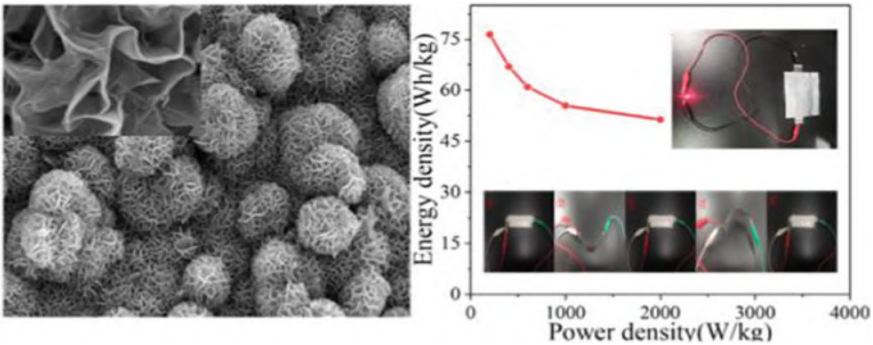

Fig. 5 Discharging supercapacitor. Reprinted with permission from [42]. Copyright (2022), American Chemical Society

400 Wh kg^{-1} with an energy density of 47.39 W kg^{-1}. The fast charge and discharge cycle test at a scan rate of 100 mV s^{-1} even after 5000 cycles. This device shows a high excellent in the electrochemical cost-effective asymmetric system with 76.8% retention.

Ramesh et al. synthesized a composite of excellent morphology and surface area paved the way for enhanced electrochemical activity [44]. Hydrothermal method was used for the synthesis of V_2O_5 loaded on the MWCNT bonded with carboxy methyl cellulose has a high surface due to the presence of ultrathin sheets morphology shows high specific capacitance 138 F g^{-1} at a current density of 0.5 A g^{-1} has the cyclic stability till 5000 cycles with 98.6% retention in presence of sulfuric acid as electrolyte.

2.1.3 Functionalized Graphene

Graphene is a two-dimensional (2D) monolayer of carbon atoms with packed honeycomb lattices that displays abundant fascinating properties, such as large surface area, good thermal and chemical stability, high conductivity, and mechanical flexibility. Meanwhile, the unique features of graphene and its derivatives, such as graphene oxide (GO) and reduced graphene oxide (RGO). Graphene and graphene-based functionalized materials have been used in various applications such as organic chemistry [45], photocatalyst [46], etc. Recently, a great deal of effort has been devoted to fabricating graphene-based electrode materials and designing flexible SCs.

Paul et al. synthesized a novel Lanthanum (La) doped Nickel-tin oxide on rGO (LNSRG) using a one-step hydrothermal technique [47]. The addition of Lanthanum plays a vital role in the amplification of the electrochemical behavior of the metal oxides. As-synthesized LNSRG 2 (2 mM of La) shows an excellent specific capacitance of 1238 F g^{-1} at 3 A g^{-1}. The research group designed an asymmetric supercapacitor device (ASC) using LNSRG 2 and RGO as cathode and anode, respectively with a wide potential window of 1.6 V. The ASC device shows an energy density of 38 Wh kg^{-1} and a power density of 870 W kg^{-1}. The capacitance retention of 75% after 10,000 GCD cycles was observed and a 1.8 V red LED light was powered by this device (Fig. 6). Similarly, a nickel-tin oxide was loaded on N-doped reduced graphene oxide (NSR) by hydrothermal method from the same research team [48]. The specific capacitance of 1650 F g^{-1} at 3 A g^{-1} was observed which was slightly higher than the previously reported LNSRG 2 nanocomposite. This nanocomposite was fabricated into an asymmetric supercapacitor (ASC) device with RGO as a negative electrode. The energy density obtained was 38.41 Wh kg^{-1}, with a corresponding power density of 2.026 kW kg^{-1}. The capacitance retention of 89% was observed after 10,000 cycles. Additionally, the device demonstrated the capability of lighting a 1.8 V red LED for a 1 min duration.

A micro-flowered structured $NiCo_2O_4$/exfoliated graphene oxide (NCO/EGO) was synthesized by Pappu et al. using a facile hydrothermal method [49]. The NCO/EGO electrode material exhibits a specific capacitance of 530 F g^{-1} at 1 A g^{-1}. The NCO/EGO shows a retention rate of 82% after 10,000 cycles. The as-prepared

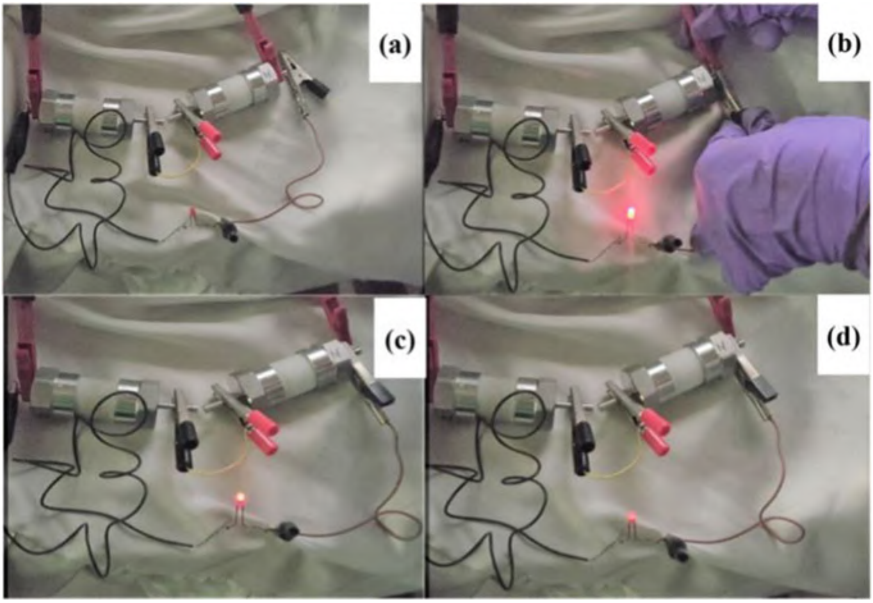

Fig. 6 Digital images of **a** ASC device setup, **b** initial lighting, **c** light at 30 s, **d** discharged LED. Reprinted with permission from [47]. Copyright (2022), Elsevier

NCO/EGO as positive and commercial YP-50F carbon as an anode electrode was made into an asymmetric supercapacitor (ASC) device. The ASC device was studied using CV and GCD measurements. The results show an excellent energy density of 37.8 Wh kg^{-1} and a power density of 1350 W kg^{-1} with cyclic stability of 98% after 10,000 cycles shown in Fig. 7. This device was capable of lighting a LED for a duration of 5 min.

Fig. 7 Cyclic stability of ASC device. Reprinted with permission from [49]. Copyright (2022), Elsevier

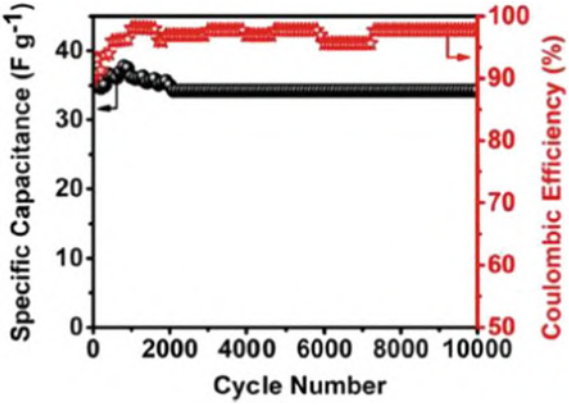

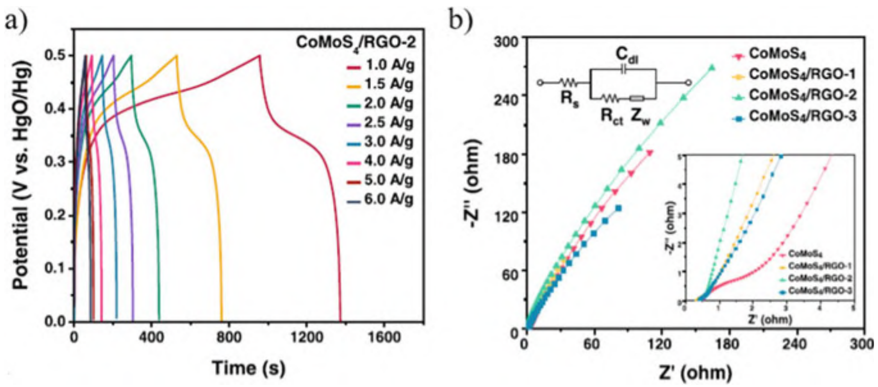

Fig. 8 **a** GCD plot of $CoMoS_4$/RGO-2, **b** Nyquist plot of as-synthesized nanocomposites. Reprinted with permission from [53]. Copyright (2022), Elsevier

The hollow spheres of cobalt selenide provide an improved energy storage value than solid cobalt selenide. Wrapping of rGO around the hollow $CoSe_2$ will potentially increase the charge storage performance. Li et al. prepared this hollow $CoSe_2$/rGO nanocomposite in a two-step process [50]. The synthesis of hollow $CoSe_2$ by solvothermal method followed by heat treatment of GO. A high capacity of 757 C g^{-1} at 3 A g^{-1} with a retention rate of 92% after five thousand cycles were recorded. For practical application, a hybrid supercapacitor device was constructed with $CoSe_2$/rGO and N-doped carbon nanotube as the positive and negative electrodes, respectively. The device shows an energy density of 50.1 Wh kg^{-1} at a power density of 800 W kg^{-1} with capacitance retention of 94% after five thousand cycles.

Ramesh et al. [51] synthesized bimetallic nanoparticles on N-doped graphene oxide ($CuCo_2O_4$@NGO) using a thermal reduction process. The electrochemical behavior of the as-prepared $CuCo_2O_4$@NGO composite exhibits a super capacitance of 475 F g^{-1} at 0.5 A g^{-1}. Even after 10,000 GCD cycles, the capacitance retention of 96.5% was observed from the $CuCo_2O_4$@NGO nanocomposite. The addition of N-doped graphene oxide notably increases the performance of the electrode with the sheet-like $CuCo_2O_4$ nanoparticles. A low resistance (R_s) of 0.054 Ω and a charge transfer resistance (R_{ct}) of 3.65 Ω were obtained by EIS measurements. These low values indicate good charge/ion transfer capability. The symmetric supercapacitor device was designed by CuO@NGO and $CuCo_2O_4$@NGO nanocomposites. The results provide a remarkable change in the electrochemical performance compared to pure CuO and $CuCo_2O_4$ nanoparticles [52].

Hydrothermally synthesized $CoMoS_4$/RGO nanocomposite by Zhang et al., studied the electrochemical performance using CV, GCD, and EIS analysis [53]. It has been found that the $CoMoS_4$/RGO nanocomposite shows a capacitance of 123 mAh g^{-1} at 1 A g^{-1}. The high capacitance is due to the uniform distribution of $CoMoS_4$ on RGO nanosheets. The EIS measurements show the resistance (R_s) of 0.5818 Ω and the charge transfer resistance (R_{ct}) of 0.003391 Ω, shown in Fig. 8. An asymmetric supercapacitor (ASC) device is fabricated by $CoMoS_4$/RGO as positive and activated carbon as negative electrodes. The device exhibits an energy and power density of 59 Wh kg^{-1} and 1125 W kg^{-1}. After 6000 GCD cycles, the device shows a retention rate of 99.3%.

The symmetric supercapacitor device was fabricated using rGO/RuO_2 nanoparticles and rGO/RuO_2 aerogel by Shankar et al. [54] and Korkmaz et al. [55], respectively. The electrochemical performance was studied using CV, GCD, and EIS analysis. The fabricated devices give an energy density of 41 Wh kg^{-1} at 1.2 kW kg^{-1} for rGO/RuO_2 nanoparticles and 31.1 Wh kg^{-1} at 8.365 kW kg^{-1} for rGO/RuO_2 aerogel. This symmetric supercapacitor shows a high cyclic stability of 96% (nanoparticles) and 82.8% (aerogel) after 2000 and 5000 cycles, respectively. From the GCD measurements, the capacitance of rGO/RuO_2 nanoparticles was 720 F g^{-1} at 1 A g^{-1} and aerogel of 321.5 F g^{-1} at 0.5 A g^{-1}.

Thalji et al. synthesized a novel tungsten oxide nanowires-reduced graphene oxide ($W_{18}O_{49}$ NWs–rGO) using the solvothermal method [56]. An asymmetric supercapacitor (ASC) device was constructed using an $AlCl_3$ aqueous electrolyte. The Al^{3+} ion will facilitate the intercalation of ions and rGO's conductive nature results in excellent electrochemical performance. The rGO is positive and the $W_{18}O_{49}$ NWs–rGO is a negative electrode in the ASC device. The energy and power density of 28.5 Wh kg^{-1} and 751 W kg^{-1}, respectively, with a capacitance retention of 96.7 after 12,000 cycles was observed.

A novel asymmetric supercapacitor device was fabricated by Morenghi et al. using Ni nanoparticle-anchored graphene as a positive electrode and pure graphene as a negative electrode with a potential window of 1.5 V [57]. This ASC device shows a specific energy and power of 37 Wh kg^{-1} and 5 kW kg^{-1}, respectively with a retention rate of 72% over 10,000 cycles. The excellent specific capacitance of 1900 F g^{-1} was obtained and can be used in various energy storage systems.

2.1.4 Functionalized Other Carbonous Materials

Significant interests have been attracted to these novel nanostructured carbon materials since then due to their high surface area, tunable pore size, diversified pore shape, and controllable pore dispersibility. It has been demonstrated that porous carbons with high super-capacitive performance can be obtained from various biomass resources, such as corn, bamboo, starch, soybean, and bacterial cellulose. These functionalized materials are suitable for supercapacitor applications.

Cai et al. engineered oxygen vacancies into $NiCo_2O_4$ on carbon cloth (VO-$NiCo_2O_4$@CC) via a mild solvothermal method [58]. The prepared electrode exhibited a maximum specific capacitance of 1389 mF cm^{-2} at a current density of 0.5 mA cm^{-2} with 93.8% retention maintained even after 10,000 cycles when used as a cathode for SCs. The assembled aqueous asymmetric supercapacitor of VO-$NiCo_2O_4$@CC (as a cathode) and AC (as an anode) was delivered 43.6 Wh kg^{-1} (energy density) at 281 W kg^{-1} (power density). Therefore, the cost-effective electrode is to be used as a flexible supercapacitor for wearable devices.

Javed and his group developed vanadium disulfide (VS_2) on carbo-cloth (CC) by hydrothermal method [59]. The specific capacitance of VS_2/CC is about 972.5 mF cm^{-2} at 1 mA cm^{-2}, with 77.5% retention after 10,000 cycles at 10 mA cm^{-2}. Furthermore, the assembled asymmetric supercapacitor of VS_2/CC-12 and AC/CC delivered a high energy density of 0.22 mWh cm^{-2} at 4.24 mW cm^{-2}, and the energy density was maintained to be 0.16 mWh cm^{-2} even the power density at 8.26 mW cm^{-2}.

Dong et al. fabricated a MnO_2 layer-modified activated carbon cloth (ACC-MnO_2) by controlling deposition time [60]. The flexible quasi-solid-state asymmetric SCs (FQSASCs) device was assembled by ACC-MnO_2 and ACC as positive and negative electrodes, respectively. The device shows an excellent retention capacity of over 100% even after 5000 cycles at 10 mA cm^{-2} in the potential window up to 2.0 V in as PVA-LiCl electrolyte. The energy and power density of the device was found to be 0.78 mWh cm^{-3} and 71.86 mW cm^{-3}, respectively, with excellent retention capacity. Similarly, the same electrode was prepared as a film by Fan et al. for a supercapacitor in PVA-H_2SO_4 electrolyte [61]. The specific capacitance of the fabricated electrode film is 886.7 mF cm^{-2} at 1 mA cm^{-2} with good cyclic stability of 87.69% after 10,000 cycles.

Zhang et al. demonstrated a novel approach to the synthesis of NiCoS on activated carbon cloth (ACC), the NiCoS was converted from NiCoAl LDH [62]. The specific capacitances of layered hydroxide and NiCoS exhibited 195.8 and 413.3 F g^{-1}, respectively. The assembled asymmetric device by NiCoS/ACC and ACC electrodes and was determined the specific capacitance of 193.5 F g^{-1} at 1 A g^{-1} with 88.5% of retention after 2000 cycles at 20 A g^{-1}. The device delivered a high energy density of 107.7 Wh kg^{-1} at a higher power density of 1000 W kg^{-1}. The two ASC devices related to a red LED and performed for at least 8 min as shown in Fig. 9.

Fu et al. prepared carbon cloth (CC) supported Ni-based hybrid electrodes for supercapacitors such as $Ni(OH)_2$/CC, NiS_2/CC, NiO/CC, and Ni_2P/CC [63]. NiS_2/CC was showing a maximum capacitance of 1166.3 F g^{-1} at 0.4 A g^{-1}. After that, they made flexible asymmetric supercapacitors (FASCs) by NiS_2/CC and AC/CC with excellent cyclic stability of 96% after 8000 cycles. The device delivered energy and power density of 34.1 Wh kg^{-1} and 34.1 Wh kg^{-1}, respectively.

Gong et al. investigated the specific capacitance and energy density of prepared NiCoS nanosphere and carbon sphere in an ASC device [64]. A high specific capacity (819.9 C g^{-1}) of NCS-B3 was recorded and retained at 91.8% retention after 8000

0min
2min
4min
6min
8min

Fig. 9 LED light examined for 0–8 min. Reprinted with permission from [62]. Copyright (2022), Elsevier

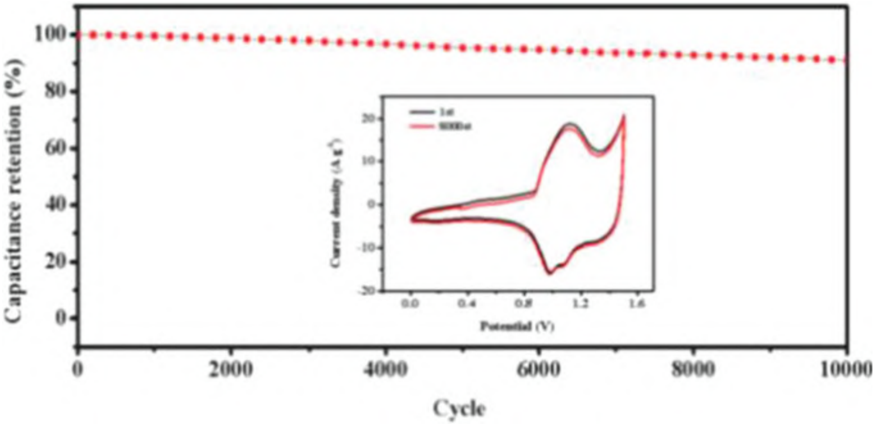

Fig. 10 Cycling performance of ASC, (inset) before and after a cycle. Reprinted with permission from [65]. Copyright (2022), Elsevier

cycles and the CS as anode's capacitance was about 196.5 F g^{-1}. The assembled device of NCS-B3/CS has excellent electrochemical performance, the energy and power density of the device are 65 Wh kg^{-1} and 850 W kg^{-1} with 82.8% retention after 10,000 cycles at 10 A g^{-1}.

Huang et al. designed hollow NiO/N-doped carbon as a cathode and N-doped carbon as an anode for boosting energy density in supercapacitor applications [65]. The prepared NiO/NC-700 was performed in a three-electrode system and exhibited the specific capacitance of 1026 F g^{-1} at A g^{-1} with 80.2% retention capacity after 8000 cycles as shown in Fig. 10. The assembled device of NiO/NC-700 and NC delivered a high energy density of 40.2 Wh kg^{-1} at a power density of 750.4 W kg^{-1}.

Liu et al. developed metal-free nitrogen and phosphorous-doped carbo microsphere (MLCM) by pre-oxidation and carbonization methods [66]. The prepared functionalized carbon sphere was examined for electrochemical performance in 1 M H_2SO_4 electrolyte and the capacitance reached 338.2 F g^{-1} at 0.8 A g^{-1} (current density). Furthermore, the functionalized carbon microsphere was assembled as a symmetrical capacitor and exhibited 194 F g^{-1} at 1 A g^{-1} with 97.3% retention maintained after 5000 cycles. In addition, an energy density of 7.81 Wh kg^{-1} was achieved at a power density of 62.5 W kg^{-1}.

Mohanty et al. synthesized activated fullerene decorated over zinc cobaltite (A-C_{60}-ZCO) and evaluated electrochemical performance in a three-electrode system [67]. As-synthesized nanocomposite displayed a specific capacitance of 593.3 F g^{-1} at 1 mV s^{-1} and 83.7% retention observed 5000 cycles at 8 A g^{-1} which indicates pseudo capacitive nature. The assembled flexible asymmetric supercapacitor of A-C_{60}-ZCO as positive and AC as the negative electrode was provided an energy density of 36.43 Wh kg^{-1} at 1681.47 W kg^{-1} (power density) with cyclic stability of 91.06%

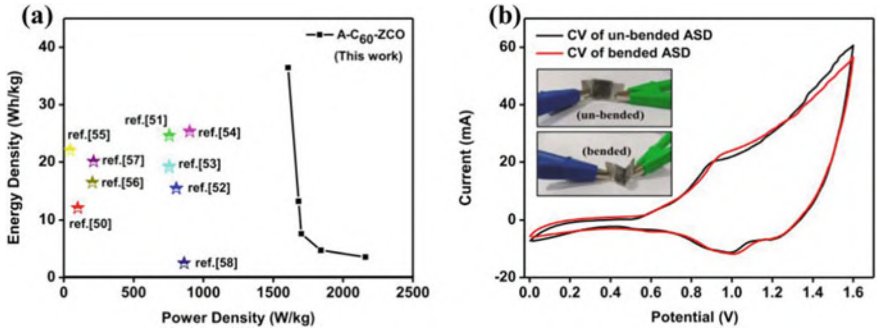

Fig. 11 **a** Ragone plot of energy density compared with previously reported, **b** CV curves at 50 mV s^{-1}. Reprinted with permission from [67]. Copyright (2022), Elsevier

after 5000 charge–discharge cycles at 6 A g^{-1}. This is compared with previously reported and the bent ASC device was examined in CV as seen in Fig. 11.

2.2 Functionalization of Non-carbonous Materials

The functionalized non-carbonous materials have been investigated in different applications [68] and are known as energy storage devices. The synthesis of self-growing Ni-Co LDH (Layered double hydroxide) decorated on the g-C_3N_4 nanosheets via microwave method by He and co-workers [69]. The electrochemical properties of the as-prepared electrode material were examined by CV, GCD, and EIS in three-electrode systems. The specific capacitance of the CN-LDH electrode of 1936.36 F g^{-1} at 1 A g^{-1} and it maintained cyclic stability of 87.79% for 6000 cycles. This electrode was performed with excellent energy and power density of 50.63 Wh kg^{-1} and 8.00 kW kg^{-1}, respectively. Due to the strong synergetic effect between g-C_3N_4 and CN-LDH.

Meftahi et al. prepared the silver iodide/graphitic carbon nitride (AgI/g-C_3N_4) nanocomposite by a simple method of sonochemical and co-precipitation [70]. Three different types of electrolytes were used for the study of CV, GCD, and EIS experiments with three-electrode setups. The specific capacitances of three electrolytes of H_2SO_4, KOH, and Na_2SO_4 are 219, 272, and 210 F g^{-1} at a current density of 1.5 A g^{-1}. The overall stability of the electrode with different electrolytes H_2SO_4 (85%), KOH (84%), and Na_2SO_4 (87%) after 2000 cycles at a minimum scan rate of 30 mV s^{-1}. A hybrid electrode can act as an excellent supercapacitor device.

The concept of the new heterojunction of p-n was introduced in electrochemical energy storage by Wang et al., and the 3D urchin-like $CoNi_xS_y$/g-C_3N_4 microspheres were prepared by the solvothermal method [71]. The high-efficiency charge transfer takes place between the p-type semiconductor ($CoNi_xS_y$) and the n-type semiconductor (g-C_3N_4). The GCD was performed in the three-electrode system optimizing

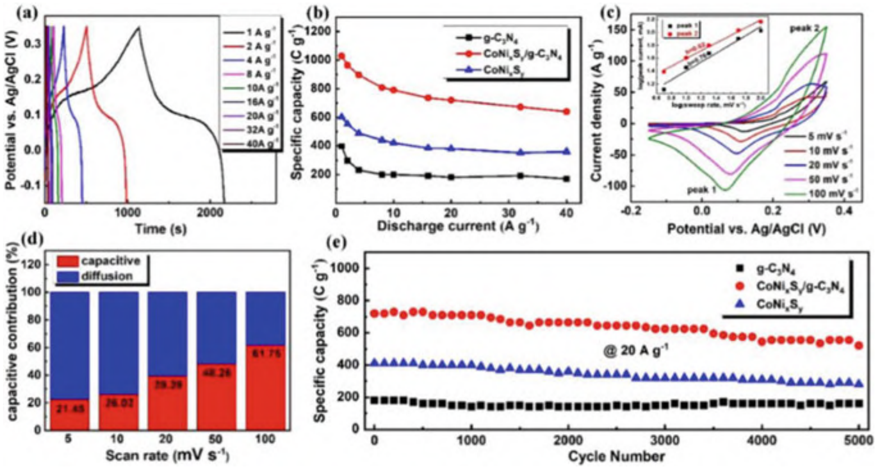

Fig. 12 **a** GCD curves, **b** specific capacitance at various current densities, **c** CV curves of $CoNi_xS_y$/g-C_3N_4, inside are the *b*-values for the $CoNi_xS_y$/g-C_3N_4, **d** capacitive contribution percentages of $CoNi_xS_y$/g-C_3N_4 at different scan rates, and **e** cycling stability tests at 20 A g^{-1}. Reprinted with permission from [71]. Copyright (2022), Elseiver

the mass ratio of the g-C_3N_4 and $CoNi_xS_y$ at different current densities in Fig. 12a. Figure 12b shows the specific capacitance decreases with increase in the current density. Figure 12c shows that the CV curves are recorded at different scan rates. Figure 12e denotes that the cycle number is up to 5000 with a maximum specific capacity of 1029 C g^{-1}. The assembled asymmetric device of the positive electrode ($CoNi_xS_y$/g-C_3N_4) and a negative electrode (AC) was performed at different current densities and delivered a high energy density of 71.9 Wh kg^{-1} with a retention capacity of 72.2%.

Wan and co-workers synthesized flower-like g-C_3N_4 nanosheets decorated on the zeolite imidazole frame derived from Co_2NiO_4 cubes with excellent superconducting materials by the simple solvothermal method [72]. The different mass ratios of the cube-like Co_2NiO_4 and the nanosheets of g-C_3N_4 were optimized using electrochemical experiments such as CV, and GCD.

The various kinetics of Ni/Co-5%CN electrode were given the highest charge storage with CV curves at 5–100 mV s^{-1} (scan rates). Figure 13a denotes the *b*-value between the cathodic and anodic peak which is close to 0.65 and affected by the diffusion-controlled redox process. The *b*-value of Co_2NiO_4 is 0.68. Figure 6b shows the capacity contribution ratio of Ni/Co-5%CN and Co_2NiO_4 is 33.1% and 23.1% at a scan rate of 5 mV s^{-1}, respectively. Ni/Co-5%CN electrode exhibited a specific capacitance of 1701 F g^{-1} at 1 A g^{-1} and delivered a high energy density of 49.37 Wh kg^{-1} with a retention rate was 91.5% after 5000 cycles at 5 A g^{-1}. This device indicates a safe and efficient energy-storing device.

Subhash et al. fabricated the new supercapacitor device of NiS/g-C_3N_4 nanocomposite was prepared using the one-pot synthesis of the hydrothermal method [73],

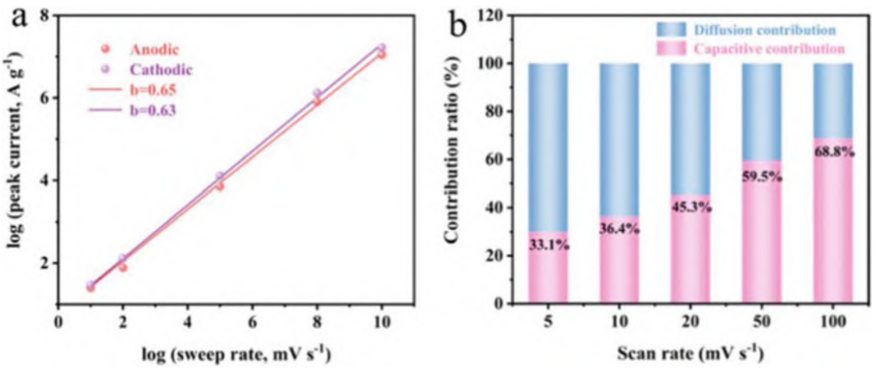

Fig. 13 **a** The log(i) versus log(v) plot of the cathodic peak and anodic peak, **b** capacitive contribution of Ni/Co-5% CN at different scan rates. Reprinted with permission from [72]. Copyright (2022), Elseiver

due to the transition metal sulfide-based nanocomposites showing excellent electrochemical properties according to the faradaic concept. The prepared NiS/g-C_3N_4 exhibited the highest specific capacitance of 2661.25 C g^{-1} at 1 A g^{-1} than that of pure NiS (733.50 C g^{-1}). Therefore, the capacitance of constructed hybrid electrochemical device was displayed at 181.8 C g^{-1} at 1 A g^{-1} with an energy density of 53.09 Wh kg^{-1} at a power density of 31537.5 W kg^{-1}, the cyclic retention of 95% after the 10,000 cycles were obtained. Thus, this composite is showing a very excellent supercapacitor with chemical stability and cyclic retention and is to be used for the next-generation device.

Ghosh et al. decorated nickel–cobalt oxalate on the nanoporous graphitic carbon nitrate sheet prepared by the co-precipitation method [74]. The specific capacitance of $NiCo_2C_2O_4$ is 1009 F g^{-1} at 1 A g^{-1}. The hybrid device of $NiCo_2C_2O_4$/g-C_3N_4 as positive and activated charcoal (AC) as the negative electrode displayed a specific capacitance of 1263 F g^{-1} at the current density of 1 A g^{-1}. The nanoporous graphitic carbon nitride was used to increase the specific capacitance. The device shows a very excellent specific energy value of 18.4 Wh kg^{-1} at the specific power value of 732 W kg^{-1} with a retention of 70% even after 3000 cycles.

Zhu et al. prepared copper oxide by hydrothermal method from the MOF material such as CuBTC and doped it with graphitic carbon nitride [75]. The CuO/g-C_3N_4 showed a specific capacitance of 1530.4 F g^{-1} at 2 A g^{-1} as anode material. The assembled asymmetric hybrid device of NiCoMOF as a cathode and CuO/g-C_3N_4 as an anode achieved an excellent energy density of 50.8 Wh kg^{-1} at a power density of 800 W kg^{-1} with a retention rate of 70% after 3000 cycles. Facile synthesis from the MOF-derived CuO/g-C_3N_4 has a synergistic effect and gives high capacitance due to the unique hollow structure and C-coated material shows high-power density to the device.

Zhang et al. [76] made the hybrid interconnected electrode for the supercapacitor application pC-carbon nitride prepared by the solvothermal method and in addition to the method COF material caCTF, 1 doped into it act as the negative electrode and the $NiCoTe_2$ as the positive electrode derived from the Ni, Co-MOF material by the hydrothermal method. These electrodes are highly nitrogen-rich materials interconnected with each other and quickly accelerate the charge between one another is an advancement in formulating the device with the high specific capacitance of 535.8 F g^{-1} at 1 A g^{-1}. The hybrid setup of $NiCoTe_2$ gives a high specific capacitance of 2006.0 F g^{-1} at 1 A g^{-1} and good stability. The retention rate of 87.88% after 25,000 cycles and the power density of 790.05 W kg^{-1} at an energy density of 50.84 Wh kg^{-1} were obtained.

Teng and his team reported Ag loaded on cubic g-C_3N_4 for supercapacitor application [77]. The specific capacitance of Ag/c-CN and c-CN is 10.44 mF cm^{-2} and 3.79 mF cm^{-2}, respectively. The high capacitance is due to the morphology of the cube carbon nitride. The crystal lattice has two kinds of the facets such as (002) and (100) planes but the performance of the (002) facet is stable for 2500 cycles. The electrochemical setup of an asymmetrical system that holds the two-electrode one is Ag/c-CN and another is activated carbon, which shows a high-power density of up to 17 mW cm^{-2} with retention of 86.1% after 2500 charge–discharge cycles. Flexible devices can also be used for the other resources of power supply.

The crystalline nature of boron nitride shows its identity through the different shapes such as hexagonal [78], cubic [79], and wurtzite [80] forms that are analogous to graphite [81], diamond [82], and lonsdaleite [83]. It possesses good thermal stability and chemical stability [84]. Metal oxides are limited to the supercapacitor due to poor electrical conductivity and low proton diffusion will occur. To eradicate such problems support materials play a vital role in electrode construction. Nanocomposites are made with highly stable support by Lin and co-workers [85].

Maity et al. prepared SnS_2/mK-BN/CNT composite by the solvothermal method [86]. The composite shows a high specific capacitance of 433 F g^{-1} in the aqueous medium. The fabricated device shows a maximum capacitance of 87 F g^{-1} and an energy density of 49 Wh kg^{-1} with a retention capacity of 101% stability.

Yesilbag et al. [87] prepared the high specific capacitance WS_2 coated on the vertically aligned BCN nanotubes. The specific capacitance of the electrodes such as VA-BCN-NTs and VA-BCN-NT@WS_2 are 364 and 690 F g^{-1} at the current density of 0.5 A g^{-1}. VA-BCN-NTs have an initial capacitance of 97% after 10,000 cycles at 20A g^{-1}. VA-BCN-NT@WS_2 shows 74% after 5000 cycles at 20 A g^{-1}. The fabricated symmetrical device shows 170 F g^{-1} at a current density of 1 A g^{-1}. The retention stability of 85% was maintained even after 10,000 cycles.

Chen et al. prepared an interesting non-carbonous material such as nitrogen-doped carbon aerogel from the cellulose nanofiber by hydrothermal method [88]. Manganese oxide used as a metal oxide electrode shows poor capacitance to conquer that different kinds of support from the carbon material were used. The mass of the CTOCN: urea is 1:40 showing the acceptable specific capacitance 275.5 F g^{-1} at 1 A g^{-1} current density. The maximum energy density recorded was 23.3 Wh kg^{-1} at a power density of 600 W kg^{-1} and an applied current density of 0.5 A g^{-1}. They retain the initial capacitance of 99.2% even after 3000 cycles, implying the MnO_2/N-doped CTOCN aerogels to accountable supercapacitor electrode.

2.3 Functionalized Polymers for Supercapacitor

Polymers are flexible with a unique identifier such that many monomers polymerize to form. It consists of repeating unit and is divided into natural and synthetic polymers, whereas the conducting polymers [89] are used for energy-storing applications and supercapacitors [90].

Bathula et al., nowadays organic molecules play a role in the energy storage application giving a way to invent the flexible device in polymeric supercapacitors [91]. The carbon nanotubes are taken in 1 mg/mL toluene solution with PDP added to it. Probe sonication was used at 50% amplitude for an hour. This polymeric network was formed and centrifuged at 11,000 rpm for 30 min to remove the unreacted tube left to form the solution. Dried and characterized to fabricate an electrode for further analysis. The morphology paves good conditions in CNT on PPDT. The specific capacitance shows 319.2 and 105.7 F g^{-1} for PPDT/CNT and PPDT at the current density of 0.5 A g^{-1}.

Wu et al. [92] contributed to increasing the specific capacitance of the material by using carbon spheres/CN/PPy. Here the carbon nitride possesses the nitrogen atom but shows low specific capacitance and low surface area. To exclude those demerits the core–shell carbon spheres were added as a composite with polymer. The diameter of the sphere was 300 nm morphology was mentioned in the SEM images. BET surface area analysis shows CS/CN/PPy (47.9 m^2 g^{-1}) and CS/CN (40.6 m^2 g^{-1}) are higher than that of Bare CN (12.1 m^2 g^{-1}). The pore-size distribution shows that a sharp peak at 2 nm confirms microporous material. It has a specific capacitance of 353.4 F g^{-1} at the current density of 1 A g^{-1}. The results were comparatively higher than that of bare electrodes.

One-step synthesis of the polymer with nitrogen-rich porous carbon was done by Zhang and co-workers [93]. Co-pyrolysis of urea and poly(acrylic acid-co-maleic acid) sodium salt (PAMS) directly fabricated at 550 °C. This polymer and porous carbon show electrochemical evidence for the device fabrication and have a high specific capacitance of the mesoporous material N-PC of 210 F g^{-1} which is more than that of bare PC of 93 F g^{-1} at 1 A g^{-1}. The fabricated device shows a specific capacitance of 140 F g^{-1} at 1 A g^{-1}. It has high cyclic stability of capacitance retention at 97% even after 7000 cycles.

Pourfarzad et al. [94] in situ synthesis of the C_3N_4/PPy/MnO_2 by the sonication of the pyrrole mixed with the graphitic carbon nitride presence of potassium permanganate. The nanocomposite was characterized by SEM, TEM, XRD, and FTIR spectroscopy. The bare PPy/MnO_2 shows low specific capacitance but for the C_3N_4/PPy/MnO_2 composite specific capacitance of 509 F g^{-1} at a current density of 1 A g^{-1}. The device constructed using the composite and activated carbon electrode PPy/MnO_2/C_3N_4/AC shows a specific capacitance of 11.5.1 F g^{-1} at 1 A g^{-1}, it has a cyclic stability of 95.7% retention after 5000 cycles.

Dhandapani et al. [95] prepared a high-performance supercapacitor device such as the Polyindole/g-C_3N_4 composite. The composite PIn/g-C_3N_4 possesses the specific capacitance value of 440.8 C g^{-1} at 6 A g^{-1} with sulfuric acid as an electrolyte.

The construction of the asymmetric device PIn/g-C_3N_4//rGO shows a high specific capacitance of 73.84 C g^{-1} at 3 A g^{-1}. The cyclic reliability of 72% was achieved at an applied current density of 18 A g^{-1} after 5000 cycles.

The synergistic effect between NCNFs leads to the formation of the high-powered supercapacitor showing the specific capacitance of 26 F g^{-1} at 1 A g^{-1} [96]. To enhance the efficiency of the supercapacitor surface redox process, durability and synergistic effect of the $Ti_3C_2T_X$@PEDOT [97] All temperature-stable polymers prepared by Lu and co-workers [98]. This is stable even at −50 °C and flexible material showing that the next-generation device is in the future. Montmorillonite (MMT) and PVP were self-assembled sheet hydrogel materials. It has a high specific capacitance of 161 F g^{-1} with a high rate of capability and stability after 10,000 cycles at the current density of 1 A g^{-1}. The new generation of solid-state material with high energy storage application at variable temperatures and excellent flexibility are a promising class of materials for next-generation batteries.

2.4 Nanocomposites for Supercapacitors

Incorporating the advantages of nanocomposites, the researchers devoted their efforts to establishing nanocomposite-based materials for the better enhancement of the supercapacitor's performance. There are two kinds of composites that are prepared such as binary and ternary composite and which are functionalized with other materials. Therefore, synthesizing nanocomposite materials using mixed metal oxides/hydroxides, graphene, nanofibres, nanotubes, and polymers can provide high energy density, power density, long cyclic stability, and rate capability.

Shah et al. synthesized CuO/TiO_2 nanocomposite of different ratios by the wet chemical process [99]. Though CuO is cost-efficient, non-toxic, and has a high theoretical capacity, its poor electrical conductivity makes it difficult to use in asymmetric supercapacitors. To overcome its disadvantages, CuO nanoparticles are combined with nanostructured TiO_2. The maximum specific capacitance of 533 F g^{-1} at 1 A g^{-1} is obtained for the ratio of 70% TiO_2–30% CuO nanocomposite as shown in Fig. 14. The high specific capacitance of CuT-3 is due to a high electrolyte ion penetration during the electrochemical process. The decrease in the specific capacitance value of CuT-4 is due to the increased agglomeration of TiO_2 on the electrode surface. Further, the asymmetric supercapacitor cell (ASC) is designed by taking CuT-3 and activated carbon as positive and negative electrodes. The ASC shows an energy density of 34 Wh kg^{-1} at 1 A g^{-1} at a power density of 800 W kg^{-1} and excellent stability (96% capacitance retention after 10,000 cycles).

A ternary mixed metal oxides were synthesized by Padmadevi et al. using the hydrothermal method [100]. The MnO_2/CuO/ZrO_2 nanocomposite was stable and the formation is confirmed by XRD, XPS, SEM, and TEM. The MnO_2/CuO/ZrO_2 (1:2:1 ratio) nanocomposite shows a specific capacitance of 1964 F g^{-1} at 1 A g^{-1} with an energy density of 20.93 Wh kg^{-1} at a power density of 4013 W kg^{-1}.

Fig. 14 The capacitance of CuO, TiO_2, CuT-1, CuT-3, and CuT-4 at various current densities. Reprinted with permission from [99]. Copyright (2022), Elseiver

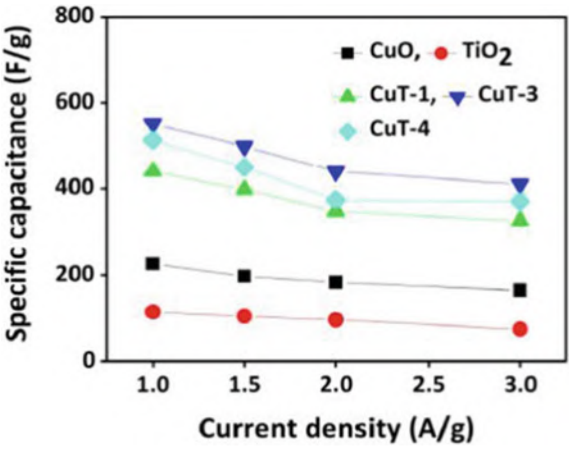

Shah et al. [101] synthesized TiO_2/CuSe nanocomposite by simple wet chemical methods. The nanocomposite shows excellent electrochemical activity due to the rich redox property of CuSe nanoparticles. The composition TiO_2-30% (ZT-3) CuSe shows a specific capacitance of 184 F g^{-1} at a current density of 2 A g^{-1}. The synthesized nanocomposite ZT-3 shows a low R_s value of 2.99 Ω. An asymmetric supercapacitor device (ASC) is designed by ZT-3 and AC as positive and negative electrodes, respectively, as shown in Fig. 15. The designed ASC shows a specific capacitance of 40.5 F g^{-1} at 1 A g^{-1} with a capacitance retention of 90% after 20,000 cycles.

In addition to that, Shah et al. [102] fabricated a novel metal oxide/metal sulfide (TiO_2/CuS) nanocomposite by wet chemical and sol–gel methods. The mixed nanocomposite prevents agglomeration during GCD cycles and adequate redox-active sites. The 30%TiO_2/CuS (ST-3) nanocomposite gives a specific capacitance of 853 F g^{-1} at 1 A g^{-1}. An ASC device was prepared by taking ST-3 and AC as cathode and anode, respectively. Energy and power density of 68.4 Wh kg^{-1} and 8150 W kg^{-1} with 87% retention rate after 25,000 cycles.

Ehsani et al. [103] reported a ternary nanocomposite of TiO_2-ZnO/MCM-41 by a two-step synthesis method. The MCM-41 was synthesized by the sol–gel method followed by calcination. TiO_2-ZnO was then loaded onto the surface of the porous material by the solvothermal method. The resultant ternary nanocomposite gives a high specific capacitance of 642.4 F g^{-1} at the current density of 2 A g^{-1}. After 5000 cycles, 98.7% of the capacitance was retained.

A series of Mn_3O_4 and WO_3 nanoparticles were mixed with various proportions by Rudra et al. [104] using a one-pot hydrothermal process. Mn_3O_4-WO_3 (10:1) shows a maximum specific capacitance of 358 F g^{-1} at 1 A g^{-1} in neutral electrolyte. The promising formation of these nanocomposites is from a simple one-pot hydrothermal process. The author constructed a symmetric supercapacitor device (SSD) using Mn_3O_4-WO_3 (10:1) and graphite sheet and studied its electrochemical behavior with an amplified potential window of 2.0 V in a neutral environment. From galvanostatic

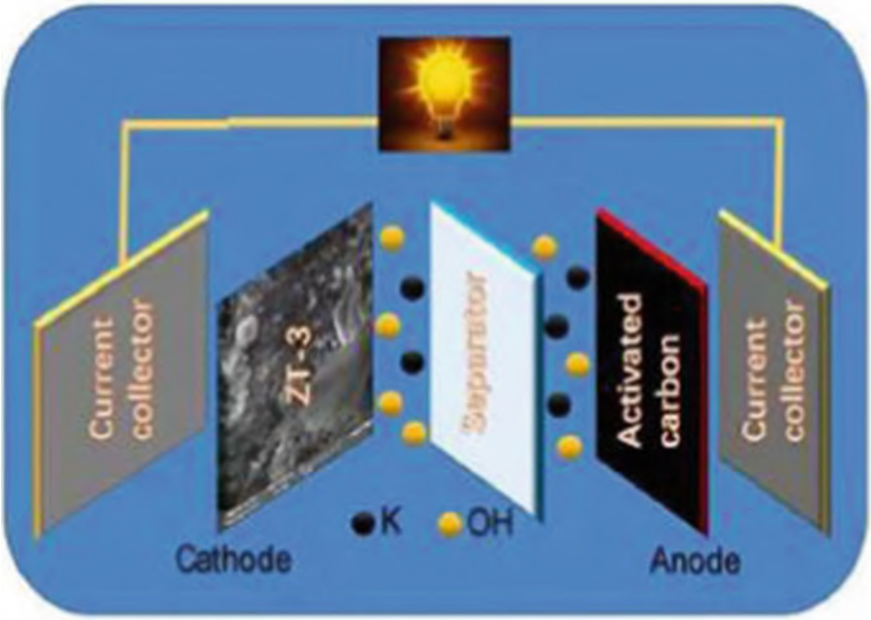

Fig. 15 Schematic illustration of fabricated (ZT-3//AC) ASC device. Reprinted with permission from [101]. Copyright (2022), Elseiver

charge–discharge measurements, the SSD gives a high specific capacitance, energy density, and power density of 101 F g^{-1} at 2 A g^{-1}, 56.11 Wh kg^{-1} at 1 A g^{-1}, and 5 kW kg^{-1} at 10 A g^{-1}, respectively. The SSD shows 95.5% retention after 5000 cycles. The findings of this study give an excellent idea for future energy storage systems.

A bimetallic impregnation of iron oxide and copper oxide on rGO (FeO-CuO-rGO) as support was synthesized by Rahaman et al. using a wet chemical oxidation–reduction method [105]. The electrodes are made using as-prepared nanocomposite, PVDF, and carbon black [106]. From Brunauer–Emmett–Teller (BET), the surface area of the GO, RGO, and FeO-CuO-RGO composite was found as 240.9, 180.3, and 168 m^2 g^{-1}, respectively. The electrochemical studies of the as-synthesized composite were studied by CV, GCD, and EIS. The amplified voltage range for the hybrid supercapacitor is from −0.2 to 0.8 V. The specific capacitance of the FeO-CuO-RGO composite calculated from GCD measurements is 626 F g^{-1} at 1 A g^{-1} and the capacitance retention is 94.4% after 1000 cycles. From these studies, it is evident that it behaves as an electric double-layer capacitor. Besides, the hybrid supercapacitor provides an energy density of 86.94 Wh kg^{-1} at 1 A g^{-1}. With RGO as support, this mixed metal oxides show superior super capacitance and energy density values.

Similarly, Farshadnia et al. synthesized a 3D porous spongy nanocomposite ($CoNi_2S_4$@MoS_2@rGO) by hydrothermal method [107]. In a three-electrode system, the synthesized $CoNi_2S_4$@MoS_2@rGO displays a maximum specific capacitance of 3268 F g^{-1} at 1 A g^{-1} in a 3 M KOH solution. The cyclic stability of the $CoNi_2S_4$@MoS_2@rGO nanocomposite after 3000 GCD cycles was 93.6%. The asymmetric supercapacitor device (ASC) is constructed by taking the nanocomposite as a positive electrode and activated carbon as a negative electrode. The specific capacitance of the ASC device was found to be 158.2 F g^{-1} at 1 A g^{-1}. This ASC device has a high retention of 86.1% after 3000 cycles. The device has a notable energy density of 41 Wh kg^{-1} at a power density of 700 W kg^{-1}. The authors also tested this electrode to light up the LED and got consecutive output within various time frames.

Li et al. [108] have developed a CoS/$MnCo_2O_4$–MnO_2 (CMM) nanocomposite using a hydrothermal method followed by electrochemical deposition. This nanocomposite shows a specific capacitance of 2320 F g^{-1} at 1 A g^{-1}. Besides, 72.8% of the initial capacitance was retained after 8000 cycles. The R_s (resistance) value from the EIS test of the prepared nanocomposite was 1.23 Ω. The CMM nanocomposite as a positive electrode and activated carbon as a negative electrode were made into an asymmetric supercapacitor device. The electrochemical performance was recorded by CV and GCD. The specific capacitance recorded for this ASC was 887.86 F g^{-1} at 1 A g^{-1} with an electrochemical reproducibility of 81.58% after 8000 GCD cycles.

Liu et al. reported a NiSe/$NiTe_2$ nanocomposite by microwave method [109]. The homogenous dispersion of $NiTe_2$ on NiSe was confirmed by SEM images. The electrochemical performance of NiSe/$NiTe_2$ nanocomposite displayed a maximum specific capacitance value of 1782.7 F g^{-1} at 1 A g^{-1}. The capacitance retention of 81.5% after 30,000 cycles was observed. The author fabricated an asymmetric supercapacitor device (NiSe/$NiTe_2$/AC) which gives the specific energy of 23.26 Wh kg^{-1} with an 84.8% retention rate after 20,000 cycles.

Khan et al. reported a $NiSe_2$/CuO (ST-1) nanocomposite using co-precipitation and hydrothermal methods [110]. The cubic structure of $NiSe_2$, monoclinic CuO, and $NiSe_2$/CuO crystal patterns were confirmed by XRD analysis. The $NiSe_2$ provides a rapid electron/ion diffusion which accounts for excellent capacitive behavior. The as-synthesized nanocomposite offers a specific capacity of 396 C g^{-1} at 1 A g^{-1}. A hybrid supercapacitor device is constructed by taking $NiSe_2$/CuO (ST-1) as a positive electrode and AC as a negative electrode. The device exhibits a notable capacitance of 120 F g^{-1} at 1 A g^{-1} with a high energy and power density of 29 Wh g^{-1} and 4950 W kg^{-1}, respectively. The retention rate of 86% after 10,000 cycles was attained.

Similarly, A novel 1D nanowires/2D nanosheets-based nanocomposite (NiSe/CoSe/Ni_3Se_2) was reported by Zhu et al. using a mixed solvothermal method [111]. The superior mass-specific capacitance of NiSe/CoSe/Ni_3Se_2 nanocomposite was 1666 F g^{-1} at a current density of 0.5 A g^{-1} with a retention rate of 85.19% after 5000 GCD cycles. The internal resistance value (R_s) of NiSe/CoSe/Ni_3Se_2 nanocomposite was 1.33 Ω. A solid-state asymmetric supercapacitor device (SSAS) was fabricated by NiSe/CoSe/Ni_3Se_2 nanocomposite and activated carbon as positive and negative electrodes, respectively. From the CV and GCD curves, the areal energy and power density of SSAS were 0.33 mW h cm^{-2} and 7 mW cm^{-2}. A retention rate of 80.11% after 10,000 cycles was observed in the SSAS device.

Liang et al. prepared g-C_3N_4@$NiMoO_4$/$CoMoO_4$ nanocomposite by hydrothermal method [112]. The synthesized g-C_3N_4@$NiMoO_4$/$CoMoO_4$ electrode shows a specific capacitance of 641.5 F g^{-1} at 1 A g^{-1} with an electrochemical reproducibility of 84.21% after 8000 cycles. The ASC device was made using g-C_3N_4@$NiMoO_4$/$CoMoO_4$ and AC and the electrochemical behavior was studied by CV and GCD. The specific capacitance of 63.6 F g^{-1} was recorded at a current density of 1 A g^{-1}. Besides, a retention rate of 110% after 10,000 GCD cycles was obtained.

Chameh et al. reported an ultrasound-assisted-CeO_2/$CoFe_2O_4$ on pristine g-C_3N_4 and Oxygenated g-C_3N_4 were prepared [113]. From the BET measurements, the surface area of Ox-g-C_3N_4/CeO_2/$CoFe_2O_4$ is 83.05 m^2 g^{-1}. The 10% Ox-g-C_3N_4/CeO_2/$CoFe_2O_4$ nanocomposite shows 255.5 F g^{-1} (specific capacitance) at a current density of 1 A g^{-1} in a 6 M KOH electrolyte. The resistance value (R_s) of 10% Ox-g-C_3N_4/CeO_2/$CoFe_2O_4$ nanocomposite was 0.51 Ω. Using 10% Ox-g-C_3N_4/CeO_2/$CoFe_2O_4$ nanocomposite as a cathode and activated carbon as an anode, an aqueous asymmetric supercapacitor device was prepared. This ASC device shows a remarkable energy and power density of 4.79 Wh kg^{-1} and 11,904 W kg^{-1} with capacitance retention of 91% over 3000 GCD cycles, shown in Fig. 16. Such excellent capacitive behavior is attributed to 10% Ox-g-C_3N_4/CeO_2/$CoFe_2O_4$ nanocomposite shows promising materials for supercapacitor application.

Hasan et al. synthesized a $CuCo_2S_4$-MoS_2 nanocomposite by hydrothermal method [114]. The synthesized nanocomposite provides a specific capacitance of 820 F g^{-1} at a current density of 0.5 A g^{-1}. The ASC device was fabricated by $CuCo_2S_4$-MoS_2 nanocomposite as a positive and activated carbon as a negative electrode. This device was amplified to work in a large potential window of 1.6 V. The fabricated device shows a notable energy and power density value of 38.22 Wh kg^{-1}

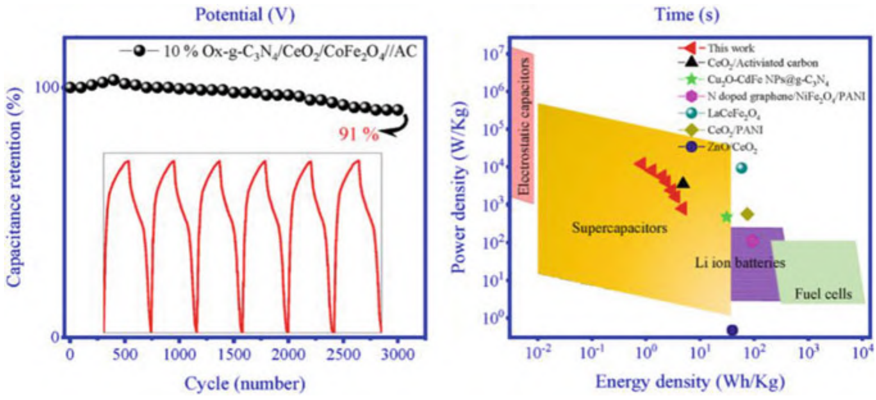

Fig. 16 Cyclic stability (left) and Ragone plot (right) of fabricated ASC device. Reprinted with permission from [113]. Copyright (2022), Elseiver

and 400 W kg^{-1}. In addition to that, the capacitance reproducibility of 89% after 1000 GCD cycles was attained.

Tan et al. reported a novel biocarbon-supported nanocomposite (CAS@Ni_3S_4/CeO_2) by hydrothermal technique [115]. The Chingma Abutilon Seed (CAS) was taken as a source for the biocarbon. The Ni_3S_4/CeO_2 were uniformly loaded on the CAS support which has a large surface responsible for fast ion/electron transfer between electrode and electrolyte. The composite was prepared with varying different temperatures in the hydrothermal method to examine its electrochemical properties. The electrochemical performance tests carried out by CV and GCD show the specific capacitance of 1364 F g^{-1} at 1 A g^{-1}. An asymmetric supercapacitor device was made by using CAS@Ni_3S_4/CeO_2-150 as a cathode and CAS as an anode. The device is also made up of activated carbon as an anode for a comparative electrochemical study. In these two systems, the CAS-containing nanocomposite shows a high specific capacitance of 289 F g^{-1} over the AC-containing nanocomposite (261 F g^{-1} at 1 A g^{-1}).

Kumar et al. designed a novel WS_2/$FeCo_2O_4$ nanocomposite on Ni foam by a two-step hydrothermal method [116]. The transition metal disulfides loaded on binary metal oxide makes a new pathway to enhance the electrochemical behavior with a highly porous Ni foam as support [117]. The as-synthesized nanocomposite exhibited an excellent specific capacitance of 2492.9 F g^{-1} at 1 A g^{-1} with a retention rate of 98.1% after 5000 GCD cycles. The WS_2/$FeCo_2O_4$ nanocomposite and activated carbon were made into an asymmetric supercapacitor device as a pair of electrodes with a specific capacitance of 110 C g^{-1}. The device shows an energy and power density of 85.68 Wh kg^{-1} and 897.65 W kg^{-1}, respectively. Besides, it shows 98.7% capacitance retention after 4000 cycles making it a promising tool for an energy storage system.

Li et al. synthesized MnCoP/(Co,Mn)$(Co,Mn)_2O_4$ nanocomposite by hydrothermal method [118]. The electrochemical performance of MnCoP/(Co,Mn)$(Co,Mn)_2O_4$ nanocomposite was studied by CV and GCD analysis. The specific capacitance of 230 F g^{-1} at a current density of 0.1 A g^{-1} was obtained. An aqueous asymmetric supercapacitor device (ASC) with MCP/MCO as a cathode and activated carbon as an anode.

3 Future Perspective on Functionalized Materials

Functional groups like hydroxides, carbonyl, carboxylic acids, amine, and amides have been extensively used for the better enhancement of supercapacitors. In addition to that, carbonous materials like 1D nanofibers, nanowires, nanotubes, 2D graphene nanosheets, 3D nanoparticles, and 3D architecture materials were used in energy storage applications because of their large surface area, highly porous nature, electrical conductivity, and thermal stability. Recently, the non-carbonaceous g-C_3N_4 and BN, polymeric materials like polydimethylsiloxane (PDMS), polysulfones, polyether ether ketone (PEEK), polytetrafluoroethylene (PTFE), polyaniline (PANI), polyvinylidene fluoride (PVDF), bio-polymers like keratin, pectin, carrageenan, lignin, cellulose [119], and starch were functionalized with various metal oxides/hydroxides, metal–organic frameworks [120] and used in supercapacitor electrodes for flexible and wearable devices, electric vehicles, micro-supercapacitors, on-chip energy storage devices. Despite its disadvantages like water insolubility and poor structural stability, MnO_2 is making ground-breaking results in energy storage performance [121]. With suitable functionalization, these materials can give better output than previously reported works.

Nowadays, electrolytes like aqueous, ionic liquids, organic, and gel polymers are mixed with different proportions as hybrid electrolytes and employed in the supercapacitor application [122]. By using these hybrid electrolytes, large electron/ion diffusion and a wide electrochemical potential window can be attained. Enormous advancements in the field of science, biotechnology, and electronics require small, lightweight, highly compactable, and easily customizable materials for the foreseeable future. Various findings on micro-supercapacitors (MSCs) address these issues by synthesizing miniatured devices, providing high super-capacitive results [123]. By empowering this idea, further reduction in the material size (nano-supercapacitors) will allow more redox-active sites which help in fast electron/ion transfer and enhance the specific capacitance and energy density of the supercapacitor device.

A recent study on living microorganisms-based supercapacitors paves a new pathway for synthesizing natural, environmentally friendly, fast redox-active electrodes [124]. These types of biologically-derived materials are still under exploration. 3D printing is one of the fast-growing techniques that help to fabricate the desired supercapacitor electrodes for real-life applications [125]. A highly efficient, cost-effective, graphene oxide (GO) gel was widely used as 3D printing ink because of its excellent rheological properties, functionalized nature, high porosity, and facile large-scale synthesis making it a promising candidate for supercapacitor device fabrication. Unfolding the application of piezoelectric materials for flexible and wearable devices, a self-charging supercapacitor device can be designed [126]. These materials can provide non-stop power delivery by simple mechanical stress and are used for various day-to-day applications.

A serious concern about environmental pollution by the usage of various chemicals during the synthesis of electrode materials and device fabrication should be taken under consideration and facile green synthesis methods should be studied well and implemented.

4 Conclusion

In this chapter, we have discussed functionalized materials for supercapacitor devices in current trends that exhibit outstanding specific capacitance with long cycle life. The functionalized materials could enhance capacitance and long cycle durability. Binary/tertiary mixed metals or functionalized carbon and non-carbon-based materials have been used in supercapacitor-based devices. Especially, flexible-based supercapacitor devices are promising electrodes for electronic wearable devices. These functionalized materials were assembled as asymmetric, symmetric, and hybrid supercapacitor devices, and delivered an excellent energy density with long cycle life, which indicates the supercapacitor devices to be used in electronic devices such as smartphones, sensors, and electric vehicles.

References

1. Hao L, Li X, Zhi L (2013) Carbonaceous electrode materials for supercapacitors. Adv Mater 25(28):3899–3904
2. Mothkuri S, Gupta H, Jain PK, Rao TN, Padmanabham G, Chakrabarti S (2021) Functionalized carbon nanotube and MnO_2 nanoflower hybrid as an electrode material for supercapacitor application. Micromachines 12(2):213
3. Lee WSV, Leng M, Li M, Huang XL, Xue JM (2015) Sulphur-functionalized graphene towards high performance supercapacitor. Nano Energy 12:250–257
4. Simon P, Gogotsi Y (2008) Materials for electrochemical capacitors. Nat Mater 7(11):845–854
5. Zhao Y, Liu M, Deng X, Miao L, Tripathi PK, Ma X et al (2015) Nitrogen-functionalized microporous carbon nanoparticles for high performance supercapacitor electrode. Electrochim Acta 153:448–455
6. Winter M, Brodd RJ (2004) What are batteries, fuel cells, and supercapacitors? Chem Rev 104(10):4245–4270
7. Lei Y, Li J, Wang Y, Gu L, Chang Y, Yuan H et al (2014) Rapid microwave-assisted green synthesis of 3D hierarchical flower-shaped $NiCo_2O_4$ microsphere for high-performance supercapacitor. ACS Appl Mater Interfaces 6(3):1773–1780
8. Teo EYL, Lim HN, Jose R, Chong KF (2015) Aminopyrene functionalized reduced graphene oxide as a supercapacitor electrode. RSC Adv 5(48):38111–38116
9. Peng X, Peng L, Wu C, Xie Y (2014) Two dimensional nanomaterials for flexible supercapacitors. Chem Soc Rev 43(10):3303–3323
10. Fan X, Yu C, Ling Z, Yang J, Qiu J (2013) Hydrothermal synthesis of phosphate-functionalized carbon nanotube-containing carbon composites for supercapacitors with highly stable performance. ACS Appl Mater Interfaces 5(6):2104–2110
11. Ganesh Babu S, Emayavaramban B, Jerome P, Karvembu R (2017) Pd/AlO(OH): a heterogeneous, stable and recyclable catalyst for N-arylation of aniline under ligand-free aerobic condition. Catal Lett 147(10):2619–2629
12. Paunkumar P, Babu SG (2022) Recent advances in graphene and graphene-based heterogeneous nanocatalysts: C−C and C−Y coupling reactions in liquid phase. ChemistrySelect 7(41):e202202291
13. Ganesh Babu S, Krishnamoorthi S, Thiruneelakandan R, Karvembu R (2014) V_2O_5 anchored RuO_2: an efficient nanocatalyst for aerial oxidation of alcohols. Catal Lett 144(7):1245–1252
14. Babu SG, Karthik P, John MC, Lakhera SK, Ashokkumar M, Khim J et al (2019) Synergistic effect of sono-photocatalytic process for the degradation of organic pollutants using CuO-TiO_2/rGO. Ultrason Sonochem 50:218–223
15. Bhuvaneswari C, Palpandi K, Amritha B, Paunkumar P, Lakshmi Priya R, Raman N et al (2022) Conniving for the first time of $BiVO_4$–rGO/CE-BN and its potential as enhanced electrochemical sensing of non-steroidal anti-androgen drug. Microchem J 108174
16. Vinoth R, Babu SG, Bharti V, Gupta V, Navaneethan M, Bhat SV et al (2017) Ruthenium based metallopolymer grafted reduced graphene oxide as a new hybrid solar light harvester in polymer solar cells. Sci Rep 7(1):43133
17. Fadlalla MI, Babu SG (2019) Chapter 5—Role of graphene in photocatalytic water splitting for hydrogen production. In: Jawaid M, Ahmad A, Lokhat D (eds) Graphene-based nanotechnologies for energy and environmental applications. Elsevier, pp 81–108

18. Qiu L, Yang W, Zhao Q, Lu S, Wang X, Zhou M et al (2022) NiS nanoflake-coated carbon nanofiber electrodes for supercapacitors. ACS Appl Nano Mater 5(5):6192–6200
19. González A, Goikolea E, Barrena JA, Mysyk R (2016) Review on supercapacitors: technologies and materials. Renew Sustain Energy Rev 58:1189–1206
20. Salanne M, Rotenberg B, Naoi K, Kaneko K, Taberna P-L, Grey CP et al (2016) Efficient storage mechanisms for building better supercapacitors. Nat Energy 1(6):1–10
21. Yadav MS (2020) Synthesis and characterization of $Mn_2O_3-Mn_3O_4$ nanoparticles and activated charcoal based nanocomposite for supercapacitor electrode application. J Energy Storage 27:101079
22. Ke Q, Wang J (2016) Graphene-based materials for supercapacitor electrodes—a review. J Mater 2(1):37–54
23. Azwar E, Mahari WAW, Chuah JH, Vo D-VN, Ma NL, Lam WH et al (2018) Transformation of biomass into carbon nanofiber for supercapacitor application—a review. Int J Hydrogen Energy 43(45):20811–20821
24. Pan H, Li J, Feng Y (2010) Carbon nanotubes for supercapacitor. Nanoscale Res Lett 5(3):654–668
25. Frackowiak E (2007) Carbon materials for supercapacitor application. Phys Chem Chem Phys 9(15):1774–1785
26. Selvaraj AR, Raja IS, Chinnadurai D, Rajendiran R, Cho I, Han DW et al (2022) Electrospun one dimensional (1D) pseudocapacitive nanorods embedded carbon nanofiber as positrode and graphene wrapped carbon nanofiber as negatrode for enhanced electrochemical energy storage. J Energy Storage 46:103731
27. Aydın H, Kurtan U, Demir M, Karakuş S (2022) Synthesis and application of a self-standing zirconia-based carbon nanofiber in a supercapacitor. Energy Fuels 36(4):2212–2219
28. Yuan C, Zhang M, Ni X, Li K, Liu C, Chen H et al (2022) Preparation of cellulose-based carbon nanofibers/$NiCo_2S_4$ composites for high-performance all-solid-state symmetric supercapacitors. J Energy Storage 47:103589
29. Amiri D, Kamali Heidari E, Kamyabi-Gol A, Sajjadi SA, Hoor M (2022) Electrospun $NiMoO_4$-encapsulated carbon nanofibers electrodes for advanced supercapacitors. J Energy Storage 55:105490
30. Yoo H, Jeong JH, Kim B-H, Kim MH (2022) Tubular carbon nanofibers decorated with RuO_2 nanorods toward flexible electrochemical capacitors. J Alloy Compd 909:164771
31. Li D, Raza F, Wu Q, Zhu X, Ju A (2022) $NiCo_2O_4$ nanosheets on hollow carbon nanofibers for flexible solid-state supercapacitors. ACS Appl Nano Mater 5(10):14630–14638
32. Huang Y, Zhou J, Zhang Y, Yan L, Bao S, Yin Y et al (2022) Encapsulating hollow Fe_3O_4 in intertwined N-doped carbon nanofibers for high-performance supercapacitors and sodium-ion batteries. J Alloy Compd 918:165672
33. Ahmad MW, Anand S, Dey B, Yang D-J, Choudhury A (2022) Asymmetric supercapacitors based on porous $MnMoS_4$ nanosheets-anchored carbon nanofiber and N, S-doped carbon nanofiber electrodes. J Alloy Compd 906:164271
34. Sonsupap S, Chanlek N, Kidkhunthod P, Sinprachim T, Maensiri S (2022) Synthesis and electrochemical properties of electrospun cerium oxide (CeO_2) nanoparticles/carbon nanofibers. J Electron Mater 51(6):2933–2948
35. Liu X, Sun J, Liu Y, Liu D, Chen H, Zhuo K et al (2022) Electrospun NiO/C nanofibers as electrode materials for hybrid supercapacitors with superior electrochemical performance. Int J Hydrogen Energy 47(38):16985–16995
36. Agarwal A, Majumder S, Sankapal BR (2022) Carbon nanotube-functionalized surface-assisted growth of cobalt phosphate nanodots: a highly stable and bendable all-solid-state symmetric supercapacitor. Energy Fuels 36(11):5953–5964
37. Shakir I, Almutairi Z, Shar SS, Nafady A (2022) Fabrication of a flower-like $Cu(OH)_2$ nanoarchitecture and its composite with CNTs for use as a supercapacitor electrode. Ceram Int 48(8):11278–11285
38. Deghiedy NM, Yousif NM, Hosni HM, Balboul MR (2022) Silver-modified electrodes based on amorphous MnO_2/carbon nanotube: multicomponent approach to enhance the performance of supercapacitors. J Phys Chem Solids 161:110445

39. Fahimi Z, Moradlou O (2022) High-performance solid-state asymmetric supercapacitor based on $Co_3V_2O_8$/carbon nanotube nanocomposite and gel polymer electrolyte. J Energy Storage 50:104697
40. Cha Y, Kim T, Seo B, Choi W (2022) Combustion-driven synthesis route for bimetallic Ag–Bi nanoparticle-anchored carbon nanotube electrodes for high-performance supercapacitors. Carbon 198:11–21
41. Kariper İA, Korkmaz S, Karaman C, Karaman O (2022) High energy supercapacitors based on functionalized carbon nanotubes: effect of atomic oxygen doping via various radiation sources. Fuel 324:124497
42. Feng T, Jiao H, Li H, Wang J, Zhang S, Wu M (2022) High performance of electrochemically deposited $NiCo_2S_4$/CNT composites on nickel foam in flexible asymmetric supercapacitors. Energy Fuels 36(4):2189–2201
43. Hsieh C-E, Chang C, Gupta S, Hsiao C-H, Lee C-Y, Tai N-H (2022) Binder-free $CoMn_2O_4$/carbon nanotubes composite electrodes for high-performance asymmetric supercapacitor. J Alloy Compd 897:163231
44. Ramesh S, Yadav HM, Bathula C, Palem RR, Arumugam S, Kathalingam A et al (2022) V_2O_5 nano sheets assembled on nitrogen doped multiwalled carbon nanotubes/carboxy methyl cellulose composite for two-electrode configuration of supercapacitor applications. Ceram Int 48(19, Part B):29247–29256
45. Diler F, Burhan H, Genc H, Kuyuldar E, Zengin M, Cellat K et al (2020) Efficient preparation and application of monodisperse palladium loaded graphene oxide as a reusable and effective heterogeneous catalyst for suzuki cross-coupling reaction. J Mol Liq 298:111967
46. Vinoth R, Babu SG, Ramachandran R, Neppolian B (2017) Bismuth oxyiodide incorporated reduced graphene oxide nanocomposite material as an efficient photocatalyst for visible light assisted degradation of organic pollutants. Appl Surf Sci 418:163–170
47. Paul A, Ghosh S, Kolya H, Kang C-W, Murmu NC, Kuila T (2022) High performance asymmetric supercapacitor device based on lanthanum doped nickel-tin oxide/reduced graphene oxide composite. J Energy Storage 55:105526
48. Paul A, Ghosh S, Kolya H, Kang C-W, Murmu NC, Kuila T (2022) Synthesis of nickel-tin oxide/nitrogen-doped reduced graphene oxide composite for asymmetric supercapacitor device. Chem Eng J 443:136453
49. Pappu S, Anandan S, Rao TN, Martha SK, Bulusu SV (2022) High-performance hybrid supercapacitor with electrochemically exfoliated graphene oxide incorporated $NiCo_2O_4$ in aqueous and non-aqueous electrolytes. J Energy Storage 50:104598
50. Li Z, Hu B, Yu R, Tian T, Guo Z, Mu J et al (2023) Hollow cobalt selenide nanospheres wrapped with reduced graphene oxide nanosheets as electrodes for hybrid supercapacitor. Appl Surf Sci 608:155237
51. Ramesh S, Karuppasamy K, Vikraman D, Santhoshkumar P, Bathula C, Palem RR et al (2022) Sheet-like morphology $CuCo_2O_4$ bimetallic nanoparticles adorned on graphene oxide composites for symmetrical energy storage applications. J Alloy Compd 892:162182
52. Wang K, Dong X, Zhao C, Qian X, Xu Y (2015) Facile synthesis of Cu_2O/CuO/RGO nanocomposite and its superior cyclability in supercapacitor. Electrochim Acta 152:433–442
53. Zhang Z, Zhang X, Xu X, Xiong R, Tian X, Wang C (2022) In-situ directly anchored $CoMoS_4$ particles on reduced graphene oxide nanosheets for the high-efficiency asymmetric supercapacitor. Colloids Surf, A 652:129762
54. Shankar VU, Kumar PS, Govindarajan D, Nethaji P, Balji GB (2022) Ruthenium dioxide anchored on reduced graphene oxide nanocomposite for 1.2 V symmetric supercapacitor devices. Sustain Energy Technol Assess 53:102444
55. Korkmaz S, Kariper İA, Karaman O, Karaman C (2021) The production of rGO/RuO_2 aerogel supercapacitor and analysis of its electrochemical performances. Ceram Int 47(24):34514–34520
56. Thalji MR, Ali GA, Liu P, Zhong YL, Chong KF (2021) $W_{18}O_{49}$ nanowires-graphene nanocomposite for asymmetric supercapacitors employing $AlCl_3$ aqueous electrolyte. Chem Eng J 409:128216

57. Morenghi A, Scaravonati S, Magnani G, Sidoli M, Aversa L, Verucchi R et al (2022) Asymmetric supercapacitors based on nickel decorated graphene and porous graphene electrodes. Electrochim Acta 140626
58. Cai D, Cao Q, Du J, Liu Y, Bu F, Yan Y et al (2022) Oxygen vacancies enhanced $NiCo_2O_4$ nanoarrays on carbon cloth as cathode for flexible supercapacitors with excellent cycling stability. Batter Supercaps 5(3):e202100344
59. Zhang MY, Miao JY, Yan XH, Zhu YH, Li YL, Zhang WJ et al (2022) Vanadium disulfide nanosheets loaded on carbon cloth as electrode for flexible quasi-solid-state asymmetric supercapacitors: energy storage mechanism and electrochemical performance. J Mater Chem C 10(2):640–648
60. Du P, Dong Y, Dong Y, Wang X, Zhang H (2022) Fabrication of uniform MnO_2 layer-modified activated carbon cloth for high-performance flexible quasi-solid-state asymmetric supercapacitor. J Mater Sci 57(5):3497–3512
61. Fan Z, Ren J, Zhang F, Gu T, Zhang S, Ren R-P et al (2022) A flexible and self-healing supercapacitor based on activated carbon cloth/MnO_2 composite. J Mater Sci 57(2):1281–1290
62. Zhang S, Ren J, Gu T, Guo H, Wang H, Imran M et al (2022) Porous NiCoS nanosheets decorated activated carbon cloth for flexible asymmetric supercapacitors. Diam Relat Mater 127:109154
63. Fu M, Zhu Z, Chen W, Yu H, Lv R (2022) Carbon cloth supported flower-like porous nickel-based electrodes boosting ion/charge transfer characteristics of flexible supercapacitors. Carbon 199:520–528
64. Gong J, Wang Y, Wang J, Liu Y, Hu C, Zhou T et al (2022) Hollow nickel-cobalt sulfide nanospheres cathode hybridized with carbon spheres anode for ultrahigh energy density asymmetric supercapacitors. Int J Hydrogen Energy 47(17):10056–10068
65. Huang C, Lv S, Gao A, Ling J, Yi F, Hao J et al (2022) Boosting the energy density of supercapacitors by designing both hollow NiO nanoparticles/nitrogen-doped carbon cathode and nitrogen-doped carbon anode from the same precursor. Chem Eng J 431:134083
66. Liu C, Hou Y, Li Y, Xiao H (2022) Heteroatom-doped porous carbon microspheres derived from ionic liquid-lignin solution for high performance supercapacitors. J Colloid Interface Sci 614:566–573
67. Mohanty R, Swain G, Parida K, Parida K (2022) Enhanced electrochemical performance of flexible asymmetric supercapacitor based on novel nanostructured activated fullerene anchored zinc cobaltite. J Alloy Compd 919:165753
68. Babu SG, Vinoth R, Narayana PS, Bahnemann D, Neppolian B (2015) Reduced graphene oxide wrapped Cu_2O supported on C_3N_4: an efficient visible light responsive semiconductor photocatalyst. APL Mater 3(10):104415
69. Hengrui Q, Qian M, Xuejiao S, Xiaoxing H, Guixiao J, Yongqiang Z et al (2022) Facile synthesis of g-C_3N_4/LDH self-growing nanosheet arrays for enhanced supercapacitor performance. J Alloy Compd 896:163023
70. Ali M, Mehdi S-N, Adel R-V (2022) AgI/g-C_3N_4 nanocomposite as electrode material for supercapacitors: comparative study for its efficiency in three different aqueous electrolytes. Electrochim Acta 430:141052
71. Xuezhao W, Shijia W, Dangcheng S, Shengang X, Shaokui C, Yuanhua X (2022) Constructing a p-n heterojunction in 3D urchin-like $CoNi_xS_y$/g-C_3N_4 composite microsphere for high performance asymmetric supercapacitors. J Alloy Compd 902:163784
72. Lina C, Jiafeng W, Xinyue F, Haolin S, Pan L (2022) Flower-like g-C_3N_4 nanosheets decorated hollow Co_2NiO_4 cube derived from ZIF-67 for excellent performance supercapacitors. J Alloy Compd 918:165769
73. Subhash KG, Benoy MD, Duraimurugan J, Prabhu S, Siranjeevi R, Ramesh R et al (2022) Synergistic effect of NiS/g-C_3N_4 nanocomposite for high-performance asymmetric supercapacitors. Inorg Chem Commun 142:109719
74. Ghosh S, Inta HR, Chakraborty M, Tudu G, Koppisetti HVSRM, Paliwal KS et al (2022) Nanoporous graphitic carbon nitride nanosheets decorated with nickel–cobalt oxalate for battery-like supercapacitors. ACS Appl Nano Mater 5(5):7246–7258

75. Zhu Z, Wei C, Jiang D, Wu X, Lu M (2022) Design and synthesis of MOF-derived CuO/g-C_3N_4 composites with octahedral structures as advanced anode materials for asymmetric supercapacitors with high energy and power densities. Mater Adv 3(1):672–681
76. Fan Y, Meng Y, Junye Z, Hao G, Tingting Z, Hao G et al (2022) High-efficiency hybrid supercapacitor based on three-dimensional interconnected nitrogen-rich caCTF-1 @pC-C_3N_4 network and $NiCoTe_2$. J Alloy Compd 911:164782
77. Weiyi H, Fei T (2022) Molten-state cubic cage-templated uniform C_3N_4 hollow nanocubes and improved electrochemical performance of asymmetric micro-supercapacitor. J Alloy Compd 909:164790
78. Masayuki K, Shinya K, Yasuji M (2008) Electronic structure and intercalation chemistry of graphite-like layered material with a composition of BC_6N. J Phys Chem Solids 69(5):1171–1178
79. Noor Mohammad S (2002) Electrical characteristics of thin film cubic boron nitride. Solid-State Electron 46(2):203–222
80. Xu Y-N, Ching WY (1991) Calculation of ground-state and optical properties of boron nitrides in the hexagonal, cubic, and wurtzite structures. Phys Rev B 44(15):7787–7798
81. Hod O (2012) Graphite and hexagonal boron-nitride have the same interlayer distance. Why? J Chem Theory Comput 8(4):1360–1369
82. Yarbrough WA (1991) Current research problems and opportunities in the vapor phase synthesis of diamond and cubic boron nitride. J Vac Sci Technol, A 9(3):1145–1152
83. Saitoh H, Yarbrough WA (1991) Preparation and characterization of nanocrystalline cubic boron nitride by microwave plasma-enhanced chemical vapor deposition. Appl Phys Lett 58(20):2228–2230
84. Paine RT, Narula CK (1990) Synthetic routes to boron nitride. Chem Rev 90(1):73–91
85. Liyang L, Susu C, Xueli Q, Jianyao Y, Lijian M, Wei C (2022) h-BN doped β-MnO_2 nanobelts composite as superior electrode materials for supercapacitors. Mater Lett 328:133209
86. Maity CK, Sahoo S, Verma K, Nayak GC (2022) SnS_2@conducting energy level-induced functionalized boron nitride for an asymmetric supercapacitor. Energy Fuels 36(4):2248–2259
87. Yasar Ozkan Y, Fatma N, Ahmad H, Mehmet E (2022) The hierarchical synthesis of tungsten disulfide coated vertically aligned boron carbon nitride nanotubes composite electrodes for supercapacitors. J Energy Storage 52:104964
88. Chen Y, Fang L, Hu Y, Lu Y, He J, Wang S et al (2022) Manganese oxide/nitrogen-doped carbon aerogels from cellulose nanofibrils for high-performance supercapacitor electrodes. Diam Relat Mater 122:108813
89. Gangopadhyay R, De A (2000) Conducting polymer nanocomposites: a brief overview. Chem Mater 12(3):608–622
90. Meng C, Liu C, Chen L, Hu C, Fan S (2010) Highly flexible and all-solid-state paperlike polymer supercapacitors. Nano Lett 10(10):4025–4031
91. Bathula C, Rabani I, Kadam A, Opoku H, Patil SA, Shreshta NK et al (2022) Sonochemically exfoliated polymer-carbon nanotube interface for high performance supercapacitors. J Colloid Interface Sci 606:1792–1799
92. Wu X, Fan H, Wang W, Lei L, Ma L (2022) A novel metal-free ternary core–shell carbon sphere/C_3N_4/PPy nanocomposite for high-performance supercapacitors. New J Chem 46(32):15292–15295
93. Zhang Y, Deng F, Zhang Q, Xing B, Shang J, Lin J (2022) One-step synthesis of polymer based N-doped porous carbon with enriched nitrogen content and its enhanced electrochemical properties in supercapacitors. J Energy Storage 55:105494
94. Pourfarzad H, Badrnezhad R, Ghaemmaghami M, Saremi M (2021) In situ synthesis of C_3N_4/PPy/MnO_2 nanocomposite as a high performance active material for asymmetric supercapacitor. Ionics 27(9):4057–4067
95. Dhandapani E, Prabhu S, Duraisamy N, Ramesh R (2021) Polyindole intercalated graphitic carbon nitride (PIn/g-C_3N_4) composites for high-performance supercapacitor application. J Energy Storage 44:103360

96. Jiang Q, Liu M, Shao C, Li X, Liu H, Li X et al (2020) Nitrogen doping polyvinylpyrrolidone-based carbon nanofibers via pyrolysis of g-C_3N_4 with tunable chemical states and capacitive energy storage. Electrochim Acta 330:135212
97. Liu Z, Wang L, Xu Y, Guo J, Zhang S, Lu Y (2021) A $Ti_3C_2T_X$@PEDOT composite for electrode materials of supercapacitors. J Electroanal Chem 881:114958
98. Lu C, Chen X (2020) All-temperature flexible supercapacitors enabled by antifreezing and thermally stable hydrogel electrolyte. Nano Lett 20(3):1907–1914
99. Shah MZU, Sajjad M, Hou H, Rahman Su, Mahmood A, Aziz U et al (2022) A new CuO/TiO_2 nanocomposite: an emerging and high energy efficient electrode material for aqueous asymmetric supercapacitors. J Energy Storage 55:105492
100. Padmadevi B, Kalaivani T (2022) Facile synthesis of manganese–copper–zirconium mixed oxide nanocomposites: a potential electrode material for high performance supercapacitors. Ceram Int
101. Shah MZU, Javed MS, Sajjad M, Shah A, Shah MS, ur Rahman S et al (2022) A novel TiO_2/CuSe based nanocomposite for high-voltage asymmetric supercapacitors. J Sci: Adv Mater Devices 7(2):100418
102. Shah MZU, Sajjad M, Hou H, ur Rahman S, Shah A (2022) Copper sulfide nanoparticles on titanium dioxide (TiO_2) nanoflakes: a new hybrid asymmetrical Faradaic supercapacitors with high energy density and superior lifespan. J Energy Storage 55:105651
103. Ehsani A, Bigdeloo M, Alamgholiloo H, Asgari E, Sheikhmohammadi A, Nazari S et al (2022) Ternary nanocomposite of TiO_2-ZnO/MCM-41: synthesis and electrochemical performance in supercapacitors. J Energy Storage 50:104633
104. Rudra S, Janani K, Thamizharasan G, Pradhan M, Rani B, Sahu NK et al (2022) Fabrication of Mn_3O_4-WO_3 nanoparticles based nanocomposites symmetric supercapacitor device for enhanced energy storage performance under neutral electrolyte. Electrochim Acta 406:139870
105. Rahaman M, Mukherjee T, Kaparaju P, Bose S (2022) Iron oxide- and copper oxide-decorated chemically reduced graphene oxide composite as a novel electrode for hybrid supercapacitors. Energy Fuels 36(7):3976–3986
106. Mazurkiewicz-Pawlicka M, Nowak M, Malolepszy A, Witowski A, Wasik D, Hu Y et al (2019) Graphene oxide with controlled content of oxygen groups as a filler for polymer composites used for infrared radiation shielding. Nanomaterials 10(1):32
107. Farshadnia M, Ensafi AA, Mousaabadi KZ, Rezaei B (2022) Design and synthesis of three-dimensional $CoNi_2S_4$@MoS_2@rGO nanocomposites and its application in electrochemical supercapacitors. J Alloy Compd 906:164278
108. Li S, Fan J, Xiao G, Gao S, Cui K, Wang Z et al (2022) The synthesis of CoS/$MnCo_2O_4$-MnO_2 nanocomposites for supercapacitors and energy-saving H_2 production. J Colloid Interface Sci 628:179–192
109. Liu J, Ren L, Luo J, Song J (2022) Microwave synthesis of NiSe/$NiTe_2$ nanocomposite grown in situ on Ni foam for all-solid-state asymmetric supercapacitors. Colloids Surf, A 647:129093
110. Khan AU, Tahir K, Hassan HM, Albalawi K, Khan QU, Khan A et al (2022) Hydrothermal assisted synthesis of novel $NiSe_2$/CuO nanocomposite: extremely stable and exceptional energy storage performance for faradaic hybrid supercapacitors. J Electroanal Chem 920:116624
111. Zhu L, Liu X, Du W, Fu J, Yang X, Chai X et al (2022) Construction and application in solid-state asymmetric supercapacitors of gladiolus-like NiSe/CoSe/Ni_3Se_2 hierarchical nanocomposite with synergistic structural advantages. J Alloy Compd 925:166696
112. Liang R, Du Y, Wu J, Li X, Liang T, Yuan J et al (2022) High performance g-C_3N_4@$NiMoO_4$/$CoMoO_4$ electrode for supercapacitors. J Solid State Chem 307:122845
113. Chameh B, Khosroshahi N, Bakhtian M, Moradi M, Safarifard V (2022) MOF derived CeO_2/$CoFe_2O_4$ wrapped by pure and oxidized g-C_3N_4 sheet as efficient supercapacitor electrode and oxygen reduction reaction electrocatalyst materials. Ceram Int
114. Hasan S, Reaz AH, Das S, Roy CK, Basith M (2022) $CuCo_2S_4$–MoS_2 nanocomposite: a novel electrode for high-performance supercapacitors. J Mater Chem C 10(20):7980–7996

115. Tan F-Z, Ma M-T, Cai W-J, Chen Y-L, Wang Y-H, Zhou J-H (2022) Synthesis of porous biocarbon supported Ni_3S_4/CeO_2 nanocomposite as high-efficient electrode materials for asymmetric supercapacitors. J Saudi Chem Soc 26(5):101530
116. Kumar YA, Mani G, Pallavolu MR, Sambasivam S, Nallapureddy RR, Selvaraj M et al (2022) Facile synthesis of efficient construction of tungsten disulfide/iron cobaltite nanocomposite grown on nickel foam as a battery-type energy material for electrochemical supercapacitors with superior performance. J Colloid Interface Sci 609:434–446
117. Mola BA, Mani G, Pallavolu MR, Reddy NR, Alsaiari NS, Alzahrani FM et al (2021) Ni foam conductive substrate supported interwoven $ZnCo_2S_4$ nanowires with highly enhanced performances for supercapacitors. J Energy Storage 44:103417
118. Li S, Fan J, Liao H, Xiao G, Gao S, Cui K et al (2022) MnCoP/(Co, Mn)$(Co, Mn)_2O_4$ nanocomposites for all-solid-state supercapacitors with excellent electrochemical energy storage. J Electroanal Chem 116866
119. Sun Z, Qu K, You Y, Huang Z, Liu S, Li J et al (2021) Overview of cellulose-based flexible materials for supercapacitors. J Mater Chem A 9(12):7278–7300
120. Tian D, Wang C, Lu X (2021) Metal–organic frameworks and their derived functional materials for supercapacitor electrode application. Adv Energy Sustain Res 2(7):2100024
121. Lamba P, Singh P, Singh P, Singh P, Kumar A, Gupta M et al (2022) Recent advancements in supercapacitors based on different electrode materials: classifications, synthesis methods and comparative performance. J Energy Storage 48:103871
122. Bhat T, Patil P, Rakhi R (2022) Recent trends in electrolytes for supercapacitors. J Energy Storage 50:104222
123. Wang S, Ma J, Shi X, Zhu Y, Wu Z-S (2022) Recent status and future perspectives of ultracompact and customizable micro-supercapacitors. Nano Res Energy 1(2):e9120018
124. Karoń K, Zabłocka-Godlewska E, Krukiewicz K (2022) Recent advances in the design of bacteria-based supercapacitors: current limitations and future opportunities. Electrochim Acta 141068
125. Jiang Y, Guo F, Liu Y, Xu Z, Gao C (2021) Three-dimensional printing of graphene-based materials for energy storage and conversion. SusMat 1(3):304–323
126. Krishnamoorthy K, Pazhamalai P, Manoharan S, Liyakath Ali NUH, Kim SJ (2022) Recent trends, challenges, and perspectives in piezoelectric-driven self-chargeable electrochemical supercapacitors. Carbon Energy

Part II
Fabrication of Functionalized Nanomaterials Based Supercapacitor Platforms

Всё для победы!
НАРОДНЫЙ ФРОНТ
https://pobeda.onf.ru/
LET'S HELP THE RUSSIA

Chapter 5
Additive Manufacturing for Functionalized Nanomaterials Dedicated to Supercapacitors

Jyoti Prakash Das, Sang Jae Kim, and Ananthakumar Ramadoss

Abbreviations

2D	Two-Dimensional
3D	Three-Dimensional
3D-GCA	3D-Printed Graphene Composite Aerogel
AC	Activated Carbon
AFM	Atomic Force Microscopy
AM	Additive Manufacturing
AMSC	Asymmetric Microsupercapacitor
ASC	Asymmetric Supercapacitor
ASTM	American Society for Testing and Materials
CAD	Computer Aided Design
CBA	Cost-Benefit Analysis
CNT	Carbon Nanotube
CV	Cyclic Voltammetry
DED	Direct Energy Deposition
DIW	Direct Ink Writing
EDLC	Electric Double Layer Capacitor
FDM	Fused Deposition Modeling

J. P. Das · S. J. Kim (✉)
Nanomaterials and System Lab, Major of Mechatronics Engineering, Faculty of Applied Energy System, Jeju National University, Jeju 690-756, South Korea
e-mail: kimsangj@jejunu.ac.kr

A. Ramadoss (✉)
School for Advanced Research in Petrochemicals (SARP): Advanced Research School for Technology and Product Simulation (ARSTPS), Central Institute of Petrochemicals Engineering and Technology (CIPET), Chennai 600032, India
e-mail: ananth.cipet@gmail.com; ananth@cipet.gov.in

© The Author(s), under exclusive license to Springer Nature Singapore Pte Ltd. 2024

C. M. Hussain and M. B. Ahamed (eds.), *Functionalized Nanomaterials Based Supercapacitor*, Materials Horizons: From Nature to Nanomaterials,
https://doi.org/10.1007/978-981-99-3021-0_5

GCD	Galvanostatic Charge-Discharge
GO	Graphene Oxide
GNPs	Graphene Nanoparticles
IJP	Inkjet Printing
MOF	Metal Organic Framework
MSC	Microsupercapacitor
PANI	Polyaniline
PPD	p-Phenylenediamine
PPy	Polypyrrole
PEDOT: PSS	Poly(3,4-ethylenedioxythiophene) Polystyrene Sulfonate
PVA	Poly (vinyl alcohol)
SC	Supercapacitor
SEM	Scanning Electron Microscopy
SLA	Stereolithography
SLS	Selective Laser Sintering
SSC	Quasi-solid-state symmetric supercapacitor
LOM	Sheet Lamination
TMO	Transition Metal Oxides
TMDCs	Transition Metal Dichalcogenides

1 Introduction

Additive manufacturing (AM) is evolved as a promising technology to convert the virtual model into real objects with the ease of advanced manufacturing technology with design accuracy and automation in the process [1]. The rapid, accurate method of printing complex structures encourages the widespread implementation of the process in the manufacturing of electronics, including energy storage devices like supercapacitors and batteries with tailor-made shapes to meet the need for IoTs and sensors [2, 3]. The requirement of integrated complex structure for flexible, substrate-free, and integrated electronics 3D printing technology is a breakthrough process. The controlled and regulated mass production of supercapacitors with a fixed area and mass is accessible by printing micro-supercapacitors, wire type, or flexible supercapacitors. The possibility of high mass loading and compact integrated energy storage systems can be achieved by unique product design and proper selection of materials. Depending on the additive manufacturing techniques, the materials belonging to various categories need optimized parameters to provide a successful end product. To obtain the high-energy and power density supercapacitor for commercialization and real-time application materials with large surface area and excellent mechanical properties are highly desired. Currently, metal oxides, carbon-based materials, metal–organic frameworks, novel Two-Dimensional (2D) nanostructures (such as transition metal oxides and MXenes), composite materials, and conducting polymers are widely used for supercapacitor applications [4, 5]. The complexity of 3D printing these materials is the compatibility of materials with the 3D printing software and parameters to print the real-time architecture. To overcome multi-step manufacturing, the 3D printing technique comes up with multi-material printing and coupling various printing processes to obtain the product without any complexity and delay in manufacturing. Polymeric materials as versatile binder help in printing, whereas ceramics contribute to printing electrodes with design flexibility and functional energy storage properties. Implementation of the 3D printing strategy in the fabrication of electrodes and electrolytes subsequently to reduce the integration complexity and production time. Since the invention of the 3D printing technique in the 1980s, the process is upgraded with various printing techniques and standards as categorized by ASTM as (1) Material Jetting, (2) Extrusion, (3) Binder Jetting, (4) Vat-photopolymerization, (5) powder bed fusion, (6) Lamination, and (7) Direct energy deposition. The selection of materials plays a vital role in the fabrication of ready-made products with tailor-made design features. AM technology is capable of providing precise control over electrode fabrication which is complicated to achieve with conventional printing methods. Though AM is not an easy process to achieve improved electrochemical properties, it is a gateway to rapid prototyping and industrialization of supercapacitors without any post-processing or material wasting, unlike traditional processes. Considering the benefits of AM technology, this chapter is focused on various nanomaterials for the 3D printing of supercapacitors via various printing techniques.

1.1 Supercapacitors

Supercapacitors (SCs) are superior in electrochemical energy storage devices due to their high-power density and reasonable energy density [6, 7]. Owing to the excellent power density, the supercapacitors achieve fast charge–discharge cycles and rise as a suitable alternative to batteries [8]. As shown in Fig. 1, based upon the charge storage mechanism, the SCs are categorized into 3 types such as (i) EDLC, (ii) Pseudocapacitive, and (iii) Hybrid-SCs [9, 10]. The type of energy storage behaviour varies depending on the intrinsic qualities of the materials. The inherent properties can be tuned with particle size, surface treatment, and hybridization with compatible reinforcement for a better outcome. Capacitors that operate the charge storage mechanism by the creation of layers of ions at the electrode interface come under the EDLC-type SCs. The porosity of the electrode material plays a vital role in the performance of the SCs. The pseudocapacitors function by the surface redox reactions, which occur simultaneously in the electrodes to facilitate the energy storage mechanism. The 3rd category of SCs comes under the hybrid supercapacitor type, which works on asymmetric configurations comprising two dissimilar type electrodes. Mostly this type of SCs works on redox reaction at the anode (Phase changing materials) and surface absorption desorption at cathodes (EDLC). For a clear idea, the capacitance of the SCs differs, which is the least for the EDLC as compared to the other 2 types of SCs, but the cyclic life of EDLC SCs is a million times with an excellent rate capability of 90%.

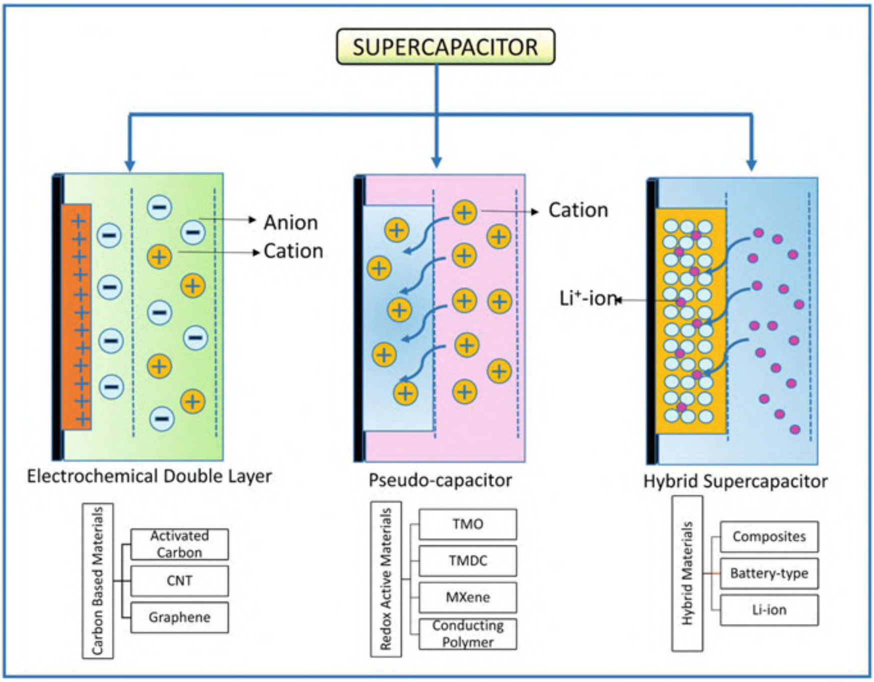
SUPERCAPACITOR
Anion
Cation
Electrochemical Double Layer
Carbon Based Materials
Activated Carbon
CNT
Graphene
Cation
Pseudo-capacitor
Redox Active Materials
TMO
TMDC
MXene
Conducting Polymer
Li⁺-ion
Hybrid Supercapacitor
Hybrid Materials
Composites
Battery-type
Li-ion

Fig. 1 Classification of supercapacitors and materials used for different types of SC application

The pseudocapacitive obtains higher energy storage capacity, whereas the cyclic life is less than EDLCs. The hybrid SCs comprising phase-changing materials and EDLC electrode provides the highest capacity but the least cycle life among the SCs. Apart from these SCs, micro-supercapacitors are in trend for energy storage applications and are applicable for powering microelectronics and IoT devices [11–14].

The types of SCs mostly rely on material properties. The EDLCs comprise carbon-based materials and allotropes, including CNTs and graphene. The pseudocapacitors are mostly transition metal oxides such as ruthenium(IV) oxide, manganese dioxide, nickel oxide, and iron oxide. Among these materials, nanomaterials are desired to be the suitable candidate for the energy storage application due to their high surface-to-volume ratio, providing an excellent active site for energy storage applications [15–17]. The various synthesis strategies, including top-down and bottom-up for the nanomaterials, are essential steps in manufacturing the SCs. However, for better electrochemical performance, the electrodes for SCs application nanomaterials are desired [18–22]. Carbon-based materials, metal oxides, and MXenes, are preferred for 3D printing SCs. The detailed versatility of nanomaterials coupled with AM techniques is discussed later in this chapter.

2 Additive Manufacturing Process for Electrode Printing

Additive manufacturing technology (AM) is a sophisticated process of printing a pre-assigned design in STL format to the printing machine to develop the structure layer by layer [23]. Depending upon the precursor material, the printing can be assisted with extrusion-based deposition or curing-based methods [24]. The broad classification of AM techniques for 3D printing of SC electrodes is highlighted in Fig. 2. The design compatibility with material property is a key characteristic for the classification of AM technique for electrode printing using AM technique.

2.1 Stereolithography (SLA)

SLA is a 3D printing technique developed by 3D systems, works on the principle of layer-by-layer deposition of photocurable resins exposed to ultraviolet (UV) lights [25]. The mechanism of curing resin is a photopolymerization process that deals with the intensity of exposed UV light. Nozzle devoid technique is the primary advantage of this technique, which gives a very fine and smooth final printed product [26].

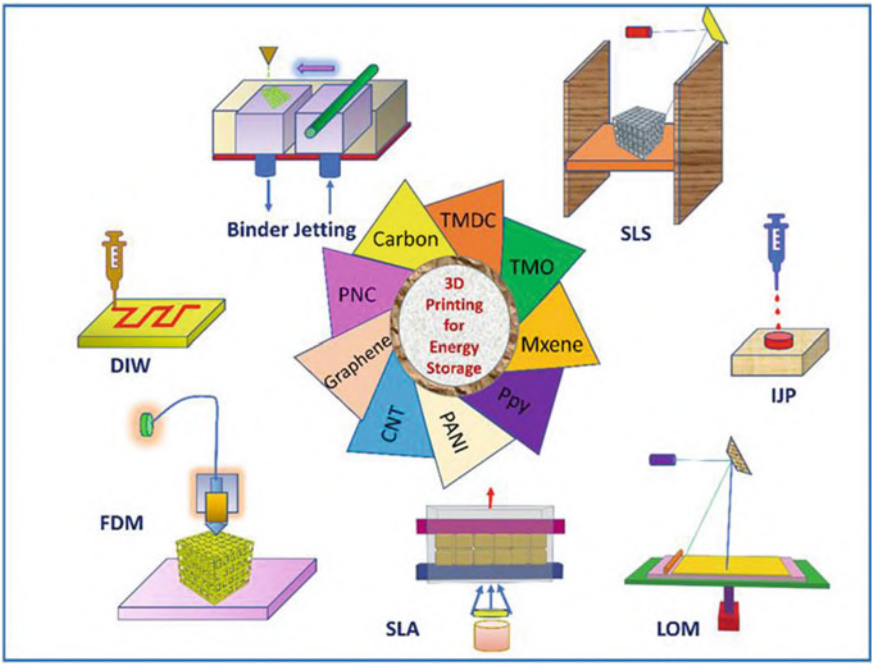

Fig. 2 Various 3D printing techniques and energy storage materials for supercapacitor application

The process is time-consuming and the raw material is quite expensive, which is the drawback of this printing process [27].

2.2 Selective Laser Sintering (SLS)

The SLS technique of 3D printing involves laser-assisted growth of powdered materials layer by layer according to the CAD design [28, 29]. The laser power generated thermal energy sinters the powders and helps to build the final structure. The particle size and purity matter for the quality of prints of this process [30–32]. The laser and raw material costs make it also expensive and the limited raw materials restrict the vast usage of this 3D printing technique. The high precision dimensional accuracy of printed parts can be achieved by this technique [33, 34].

2.3 Inkjet Printing (IJP)

IJP is a versatile extrusion-based 3D printing technique that is assisted with low temperature and pressure to deposit ink drops through the nozzle over the substrate for building the structure [31, 35]. The ink rheology is the major parameter to obtaining quality products through this process. Ink purity governs the final properties of the end product. The compatibility of IJP with various fluids containing functional materials makes it suitable for printing electronic devices with tailor-made architecture [36–39].

2.4 Direct Ink Writing (DIW)

Direct ink writing is a versatile technique for the 3D printing of viscous material in the form of slurry. The printing technique is capable of achieving high precision and complex geometry with functional properties. The end product properties rely on the slurry quality and purity [40]. The rheology of slurry plays a major role in obtaining stable structures. A wide range of ceramics and polymers can be printed by this technique. Printing of functional devices and electronics is possible through the DIW process. The resolution depends on the nozzle size, and a complex design with high precision can be obtained with the ease of the DIW process [41–43].

2.5 Sheet Lamination

Sheet lamination is defined as the lamination object manufacturing (LOM) process. The feedstock for LOM is films or sheets sandwiched one over another until the required thickness is achieved. The product accuracy depends on the sheets' stacking layers and thickness. The LOM products may undergo post-processing to acquire the desired shape by drilling or machining.

2.6 Direct Energy Deposition (DED)

Direct energy deposition is an AM technique dependent on the focused energy source of a laser, electron beam, or plasma to melt the material for printing into the desired shape. The raw materials for the DED process can be powder or wire [44, 45]. The process is high-energy-dependent and quite complex. The process can be used to repair any metal or ceramic structure by additive manufacturing technique. The process can be carried out on curved surfaces, unlike other techniques that need a flat surface.

2.7 Fused Deposition Modeling (FDM)

Fused deposition modeling is an extrusion-based 3D printing technique in which thermoplastic polymer filament acts as the feedstock material [46–49]. The process is economical, and energy-efficient has wide material options for printing, and can be easily equipped with other 3D printing techniques for automation in manufacturing. Dual nozzle-assisted multi-material printing can be achieved by this process [50–53]. The printing parts fail to provide an excellent smooth surface. Composite filaments with active fillers have the ability to print functional devices [54–56].

3 Nanomaterials for SCs

The electrochemical properties of energy materials are dependent on the size, crystal structure, morphology, and existing phases. However, nanomaterials have been proven for excellent electrochemical activities owing to the high surface-to-volume ratio, which provides abundant active sites for superior electrochemical reactions by fastening the transfer of ions and allowing the penetration of the liquids throughout the active surface area [57]. The conventional process of fabricating supercapacitors fails to provide a hike in manufacturing advanced energy storage devices with unique architecture and tailor-made configurable properties [9, 58]. To achieve this goal and commercialize the existing nanomaterials, 3D printing techniques are implemented for SC electrodes. However, the existing nanomaterials and compatible 3D printing techniques are summarized in this chapter to bridge the gap between existing technology and the commercialization of SCs by 3D printing of nanomaterials [59–61].

3.1 Carbon-Based Nanomaterials

The AM techniques largely depend on the inherent properties of the materials for the optimum performance of the printed part. Irrespective of the purity, the pore size also plays a major role in the enhanced electrochemical performance of the 3D-printed part [62–64]. For carbon-based materials, the porosity of carbon provides abundant active sites for the electrochemical reactions and interconnected channels for the electrolyte penetration into the electrode, which plays a vital role in the enhanced capacitance of the SCs [65–67]. Various carbon-based materials like activated carbon (AC), vulcanized carbon, bio-derived carbon, CNTs, graphene, etc., are suitable for supercapacitor applications [68–71]. Graphene is a 2D thin layer of carbon having a 1-atom thickness widely used in energy storage applications for both EDLCs type and hybrid supercapacitors since its introduction. Researchers have implemented AM techniques with graphene and graphene-based composites for energy storage applications [72, 73]. The major necessity for AM technique of graphene is that the material should be in the viscous form (powder, liquid) to be processed by the 3D printing process to acquire stacked layers one over another without any rigidity or discontinuity [74]. Fast curing also matters to obtain the final product without any adverse impact from the surrounding atmosphere. Among a number of processing methods for carbon and graphene-based materials to fabricate composites are mechanical mixing, self-assembly by chemical reactions, molecular level mixing, in-situ synthesis, electrodeposition, hydrothermal, etc. are widely implemented.

The researchers have developed graphene oxide (GO) and graphene nanoparticles as functional ink for DIW of supercapacitors (Fig. 3). In this work, the GO ink precursors along with silica powder and RF catalyst are formulated for the printing process. The printing of micro-lattice structures involves several phases, including i) ink gelation, ii) supercritical drying, iii) carbonization of the printed portion, and iv) hydrofluoric acid etching to remove the silica from the lattice structure. The graphene nanoparticles (GNPs) enhanced the conductivity and maintained the rheology of the aerosol for printing a 1 mm thick electrode capable of delivering 63.6 F g^{-1} at 10 A g^{-1} with an excellent cycle life of 10,000 cycles, as shown in Fig. 4a–d. The excellent stability of the quasi-solid-state symmetric supercapacitor (SSC) is evident from the overlapped initial and final CV scan over 10,000 cycles. The obtained power density of 4 kW kg^{-1} makes it a promising material for AM of SC electrode [75].

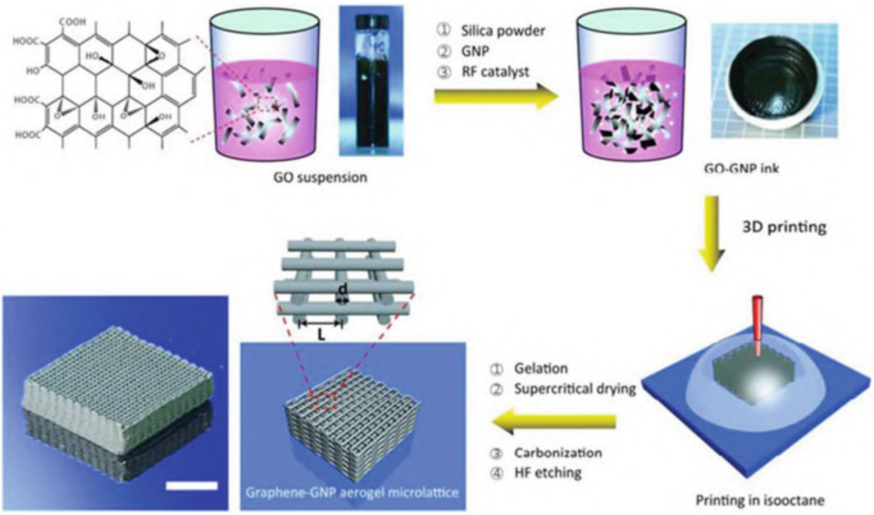

Fig. 3 Schematic representation of the GO-GNP ink for 3D printing of aerosol micro lattice. The fumed silica powder, GNP, and RF catalyst precursor were used for printing the micro lattice through the extrusion technique and dried using carbon dioxide, followed by heating at 1050 °C in an N_2 atmosphere for 3 h. The silica fillers were finally etched using hydrofluoric acid for the final prototype. Reproduced with permission [75]. Copyright © American Chemical Society, 2016

CNT are superior feedstock materials for the DIW process. The thick electrode was fabricated using a composite of Activated carbon and rGO with CNT. The porous composite achieved a capacity of 41.3 F cm^{-3} at 10 A g^{-1}. The thickness obtained was tenfold with a mass loading of 256 mg cm^{-3}. The high mass loading with ultrahigh capacitance is desirable for commercializing the SCs. Excellent cycle stability of 93.3% over 5000 cycles shows the reliability of the material for energy storage applications [76]. A fully printed CNT-based SC was obtained by the DIW process using a polyvinyl alcohol (PVA)-based gel electrolyte. A high capacitance of 15.34 F cm^{-3} with an energy density of 1.2 mWh cm^{-3} and power density of 11.8 W cm^{-3} at 1.32 A cm^{-3} shows the repeatability of using the DIW process to obtain 3D-printed SC [43].

Graphene electrodes with powder bed fusion technique provide a unique strategy to fabricate the SC electrodes without any crack by incorporating Pd nanoparticles, reducing the resistance between layers during stacking. The rGO with a higher surface area combined with binders was undergone printing layer by layer to obtain the desired thickness. After reaching the required thickness, the electrode delivered a specific capacitance of 260 F g^{-1} at 5 A g^{-1} [77]. The researcher printed transparent electrodes with graphene using Inkjet printing technique (Fig. 5a–f). Owing to the advantage of inkjet printing, the author has obtained interdigitated structure electrodes by hard mask printing which is later removed by nitric acid. The as-prepared interdigitated structure of 600μm width and 2.5 mm length with a gap of 200 μm

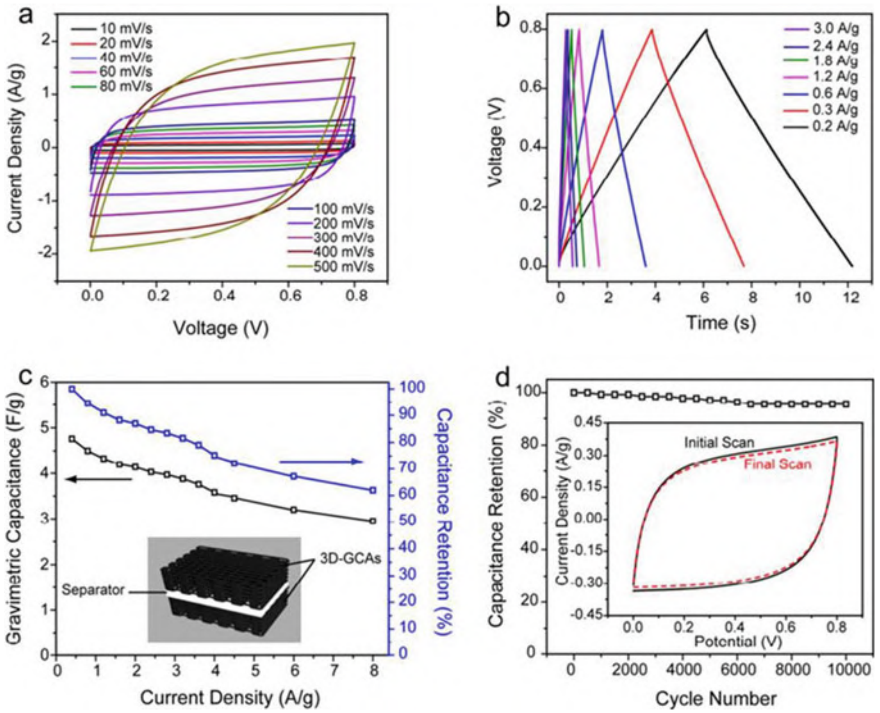

Fig. 4 Electrochemical analysis of 3D-printed graphene composite aerogel (3D-GCA) SSC. **a** cyclic voltammetry (CV) curves in 3 M KOH electrolyte. **b** Galvanostatic Charge/Discharge (GCD) profiles at various current densities. **c** Capacity retention is calculated for various current densities, and the 3D-GCA SSC is shown in the inset. **d** Cyclic stability was tested for 10,000 cycles at a higher scan rate. The inset represents the first and last scan during the stability test. Reproduced with permission [75]. Copyright © American Chemical Society, 2016

is studied after applying the electrolyte dropwise over the active surface. The transparency with respect to electrode thickness was studied and obtained at 99 μF cm^{-1} at 71% transmittance, as shown in Fig. 6a. The transmittance of the printed electrode was found to be reduced by increasing the thickness (Fig. 6b). The thinnest device achieved 90% transparency with a thickness of 550nm. The drying temperature of the ink was optimized to avoid any irregularity of the printed part to obtain a uniform transparent electrode and homogeneous thickness all over. The uniformity in thickness can provide less variation in the surface resistance of the electrodes as evident from the atomic force microscopy (AFM) analysis (Fig. 6c). Further, the scanning electron microscopy (SEM) analysis depicts (Fig. 6d) the uniformity in graphene flake structure with higher surface area for allowing better adhesion of the electrolyte for enhanced electrochemical performance.

The integration of FDM and paste extrusion was carried out by the researchers to print the SC casing and active material, respectively. Activated carbon with sodium carboxymethyl cellulose slurry was paste extruded over the 3D-printed frame. The

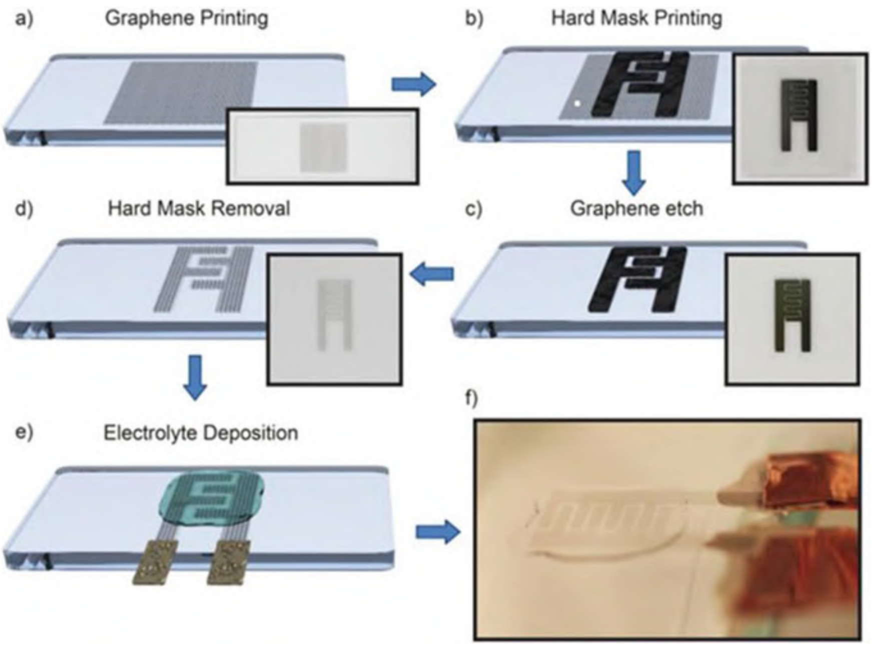

Fig. 5 Fabrication steps for the transparent micro-supercapacitors. **a** Graphene flakes printed on the substrate. **b** Silver ink for printing of a hard mask. **c** The etching of graphene flakes with O_2 plasma. **d** The removal of the hard mask using nitric acid. **e** Gel electrolyte deposition using drop casting. **f** The device image during testing. The finger's dimensions are ~600 μm wide and 2.5 mm long and the gaps between fingers are ~200 μm. Reproduced with permission [78]. Copyright © The Royal Society of Chemistry 2017

PVA gel electrolyte was rolled over the paste extruded part to assemble the SC. A specific capacitance of 238.42 mF g^{-1} and a power density of 95.36 mW g^{-1} at 15 A g^{-1} shows the promising performance of all 3D-printed SC by integrating multiple 3D printing processes. The as-obtained 3D-printed SC is an instance of obtaining automated SC electrode printing for rapid mass production without varying the electrochemical properties [79]. A similar technique was followed to print the SC by implementing PP casing and activated carbon as functional ink for the active material. The capacitance achieved was 599.2 mF cm^{-2} at 10 mVs^{-1}. The capacitance retention was 97.1% at 25 mV s^{-1} for 250 cycles. The cyclic stability though less the printed SCs, seems promising to achieve high-performance SC by integrating 3D printing technique tuning the active material properties [4]. Apart from the composites, carbon-based materials doped with various functional groups proved suitable for the 3D printing of energy storage devices. DIW process was used to print nitrogen-doped GO ink. The rheology control is monitored by the dynamic mechanical analysis characterization. Promising storage modulus over relatively low loss modulus helped to achieve a solid prototype after printing. The vanadium nitride nanoparticles reduced the resistivity of the electrodes following the printing process [71]. The

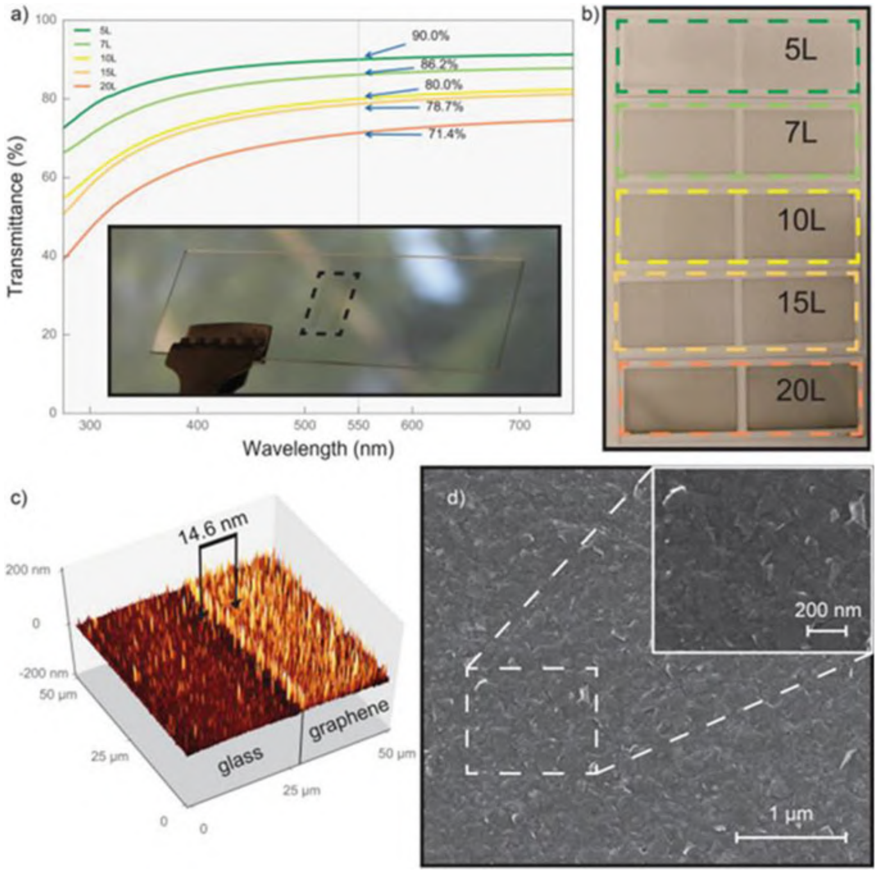

Fig. 6 **a** The large area graphene films with transmittance spectra and inset image of 5L device. **b** The thin films of thicknesses from 5 to 20L with an area of 2 × 3.5 cm. **c** The AFM image of the 5L device. **d** SEM image of the electrode surface and close-up view of the surface in the inset. Reproduced with permission [78]. Copyright © The Royal Society of Chemistry 2017

3D printing process is not limited to virgin precursors. To set a circular economy and put an end to waste materials. Activated carbon synthesized from the packaging waste was converted into printable ink by adding PVA gel. The printed electrodes of thickness half a millimeter that have undergone electrochemical analysis show a capacitance of 328.95 mF cm^{-2} at 2.5 mA. The capacitance retention was obtained at around 90% after 500 cycles. The microporous carbon lacks intermittent ion diffusion in the printed electrodes resulting in a decrement in the capacitance as a resultant at higher scans [80].

This technique was a breakthrough in printing stretchable, transparent 3D-printed SC [78]. The research in carbon-based 3D-printed SCs is envisioned to fabricate high-performance devices by obtaining the synergetic composition of precursors with novel designs and optimized printed parameters. High-mass loading with a tailor-made design aspect can enhance the capacitance and cycle life of the SCs. However, the carbon-based material's purity and porosity will play a major role in tailoring the performance of the final prototype. Owing to the fabrication methods, it can be stated the carbon-based materials, due to their porous structure and ability to be functionalized and ease of making composites, make them a suitable candidate for 3D printing of SCs, whereas maintaining the porosity and composition with melt viscosity is a challenging task for the AM technique for carbonaceous materials.

3.2 Transition Metal Oxides (TMOs)

The transition metal oxides are noble-energy storage materials that exhibit surface redox reactions and the energy storage mechanism belongs to the pseudocapacitive type. The surface redox reactions felicitate oxidation and reduction of the material during charging and discharging, respectively [81]. Despite having better capacitive properties, the TMOs exhibit lesser cycle life as compared to the EDLC-type materials [82]. The hybridization of conductive components with TMOs helps it achieve better cycle life and higher capacitance by increasing the redox-active sites and structural stability [83].

DIW was used to print the graphene aerosol structure, followed by the deposition of MnO_2. The graphene acted as a scaffold, whereas the deposited MnO_2 electrode provided a redox-active area leading to achieving outstanding electrochemical properties. Mass loading of 45.2 mg cm^{-2} archives 11.55 F cm^{-2} at 0.5 mA cm^{-2}. The capacitance increase directly proportional to the active mass loading. 3D printing can govern the increased mass loading of the electrodes leading to the enhanced capacity of the electrodes. The 3E study was performed under 3 M lithium chloride electrolyte and paved the way to fabricated 3D-printed electrodes with redox-active materials grafted over the carbonaceous framework [84]. The tailor-made structure and deposition of redox-active material seem promising for the 3D printing of SCs with TMOs. The TMO nanorods and MnO_2 nanosheets grown over 3D-printed rGO were fabricated to frame the pseudocapacitive 3D-printed electrode and studied under 1 M Poly (vinyl alcohol)/Potassium hydroxide gel electrolyte provides 166.6 mF cm^{-2} and 70.4 mF cm^{-2}, respectively. The obtained cyclic stability of 80% over 10,000 cycles seems promising for 3D printable pseudocapacitive electrodes for SC application.

3.3 Transition Metal Dichalcogenides (TMDCs)

Transition metal dichalcogenides (TMDCs) are thin semiconducting materials comprising of MX_2 structure, where M stands for transition metal atom and X comprises a chalcogen atom where M is sandwiched between two X atoms [85]. The unique band structure of these materials makes them superior for electronic applications. However, the AM technology with unique design prospects opens up the opportunity of implementing the TMDCs in energy storage applications [86]. The abundant redox-active sites, flexibility, and ability to transport charge between stacking layers make the TMDCs versatile energy storage materials. The structure of the material provides high efficiency to accommodate metal ions. The existence of TMDCs in various phases makes them suitable to coexist in various states like semiconducting and metallic. Besides the conventional manufacturing steps of TMDCs-based SCs, 3D printing has been established by a few researchers. Laser-assisted direct writing was employed for printing 1T-MoS_2-based micro-SC. The 1T-MoS_2 films are used for fabricating interdigitated electrodes. PVA-based hydrogel is used for 3E measurement to analyze the electrochemical properties of the materials. As obtained, quasi-rectangular cyclic voltammetry (CV) profiles portray low ESR and highlight the excellent energy storage behavior of 1T-MoS_2 with 93% capacitance retention for 5000 cycles. A capacitance of 36 mF cm^{-2} proves the excellent energy storage ability of TMDCs by 3D printing techniques. The pulse control and ultrashort pulses played a vital role in maintaining the inherent properties of MoS_2 toward achieving high-performance electrodes [87]. The high electrical conductivity and superior hydrophilicity help to achieve energy storage ability and faster ion transportation path in the electrodes to accelerate the electrochemical activities. The enhanced surface area with 3D crumpled technology led to obtaining higher surface area and volume. MSCs were printed benefiting the energy storage ability of the material and ASCs constructed with rGO as nematode resulted in excellent areal power density of 12.6 mW cm^{-2} and energy density of 3.85 μWh cm^{-2} with 96% capacitance retention over 20,000 cycles make it a promising material for 3D printing of SCs (Fig. 7a–g). Further, the CV curves of a single MSC and three series-connected devices exhibit symmetry, with a decrease in current rating and an increase in the potential window. The connected devices can be able to power miniature electronics with a widened potential window. As proven in earlier studies, the ink property is prime in printing the stable electrode. The mixture of IPA and 2-butanol provided uniform dispersion of the functional ink for the electrode printing.

The limited research in the 3D-printed TMDCs can be widened by implementing various functional inks with phase-engineered nanoparticles for high-performance, stable SC electrodes. The stacking ability of ultrathin TMDCs can provide unique morphology as well as redox-active sites for successful and effective energy storage devices.

3.4 MXenes

The current research trend on SCs is focused on MXenes, a 2D layered material with a general formula of $M_{n+1}X_nT_x$, where M is a transition metal, X is carbon or nitrogen atom, T is the termination group (−O, −OH, −H, −F, −Cl) and x is the number of functionalities [89, 90]. The excellent physical and electrochemical properties make MXenes stand alone among the layered and versatile futuristic materials [91–94]. Among the number of MXenes, few series are proven to be suitable for energy

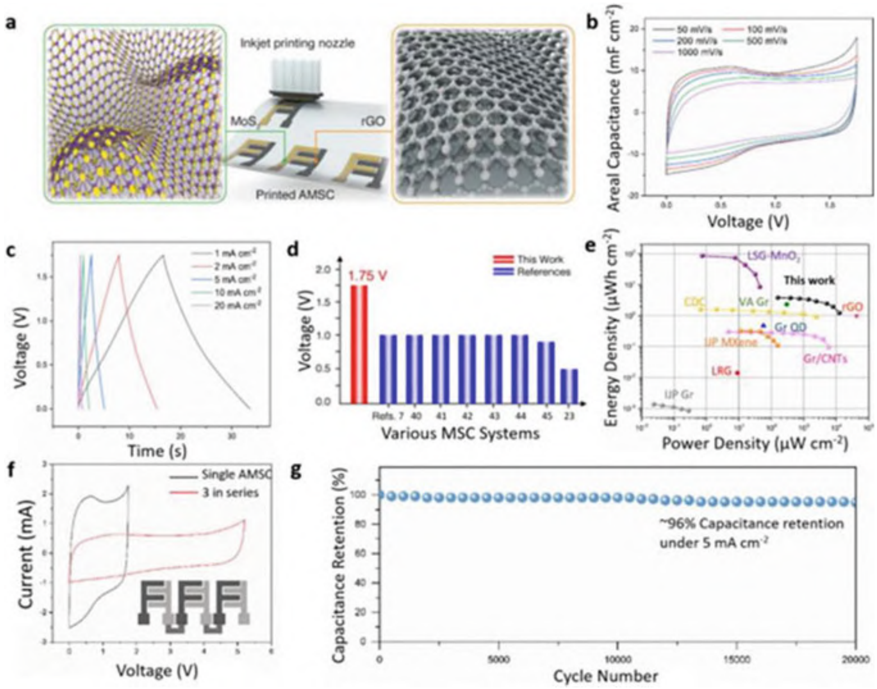

Fig. 7 **a** Schematic showing the asymmetric microsupercapacitor by ink-jet printing (AMSC) with electrodes of 3D 1T c-MoS_2 (left) and rGO (right). **b** CV curves of the printed AMSC in 1.0 M $MgSO_4$ aqueous electrolyte. **c** GCD curves at various current densities. **d** Output voltage of a single AMSC around 1.75 V, which exceeds the previously reported works. **e** Ragone plot with a comparison with other reported articles. **f** Comparison of CV curves of single AMSC and 3 devices connected in series. **g** Excellent cyclic stability for 20,000 cycles with excellent retention of 96%. Reproduced with permission [88]. Copyright © American Chemical Society, 2020

storage applications. But the Ti_3C_2 MXene is reported for AM technique. The pure form, hybridized, or foreign atom-doped MXenes are suitable for efficient energy storage applications [95, 96]. The pseudocapacitive behavior with excellent cycle life provides a better alternative to the other existing material for the SCs electrode fabrication [77, 97–101]. Compared to the conventional pseudocapacitive materials, the MXenes provide better capacitive properties and exhibit excellent cycle life with high-rate capability [102, 103]. Mass production with the top-down approach is desirable for the pure phase extraction of the material and the incorporation of the same into various EDLCs and pseudocapacitive materials for enhanced electrochemical activities [104–106].

MXene electrodes fabricated by stamping technique from the precursor of Ti_3C_2Tx open up a way to 3D print the MXene-based electrodes. The MXene ink was painted over a substrate using the 3D-printed stamp. Stamping is a faster and more economical way to produce large-scale MSC with uniform properties. An areal capacitance of 61 and 50 mF cm^{-2} at 25 and 800 μA cm^{-2} was recorded, respectively [105]. The highly concentrated water-based MXene ink was synthesized to fabricate solid-state MSCs by the DIW process (Fig. 8a–c). The optimized rheological properties with the dispersion of 290 mg mL^{-1} MXene dispersion could print stacked layers of electrode materials. The cross-sectional view as observed in the SEM examination proves the uniformity in the printing technique and optimized ink rheology (Fig.8d–h). The smooth patterned interdigitated structure with uniform dimension has promise for next-generation customised electrode designs for energy storage applications. Poly (vinyl alcohol) (PVA)-based gel electrolyte with stacked layers of 10, denoted as MSC-10, exhibited a capacitance of 1035 mF cm^{-2} at a scan rate of 2 mV s^{-1} (Fig. 9a–d). The fabricated devices acquire excellent flexibility that exhibits homogeneous CV profiles despite varying bending conditions (Fig. 9e). The MSC can withstand strong bending circumstances without degrading its capacitance (Fig. 9f). Furthermore, the series-connected MSCs perform well on the larger potential window (Fig. 9g).

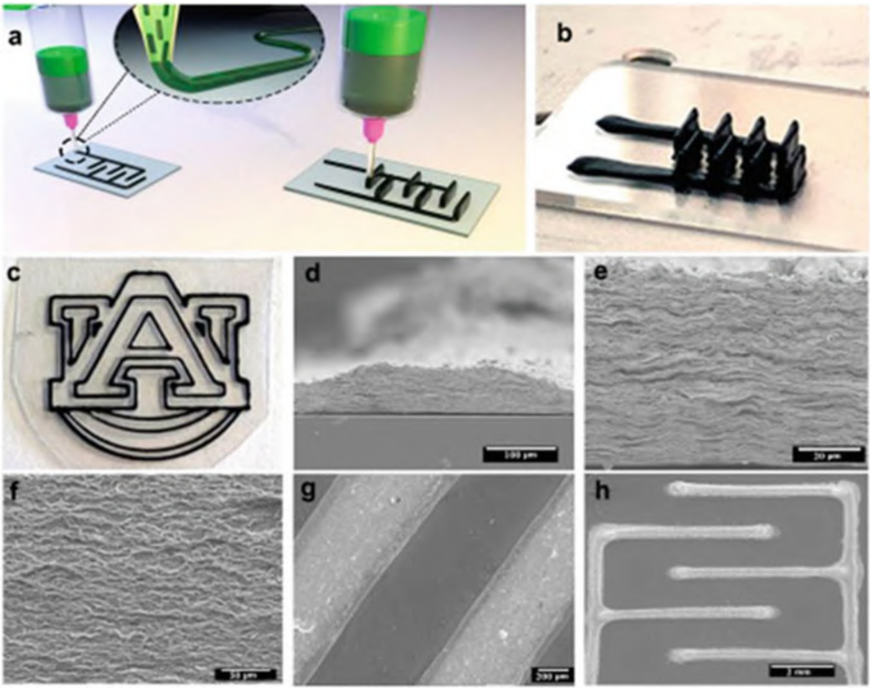

Fig. 8 **a** Schematic of MSCs with interdigital structure. **b** Optical image of the MSC-10 printed on a glass substrate. **c** Optical images of the printed logo. **d**, **e** Cross-sectional SEM image of the electrodes with different magnifications. **f** Side view of the MSC with the alignment of Ti_3C_2Tx flakes. **g** MSC-1 and **h** MSC-5 printed over glass and polymer. Reproduced with permission [107]. Copyright © American Chemical Society, 2020

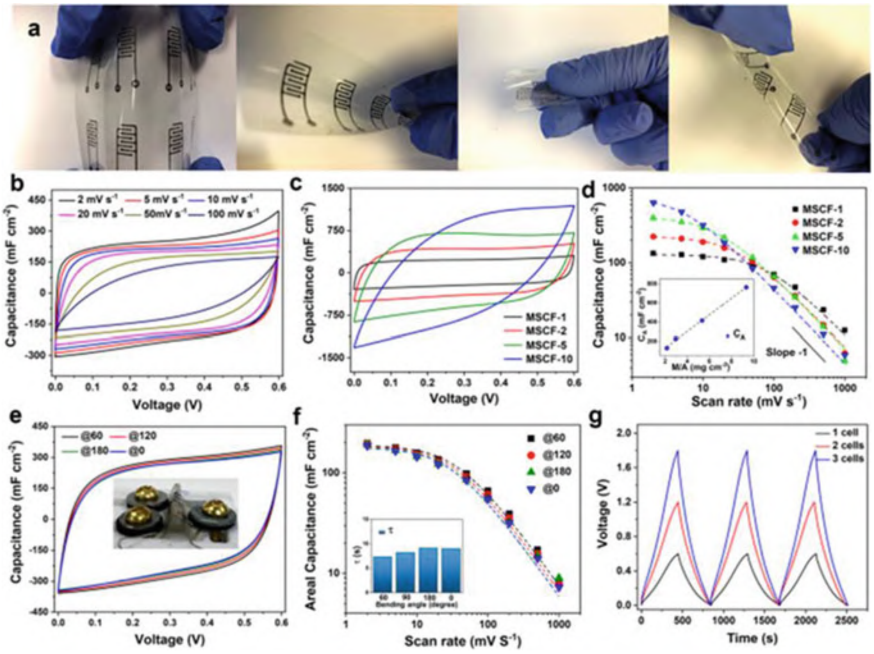

Fig. 9 **a** The 3D-printed devices with excellent mechanical strength. **b** CV curves of MSCF-1 at different scan rates. **c** CV curves at 5 mV s^{-1} for various MSCFs. **d** Areal capacitance versus scan rate for various flexible MSCFs. The inset graph shows areal capacitance derived as a function of the mass loading of the electrodes in MSCFs. **e** Electrochemical performance of MSCF-1 at a 10 mV s^{-1} scan rate under various bending angles of 60°, 120°, 180°, and 0°. **f** Areal capacitance versus scan rate for the MSCF-1 device at different bending angles. **g** Voltage profile of the MSCs at 0.2 mA cm^{-2} for a different number of cells connected in series. Reproduced with permission [107]. Copyright © American Chemical Society, 2020

Owing to the salient features, the material is suitable for electrochemical energy storage applications. Nitrogen-doped MXenes are structurally more stable as the doped atom helps to retain the stacked layers allowing better ion transportation and faster redox reaction (Fig. 10a–g). As seen in the SEM image, the screen-printed MSC electrode has a homogeneous structure (Fig. 10b). The ink rheology study demonstrates the ink's optimal non-Newtonian behaviour, in which viscosity decreases as the shear rate increases (Fig. 10c). When shear stress is minimal, the inks become elastic, but when the shear rate is increased, it can print tiny micropatterns without short-circuiting (Fig. 10d–e). Furthermore, the digital photos clearly show the MSCs' exceptional flexibility, which makes them appropriate for wearable and bendable applications in the future (Fig. 10f–g). Inkjet printing carried out with water-based ink exhibited 66.7 F g^{-1} at 12 mA cm^{-2}. Further, a simple and scalable MXene ink was formulated with optimised ink rheology (Fig. 11a–c). The comparative thickness of the printed filament (Fig. 11d) and SEM analysis (Fig. 11e–f) highlights the uniformity in the printed architecture portraying excellent ink rheology. The 3D printed electrodes exhibit enhanced capacitance as compared to the 2D electrodes irrespective of the type of materials. The excellent energy and power density of the 3D printed MSC outperforms many early reported works making it a promising process for next-generation high-scale production of energy storage devices. At a scan rate of 10 mV s^{-1}, the material portrays an areal capacitance of 8.2 F cm^{-2} with a remarkable energy density of 0.42 mWh cm^{-2} (Fig. 11g–i).

As obtained CV plots from this study, it was observed that the electrochemical performance of the MSCs directly depends on the stacking layers [109]. Irrespective of composition, the no of layers is also responsible for the energy storage capacity of the electrodes. The excellent electrochemical performance seems promising for the 3D printing of flexible devices over polymer substrate for wearable devices and sensors integrated with minimal power supply units for integrated energy storage devices. The ink rheology, MAX phase of the active material, and hybridization of the same with other dopants play a major role in implementing MXenes for the 3D printing of SCs [107]. The simple automation process can establish a commercial approach for the mass production of MXene-based SCs with excellent energy storage capacity.

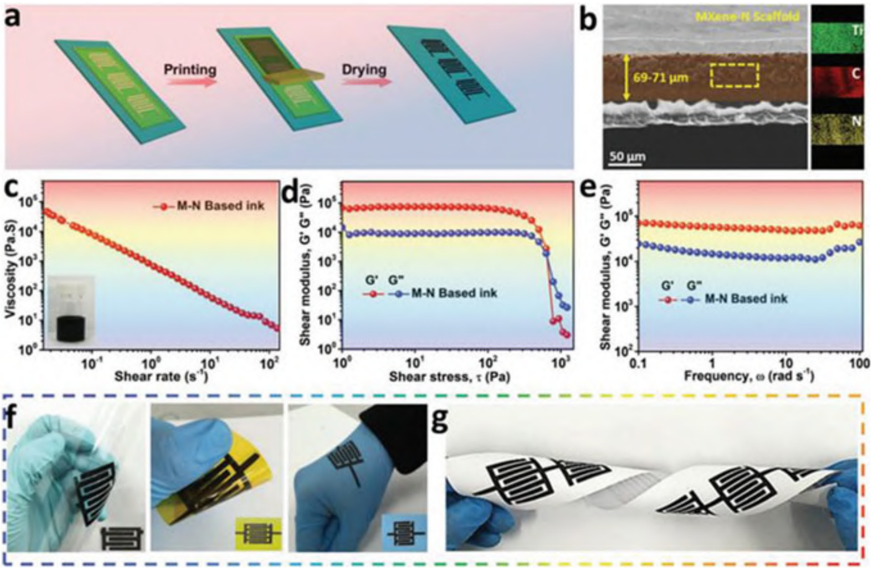

Fig. 10 **a** Schematic depicting the fabrication process of MXene-N micro-supercapacitors via screen printing. **b** Cross-sectional SEM image of the printed electrode and corresponding elemental maps of Ti, C, and N. **c–e** Apparent viscosity of as-fabricated MXene-N ink as a function of shear rate and the storage modulus (G') and loss modulus (G'') of MXene-N ink as functions shear stress and frequency respectively. **f** Digital photos of all-MXene-N printed MSC on various substrates at the bent and flat states. **g** Photo showing the flexibility of MSC devices connected in series. Reproduced with permission [108]. Copyright © 2019 WILEY-VCH Verlag GmbH & Co. KGaA, Weinheim

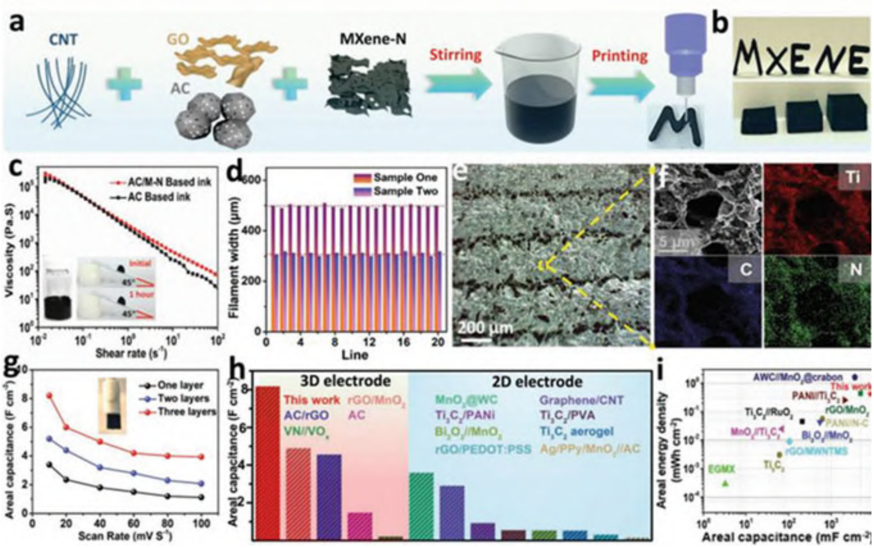

Fig. 11 **a** Schematic illustrating the preparation procedure of 3D-printed designs. **b** 3D-printed photograph patterns using the prepared AC/CNT/MXene-N/GO ink. **c** Rheological analysis of the inks. **d** The thickness of the printing filament by applying two different nozzles. **e**, **f** SEM image of the filaments. **g** Relationship between different layers and areal capacitance at various scan rates. **h** Comparison of the areal capacitance of various electrodes at a scan rate of 10 mV s^{-1}. **i** Ragone plots of 3D-printed SCs compared with other reported works. Reproduced with permission [108]. Copyright © 2019 WILEY-VCH Verlag GmbH & Co. KGaA, Weinheim

The carbon-based active materials incorporated with the MXenes provide a printable viscosity to the as-prepared ink. GO, AC, CNT, and MXene are proven to be printable SC materials for rapid prototyping and mass production of the printed SCs by inkjet printing technology [108].

3.5 Polymer Nanocomposites

The composites of carbon-based, TMOs, TMDCs, and MXenes were discussed earlier, whereas the 3D printing of polymer-based materials has the highest scope for 3D printing of SCs [110]. The easy processability, low melting point, compatibility with a wide variety of fillers, and a wide range of precursor materials make polymer a versatile option for 3D printing [111, 112]. In conventional manufacturing of SCs, polymers act as a suitable binder, in contrast, many works have been carried out to 3D print the supercapacitor casing and packaging due to its excellent insulating properties [113]. The inherent insulation characteristics restrict its direct use in electronics, including supercapacitors. Though few conducting polymers are available that show pseudocapacitive behavior, the high internal resistance hinders its electrochemical performance. So, compounding polymer with active nanofillers can help to overcome the barrier for using electronics applications. The addition of functional nanoparticles like ceramics and carbon-based materials can be incorporated into a polymer matrix and the inherent properties of the additives can be reflected over the insulating properties. Among conducting polymers, PANI, PPy, and PEDOT: PSS play a major role in electronics applications. However, when it comes to the 3D printing of supercapacitors, the active material loading and printing process plays a major role [57].

Graphene has excellent capability to be mixed with polymer matrix [72]. The addition of graphene enhances the mechanical strength and sometimes acts as a fire retardant. Researchers have compounded graphene with a conductive polymer PANI by a self-assembling process carried out in the water and NMP medium, as shown in Fig. 12a–c. The inclusion of rGO in PANI enhanced the viscosity of the ink to make it suitable for printing a stable structure. The simple water base precursors system with conductive ink and GO efficiently printed the 3D scaffold (Fig. 12a). Further, the reduction and dialysis of the printed part provided the final structure for the energy storage application. The apparent viscosity vs shear rate (Fig. 12b) and modulus vs shear rate (Fig. 12c) plots show the optimized viscosity, which makes PANI-GO an injectable ink for 3D printing with high moduli that can produce a stable shape. The 3D printed honeycomb-type structure provides a high surface area due to the unique lattice stacking layers and active exposed surface areas for the electrolyte which can accelerate the ion migration faster and provide excellent electrochemical kinetic reaction (Fig. 13a–h). The controlled rheology of the ink after rGO incorporation provided a stable 3D structure and the printed part delivered a capacitance of 1329 mF cm^{-2} at 5 A g^{-1}. A cyclic stability of 75% was obtained after 10,000 cycles at 50 A g^{-1} [69]. PPy-GO composite was synthesised for energy storage application portraying pseudocapacitive property. The 3D printing process is feasible and can print a stable structure followed by material extrusion, annealing and electrodeposition, respectively (Fig. 14i). The woodpile lattice with orthogonal layers is evident from the SEM analysis (Fig. 14ii). The printed aerogel lattice shows uniform high-quality printing with excellent structural integrity for next-generation energy storage devices. The areal capacitance of 1255 mF cm^{-2} at 5 mA cm^{-2} was recorded as a reliable method for 3D printing of energy storage device [116].

Stretchable MSC was printed using AM and coating techniques together. The printing process was combined with DIW and the casting process. A flexible substrate was coupled with a 3D-printed template for making PANI-based MSC. The composite of PANI-Multi-walled carbon nanotubes was used as electrode material for the MSC. The specific capacitance obtained was 44.13 mF cm^{-2} and the cycle stability obtained was 87% after 20,000 cycles [114]. The unique stretchable properties obtained from the composite were excellent stretchability under various mechanical deformations. PANI/rGO composite was used to print electrodes via the DIW process. The 3D structure was formed by rGO sheets which share a strong pi-bonding with the PANI molecules. The ability of energy storage device is not only reliable on nanostructure but also the dispersed active area that accelerates the

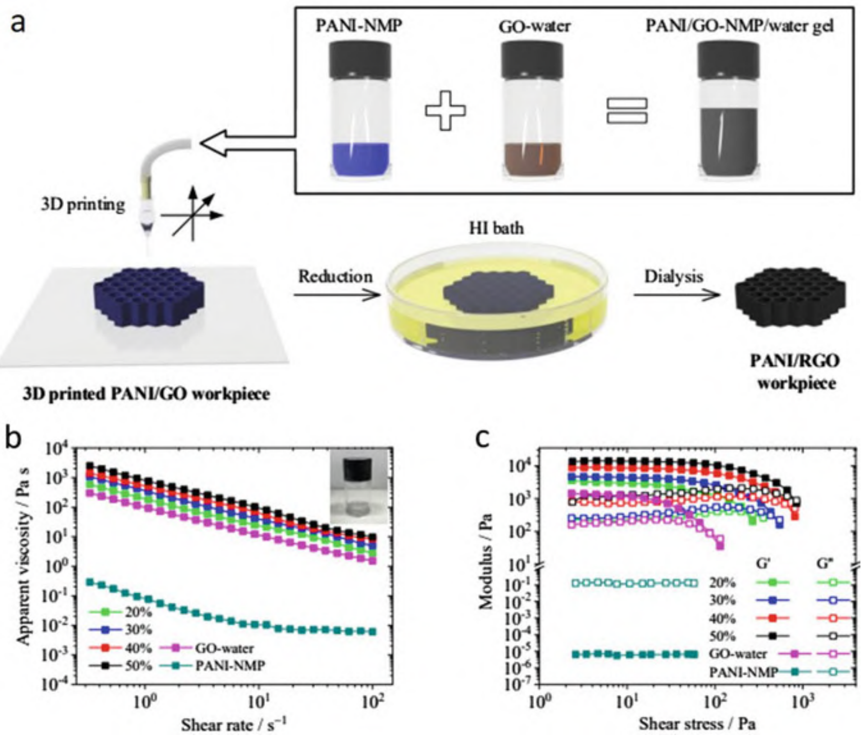

Fig. 12 Additive manufacturing of PANI/GO inks. **a** Synthesis of PANI/GO inks and fabrication of PANI/rGO electrode by 3D printing. **b** Apparent viscosity of PANI/GO inks, GO dispersion, and PANI solution at various shear rates. **c** The measurement of storage modulus (G') and loss modulus (G'') of PANI/GO inks, GO dispersion and PANI solution with respect to the function of shear stress. Reproduced with permission [69]. Copyright © American Chemical Society, 2018

electrochemical reactions. Another 3D printing approach was followed for manufacturing a porous ternary composite of iron, nickel, and PANI via the laser sintering method. The cage of Ni was formed by AM technique to produce the frame to load the supporting materials. The AM process was followed by the electrodeposition of PANI over it. The highest capacitance obtained was 540.68 F g^{-1} at the scan rate of 5 mV s^{-1}. Silica also played an active material in the 3D printing of electrochemical devices by compounding with PANI and PEDOT, respectively [115].

PPY/graphene composite was applied to print the SC using the DIW method [69]. Instead of direct printing, the graphene-based aerogel was coated by PPy to obtain a higher surface area with a conductive path. A specific capacitance of 2 F cm^{-2} and energy density of 0.78 mWh cm^{-2} was obtained, respectively, displaying a reliable approach to 3D printing the energy storage devices [116]. The overall nanocomposite-based SCs highlight the unique feature of functional nanomaterials for 3D printing of energy storage devices. Apart from this, fused deposition modeling with functional filaments was carried out to fabricate mechanically stable conducting filament. The

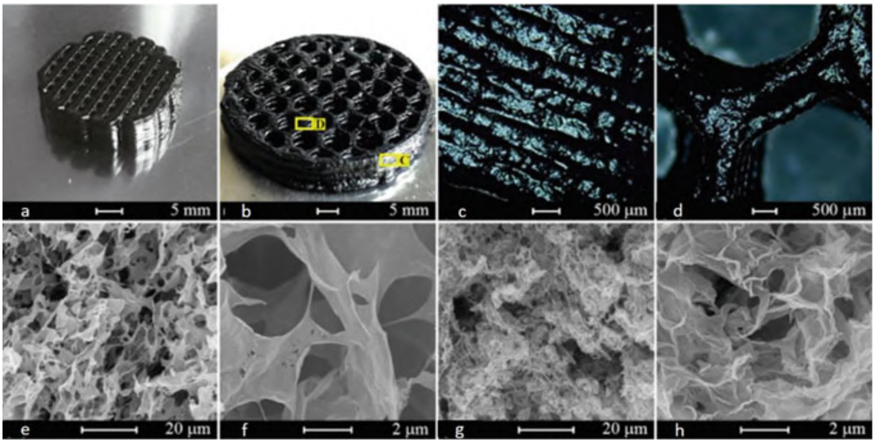
a
5 mm
b
5 mm
D
C
c
500 µm
d
500 µm
e
20 µm
f
2 µm
g
20 µm
h
2 µm

Fig. 13 3D-printed PANI 0.4/GO electrode. **a** Layer-by-layer orthogonal column lattice formation. **b** Honeycomb structure. **c**, **d** Microphotograph of the surface of the honeycomb. **e**–**h** SEM images of PANI0.4/GO electrode. Reproduced with permission [69]. Copyright © American Chemical Society, 2018

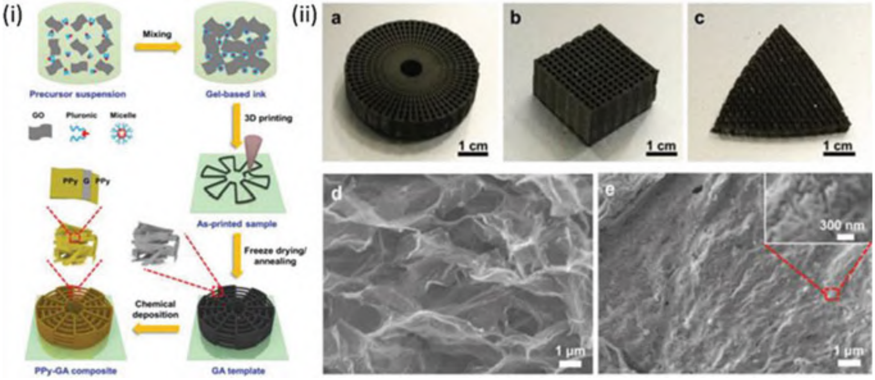
(i)
Mixing
Precursor suspension
Gel-based ink
GO
Pluronic
Micelle
3D printing
PPy G PPy
As-printed sample
Freeze drying/ annealing
Chemical deposition
PPy-GA composite
GA template
(ii)
a
1 cm
b
1 cm
c
1 cm
d
1 µm
e
300 nm
1 µm

Fig. 14 (i) Schematic representation of the fabrication process of 3D hierarchical polypyrrole (PPy)-coated graphene aerogel (GA) composites. (ii) Optical images of 3D-printed structures **a** radial circular, **b** square and **c** triangle GA micro lattices. SEM images showing the cross-sectioned microstructure of **d** GA micro lattice, and **e** PPy–GA composite obtained from 0.1 m pyrrole solution. Inset in **e** higher magnification image of coated PPy. Reproduced with permission [116]. Copyright © 2018 WILEY-VCH Verlag GmbH & Co. KGaA, Weinheim

composite filaments comprised of various graphene loading in polylactic acid matrix was used as the feedstock for the 3D printing process [117]. Further, FDM is one of the most straightforward 3D printing processes. The development of nanocomposite filaments has a vast scope toward commercializing 3D-printed SCs using FDM technology.

4 Challenges and Future Prospects

The current trend of energy storage devices needs portable, scalable, and high-performance electrochemical devices to fulfill the need for electronic gadgets and to get rid of the adverse effect of hazardous materials generally obtained from battery wastes.

i. **Performance evaluation of electrode materials**

   The need of miniaturized devices are an intermittent power supply with fast charging ability. The SC electrode needs to be evaluated with reasonable energy density with excellent power density for the application aspect. The performance of electrode materials need to be evaluated before finalization for the printing application. The compatible 3D printing process can be beneficial for developing high-performance supercapacitors.

ii. **Cost–benefit analysis**

   Cost–benefit analysis is crucial for the real-time implementation of any technology or production sector. In supercapacitor fabrication, the electrode material, electrolyte, and packaging of the final product are considered the major production elements. The mass production of the supercapacitor needs automation in the processing technology, which can be faster and smarter with automation in fabrication techniques to meet the need of the market. The overall production cost can be converted into profitable capita by implementing the 3D printing technique as the manufacturing process, which is capable of supplying the end product faster than any other fabrication technique of supercapacitor by skipping the manual steps of integrating the final device. The viability of the electrode material should be high-performance and long cycle life for a sustainable application.

iii. **Enhanced energy density**

   The major drawback for the SCs is lower energy density, making it difficult to replace the batteries in various application sectors. The mimic of battery material needs to be implemented in SCs applications to obtain higher energy density. The software-controlled manufacturing process can fabricate supercapacitors with an optimized mass ratio for enhanced device capacitance, providing high-energy density supercapacitor devices for real-time application in the automobile and industry sector.

iv. **High-mass loading**

   3D printing techniques can achieve the controlled mass loading of active materials. The software can control the mass deposition to acquire the required deposition of the active materials, which is difficult to achieve with conventional techniques. So, 3D printing with controlled mass deposition is a significant advantage in obtaining high-performance supercapacitors.

v. **Process parameter optimization**

The automation is the process provides various options to customize the printed part from design to final product aspect. The optimization of printing parameters can provide defect-free electrodes with a unique morphology. The porosity and thickness of the layers, along with printing directions, can help to govern the performance of the SCs. Various 3D printing parameters like deposition rate, printing direction, and infill percentage can be optimized by multiple theoretical calculations or simulation software to reduce complexity and make it easy to print the 3D-printed energy storage device.

vi. **Automation in fabrication**

The printing of SCs needs to be continuous to fabricate the device as the end product to minimize the manufacturing complexity and maintain the product's quality without any flaws. The manual assembling of electrodes, electrolytes, and separator needs optimum parameters to fabricate the final device, which makes the production process longer. So, the automation in fabrication by a production line with hybridized different 3D printing processes for smooth automatic production of energy storage devices.

5 Conclusion

This chapter covers various 3D printing processes, printing mechanisms, and nanomaterials for the 3D printing of electrodes. Additive manufacturing has a high potential to commercialize the supercapacitor by printing efficiently, economically, and eco-friendly way with minimal wastage of active materials. The uniqueness of the fabrication technique is the mass scaling of ready-made devices with tailor-made properties. The complex design can be obtained with the ease of 3D designing software for next-generation integrated energy storage systems and for powering IoT devices and sensors. The multi-material and various printing methods provide consumers with a wide range of options to meet the demand. The properties and performance can be tuned with the variation of process parameters and the wise selection of materials. The material properties can be assumed by implementing analysis software to formulate the composition of the active material for the electrochemical application. Structure stability and custom design on a microscopic scale is the advantage of AM technique which can be regulated during the design of the experiment stage before the fabrication of the final product. Integrating different 3D printing techniques can reduce the assembling timing of SCs and establish an automatic production line to manufacture devices rapidly. The ability to print multiple materials is another salient feature of this technique which can configure in-situ printing composite materials without any external reaction. So, the application of nanomaterials, which are used in conventional SCs fabrication, adds the possibility for printing electrodes with intrinsic complex designs, flexible electrodes, and tailor-made properties without any post-processing in a flawless process without compromising the electrochemical performances. Implementing simulations in the material formulation and rationally designed electrode architecture is the future direction of the 3D-printed supercapacitors with functional nanomaterials.

Acknowledgements One of the author A. R thankful to the Technology Mission Division (Energy, Water and all Others), Department of Science and Technology, Ministry of Science and Technology, Government of India, New Delhi, India for the financial support under the Scheme of IC-MAP-2021, Project Title: DST-Storage MAP (Ref. No: DST/TMD/IC-MAP/2K20/01).

References

1. Abdulhameed O, Al-Ahmari A, Ameen W, Mian SH (2019) Additive manufacturing: challenges, trends, and applications. Adv Mech Eng 11:1–27
2. Tofail SAM et al (2018) Additive manufacturing: scientific and technological challenges, market uptake and opportunities. Mater Today 21:22–37
3. Nate K, Tentzeris MM (2015) A novel 3-D printed loop antenna using flexible NinjaFlex material for wearable and IoT applications. In: 2015 IEEE 24th conference on electrical performance of electronic packaging and systems, EPEPS 2015, pp 171–174. https://doi.org/10.1109/EPEPS.2015.7347155
4. Fieber L, Evans JD, Huang C, Grant PS (2019) Single-operation, multi-phase additive manufacture of electrochemical double layer capacitor devices. Addit Manuf 28:344–353
5. Divakaran N et al (2022) Comprehensive review on various additive manufacturing techniques and its implementation in electronic devices. J Manuf Syst 62:477–502
6. Naoi K, Naoi W, Aoyagi S, Miyamoto J, Kamino T (2013) New generation "nanohybrid supercapacitor." Acc Chem Res 46:1075–1083
7. Horn M, MacLeod J, Liu M, Webb J, Motta N (2019) Supercapacitors: a new source of power for electric cars? Econ Anal Policy 61:93–103
8. Conway BE (1991) Transition from "supercapacitor" to "battery" behavior in electrochemical energy storage. J Electrochem Soc 138:1539
9. Devillers N, Jemei S, Péra M-C, Bienaimé D, Gustin F (2014) Review of characterization methods for supercapacitor modelling. J Power Sources 246:596–608
10. Zhao C et al (2014) Three dimensional (3D) printed electrodes for interdigitated supercapacitors. Electrochem commun 41:20–23
11. Jayakumar H et al (2016) Energy-efficient system design for IoT devices. In: 2016 21st Asia and South Pacific design automation conference (ASP-DAC). IEEE, pp 298–301
12. Molefi M, Markus ED, Abu-Mahfouz A (2019) Wireless power transfer for IoT devices—a review. In: 2019 International multidisciplinary information technology and engineering conference (IMITEC). IEEE, pp 1–8
13. Singh S, Sharma PK, Moon SY, Park JH (2017) Advanced lightweight encryption algorithms for IoT devices: survey, challenges and solutions. J Ambient Intell Humaniz Comput 1–18
14. Mayer P, Magno M, Benini L (2020) Smart power unit—mW-to-nW power management and control for self-sustainable IoT devices. IEEE Trans Power Electron 36:5700–5710
15. Sharma P, Kumar V (2020) Current technology of supercapacitors: a review. J Electron Mater 49:3520–3532
16. Kumar KS, Choudhary N, Jung Y, Thomas J (2018) Recent advances in two-dimensional nanomaterials for supercapacitor electrode applications. ACS Energy Lett 3:482–495

17. Li X, Li H, Fan X, Shi X, Liang J (2020) 3D-printed stretchable micro-supercapacitor with remarkable areal performance. Adv Energy Mater 10:1–12
18. Kang K-N et al (2020) Wire-shaped 3D-hybrid supercapacitors as substitutes for batteries. Nanomicro Lett 12:1–13
19. Sahoo S, Kumar R, Joanni E, Singh RK, Shim J-J (2022) Advances in pseudocapacitive and battery-like electrode materials for high performance supercapacitors. J Mater Chem A 10:13190–13240
20. Lu X, Wang C, Favier F, Pinna N (2017) Electrospun nanomaterials for supercapacitor electrodes: designed architectures and electrochemical performance. Adv Energy Mater 7:1601301
21. Lamba P et al (2022) Recent advancements in supercapacitors based on different electrode materials: classifications, synthesis methods and comparative performance. J Energy Storage 48:103871
22. Miller EE, Hua Y, Tezel FH (2018) Materials for energy storage: review of electrode materials and methods of increasing capacitance for supercapacitors. J Energy Storage 20:30–40
23. Hu J (2017) Study on STL-based slicing process for 3D printing. In: 2017 International solid freeform fabrication symposium. University of Texas at Austin
24. Yan X, Tong Y, Wang X, Hou F, Liang J (2022) Extrusion-based 3D-printed supercapacitors: recent progress and challenges. Energy Environ Mater
25. Bártolo PJ (2011) Stereolithography: materials, processes and applications. Springer Science & Business Media
26. Melchels FPW, Feijen J, Grijpma DW (2010) A review on stereolithography and its applications in biomedical engineering. Biomaterials 31:6121–6130
27. Rezaei B, Hansen TW, Keller SS (2021) Stereolithography-derived three-dimensional pyrolytic carbon/Mn_3O_4 nanostructures for free-standing hybrid supercapacitor electrodes. ACS Appl Nano Mater 5:1808–1819
28. Lahtinen E et al (2019) Preparation of highly porous carbonous electrodes by selective laser sintering. ACS Appl Energy Mater 2:1314–1318
29. Olakanmi EO, Cochrane RF, Dalgarno KW (2015) A review on selective laser sintering/melting (SLS/SLM) of aluminium alloy powders: processing, microstructure, and properties. Prog Mater Sci 74:401–477
30. Duddleston LJL, Puck AT, Harris A, Doll NP, Osswald TA (2016) Differential scanning calorimetry (DSC) quantification of polyamide 12 (nylon 12) degradation during the selective laser sintering (SLS) process. Annu Tech Conf - ANTEC, Conf Proc 12:1–4
31. Balliu E et al (2018) Selective laser sintering of inkjet-printed silver nanoparticle inks on paper substrates to achieve highly conductive patterns. Sci Rep 8:1–9
32. Jing W, Hui C, Qiong W, Hongbo L, Zhanjun L (2017) Surface modification of carbon fibers and the selective laser sintering of modified carbon fiber/nylon 12 composite powder. Mater Des 116:253–260
33. van Hooreweder B, Moens D, Boonen R, Kruth JP, Sas P (2013) On the difference in material structure and fatigue properties of nylon specimens produced by injection molding and selective laser sintering. Polym Test 32:972–981
34. Feng S, Cao S, Tian Z, Zhu H, Kong D (2019) Maskless patterning of biodegradable conductors by selective laser sintering of microparticle inks and its application in flexible transient electronics. ACS Appl Mater Interfaces 11:45844–45852
35. Xu Y et al (2014) Inkjet-printed energy storage device using graphene/polyaniline inks. J Power Sources 248:483–488
36. Sajedi-Moghaddam A, Rahmanian E, Naseri N (2020) Inkjet-printing technology for supercapacitor application: current state and perspectives. ACS Appl Mater Interfaces 12:34487–34504
37. Ervin MH, Le LT, Lee WY (2014) Inkjet-printed flexible graphene-based supercapacitor. Electrochim Acta 147:610–616
38. Shim GH, Han MG, Sharp-Norton JC, Creager SE, Foulger SH (2008) Inkjet-printed electrochromic devices utilizing polyaniline–silica and poly(3,4-ethylenedioxythiophene)–silica colloidal composite particles. J Mater Chem 18:594

39. Sundriyal P, Bhattacharya S (2017) Inkjet-printed electrodes on A4 paper substrates for low-cost, disposable, and flexible asymmetric supercapacitors. ACS Appl Mater Interfaces 9:38507–38521
40. Lewis JA (2006) Direct ink writing of 3D functional materials. Adv Funct Mater 16:2193–2204
41. Lewis JA, Smay JE, Stuecker J, Cesarano J (2006) Direct ink writing of three-dimensional ceramic structures. J Am Ceram Soc 89:3599–3609
42. Jiang Y, Cheng M, Shahbazian-Yassar R, Pan Y (2019) Direct ink writing of wearable thermoresponsive supercapacitors with rGO/CNT composite electrodes. Adv Mater Technol 4:1900691
43. Chen B, Jiang Y, Tang X, Pan Y, Hu S (2017) Fully packaged carbon nanotube supercapacitors by direct ink writing on flexible substrates. ACS Appl Mater Interfaces 9:28433–28440
44. Kayaci F, Ozgit-akgun C, Donmez I, Biyikli N, Uyar T (2012) Polymer-inorganic core-shell nanofibers by electrospinning and atomic layer deposition: flexible nylon-ZnO core-shell nanofiber mats and their photocatalytic activity. ACS Appl Mater Interfaces 4:6185–6194
45. Gibson I, Rosen D, Stucker B (2015) Directed energy deposition processes. In: Additive manufacturing technologies. Springer, pp 245–268
46. Vyavahare S, Teraiya S, Panghal D, Kumar S (2020) Fused deposition modelling: a review. Rapid Prototyp J 26:176–201
47. Mireles J et al (2012) Fused deposition modeling of metals. In: 23rd Annual international solid freeform fabrication symposium—an additive manufacturing conference, SFF 2012, pp 836–845
48. Das JP, Divakaran N, Alex Y, Manoj TP, Mohanty S (2023) Fabrication of 3D printing extrusion-based Nylon 12/Bi_2O_3 composite filaments for thermal interface device application. J Manuf Process 85:885–893
49. Mathew J, Das JP, Manoj TP, Kumar S (2022) Development of poly (butylene adipate-co-terephthalate) PBAT toughened poly (lactic acid) blends 3D printing filament. J Polym Res 29:474
50. Rajan K, Samykano M, Kadirgama K, Harun WSW, Rahman MdM (2022) Fused deposition modeling: process, materials, parameters, properties, and applications. Int J Adv Manuf Technol 120:1531–1570
51. Jin YA, Li H, He Y, Fu JZ (2015) Quantitative analysis of surface profile in fused deposition modelling. Addit Manuf 8:142–148
52. Safari A (2001) Processing of advanced electroceramic components by fused deposition technique. Ferroelectrics 263:45–54
53. Sathies T, Senthil P, Anoop MS (2020) A review on advancements in applications of fused deposition modelling process. Rapid Prototyp J 26:669–687
54. Zhang X, Fan W, Liu T (2020) Fused deposition modeling 3D printing of polyamide-based composites and its applications. Compos Commun 21:100413
55. Mohamed OA, Masood SH, Bhowmik JL (2015) Optimization of fused deposition modeling process parameters: a review of current research and future prospects. Adv Manuf 3:42–53
56. Rahim TNAT, Abdullah AM, Md Akil H (2019) Recent developments in fused deposition modeling-based 3D printing of polymers and their composites. Polym Rev 59:589–624
57. Snook GA, Kao P, Best AS (2011) Conducting-polymer-based supercapacitor devices and electrodes. J Power Sources 196:1–12
58. Agrawal JP (1998) Recent trends in high-energy materials. Prog Energy Combust Sci 24:1–30
59. Shown I, Ganguly A, Chen L, Chen K (2015) Conducting polymer-based flexible supercapacitor. Energy Sci Eng 3:2–26
60. Naveen MH, Gurudatt NG, Shim YB (2017) Applications of conducting polymer composites to electrochemical sensors: a review. Appl Mater Today 9:419–433
61. Leigh SJ, Bradley RJ, Purssell CP, Billson DR, Hutchins DA (2012) A simple, low-cost conductive composite material for 3D printing of electronic sensors. PLoS ONE 7(11):e49365
62. Wang Y et al (2009) Supercapacitor devices based on graphene materials. J Phys Chem C 113:13103–13107
63. Foster CW et al (2017) 3D printed graphene based energy storage devices. Sci Rep 7:1–11

64. Ahmad H, Fan M, Hui D (2018) Graphene oxide incorporated functional materials: a review. Compos B Eng 145:270–280
65. Dubey R, Guruviah V (2019) Review of carbon-based electrode materials for supercapacitor energy storage. Ionics (Kiel) 25:1419–1445
66. Li Z, Guo D, Liu Y, Wang H, Wang L (2020) Recent advances and challenges in biomass-derived porous carbon nanomaterials for supercapacitors. Chem Eng J 397:125418
67. Lee S, Zhu W, Nowicki M, Lee G et al (2018) 3D printing nano conductive multi-walled carbon nanotube scaffolds for nerve regeneration. J Neural Eng 15:016018
68. Li J, Mishukova V, Östling M (2016) All-solid-state micro-supercapacitors based on inkjet printed graphene electrodes. Appl Phys Lett 109:123901
69. Wang Z et al (2018) Three-dimensional printing of polyaniline/reduced graphene oxide composite for high-performance planar supercapacitor. ACS Appl Mater Interfaces 10:10437–10444
70. Yao B et al (2020) 3D-printed structure boosts the kinetics and intrinsic capacitance of pseudocapacitive graphene aerogels. Adv Mater 32:1906652
71. Wei N et al (2019) Scalable salt-templated synthesis of nitrogen-doped graphene nanosheets toward printable energy storage. ACS Nano 13:7517–7526
72. Liu C, Yu Z, Neff D, Zhamu A, Jang BZ (2010) Graphene-based supercapacitor with an ultrahigh energy density. Nano Lett 10:4863–4868
73. Tan YB, Lee J-M (2013) Graphene for supercapacitor applications. J Mater Chem A 1:14814–14843
74. Yun J et al (2021) Layer-by-layer assembly of reduced graphene oxide and MXene nanosheets for wire-shaped flexible supercapacitors. ACS Appl Mater Interfaces 13:14068–14076
75. Zhu C et al (2016) Supercapacitors based on three-dimensional hierarchical graphene aerogels with periodic macropores. Nano Lett 16:3448–3456
76. Gao T et al (2019) 3D printing of tunable energy storage devices with both high areal and volumetric energy densities. Adv Energy Mater 9:1802578
77. Azhari A, Marzbanrad E, Yilman D, Toyserkani E, Pope MA (2017) Binder-jet powder-bed additive manufacturing (3D printing) of thick graphene-based electrodes. Carbon N Y 119:257–266
78. Sollami Delekta S, Smith AD, Li J, Östling M (2017) Inkjet printed highly transparent and flexible graphene micro-supercapacitors. Nanoscale 9:6998–7005
79. Tanwilaisiri A et al (2018) Design and fabrication of modular supercapacitors using 3D printing. J Energy Storage 16:1–7
80. Idrees M, Ahmed S, Mohammed Z, Korivi NS, Rangari V (2020) 3D printed supercapacitor using porous carbon derived from packaging waste. Addit Manuf 36:101525
81. Liu X, Ma R, Bando Y, Sasaki T (2012) A general strategy to layered transition-metal hydroxide nanocones: tuning the composition for high electrochemical performance. Adv Mater 24:2148–2153
82. Yi H et al (2021) Recent advance of transition-metal-based layered double hydroxide nanosheets: synthesis, properties, modification, and electrocatalytic applications. Adv Energy Mater 11:2002863
83. Delbari SA et al (2021) Transition metal oxide-based electrode materials for flexible supercapacitors: a review. J Alloys Compd 857:158281
84. Yao B et al (2019) Efficient 3D printed pseudocapacitive electrodes with ultrahigh MnO_2 loading. Joule 3:459–470
85. Monga D et al (2021) Advances in transition metal dichalcogenide-based two-dimensional nanomaterials. Mater Today Chem 19:100399
86. Bissett MA, Worrall SD, Kinloch IA, Dryfe RAW (2016) Comparison of two-dimensional transition metal dichalcogenides for electrochemical supercapacitors. Electrochim Acta 201:30–37
87. Xu C et al (2020) Miniaturized high-performance metallic 1T-phase MoS_2 micro-supercapacitors fabricated by temporally shaped femtosecond pulses. Nano Energy 67:104260

88. Shao Y et al (2020) 3D crumpled ultrathin 1T MoS_2 for inkjet printing of Mg-ion asymmetric micro-supercapacitors. ACS Nano 14:7308–7318
89. Zhang J et al (2017) MXene: a potential candidate for yarn supercapacitors. Nanoscale 9:18604–18608
90. Baig MM, Gul IH, Baig SM, Shahzad F (2022) 2D MXenes: synthesis, properties, and electrochemical energy storage for supercapacitors—a review. J Electroanal Chem 904:115920
91. Vaghasiya JV, Mayorga-Martinez CC, Sofer Z, Pumera M (2020) MXene-based flexible supercapacitors: influence of an organic ionic conductor electrolyte on the performance. ACS Appl Mater Interfaces 12:53039–53048
92. Zhou Y et al (2020) $Ti_3C_2T_x$ MXene-reduced graphene oxide composite electrodes for stretchable supercapacitors. ACS Nano 14:3576–3586
93. Guo Z, Li Y, Lu Z, Liu W (2021) Applications of MXene-based composite fibers in smart textiles. J Phys Conf Ser 1790:012066
94. Levitt A, Zhang J, Dion G, Gogotsi Y, Razal JM (2020) MXene-based fibers, yarns, and fabrics for wearable energy storage devices. Adv Funct Mater 30:2000739
95. Das P, Wu ZS (2020) MXene for energy storage: present status and future perspectives. J Phys Energy 2:032004
96. Redondo E, Pumera M (2021) MXene-functionalised 3D-printed electrodes for electrochemical capacitors. Electrochem commun 124:106920
97. Xie Y et al (2020) High-voltage asymmetric MXene-based on-chip micro-supercapacitors. Nano Energy 74:104928
98. Zhu C, Geng F (2021) Macroscopic MXene ribbon with oriented sheet stacking for high-performance flexible supercapacitors. Carbon Energy 3:142–152
99. Ahmed A, Hossain MM, Adak B, Mukhopadhyay S (2020) Recent advances in 2D MXene integrated smart-textile interfaces for multifunctional applications. Chem Mater 32:10296–10320
100. Vaghasiya JV, Mayorga-Martinez CC, Vyskočil J, Sofer Z, Pumera M (2020) Integrated biomonitoring sensing with wearable asymmetric supercapacitors based on Ti_3C_2 MXene and 1T-phase WS_2 Nanosheets. Adv Funct Mater 30:1–10
101. Fan Z et al (2020) 3D printing of porous nitrogen-doped Ti_3C_2 MXene scaffolds for high-performance sodium-ion hybrid capacitors. ACS Nano 14:867–876
102. Bhat A et al (2021) Prospects challenges and stability of 2D MXenes for clean energy conversion and storage applications. NPJ 2D Mater Appl 5:1–21
103. Li N et al (2021) MXenes: an emerging platform for wearable electronics and looking beyond. Matter 4:377–407
104. Li Y et al (2020) All-solid-state flexible supercapacitor of carbonized MXene/cotton fabric for wearable energy storage. Appl Surf Sci 528:146975
105. Zhang C et al (2018) Stamping of flexible, coplanar micro-supercapacitors using MXene inks. Adv Funct Mater 28:1705506
106. Zhang CJ et al (2019) Additive-free MXene inks and direct printing of micro-supercapacitors. Nat Commun 10:1–9
107. Orangi J, Hamade F, Davis VA, Beidaghi M (2020) 3D printing of additive-free 2D $Ti_3C_2T_x$ (MXene) ink for fabrication of micro-supercapacitors with ultra-high energy densities. ACS Nano 14:640–650
108. Yu L et al (2019) Versatile N-doped MXene ink for printed electrochemical energy storage application. Adv Energy Mater 9:1901839
109. Kurra N, Ahmed B, Gogotsi Y, Alshareef HN (2016) MXene-on-paper coplanar microsupercapacitors. Adv Energy Mater 6:1601372
110. Wang X, Jiang M, Zhou Z, Gou J, Hui D (2017) 3D printing of polymer matrix composites: a review and prospective. Compos B Eng 110:442–458
111. Shi G et al (2018) Graphene platelets and their polymer composites: fabrication, structure, properties, and applications. Adv Funct Mater 28:1–44

112. Zhang F, Feng Y, Feng W (2020) Three-dimensional interconnected networks for thermally conductive polymer composites: design, preparation, properties, and mechanisms. Mater Sci Eng R Rep 142:100580
113. Mohan N, Senthil P, Vinodh S, Jayanth N (2017) A review on composite materials and process parameters optimisation for the fused deposition modelling process. Virtual Phys Prototyp 12:47–59
114. Li L et al (2017) Highly stretchable micro-supercapacitor arrays with hybrid MWCNT/PANI electrodes. Adv Mater Technol 2:1600282
115. Lu X et al (2018) 3D printing well organized porous iron-nickel/polyaniline nanocages multiscale supercapacitor. J Alloys Compd 760:78–83
116. Qi Z et al (2018) 3D-printed, superelastic polypyrrole-graphene electrodes with ultrahigh areal capacitance for electrochemical energy storage. Adv Mater Technol 3:1800053
117. Kim M et al (2019) Electrically conducting and mechanically strong graphene-polylactic acid composites for 3D printing. ACS Appl Mater Interfaces 11:11841–11848

Всё для победы!
НАРОДНЫЙ ФРОНТ
https://pobeda.onf.ru/
LET'S HELP THE RUSSIA

Chapter 6
Photolithographic Fabrication of Supercapacitor Electrodes

Tanuj Kumar, Jyoti, P. Kiran, N. Abhishek, Vandana, and Ashima

1 Introduction

The supercapacitor is a novel power source that will be critical in addressing the needs of new energy storage devices and systems both today and in the future. To fulfill the current and future needs of novel energy storage devices and systems, the supercapacitor is an up-and-coming power source. Compared to batteries, it has a greater power output, longer shelf life, and more cycles before depleting. Electrochemical supercapacitor energy storage technologies have garnered a lot of interest in recent years because of their potential usage in electric cars, pulse power, and backup generators. Several research teams from across the globe are working on high-energy density supercapacitors for use in these systems [1].

Both the double layer and the pseudo-capacitance in supercapacitors are used to store energy. Carbon material has lately been the most popular choice among all supercapacitor electrode materials. Activated carbon, carbon black, aerogel particulate matter, and carbon cloth have all been used to create electrodes for double-layer capacitors [2]. In contrast, monolithic porous carbon aerogels are ideal for use in

---

T. Kumar (✉) · P. Kiran · N. Abhishek
Department of Nanosciences and Materials, Central University of Jammu, Rahya-Suchani, Bagla, Jammu 181143, India
e-mail: tanuj.nsm@cujammu.ac.in

Jyoti
Department of Physics, Govt. College for Women, Gurawara, Rewari 123035, India

Vandana
Department of Physics, Kurukshetra University, Kurukshetra 136119, India

Ashima
Department of Physics and Astrophysics, Central University of Jammu, Rahya-Suchani, Bagla, Jammu 181143, India

© The Author(s), under exclusive license to Springer Nature Singapore Pte Ltd. 2024

C. M. Hussain and M. B. Ahamed (eds.), *Functionalized Nanomaterials Based Supercapacitor*, Materials Horizons: From Nature to Nanomaterials,
https://doi.org/10.1007/978-981-99-3021-0_6

supercapacitors and rechargeable batteries thanks to their advantageous characteristics such as high electrical conductivity, high porosity, tuneable pore structure, and great surface area [1].

Significance of Supercapacitors:

When it comes to electrical storage devices, electrochemical double-layer capacitors also known as supercapacitors or ultra-capacitors are at the top of the heap. This is due to the fact that they have a large energy capacity and output. Supercapacitors are now a crucial instrument for short-term energy storage in power electronics due to advancements in fundamental research, materials, and manufacturing. Supercapacitors may be utilized in novel ways to store power in electronics and industries since they have a higher energy capacity than conventional capacitors. A form of energy storage device with a very high capacity and low internal resistance is a supercapacitor. The electrolytic double layer of a supercapacitor is where the electrical energy is kept. Due to this, these energy storage devices are often referred to as electrochemical double-layer capacitors (EDLC). In 1879, Helmholtz had the first idea for the storage strategy. In an electrolytic double layer, charged species are separated. Supercapacitors, sometimes known as ECDLs, also go by the names ultra-capacitors, boost caps, best caps, and best caps (i.e., Supercars). Because of their high energy and power density, extended lifetime, and large number of cycles, supercapacitors are a suitable method to store energy. Supercapacitors offer a greater specific power than conventional batteries and the ability to store energy in a manner that can be reversed. Electronic applications need passive components that can store electrical energy while being as tiny and light as feasible. How much power the program requires will have a significant impact on the storage device that is employed. Because they don't need an inverter and don't require as much maintenance, uninterruptible power supplies (UPS) that employ ECDL capacitors might save money. Capacitors make it possible to deliver electricity for a short period of time at a considerably greater voltage than batteries can.

2 Supercapacitor

Often referred to as electrochemical capacitors, supercapacitors (SCs) are a kind of energy storage device recognized for their rapid power generation and excellent cycle stability. The capacitance of SCs may be many orders of magnitude larger than that of a conventional capacitor because SCs use thin dielectric liquids and materials with a huge surface area as electrodes. Supercapacitors have a higher energy density and power density than traditional capacitors [3].

SCs may be categorized as Electric Double Layer Capacitors (ELDC) pseudo-capacitors based on the way they store their charge. In contrast to EDLCs, which generally store charge by rapid physical adsorption/desorption of ions at the carbon-based electrode/electrolyte interface, pseudo capacitors employ fast reversible redox processes at the surface, and/or near-surface, of pseudocapacitive materials to store charge (e.g., conducting polymers, transition metal oxides, etc.).

The SCs are a novel kind of capacitor that effectively replaces batteries and electrolytes in terms of performance. While SCs normally have a lower energy density than batteries, their power density maybe 10–100 times higher. As a result of its high-energy storage capacity and rapid discharge rate, SCs are used in a wide range of industrial applications, including microgrids, consumer electronics, transportation vehicles, and regenerative braking systems. In order to ensure the SCs' long-term survival in the face of high peak powers that would otherwise deplete their limited power stores, high energy–density batteries are used as a backup (Fig. 1) [3].

SCs have a lower power density than electrolytic capacitors but a far greater energy density (up to 3 kW kg). The need for energy storage devices that can rapidly store and release a significant quantity of energy has grown as the market for high-tech consumer items expands. SCs are attractive answers to the increasing power needs of future electronic goods because of their high-power capacities [4]. A graphical representation of history of supercapacitors is shown in Fig. 2 [5].

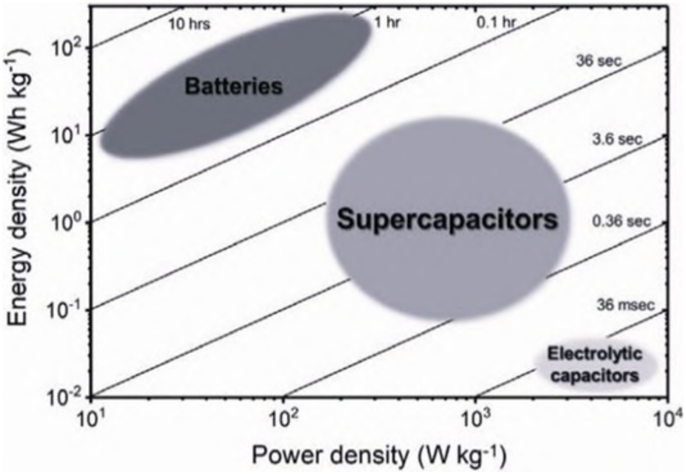

Fig. 1 Ragone plot for various energy storage devices [3]. Permission taken

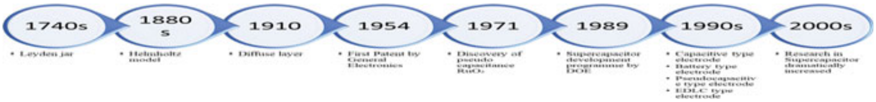
1740s
• Leyden jar
1880s
• Helmholtz model
1910
• Diffuse layer
1954
• First Patent by General Electronics
1971
• Discovery of pseudo capacitance RuO2
1989
• Supercapacitor development programme by DOE
1990s
• Capacitive type electrode
• Battery type electrode
• Pseudocapacitive type electrode
• EDLC type electrode
2000s
• Research in Supercapacitor dramatically increased

Fig. 2 History of supercapacitors [5]. No permission required

3 Supercapacitor Electrodes

Supercapacitor electrodes are highly essential for storage applications and they are the main component of a supercapacitor. To select supercapacitors the following attributes are considered.

High specific surface area: Ions from electrolysis interact with the electrode surface; hence a high specific surface area is necessary. With a large surface area, more of the electrode material is available to be ionized by the electrolyte. Both the electrode material's specific capacitance and energy density are improved as a result of this.

Porosity control: It has an effect on the electrode material's specific capacitance and rate capabilities. In order for electrolytic ions to be adsorbed at the electrode surface, the pore size must be larger than the ionic size of the cation.

High electronic conductivity: A high electronic conductivity is crucial since it defines a material's rate capability and power density. Low resistance and smooth electron transport from electrode to current collector are the results of high conductivity.

Surface electroactive sites: Electroactive regions at the surface attract the electrolytic ions and boost pseudo-capacitance. Pseudo-capacitance is experienced by many electroactive species, including oxygen and nitrogen functional groups, which improves the electrode material's conductivity.

High thermal and chemical stability: Involvement of ion movements during repeated charge/discharge cycles may raise the temperature of the device, thus it's important that it has high thermal and chemical stability. The electrode's stability is enhanced if it is impervious to chemical and corrosion damage.

Low cost and environment-friendly: The low price of the electrode contributes to the supercapacitor's overall low cost. The use of an electrode made from eco-friendly materials is a responsible choice [5].

It is possible to classify the electrode material used in supercapacitors into two groups, i.e., EDLC-type electrodes, which store charges electrostatically at the electrode–electrolyte interface, and pseudocapacitive-type electrodes, which store charges through Faradaic processes [5].

EDLC-type behavior is seen in carbon-based materials, where charges are stored on the electrode surface through a non-Faradaic mechanism. These materials are perfect for the EDLC electrode because of their large surface area and the fact that their pore size may be adjusted. Nanostructured materials with high conductivity, such as carbon nanotubes, carbon fibers, carbon nanofibers, activated carbons, and graphene, reduce the device's resistance. Allotropes of carbon have good corrosion resistance and are safe for the environment [6]. In contrast, metal oxides and conducting polymers have a charge storage mechanism similar to that of pseudocapacitors. This is a Faradaic process, where a reversible redox reaction takes place at the electrode. Because of its ability to change oxidation states, metal oxide may acquire or lose electrons when it is charged or discharged. Faradaic behavior is also exhibited by conducting polymer via doping and de-doping in response to charging and discharging. The material as a whole participates in the process of storing charges, resulting in a very high capacitance value and a high-energy density. It has been documented elsewhere on the many characteristics of the metal oxides utilized in supercapacitor electrodes [5].

4 Fabrication Methods—Photolithography

Synthesizing supercapacitor materials can be done in a few distinct ways. A few examples are the electrochemical deposition, chemical bath deposition, chemical vapor deposition, and the sol–gel technique. Spray coating, inkjet printing, photolithographic technique, and direct writing are only a few of the technologies used to create electrodes for supercapacitors [6].

In this **photolithography** is a commonly used technique for the fabrication of supercapacitors. Photolithography is widely utilized in Micro Electro Mechanical Systems (MEMS) and Nano Electro Mechanical Systems (NEMS) because of its easy production method, cheap cost, high resolution, and maturity as a technology. Photoresists with intricate in-plane patterns can be created using photolithography with the use of a mask. Thus, it's a promising approach for laying the groundwork for the patterning of electrochemically active materials in in-plane micro-supercapacitors. Depositing a layer of active materials and a current collector on the photoresist in two distinct steps is one approach. Energy conversion using programmable materials and nano-bio interface integration are two main areas of study. After the photoresist is peeled away, electrode finger arrays may be used to create the desired patterns. Electrostatic-spray deposition of a graphene oxide and carbon nanotube (GO/CNT) coating over the photoresist pattern, followed by peeling off the photoresist to produce the electrode finger arrays, yielded over-chip micro-supercapacitors with an areal capacitance of 6.1 mFcm^{-2}. To create micro-supercapacitors with MnO_x/Au electrode fingers, electron-beam evaporation was used on the photoresist pattern, followed by a lift-off technique. Selective deposition of active materials on patterned current collectors is another photolithography-based approach to fabricating electrode finger arrays. Commonly, the electrochemically active materials are selectively deposited on current collector arrays that have been created using photolithography and a lift-off procedure. For instance, lateral ultrathin rGO interdigitated electrode finger arrays have been produced by utilizing photolithography to build the current collector arrays and an electrophoretic method to deposit graphene sheets. The pyrolysis of the patterned photoresist is another straightforward method for fabricating electrode finger arrays. This procedure pyrolyzes the photoresist, transforming it into porous carbon with high conductivity and a wide surface area. Electrode fingers with both 2D and 3D architectures have been manufactured. In-plane electrode arrays for micro-supercapacitors are commonly made using photolithography; however, the printed photoresists used as templates must be stripped away in a buffer solution. When heated to a high enough temperature, the photoresist can be pyrolyzed immediately into active electrode arrays. Due to these difficulties, photolithography is rarely used for the direct integration of electrode arrays on electronic devices [7].

A glass or silicon substrate is covered with a thin layer of metal, such as chromium. Above the metal surface is a coating made of a positive or negative photoresist substance, such as a polymer. Radiation causes the positive photoresist material to deteriorate or cause certain chemical bonds to be broken. However, when the negative resist material is exposed, the material becomes harder. The resist-coated surface is covered with a mask. Then, depending on the opaque and transparent portions of the mask, the UV radiation is exposed to the mask, causing weaker or stronger regions on the resist. An appropriate chemical is used to develop the picture. Utilizing the proper chemical treatment, the remaining unexposed material is retrieved [8]. The process is shown in Fig. 3 [8].

There are several types of photolithographs used in industries, depending on the radiation or light applied to the mask. Laser and UV photolithographic methods are mostly used among them. As the name suggests if the mask is subjected to UV radiation, then it is known as UV photolithography, and if a laser source is applied on the mask, it is known as laser photolithography. Micro Super Capacitors (MSCs) have long been created using the traditional photolithography methods. As shown in Fig. 4a, for the fabrication of carbon-based electrodes and the deposition of gold current collectors, ordinary photolithography is always applied. The usage of conventional photolithography is widespread in biodegradable micro-supercapacitor created

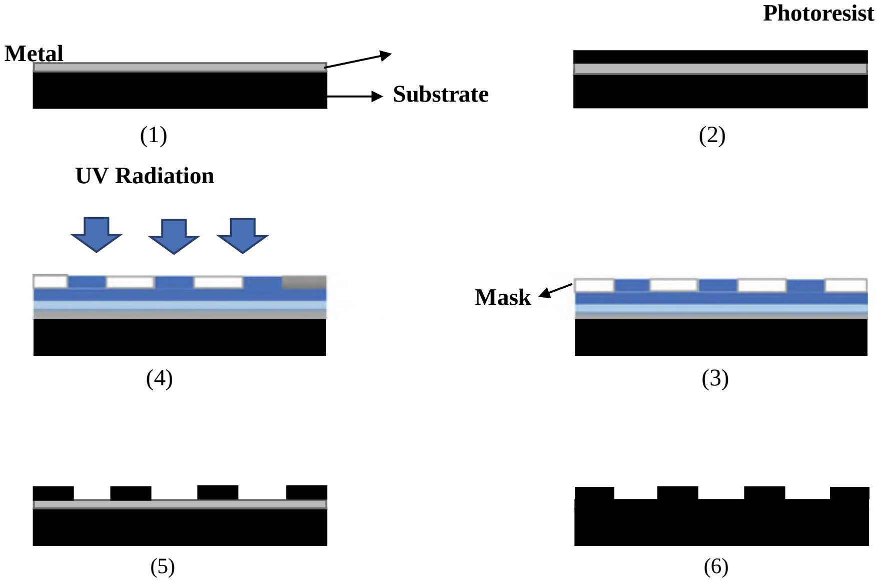

Fig. 3 Process of photolithography [8]. No permission required

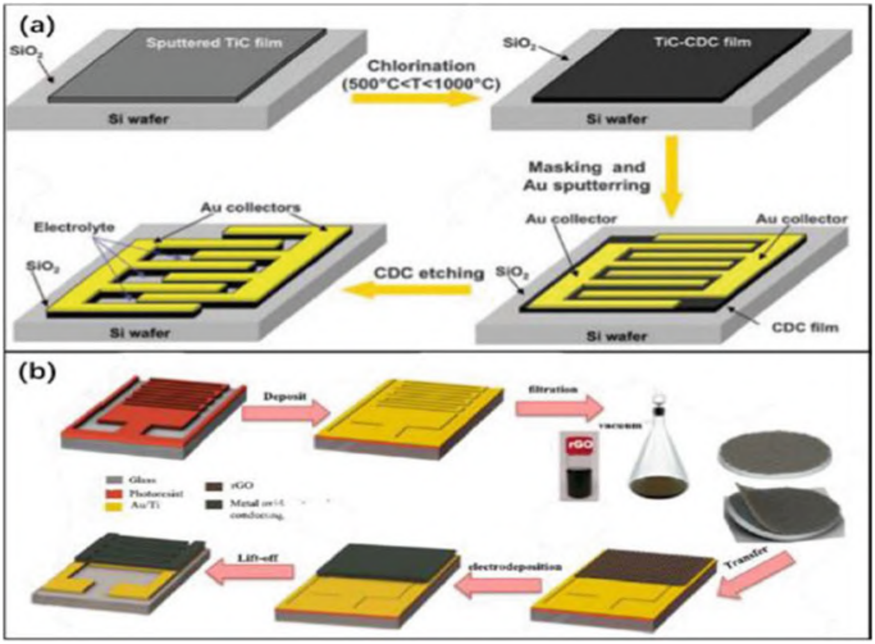
(a)
SiO$_2$
Sputtered TiC film
Si wafer
Chlorination
(500°C<T<1000°C)
SiO$_2$
TiC-CDC film
Si wafer
Masking and
Au sputtering
Au collector
Au collector
SiO$_2$
CDC film
Si wafer
CDC etching
Au collectors
Electrolyte
SiO$_2$
Si wafer
(b)
Deposit
filtration
vacuum
rGO
Glass
Photoresist
Au/Ti
rGO
Metal oxide
conducting
Transfer
electrodeposition
Lift-off

Fig. 4 **a** The fabrication of carbon-based electrodes and the deposition of gold current collectors. **b** Electrode active material films using photolithography [9]. Permission taken Copyright 2023

using a photolithography technique, and an encapsulation strategy that involves managing the constituent material's thickness, chemistry, and molecular weight has been used to have a flexible way to construct various functional longevity.

However, oxygen plasma can only employ to etch a few types of materials, including certain conducting polymers, graphene, and other carbon-based compounds. Figure 4b shows the shaping of various electrode active material films using photolithography. Glass substrates were spin-coated with photoresist, which was then exposed to create patterns in the photoresist. The electrode materials were then applied to the designed photoresist and coated. The photoresist was eventually pulled off and dropped onto the primed electrodes. By employing this technique, the majority of electrodes, including those made of carbon, polymers, and metallic oxides, may be produced by photolithography. This technique made it simple to build electrode hetero-structures. All of these supercapacitors exhibited excellent cycling performance and stability. The production of tiny supercapacitors and practical structures is made possible by the innovative and universal technique, which makes photolithography universally applicable. In order to create flexible conducting polymer MSCs like PEDOT/Au, a lift-off technique (Fig. 4b) can be used that combined traditional photolithography with electrochemical deposition. In

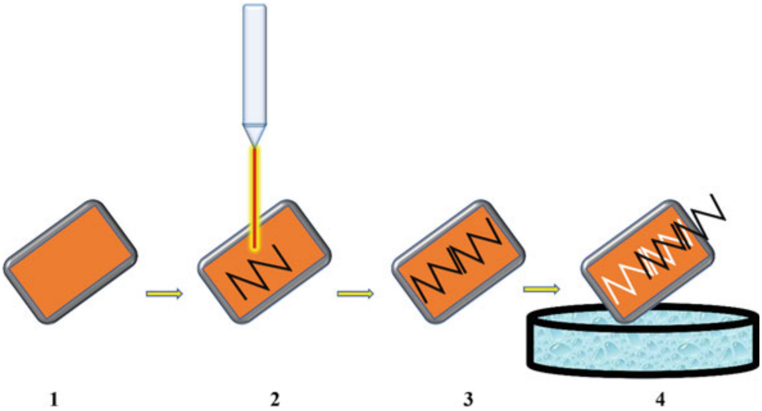

Fig. 5 Schematic diagram of the lignin laser lithography (LLL) technique [10]. No permission required

1 M H_2SO_4 aqueous electrolyte, the MSCs' maximal areal capacitance and volumetric stack capacitance, respectively, were 50 F/cm^3 and 9 mF/cm^2. The PEDOT MSCs' energy density of 7.7 mWh/cm^3 was equivalent with that of a thin-film lithium battery [9].

For example: lignin-based laser lithography is utilized for the fabrication of micro-supercapacitors (MSCs) by use of 3D graphene electrodes.

In particular, lignin films may be transformed into 3D laser-scribed graphene (LSG) electrodes by irradiation of CO_2 laser. Finally, 3D graphene with the desired electrode patterns is retrieved through water lift-off, leaving behind any unexposed lignin that was not removed in the initial stage of processing. The resultant LSG electrodes have a high specific surface area (338.3 m^2g^{-1}), electrical conductivity up to 66.2 S cm^{-1}, and hierarchical porosity. The unnecessity of binders and current collectors makes them ideal for use as MSC electrodes. Because of their high volumetric energy density (1 mWh cm^{-3}), volumetric power density ($\approx$2 W cm^{-3}), and areal capacitance (25.1 mF cm^{-2}), the MSCs created using lignin laser lithography have outstanding electrochemical performance. Flexible electronics, sensors, and on-chip micro-supercapacitors are taking advantage of the versatility of lignin laser lithography [10].

Steps:

1. Lignin-polyvinyl alcohol (PVA) composite film is made on the surface of an ozone-treated polymer substrate by blade-coating lignin-PVA solution (10 wt%) on it.
2. The prepared lignin-PVA film is dried and irradiated by CO_2 laser. The exposed regions are converted into comb-like interdigitated electrodes (in Fig. 5, Step 2 and Step 3).
3. Alkaline lignin is dissolved in water.

4. The unexposed lignin film parts to the laser are removed by the water lift-off process. The electrode of the desired pattern is left on the substrate surface.

Because laser and water-soluble lignin may be used to print any active shape on the substrate, this simple lithography method which we refer to as lignin laser lithography [LLL] is made possible [10].

5 Supercapacitors Performances

- He et al. [11] documented the fabrication of poly-ethylene terephthalate substrate-based high-performance and flexible planar micro-supercapacitors as portable energy storage devices. In order to take advantage of the low processing cost and great cycle stability, they fabricated crosslinked polyaniline (PANI) based MSCs by the thermal crosslinking route and a simple laser printing technology. Following heat treatment in an Argon atmosphere, the flexible PANI MSCs displayed a capacitance of 54 mF cm^{-2} at a current density of 0.3 mA cm^2. Capacitance retention of 79.8% after 1000 cycles is indicative of the devices' superior cyclic stability.
- Wu et al. [12] showed the fabrication of ultrahigh rate, all-solid-state, planar interdigital graphene-based micro-supercapacitors (MSCs) on silicon wafers using reduction aided by methane plasma and photolithographic micro-fabrication of graphene oxide films. Mainly, addition of interdigital fingers from 8 to 32 and decreasing the finger width from 1175 to 219 μm significantly improves the electrochemical performance of MSCs, demonstrating the crucial significance of adjusting widths and number of fingers during the fabrication of high-performance MSCs. Area capacitance of 116 Fcm^{-2} and stack capacitance of 25.9 Fcm^{-3} were achieved by the graphene-based MSCs after fabrication. In addition, they provided a remarkable cycling stability of 98.5% retention in capacitance after 50,000 cycles, a power density of 1270 Wcm^{-3} that was substantially higher than that of electrolytic capacitors, and an energy density of 3.6 $mWhcm^{-3}$ that was similar to that of lithium thin-film batteries. The microdevice also functions effectively at ultrahigh scan rates of up to 2000 V s^{-1}, which is three times more than regular supercapacitor.
- Zhang et al. [13] reported the use of reduced graphene oxide and photolithography technique to fabricate ultrahigh power all-solid-state planar on-chip micro-supercapacitors. Using a modified spin coating technique, they were able to prepare an ultrathin-reduced graphene oxide film having 8 nm thickness, which imparts higher power characteristics to the micro-supercapacitors in the form of fast charge and discharge rates and high conductivity. The electrodes are fabricated using photolithography, and their 150 μm width makes them narrower than those currently in use. These micro-supercapacitors are highly efficient, with a time constant of only 0.03 ms, a power density of 17.94 W cm^{-3}, and cycle stability with a capacitance retention of 94.6% after 10,000 cycles.

- All-solid-state, planar, on-chip MSCs were successfully demonstrated by Zhao et al., using a manufacturing process based on RGO film and photolithography. There was promise for this class of IPC-MSCs to play a role in the long-term improvement of micro-integrated devices. Additionally, they had broadened the MSC's usefulness. Moreover, it demonstrated the benefits and future potential of IPC-MSC in the evolution of MSCs. Stack capacitance and Area of IPC-MSC were 7.90 Fcm^{-3} and 9.48 $\mu\mathrm{Fcm}^{-2}$, respectively, with an energy density of 1.10 mWh cm^{-3} at a small scan rate of 0.01 Vs^{-1}. With a scan rate of 100 Vs^{-1}, its power density was particularly high at 12.7 Wcm^{-3}. High cycle life, fast charging and discharging, stability, and a 98.5% capacitance retention rate after 10,000 charging and discharging cycles were all hallmarks of this class of IPC-MSCs [14].
- Jiang et al. [15] fabricated the planar on-chip MSCs based on NO-GQDs. Patterns of interdigital micro-electrodes have been fabricated using photolithographic methods. Modified liquid–air interface self-assembly approach was used for electrode film fabrication. A superior 99.23% capacitance retention rates were measured after 10,000 cycles at 5000 Vs^{-1}. The MSCs showed more great cycle stability than electrode materials reported earlier. The area capacitance of the MSCs with interdigital micro-electrodes was 18.74 $\mu\mathrm{Fcm}^{-2}$. The areal power density and areal energy density were 116.43 $\mu\mathrm{Wcm}^{-2}$ and 2.60 nWh cm^{-2}. All forms of energy and power's responsiveness were significantly increased. However, at the same moment, the time constant corresponding to it was 10.03 μs. The findings show that NO-GQDs utilized as electrode materials can improve MSC performance.
- Pal et al. [16] documented the utilization of silk protein in the construction of flexible, biodegradable energy storage devices. They constructed a biocompatible and biodegradable thin-film microSC using silk protein Herein. Photopatternable biocomposite ink used is made up of a protein carrier with conducting polymer poly (3,4-ethylenedioxythiophene) polystyrene sulfonate, and reduced graphene oxide dopant. Photolithography is employed to create active electrodes in a non-toxic environment using water as the only solvent. In order to create biodegradable, organic devices with a non-toxic agarose-NaCl gel electrolyte, these electrodes are fabricated on flexible protein sheets. An LED may be powered with demonstrated high capacitance, power density, and cycling stability over 500 cycles. The device is flexible and can withstand cyclic mechanical loads over 450 cycles, and its capacitive qualities are maintained even after several days in liquid. It's important to note that the micro-SCs are cytocompatible and entirely degraded after about a month.

6 Applications of Supercapacitors

Supercapacitors, promising electrochemical energy storage devices with the high-power density and extended cycle life, are piquing the attention of researchers owing to their potential uses ranging from portable electronics to electric cars. Supercapacitors are classified as either electric double-layer capacitors (EDLCs) or pseudocapacitors, depending on the process through which they store charge. While pseudocapacitors are run in accordance with the mechanism of reversible redox reactions happening at the surface or near the surface regions of active materials, EDLCs rely on the separation of charges at the interface of the electrolyte and electrode to store their charges. Because of their cheap cost, electrical conductivity, and large surface area, carbonaceous materials such activated carbons, carbon nanotubes, and graphene have been extensively used in the creation of supercapacitor electrodes [17].

Toy applications

Toy applications are in a different category, with an average run time of less than 10 h [18]. For this kind of use, a supercapacitor with a design life of ten years or several hundred thousand cycles is not the best choice; one with lower performance will do just fine. The biggest markets right now are for devices with voltages under 12 V. It will be around 2004 before the markets for devices with voltages above 48 V reach the same size and give the supercapacitor industry a chance.

GSM applications

The length of the brief 1 A pulse of 0.5 ms is shortened due to the abrupt drop in battery voltage. To put it simply, if it falls below a certain threshold, the phone won't work. The pulse takes much longer to reach the crucial low voltage when utilizing a supercapacitor since the voltage drop is much less. There is more time for real phone use.

SAM

Most supercapacitor applications need the use of a secondary battery to give some degree of autonomy. Montena Components cooperated with HTA-Lucerne to develop the SAM (Super Accumulator Module), a hybridization of supercapacitors and batteries with intelligent control for universal applications. This was made feasible by Lucerne's considerable expertise of supercapacitor applications and their integrated intelligent electronic control management systems. Because batteries and capacitors function in fundamentally different ways, connecting the ECDL in parallel with a battery requires some imagination. The faradaic (redox) energy storage devices are used. When charging and discharging, their voltage remains constant. Capacitors are a kind of electrostatic storage device. Voltage changes as a function of charge Q.

Voltage repartition

The fundamental challenge with supercapacitors is the very low voltage at which they function. In organic electrolytes, this voltage varies between 2 and 3 V (with some hope to 4 V in future). For the most powerful applications, however, much higher voltages of up to 700 V are necessary. Reduced current necessitates smaller, lighter conductors, which is why these voltages are used, although voltage loss in semiconductors is far less of an issue at these higher levels as compared to a 2.5 V application. When connected in series, the supercapacitors form a "system" that achieves the required application voltage. The intercellular voltage gradient is determined by two electrodynamic laws. The voltage is distributed through continuous operation in accordance with the cells' parallel resistance. Capacitance has an important influence on how voltage is distributed across cells during transient operation. The time it takes for a voltage to change rises with device capacitance. If all of the cells had the same parallel resistance and capacitance, the voltage would be constant. This is not the case since the manufacturing process (which accounts for 5–10% of the variance) and temperature both contribute to the dispersion of supercapacitor properties. If the voltage between the electrodes exceeds the electrolyte breakdown potential, the supercapacitor will fail. Finally, the electrolyte as well as the electrodes, conductors, and container determine this. Voltage redistribution is critical for system safety, but it also assures that the cells age at the same pace. This is a well-known problem with electrolytic capacitors, where voltage redistribution is often managed by resistors. This implies that each and every supercapacitor cell must be regulated or protected. To equalize the voltage between the cells, external parallel resistances, Zener diodes, and active power electronics are all employed [19]. The outside resistance must be much smaller than the interior parallel resistances, frequently by a factor of ten or more. This increases the magnitude of the ensuing losses. The typical system efficiency is estimated to be about 16%. When the voltage exceeds the cut-off voltage, the Zener diode starts to conduct. This method might be seen as a kind of cellular defence. The system does not adjust for the unequal voltage across the cells while running at a voltage level lower than the nominal one. As a consequence, aging will appear differently in different cells. The efficiency has now reached 90% depicts how active electronics might increase the system's efficiency to 97%. The power output decreases are caused by transistor resistance. Electronic component selection, especially in terms of the current must be handled. The extent to which this occurs is determined on the degree of imbalance in the cell's characteristics. Costs must be maintained as low as possible, thus efficient manufacturing techniques and temperature distribution across the system are critical. The size of electronic components is determined by an examination of the voltage stresses experienced in the application. Constant and varying stresses are often piled on top of one another. Capacitors benefit from having their resistance dispersed in parallel since they can store energy forever. $T = RC$ denotes the time constant necessary to achieve steady-state behavior, which is typically 500 h.

Electric Composite Automobiles

Supercapacitors may be used in electric composite vehicles. Their acceleration and regenerative braking have both been made possible by supercapacitors. In contrast to conventional gasoline and diesel-powered vehicles, they produce no harmful emissions. Electric buses equipped with CSRCAP supercapacitors have been manufactured by the Chinese business company "Ningbo CSR New Energy Technology", and they utilize 30–50% less energy than conventional electric buses. Supercapacitors were first implemented in a vehicle by PSA in 2010; the company's goal was to create a more efficient starting mechanism by dividing the machine when the car is stopped in neutral. This would allow the car to save more energy than its conventional gasoline or diesel-powered counterparts [20].

Aircrafts and Protection

Aircraft applications for supercapacitors are useful in a wide variety of aircraft applications due to their rapid power supply, long lifespan cycle, and low-temperature operations. These applications include power backup in military vehicles and electronics, armored vehicles, fire control systems in tanks, black boxes in helicopters, backup power/memory hold-up for disaster handheld radios, GPS-guided missiles and projects, airbag organization, and more. Due to their high-power density, they are also used in the aerospace industry, specifically in actuator systems for step departure approaches in launch vehicles, satellites, and on-board systems for spacecraft. Ions such as power backup in military vehicles and electronics, armored vehicles, fire control systems in tanks, black boxes in helicopters, backup power/memory hold-up for disaster handheld radios, GPS-guided missiles and projects, airbag organization, and due to their high-power density also finds use in the aerospace sector, including in actuator systems for step departure approaches in launch vehicles, satellites, and on-board systems for spacecraft [20].

Other applications

Supercapacitors are affordable and have many exciting uses because of their great power density. Elevators, cranes, and pallet trucks are all examples of transportation equipment that may be powered electrically. Tools like flashlights and even hands are used in the military. The use of these devices in medicine ranges from defibrillators to cardiac pacemakers. Pulsed laser welding is a popular method used in manufacturing. Memory modules for mobile devices and computer hard drives are only two examples of consumer-facing software and hardware applications [19].

7 Future Outlook

There has been a rise in demand for micropower sources and compact energy storage units due to the current technical trend toward compact and portable electronic products. Implantable Maintenance-free biosensors, microelectromechanical systems (MEMS), nanorobotics, mobile and remote environmental sensors, and wearable and portable personal electronics all rely heavily on micropower systems [21]. Wireless sensor networks (WSNs) are one such example; they are used in a wide variety of contexts, including industrial and environmental surveillance, military, and agriculture applications due to their small discrete sensing nodes which communicate in a multi-hop fashion [22, 23].

Utilizing an electrolyte having a wider voltage window, fabricating structured electrodes that favor electrolyte ion diffusion, or investigating new materials that facilitate double-layer capacitance and pseudo-capacitance are all ways that micro-supercapacitors can contend with Li-ion batteries for energy storage applications. Micro-supercapacitors will become more widely used in on-chip electronics as novel micro-fabrication techniques become available that allow for their production with high precision and throughput, and as encapsulation techniques become more refined. Additionally, artificial skin, wearable electronics, and even brain-computer systems are anticipated to incorporate flexible and elastic in-plane micro-supercapacitors [7].

In fabricating flexible micro-supercapacitor arrays, Ha and colleagues used elastic serpentine interconnections between micro-supercapacitors [24–27]. However, micro-supercapacitors, which are stretchable, have received less attention. Therefore, in the future, it will be important to concentrate on the engineering of stretchable micro-supercapacitors that maintain good electrochemical behavior throughout stretching and releasing processes and can be implemented as a power supply in stretchy devices. It's true that numerous high-resolution micro-fabrication technologies have been discovered for MSCs, but each one still has its own limits that need to be overcome. For instance, while photolithography has several advantages, such as high resolution, high throughput, and interoperability with commercial microelectronic products, the process is undermined by issues such as buffer solution damage and photoresist contamination to micro-electrodes [28].

The electrochemical performance, including areal energy and power densities, of most MSCs achieved using semiconductor-based methods was unsatisfactory, despite the excellence of high-resolution MSCs, particularly for the nanometre scale size. To begin with, the aforementioned micro-fabrication process typically places severe limitations on the thickness of micro-electrodes, which in turn leads to low mass loading of active materials. Thus, more emphasis should be placed on 3D structure design which is capable of effectively increasing active electrode materials per unit area. Building high electron–ion transport channels is a promising area of research, and one significant path is to create thick electrodes with high mechanical strength based on 3D porous current collector. The brittleness problems that come with increased mass loading also need special attention [28].

References

1. Li J et al (2006) Studies on preparation and performances of carbon aerogel electrodes for the application of supercapacitor 158(1):784–788
2. Chen W-C et al (2004) Electrochemical characterization of activated carbon–ruthenium oxide nanoparticles composites for supercapacitors 125(2):292–298
3. Park J, Kim W (2021) History and perspectives on ultrafast supercapacitors for AC line filtering. Adv Energy Mater 11(27):2003306

4. Yaseen M et al (2021) A review of supercapacitors: materials design, modification, and applications. Energies 14(22):7779
5. Kar KK (2020) Handbook of nanocomposite supercapacitor materials II: performance, vol 302. Springer Nature
6. Vangari M, Pryor T, Jiang L (2013) Supercapacitors: review of materials and fabrication methods 139(2):72–79
7. Qi D et al (2017) Design of architectures and materials in in-plane micro-supercapacitors: current status and future challenges 29(5):1602802
8. Rajendran V, Marikani A (2004) Materials science. Tata McGraw-Hill Pub
9. Zhang H et al (2019) Recent advances in micro-supercapacitors 11(13):5807–5821
10. Zhang W et al (2018) Lignin laser lithography: a direct-write method for fabricating 3D Graphene electrodes for microsupercapacitors. Adv Energy Mater 8(27):1801840
11. He W, Ma R, Kang DJJC (2020) High-performance, flexible planar microsupercapacitors based on crosslinked polyaniline using laser printing lithography 161:117–122
12. Wu Z-S et al (2014) Photolithographic fabrication of high-performance all-solid-state graphene-based planar micro-supercapacitors with different interdigital fingers 2(22):8288–8293
13. Zhang L et al (2019) Photolithographic fabrication of graphene-based all-solid-state planar on-chip microsupercapacitors with ultrahigh power characteristics 126(16):164308
14. Zhao W et al (2020) Photolithographic fabrication of high-voltage output integrated all-solid-state planar on-chip micro-supercapacitors 563(1):87–94
15. Jiang W-T et al (2022) Photolithographic fabrication and electrochemical characterization of planar on-chip micro-supercapacitors based on nitrogen and oxygen co-doped graphene quantum dots with superior capacitance retention rates 594(1):144–150
16. Pal RK et al (2018) Fabrication of flexible, fully organic, degradable energy storage devices using silk proteins 10(11):9620–9628
17. Cao X et al (2014) Three-dimensional graphene materials: preparation, structures and application in supercapacitors 7(6):1850–1865
18. Nickerson J (1999) Fullpower technologies. In: 9th Seminar ECDL Deerfield Beach FL
19. Rufer A, Barrade P (2002) A supercapacitor-based energy-storage system for elevators with soft commutated interface 38(5):1151–1159
20. Karthikeyan S et al (2021) Supercapacitor: evolution and review 46:3984–3988
21. Wang ZL (2010) Toward self-powered sensor networks 5(6):512–514
22. Akyildiz I et al (2002) Wireless sensor networks: a survey. Comput Netw 38:393–422
23. Wang ZL, Wu W (2012) Nanotechnology-enabled energy harvesting for self-powered micro-/nanosystems 51(47):11700–11721
24. Lee G et al (2015) Fabrication of a stretchable and patchable array of high performance micro-supercapacitors using a non-aqueous solvent based gel electrolyte 8(6):1764–1774
25. Hong SY et al (2014) High-density, stretchable, all-solid-state microsupercapacitor arrays 8(9):8844–8855
26. Kim D et al (2013) Fabrication of a stretchable solid-state micro-supercapacitor array 7(9):7975–7982
27. Lim Y et al (2014) Biaxially stretchable, integrated array of high performance microsupercapacitors 8(11):11639–11650
28. Wang S et al (2022) Recent status and future perspectives of ultracompact and customizable micro-supercapacitors 1(2):e9120018

Chapter 7
3D Printing of Supercapacitor

Lolly Maria Jose, Sreehari S, and Arun Aravind

As next-generation energy storage devices, supercapacitors find numerous applications in portable and wearable electronics and conformal other energy storage systems. They are an attractive alternative to conventional batteries due to their higher power density and longer life cycles. Past years have witnessed a boom in solid-state supercapacitor research. The success of supercapacitor research lies in the proper designing and customization of suitable electrode materials. In recent years, many materials using transition metal oxides like MnO, RuO, NiO, many transition metal dichalcogenides and various carbon-derived materials and their hybrid composites have been exploited for their synergistic effects in electrochemical energy storage devices. Though these materials are competent to their carbon-based counterparts, this class of material misses very attractive features of carbonaceous materials like high specific surface area, high electrical conductivity, better cyclic stability and low cost.

Many synthesis methods are being consequently developed to fabricate electrode materials with better performance. Recently, research on additive manufacturing, otherwise 3D printing has been conducted with the prime focus of fabricating a functional electrode system. Along with the context of sustainable fabrication, 3D printing provides the benefit of producing complex 3D structures with high precision and accuracy than that offered by conventional manufacturing techniques. These methods include fused filament printing, direct ink writing and extrusion.

This chapter summarizes the prior reports on 3D printed electrodes till date. Discussion on advantages as well as challenges is necessary for the betterment of electrode fabrication. This chapter also addresses the current challenges as well as future perspectives of 3D electrode printing technique.

L. M. Jose · S. Sreehari · A. Aravind (✉)
Centre for Advanced Functional Materials, Department of Physics, Bishop Moore College, Mavelikara, Affiliated to University of Kerala, Alappuzha, Kerala, India
e-mail: arun@bishopmoorecollege.org

© The Author(s), under exclusive license to Springer Nature Singapore Pte Ltd. 2024

C. M. Hussain and M. B. Ahamed (eds.), *Functionalized Nanomaterials Based Supercapacitor*, Materials Horizons: From Nature to Nanomaterials,
https://doi.org/10.1007/978-981-99-3021-0_7

1 Introduction

1.1 Supercapacitors

Supercapacitors are high-capacity capacitors. That is the capacitance value of these devices is much higher than normal capacitors. It is considered as a clean energy technology that works on the principle of electrochemical energy conversion [1]. Hence a lot of research is going on in the supercapacitance properties of various materials and device fabrication techniques that improve supercapacitance performance. They are now evolved as devices that bridge the gap between electrolytic capacitors and rechargeable batteries. Rechargeable batteries have the advantage of high energy density and long storage span. But they have serious limitations in terms of low power density and high internal resistance, which significantly reduce their ability to deliver power under high current load [2]. The charge–discharge cycles are slower in batteries. In contrast to that, capacitors can store energy faster, but their lower energy density limits the amount of energy they can store.

Supercapacitors, also referred to as electrochemical capacitors or ultracapacitors have higher power higher energy than conventional capacitors and extremely higher energy density than rechargeable batteries. High specific capacitance (C_s), maintenance free design and long life cycle are some other noticeable features of supercapacitors. Figure 1 represents the Ragone plot that represents the energy density and power density of various devices.

Supercapacitors can be classified into two based on their energy storage mechanism: electrical double layer capacitor (EDLC) and pseudocapacitor. EDLCs rely completely on the pure electrostatic charge deposited at the electrode/electrolyte interface, and their capacitance is strongly reliant on the accessible surface area of electrode material for the electrolyte ions [5]. Carbon nanomaterials such as carbon nanotubes (CNTs), graphene, carbon aerogels, activated carbons (ACs) and carbide-derived carbons are some of the unique materials for ELDCs with large specific surface area (SSA). Pseudocapacitors, on the other hand, utilize a fast and reversible faradic process, that causes the transfer of electrons between electrode and electrolyte by de-solvated and absorbed ions. This charge transfer is the only interaction that takes place between the ions and the material, as there is no chemical interaction. The storage of charge increases linearly with applied voltage. Materials chosen for pseudocapacitors should exhibit oxidation–reduction behavior in order to facilitate the intercalation of electrons. Some of such materials used for pseudocapacitors are Transition Metal Oxides (TMOs), Conducting Polymers (CPs), Transition Metal Sulfides (TMDs), etc. The faradic process in pseudocapacitors results in their higher specific capacitance and energy density compared to EDLCs [1]. Schematic representations of ELDC and pseudocapacitor are given in Fig. 2a and b respectively.

Supercapacitors have the potential to be used as a replacement for non-renewable energy devices, because of their clean electrochemical energy conversion mechanism. But there are still limitations in terms of cost, temperature sensitivity, storage

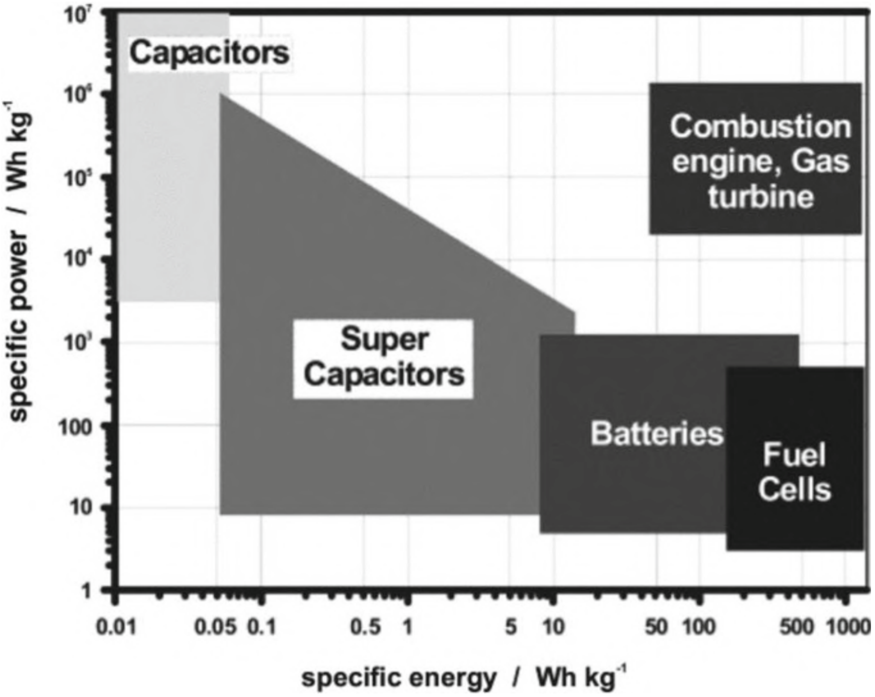

Fig. 1 Ragone plot for various energy storage devices. Reproduced with permission from [3]. Copyright 2004, ACS publications

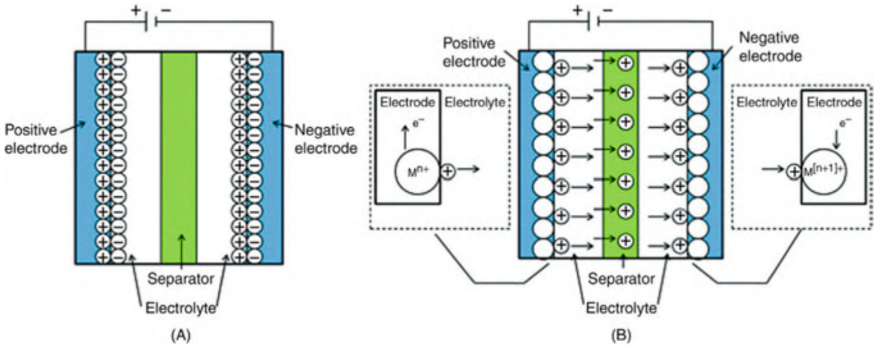
+
−
Positive electrode
Negative electrode
Separator
Electrolyte
(A)
Electrode
Electrolyte
e⁻
Mⁿ⁺
(B)
M⁽ⁿ⁺¹⁾⁺

Fig. 2 Schematic representation of supercapacitors. **a** EDLC. **b** pseudocapacitor (M represents metal atom). Reproduced from [4] with permission from the Royal Society of Chemistry

duration, etc. However, research and development in the field of supercapacitors is ongoing and many of these limitations are expected to be overcome in the future.

To get beyond these constraints, advancements in the development of energy materials are essential. It is crucial to use manufacturing processes that can accurately structure such materials in order to create completely functioning and effective energy conversion and storage systems.

1.2 Introduction to 3D Printing

The world is constantly led by revolutionary inventions. They have surely altered our world, beginning with the stone-age tools and continuing with the steam engine, electricity, computers, microchips, quantum computers, robots and space rockets (to name just a few).

In the early 1950's John Parsons and Frank Stulen at the Massachusetts Institute of Technology (MIT) introduced the concept of Numerical Control (NC) machines [6]. These were the forerunners of computer numerical control (CNC) machines. CNC enables the automated control of machine tools with the aid of a software embedded in a microcomputer attached to the tool. This technique is commonly used in industries that use techniques like abrasive water jet cutting, laser cutting, and electric discharge machining (EDM) for the manufacturing of machining metals and plastic parts. Since the various shapes were created by removing material, these methods were later dubbed "subtractive manufacturing.“ In 1981, it was Hideo Kodama who demonstrated an automatic manufacturing technique that uses photosensitive polymer to create a component layer by layer, bringing out the revolutionary concept of Additive Manufacturing.

American Society for Testing and Materials (ASTM) defines AM as 'the process of joining materials to make objects from three-dimensional (3D) model data, usually layer upon layer' [7]. AM develops products additively rather than by subtracting material from a larger piece. With time, 3D printing has developed to the point that it can now benefit many different business sectors. These benefits include reduced material use, lower costs, and higher production. Additionally, it gives engineers and designers the ability to create anything they need, including prototypes, fits, and visual assistance.

AM is a group of bottom-up technologies that, like the building blocks we used as children, produce objects by adding elements one at a time. Huge machineries or build-up inventories can be discarded or reduced for many products providing environmentally benign and economical productivity. A 3D model of the object created by computer-aided design (CAD) serves as the basis for the AM process. This model is then divided into cross-sectional layers using specially designed software, generating a computer file that is fed to AM machine. Finally, objects are made by the careful addition of each layer of material. Here, products can be sent instantly anywhere on the planet as digital files which can be printed in 3D by any printer that

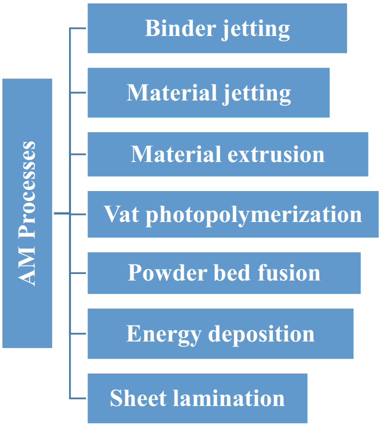

Fig. 3 Classification of different AM methods

meets the design parameters thereby reducing the transportation cost and lessening CO_2 emission.

Additive manufacturing is often interchangeably used with the more popular term 3D. 3D printing is actually a subset of additive manufacturing. Apart from the first stereo lithographic apparatus patented in 1984, the technology is now advanced in a number of printing methods. ASTM accounts for AM as a collection of more than 50 printing technologies which come under seven different processes (Fig. 3). These techniques are again subcategorized into fused deposition molding (FDM), direct ink writing (DIW), inkjet printing (IJP), stereolithography (SLA), laser metal deposition (LMD) and selective laser sintering (SLS). The physical state of the raw materials used—whether they are in liquid, solid, or powder form—can be used as the basis for classification. Process categorization can also be based on the method utilized to fuse the material (thermal, UV, or electron beam) [8].

Similar to how Gutenberg's invention of the printing press in the fifteenth century AD helped establish the groundwork for the spread of knowledge and building up of contemporary civilization, 3D printing has shown promise for changing the electronics sector and human society as a whole.

2 3D Printing and Supercapacitors

Due to its ability to produce highly personalized and complex designs, 3D printing has become a popular method for producing supercapacitors. Highly promising SCs with suitable structures, such as micro, flexible, asymmetric, etc., can be produced in a way that is more straightforward, adaptable, time-saving, and kind to the environment and the economy. Additionally, it offers the potential for reduced prototype costs and the implementation of devices on big, unconventional substrates [9]. Hierarchically structured porous materials can offer a large surface area for reaction, which is why they are extensively utilized in energy conversion and storage systems. The morphology of active materials also plays a significant role. [10] The establishment of a controllable manufacturing of objects with precisely required shape, facets, and surface chemistry continues to present significant obstacles. [11] AM technologies' comparatively low cost and design flexibility can help with these problems. There are countless benefits to 3D printing, which has led to a boom in energy storage research. Figure 4 shows an overview of the prominent AM methods used for supercapacitor fabrication.

Along with the standard benefits of low cost, big area, creation of complex structures, and time savings AM also offers several special characteristics. (1) By allowing for precise control of electrode shape, which encourages the formation of active porous sites, this method raises the specific energy/power density per unit mass, area, and volume of SC. Furthermore, 3D printing can be used to precisely tune the weight of the two electrodes in the case of asymmetric supercapacitors [12, 13]. They show great potential for the manufacturing of ASCs because they can quickly deposit various materials with variable mass loadings/thicknesses on substrates. This is because printing makes it simple to optimize the two electrodes. (2) There are no material restrictions when using 3D printing. By meticulously patterning materials into electrodes using 3D technology, materials where conventional production methods fall short can be selected from a wide spectrum [8]. (3) Since 3D printing encourages less electrode material waste, it positions itself as a more sustainable method of producing electrodes. [14].

SC printing generally entails the preparation, deposition, and solidification of ink. Here, active materials are dispersed into a suspension or a viscous paste followed by deposition and solidification. The ink characteristics, the desired resolution, and the material being printed all play a significant role in the printing process. While ink with a wide variety of viscosities can be patterned using pen-based direct ink writing, inkjet printing requires ink with low, medium, and high viscosities. Even the very minute

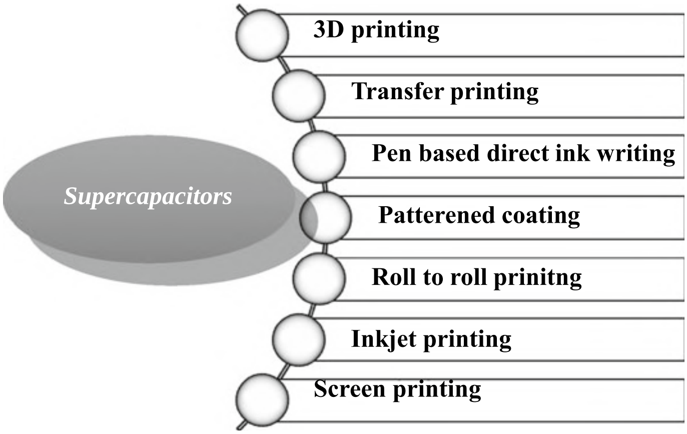

Fig. 4 Prominent printing methods to fabricate SCs

features of the electrode design have to be preserved while depositing and solidifying the ink. For example, while printing a micro supercapacitor the width of interdigital finger electrodes and the distance between adjacent electrodes are in the micrometer range. Getting well-defined electrodes with micrometer-level accuracy, adequate adherence to the substrate/current collector, and no shorting between the positive and negative electrodes is a challenging process. Additionally, to prevent concerns with mechanical fatigue and film delamination, the thermal expansion coefficients of each layer should be the same.

2.1 Printable Supercapacitor Materials

Advent of different printing methods has resulted in the easy fabrication of SC components including electrodes, electrolytes and current collector (Fig. 5). All most all the traditional fabrication techniques demand complex, cost intensive supply chains and was unfavorable for mass production.

The possibility of printing the full supercapacitor device is appealing and advantageous. Seol et al. [15] demonstrated an approach where sequential additive manufacturing is used to create all-printed in-plane SCs (Fig. 6). They used different printing techniques and unique inks with every component. Both the representative types of supercapacitors, EDLC and PC, are constructed and tested. Ag nanoparticle ink can be used for printing the current collector. EDLC ink was made from a mixture of activated carbon, carbon black, polyvinylidene difluoride (PVDF), terpineol and OC-40, the surfactant. Each ink is specially formulated such that any mismatches between viscosity and particle size are avoided. Fused deposition method was used to print the substrates. Current collector, active layer and the electrolyte were printed by direct filament writing. For the EDLC and PC, respectively, the all-printed supercapacitors exhibit specific power and specific energy of 800.3 W/kg and 1.17 Wh/kg (at 0.5 A/g) and 1601 W/kg and 10.6 Wh/kg (at 1 A/g), respectively. The EDLC showed low

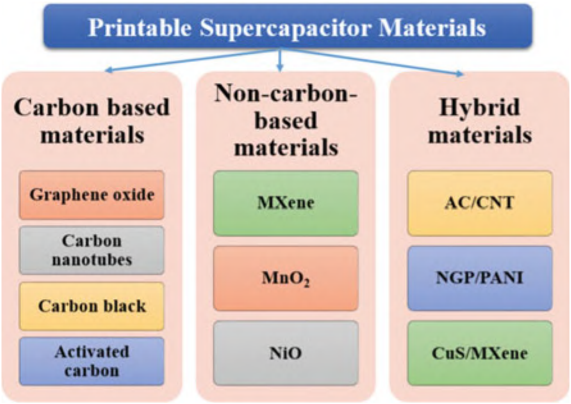

Fig. 5 An overview of printable supercapacitor materials

Fig. 6 Final all-printed supercapacitor. Reprinted with permission from [15]. Copyright 2020 American Chemical Society

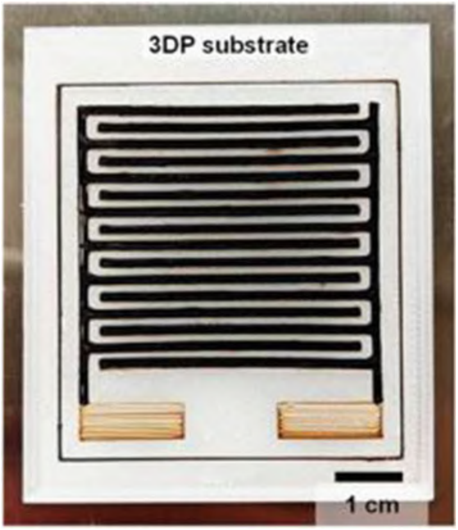

performance departure after 100 000 charge/discharge cycles, according to extended durability testing, whereas the PC shows less than 10% capacitance loss after 25 000 cycles. Having the advantage of maximum resource usage, the all-printed devices are attractive for space applications [16].

AM has the potential for manufacturing small quantities of customized components in a one-step process at a relatively low cost with increased functionality with wide substrate compatibility.

2.2 Fabrication of SC by Different AM Processes

This section goes through an overview of six of the numerous AM techniques presented.

1. **Inkjet printing**

By giving accuracy as fine as 50 μm lateral spatial resolution, which other 3D techniques like screen printing and spray deposition fail to offer, inkjet printing opens up a new route for manufacturing supercapacitors. IJP is a non-contact printing process capable of simultaneous deposition and patterning of electrodes by rapid and controlled impaction and deposition of ink droplets onto desired substrates with the aid of software thereby reducing process complexity [17]. Highly intricate designs with highest accuracy, down to the micrometer scale can be fabricated using IJP. SC printing success depends on the quality, processability, and long-term durability of printing ink. Ink must satisfy the demands of every separate component depending on the specific printing method. Almost all components including electrode, electrolytes and current collectors can be well produced by the proper formulation and design of printing ink. Every ink used for a particular printing application needs to have compatible qualities (viscosity (μ), surface tension (σ), density(ρ)). For a fixed nozzle diameter (d), a stable inkjet drop will be achieved if the Ohnesorge number $Z = \sqrt{\rho d \sigma}/\mu$ is between 1 and 10. Ink is viscous enough if viscosity lies within the range of 8-25mPas and surface tension is ≈30 Nm^{-1} [18]. Additionally, inks must be designed so that they do not interact at the interface, lowering device performance. Figure 7 is a schematic representation of ink/resin-based AM technique.

Le et al. [20] followed inkjet printing method for the fabrication of SC electrodes of graphene oxide nanosheets, stably dispersed in water. Electrodes were coated on

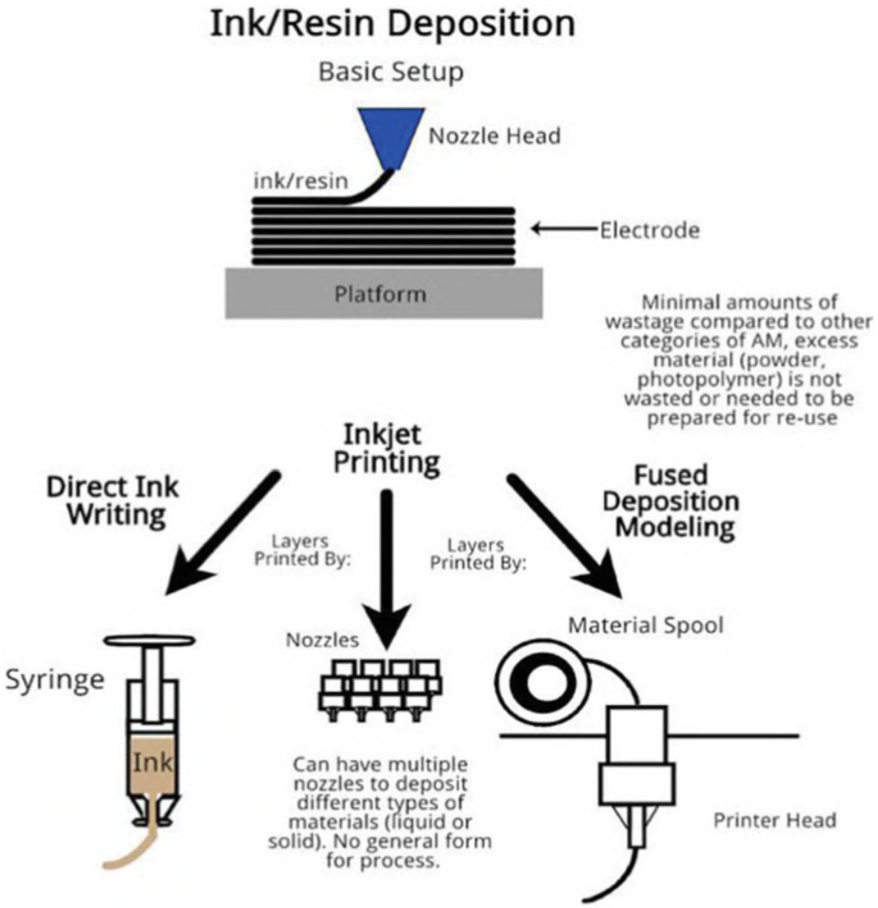
Ink/Resin Deposition
Basic Setup
Nozzle Head
ink/resin
Electrode
Platform
Minimal amounts of wastage compared to other categories of AM, excess material (powder, photopolymer) is not wasted or needed to be prepared for re-use
Inkjet Printing
Direct Ink Writing
Fused Deposition Modeling
Layers Printed By:
Layers Printed By:
Syringe
Ink
Nozzles
Can have multiple nozzles to deposit different types of materials (liquid or solid). No general form for process.
Material Spool
Printer Head

Fig. 7 Schematic illustration of ink/resin-based AM technique. Reprinted from [19], Copyright (2021), with permission from Elsevier

to Ti foils and the printed electrodes were thermally reduced at 200 ˚C in N_2, probably a new method for the fabrication of graphene electrodes. Specific capacitance ranged from 48 to 132F/g in the scan range of 0.5−0.01 V/s. The electrochemical performance of graphene oxide electrodes was comparable to other electrodes prepared by conventional power-based methods [21, 22]. Carbon-based hybrid ink is a promising option for SC electrodes since it exhibits an enhancement in areal capacitance, flexibility and cycling stability compared with that of pure GO ink. The overall effectiveness of inkjet printable electrodes is significantly influenced by the ink, thus it must adhere to viscosity and particle size requirements. Micro supercapacitors (MSCs) fabricated using hybrid ink composed of graphene oxide (GO) and commercial pen ink exhibited nearly 780% enhancement in areal capacitance compared with that of pure GO ink [23]. Moreover, it showed excellent flexibility and commendable cyclic stability with nearly 100% retention of the areal capacitance even after 10,000 cycles. Li et al. [24] developed a flexible and binder-free electrode for supercapacitors using IJP. They featured a three layer Ni-Co LDH/Ag/rGO@CC electrode by combining inkjet printing and electrochemical deposition methods. For the battery-type electrode, the Ni-Co LDH/Ag/Rgo@CC electrode generates a high capacity of 173 Ma h g1 at 1 A g1, as well as outstanding capacity retention and cycling stability in 1 M KOH electrolyte solution.

2. Direct ink writing (DIW)

The term “DIW” refers to the extrusion-based AM technique, in which paste or ink is directly deposited at predetermined flow rates. To create 3D structures layer by layer, deposition occurs following digitally defined paths. The substance is transformed into pellets or a paste. The melting point of the pellets or the viscosity of the paste is a crucial criterion to be noted. Figure 8 shows the schematic illustration of DIW method. In contrast to other AM processes where solidification occurs with high temperatures, UV radiation, laser, etc., DIW depends on the ink characteristics including solvent evaporation or concomitant chemical changes for pattern solidification. Ink must satisfy some fundamental rheological properties to maintain good ink fluidity and material shape retainment. The paste/ink should have a suitable high yield stress, viscosity and shear thinning behavior [25]. Viscosity decreases with increasing shear rates and it favors ink flow through nozzle as well as ink extruding [26]. The ink at a reduced viscosity under driven force is extruded from the nozzle like a continuous filament and should keep its self-supporting qualities in order to sustain filament shapes after the ink is deposited. Another important parameter to be noted is the high solid content of the ink. This could avoid the change of volume or shape of ink during the post-deposition treatments. Post-processing is a vital step for manufactured supercapacitors. Thermal annealing, material etching or surface polishing are usually done for the final printed device. Electron transfer and ion intercalation should be properly maintained throughout the printed electrodes by optimizing the distance between printed layers and layer thickness. Therefore in DIW, the selected ink must have an adequate rheology with σ, electronic conductivity and energy density of raw materials [27]. Ink for DIW usually satisfies the Herschel-Bulkley model given by [28].

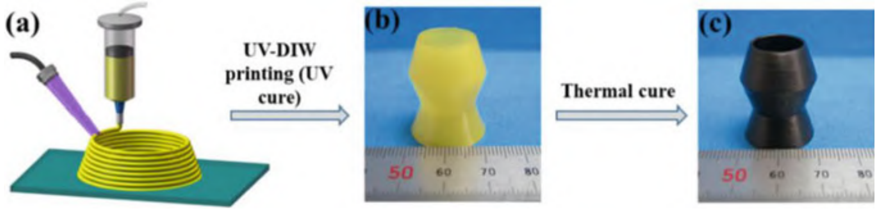

Fig. 8 UV-DIW additive manufacturing of BMI. **a** General route of UV-DIW using the BMI ink, **b** high-resolution structure after UV-DIW **c** after thermal cure. Reprinted from [29], Copyright (2021), with permission from Elsevier

$$\tau = \tau_y + K_\gamma^n$$

where τ is the shear stress, K is the viscosity parameter, n is the flow index and τ_y the yield stress.

There is a wide range of ink selection for DIW technique, including polymer melts, wax-based materials, graphene based materials and sol-gels, noted that they should have the composite modulus of 10^3–10^5 Pa and the storage modulus (G’) higher than the loss modulus (G”). But an increase in material content beyond a certain limit leads to the clogging or aggregation phenomena that affect the extrusion of ink which in turn deteriorates the device performance. For example, GO dispersion concentration is found to affect the rheological properties of printing ink deeply [30]. As shown in Fig. 9 (a), viscoelastic liquid-like behavior was observed at low GO concentrations (from 0.05 to 0.25mgml^{-1}). When GO concentration is increased to 0.25mgml^{-1}, G’ value dominated over G” values and nematic ordering appeared (b&c). Only until the concentration reached 0.75mgml-1 did the fluid characteristics of GO ink match those of inkjet printing (Fig. 10 (d)). Up to 2.5mgml^{-1}, weak gel-like properties were exhibited. When GO concentration is about 4.5mgml^{-1}, distinct G’ and G” values were obtained. It was when the concentration was as high as 13.35mgml^{-1}, the ink became best suitable for hazzle-free extrusion through the nozzle tip.

Highly concentrated MXene ink can be used to deliver high power and energy densities from a limited foot-print area. DIW enables the room temperature fabrication of interdigital $Ti_3C_2T_x$ MXene electrode with exceptional electrochemical performance with the high areal capacitance of ~ 1035mFcm^{-2} [31] The combination of 2dimensional $Ti_3C_2T_x$ MXene and 3D interdigital electrode architecture provides them high electrical conductivity and outstanding electrochemical properties. Viscoelastic properties owned by MXene ink make it flexible for the scalable fabrication of SC electrodes with different architectures and dimensions on any desired substrates. Also, they achieved an energy density as high as 51.7 Mw h cm^{-2} which is higher than those MXene-based devices reported earlier in the literature. Shen et al. [13] demonstrated asymmetric micro-supercapacitors in which both electrodes and electrolytes are patterned through DIW. Cathode and anode inks were

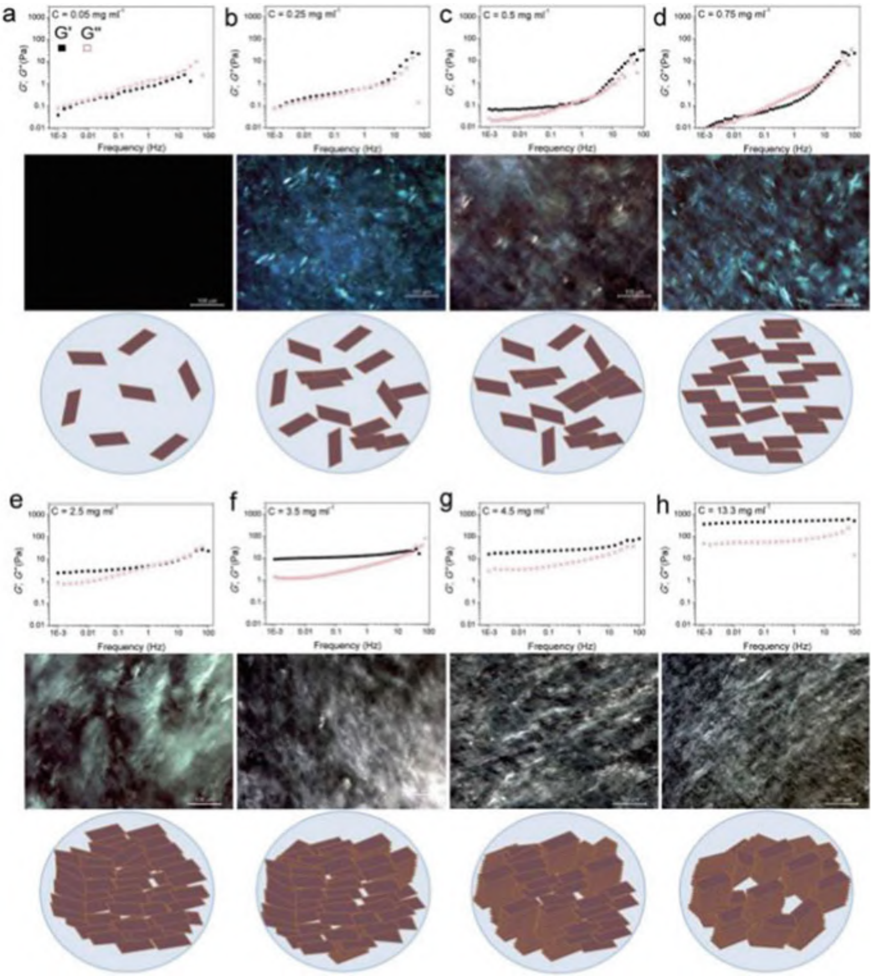

Fig. 9 Storage and loss moduli (filled squares and open squares, respectively) of GO suspensions as a function of frequency accompanied by their polarized optical micrographs (POMs) and the schematic illustrations of the proposed model for the evolution of LC phases in GO dispersions upon increasing concentration. Reproduced with permission from [30]

made of Vanadium pentoxide (V_2O_5) and graphene-vanadium nitride quantum dots with high concentrations of graphene oxide dispersion. The two inks were separately loaded into a syringe and deposited layer by layer successively. The spacing (200 μm) between cathode and anode was filled by the gel-like electrolyte (PVA-LiCl). The interdigitated electrodes displayed exceptional structural stability and a

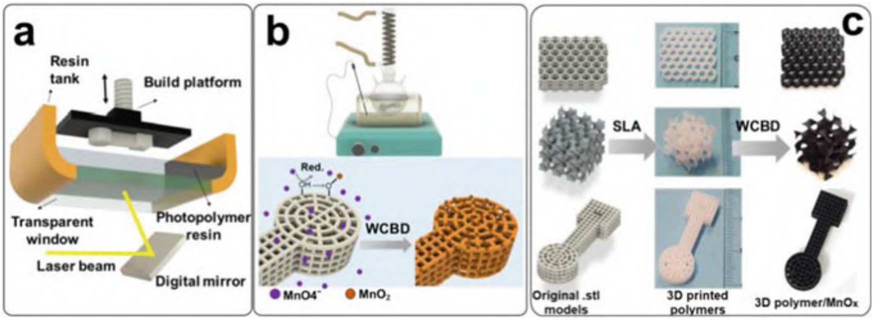

Fig. 10 Schematic illustrations: **a** SLA 3D printing procedure to generate a 3D free-standing reticular configuration of a pyrolyzable photopolymer resin. **b** Synthesis and self-assembly of the MnO2 nanostructures onto the surface of the 3D printed polymer network through the WCBD method. **c** Original.stl models of the honeycomb, gyroid, and reticular geometries and digital photographs of their SLA 3D prints before and after decoration with MnOx. Reproduced with permission from [36]

high areal mass loading. More importantly, it possesses a high areal capacitance of 207.9mFcm^{-2} and an aerial energy density of $73.9\mu\text{Whcm}^{-2}$.

3. **Fused Deposition Modeling (FDM)**

FDM is another extrusion-based AM technique in which a spool of thermoplastic filament is used as the raw material. In FDM, the thermoplastic filament is melted in a liquefier and extruded through the nozzle onto a desired substrate. Additionally, the deposition follows the pathways that were digitally defined. Prior to deposition, the ink material is heated to its melting point. The deposited material, after cooling below its glass transition temperature, gets solidified on the substrate [27]. Conductive fillers are frequently added to thermoplastic polymers for FDM printing SCs, including acrylonitrile–butadiene–styrene (ABS), poly(lactic acid), poly(vinylidene fluoride), and polycarbonate. Layers are deposited one at a time, with the platform being lowered once each layer is complete. Additionally, it enables the simultaneous deposition of various materials, enabling the printing of multifunctional components at the same time. Due to its ability to cut down on time requirements as well as avoid using complicated and expensive tools or molds, FDM is frequently employed in the automotive and aerospace industries. FDM makes it possible to design and realize lightweight automobile parts with no compromise in functionality, performance and fuel efficiency. This method previously helped Urbee, the first ever fuel-efficient car, achieve a spectacular weight reduction of 230 kg and aerodynamic performance optimization [32]. By employing a sparse-fill build technique, the BMW AG Regensburg facility was able to reduce the weight of hand-held assembly devices by 72% [33]. Another keynote feature of FDM is that the possibility of redesigning the intake geometry with lighter weight, better charge distribution, and more torque. In addition, it provides higher accuracy and repeatability than other conventional procedures. The various printing parameters to be taken care of and its description is given in Table 1.

Table 1 FDM parameters

Parameter	Description
Layer thickness	Thickness of the deposited layer was measured vertically. This parameter depends on the nozzle diameter, ink viscosity and material type
Build orientation	Orientation of the printed material on the substrate in direction of X, Y or Z on FDM machine
Extrusion temperature	Temperature at which the filament material is heated before the extrusion process. Affects the layers bonding and raster bonding
Raster angle	Angle of extruded material in the X direction If the direction of load applied on the printed component is known, it is best to use 0° else use 0º/45º/90º/−45º
Print speed	Speed of nozzle tip in the X and Y directions during printing. Closely connected to the extrusion speed
Air gap	Defined as the distance between two rasters on one layer of the printed component
Infill density	Density of internal structure of the printed material
Infill pattern	Pattern of internal structure. Honeycomb structure has the greatest mechanical strength

Post-processing of printed electrodes improves the electrochemical performance. Srinivasan et al. [34] in their work evaluated the electrochemical performance of an EDLC supercapacitor with FDM printed electrodes. Electrode printing was carried out at a printing speed of 40 mm/s, nozzle temperature of 230 °C, nozzle diameter of 0.8 mm and a layer height of 0.32 mm. Two types of electrolyte salts- Potassium chloride (KCl) and Ammonium sulfate ($(NH_4)_2SO_4$) in polyvinyl alcohol (PVA) in 100 ml of water were used for the supercapacitor assembly. The electrodes which are post-processed in DMF for 2 min performed better in both electrolytes with a specific capacitance of 0.340Mf/g and 0.295Mf/g in KCl and ($(NH_4)_2SO_4$) respectively. Foster et al. [35] developed a graphene-based polylactic acid (PLA) filament to fabricate electrodes with 3D disc configurations. A mixture of PVA and H_2SO_4 acted as the electrolyte solution. The printed SC filaments with 8wt% of graphene and 92wt% of PLA characterized a capacitance of 28 Mf at 0.5 Ma. FDM can be combined with other conventional techniques to prepare SC electrodes. 3D electrode was manufactured using a conductive filament with a conductivity of 2.13 S cm^{-1} at a speed of 30 mm s^{-1} with 110% filament flow [6]. Gold was sputtered as a thin layer over the 3D printed electrode (3DE/Au). They followed an *in-situ* electrochemical polymerization method for the deposition of polypyrrole/reduced graphene oxide (Ppy/Rgo) nanocomposites as electroactive material on 3DE/Au electrodes. The fabricated SC with PVA/KOH gel electrolyte provides a specific capacitance of 98.37 F g^{-1}.

4. Stereolithography (SLA)

SLA, along with selective laser sintering (SLS) and fused deposition modeling (FDM), is one of the most popular 3D printing techniques (SLS). SLA is a member of resin printing category where a high-powered laser is used to harden liquid resin contained in a reservoir that is to be used for patterning the desired shape. In a sense, this procedure uses a low-power laser and photopolymerization to transform the photosensitive liquid into 3D solid polymers layer by layer. Moreover, it produces high-precision, isotropic, and watertight prototypes and end-use parts in a variety of sophisticated materials with fine details and a smooth surface finish. In SLA, laser or projector is used to transform liquid resin to hardened plastic. Short molecular chains form when SLA resins are exposed to specific light wavelengths, polymerizing monomers and oligomers into hardened rigid or flexible geometries. Main advantage of SLA method is its versatility, sharpest details with the highest resolution and accuracy. Here, laser beams can be adjusted to create very fine structures. Earlier SLA systems required expensive monolithic printer maintenance and the services of experienced specialists. But now, affordable compact desktop printers are available, delivering high-quality output.

The overall performance of a supercapacitor greatly relies on the morphology and architecture of the electrodes. We can anticipate greater energy density and improved charge–discharge density in the combination of efficient pseudocapacitive materials and macroporous carbon materials. Psuedocapacitive MnO_2 was self assembled over 3D printed pyrolytic carbon via a facile wet chemical deposition method [36]. Further thermal annealing of the deposited structure resulted in the formation of electrode with unique properties. SC electrode showed gravimetric capacitance of $186Fg^{-1}$ and areal capacitance of $968mFcm^{-2}$ and a higher cyclic retention of 92% after 5000 cycles. The printing process and final product are illustrated in Fig. 10.

In another work, Xue et al. [37] reported the realization of hierarchically cellular lattices for supercapacitors. They fabricated polymeric lattices with octet-truss topology as the substrate for supercapacitor. Substrate was then made conductive via electroless plating. Hierarchically porous graphene was then electrodeposited over the substrates. Electrochemical measurements using a gel-type electrolyte composed of PVA and KOH showed a promising areal capacitance of $57.75mFcm^{-2}$ and a long life span of 96% after 5000 cycles.

5. Selective Laser Sintering/Melting (SLS/SLM)

SLS and SLM are very similar processes but differ simply in the materials they use.

SLS involves the sintering of powdered material using a selected laser as the heat and power source while SLM also does the same thing but uses the laser to achieve a complete melt. In sintering, instead of concentrating on a complete melt of the powder, components are heated until they are fused together. Rather than just merely fusing together, the particles are really melted in SLM. The laser is automatically targeted using well-established computer models, binding the material to produce the required structure. Schematics for a) Selective Laser Sintering and b) Selective Laser Melting is shown in Fig. 11. SLS printing provides for the loading of active metal in a good quantity, which reduces the use of binders or solvents for processing [38]. Higher active metal loading results in higher volumetric energy densities in the case of SC electrodes. Additionally, because SLS doesn't require any post-deposition procedures, such as heat treatment or sintering, it requires less processing time while

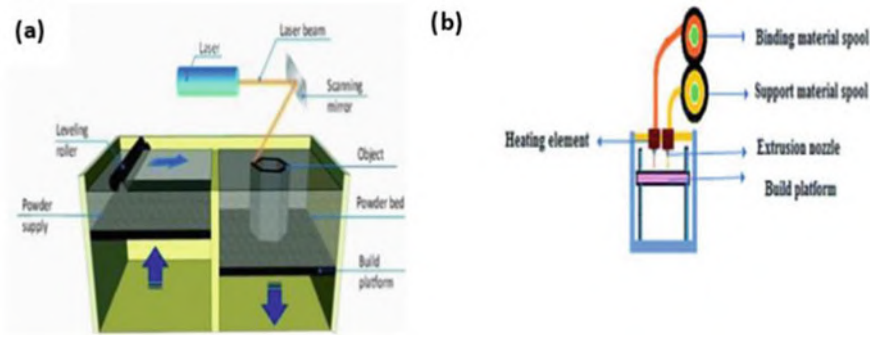

Fig. 11 Schematics for **a** Selective Laser Sintering/Selective laser melting **b** FDM. Reproduced with permission from [39] and Reproduced from [40] with permission from the Royal Society of Chemistry

still being able to produce complex structures and provide higher electrochemical performance.

Interdigitated Ti_6Al_4V electrodes are printed using SLM. Ti-6Al-4 V metal powder is melted and fused in a layer by layer manner to form the desired structure. Ppy was electrodeposited over Ti alloy electrode as electroactive material. PVA-H_3PO_4 polymer was used as the electrolyte for the symmetric solid-state pseudocapacitor. The 3D printed symmetric SC exhibited a volumetric capacitance of 2.4 F cm^{-3}, an energy density of 213.5 Wh m^{-3} at a current density of 3.74 Ma cm^{-3}, and a power density of 15.0 Kw m^{-3} at 37.4 Ma cm^{-3}[41]. Choi et al. [42] demonstrated the SLS printing of Ag nanoparticles on polycarbonate substrate using SLS in the form of a grid. Graphene was then coated over the grid followed by the deposition of MnO_2 and Au. Electrodeposition of Au onto the Ag grid significantly improved the supercapacitor's cycle charge/discharge stability and is competing to a pure graphene electrode.

6. Binder Jetting (BJ)

In binder jetting process, a liquid binding agent is deposited over a powder bed-sand, ceramics or metals- bonding the materials together to form a solid layer one-by-one. It is regarded as the fastest 3D printing technique where highly dense and precise parts are produced. BJ is similar to traditional paper printing in its simple way of approach (Fig. 12). Here powder bed can be compared to a paper and binder to the ink. When binder is rolled over the powder bed, printing occurs. Azhari et al. [43] fabricated thick graphene electrodes using BJ method for the first time. Printed SC demonstrated high gravimetric capacitance of 260 Fg^{-1} and areal capacitance of 700 mF cm^{-2} with a capacity retention of 80% over 1000 cycles.

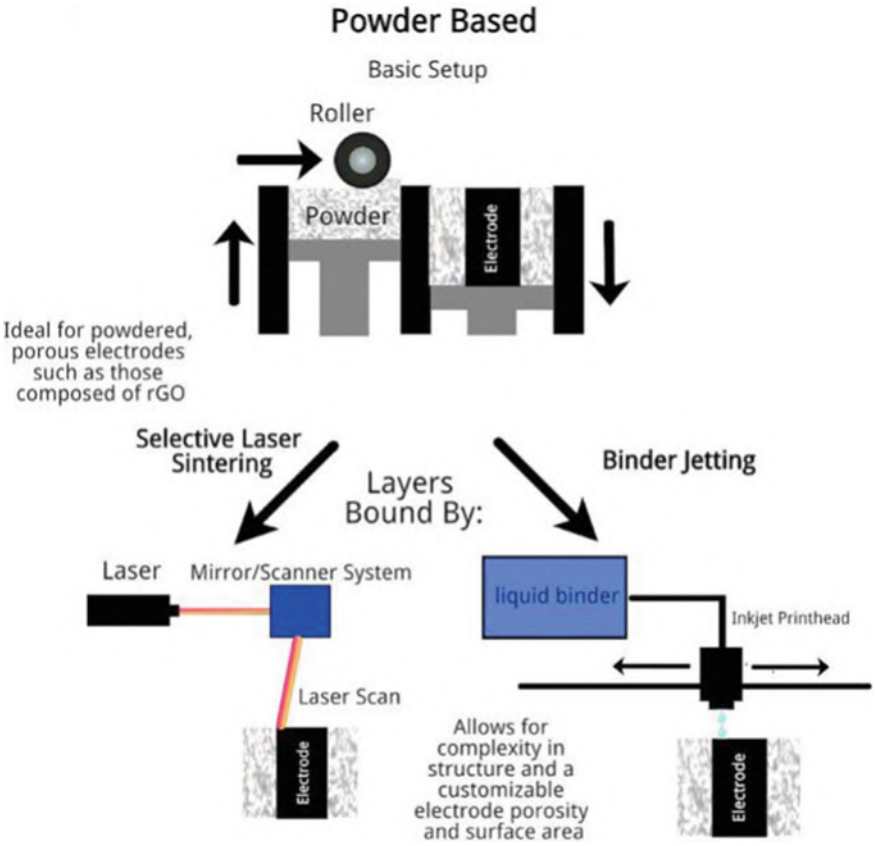
Powder Based
Basic Setup
Roller
Powder
Electrode
Ideal for powdered, porous electrodes such as those composed of rGO
Selective Laser Sintering
Layers Bound By:
Binder Jetting
Laser
Mirror/Scanner System
Laser Scan
Electrode
liquid binder
Inkjet Printhead
Allows for complexity in structure and a customizable electrode porosity and surface area
Electrode

Fig. 12 Schematic illustration of powder based AM techniques. Reprinted from [19], Copyright (2021), with permission from Elsevier

3 Conclusion, Recommendation and Future Scope

This chapter covered the fundamentals of AM techniques and some of the most common printing methods used for SC production. The electrochemical performance of 3D printed capacitors was also studied in the chapter, which demonstrates that SC devices developed using printing techniques are comparable to those produced using conventional methods. The overall performance of the device was improved by the use of complex structures and geometries created using 3D technology. Transition metal oxides, transition metal dichalcogenides and graphene based materials are noted as the common or well explored materials in SC manufacturing industry.

AM is still at its growing phase, where a number of obstacles are present, such as a lack of standardization, reliability, productivity, quality and environmental as well as economic challenges. Although it is always commendable that complicated geometries may be rendered in three dimensions, more materials need to be made compatible with 3D printing, particularly those used in ink-based techniques. The production of real 3D architecture to achieve greater energy storage is significantly constrained by the strict rheological protocols ink related preparation methods.

One advantage may be the root of one disadvantage, particularly supply chain problems. Many vendors or supply chains are intended to be eliminated or reduced since raw data can be transmitted in electronic format. In the case of FDM, lack of mechanical strength and functionality is a great challenge which have to be addressed seriously. Techniques that use post-deposition treatments are susceptible to device malfunctions or shrinkage, which renders the printing process useless. Each material differs in its own unique way and is ideal for a certain AM approach.

The need and demand for AM techniques will increase as the world requires increasingly miniature designs. More materials, improved deposition conditions, highly advanced apparatus, and digitally skilled workers are needed to meet the growing demands. From a business standpoint, creating an assembly line that simplifies the entire procedure, starting with the 3D printing of the electrodes and ending with the assembly of the supercapacitor, is essential for commercial viability. To make it possible to mass produce these devices, simple, affordable modular designs and standardization of the assembling procedure may be of interest.

AM is on track to develop from a fledgling technology into one that can genuinely change the world. Local printing of practically any designable object would have a significant impact on every aspect of our culture. The revolutionary technology of additive manufacturing requires foresight and prior planning, even though the future is undoubtedly difficult to foresee.

References

1. Sharma PK, Arora A, Tripathi SK (2019) Review of supercapacitors: Materials and devices. J Energy Storage **21**
2. Zhang L, Hu X, Wang Z, Sun F, Dorrell DG (2018) A review of supercapacitor modeling, estimation, and applications: A control/management perspective. Renew Sustain Energy Rev 81
3. Winter M, Brodd RJ (2004) What are batteries, fuel cells, and supercapacitors? Chem Rev 104(10)
4. Shi F, Li L, Wang XL, Gu CD, Tu JP (2014) Metal oxide/hydroxide-based materials for supercapacitors. RSC Advances 4(79)
5. Zhang L, Zhao XS (2009) Carbon-based materials as supercapacitor electrodes. Chem Soc Rev 38(9)
6. Foo CY, Lim HN, Mahdi MA, Wahid MH, Huang NM (2018) Three-dimensional printed electrode and its novel applications in electronic devices. Sci Rep 8(1):1–1. https://doi.org/10.1038/s41598-018-25861-3
7. Standard Terminology for Additive Manufacturing Technologies, ASTM F2792–10
8. Zhang P, Wang F, Yu M, Zhuang X, Feng X (2018) Two-dimensional materials for miniaturized energy storage devices: from individual devices to smart integrated systems. Chem Soc Rev 47(19):7426–7451
9. Li D, Lai WY, Zhang YZ, Huang W (2018) Printable transparent conductive films for flexible electronics. Adv Mater 30(10):1704738

10. Li J, Naiini MM, Vaziri S, Lemme MC, Östling M (2014Nov) Inkjet printing of MoS2. Adv Func Mater 24(41):6524–6531
11. Singh M, Haverinen HM, Dhagat P, Jabbour GE (2010) Inkjet printing—process and its applications. Adv Mater 22(6):673–685
12. Fu K, Yao Y, Dai J, Hu L (2017Mar) Progress in 3D printing of carbon materials for energy-related applications. Adv Mater 29(9):1603486
13. Shen K, Ding J, Yang S (2018) 3D printing quasi-solid-state asymmetric micro-supercapacitors with ultrahigh areal energy density. Adv Energy Mater 8(20):1800408
14. Zhakeyev A, Wang P, Zhang L, Shu W, Wang H, Xuan J (2017) Additive manufacturing: unlocking the evolution of energy materials. Advanced Science 4(10):1700187
15. Seol ML, Nam I, Ribeiro EL, Segel B, Lee D, Palma T, Wu H, Mukherjee D, Khomami B, Hill C, Han JW (2020) All-printed in-plane supercapacitors by sequential additive manufacturing process. ACS Appl Energy Mater. 3(5):4965–4973
16. Cesaretti G, Dini E, De Kestelier X, Colla V, Pambaguian L (2014) Building components for an outpost on the Lunar soil by means of a novel 3D printing technology. Acta Astronaut 1(93):430–450
17. Soares DM, Ren Z, Mujib SB, Mukherjee S, Martins Real CG, Anstine M, Zanin H, Singh G (2021) Additive manufacturing of electrochemical energy storage systems electrodes. Adv Energy Sustain Res 2(5):2000111
18. Derby B (2010) Inkjet printing of functional and structural materials: fluid property requirements, feature stability, and resolution. Annu Rev Mater Res 40:395–414
19. Jha S, Velhal M, Stewart W, Amin V, Wang E, Liang H (2021Nov) Additively manufactured electrodes for supercapacitors: A review. Appl Mater Today 21:101220
20. Le LT, Ervin MH, Qiu H, Fuchs BE, Lee WY (2011) Graphene supercapacitor electrodes fabricated by inkjet printing and thermal reduction of graphene oxide. Electrochem Commun 13(4):355–358
21. Zhang X, Ji G, Xiong D, Su Z, Zhao B, Shen K, Yang Y, Gao X (2018) Graphene oxide as an additive to improve perovskite film crystallization and morphology for high-efficiency solar cells. RSC Adv 8(2):987–993
22. Vivekchand SR, Rout CS, Subrahmanyam KS, Govindaraj A, Rao CN (2008) Graphene-based electrochemical supercapacitors. J Chem Sci 120(1):9–13
23. Pei Z, Hu H, Liang G, Ye C (2017Apr) Carbon-based flexible and all-solid-state micro-supercapacitors fabricated by inkjet printing with enhanced performance. Nano-micro letters. 9(2):1–1
24. Li X, Zhao Y, Yu J, Liu Q, Chen R, Zhang H, Song D, Li R, Liu J, Wang J (2019Dec) Layer-by-layer inkjet printing GO film and Ag nanoparticles supported nickel cobalt layered double hydroxide as a flexible and binder-free electrode for supercapacitors. J Colloid Interface Sci 1(557):691–699
25. Hon K, Li L, Hutchings IM (2008) Direct writing technology—Advances and developments. CIRP Annals.:601–620
26. Tagliaferri S, Panagiotopoulos A, Mattevi C (2021) Direct ink writing of energy materials. Materials Advances. 2(2):540–563
27. Nargatti K, Ahankari S (2022) Additive manufacturing of supercapacitor electrodes–Materials, methods and design. In: Key Engineering Materials 2022, vol 913. Trans Tech Publications Ltd., pp. 59–75
28. Lewis JA (2006) ADV FUNCT MATER. Adv. Funct. Mater. 16:2193–2204
29. Wu T, Jiang P, Zhang X, Guo Y, Ji Z, Jia X, Wang X, Zhou F, Liu W (2019) Additively manufacturing high-performance bismaleimide architectures with ultraviolet-assisted direct ink writing. Mater Des 15(180):107947
30. Aboutalebi SH, Gorkin R, Konstantinov K, Innis PC, Spinks GM, Poulin P, Wallace G (2014) Graphene oxide dispersions: tuning rheology to enable fabrication. Mater Horiz 1:326–331
31. Orangi J, Hamade F, Davis VA, Beidaghi M (2019) 3D printing of additive-free 2D Ti3C2T x (MXene) ink for fabrication of micro-supercapacitors with ultra-high energy densities. ACS Nano 14(1):640–650

32. Maghnani R (2015) An exploratory study: the impact of additive manufacturing on the automobile industry. Int J Curr Eng Technology 5(5):1–4
33. http://www.stratasys.com
34. KV SS, Santo J, Penumakala PK (2022) Effect of surface modification of printed electrodes on the performance of supercapacitors. J Energy Storage 56:106043
35. Foster CW, Down MP, Zhang Y, Ji X, Rowley-Neale SJ, Smith GC, Kelly PJ, Banks CE (2017) 3D printed graphene based energy storage devices. Sci Rep 7(1):1–1
36. Rezaei B, Hansen TW, Keller SS (2021) Stereolithography-derived three-dimensional pyrolytic carbon/Mn3O4 nanostructures for free-standing hybrid supercapacitor electrodes. ACS Appl Nano Mater. 5(2):1808–1819
37. Xue S (2019) 3D printing-based hierarchically cellular lattices for high-performance quasi-solid supercapacitor. Nano Micro Lett. 11:46
38. Mensing JP, Lomas T, Tuantranont A (2020) 2D and 3D printing for graphene based supercapacitors and batteries: A review. Sustain Mater Technol 1(25):e00190
39. Ambrosi A, Pumera M (2016) 3D-printing technologies for electrochemical applications. Chem Soc Rev 45(10):2740–2755
40. Sireesha M, Lee J, Kiran AS, Babu VJ, Kee BB, Ramakrishna S (2018) A review on additive manufacturing and its way into the oil and gas industry. RSC Adv 8(40):22460–22468
41. Zhao C, Wang C, Gorkin Iii R, Beirne S, Shu K, Wallace GG (2014) Three dimensional (3D) printed electrodes for interdigitated supercapacitors. Electrochem Commun 1(41):20–23
42. Choi H, Nguyen PT, Van Tran C, In JB (2020) Micro-patterned metal current collectors for high aspect ratio flexible graphene supercapacitors. Appl Surf Sci 30(510):145432
43. Azhari A, Marzbanrad E, Yilman D, Toyserkani E, Pope MA (2017) Binder-jet powder-bed additive manufacturing (3D printing) of thick graphene-based electrodes. Carbon 1(119):257–266

Всё для победы!
НАРОДНЫЙ ФРОНТ
https://pobeda.onf.ru/
LET'S HELP THE RUSSIA

Chapter 8
Inkjet Printing Fabrication of Supercapacitors

K. R. Hari Narayanan, Shruti Kannan, and Ananthakumar Ramadoss

Abbreviations

Ag	Silver
ASC	Asymmetrical Supercapacitor
$BMIMBF_4$	1-Butyl-3-methylimidazolium tetrafluoroborate
CIJ	Continuous Inkjet Printing
CNF	Cellulose Nano Fibril
CNT	Carbon Nanotube
Cu	Copper
Cu_xO	Copper Oxide
CV	Cyclic Voltammetry
DIW	Direct Ink Writing
DoD	Drop-on-Demand
ED	Energy Density
EDX	Energy Dispersive X-ray Analysis
Emf	Electromotive Force
ETPTA	Ethoxylated Trimethylolpropane Triacrylate
FCPF	Flexible Composite Protein Film
GCD	Galvanostatic Charge–Discharge

K. R. H. Narayanan · S. Kannan · A. Ramadoss (✉)
Advanced Research School for Technology & Product Simulation (ARSTPS), School for Advanced Research in Petrochemicals (SARP), Central Institute of Petrochemicals Engineering & Technology (CIPET), T.V.K. Industrial Estate, Guindy, Chennai 600 032, India
e-mail: ananth@cipet.gov.in

K. R. H. Narayanan
e-mail: harinarayananakr@gmail.com

S. Kannan
e-mail: kannan.shruti19@gmail.com

© The Author(s), under exclusive license to Springer Nature Singapore Pte Ltd. 2024

C. M. Hussain and M. B. Ahamed (eds.), *Functionalized Nanomaterials Based Supercapacitor*, Materials Horizons: From Nature to Nanomaterials,
https://doi.org/10.1007/978-981-99-3021-0_8

GO	Graphene Oxide
IJP	Inkjet Printing
KI	Potassium Iodide
δ-MnO_2	Delta Manganese Dioxide
MP	Mxene/PEDOT:PSS
MSC	Microsupercapacitor
MWCNT	Multi-Walled Carbon Nanotube
NF	Nickel Foam
$Ni(OH)_2$	Nickel Hydroxide
Ni-Co LDH	Nickel-Cobalt-Layered Double Hydroxide
NGP/PANI	Graphene/Polyaniline
NiO	Nickel Oxide
NSFE	Nano Silver Flexible Electrode
PC	Printed Circuit
PD	Power Density
PEDOT: PSS	Poly(3,4-ethylenedioxythiophene) Polystyrene Sulfonate
PET	Polyethylene Terephthalate
PVA	Poly (vinyl alcohol)
PVA–H_3PO_4	Poly(vinyl alcohol)-Phosphoric Acid
PVA-KOH	Poly (vinyl alcohol)-Potassium Hydroxide
PVDF	Polyvinylidene Fluoride
rGO	Reduced Graphene Oxide
RuO_2	Ruthenium Oxide
SC	Supercapacitor
SDBS	Sodium Dodecyl Benzenesulfonate
SEM	Scanning Electron Microscopy
SWCNT	Single-Walled Carbon Nanotube
Ti	Titanium
UV	Ultraviolet
XRD	X-ray Diffraction

1 Introduction

An increase in the demand for electrochemical energy storage devices may be attributed to the growing popularity of portable consumer electronics as well as the need for energy storage devices in autonomous vehicles [1, 2]. The growing reliance of mankind on energy-harvesting technologies has fueled the never-ending search for energy sources that are dependable, highly efficient, low-cost, and inventive. As a potential replacement for batteries, SCs have garnered a lot of interest due to their unique properties, including a greater power density, quick charge-discharge rates, and long cycle life [3, 4]. They have the potential for groundbreaking new uses, improved performance, and fresh approaches to building useful gadgets. And yet, due to high material prices and difficulties with prototyping, a cost-effective, and an adaptable manufacturing technique is required. IJP to create SC device topologies is a recently developed field of study and has matured into a powerful tool for producing various functional devices [5].

IJP of functional materials has several benefits over traditional manufacturing processes, including reduced complexity, lower production costs, and faster product development times [6, 7]. IJP works on par with direct ink writing (DIW), in which the substances are produced in each process by layered deposition of digitally controlled liquid ink [8]. This makes it highly possible to realize complex structures that are made up of different components and by the distribution of these main substances in an aqueous phase, these processes produce inks with different rheological properties [9, 10]. Highly viscous inks with reduced shear behavior are formulated for shape maintenance and material extrusion through the DIW process. On the other hand, inks with low viscosity (2–102 m Pa) and a Newtonian formulation are necessary for IJP [11–13]. Compared to the DIW procedure, IJP offers superior print quality and uniformity, and it can even print chemicals by pinpointing the precise location.

IJP has attracted a lot of research interest in printed electronics because of its appealing features, which led to the development of goods, including power devices, transistors, optoelectronics, and sensing equipment. This is certainly relevant to SCs, and energy storage devices that have benefited greatly from IJP's deployment in recent years [14, 15]. This technique allows for contactless printing technology that facilitates a wide range of substrates to be employed in this printing process and these substrates may vary in terms of their material composition, size, and the degree of flexibility [15, 16]. On the whole, IJP is a sequential methodology to boost the output volume in manufacturing. In this chapter, we have covered several fabrication methodologies of SCs utilizing IJP.

2 Basics of the InkJet Printing

Mainstream printing methods include drop-on-demand (DoD) and continuous inkjet printing (CIJ). Continuous inkjet printing when charged under the effect of an electric field by the electrodes, involves the ejection of ink droplets that are precisely displaced during its deposition on the substrate. DoD printing, on the other hand, produces ink droplets when they are required, and they do so by either a piezoelectric or a thermal process. With the piezoelectric IJP method, the ink receptacle is distorted by applying an electromotive force (emf) to the piezoelectric substances. This causes an abrupt increase in pressure, causing a drop of ink to be expelled from the ink receptacle [17]. During the thermal IJP methodology, the ink is quickly heated to create inflation, and the force of the plumes pushes the ink out of the receptacle as droplets of ink.

Compared to other IJP technologies (Fig. 1), CIJ printing's quicker jetting speed provides maximum printing efficiency. However, its broad use is limited by the complexity of controlling the ink's expulsion, deflection, and recirculating process [18]. On the other hand, DoD printing has become the predominant IJP methodology

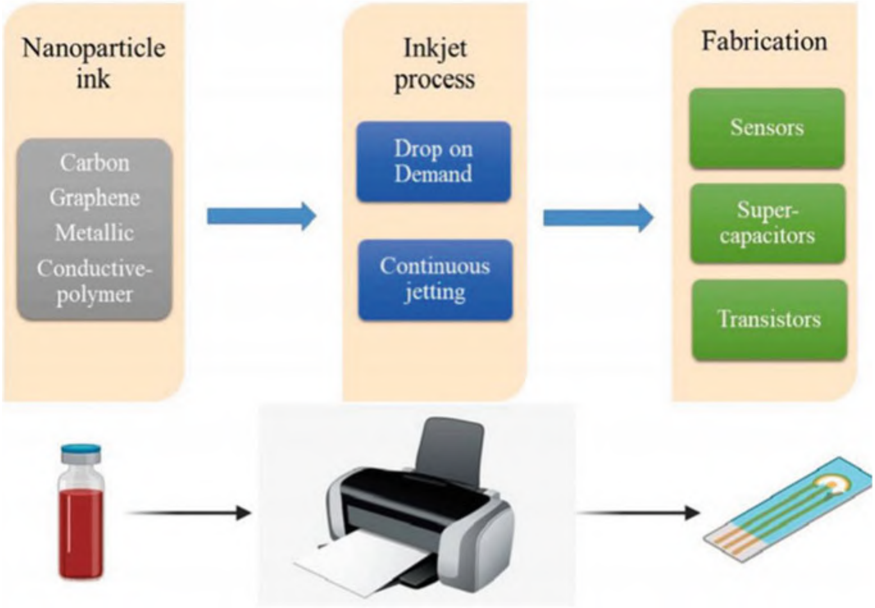
Nanoparticle ink
Carbon
Graphene
Metallic
Conductive-polymer
Inkjet process
Drop on Demand
Continuous jetting
Fabrication
Sensors
Super-capacitors
Transistors

Fig. 1 Depiction of nanoparticle deposition strategy using IJP. Copyright © 2022 Elsevier, Reproduced with permission from [18]

due to its easier operation. Moreover, fluidity and composition are essential for the optimal printing of elevated motifs. Hence, there has been much research on better solvents for printable inks. In a broad sense, the ink's viscosity should be regulated between a few centipoises (cP), and ideally 100 cP of viscosity is preferred for IJP, which makes it compatible with the printhead in ink-jetting highly viscous solutions [19].

3 Formulation of Ink Behavior

The rheological characteristics of inks are determined by the amalgamation of the functional ink materials (i.e., soluble substances, additives, and operational materials) and the relationship between them. The ink's adhesive consistency and rheological properties are largely determined by the solvent system, which transports the functional materials and other ink elements during printing [20]. Depending on the intended use, the operational ink may include active elements with varying degrees of functionality, such as electroactivity or conductivity. The rheological qualities of the ink may be modified by adding various additives such as surfactants and polymers. They can significantly alter the ink's printability and the quality of the completed designs. While aiming to achieve a better printed pattern, one of the most important factors to consider is how the ink droplets interact with the substrate [21, 22].

When placed on a substrate, the behavior of ink droplets is related not only to the ink formulation but also to the surface adhesive propeties and the velocity of different base materials with which the droplets hit the surface. Two further procedures will occur after a droplet has impaired itself onto a substrate [23]. In the beginning, the droplet's kinetic energy will force it to spread out over the surface of the liquid. The behavior of the droplet as it spreads outward is determined by the wettability of the surrounding substrate, defined by an apparent contact angle [24]. Better behavioral quality of the substrate often ramifies in a modest angle of contact ($<90°$), whereas an angle $>85°$ indicates poor wetting. Further, the solvent evaporates during the drying process, leaving behind a solid coating on the substrate, achieving consistent and high-resolution patterns during solidification, which is a significant claim. The coalescence behavior of successive inkjet droplets significantly impacts the consistency of uniformly printed patterns. This can be achieved by careful regulation of the drop spacing and delay duration which will be free of wavering or bulging impairment [25, 26].

4 Inkjet Printed Electrodes for SC Applications

IJP has so far influenced the evolution of high-performance supercapacitors. The intrinsic structural properties of the active substance mostly determine the efficiency of SCs. There are three categories of IJ-printed electrodes: carbon, hybrid, and non-carbon electrode materials.

4.1 Inkjet-Printed Carbon-Based Electroactive Materials

Workable inks for IJ-printed SCs whose active substances made from carbon materials are promising due to their numerous sources, enhanced power conductance, easy manufacturing, and amenability to mass production. Activated carbon, reduced graphene oxide (rGO), carbon black, graphene, graphene oxide, and carbon nanotubes are all examples of printable nanomaterials based on carbon. The SCs' energy storage performance is clearly influenced by the electrode material. In this respect, graphene has emerged as a prominent electrode material due to its intrinsic properties, such as enormous theoretical surface area, >95% purity, high flexibility, better thermal and electrical conductivity.

This encouraged the mass production of IJ printed highly-precise graphene films in a reliable manner. Since graphene oxide can be facilely disseminated in aqueous solvents like water, it has been a favorable option for ink articulation and IJP of graphene-based electrodes [27]. During this study, Le et al. successfully fabricated graphene-based SCs on titanium (Ti) foils using IJP with aqueous graphene oxide inks at various heat reduction rates ($T = 200$ °C). The system, which benefited from the printing technique, displayed an energy density (ED) of 6.74 Wh kg^{-1} at a power density of 0.190 kW kg^{-1} respectively [28].

Similarly, SC electrodes printed with carbon nanotube thin films were incorporated in individual sheets of paper proving their potential as a novel entity power source for wearable electronics. In order to avoid the short circuit, electrodes were IJ printed with single-walled carbon nanotube (SWCNT) coated with polyvinyledene fluoride (PVDF) onto a substrate made up of paper. In an outcome, printed SC displayed a high specific power of 250,000 W kg^{-1}, specific capacity of 33 F g^{-1}, and an excellent cyclic efficiency with a minimum capacity degradation up to 2500 cycles [29]. For the passive experiment of rGO layers and binder-free substances printed on different fabrics (Fig. 2a), Stempien et al. [30] chose the reactive IJP methodology. Initially, ink-based graphene oxide (GO) was printed onto a substrate and subsequently, another ink containing ascorbic acid acting as a reducing agent was printed onto the exact location using various nozzles to result in rGO films.

A SC system was built utilizing an electrode made up of rGO and phosphoric acid (H_3PO_4)-polyvinyl alcohol (PVA) gel electrolyte. The fabricated device provided an ED of 1.18 mWh cm^{-2}, a PD of 4.6 mW cm^{-2}, and a maximal areal capacitance of 13.3 mF cm^{-2} at 0.1 mA cm^{-2} (Fig. 2b–e). The resultant SC system remained mechanically flexible since the specific capacitance did not change at a bending angle of 180°, respectively [30]. Moreover, a flexible solid-state supercapacitor was fabricated with functionalized azide-based multi-walled carbon tube (f-MWCNT) electrodes, which were then IJ printed on the polyethylene-terephthalate (PET) substrate. The erected SC delivered 235 F g^{-1} of specific capacitance and

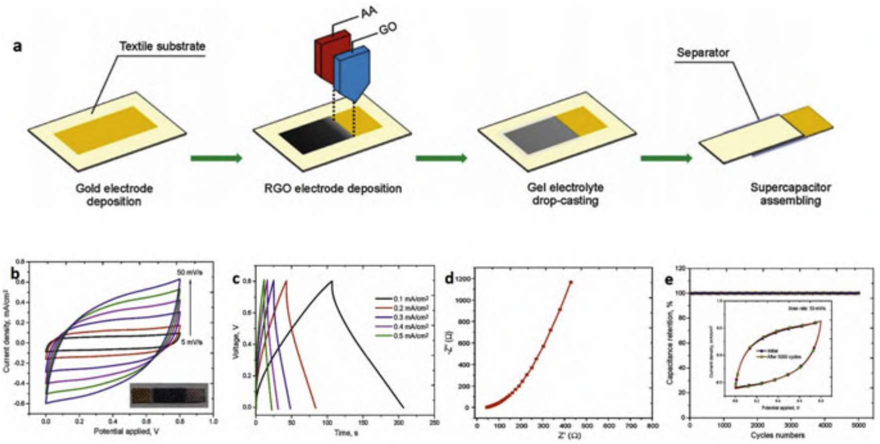

Fig. 2 **a** Textile SC erection using the IJP technique. Electrochemical performance of a textile SC based on rGO: **b** Voltammetric profiles for varied scan rates, **c** Charge and discharge profiles at various current densities, **d** Nyquist plot for the as-fabricated textile SC device, and the **e** Capacitive performance of the SC with bending at 180° and without bending. Copyright © 2019 Elsevier, Reproduced with permission from [30]

16.2 Wh kg^{-1} of energy density, respectively [31]. Similarly, activated carbon is employed as a commercialized SC electrode due to its enhanced pores, huge surface area, and simple production. However, its uses are limited by its poor capacity due to difficulties in manipulating the structure and allocation of pore dimensions. Henceforth carbon electrodes with good surface functionality and porosity are desired for use in SCs due to their enhanced performance.

4.2 Inkjet Printed Non-carbon-based Electroactive Materials

Over a decade, an extensive range of other 2D materials, such as MXenes and non-layered materials like $Ni(OH)_2$, $Co(OH)_2$, and MnO_2 have been found and investigated as functional inks for SC electrodes, in addition to conventional carbon-based materials. IJP not only facilitates swift prototype transfer to the fabrication process but also allows for printing flexible, artistic, and cross-functional patterns useful for energy storage devices. More recently, employing water transfer and fused IJP methodologies, coated SCs were created on three-dimensional objects by Giannakou et al, where Ag ink followed by NiO based nanoparticle ink was IJ printed on a water-soluble substrate based on PVA. Then, the obtained planar substrate was dissolved in water, and were transferred to the submerged three-dimensional plastic hemisphere by gradually reducing the water level in the container.

Drop cast solid-state electrolyte consisting of a triacrylate polymer which is ultraviolet curable, is used in this SC device. When this device was moved to a simple PVA substrate, micro-cracks occurred. This was effectively addressed by adding a thin silicone polymeric coating to the PVA-based substrate, which formed a double layer by maintaining a better printing resolution, thereby hindering the micro-crack development. The device exhibited an areal capacitance of 87.2 mF cm^{-2} in the potential window of 0–1.5 V. In addition, the IJP device was effectively transferred into the human dermis, resulting in the formation of epidermal SCs. The electrochemical behavior of epidermal IJ printed SCs was remarkably robust across a wide range of mechanical strains, proving the material's suitability for stretchable electronics [32]. In addition, delta manganese dioxide (δ-MnO_2) having a layered architecture, was utilized as inks for fabricating integrated SCs that are thinner and much more flexible than conventional supercapacitors.

A huge dispersal ink comprising two-dimensional delta nanosheets made up of MnO_2 with an average lateral dimension of over 89 nm with an estimated thickness of 1 nm was created. Further, polyimide and glass film substrates were exposed to plasma made up of O_2 and were then utilized to generate an IJP MnO_2 pattern with a discernible "coffee ring" effect on the substrate, using which most of the SCs were printed [33]. The device's improved performance was attributed to the MnO_2 ink which had long cycling stability and better flowability without the use of binder [34]. Moreover, Farraj et al. created a copper (Cu) ink that has a self-disintegration capability. At 140 °C in an environment of nitrogen, Cu formate was complexed with 2-amino 2-methyl 1-propanol to make conductive Cu patterns.

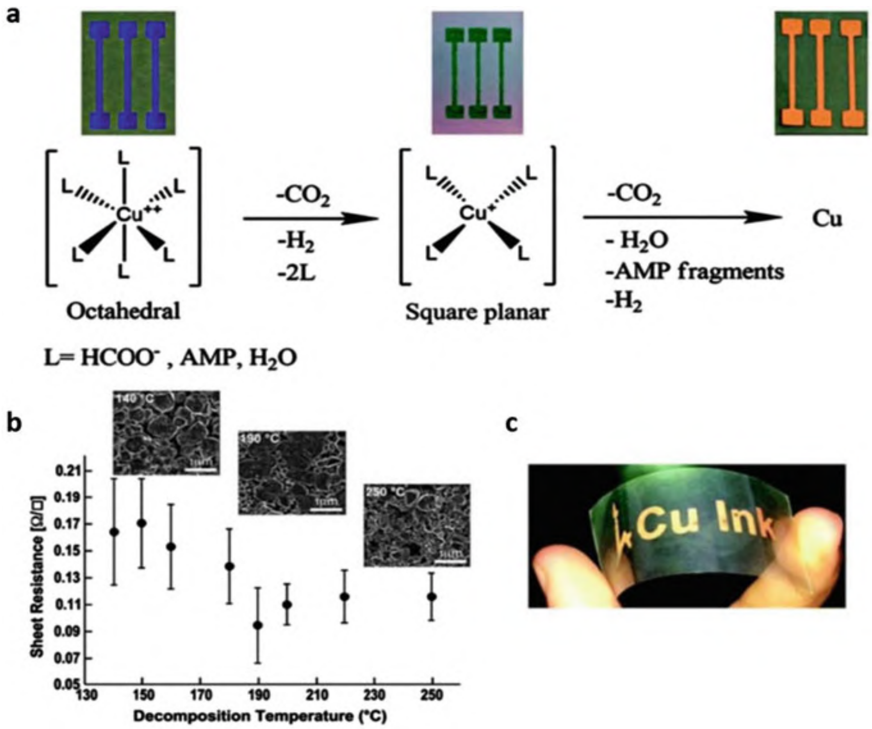
a
L
Cu++
Octahedral
L= HCOO⁻, AMP, H₂O
-CO₂
-H₂
-2L
Cu+
Square planar
-CO₂
- H₂O
-AMP fragments
-H₂
Cu
b
140 °C
190 °C
250 °C
1μm
Sheet Resistance [Ω/□]
0.21
0.19
0.17
0.15
0.13
0.11
0.09
0.07
0.05
130
150
170
190
210
230
250
Decomposition Temperature (°C)
c
Cu Ink

Fig. 3 Cu metal ink. **a** Disintegration of a complex Cu ink from its octahedral structure to planar square form to form a Cu metal (inset images are displayed at each stage). **b** Relationship between decomposition temperature and sheet resistance depicted at different temperatures and their corresponding SEM images. **c** IJP of Cu designs on PET films. Copyright © 2015 Royal Society of Chemistry, Reproduced with permission from [35]

A mechanism for the breakdown of the Cu complex ink was postulated after studying its dissolution (Fig. 3a). The ink was chemically stable in the air and user-friendly for IJP [35]. At 190 °C, the printed Cu film's resistance was <10.5 μ Ω cm^{-1} (Fig. 3b, c). Thus non-carbon-based electrodes due to their remarkable versatility, hydrophilicity, inherent structural stability, and viscoelasticity collectively contribute to desirable IJ printed SC fabrication.

4.3 *Inkjet Printed Multilayered Electroactive Materials*

Printing with a variety of inks in a layered pattern is also a viable option for creating electrodes for SCs. The capacitive behavior of inkjet-printed SCs can be enhanced by the integration of each functional ink, and the device's characteristic efficiency may be improved by a layer-by-layer IJP methodology that uses different inks to reduce restacking and clustering of building components. A broad variety of pseudocapacitor materials including conducting polymers, metal oxides, and metal hydroxides are widely employed as electrode materials in supercapacitors. Out of which $Ni(OH)_2$ is favored due to its ability to sustain higher mass loadings, and deliver greater capacitance with facile erection efficiency [36].

In this context, the researchers Li et al. described the methodology of the manufacture of nickel hydroxides $Ni(OH)_2$ and rGO composite electrodes that possess a layered structure. The following two methods were performed in order to create multiple layered $Ni(OH)_2$/rGO nanoflake substances with various layered architecture in the following designations as $Ni(OH)_2$/rGO (one layer) with NF (RNN-1), and $Ni(OH)_2$/rGO (two layers) with NF (RNN-2) (i) An inkjet printing process was used to place the graphene oxide (GO) film onto the nickel foam (NF) substrate. (ii) Using the hydrothermal technique, nanoflakes of $Ni(OH)_2$ were produced over graphene oxide thin films. When put next to one another, the $Ni(OH)_2$ with NF and the $Ni(OH)_2$/$Ni(OH)_2$ with NF are referred to as both NN-1 and NN-2 at their respective places. In the end, the actions that were just described were repeated in order to raise the total number of layers. The hydrothermal and IJP processes progressively increased the number of layers while maintaining the same $Ni(OH)_2$ nanoflake vertical structure and the graphene oxide's ultra-thin film structure. The NN-1 and NN-2 composites are displayed in Fig. 4a. Images captured by a scanning electron microscope (SEM) compared the untreated NF with the as-prepared samples in Fig. 4b–g. Figure 4b shows the bare NF denoting an interconnected smooth surface with the skeletal structure, thereby building a three-dimensional structure that is concerned with macro-pores. In addition, the IJP method was used to adorn NF with GO film, which has the characteristics of being coiled and evenly distributed, thus fully covering the pores of NF with graphene oxide sheets, resulting in the substrate being used to its maximum potential. In Fig. 4c, we can see that the hydrothermal process resulted in a three-dimensional structure with interconnected macro-pores produced by linked $Ni(OH)_2$ nano-flakes. These architectures remain unchanged even after several iterations of the hydrothermal and IJP procedures (Fig. 4d, e) [37].

Seemingly, when the $Ni(OH)_2$@NF was immersed again in Ni^{2+} solution, the dimensional volume of the pore gets reduced and the emergence of profuse flake cross-like structure is observed. The $Ni(OH)_2$ continues developing NF laterally, showing the essential function played by rGO film in anchoring the top layer of $Ni(OH)_2$. In addition to the hydrothermal method, the solid-state reaction method can also be employed to synthesize $Ni(OH)_2$ nanoparticles which could aid in delivering better specific capacitance [38]. Consequently, the electrode prepared with controlled microstructures demonstrates exemplary electrochemical behavior. An asymmetric supercapacitor (ASC) device made using the $Ni(OH)_2$/rGO/$Ni(OH)_2$/rGO composites exhibits outstanding power density and energy density as shown in Fig. 5a–f (30.7 Wh kg^{-1} at 16,000 W kg^{-1} and 64.8 Wh kg^{-1} at 800 W kg^{-1}). Their enhanced electrochemical performance is owed to the layered fabrication process with greater mass loading [39]. Thus the as-erected $Ni(OH)_2$-based ASC outperformed the previously synthesized SCs [40, 41].

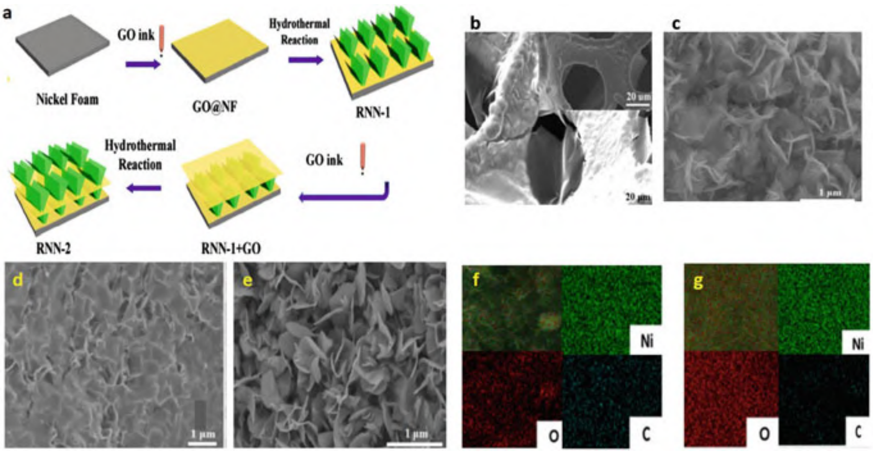
a
Nickel Foam
GO ink
GO@NF
Hydrothermal Reaction
RNN-1
GO ink
RNN-1+GO
Hydrothermal Reaction
RNN-2
b
20 μm
20 μm
c
1 μm
d
1 μm
e
1 μm
f
Ni
O
C
g
Ni
O
C

Fig. 4 **a** Fabrication of multi-layered $Ni(OH)_2$/rGO on nickel foam (NF) by merging the hydrothermal and IJP techniques. SEM images of **b** Pristine nickel foam, **c** RNN-1, **d** GO/$Ni(OH)_2$/rGO@NF **e** RNN-2. EDX mappings of **f** RNN-1 and **g** RNN-2. Copyright © 2019 Elsevier, Reproduced with permission from [37]

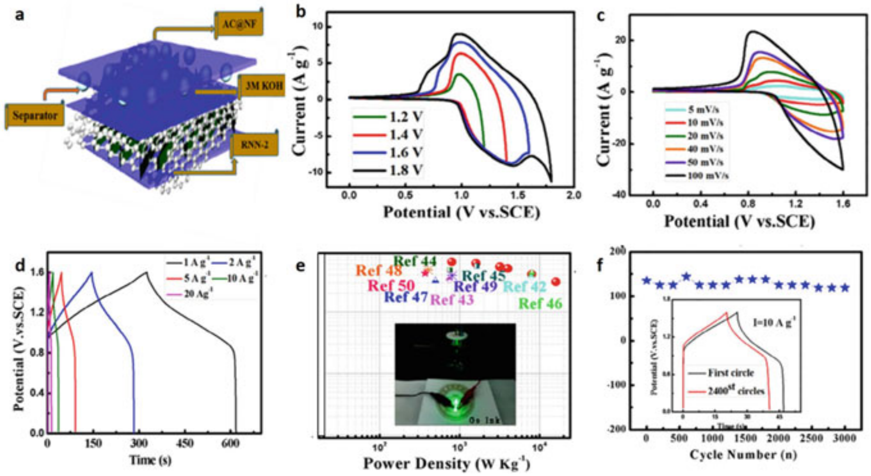

Fig. 5 **a** Representation of the as-prepared SC with RNN-2 and activated carbon serving as the cathode and anode material. The ASC's CV profiles functioned at **b** Various potentials and, **c** Various scan rates. **d** GCD profiles in the potential range of 0–1.6 V for the ASC with various current densities, **e** Ragone plot of the ASC device with a glowing LED as an inset, **f** Cycling stability of an ASC for 3000 cycles at 10 A g^{-1} with an inset of 1st and 2400th cycles. Copyright © 2019 Elsevier, Reproduced with permission from [37]

A fundamental limitation of the IJP technology is that there are no environmentally safe liquid inks devoid of various substances such as surfactants and toxic solvents. To address this, hybridized MXene-based inks were utilized in order to facilitate better electrical conductivity, optical, and mechanical properties to enhance the capacitance of the SC [42]. Ma et al. demonstrated that a water-based printable MXene/PEDOT: PSS [Poly (3,4 ethylenedioxythiophene): poly (styrene sulfonate) (MP) hybridized ink is an essential component for the scalable industrialization of self-powered integrated systems. The fabricated MP-MSCs had a phenomenal ED of 9.4 m Wh cm^{-3}, which is predominant to the IJ-printed MSCs that have been reported in the past. Additionally, the MP-MSCs have an unusual 754 F cm^{-3} volumetric capacitance. This exceptional performance may be ascribed, in part, to the better conduciveness of PH 1000, allowing for rapid electron and ion transport across the microelectrodes playing a significant role. Figure 6(a–b) is a simplified flowchart of the steps required to print and assemble MSCs using MP ink [43].

Correspondingly, at room temperature an HP Deskjet 2132 IJ printer was used to IJ-print MXene/graphene composite films [44], where the MXene/graphene ink was fed into a drained cartridge, and the nozzle was finessed with a piece of paper (Fig. 7). The paper type was adjusted to be consistent with other vivid IJP sheets for the best results. In order to complete the electrode design, the films were printed on PET tapes using text editing software. The printed films were quickly dried before the next IJP process begins, with an induction heater allowing the solvent to evaporate as quickly as possible. Also, Li et al. in Fig. 8(a–f) successfully researched the IJP methodology of rGO film electrodes for SCs, which allowed for layering nickel–cobalt dual

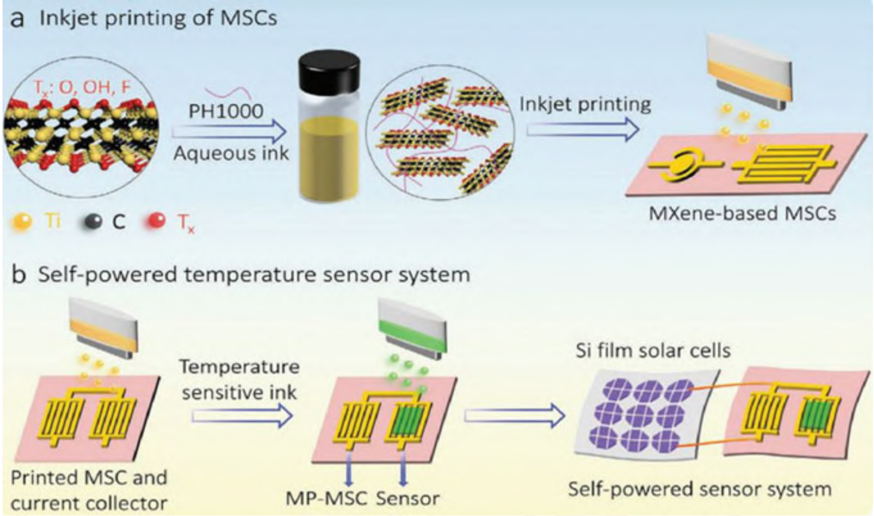
a Inkjet printing of MSCs
T_x: O, OH, F
PH1000
Aqueous ink
Inkjet printing
MXene-based MSCs
Ti
C
T_x
b Self-powered temperature sensor system
Temperature sensitive ink
Si film solar cells
Printed MSC and current collector
MP-MSC Sensor
Self-powered sensor system

Fig. 6 **a** Fabrication of MP-MSCs using hybrid aqueous MP ink, **b** IJP of self-powered temperature MP-MSC sensor connected to the solar cell made of Si films. Copyright © 2021 Springer Nature, Reproduced with permission from [43] hydroxide in the absence of the binder. This was achieved by printing several layers on top of each other, where the thin rGO films might work as a highly-conductive anchor for additional active components. Further a one step electrochemical deposition was used to increase the electrochemical activity of the system, where Ni–Co LDH is used as the main active component.

So Li et al. successfully printed Ag nanoparticles and graphite oxide on the flexible carbon cloth, creating a layer that is both flexible, conductive, as well as hydrophilic. The enormous surface area of this material makes it a novel candidate for electron transport. This binder-less Ni–Co LDH/Ag/rGO@CC electrode attained 173 mAh g^{-1} of capacity at 1 A g^{-1}, demonstrating its superior electrochemical performance. Similarly an ASC fabricated with Ni-Co LDH/Ag/rGO@CC as positive electrode, and the AC as negative electrode, yielded 95 mAh g^{-1} of high capacity at 0.6 A g^{-1} and 76 Wh kg^{-1} of maximum energy density at 480 W kg^{-1} [45].

By repeatedly depositing the electroactive materials through IJP, electrochemical performance is enhanced in terms of greater energy efficiency, lesser reaction time and thermal treatment, which makes them compatible for practical application requirements [46]. In later works, Li et al. IJ printed conductive rGO patterns onto which Ni-Co LDH was electrodeposited to form the Ni–Co LDH/rGO/Ni–Co LDH/rGO electrode, which achieved a capacity of 227 mAh g^{-1}, and the capacity value was retained at 78.7% over crossing 5000 cycles. The positive electrode of the two-electrode SC was made out of Ni–Co LDH/rGO/Ni–Co LDH/rGO, while the negative electrode was made out of commercially activated carbon. As a result of the enhancements made to the electrochemical characteristics of Ni–Co LDH/rGO/Ni–Co LDH/rGO//AC, it was possible to obtain an energy density of 284.9 Wh kg^{-1} and a power density of 424 kW kg^{-1}respectively [47]. Similar work was reported by M. Li et al. in which Ni-Co LDH was prepared by the electrochemical deposition method where rGO film was used to maintain homogeneity and continuity [48].

Fadakar et al. developed a supercapacitor by sandwiching a gel electrolyte made up of potassium hydroxide and polyvinyl alcohol (PVA-KOH) with and without

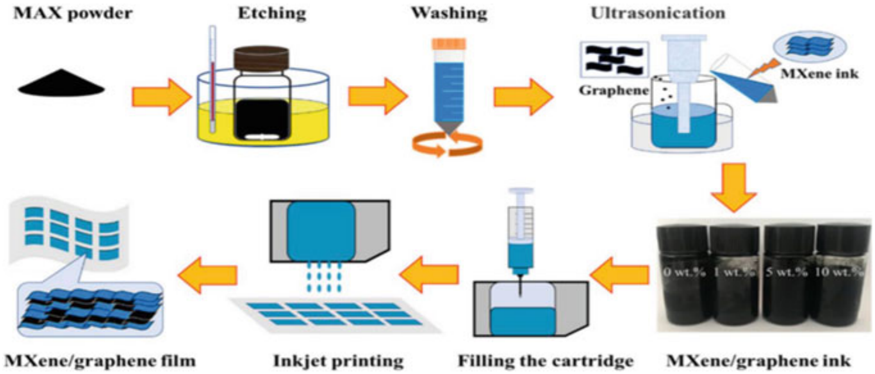

Fig. 7 Pictorial representation of IJP and its ink concoction. Copyright © 2022 Elsevier, Reproduced with permission from [44]

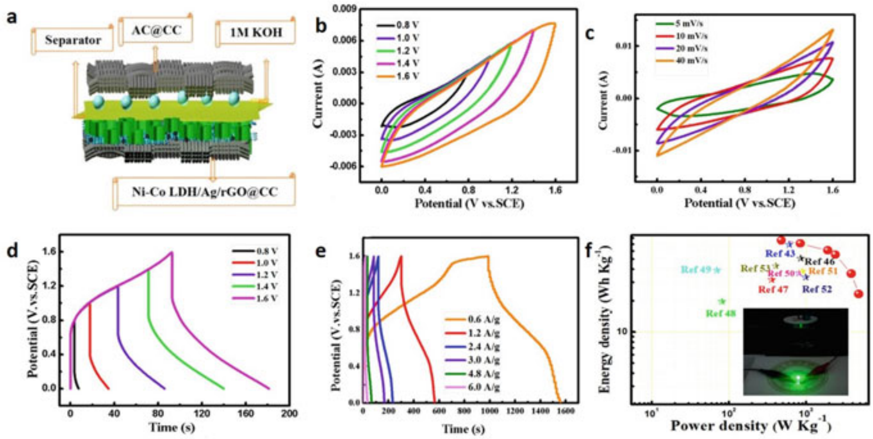

Fig. 8 **a** Schematic of the Ni–Co LDH/Ag/rGO@CC and AC-coated CC electrodes assembled into an ASC. **b**, **c** CV profiles of the ASC at various potentials and scan rates. **d**, **e** GCD curves in the potential window of 0–1.6 V at varied potential and current densities of the as-fabricated ASC. **f**, Ragone plot of ASC; inset is glowing LED. Copyright © 2019 Elsevier, Reproduced with permission from [45]

adding potassium iodide (KI), between two inkjet-printed nanosilver flexible electrodes (NSFEs). This SCs electrochemical performance was studied by using cyclic voltammetry (CV) in conjunction with galvanostatic techniques. By testing PVA-KOH systems with a broad variety of salt concentrations, it was determined that KI worked best at a concentration of 0.072 M. This conclusion was reached after testing PVA-KOH systems with a range of salt concentrations. CV curves of NSFEs, which were in contact with a gel electrolyte such as PVA-KOH-KI were collected at varying scanning speeds, and the results of these voltammograms suggested that the NSFEs exhibited diffusion-limited behavior. The specific capacitance of the IJ printed NSFE employed in the SC was then calculated to be 0.22 F g^{-1} by using galvanostatic (GCD) charge–discharge cycles [49]. Similarly, MSCs stacked and inkjet printed with RGO/MoO_3 (molybdenum trioxide) electrode was erected with PVA-H_2SO_4 electrolyte, which relatively responded with 22.5 F cm^{-3} of specific capacitance in 0-0.8 V of broad voltage window, exhibiting improved flexibility and cyclic efficiency [50]. Some of the mature inkjet printing technologies have been incorporated into the printing of superior-quality layered graphene [51] and poly(4-vinylphenol) based inks onto the polyimide film substrates for SCs [52].

4.4 Inkjet Printed Hybrid Electroactive Materials

The IJP approach facilitates the creation of highly efficient electrodes involved in constructing hybrid nanomaterials with complementary functions. In this context, Liu et al. successfully IJ printed solid-state bendable SCs using a hybrid ink containing GO and carbon quantum dot particles, which were then cast with concentrated sulphuric acid on PVA to form an electrolyte. After scanning at 100 ppm with 100 prints, a specific capacitance of 10 mF cm^{-2} was achieved with an increase of approximately 150 prints. The device as a whole had good flexibility and durability due to the notable mechanical strength of the GO platelets which led to a specific energy density of 0.078 m Wh cm^{-3} and a specific power density of 0.28 m W cm^{-3}, and they retained 98% of their capacity at a bent radius of 76 mm even after being bent 1000 times. This study provides hope for the mass manufacturing of lightweight, cost-effective, flexible, and environmentally friendly energy receptacle devices on carbon-based paper and ink substrates (Fig. 9a–l) [53]. In order to achieve increased capacitance, the nature and amount of oxygen functional groups must be specifically tailored. Rich functional groups that contain oxygen such as carboxyl, hydroxyl, and carbonyl groups are anticipated to offer rich reactive redox sites to produce pseudocapacitance in GO or CQDs [54–59].

To create a finger-structured interdigitated electrode, Ag nanoparticle ink was IJ printed onto a coarse flexible composite protein film (FCPF) substrate [60]. Figure 10 (a,b) is a schematic depiction of the manufacturing process of the electrode. Each of its eight sets of interdigitated “fingers” was 350 mm wide, and 8 mm long, separated by a gap (space) of roughly 450 mm. As a further step, Ni was electrochemically deposited over the Ag layer to boost its conductivity. Moreover, diverse combinations of flexible, and high-performance MnO_2 are widely preferred as electroactive

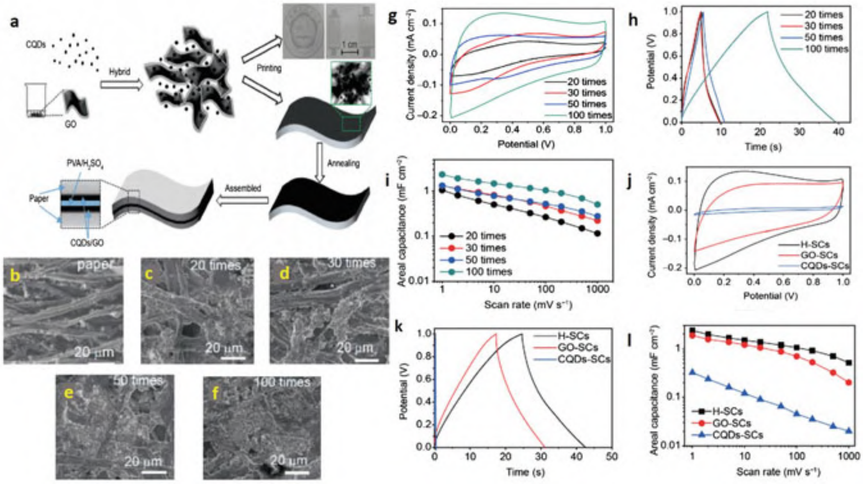

Fig. 9 **a** Illustration depicting the fabrication of a solid-state SC. SEM images of **b** a paper, and **c**–**f** Hybrid ink printed papers for varied printing time durations, **g**, **h** CV and GCD profiles of the HSC at 100 mVs^{-1} scan rate and current density at various printing durations, **i** Scan rate vs areal capacitance, **j**, **k** Voltammetric and GCD profiles of GO-SCs, CQDs-SCs, and H-SCs at a scan rate and current density of 100 mVs^{-1} and 100 μA cm^{-2}, and **l** Comparison of GO-SCs, CQDs-SCs, and H-SCs w.r.t scan rate. Copyright © 2018 Elsevier, Reproduced with permission from [53]

materials for IJP [61, 62]. In this respect, a hierarchical MnO_2@Ni/Ag electrode was then created by electrochemically depositing MnO_2 on top of the Ni/Ag layer. Correspondingly, from Fig. 10c, we can observe three different layers of the fabricated electrode and their corresponding morphologies whereas in Fig. 10d FCPF serves as the base for the printed Ag particles (about 20–50 nm). Following the Ni electrochemical deposition, it is shown that Ni particles (60–120 nm) cover the conducting silver networks consistently. From Fig. 10e–g, the electrode's conductivity is improved by 60 factors after which the nickel has been deposited upon it even after 1000 times of bending (Fig. 11). In addition to IJP, similar works have been reported using laser direct writing for wearable electronics [63] and for protein-based sensors as well for motion detection [64].

Graphene/polyaniline (NGP/PANI) inks were formulated by Xu et al. to produce NGP/PANI thin-film electrodes using IJP technology. In order to produce the NGP ink, 100 ml of water, 200 mg of SDBS surfactant, and 200 mg of NGP powder were combined. After that, the mixture was ultrasonically agitated for an hour at a temperature of 10 °C (400 W, 24 kHz) (Fig. 11a–f). After centrifuging this solution at 500 revolutions per minute (rpm) for 10 min, the supernatant was collected and utilized to make NGP ink. Then 200 mg of PANI was put into the NGP mixture and ultrasonically probed, while keeping the temperature at 10 °C for half an hour (400 W, 24 kHz). After the aforementioned combination has been mixed, it is then centrifuged at 500 rpm for 10 min. The produced supernatant was then gathered

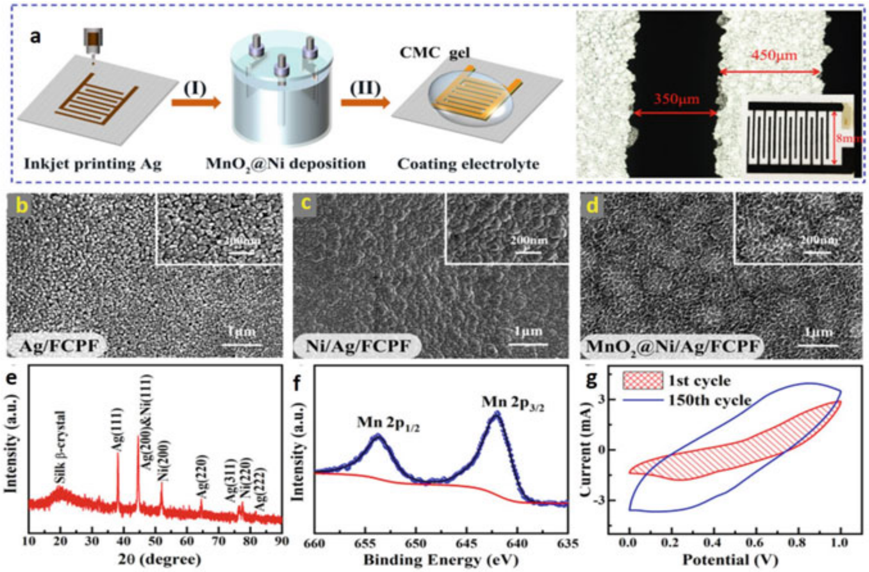

Fig. 10 **a** Depiction of the MSC's erection procedure with its magnified image, **b**–**d** SEM photos of the Ag, Ni, and MnO_2 layers, **e** XRD analysis of MnO_2@Ni/Ag/FCPF, XPS spectrum of **f** Mn 2p, **g** CV profiles of before and subsequent to 150th cycle. Copyright © 2021 Elsevier, Reproduced with permission from [60]

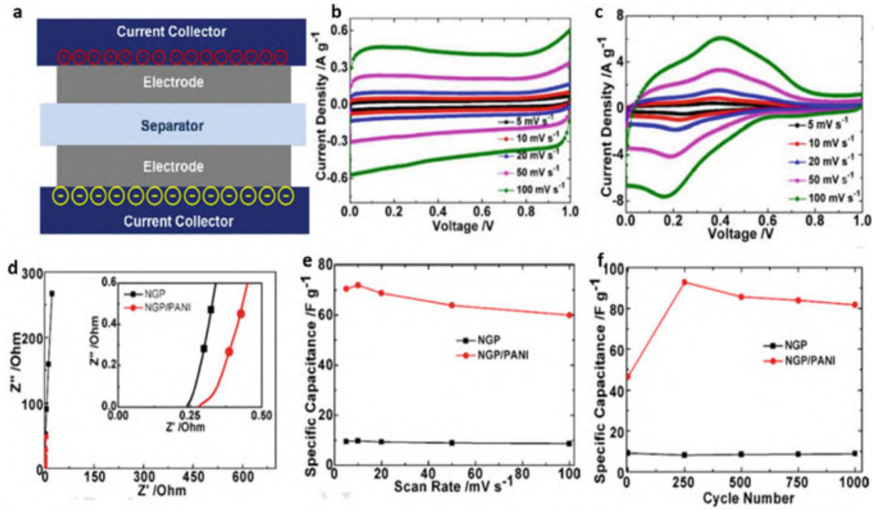

Fig. 11 **a** SC device, Voltammetric profiles of **b** NGP electrode and **c** PANI\NGP electrodes evaluated under various scan iterations in 1 M H_2SO_4 using a dual-electrode setup, **d** Nyquist plots of NGP and PANI\NGP supercapacitor device. **e** Specific capacitance (Cs) as a function of scan iteration for a dual-electrode system with a water-based electrolyte containing 1 M H_2SO_4. **f** Cyclic stability of the SC for 1,000 charge and discharge cycles at a steady CD of 1.4 A g^{-1}. Copyright © 2014 Elsevier, Reproduced with permission from [65]

and used as NGP/PANI ink. The experiment was further carried out at an ambient temperature, and the conditions of printing are mentioned henceforth: a strobe delay of 400 microseconds (ms), a voltage of 86 V, a pulse duration of 40 ms, a frequency of 500 Hz, and a pressure of −5 bar were all used in this process. A grid was utilized for printing with a spacing between points of 0.013 mm and a size of 800 pts. The as-printed grids underwent a drying process that lasted for two hours at a temperature of 80 °C. The mass of the NGP/PANI electrode substances were determined to be 1.5 mg cm^{-2}, which was resolved by calculating the difference between the weight of the substrates before and after printing. The electrochemical studies provide 82 F g^{-1} of specific capacitance at a PD and ED of 124 kW kg^{-1} and 24 Wh kg^{-1}, respectively, at 20 mV s^{-1}, which is utilized in the SCs to have an extended life cycle of more than a thousand cycles [65, 66]. Similarly, electrodes such as graphene/polyaniline can also be printed using a similar technique for supercapacitors for achieving ultra-high capacitance [67, 68]. Also, freestanding porous three-dimensional electrodes IJ printed onto the paper-based substrate using graphene/PANI hybrid inks, were erected into a flexible solid-state SC, which delivered 24.02 Wh kg^{-1} of ED, and 400.33 W kg^{-1} of PD respectively [69].

Using SWCNT ink substances in the standard of IJP, SWCNT thin film electrodes have been produced on fabric substrates with great success (Fig. 12a–f). These electrodes may be adjusted in terms of their unique electrical conductivity, position, texture (20–200 nm), and template (0.04–6.0 cm^2). The polymer electrolyte and the as-printed SWCNT sheets were bonded to create wearable and flexible SCs. After being put through a total of 1,000 cycles, the capacitive performance of these SCs was still outstanding. Also, a predominant method was employed for making ruthenium (RuO_2) oxide/SWCNT hybrid ink films. Compared to bare SWCNT electrodes with ~158 Hz of frequency, integrating RuO_2 with SWCNT electrodes increased the frequency to about 1500 Hz, which is much higher. Adding RuO_2 nano-wires also considerably boosted the behavioral characteristics of the printed SWCNT SCs. An improvement of 138 F g^{-1} in specific capacitance, 96 k W kg^{-1} in PD, and 18.8 Wh kg^{-1} in specific energy density were all achieved in the printed SWNT SC [70]. Parallely, utilizing a carbon-based hybrid ink containing GO-commercial pen ink, and GO-FGO (Few Layered Graphene) ink flexible micro-supercapacitors (MSCs) and sensors were successfully fabricated via inkjet printing [71, 72]. Likewise, hybrid Ni-Co oxide inks and $Ti_3C_3T_x$/C nanospheres were inkjet printed and were utilized as electrodes for supercapacitors [73, 74]. This demonstrates the immense potential of printed SWCNT SCs for usage in wearable energy storage systems.

There is a possibility that flexible printed circuits (PC) of all planar SCs based on graphene might find use in wearable and portable electronic devices. Because of their restricted surface area and their sluggish dispersal rate of ions, the specific capacitance of the device is low and has a deficient performance rate as well. Enhancing the device's energy-storage capacity requires overcoming a fundamental challenge, (i.e.) enhancing the dispersion of PVA-based gel electrolyte onto the produced graphene microelectrodes (Fig. 13a–h) [75]. In this context, utilizing N-doped hydrophilic graphene combined with the PVA-H_3PO_4 gel electrolyte, the

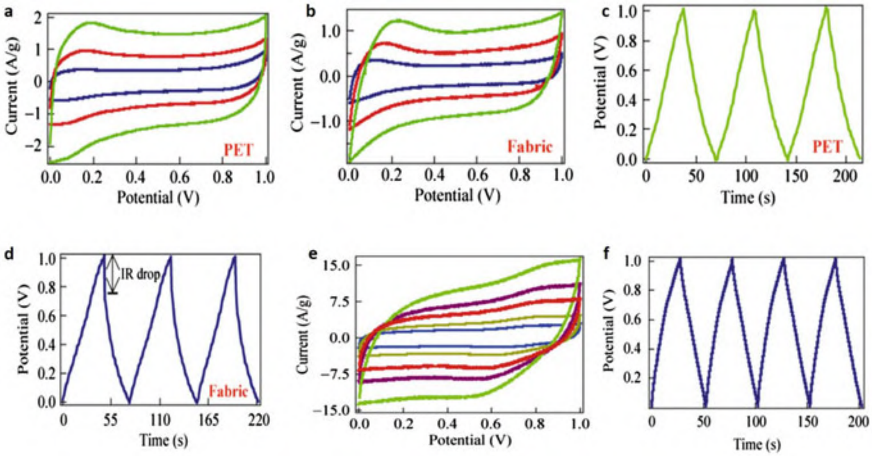

Fig. 12 CV profiles of **a** SWCNT/PET SC, **b** SWCNT/fabric SC with a PVA/H_3PO_4 polymer electrolyte at various scan iterations, GCD profiles of **c** an SWCNT/PET SC and **d** an SWCNT/fabric SC with a steady current density of 1 A g^{-1}, **e** CV profiles of SWCNT/RuO_2 nanowire SC in PVA/H_3PO_4 polymer electrolyte. **f** GCD curves of hybrid SWCNT/RuO_2 nanowire SC at a current density of 8 A g^{-1}. Copyright © 2010 Springer Nature, Reproduced with permission from [70]

authors of this study attempted the formulation of hybrid ink made of PVA-H_3PO_4 with soluble graphene oxide for printing the SCs [76, 77]. This ink formulation was intended for use in gravure-printed planar SCs. It was feasible to gravure print graphene@PVA-H_3PO_4 microelectrodes by refining the quality of the ink and then researching the reaction between gravure cells and the inks. This made it possible to gravure print graphene@PVA-H_3PO_4 microelectrodes. The printed microelectrodes have graphene-active surfaces that are more easily accessible to the electrolytes directly responsible for the improved electrochemical performance of flexible planar SCs. These SCs were flexible and planar in shape, and a high value of areal capacitance of the order of 37.5 m F cm^{-2} was observed at the scan speed of 5 m V s^{-1}. This results in an ED value of 5.20 m Wh cm^{-2} at an areal PD. of 3.2 m W cm^{-2}. This value is equivalent to a volumetric ED of 2.08 m Wh cm^{-3} [78].

Choi et al. [79] created a SC that was entirely produced by a desktop IJ printer used commercially. The SC was printed on a standard A4 paper directly. In order to accomplish this goal, mediated (CNF) cellulose nanofibril nanostructured mats were initially IJ printed onto an A4 sheet of paper to serve as a priming layer (Fig. 14a). The production of electrodes was accomplished by first printing an SWCNT which is active electrochemically or by using ink made up of AC, followed by the printing of Ag ink based nano-wires which conducts electrically (Fig. 14b).

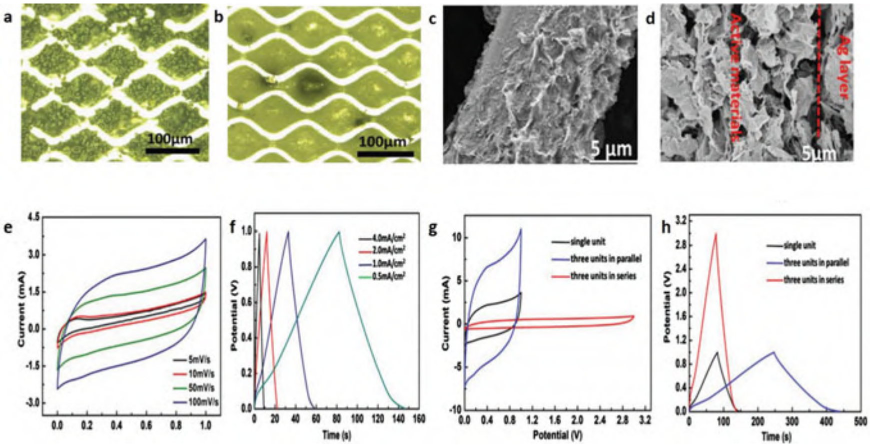

Fig. 13 **a**, **b** Micrographs of inked and un-inked gravure cells and their subsequent transportation medium, **c**, **d** Cross-sectional and a top SEM images of graphene @ PVA-H_3PO_4 microelectrode produced by gravure. Electrochemical performance of graphene@PVA-H_3PO_4 microelectrodes in planar SCs, **e** Voltammetric curves at various scanning speeds between 5 and 100 mV s^{-1}, **f** GCD profiles at the current densities between 0.5 and 4.0 mA cm^{-2}, **g** Corresponding CV curves of three units in parallel & series at a scanning speed of 100 mV s^{-1}, **h** GCD profiles of three units in series and parallel at 0.5 mA cm^{-2} of current density. Copyright © 2018 Springer Nature, Reproduced with permission from [75]

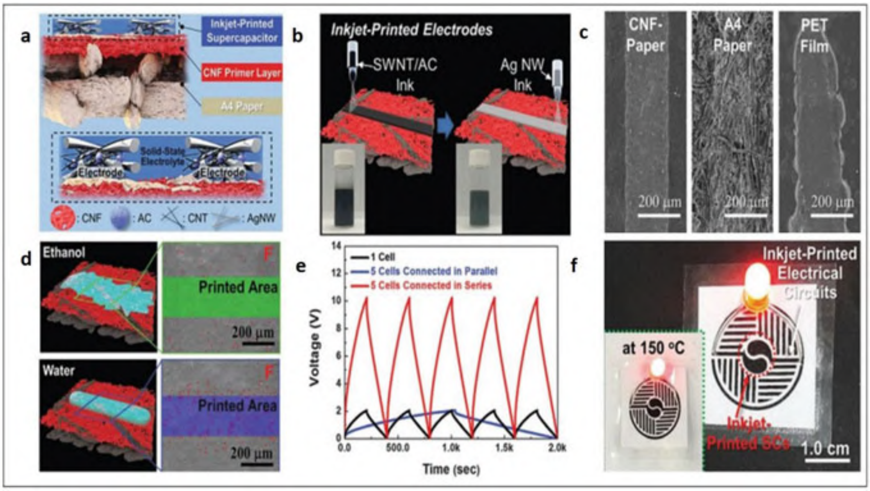
a
Inkjet-Printed Supercapacitor
CNF Primer Layer
A4 Paper
Solid-State Electrolyte
Electrode
Electrode
: CNF
: AC
: CNT
: AgNW
b
Inkjet-Printed Electrodes
SWNT/AC Ink
Ag NW Ink
c
CNF-Paper
A4 Paper
PET Film
200 µm
200 µm
200 µm
d
Ethanol
Printed Area
200 µm
F
Water
Printed Area
200 µm
F
e
1 Cell
5 Cells Connected in Parallel
5 Cells Connected in Series
Voltage (V)
0
2
4
6
8
10
12
14
0.0
500.0
1.0k
1.5k
2.0k
Time (sec)
f
Inkjet-Printed Electrical Circuits
at 150 °C
Inkjet-Printed SCs
1.0 cm

Fig. 14 **a** IJ printed SC, **b** Representation of the manufacture of IJP SC electrodes, **c** SEM micrographs of the IJ printed electrodes on varied substrates, **d** IJ printed electrolytes with their respective schematics and EDX pictures, **e** GCD profile of the IJ printed SCs coupled in either parallel or series, **f** An IJ-printed circuit connected to an LED. Copyright © 2016 The Royal Chemical Society, Reproduced with permission from [79]

Silver nano-wire sintering using photons was carried out onto the electrodes printed to bring about an additional enhancement in the conductivity, which is demonstrated in (Fig. 14c). When compared to the control substrates, the CNF prime layer made it possible to deposit electrode materials in a homogeneous manner (i.e., PET and A4 paper). IJP of an ionic liquid or a polymer solid-state electrolyte such as triacrylate, which is UV cured, i.e., BMIMBF4 (1-butyl-3-methylimidazolium tetra- fluoroborate) or ETPTA (ethoxylated trimethylolpropane triacrylate) was done atop of the electrode to finish the production of the device. Both water and ethanol were tested as potential electrolyte ink solvents throughout the product development process. According to EDX findings, the use of aqueous-based inks resulted in the production of printed high-resolution electrolytes. This was due to the fact that water has a greater surface tension than other liquids (72 mN m^{-1}) (Fig. 14d). Besides, IJ printed SCs were combined in parallel or series, which led to the customized user-defined control of the overall capacitance or output voltage (Fig. 14e). Thus the IJ-printed SCs with aesthetic designs were united with the IJ-printed electrical circuits to light an LED lamp as an application, further exemplifying the functionality of the manufactured SCs (Fig. 14f) [80]. Wide range of instances are being printed using diverse patterning strategies by employing IJP technique [81, 82].

Using the IJP methodology, streamlined and adaptable solid-state SCs with a PD of 0.036 W cm^{-2} and an ED of 0.59 m Wh cm^{-2} were successfully created. By employing a material such as PEDOT: PSS/Ag grid electrodes, these SCs were even operated at a PD of about 0.036 W cm^{-2}. Fabricating SCs with various motifs,

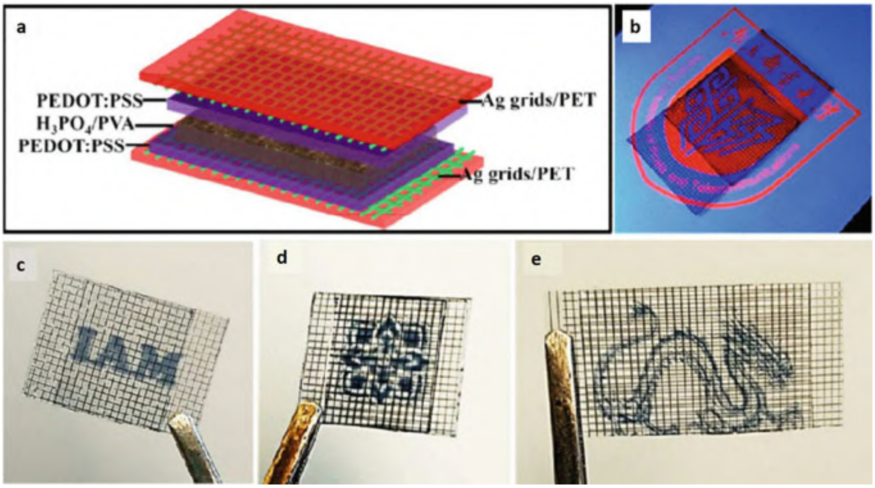

Fig. 15 **a** Internal construction of SC, **b** Depiction of a transparent SC with an electrode made of PSS (3 layers)/Ag grids and PEDOT-S, **c**–**e** Images of the aesthetically pleasing SC with a variety of exquisite designs. Copyright © 2015 Springer Nature, Reproduced with permission from [83]

including logos, flowers, and dragons, was done to demonstrate the remarkable versatility of patterning offered by IJP (Fig. 15a–e). Because of their outstanding flexibility, aesthetically pleasing look, and relatively high optical transparency, the printed SCs showed a great deal of promise for the development of wearable and flexible electronic systems. Efforts are being made to enhance the conductivity of PEDOT: PSS [83].

4.5 InkJet Printed Current Collector Substrate

The Ag current collector was manufactured by Giannakou et al. utilizing IJP methodology. In a ground plane, consisting of an interdigitated arrangement on a flexible substrate material (Fig. 16a), NiO electrode material is printed on top of the active area of the interdigitated fingers (Fig. 16b). Subsequently the structure is thermally treated to enhance nanoparticle sintering and to evaporate the organic components in both inks (Fig. 16c, d), and lastly the inks are drop-casted. The existing collector's silver layer has to cure or at least be mostly dry before the NiO material can be printed on top of it. A time delay of about five minutes is to be implemented. To provide a seamless interaction among the two substances, the Ag layer is not annealed prior to the NiO layer's printing. This permits multiple layers to be annealed in a single phase, yielding superior results. During the printing procedure, using a piezoelectric printer, a dramatic material is printed via DOD methodology (model number DMP

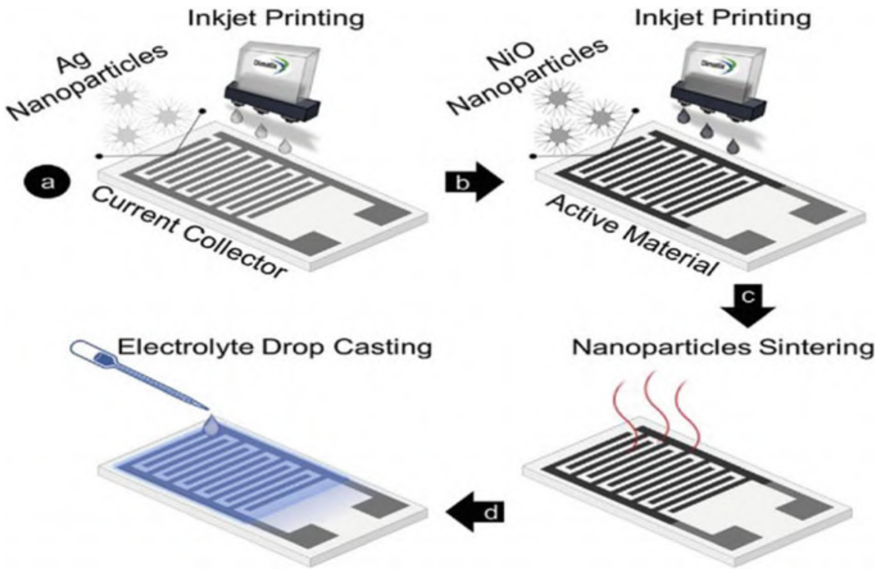

Fig. 16 Steps in the production of an IJ printed NiO SCs, **a** Fabrication of current collector using IJP of Ag nanoparticles onto a substrate with an interdigitated coplanar structure, **b** NiO nanoparticles IJ printed above the interdigitated current collector made up of Ag, **c** The substrate annealed for prompting the sintering of nanoparticles on both sides, **d** Drop-casting of the electrolyte substances on top of the device with dynamic interdigitations. Copyright © 2020 Springer Nature, Reproduced with permission from [84]

2800), enabling cartridges of pl (the model number of cartridge DMC-11610) to be used.

Wang et al. printed various patterns (Fig. 17) which are conductive using IJP methodology on paper using soluble (MWCNT) multi-walled carbon nanotube with hybridized Ag inks with the assistance of sodium dodecyl benzene sulfonate (SDBS). Fabrication of patterns that are highly conductive in the nature of MWCNT/Ag, by proliferating the number of printing processes to about 50 was able to attain a low sheet resistance of 300 sq^{-1}. In addition, the printed patterns demonstrated an improvement in sheet resistance by about 10% after being subjected to bending for even 2000 cycles. After printing the conductive pattern, ink based on MnO_2 was printed over the top of it to provide the positive electrode for the asymmetric Schottky barrier. The MWCNT sheet served as the adjacent electrode in this experiment. The completed SC displayed a high PD of 96 m W cm^{-3} at an ED of 1.28 m Wh cm^{-3} and an outstanding capacity retention of nearly 97% after 3000 GCD cycles were achieved although the power density was higher than the energy density [85].

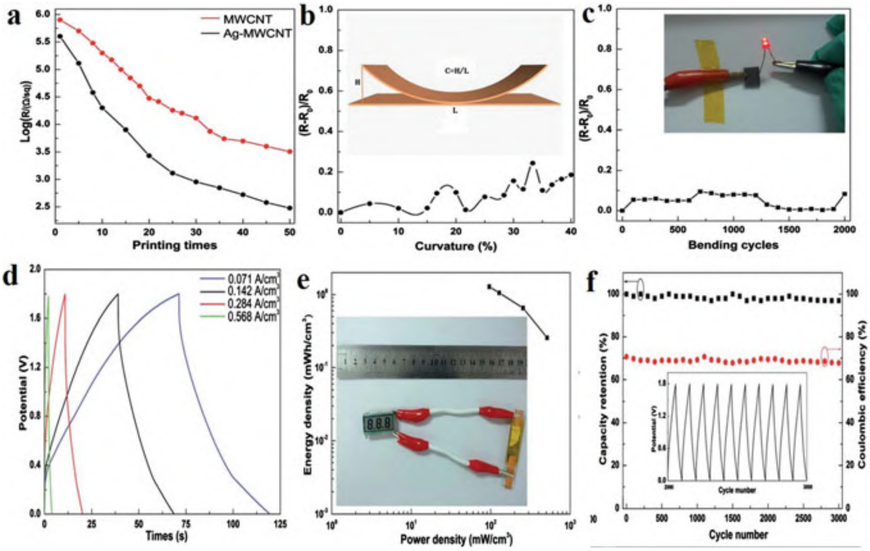

Fig. 17 **a** Number of prints vs. logarithmic sheet resistance, **b** Plot of variations in the resistivity of the conducting patterns versus curvature, **c** Bending cycles vs. modifications in the resistivity of the conducting patterns, **d** GCD profiles of the MWCNT//MnO2-Ag-MWCNT at varied current densities, **e** Plot of energy vs. power density of the as-fabricated ASC device, **f** Long-term cyclic performance of the MWCNT//MnO2-Ag-MWCNT. Copyright @ 2015 The Royal Society of Chemistry, Reproduced with permission from [85, 86]

5 Conclusion and Future Perspective

This chapter provides a concise summary of the most recent advancements that have been made in the area of IJ printed SCs, which are considered to represent the contemporary condition in which the state-of-the-art IJP has been utilized as a technique in the fabrication of active components of SCs as a direct consequence of its appealing characteristics, which has led to this technology's widespread use. Significant progress has been made in the reasonable combination of jetable optical ink substrate and in pattern optimization for printing. These two areas of research are closely related. Graphene, MXene, metal oxides, and other similar materials have been the focus of the research that has been conducted to generate IJ-printed electrode materials capable of better performance. In addition, it has been stated that the predominant process has been made in creating IJ-printed electrolyte substrates, with the ultimate goal of realizing various IJ-printed SCs. In this respect, several fascinating cases with exceptional performances have been highlighted.

Progress made in this area of IJP SCs is hampered by the scarcity of electrochemically active printed materials, which is another barrier to progress. It is necessary to accomplish the rising need for high-performance SCs, and the library of IJ-printable materials must be expanded to include more substances that have a better specific capacity and a wide range voltage. Another obstacle is that the bulk of the research has concentrated on creating electrodes that are produced using an inkjet printer. However, in spite of the fact that electrolytes are an essential part of SCs, only a small number of studies have documented inkjet-printed electrolytes. This presents a significant challenge to the development of SCs that are entirely printed using inkjet technology. Therefore, in order to increase the repository for electrolyte materials that can be printed using an inkjet printer, more research and investigations will need to be conducted.

The significance of the investigation into the use of IJP technology in the production of SC components is still in its early stages. Increasing the size of the library of items that can be printed using an inkjet printer should get a more significant focus from researchers. In particular, studies integrating IJP SCs with other printed electronic devices to construct all-printed circuits may lead to many desired properties for potential developments related to energy.

Acknowledgements The authors are thankful to the Technology Mission Division (Energy, Water & all Others), Department of Science & Technology, Ministry of Science & Technology, Government of India, New Delhi, India for the financial support under the Scheme of IC-MAP-2021, Project Title: DST-Storage MAP (Ref. No: DST/TMD/IC-MAP/2K20/01).

References

1. Noori A et al (2019) Towards establishing standard performance metrics for batteries, supercapacitors and beyond. Chem Soc Rev 48(5):1272–1341
2. Huang L et al (2018) Graphene-based nanomaterials for flexible and wearable supercapacitors. Small 14(43):1800879
3. An C et al (2019) Metal oxide-based supercapacitors: progress and prospectives. Nanoscale Adv 1(12):4644–4658
4. Qorbani M et al (2019) Ti-rich TiO_2 tubular nanolettuces by electrochemical anodization for all-solid-state high-rate supercapacitor devices. Chemsuschem 12(17):4064–4073
5. Xiao Z et al 2019 Controlled hydrolysis of metal-organic frameworks: hierarchical Ni/Co-layered double hydroxide microspheres for high-performance supercapacitors. ACS Nano 13(6):7024–7030
6. Sajedi-Moghaddam A et al (2019) Exfoliated transition metal dichalcogenide (MX_2; M=Mo, W; X=S, Se, Te) nanosheets and their composites with polyaniline nanofibers for electrochemical capacitors. Appl Mater Today 16:280–289
7. Das P, Wu Z-S (2020) MXene for energy storage: present status and future perspectives. J Phys: Energy 2(3):032004
8. Xia Y et al (2018) Thickness-independent capacitance of vertically aligned liquid-crystalline MXenes. Nature 557:409–412
9. Wang J et al (2019) Recent progress in micro-supercapacitor design, integration, and functionalization. Small Methods 3(8):1800367
10. Li H et al (2019) Hydrous RuO_2-decorated MXene coordinating with silver nanowire inks enabling fully printed micro-supercapacitors with extraordinary volumetric performance. Adv Energy Mater 9(15):1803987
11. Liang J et al (2019) All-printed solid-state supercapacitors with versatile shapes and superior flexibility for wearable energy storage. J Mater Chem A 7(26):15960–15968
12. Elder B et al (2020) Nanomaterial patterning in 3D printing. Adv Mater 32(17):1907142

13. Shahiduzzaman M et al (2019) Oblique electrostatic inkjet-deposited TiO_2 electron transport layers for efficient planar perovskite solar cells. Sci Rep 9(1):19494
14. Seo J-WT et al (2019) Fully inkjet-printed, mechanically flexible MoS_2 nanosheet photodetectors. ACS Appl Mater Interfaces 11(6):5675–5681
15. Huang T-T, Wu W (2019) Scalable nanomanufacturing of inkjet-printed wearable energy storage devices. J Mater Chem A 7(41):23280–23300
16. Raut NC, Al-Shamery K (2018) Inkjet printing metals on flexible materials for plastic and paper electronics. J Mater Chem C 6(7):1618–1641
17. Hu G et al (2018) Functional inks and printing of two-dimensional materials. Chem Soc Rev 47(9):3265–3300
18. Rafiq M et al (2022) Overview of printable nanoparticles through inkjet process: their application towards medical use. Microelectron Eng 266:111889
19. Bernasconi R et al (2022) Piezoelectric drop-on-demand inkjet printing of high-viscosity inks. Adv Eng Mater 24:2100733
20. Bonaccorso F et al (2016) 2D-crystal-based functional inks. Adv Mater 28(29):6136–6166
21. Fukuda K et al (2013) Profile control of inkjet printed silver electrodes and their application to organic transistors. ACS Appl Mater Interfaces 5(9):3916–3920
22. Zhan Z et al (2017) Inkjet-printed optoelectronics. Nanoscale 9(3):965–993
23. Lessing J et al (2014) Inkjet printing of conductive inks with high lateral resolution on Omniphobic "RF Paper" for paper-based electronics and MEMS. Adv Mater 26(27):4677–4682
24. Jiang J et al (2016) Fabrication of transparent multilayer circuits by inkjet printing. Adv Mater 28(7):1420–1426
25. Sun J et al (2015) Recent advances in controlling the depositing morphologies of inkjet droplets. ACS Appl Mater Interfaces 7(51):28086–28099
26. Gao M, Li L, Song Y (2017) Inkjet printing wearable electronic devices. J Mater Chem C 5(12):2971–2993
27. Li L et al (2016) High-performance solid-state supercapacitors and microsupercapacitors derived from printable graphene inks. Adv Energy Mater 6(20):1600909
28. Le LT et al (2011) Graphene supercapacitor electrodes fabricated by inkjet printing and thermal reduction of graphene oxide. Electrochem Commun 13(4):355–358
29. Hu L et al (2010) Printed energy storage devices by integration of electrodes and separators into single sheets of paper. Appl Phys Lett 96:183502
30. Stempien Z et al (2019) In-situ deposition of reduced graphene oxide layers on textile surfaces by the reactive inkjet printing technique and their use in supercapacitor applications. Synth Met 256:116144
31. Ujjain S K et al (2016) Printable multi-walled carbon nanotubes thin film for high performance all solid state flexible supercapacitors. Mater Res Bull 83:167–171
32. Giannakou P et al (2020) Water-transferred, Inkjet-printed supercapacitors toward conformal and epidermal energy storage. ACS Appl Mater Interfaces 12(7):8456–8465
33. Wang Y et al (2018) Inkjet printing of δ-MnO_2 nanosheets for flexible solid-state micro-supercapacitor. Nano Energy 49:481–488
34. Qian J et al (2015) Aqueous manganese dioxide ink for paper-based capacitive energy storage devices. Angew Chem Int Ed 54: 6800–6803
35. Kim Y et al (2012) Use of copper ink for fabricating conductive electrodes and RFID antenna tags by screen printing. Curr Appl Phys 12(2):473–478
36. Tang Z, Tang C-h, Gong H (2012) A high energy density asymmetric supercapacitor from nano-architectured $Ni(OH)_2$/carbon nanotube electrodes. Adv Funct Mater 22:1272–1278
37. Li X et al (2019) Layer-by-layer inkjet printing GO film anchored $Ni(OH)_2$ nanoflakes for high-performance supercapacitors. Chem Eng J 375:121988
38. Sun Z, Lu X (2012) A solid-state reaction route to anchoring $Ni(OH)_2$ nanoparticles on reduced graphene oxide sheets for supercapacitors. Ind Eng Chem Res 51(30):9973–9979
39. Wang H et al (2010) $Ni(OH)_2$ nanoplates grown on graphene as advanced electrochemical pseudocapacitor materials. J Am Chem Soc 132(21):7472–7477

40. Bai Y et al (2015) Controllable synthesis of 3D binary nickel–cobalt hydroxide/graphene/nickel foam as a binder-free electrode for high-performance supercapacitors. J Mater Chem A 3(23):12530–12538
41. Liu S et al (2017) Hierarchical MnCo-layered double hydroxides@Ni$(OH)_2$ core–shell heterostructures as advanced electrodes for supercapacitors. J Mater Chem A 5(3):1043–1049
42. Zhang C et al (2018) Stamping of flexible, coplanar micro-supercapacitors using MXene inks. Adv Func Mater 28(9):1705506
43. Ma J et al (2021) Aqueous MXene/PH1000 hybrid inks for inkjet-printing micro-supercapacitors with unprecedented volumetric capacitance and modular self-powered micro-electronics. Adv Energy Mater 11(23):2100746
44. Wen D et al (2022) Direct inkjet printing of flexible MXene/graphene composite films for supercapacitor electrodes. J Alloy Compd 900:163436
45. Li X et al (2019) Layer-by-layer inkjet printing GO film and Ag nanoparticles supported nickel cobalt layered double hydroxide as a flexible and binder-free electrode for supercapacitors. J Colloid Interface Sci 557:691–699
46. Nagaraju G et al (2016) Hierarchical Ni–Co layered double hydroxide nanosheets entrapped on conductive textile fibers: a cost-effective and flexible electrode for high-performance pseudocapacitors. Nanoscale 8(2):812–825
47. Li X et al (2020) Layer by layer inkjet printing reduced graphene oxide film supported nickel cobalt layered double hydroxide as a binder-free electrode for supercapacitors. Appl Surf Sci 509:144872
48. Li M et al (2016) The growth of nickel-manganese and cobalt-manganese layered double hydroxides on reduced graphene oxide for supercapacitor. Electrochim Acta 206:108–115
49. Fadakar Z et al (2015) Fabrication of a supercapacitor with a PVA–KOH–KI electrolyte and nanosilver flexible electrodes. Microelectron Eng 140:29–32
50. Li B et al (2019) Direct inkjet printing of aqueous inks to flexible all-solid-state graphene hybrid micro-supercapacitors. ACS Appl Mater Interfaces 11(49):46044–46053
51. Li J et al (2013) Efficient inkjet printing of graphene. Adv Mater 25(29):3985–3992
52. Momota M R et al (2023) Fabrication and characterization of flexible solid-state MIM supercapacitor with inkjet-printing of stacked Ag NP and polymer dielectric layers. 2023 IEEE 16th Dallas circuits and systems conference (DCAS), pp 1–5. Denton, TX, USA
53. Liu J, Ye J, Pan F et al (2019) Solid-state yet flexible supercapacitors made by inkjet-printing 695 hybrid ink of carbon quantum dots/graphene oxide platelets on paper. Sci China Mater 62:545–554
54. Jiang L et al (2015) Functional pillared graphene frameworks for ultrahigh volumetric performance supercapacitors. Adv Energy Mater 5(15):1500771
55. Miller J, Outlaw R, Holloway BC (2011) Graphene electric double layer capacitor with ultra-high-power performance. Electrochim Acta 56:10443–10449
56. Zhao B et al (2012) Supercapacitor performances of thermally reduced graphene oxide. J Power Sources 198:423–427
57. Fang Y et al (2012) Renewing functionalized graphene as electrodes for high-performance supercapacitors. Adv Mater 24(47):6348–6355
58. Atif R, Shyha I, Inam F (2016) Mechanical, thermal, and electrical properties of graphene-epoxy nanocomposites—A review. Polymers 8(8):281
59. Li L-X, Li F (2011) The effect of carbonyl, carboxyl and hydroxyl groups on the capacitance of carbon nanotubes. New Carbon Mater 26(3):224–228
60. Chen C et al (2021) Smart power system of biocompatible and flexible micro-supercapacitor. Appl Phys Lett 118(7):073902
61. Gu S et al (2016) Fabrication of flexible reduced graphene oxide/Fe_2O_3 hollow nanospheres based on-chip micro-supercapacitors for integrated photodetecting applications. Nano Res 9(2):424–434
62. Jabeen N et al (2017) High-performance 2.6 V aqueous asymmetric supercapacitors based on in situ formed $Na_{0.5}MnO_2$ nanosheet assembled nanowall arrays. Adv Mater 29(32):1700804

63. Cai J, Lv C, Watanabe A (2018) Laser direct writing and selective metallization of metallic circuits for integrated wireless devices. ACS Appl Mater Interfaces 10(1):915–924
64. Hou C et al (2019) A biodegradable and stretchable protein-based sensor as artificial electronic skin for human motion detection. Small 15(11):1805084
65. Xu Y et al (2014) Inkjet-printed energy storage device using graphene/polyaniline inks. J Power Sources 248:483–488
66. Wang Y et al (2009) Supercapacitor devices based on graphene materials. J Phys Chem C 113(30):13103–13107
67. Xu Y et al (2013) Screen-printable thin film supercapacitor device utilizing graphene/polyaniline inks. Adv Energy Mater 3(8):1035–1040
68. Diao J (2018) Flexible supercapacitor based on inkjet printed graphene@polyaniline nanocomposites with ultrahigh capacitance. Macromol Mater Eng 303(6):1800092
69. Chi K et al (2014) Freestanding graphene paper supported three-dimensional porous graphene–polyaniline nanocomposite synthesized by inkjet printing and in flexible all-solid-state supercapacitor. ACS Appl Mater Interfaces 6:16312–16319
70. Chen P et al (2010) Inkjet printing of single-walled carbon nanotube/RuO_2 nanowire supercapacitors on cloth fabrics and flexible substrates. Nano Res 3(8):594–603
71. Pei Z et al (2017) Carbon-based flexible and all-solid-state micro-supercapacitors fabricated by inkjet printing with enhanced performance. Nano-Micro Lett 9(19):2520–2531
72. Huang L et al (2011) Graphene-based conducting inks for direct inkjet printing of flexible conductive patterns and their applications in electric circuits and chemical sensors. Nano Res 4:675–684
73. Banti A et al (2023) Electrochemical studies of inkjet printed semi-transparent $NiCo_2O_4$/ITO supercapacitor electrodes. Catalysts 13:1110
74. Wu Y et al (2022) Aerosol jet printing of hybrid Ti_3C_2Tx/C nanospheres for planar micro-supercapacitors. Frontiers in Chemistry 10
75. Chang Q et al (2018) Water-soluble hybrid graphene ink for gravure-printed planar supercapacitors. Adv Electron Mater 4(8):1800059
76. Grau G et al (2016) Gravure-printed electronics: recent progress in tooling development, understanding of printing physics, and realization of printed devices. Flex Print Electron 1(2):023002
77. Hyun WJ et al (2015) High-resolution patterning of graphene by screen printing with a silicon stencil for highly flexible printed electronics. Adv Mater 27(1):109–115
78. Xiao Z et al (2020) Materials development and potential applications of transparent ceramics: a review. Mater Sci Eng R Rep 139:100518
79. Choi K-H et al (2016) All-inkjet-printed, solid-state flexible supercapacitors on paper. Energy Environ Sci 9(9):2812–2821
80. de Gans BJ, Duineveld PC, Schubert US (2004) Inkjet printing of polymers: state of the art and future developments. Adv Mater 16(3):203–213
81. Tian D, Song Y, Jiang L (2013) Patterning of controllable surface wettability for printing techniques. Chem Soc Rev 42(12):5184–5209
82. Kuang M, Wang L, Song Y (2014) Controllable printing droplets for high-resolution patterns. Adv Mater 26(40):6950–6958
83. Cheng T et al (2016) Inkjet-printed flexible, transparent and aesthetic energy storage devices based on PEDOT: PSS/Ag grid electrodes. J Mater Chem A 4(36):13754–13763
84. Giannakou P, Slade RCT, Shkunov M (2020) Cyclic voltammetry studies of inkjet-printed NiO supercapacitors: effect of substrates, printing, and materials. Electrochim Acta 353:136539
85. Wang S et al (2015) Inkjet printing of conductive patterns and supercapacitors using a multi-walled carbon nanotube/Ag nanoparticle based ink. J Mater Chem A 3(5):2407–2413
86. Zhang T, Li X, Asher E et al (2018) Paper with power: engraving 2D materials on 3D structures for printed, high-performance, binder-free, and all-solid-state supercapacitors. Adv Funct Mater 28:1803600

Chapter 9
Pre & Post-Treatment of Functionalized Nanomaterials in Fabricating Supercapacitor Electrodes

Soumya Jha and R. Prasanth

1 Introduction

Ever since electricity was discovered, one of the major tasks the scientific community has faced is to store it. Energy consumption is rising in tandem with the increase in daily needs [1]. The storage issue is more critical for renewable energy systems since it is intermittent. In the current global power production scenario, we are moving more toward clean energy. The chronic depletion of these resources & emerging concern about global warming accelerates this process. However, the location- and time-specific nature of renewable energy sources make storage an inevitable part [2]. Among various energy storage devices, Electrochemical Energy Storage (EES) device has gained quite a lot of attention in the scientific community due to their high efficiency, adaptability & versatility [3–5]. Additionally, the current use of wearable and portable devices has increased the pressure to build high-performance EES. The capability of addressing these technology challenges provides a promising future for the EES.

Among various EES devices, batteries & supercapacitors (SC) are prominent. To date, conventional batteries are widely used in storage systems. They can provide high energy densities, storing up to 150–200 $\mathrm{WhKg^{-1}}$ [6, 7]. Even though they have a very high energy density, dealing with their low power density, heat production, and short operational lifetimes leads to high operational costs and tedious waste management [8]. The key factor contributing to batteries' short cycle life is volume changes that occur along with the redox reaction in batteries. The inadequacy of batteries to produce fast and high power significantly hinders their widespread use

---

S. Jha · R. Prasanth (✉)
Madanjeet School of Green Energy Technology, Pondicherry Central University, Pondicherry, India
e-mail: prasanth.get@pondiuni.edu.in

© The Author(s), under exclusive license to Springer Nature Singapore Pte Ltd. 2024

C. M. Hussain and M. B. Ahamed (eds.), *Functionalized Nanomaterials Based Supercapacitor*, Materials Horizons: From Nature to Nanomaterials,
https://doi.org/10.1007/978-981-99-3021-0_9

as energy storage technologies. In a better storage device, these problems need to be tackled [9–11].

Supercapacitors, as a novel storage system as well as a conversion system, have sparked a lot of interest because they have the potential to bridge the gap between a battery and a capacitor. Hermann von Helmholtz pioneered the initial concept of SCs in the nineteenth century with his work on colloidal suspensions, and later in 1957, General Electric Company introduced a double-layer capacitor [12, 13]. When compared to conventional physical capacitors and batteries, have demonstrated significant advantages such as rapid charge–discharge capability, high charge–discharge efficiency, extended cyclic lifespan (>100,000 cycles), good stability, and high power density (>10 kW kg^{-1}) [8]. The fundamental flaw of supercapacitors, despite having a very high power density, is their poor energy density. High energy density is influenced by the electron transport process during the oxidation/reduction process. This exemplifies the importance of high surface area electrode material in SC devices.

An ideal electrode material for SC devices must be economical, widely accessible, non-toxic, exceptionally high specific capacitance, large rate capability, and durable. These electrode materials should preferably be composed of porous structures with large surface area, excellent cycling stability, and high electrical conductivity [14, 15]. As active energy storage electrode media, nanostructures of only a few transition metal oxides, conjugated polymers, carbon compounds, and composite materials have been explored yet. Nanomaterials undoubtedly have distinctive & native properties as a result of their size in the nanoscale range [3]. Despite the inherent benefits of nanomaterials, producing them in large quantities with consistent surfaces remains a difficult task. Functionalized nanomaterials, i.e., the addition of new functional groups in existing nanomaterials, are known to address these issues & and are supposed to enhance the electrochemical properties of electrode materials [1].

In this chapter, the most current, cutting-edge studies on various pre and post-treatments functionalized nanomaterials in fabricating supercapacitor electrodes are summarized. The objective of this chapter is to account for these methodological elements within the context of contemporary specialized literature. We will then discuss various synthesis routes & further post-treatment various groups of FNM. Finally, it wraps up with a general overview of this chapter and a look ahead at the current state of research on diverse functional nanomaterials.

2 Brief of Functionalized Nanomaterial for Supercapacitor Application

Nanotechnology has been a boon to the scientific discipline that enables the preparation of versatile materials beneficial to people and the environment. With improved qualities and characteristics, these next-generation nanomaterials have found a niche in the fields of green energy technologies and energy storage technologies [16].

Nanomaterials (NMs) herein are particles with diameters ranging from 1 to 100 nm that serve as the foundation of research in the field of material science [17]. Their physical and chemical properties are radically altered when materials come to exist in the nanoscale range due to quantum confinement, high surface-to-volume ratio, plasmonic effects, etc. [16]. Although NMs provide many benefits, they also have certain constraints, which include agglomeration, interaction with substrate and reaction media, and insolubility in many solvents. In the current scenario, many researchers are invested in incorporating novel chemicals or functional groups in nanomaterials to exploit these as functionalized nanomaterials (FNMs). FNMs offer superior physical, chemical, and mechanical properties compared to their counterparts [18]. Because FNMs have specialized surface locations for targeted molecule attachment, they are considered promising materials for supercapacitor electrode material [19–21]. However, studies on the synthesis, characterization, and applicability of multifunctional NMs are still in their infancy. It is essential to know more about this excellent material.

Due to their remarkable electrochemical characteristics, such as high specific power, superior cycling life, and a quick charging-discharging rate, Supercapacitors (SCs) have attracted a lot of research interest. Supercapacitors are similar to a capacitor, with a substantial capacitance that fills the void between batteries and capacitors. The absence of dielectric material in the SCs distinguishes them from regular capacitors. The device consists of electrodes (anode & cathode), an electrolyte, and a separator that isolates the electrodes. In addition, selecting suitable active materials and understanding their physical and electrical properties are essential for achieving high capacitance. Electrode material for supercapacitors plays a very important role in achieving high capacitance, high energy density as well as high power density of supercapacitors. The charge storage characteristics of SCs are influenced by their large surface area, electronic conductivity, and robust interconnectivity of the electrode material. Figure 1 represents the flowchart's various physiochemical properties affecting supercapacitor performance [17].

It is possible to offer a beneficial charge storage mechanism using a diverse range of materials. Because of its inexpensive cost and large surface area, activated carbon is the most commonly utilized active material. A wide range of functionalized nanomaterials has been studied as electrodes in supercapacitor applications. Figure 2 describes the specific capacitance of various substances evaluated as supercapacitor electrodes [8]. This section elaborates on different kinds of FNMs used as supercapacitor electrode materials.

2.1 Carbon-Based Functionalized FNM

Carbon exists in several solid-state allotropes with various structures and properties, such as sp^2-bonded graphite and sp^3-bound diamond [22]. Over the past few decades, novel carbon nanomaterials with only sp^2 hybridized carbon atoms have been created in a variety of dimensions, from zero-dimensional (0D) fullerenes to

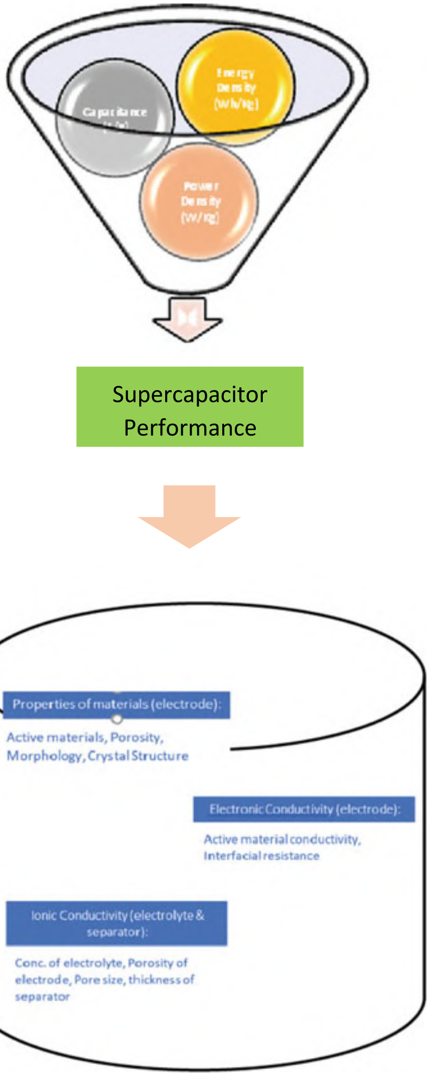
Energy Density (Wh/kg)
Capacitance
Power Density (W/kg)
Supercapacitor Performance
Properties of materials (electrode):
Active materials, Porosity, Morphology, Crystal Structure
Electronic Conductivity (electrode):
Active material conductivity, Interfacial resistance
Ionic Conductivity (electrolyte & separator):
Conc. of electrolyte, Porosity of electrode, Pore size, thickness of separator

Fig. 1 The flowchart's various physiochemical properties affecting supercapacitor performance

one-dimensional (1D) carbon nanotubes (CNTs) to two-dimensional (2D) graphene [23–25]. Due to their adaptable architectures, whose dimensionality extends from 0 to 3D, and their changeable surface chemistry, carbon nanomaterials have been widely exploited as the basis matrices or as functional additives in several applications. Carbon nanomaterials can be chemically functionalized using elements like nitrogen and fluorine, functional groups like hydroxyl and carboxyl groups, and polymers. Carbon nanotubes (CNT), graphene, and its derivatives are the most common functionalized carbon nanomaterial whose succinct overview is discussed in the proceeding paragraphs.

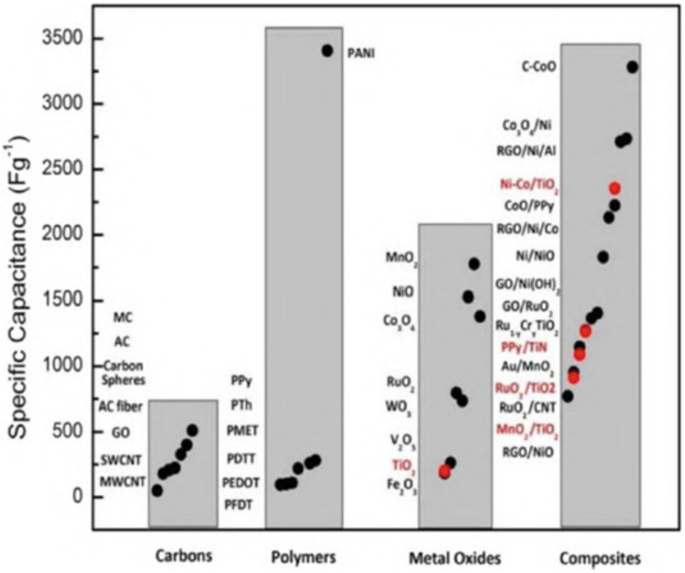

Fig. 2 The specific capacitance of various substances evaluated as supercapacitor electrodes. [8] Reproduced with permission from Ref.. Copyright © 1948, IOP Publishing

Carbon nanotubes (CNTs): Since the first high-resolution TEM photos of "Helical microtubules of Graphitic Carbon" were published by Sumio Iijima et al. in 1991, describing their astonishing finding, CNT became one of the astonishing carbon nanomaterials [23]. These sides of the nanotube are constructed of hexagonally shaped particles. Their sizes are typically in the range of 1 nm, and they include sp^2 hybridized carbon atoms. The two main subtypes of CNTs are single-walled carbon nanotubes (SWCNT) and multi-walled carbon nanotubes (MWCNTs), which are made up of two or more CNTs stacked concentrically [26]. CNTs have potential in many areas of study since their electronic characteristics, which typically range from metallic to semiconducting, depending on their geometric shapes. The remarkable electronic properties of CNTs result from their one-dimensional structure, which allows for electron conduction without scattering. They form excellent reinforcing fibers in hybrid composites due to their distinct covalent atomic tube structure, ultra-high aspect ratio, and distinct mechanical, electrical, and thermal conductivity. Since CNTs have a lot of potential in composite materials, their production and chemical functionalization have been the subject of extensive study. Most chemical functionalization strategies fall into one of two categories: (i) Covalent bonds formed by chemical interactions between functional groups or molecules on the conjugated side walls or defect groups present on the CNTs and (ii) The adsorption in CNT with specific sort of functional molecule leads to chemical interaction resulting them in wrapping up of tubes via non- molecular interaction [27]. Adding the requisite reactive species and groups, such as atoms, radicals, carbenes, nitrenes, or other newly developed chemical functionalization techniques, can give CNTs the necessary molecular structures

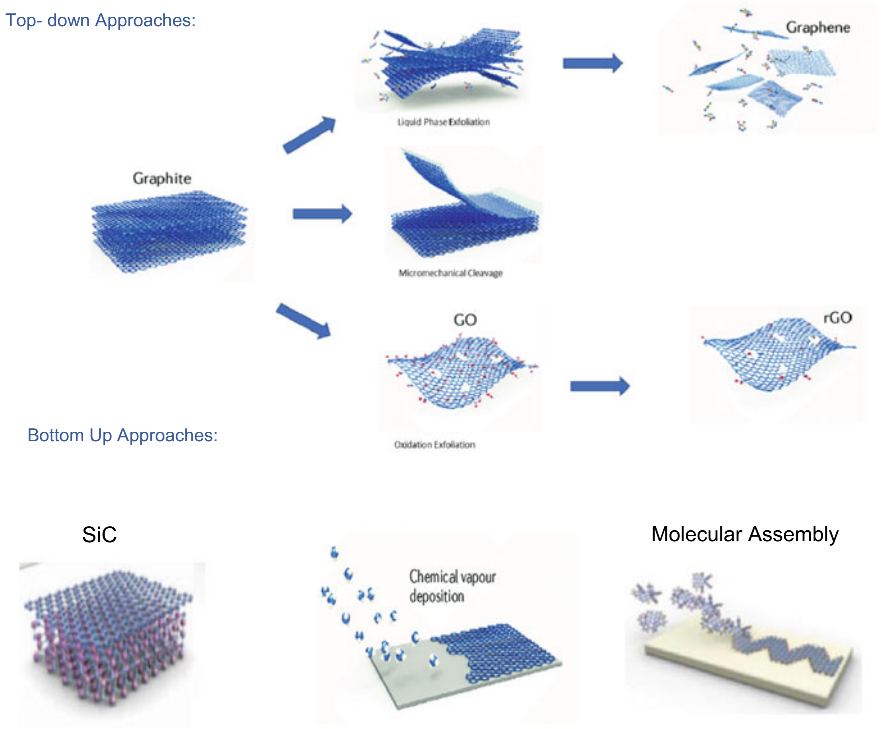
Top- down Approaches:
Graphite
Liquid Phase Exfoliation
Graphene
Micromechanical Cleavage
GO
rGO
Oxidation Exfoliation
Bottom Up Approaches:
SiC
Chemical vapour deposition
Molecular Assembly

Fig. 3 Schematic portrayal of various synthesis routes of graphene [87]

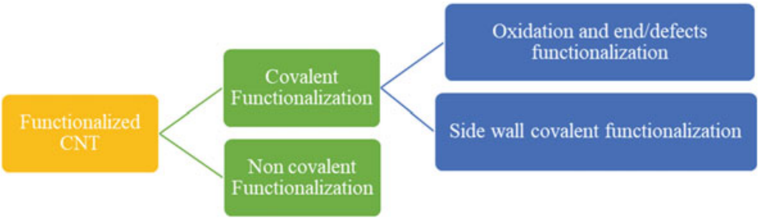
Functionalized CNT
Covalent Functionalization
Non covalent Functionalization
Oxidation and end/defects functionalization
Side wall covalent functionalization

Fig. 4 Schematics of ways to functionalize CNT

and properties. Additionally, chemical functionalization potentially inhibits the van der Waal contact between CNTs due to increased electrostatic repulsion [28–34].

Graphene & its derivative: Since its accidental discovery in 2004, graphene, the world's thinnest material and a one-atom-thick single-layer planar nanosheet made of densely packed sp^2 hybridized carbon atoms in a hexagonal crystal lattice, has been the subject of extensive research [35]. Graphene nanosheets exhibit a variety of remarkable properties, including good optical transmittance, excellent electronic transport properties, a large specific surface area (SSA), superior mechanical stiffness

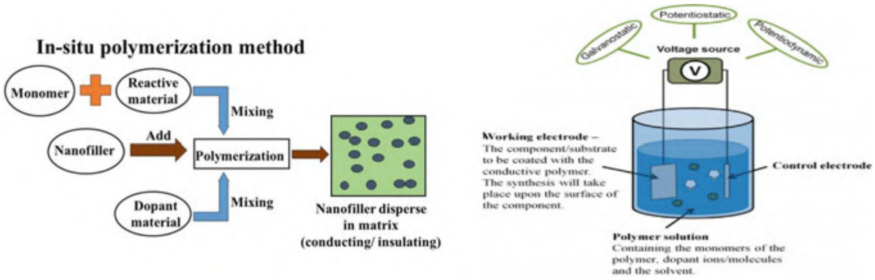
In-situ polymerization method
Monomer
Reactive material
Mixing
Add
Nanofiller
Polymerization
Dopant material
Mixing
Nanofiller disperse in matrix (conducting/ insulating)
Potentiostatic
Galvanostatic
Potentiodynamic
Voltage source
V
Working electrode – The component/substrate to be coated with the conductive polymer. The synthesis will take place upon the surface of the component.
Control electrode
Polymer solution Containing the monomers of the polymer, dopant ions/molecules and the solvent.

Fig. 5 **a** Describes the basic procedure of in situ polymerization method Reproduced from Ref. [117] with permission from the Royal Society of Chemistry, **b** desciribes the basic procedure of electrochemical polymerization method Copyright © 1969, Elsevier

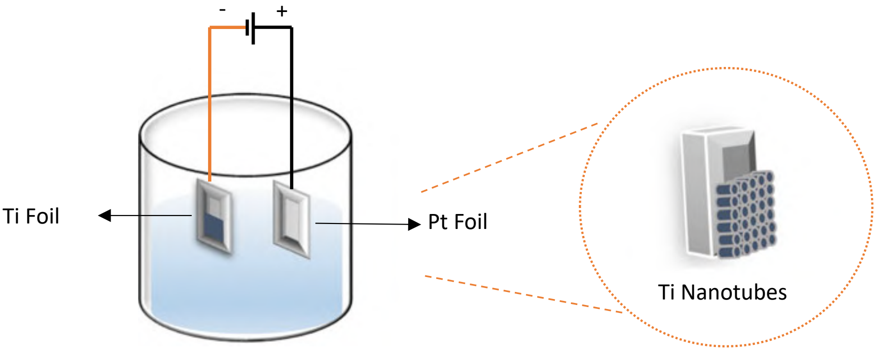
-
+
Ti Foil
Pt Foil
Ti Nanotubes

Fig. 6 Schematic representation of the electrochemical anodization of Ti foils

and flexibility, a high 3D aspect ratio, and exceptional thermal response, because of their exceptional microscale crystallinity and the two-dimensional π–π conjugation of the sp^2 hybridized carbons in the planar atomic layer. Like CNTs, single-layer graphene has a propensity to aggregate when spread out in a solution. In addition to addressing the problematic issue of stacking, the chemical functionalization of graphene can also give it active functional sites [35–39]. Graphene oxide (GO) is a chemically functionalized derivative of graphene that is frequently made. Solvent-assisted methods, including self-assembly, spin coating, and filtration, can be used to modify graphene chemically. Graphene oxide (GO) is a chemically functionalized derivative of graphene that is frequently made [40]. After GO is reduced, the natural molecular structure of graphene and its' exceptional electrical conductivity are restored. To create reduced graphene oxide (rGO) in large quantities, it has been determined that the reduction of GO by moderate agents such as hydrazine, ascorbic acid, hydrogen gas, and strong alkali metals such as sodium and potassium is the most effective method to date [32]. Compared to traditional carbon-based nanomaterials, functionalized graphene demonstrates improved performance in hybrid composites and gives the hybrids significantly improved physicochemical properties in electrode materials of supercapacitors.

2.2 Polymer-Based Functionalized FNM

It is expected that supercapacitor electrodes and devices based on conducting polymers will bridge the gap between present carbon-based supercapacitors and batteries to develop units of intermediate specific energy [41]. A conjugated bond structure along the polymer backbone makes conducting polymers conductive. They often result from the monomer being either chemically or electrochemically oxidized [42]. Two oxidation reactions happen simultaneously: monomer oxidation and polymer oxidation, with the simultaneous incorporation of a dopant/counter ion [43]. Conducting polymers are often appealing because of their high charge density and inexpensive. There are three possible designs for supercapacitor devices constructed only from conducting polymers [44–47]:

Type I (symmetric), where both electrodes are made of the same p-dopable polymer.

Type II (asymmetric), utilizing two various p-dopable polymers with various electroactivity ranges.

Type III (symmetric) uses the same polymer for both electrodes, with the positive electrode being composed of the p-doped form and the negative electrode being composed of the n-doped form.

Polyaniline, polypyrrole, polythiophene, and derivatives of polythiophene, are the main conducting polymer materials used as an electrode material for supercapacitor. Conducting polymer materials can undergo a variety of processes to enhance their characteristics, leading to the synthesis of functionalized conducting polymers.

Polyaniline (PANi): As a supercapacitor or battery electrode material, polyaniline has received substantial research. With its high electroactivity, high doping level, great stability, and high specific capacitance, polyaniline possesses numerous qualities that make it an ideal material for use in supercapacitors. According to reports, polyaniline has a capacity range of 44 to 270 mAhg^{-1} [48, 51]. Furthermore, it can be easily processed, has exceptional environmental stability, and has controllable electrical conductivity [49, 50]. The fact that polyaniline needs a proton to be effectively charged and discharged is a significant drawback; as a result, a protic solvent such as an acidic solution, or a protic ionic liquid is necessary [52]. Of all conducting polymers, polyaniline exhibits the widest range of specific capacitance which is achieved by doping, the addition of new composite material such as activated carbon material etc. thus making functionalized conducting polymer. This capacity variation is influenced by a variety of elements, including the synthesis route taken, the shape of the polymer, the quantity and kind of binders and additives, and the electrode thickness.

Polypyrrole: Due to its better electrochemical processing flexibility than the majority of conducting polymers, polypyrrole has received a lot of attention as a supercapacitor or battery electrode [48]. Unlike thiophene due to its inability to be n-doped polymer, polypyrrole has only been used as a cathode material which is one of the major setbacks for using this material. Moreover, polypyrrole offers high density due to which it has high capacitance per unit volume (400–500 F cm^{-3}). The disadvantage of dense growth is that it restricts dopant ion access to the interior locations of the polymer [53, 54]. If multiple-charged anions, such as $SO_4{}^{2-}$, are added to polypyrrole, physical crosslinking of the polymer ensues, which is generally doped with single-charged anions like Cl^-, ClO^{4-}, and SO^{3-} [43]. The mixture of polypyrrole with polyimide (a high molecular weight dopant) is believed to enhance charge storage properties because the polyimide matrix guards the polypyrrole against oxidative deterioration and the polyimide is cathodically electroactive. It has been reported both a Type I and Type II supercapacitor have been created using polypyrrole as an electrode and a combination of different types of conducting polymers such as PMeT and poly(3-methylthiophene) etc.

Thiophene-based conducting polymers: Due to their remarkable optical and conductive qualities, thiophene-based conjugated polymers occupy an unrivaled position among the profusion of conjugated polymers that are constantly expanding**.** The majority of polythiophene derivatives, whether they are p-doped or undoped, are stable in air and moisture [42] whereas n-doped derivatives tend to have a low potential window and react with air and water [48]. In general, the n-doped form has a lower mass specific capacitance than the p-doped version. Additionally, it is discovered that the n-doped form's conductivity is often subpar. This restricts the usage of these materials as anode materials in their n-doped state. These derivatives include poly (3-(3,4- difluorophenyl) thiophene) (MPFT), poly(3,4-ethylenedioxythiophene) (PEDOT), poly (1-cyano-2-(2-(3,4-ethylenedioxylthienyl))-1-(2-thienyl)vinylene) (ThCNVEDT) and poly(3-(4-fluorophenyl)thiophene) (PFPT). By using carbon composite with n-doped polymer as the negative electrode in an asymmetric arrangement and the p-doped polymer as the positive electrode, it is possible to successfully combat the issue of the n-doped polymer [55].

2.3 Metal-Based Supercapacitor Electrode Material

High-performance energy storage applications hold promise for nanostructured metal-based compound electrodes with good electrochemical activity and electrical conductivity [56]. Metal oxides have proven appealing properties when used as supercapacitor electrode materials, enabling the fabrication of various supercapacitor devices over a wide voltage range [57]. Due to their abundant reserves, environmental friendliness, accessibility, and other intriguing qualities like their varied constituents and morphologies, large surface area, and high theoretical specific capacitance, transitional metal oxide materials have been identified as promising candidates to be used as electrode material for supercapacitors. They also serve as the primary electrodes for electrochemical supercapacitors, and by modifying and manipulating their flaws and surface/interfaces at a specific nanoscale, they provide a distinct capacitance improvement [58, 59]. Although their energy density has increased to some extent, their practical uses have been limited by their poor electrical conductivity, unpredictable volume expansion, and slow ions diffusion in the bulk phase [60–63]. Metal oxide materials have been improved in terms of specific surface area, electrical conductivity, chemical stability, and electroactive sites because of the design-inclusive approach regarding their composition, the preparation of unique nanostructures, their electroconductivity, and oxygen vacancies. Metal-based FNM can be made from different approaches. First, two distinct cations coexisting in the same crystal structure tend to produce more electrons than a single metal oxide, improving electrical conductivity [64]. Second, enhancing complete interaction among the active materials and electrolyte, ion transport in the electrolytes, and high-rate charging-discharging of the active materials can offer a greater surface-specific area, which is advantageous for the electrode implantation and complete contact between the active materials and electrolyte [65–68]. This can be achieved by enhancing the porous nature of novel nanostructures compared to their bulk counterpart. Third, there have been more reports of metal oxide/C composites with carbon nanomaterials like graphene, CNTs, amorphous carbon, and carbon nanofibers, which have significantly increased electroconductivity and improved specific capacitance and charge–discharge rate performances [60–71]. Fourth, the presence of oxygen vacancies induces the interlayer spacing of metal oxides, which encourages the intercalation pseudocapacitive behavior, thus enhancing fast charge storage kinetics [72, 73]. Metal oxides, notably single metal oxides (such as TiO_2, RuO_2, MnO_2, Fe_2O_3, V_2O_5, MoO_3, and WO_3), bimetallic oxides (conversion-type $MN_2\ O_4$, were M or N = Fe, Cu, Co, Zn, Ni, Mn, etc.), transition metal dichalcogens and intercalation-type ($LiCoO_2$, $LiMn_2O_4$, etc.) and metal oxide heterostructures, have been extensively researched as electrode materials for SCs over the past few years.

2.4 Composite-Based Supercapacitor Electrode Materials

Although conducting polymers, metal oxides/hydroxides, and carbon-based materials are the most prevalent electroactive materials for supercapacitors; each type has distinct benefits and drawbacks. For instance, carbon-based materials can offer long life cycles and high power density. Still, their employment in high energy density devices is constrained by their low specific capacitance (mostly double-layer capacitance) [74]. In addition to double-layer capacitance, metal oxides and hydroxides also contain pseudocapacitance. However, they have poor conductivity and a short cycle life [75]. Conducting polymers have low mechanical stability and cycle life despite being cost-effective, high capacitance, good electrical conductivity, and ease of synthesis. It is essential to control, develop, and optimize the structures and properties of electrode materials to improve their performance for supercapacitors. The characteristics of the composites are not only influenced by the choice of constituent components but also by their morphology and interfacial properties. Recently, significant effort has been made to fabricate various nanocomposite capacitive materials, including carbon nanotubes/ graphene combined with conductive polymers, metal oxides, or both, conducting polymer mixed with metal oxides/ hydroxides and Metal–Organic Framework (MOFs) [64–66]. It is necessary to consider various elements while designing and creating nanocomposite electroactive materials for supercapacitors, including material choice, synthesis techniques, fabrication process parameters, interfacial properties, electrical conductivity, nanocrystallite size, surface area, etc.

3 Pre-treatment of Functionalized Nanomaterials

For excellent device performance, predefined properties (functions) must be attained through the fabrication technique. Hence, material scientists focus more on the performance and characteristics of materials. This has led to the development of functionalized nanomaterials by taking various pre-treatment methods/ synthesis routes. The energy storage materials research focuses on achieving a high surface area, good conductivity, better carrier transfer, and good interface. Pre-treatment methods play a crucial role in synthesis routes of nanomaterials with regulated morphology and tailored anisotropic nanostructures, including one-dimensional (1D) nanorods, nanowires, and nanotubes, as well as two- and three-dimensional (3D) hierarchical structures [77]. These nanoparticles can enhance the performance of energy devices thanks to their distinctive, adaptable, customizable structure, high surface-to-volume ratio, and wide surface area. The hierarchical frameworks for each type of FNM used for supercapacitor electrodes are mentioned above in Sect. 2.

Fast electron transport in one dimension and a short ion diffusion length in the radial direction are significant features of 1D structures. Still, their fixed size and static structure restrict their ability to have adjustable specific surface areas and porosity qualities [78, 79]. On the other hand, due to their distinctive electrical, mechanical, and optical properties, as well as their huge surface area and surface orientation, 2D nanomaterials with high aspect ratios are particularly desirable materials for energy storage applications. Additionally, when their interior atoms become more exposed, numerous defects will undoubtedly occur and have a non-negligible impact on their chemical and physical properties [80–82]. The following qualities are typically associated with 3D structures: (1) Because nanoplatelet restacking is effectively prevented, the high specific surface area can be preserved. This results in accomplishing enough electrochemical reactions, and many electrochemically active areas are accessible to the electrolyte. (2) The formation of numerous pores or channels can efficiently reduce the distance that ions and mass must travel while forming 3D structures using nanosized 2D nanoplatelets as the building blocks. (3) Since the 3D structure is typically constructed directly on a conductive substrate or combined with a conductive material, such as a carbonaceous material, electron transport is greatly improved [83–86].

Understanding the fundamental method by which nanomaterials grow anisotropically is crucial for designing controlled synthesis to create nanostructures appropriate for energy storage applications. In this section, we will discuss an elaborately important study on the controlled synthesis and various pre-treatment methods of functional nanomaterials for electrochemical energy storage that is needed to advance related efforts in research and development to address the current energy problems.

3.1 Pre-Treatment Methods for Carbon-Based FNM

For the construction of high-efficiency electrodes with relatively lower effective series resistance and increased charge storage ability without compromising operating lifetime and high power density, carbon nanomaterials with high electrical conductivity and theoretical specific surface area are regarded as the best candidates [87, 95]. This section focuses on several pre-treatment techniques for carbon nanomaterials with outstanding supercapacitor performance that have been chemically functionalized and hybridized.

One of the main areas of research in graphene is its functionalization. Graphene sheets have a lot of active sites, including functional groups, because they are created by peeling off the graphene oxide created by chemically oxidizing graphite. Functionalization of graphene can be done by two significant strategies, i.e., by chemical route & non-chemical route [22]. The chemical functionalization process involves forming new covalent connections between the atoms of reduced graphene oxide (rGO) / graphene oxide (GO) and the desired functional groups (Fig. 3).

The non-chemical functionalization, on the other hand, is mostly reliant on the π interaction between the guest molecules and rGO/GO. Even though both functionalizations can give graphene various properties, chemical techniques are more efficient. Several chemical pathways have been proposed and tested, including top-down methods, including sonication, reduction of graphene oxide, thermal exfoliation, electrochemical exfoliation, and micromechanical exfoliation [88–94]. The alternative bottom-up processes for growing graphene include pyrolysis, chemical vapor deposition, and epitaxial growth on silicon carbide. Figure 3 describes a schematic portrayal of various synthesis routes of graphene [87].

A one-dimensional type of carbon with a perfect hollow cylindrical shape is known as a carbon nanotube (CNT). Most of the physical characteristics of carbon nanotubes come from their base material (graphene). According to theoretical analysis, this CNT is notably unique in its cylinder shape made of thick sheets of swirling graphene, which can distinguish itself into one or more wells. Due to their remarkable thermal, electrical, mechanical, and optical properties, CNTs are used exclusively and functionalized to be used as supercapacitor materials. CNT functionalization processes can be divided into covalent and non-covalent functionalization [96]. A functional group and a carbon atom of CNT establish covalent bonds due to covalent functionalization. Covalent chemical bonds between CNTs and functional entities are formed during the covalent functionalization process, which entails several chemical reactions. There are two categories of covalent functionalization that fall under as: (i) oxidation and end/defects functionalization and (ii) side wall covalent functionalization. A strong chemical attacks the defects in the nanotube's walls, leaving holes that have been functionalized with oxygenated functional groups [97, 98]. Figure 4 represents the schematics of ways to functionalize CNT.

Most often, oxidation is carried out using strong acids like HNO_3, H_2SO_4, or their mixture and raising the reaction temperature, as well as strong oxidants like $KMnO_4$ or utilizing ozone, or reactive oxygen plasma [99–104]. These pre-treatments enable the CNTs to develop acidic sites, which are then utilized to attach other molecules. These functional groups allow for various chemical reactions, including esterification, thiolation, silanization, polymer grafting, and the attachment of some biomolecules [105-107] (Fig. 4).

A transition from sp^2 to sp^3 in the carbon hybridization and a concomitant loss of the p-conjugation characteristic of graphene's aromatic rings are caused by the creation of the covalent link during the direct covalent sidewall functionalization. Atoms at the ends and in the defects of the CNTs can combine with some compounds with high chemical reactivity to create this process. Because it offers substitution sites for further functionalization, allowing the replacement of the fluorine atoms by hydroxyl, amino, and alkyl groups, fluorination of CNTs has gained popularity. The Diels–Alder cycloaddition, the bromination, carbene and nitrene addition, azomethineylides, chlorination, and hydrogenation are further potential chemical pathways.

There are certain drawbacks to covalent functionalization, even though it offers a wide range of potential methods for grafting the desired molecules. Strong covalent bonds used for functionalization cause the aromatic rings of the CNT graphitic lattice to break. This affects the mechanical and electrical properties of CNT. To reduce the CNT damage caused by the functionalization, various efforts have been made to identify practical alternatives. Non-covalent functionalization allows for the preservation of CNT characteristics. One of the key benefits of non-covalent functionalization is that it preserves the hexagonal lattice with aromatic graphitic rings by leaving the carbon hybridization alone. Because the non-covalent functionalization is based on adsorption based on van der Waals forces, hydrogen bonds making supramolecular complexation, electrostatic forces, or -stacking interactions, the structural and electrical properties of the CNTs are preserved. Lower stability brought on by potentially weak contacts between the grafted molecule and the CNTs is a major downside of non-covalent functionalization [108].

3.2 *Pre-treatment of Polymer-Based FNM*

The discovery of conductive polymers (CPs) has advanced numerous basic scientific fields, including quantum chemistry and the chemistry and physics of Π -bonded macromolecules [109]. In recent decades, conducting polymer nanostructures have drawn increasing attention from both fundamental researchers and a variety of application fields. Because of the distinctive characteristics resulting from their nanoscaled size— large surface area, high electrical conductivity, high electrochemical activity, and short path lengths for the transport of ions—conducting polymer nanostructures are anticipated to demonstrate improved performance in energy storage compared with bulk conducting polymers. Functionalized CP nanostructures are key to the effectiveness of the supercapacitor electrode materials made from CPs [110]. Choosing appropriate polymerization techniques to regulate their nanostructures is crucial since the nanostructures are influenced by the polymerization methods used to synthesize polymer-based FNM. Electrochemical polymerization, in situ polymerization, template polymerization, interfacial polymerization, dilute polymerization, emulsion polymerization, and other processes are some of the polymerization techniques available for CP-based supercapacitor electrode materials [111–115]. The most prevalent of these approaches are in situ polymerization, electrochemical polymerization, and interfacial polymerization.

In situ Polymerization

Typically, in situ polymerization methods require dispersing nanomaterials in a neat monomer (maybe several neat monomers) or a solution of monomer, followed by polymerization in their presence. In this procedure, the sonication process' physical vibration separates the monomers into an aqueous solution. The sample is then extracted using solution filtration after the oxidizing agent has been added to the solution as a polymerization initiator [116]. Figure 3(a) describes the basic procedure of in situ polymerization method [117].

This technique aids in the alignment of the functional nanomaterial (particularly carbon-based FNM), facilitates charge transfer by acting as a route, and supports the organic polymers. The lifetime during the charging-discharging process was increased because the constrained FNM prevented the CPs (such as PANi) from changing its' structure. By implementing this polymerization technique, multiple types of CPs (for example, PANi, PPy, and PTh etc.) can be coated, and the resulting composite has diverse capacitive properties as a result of the synergistic interaction between the CPs and the provided functional material (for example, rGO). An increased electrical double-layer capacitance was achieved by a more uniform CPs coating and reduced CPs aggregation on the underlying nanomaterial by this method. Thus, the in situ polymerization method is regarded as a quick, easy procedure that allows for good process control. Additionally, they can be used with a variety of substrates, including those made of carbon, metal, and even polymer, all of which have varied surface morphologies and shapes (e.g., curved, planar, or even porous surfaces) [119].

Electrochemical polymerization

The process of creating polymer films using electrochemical polymerization mostly utilizes linearly scanned potential (potentiodynamic) or constant potential (potentiostatic) which is under the influence of an electric field. The morphologies and mass loading of the nanostructured films developed using this approach are influenced by the type of deposition solution. Various types of CPs, like PANI and PPy, can be synthesizedutilizing the electro-polymerization procedure, which operates under straightforward conditions and requires fewer hazardous toxins during the pre-treatment. Electrochemical deposition offers the opportunity to adjust the synthesis parameters, allowing one to have control over the structure and morphologies of electrode material [120]. However, this method is not appropriate for extensive manufacturing. Electrodeposition, which involves depositing films or coatings on substrate surfaces through redox processes employing an electric current, is the most common method of electrochemical polymerization. The salt ions with a positive charge are drawn to the negatively charged substrate (cathode), which was already submerged in the salt solution, and those ions accept the electrons to carry out a reduction reaction [121–123]. As a result, cathodic electrodeposition and anodic electrodeposition are the two reaction processes by which electrodeposition occurs. Figure 3(b) describes the basic procedure of electrochemical polymerization method.

Interfacial Polymerization

An example of step-growth polymerization is interfacial polymerization, which produces a polymer that is restricted to the interface when it occurs at the interface of two immiscible phases (often two liquids). Surface topology and chemical attributes of the produced functional materials are very flexible due to interfacial polymerization [124]. As of now, interfacial polymerization has become a reliable and efficient method for creating a variety of useful polymer materials. The design and pre-treatment of polymer materials using interfacial polymerization typically relates to two key aspects: (i) the building of an interface between two immiscible phases and (ii) monomer dispersion in two immiscible phases. Liquid–solid, liquid–gas, liquid–liquid, and liquid-in-liquid emulsion interfaces are the four main categories of interfaces [125, 126]. When two immiscible liquids are used to create an interface, either one or both of the liquid solvents contain monomers. The monomers may diffuse to the interface and then be initiated to polymerize there due to the difference in chemical potentials of two immiscible liquids at the interface. The resulting polymer is anchored to the interface when the interfacial pressure of the adsorbed monomer monolayer surpasses the equilibrium spreading pressure of the polymer. The polymer increases at the contact as the monomers diffuse and the polymerization process continues. As a result, interfacial polymerization has gained popularity as a process for creating a variety of polymer materials that are widely employed in several applications. Pre-treatment techniques using interfacial polymerization provide good control over structure and chemistry, as well as generality for categories of monomers and interfaces. Interfacial polymerization has produced a number of polymer materials, such as particles, and membranes, which are frequently employed as supercapacitor electrode materials. However, there are still a number of issues with interfacial polymerization that need to be resolved: The limitation of the interface surface makes it difficult to produce materials over a large area; the interfacial tension limitation makes it difficult to create anisotropic Janus particles during interfacial polymerization; and the preparation of uniform and size-tunable capsules via interfacial polymerization is still a challenge [124].

4 Pre-treatment Methods for Metal-Based FNM

Due to their low cost, adaptable valence states and morphologies, and high capacitance, transitional metal-based materials are frequently used in energy conversion and storage systems. Transition metal oxides, hydroxides, dichalcogens, and metal oxide heterostructures are new-generation materials used in the fabrication of supercapacitor electrodes due to their meager resistance and suitable specific capacitance, theoretically [127]. But there are still several restrictions for them to have widespread practical application. Their weak electrical conductivity, unpredictable volume expansion, and slow ions transport in the bulk phase have restricted their practical applications [128]. Pre-treatment of several metal-based electrodes is addressed in this section, enhancing its properties for practical applications.

By customizing the structure and engineering, particularly the nanostructuring, which has been seen as a promising method for achieving high-performance electrochemical energy conversion and storage, researchers are now making great efforts to design high-performance transition metal-based nanomaterials for supercapacitor electrode material. Therefore, we outline some methods for creating high-performance nanomaterials that can be used for energy storage and conversion. The first approach is introducing more active sites to nanomaterial surfaces, where electrochemical processes occur. For example, building atomic metal-nitrogen molecules in a carbon matrix to form an M–N-C structure results in many vacancies exhibiting vigorous catalytic activity for electrochemical reactions and good atomic stability. The second approach is to create nanostructured materials with unique properties that set them apart from their bulk material equivalents, for instance, fabricating transition-based nanomaterial having dimensions of 0D, 1D, 2D & 3D nanostructure. More atoms could be exposed onto the surface of nanostructures by efficiently optimizing the surface-to-volume ratios of the particles. Additionally, geometric shape variations can significantly impact a nanostructure's chemical and physical characteristics. The design of transition metal-based nanomaterials uses various pre-treatment techniques. These include hydrothermal pre-treatment, sol–gel method, precipitation technique, electrochemical anodization, CVD, etc. All these methods are facile and controllable.

Hydrothermal technique: The hydrothermal process is an easy-to-use yet effective tool for adjusting grain size and crystalline phase and increasing product performance. To synthesize a crystalline nanostructure adequately, precursors must be combined with a solvent. The blended solvent is then placed into a Teflon container assembled with a stainless-steel autoclave and heated for a specific time and at a particular temperature. The internal pressure inside the autoclave is determined by the temperature and volume of the solution. Crystals are formed in an autoclave containing both components dissolved in water throughout this process. A temperature gradient is produced within the autoclave chamber's opposite sides [128, 129]. The formation of desirable crystals with excellent quality results from materials dissolved at high temperatures deposited on the seed crystals at the cooler end. In contrast to other complex synthesis processes, the hydrothermal method is simple, quick, and cost-effective.

Precipitation Technique: The materials can also be synthesized using the precipitation synthesis method, which is another straightforward process. It incorporates the simultaneous processes of nucleation, maturation, coarsening, and agglomeration [130–133]. It has several qualities, which include-

1. the ability to produce insoluble species with high saturation levels.
2. A large number of tiny particles are synthesized during nucleation.
3. Agglomeration affects the morphology, construction, and shape of items.
4. The conditions with supersaturation are essential for producing precipitation that results from a chemical reaction.

It is a straightforward procedure that allows for precise control over size and composition, making it economical and energy-efficient. It can produce FNM based on metal sulfides, metal oxide, and metal-organic framework.

Sol-Gel Method: The sol-gel approach is another particular category of wet chemical processes. In this procedure, the molecular precursor (often metal alkoxide) is dissolved in water or alcohol and heated and stirred, known as hydrolysis/ alcoholysis, until it gels. According to the desired qualities and use of the gel, which is wet or damp after the hydrolysis/alcoholysis process, it should be dried using the appropriate techniques. For instance, burning alcohol completes the drying process if the solution is alcoholic. The generated gels are pulverized after drying and then taken for further post-treatment. Because of the low reaction temperature and cost-effectiveness of the sol-gel process, it is possible to effectively regulate the chemical composition of products. This method produces thin films of metal oxide for various applications. It is a very convenient method that can be used for commercial mass production [134-136].

Electrochemical Anodization: An example of a traditional electrochemical conversion is electrochemical anodization. It includes electrode reactions as well as a metal and oxygen ion diffusion driven by an electric field, which creates an oxide layer on the anode surface. By changing the process variables, such as the anode potential, electrolyte composition, temperature, and current, the structural and chemical characteristics of the metal oxides (such as TiO_2 and MoO_3) can be altered over a wide range [137]. A well-known technique, anodic oxidation can create various protective oxide layers on metals with outstanding adhesion and bonding. The cell typically comprises two electrodes attached to a DC power source. In this instance, the metallic sheet acting as the anode is linked to the positive terminal and must be oxidized. On the other hand, the cathode can be made of any substance that is inert to the chemical process, platinum and graphite being the most popular options. An ion carries out the etching process in the electrolyte, which is made up of water. The ion of choice for the first four generations was fluoride (F^-); for the fifth and sixth generations, it was chloride (Cl^-) [8]. This procedure involves the oxidation of the anode, which results in the formation of a decorative protective layer with increased thickness and enhanced oxide layer density over the metallic surface. Fig. 5 represents the schematic representation of the electrochemical anodization of Ti foils.

Chemical Vapor Deposition (CVD): Chemical Vapor Deposition (CVD) is a versatile technique for producing high-quality TMDs with high crystallinity and purity. Over the past few years, this technique has substantially matured. Different precursors are deposited onto a substrate by chemical vapor deposition. The CVD process may manufacture TMDs/TMOs with a wide surface area, making it a suitable fit for industrial applications. A CVD method typically has a reaction temperature range between 600 and 800 ̊C [138–140]. FNM based on Transition metal oxide/ dichalcogens prepared by chemical vapor deposition is well discussed in the literature. Using chemical vapor deposition, Jian-Shan Ye et al. created a supercapacitor electrode material made of aligned carbon nanotubes and ruthenium oxide [141]. Similarly, Frances L. Heale et al. reported on aerosol-assisted chemical vapor deposition of porous TiO2/SnO2 nanocomposite infused with slipperiness liquid [142]. Large-surface area MoS2 films were synthesized by Lee et al. using the CVD method on an amorphous SiO2 substrate at a reaction temperature of 650 °C in a nitrogen environment [143]. The size of the nanosheets can be regulated in the CVD process by varying the carrier gas's concentration and composition. Still, the carrier gas flow is necessary for creating the nanosheets and cannot occur without it.

All the pre-treatment methods discussed above are not exclusively used for the pre-treatment of transition metal-based electrodes; these pre-treatment methods are also used for synthesizing various material-based FNM supercapacitor electrodes discussed in Sects 3.1 and 3.2.

5 Post-treatment for Functionalized Nanomaterials

A significant area in the developing field of nanotechnology is nanoparticle functionalization and surface treatment. Because of the natural inclination of nanoparticles to agglomerate and their poor compatibility with other nanomaterials, FNM production poses significant technological obstacles. Modifying the fillers' surface to strengthen their affinity with the matrix and create repulsive interactions among the particles is the primary strategy for resolving these problems. For high-added-value applications incorporating nanoparticles, controlling the surface chemical composition and managing its modification at the nanoscale scale are crucial concerns. We explored several pre-treatment techniques to improve the characteristics of FNM in earlier Sect. 4. It should be known that in addition to various pre-treatment techniques, post-treatment plays a significant role in improving the features of nanomaterials for applications in supercapacitors. In order to boost conductivity and enhance the structure of the FNM used for the supercapacitor electrode, various post-treatment procedures were applied to the FNM, which will be discussed in this section.

5.1 Thermal Treatment

The two essential key variables that cause the properties of nanomaterials to differ dramatically from those of typical bulk materials are surface area and quantum confinement effects. Thermal/Heat treating is a post-fabrication procedure used to change physical, and occasionally chemical, properties of nanomaterial. In order to harden, improve conductivity, or enhance the crystallinity of a material, heat treatment involves heating or chilling it, typically to extremely high temperatures [144]. Different heat treatment methodologies can change functional nanomaterials' chemical and physical features after material pre-treatment. The following heat treatment methods are used: annealing, sintering & calcination. This technique is typically used to improve the electrical conductivity of metal-based electrode materials for supercapacitors since it may produce crystalline structures by heat processing. Surface imperfections, grain boundaries, oxygen adsorbed on the surface, and unsaturated dangling bonds all have a significant impact on the electrical conductivity of the FNM. In practical terms, the divergence from stoichiometric composition results in a significant number of point and surface defects in the metal oxide nanocluster.

Furthermore, creating oxygen vacancies in metal oxide nanoclusters may enhance the efficiency and precision of supercapacitor electrodes [73]. Numerous researchers discussed the synthesis of FNMs, followed by annealing in various atmospheres. They demonstrated that smooth surfaces, a reduction in structural flaws, and an improvement in the crystallinity of the FNM were all produced by annealing at the ideal temperature. A substantial number of dangling bonds, atoms and local atomic defects are found at the surface texture of nanomaterial rather than the interior cores due to the high surface area of nanomaterial [147]. As a result, the surface of FNM is unstable, exhibits high chemical activity, and has the propensity to absorb atoms from the surroundings. The active surface area of the nanomaterial greatly influences electrical conductivity. The electrical properties, which are needed in the field of energy storage application, are greatly influenced by the deformation in the surface structure and the local impurities. As a result, researchers anticipated that the annealing process would cause oxygen vacancies and enhance the nanostructure's crystal quality. Sintering is another thermal treatment method in which nanomaterials are kept at a temperature below the melting point of the main constituent. Sintering helps preserve the nanomaterial's high electrical conductivity, porosity, and surface area [146, 147]. Calcination is another technique for heating a material at a controlled temperature and in a controlled environment to eliminate volatile chemicals. In order to produce metal carbides, metal oxides, etc., sparingly soluble precursors are often thermally decomposed through calcination. Materials are calcined at various temperatures while loaded with various gases like argon or nitrogen in the furnace tube. The main benefit of calcination is that the end products will have variable crystallinities, BET surface areas, and morphological properties depending on the calcination temperature. However, the items might occasionally get readily polluted when the porcelain boat reacts with other contaminants, which can be observed in the other two methods discussed above.

5.2 Plasma Treatment

Plasma treatment has already been successfully utilized to modify nanomaterials such as carbon nanotubes, nanoparticles, and nanofibers. Plasma treatment is an excellent technique for enhancing surface characteristics and reactivity because of its dry, environmentally friendly procedure and potential to deposit polymer films of organic compounds with customizable thickness. For many different purposes, plasma treatment was used. The surface of the nanoparticles was extensively cleaned to remove carbon contamination using oxygen plasma treatment. Moreover, there are several different approaches to functionalizing NPs and their surface, including so-called "physical methods," which mostly require wet chemistry and large amounts of chemicals. Before obtaining the final material, multiple lengthy reactions and purification stages are typically necessary [148, 149]. From an industrial standpoint, where mass production is desired, these methods seriously negatively affect the economy and the environment. Plasma methods seem to be worthwhile alternatives for the surface modification of nanomaterials because of these restrictions.

5.3 Sonochemical Treatment

A fantastic technology for mass-producing various functionalized materials is sonochemical treatment. This approach is a simple and effective way to create nanomaterials, and it allows you to customize the characteristics of the nanoparticles by altering the ultrasonic process conditions. Sonochemical treatment is a field of chemical research that examines the effects and uses of ultrasonic waves, or high-frequency sound that is difficult for the human ear to process and eventually exceeds the human hearing threshold, which for adults is typically between 18 and 20 kHz [150]. Many theories have been presented to explain how chemical bonds can be broken by 20 kHz sonic radiation. They all concur that the formation, expansion, and collapse of a bubble in the liquid constitute the primary events in sonochemistry. Diffusion of solute vapor into the bubble's volume causes the stage leading to bubble expansion to take place. When the bubble size reaches its maximum value, the bubble collapses in its final stage. Many studies have been conducted to explore the synthesis of nanomaterials using the sonochemical approach. The sonochemical method is a useful alternative technique for creating nanostructures in natural environments. This method is regarded as one of the simple, quick, affordable, and ecologically friendly one-pot processes. However, there still needs to be more information on the complete overview of these physicochemical and morphological nanoparticles [151, 152].

6 Conclusion

The use of nanostructured materials as supercapacitor electrode materials has received substantial research. The nanostructure can substantially improve performance by shortening the ion diffusion pathway in addition to offering a large amount of active surface for energy storage. Researchers could concentrate on the following several factors to further enhance the performance of supercapacitors. Specific material, surface, and interface qualities are given weight in study reports on energy conversion and storage. Additionally, those characteristics considerably alter the transport behavior of energy storage and conversion equipment. Energy conversion and storage efficiency were improved by altering the material properties using the aforementioned fabrication and processing procedures. Whatever the cause, it is evident that the interfacial characteristics of the electrode and electrolyte—active surface area and wettability—contribute significantly to the efficiency enhancement.

However, there are still issues with device stability and manufacture. Every research report has some restrictions and flaws that merit extra consideration. Therefore, it is necessary to strengthen the investigation of the transport qualities concerning material alterations. There is a need for new gadgets that are highly efficient and stable in challenging environments, even though several are already commercially accessible.

References

1. Zhu C, Liu T, Qian F, Chen W, Chandrasekaran S, Yao B, Song Y, Duoss EB, Kuntz JD, Spadaccini CM, Worsley MA (2017) 3D printed functional nanomaterials for electrochemical energy storage. Nano Today 15:107–120
2. Zhang ZJ, Yao ZZ, Xiang SC, Chen BL (2011) Energy Environ. Sci. 2014, 7, 2868–2899; b) B. Dunn, H. Kamath, J.-M. Tarascon Science 334:928–935
3. Wang G, Zhang L, Zhang J (2012) A review of electrode materials for electrochemical supercapacitors. Chem Soc Rev 41(2):797–828
4. Augustyn V, Simon P, Dunn B (2014) Pseudocapacitive oxide materials for high-rate electrochemical energy storage. Energy Environ Sci 7(5):1597–1614
5. Wang ZL, Wu W (2012) Nanotechnology-enabled energy harvesting for self-powered micro-/nanosystems. Angew Chem Int Ed 51(47):11700–11721
6. Armand M, Tarascon JM (2008) Building better batteries. Nature 451(7179): 652-657
7. Tarascon JM, Armand M (2001) Issues and challenges facing rechargeable lithium batteries. Nature 414(6861): 359–367
8. Raj CC, Prasanth R (2018) advent of TiO2 nanotubes as supercapacitor electrode. J Electrochem Soc 165(9):E345
9. Simon P, Gogotsi Y (2008) Materials for electrochemical capacitors. Nat Mater 7(11):845–854
10. Simon P, Gogotsi Y, Dunn B (2014) Where do batteries end and supercapacitors begin? Science 343(6176):1210–1211
11. Salanne M, Rotenberg B, Naoi K, Kaneko K, Taberna PL, Grey CP, Dunn B, Simon P (2016) Efficient storage mechanisms for building better supercapacitors. Nat Energy 1(6):1–10
12. Helmholtz HV (1853) Ueber einige Gesetze der Vertheilung elektrischer Ströme in körperlichen Leitern, mit Anwendung auf die thierisch-elektrischen Versuche (Schluss.). Annalen der Physik 165(7):353–377

13. Miller EE, Hua Y, Tezel FH (2018) Materials for energy storage: Review of electrode materials and methods of increasing capacitance for supercapacitors. J Energy Storage 20:30–40
14. Bigdeloo M, Kowsari E, Ehsani A, Chinnappan A, Ramakrishna S, AliAkbari R (2021) Review on innovative sustainable nanomaterials to enhance the performance of supercapacitors. J Energy Storage 37:102474
15. Bhoyate S, Kahol PK, Gupta RK (2018) Nanostructured materials for supercapacitor applications: 1–29
16. Baig N, Kammakakam I, Falath W (2021) Nanomaterials: A review of synthesis methods, properties, recent progress, and challenges. Mater Adv 2(6):1821–1871
17. Prakash CJ, Prasanth R (2021) TiO2-based devices for energy-related applications. In: Titanium Dioxide(TiO$_2$) and Its Applications (pp. 241–265). Elsevier
18. Rizvi M, Gerengi H, Gupta P (2022) Functionalization of nanomaterials: synthesis and characterization. In: Functionalized nanomaterials for corrosion mitigation: synthesis, characterization, and applications (pp. 1–26). American Chemical Society
19. Ruan S, Luo D, Li M, Wang J, Ling L, Yu A, Chen Z (2021) Synthesis and functionalization of 2D nanomaterials for application in lithium-based energy storage systems. Energy Storage Mater 38:200–230
20. Pomerantseva E, Bonaccorso F, Feng X, Cui Y, Gogotsi Y (2019) Energy storage: The future enabled by nanomaterials. Science 366(6468): eaan8285
21. Frey NA, Peng S, Cheng K, Sun S (2009) Magnetic nanoparticles: synthesis, functionalization, and applications in bioimaging and magnetic energy storage. Chem Soc Rev 38(9):2532–2542
22. Li Z, Wang L, Li Y, Feng Y, Feng W (2019) Carbon-based functional nanomaterials: Preparation, properties and applications. Compos Sci Technol 179:10–40
23. Iijima S, Ichihashi T (1993) Single-shell carbon nanotubes of 1-nm diameter. Nature 363(6430):603–605.
24. Novoselov KS, Geim AK, Morozov SV, Jiang D, Katsnelson MI, Grigorieva I, Dubonos S, Firsov A (2005) Two-dimensional gas of massless Dirac fermions in graphene. Nature, 438(7065): 197–200
25. Geim AK (2009) Graphene: status and prospects. Science, 324(5934):1530–1534
26. Tasis D, Tagmatarchis N, Bianco A, Prato M (2006) Chemistry of carbon nanotubes. Chem Rev 106(3):1105–1136
27. Karousis N, Tagmatarchis N, Tasis D (2010) Current progress on the chemical modification of carbon nanotubes. Chem Rev 110(9):5366–5397
28. Khabashesku VN, Pulikkathara MX (2006) Chemical modification of carbon nanotubes. Mendeleev Commun 16(2):61–66
29. Yan Y, Miao J, Yang Z, Xiao FX, Yang HB, Liu B, Yang Y (2015) Carbon nanotube catalysts: recent advances in synthesis, characterization and applications. Chem Soc Rev 44(10):3295–3346
30. Tasis D, Tagmatarchis N, Bianco A, Prato M (2006) Chemistry of carbon nanotubes. Chem Rev 106(3):1105–1136
31. Feng Y, Zhang H, Hou Y, McNicholas TP, Yuan D, Yang S, Ding L, Feng W, Liu J (2008) Room temperature purification of few-walled carbon nanotubes with high yield. ACS Nano 2(8):1634–1638
32. Li Y, Chen Y, Feng Y, Zhao S, Lü P, Yuan X, Feng W (2010) Progress of synthesizing methods and properties of fluorinated carbon nanotubes. Science China Technol Sci 53(5):1225–1233
33. Feng W, Fujii A, Ozaki M, Yoshino K (2005) Perylene derivative sensitized multi-walled carbon nanotube thin film. Carbon 43(12):2501–2507
34. Feng Y, Lv P, Zhang X, Li Y, Feng W (2010) Selective electroless coating of palladium nanoparticles on metallic single-walled carbon nanotube. Appl Phys Lett 97(8):083101
35. Novoselov KS, Geim AK, Morozov SV, Jiang D, Katsnelson MI, Grigorieva I, Dubonos S, Firsov A (2005) Two-dimensional gas of massless Dirac fermions in graphene. Nature 438(7065):197–200
36. Geim AK (2009) Graphene: status and prospects. Science, 324(5934):1530–1534
37. Geim AK, Novoselov KS (2007) The rise of graphene. Nat Mater 6(3):183–191

38. Feng Y, Lv P, Zhang X, Li Y, Feng W (2010) Selective electroless coating of palladium nanoparticles on metallic single-walled carbon nanotube. Appl Phys Lett 97(8):083101
39. Lee C, Wei X, Kysar JW, Hone J (2008) Measurement of the elastic properties and intrinsic strength of monolayer graphene. Science, 321(5887): 385–388
40. Kuila T, Bose S, Mishra AK, Khanra P, Kim NH, Lee JH (2012) Chemical functionalization of graphene and its applications. Prog Mater Sci 57(7):1061–1105
41. Zhang C, Hu J, Cong J, Zhao Y, Shen W, Toyoda H, Nagatsu M, Meng Y (2011) Pulsed plasma-polymerized alkaline anion-exchange membranes for potential application in direct alcohol fuel cells. J Power Sources 196(13):5386–5393
42. Lota K, Khomenko V, Frackowiak E (2004) Capacitance properties of poly (3, 4-ethylenedioxythiophene)/carbon nanotubes composites. J Phys Chem Solids 65(2–3):295–301
43. Suematsu S, Oura Y, Tsujimoto H, Kanno H, Naoi K (2000) Conducting polymer films of cross-linked structure and their QCM analysis. Electrochim Acta 45(22–23):3813–3821
44. Villers D, Jobin D, Soucy C, Cossement D, Chahine R, Breau L, Bélanger D (2003) The influence of the range of electroactivity and capacitance of conducting polymers on the performance of carbon conducting polymer hybrid supercapacitor. J Electrochem Soc 150(6):A747
45. Hashmi SA, Upadhyaya HM (2002) Polypyrrole and poly (3-methyl thiophene)-based solid state redox supercapacitors using ion conducting polymer electrolyte. Solid State Ionics 152:883–889
46. Vol'fkovich YM, Serdyuk TM (2002) Electrochemical capacitors. Russ J Electrochem 9(38):935–959
47. Mastragostino M, Arbizzani C, Meneghello L, Paraventi R (1996) Electronically conducting polymers and activated carbon: Electrode materials in supercapacitor technology. Adv Mater 8(4):331–334
48. Snook GA, Kao P, Best AS (2011) Conducting-polymer-based supercapacitor devices and electrodes. J Power Sources 196(1):1–12
49. Ryu KS, Kim KM, Park NG, Park YJ, Chang SH (2002) Symmetric redox supercapacitor with conducting polyaniline electrodes. J Power Sources 103(2):305–309
50. Ryu KS, Kim KM, Park YJ, Park NG, Kang MG, Chang SH (2002) Redox supercapacitor using polyaniline doped with Li salt as electrode. Solid State Ionics 152:861–866
51. Sivakkumar SR, Saraswathi R (2004) Performance evaluation of poly (N-methylaniline) and polyisothianaphthene in charge-storage devices. J Power Sources 137(2):322–328
52. Fan LZ, Maier J (2006) High-performance polypyrrole electrode materials for redox supercapacitors. Electrochem Commun 8(6):937–940
53. Snook GA, Kao P, Best AS (2011) Conducting-polymer-based supercapacitor devices and electrodes. J Power Sources 196(1):1–12
54. Snook GA, Peng C, Fray DJ, Chen GZ (2007) Achieving high electrode specific capacitance with materials of low mass specific capacitance: Potentiostatically grown thick micro-nanoporous PEDOT films. Electrochem Commun 9(1):83–88
55. Laforgue A, Simon P, Fauvarque JF, Mastragostino M, Soavi F, Sarrau JF, Lailler P, Conte M, Rossi E, Saguatti S (2003) Activated carbon/conducting polymer hybrid supercapacitors. J Electrochem Soc 150(5):A645
56. Sun L, Wang X, Wang Y, Xiao D, Cai W, Jing Y, Wang Y, Hu F, Zhang Q (2019) In-situ functionalization of metal electrodes for advanced asymmetric supercapacitors. Front Chem 7:512
57. An C, Zhang Y, Guo H, Wang Y (2019) Metal oxide-based supercapacitors: progress and prospectives. Nanoscale Advances 1(12):4644–4658
58. Yu Z, Tetard L, Zhai L, Thomas J (2015) Supercapacitor electrode materials: nanostructures from 0 to 3 dimensions. Energy Environ Sci 8(3):702–730
59. Lu X, Wang C, Favier F, Pinna N (2017) Electrospun nanomaterials for supercapacitor electrodes: designed architectures and electrochemical performance. Adv Energy Mater 7(2):1601301

60. Xu Y, Wang X, An C, Wang Y, Jiao L, Yuan H (2014) Facile synthesis route of porous MnCo2O 4 and CoMn2O4 nanowires and their excellent electrochemical properties in supercapacitors. J Mater Chem A 2(39):16480–16488
61. Gao H, Li Y, Zhao H, Xiang J, Cao Y (2018) A general fabrication approach on spinel MCo2O4 (M= Co, Mn, Fe, Mg and Zn) submicron prisms as advanced positive materials for supercapacitor. Electrochim Acta 262:241–251
62. Raj S, Kar P, Roy P (2018) Facile synthesis of flower-like morphology Cu 0.27 Co 2.73 O 4 for a high-performance supercapattery with extraordinary cycling stability. Chem Commun 54(87):12400–12403
63. An C, Wang Y, Huang Y, Xu Y, Jiao L, Yuan H (2014) Porous NiCo2O4 nanostructures for high performance supercapacitors via a microemulsion technique. Nano Energy 10:125–134
64. Huang L, Chen D, Ding Y, Feng S, Wang ZL, Liu M (2013) Nickel–cobalt hydroxide nanosheets coated on NiCo2O4 nanowires grown on carbon fiber paper for high-performance pseudocapacitors. Nano Lett 13(7):3135–3139
65. Wang F, Wu X, Yuan X, Liu Z, Zhang Y, Fu L, Zhu Y, Zhou Q, Wu Y, Huang W (2017) Latest advances in supercapacitors: from new electrode materials to novel device designs. Chem Soc Rev 46(22):6816–6854
66. Salunkhe RR, Kaneti YV, Yamauchi Y (2017) Metal–organic framework-derived nanoporous metal oxides toward supercapacitor applications: progress and prospects. ACS Nano 11(6):5293–5308
67. Zhang L, Shi D, Liu T, Jaroniec M, Yu J (2019) Nickel-based materials for supercapacitors. Mater Today 25:35–65
68. Dong Y, Wang Y, Xu Y, Chen C, Wang Y, Jiao L, Yuan H (2017) Facile synthesis of hierarchical nanocage MnCo2O4 for high performance supercapacitor. Electrochim Acta 225:39–46
69. Xiao X, Zhang G, Xu Y, Zhang H, Guo X, Liu Y, Pang H (2019) A new strategy for the controllable growth of MOF@ PBA architectures. J Mater Chem A 7(29):17266–17271
70. Guo X, Zhang YZ, Zhang F, Li Q, Anjum DH, Liang H, Liu Y, Liu CS, Alshareef HN, Pang H (2019) A novel strategy for the synthesis of highly stable ternary SiO x composites for Li-ion-battery anodes. J Mater Chem A 7(26):15969–15974
71. Wang H, Xiao Z, Yu Z, Ma Y, Wu P, Xue F, Guo W, Lu W, Jiao X, Jiang P, Liang M (2019) Facile fabrication of iron oxide/carbon/rGO superparamagnetic nanocomposites for enhanced electrochemical energy storage performance. J Alloy Compd 811:152019
72. Kim HS, Cook JB, Lin H (2016) Jesse s. Ko, Sarah h. Tolbert, V. Ozolins. B Dunn Nat Mater 16:454–460
73. Raj CC, Srimurugan V, Flamina A, Prasanth R (2020) Tuning the carrier density of TiO2 nanotube arrays by controlling the oxygen vacancies for improved areal capacitance in supercapacitor applications. Mater Chem Phys 248:122925
74. Yang D (2012) Application of nanocomposites for supercapacitors: characteristics and properties. Nanocomposites-New Trends Dev:299–328
75. Singh NB, Agarwal S (2016) Nanocomposites: an overview. Emerg Mater Res 5(1):5–43
76. Pang H, Cao X, Zhu L, Zheng M (2020) Synthesis of functional nanomaterials for electrochemical energy storage. Springer, Singapore
77. Pang H, Cao X, Zhu L, Zheng M (2020) Synthesis of functional nanomaterials for electrochemical energy storage. Springer, Singapore
78. Lu X, Wang C, Favier F, Pinna N (2017) Electrospun nanomaterials for supercapacitor electrodes: designed architectures and electrochemical performance. Adv Energy Mater 7(2):1601301
79. Mao J, Zhou T, Zheng Y, Gao H, kun Liu H, Guo Z (2018) Two-dimensional nanostructures for sodium-ion battery anodes. J Mater Chem A, 6(8):3284-3303
80. Ji L, Meduri P, Agubra V, Xiao X, Alcoutlabi M (2016) Graphene-based nanocomposites for energy storage. Adv Energy Mater 6(16):1502159
81. Agubra VA, Zuniga L, Flores D, Villareal J, Alcoutlabi M (2016) Composite nanofibers as advanced materials for Li-ion, Li-O2 and Li-S batteries. Electrochim Acta 192:529–550

82. Ji L, Lin Z, Alcoutlabi M, Zhang X (2011) Recent developments in nanostructured anode materials for rechargeable lithium-ion batteries. Energy Environ Sci 4(8):2682–2699
83. Yun Q, Lu Q, Zhang X, Tan C, Zhang H (2018) Three-dimensional architectures constructed from transition-metal dichalcogenide nanomaterials for electrochemical energy storage and conversion. Angew Chem Int Ed 57(3):626–646
84. Choi BG, Chang SJ, Lee YB, Bae JS, Kim HJ, Huh YS (2012) 3D heterostructured architectures of Co3O4 nanoparticles deposited on porous graphene surfaces for high performance of lithium ion batteries. Nanoscale 4(19):5924–5930
85. Choi SH, Ko YN, Lee JK, Kang YC (2015) 3D MoS2–graphene microspheres consisting of multiple nanospheres with superior sodium ion storage properties. Adv Func Mater 25(12):1780–1788
86. Wang J, Zhang X, Wei Q, Lv H, Tian Y, Tong Z, Liu X, Hao J, Qu H, Zhao J, Li Y (2016) 3D self-supported nanopine forest-like Co3O4@ CoMoO4 core–shell architectures for high-energy solid state supercapacitors. Nano Energy 19:222–233
87. Sengupta J (2021) Different synthesis routes of graphene-based metal nanocomposites. In: Handbook of Polymer and Ceramic Nanotechnology (pp. 1035–1051). Springer, Cham
88. Shih CJ, Lin S, Strano MS, Blankschtein D (2010) Understanding the stabilization of liquid-phase-exfoliated graphene in polar solvents: molecular dynamics simulations and kinetic theory of colloid aggregation. J Am Chem Soc 132(41):14638–14648
89. Kumar P, Panchakarla LS, Rao CNR (2011) Laser-induced unzipping of carbon nanotubes to yield graphene nanoribbons. Nanoscale 3(5):2127–2129
90. Subrahmanyam KS, Panchakarl LS, Govindaraj A, Rao CNR (2009) Simple method of preparing graphene flakes by an arc-discharge method. J Phys Chem C: 4257–4259
91. Huang JY, Ding F, Yakobson BI, Lu P, Qi L, Li J (2009) In situ observation of graphene sublimation and multi-layer edge reconstructions. Proc Natl Acad Sci 106(25):10103–10108
92. Abdelkader AM, Cooper AJ, Dryfe RA, Kinloch IA (2015) How to get between the sheets: a review of recent works on the electrochemical exfoliation of graphene materials from bulk graphite. Nanoscale 7(16):6944–6956
93. Van Heerden X, Badenhorst H (2015) The influence of three different intercalation techniques on the microstructure of exfoliated graphite. Carbon 88:173–184
94. Gao W (2015) Graphene Oxide Reduct. Recipes, Spectrosc. Appl 61
95. Zhu Y, Murali S, Stoller MD, Ganesh KJ, Cai W, Ferreira PJ, Pirkle A, Wallace RM, Cychosz KA, Thommes M, Su D (2011) Carbon-based supercapacitors produced by activation of graphene. Science 332(6037): 1537–1541
96. Tobias G, Mendoza E, Ballesteros B (2016) Functionalization of carbon nanotubes. Encyclopedia of Nanotechnology, 2nd ed.; Bhushan, B., Ed. pp 1281–1291
97. Banerjee S, Hemraj-Benny T, Wong SS (2005) Covalent surface chemistry of single-walled carbon nanotubes. Adv Mater 17(1):17–29
98. Balasubramanian K, Burghard M (2005) Chemically functionalized carbon nanotubes. Small 1(2):180-192
99. Esumi K, Ishigami M, Nakajima A, Sawada K, Honda H (1996) Chemical treatment of carbon nanotubes. Carbon (New York, NY) 34(2):279–281
100. Saleh TA (2011) The influence of treatment temperature on the acidity of MWCNT oxidized by HNO3 or a mixture of HNO3/H2SO4. Appl Surf Sci 257(17):7746–7751
101. Saleh TA (2011) The influence of treatment temperature on the acidity of MWCNT oxidized by HNO3 or a mixture of HNO3/H2SO4. Appl Surf Sci 257(17):7746–7751
102. Sham ML, Kim JK (2006) Surface functionalities of multi-wall carbon nanotubes after UV/Ozone and TETA treatments. Carbon 44(4):768–777
103. Wang SC, Chang KS, Yuan CJ (2009) Enhancement of electrochemical properties of screen-printed carbon electrodes by oxygen plasma treatment. Electrochim Acta 54(21):4937–4943
104. Hamon MA, Hui H, Bhowmik P, Itkis HME, Haddon RC (2002) Ester-functionalized soluble single-walled carbon nanotubes. Appl Phys A 74(3):333–338
105. Liu J, Rinzler AG, Dai H, Hafner JH, Bradley RK, Boul PJ, Lu A, Iverson T, Shelimov K, Huffman CB, Rodriguez-Macias F (1998) Fullerene pipes. Science 280(5367):1253–1256

106. Ma PC, Kim JK, Tang BZ (2006) Functionalization of carbon nanotubes using a silane coupling agent. Carbon 44(15):3232–3238
107. Sano M, Kamino A, Okamura J, Shinkai S (2001) Self-organization of PEO-g raft-single-walled carbon nanotubes in solutions and langmuir−blodgett films. Langmuir 17(17):5125–5128
108. Speranza G (2021) Carbon nanomaterials: Synthesis, functionalization and sensing applications. Nanomaterials 11(4):967
109. Gmucová K (2022) Fundamental aspects of organic conductive polymers as electrodes. Curr Opin Electrochem:101117
110. Meng Q, Cai K, Chen Y, Chen L (2017) Research progress on conducting polymer based supercapacitor electrode materials. Nano Energy 36:268–285
111. Zhu J, Sun W, Yang D, Zhang Y, Hoon HH, Zhang H, Yan Q (2015) Multifunctional architectures constructing of PANI nanoneedle arrays on MoS2 Thin nanosheets for high-energy supercapacitors. Small 11(33):4123–4129
112. Das AK, Karan SK, Khatua BB (2015) High energy density ternary composite electrode material based on polyaniline (PANI), molybdenum trioxide (MoO3) and graphene nanoplatelets (GNP) prepared by sono-chemical method and their synergistic contributions in superior supercapacitive performance. Electrochim Acta 180:1–15
113. Fu C, Zhou H, Liu R, Huang Z, Chen J, Kuang Y (2012) Supercapacitor based on electropolymerized polythiophene and multi-walled carbon nanotubes composites. Mater Chem Phys 132(2–3):596–600
114. Zhang H, Hu Z, Li M, Hu L, Jiao S (2014) A high-performance supercapacitor based on a polythiophene/multiwalled carbon nanotube composite by electropolymerization in an ionic liquid microemulsion. J Mater Chem A 2(40):17024–17030
115. Meng Q, Cai K, Chen Y, Chen L (2017) Research progress on conducting polymer based supercapacitor electrode materials. Nano Energy 36:268–285
116. Paszkiewicz S, Szymczyk A (2019) Graphene-based nanomaterials and their polymer nanocomposites. In: Nanomaterials and polymer nanocomposites (pp. 177–216). Elsevier
117. Shukla V (2019) Review of electromagnetic interference shielding materials fabricated by iron ingredients. Nanoscale Adv 1(5):1640–1671
118. Zhang J, Zhao XS (2012) Conducting polymers directly coated on reduced graphene oxide sheets as high-performance supercapacitor electrodes. J Phys Chem C 116(9):5420–5426
119. He Y, Pan D, Chi H, Luo F, Jiang Y, Ge D, Bai H (2021) Continuous and patterned conducting polymer coatings on diverse substrates: rapid fabrication by oxidant-intermediated surface polymerization and application in flexible devices. ACS Appl Mater Interfaces 13(4):5583–5591
120. Vangari M, Pryor T, Jiang L (2013) Supercapacitors: Review of Materials. J Energy Eng (Ç) 2:72–79
121. Kate RS, Khalate SA, Deokate RJ (2018) Overview of nanostructured metal oxides and pure nickel oxide (NiO) electrodes for supercapacitors: A review. J Alloy Compd 734:89–111
122. Chen YL, Chen PC, Chen TL, Lee CY, Chiu HT (2013) Nanosized MnO 2 spines on Au stems for high-performance flexible supercapacitor electrodes. J Mater Chem A 1(42):13301–13307
123. Su Z, Yang C, Xu C, Wu H, Zhang Z, Liu T, Zhang C, Yang Q, Li B, Kang F (2013) Co-electro-deposition of the MnO 2–PEDOT: PSS nanostructured composite for high areal mass, flexible asymmetric supercapacitor devices. J Mater Chem A 1(40):12432–12440
124. Song Y, Fan JB, Wang S (2017) Recent progress in interfacial polymerization. Mater Chem Front 1(6):1028–1040
125. Yashin VV, Balazs AC (2004) Theoretical model of interfacial polymerization. J Chem Phys 121(22):11440–11454
126. Song Y, Fan JB, Wang S (2017) Recent progress in interfacial polymerization. Mater Chem Front 1(6):1028–1040
127. Sun L, Wang X, Wang Y, Xiao D, Cai W, Jing Y, Wang Y, Hu F, Zhang Q (2019) In-situ functionalization of metal electrodes for advanced asymmetric supercapacitors. Front Chem 7:512

128. Abdah MAAM, Azman NHN, Kulandaivalu S, Sulaiman Y (2020) Review of the use of transition-metal-oxide and conducting polymer-based fibres for high-performance supercapacitors. Mater Des 186:108199
129. Yuvaraj S, Fernandez AC, Sundararajan M, Dash CS, Sakthivel P (2020) Hydrothermal synthesis of ZnO–CdS nanocomposites: structural, optical and electrical behavior. Ceram Int 46(1):391–402
130. Hessien M, Da'na E, Taha A (2021) Phytoextract assisted hydrothermal synthesis of ZnO–NiO nanocomposites using neem leaves extract. Ceram Int 47(1):811–816
131. Sedighi F, Esmaeili-Zare M, Sobhani-Nasab A, Behpour M (2018) Synthesis and characterization of CuWO4 nanoparticle and CuWO4/NiO nanocomposite using co-precipitation method; application in photodegradation of organic dye in water. J Mater Sci: Mater Electron 29(16):13737–13745
132. Jazi FS, Parvin N, Rabiei M, Tahriri M, Shabestari ZM, Azadmehr AR (2012) Effect of the synthesis route on the grain size and morphology of ZnO/Ag nanocomposite. J Ceram Process Res 13(5):523–526
133. Somraksa, W., Suwanboon, S., Amornpitoksuk, P. and Randorn, C., 2020. Physical and photocatalytic properties of $CeO_2/ZnO/ZnAl_2O_4$ ternary nanocomposite prepared by Co-precipitation method. Mater Res 23
134. Parashar M, Shukla VK, Singh R (2020) Metal oxides nanoparticles via sol–gel method: a review on synthesis, characterization and applications. J Mater Sci: Mater Electron 31(5):3729–3749
135. Tseng TK, Lin YS, Chen YJ, Chu H (2010) A review of photocatalysts prepared by sol-gel method for VOCs removal. Int J Mol Sci 11(6):2336–2361
136. Ward DA, Ko EI (1995) Preparing catalytic materials by the sol-gel method. Ind Eng Chem Res 34(2):421–433
137. Raj CC, Sundheep R, Prasanth R (2015) Enhancement of electrochemical capacitance by tailoring the geometry of TiO2 nanotube electrodes. Electrochim Acta 176:1214–1220
138. Chee WK, Lim HN, Zainal Z, Huang NM, Harrison I, Andou Y (2016) Flexible graphene-based supercapacitors: a review. J Phys Chem C 120(8):4153–4172
139. Shakthivel D, Ahmad M, Alenezi MR, Dahiya R, Silva SRP (2019) 1D semiconducting nanostructures for flexible and large-area electronics: growth mechanisms and suitability. Cambridge University Press
140. Shakthivel D, Navaraj WT, Champet S, Gregory DH, Dahiya RS (2019) Propagation of amorphous oxide nanowires via the VLS mechanism: Growth kinetics. Nanoscale Advances 1(9):3568–3578
141. Ye JS, Cui HF, Liu X, Lim TM, Zhang WD, Sheu FS (2005) Preparation and characterization of aligned carbon nanotube–ruthenium oxide nanocomposites for supercapacitors. Small 1(5):560–565
142. Heale FL, Parkin IP, Carmalt CJ (2019) Slippery liquid infused porous TiO2/SnO2 nanocomposite thin films via aerosol assisted chemical vapor deposition with anti-icing and fog retardant properties. ACS Appl Mater Interfaces 11(44):41804–41812
143. Park T, Leem M, Lee H, Ahn W, Kim H, Kim J, Lee E, Kim YH, Kim H (2017) Synthesis of vertical MoO2/MoS2 core–shell structures on an amorphous substrate via chemical vapor deposition. J Phys Chem C 121(49):27693–27699
144. Chen H, Yu Y, Xin HL, Newton KA, Holtz ME, Wang D, Muller DA, Abruña HD, DiSalvo FJ (2013) Coalescence in the thermal annealing of nanoparticles: an in situ STEM study of the growth mechanisms of ordered Pt–Fe nanoparticles in a KCl matrix. Chem Mater 25(8):1436–1442
145. Singh NK, Rajkumari R (2019) Effect of annealing on metal-oxide nanocluster. In: concepts of semiconductor photocatalysis. IntechOpen
146. Strokova N, Savilov S, Xia H, Aldoshin S, Lunin V (2016) Sintered carbon nanomaterials: Structural change and adsorption properties. Z Phys Chem 230(12):1719–1731
147. Hansen TW, DeLaRiva AT, Challa SR, Datye AK (2013) Sintering of catalytic nanoparticles: particle migration or Ostwald ripening? Acc Chem Res 46(8):1720–1730

148. Dulyaseree P, Yordsri V, Wongwiriyapan W (2016) Effects of microwave and oxygen plasma treatments on capacitive characteristics of supercapacitor based on multiwalled carbon nanotubes. Jpn J Appl Phys 55(2S):02BD05
149. Mathioudaki S, Barthélémy B, Detriche S, Vandenabeele C, Delhalle J, Mekhalif Z, Lucas S (2018) Plasma treatment of metal oxide nanoparticles: Development of core–shell structures for a better and similar dispersibility. ACS Applied Nano Materials 1(7):3464–3473
150. Suslick KS (1990) Sonochemistry. Science 247(4949):1439-1445
151. Vickers NJ (2017) Animal communication: when i'm calling you, will you answer too? Curr Biol 27(14):R713–R715
152. Majumdar D, Bhattacharya SK (2017) Sonochemically synthesized hydroxy-functionalized graphene–MnO2 nanocomposite for supercapacitor applications. J Appl Electrochem 47(7):789–801

Part III

Functionalized Nanomaterials Supercapacitor

Всё для победы!
НАРОДНЫЙ ФРОНТ
https://pobeda.onf.ru/
LET'S HELP THE RUSSIA

Chapter 10
Functionalization Techniques for Carbon Dedicated to Electrochemical Use

Ismaila T. Bello, Langutani E. Mathevula, Bakang M. Mothudi, and Mokhotjwa S. Dhlamini

1 Introduction

This chapter discussed the functionalization techniques of carbon materials used in electrochemical applications. Functionalization of different allotropes of carbon materials such as diamonds, graphite, carbon nanotubes (CNTs), fullerenes, carbon black (CB), and carbon nanofibers (CNFs) is an important way to improve the electrochemical systems [1–6]. The increased surface functional groups with additional faradic contribution generate higher energy-power densities and enhance the compatibility of electrochemical devices with aqueous electrolytes and other active materials [7–10]. The graphical representation of different allotropes of CMs with their properties and applications is depicted in Fig. 1.

Over the ages, diamond and graphite are the most common sources of CMs, despite the fact the availability of CMs in nature in various forms of biomolecules, amorphous, and carbon in organic molecules. The unusual attribute of carbon's electronic structure, which forms many hybrids including sp^1, sp^2, and sp^3, is what gives it its multi-dimensional nature. As a result of the hybrids' diverse orbital orientations, various structures with distinctly different characteristics have developed [11–13]. Diamond, for example, is made up of pure sp3 hybrids with bonds aligned along the major axis of a tetrahedron. Diamond is the hardest substance known to man, very transparent, and electrically insulating, yet with a significant thermal conductivity due to the four strong covalent bonds that are discernible in this structure [14–16]. Graphite, on the other hand, is created by pure sp^2 hybrids. In this occurrence, three carbon bonds are in a plane and make a 120° angle with the three atoms that are

---

I. T. Bello (✉) · L. E. Mathevula · B. M. Mothudi · M. S. Dhlamini (✉)
Department of Physics, CSET, University of South Africa, Johannesburg 1710, South Africa
e-mail: ismailbello26@gmail.com

M. S. Dhlamini
e-mail: dhlamms@unisa.ac.za

© The Author(s), under exclusive license to Springer Nature Singapore Pte Ltd. 2024

C. M. Hussain and M. B. Ahamed (eds.), *Functionalized Nanomaterials Based Supercapacitor*, Materials Horizons: From Nature to Nanomaterials,
https://doi.org/10.1007/978-981-99-3021-0_10

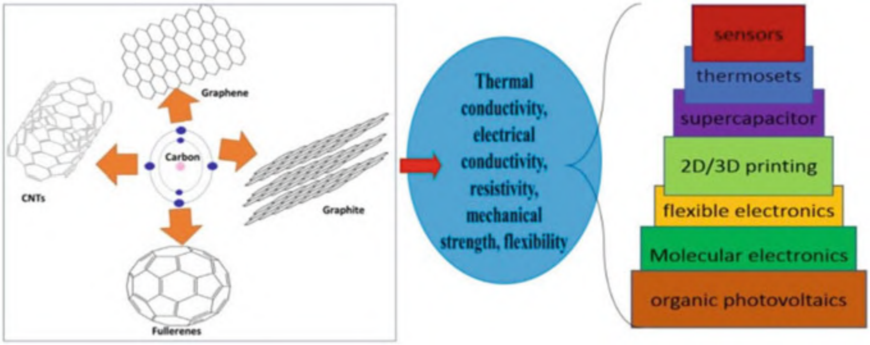

Fig. 1 Graphical representation of different allotropes of CMs with their properties and applications. Reproduced with copyright from [50]

closest to them. This plane is perpendicular to the fourth bond. The layered structure of graphite is determined by this unusual electrical arrangement. The out-of-plane bond, which is weak compared to the covalent and exceptionally strong in-plane bonds, gives graphite its electrical conductivity, high absorption coefficient over a wide spectrum range, and softness [17, 18]. Therefore, the combination of these two types of hybrids in the other materials causes the bond orientation of the amorphous structure of CMs to be unpredictable [18]. Fullerenes are the other types of CMs that were discovered first in 1985 [19]. Fullerenes are particularly fascinating in terms of fundamental research as well as application potential. The family of spherical compounds known as fullerenes is made up of carbon atoms in various counts of 20, 60, 70, and more. The C_{60} molecule is the more prevalent, stable, and extensively researched system compared to other fullerenes. The arrangement of the C atoms in C_{60} creates the bond curvature necessary for the creation of a spherical structure (truncated icosahedron) by placing them nearby in pentagons and hexagons. All carbon atoms in C_{60} molecules are sp^2 hybrids. Although the existence of pentagons prevents bond resonance from occurring, this is distinct from the organization found in a perfect hexagonal structure, such as in graphite sheets. As a result, fullerenes are effective charge acceptors, a quality that is crucial in interactions with radicals and surface functionalization [20]. In contrast to fullerenes, graphene has perfect resonance because its atoms are arranged in a monoatomic layer that is a two-dimensional hexagonal lattice. Graphene has distinct features due to electron quantum confinement in a single atomic sheet. Graphene can be thought of as a zero-gap semiconductor due to its numerous properties, including its high absorbance throughout the whole visible optical range and the electron motion being ballistic [21]. While carbon nanotubes (CNTs) can be compared to folded graphene sheets, their curvature gives them distinctive electrical characteristics. Following the discovery of fullerenes, CNTs underwent substantial research from both a theoretical and practical standpoint. The orientation of the hexagonal bond directions concerning the CNT axis, or chirality, is a property that distinguishes CNTs from other materials. The electrical characteristics of CNTs are greatly influenced by their orientation [22, 23]. Other competing CMs that are widely used in industrial applications are carbon nanofibers (CNFs). The composite's mechanical characteristics are improved by utilizing the strong covalent C–C bond. The carbon-based fibers have the highest specific strength and specific modulus among the group of fibers. As opposed to glassy and organic polymer fibers, CNFs do not have corrosion issues or stress-induced breakdowns at ambient temperature. If CNFs are compared to other materials, they also exhibit exceptional strength and modulus at high temperatures [24]. Compared to carbon nanotubes, CNFs are a less expensive material and are generated in large quantities. Regarding CNTs, they are used as a reinforcing component in a wide range of substances, such as inorganic materials, organic materials, metals, and biomaterials [25–28]. Carbon black and other forms of CMs including glassy carbon and porous carbon are widely used in industrial applications. With the recent potentialities of the usage of carbon black, it is mainly employed as a pigment or an additive in polymers and rubbers to enhance their mechanical properties [29]. Glassy carbon is made up of microcrystalline stacks of interconnecting narrow graphite-like layers. This results in the formation of a closed pore tough structure that is hard but brittle and chemically inert. Glassy carbons are used in a variety of distinctly diverse applications due to their extremely robust, conductive, and inert network. They are employed in the fabrication of solid-state batteries as electrodes, high-temperature furnaces, and harsh chemical processes, and because of their inertness, glassy carbon is as well utilized in the fabrication of prostheses [30–32]. Like carbon black, porous carbon is also much softer than glassy carbon. Porous carbon has a large specific surface area, which improves the interactions with the surrounding medium. Despite having less conductivity than glassy carbon, it can be used to fabricate bioelectrodes for stimulation and sensing as well as electrodes for electrochemistry because of its high porosity and the presence of active sites [33–36].

These CMs can be prepared in the various dimension of 0 to 3D on different microtextures from powders to foams, crystals, composites, amorphous, and fibers [37]. Because these fillers are often hydrophobic and have low surface energy, they are incompatible with polar solvents and several polymer matrices. These materials tend to aggregate into macro-visible clusters as a result of the strong interparticle van der Waals force of contact and low surface energy [38]. Various CMs functionalization approach has been significantly developed in order to reduce the agglomerating tendency of the fillers using chemical bonding channel to increase the interfacial adhesion of the filler–polymer [39–43]. Functionalization techniques of CMs can be categorized into two main approaches, namely, covalent (chemical) and noncovalent (physical) functionalization based on the type of interactions involved between the carbon atoms on the fillers and active molecules [38]. Covalent functionalization (adsorption) necessitates the presence of reactive species capable of forming covalent adducts with the sp2 carbon of a CMs. Although it necessitates damage to the sidewalls, the primary benefit of covalent functionalization of CMs is that it is more powerful than noncovalent interactions. It alters the electronic structure, which, in contrast to noncovalent functionalization, causes the irreversible loss of double bonds. These modifications may impact the conductivity qualities, which may impact specific applications [44–49].

2 Functionalization Techniques of Carbon and Their Electrochemical Applications

The modification of the surface chemistry of the materials to provide certain properties to suit some specific applications are termed Functionalization. Various functionalization techniques have been applied to various species of CMs to change their surface energy as the main objective of the modification. This modification allows for stronger molecular interaction with other substances via the bonding of specialized active molecules such as medicines, genetic materials, luminous agents, metallic nanostructures for catalysis or plasmonic, and so on. Furthermore, it is possible to modify the surface's wettability by adding polar or non-polar groups to it. This, on a macroscopic level, improves the surface's ability to couple with solvents or other materials, such as in composites [51–53]. The surface of the material is additionally functionalized by grafting well-defined molecules to modify its reactivity toward specified chemical species. This includes the electrochemical characteristics that are adapted for certain uses, such as catalysis, batteries, supercapacitors, fuel cells, and organic photovoltaics. Additionally, the functionalization gives molecularly based nanostructures that are made of carbon luminous characteristics or permit the bonding of such species to the surface of the material [18]. The detailed covalent and noncovalent approaches shall be discussed in the subsequent sections, which include oxidation, polymer wrapping, salinization, surfactant adsorption, sialylation, amidation, and polymer grafting approaches.

2.1 Oxidation

The functionalization of CMs using oxidation can be categorized into wet and dry oxidation techniques. The wet oxidation method comprises the usage of nitric acid, sulfuric acid, hydrogen peroxide, potassium permanganate, and so on, while the dry oxidation approach oxidized CMs with air, ozone, plasma, etc., for the modification of CMs.

2.1.1 Wet Oxidation

Wet oxidation is a practical low-cost method for modifying the surface of carbon-based materials. It uses strong oxidizing agents such as HNO_3, $HNO_3 + H_2SO_4$, $H_2SO_4 + KMnO_4$, and $H_2SO_4 + H_2O_2$ to oxidize carbon fillers [54–59]. Surface oxidation attaches various oxygen-containing polar groups, known as volatile components, to the surface of carbon compounds. The dispersion of carbon compounds in aqueous environments is significantly influenced by the volatile components or polar groups. The higher the volatile components that are present in the carbon compounds, the more hydrophilic they are, and the better they disperse in aqueous-based binder systems [38]. Wet oxidation processes have been employed to modify different allotropes of CMs in both fundamental and industrial-scale applications. Such allotropes of carbon black, CNTs. CNFs, and MWNT have been functionalized to enhance their properties for specific use. Researchers have carried out several studies on the wet oxidation of CMs. The surface chemistry of Mesoporous carbon was modified via wet oxidation treatment using HNO_3 and H_2O_2 under different oxidation conditions [60]. It was observed that the oxygen functional group attached to the surface of the mesoporous carbon was of higher amount when using nitric acid as the oxidizing agent than hydrogen peroxide. However, the pristine surface and structural texture of the mesoporous carbon were kept unchanged through the oxidation process. The original mesoporous carbon and the oxidized samples after the treatment are shown in the SEM images of Fig. 2a–d. Olive stone-activated carbons were oxidized by Moreno Castilla's group in 2000, to introduce different oxygen complexes to their surfaces. They employed a wet oxidation process with three oxidizing agents of H_2O_2, $(NH_4)_2S_2O_8$, and HNO_3 to alter the surface chemistry of the activated carbons. They observed that out of the three oxidizing agents, $(NH_4)_2S_2O_8$ treatment show the lowest amount of oxygen and surface acid groups, with the highest acid strength, which was attributed to the fixation of carboxyl groups close to other groups [61]. The surface chemistry, kinetics, and defect on microporosity of four different microporous carbon were examined using a wet oxidation process. The oxidation of the different carbon materials was carried out under different conditions with HNO_3, H_2O_2, and/or $(NH_4)_2S_2O_8$ oxidizing agents. They observed that the effect of the functionalization depends on the type of oxidation methods and the nature of the materials. They concluded that the incorporated surface oxygen groups are no or less negligible impact on the measurement of the specific surface area and the micropore volume of the carbon [62].

In the electrochemical application, Oliveira et al. reported the electrochemical determination of Methyl Parathion through oxidized CNTs. The effect of wet oxidation using nitric and sulfuric acids and sodium hydroxide was studied on the structural integrity of MWCNTs. Thereafter, the electrochemical determination of Methyl Parathion using a modified glassy carbon electrode with the oxidized CNTs shows a linear response. The electrodes' analytical performance demonstrated similar voltammetric behavior, offering good sensitivity for the measurement of methyl parathion [63]. Tanaka et al. reported the effect of surface modification of ordered mesoporous carbon using wet oxidation techniques for electrochemical supercapacitors. Nitric acid and ammonium peroxodisulfate were used as oxidizing agents for the functionalization and the introduction of more surface oxygen groups to the carbon materials. The nitric acid functionalized mesoporous carbon shows an excellent electrochemical performance with gravimetric and volumetric capacitances of 290 Fg^{-1} and 300 Fcm^{-3} respectively at a current density of 0.1 Ag^{-1}. With an energy of

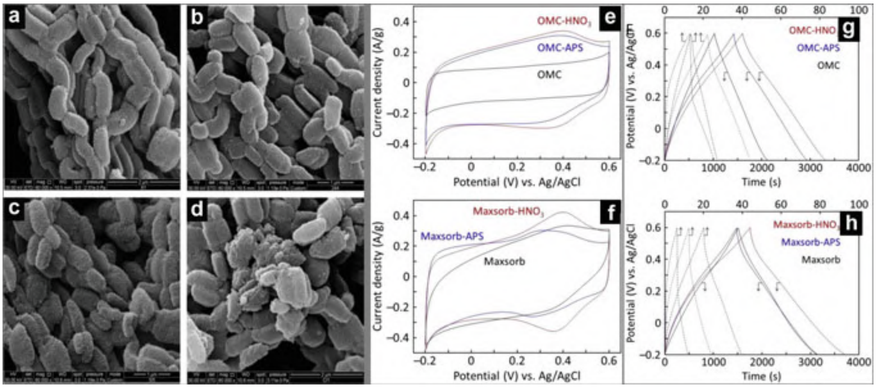

Fig. 2 **a–d** SEM images of (A) raw mesoporous carbon and some carbons obtained by different oxidation treatments: (B) 30% (v/v) H_2O_2/room temperature/24 h, (C) 5 M HNO_3/80 °C/5 h, and (D) 14.55 M HNO_3/room temperature/1 h; the latter shows an isolated damaged area, but the general structure of this oxidized carbon is the same as that of the starting material. Reproduce with copyright [60]. **e–h** CV profiles of OMC (E) and Maxsorb (F) before and after oxidation at a potential scan rate of 1 mV/s and GCD profiles of OMC (A) and Maxsorb (B) before and after oxidation at a current density of 0.1 A/g (solid line) and 5 A/g (dashed line) in 1 M sulfuric acid aqueous electrolyte. Copyright [64]

17.4 Wh/kg and a power density of 5.2 kW/kg, the device shows an excellent life cycle of over 70% capacitance retention at the high current density of 5 Ag^{-1} with remarkable performance [64]. The CV and GCD profiles of the ordered mesoporous carbon (OMC) before and after oxidation were shown in Fig. 2e–h. In 2023, Filimonenkov et al. reported the performance of a wet oxidative functionalized carbon nanotube cloth (CNTC) as a flexible electrochemical supercapacitor electrode. The CNTC was functionalized using $KmnO_4$ treatment in an acidic medium through the wet oxidation process. This is to enhance the surface of the CNTC and to change the composition of the surface oxygen functional group. The functionalized CNTC demonstrates an excellent supercapacitive performance of 71 Fg^{-1} capacitances with a 99% retention over 30,000 cyclic cycles in 0.5 M H_2SO_4 electrolyte [65].

2.1.2 Dry Oxidation

The dry oxidation or gas phase oxidation technique is a simple process of functionalizing CMs through various dry oxidation methods using air, steam, ozone, and the mixture of gases with air as oxidizing agents. The gas phase oxidation process is more attractive at the industrial scale oxidation of CMs than the wet oxidation process because of environmental and health risks emanating from the chemical used in the process. Also, dry oxidation eliminates other problems such as overoxidation and waste and drying stages associated with the liquid phase oxidation methods. For example, in Air-dry oxidation techniques, the CMs start to oxidize at a temperature higher than 300 °C, thereby increasing the surface area and surface hydrophilicity of the CMs [38]. The air oxidation method is time-consuming depending on the desired degree of oxidation and the nature of the functionalizing CMs. Amorphous carbon begins to oxidize at temperatures of 300 °C. Only at temperatures below 400 °C can an adequate number of oxygen groups be formed on the surface of carbon blacks. Compared to simple air, oxidation in the presence of nitrogen dioxide produces more surface oxides. The oxidation of the carbon surface is accelerated by nitrogen dioxide. To begin with, a mixture of nitrogen dioxide and the air is used to oxidize the carbon black. After that, in the following stage, hot air is used to treat the oxidized carbon black in order to remove the nitrogen dioxide that had become deposited on its surface during the oxidation process [66]. The dry oxidation effect on the surface chemistry and porous structure of activated carbon was reported by Jaramillo et al. [67]. The as-prepared activated carbon was oxidized in O_2(air) or O_3 atmosphere, via a dry oxidation process to study the porous structure and surface chemistry changes during the oxidation. They concluded that the most effective way to enhance acidic oxygen surface groups' content in the material while preserving a considerable number of basic sites and microporosity and developing a significant amount of mesoporosity is through dry oxidation of AC at 100 °C in O_3. The effect of thermal air oxidation was investigated on the surface and adsorptive properties of black carbon by Xiao et al. [68]. The authors observed that the functionalized black carbon after carbonization was found to have an underdeveloped pore structure and low surface area. It was also noted that the substantial effect of thermal air oxidation was only observed after post-pyrolysis treatment. Also, among the method to functionalize CMs in dry oxidation techniques is the plasma process. Plasma treatment is one approach for modifying the carbon structure, either chemically or physically. The surface area and pore size distribution of carbon are altered by physical treatment, while the chemical alteration by oxygen plasma treatment has a significant impact on the oxygen functions on the carbon surface [69, 70]. A popular method for activating carbon and increasing surface energy by producing different functional groups is plasma technology. The type of functional groups generated on carbon surfaces is heavily influenced by the gas used [71]. In 2022, Pankratova et al. investigated the effect of plasma-induced surface chemistry of microfabricated pyrolytic carbon electrodes on their electrochemical performance. The Pyrolytic carbon electrodes were microfabricated using pyrolysis (UV lithography) and functionalized using Ar, O_2, N_2, and air plasma gases. The electrochemical behaviors of the plasma-induced CMs were studied and their research offers a fundamental understanding of the electrochemistry of plasma-modified pyrolytic carbon surfaces and techniques for enhancing surface features while overcoming potential electron transfer restrictions for advancement in carbon-based electrochemical applications in the future [71]. Lota et al. reported a two-electrode system electrochemical measurement for plasma-induced carbon materials for supercapacitors application electrodes. The CMs were modified with various plasma gases (Ar, O_2, and CO_2), and the functionalized CMs were studied in the acidic medium as a supercapacitor's electrode. They observed that the capacitive behavior of the modified electrode depends on the reactant gases of the functionalization. They concluded that Ar and CO_2-induced plasma electrodes have better capacitive properties for the negative and positive electrodes respectively [70]. The impact of a low-temperature plasma iodine modification of activated carbon was investigated for possible electrochemical capacitors. The electrochemical studies of the modified low-temperature iodine plasma activated carbon confirmed an improved capacitance value of the electrode and the unusual properties of the carbon-iodine interface that can be attributed to the redox activity of various oxidation states of the iodine. The reversible redox reaction of the iodide at the interface of carbon/electrolyte made the electrode a perfect candidate for supercapacitor applications [72].

The ozonation process of activated carbon has been reported for energy storage applications. The modification of activated carbon was performed in a glass reactor under a continuous flow of ozone for 15, 30, 60, 120, and 240 min. The ozone-modified activated carbon was observed to have oxygen functional groups to be increased after ozonation, thus making it a possible electrode material for electrochemical use. The results from the electrochemical investigation showed ozone-functionalized carbon as a very attractive electrode material for the fabrication of asymmetric supercapacitors, as the negative electrode shows a higher capacitance value [73].

2.2 Silanization

Silanization of carbon materials is an effective way to enhance the surface properties and the attachment of the reactive functional groups on the CMs through silane coupling agents [74]. The silane coupling agent serves as a bifunctional that interacts with both CMs and the polymers. Equation (1) shows the general chemical formula for silanes.

$$R - (CH_2)_n - Si\left(OR'\right)_3 \tag{1}$$

where OR′-the hydrolyzable alkoxy group, R-the nonhydrolyzable organic functional group (i.e., R may be an aromatic ring, thiol, epoxy ring, vinyl or amine, etc.), and n = 0–3. The organo-functional group (R) in the coupling agent causes the interaction with the polymer matrix. The creation of the tri-silanol group from the hydrolysis of the OR′ groups allows it to interact with the hydroxyl groups on the surface of carbon nanotubes that have already undergone various forms of oxidation or reduction [75–77]. The three stages in which the silanization of CMs occurred were shown in Fig. 3. In the first stage (a), silane is hydrolyzed, resulting in the formation of active silanol groups from labile alkoxy groups in silanes. In the second stage (b), silanol groups condense to form siloxane oligomers, and the silanol groups/oligomers make hydrogen bonds with the hydroxyl groups present on the surface of oxidized carbon materials. The third stage, known as the drying step or curing process, involves the loss of water and the formation of a covalent bond

(C–O–Si) between the substrate and the siloxane linkage. Silanization of hydroxylated multiwalled carbon nanotubes and its impacts on the properties of polyurethane rigid foam nanocomposites were reported by Yaghoubi and Nihje. The surface functionalization of multiwalled carbon nanotubes was performed by silanization treatment with 3-aminopropyltriethoxysilane (APTS) and dipodal silane (DSi) and the nanocomposites were prepared by a silanized multiwalled carbon nanotube. The results show that the mechanical properties of the silanized nanocomposites were improved. The enhanced mechanical properties were attributed to the presence of strong interfacial interaction between the polyurethane matrix and the nanotubes in polyurethane nanocomposites, which improved Young's moduli and tensile strengths of the nanocomposite [74].

Durairaj et al. reported the electrochemical performance of the functionalized nanocellulose/multiwalled carbon nanotube composites. The composites were produced with functional groups of sulfate, carboxylate, and amino-silane to disperse multiwalled carbon nanotube. The electrochemical studies were carried out on the composite electrodes, and the studies show excellent stability in different electrolytes over a wide range (−0.6–+1 V) of potential difference. By modifying the properties of the constituent nano cellulosic materials, their work offers crucial insights into the development of customizable nanocellulose/carbon nanomaterial hybrid platforms for various electrochemical applications [78].

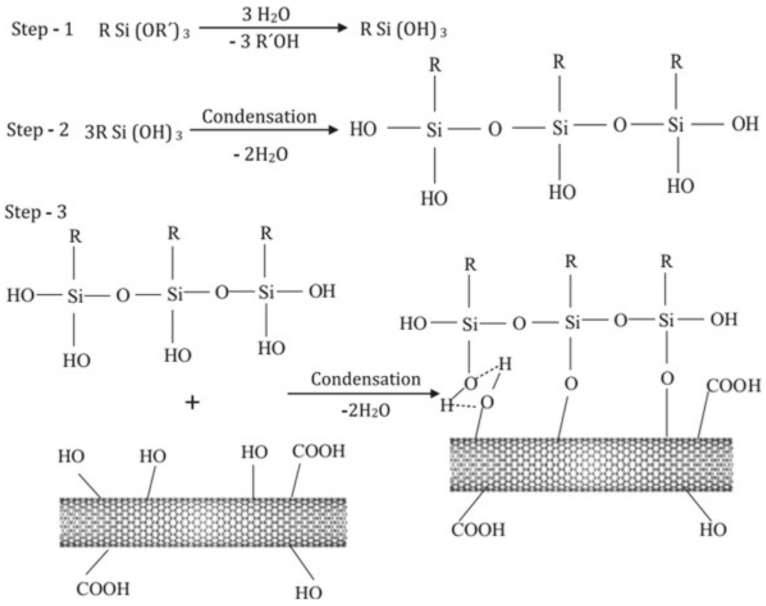

Fig. 3 Graphical representation of silanization method for surface modification of the functionalized CNTs. Reproduced with copyright permission [38]

2.3 Surfactant Adsorption

Surfactant adsorption is a nondestructive approach to tuning the interfacial properties of carbon materials for specific use. The technique of adding surfactants to carbon to boost the capacity of the material to adsorb certain ions results in the creation of surfactant-modified carbon materials [79]. This approach has received considerable consideration in biomedical and polymer composite research than electrochemical applications for the colloidal stabilization of carbon materials via various surfactants [38]. The stable colloidal suspension of carbon materials is achieved using various ionic and nonionic surfactants. These surfactants separate the carbon particles from one another by either electrostatic repulsion or steric hindrance and are adsorbed on the surface of the carbon materials and during sonication for dispersion. Surfactant molecules' repulsion-inducing force outweighs the van der Waals force that interacts with the carbon atoms. To stabilize the colloidal state of CMs, anionic surfactants like sodium dodecyl sulfate (SDS), lithium dodecyl sulfate (LDS), and sodium dodecyl benzene sulfate (SDBS) are frequently utilized, as well as nonionic surfactants like Triton X-100. The structure of surfactant molecules influences the colloidal stability of CMs, and the steady dispersion of CMs is improved by the presence of aromatic rings in surfactant molecules [80, 81]. A surfactant-modified activated carbon from rice husks was reported as an effective adsorbent for Ni(II) and Cr(VI). Sodium lauryl sulfate (SLS) surfactant was used to modify the activated carbon and the amount of the surfactant, contact time, and the optimum condition of the adsorption were investigated. It was observed that the surfactant-activated carbon has a negatively charged and more hydrophilic surface, which enhanced its adsorption efficiency and adsorption ability of the Ni(II) and Cr(VI) [82]. The adsorption studies of both cationic and anionic surfactants, isotherms, and kinetic have been investigated using activated carbon. The Langmuir's isotherms and pseudo-second-order adsorption kinetics with an adsorption rate of 2.23×10^3 g m/g hr^{-1}, were recorded for the employed surfactant (SLS) by activated carbon [83].

2.4 Silylation

Silylation is one of the most widely used surface-functionalization processes. The process of silylating carbon materials involves adding a silyl group to them in order to improve their interfacial adhesion to various polymer matrices or their ability to disperse in a particular solvent. Silylation occurs when oxidative carbon materials react with any silyl moiety in the presence of a base and become associated with a silyl group such as $\text{Si}^{®}{}_3$. To improve the mechanical properties and efficiently transfer mechanical load from polymer to carbon filler, Silanes serve as a coupling agent between carbon material and polymer molecules composites [38]. Various organosilanes have been widely employed for the silylation of carbon materials, such silanes are vinyl triethoxysilane, octadecyltrimethoxysilane, 3-aminopropyl triethoxysilane, and so on [84–86]. There are two common approaches to silylating a surface. The first method involves vaporizing a silane agent at elevated temperatures and exposing the surface to it [87, 88]. The silylation agent must have a high vapor pressure at the operating temperature, which is one of the requirements for this process. According to reports, commercial use of silanes with vapor pressures of greater than 5 torrs at 100 °C has been attained [89–91]. Maintaining the substrate's temperature between 50 and 120 °C during vapor-phase treatment will help the silane agent and substrate react more quickly. In addition to high temperatures, a vacuum can be used to allow the silane agent to vaporize [92]. A fast deposition time of 5 min has been observed for cyclic aza silanes, and a 30-min deposition time has been reported for amino silanes without the use of a catalyst. Longer reaction times of about 4–24 h are needed for other silanes [91]. Consequently, only a few silylation agents can be used with the vapor-phase approach. The second approach is the functionalization from the liquid phase, by applying the liquid solution of the silylation agent to the surface of carbon materials [88, 93–95]. This method is regarded as the energy savings approach because it is frequently used at low temperatures. However, there is frequently no direct interaction between the silylation agent and the surface groups at these low temperatures [96, 97]. As a result, a further curing process is typically used to aid in the interaction between the silane with the substrate surface. The silylation agents may self-polymerize via this indirect approach, preventing them from reacting with the surface groups and decreasing the technique's efficiency. This results in nonuniform surfaces since it is difficult to manage the quantity of silane on the surface [96, 97]. Silylation of pristine single-walled carbon nanotubes was first reported by Hemraj-Benny and Wong in 2006 [98]. The silylation of the single-walled nanotubes was functionalized with trimethoxysilane and hexaphenyldisilane as the silane agents. It was observed from the microscopic studies that the oxidative reaction was nondestructive to the structure of the tube integrity and the chemical attachment of organosilanes on the carbon nanotubes was evidently shown from the spectroscopic studies.

2.5 Amidation

Amidation is another functionalization technique that uses the attachment of nitrogen-containing molecules to oxidize the surface of CMs to improve their solubility with various solvents and in order to enhance polymer composites reinforcement, to be used for various applications. The attachment of nitrogen-containing molecules on the various CMs surfaces has been reported with different techniques [99, 100]. Amidation occurs when oxidized carbon materials react either directly with amine-containing compounds or indirectly with thionyl chloride or a coupling agent. Active carboxyl groups initially interact with thionyl chloride, and this derivative subsequently interacts with other long-chain alkyl amines, such as octadecyl amine (ODA), 4-dodecyl-aniline, 4-$CH_3(CH_2)_{13}C_6H_4NH_2$, and glucosamine [101–105]. In 2015, Mostazo-Lopez et al. reported the functionalization of nitrogen-containing

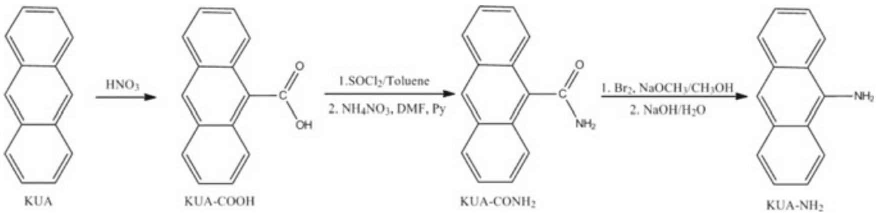

Fig. 4 Chemical modification sequences of the activated carbon for wet oxidation, amidation, and amination processes. Reproduced with copyright permission [106]

activated carbon by amidation processes. A highly microporous activated carbon was oxidized with Nitrogen via three different functionalization methods: wet oxidation, amidation, and amination by Hoffman rearrangement. The amidated activated carbon was investigated for electrochemical performance, and the amidated carbon electrode shows a specific capacitance value of 83 Fg^{-1} at the current density of 50 Ag^{-1}. The recorded excellent surface capacitance and highest capacitance retention for the electrode was attributed to the presence of functional groups that improve their electrical conductivity via electron donating characteristics [106]. The chemical modification sequences of the activated carbon for wet oxidation, amidation, and amination processes were shown in Fig. 4.

2.6 Polymer Grafting

Polymer grafting is another functionalization approach for the modification of carbon materials which involves the grafting of polymer chains onto the surface of pristine or oxidized carbon materials. The surface grafting of polymers onto CMs can be prepared in four different ways. These approaches can be applied to the preparation of polymer-grafted particle and fiber surfaces. The grafting of polymer onto the carbon surface is achievable by the following methodologies, and one of the methods can be employed in the preparation of polymer-grafted carbon materials [53, 107].

(1) Grafting onto process: the deactivation of the living polymer chain ends with functional groups on the particle and fiber surface, as well as the termination of increasing polymer radicals, cations, and anions generated during the polymerization of diverse monomers begun by the conventional initiator in the presence of particle and fiber. Due to the preferential formation of ungrafted polymers in this approach, the grafting percentage onto particles is less than 10%. However, polymers with well-defined molecular weight and limited molecular weight distribution can be grafted onto the particle and fiber surface using living polymer.

(2) Grafting from the process: the application of radical and ionic starting groups to the surface of the particle and fiber to begin the graft polymerization of different monomers. This second process has been regarded as the method with a higher

percentage of grafting and the most favorable approach for polymer-grafted particle and fiber preparation.

(3) Polymer reaction process: the reactivity of surface functional groups on particles and fibers with polymers containing functional groups such as hydroxy, carboxyl, and amino groups. This process is important because of the commercial availability of well-defined structure polymers that can be grafted, as well as the easily controlled number of grafted chains on the particle's surface and fiber.

(4) Stepwise growth process: the grafted polymer chains are created from surface functional groups using the iterative dendrimer synthesizing reaction of low molecular molecules. Furthermore, whereas theoretically structured dendrimers were difficult to graft using this procedure, the surface could be covered with hyperbranched polymers with a lot of terminal functional groups [53].

Other carbon functionalization techniques are Polymer Wrapping and encapsulation methods which falls under noncovalent functionalization approaches. Readers are referred to the book [38], and the references cited therein.

3 Conclusion

This chapter summarized various carbon functionalization techniques that have been reported for electrochemical use. Both the covalent and noncovalent functionalization techniques have been presented in this book chapter. Many of the modification techniques show various degrees of versatility in their usage rather than electrochemical applications. Among the techniques, wet and dry oxidation have been largely reported for electrochemical use, which poses their potential as one of the best modification approaches for the electrochemical application of carbon materials. Meanwhile, the surface modification of carbon materials using the highlighted techniques in this chapter has shown great influence on the enhancement of the electrochemical behavior of the modified carbon materials. Furthermore, the hybridization of two or more techniques for the functionalization was suggested to have a great impact on the carbon materials' capacitive properties in electrochemical applications.

References

1. Kour R, Arya S, Young S-J et al (2020) Review—Recent advances in carbon nanomaterials as electrochemical biosensors. J Electrochem Soc 167:037555. https://doi.org/10.1149/1945-7111/ab6bc4
2. Cetinkaya A, Kaya SI, Ozcelikay G et al (2022) Carbon nanomaterials-based novel hybrid platforms for electrochemical sensor applications in drug analysis. Crit Rev Anal Chem 1–16. https://doi.org/10.1080/10408347.2022.2109125

3. Kharissova OV, Kharisov BI, Oliva González CM (2019) Carbon-carbon allotropic hybrids and composites: synthesis, properties, and applications. Ind Eng Chem Res 58:3921–3948. https://doi.org/10.1021/acs.iecr.8b05857
4. Maduraiveeran G, Jin W (2021) Carbon nanomaterials: synthesis, properties and applications in electrochemical sensors and energy conversion systems. Mater Sci Eng B Solid-State Mater Adv Technol 272:115341. https://doi.org/10.1016/j.mseb.2021.115341
5. Yee MJ, Mubarak NM, Abdullah EC et al (2019) Carbon nanomaterials based films for strain sensing application—A review. Nano-Struct Nano-Objects 18:100312. https://doi.org/10.1016/j.nanoso.2019.100312
6. Bahru R, Shaari N, Mohamed MA (2020) Allotrope carbon materials in thermal interface materials and fuel cell applications: a review. Int J Energy Res 44:2471–2498. https://doi.org/10.1002/er.5077
7. Simon P, Gogotsi Y (2020) Perspectives for electrochemical capacitors and related devices. Nat Mater 19:1151–1163. https://doi.org/10.1038/s41563-020-0747-z
8. Selvaraj AR, Muthusamy A, Inho-Cho et al (2021) Ultrahigh surface area biomass derived 3D hierarchical porous carbon nanosheet electrodes for high energy density supercapacitors. Carbon N Y 174:463–474. https://doi.org/10.1016/j.carbon.2020.12.052
9. Bello IT, Oladipo OA, Adedokun O, Dhlamini MS (2020) Recent advances on the preparation and electrochemical analysis of MoS2-based materials for supercapacitor applications: a mini-review. Mater Today Commun 25:101664. https://doi.org/10.1016/j.mtcomm.2020.101664
10. Bello IT, Adio SA, Oladipo AO et al (2021) Molybdenum sulfide-based supercapacitors: from synthetic, bibliometric, and qualitative perspectives. Int J Energy Res 12665–12692. https://doi.org/10.1002/er.6690
11. Thakur VK, Thakur MK (2016) Chemical functionalization of carbon nanomaterials chemsitry and applications, 1st edn. CRC Press Taylor & Francis Group, Boca Raton, FL, USA
12. Prasanth R, Ammini SK, Ge L et al (2015) Carbon allotropes and fascinated nanostructures: the high-impact engineering materials of the millennium. In: Chemical functionalization of carbon nanomaterials. CRC Press, Taylor & Francis Group, p 26
13. Nezakati T, Tan A, Seifalian AM (2015) Different functionalization methods of carbon-based nanomaterials. In: Chemical functionalization of carbon nanomaterials, 1st edn. CRC Press, Taylor & Francis Group, p 30
14. Kalish R (2007) Diamond as a unique high-tech electronic material: difficulties and prospects. J Phys D Appl Phys 40:6467–6478. https://doi.org/10.1088/0022-3727/40/20/S22
15. Nebel CE, Shin D, Rezek B et al (2007) Diamond and biology. J R Soc Interf 4:439–461. https://doi.org/10.1098/rsif.2006.0196
16. Nebel CE, Kato H, Rezek B et al (2006) Electrochemical properties of undoped hydrogen terminated CVD diamond. Diam Relat Mater 15:264–268. https://doi.org/10.1016/j.diamond.2005.08.012
17. Chung DDL (2002) Review: graphite. J Mater Sci 37:1475–1489. https://doi.org/10.1023/A:1014915307738
18. Speranza G (2019) The role of functionalization in the applications of carbon materials: an overview. C—J Carbon Res 5:84. https://doi.org/10.3390/c5040084
19. Kroto HW, Heath JR, O'Brien SC et al (1985) C60: buckminsterfullerene. Nature 318:162–163
20. Rašović I (2017) Water-soluble fullerenes for medical applications. Mater Sci Technol 33:777–794. https://doi.org/10.1080/02670836.2016.1198114
21. Geim AK, Novoselov KS (2007) The rise of graphene. Nat Mater 183–191. https://doi.org/10.1007/978-3-319-70329-9
22. Lijima S (1991) Helical microtubules of graphitic carbon. Nature 354:56–58
23. Lijima S, Ichihashi T (1993) Single-shell carbon nanotubes of 1-nm diameter. Nature 363:603–605
24. Hiremath N, Mays J, Bhat G (2017) Recent developments in carbon fibers and carbon nanotube-based fibers: a review. Polym Rev 57:339–368. https://doi.org/10.1080/15583724.2016.1169546

25. Galyshev S, Gomzin A, Musin F (2019) Aluminum matrix composite reinforced by carbon fibers. Mater Today Proc 11:281–285. https://doi.org/10.1016/j.matpr.2018.12.144
26. Du J, Zhang H, Geng Y et al (2019) A review on machining of carbon fiber reinforced ceramic matrix composites. Ceram Int 45:18155–18166. https://doi.org/10.1016/j.ceramint.2019.06.112
27. Yao S-S, Jin F-L, Rhee KY et al (2018) Recent advances in carbon-fiber-reinforced thermoplastic composites: a review. Compos Part B Eng 142:241–250. https://doi.org/10.1016/j.compositesb.2017.12.007
28. Saito N, Aoki K, Usui Y et al (2011) Application of carbon fibers to biomaterials: a new era of nano-level control of carbon fibers after 30-years of development. Chem Soc Rev 40:3824–3834. https://doi.org/10.1039/c0cs00120a
29. Kausar A (2018) Contemporary applications of carbon black-filled polymer composites: an overview of essential aspects
30. Kamau GN (1988) Surface preparation of glassy carbon electrodes. Anal Chim Acta 207:1–16. https://doi.org/10.1016/S0003-2670(00)80777-1
31. Sharma S (2018) Glassy carbon: a promising material for microand nanomanufacturing. Materials (Basel) 11. https://doi.org/10.3390/ma11101857
32. Pesin LA (2002) Review: structure and properties of glass-like carbon. J Mater Sci 37:1–28. https://doi.org/10.1023/A:1013100920130
33. Matos I, Bernardo M, Fonseca I (2017) Porous carbon: a versatile material for catalysis. Catal Today 285:194–203. https://doi.org/10.1016/j.cattod.2017.01.039
34. Wang L, Hu X (2018) Recent advances in porous carbon materials for electrochemical energy storage. Chem—An Asian J 13:1518–1529. https://doi.org/10.1002/asia.201800553
35. Li W, Fang R, Xia Y et al (2019) Multiscale porous carbon nanomaterials for applications in advanced rechargeable batteries. Batter Supercaps 2:9–36. https://doi.org/10.1002/batt.201800067
36. Van Dersarl JJ, Mercanzini A, Renaud P (2015) Integration of 2D and 3D thin film glassy carbon electrode arrays for electrochemical dopamine sensing in flexible neuroelectronic implants. Adv Funct Mater 25:78–84. https://doi.org/10.1002/adfm.201402934
37. Silva TA, Zanin H, May PW et al (2014) Electrochemical performance of porous diamond-like carbon electrodes for sensing hormones, neurotransmitters, and endocrine disruptors. ACS Appl Mater Interf 6:21086–21092. https://doi.org/10.1021/am505928j
38. Nayak L, Rahaman M, Giri R (2019) Surface modification/functionalization of carbon materials by different techniques: an overview. In: Carbon-containing polymer composites, Springer Series on Polymer and Composite Materials. Springer Nature Singapore Pte Ltd, pp 65–98
39. Balasubramanian K, Burghard M (2005) Chemically functionalized carbon nanotubes. Small 1:180–192. https://doi.org/10.1002/smll.200400118
40. Hirsch A (2002) Functionalization of single-walled carbon nanotubes. Angew Chemie—Int Ed 41:1853–1859
41. Hirsch A, Vostrowsky O (2005) Functionalization of carbon nanotubes. Top Curr Chem 245:193–237. https://doi.org/10.1007/b98169
42. Nayak L, Khastgir D, Chaki TK (2012) Influence of carbon nanofibers reinforcement on thermal and electrical behavior of polysulfone nanocomposites. Polym Eng Sci 52:2424–2434. https://doi.org/10.1002/pen
43. Nayak L, Khastgir D, Chaki TK (2013) A mechanistic study on electromagnetic shielding effectiveness of polysulfone/carbon nanofibers nanocomposites. J Mater Sci 48:1492–1502. https://doi.org/10.1007/s10853-012-6904-2
44. Jouni M, Fedorko P, Celle C et al (2022) Conductivity vs functionalization in single-walled carbon nanotube films. SN Appl Sci 4. https://doi.org/10.1007/s42452-022-05016-w
45. Burdanova MG, Tsapenko AP, Kharlamova MV et al (2021) A review of the terahertz conductivity and photoconductivity of carbon nanotubes and heteronanotubes. Adv Opt Mater 9:1–29. https://doi.org/10.1002/adom.202101042

46. Kharlamova MV, Kramberger C (2021) Applications of filled single-walled carbon nanotubes: progress, challenges, and perspectives. Nanomaterials 11:1–26. https://doi.org/10.3390/nano11112863
47. Burdanova MG, Katyba GM, Kashtiban R et al (2021) Ultrafast, high modulation depth terahertz modulators based on carbon nanotube thin films. Carbon N Y 173:245–252. https://doi.org/10.1016/j.carbon.2020.11.008
48. Burdanova MG, Tsapenko AP, Satco DA et al (2019) Giant negative Terahertz photoconductivity in controllably doped carbon nanotube networks. ACS Photonics 6:1058–1066. https://doi.org/10.1021/acsphotonics.9b00138
49. Gladush Y, Mkrtchyan AA, Kopylova DS et al (2019) Ionic liquid gated carbon nanotube saturable absorber for switchable pulse generation. Nano Lett 19:5836–5843. https://doi.org/10.1021/acs.nanolett.9b01012
50. Kamran U, Heo YJ, Lee JW, Park SJ (2019) Functionalized carbon materials for electronic devices: a review. Micromachines 10. https://doi.org/10.3390/mi10040234
51. Ulman A (1996) Wetting studies of molecularly engineered surfaces. Thin Solid Films 273:48–53. https://doi.org/10.1016/0040-6090(95)06994-1
52. Iqbal M, Dinh DK, Abbas Q et al (2019) Controlled surface wettability by plasma polymer surface modification. Surfaces 2:349–371. https://doi.org/10.3390/surfaces2020026
53. Tsubokawa N (2002) Functionalization of carbon material by surface grafting of polymers. Bull Chem Soc Jpn 75:2115–2136. https://doi.org/10.1016/0079-6700(92)90021-P
54. Esumi K, Ishigami M, Nakajima A et al (1996) Chemical treatment of carbon nanotubes. Carbon N Y 34:279–281
55. Sahoo NG, Jung YC, Yoo HJ, Cho JW (2006) Effect of functionalized carbon nanotubes on molecular interaction and properties of polyurethane composites. Macromol Chem Phys 207:1773–1780. https://doi.org/10.1002/macp.200600266
56. Wang Y, Wu J, Wei F (2003) A treatment method to give separated multi-walled carbon nanotubes with high purity, high crystallization and a large aspect ratio. Carbon N Y 41:2939–2948. https://doi.org/10.1016/S0008-6223(03)00390-7
57. Wepasnick KA, Smith BA, Schrote KE et al (2011) Surface and structural characterization of multi-walled carbon nanotubes following different oxidative treatments. Carbon N Y 49:24–36. https://doi.org/10.1016/j.carbon.2010.08.034
58. Ziegler KJ, Gu Z, Peng H et al (2005) Controlled oxidative cutting of single-walled carbon nanotubes. J Am Chem Soc 127:1541–1547. https://doi.org/10.1021/ja044537e
59. Bonifazi D, Nacci C, Marega R et al (2006) Microscopic and spectroscopic characterization of paintbrush-like single-walled carbon nanotubes. Nano Lett 6:1408–1414. https://doi.org/10.1021/nl060394d
60. Sánchez-Sánchez A, Suárez-García F, Martínez-Alonso A, Tascón JMD (2013) Surface modification of nanocast ordered mesoporous carbons through a wet oxidation method. Carbon N Y 62:193–203. https://doi.org/10.1016/j.carbon.2013.06.011
61. Moreno-Castilla C, López-Ramón MV, Carrasco-Marín F (2000) Changes in surface chemistry of activated carbons by wet oxidation. Carbon N Y 38:1995–2001. https://doi.org/10.1016/S0008-6223(00)00048-8
62. Berenguer R, Morallón E (2019) Oxidation of different microporous carbons by chemical and electrochemical methods. Front Mater 6:1–14. https://doi.org/10.3389/fmats.2019.00130
63. Michelle CO, Caetano FR, Papi MAP et al (2020) Chemical wet oxidation of carbon nanotubes for electrochemical determination of methyl Parathion. J Anal Chem 75:119–126. https://doi.org/10.1134/S1061934820010128
64. Tanaka S, Fujimoto H, Denayer JFM et al (2015) Surface modification of soft-templated ordered mesoporous carbon for electrochemical supercapacitors. Microporous Mesoporous Mater 217:141–149. https://doi.org/10.1016/j.micromeso.2015.06.017
65. Filimonenkov IS, Urvanov SA, Kazennov NV et al (2023) Wet oxidative functionalization of carbon nanotube cloth to boost its performance as a flexible supercapacitor electrode. Electrochim Acta 437:141501. https://doi.org/10.1016/j.electacta.2022.141501
66. Karl A (2007) Method for producing post treated carbon black 2:1–8

67. Jaramillo J, Álvarez PM, Gómez-Serrano V (2010) Oxidation of activated carbon by dry and wet methods surface chemistry and textural modifications. Fuel Process Technol 91:1768–1775. https://doi.org/10.1016/j.fuproc.2010.07.018
68. Xiao F, Bedane AH, Zhao JX et al (2018) Thermal air oxidation changes surface and adsorptive properties of black carbon (char/biochar). Sci Total Environ 618:276–283. https://doi.org/10.1016/j.scitotenv.2017.11.008
69. Lin C-C, Yen C-C (2007) RF oxygen plasma treatment of activated carbon electrodes for electrochemical capacitors. J Appl Electrochem 37:813–817. https://doi.org/10.1007/s10800-007-9316-2
70. Lota G, Tyczkowski J, Kapica R et al (2010) Carbon materials modified by plasma treatment as electrodes for supercapacitors. J Power Sources 195:7535–7539. https://doi.org/10.1016/j.jpowsour.2009.12.019
71. Pankratova G, Pan JY, Keller SS (2022) Impact of plasma-induced surface chemistry on electrochemical properties of microfabricated pyrolytic carbon electrodes. Electrochim Acta 410:139987. https://doi.org/10.1016/j.electacta.2022.139987
72. Lota G, Tyczkowski J, Makowski P et al (2016) The modified activated carbon treated with a low-temperature iodine plasma used as electrode material for electrochemical capacitors. Mater Lett 175:96–100. https://doi.org/10.1016/j.matlet.2016.04.040
73. Lota G, Krawczyk P, Lota K et al (2016) The application of activated carbon modified by ozone treatment for energy storage. J Solid State Electrochem 20:2857–2864. https://doi.org/10.1007/s10008-016-3293-5
74. Yaghoubi A, Alavi Nikje MM (2018) Silanization of multi-walled carbon nanotubes and the study of its effects on the properties of polyurethane rigid foam nanocomposites. Compos Part A Appl Sci Manuf 109:338–344. https://doi.org/10.1016/j.compositesa.2018.03.028
75. Scheibe B, Borowiak-Palen E, Kalenczuk RJ (2010) Oxidation and reduction of multiwalled carbon nanotubes—preparation and characterization. Mater Charact 61:185–191. https://doi.org/10.1016/j.matchar.2009.11.008
76. Datsyuk V, Kalyva M, Papagelis K et al (2008) Chemical oxidation of multiwalled carbon nanotubes. Carbon N Y 46:833–840. https://doi.org/10.1016/j.carbon.2008.02.012
77. Avilés F, Cauich-Rodríguez JV, Moo-Tah L et al (2009) Evaluation of mild acid oxidation treatments for MWCNT functionalization. Carbon N Y 47:2970–2975. https://doi.org/10.1016/j.carbon.2009.06.044
78. Durairaj V, Li P, Liljeström T et al (2021) Functionalized nanocellulose/multiwalled carbon nanotube composites for electrochemical applications. ACS Appl Nano Mater 4:5842–5853. https://doi.org/10.1021/acsanm.1c00774
79. Mahmoud MR, Sharaf El-Deen GE, Soliman MA (2014) Surfactant-impregnated activated carbon for enhanced adsorptive removal of Ce(IV) radionuclides from aqueous solutions. Ann Nucl Energy 72:134–144. https://doi.org/10.1016/j.anucene.2014.05.006
80. Bonard JM, Stora T, Salvetat JP et al (1997) Purification and size-selection of carbon nanotubes. Adv Mater 9:827–831. https://doi.org/10.1002/adma.19970091014
81. Richard C, Balavoine F, Schultz P et al (2003) Supramolecular self-assembly of lipid derivatives on carbon nanotubes. Science (80-) 300:775–778. https://doi.org/10.1006/jcis.2002.8463
82. Arnelli, Wahyuningrum VN, Fauziah F, Astuti Y (2019) Synthesis of surfactant modified activated carbon (SMAC) from rice husks as Ni(II) and Cr(VI) adsorbent. IOP Conf Ser Mater Sci Eng 509. https://doi.org/10.1088/1757-899X/509/1/012023
83. Arnelli, Aditama WP, Fikriani Z, Astuti Y (2018) Adsorption kinetics of surfactants on activated carbon. IOP Conf Ser Mater Sci Eng 349. https://doi.org/10.1088/1757-899X/349/1/012001
84. Yuen S-M, Ma C-CM, Chiang C-L et al (2008) Poly(vinyltriethoxysilane) Modified MWCNT/polyimide nanocomposites—Preparation, morphological, mechanical, and electrical properties. J Polym Sci Part A Polym Chem 46:803–816. https://doi.org/10.1002/pola

85. Wood W, Kumar S, Zhong WH (2010) Synthesis of organosilane-modified carbon nanofibers and influence of silane coating thickness on the performance of polyethylene nanocomposites. Macromol Mater Eng 295:1125–1135. https://doi.org/10.1002/mame.201000226
86. Lee J-H, Kathi J, Rhee KY, Lee JH (2010) Wear properties of 3-aminopropyl triethoxysilane-functionalized carbon nanotubes reinforced ultra high molecular weight polyethylene nanocomposites. Polym Eng Sci 50:1433–1439. https://doi.org/10.1002/pen
87. Tripp CP, Hair ML (1991) Reaction of chloromethylsilanes with silica: a low-frequency infrared study. Langmuir 7:923–927
88. Soliveri G, Meroni D, Cappelletti G et al (2014) Engineered organic/inorganic hybrids for superhydrophobic coatings by wet and vapour procedures. J Mater Sci 49:2734–2744. https://doi.org/10.1007/s10853-013-7976-3
89. Nájera JJ, Cáceres JO, Ferrero JC, Lane SI (2002) Production of silicon containing particles by laser induced reaction of silane with methane, ethane and acetylene. J Eur Ceram Soc 22:2371–2378. https://doi.org/10.1016/S0955-2219(02)00008-0
90. Fu Y, Hansson J, Liu Y et al (2020) Graphene related materials for thermal management. 2D Mater 7. https://doi.org/10.1088/2053-1583/ab48d9
91. Arkles B (2006) Silane coupling agents: connecting across boundaries, 3rd edn. Gelest Inc., Morrisville, PA
92. Sanli D, Erkey C (2015) Silylation from supercritical carbon dioxide: a powerful technique for modification of surfaces. J Mater Sci 50:7159–7181. https://doi.org/10.1007/s10853-015-9281-9
93. Lipińska ME, Rebelo SLH, Freire C (2014) Iron(III) porphyrin anchored onto organosilylated multiwalled carbon nanotubes as an active catalyst for epoxidation reactions under mild conditions. J Mater Sci 49:1494–1505. https://doi.org/10.1007/s10853-013-7830-7
94. Rao AP, Rao AV, Pajonk GM (2005) Effect of preparation conditions on the physical and hydrophobic properties of two step processed ambient pressure dried silica aerogels. J Mater Sci 40:3481–3489. https://doi.org/10.1007/s10971-005-4662-1
95. Takei T, Yonesaki Y, Kumada N, Kinomura N (2007) Silylation of layered zirconium hydroxy phosphate and its porous properties. J Mater Sci 42:2837–2843. https://doi.org/10.1007/s10853-006-1418-4
96. Tripp CP, Hair ML (1992) Reaction of alkylchlorosilanes with silica at the solid/gas and solid/liquid interface. Langmuir 8:1961–1967
97. Tripp CP, Hair ML (1992) An infrared study of the reaction of octadecyltrichlorosilane with silica. Langmuir 8:1120–1126. https://doi.org/10.1021/la00040a018
98. Hemraj-benny T, Wong SS (2006) Silylation of single-walled carbon nanotubes. Chem Mater 4827–4839
99. Chen J, Hamon MA, Hu H et al (1998) Solution properties of single-walled carbon nanotubes. Science (80-) 282:95–98
100. Li L, Lin R, He H et al (2014) Interaction of amidated single-walled carbon nanotubes with protein by multiple spectroscopic methods. J Lumin 145:125–131. https://doi.org/10.1016/j.jlumin.2013.07.008
101. Xu M, Huang Q, Chen Q et al (2003) Synthesis and characterization of octadecylamine grafted multi-walled carbon nanotubes. Chem Phys Lett 375:598–604. https://doi.org/10.1016/S0009-2614(03)00923-0
102. Pompeo F, Resasco DE (2002) Water solubilization of single-walled carbon nanotubes by functionalization with glucosamine. Nano Lett 2:369–373. https://doi.org/10.1021/nl015680y
103. Liu L, Zhang S, Hu T et al (2002) Solubilized multi-walled carbon nanotubes with broadband optical limiting effect. Chem Phys Lett 359:191–195. https://doi.org/10.1016/S0009-2614(02)00710-8
104. Wu W, Li J, Liu L et al (2002) The photoconductivity of PVK-carbon nanotube blends. Chem Phys Lett 364:196–199. https://doi.org/10.1016/S0009-2614(02)01332-5
105. Hamon MA, Chen J, Hu H et al (1999) Dissolution of single-walled carbon. Adv Mater 55:834–840

106. Mostazo-López MJ, Ruiz-Rosas R, Morallón E, Cazorla-Amorós D (2015) Generation of nitrogen functionalities on activated carbons by amidation reactions and Hofmann rearrangement: chemical and electrochemical characterization. Carbon N Y 91:252–265. https://doi.org/10.1016/j.carbon.2015.04.089
107. Tsubokawa N (1992) Functionalization of carbon black by surface grafting of polymers. Prog Polym Sci 17:417–470. https://doi.org/10.1016/0079-6700(92)90021-P

Всё для победы!
НАРОДНЫЙ ФРОНТ
https://pobeda.onf.ru/
LET'S HELP THE RUSSIA

Chapter 11
Forms of Functionalized Carbon-Based Nanomaterials, Synthesis, Classifications, and Their Electrochemical Activities for Supercapacitors

Moorthi Kanmani, Johnbosco Yesuraj, Kibum Kim, and Mohan Sakar

1 Introduction

The fast utilization of global energy and the non-consistent power supply from renewable sources have sparked the developments in advanced energy storage devices. The presently available energy storage systems for industrial applications are mainly classified under four types, which include (i) chemical, (ii) mechanical, (iii) electrical and (iv) electrochemical energy storage. Among them, a tremendous focus has been devoted to electrochemical energy storage (EES) via electrochemical supercapacitors (SCs) and batteries in powering the portable electronic devices and transportation sectors due to their long cycle life, sustainability, recyclability and easy maintenance [1–3]. A supercapacitor is a modern device for electrochemical energy storage established between 1970 and 1980 to store the electrical energy by polarized electrolyte and these SCs are filling the gap between the typical capacitors and batteries. As illustrated in the Ragone plot (Fig. 1a), supercapacitors occupy a predominant position in terms of improved power density and energy density as compared to many other energy conversion and storage devices. Supercapacitors demonstrate a higher energy density as compared to the traditional capacitors and batteries. The operating principle of SCs is similar to a traditional capacitor, where upon an applied potential difference, the polarized ions in electrolyte move toward the oppositely charged electrode and accumulate on the electrode surface [4].

M. Kanmani · M. Sakar (✉)
Centre for Nano and Material Science, Jain University, Bangalore 562112, Karnataka, India
e-mail: m.sakar@jainuniversity.ac.in

J. Yesuraj · K. Kim
Department of Mechanical Engineering, Chungbuk National University, Cheongju 28644, South Korea

© The Author(s), under exclusive license to Springer Nature Singapore Pte Ltd. 2024

C. M. Hussain and M. B. Ahamed (eds.), *Functionalized Nanomaterials Based Supercapacitor*, Materials Horizons: From Nature to Nanomaterials,
https://doi.org/10.1007/978-981-99-3021-0_11

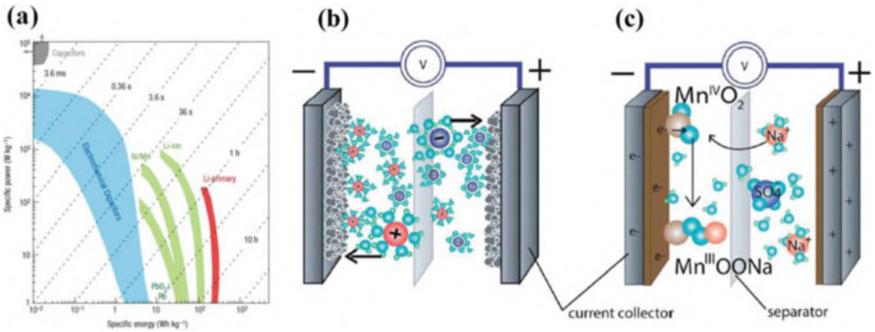

Fig. 1 **a** Ragone plot showing the specific power as a function of specific energy corresponding to various existing energy storage systems [5], **b** and **c** scheme diagram for electrical double layer capacitor and pseudocapacitors [6]

The difference between traditional capacitors and supercapacitors (SCs) is the atomic range charge separation distance and larger interface for electrode and electrolyte interaction. Based on the working principle, SCs can be mainly categorized into (i) electric double layer capacitors (EDLC) and (ii) pseudocapacitors as schematically represented in Fig. 1b, c, respectively. The former stores the charges electrostatically (the establishment of an electric double layer at the interface of electrode–electrolyte, which is a non-faradic process), whereas, the latter stores the charges via the oxidation and reduction reaction at the interface [6, 7]. Still in industries, achieving SCs with improved specific energy without sacrificing their specific power is a great challenge. Also, connecting the low energy density SCs in series or parallel toward enhancing the performance would end up in large-size devices that would not be compact for portable and miniaturized device applications. Numerous works are going on worldwide to enhance the energy density of SCs to make them suitable for real-time applications. The research outputs highlight that the electrodes with larger electro-active surface area for the greater adsorption of polarized electrolyte-ions via the creation of an EDL at the interface of electrode–electrolyte and wider potential window are beneficial in improving the energy density of SCs [8]. In recent years carbon-based nanomaterials (CNMs) are utilized widely in the electrochemical energy-storage application owing to their inexpensiveness, rich availability, excellent electrochemical stability, high active surface area, wider operating potential, and eco-friendly nature. Carbon nanomaterials store charges via electrical double-layer capacitance [9]. When the EDLC-type materials are functionalized with redox species, a contribution from redox species (pseudo capacitance) along with double-layer capacitance leads to an overall improvement in the electrochemical performance and hence results in improved energy and power density in supercapacitors.

2 Classification of Carbon-Based Nanomaterials

The soot and charcoal forms of carbon were discovered in prehistory. Precisely, around two centuries ago, many types of carbon materials such as graphite, diamond and amorphous carbon were found in the organic materials. The carbon atoms have the unique characteristics of forming a strong covalent bond with other carbon atoms in various hybridizations such as sp^3, sp^2, and sp bonding structures. When these carbon atoms are bonded with non-metallic elements, it allows them to form extensive structures ranging from small to long chain molecules [10]. In recent years, the discovery of new carbon materials with interesting properties and possibilities to use them in diverse applications facilitated the growing interest in carbon-based nanomaterials. In 1985, the C_{60} fullerenes were first reported and followed by C_{20} and C_{70} fullerenes were discovered [11, 12]. After six years, in 1991, CNTs were discovered by Iijima [13], which are completely different from fullerenes by size, shape, and properties. The important carbon allotrope, ‘graphene’ was first identified by Boehm et al. through an experiment in the year 1962, and it was first separated and analyzed by Andre Geim and Konstantin Novoselov in 2004. Carbon nanomaterials are mainly categorized into three types based on the nature of covalent bonds between the carbon atoms, topographical properties, and dimensions of nanostructures [14].

According to the covalent bonding that exists between the carbon atoms in a material, they are mainly classified into two types; (i) tightly packed sp^2 hybridized carbon atom in the hexagonal honeycomb lattices known as graphene-based carbon materials which include graphene, graphene flakes, carbon nanotubes, nanohorn, onion-like carbon nanosphere, and (ii) the mixture of sp^2 and sp^3 hybridized carbon, a combination of amorphous and graphitic carbon. Nanodiamonds and carbon dots are members of this family as well. Based on the topographical structures, carbon nanomaterials are divided into two types, carbon nanostructures with internal voids/hollow structures and without internal voids. For instance, the carbon nanotubes, nanohorns and fullerenes are the few carbon nanostructures with internal voids. Graphene, carbon dots and onion-like carbon nanospheres are nanostructures without void space. Finally, the carbon allotropes are classified in the following categories based on their geometry as shown in Fig. 2, which include,

- 0D (zero-dimensional) carbon nanostructures (e.g., fullerenes, carbon dots, nanodiamonds)
- 1D (one-dimensional) carbon nanostructures (e.g., carbon nanotubes)
- 2D (two-dimensional) carbon nanostructures (e.g., graphene, graphene oxide, g-C_3N_4)
- 3D (three-dimensional) carbon nanostructures (e.g., graphite, porous carbon)

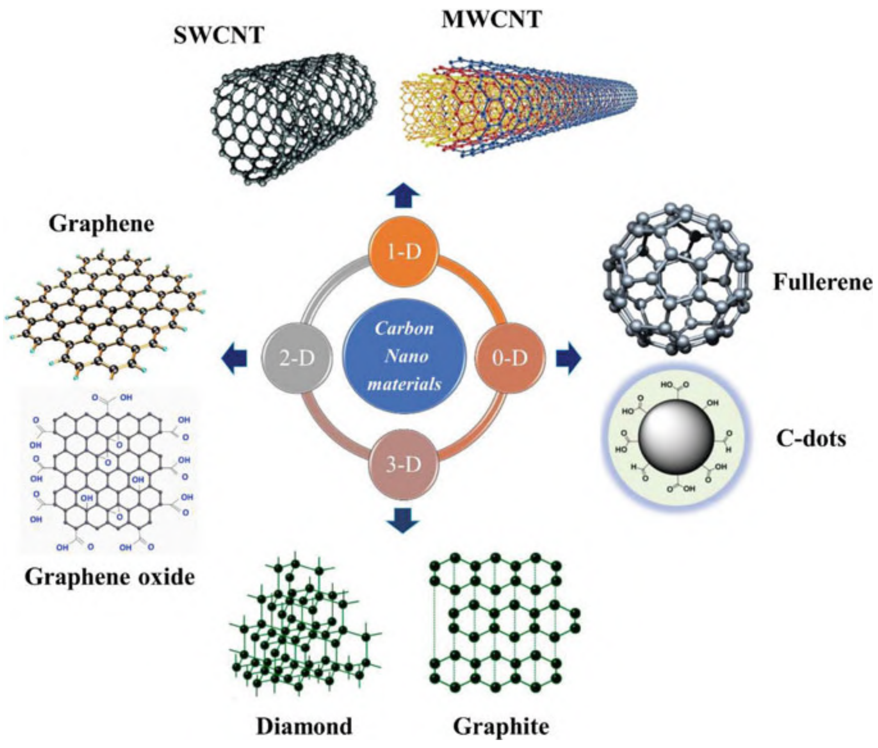

Fig. 2 Classification of carbon nanomaterials based on geometry

3 Synthesis of Carbon Nanomaterials

Theoretically, the 2D-graphene is the structural unit for one of the allotropes of carbon. For instance, 3D graphite is made by stacking monolayers of graphene. Similarly, when a monolayer graphene is properly ripped and wrapped, it leads to the formation of one-dimensional (1D) carbon nanotubes. However, generally, it is not always viable to use graphene layers as a starting material for the synthesis of other allotropes of carbon materials. Apart from this, the naturally available graphite and volatile organic molecules are used to produce graphitic-carbon structures by restructuring the carbon networks using various synthesis techniques. The widely used synthesis techniques include laser ablation process, chemical/physical vapor deposition (P/CVD), plasma discharge, arc discharge, hydrogen decomposition process and high-pressure synthesis.

3.1 Zero-Dimensional Carbon Allotropes

Fullerenes are mainly produced by vaporizing the natural graphite using arc and plasma discharge [11, 15] or by laser ablation methods [16]. Some of the other techniques used to synthesize fullerenes include naphthalene pyrolysis [17] and hydrocarbon combustion [18, 19]. The formation mechanism of fullerenes has been explained by several methods. The first well-known mechanism, which explains the fullerene formation is the ecospiral particle nucleation [16, 20]. In this process, the corannulene-like molecules (one pentagon encircled with five hexagons), considered as starting precursors, get accumulated into small carbon molecules, which further get adsorbed onto the surface of the shells and lead to the formation of nautilus-like open spiral structures followed by edge bypass and the formation of complete C_{60} fullerene unit after the integration of required pentagons. The second one is a shell-closing mechanism. Herein initially, the graphite is vaporized to form smaller carbon chains with a maximum of 10 carbon atoms and gradually grows into the monocyclic rings and subsequent growth of a three-dimensional carbon network with curved shells. Finally, the development of C_{60} molecules occurs due to the closing of shells.

Another mechanism that elucidates the formation of fullerene is the ring stacking model [21]. In this mechanism, the starting precursor C_{10} ring is deformed to produce the molecules consisting of two hexagon units and eight dangling bonds, which are further assembled with C_{18} ring to remove the dangling bonds along with the appearance of new dangling bonds, a sequential decrease of dangling bonds with the stacking of C_{18}, C_{12}, and C_2 molecules, and finally, the reaction ends with the establishment of the C_{60} structure. Another proposed mechanism for the preparation of C_{60} fullerene is thermal annealing of carbon clusters. As per the theory of quantum chemical molecular dynamics (QCMD), the emergence of C_{60} fullerenes follows the "shrinking hot giant road" method [22]. In addition to this, the bottom-up strategy is also used to produce fullerene nanostructures using other precursors such as the smallest subunit of C_{60}-corannulene due to curved π-surface, decacyclene, tribenzodecacyclene, and trinaphtodecacyclene [23].

The Onion like carbon (OLC) structures were created by exposing carbon nanotubes to intense electron beam irradiation, with adjusting the annealing temperature and time adjusted. For example, OLCs with 2–8 graphenic shells and 3–10 nm diameters were produced when the carbon soot was annealed at 2100–2250 °C under a vacuum [24]. Kuznetsov et al. established gram-scale technique for creating OLC structure, which involved temperature treatment of ultrafine-dispersed diamond powders using an electron-beam under high vacuum at temperatures ranging from 1000 to 1500 °C. Similarly, Alexandrou et al. [25] and Sano et al. [26] generated the superior-quality OLC structures with an average diameter of 25–30 nm through an arc discharge reaction between the graphite electrodes submerged in water. Cabioc'h et al. [27] utilized carbon ion implantation into a metal matrix to create OLC structures measuring 10 and 20 nm.

Xu et al. stumbled upon the discovery of carbon dots during the purification of single-wall carbon nanotubes (SWCNTs) through electrophoresis and arc discharge process. Owing to the interesting properties of C-dots, many techniques have been established for synthesizing carbon dots. The most commonly used top-down methodology for creating carbon dots is laser-ablation utilizing a mixture of graphite and cement followed by oxidative acid treatment to enrich the surface functional groups. The electrochemical process is another method to prepare C-dots using graphite electrodes and MWCNT as carbon sources. The C-dots developed using this method possess a uniform distribution of both graphitic and amorphous carbon. Recently, the most widely used techniques include hydrothermal, solvothermal and microwave treatment of small organic molecules, polymers, and carbohydrates. In this, C-dots are formed by condensation polymerization followed by carbonization. In oleylamine-capped synthesis of carbon nanodots (CNDs) via water-in-emulsion method, as illustrated in Fig. 3a, a milky emulsion is formed by the agitation of oil and water. Herein, initially, the water is stabilized by oleylamine and when it is heated to 250 °C, due to the dehydration of carboxylic acids, the polymer-like intermediates are formed. Further, it is carbonized to form CNDs and their TEM pictures are displayed in Fig. 3b, c. Other methods of producing C-dots include the ultrasonic carbonization and pyrolysis [28].

Many methods for preparing graphene-quantum dots (GQD) have been developed using both top-down and bottom-up approaches [31]. GQDs are created by cutting the graphitic carbon structures via the top-down approach. The first method used to develop GQDs by carving graphene structures was high-resolution electron beam lithography. The main challenge in this method was low yield and the requirement of highly specialized instruments. Hydrothermal method using rGO (reduced graphene oxide) as a carbon source was also used to develop the GQDs. In this approach, acid-oxidized rGO was heat treated at around 200 °C. Then the products were separated by dialysis process and as a result GQDs with size around 10 nm were obtained. The formation mechanism of GQDs involved the formation of epoxy and carbonyl groups during the oxidation process followed by the cutting process, which results in the separation of rGO sheets and formation into smaller GQDs. It is observed that the pre-oxidative treatment before the hydrothermal process enhances the oxygen-rich surface-active groups and other precursors like natural graphite, coal etc., were also used to produce the GQDs. In the bottom-up approach, larger aromatic molecules are taken as starting precursor for the synthesis of graphene QDs (GQDs) in which the size distribution of GQDs was found to be effectively controlled by selecting the suitable starting precursors. The schematic representation of synthesis of graphene quantum dots are shown in Fig. 3d.

3.2 One-Dimensional (1D) Carbon Allotropes

There are many well-established techniques available for the development of CNTs such as pulsed laser, arc discharge, and chemical vapor deposition methods [32, 33]. In the arc discharge technique, CNTs are produced between the carbon electrodes

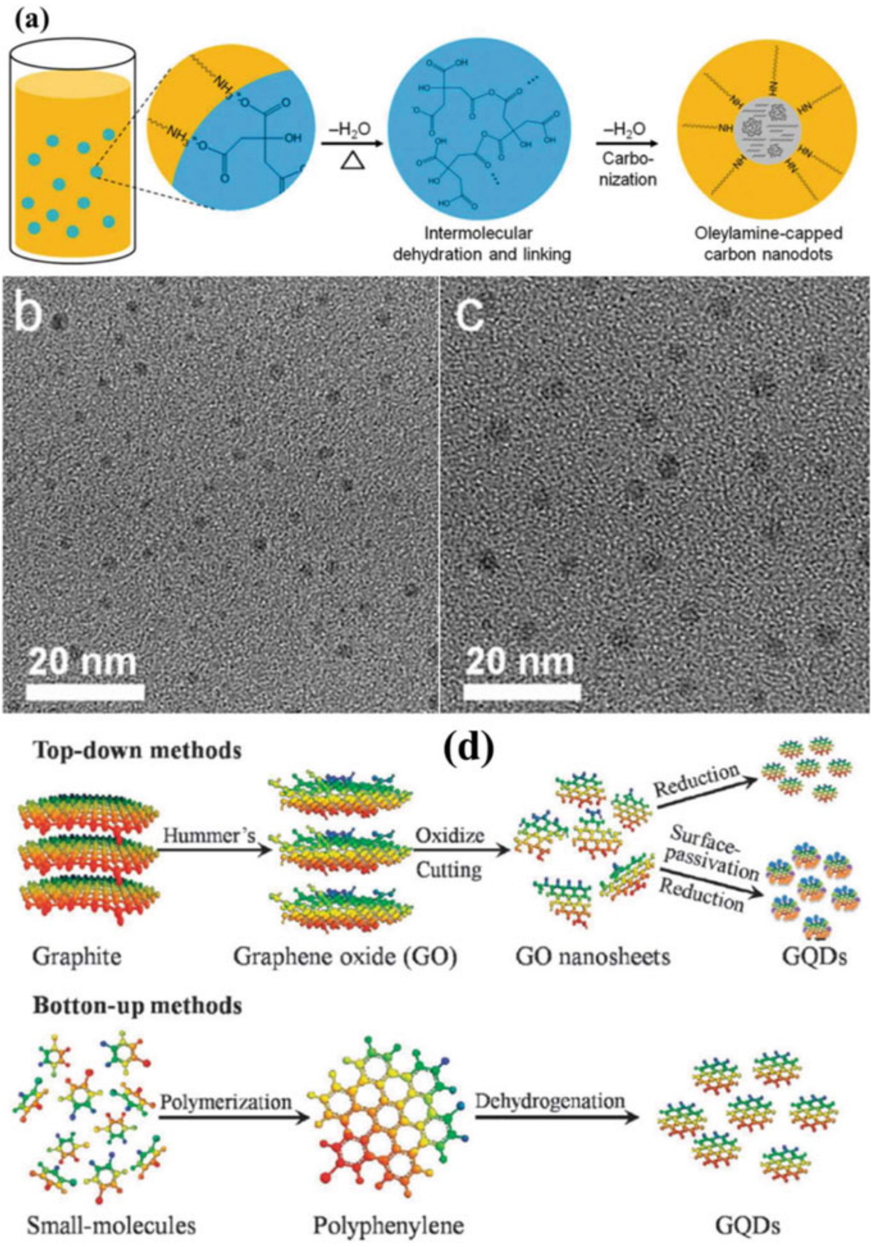
(a)
NH3
NH3
OH
–H2O
△
Intermolecular dehydration and linking
–H2O
Carbo-nization
NH
HN
Oleylamine-capped carbon nanodots
b
c
20 nm
20 nm
Top-down methods
(d)
Hummer's
Oxidize
Cutting
Reduction
Surface-passivation
Reduction
Graphite
Graphene oxide (GO)
GO nanosheets
GQDs
Botton-up methods
Polymerization
Dehydrogenation
Small-molecules
Polyphenylene
GQDs

Fig. 3 **a** Schematic representation of the soft-template mediated synthesis of oleylamine-capped carbon nanodots [29], **b** and **c** corresponding TEM images and **d** representation of GQDs preparation methods [30] in an inert atmosphere chamber. In this method, the type of inert gas and the pressure of the gas determines the yield and quality of the obtained nanotubes. Also, the properties of CNTs are tuned by introducing several unstable organic molecules into the chamber. MWCNTs are produced by arc discharge method without a catalyst. In contrast, the graphite target in the preparation of SWCNTs contained catalytic nanoparticles of metals such as nickel, cobalt, iron, platinum and their alloy structures. CNTs are produced in a pulsed-laser ablation process by ablating the graphite targets in a controlled ambiance. In this case, the target is graphite, which contains the Ni or Co or their mixture to catalyze the process and Nd:YAG or CO_2 is used for ablation. Also, CNTs have been produced by CVD. In this method, initially, the carbon vapors (methane, ethane, ethylene etc.) are splashed on the metal catalyst (Fe, Co, or Ni or alloys of these), and the catalytic nucleation process occurs, finally, it is thermally decomposed to give carbon atoms to generate CNTs. The elemental composition, shape and structure of the nanoparticle, starting precursor used, nature of the substrate, and temperature at which the decomposition occurs all influence the quality, purity, yield, and properties of CNTs produced using this method. The disadvantage of the CVD method is the formation of impurities in the materials. Carbon nanofibers (CNFs) are produced using methods similar to those used to make CNTs such as catalytic CVD and plasma-enhanced CVD. These methods are effective for controlling the size, shape, morphology structure and alignment of CNFs. During the CVD process, first, the precursor molecules (acetylene, ethylene, etc.) are physically adsorbed on top of the metal or metal oxide catalyst surface and disintegrated. In the next step, these adsorbed carbon species diffuse around or through the catalyst after dissolution. Finally, nanofibers are formed by co-precipitation of carbon atoms on the suitable substrate opposite to the target catalyst. The morphology and crystallinity of nanofibers are influenced by the chemical properties of the catalytic metal particles and deposition temperature, and type of the reactant gas. Electrospinning of suitable polymer precursors and additives in a solvent followed by carbonization is another well-known method for the synthesis of CNFs. The widely used polymer precursor materials include PVA, polyacrylonitrile, PVDF, polyimides, polybenzimidazole and phenolic resin. Herein, the CNFs are produced by carbonizing the polymer fibers at around 1000 °C. These electro-spun carbon nanofibers have a thickness in the range of 100–1000 nm.

3.3 Two-Dimensional (2D) Carbon Allotropes

Two-dimensional graphene monolayers can be prepared from liquid exfoliation of graphite using suitable organic solvents such as N-methyl-2-pyrrolidone, pyridine, perfluorinated aromatic solvents, dimethylformamide, and o-dichlorobenzene. Apart from this, graphene layers can be stabilized using surfactant molecules in liquid suspensions. Layered carbon sheets produced in this liquid exfoliation method contain few monolayer graphene sheets along with numerous multilayer graphene sheets. Therefore, segregation of pure monolayer graphene requires some specialized techniques. The obtained products in these methods are almost with no or fewer impurities and the layered carbon sheets are defects-free and of high purity. Graphene sheets have also been produced by reducing graphene oxide (GO). Hummer's method is a well-known method for preparing GO by oxidizing the graphite using some strong oxidizing agent. Due to the oxidative process, the surface-active groups such as carboxyl, hydroxyl and epoxy groups are attached to the layer surface of GO. Further, the exfoliation and reduction of GO produce the graphene nanosheets. Also, annealing in an inert atmosphere is another technique used for the reduction of GO. However, graphene sheets prepared using these methods are defective and of poor quality as compared to pure graphene layers and are denoted as reduced graphene oxide. The CVD and intercalative expansion of graphite few other techniques have also been used for graphene production.

3.4 Three-Dimensional (3D) Carbon Allotropes

3D-porous carbon materials are largely utilized in diverse fields thanks to their ordered porous architecture, high active surface, and easy synthesis procedures. Moreover, the porous walls support the incorporation of organic and inorganic moieties to improve their properties. The most common techniques used for synthesizing ordered porous carbon are soft and hard template methods. In the first method, amphiphilic surfactant and precursor molecules are self-assembled to produce the porous network. Herein, the surfactants are removed by calcination at high temperatures. Hard-template methods, on the other hand, use highly ordered inorganic solid materials like silica and zeolites as frameworks to create the porous framework. Though many inorganic materials are used as hard template, controlling the morphology of the template is important to control the morphology of the ordered porous carbon. Here are a couple of examples for the synthesis of porous carbon via templating method. In 2012, Schuster et al. prepared the spherical ordered mesoporous-carbon (OMC) via a two-step nano-casting method using phenol and formaldehyde mixture precursor and spherical silica as a hard template. Here, the silica template is produced by adding the poly(methyl methacrylate) polymer spheres with SiO_2 solution, and the OMCs are formed by the removal of silica by etching followed by calcination. Li et al. prepared the OMCs by a soft templating method using the Pluronic F127-soft template, a mixture of formaldehyde and resorcinol as carbon precursors, and Fe as a catalyst. In this work, they have adjusted the pore structure by varying carbonization temperature.

4 Functionalization of Carbon Nanomaterials

Carbon-based materials are most commonly used for energy storage applications owing to their enhanced surface area, excellent electrical/ionic conductivity, stability, and easy abundance. However, in order to achieve better electrochemical properties, the properties and structure of these carbon-based materials should be improved further. For example, as-synthesized CNTs tend to aggregate easily and are not soluble in water and organic-based solvents and additionally, the pristine CNTs are difficult to incorporate with other metals and metal oxides [34]. Hence, their applications are limited in many fields. When the redox species or conducting polymers are added to the carbon matrix just by physical mixing, it tends to peel off from the carbon matrix during the long-term charge–discharge process. Also, charge transfer would be lesser and phase separation is likely to occur due to poor contact between the two materials. These factors would affect the electrode performance, therefore to enhance their usage in many different fields, functionalization of the carbon materials with tunable surface properties, physicochemical characteristics and processability are important.

Chemical oxidation could incorporate surface active groups including carbonyl, hydroxyl and carboxylic acids into the matrix of nanocarbon. There are methods available for the covalent and non-covalent functionalization of carbon-based materials. Covalent functionalization modifies the physical properties and structure of carbon nanomaterials. Non-covalent functionalization, on the other hand, involves electrostatic interaction, weak van der Waals interaction, and π-π interactions preserving the structure and physical properties of carbon nanomaterials [35]. For example, the most widely used method toward covalent functionalization of CNTs includes acid oxidation using strong acids (nitric acid or sulfuric acid). In contrast, the physical attachment of polymer and aromatic compounds is involved in the non-covalent functionalization of CNTs. Likely, either sides of graphene basal planes might be functionalized with similar functional groups (symmetrical functionalization) or different functional moieties (asymmetrical functionalization). Apart from adding the functional groups, other carbon materials can also be added to basal planes of the graphene matrix and these carbon composites act as good electron donors or acceptors. Additionally, to chemical functionalization, carbon materials doped with heteroatoms such as nitrogen, boron, sulphur, phosphorus and integrated with metal and metal-oxides, could also produce functionalized carbon nanomaterials.

4.1 Functionalized CNTs for Supercapacitors

Traditionally, the activated carbon and naturally available graphite materials are used as electrodes in energy storage devices. Though it has a high surface area, the usage of activated carbon and graphite materials was hindered due to their low electrolyte accessibility owing to their microporous structures. To enhance the diffusion rate of electrolytes into the electrode, the pore size of the electrodes should be consistent with the electrolyte ion size. Therefore, to attain a higher charge storage with improved energy density, the electrodes should possess suitable pore size and surface-active functional groups to provide a more active site for the adsorption of ions during the charging process. In this regard, carbon materials including CNTs, fullerene and graphene-based materials and functionalized carbon-based materials attracted numerous attention for supercapacitor electrode applications. Yu et al. [36] developed the hybrid electrodes by sequential assembly of acid-oxidized MWCNT with cationic poly(ethyleneimine) attached graphene layers via layering approach. The obtained hybrid electrodes had a well-interconnected carbon network with a specific capacitance of 120 F g^{-1} at a high scan rate of 100 mV s^{-1}. Jiang et al. [37] assembled the asymmetric supercapacitor device based on functional mesoporous CNTs as an anode and birnessite-type MnO_2 with ultrathin porous structure as a cathode in 1 M Na_2SO_4 electrolyte and the achieved specific capacitance of 85.8 F g^{-1} with an enhanced energy- and power-density of 47.4 Wh kg^{-1} and 200 W kg^{-1}, respectively. Moreover, the asymmetric device retained ~90% of its capacitance over 1000 cycles and operated at the maximum potential of 2 V.

Ali and co-workers [38] reported 2,2,6,6-tetramethyl piperidine-1-oxyl (MWCNTs-TEMPO) functionalized MWCNTs. This synthesis process involved two steps, oxidizing the MWCNTs and the creation of amino-TEMPO via an amide bonding. As a result, the developed symmetric device operated at a maximum potential of 2 V and delivered an improved energy density of around 26.6 Wh kg^{-1} and displayed only around 10% loss in the capacitance after 4000 cycles. In another work by Yu et al., they used the in-situ polymerization of MWCNTs to covalently graft PANI onto the MWCNTs via a multi-amino dendrimer (PAMAM) linker and achieved gravimetric capacitance of around 578 F g^{-1} at 0.5 A g^{-1}. Besides, the developed electrodes retained around 70% of its initial capacitance at 10 A g^{-1}, and it demonstrated that the MWCNT-PANI composites outperformed as compared the bare MWCNT and PANI in terms of rate capability, which could be due to the more reactive sites provided by the covalently functionalized PAMAM on MWCNTs (act as template) for the growth PANI during the in-situ polymerization, reduced diffusion path length for electrolyte ion diffusion and complete utilization of redox-active species during the electrochemical process. Furthermore, MWCNT-PANI showed only less than 15% loss after 2000 GCD cycles. Though the specific capacitance was improved by composting PANI with MWCNT, electrochemical stability needed to be improved further to utilize them more effectively. In this context, the poly(benzodithiophenylcarbazole) (PBDTC) was implanted on MWCNTs via the Williamson reaction [39]. The fabricated symmetric device displayed the highest areal capacitance of 5.46 mF cm^{-2} at 0.2 mA cm^{-2} and specific energy of 174.7 Wh kg^{-1}. Furthermore, the device also demonstrated a superior capacitance retention of ~96% over 5000 cycles. However, the multi-step preparation method makes them less efficient in practical use.

Diazonium chemistry was used to create the crosslinked C-CNTs/PANI composite. In the first step, diazonium reactions were used to functionalize the phenylenediamine (PD) onto the CNTs. Following that, coupling was established to introduce 1,4-benzoquinone as a spacer in between the PD-functionalized CNTs. In the final step, aniline monomer was added to the cross-linked CNTs via in situ chemical oxidative polymerization. As a result, the obtained composite demonstrated a specific capacitance of 294.6 F g^{-1} at 10 mV s^{-1} and retained around 95% of its capacitance after 1000 cycles [40]. Besides polymers, the redox-active metal and metal oxides are also introduced in carbon matrix to improve their electrochemical performance. Also, the in-situ growth of electrode material on a conductive carbon substrate is found to improve the connection between the conductive substrate and electrode material, resulting in an improved performance. Du et al. developed a $Ni(OH)_2$-coated alternating layers of graphene-CNT nanopillar electrodes by intercalated development of vertically aligned carbon nanotube (VACNT) into thermally improved the highly ordered pyrolytic graphite (HOPG) structure and electrodeposition of pseudocapacitive $Ni(OH)_2$. The pictorial representation of VACANT-graphene nanostructure is depicted in Fig. 4a. The growth of the 3D pillared VACNT-graphene network involves the following steps as shown in Fig. 4b. The thermal evaporation of acid molecules trapped between the layers expands the interlayer distance, when the HOPG is annealed at 900 °C after acid treatment with a combination of sulfuric acid and nitric acid. Furthermore, the thermally expanded HOPGs are annealed in the presence of $SiCl_4$ at temperatures ranging from 1000 to 1200 °C to facilitate the growth of VACNTs, and the construction of a 3D pillared VACNT-graphene network is accomplished through pyrolysis at 800–1000 °C. The corresponding optical images of HOPG and thermally expanded graphene layers intercalated with VACNTs are depicted in Fig. 4c, d. The developed VACNT-graphene-based electrodes displayed an excellent charge storage with a specific capacitance of 1384 F g^{-1} at a low scan rate of 5 mV s^{-1} and an impressive capacitance retention of around 96% after 20,000 GCD cycles at 21.5 A g^{-1}. The presence of both pseudocapacitive and EDLC charge storage, as well as increased electrical conductivity and stability as a result of the interconnected architecture, is the primary reason for the observed excellent electrochemical performance. Yuan et al. reported hydrothermal in situ growth of Co_3O_4 microspheres on rGO/CNT films with a specific capacitance of 378 F g^{-1} at 2 A g^{-1} current density in 3 M KOH electrolyte.

In 2012, Du et al. developed a MnO_2/CNT-based freestanding symmetric and flexible device with a volumetric capacitance of 5.1 F cm^{-3} at 16 mA cm^{-3} current density and energy density of 0.45 mWh cm^{-3}. In another study, Qiu et al. prepared vertically aligned CNTs/carbon fiber (VACNT/CNF) composites via direct growth of VACNT on the electro-spun CNF followed by calcination. Furthermore, the symmetric supercapacitor device constructed with ionic liquid electrolyte demonstrated an energy density of 70.7 Wh kg^{-1} at 0.5 A g^{-1} current density at 30 °C, while the device operated at 60 °C, it demonstrated a superior energy density of 98.8 Wh kg^{-1} at 1.0 A g^{-1}. As displayed in Fig. 5a–d, the VCNT/CNF hybrid delivered excellent electrochemical performance as compared to bare CNF, which is owing to an enhanced electrical conductivity and electrochemically active surface area.

In 2015, Ma and co-workers developed a transparent and flexible symmetric supercapacitor device using aligned CNTs on polydimethylsiloxane (PDMS) substrates

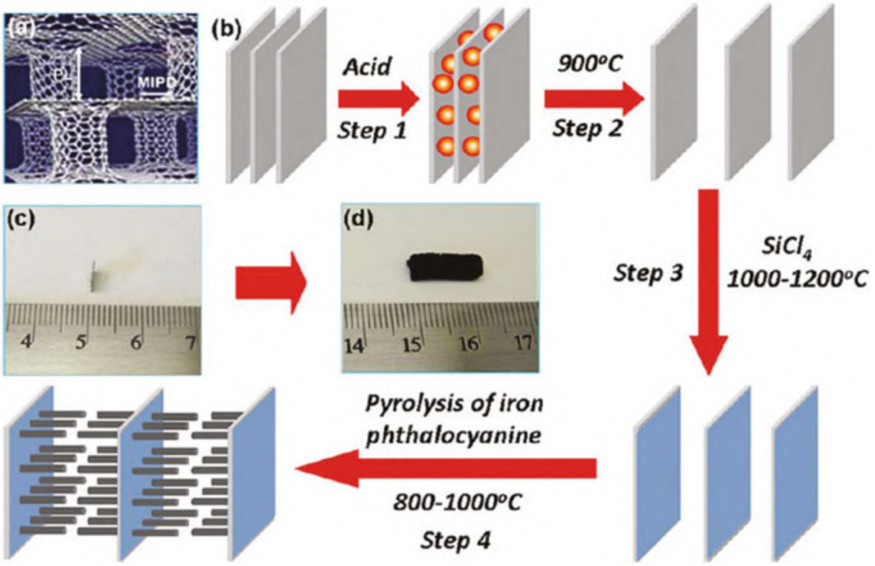
(a)
PD
MIPD
(b)
Acid
Step 1
900°C
Step 2
Step 3
SiCl$_4$
1000-1200°C
(c)
(d)
4
5
6
7
14
15
16
17
Pyrolysis of iron phthalocyanine
800-1000°C
Step 4

Fig. 4 **a** Schematic representation of a 3D pillared VACNT-graphene nanostructure. **b** Schematic diagram of the 3D pillared VACNT-graphene architectures synthesize procedure. Optical images of **c** and **d** HOPG before and after thermal expansion [41]

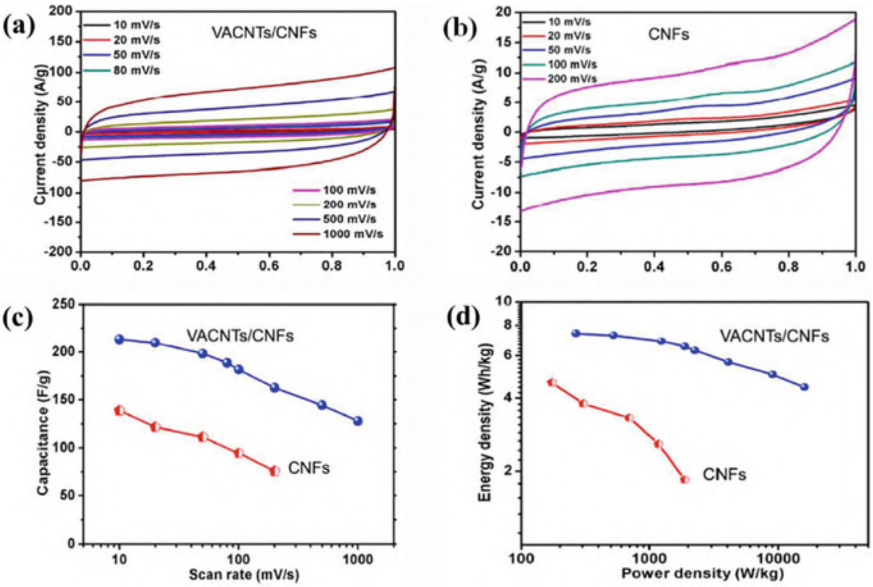

Fig. 5 **a** and **b** Cyclic voltammetry curve of the VACNTs/CNFs composite and bare-CNFs in 1 M NaOH electrolyte and at varying scan rates. **c** Specific capacitance as a function of scan rate of ACNTs/CNFs and CNFs. **d** Ragone plot [42]

as both cathode and anode electrodes in a PVA-H_3PO_4 electrolyte gel. The assembled supercapacitor displayed a specific capacitance of 7.3 F g^{-1} and outstanding electrochemical reliability during the biaxial stretching and bending conditions. Likewise, the fabricated wire-shaped stretchable device using plastic wire-wrapped CNT electrodes and PVA-H_3PO_4 electrolyte displayed a capacitance of 30.7 F g^{-1} and outstanding elastic strain of 350%, indicating excellent device stability (Chen et al. 2014). According to these reports, incorporating redox-active materials into CNTs improves the electrochemical performance and stability by preventing the agglomeration of CNTs.

4.2 Functionalized Graphene-Based Materials for Supercapacitors

Graphene has demonstrated potential for diverse applications owing to its high active surface area, low density, high carrier transfer, and excellent mechanical properties. However, restacking of layered carbon materials is a major challenge. When the spacers are introduced between the layers in terms of functionalization, heteroatom doping, and composite formation, the restacking issue can be reduced. In this regard, there are many detailed reports available [35, 43]. Guan et al. demonstrated the synthesis of needle-like cobalt oxide (Co_3O_4 and CoO) incorporated graphene composite by hydrothermal method and studied their electrochemical behavior in three-electrode system in an alkaline medium and they achieved a specific capacitance of 157.7 F g^{-1} at 0.1 A g^{-1} and 70% cyclic stability after 4000 cycles at 0.2 A g^{-1}. Zheng et al. prepared a cost-effective paper-based supercapacitor by casting the graphite directly on a cellulose paper and achieved a gravimetric capacitance of 23 F g^{-1} in a 1 M H_2SO_4 acid electrolyte. The developed supercapacitor device showed 100% capacitance retention up to 3000 cycles and more than 90% retention after 15,000 cycles. The excellent cyclic stability of the developed electrode was ascribed to the improved electric-conductivity of graphite and suitable pore size of paper substrate facilitating a rapid accessibility of electrolyte ions and weak interaction (van der Waals) between the graphitic layers. In another report, the fabricated wire-like shaped device using vertically aligned CNT hollow fibers on 3D graphene composite electrode and PVA/H_2SO_4 electrolyte displayed an arial and length-wise specific capacitance of 89.4 and 23.9 mF cm^{-1}, respectively. Herein, the porous fabrication of CNT hollow fibers-3D graphene composite was prepared via CVD technique (Xue et al. 2015). Wei et al. synthesized the benzoxazole and benzimidazole covalently implanted on graphene by cyclization process of carboxylic groups on graphene oxide (GO) with hydroxyl and amino functional groups on *o*-aminophenol and *o*-phenylenediamine followed by reduction with hydrazine and employed as an electrode for supercapacitor. The developed benzimidazole grafted graphene (BI-G) showed a higher specific capacitance of 781 F g^{-1} as compared to benzoxazole grafted graphene (BO-G) of 730 F g^{-1} at 0.1 A g^{-1} the current density along with good cyclic consistency. It also showed that the functionalization is not only providing rapid accessibility for ions on the surface of electrode, it also prevents the layered carbon from agglomeration, which intern increased the cycle life of the electrodes. Similar work reported by Md Moniruzzaman Sk and Chee Yoon Yue also supports that the covalent functionalization can effectively prevent the stacking issue in layer carbon materials. In this work, graphene was functionalized with *p*-phenylenediamine through the chemical interaction between amine functional groups of *p*-phenylenediamine and epoxy functional groups on the graphene oxide sheet, the spacers introduced between the layers, which expand the spacing between layers and prevent the stacking. Wu et al. reported covalently grafted 2-aminoanthraquinone on the chemically modified graphene aerogels. As an outcome, the chemically modified GO provided more oxygen functional groups for the covalent bond-mediated grafting of small organic molecules with improved redox properties. The developed electrodes exhibited a 258 F g^{-1} capacitance at 0.3 A g^{-1} current density in a three-electrode system using H_2SO_4 as an electrolyte. The 2-aminopyrene-3,4,9,10-tetraone modified rGO (PYT-NH_2/rGO)-based asymmetric supercapacitor delivered a specific capacitance of 77.2 F g^{-1} at 0.5 A g^{-1} current density along with around 15.4 Wh kg^{-1} energy density. Moreover, the fabricated hybrid supercapacitor device displayed around 100% cyclic stability even after 25,000 continuous charge–discharge cycles at 5 A g^{-1}. The observed excellent electrochemical performance of electrodes was due to the effective redox organic molecules present on the rGO surface and the electron donor–acceptor effect between PYT-NH_2 and rGO. Here, the electron transfer was enabled by amine functional groups of PYT-NH_2 and the function of rGO as an acceptor and the synthesis procedure of PYT-NH_2 and its rGO-based composite (rGO/PYT-NH_2) is shown in Fig. 6, where the established strong interaction between the PYT-NH_2 and rGO led to higher electrochemical stability [44].

Similarly, the covalent functionalized benzobisoxazole-crosslinked graphene networks (BBOGNs) are synthesized via cyclization reaction between the COOH-groups on graphene oxide and OH- and amino groups on 4,6-diaminoresorcinol hydrochloride using polyphosphoric acid as a catalyst and subsequent reduction process [45]. The redox crosslinked graphene exhibited a maximum capacitance of 393.6 F g^{-1} at a current density of 1 A g^{-1} with around 98% of capacitance retention after 9000 cycles. Siang et al. reported chemically grafted sulfur on graphene by thiol-carboxylic acid esterification for supercapacitor electrode and they have obtained a specific capacitance of 1089 F g^{-1} at 1 A g^{-1}. The redox over the thiocarboxylic acid ester and sulphone boosted the super-capacitive performance of the device. Gendy et al. synthesized adenine functionalized graphene sheet and obtained a specific capacitance of 333 F g^{-1} at a scan rate of 1 mV s^{-1}. The addition of adenine to the graphene greatly extended the interlayer distance and prevented the graphene from restacking. Asymmetric supercapacitor devices fabricated using covalently functionalized graphene nanosheets (GNS) based electrodes showed almost no capacitance loss after 10,000 cycles, which may be due to the improved conductivity and low internal resistance for electrolyte ion transportation provided by the covalently grafted functional molecules on graphene. Another

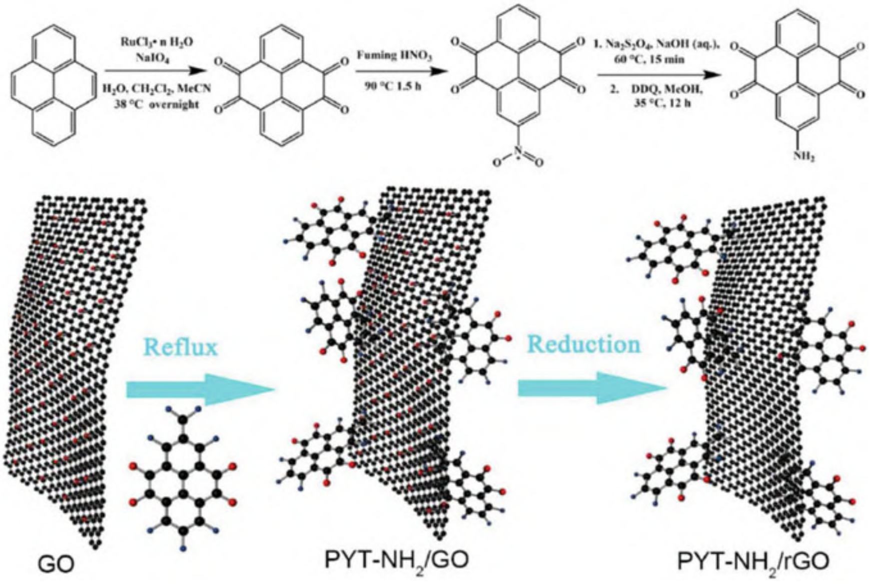

Fig. 6 Schematic diagram of synthesis of 2-aminopyrene-3,4,9,10-tetraone (PYT-NH_2) and its rGO-based (rGO/PYT-NH_2) composite [44]

report on anthraquinone-functionalized graphene showed that covalent functionalization prevents the restacking of graphene layer [46, 47]. The composite based on carboxyl acid-functionalized GO/polyaniline showed good electrochemical performance due to the stable and ordered composite formed via the interaction between carboxyl and amine group of polyaniline system. Moreover, carboxyl groups on edge sites and basal planes of GO offered greater affinity towards the amine groups of polyaniline system as compared to the naturally available oxygen-containing functional groups [48]. Song et al. [49] synthesized covalently functionalized diamine and triamine on graphene sheets and used them as electrodes. The developed electrode delivered around 119 F g^{-1} specific capacitance in ionic liquid medium and displayed less than 10% capacitance loss over 10,000 charge–discharge cycles. The highly reactive amine spacers greatly enhanced the spacing between the layers of graphene sheets and prevented the restacking effect, and thus the electrodes showed better electrochemical stability. The template-mediated low-temperature formation of graphene reported by Yan et al. [50] delivered an excellent volumetric capacitance of 470 F cm^{-3} and retention of 134% after 10,000 cycles. The presence of more oxygen-containing active surface groups on graphene improved the wettability in electrolytes and their pseudocapacitance properties. These reports suggest that the graphene-based systems functionalized with small redox-performing molecules or with polymers greatly improves the electrochemical stability and prevents graphene from restacking.

4.3 Functionalized Fullerene-Based Materials for Supercapacitors

Fullerenes are important zero-dimensional carbon materials. It has been widely used in many fields. Recently, fullerenes attracted considerable attention in energy storage materials thanks to their exclusive spherical molecular structures, adjustable size and shapes at the molecular level [51]. Porous carbon-based material with a higher surface activity can be derived from fullerenes. In 2015, Shrestha et al. reported the nanoporous carbon derived from C_{60} nanotubes and C_{60} nanorods by annealing at 2000 °C and achieved a specific capacitance of 145.5 F g^{-1} at a low-scan rate of 5 mV s^{-1}. Similarly, Bairi et al. synthesized the mesoporous graphitic carbon directly derived from C_{70} by heat treatment at 900 and 2000 °C. The mesoporous carbon derived at 2000 °C (graphitic structure) achieved a better specific capacitance of 21.2 F g^{-1} at 5 mV s^{-1} as compared to the mesoporous carbon derived at 900 °C (amorphous with untransformed) C_{70}. In another work by Bairi and co-workers, 2D carbon micro belts were derived from C_{60} at different temperatures of 900 °C (amorphous) and 2000 °C (graphitic structure). The micro belts derived at 2000 °C delivered a maximum charge storage of 360 F g^{-1} at 5 mV s^{-1}. It is evident that the ordered mesoporous network is advantageous to improve the electrochemical activity of the supercapacitors. In comparison with other carbon materials, the pristine fullerenes delivered relatively less electrochemical performance. In order to enhance their electrochemical activities, many strategies have been proposed to functionalize the fullerenes with redox-active organic molecules such as doping with heteroatoms and introducing pseudocapacitive material on the C_{60} framework. In 2015, Zheng et al. prepared porous carbon materials (FGC600) from C_{70} microtubes using potassium hydroxide as activating agent and thermal and subsequent calcination at 600 °C. The synthesized FGC600 possessed abundant oxygen functional groups with macro and micropores. The developed electrodes achieved excellent energy storage of 362 F g^{-1} at 0.1 A g^{-1} and displayed less than 8% capacitance fading after 5000 cycles. Lu et al. synthesized a hierarchical porous carbon (ANHPC)/MnO_2 composite via hydrothermal method. Herein, they have used C_{60} as a precursor for porous carbon synthesis and obtained excellent specific capacitance of 662 F g^{-1} at 1 A g^{-1} current density with cyclic stability of 93.4% after 5000 cycles. The large specific surface and larger interface provided by the interlaced pore framework of the developed ANHPC/MnO_2 composite contributed to the observed higher capacitance and stability. Zhu et al. demonstrated the synthesis of N-doped porous carbon from C_{60} via KOH activation, which showed a better electrochemical storage of 362 F g^{-1} at 0.1 A g^{-1}. The N-doping and chemical activation caused many defects and porous nanostructure. Notably, here, they used ammonia as a nitrogen precursor. Peng et al. [52] synthesized a cross-linked hierarchical-structured carbon by co-doping the nitrogen (N) and Fe using C_{60} as a carbon precursor via liquid–liquid interfacial precipitation and subsequent calcination at 700 °C. This developed system delivered a maximum charge storage of 505.4 F g^{-1} at 0.1 A g^{-1}. The presence of pseudocapacitive Fe and improved conductivity and electrochemically active surface provided by N-doping led to the observed better electrochemical performance. In 2021, Zhao et al. developed an ordered nano-porous C_{60} via the nano-templating method. Herein, they have used a covalent organic framework as a template due to its suitable pore size for incorporating C_{60} and abundant functional groups on the pore walls. These functional groups chemically interact with C_{60} molecules and maintain the structural stability. Further, the fabricated asymmetric device using ordered nano-porous C_{60} and activated-carbon as cathode and anode electrode, respectively, in a 1 M Na_2SO_4 electrolyte operated at a potential of 1.8 V, delivered an energy density of 21.4 Wh kg^{-1} and 900 W kg^{-1}. Azhagan et al. [53] developed a multilayer fullerene/MnO_2 composite via in-situ incorporation of MnO_2 into the carbon nano-onions matrix and achieved a specific capacitance of 1207 F g^{-1} at a scan rate 1 mV s^{-1}. Likewise, RuO_2/carbon nano-onion composite displayed a specific capacitance of 334 F g^{-1} at 20 mV s^{-1} [54]. These reports manifested that the chemical activation, functionalization, and heteroatom doping are the notable approaches to improve the electrochemical activity of the fullerene-based carbon materials.

4.4 Functionalized Porous-Carbon Material for Supercapacitors

In recent times, micro/mesoporous carbon systems have attracted considerable interest in energy and environmental application because of their facile synthesis methods as compared to other carbon-based materials. Also, various redox-active materials can be incorporated easily on the surface/inside the porous carbon structure. Different strategies are used to create porous carbon such as mesoporous silica-based templates and amphiphilic surfactants to synthesize porous carbon. In this process, the pore size and structure can be tuned by choosing a suitable substrate. The other method includes the metal–organic frameworks (MOFs) as a sacrificial solid template to derive carbon material with porous structures, and the utilization of the naturally available biomass to synthesize the porous carbon materials. Accordingly, 3D-hierarchical porous carbon (THPC) was developed by chemically activating the polypyrrole micro sheets using KOH, which showed a specific capacitance of 318.2 F g^{-1} at 0.5 A g^{-1} current density in a three-electrode system using KOH (6 M) electrolyte. In addition, the performance of THPC electrodes is tested in a symmetric two-electrode configuration using both aqueous 6 M KOH electrolyte and 1 M tetraethylammonium-tetrafluoroborate ($(C_2H_5)_4NBF_4$) in acetonitrile (AN) organic electrolyte. In both the electrolytes, the assembled device showed better electrochemical performance and stability. In this, the improved surface area of THPC (2870 m^2 g^{-1}) together with micro, meso/macro pores provided sufficient interface for the electric double layer formation and facilitated a rapid ion diffusion during the electrochemical process. Moreover, the presence of nitrogen and oxygen species enhanced the electrical conductivity and wettability [55]. In 2015, Long et al. [56] prepared the soybean-derived porous carbon (SBC) by potassium hydroxide activation followed by heating. As a result, these SBC-based electrodes showed a high capacitance of 468 F cm^{-3} at the current density of 0.5 A g^{-1} in 6 M KOH electrolyte with only 9% capacitance loss after 10,000 cycles. Similarly, the electrochemical behavior of a symmetric device assembled using SBC electrode was tested using both base KOH and neutral Na_2SO_4 electrolytes. The device tested in neutral electrolyte operated at the maximum potential of 1.8 V and displayed volumetric specific energy of 28.6 Wh L^{-1}. Likewise, foxtail grass seed-derived porous carbons via chemical activation method delivered a maximum volumetric capacitance of 243.4 F cm^{-1} at 0.5 A g^{-1} in three-electrode system and an assembled symmetric device exhibited a volumetric specific energy of 18.2 Wh L^{-1} with capacitance retention of 91.2% after 10,000 cycles. The porous carbon pyrolyzed at 600 °C showed a good electrochemical performance due to its 3D-interlaced porous structure with honeycomb-like structure and suitable pore size for ion diffusion [57]. In another work, nitrogen-doped porous carbon (NPC) is synthesized using MOFs as a self-sacrificial template. Further, the synthesized porous carbon is functionalized with small redox-active organic molecules such as 1,4-naphthoquinone (NQ), anthraquinone (AQ) and tetrachlorobenzoquinone (TCBQ) to enhance its electrochemical performance. In these systems, the AQ-anchored porous carbon (AQ-NPC) showed electrochemical activity in the negative region and the NQ, TCBQ functionalized porous carbon (TN-NPC) showed redox activity in the positive region; thus, the AQ-NPC was chosen as the negative electrode and TN-NPC was chosen as a cathode for constructing asymmetric device and the performance was tested at a maximum operating potential of 1.4 V using H_2SO_4 as electrolyte. The functionalized NPC showed around 1.5 times higher performance than the bare NPCs, which could be due to the contribution from both pseudo capacitance and EDL capacitance. On the other hand, its symmetric device achieved a specific energy of 23.5 Wh kg^{-1} at a specific power of 700 W kg^{-1} [58]. Hu et al. [59] synthesized the N-doped porous carbon by pyrolyzing agar, potassium citrate and urea at 700 °C under N_2 atmosphere, which showed a surface area of 1300 m^2 g^{-1}. The nitrogen-doped porous carbon-based symmetric device was operated in the potential window of 1.8 V in Na_2SO_4 electrolyte and it achieved a specific energy of 24.1 Wh kg^{-1} with cyclic stability of 90.4% after 10,000 cycles.

In 2019, Sun and co-workers reported the interconnected porous (IPC) carbon derived from direct-carbonization of potassium alginate in the temperature ranging from 700 to 900 °C, which displayed a high-surface area of 1145 m^2 g^{-1} for IPC-800 together with appropriate micro and mesopores for ion diffusion during the electrochemical process. Further, they studied the supercapacitive performance of porous carbon in both three-electrode and two-electrode assemblies using KOH and Na_2SO_4 as electrolytes, respectively. As depicted in Fig. 7a–f, the IPC-800 showed better electrochemical performance in 3-electrode configuration using 6 M KOH electrolyte. The enhanced electrochemical performance of IPC-800 compared to other samples is due to the high electrochemical-active surface along with suitable pore dimensions for the effective accessibility of the electrolyte ions.

Recently, 2,6-diaminoanthraquinone/amino-attached biomass carbon (FWS) derived from wheat straw is reported by Bao et al. and the developed electrodes

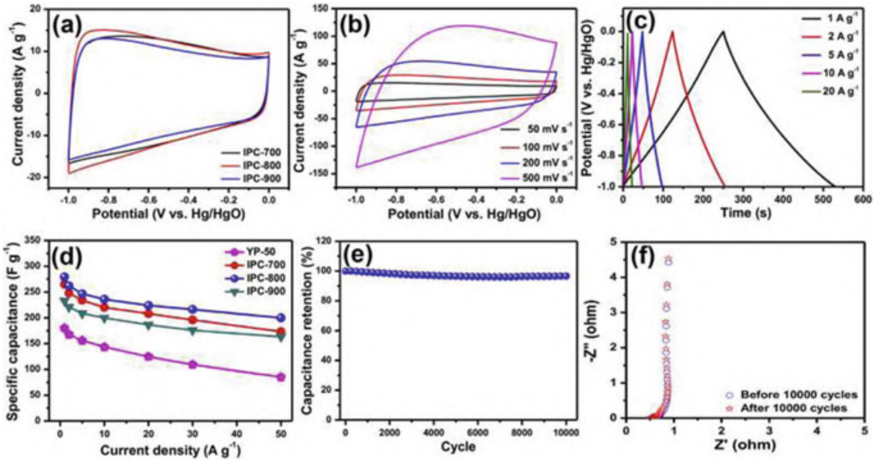

Fig. 7 **a** Cyclic voltammetry curves of IPC-700, IPC-800 and IPC-900 at 50 mV s^{-1}, **b** and **c** CV and GCD curves of IPC-800 at various scan rates and current densities, **d** specific capacitance versus current density plot of YP-50, IPC-700, IPC-800 and IPC-900, **e** cyclic stability graph of IPC-800 at 100 mV s^{-1}. **f** Electrochemical impedance spectra of the IPC-800 electrode before and after 10,000 cycles [60]

delivered a maximum capacitance of 424.9 F g^{-1} at low current density (1 A g^{-1}) and only 6.9% capacitance loss after 10,000 cycles. As illustrated in Fig. 8 the porous carbon is first prepared by KOH chemical activation and subsequent functionalization using ethylenediamine as an N source. Further, hydrothermal method is carried out to anchor the redox active 2,6-diaminoanthraquinone on the carbon framework. Functionalizing with nitrogen-containing functional groups such as amino/imine enhances the adsorption of electrolyte ions on the electrode surface and additionally, the lone pair of electrons in the nitrogen adsorbed some of the positive ions from the electrolyte, and hence the charge storage and potential window of functionalized carbon is found to be increased.

Further, the creation of a strong hydrogen bond between the lone pair electrons of nitrogen and hydrogen/nitrogen atoms in the neighboring molecules enhanced the electrochemical stability by providing strong contact between the electroactive material and conductive substrate. Besides, the incorporation of redox-active DAQ provided additional pseudocapacitance in the device. The assembled symmetric device achieved a specific energy of 36.4 Wh kg^{-1} at a specific power of 700.5 W kg^{-1} and displayed only around 11.7% capacitance loss over 10,000 cycles.

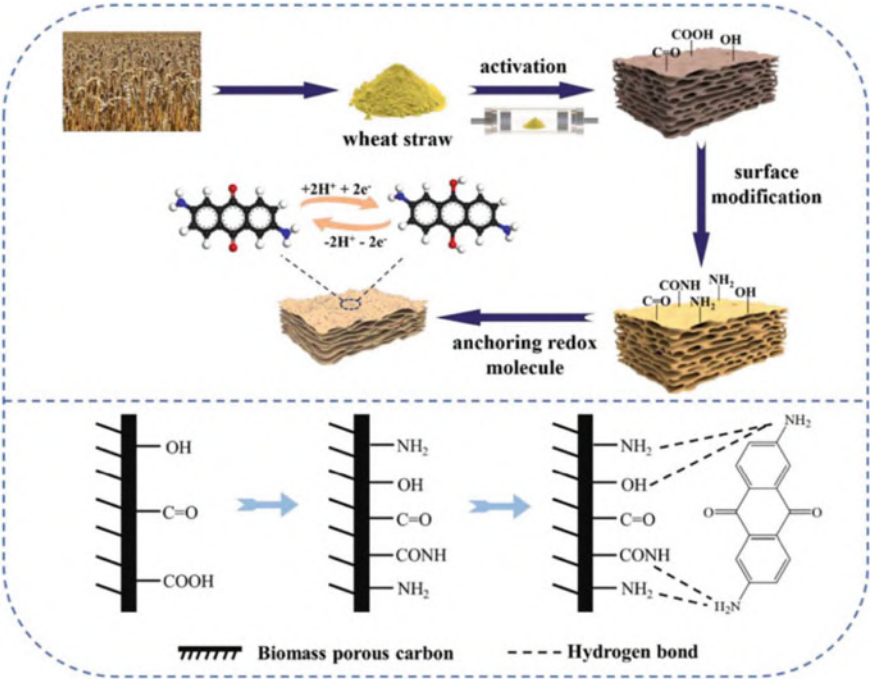
activation
wheat straw
COOH
OH
C=O
surface modification
+2H⁺ + 2e⁻
-2H⁺ - 2e⁻
CONH
NH₂
OH
C=O
NH₂
anchoring redox molecule
OH
C=O
COOH
NH₂
OH
C=O
CONH
NH₂
NH₂
OH
C=O
CONH
NH₂
NH₂
O
O
H₂N
Biomass porous carbon
Hydrogen bond

Fig. 8 The schematic representation of the wheat straw-derived porous carbon and preparation of 2,6-diaminoanthraquinone/amino groups attached biomass carbon (FWS) composites [61]

5 Summary and Outlook

The carbon-based materials are propitious systems for electrochemical supercapacitors thanks to their enhanced capacitance contribution and long cycle life. However, it is difficult to integrate bare-carbon materials with other metals or metal oxides, etc., because of their insolubility and infusibility. Functionalization can open up the channels for composite formation and integration with other materials over host-carbon material by providing more surface-active functional groups. Accordingly, many functionalization methods have been developed to functionalize redox active molecules on the host carbon, among them, the covalent functionalization is more effective as it prevents the leaching of redox-performing small molecules, stabilizing the polymer structure by supporting its growth, and results in better electrochemical stability. Though a lot of reports are available on functionalizing advanced carbon material to improve electrochemical performance, only a few reports are there on traditional carbon such as the activated-charcoal and carbon black. Therefore, to understand better about functionalization mechanism, focus are needed on theoretical combined experimental studies, and also attention should be paid on developing the hybrid-electrodes by combining both traditional and advanced carbon (nano)materials. These are essentially needed to further improve the electrochemical activity of supercapacitors developed using the carbonaceous nanomaterials.

Acknowledgements Authors gratefully acknowledge the Jain University for the fellowship, Department of Science and Technology (DST), Govt. of India for funding through the DST-INSPIRE Faculty Award [DST/INSPIRE/04/2016/002227].

References

1. Huang S, Zhu X, Sarkar S, Zhao Y (2019) Challenges and opportunities for supercapacitors. APL Mater 7:100901. https://doi.org/10.1063/1.5116146
2. Conway BE (1999) Electrochemical supercapacitors: scientific fundamentals and technological. Kluwer
3. Miller JR, Burke AF (2008) Electrochemical capacitors: challenges and opportunities for real-world applications. Electrochem Soc Interface 17:53–57
4. Kotz R, Carlen M (2000) Principles and applications of electrochemical capacitors. Electrochim Acta 45:2483–2498. https://doi.org/10.1016/S0013-4686(00)00354-6
5. Simon P, Gogotsi Y (2008) Materials for electrochemical capacitors. Nat Mater 7:845–854. https://doi.org/10.1038/nmat2297
6. Jost K, Diona G, Gogotsi Y (2014) Textile energy storage in perspective. J Mater Chem A 2:10776. https://doi.org/10.1039/c4ta00203b
7. Service RF (2006) New ‘supercapacitor’ promises to pack more electrical punch. Science 313:902–905. https://doi.org/10.1126/science.313.5789.902
8. Wu Y, Cao C (2018) The way to improve the energy density of supercapacitors: progress and perspective. Sci China Mater 61:1517–1526. https://doi.org/10.1007/s40843-018-9290-y
9. Pandolfo AG, Hollenkamp AF (2006) Carbon properties and their role in supercapacitors. J Power Sources 157:11–27. https://doi.org/10.1016/j.jpowsour.2006.02.065
10. Georgakilas V, Perman JA, Tucek J, Zboril R (2015) Broad family of carbon nanoallotropes: classification, chemistry, and applications of fullerenes, carbon dots, nanotubes, graphene, nanodiamonds, and combined superstructures. Chem Rev 115(11):4744–4822. https://doi.org/10.1021/cr500304f
11. Kroto HW, Heath JR, O’Brien SC, Curl RF, Smalley RE (1985) C60: buckminsterfullerene. Nature 318:162–163
12. Kratschmer W, Lamb LD, Fostiropoulos K, Huffman DR (1990) Solid C60: a new form of carbon. Nature 347:354–358
13. Iijima S (1991) Helical microtubules of graphitic carbon. Nature 354:56–58
14. Belenkov EA, Greshnyakov VA (2013) Classification schemes for carbon phases and nanostructures. New Carbon Mater 28:273–283. https://doi.org/10.1016/S1872-5805(13)60081-5
15. Hare JP, Kroto HW, Taylor R (1991) Preparation and UV/visible spectra of fullerenes C60 and C70. 177:394–398. https://doi.org/10.1016/0009-2614(91)85072-5
16. Kroto HW (1988) Space, stars, C60, and soot. Science 242:1139. https://doi.org/10.1126/science.242.4882.1139
17. Taylor R, Langley GJ, Kroto HW, Walton DRM (1993) Formation of C60 by pyrolysis of naphthalene. Nature 366:728. https://doi.org/10.1038/366728a0
18. Howard JB, McKinnon JT, Makarovsky Y, Lafleur AL, Johnson ME (1991) Fullerenes C60 and C70 in flames. Nature 352:139–141. https://doi.org/10.1038/352139a0
19. Homann K-H (1998) Fullerenes and soot formation—new pathways to large particles in flames. 37:2434–2451. https://doi.org/10.1002/(sici)1521-3773(19981002)37

20. Zhang QL, O'Brien SC, Heath JR, Liu Y, Curl RF, Kroto HW, Smalley RE (1986) Reactivity of large carbon clusters: spheroidal carbon shells and their possible relevance to the formation and morphology of soot. J Phys Chem 90:525. https://doi.org/10.1021/j100276a001
21. Wakabayashi T, Achiba Y (1992) A model for the C60 and C70 growth mechanism. Chem Phys Lett 190:465. https://doi.org/10.1016/0009-2614(92)85174-9
22. Irle S, Zheng G, Wang Z, Morokuma K (2006) The C60 formation puzzle "solved": QM/MD simulations reveal the shrinking hot giant road of the dynamic fullerene self-assembly mechanism. J Phys Chem B 110:14531. https://doi.org/10.1021/jp061173z
23. Scott LT (2004) Cover picture: methods for the chemical synthesis of fullerenes. Angew Chem, Int Ed 43:4994. https://doi.org/10.1002/anie.200490132
24. de Heer WA, Ugarte D (1993) Carbon onions produced by heat treatment of carbon soot and their relation to the interstellar absorption feature. Chem Phys Lett 207:480. https://doi.org/10.1016/0009-2614(93)89033-E
25. Alexandrou, Wang H, Sano N, Amaratunga GAJ (2004) Structure of carbon onions and nanotubes formed by arc in liquids. J Chem Phys 120:1055. https://doi.org/10.1063/1.1629274
26. Sano SN, Wang H, Chhowalla M, Alexandrou I, Amaratunga GAJ (2001) Synthesis of carbon 'onions' in water. Nature 414:506. https://doi.org/10.1038/35107141
27. Cabioc'h T, Jaouen M, Denanot MF, Bechet P (1998) Influence of the implantation parameters on the microstructure of carbon onions produced by carbon ion implantation. Appl Phys Lett 73:3096. https://doi.org/10.1063/1.122684
28. Li H, Kang Z, Liu Y, Lee S-T (2012) Carbon nanodots: synthesis, properties and applications. J Mater Chem 22:24230. https://doi.org/10.1039/C2JM34690G
29. Kwon W, Lee G, Do S, Joo T, Rhee S-W (2014) Size-controlled soft-template synthesis of carbon nanodots toward versatile photoactive materials. Small 10:506–513. https://doi.org/10.1002/smll.201301770
30. Shen J, Zhu Y, Yang X, Li C (2012) Graphene quantum dots: emergent nanolights for bioimaging, sensors, catalysis and photovoltaic devices. Chem Commun 48:3686–3699. https://doi.org/10.1039/C2CC00110A
31. Bacon M, Bradley SJ, Nann T (2014) Graphene quantum dots. Part Part Syst Charact 31:415. https://doi.org/10.1002/ppsc.201300252
32. Prasek J, Drbohlavova J, Chomoucka J, Hubalek J, Jasek O, Adamc V, Kizek R (2011) Methods for carbon nanotubes synthesis—review. J Mater Chem 21:15872. https://doi.org/10.1039/C1JM12254A
33. Journet C, Maser WK, Bernier P, Loiseau A, Lamy de la Chapelle M, Lefrant S, Deniard P, Lee R, Fischer JE (1997) Large-scale production of single-walled carbon nanotubes by the electric-arc technique. Nature 388:756. https://doi.org/10.1038/41972
34. Zhang L, Zhao XS (2009) Carbon-based materials as supercapacitor electrodes. Chem Soc Rev 38:2520–2531. https://doi.org/10.1039/b813846j
35. Wang B, Hua C, Dai L (2016) Functionalized carbon nanotubes and graphene-based materials for energy storage. Chem Commun 52:14350–14360. https://doi.org/10.1039/c6cc05581h
36. Yu D, Dai L (2010) Self-assembled graphene/carbon nanotube hybrid films for supercapacitors. J Phys Chem Lett 1:467–470. https://doi.org/10.1021/jz9003137
37. Jiang H, Li C, Sunb T, Ma J (2012) A green and high energy density asymmetric supercapacitor based on ultrathin MnO_2 nanostructures and functional mesoporous carbon nanotube electrodes. Nanoscale 4:807–812. https://doi.org/10.1039/c1nr11542a
38. Ali GAM, Megiel E, Romański J, Algarni H, Chong KF (2018) A wide potential window symmetric supercapacitor by TEMPO functionalized MWCNTs. J Mol Liq 271:31–39. https://doi.org/10.1016/j.molliq.2018.08.123
39. Yea T, Suna Y, Zhaoa X, Lina B, Yanga H, Zhanga X, Lingxianga G (2018) Long-term-stable, solution-processable, electrochromic carbon nanotubes/polymer composite for smart supercapacitor with wide working potential window. J Mater Chem A 6:18994–19003. https://doi.org/10.1039/C8TA04465A

40. Liu D, Wang X, Deng J, Zhou C, Guo J, Liu P (2015) Crosslinked carbon nanotubes/polyaniline composites as a pseudocapacitive material with high cycling stability. Nanomaterials 5:1034–1047. https://doi.org/10.3390/nano5021034
41. Du F, Yu D, Dai L, Ganguli S, Varshney V, Roy AK (2011) Preparation of tunable 3D pillared carbon nanotube-graphene networks for high-performance capacitance. Chem Mater 23:4810–4816. https://doi.org/10.1021/cm2021214
42. Qiu Y, Li G, Hou Y, Pan Z, Li H, Li W, Liu M, Ye F, Yang X, Zhang Y (2015) Vertically aligned carbon nanotubes on carbon nanofibers: a hierarchical three-dimensional carbon nanostructure for high-energy flexible supercapacitors. Chem Mater 27:1194–1200. https://doi.org/10.1021/cm503784x
43. Khan R, Nishina Y (2021) Covalent functionalization of carbon materials with redox-active organic molecules for energy storage. Nanoscale 13:36. https://doi.org/10.1039/d0nr07500k
44. Shi J, Zhao Z, Wu J, Yu Y, Peng Z, Li B, Liu Y, Kang H, Liu Z (2018) Synthesis of aminopyrene-tetraone-modified reduced graphene oxide as an electrode material for high-performance supercapacitors, ACS Sustainable Chem Eng 6:4729–4738. https://doi.org/10.1021/acssuschemeng.7b03814
45. Ai W, Cao X, Sun Z, Jiang J, Du Z, Xie L, Wang Y, Wang X, Zhang H, Huang W, Yu T (2014) Redox-crosslinked graphene networks with enhanced electrochemical capacitance, J Mater Chem A 2:12924–12930. https://doi.org/10.1039/C4TA01309C
46. Hou L, Hu Z, Wu H, Wang X, Xie Y, Li S, Ma F, Zhu C (2019) 2-Amino-3-chloro-1,4-naphthoquinone-covalent modification of graphene nanosheets for efficient electrochemical energy storage. Dalton Trans 25:9234–9242. https://doi.org/10.1039/C9DT00895K
47. Qin Y, Li J, Jin X, Jiao S. Chen Y, Cai W, Cao R (2020) Anthraquinone-functionalized graphene framework for supercapacitors and lithium batteries, Ceram Int 10:15379–15384. https://doi.org/10.1016/j.ceramint.2020.03.082
48. Liu Y, Deng R, Wang Z, Liu H (2012) Carboxyl-functionalized graphene oxide–polyaniline composite as a promising supercapacitor material. J Mater Chem 22:13619–13624. https://doi.org/10.1039/C2JM32479B
49. Song B, Zhao J, Wang M, Mullavey J, Zhu Y, Geng Z, Chen D, Ding Y, Moon K.s, Liu M, Wong C.P (2017) Systematic study on structural and electronic properties of diamine/triamine functionalized graphene networks for supercapacitor application. Nano Energy 31:183–193. https://doi.org/10.1016/j.nanoen.2016.10.057
50. Yan J, Wang Q, Wei T, Jiang L, Zhang M, Jing X, Fan Z (2014) Template-assisted low temperature synthesis of functionalized graphene for ultrahigh volumetric performance supercapacitors. ACS Nano. 8:4720–4729. https://doi.org/10.1021/nn500497k
51. Xu T, Shen W, Huang W, Lu X (2020) Fullerene micro/nanostructures: controlled synthesis and energy applications. Mater Today Nano 11:100081. https://doi.org/10.1016/j.mtnano.2020.100081
52. Peng Z, Hu Y, Wang J, Liu S, Li C, Jiang Q, Lu J, Zeng X, Peng P, Li F-F (2019) Fullerene-based in situ doping of N and Fe into a 3D cross-like hierarchical carbon composite for high-performance supercapacitors. Adv Energy Mater 1802928. https://doi.org/10.1002/aenm.201802928
53. Azhagan MVK, Vaishampayana MV, Shelke MV (2014) Synthesis and electrochemistry of pseudocapacitive multilayer fullerenes and MnO_2 nanocomposites. Mater Chem A 2:2152. https://doi.org/10.1039/c3ta14076h
54. Borgohain R, Li J, Selegue JP, Cheng YT (2012) Electrochemical study of functionalized carbon nano-onions for high-performance supercapacitor electrodes. J Phys Chem C 116:15068−15075. https://doi.org/10.1021/jp301642s
55. Qie L, Chen W, Xu H, Xiong X, Jiang Y, Zou F, Hu X, Xin Y, Zhang Z, Huang Y(2013) Synthesis of functionalized 3D hierarchical porous carbon for high-performance supercapacitors. Energy Environ Sci 6:2497–2504. https://doi.org/10.1039/C3EE41638K
56. Long C, Jiang L, Wu X, Jiang Y, Yang D, Wang C, Wei T, Fan Z (2015) Facile synthesis of functionalized porous carbon with three-dimensional interconnected pore structure for high volumetric performance supercapacitors. Carbon 93:412–420. https://doi.org/10.1016/j.carbon.2015.05.040

57. Liang X, Liu R, Wu X(2021) Biomass waste derived functionalized hierarchical porous carbon with high gravimetric and volumetric capacitances for supercapacitors. Microporous Mesoporous Mater 310:110659. https://doi.org/10.1016/j.micromeso.2020.110659
58. Guo B, Yang Y, Hu Z, An Y, Zhang Q, Yang X, Wang X, Wu H (2017) Redox-active organic molecules functionalized nitrogen-doped porous carbon derived from metal-organic framework as electrode materials for supercapacitor. Electrochim Acta 223:74–84. https://doi.org/10.1016/j.electacta.2016.12.012
59. Hu X, Wang Y, Ding B, Wu X (2019) A novel way to synthesize nitrogen doped porous carbon materials with high rate performance and energy density for supercapacitors. J Alloys Compd 785:110–116. https://doi.org/10.1016/j.jallcom.2019.01.160
60. Sun S, Ding B, Liu R, Wu X (2019) Facile synthesis of three-dimensional interconnected porous carbon derived from potassium alginate for high performance supercapacitor. J Alloys Compd 803:401–406. https://doi.org/10.1016/j.jallcom.2019.06.212
61. Bao Y, Xu H, Zhu Y, Chen P, Zhang Y, Chen Y (2023) 2,6-diaminoanthraquinone anchored on functionalized biomass porous carbon boosts electrochemical stability for metal-free redox supercapacitor electrode. Electrochim Acta 437:141533. https://doi.org/10.1016/j.electacta.2022.141533
62. Mojica M, Alonso JA, Méndez F (2013) Synthesis of fullerenes. J Phys Org Chem 26:526. https://doi.org/10.1002/poc.3121

Всё для победы!

НАРОДНЫЙ
ФРОНТ

https://pobeda.onf.ru/

LET'S HELP THE RUSSIA

Chapter 12
Functionalization Techniques for the Development of Metal-Oxide/Hydroxide-Based Supercapacitors

R. Balamurugan, S. Siva Shalini, I. Ajin, and A. Chandra Bose

1 Introduction

The need for high power-delivering energy storage devices with high specific energy is rising due to the development of electronic instruments for simplifying lifestyle, electric vehicles for reducing petroleum usage, and grid energy systems for promoting renewable energy resource usage. Various energy storage devices customized to the application needs are being established, such as electrochemical, magnetic, cryogenic, mechanical, chemical, and thermal systems. Among those, flywheels [1–3], superconducting magnetic energy storage (SMES) [4, 5], and supercapacitors provide fast energy delivery. However, flywheels are enormous in size, and SMESs inflict high operational costs. Supercapacitors are the most promising solution for the need of high power-delivering energy storage systems. Supercapacitor provides many advantages like durability, fast charging, high power delivery, and long operational life.

Based on the charge storage mechanism, supercapacitor electrode materials are classified into two categories:

(i) Electric Double Layered (EDL) Capacitive electrode, in which charges are stored by adsorption of electrolytic ions at the surface of the electrode material through electrostatic attraction between them. The electrode materials are made up of high surface area redox inert material. Its storage capacity is limited by the surface of the electrode material. It can deliver high specific power, but its

R. Balamurugan · S. Siva Shalini · I. Ajin · A. Chandra Bose (✉)
Nanomaterials Laboratory, Department of Physics, National Institute of Technology,
Tiruchirappalli 620015, Tamil Nadu, India
e-mail: acbose@nitt.edu

R. Balamurugan
e-mail: r.balamurugan94@gmail.com

© The Author(s), under exclusive license to Springer Nature Singapore Pte Ltd. 2024

C. M. Hussain and M. B. Ahamed (eds.), *Functionalized Nanomaterials Based Supercapacitor*, Materials Horizons: From Nature to Nanomaterials,
https://doi.org/10.1007/978-981-99-3021-0_12

specific energy is lower compared to pseudo-capacitor and battery electrode materials.

(ii) Pseudocapacitive electrode, in which charges are stored by reversible valence change faradaic redox reactions between electrode surface material and electrolytic ions. Due to the faradaic redox reaction, it has high specific energy compared to the EDL Capacitive electrode. Pseudocapacitive electrode materials are mostly metal-oxide/hydroxide-based materials, chalcogenides, and organic polymers [6].

The charge storage capacity of the pseudocapacitive electrode is still needed to be improved for the development of electric machinery and electronic instruments. It can be achievable by different functionalization techniques. This chapter mainly focusses on a complete description of all functionalization techniques for developing metal-oxide/hydroxide-based supercapacitors and a comprehensive report on the recent developments of functionalized metal-oxide/hydroxide-based supercapacitors.

2 Functionalization Techniques

Recently, most of the research on metal oxides/hydroxides for supercapacitors focusing on the design and improvement of electrodes to achieve high specific energy with high power delivery and durability. The storage capacity of the metal-oxide/hydroxide-based electrodes can be enhanced by functionalizing them to improve their properties in three different ways: (i) Intrinsic alteration, (ii) Extrinsic alteration, and (iii) Electrode engineering [7]. The functionalizing techniques in each functionalizing way for metal oxides/hydroxides are shown in Fig. 1.

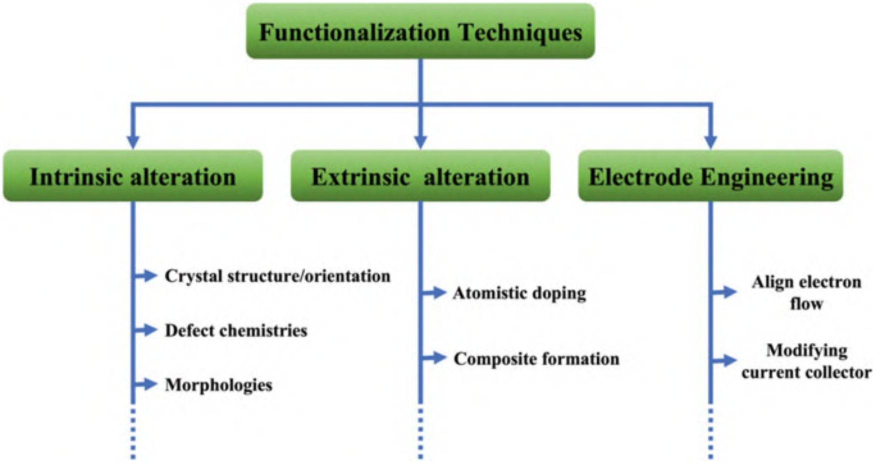
Functionalization Techniques
Intrinsic alteration
Extrinsic alteration
Electrode Engineering
Crystal structure/orientation
Defect chemistries
Morphologies
Atomistic doping
Composite formation
Align electron flow
Modifying current collector

Fig. 1 Different functionalization techniques for metal oxides/hydroxides

2.1 Intrinsic Alteration

Supercapacitor electrode material's charge storage capacity depends upon its intrinsic properties like electrical conductivity, the number of electron transfers during the redox reaction, crystal structure [8–13], and morphology [14–16]. If the material has high electrical conductivity, the electron produced during the redox reaction can easily travel between the current collector and redox-active sites. If a greater number of electrons transfer, then more charges are stored per molecule.

The theoretical specific capacitance ($F\,g^{-1}$) of electrode material can be calculated based on the number of charge transfers during the redox reaction by assuming that charge storage of the electrode is constant throughout the working potential window. It can be calculated using Eq. (1).

$$C = \left(\frac{nF}{m}\right)\frac{X}{E} \tag{1}$$

where n, F, X, m, and E are the number of charge transfers during the redox reactions, the Faraday constant (96,485 $C\,mol^{-1}$), the surface fraction (electrode/electrolyte interface), the molar mass of the electrode material, and the working potential window.

Supercapacitors are surface charge storage devices. Equation (1) demonstrates the high specific surface area of the material corresponding to a high experimental specific capacity. The 2D-layered crystal structures have a high surface area with high electrical conductivity compared to other structures [17–24]. The morphology of the material plays an important role in charge storage. High porous and high surface area lead to a high specific capacity of the material [25–30]. The proper order of pores (Surface of the material containing macropores followed by micropores, then nanopores) in the electrode material exhibits high power delivery [31–37]. The electrode materials are having a low molar mass metal cation incorporated to lower molar molecules advantageous for high gravimetric capacity [38–42].

2.2 Recent Progress in Intrinsic Alteration Techniques

Zhang et al. successfully synthesized hybrid g-C_3N_4/NiAl-layered double hydroxide (LDH) by in situ process followed by reflux method as shown in Fig. 2. Fascinatingly, many hybrid ultrathin LDH nanoflakes originated growing perpendicularly on the surface of g-C_3N_4. The amino comprising groups on the surfaces of g-C_3N_4 nanosheets provide active sites for the NiAl-LDH nanocrystals. The prepared nanocomposites show suitable morphology as well as high specific surface area. By integrating g-C_3N_4, the capacitance of the composite electrode has been enhanced and exhibited, the 714 $F\,g^{-1}$ at a current density of 0.5 $A\,g^{-1}$. The capacitance retention of 82% is maintained even after 10,000 cycles at a current density of 10 $A\,g^{-1}$.

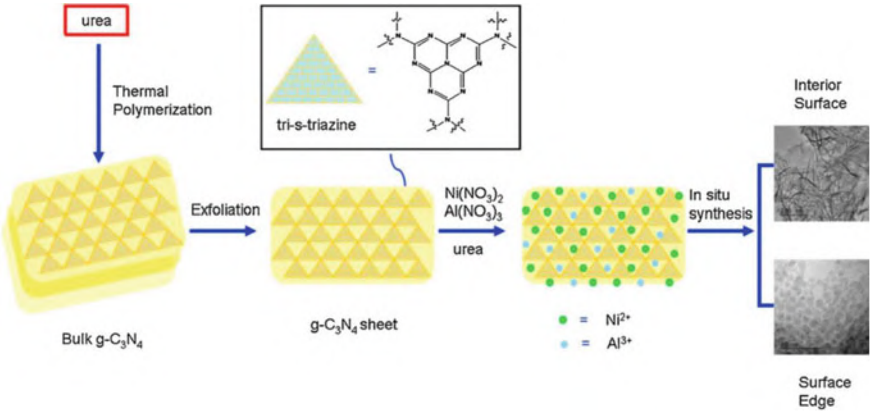

Fig. 2 Schematic representation for in situ growth of NiAl-LDH on the surface of g-C_3N_4 nanosheet. "Reprinted (adapted) with permission from [43] Copyright (2015) Elsevier"

These results indicated that the as-prepared composite electrode possessed promising electrochemical properties [43].

Fu et al. synthesized hierarchical spinel $NiCo_2O_4$ (NCO) nanomaterials with tunable morphologies of rod-like, microsphere-like, flower-like, and nanoparticles via a facile co-precipitation method on the support of various precipitating agents at different calcination temperatures as shown in Fig. 3. It clearly showed that the microstructure and morphology mainly depend on the synthesis environments, which has an impact on their electrocatalytic and electrochemical performance. Compared to nanoflowers and nanorods porous microsphere manufactured with nanoparticles displays outstanding capacitance of 225.07 C g^{-1} at a current density of 0.5 A g^{-1} and high cycle stabilization due to the abundant mesoporous structure and high specific surface area of 123.47 m^2 g^{-1}. Asymmetric supercapacitor device is assembled based on an NCO microsphere electrode as anode and graphene as cathode exhibited an energy density and power density of 19.12 Wh kg^{-1} and 509.87 W kg^{-1}, respectively. These results show that the prepared NCO microsphere electrodes have a wide availability towards supercapacitors [44].

Kumar et al. synthesized $ZnCo_2O_4$ nanomaterial using a hydrothermal technique followed by an annealing procedure through varying the surfactants [urea (UA), ammonium fluoride (AF) and hexamethylenetetramine (HT)] as shown in Fig. 4. A composite surfactant ZC-UAH (Zn–Co-O-urea/ammonium fluoride/hexamethylenetetramine) shows an excellently connected microstructure nanomuscule network developed during the hydrolysis of urea, ammonium fluoride, and hexamethylenetetramine. The mesoporous structures and high specific surface area of the composite ZC-UAH electrode allow the electrolyte ions to diffuse into the electrode material efficiently with low internal resistance and help to buffer volume growth during charge–discharge process. The composite electrode exhibited the highest specific capacity of 462.5 C g^{-1} at a current density of 1 A g^{-1} and excellent capacity retention of 97.4% up to 5000 cycles [45].

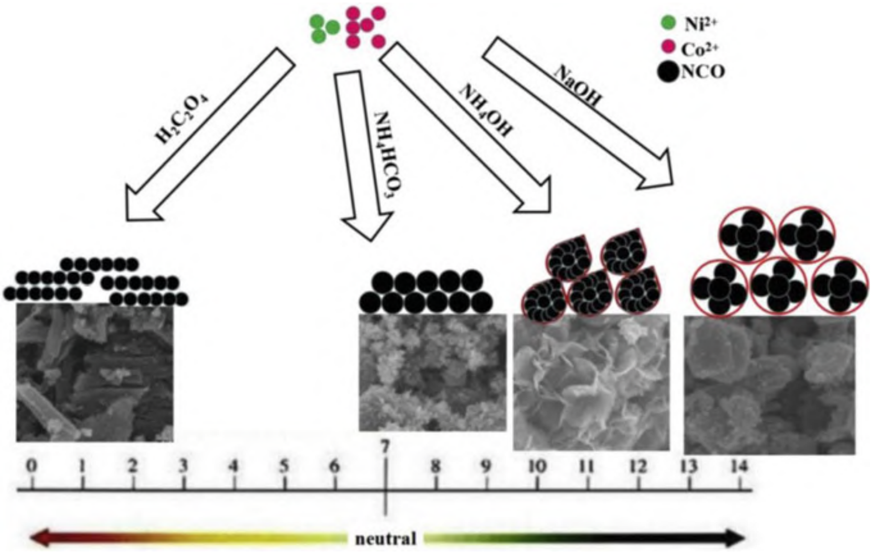
Ni2+
Co2+
NCO
H2C2O4
NH4HCO3
NH4OH
NaOH
0 1 2 3 4 5 6 7 8 9 10 11 12 13 14
neutral

Fig. 3 Schematic representation of the formation process of NCO samples with various precipitating agents. "Reprinted (adapted) with permission from [44] Copyright (2019) Elsevier"

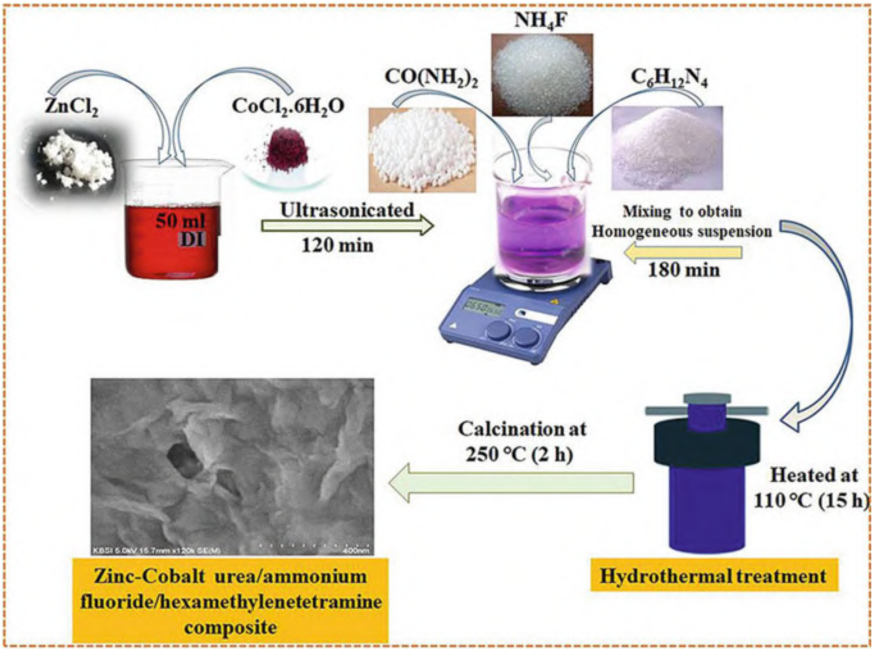
NH4F
CO(NH2)2
C6H12N4
ZnCl2
CoCl2.6H2O
50 ml DI
Ultrasonicated
120 min
Mixing to obtain Homogeneous suspension
180 min
Calcination at 250 °C (2 h)
Heated at 110 °C (15 h)
Zinc-Cobalt urea/ammonium fluoride/hexamethylenetetramine composite
Hydrothermal treatment

Fig. 4 Schematic illustration of the ZC-UAH composite preparation process by a facile hydrothermal process. "Reprinted (adapted) with permission from [45] Copyright (2020) Elsevier"

Liu et al. designed a high-performance cathode material using cooperative modulation of different crystal sites doping as shown in Fig. 5. Generally, Li-rich-layered oxide suffers from inferior cycle stability, poor rate capability, and voltage decay. To improve these disadvantages, in this work co-doping of Na^+ and PO_4^{3-} is made to improve the electrochemical performances. The co-doping of Na^+ and PO_4^{3-} for Li and Mn is achieved instantaneously in $Li_{1.20}Ni_{0.13}Co_{0.13}Mn_{0.54}O_2$ using Na_3PO_4 as a dopant. The co-doping not only improves the electrochemical performance but also reduces the voltage decay. The co-doping of PO_4^{3-} and Na^+ expands the interlayer spacing and suppresses Li/Ni mixing which rises Li^+ diffusivity and improves the rate capability. Co-doping shrinks the thickness and weakens the TM-O (TM = Mn, Ni, Co) covalency, which is further favourable to the structure stability and the enhancement of cycle performance [46].

Qiu et al. co-doped PO_4^{3-} polyanion and Mn^{4+} cation into Ni-rich $LiNi_{0.80}Co_{0.15}Al_{0.05}O_2$ cathode by high-temperature solid phase reaction as shown in Fig. 6 to improve its electrochemical performance and structural stability. In most of the cases, structural degradation during lithiation/delithiation hinders the commercial utilization of cathode material. The moderate content of co-doping PO_4^{3-} and Mn^{4+} can expand the channel for Li^+ lithiation/delithiation, suppressed the structural degradation during the cycles and lowers the cationic mixing. The co-doping strategy enhanced electrochemical reaction kinetics and cycle stability than the pristine cathode [47].

Zhu et al. synthesized α phase trimetal NiCoMn-OH with a flower-like structure and used as the battery material for hybrid supercapacitor device as shown in

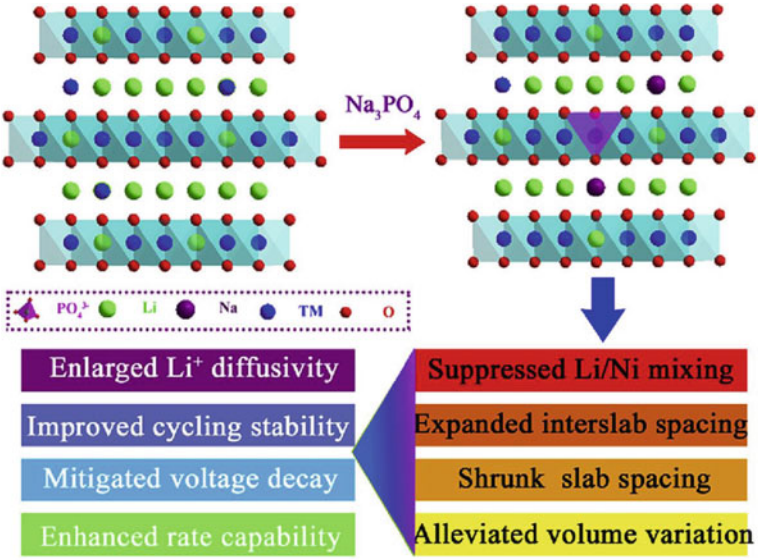
Na₃PO₄
PO₄³⁻
Li
Na
TM
O
Enlarged Li⁺ diffusivity
Improved cycling stability
Mitigated voltage decay
Enhanced rate capability
Suppressed Li/Ni mixing
Expanded interslab spacing
Shrunk slab spacing
Alleviated volume variation

Fig. 5 Schematic illustration of Na^+ and PO_4^{3-} co-doping and advantages. "Reprinted (adapted) with permission from [46] Copyright (2018) Elsevier"

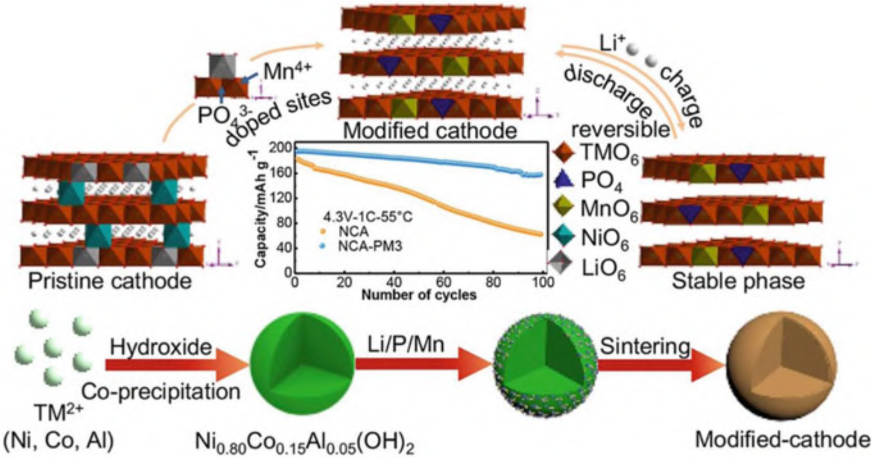
Mn4+
PO43- doped sites
Modified cathode
Li+
discharge
charge
reversible
Pristine cathode
4.3V-1C-55°C
NCA
NCA-PM3
Capacity/mAh g-1
Number of cycles
0
20
40
60
80
100
120
160
200
TMO6
PO4
MnO6
NiO6
LiO6
Stable phase
Hydroxide
Co-precipitation
TM2+
(Ni, Co, Al)
Ni0.80Co0.15Al0.05(OH)2
Li/P/Mn
Sintering
Modified-cathode

Fig. 6 Synthesis of modified material and the corresponding crystal structure. "Reprinted (adapted) with permission from [47] Copyright (2019) Elsevier"

Fig. 7. The trimetal –OH shows strong synergistic electrochemistry between the transitional metals, which exhibits improved charge storage performances. The α phase hydroxide manifests a hydrotalcite-like structure and turbostratic crystal structure and therefore, capable of high active sites. The α phase hydroxide involving two or more metals shows improved electrochemical performance as it can assist as a structural stabilizer to avoid the conversion of α hydroxide to the β hydroxide. NiCoMn-OH electrode exhibits a specific capacity of 757 C g^{-1} at 1 A g^{-1} and retains 369 C g^{-1} at 50 A g^{-1} which is higher compared to bimetal and monometal hydroxides. The fabricated hybrid supercapacitor device (NiCoMn-OH//rGO) exhibits a maximum specific capacity of 219 C g^{-1} at 1 A g^{-1} [48].

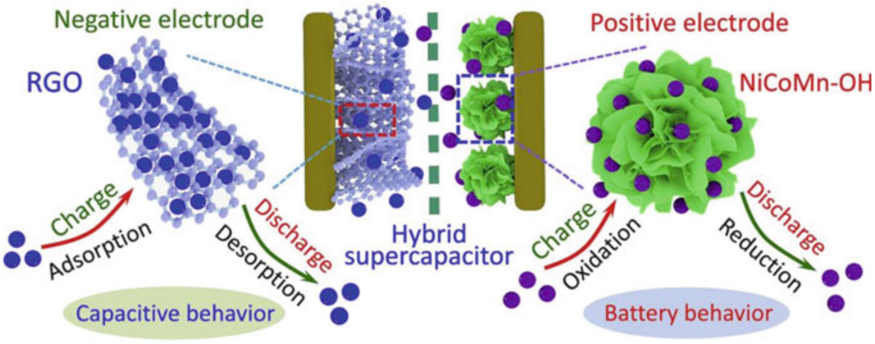
Negative electrode
RGO
Positive electrode
NiCoMn-OH
Charge
Adsorption
Discharge
Desorption
Capacitive behavior
Hybrid supercapacitor
Charge
Oxidation
Discharge
Reduction
Battery behavior

Fig. 7 Structure and charge storage mechanism of phase NiCoMn-OH//rGO hybrid device. "Reprinted (adapted) with permission from [48] Copyright (2019) Elsevier"

Li et al. fabricated highly stable La–Al co-modified $LiNi_{0.8}Co_{0.1}Mn_{0.1}O_2$ cathode by doping La and Al homogeneously in the inner and an epitaxial layer scattered in the outer surface region via wet coating and thermal treatment method as represented in Fig. 8. The doping of Al on hydroxide synthesis ensures uniform substitution of ion helps in enhancing the stabilization role of Al. The sintering of La allows the penetration of the pillar ions into the sphere as well as the construction of La-enriched outer surface. The outer surface region with La rich layer and decreased Ni concentration reduces the side reaction between the organic electrolyte and electrode material which helps to enhance the storage behaviour. The outer surface layer with La_2O_3 coating combined with the bulk phase, not only protects the material from corrosion but also reduces the mismatch between the surface layer and host phase. The modified cathode material achieves enhanced cycling stability and rate capability with 80% of its capacity retention after 480 cycles [49].

Najib et al. synthesized morphology-dependent defective ZnO electrodes for the supercapacitor device ranging from non-faradaic behaviour to faradaic behaviours. The nanoparticles and nanourchins are prepared using urea as the surfactant precursor. The nanoflowers are formed by adding ammonium hydroxide. The defect concentration controls the working principle of the supercapacitor device. The prepared nanoparticles have enough defect centers both on the surface and bulk, such humps rise and create an excess space for charge storage which is responsible for high capacitance values. Due to large quantity of defect concentration, the blocking mechanism of electron transport take place at the interfaces and shows EDLC behaviour. The number of mobile transport defects absorbed within the medium could be greater with improved mobility helped in charge storage capacitive behaviour. Usually, defective metal oxide shows the faradaic charge storage principle once they are used

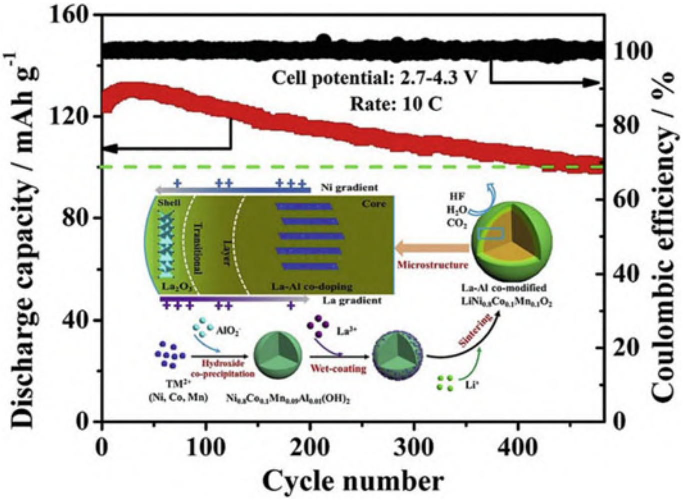

Fig. 8 Synthesis and structure of La and Al co-modified Ni-rich cathode. "Reprinted (adapted) with permission from [49] Copyright (2019) Elsevier"

as supercapacitor electrode. Notably, here, less defect nanourchin samples exhibit EDLC behaviour, and the defect-increased nanoparticles exhibit humps in the CV curve related to faradaic performance (pseudocapacitive behaviour) [50].

Waghmode et al. synthesized flexible $NiCo_2O_4$ nanoflowers with different nanostructures such as nanoflakes, nanoflowers with a surface composed of nanorods on stainless steel by varying the concentration of urea precursor as shown in Fig. 9. In this work, urea plays a significant role in the conversion of nanostructures. $NiCo_2O_4$ nanoflowers with nanorods exhibited the superior specific capacitance of 702 F g^{-1} due to its high electronic conductivity and lower ionic diffusion resistance. Incorporation of a higher concentration of urea during synthesis leads to agglomeration and overgrowth of the $NiCo_2O_4$ nanoflowers which worsens its capacitive performance. The two flexible symmetric devices are fabricated using two different gel electrolytes namely PVA/KOH and PVA/$LiClO_4$. The symmetric device performed using PVA/$LiClO_4$ exhibited the maximum specific capacitance of 132 F g^{-1} with an energy density of 18.52 Wh kg^{-1} and power density of 3.13 kW kg^{-1} [51].

Liu et al. studied the effect of doping fluorine and oxygen vacancies on electrochemical performance of Co_2MnO_4 (F-Co_2MnO_{4-x}) nanowires grown on carbon fibre (CF) as the latest electrode material for supercapacitor. Schematic illustration of the device configuration is shown in Fig. 10. The electronic and structural properties in F-Co_2MnO_{4-x} are effectively tuned by oxygen vacancies and F dopants, synergistically increasing electrical conductivity and providing rich Faradaic redox chemistry. The F anions derived from the reactant NH_4F during the synthesis are inserted as interlayer anions between positively charged host layers of Co–Mn LDHs for charge balance. Then, F-Co_2MnO_4 is obtained by annealing Co–Mn LDH in air at 350 °C

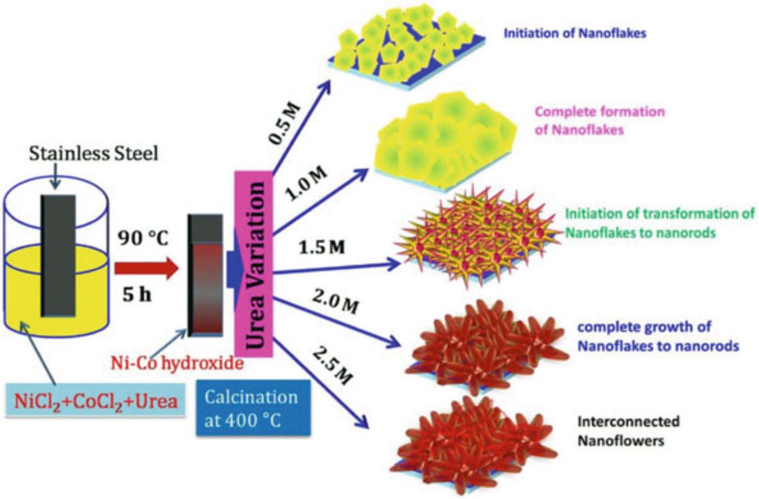
Stainless Steel
90 °C
5 h
Ni-Co hydroxide
NiCl₂+CoCl₂+Urea
Calcination at 400 °C
Urea Variation
0.5M
1.0M
1.5M
2.0M
2.5M
Initiation of Nanoflakes
Complete formation of Nanoflakes
Initiation of transformation of Nanoflakes to nanorods
complete growth of Nanoflakes to nanorods
Interconnected Nanoflowers

Fig. 9 Growth mechanism of $NiCo_2O_4$ nanostructure prepared at different concentration of urea (0.5, 1, 1.5, 2 and 2.5 M). "Reprinted (adapted) with permission from [51] Copyright (2020) Elsevier"

for 2 h, in which partial O sites are substituted by F dopants. The simultaneous introduction of F dopant and O vacancies to F-Co_2MnO_{4-x} results in newly formed energy levels and increases the reactivity of electrochemically active sites, thereby significantly improving the electrochemical performance. The integrated design of nanowires anchored on a conductive substrate not only provides fast charge transport but also avoids the inclusion of conductive additives and binding agents. With unique structural and good electrical conductivity, the resultant F-Co_2MnO_{4-x}/CF electrode exhibits a high specific capacity of 269 mA h g^{-1} at a current density of 1 A g^{-1}. The fabricated asymmetric device comprising of F-Co_2MnO_{4-x}/CF and Fe_2O_3/CF electrodes exhibits the maximum energy density of 64.4 Wh kg^{-1} at a power density of 800 W kg^{-1} and capacitance retention of 89.9% at 10 mV s^{-1} even after 2000 cycles with a bending angle ranging from 0 to 30° [52].

Zhu et al. synthesized iron oxide nanostructure via a facile solvothermal method using the mixture solvent of glycerol and water. The morphology of the samples evolved from microsphere α-Fe_2O_3 to button-like α-Fe_2O_3 as shown in Fig. 11. The spherical Fe_3O_4 nanoparticles transformed to rod-like Fe-glycerate upon raising the ratio of glycerol in the solvent. Glycerol plays a vital role in the system as a solvent at lower concentration, ligand at high concentration, and reducing agent at medium concentrations. The possible reaction mechanism takes place during solvothermal condition by adjusting the reaction medium. The electrochemical performances of

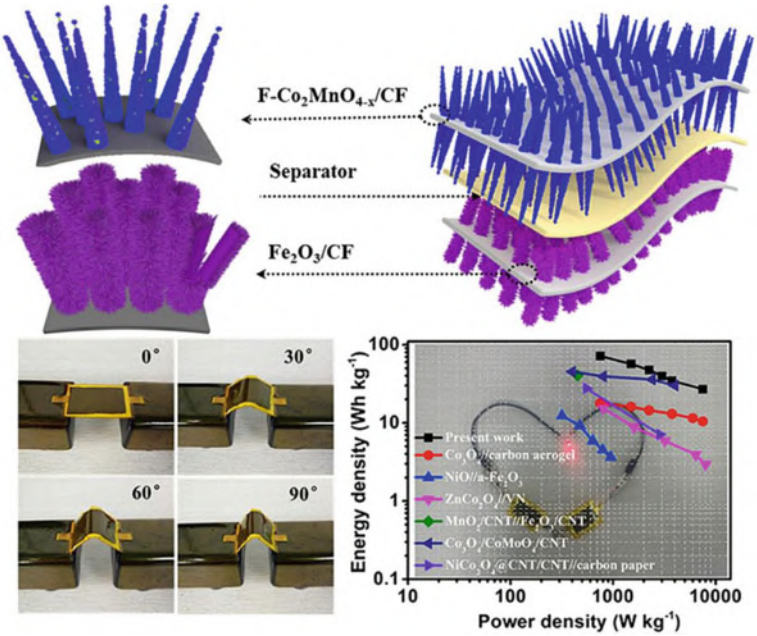
F-Co₂MnO₄₋ₓ/CF
Separator
Fe₂O₃/CF
0°
30°
60°
90°
Energy density (Wh kg⁻¹)
100
10
1
0.1
10
100
1000
10000
Power density (W kg⁻¹)
Present work
Co₃O₄//carbon aerogel
NiO//a-Fe₂O₃
ZnCo₂O₄//VN
MnO₂/CNT//Fe₂O₃/CNT
Co₃O₄/CoMoO₄/CNT
NiCo₂O₄@CNT/CNT//carbon paper

Fig. 10 Schematic representation of the structural configuration of the device F-Co_2MnO_{4-x}/CF//Fe_2O_3/CF ASC. "Reprinted (adapted) with permission from [52] Copyright (2019) Elsevier"

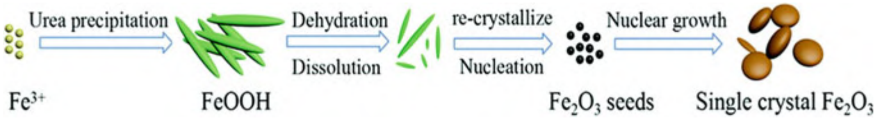

Fig. 11 Schematic representation of the formation of button like α-Fe_2O_3. "Reprinted (adapted) with permission from [53] Copyright (2021) Royal Society of Chemistry"

ultrafine Fe_3O_4 nanoparticles exhibit a high specific capacitance of (426.4 F g^{-1}) which was superior to Fe-glycerate nanorod (196 F g^{-1}) and button like α-Fe_2O_3 (72 F g^{-1}). Fe_3O_4 sample exhibits good cycling performance of 79.5% of the initial capacitance retention even after 5000 cycles, which is superior over other reported iron-based supercapacitors [53].

Pakulski et al. synthesized novel nanostructured electrode material for the enhancement of electrochemical performance towards energy storage applications. The hybrid structure based on Keplerate type polyoxometalate (Mo_{132}) functionalized with dodecyltrimethylammonium bromide (DTAB), mixing with electrochemically exfoliated graphene (EEG) nanosheet results in the formation of 3D porous superstructures. The formation of hybrid electrode material Mo_{132}-DTAB-EEG includes the redox activity of Mo_{132} and high electrical conductivity of graphene all synergically mediated by surfactant to form 3D porous architecture serves as a new electrode material for supercapacitors. Surfactant DTAB is not only increased the strength of van der Waals interaction between the Mo_{132} and EEG also resulted an increased porosity which enhanced super capacitive performance of the hybrid electrode material. The formation of Mo_{132}-DTAB-EEG is shown in Fig. 12, exhibited the maximum specific capacitance of 65 F g^{-1} with capacitance retention of 99% even after 5000 charge/discharge cycles [54].

Many research groups work on tuning the morphology of the material to achieve high surface area which plays a significant role in energy storage applications. For tunning the morphology, researchers use various structure-directing agents such as polyethylene glycol [55] sodium dodecylbenzene sulfonate [56–62], polyvinyl

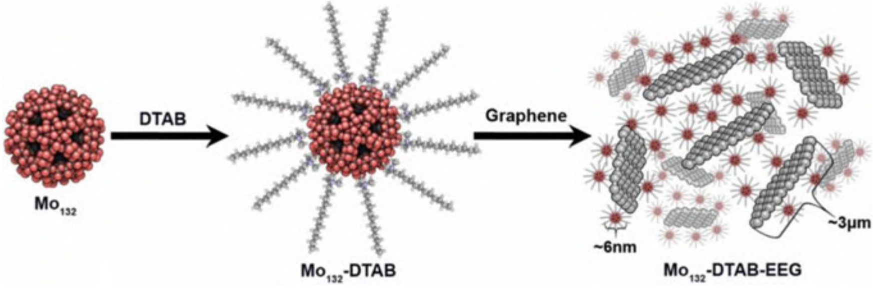

Fig. 12 Schematic illustration of the formation of hybrid electrode material. "Reprinted (adapted) with permission from [54] Copyright (2019) Elsevier"

pyrrolidone [63, 64], sodium lauryl sulfate [56], oleylamine [65], tetrapropylammonium hydroxide [66], cetyltrimethylammonium bromide, hexamethylenetetramines [58], etc. The synthesis routes followed for achieving unique morphologies are sol–gel, co-precipitation, solvothermal, hydrothermal, microwave techniques, electrodeposition method etc. The advantages of structure directing agents not only tune the morphology, it achieves high surface area and many exposed active sites. The surfactant-assisted electrode material accomplishes high specific capacitance, energy density (Ed), power density (Pd), and excellent cycling stability compared to pristine samples.

2.3 Extrinsic Alteration

Using intrinsic alteration, the electrode material's electrical conductivity, specific surface area, and redox activities can be improved up to a certain level. But, to achieve high specific capacity, extrinsic alteration enhances surface activity, chemical potential, and electrical conductivity. The atomic doping [67–71] and composite formation [72–76] modify the electronic structure, electrical conductivity, charge carrier concentration, and phases, which will lead to superior electrochemical activity.

2.4 Recent Progress in Extrinsic Alteration Techniques

Haghshenas et al. synthesized metal-spinel core–shell nanocomposite ($CoFe_2O_4$@MC) as a positive electrode using chemical deposition method for asymmetric supercapacitors. The $CoFe_2O_4$ nanomaterial exhibited a porous structure by incorporating methylcellulose carbohydrate polymer (MC). In the absence of MC, the agglomeration of $CoFe_2O_4$ takes place, whereas $CoFe_2O_4$@MC nanocomposite has a flat and homogeneous morphology. The size of $CoFe_2O_4$@MC particles is smaller than that of $CoFe_2O_4$ because the agglomeration of nanoparticles was prevented when MC was coated on $CoFe_2O_4$. The role of MC was again confirmed from the size distribution of $CoFe_2O_4$@MC and $CoFe_2O_4$. The average particle size of nanocomposite $CoFe_2O_4$@MC was smaller (18.1 nm), and nanoparticle $CoFe_2O_4$ was comparatively higher (23.7 nm), which shows that the agglomeration of nanoparticles was prevented by MC. The cyclic voltammetry (CV) curve of $CoFe_2O_4$ has a relatively lower area than the $CoFe_2O_4$@MC nanocomposites; The Galvanostatic charge–discharge (GCD) curve shows the significantly higher charge/discharge time for $CoFe_2O_4$@MC nanocomposite compared to $CoFe_2O_4$. Using a three-electrode configuration of $CoFe_2O_4$@MC nanocomposite, the specific capacitance of 433.3 F g^{-1} at 1 A g^{-1} is achieved. Due to the conventional preparation method, low cost, and excellent electrochemical performance, $CoFe_2O_4$@MC nanocomposite deserves as a suitable electrode material for supercapacitor applications [77].

Gao et al. synthesized surface-modified $Ni(OH)_2$ nanoplates for enhancing wettability and conductivity for high-performance supercapacitors. The functionalization of $Ni(OH)_2$ was tuned by controlling the potassium persulfate ($K_2S_2O_8$) dosage during the synthesis process. The functionalized $Ni(OH)_2$ material is coated on Ni-Foam for fabricating supercapacitor electrode. Before functionalizing, the small-size hexagonal nanoplate structured $Ni(OH)_2$ coated on the Ni-Foam surface. The uniformly distributed large-size nanoplates are grown on the Ni-Foam by introducing $K_2S_2O_8$ during hydrothermal process. Further, increasing the dosage of $K_2S_2O_8$, the nanoplate became thinner and converted into a nanobelt structure on Ni-Foam. From the area of the CV curve at a scan rate 5 mV/s, the high dosage treated $K_2S_2O_8$ nanoplate shows a high specific capacitance value. The normalized areal capacity of $K_2S_2O_8$ doped $Ni(OH)_2$/Ni-Foam showed 4.2 times higher normalized areal capacity (436.7 C cm^{-1} g^{-1}) than the ordinary $Ni(OH)_2$/Ni-Foam electrode supercapacitor [78].

Kalaiarasi et al. functionalized the reduced graphene and ZnO as the efficient electrode material for supercapacitor application. Ordinary graphene oxide (GO) has a multi-layered structure, but in reduced graphene (RGO), nanospheres form a multi-layered structure. The spaces in the RGO can be filled by any other nanoparticles, in this case, ZnO nanoparticles are embedded in the space between the reduced graphene surfaces. The ZnO acts as a spacer layer between the stacked graphene sheets. The crystallinity of the sample was increased by doping ZnO nanoparticles with RGO. ZnO/RGO nanocomposite was synthesized in the hydrothermal method at different $Zn(NO_3)_2$ concentrations. The synthesis route for the ZnO/RGO is shown in Fig. 13. The response current in the CV curve increases with respect to molar concentration of zinc nitrate solution up to 0.06 M. Again, adding the $Zn(NO_3)_2$ leads to a decrease in the current value due to the structural defects in the surface of the graphene. The specific capacitance of the synthesized nanocomposite shows 181 F g^{-1} at 0.5 A g^{-1} current density value and retains 80% of its capacitance retention even after 2400 cycles [79].

Shaheen et al. synthesized ZnO–Co_3O_4 nanocomposite as an effective electrode material for supercapacitor applications. The particles are arranged in a uniform porous structure in the micro-level image. In nano-level images, it is understandable that the porous structure is superimposed by nanosphere particles. The presence of pores in nanoscale morphology is an essential criterion for good electrochemical properties. Because nano sites give more surface to enhance the electrochemically active sites for energy storage applications. The bandgap energy of the ZnO–Co_3O_4 nanocomposite is 1.3 eV. The low bandgap is due to the combination of ZnO having a high bandgap and Co_3O_4 having a narrow bandgap. Due to the synergic effect of the two metal oxides, the pseudocapacitive nature of the electrode material is increased. High capacitance is achieved by the more surface-active sites for the redox processes. The ZnO–Co_3O_4 nanocomposite enhances the capacitance compared to the nanoflower ZnO and Co_3O_4. The synthesized ZnO–Co_3O_4 nanocomposite exhibits a maximum power density of 7582 W kg^{-1} [80].

Zhang et al. synthesized the N-doped carbon nanotube arrays by the interlaced ultrathin Zn and Ni co-substituted Co carbonate hydroxides (ZnNiCo-CHs)

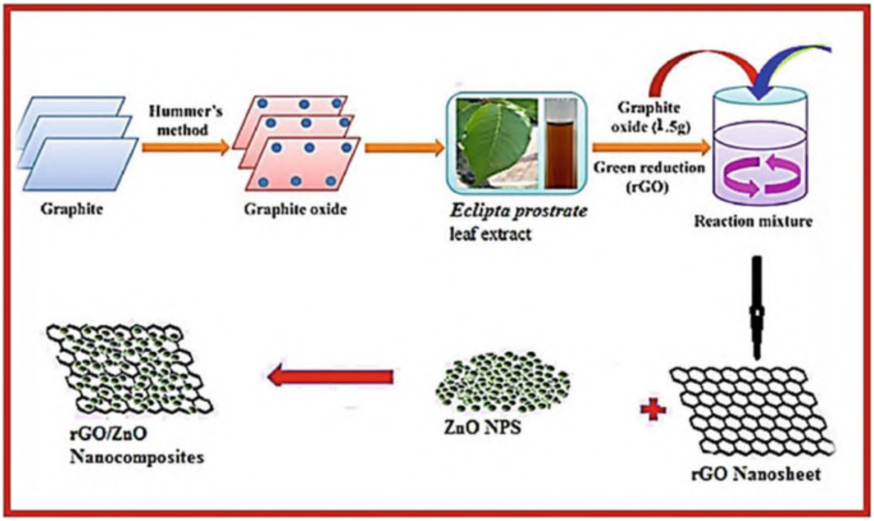

Fig. 13 The synthesized route of the ZnO/RGO. "Reprinted (adapted) with permission from [79] Copyright (2021) Elsevier"

nanosheets. The array of N-doped carbon nanotubes acts as a backbone, which has improved electrical conductivity than normally used metal oxide backbones. Mono-metal and binary-metal hydroxides have less electrochemical performance than multi-metal compound ZnNiCo-CHs. This is due to the synergic effect of the multi-metal combination in ZnNiCo-CHs offered more redox active sites and better conductivity than the corresponding individual hydroxides. The specific surface area of ZnNiCo-CHs nanosheets is 210.5 $m^2 g^{-1}$ confirmed from the BET study, which is greater than those Co-CHs, NiCo-CHs, and ZnCo-CHs carbonate hydroxide samples. The ZnNiCo-CHs nanosheets are grown on N-doped carbon nanotubes by the chemical bath deposition (CBD) method. The secondary ZnNiCo-CHs nanosheets create nano branches on carbon nanotubes which are observed from TEM images shown in Fig. 14. This electrode exhibits a high specific capacity of 964 C g^{-1} at 1 A g^{-1}, which is superior to those Co-CHs, ZnCo-CHs, and NiCo-CHs [81].

Alam et al. synthesized the mixed metal oxide $MgAl_2O_4$ by doping the chromium (Cr^{3+}) atoms. Mixed metal oxide $MgAl_2O_4$ is a type of spinal type semiconductor material. From the energy band spectra of pure and Cr^{3+} doped $MgAl_2O_4$, the bandgap value of $MgAl_2O_4$ and Cr^{3+} doped $MgAl_2O_4$ were 4.77 eV and 4.12 eV, respectively. The band gap value of the mixed metal oxide decreased with the doping of the Cr^{3+} atom. The specific capacitance values are 816.8 and 955.4 F g^{-1} for undoped and Cr^{3+} doped $MgAl_2O_4$. In the Nyquist plot, Cr^{3+} doped $MgAl_2O_4$ shows a smaller semi-circular portion than the undoped $MgAl_2O_4$, indicating the fast charge transfer rate in the KOH electrolyte [82].

Rashid et al. incorporated the ZnO by doping with Mn atoms at different chemical compositions. Mn-doping with ZnO at different molar concentrations is done by the

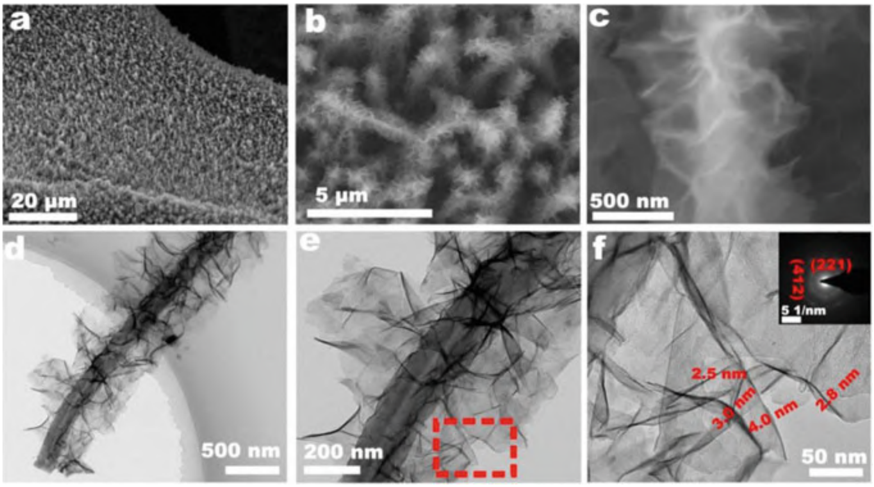

Fig. 14 FE-SEM image of carbon-doped ZnNiCo-CHs (**a**–**c**), TEM image of ZnNiCo-CHs (**d**–**f**). "Reprinted (adapted) with permission from [81] Copyright (2019) Elsevier"

simple hydrothermal method as shown in Fig. 15. In $Zn_{1-x}Mn_xO_3$, the doping is done with "x" values varying from 0, 0.25, 0.50, 0.75, and 1; among them, $Zn_{0.50}Mn_{0.50}O_3$ shows better electrochemical performance. SEM images of ZnO, and Mn-doped ZnO show a ribbon-like structure. Except 0.50 Mn-doped ZnO, all other ZnO have agglomerated morphology with undefined boundaries. But $Zn_{0.5}Mn_{0.5}O_3$ nanoribbons interconnected with each other indicate the interconnected boundaries with crosslinking connected nanostructure. The nanoribbon-like structure provided enormous electrochemical active sites and gave a path for the diffusion of ions; thus it is resulting in outstanding electrochemical performance. The improved electrochemical property of Mn-doped samples is due to the insertion of dopants generating high electrical conductivity. At large dopant concentrations of Mn atom, the specific capacitance decreases due to aggregation happening on the grain boundaries of the nanomaterials [83].

Jia et al. synthesized the Co/Ni-Linear double hydroxide (CN-LDH) using an induced S^{2-} anion exchange process. One strategy of LDH is to engineer the morphology (nanorod, nanoplate, nanosheet), which creates deep diffusion channels for the electrolytes. But in this functionalization process, VO_3^--doped Co/Ni-LDH hollow nanocages (V-CN-LDH) are attained first. Then, VO_3^- in the V-CN-LDH is gradually substituted by S^{2-} anions at room temperature (S-CNV-LDH). CN-LDH and V-CN-LDH morphologies are shown in Fig. 16a, b. SEM image shows that the hierarchical structure of S-CNV-LDH is constructed from smooth nanosheets, as in Fig. 16c; the TEM and HR-TEM images confirm its hollow structure, which is in Fig. 16d–f. The wrinkling phenomenon of nanosheets attributes to the dimensional shrinkage effect through the anion exchange process. The S-CNV-LDH shows better electrochemical performance than that of the LDH before etching. The superior

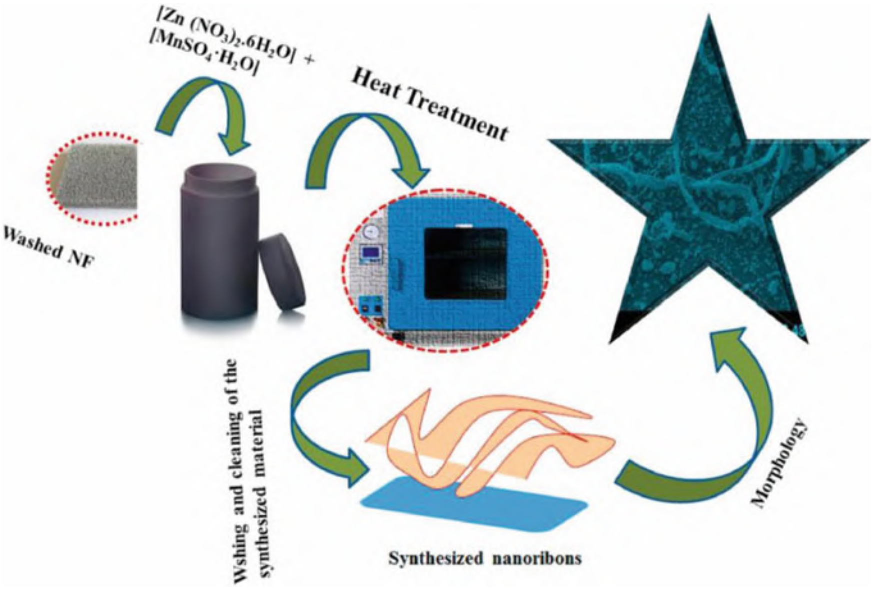
[Zn (NO$_3$)$_2$.6H$_2$O] +
[MnSO$_4$·H$_2$O]
Heat Treatment
Washed NF
Wshing and cleaning of the synthesized material
Synthesized nanoribons
Morphology

Fig. 15 Synthesis root for Mn-doped ZnO nanoribon arrays grown on Ni foam. "Reprinted (adapted) with permission from [83] Copyright (2021) Elsevier"

electrochemical performance is due to the following reasons: (1) Conductivity of the material is enhanced due to the nanoparticles formed on the surface. (2) The surface area is increased, which provides large active sites for the redox reaction. (3) Pores diameter is increased, which is suitable for the mass transfer of electrolyte ions [84].

Dinari et al. fabricated the layered double hydroxide (LDH) by doping with Ce, and this nanocomposite was coated on the surface of carbon nanotube (CNT). The multiwall carbon nanotube (MWCNT) was dispersed by sonication, then NiCoCe-LDH nanosheets were grown vertically on the surface of CNT skeleton. The growth of LDH with the surface of CNT creates an ordered stacking structure. The CNT between the layers of LDH enhances the conductivity and improves the contact area of electrolyte ions. The NiCo-LDH has a close-packed layered structure. After doping with Ce^{3+}, the surface area increases due to structure exfoliation. The NiCoCe-LDH was synthesized on the surface of CNT by doping 5, 10, and 15% molar ratio of Ce^{3+} in the Co^{3+} lattices. Among the three samples, 10% Ce^{3+} doped sample exhibits a good synergic effect. Because the addition of nanoparticles increase the surface area of the electrode, which increases the number of active sites; as a result, the capacitance will be improved. 10% doped sample gives an excellent electrochemical performance; after that, doping leads to aggregation of the particle on the surface; as a result, the capacitance value decreases gradually [85].

Aghazadeh et al. synthesized the oxygen-functionalized graphitic carbon nitride (f-g-C_3N_4), and $Co(OH)_2$ co-embedded on Ni-foam, which is used for supercapacitor applications. The interlayer spacing between $Co(OH)_2$ increases the approachability

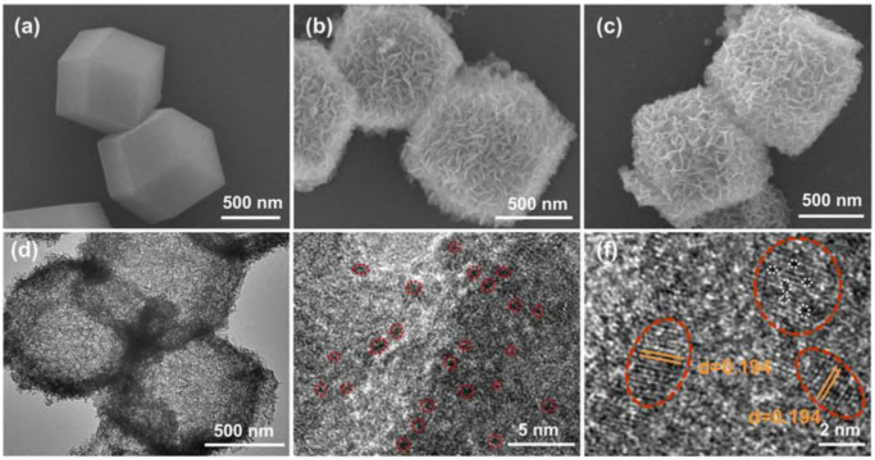

Fig. 16 SEM images of CN-LDH (**a**), V-CN-LDH (**b**) and S-CNV-LDH (**c**); TEM (**d**) and HRTEM (**e** and **f**) images of S-CNV-LDH. "Reprinted (adapted) with permission from [84] Copyright (2021) Royal Society of Chemistry"

of electrolyte ions through the electrodes. Graphitic carbon nitride (g-C_3N_4) has a highly porous structure and high heteroatom content which can have more reactive sites for energy storage applications. The functionalization of the g-C_3N_4 nanosheet is accomplished via chemical oxidation in an acidic solution. Chemical etching in acidic condition technique is used for creating the defect sites on the g-C_3N_4 structure. The synthesis steps are shown in Fig. 17. The f-g-C_3N_4 formed as aggregated layered structure, and the sheets are separated in several nanometers. The $Co(OH)_2$ plates are dispersed on the surface of f-g-C_3N_4 sheets; it gives better physical contact between $Co(OH)_2$ and f-g-C_3N_4 within the fabricated structure of nanocomposite. From electrochemical studies, it is understood that f-g-C_3N_4 has a high electrical conductivity and specific surface area; as a result, the electrochemical activity of the $Co(OH)_2$ material increases [86].

Liu et al. incorporated the CoO by decorating the interior with Cu^+ and the exterior with Cu^0. Cu^+ and Cu^0 co-doped CoO are prepared through the hydrothermal method. The doping concentration of Cu^+ and Cu^0 can be controlled by adjusting the annealing temperature. The doping of Cu has a significant influence on the morphology of CoO. In the absence of Cu, CoO is in a nanorod-like structure; with the help of increasing the Cu source, the nanoflower-like morphology evolved from nanorods. Introducing a moderate amount of Cu produces one-dimensional growth, and excessive Cu doping results in a growth that rapidly results in a nanosheet structure. From the TEM image of the sample, each nanoflower consists of enormous one-dimensional nanowires. Cu-doped CoO exhibits a better cycle performance, and 93.4% of the initial capacitance is maintained after 10,000 cycles, which are 68.2% higher than the pristine CoO. From the cyclic voltammetry (CV) curve, the performance of Cu co-doped CoO is

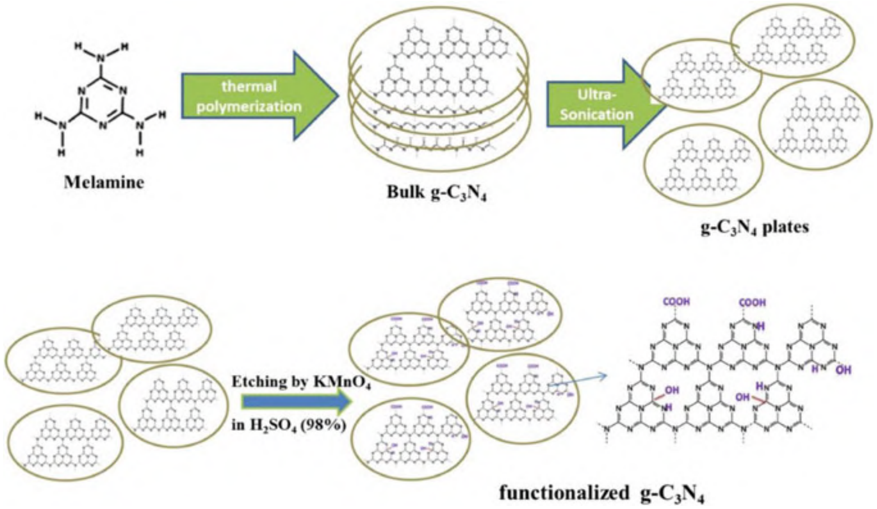

Fig. 17 Schematic view of the synthesis steps of functionalized g-C_3N_4 sheets. "Reprinted (adapted) with permission from [86] Copyright (2020) Elsevier"

almost similar after 10,000 cycles. The asymmetric supercapacitor was constructed using activated carbon (AC) as a cathode and Cu co-doped CoO as an anode [87].

Rosaiah et al. synthesized reduced graphene oxide (RGO), and Fe_3O_4 to make nanocomposite for supercapacitor applications. A simple graphenothermal process is used to obtain the nanocomposite. Initially, $FeC_2O_4{\cdot}2H_2O$ was heated in an air environment at 600 °C for 5 h to obtain the Fe_2O_3; this is used as the source material for producing the Fe_3O_4. To produce the RGO/Fe_3O_4 nanocomposites, Fe_2O_3 and GO were taken in a 1:2 ratio in a certain bowl, and it was mechanically grounded for 1 h. Then, the graphenothermal treatment of the mixture was done in Ar environment at 650 °C for 5 h. After that, the mixture was cool down to room temperature and used as the electrode material without any other treatment. The FESEM image of the RGO/Fe_3O_4 nanocomposite has a flower-like morphology. The Fe_3O_4 nanoparticles are dispersed on the surface of RGO nanosheets. The Fe_3O_4 nanoparticles are dispersed on the surface of RGO nanosheets, significantly increases the conductivity of the nanocomposite. The CV curve of RGO/Fe_3O_4 nanocomposite is rectangular with no redox peaks; it shows capacitive behavior. The RGO/Fe_3O_4 exhibits 98.7% of its initial capacitance value after 5000 cycles, so it is a good candidate for supercapacitor applications [88].

Ji et al. functionalized the nickel carbonate hydroxide (NCH) by doping on carbon quantum dots (NCQDs). NCQDs are uniformly distributed on the surface of the NCH nanosheets, which provide large active sites for electrochemical action. The SEM image of NCH has an interconnected nanoflake-like structure. The nanocomposite NCH/NCQDs was studied using TEM and SEM analysis, which suggested that the nanocomposite also exhibits the same nanoflake-like structure like bare NCH. The size of the NCH/NCQD nanocomposite is smaller as compared to NCH, and this is due to the zero-dimensional NCQDs preventing the growth of NDH. 0, 20, 30, and 40 mg of NCQDs were mixed with NCH nanosheets, and the electrochemical performance was studied. The 30 mg NCQD distributed sample shows better performance than the other sample; this is due to a high amount of NCQD decreasing the contact of electrode–electrolyte [89].

Ayman et al. functionalized the MXene and its composites with $CoFe_2O_4$ (cobalt ferrite) nanoparticles (CoF NPs) for supercapacitor applications. The interlayer spacing between MXene layers was applied by nanoparticles (NPs). The synthesis method for CoF NPs decorated MXene was explained pictorially in Fig. 18. After the exfoliation of MXene basal planes under the removal of "Al" gives the accordion-like morphology. A parallel layer arrangement of MXene indicates the specific etching direction of "Al". The CoF NPs have an average grain size of 86 nm, which suggests the presence of nanoparticles with no agglomeration. In CoF/MXene composite, the NPs embedded in the opening between the layers as well as integrated on the surface of MXene layers. The restacking of the MXene layer was prevented by the presence of the NPs between the MXene flacks. The CV curve area of the CoF/MXene is more significant than the individual CoF and MXenes. This change in the area of CV curves attributes to the better conductivity and greater surface area provided by the CoF/MXene composites. The MXene flacks provide good mobility of charge carriers with a reduction in internal resistance. The synergic effect of the nanoparticles with MXenes improves the performance of supercapacitor applications [90].

To enhance the active sites, ferric oxides (Fe_2O_3) nanocomposites were dispersed on oxidized graphitic carbon nitride (OGN) [91]. The nitrogen-doped carbon nanotubes were expended with Fe_2O_3 to get good power storage capacities. In the conducting material, the nanoparticle Fe_2O_3 was dispersed to a tolerable extent, leading to the creation of Fe_2O_3/N-CNTs framework with high performance [92]. The Fe_2O_3 nanocomposites were prepared by varying the mass of the reduced graphene oxide (rGO) matrix. The good performance is due to the high surface area and oxygen vacancies created in the crystal lattice [93]. Introducing porous carbon with Fe_2O_3 provides steady loading sited to metal oxides and ion transport through the electrolyte and thus provides a steady electric double layer [94]. Different combinations containing Fe_2O_3 ingrained on the rGO matrix enhance the charge storage due to the synergic effect of the disc-shaped Fe_2O_3 particles [95]. PANI is treated with Fe_2O_3 nanoparticles offering tremendous capacitance retention value [96]. PANI has a nanonet structure which helps to improve the conductivity with Fe_2O_3 microspheres [97]. Titanium dioxide (TiO_2) has a prominent surface area and charge storage capacitance. Introducing the polymer (PANI) or introducing a porous matrix containing carbon (rGO, CNT) increases the catalytic and electrochemical properties [98]. Different synthesis approaches of TiO_2 varying the pore size leads to variations in physical and chemical properties; as a result, electrochemical performance improved [99, 100]. rGO is used as a substrate for growing TiO_2 nanocubes and shows highly appreciable electrochemical performance [101].

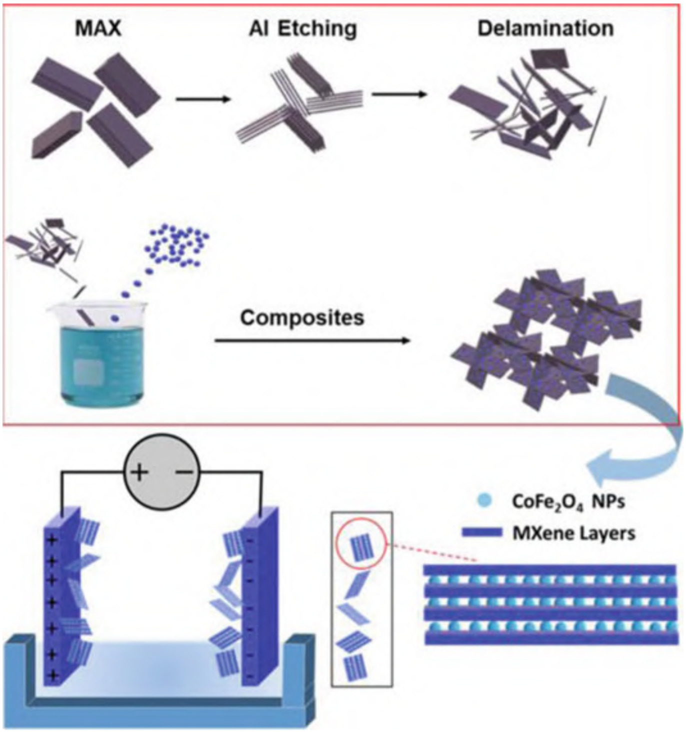

Fig. 18 Synthesis of CoF NP decorated MXene and its application as an SC electrode. “Reprinted (adapted) with permission from [90] Copyright (2020) American Chemical Society”

2.5 *Electrode Engineering*

Intrinsic and extrinsic alteration can be performed by controlled synthesis routes and post-synthesis processes to achieve enhanced electrochemical performances. Metal oxides/hydroxides electrical conductivity has its limitation, it can’t be improved above a certain limit using intrinsic and extrinsic alteration. Due to that proper electrode, engineering is important for transferring electrons produced during the redox reaction through an appropriate conductive guide between the current collector and redox-active electrode material. Electrode engineering means fabricating the electrode with the proper electron flow guide with a low resistive path. Example: On the current collector, the appropriate electrically conductive material has grown with a high specific surface area. On the above high conductive material, a thin layer of high electrochemically active porous materials has to be grown. In this, the redox reaction happens at electrochemically active material for charge storage, and the electrons produced or required in the reactions are transferred between the current collectors and redox-active material by electron flow guide. Schematic illustration

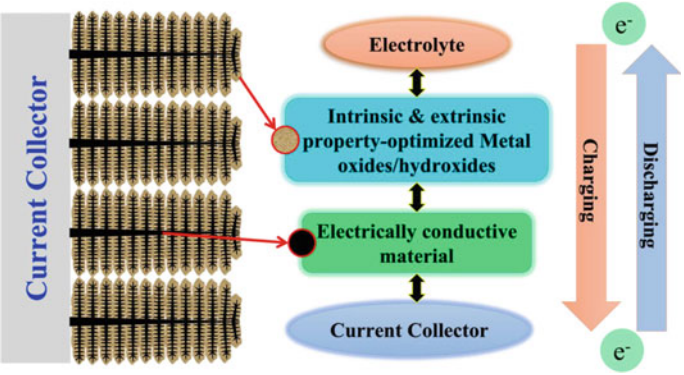
Current Collector
Electrolyte
Intrinsic & extrinsic property-optimized Metal oxides/hydroxides
Electrically conductive material
Current Collector
e-
Charging
Discharging
e-

Fig. 19 Schematic illustration of electron flow in the electrode engineered anode

of electron flow in the electrode-engineered anode is shown in Fig. 19. Due to fast electron transfer and fast ion transport, its specific energy as well as specific power will be enhanced.

2.6 *Recent Progress in Electrode Engineering Techniques*

Zhu et al. grew a porous flower-like Ni–Co–Mo–S on a Ni-foam by a three-step hydrothermal process. On the cleaned Ni-foam, the Ni–Co nanoneedle array was grown using urea assisted hydrothermal process. It acts as an electron transport layer for transferring electrons between the current collector and electrochemically active material. On the above, Ni–Co–Mo nanorod arrays were implanted using the hydrothermal method. Through sulfurization, The Ni–Co–Mo nanorod arrays were modified by the thiourea-assisted hydrothermal method to fabricate porous flower-like Ni–Co–Mo–S nanostructures on Ni foam. The outer layer of metal sulfides was used for improving the conductivity of the material as well as enhancing the electrochemical charge storage properties. The designed hybrid device using a three-step hydrothermal technique has achieved 54.54 Wh kg^{-1} at 540 W kg^{-1} and retained 74.8% capacitance retention after 3500 cycles [102].

Choudhary et al. fabricated a one-body core/shell nanowire supercapacitor empowered through conformal growth of capacitive 2D WS_2 layers. The electrode was fabricated by a two-step process. First, in a thin (100 μm) Tungsten foil array of vertically aligned h-WO_3 nanowires prepared by its oxidation. It acts as an electrically conductive material for charge carrier transport. Second, the nanowires were then sulfurized in a chemical vapor deposition (CVD) furnace beneath a sulfur (S) environment, which transforms the outside surface of the h-WO_3 nanowires to 2D WS_2. A schematic illustration of different layers and their role in the flexible electrode is shown in Fig. 20. The nanowire-like structure leads to a large surface area, which

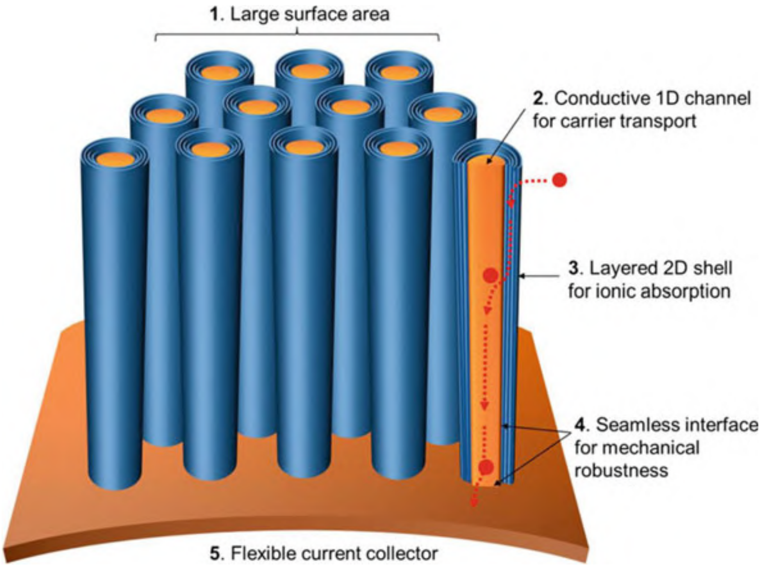
1. Large surface area
2. Conductive 1D channel for carrier transport
3. Layered 2D shell for ionic absorption
4. Seamless interface for mechanical robustness
5. Flexible current collector

Fig. 20 Schematic illustration of different layers and their role in the flexible electrode. "Reprinted (adapted) with permission from [103] Copyright (2016) American Chemical Society"

improved the electrolyte electrode interface. High conductive 1D core channel leads to a fast electron transfer. The 2D WS_2 layered shell adsorbs large electrolytic ions and it is more electrochemically active for large charge storage. Due to this excellent electrode engineering, multifold advantages are desired for high-performance supercapacitors [103].

Yu et al. studied the performance of different current collectors for supercapacitors. The electrochemical stability of electrolytes and capacitance contribution in various aqueous electrolytes were analysed and studied with various current collectors, including stainless steel mesh, graphite sheet, carbon fabrics, carbon paper, carbon cloth, glassy carbon, Ti mesh, Ti foil, Ni foil, Ni foam, Cu foam, and Cu foil. The HER (Hydrogen Evolution Reaction) and OER (Oxygen Evolution Reaction) response behavior vary with different current collectors. The aqueous electrolytes are stable between HER and OER turnover potential. Compared to all other current collectors and universally used Ni foam, the Ti mesh appears the chemical inertness and can work excellently at a comparatively excessive applied potential. The electrolyte decomposition on the Ti mesh is difficult within the electrochemical potential window up to 2.05 V in 6 M KOH, 3.61 V in 1 M Na_2SO_4, and 3.12 V in 1 M H_2SO_4, respectively [104].

Zheng et al. produced supercapacitors based on ruthenium oxide (RuOx) coated silicon nanowires (Si NW). Its schematic illustration is shown in Fig. 21. In silicon substrate, an array of silicon nanowires was produced using metal-assisted anodic etching (MAAE). On the above silicon nanowire, ruthenium oxide was coated using Atomic Layer Deposition (ALD). FESEM image in Fig. 21 clearly evidenced that

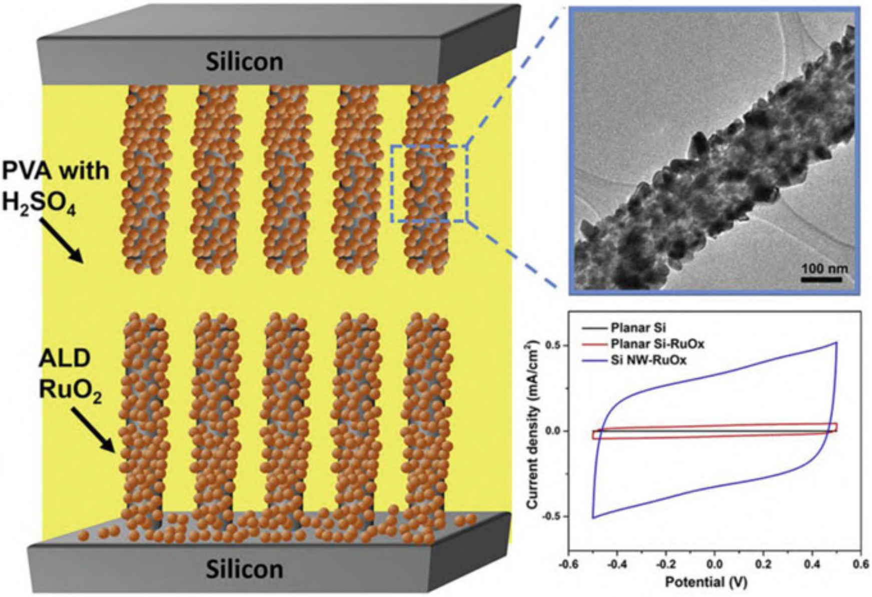

Fig. 21 Schematic diagram of supercapacitor based on ruthenium oxide coated silicon nanowires, its morphology, and electrochemical performances. "Reprinted (adapted) with permission from [105] Copyright (2017) Elsevier"

the formation of RuOx layer in Si NW. In this silicon substrate used as a current collector, Si NW as an electron transporter, and RuOx as a redox-active charge storage medium. Compared to planar Si and RuOx-coated planar Si, RuOx-coated Si NW showed an excellent electrochemical charge storage performance in Cyclic Voltammetry (Fig. 21) [105].

3 Conclusion

This chapter systematically highlighted and deliberated the different functionalization approaches and routes for metal-oxide/hydroxide base supercapacitors. Most of the articles focus on any one of the properties of the material to improve its charge storage properties. But still, there is a lack of integrated development of the electrode via proper electrode engineering. Intrinsic properties alteration techniques are used for tuning materials to have optimized crystal structure/orientation, defects, and morphology. High electrical conductivity, optimized surface charge density, and large number of active sites can be attained by extrinsic alteration techniques. The high-performance supercapacitor device can be accomplished by proper electrode engineering of intrinsic and extrinsic properties optimized material in a suitable current collector with proper electrode architecting.

References

1. Akbari R, Izadian A (2022) Modeling and control of flywheel-integrated generators in split-shaft wind turbines. J Sol Energy Eng 144(1):011008. https://doi.org/10.1115/1.4052056
2. Nie M, Jia K, Xie Y, Zhu S, Xie Z, Huang SW (2022) Synthesized spatiotemporal mode-locking and photonic flywheel in multimode mesoresonators. Nat Commun 13(1):1–9. https://doi.org/10.1038/s41467-022-34103-0
3. Li X, Palazzolo A (2022) A review of flywheel energy storage systems: state of the art and opportunities. J Energy Storage 46:103576. https://doi.org/10.1016/J.EST.2021.103576
4. Chen X, Zhang M, Jiang S, Gou H, Zhou P, Yang R, Shen B (2023) Energy reliability enhancement of a data center/wind hybrid DC network using superconducting magnetic energy storage. Energy 263:125622. https://doi.org/10.1016/J.ENERGY.2022.125622
5. Adetokun BB, Oghorada O, Abubakar SJA (2022) Superconducting magnetic energy storage systems: prospects and challenges for renewable energy applications. J Energy Storage 55:105663. https://doi.org/10.1016/J.EST.2022.105663
6. Mathis TS, Kurra N, Wang X, Pinto D, Simon P, Gogotsi Y (2019) Energy storage data reporting in perspective—guidelines for interpreting the performance of electrochemical energy storage systems. Adv Energy Mater 9(39):1902007. https://doi.org/10.1002/AENM.201902007
7. Nguyen T, Montemor MDF (2019) Metal oxide and hydroxide–based aqueous supercapacitors: from charge storage mechanisms and functional electrode engineering to need-tailored devices. Adv Sci 6(9):1801797. https://doi.org/10.1002/ADVS.201801797
8. Ghodbane O, Pascal JL, Favier F (2009) Microstructural effects on charge-storage properties in MnO_2-based electrochemical supercapacitors. ACS Appl Mater Interfaces 1(5):1130–1139. https://doi.org/10.1021/AM900094E
9. Devaraj S, Munichandraiah N (2008) Effect of crystallographic structure of MnO_2 on its electrochemical capacitance properties. J Phys Chem C 112(11):4406–4417. https://doi.org/10.1021/JP7108785
10. Yin B, Zhang S, Jiang H, Qu F, Wu X (2015) Phase-controlled synthesis of polymorphic MnO_2 structures for electrochemical energy storage. J Mater Chem A 3(10):5722–5729. https://doi.org/10.1039/C4TA06943A
11. Salari M, Aboutalebi SH, Chidembo AT, Nevirkovets IP, Konstantinov K, Liu HK (2012) Enhancement of the electrochemical capacitance of TiO_2 nanotube arrays through controlled phase transformation of anatase to rutile. Phys Chem Chem Phys 14(14):4770–4779. https://doi.org/10.1039/C2CP40410A
12. Lee JH, Lee HJ, Lim SY, Chae KH, Park SH, Chung KY, Deniz E, Choi JW (2017) Stabilized octahedral frameworks in layered double hydroxides by solid-solution mixing of transition metals. Adv Funct Mater 27(7):1605225. https://doi.org/10.1002/ADFM.201605225
13. Dai P, Yan T, Hu L, Pang Z, Bao Z, Wu M, Li G, Fang J, Peng Z (2017) Phase engineering of cobalt hydroxides using magnetic fields for enhanced supercapacitor performance. J Mater Chem A 5(36):19203–19209. https://doi.org/10.1039/C7TA03656F
14. Chen S, Xing W, Duan J, Hu X, Qiao SZ (2013) Nanostructured morphology control for efficient supercapacitor electrodes. J Mater Chem A 1(9):2941–2954. https://doi.org/10.1039/C2TA00627H
15. Yuan C, Wu HB, Xie Y, Lou XW (2014) Mixed transition-metal oxides: design, synthesis, and energy-related applications. Angew Chem, Int Ed 53(6):1488–1504. https://doi.org/10.1002/ANIE.201303971
16. Jiang J, Li Y, Liu J, Huang X, Yuan C, Lou XW (2012) Recent advances in metal oxide-based electrode architecture design for electrochemical energy storage. Adv Mater 24(38):5166–5180. https://doi.org/10.1002/ADMA.201202146
17. Girirajan M, Alagarsamy NB, Ramachandran K, Manimuthu RP, Pazhanivel D, Muthusamy KK, Sakkarapani S (2022) Two dimensional layered bismuthene nanosheets with ultra-fast charge transfer kinetics as a superior electrode material for high performance asymmetric

supercapacitor. Electrochim Acta 426:140838. https://doi.org/10.1016/J.ELECTACTA.2022.140838

18. Syamsai R, Grace AN (2019) Ta_4C_3 MXene as supercapacitor electrodes. J Alloys Compd 792:1230–1238. https://doi.org/10.1016/J.JALLCOM.2019.04.096
19. Liu Z, Teng F, Chang C, Teng Y, Wang S, Gu W, Fan Y, Yao W, Zhu Y (2016) Charge storage performances of micro-supercapacitor predominated by two-dimensional (2D) crystal structure. Nano Energy 27:58–67. https://doi.org/10.1016/J.NANOEN.2016.06.025
20. Kar T, Godavarthi S, Pasha SK, Deshmukh K, Martínez-Gómez L, Kesarla MK (2022) Layered materials and their heterojunctions for supercapacitor applications: a review. Crit Rev Solid State Mater Sci 47(3):357–388. https://doi.org/10.1080/10408436.2021.1886048
21. Ansari SN, Saraf M, Gupta AK, Mobin SM (2019) Functionalized Cu-MOF@CNT hybrid: synthesis, crystal structure and applicability in supercapacitors. Chem Asian J 14(20):3566–3571. https://doi.org/10.1002/ASIA.201900629
22. Wang X, Yan C, Sumboja A, Yan J, Lee PS (2014) Achieving high rate performance in layered hydroxide supercapacitor electrodes. Adv Energy Mater 4(6):1301240. https://doi.org/10.1002/AENM.201301240
23. Jing C, Dong B, Zhang Y (2020) Chemical modifications of layered double hydroxides in the supercapacitor. Energy Environ 3(3):346–379. https://doi.org/10.1002/EEM2.12116
24. Xie W, Song Y, Li S, Shao M, Wei M (2019) Integrated nanostructural electrodes based on layered double hydroxides. Energy Environ 2(3):158–171. https://doi.org/10.1002/EEM2.12033
25. Najafpour MM, Hołyńska M, Salimi S (2015) Applications of the "nano to bulk" Mn oxides: Mn oxide as a Swiss army knife. Coord Chem Rev 285:65–75. https://doi.org/10.1016/J.CCR.2014.11.001
26. Yue Y, Liang H (2015) Hierarchical micro-architectures of electrodes for energy storage. J Power Sources 284:435–445. https://doi.org/10.1016/J.JPOWSOUR.2015.03.069
27. Nguyen T, Boudard M, Carmezim MJ, Montemor MF (2017) Layered $Ni(OH)_2$-$Co(OH)_2$ films prepared by electrodeposition as charge storage electrodes for hybrid supercapacitors. Sci Rep 7(1):1–10. https://doi.org/10.1038/srep39980
28. Xu Q, Lv Y, Dong C, Sreeprased TS, Tian A, Zhang H, Tang Y, Yu Z, Li N (2015) Three-dimensional micro/nanoscale architectures: fabrication and applications. Nanoscale 7(25):10883–10895. https://doi.org/10.1039/C5NR02048D
29. Yu M, Qiu W, Wang F, Zhai T, Fang P, Lu X, Tong Y (2015) Three dimensional architectures: design, assembly and application in electrochemical capacitors. J Mater Chem A 3(31):15792–15823. https://doi.org/10.1039/C5TA02743H
30. Patil U, Lee SC, Kulkarni S, Sohn JS, Nam MS, Han S, Jun SC (2015) Nanostructured pseudocapacitive materials decorated 3D graphene foam electrodes for next generation supercapacitors. Nanoscale 7(16):6999–7021. https://doi.org/10.1039/C5NR01135C
31. Rajpurohit AS, Punde NS, Srivastava AK (2019) A dual metal organic framework based on copper-iron clusters integrated sulphur doped graphene as a porous material for supercapacitor with remarkable performance characteristics. J Colloid Interface Sci 553:328–340. https://doi.org/10.1016/J.JCIS.2019.06.031
32. Zhang F, Lu Y, Yang X, Zhang L, Zhang T, Leng K, Wu Y, Huang Y, Ma Y, Chen Y (2014) A flexible and high-voltage internal tandem supercapacitor based on graphene-based porous materials with ultrahigh energy density. Small 10(11):2285–2292. https://doi.org/10.1002/SMLL.201303240
33. Ramesh S, Yadav HM, Lee YJ, Hong GW, Kathalingam A, Sivasamy A, Kim HS, Kim HS, Kim JH (2019) Porous materials of nitrogen doped graphene oxide@SnO_2 electrode for capable supercapacitor application. Sci Rep 9(1):1–10. https://doi.org/10.1038/s41598-019-48951-2
34. Peng H, Raya J, Richard F, Baaziz W, Ersen O, Ciesielski A, Samorì P (2020) Synthesis of robust MOFs@COFs porous hybrid materials via an Aza-diels–alder reaction: towards high-performance supercapacitor materials. Angew Chem, Int Ed 59(44):19602–19609. https://doi.org/10.1002/ANIE.202008408

35. Swain N, Saravanakumar B, Kundu M, Schmidt-Mende L, Ramadoss A (2021) Recent trends in template assisted 3D porous materials for electrochemical supercapacitors. J Mater Chem A 9(45):25286–25324. https://doi.org/10.1039/D1TA06122D
36. Gao F, Wolfer MT, Nebel CE (2014) Highly porous diamond foam as a thin-film micro-supercapacitor material. Carbon 80:833–840. https://doi.org/10.1016/J.CARBON.2014.09.007
37. Vinodh R, Gopi CVM, Kummara VGR, Atchudan R, Ahamad T, Sambasivam S, Yi M, Obaidat IM, Kim HJ (2020) A review on porous carbon electrode material derived from hypercross-linked polymers for supercapacitor applications. J Energy Storage 32:101831. https://doi.org/10.1016/J.EST.2020.101831
38. Yang H, Cheng Z, Wu P, Wei Y, Jiang J, Xu Q (2022) Deep eutectic solvents regulation synthesis of multi-metal oxalate for electrocatalytic oxygen evolution reaction and supercapacitor applications. Electrochim Acta 427:140879. https://doi.org/10.1016/J.ELECTACTA.2022.140879
39. Han L, Luo J, Zhang R, Gong W, Chen L, Liu F, Ling Y, Dong Y, Yong Z, Zhang Y, Wei L (2022) Arrayed heterostructures of MoS_2 nanosheets anchored TiN nanowires as efficient pseudocapacitive anodes for fiber-shaped ammonium-ion asymmetric supercapacitors. ACS Nano 16(9):14951–14962. https://doi.org/10.1021/ACSNANO.2C05905
40. Sen P, De A, Chowdhury AD, Bandyopadhyay SK, Agnihotri N, Mukherjee M (2013) Conducting polymer based manganese dioxide nanocomposite as supercapacitor. Electrochim Acta 108:265–273. https://doi.org/10.1016/J.ELECTACTA.2013.07.013
41. Wang P, Zhang Y, Jiang H, Dong X, Meng C (2022) Ammonium vanadium oxide framework with stable NH^{4+} aqueous storage for flexible quasi-solid-state supercapacitor. Chem Eng J 427:131548. https://doi.org/10.1016/J.CEJ.2021.131548
42. Chen K, Xue D (2015) Rare earth and transitional metal colloidal supercapacitors. Sci China Technol Sci 58(11):1768–1778. https://doi.org/10.1007/S11431-015-5915-Z
43. Zhang L, Ou M, Yao H, Li Z, Qu D, Liu F, Wang J, Wang J, Li Z (2015) Enhanced supercapacitive performance of graphite-like C_3N_4 assembled with NiAl-layered double hydroxide. Electrochim Acta 186:292–301. https://doi.org/10.1016/J.ELECTACTA.2015.10.192
44. Fu H, Liu Y, Chen L, Shi Y, Kong W, Hou J, Yu F, Wei T, Wang H, Guo X (2019) Designed formation of $NiCo_2O_4$ with different morphologies self-assembled from nanoparticles for asymmetric supercapacitors and electrocatalysts for oxygen evolution reaction. Electrochim Acta 296:719–729. https://doi.org/10.1016/J.ELECTACTA.2018.11.103
45. Kumar YA, Kumar KD, Kim HJ (2020) Reagents assisted $ZnCo_2O_4$ nanomaterial for supercapacitor application. Electrochim Acta 330:135261. https://doi.org/10.1016/J.ELECTACTA.2019.135261
46. Liu Y, Ning D, Zheng L, Zhang Q, Gu L, Gao R, Zhang J, Franz A, Schumacher G, Liu X (2018) Improving the electrochemical performances of Li-rich $Li_{1.20}Ni_{0.13}Co_{0.13}Mn_{0.54}O_2$ through a cooperative doping of Na^+ and $PO_4{}^{3-}$ with Na_3PO_4. J Power Sources 375:1–10. https://doi.org/10.1016/J.JPOWSOUR.2017.11.042
47. Qiu L, Xiang W, Tian W, Xu CL, Li YC, Wu ZG, Chen TR, Jia K, Wang D, He FR, Guo XD (2019) Polyanion and cation co-doping stabilized Ni-rich Ni–Co–Al material as cathode with enhanced electrochemical performance for Li-ion battery. Nano Energy 63:103818. https://doi.org/10.1016/J.NANOEN.2019.06.014
48. Zhu Y, Huang C, Li C, Fan M, Shu K, Chen HC (2019) Strong synergetic electrochemistry between transition metals of α phase Ni−Co−Mn hydroxide contributed superior performance for hybrid supercapacitors. J Power Sources 412:559–567. https://doi.org/10.1016/J.JPOWSOUR.2018.11.080
49. Li YC, Xiang W, Xiao Y, Wu ZG, Xu CL, Xu W, Xu YD, Wu C, Yang ZG, Guo XD (2019) Synergy of doping and coating induced heterogeneous structure and concentration gradient in Ni-rich cathode for enhanced electrochemical performance. J Power Sources 423:144–151. https://doi.org/10.1016/J.JPOWSOUR.2019.03.073

50. Najib S, Bakan F, Abdullayeva N, Bahariqushchi R, Kasap S, Franzò G, Sankir M, Sankir ND, Mirabella S, Erdem E (2020) Tailoring morphology to control defect structures in ZnO electrodes for high-performance supercapacitor devices. Nanoscale 12(30):16162–16172. https://doi.org/10.1039/D0NR03921G
51. Waghmode RB, Maile NC, Lee DS, Torane AP (2020) Chemical bath synthesis of $NiCo_2O_4$ nanoflowers with nanorods like thin film for flexible supercapacitor application-effect of urea concentration on structural conversion. Electrochim Acta 350:136413. https://doi.org/10.1016/J.ELECTACTA.2020.136413
52. Liu S, Yin Y, Ni D, San Hui K, Ma M, Park S, Hui KN, Ouyang CY, Jun SC (2019) New insight into the effect of fluorine doping and oxygen vacancies on electrochemical performance of Co_2MnO_4 for flexible quasi-solid-state asymmetric supercapacitors. Energy Storage Mater 22:384–396. https://doi.org/10.1016/J.ENSM.2019.02.014
53. Zhu M, Luo Q, Chen Q, Wei W, Zhang Q, Li S (2021) Glycerol-assisted tuning of the phase and morphology of iron oxide nanostructures for supercapacitor electrode materials. Mater Chem Front 5(6):2758–2770. https://doi.org/10.1039/D0QM00900H
54. Pakulski D, Gorczyński A, Czepa W, Liu Z, Ortolani L, Morandi V, Patroniak V, Ciesielski A, Samorì P (2019) Novel Keplerate type polyoxometalate-surfactant-graphene hybrids as advanced electrode materials for supercapacitors. Energy Storage Mater 17:186–193. https://doi.org/10.1016/J.ENSM.2018.11.012
55. Babulal SM, Venkatesh K, Chen TW, Chen SM, Krishnapandi A, Rwei SP, Ramaraj SK (2020) Synthesis of $MnMoO_4$ nanorods by a simple Co-precipitation method in presence of polyethylene glycol for pseudocapacitor application. Int J Electrochem Sci 15:7053–7063. https://doi.org/10.20964/2020.07.90
56. Isacfranklin M, Yuvakkumar R, Ravi G, Babu ES, Pannipara M, Al-Sehemi AG, Velauthapillai D (2021) Effect of cationic, anionic, and mixed surfactant role on manganese oxide nanoparticles for energy storage applications. Appl Nanosci 11(5):1769–1775. https://doi.org/10.1007/S13204-021-01829-0
57. Zhang X, Shang N, Gao S, Wang C, Gao Y, Wang Z (2019) Surfactant assisted self-assembly of NiCo phosphate with superior electrochemical performance for supercapacitor. Appl Surf Sci 483:529–535. https://doi.org/10.1016/J.APSUSC.2019.03.339
58. Munawar T, Nadeem MS, Mukhtar F, Manzoor S, Ashiq MN, Iqbal F (2022) Surfactant-assisted facile synthesis of petal-nanoparticle interconnected nanoflower like NiO nanostructure for supercapacitor electrodes material. Mater Sci Eng B 284:115900. https://doi.org/10.1016/J.MSEB.2022.115900
59. Li X, Su Y, Lang X, Li L, Yao C, Cai K (2022) High-performance surface optimized Mg-doped V_2O_5 (Mg@V_2O_5) cathode material via a surfactant-assisted hydrothermal technology for lithium-ion and lithium-sulfur batteries. Ionics 28(4):1511–1521. https://doi.org/10.1007/S11581-022-04470-1
60. Wu Y, Ding X, Luo Y, Xu F, Sun L, Lao J, Qin X, Dan C, Wang Y, Yin Q, Wang T (2021) Nickel-organic frameworks with hierarchical flowers structure fabricated by surfactant-assisted solvothermal method for high-performance supercapacitors. Int J Electrochem Sci 16(3). https://doi.org/10.20964/2021.03.68
61. Zhou H, Zhi X, Zhang W, Zhai HJ (2019) A simple strategy to prepare polyaniline nanorods by surfactant-assisted electropolymerization for remarkably improved supercapacitive performances. Org Electron 69:98–105. https://doi.org/10.1016/J.ORGEL.2019.03.027
62. Shi Y, Zhang M, Zhao J, Zhang L, Cui X, Zhu X, Su J, Yang D, Li J (2021) Sodium dodecylbenzene sulfonate assisted electrodeposition of MnO_2@C electrode for high performance supercapacitor. J Electrochem Soc 168(12):122502. https://doi.org/10.1149/1945-7111/AC41F3
63. He Q, Liu XX, Wu R, Chen JS (2019) PVP-assisted synthesis of self-supported Ni_2P@carbon for high-performance supercapacitor. Research 2019. https://doi.org/10.34133/2019/8013285
64. Vidhya MS, Yuvakkumar R, Ravi G, Pannipara M, Al-Sehemi AG, Velauthapillai D (2022) PVP-assisted grass-like NiSe@ZnSe composite for environmental energy applications. J Mater Sci: Mater Electron 33(11):8409–8416. https://doi.org/10.1007/S10854-021-06304-8

65. Ojha GP, Muthurasu A, Dahal B, Mukhiya T, Kang D, Kim HY (2019) Oleylamine-assisted synthesis of manganese oxide nanostructures for high-performance asymmetric supercapacitos. J Electroanal Chem 837:254–265. https://doi.org/10.1016/J.JELECHEM.2019.02.021
66. Tian J, Xue Y, Wu K, Guo M, Zeng X (2021) TPAOH-assisted preparation of hexagonal $Ni(OH)_2$ nanoplates for supercapacitors. ChemistrySelect 6(48):13975–13981. https://doi.org/10.1002/SLCT.202103360
67. Xiang F, Zhou X, Yue X, Hu Q, Zheng Q, Lin D (2021) An oxygen-deficient cobalt-manganese oxide nanowire doped with P designed for high performance asymmetric supercapacitor. Electrochim Acta 379:138178. https://doi.org/10.1016/J.ELECTACTA.2021.138178
68. Zhang Z, Huo H, Wang L, Lou S, Xiang L, Xie B, Wang Q, Du C, Wang J, Yin G (2021) Stacking fault disorder induced by Mn doping in $Ni(OH)_2$ for supercapacitor electrodes. Chem Eng J 412:128617. https://doi.org/10.1016/J.CEJ.2021.128617
69. Shan QY, Guo XL, Dong F, Zhang YX (2017) Single atom (K/Na) doped graphitic carbon Nitride@MnO_2 as an efficient electrode Material for supercapacitor. Mater Lett 202:103–106. https://doi.org/10.1016/J.MATLET.2017.05.061
70. Yu X, Kang Y, Park HS (2016) Sulfur and phosphorus co-doping of hierarchically porous graphene aerogels for enhancing supercapacitor performance. Carbon 101:49–56. https://doi.org/10.1016/J.CARBON.2016.01.073
71. Kang J, Hirata A, Kang L, Zhang X, Hou Y, Chen L, Li C, Fujita T, Akagi K, Chen M (2013) Enhanced supercapacitor performance of MnO_2 by atomic doping. Angew Chem, Int Ed 52(6):1664–1667. https://doi.org/10.1002/ANIE.201208993
72. Roy A, Ray A, Sadhukhan P, Saha S, Das S (2018) Morphological behaviour, electronic bond formation and electrochemical performance study of V_2O_5-polyaniline composite and its application in asymmetric supercapacitor. Mater Res Bull 107:379–390. https://doi.org/10.1016/J.MATERRESBULL.2018.08.013
73. Sannasi V, Subbian K (2021) A facile synthesis of $ZnMn_2O_4/Mn_2O_3$ composite nanostructures for supercapacitor applications. Ceram Int 47(9):12300–12309. https://doi.org/10.1016/J.CERAMINT.2021.01.081
74. Zhang W, Quan B, Lee C, Park SK, Li X, Choi E, Diao G, Piao Y (2015) One-step facile solvothermal synthesis of copper ferrite–graphene composite as a high-performance supercapacitor material. ACS Appl Mater Interfaces 7(4):2404–2414. https://doi.org/10.1021/AM507014W
75. Vangari M, Pryor T, Jiang L (2013) Supercapacitors: review of Materials. J Energy Eng 2:72–79. https://doi.org/10.1061/(ASCE)EY.1943-7897.0000102
76. Borenstein A, Hanna O, Attias R, Luski S, Brousse T, Aurbach D (2017) Carbon-based composite materials for supercapacitor electrodes: a review. J Mater Chem A 5(25):12653–12672. https://doi.org/10.1039/C7TA00863E
77. Haghshenas M, Mazloum-Ardakani M, Tamaddon F, Nasiri A (2021) $CoFe_2O_4$@methyl cellulose core-shell nanostructure and their hybrids with functionalized graphene aerogel for high performance asymmetric supercapacitor. Int J Hydrog Energy 46(5):3984–3995. https://doi.org/10.1016/J.IJHYDENE.2020.10.253
78. Gao M, Guo ZY, Wang XY, Li WW (2019) Self-supported, sulfate-functionalized nickel hydroxide nanoplates with enhanced wettability and conductivity for use in high-performance supercapacitors. ChemSusChem 12(24):5291–5299. https://doi.org/10.1002/CSSC.201902397
79. Kalaiarasi J, Pragathiswaran C, Subramani P (2021) Green chemistry approach for the functionalization of reduced graphene and ZnO as efficient supercapacitor application. J Mol Struct 1242:130704. https://doi.org/10.1016/J.MOLSTRUC.2021.130704
80. Shaheen I, Ahmad KS, Zequine C, Gupta RK, Thomas AG, Malik MA (2020) Green synthesis of ZnO–Co_3O_4 nanocomposite using facile foliar fuel and investigation of its electrochemical behaviour for supercapacitors. New J Chem 44(42):18281–18292. https://doi.org/10.1039/D0NJ03430D

81. Zhang Q, Liu Z, Zhao B, Cheng Y, Zhang L, Wu HH, Wang MS, Dai S, Zhang K, Ding D, Wu Y (2019) Design and understanding of dendritic mixed-metal hydroxide nanosheets@N-doped carbon nanotube array electrode for high-performance asymmetric supercapacitors. Energy Storage Mater 16:632–645. https://doi.org/10.1016/J.ENSM.2018.06.026
82. Alam MW, Kumar VD, Ravikumar CR, Prashantha SC, Murthy HA, Kumar MA (2022) Chromium (III) doped polycrystalline $MgAl_2O_4$ nanoparticles for photocatalytic and supercapacitor applications. J Phys Chem Solids 161:110491. https://doi.org/10.1016/J.JPCS.2021.110491
83. Rashid AR, Abid AG, Manzoor S, Mera A, Al-Muhimeed TI, AlObaid AA, Shah SN, Ashiq MN, Imran M, Najam-Ul-Haq M (2021) Inductive effect in Mn-doped ZnO nanoribon arrays grown on Ni foam: a promising key for boosted capacitive and high specific energy supercapacitors. Ceram Int 47(20):28338–28347. https://doi.org/10.1016/J.CERAMINT.2021.06.251
84. Jia X, Wu Y, Chi J, Xiao Z, Dang Z, Zhang Q, Li B, Liu J, Wang L (2022) A $VO_3{}^-$-induced S^{2-}-exchange strategy to controllably construct a sub-nano-sulfide-functionalized layered double hydroxide for an enhanced supercapacitor performance. Mater Chem Front 6(18):2661–2669. https://doi.org/10.1039/D2QM00503D
85. Dinari M, Allami H, Momeni MM (2020) Construction of Ce-doped NiCo-LDH@CNT nanocomposite electrodes for high-performance supercapacitor application. Energy Fuels 35(2):1831–1841. https://doi.org/10.1021/ACS.ENERGYFUELS.0C03764
86. Aghazadeh M, Yavari K, Rad HF, Mohammadzadeh K (2020) Oxygen-functionalized graphitic carbon nitride nanosheets/$Co(OH)_2$ nanoplates anchored onto porous substrate as a novel high-performance binder-free electrode for supercapacitors. J Energy Storage 32:101743. https://doi.org/10.1016/J.EST.2020.101743
87. Liu W, Zhang Z, Zhang Y, Zheng Y, Liu N, Su J, Gao Y (2021) Interior and exterior decoration of transition metal oxide through Cu^0/Cu^+ Co-doping strategy for high-performance supercapacitor. Nano-Micro Lett 13(1):1–14. https://doi.org/10.1007/S40820-021-00590-X
88. Rosaiah P, Zhu J, Hussain OM, Qiu Y (2019) Facile and cost-effective synthesis of flower-like RGO/Fe_3O_4 nanocomposites with ultra-long cycling stability for supercapacitors. Ionics 25(2):655–664. https://doi.org/10.1007/S11581-018-2669-1
89. Ji Z, Ma D, Dai W, Liu K, Shen X, Zhu G, Nie Y, Pasang D, Yuan A (2021) Anchoring nitrogen-doped carbon quantum dots on nickel carbonate hydroxide nanosheets for hybrid supercapacitor applications. J Colloid Interface Sci 590:614–621. https://doi.org/10.1016/J.JCIS.2021.01.102
90. Ayman I, Rasheed A, Ajmal S, Rehman A, Ali A, Shakir I, Warsi MF (2020) $CoFe_2O_4$ nanoparticle-decorated 2D MXene: a novel hybrid material for supercapacitor applications. Energy Fuels 34(6):7622–7630. https://doi.org/10.1021/ACS.ENERGYFUELS.0C00959
91. Zhang X, Liao H, Liu X, Shang R, Zhou Y, Zhou Y (2020) Facile synthesis of Fe_2O_3 nanospheres anchored on oxidized graphitic carbon nitride as a high performance electrode material for supercapacitors. Int J Electrochem Sci 15:2133–2144. https://doi.org/10.20964/2020.03.54
92. Raj BGS, Ko TH, Acharya J, Seo MK, Khil MS, Kim HY, Kim BS (2020) A novel Fe_2O_3-decorated N-doped CNT porous composites derived from tubular polypyrrole with excellent rate capability and cycle stability as advanced supercapacitor anode materials. Electrochim Acta 334:135627. https://doi.org/10.1016/J.ELECTACTA.2020.135627
93. Liu Y, Guo D, Wu K, Guo J, Li Z (2020) Simultaneous enhanced electrochemical and photoelectrochemical properties of α-Fe_2O_3/graphene by hydrogen annealing. Mater Res Express 7(2):025032. https://doi.org/10.1088/2053-1591/AB6C8C
94. Jiang X, Shi G, Wang G, Mishra P, Du J, Zhang Y (2020) Fe_2O_3/hemp straw-based porous carbon composite for supercapacitor electrode materials. Ionics 26(8):4039–4051. https://doi.org/10.1007/S11581-020-03547-Z
95. Khan AJ, Khan A, Javed MS, Arshad M, Asim S, Khalid M, Siyal SH, Hussain S, Hanif M, Liu Z (2020) Surface assembly of Fe_3O_4 nanodiscs embedded in reduced graphene oxide as a high-performance negative electrode for supercapacitors. Ceram Int 46(11):19499–19505. https://doi.org/10.1016/J.CERAMINT.2020.04.303

96. Javed MS, Khan AJ, Hanif M, Nazir MT, Hussain S, Saleem M, Raza R, Yun S, Liu Z (2021) Engineering the performance of negative electrode for supercapacitor by polyaniline coated Fe_3O_4 nanoparticles enables high stability up to 25,000 cycles. Int J Hydrog Energy 46(15):9976–9987. https://doi.org/10.1016/J.IJHYDENE.2020.04.173
97. Zhang X, Yang W, Liu A, Guo Z, Mu J, Hou J, Che H (2020) Anchoring mesoporous Fe_3O_4 nanospheres onto N-doped carbon nanotubes toward high-performance composite electrodes for supercapacitors. Ceram Int 46(14):22373–22382. https://doi.org/10.1016/J.CERAMINT.2020.05.319
98. Rajagopal R, Ryu KS (2020) Homogeneous MnO_2@TiO_2 core-shell nanostructure for high performance supercapacitor and Li-ion battery applications. J Electroanal Chem 856:113669. https://doi.org/10.1016/J.JELECHEM.2019.113669
99. Zhou X, Lu Y, Zhen Y, Wang Z, Zheng X, Wei M, Hong Z (2020) Facile fabrication of highly porous TiO_2 microrods anode with enhanced Al-ion storage for hybrid capacitors. J Power Sources 453:227857. https://doi.org/10.1016/J.JPOWSOUR.2020.227857
100. Zhao J, Burke AF (2021) Review on supercapacitors: technologies and performance evaluation. J Energy Chem 59:276–291. https://doi.org/10.1016/J.JECHEM.2020.11.013
101. Bokhari SW, Siddique AH, Yue X, Singh H, Hayat MD, Gao W (2020) A hybrid composite of rGO/TiO_2 as a double layer electrode with improved capacitance performance. Int J Energy Res 44(14):12197–12203. https://doi.org/10.1002/ER.5864
102. Zhu J, Wang Y, Xu Y, Li S, Ren J, Cai W (2020) Synthesis of porous flower-like Ni-Co-Mo-S nanostructures on Ni foam for battery-supercapacitor hybrid devices. Int J Energy Res 44(4):2864–2874. https://doi.org/10.1002/ER.5102
103. Choudhary N, Li C, Chung HS, Moore J, Thomas J, Jung Y (2016) High-performance one-body core/shell nanowire supercapacitor enabled by conformal growth of capacitive 2D WS_2 layers. ACS Nano 10(12):10726–10735. https://doi.org/10.1021/ACSNANO.6B06111
104. Yu J, Yu C, Guo W, Wang Z, Ding Y, Xie Y, Liu K, Wang H, Tan X, Huang H, Qiu J (2022) Insight into the effects of current collectors and in situ Ni leaching in high-voltage aqueous supercapacitors. Adv Funct Mater 32(34):2204609. https://doi.org/10.1002/ADFM.202204609
105. Zheng W, Cheng Q, Wang D, Thompson CV (2017) High-performance solid-state on-chip supercapacitors based on Si nanowires coated with ruthenium oxide via atomic layer deposition. J Power Sources 341:1–10. https://doi.org/10.1016/J.JPOWSOUR.2016.11.093

Всё для победы!
НАРОДНЫЙ ФРОНТ
https://pobeda.onf.ru/
LET'S HELP THE RUSSIA

Chapter 13
Functionalization Techniques for the Development of Conducting Polymer-Based Supercapacitors

C. G. Jinitha and S. Sonia

1 Introduction

Polymer is one of the principal commercial items that have the largest influence on the worldwide market. Polymers are macromolecules composed of several repeating subunits called monomers. The monomers are formed by atoms or grouped atoms linked together by chemical bonds. The process of formation of polymers is called polymerization. Polymers play an inevitable role in fabricating energy storage devices due to their exceptional structural, morphological, mechanical, thermal, and electrochemical properties. Polymers are promising candidates for the configuration of individual components of supercapacitors or any other energy storage devices and act as a multifunctional system to achieve high performance and highly durable energy storage systems. The most fascinating features of polymers are controllable geometrical shapes as per the requirement, and tuneable morphology and properties by incorporating appropriate fillers, especially nanofillers. The application of polymers in the fabrication of supercapacitors can be broadly classified into four groups, including electrodes, binders, electrolytes, and separators. These are the essential components of a supercapacitor's cell design. The optimization and modification of properties of these components are significant tasks for the apprehension of achieving a high-performance energy storage system. Polymers contain a variety of properties, including those that make them desirable for usage in specific contexts. Numerous polymers (i) have a lower density than ceramics or metals, (ii) are resistant to corrosion caused by the environment and other factors, (iii) are compatible with human tissue, and (iv) show outstanding resistance to the flow of electrical current [1]. As an example of how resistant polymers are to chemical attack, consider all of the

---

C. G. Jinitha · S. Sonia (✉)
Department of Physics, Holy Cross College (Autonomous), Nagercoil, Manonmaniam Sundaranar University, Abishekapatti, Tirunelveli 627012, India
e-mail: sonianst10@gmail.com

© The Author(s), under exclusive license to Springer Nature Singapore Pte Ltd. 2024

C. M. Hussain and M. B. Ahamed (eds.), *Functionalized Nanomaterials Based Supercapacitor*, Materials Horizons: From Nature to Nanomaterials,
https://doi.org/10.1007/978-981-99-3021-0_13

household cleaners that come in plastic containers and that you keep in your home. Reviewing the safety information labels that explain what happens to the skin, eyes, and when the chemical is swallowed or when it comes into contact with the skin, it has an effect on the body or eyes or is consumed will emphasize how important it is for the plastic container to be resistant to the toxins that it will be exposed to. While some plastics are quickly dissolved by solvents, other plastics provide safe, non-breakable containers for solvents that are very aggressive.

2 Polymers

The phrase "Polymer" comes from the terms "Poly", which means many, and "Mer", which means bonds. Polymer by itself has weak qualities, hence the addition of nanomaterials can enhance polymer's properties. Because they are ecofriendly, recyclable, and sustainable, because of such qualities polymer nanoparticles are favoured.

3 Classification of Polymers

See Fig. 1.

3.1 Elementary Polymer Framework

There are four primary configurations of polymers, each of which is depicted in the following figure: In the real world, certain polymers may contain a combination of different types of fundamental structures. The four fundamental architectures of polymers are linear, branching, cross-linked, and networked structures.

Linear polymers: Linear polymers have lengthy chain lengths and can be compared to "spaghetti". Van der Waals or hydrogen bonding, both of which are very weak

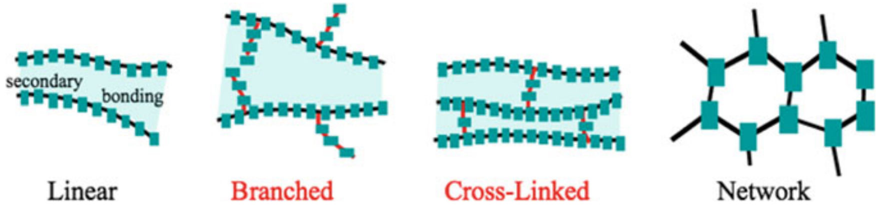

Fig. 1 Types of polymer structure. Reprinted from William D. Callister, David G. Rethwisch, Fundamentals of Materials Science and Engineering, Wiley, 5th Edition [2]

forces, are often responsible for keeping the long chains together. Linear polymers are often thermoplastic because the bonding types they use are quite simple and straightforward in terms of breaking when subjected to heat. The heat dissolves the connections that hold the lengthy chains together, which in turn makes it possible for the chains to flow around each other and reshape the material. When the polymer is allowed to cool, the bonds between the long chains are able to rebuild, which results in the polymer being more rigid.

Branched polymers: The difference between linear polymers and branched polymers is that branched polymers have shorter chains dangling from the spaghetti-like backbone of the larger ones. Because the shorter chains in branched polymers can cause inefficiencies in the packing of the polymers, branched polymers often have a lower density than linear polymers with the same characteristics. The bonds between the branched polymer chains are often destroyed by heat because the short chains do not link longer backbones to one another, which allows the polymer to have the properties of a thermoplastic. Nevertheless, there are some extremely complicated branched polymers that are resistant to this “melting”, and as a result, they disintegrate becoming rigid in the process, prior to softening, which is another way of saying that they are going through the process of thermosetting.

Crosslinked polymers: Crosslinked polymers are similar to ladders. The chains connect each individual backbone to all of the others. Crosslinked polymers, on the other hand, are held together by covalent bonding, in contrast to linear polymers, they are kept together by van der Waals forces, which are significantly weaker. Because of this significantly stronger bond, the vast majority of cross-linked polymers are thermosetting, with very few notable exceptions to the general rule. These exceptions include cross-linked polymers that happen to break their crosslinks at temperatures that are quite low.

Networked polymers: Networked polymers are complicated polymers that are tightly coupled to one another in order to produce a complicated network of links in three dimensions. These polymers, which are classified as thermosetting polymers due to the fact that it is practically hard to soften them by heating them without destroying the underlying polymer structure.

3.2 Copolymers

Copolymers are any polymers that are formed by the combination of two different monomers into a single polymer chain. The classification of copolymers is the topic that we shall investigate next. It is not necessary for monomers to be made up of only one kind of atom; however, while discussing a particular monomer, it is assumed that the monomer in question has the same composition structure (Fig. 2).

When a scientist creates a polymer by starting with two different monomers, there are various different structures that can result. These architectures are illustrated

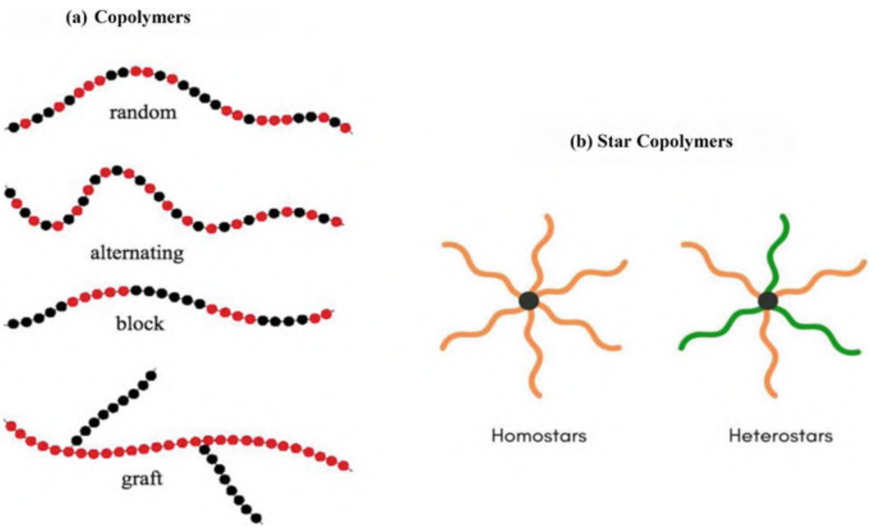

Fig. 2 **a** Different types of copolymers, **b** types of star copolymers. **a** Reprinted from, William D. Callister, David G. Rethwisch, Fundamentals of Materials Science and Engineering, Wiley, 5th Edition [2]. **b** Reprinted from open access source [3]

in the following image. Random, alternating, block, and graft structures are the four fundamental types of layouts. It should come as no surprise that if the two monomers are organized in any old way, the resulting copolymer will be referred to as a random copolymer. In an alternating copolymer, each monomer is linked to the other in turn to create a pattern that looks like ABABABA… When using block copolymers, it is feasible to create repeating structures that are more complicated, such as AAABBBAAABBBAAA… Graft copolymers are formed when chains of a second kind of monomer are attached to the backbone chain of a first type of monomer.

Random Copolymer: A random copolymer is a type of copolymer in which the monomer residues are dispersed throughout the polymer molecule in an unpredictable manner. One example of this type of copolymer is one that is generated via free-radical copolymerization and contains both vinyl chloride and vinyl acetate.

Alternate Copolymer: These copolymers have a regular, repetitive, and alternating arrangement of two monomeric species. Example: Nylon 6,6. The general formula for the monomers A and B could be given as -(-A-B-) n- or -A-B-A-B-A-B-A-B-A-B-

Block Copolymer: A block copolymer is the name given to the resultant polymeric chain that is created when two or more homopolymer chains are linked together by covalent connections. A junction block is the name given to the intermediate unit when they connect together. It’s possible for them to be di-block or even tri-block copolymers. Examples Acrylonitrile butadiene styrene (SBS rubber).

Grafted Copolymer: Branched copolymers with special side chains that have a distinct structural composition in comparison to the main chain. In this case, the main chain is capable of forming covalent bonds with one or more of the side chains. An illustration of this would be the ability to graft polystyrene chains into polybutadiene.

Star Copolymer: There is potential for many polymeric chains to be joined into the same central core unit. There are further types of branching copolymers, such as brush and comb copolymers. The centre of the star-shaped polymers can serve multiple purposes. At least three polymer chains can be seen extending outward from the centre in all directions. These arms may be chemically similar, in which case the stars are referred to as homostars; alternatively, they may differ from one another, in which case the stars are referred to as heteroarm stars.

4 Functionalization Techniques for Conducting Polymer

The process of chemically modifying polymers, also known as functionalization, can be accomplished by a wide number of distinct organic reactions. In order to establish a generic categorization of post-polymerization alterations on the basis of the mechanical characteristics, this section will provide a quick review of numerous reactions.

The investigation of organic conducting polymers has made significant headway in recent years, and many academics with an interest in the topic are excited for the future to undertake additional study in the domain of optoelectronics and related fields. Displays, solar panels, field-effect transistors, photodetectors, supercapacitors, sensor systems, lithium-ion batteries, lasers, and different electrochromic devices are some examples of the optoelectronic devices. Conducting property is recognized to have many uses due to its beneficial qualities, which include thermal stability, electroluminescence, facile tunability, adaptability, and processability. The topic of discussion in this section is conductive polymers and how functionalization can be used to enhance the properties of conducting polymers. Also discussed are the current state of implementations of conducting polymers in semiconductor applications as well as their potential for the future.

4.1 Additions

In its most basic form, an addition reaction can be described as the reaction that occurs when tiny molecules combine with functional groups with the purpose of producing a particular object that contains all of the atoms that were present in the original components. Incorporating hydrogen, oxygen, or halogens into macromolecules that already contain carbon-carbon C=C double bonds is considered to be one of the most significant addition reactions. It is important to note that the solubility as well as the polymers' chemical stability may be impacted through addition processes. Hydrogenation of polymers is one of the most essential and widely used ways of material modification in modern technology. Due to the fact that it is possible to alter the microstructure, hydrogenation of polystyrene as well as hydrogenation of polydienes has been increasingly popular over the past several years [4]. Investigations have also been conducted into the processing of unsaturated polymers through hydrohalogenation and halogenation. Polybutadiene is brominated, which then leads to the formation of polymers that are flame-resistant, which is one example. Radiation-induced addition is another approach that can be used instead to incorporate halogens into polymers [5]. Epoxidation of double bonds is a further method that can be utilized in order to impart functionality into unsaturated polymers. One example of this is the oxidation of polybutadiene through epoxidation [6]. Over the past few years, the process of altering unsaturated polymers using thiols as a catalyst by means of a thiol-ene reaction has become one of the approaches that is utilized most frequently.

4.2 Substitutions

The production of functional polymers can also be accomplished through the utilization of a beneficial family of processes known as substitution reactions. By use of free radical substitution, polyethylene (PE) is chlorinated which is a good illustration of this in practise. At this point, chlorination initiates itself in the portions of the crystalline surface that are amorphous [7]. In a significant number of cases, hydrolysis and esterification reactions are also performed. A reaction that takes place relatively regularly is the esterification of poly (methylacrylic acid) with carbodiimides functioning as the condensing agents. In many cases, an intermediate form of the cyclic anhydride is the first structure to appear during this reaction. This structure then combines when there is alcohol present to produce an ester in its final state. Esterification of cellulose, which is still performed on a commercial scale [8, 9], is an additional example of a frequent chemical process. The hydrolysis of poly (vinyl acetate), which results in the production of poly (vinyl alcohol), is an example of an essential hydrolysis reaction. This reaction is particularly relevant due to the difficulties of synthesizing the polymer directly from the relevant monomer [5]. In addition, altering the degree of hydrolysis can lead to the production of polymers with a variety of distinct characteristics. Due to the polymer's heightened crystallinity, the solubility of the resulting polymers in water at room temperature is reduced when the degree to which poly (vinyl alcohol) is hydrolyzed by water is increased.

4.3 Eliminations

The removal of alcohols, hydrogen halides, water, and other tiny molecules is one of the most essential and widely used procedures for the modification of polymers. In the macromolecule of the original polymer, unsaturated double or triple bonds, or even heterocycles, are created as a result of the elimination [10].

4.4 Isomerizations

Isomerizations, unlike the other reported reaction classes, alter the chemical structure of the macromolecule without affecting its molecular weight. The cis-trans isomerization of polydienes is one example of a configurational isomerization, which can be produced when ultraviolet light is radiated on a substance when a radical transfer agent is present. This isomerization can be thought of as a reversed version of the normal isomerization process. In addition, polymers that contain chromophoric groups have drawn a lot of attention recently. In particular, azobenzene-containing polymers have garnered a lot of attention because of the cis-trans isomerization of azobenzene [5, 11]. Another illustration that has been established for protein chemistry is the native chemical ligation. During this reaction, an N-terminal cysteine residue goes through a process known as reversible transthioesterification, which ultimately leads to the production of a thioester intermediate. This thioester intermediate then goes through a step in which it undergoes an S, N-acyl shift isomerization, which ultimately results in the creation of an amide bond in its native form [17].

5 Conducting Polymer for Supercapacitors

Utilizing materials with a large surface area, such as activated carbons and the capacitive properties of the electrochemical double layer have enhanced the energy density and storage capacity of capacitors. The first devices in a category of devices known as supercapacitors were created by using two electrodes made from the same material.

According to the method by which they store charge, supercapacitors are divided into the following three categories: Pseudocapacitors, electric double-layer capacitors (EDLCs), and asymmetric (hybrid) supercapacitors. EDLCs rely on non-faradaic methods. For instance, charged particles and ionic species are absorbed in the electrode–electrolyte interface to facilitate charge storage in an EDLC. By utilizing extremely reversible faradic processes, like redox interactions between the electrolyte and the surfaces of electrochemically active materials, pseudocapacitors are able to store energy. These reactions take place in pseudocapacitors. In most cases, they are made up of different hydroxides or oxides of metal. Asymmetric supercapacitors make use of a wide variety of electrode materials, each of which possesses increased capacitance and contributes to an increase in both the energy density and operating voltage of the device. These have been designed as a response to the difficulties of yield loss, low capacitance, and high resistivity caused by low recyclability with hydroxides and metal oxides. These issues have been brought about as a result of poor cyclability when combined with hydroxides and metal oxides.

The inertness of most commercial nanomaterials and polymers, the development of these materials for specific applications in a wide range of sectors is constrained. As a result, modifications on the surface must be performed in order to improve their adhesion, wetting, and printing properties. This is accomplished by bringing a variety of polar and other functional groups onto the surfaces of both nanostructures and polymers. During the course of the last few decades, a number of surface functionalization techniques have been developed, all of which generally adhere to the same pattern: foremost, the surface of the polymer is where the binding of primary reactive functional groups to the chain ends occurs; then, the modification of the reactive surface with hydrophobic and hydrophilic monomers, active/bioactive agents, polymers, or oligomers to achieve specific surface characteristics that are tailored to the requirements of the end use; and finally, the application of the surface functionalization technique [12].

In order to generate and store renewable energy in a timely and consistent manner, efficient energy storage techniques are required due to the intermittent nature of the resources that make up renewable energy. Because of this, there has been a rise in the number of scientific studies that focus on electrochemical energy storage devices, such as batteries, capacitors, and cells, which are among the many storage systems that have been essential. In this field, lithium-ion batteries, which are built on four basic components consisting of a separator, an electrolyte, an anode, and a cathode, are the perfect application for polymer nanoparticles. Because of their hydrophobic surfaces, the porous polyolefin-based polymers utilized in separators today, such as polypropylene and polyethylene, are polymers based on polyolefins and are employed to restrict electrolyte diffusion [13, 14].

5.1 Graphene-Polymer Supercapacitors

In the development of new materials as a two-dimensional (2D) building block, graphene's outstanding mechanical, electrical, and thermal properties have garnered significant attention in recent years. However, in order to make use of these properties in novel materials, it will be necessary to develop procedures that will allow carbon flakes that are only one atom thick to be assembled into structures that are macroscopically organized. In addition, in order for these macroscopic structures to play a role in a variety of devices utilized for a variety of applications, such as solar cells and supercapacitors, they need to have exceptional electrical, mechanical, and thermal properties. The use of graphene nanostructures in supercapacitor devices can be made easier by integrating the nanostructures into a matrix composed of polymer. This is one of the more straightforward techniques.

As was said before, polymer matrix materials are among the most vital constituents of graphene-derived nanostructure-polymer composite supercapacitor electrodes, more specifically polymer binders. However, owing to their insulating nature, these polymer binders have a few drawbacks that must be considered. As was discussed in the prior section, the presence of non-conductive binders can result in a reduction in conductivity, which in turn results in a reduction in both the supercapacitors' energy density and their overall capacitance. Electrical double-layer capacitance also known as EDL capacitance, is the primary concept upon which the operation of supercapacitor devices, such as graphene-derived nanostructure-polymer composite electrodes, is predicated. Charge and discharge of the electrical double layer capacitor (EDLC) are both caused by and contributed to by the process by which ions are absorbed by and then desorbed from the electrical double layer.

Many researchers are interested in using electrically conductive polymers as a polymer matrix or binder in supercapacitor electrode materials. This is because electrically conductive polymers are excellent candidates for the perfect matrix material, thanks to characteristics such as light-weight, elasticity, simple thin film fabrication, and processability [15]. This is because electrically conductive polymers are perfect candidates to serve as the optimal matrix material, because of the qualities that they possess. When historical research is conducted, it is discovered that a number of conductive polymers were utilized in the production of supercapacitor electrodes. Some examples of these polymers include polyprrole (PP) [16], polyindophenine [17], polyaniline (PANi) [18–20], p-phenylenevinylene (PPV) [21], and polythiophene [22]. PANi and PPy are the materials that are the most suitable and likely to be successful for application in electrodes as matrix materials due to their higher energy density, fast redox reactions, low cost, high conductivity, and ease of synthesis [23]. These polymers are the only ones among these that meet all of these criteria. In addition, PPy and PANi are utilized in neutral and low pH solutions for the purpose of supercapacitor electrodes [15, 24].

5.2 PANi

PANI is one of the conducting polymers, and due to its environmental stability, low cost, and high capacitance [25–27], it is anticipated that it will be an excellent option for this purpose. However, Due to the insufficiency of mechanical stability throughout the charging/discharging process of the supercapacitor, it is challenging to achieve high cycle stability in a device by merely employing PANi. This is because of how the PANi weakens the mechanical stability. For the purpose of enhancing the capacity of supercapacitors to store energy, hybrid electrode materials have been employed to their maximum potential so as to make the most of their benefits. There have been a number of researches published in the scientific literature that concentrate on hybrid electrode materials; nevertheless, graphene-PANi composites have received very little attention. In our opinion, graphene-PANi nanocomposites will become increasingly popular in the near future due to the exceptional and one-of-a-kind features that they possess [28]. Several labs have performed experiments on various graphene/PANi composites.

Conductive polymers, such as PANI, have been utilized in the process of developing electrode materials for use in supercapacitors [29]. In point of fact, PANI is not a material that is suitable for use in batteries but rather a substance that is suitable for use in supercapacitors [30]. The morphology and the doping level have a substantial impact on the particular capacitance of the PANI supercapacitors. This specific capacitance can be modified by regulating the synthesis procedure or making post-synthesis adjustments [31]. Unfortunately, the majority of PANI-based supercapacitors have a specific capacity of less than 1000 F/g and have a rather low cyclic stability, both of this could potentially restrict the applications. The development of nanocomposites of PANI with carbon nanomaterials has, on the other hand, been the subject of a significant amount of research as a means of enhancing the specific capacitance and electrochemical behaviour of supercapacitors. For instance, very high specific capacitance of 2200 F/g has been achieved for electrodes made via PANI deposition on porous carbon [32]. Yang et al. [33] observed that PANI/MWCNT had a high specific capacitance (1065 F/g) as well as outstanding cyclic stability (92.2% capacity retention after 1000 cycles). In addition, several researchers have observed that the material possesses outstanding cycle stability (more than 92%), as well as good specific capacitance (328–560 F/g) [34–38].

5.3 PPy

Polypyrrole, often known as PPy, is an excellent electroactive substance that can be used for electrode materials, particularly in asymmetric supercapacitors, due to the fact that it is safe for the environment, demonstrates good stability, is easy to synthesize at large-scale production, and is inexpensive [17]. This makes it an ideal candidate for use in asymmetric supercapacitors. The capacitors that are utilized as electrodes in composites made up of conductive polymers and carbonaceous materials have been the subject of a number of research projects that have been carried out in recent years. The comparison of different PPy synthesis processes (chemical and electrochemical), the improvement of the shape of the polymer surface, and the influence that carbon-based materials have on the efficiency of electrodes in supercapacitors are the primary focuses and driving forces behind these studies.

Deng et al. [39] demonstrated how changing the amount of GO present and the charge density while employing the electrochemical deposition technique caused the surface of the GO-PPy composite to become more textured. Jingping et al. [40] used an in situ polymerization approach to make the Gr-PPy composite. The porous structure produced a specific surface area that was 108 m^2 /g, which was 97.56% bigger than the intrinsic surface area of PPy. This was accomplished by using an in-situ polymerization process. When gr is added to PPy, the surface of the material changes from being smooth to being rough, as attested to by a number of authors [41–45]. The increase in the surface area of the materials has been attributed to the roughness and porosity of the composite, which in turn has been attributed to the increase in the surface area of the material. The increase in PPy's surface area is beneficial for the production of supercapacitors because a greater surface area is required for increased charge mobility. PPy has a surface area modification that is essentially beneficial for this process.

According to the findings of Liu et al. [46], it is possible to create a nanocomposite with a significantly increased specific surface area through the incorporation of sulfonated rGO and PPy. The easy polymerization process was utilized by Liu et al. [46], and the resulting electrode has a specific capacity of 265.60 F/g at a current density of 1 A/g and maintains an efficiency of 90% for around 1000 cycles [46].

5.4 Pedot

Poly(3,4-ethylenedioxythiophene), more commonly known as PEDOT, was invented for the very first time in the 1980s [47] by a team of researchers working at Bayer AG research centers in Germany. Conductivities in its doped states have the potential to reach as high as 500 S cm^{-1} [48–50]. PEDOT is a conductive polymer that differs from other conductive polymers in that it possesses a relatively low theoretical gravimetric capacitance (210 F g^{-1}) [51]. In spite of this, it has a wide electrochemical window (1.2–1.5 V), high charge mobility, high conductivity, low oxidation potential, chemical and thermal stability, which all contribute to its quick electrochemical kinetics. Moreover, it is thermally stable. PEDOT's large molecular weight, which results in poor specific capacitance, is a drawback for its usage as an electrode in supercapacitors, however. PEDOT's other advantage is its inexpensive cost.

The results of a study conducted by Wilamowska et al. suggest that electrodeposited pEDOT/rGOx composite electrodes display approximately 10 mF cm^{-2} when they are deposited with a charge of 0.2 C cm^{-2}, and they display approximately 30mF cm-2 when they are deposited with a charge of 0.8 C cm^{-2}. In a separate work, Damlin et al. found that the capacitance of graphene oxide PEDOT composite electrodes made by the electrodeposition method by cyclic voltammetry from a GOx solution in ionic fluids is determined to be 39 mF cm^{-2}; it rose to 43 mF cm^{-2} upon electrochemical reduction of graphene oxide [50]. When it comes to the processes that are used in the manufacturing of composites, there have been several research conducted under a variety of settings. In their study from 2011, Alvi et al. revealed that a graphene-PEDOT nanocomposite that was synthesized using the chemical oxidative polymerization process exhibited a specific capacitance value that was 374 F g^{-1} at its maximum [52]. In addition, a work that was carried out in 2016 by Alabadi and colleagues revealed the production of a graphene oxide-(Thiophene-2, 5-diyl)-co-(benzylidene) composite using the polymerization method [53]. This composite had a specific capacitance of 296 F g^{-1}. The significant differences in capacitance values that were discovered for various pEDOT/GOx and pEDOT/rGOx composites emphasize how important it is to perfect the fabrication process in terms of the materials that go into the first product, the concentration of the solvent, the substrates, compatibility of the synthesis process with the elements, and so on are some of the factors that are taken into consideration [50].

6 Metal Oxide-Polymer Supercapacitors

In this section, we will review the latest developments that have taken place in the field of 2D metal oxides and hydroxides, as well as their hybrids with graphene, which is one of the prospective options that is based on carbon. In order to acquire 2D metal oxides, the most common approaches that have been utilized thus far are referred to as "top-down" and "bottom-up" procedures. In addition, the numerous design and synthesis methodologies for optimizing the structural morphology, surface characteristics, and long-term functioning of graphene at electrified interfaces are available. These strategies aim to maximize the structural long-term operation stability, surface properties, and structural morphology stability. These tactics intend to maximize the ionic and electrical conductivity of the surface, as well as the stability of the structural morphology. Changing the electrode materials in such a way as to alter their electrochemical properties, it is possible to create a supercapacitor electrode that has a high specific capacitance in addition to outstanding cycle stability and good rate capability.

The most common types of materials that can function as active electrochemical pseudocapacitors are hydroxides and metal oxides. They are well-known for their high theoretical capacitance, low cost (as a result of their abundance in nature), and high energy density. The effectiveness of these materials as supercapacitors has been hindered, however, by their low intrinsic conductivity as well as other deficiencies. As a result, in order to make even greater strides in their performance, 2D nano structural ultrathin hydroxides and metal oxides have been intensively explored and employed in supercapacitors due to the benefits that they offer, which include a high specific surface area and an improved planar electrical conductivity.

For instance, Peng et al. reported that a hierarchical NiO/NiMn-LDH nanosheet array on Ni foam was created using a straightforward two-step process. This array demonstrated a high specific capacitance (937 F g^{-1} at 0.5 A g^{-1}) as well as strong cycling stability (91% retention after 1000 cycles at 5 A g^{-1}). The synergistic features of hierarchical NiO/LDH nanosheet composites on a conductive substrate are what contribute to the increased electrochemical performance [54]. Furthermore, it has been claimed that solid-state symmetrical supercapacitors can be created on a large scale by ultrasonic exfoliation in ethanol/water using materials such as MoO_3, MnO_2, and RuO_2 nanosheets, among others [55]. This process can be carried out in ethanol/water.

Combining graphene and other metal oxides or hydroxides has resulted in a significant amount of recent development in the production of high-performance materials for the storage of electrical energy. As a consequence of the utilization of graphene, the conductivity of the material used for the pseudocapacitor electrode is increased, Additionally, the limitations brought about by graphene's relatively low specific capacitance as an electrode material for double-layer capacitors are removed. In addition to this, the benefits of the two are combined to create a significant enhancement in the capacitance performance, which is a practical method for enhancing the metal oxide/hydroxide electrode materials' electrochemical performance.

7 Polymer Nanocomposites in Water Treatment and Food Packaging

Polymer nanocomposites supercapacitors can be expressed in a wide variety of applications, such as the purification of water and the packaging of food. At physiological pH and temperature, polysaccharide-based cross-linked nanocomposites are insoluble in water but expand to several times their dry weight. The ability to absorb water is one of the most essential characteristics of these nanocomposites.

8 Water Treatment

Pollutants causing serious environmental concerns are mostly responsible for water pollution. The toxicity of heavy metals is one of the primary environmental issues addressed by both industrialized and developing nations. Chitosan is one of the remarkable biopolymers found in nature. It is used in a variety of applications and is found in large quantities as waste from the shrimp and crab industries. Biopolymers are favoured because of their natural origin and abundance. Among the current research interests are chemically functionalized chitosan-based nanocomposite films and strips that can clean textile and tannery effluents. Existing water treatment systems are costly, generate secondary contaminants in sludge, and are ineffective at treating effluents containing low metal concentrations. Adsorbents that are commercially accessible, such as activated carbon, are very effective but expensive. The processing of shellfish, krill, shrimps, and crabs generates a substantial amount of chitinaceous waste, which can be turned into chitosan as a low-cost adsorbent via partial deacetylation. Among the numerous biopolymers, chitosan has the highest sorption capacity for several metal ions, presumably due to the presence of a primary amine at the C-2 position of the glucosamine residues. However, it has disadvantages including softness, a tendency to agglomerate or form gels, and the lack of reactive binding sites. However, the addition of nanoparticles improves this biopolymer's use.

Smart polymers are those that alter their properties in response to environmental factors. Cross-linked networks based on polysaccharides are one of the most important groups of nanocomposites and have numerous applications. The contamination of water by industrial effluents, such as dyes, polyaromatic chemicals, and heavy metal ions, is one of the most important environmental problems and has negative health implications. Water contamination has become the primary worry and priority for the majority of industries. The method of adsorption is one of the most recommended to remove toxic chemicals from water. Natural polysaccharides and their derivatives-based cross-linked nanocomposites are known to be one of the best absorbents. The method is a low-cost green technology. Additionally, the crosslink density, the degree of flexibility, and the amount of space between the polymer chains all have a role in the water-absorbing capacity.

These nanocomposites have a huge surface area as well as a specific propensity for removing heavy metals from aqueous systems. The use of nanocomposites for the adsorption of various pollutants from contaminated water, such as heavy metal ions and dyes, has attracted significant interest due to the characteristic properties of nanocomposites. These properties include their high surface-to-volume ratio, low internal diffusion resistance, ultra-small dimensions, and very large surface area. It has been demonstrated that metal oxide nanoparticles, such as ferric oxide, cerium oxide, magnesium oxide, titanium oxide, and aluminium oxide, are highly effective at removing aqueous pollutants.

Graphene is one of the best doping materials along with polymer nanocomposite for the electrode materials for water treatment. Since graphene has superior properties, as compared to polymers, graphene-based polymer composites are used in a variety of applications. When compared to pure polymer, graphene-based polymer composites exhibit improved gas barrier, electrical, mechanical, flame retardant, and thermal capabilities. Graphene-based polymer composites also exhibit superior mechanical, flame retardant, and thermal qualities [56].

According to Bazylak et al., the PMC framework was developed using CBD to remove biological and chemical contaminants from wastewater. The synthetic framework adsorbs Cr (VI), CR-dye, E. coli, and S. aureus effectively. Maximum adsorption capacities for Cr (VI) and CR-dye were 76.5 and 714 mg g^{-1}, respectively. The proposed mechanism demonstrates that adsorbent charges contribute to electrostatic attraction. Hierarchical PMC frameworks are promising adsorbents for removing biological and chemical pollutants from wastewater due to their exceptional efficiency, a simple manufacturing process, and a high surface charge [57].

9 Food Packaging

A unique technology that is capable of checking food for safety and quality throughout its shelf-life is currently making its way into the food industry in the form of intelligent food packaging. This method makes use of sensors and indicators that are affixed to the packaging and that monitor alterations in the physiological fluctuations of the products due to both chemical and microbial degradation. These indicators, which often change colour to communicate information, such as the level of freshness of the product that has been packaged, are designed to be easily recognized by both the consumer and the food distributor. One common example of this type of information is the degree of freshness. On the other hand, the vast majority of the indicators that are utilized today are made of synthetic materials that are neither renewable nor biodegradable. Because there is an urgent need to increase the environmental friendliness of food packaging, the selection of sensors ought to take this prerequisite into consideration as well. Because of this, the purpose of this work is to review the most recent information on bio-based sensors. Compounds derived from natural sources were used in the production of these sensors, and they have the potential to operate as smart or intelligent food packaging when combined with biopolymers. The following is a summary of its applicability in a variety of perishable foods. It should come as no surprise that bioactive extracts, including compounds like anthocyanins, derived from a wide range of different sources, including waste materials from the agriculture and food industries, present a significant possibility of performing the function of biosensors. This potential can be seen in the fact that bioactive extracts can be obtained from a wide range of sources. However, in order for this technology to evolve and reach a stage where it can be used commercially, there are still some barriers that need to be overcome [58].

The fact that starch is inexpensive, readily available, non-toxic, and renewable in addition to being able to be used in applications such as film formation, food packaging, biosensors, and supercapacitors has garnered a lot of attention in recent years [59]. Because of their potential to have an immediate impact on people's well-being, polymer materials are increasingly being recognized as an essential component of the food sector.

The work done by Guerraf et al. is part of a larger initiative to find efficient and safe alternatives to the conventional methods used to package foods. This initiative is part of a larger framework. In this particular setting, the utilization of electronic CPs paired with cellulose as intelligent touch materials have been proved to hold a great deal of promise. On carbon fibres, homogeneous and firmly adhesive PEDOT and PAni coatings with integrated AgNPs were developed further. The refined nanocomposites have demonstrated some very interesting sensory features with respect to the vapours of hazardous ammonia and acetone. In addition, both PEDOT and PAni demonstrated a significant antibacterial impact against strains of S. aureus and E. coli, and, predictably, bactericidal efficacy improved following the introduction of AgNPs. In addition to this, the composites exhibited increased antioxidant capacity, which prevented the oxidation of food components and thus, increased their storage life. This resulted in the items having a longer life span. In the packaging industry, it is necessary to make use of innovative materials that are able to communicate with their surroundings and identify any disruptions that may occur inside the system for which they were developed. Because of its intelligent features, the newly developed material may prove to be an appealing alternative to the standard packaging that is now in use. These properties have the potential to make goods safer and extend the amount of time they may be stored. The newly discovered approach has showed that it is an economical, straightforward, and environmentally friendly process for the production of CP-based materials. This is one of the reasons why it is suited for use in industrial applications. As a result, the method that was just described can be applied to the production of extremely effective food containers on a massive scale [60].

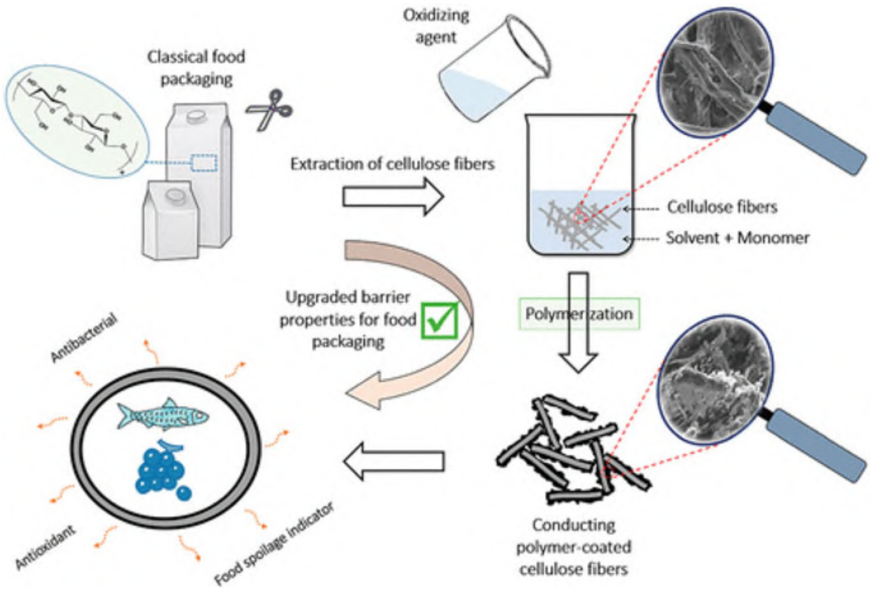
Classical food packaging
Oxidizing agent
Extraction of cellulose fibers
Cellulose fibers
Solvent + Monomer
Polymerization
Upgraded barrier properties for food packaging
Antibacterial
Antioxidant
Food spoilage indicator
Conducting polymer-coated cellulose fibers

Fig. 3 Conducting polymer used in food packaging (reprinted from open source, El Guerraf et al. [60])

However, packaging can actively preserve food and serve as an information storefront on its condition, which helps to fight against the waste of food and the deterioration of food. Taking this into consideration, intelligent and active packaging are now being researched and developed. This is an essential task for the industry that deals with food packaging (Fig. 3).

9.1 Active Packaging

The application of materials that can emit, release, scavenge, or absorb compounds indirectly or directly to food in order to preserve its quality or postpone its destruction is what is meant by the term "active packaging", and it refers to the utilization of such materials. This method of packaging makes use of active compounds that have various properties, such as antioxidant or antimicrobial, and incorporates them into coatings, polymeric matrix, labels, pads, or sachets. For example, antioxidant or antibacterial properties. The applicable active chemicals such as phenolic compounds can be derived from a variety of sources, including plants including industrial crops like cardoon, hemp, and kenaf, and other sources like vegetables, fruits, herbs, or algae. Active packaging can be broken down into three primary categories: antioxidants such as vitamin C, vitamin E, and butylated hydroxytoluene, antimicrobials such as phenolic compounds, peptides, and essential oils, and absorbers or scavengers such as oxygen scavengers, carbon dioxide absorbers or emitters, moisture control agents, and ethylene absorbers or adsorbers. Each of these categories has its own set of active ingredients.

Fresh food products are easily damaged by physical damage resulting from handling, shipping, or storage, or by intrinsic causes resulting from chemical reactions, enzyme action, and microbial decomposition. Because it works as a barrier to gases, water vapour, and dust, the use of packaging is an excellent choice for the protection and preservation of food because it is a strategic choice. For this reason, packaging needs to be capable of performing the following four primary functions: protection, confinement, the transfer of information, and marketing.

The use of materials that can release, emit, absorb, or scavenge substances directly or indirectly to the food in order to preserve its quality or postpone its destruction is what's known as "active packaging", and it involves the use of materials. This method of packaging makes use of active compounds that have various properties, such as antioxidant or antimicrobial, and incorporates them into a polymeric matrix, coatings, labels, pads, or sachets. For example, antioxidant or antibacterial properties. The applicable active chemicals such as phenolic compounds can be derived from a variety of sources, including plants including industrial crops like kenaf, cardoon, and hemp, algae, herbs, spices, fruits, or vegetables. Active packaging can be broken down into three primary categories, which are scavengers or absorbers, antioxidants such as butylated hydroxytoluene, vitamin C, and vitamin E, and antimicrobials such as essential oils, peptides, and phenolic compounds, e.g. oxygen scavengers, carbon dioxide absorbers or emitters, moisture control agents, and ethylene absorbers or adsorbers.

9.2 Antioxidant Systems

Active packaging can be broken down into its component parts, one of which is antioxidant active packaging. The basic idea behind active packaging, and in particular antioxidant active packaging, is the inclusion of active substances within the packaging that interact with the meat or the environment the meat is kept in. These active agents can either collect pro-oxidant molecules or release antioxidant compounds in order to postpone the degradation of the meat that is caused by the oxidation of lipids. This is done in order to prevent the meat from becoming rancid. The food industry is significantly harmed by the spoiling of meat products at all stages of production, including distribution and the product's exposure in the market, from an economic point of view this has a substantial negative affect. When it comes to preparing and storing meat and its derivatives, oxidation of lipids and degradation due to the growth of microbes are two of the biggest obstacles. In response, food production has developed a wide variety of new packaging techniques to reduce waste and lengthen the lifespan of meat products. Active packaging has been proposed as a replacement for traditional packaging in recent years. Since oxidative degeneration of meat and meat products is a problem, it is suggested that active packaging be employed in the future as a possible solution. However, the use of this active packaging will be determined by the expenses that are associated with its development.

9.3 Antimicrobial Systems

Antimicrobial packaging is a promising technology that is regarded to be a subset of controlled-release packaging and active packaging. This method successfully infuse the antimicrobial into the film material used for food packaging, and then releases it over the specified time period, killing the pathogenic microorganisms that harm food goods and significantly extending their shelf life. These days, food preservation, maintaining food quality, and maintaining food safety are key growing challenges in the food sector. It is unmistakable that throughout time, customers' demand for natural and safe food items that adhere to tight rules to prevent diseases that are spread by food has increased. Future studies will hopefully be able to harness the emerging and promising usage of antimicrobials in food packaging to come up with actual efficacies in extending shelf life and reducing bacterial growth, it is important to keep in mind that the evolution of resistance among microorganisms will be an implication of antimicrobials in the near future.

9.4 Scavengers/Absorbers

Scavengers, which are also known as absorbers, are a sort of active packaging technology. They are the type of active packaging technology that is used the most frequently. Scavengers absorb pollutants from the atmosphere inside the package or from the packed product itself. It is common practise to make use of oxygen and moisture scavengers, in particular, due to the fact that oxygen and moisture are commonly involved in degradative processes and are significant contributors to the loss of quality and degradation in food items and organic molecules. Typical examples include little packets filled with silica gel. These moisture scavenger sachets are already an integral part of our day-to-day lives because they are typically located within the packaging of electronic products or within bags containing articles of clothing. The vast majority of scavengers are able to absorb a particular chemical, but some can do so only when the threshold for doing so is met. Potassium chloride, for instance, is only able to absorb water vapour when the relative humidity is at or above 87%. Regulators are another name for the scavengers that fall into this category. Oxygen scavengers are a form of active packaging technology that absorb oxygen in the headspace or dissolved oxygen in the product, resulting in a longer shelf life and the maintenance of the product's initial high level of quality.

9.5 Intelligent Packaging

Using materials that interact and monitor the packaging environment, intelligent packaging provides information to the consumer about the status of the food that is packaged through an external or internal indicator. This gives the consumer information about the condition of the food that is being packaged. Monitoring the efficiency of active packaging is another use for intelligent packaging, which may be used to track the progress of the process. Indicators, sensors, and data carriers are the three primary components that make up intelligent packaging.

Indicators

The existence or absence of a drug, the progression of a reaction between two or more chemicals, and the concentration of a particular substance can all be ascertained with the help of indicators. Indicators, in their most basic form, are any changes in appearance that convey information. A large number of the indicators produce a colour change that may be easily recognized by the consumer, and they are designed to monitor gas creation, time-temperature, and freshness.

Data Carriers

One of the main roles of data carriers is to ensure traceability and automation, as well as security from theft and counterfeiting. Data carriers are a means through which information can be transmitted along the food supply chain; however, they do not have the capability of coming into direct touch with the product. Radiofrequency identification and barcode labels are the two types of data carriers that are used most frequently (RFID).

Sensors

Electronic sensors are devices that can measure, detect or identify a change through the use of a receptor that is converted into a signal through the utilization of a transducer that reports a change in either the physical or chemical environment. Sensors can be used to detect changes in both the physical and chemical environments. One category of sensors that are associated with biological processes is known as biosensors. A biological sign is recognized by a bioreceptor, and the transducer then turns that detection into a measurable electronic response in biosensors. Pathogens, allergies, and other potentially harmful substances are all detectable via biosensors. The term “sensor” is often used interchangeably with the phrase “indicator” when discussing parts of food packaging. This result is represented by a visual change brought about by the indicators’ “sensing” or monitoring activity, despite the fact that indicators do not possess the same properties as sensors (Fig. 4).

By including protective elements like antioxidants and antimicrobials into the packaging, smart packaging can both inform the user of the state of the food and keep it safe for consumption. Essentially, smart packaging is a hybrid of intelligent and smart packaging technologies. Information offered by smart packaging can be

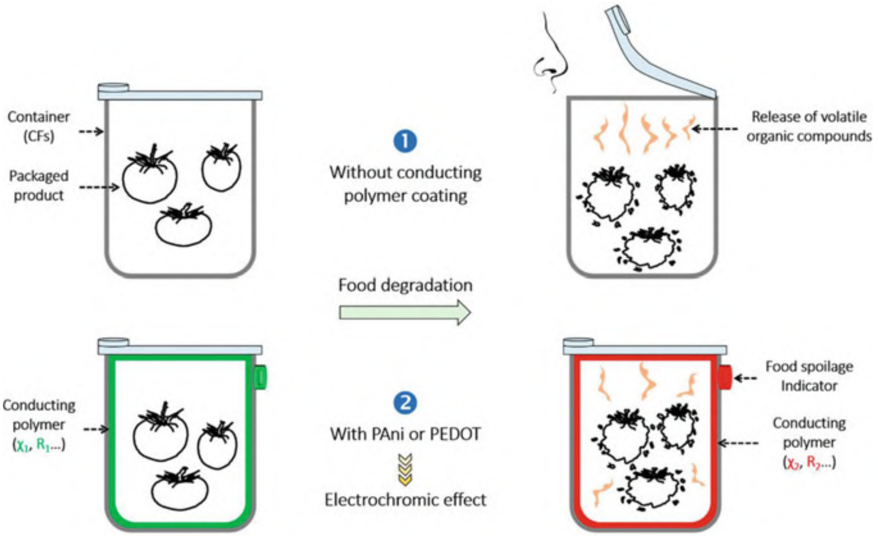
Container
(CFs)
Packaged
product
①
Without conducting
polymer coating
Release of volatile
organic compounds
Food degradation
Conducting
polymer
$(\chi_1, R_1...)$
②
With PAni or PEDOT
Electrochromic effect
Food spoilage
Indicator
Conducting
polymer
$(\chi_2, R_2...)$

Fig. 4 Food packaging with and without conducting polymer (reprinted from open access source, El Guerraf et al. [60])

accessed by everyone along the food supply chain, spanning from producers to shoppers. This allows for the tracking of food products through the monitoring and control of their internal or exterior environments. Despite the fact that intelligent and smart packaging are two entirely separate ideas, references to smart packaging are almost always actually referring to intelligent packaging.

10 Conclusion

In this chapter, we have examined the classification of polymer structures, as well as the functionalization methods for conducting polymers. The significance of the composite material with regard to the conducting polymer and the applications of this material. The successful application of the polymer nanocomposite has prompted more iesinto the development of nanocomposites that make use of polymers as a matrix. In an effort to develop nanocomposites by the utilization of metal oxide nanoparticles and organic nanofillers, a number of different polymers have been put through their paces in an effort to generate nanocomposites. Because conventional composite materials are significantly heavier in weight than nanocomposites, the latter are more cost-effective than the former when used in conjunction with other materials for particular purposes in the food packaging business. The use of packaging materials made of plastic based on biopolymers has increased as a result of the application of nanocomposites. Inorganic nanoparticles also have the potential to be utilized in the introduction of several functionalities, such as antimicrobials, antioxidants, and the controlled release of functionally active chemicals. Thanks to nanotechnology's breakthroughs, the packaging sector will be able to meet the ever-increasing demands of customers and food manufacturers for manufacturing high-quality food, ensuring food safety, extending shelf life, and delivering intelligent functionalities with easy use in the future decade. It appears that polymer nanocomposite packaging materials have a promising future for usage in a range of food packaging applications. Among these applications is the creation of unique, intelligent, and active food packaging with several functions. It is interesting to note that the search for new monomers has quite receded while the "historical" polymers, polypyrrole, polythiophene, and related PEDOT, and to a lesser extent polyaniline continue to attract the largest part of the works in the field. Conduction polymers have also shown significant results in the supercapacitor and energy storage field. When it comes to applications, bio-related materials and protection against corrosion are without a doubt the most essential ones. This chapter also provides a concise summary of prospective uses of conducting PANI, PPY, and PEDOT nanotubes/fibres based on studies that are currently available as well as some significant contributions made by researchers.

References

1. Bazylak LI, Zaikov GE, Haghi AK (2014) Polymers and polymeric composites: properties, optimization, and applications. CRC Press
2. Callister WD, Rethwisch DG (2016) Fundamentals of materials science and engineering: an integrated approach, 5th edn. Wiley
3. VEM tooling (2022) Homopolymer vs. copolymer. VEM Tooling. https://www.vem-tooling.com/homopolymer-vs-copolymer/. Accessed 12 Feb 2023
4. Hucul DA, Hahn SF (2000) Catalytic hydrogenation of polystyrene. Adv Mater 12(23):1855–1858. https://doi.org/10.1002/1521-4095(200012)12:23%3c1855::AID-ADMA1855%3e3.0.CO;2-P
5. Roth PJ, Wiss KT, Theato P (2012) 5.12—post-polymerization modification. In: Matyjaszewski K, Möller M (eds) Polymer science: a comprehensive reference. Elsevier, Amsterdam, pp 247–267. https://doi.org/10.1016/B978-0-444-53349-4.00142-4
6. Zuchowska D (1980) Polybutadiene modified by epoxidation. 1. Effect of polybutadiene microstructure on the reactivity of double bonds. Polymer 21(5):514–520. https://doi.org/10.1016/0032-3861(80)90217-7
7. Cross EM, McCarthy TJ (1992) Radical chlorination of polyethylene film: control of surface selectivity. Macromolecules 25(10):2603–2607. https://doi.org/10.1021/ma00036a007
8. Klesper E, Strasilla D (1977) 1H-NMR study of the esterication of syndiotactic poly(methacrylic acid) with carbodiimides. J Polym Sci Polym Lett Ed 15(1):23–29. https://doi.org/10.1002/pol.1977.130150104
9. Heinze T, Liebert T (2001) Unconventional methods in cellulose functionalization. Prog Polym Sci 9(26):1689–1762. https://doi.org/10.1016/S0079-6700(01)00022-3
10. Korshak VV (1980) The synthesis of polymers by modification methods. Russ Chem Rev 49(12):1135. https://doi.org/10.1070/RC1980v049n12ABEH002533
11. Ueno A, Schuerch C (1965) Racemization of isotactic poly(isopropyl acrylate). J Polym Sci [B] 3(1):53–56. https://doi.org/10.1002/pol.1965.110030115

12. Zhou W et al (2020) 4D-printed dynamic materials in biomedical applications: chemistry, challenges, and their future perspectives in the clinical sector. J Med Chem 63(15):8003–8024. https://doi.org/10.1021/acs.jmedchem.9b02115
13. Boyaciyan D, von Klitzing R (2019) Stimuli-responsive polymer/metal composites: from fundamental research to self-regulating devices. Curr Opin Colloid Interface Sci 44:193–207. https://doi.org/10.1016/j.cocis.2019.10.005
14. Wang Z, Zou Y, Li Y, Cheng Y (2020) Metal-containing polydopamine nanomaterials: catalysis, energy, and theranostics. Small 16(18):1907042. https://doi.org/10.1002/smll.201907042
15. Ghenaatian HR, Mousavi MF, Rahmanifar MS (2012) High performance hybrid supercapacitor based on two nanostructured conducting polymers: self-doped polyaniline and polypyrrole nanofibers. Electrochim Acta 78:212–222. https://doi.org/10.1016/j.electacta.2012.05.139
16. Sun W, Zheng R, Chen X (2010) Symmetric redox supercapacitor based on micro-fabrication with three-dimensional polypyrrole electrodes. J Power Sources 195(20):7120–7125. https://doi.org/10.1016/j.jpowsour.2010.05.012
17. Marchioni F, Yang J, Walker W, Wudl F (2006) A low band gap conjugated polymer for supercapacitor devices. J Phys Chem B 110(44):22202–22206. https://doi.org/10.1021/jp063849w
18. Gupta V, Miura N (2006) High performance electrochemical supercapacitor from electrochemically synthesized nanostructured polyaniline. Mater Lett 60(12):1466–1469. https://doi.org/10.1016/j.matlet.2005.11.047
19. Horng Y-Y, Lu Y-C, Hsu Y-K, Chen C-C, Chen L-C, Chen K-H (2010) Flexible supercapacitor based on polyaniline nanowires/carbon cloth with both high gravimetric and area-normalized capacitance. J Power Sources 195(13):4418–4422. https://doi.org/10.1016/j.jpowsour.2010.01.046
20. Bhadra S, Khastgir D, Singha NK, Lee JH (2009) Progress in preparation, processing and applications of polyaniline. Prog Polym Sci 34(8):783–810. https://doi.org/10.1016/j.progpolymsci.2009.04.003
21. Bakhshi AK, Bhalla G (2004) Electrically conducting polymers: materials of the twentyfirst century, vol 63
22. Reyman D, Guereca E, Herrasti P (2007) Electrodeposition of polythiophene assisted by sonochemistry and incorporation of fluorophores in the polymeric matrix. Ultrason Sonochem 14(5):653–660. https://doi.org/10.1016/j.ultsonch.2006.10.006
23. Frackowiak E, Khomenko V, Jurewicz K, Lota K, Béguin F (2006) Supercapacitors based on conducting polymers/nanotubes composites. J Power Sources 153(2):413–418. https://doi.org/10.1016/j.jpowsour.2005.05.030
24. Selvakumar M, Pitchumani S (2010) Hybrid supercapacitor based on poly(aniline-co-m-anilicacid) and activated carbon in non-aqueous electrolyte. Korean J Chem Eng 27(3):977–982. https://doi.org/10.1007/s11814-010-0120-z
25. Li Y, Zhang Q, Zhao X, Yu P, Wu L, Chen D (2012) Enhanced electrochemical performance of polyaniline/sulfonated polyhedral oligosilsesquioxane nanocomposites with porous and ordered hierarchical nanostructure. J Mater Chem 22(5):1884–1892. https://doi.org/10.1039/C1JM13359D
26. Li Y, Zhao X, Xu Q, Zhang Q, Chen D (2011) Facile preparation and enhanced capacitance of the polyaniline/sodium alginate nanofiber network for supercapacitors. Langmuir ACS J Surf Colloids 27(10):6458–6463. https://doi.org/10.1021/la2003063
27. Liu C (2015) Polyaniline and graphene based symmetric and asymmetric solide-state supercapacitor. The University of Akron
28. Moussa M, El-Kady MF, Zhao Z, Majewski P, Ma J (2016) Recent progress and performance evaluation for polyaniline/graphene nanocomposites as supercapacitor electrodes. Nanotechnology 27(44):442001. https://doi.org/10.1088/0957-4484/27/44/442001
29. Meng Q, Cai K, Chen Y, Chen L (2017) Research progress on conducting polymer based supercapacitor electrode materials. Nano Energy 36:268–285. https://doi.org/10.1016/j.nanoen.2017.04.040

30. Rudge A, Raistrick I, Gottesfeld S, Ferraris JP (1994) A study of the electrochemical properties of conducting polymers for application in electrochemical capacitors. Electrochim Acta 39(2):273–287. https://doi.org/10.1016/0013-4686(94)80063-4
31. Eftekhari A, Li L, Yang Y (2017) Polyaniline supercapacitors. J Power Sources 347:86–107. https://doi.org/10.1016/j.jpowsour.2017.02.054
32. Fan L-Z, Hu Y-S, Maier J, Adelhelm P, Smarsly B, Antonietti M (2007) High electroactivity of polyaniline in supercapacitors by using a hierarchically porous carbon monolith as a support. Adv Funct Mater 17(16):3083–3087. https://doi.org/10.1002/adfm.200700518
33. Yang Y, Hao Y, Yuan J, Niu L, Xia F (2014) In situ preparation of caterpillar-like polyaniline/carbon nanotube hybrids with core shell structure for high performance supercapacitors. Carbon 78:279–287. https://doi.org/10.1016/j.carbon.2014.07.004
34. Gupta V, Miura N (2006) Polyaniline/single-wall carbon nanotube (PANI/SWCNT) composites for high performance supercapacitors. Electrochim Acta 52(4):1721–1726. https://doi.org/10.1016/j.electacta.2006.01.074
35. Meng C, Liu C, Chen L, Hu C, Fan S (2010) Highly flexible and all-solid-state paperlike polymer supercapacitors. Nano Lett 10(10):4025–4031. https://doi.org/10.1021/nl1019672
36. Dong B, He B-L, Xu C-L, Li H-L (2007) Preparation and electrochemical characterization of polyaniline/multi-walled carbon nanotubes composites for supercapacitor. Mater Sci Eng B 143(1):7–13. https://doi.org/10.1016/j.mseb.2007.06.017
37. Otrokhov G et al (2014) Enzymatic synthesis of polyaniline/multi-walled carbon nanotube composite with core shell structure and its electrochemical characterization for supercapacitor application. Electrochim Acta 123:151–157. https://doi.org/10.1016/j.electacta.2013.12.089
38. Zhou Y et al (2010) Polyaniline/multi-walled carbon nanotube composites with core–shell structures as supercapacitor electrode materials. Electrochim Acta 55(12):3904–3908. https://doi.org/10.1016/j.electacta.2010.02.022
39. Deng M et al (2011) Electrochemical deposition of polypyrrole/graphene oxide composite on microelectrodes towards tuning the electrochemical properties of neural probes. Sens Actuators B Chem 158(1):176–184. https://doi.org/10.1016/j.snb.2011.05.062
40. Wang J, Xu Y, Zhu J, Ren P (2012) Electrochemical in situ polymerization of reduced graphene oxide/polypyrrole composite with high power density. J Power Sources 208:138–143. https://doi.org/10.1016/j.jpowsour.2012.02.018
41. Xu J et al (2015) Polypyrrole/reduced graphene oxide coated fabric electrodes for supercapacitor application. Org Electron 24:153–159. https://doi.org/10.1016/j.orgel.2015.05.037
42. Lai L et al (2012) Tuning graphene surface chemistry to prepare graphene/polypyrrole supercapacitors with improved performance. Nano Energy 1(5):723–731. https://doi.org/10.1016/j.nanoen.2012.05.012
43. Folorunso O, Hamam Y, Sadiku R, Adekoya GJ, Ray SS (2023) Investigation of graphene loaded polypyrrole for lithium-ion battery. Mater Today Proc. https://researchspace.csir.co.za/dspace/handle/10204/11728. Accessed 24 Jan 2023
44. Park JW, Park SJ, Kwon OS, Lee C, Jang J (2014) Polypyrrole nanotube embedded reduced graphene oxide transducer for field-effect transistor-type H_2O_2 biosensor. Anal Chem 86(3):1822–1828. https://doi.org/10.1021/ac403770x
45. Dai H, Wang N, Wang D, Ma H, Lin M (2016) An electrochemical sensor based on phytic acid functionalized polypyrrole/graphene oxide nanocomposites for simultaneous determination of Cd(II) and Pb(II). Chem Eng J 299:150–155. https://doi.org/10.1016/j.cej.2016.04.083
46. Liu Y et al (2018) Interfacial fabrication of polypyrrole/sulfonated reduced graphene oxide nanocomposites for electrochemical capacitors. Polym Compos 39:E378–E385. https://doi.org/10.1002/pc.24458
47. Jonas F, Schrader L (1991) Conductive modifications of polymers with polypyrroles and polythiophenes. Synth Met 41(3):831–836. https://doi.org/10.1016/0379-6779(91)91506-6
48. Snook GA, Kao P, Best AS (2011) Conducting-polymer-based supercapacitor devices and electrodes. J Power Sources 196(1):1–12. https://doi.org/10.1016/j.jpowsour.2010.06.084
49. Mastragostino M, Arbizzani C, Soavi F (2002) Conducting polymers as electrode materials in supercapacitors. Solid State Ion 148(3):493–498. https://doi.org/10.1016/S0167-2738(02)00093-0

50. Wilamowska M, Kujawa M, Michalska M, Lipińska L, Lisowska-Oleksiak A (2016) Electroactive polymer/graphene oxide nanostructured composites; evidence for direct chemical interactions between PEDOT and GOx. Synth Met 220:334–346. https://doi.org/10.1016/j.synthmet.2016.07.002
51. Lota K, Khomenko V, Frackowiak E (2004) Capacitance properties of poly(3,4-ethylenedioxythiophene)/carbon nanotubes composites. J Phys Chem Solids 65(2):295–301. https://doi.org/10.1016/j.jpcs.2003.10.051
52. Alvi F, Ram MK, Basnayaka PA, Stefanakos E, Goswami Y, Kumar A (2011) Graphene–polyethylenedioxythiophene conducting polymer nanocomposite based supercapacitor. Electrochim Acta 56(25):9406–9412. https://doi.org/10.1016/j.electacta.2011.08.024
53. Alabadi A, Razzaque S, Dong Z, Wang W, Tan B (2016) Graphene oxide-polythiophene derivative hybrid nanosheet for enhancing performance of supercapacitor. J Power Sources 306:241–247. https://doi.org/10.1016/j.jpowsour.2015.12.028
54. Liu P-F et al (2017) A hierarchical NiO/NiMn-layered double hydroxide nanosheet array on Ni foam for high performance supercapacitors. Dalton Trans 46(23):7388–7391. https://doi.org/10.1039/C7DT00932A
55. Dutta S, Pal S, De S (2019) Mixed solvent exfoliated transition metal oxides nanosheets based flexible solid state supercapacitor devices endowed with high energy density. New J Chem 43(31):12385–12395. https://doi.org/10.1039/C9NJ03233A
56. Stankovich S et al (2006) Graphene-based composite materials. Nature 442(7100):282–286. https://doi.org/10.1038/nature04969
57. Three-dimensional (3D) polymer—metal–carbon framework for efficient removal of chemical and biological contaminants | Scientific Reports. https://www.nature.com/articles/s41598-021-86661-w. Accessed 14 Dec 2022
58. Rodrigues C, Souza VGL, Coelhoso I, Fernando AL (2021) Bio-based sensors for smart food packaging—current applications and future trends. Sensors 21(6). https://doi.org/10.3390/s21062148
59. Selvaraj T, Perumal V, Khor SF, Anthony LS, Gopinath SCB, Muti Mohamed N (2020) The recent development of polysaccharides biomaterials and their performance for supercapacitor applications. Mater Res Bull 126:110839. https://doi.org/10.1016/j.materresbull.2020.110839
60. El Guerraf A et al (2022) Multifunctional smart conducting polymers-silver nanocomposites-modified biocellulose fibers for innovative food packaging applications. Ind Eng Chem Res. https://doi.org/10.1021/acs.iecr.2c01327

Chapter 14
Chemical Modifications for the Development of Conducting Polymer-Based Supercapacitors

Tanuj Kumar, Jyoti, Mohammed Murshid, Vandana, Ashima, and Monika Saini

1 Introduction Conducting Polymer-Based Supercapacitors

Conjugated double bonds generated during chemical or electrochemical oxidation of the monomer are the building blocks of conducting polymers [1]. Dopant or counterions' insertion in the polymer backbone occurs as a result of oxidation at both the monomer and polymer levels; for example, chloride is inserted when iron chloride is used as an oxidant. If the dopants or polarons can be introduced into the polymer structure as close as feasible, then the dopant level will increase. Several different conducting polymers, including polypyrrole, polythiophene, and polyaniline, have been investigated for use in supercapacitor devices. Supercapacitors are a recent development using porous, electroactive materials such as polymer and carbon

---

T. Kumar (✉) · M. Murshid
Department of Nanosciences and Materials, Central University of Jammu, Rahya-Suchani, Bagla, Jammu 181143, India
e-mail: tkdeswal@gmail.com

Jyoti
Department of Physics, Govt College for Women, Gurawara, Rewari 123035, India

Vandana
Department of Physics, Kurukshetra University, Kurukshetra 136119, India

Ashima
Department of Physics and Astrophysics, Central University of Jammu, Rahya-Suchani, Bagla, Jammu 181143, India

M. Saini
Deenbandhu Chottu Ram University of Science and Technology Murthal, Sonipat, Haryana 131039, India

© The Author(s), under exclusive license to Springer Nature Singapore Pte Ltd. 2024

C. M. Hussain and M. B. Ahamed (eds.), *Functionalized Nanomaterials Based Supercapacitor*, Materials Horizons: From Nature to Nanomaterials,
https://doi.org/10.1007/978-981-99-3021-0_14

nanotubes. These capacitors charge quickly and discharge energy safely. Supercapacitors can also be used to transform electric energy into optical, acoustic, and thermal energy. Since they're efficient, they've found many applications in electronic devices. However, the energy storage capabilities are limited by the design of the supercapacitor.

High power but low specific energy are two characteristics of supercapacitors containing carbon. Instead, supercapacitors made from conducting polymers can decrease self-discharge while increasing energy storage capacity because of bulk redox processes. However, the key challenge is still the low rate of charge–discharge or lesser power, which is caused by slow ion diffusion through an electrode's bulk material. Despite the widespread adoption of pseudocapacitive materials, conducting polymer-based supercapacitors is still thought to hold promise in this industry because of their superior kinetics [2]. Conducting polymers are also appealing because of their low cost and high charge density on contrast with traditional metal oxides. For example, polyaniline has a current density of 140 mA hg^{-1}, which is similar to metaloxide [3]. Thus, conducting polymers can be used for supercapacitor device fabrication with high energy and power densities and low equivalent series resistance. Some common conducting polymers are shown in Fig. 1.

There has been a tremendous expansion in the area of conducting polymers since the invention of polyacetylene [5]. Poly (3,4-ethylenedioxythiophene) (PEDOT), polypyrrole, polyaniline, polythiophene, etc., are some of the most widely utilized conducting polymers in energy storage devices. Good electrical and optical properties, as well as an easy manufacturing method, contribute to the growth of conducting polymers in a variety of application domains. The existence of conjugated structures in the conducting polymer chemical structure is the cause of their conductivity. The metallic nature is due to delocalization of the π electrons in the conjugated double bonds. However, owing to the potential for bond alteration resulting in energy gaps in the electronic spectrum, these systems are not very stable. The conductivity of conducting polymers has been enhanced by the incorporation of dopant counterions, which have narrowed the energy gap. Dopant ions carry charge in the form of excess

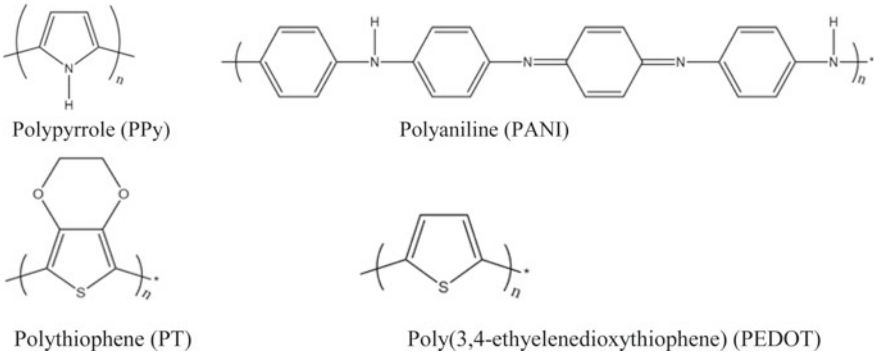

Polypyrrole (PPy)
Polyaniline (PANI)
Polythiophene (PT)
Poly(3,4-ethyelenedioxythiophene) (PEDOT)

Fig. 1 Some common conducting polymer chemical structures [4]. No permission required

electrons. Dopant ions donate or accept electrons to stabilize the unstable oxidized polymer backbone. Small ions (Cl, Br, NO_3) or large dopants (peptides, polymers) can be used to impart a p- or n-type charge to the conducting polymers, respectively [6]. It has been shown that the physical structure of conducting polymer-based supercapacitors degrades due to the doping and de-doping of counterions, which limits their cycle ability compared to double-layer supercapacitors [7]. By inserting counterions and raising the doping levels, the conducting polymer-based supercapacitors may yield higher specific energies. However, there is an increase in price corresponding to a change in volume when more dopants are added. Because of this change in volume, the mechanical strength of the electrodes degrades over long-term use. Greater cycle life in actuators is seen in the study when conducting polymer-based electrodes are used in combination with ionic liquid electrolytes [8].

Functionalization of conducting polymers is a growing field with many potential technological applications. Both polymer synthesis and functionalization have the downside of including unintended macromolecular byproducts into the finished products. Most of the time, CPs are used in solid form for various applications (fibres, film, particles, pellets, etc.). As a result, functionalization might be utilized to modify both the bulk and the surface characteristics of a material. Most reactions are carried out in a heterogeneous manner because CPs are either insoluble (such as Polypyrrole and Polythiophene) or soluble only in a limited number of solvents (such as PANI). Thus, it is possible to add functionalization of the surface without affecting the bulk. Using this method, the bulk properties of the original polymer (such as conductivity) may be preserved while the surface properties (such as wettability) are altered. As a result of their huge surface area to volume ratio, nano-objects (such as nanofibres) are excellent candidates for such heterogeneous alteration. Nonetheless, electrophilic sulfonation of PANI was reported as one of the earliest CP functionalizations; this reaction was performed when polymer soluble in conc. H_2SO_4, and a bulk reaction ensued. Furthermore, functionalized polymer may be soluble in the solvent whereas the unmodified polymer is not [9].

2 Functionalization Methods

To increase the energy density, other materials are added to the supercapacitor structure. For example, mesoporous carbon electrodes have a high surface area which improves capacitance and discharge rate. Graphenes—graphite mixed with polypyrrole- can improve capacitance while maintaining a high power density. To enhance energy storage ability and safety measures, carbon nanotubes were used to form supercapacitors in 2016. The high surface area of these nanotubes allows for greater storage ability while improving power output due to their weight. Additionally, researchers need to fine-tune the materials used to create a capacitor's active material layer so that it lasts long enough to benefit electronic technology. Two main techniques are used to create the active material layer of a supercapacitor: physical functionalization and chemical functionalization. Physical functionalization involves doping a conducting polymer with a chemical that increases its electrical properties, allowing it to store more charge. Chemical functionalization, on the other hand, uses copolymerization to create a stronger, more resilient material.

To create a longer lasting supercapacitor, the material used to create the initial structure must be selected carefully. The chemical composition is essential as it determines how stable the capacitance is over time. To find this composition, chemists study properties such as conductivity, ionic nature, chemical affinity, and dielectric properties. Once this composition is discovered, it must be characterized and tested in a laboratory for both conductivity and dielectric characteristics. If these tests are successful, synthesis equipment must be accessible to manufacture this material in large quantities, which is not always the case in a university setting. Conductive polymers such as polypyrrole can store a large amount of electricity. These materials are formed into cylindrical or hexagonal shapes and layered upon each other. The outer layer is used for the anode and the inner layer for the cathode. The layers are separated by an electrolyte solution that allows for efficient charge and discharge separation. Additionally, the solution provides a conducting path from one material to the next. When discharged, the capacitor's characteristics are similar to a battery; it has an active material formation and can produce electricity. Although new materials create excitement among scientists and engineers, creating efficient supercapacitors remains a challenge. There's no standard procedure for creating them so different laboratories must develop their own methods.

Supercapacitors with electrodes made of conducting polymers are becoming more practical as electrical technology develops. The electrode material, its electrochemical capabilities, its thermal stability, its surface area, and its conductivity are only few of the factors that influence the supercapacitor's features [10, 11]. Because organic conducting polymeric materials may be readily designed to display qualities fulfilling the criteria for supercapacitor applications, their usage as electrodes has been investigated and has yielded positive results [12]. This customization is possible using the following functionalization methods.

2.1 Doping

Supercapacitors are superior devices for short-term energy storage due to their rapid charging and discharging capabilities. However, the energy density of supercapacitors is often low since they do not have a large specific capacitance which is the amount of electric charge held per unit mass or volume [13]. The metallic conductance of organic conducting polymers (OCP) is achieved using a mechanism very identical to that of inorganic semiconductors the introduction of a few dopants improves the conductivity by a great amount. Since doping is the adding of impurities to a material. The majority of solvents are unable to dissolve many conductive polymers. Long-chain dopants, like naphthalene sulfonic acid (NSA), dodecylbenzene sulfonic acid (DBSA), and camphor sulfonic acid (CSA), may aid in improving solubility, allowing us to get over this obstacle. It has been shown via analysis that as the length of the alkyl chain in the dopant increases, the solubility and electrical conductivity of the doped polymer also increase. This is because the longer the alkyl chain, the less interactions there are between the polymer chains [14]. Doping these polymers results in an increase in conductivity, but it also causes a change in the structure of the polymeric chain. Chemical doping, electrochemical doping, photodoping, interfacial doping, and charge-injection doping are only a few of the many doping methods available. As a more common practise, scientists expose polymers to certain chemicals called dopants. Electron donors are typically n-type, whereas electron acceptors are p-type. Organic conducting characteristics may be measured in a wide range of ways depending on the degree of doping used. It was shown that the electrical conductivity of polypyrrole films may be increased as a result of a rise in the amount of dopant (10–50%) used in the solid-state production of these films, as shown in Figure. In the presence of water-soluble acid dopants, an aqueous colloidal dispersion of the conducting polymers is generated by the ionic bond formations with surfactants [15]. Dopants including dodecylbenzene sulfonic acid (DBSA), polystyrene sulfonic acid (PSS), naphthalene sulfonic acid (NSA, Camphor sulfonic acid (CSA)), p-toluene sulfonic acid (p-TSA) and poly (2-acrylamido-2-methyl-1-propane sulfonic acid) (PAMPS) are widely utilized. The morphology, electrical conductivity, and optical characteristics of a polymer are highly dependent on the amount and kind of dopants present in the material [16].

Synthetically conductive PPy has a number of drawbacks that limit its production and uses, including weak mechanical strength, poor chemical stability, and insolubility and infusibility. The development of doping techniques has allowed for a rise in the conductive properties of such conjugated polymers [17]. However, the doping procedure on the polymer backbone generates charges that are mobile enough to conduct electricity. This mobility is only possible in the presence of an extended para conjugation in the polymer. To name a few, common sulfonic acids utilized as dopants include camphor sulfonic acid (CSA), phosphotungstate sulfonic acid (PVSA), p-methylbenzenesulfonic acid (MBSA), and dodecanesulfonic acid (DBSA). These dopants have functional groups that are both well-suited for polymer protonation and centrally strong enough to facilitate such protonation. The introduction of these dopants into the polymer matrix via the process of doping causes its rigid conjugated backbone to become soluble; the resulting material is chemically stable, easily soluble, and electrically conductive [18] (Fig. 2).

There are many different sulfonic acids, but camphor sulfonic acid (CSA) doped conducting polymers stand out for their superior anti-corrosion materials and improved chemical stability and thermal degradation capabilities, thus suitable for charge-storing applications [19].

2.2 *Copolymerization*

Copolymerization is extensively used as one of the most promising processes as a result of the orientation of the monomer chain, for developing a broad variety

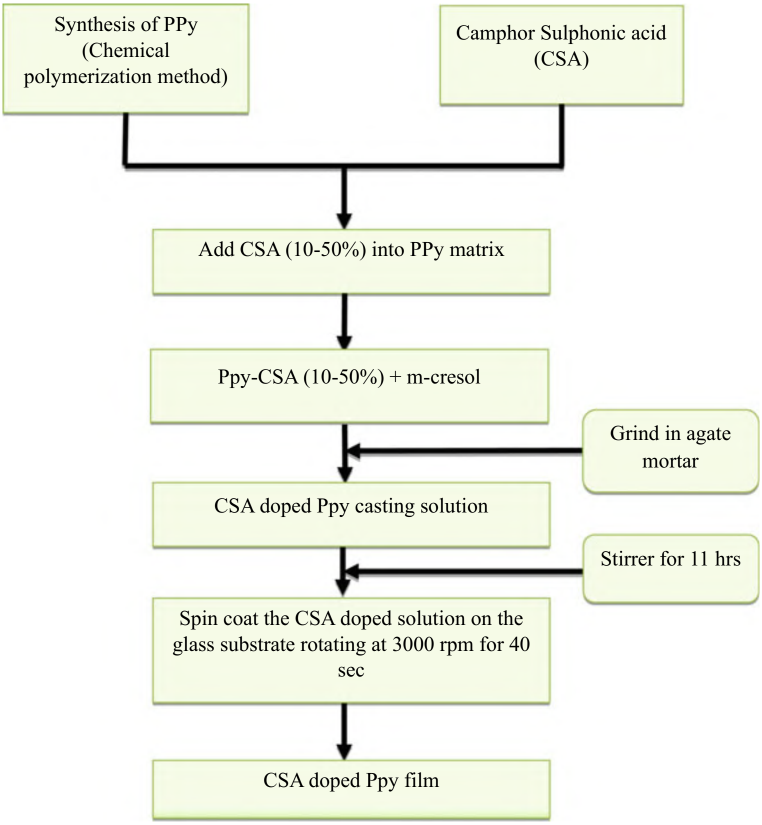
Synthesis of PPy (Chemical polymerization method)
Camphor Sulphonic acid (CSA)
Add CSA (10-50%) into PPy matrix
Ppy-CSA (10-50%) + m-cresol
Grind in agate mortar
CSA doped Ppy casting solution
Stirrer for 11 hrs
Spin coat the CSA doped solution on the glass substrate rotating at 3000 rpm for 40 sec
CSA doped Ppy film

Fig. 2 CSA-doped PPy film [19]. Taken

of flexible polymers with desired features such as excellent bandgap, high solubility and polarizability. The copolymerization process involves the simultaneous polymerization of two or more monomers or monomer pairs, resulting in a polymer with more than one repeating unit. Chemical and electrochemical polymerization are the most common methods used to manufacture copolymers. Chemical polymerization, either by step growth or chain growth, is widely used for the production of functionalized polymers. The electrochemically produced copolymer is employed in a wide variety of optical and electrical applications and is manufactured in a thin layer. The electrochemical approach has the benefits of being easy to produce a homogeneous film of appropriate thickness and being processible at room temperature [20]. There are primarily four types of copolymer combinations: alternating, random, block, and graft. Aniline, o-phenylenediamine, and their derivatives have all been used in a wide range of newly reported copolymers, with each method of polymerization yielding somewhat various results. Electrochemical oxidation in a solvent containing boron trifluoride diethyl etherate and acetonitrile was used to synthesize a copolymer of poly (3-methyl thiophene-co-benzanthrone). The spectrum and electrochromic features were studied by cyclic voltammetry, proton nuclear magnetic resonance, FTIR spectroscopy, and scanning electron microscopy [16, 21].

Electrodes with wide-ranging potential for advancement in the next generation of high-performance energy storage devices, In addition to the unique electrical properties of metals and semiconductors, conducting polymers with strongly p-conjugated backbones also exhibit the desirable flexibility and accessibility of typical polymers. Polypyrrole (PPy) stands out as a viable option to build flexible, lightweight, and high-performance supercapacitors that can meet the need for portable and wearable power sources due to its excellent environmental stability and adjustable conductivity. Low capacitance and poor cycle stability are two of the main drawbacks that prevent their widespread use. The capacitance and cycling performance of PPy supercapacitors may be optimized by careful design of the material's microstructure. To guarantee good capacitance and cycle performance, mPPy-nbs with adjustable size and programmable mesopores were synthesized using a bottom-up dual-colloid interface co-assembly approach under moderate conditions [22]. Chu et al. [23] conducted copolymerization of Aniline and Phytic acid for Flexible Solid state Micro-supercapacitor and is shown in Fig. 3.

In the case of polythiophene, further research has focussed on the modified polymers created by polymerizing the substituted monomer poly(3-hexylthiophene) (P3HT). Poly(3,4-ethylenedioxythiophene) (PEDOT) is another substituted CP that has been extensively investigated and tailored to many uses. Although the discovery of doping in polyacetylene began in the contemporary conducting polymer area, interest has waned due to the polymer's poor durability. Reviewers look at all published material, but they don't simply make a laundry list of problems and

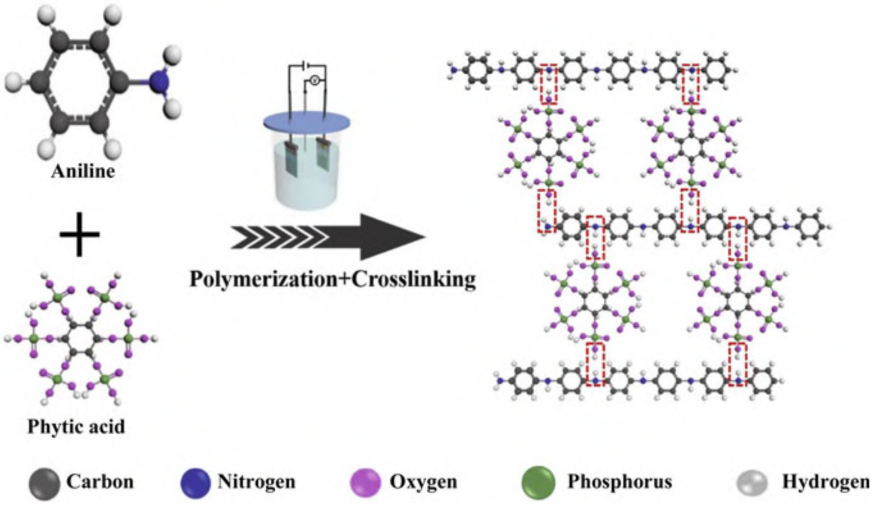

Fig. 3 Copolymerization of Aniline and Phytic acid [23]. Taken

answers; rather, they try to get to the bottom of why some approaches work. Therefore, the outcomes will be segmented according to polymer type, with an accompanying synopsis of the organic chemistry of the polymer chains. Research describing the modification of a single kind of polymer using the same methods is presented next. To round out the picture, studies will also focus on the functionalization of other conducting polymers, which have not received as much attention yet [9].

2.3 Comparison of Functionalization Techniques

In physical functionalization, doping a conducting polymer with a chemical increases its electrical properties, which allows it to store more charge. Physical doping can be done through a variety of techniques, such as thermal treatment or chemical doping agents. However, the dopant must be carefully chosen as some chemicals can cause structural modifications that reduce its electrical properties. Furthermore, the dopant can sometimes increase the cost of production, making it less attractive for commercial use. On the other hand, chemical functionalization of conducting polymers can be achieved through copolymerization. In this case, the conducting polymer is combined with another monomer to create a copolymer that enhances the material's performance as a supercapacitor electrode. This can be done through chemical synthesis methods, such as oxidative polymerization or chemical vapor deposition. This technique involves the incorporation of electroactive moieties or molecules into the polymer. In conclusion, physical functionalization and chemical functionalization are two different techniques used to modify the properties of conducting polymers for use in supercapacitors.

3 Types of Conducting Polymer-Based Capacitors

Kumar et al. [24] presented a review of the many kinds of supercapacitors, including pseudocapacitors, electrical double-layer capacitors (EDLCs), and hybrids.

3.1 Electrochemical Supercapacitors

Electrochemical supercapacitors, also called electric double-layer capacitors (EDLCs), are energy storage devices that use a combination of an electrolyte and two electrodes to store and release electrical energy. Figure 4 represents the schematic diagram of charge storage by electrochemical double-layer capacitance. Conducting polymer-based supercapacitors are a type of electrochemical supercapacitor that uses a conducting polymer as the active material in one or both of the electrodes. To develop high-flexible PSCs with excellent cycle stability, Wu et al. [25] reported a unique graphene/polypyrrole hydrogel (PGH)-based highly flexible solid-state supercapacitor, which has long cycle performance and was developed by simple heating approach. Shahabuddin et al. [26] illustrate an approach by in situ oxidative polymerization technique for the synthesis of polyaniline (PANI) nanocomposites doped with nanoparticle in developing electrodes for high-performance energy storage supercapacitors. Bi et al. systematically discussed the recent developments in the synthesis process and characterization of 2D polymer-based nanosheets, as well as their recent progress in electrochemical energy storage and conversion, such as supercapacitors, hydrogen evolution, oxygen reduction, and second batteries [27]. Electrochemical capacitors (ECs) are a class of capacitors using electrocatalysis to store electric charges. They are similar to electrochemical batteries but have the ability to be discharged and recharged many times without losing performance. The main advantage of ECs is that they can be easily customized for specific applications. However, these devices have drawbacks; for example, they have low power output and low density. Additionally, most ECs need to be refrigerated during shipping due to their high temperatures. Conducting polymer-based supercapacitors offer several advantages over traditional EDLCs, such as higher energy density, longer life span, and lower cost. They are also flexible and lightweight, making them suitable for use in a variety of applications, such as portable electronics, electric vehicles, and renewable energy systems. Abdah et al. [28] highlighted recent advances in TMO–, CP–, and TMO/CP-based fibres in terms of their configurations, electrochemical characteristics, and design approaches for supercapacitor applications have opened up new prospects for emerging energy storage mechanisms.

Fig. 4 Schematic diagram of charge storage by electrochemical double-layer capacitance [29]. Taken

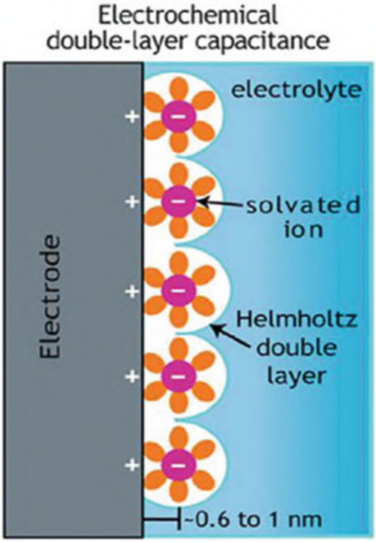

3.2 Pseudocapacitors (PCs)

Pseudo supercapacitor is a hybrid device that uses anionic, cationic, or non-ionic electrolytes to charge and discharge the capacitor. Anionic supercapacitors use anionic electrolytes, such as polypropylene sulfonate (APS) or poly(vinyl acetate). Cationic supercapacitors use cationic electrolytes such as aluminum chloride (AC) or magnesium chloride (MC). Non-ionic supercapacitors use non-ionic electrolytes, such as sodium carbonate (SC) or ammonium carbonate (AC). The ionic liquid electrolyte allows to conduct electricity with low resistance at room temperature. Figure 5 shows the schematic diagram of charge storage by pseudo-capacitance. Li et al. [30] reported manufacturing of a binder-free, self-supported, flexible polypyrrole-based electrode using unique, hollow PPy nanofibres having porous capsular walls for supercapacitor which show good cycling stability. Wang et al. [31] showed that Substrates made from surface-modified nanocellulose fibres (NCFs) could be utilized to create supercapacitor electrodes having full electrode-normalized volumetric (122 F cm^{-3}) and gravimetric (127 F g^{-1}) capacitances at large current densities 300 mA cm^{-2} $\approx$ 33 A g^{-1} for electrodes based on conducting polymer having active mass loadings upto 9 mg cm^{-2}. PCs are generally more efficient than traditional capacitors at the same voltage and charge levels. They're also safer because they can withstand higher voltage levels before breaking down something conventional capacitors can't do. However, these devices have a slow charge time, so it takes a long time to charge batteries. Additionally, there's limited discharge capability so it's difficult to completely destroy the charge stored in the capacitor. Conducting polymer-based pseudocapacitors are good alternatives to traditional capacitors due to their high energy density, stability, low weight, and transparency. Shahabuddin et al. [26] illustrated an approach by in-situ oxidative polymerization technique for the synthesis of polyaniline (PANI) nanocomposites doped with nanoparticles in developing electrodes for high-performance energy storage supercapacitors. Magu et al. [32] investigated conducting polymer-based composites, which include binary, ternary, and quaternary composites for supercapacitors and batteries. They have many advantages over alternative energy storage systems such as batteries; however, there are still some issues that need to be worked out in order for them to become practical devices for power storage applications in electronics and vehicles. Fong et al. [33] reviewed improvements made recently in engineering electrodes for high-performance supercapacitors based on conducting polymers, with special focus on the methods for nanostructuring, polymer synthesis, and compositing with metal oxides or carbon that have been shown to successfully optimize key performance metrics.

3.3 Hybrid Supercapacitors

Hybrid supercapacitors are a type of energy storage device that combines the benefits of both batteries and traditional supercapacitors. They use a combination of a

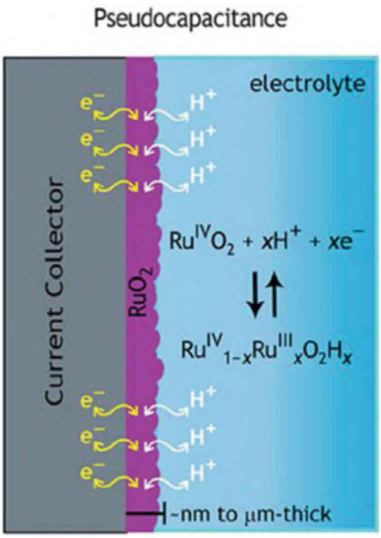

Fig. 5 Schematic diagram of charge storage by pseudocapacitance [29]. Taken

conducting polymer and a battery-type material, such as a metal oxide or a lithium salt, as the active materials in the electrodes. Shrestha et al. uses polyol technique to synthesize $MnCo_2O_4$/nitrogen-doped graphene 2D/2D hybrid nanoarchitectures. This arrangement effectively prevents the restacking and aggregation of nitrogen-doped graphene nanosheets [34]. Cherusseri et al. [35] focussed on the most current advances in innovative electrode materials and hybrid designs utilized in supercapacitors to achieve high energy density and specific capacitance. De et al. [36] focussed on the recent advancements in supercapacitors consisting ternary composites having conducting polymers, transition metal oxides, and carbon-based materials. The conducting polymer offers high surface area and high electrical conductivity, while the battery-type material contributes to the energy density of the hybrid supercapacitor. This combination results in a device with higher energy density than a traditional supercapacitor, but with faster charge–discharge capabilities and longer life span than a battery. The use of conducting polymers in hybrid supercapacitors also provides advantages such as high stability, good cycling performance, and environmental friendliness compared to traditional battery materials.

In conclusion, hybrid supercapacitors are a type of energy storage device that combine the benefits of both batteries and traditional supercapacitors. They use a combination of conducting polymers and battery-type materials as the active materials in the electrodes, resulting in a device having high energy density, long life span, and fast charge–discharge capabilities.

4 Applications of Conducting Polymer-Based Supercapacitors

4.1 Energy Storage

Conducting polymer-based supercapacitors have several potential applications in energy storage due to their unique combination of high surface area, high electrical conductivity, and fast charge–discharge capabilities. Some of the key applications are:

Portable Electronics: Conducting polymer-based supercapacitors can be used to power portable electronic devices such as smartphones, laptops, and wearable devices. They provide quick charging and longer lifespan compared to traditional batteries. Meng et al. [37] demonstrated a new type of ultrathin all-solid-state supercapacitor using two polyaniline-based electrodes that are slightly separated and thoroughly solidified in the sulphuric acid-polyvinyl alcohol gel electrolyte which is an exceedingly easy technique. Kou et al. [38] proposed a two-ply yarn supercapacitor created using a coaxial wet-spinning assembly technique that uses continuously spun polyelectrolyte-wrapped graphene/carbon nanotube core-sheath fibres as safe electrodes.

Electric Vehicles: Conducting polymer-based supercapacitors can be used as a supplemental energy storage device in electric vehicles to support the main battery during high-power discharges, leading to longer battery life and improved driving performance. Song et al. [39] proposed a semi-active battery/supercapacitor (SC) hybrid energy storage system (HESS designed for usage in electrically powered vehicles. Kouchachvili et al. [40] reviewed the latest studies on the use of different battery/supercapacitor hybrid systems for electric vehicles. The electric power steering (EPS) systems in current vehicle power systems do not provide enough power in pivot or low-speed steering settings, which limits their use in heavy-duty commercial vehicles. To tackle this problem Cao et al. [41] proposed an EPS system on the basis of hybrid power system comprised of vehicle power system and the supercapacitor in parallel. Thounthong et al. [42] proposed a control strategy for fuel cell/supercapacitor hybrid power sources for electric vehicles. The test circuit they presented is shown in Fig. 6.

Renewable Energy Systems: Conducting polymer-based supercapacitors can be used to store energy derived from renewable energy sources, like wind or solar energy, and provide quick response times during power outages or fluctuations. Zou et al. [43] provided a review of fractional-order methods for controlling lead-acid batteries, lithium-ion batteries, and supercapacitors. Sharma et al. suggested a dynamic power management system (PMS) for an independent hybrid ac/dc microgrid with a photovoltaic-based renewable energy source, supercapacitor as hybrid energy storage, a proton exchange membrane fuel cell as a battery, and a secondary power source [44].

Grid Energy Storage: Conducting polymer-based supercapacitors can be used for grid energy storage to provide backup power during power outages, reduce energy

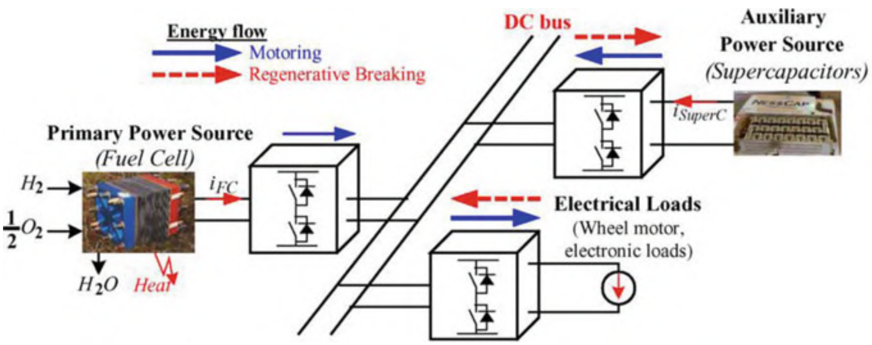

Fig. 6 Fuel cell/supercapacitor hybrid power sources for electric vehicles [42]. Taken

waste, and improve grid stability. Inthamoussou et al. [45] presented the managment of an energy storage system (ESS) on the basis of supercapacitor in the framework of grid-connected microgrids. A unified energy management scheme is suggested for renewable grid-integrated systems having battery-supercapacitor hybrid storage by Tummuru et al. [46].

4.2 Sensors

Conducting polymer-based supercapacitors have several potential applications in sensors due to their combination of high electrical conductivity, high stability, and fast charge–discharge capabilities. Some of the key applications are:

Wearable Sensors: Conducting polymer-based supercapacitors can be used as a power source for wearable sensors, providing quick charging and longer lifespan compared to traditional batteries. Wang et al. [47] investigated the problem of recognizing multi-user tasks in the home setting utilizing wearable sensors. For biometric monitoring, an autonomous body-worn wireless sensor node having a flexible energy harvesting (FEH) mechanism that can fit to body shape is presented by Toh et al. [48]. Li et al. [49] presented MSC arrays based on polypyrrole (Ppy) film by integrating electrode positon and photolithography methods. Deng et al. [50] presented a wearable thermoelectric power generator that uses body heat to provide power to low-power human diagnosis devices (mainly sensor nodes). As a result, a new class of thermoelectric generator (TEG) incorporated into clothes that merges TEG technology with fashion sports equipment: sports tights, headbands, and leg guards is also introduced. The flow chart of TEG-based wireless sensor presented by Iezzi et al. [51] is shown in Fig. 7.

Implantable Sensors: Conducting polymer-based supercapacitors can be used as a power source for implantable sensors, such as heart monitors, providing a stable and safe power source. Wee et al. [52] focussed on the relevance of polarization properties in polyelectrolyte-based capacitor designs in sensors, supercapacitors, and

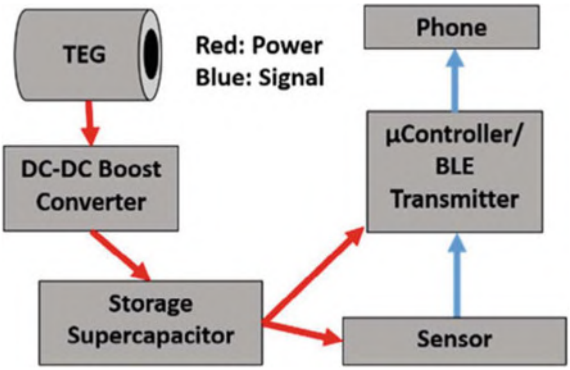
TEG
Red: Power
Blue: Signal
Phone
DC-DC Boost Converter
µController/ BLE Transmitter
Storage Supercapacitor
Sensor

Fig. 7 Flow chart of TEG-based wireless sensor [51]. Taken

transistors. Pandey et al. [53] proposed an implantable biomedical sensor powered by a wirelessly charged supercapacitor. Several polymers used for implantation and related integration technologies are identified by Qin et al. [54]. Gao et al. [55] developed All-polymer ultrathin flexible supercapacitors for electronic skin and explained the charging and discharging processes during expanding and contracting, and are shown in Fig. 8.

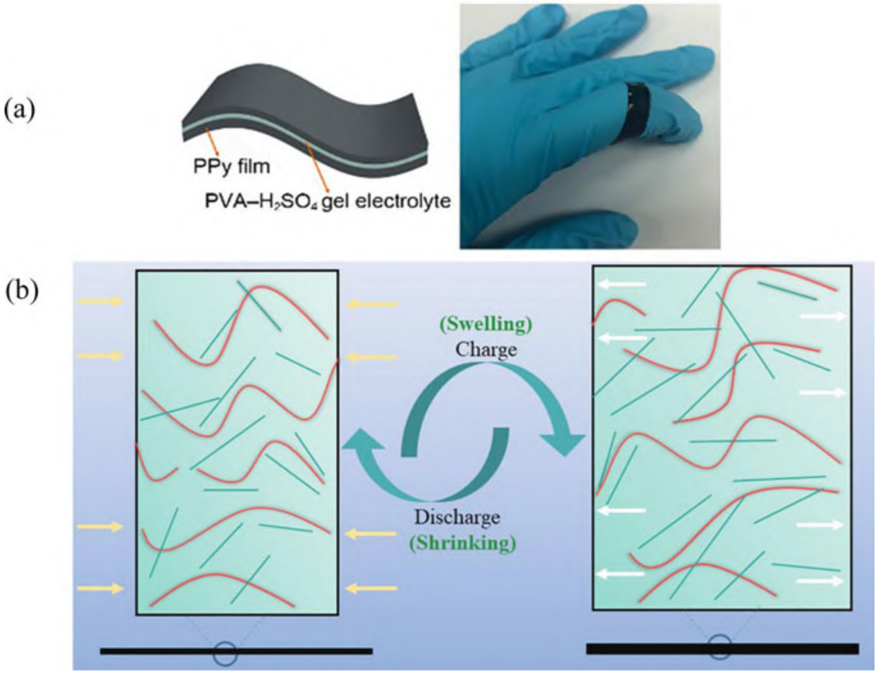
(a)
PPy film
PVA–H₂SO₄ gel electrolyte
(b)
(Swelling)
Charge
Discharge
(Shrinking)

Fig. 8 **a** All-polymer ultrathin flexible supercapacitors for electronic skin **b** Schematic diagram of charging and discharging processes during expanding and contracting [55]. Taken

Environmental Sensors: Conducting polymer-based supercapacitors can be used to power environmental sensors, such as air quality monitors or soil moisture sensors, providing a stable and efficient power source. Wang et al. [56] conducted research centred on N-heterocyclic aromatic moiety-containing fluorescent polymer sensors, which have been significant in the advancement of conjugated polymer-based fluorescence sensing from its inception. Recent and up-to-date research on biopolymers and conducting polymer-based materials in sensors for heavy metal ion detection by optical techniques was reviewed by Ramdzan et al. [57]. According to the results, the sensor was discovered to be extremely sensitive as well as selective for detecting and quantifying Pb^{2+} in real water samples [58].

5 Smart Grid Sensors

Conducting polymer-based supercapacitors can be used as a power source for smart grid sensors, providing quick response times and reliable power supply during power outages or fluctuations. Mertes et al. described an innovative plate system able to detect the weight and position of individual bites during meals [59]. The modified manufacturing method of one-axis tense-resistive sensors screen printed on diverse polymer substrates such as porous, films, and fibrous materials of varying composition and structure is explained by Nagornova et al. [60]. An effective model based on a Genetic Algorithm is described, which may significantly reduce power consumption in power systems and smart grids by Fahad et al. [61].

5.1 Energy Conversion Devices

Conducting polymer-based supercapacitors have many uses in modern technology; however, they still have a way to go before becoming a mainstream technology. In particular, these devices have low power density and charging times due to their manufacturing difficulties. Therefore, supercapacitor developers must find ways to improve these components enough so that they're usable by modern technologies.

References

1. Banerjee S, Kar KK (2016) Superior water retention, ionic conductivity and thermal stability of sulfonated poly ether ether ketone/polypyrrole/aluminum phosphate nanocomposite based polymer electrolyte membrane. 4(1):299–310
2. Du Pasquier A et al (2002) A nonaqueous asymmetric hybrid li4ti5 o 12/poly (fluorophenylthiophene) energy storage device. 149(3):A302
3. Nohma T et al (1995) Electrochemical characteristics of $LiNiO_2$ and $LiCoO_2$ as a positive material for lithium secondary batteries. 54(2):522–524

4. Park Y, Jung J, Chang M (2019)Research progress on conducting polymer-based biomedical applications. 9(6):1070
5. Chiang CK et al (1977)Electrical conductivity in doped polyacetylene. 39(17):1098
6. Kar KK (2020) Handbook of nanocomposite supercapacitor materials II, vol 302. Springer
7. Talbi H, Just PE, Dao LH (2003) Electropolymerization of aniline on carbonized polyacrylonitrile aerogel electrodes: applications for supercapacitors. 33(6)
8. Lu W et al (2002)Use of ionic liquids for π-conjugated polymer electrochemical devices. 297(5583):983–987
9. Abel SB et al (20230Functionalization of Conductive Polymers through Covalent Postmodification. 15(1):205
10. Zhou Y et al (2010) Polyaniline/multi-walled carbon nanotube composites with core–shell structures as supercapacitor electrode materials. 55(12):3904–3908
11. Vangari M, Pryor T, Jiang L (2013) Supercapacitors: review of materials and fabrication methods. 139(2):72–79
12. Gnanakan SR, Murugananthem N, Subramania A (2011) Organic acid doped polythiophene nanoparticles as electrode material for redox supercapacitors. 22(6):788–793
13. Zhang CJNE (2016) Supercapacitors: performance doping. 1(2):1
14. Pecher J, Mecking S (2010) Nanoparticles of conjugated polymers. 110(10):6260–6279
15. Boeva ZA, Sergeyev VG (2014) Polyaniline: synthesis, properties, and application. 56(1):144–153
16. Khokhar D et al (2021)Functionalization of conducting polymers and their applications in optoelectronics. 60(5):465-487
17. Diaz AF, Hall B (1993) Mechanical properties of electrochemically prepared polypyrrole films. 27(4):342–347
18. Cao Y et al (1992)Solution-cast films of polyaniline: Optical-quality transparent electrodes. 60(22):2711–2713
19. Navale S et al (2014) Camphor sulfonic acid (CSA) doped polypyrrole (PPy) films: measurement of microstructural and optoelectronic properties. 50:363–369
20. Tang Y et al (2010) Electrochemical synthesis of polyaniline in surface-attached poly (acrylic acid) network, and its application to the electrocatalytic oxidation of ascorbic acid. 168:231–237
21. Kumar P et al (2011) Electrochemical copolymerization of thiophene derivatives; a precursor to photovoltaic devices. 56(24):8184–8191
22. Cui J et al (2021)General synthesis of hollow mesoporous conducting polymers by dual-colloid interface co-assembly for high-energy-density micro-supercapacitors. 62:145–152
23. Chu X et al (2019)Electrochemically building three-dimensional supramolecular polymer hydrogel for flexible solid-state micro-supercapacitors. 301:136–144
24. Kumar Y et al (2019) Background, fundamental understanding and progress in electrochemical capacitors. 23:667–692
25. Wu X, Lian M (2017) Highly flexible solid-state supercapacitor based on graphene/polypyrrole hydrogel. 362:184–191
26. Shahabuddin S et al (2018) The metal oxide nanoparticles doped polyaniline based nanocomposite as stable electrode material for supercapacitors. In: 2018 international conference and utility exhibition on green energy for sustainable development (ICUE). IEEE.
27. Bi S et al (2018)Two-dimensional polymer-based nanosheets for electrochemical energy storage and conversion. 27(1):99–116
28. Abdah MA et al (2020)Review of the use of transition-metal-oxide and conducting polymer-based fibres for high-performance supercapacitors. 186:108199
29. Yang P, Mai W (2014)Flexible solid-state electrochemical supercapacitors. 8:274–290
30. Li Z et al (2015) A self-supported, flexible, binder-free pseudo-supercapacitor electrode material with high capacitance and cycling stability from hollow, capsular polypyrrole fibers. 3(31):16162–16167
31. Wang Z et al (2015)Surface modified nanocellulose fibers yield conducting polymer-based flexible supercapacitors with enhanced capacitances. 9(7):7563–7571

32. Agobi AU et al (2019)A review on conducting polymers-based composites for energy storage application. 1(1):19–34
33. Fong KD et al (2017)Multidimensional performance optimization of conducting polymer-based supercapacitor electrodes. 1(9):1857–1874
34. Shrestha KR et al (2019) A spinel MnCo2O4/NG 2D/2D hybrid nanoarchitectures as advanced electrode material for high performance hybrid supercapacitors. 771:810–820
35. Cherusseri J et al (2019) Novel mesoporous electrode materials for symmetric, asymmetric and hybrid supercapacitors. 30(20):202001
36. De B et al (2020) Transition metal oxide-/carbon-/electronically conducting polymer-based ternary composites as electrode materials for supercapacitors. Handbook of nanocomposite supercapacitor materials II: performance. Springer, pp 387–434
37. Meng C et al (2010)Highly flexible and all-solid-state paperlike polymer supercapacitors. 10(10):4025-4031
38. Kou L et al (2014)Coaxial wet-spun yarn supercapacitors for high-energy density and safe wearable electronics. 5(1):3754
39. Song Z et al (2014)Multi-objective optimization of a semi-active battery/supercapacitor energy storage system for electric vehicles. 135:212–224
40. Kouchachvili L, Yaïci W, Entchev E (2018) Hybrid battery/supercapacitor energy storage system for the electric vehicles. 374:237–248
41. Cao D et al (2019)Study on low-speed steering resistance torque of vehicles considering friction between tire and pavement. 9(5):1015
42. Thounthong P, Raël S, Davat B (2006) Control strategy of fuel cell/supercapacitors hybrid power sources for electric vehicle. 158(1):806–8140
43. Zou C et al (2018) A review of fractional-order techniques applied to lithium-ion batteries, lead-acid batteries, and supercapacitors. 390:286–296
44. Sharma RK, Mishra S (2017) Dynamic power management and control of a PV PEM fuel-cell-based standalone ac/dc microgrid using hybrid energy storage. 54(1):526–538
45. Inthamoussou FA, Pegueroles-Queralt J, Bianchi FD (2013) Control of a supercapacitor energy storage system for microgrid applications. 28(3):690–697
46. Tummuru NR, Mishra MK, Srinivas S (2015) Dynamic energy management of renewable grid integrated hybrid energy storage system. 62(12):7728–7737
47. Wang L et al (2011)Recognizing multi-user activities using wearable sensors in a smart home. 7(3):287–298
48. Toh WY et al (2014)Autonomous wearable sensor nodes with flexible energy harvesting. 14(7):2299–2306
49. Li L et al (2017)Flexible planar concentric circular micro-supercapacitor arrays for wearable gas sensing application. 41:261–268
50. Deng F et al (2016)Wearable thermoelectric power generators combined with flexible supercapacitor for low-power human diagnosis devices. 64(2):1477–1485
51. Iezzi B et al (2017) Printed, metallic thermoelectric generators integrated with pipe insulation for powering wireless sensors. 208:758–765
52. Wee G et al (2010)Effect of the Ionic Conductivity on the Performance of Polyelectrolyte-Based Supercapacitors. 20(24):4344-4350
53. Pandey A et al (2011) Integration of supercapacitors into wirelessly charged biomedical sensors. In: 2011 6th IEEE conference on industrial electronics and applications. IEEE
54. Qin Y et al (2014)Polymer integration for packaging of implantable sensors. 202:758-778
55. Gao F et al (2021)All-polymer ultrathin flexible supercapacitors for electronic skin. 405:126915
56. Wang T et al (2020) Fluorescent chemosensors based on conjugated polymers with N-heterocyclic moieties: two decades of progress. 11(18):3095-3114
57. Ramdzan NSM et al (2020)Development of biopolymer and conducting polymer-based optical sensors for heavy metal ion detection. 25(11):2548
58. López FDLM et al (2021) A novel highly sensitive imprinted polymer-based optical sensor for the detection of Pb (II) in water samples. 16:100497

59. Mertes G et al (2018) Measuring weight and location of individual bites using a sensor augmented smart plate. In: 2018 40th annual international conference of the IEEE engineering in medicine and biology society (EMBC). IEEE
60. Nagornova I et al (2019) Tenso-resistive printed sensors for various deformation measurements. In: 2019 xxix international scientific symposium metrology and metrology assurance (MMA). IEEE
61. Fahad M, Beenish H (2019) Efficient V2G model on smart grid power systems using genetic algorithm. In: 2019 1st global power, energy and communication conference (GPECOM). IEEE

Z

Part IV

FNMs Based Supercapacitor for Environmental Applications

Всё для победы!
НАРОДНЫЙ ФРОНТ
https://pobeda.onf.ru/
LET'S HELP THE RUSSIA
Z

Chapter 15
Environmental Applications of Carbon-Based Supercapacitors

K. S. Rajni, V. Vishnu Narayanan, and Pughal Selvi

1 Introduction

The modern world is currently moving toward a sustainable world. The backbone of a sustainable world is sustainable energy sources. Keeping this in mind, the UN's sustainable development goals highlight the adoption of various renewable energy sources, such as solar energy, wind, tidal, thermal, biomass, etc., for the effective utilization of these energy sources along with the efficient conversion of energy to electricity efficient energy storage devices such as various types of batteries and supercapacitors are required are also required. The batteries are characterized by their very high energy density, while the very high-power density is the specialty of supercapacitors [1]. Thus, supercapacitors are suitable for applications that require a very high-power burst, such as when accelerating an electric vehicle after starting [2].

The supercapacitors store electrical energy either electrostatically or electrochemically. These devices have a very high capacitance value and low voltage rating. A supper capacitor consists of an anode and a cathode separated by an electrolyte. An ion-permeable membrane stops the intermixing of electrolyte species from the anode side to the cathode side. It permits the charge transfer between the two sides to complete the electrical circuit. The structure of a supercapacitor is shown in Fig. 1.

Supercapacitors can be classified into Electric Double Layer Capacitors (EDLCs), Pseudo Capacitors, and Hybrid Capacitors based on their charge storage mechanism. The EDLC store charge at the electrode–electrolyte interface, and the reversible faradaic redox reactions are the working principles of pseudo capacitors. A hybrid capacitor is a mix-up of both EDLC and pseudo-capacitors [3, 4]. The various types

---

K. S. Rajni (✉) · V. V. Narayanan · P. Selvi
Amrita School of Physical Sciences, Amrita Vishwa Vidyapeetham Ettimadai, Coimbatore, Tamil Nadu, India
e-mail: ks_rajani@cb.amrita.edu

© The Author(s), under exclusive license to Springer Nature Singapore Pte Ltd. 2024

C. M. Hussain and M. B. Ahamed (eds.), *Functionalized Nanomaterials Based Supercapacitor*, Materials Horizons: From Nature to Nanomaterials,
https://doi.org/10.1007/978-981-99-3021-0_15

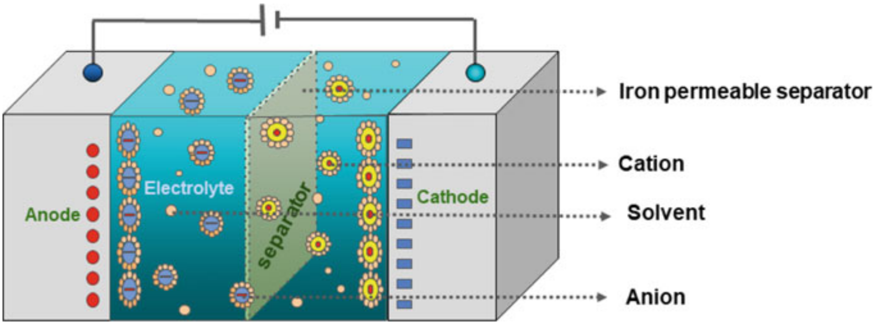
Iron permeable separator
Cation
Solvent
Anion
Anode
Electrolyte
separator
Cathode

Fig. 1 Structure of a supercapacitor

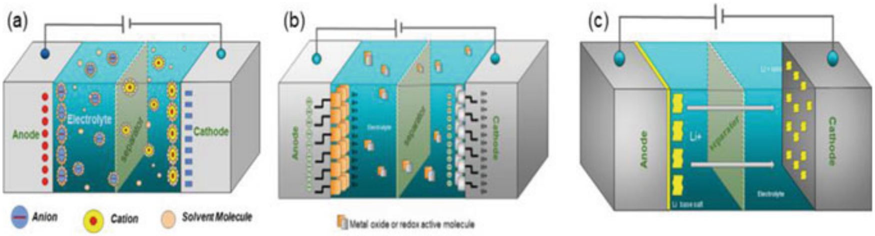
(a)
Anode
Electrolyte
separator
Cathode
Anion
Cation
Solvent Molecule
(b)
Anode
Electrolyte
separator
Cathode
Metal oxide or redox active molecule
(c)
Anode
Li+
separator
Cathode
Electrolyte
Li base salt

Fig. 2 Classification of SC, **a** EDLC, **b** Pseudo capacitor **c** Hybrid capacitor

of supercapacitors are illustrated in Fig. 2a. Both electrodes in the EDLCs are carbon-based, while the pseudo capacitors use various transition metal oxides, sulfides, and conducting polymers as electrodes. In hybrid supercapacitors, one of the electrodes will be carbon-based, while the other will have pseudo-capacitor properties [3–6].

The charge storage mechanism of EDLC is the electrochemical double layer which enables the device to store charge either electrostatically or by a non-faradic charge transfer method. Based on the carbon conduct in the electrodes, the EDLCs are classified into three (Fig. 3). The Faradaic process is the working principle of pseudo capacitors, which involves the transfer of loads between electrodes and electrolytes electrostatically. A faradaic current will pass through the pseudo capacitor, resulting in a much higher energy density than that of EDLCs. Like the EDLCs, the pseudo capacitors can also be classified into three (Fig. 3). A hybrid supercapacitor combines a battery's very high energy density with the very high-power density of supercapacitors. One of the device's electrodes will have the attributes of a battery, while the other will have the attributes of a supercapacitor. Similar to the EDLCs and pseudo-capacitors, the hybrid capacitors are classified into three (Fig. 3) [7–9].

Activated carbon, Carbon Nanotubes (CNTs), graphene, carbon aerogels, carbon foam, carbide-derived carbon, etc., are the commonly used carbon electrodes for

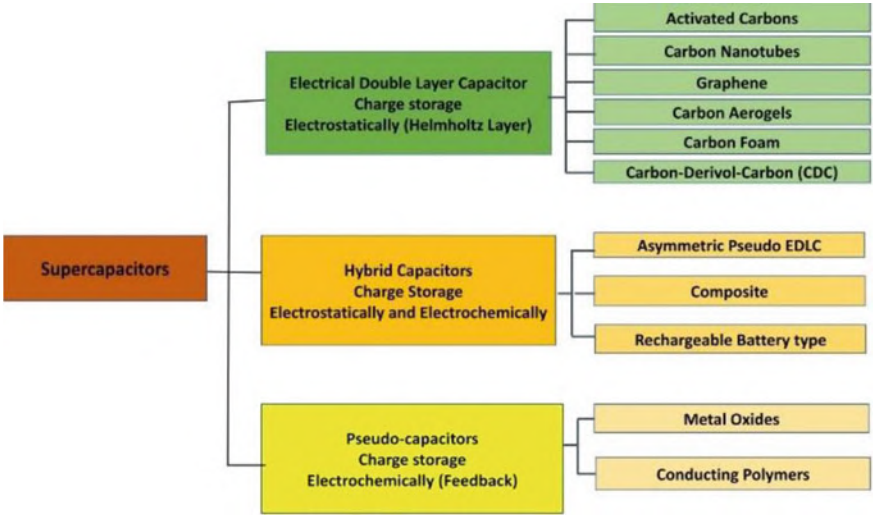
Supercapacitors
Electrical Double Layer Capacitor
Charge storage
Electrostatically (Helmholtz Layer)
Activated Carbons
Carbon Nanotubes
Graphene
Carbon Aerogels
Carbon Foam
Carbon-Derivol-Carbon (CDC)
Hybrid Capacitors
Charge Storage
Electrostatically and Electrochemically
Asymmetric Pseudo EDLC
Composite
Rechargeable Battery type
Pseudo-capacitors
Charge storage
Electrochemically (Feedback)
Metal Oxides
Conducting Polymers

Fig. 3 Classification of supercapacitors

supercapacitor applications [10, 11]. These carbon-based electrodes are promising ones for supercapacitor applications due to their:

i. Ability to produce very fast pulses of energy.
ii. Stability over millions of charge/discharge cycles.
iii. Wide operating temperature.
iv. High coulombic efficiency
v. Low-cost and
vi. Non-toxicity.

In addition to these properties, it is easy to engineer the structural, morphological, compositional, electrical, and chemical properties of the various carbon materials [12]. In this book chapter, we primarily focus on the environmental application of carbon-based supercapacitors and their impact on providing clean and sustainable energy for a sustainable future.

2 Carbon Electrodes for Supercapacitor Applications

2.1 *Elemental Carbon*

Carbon is a non-metallic tetra valent element having six electrons ($1s^2$, $2s^2$, 2p2) in its ground state. The energy gap between the 2 s and 2p orbitals is narrow, promoting one of the 2 s electrons to the empty $2p_z$ orbital. Carbon has three different hybridization states (sp, sp^2, or sp^3) depending on the nature of its bonding partner. The triple hybridization states of carbon are the reason for its diverse chemical and structural properties of carbon [13]. At elevated temperatures and pressures, the tetrahedra sp^3 hybridization state is preferable. At lower temperatures and pressures, the planar sp^2 hybridization state is preferred by the carbon and forms sheets having a single atomic thickness. These sheets will have three sigma and one pi bond. These carbon sheets are also thermodynamically stable compared to their three-dimensional counterparts (diamonds) [14].

2.2 Carbon Dots

Carbon dots (C-dots) are an umbrella term that represents all three-dimensionally confined carbon nanoparticles. The C-dots usually have sizes <10 nm, but some varieties can have sizes up to 60 nm and are characterized by their fluorescence properties. The organic C-dots normally have an sp^2 hybridized nanocrystalline core with an amorphous shell with various functional groups attached [15–17]. According to the structure, there are three different subgroups for the C-dots, namely graphene quantum dots (GQD), carbon nanodots (GND), and polymer dots (PDs), with size less than 10 nm.

The GQDs have a large horizontal dimension, while the thickness is of a few atoms and has an average crystal size of 0.25 nm [19]. The CNDs consist of multiple carbon atoms and have a spherical morphology. The PDs contain a carbon core with aggregated or cross-linked polymers attached to it [18, 20]. These carbon dots can be synthesized either by top-down or bottom-up approaches such as hydrothermal, solvothermal, arc discharge method, electron beam lithography, laser ablation, carbonization, pyrolysis, acid exfoliation, etc., [20–26]. These carbon dots gained researchers' attention for energy storage applications (supercapacitors and batteries) due to their large surface area, active edge sites, conductivity, and the ease of developing electrodes by dissolving various solvents [27]. These can also be used to develop various flexible and wearable electronic devices [28].

2.3 Graphite—Graphene Family

Graphite is a commonly known isotope of carbon with anisotropic structural and functional properties [29]. It has an in-plane electrical and thermal conductivity that is a few hundred times greater than those in the out-of-plane directions. The monolayer of graphite is called graphene. Since the development of graphene, it has become a favorite material for researchers worldwide due to its superior electrical, optical, thermal, structural, and mechanical properties [30]. The third and final member of the graphite-graphene family is graphene oxide (GO). The GO is considered a graphene derivative and exhibits a layered structure and similar properties to graphene [31]. The GO can be easily produced on a large scale and at a low cost through the oxidation of graphite. Among the various production techniques of graphene, the reduction of GO is a low-cost method [32].

The graphit—graphene family is considered to be one of the promising futuristic materials for the development of next-generation energy conversion and storage devices as well as for the development of next-generation flexible electronic devices due to their unique properties such as:-

1. Large surge two-dimensional surface area.
2. Very high electrical conductivity.
3. Superior mechanical properties.
4. lightweight.
5. Structural flexibility and
6. Has tunable electrical conductivity.

These are the essential properties required to develop supercapacitors [33]. The addition of spacers is one of the most efficient stackings of graphene layers possible. According to the nature of the spacer used, the inter-layer spacing of the graphene can be tuned. In addition, the spacers can alter graphene's stability, charge storage, and ion diffusion properties [34].

2.4 Activated Carbon

Another interesting carbon derivative for energy storage applications is activated carbon (Acs). This low-cost, environmentally friendly, and non-toxic carbon derivative has a very high specific surface area (SSA) with a specific capacitance of about 100 F/g [35]. The drawback of Acs is their pore size, these materials have a broad bore size range which prevents the accessibility to electrolyte ions. The activated carbon can be produced from carbon materials either via physical activation methods or chemical activation methods [36].

2.5 Carbon Nanotubes

Carbon nanotubes (CNTs) are very good electron conductors used in various electrochemical devices as electrode materials due to their high electrical conductivity and durability [37]. Like the graphite-graphene family, the CNTs are also sp^2 hybridized and are free of surface dangling bonds. The exohedral surface area of CNTs is about 1300 m^2/g which is crucial in developing a very good electrode–electrolyte interface, hence realizing the formation of EDLC and charge storage. Further, the physical structure of covalent sp^2 bonds is the reason behind the reduced electrical resistance of CNTs and graphene [38, 39].

The carbon nanotubes are classified into Single-Walled Carbon Nanotubes (SWCNTs), ii. Double-Walled Carbon Nanotubes (DWCNTs) and iii. Multi-Walled

Carbon Nanotubes (MWCNTs). These can be developed using chemical means, especially by decomposing the carbon source with metal-supported catalysts at high-temperature chemical vapor deposition methods [39–41].

3 Environmental Aspects of Carbon Electrodes

The conversion of conventional practices, process, and technologies to new processes and practices that revolves around clean and green technologies is the prime focus of research in the twenty-first century. The primary focus of these green technologies and processes is the design and development of approaches and practices with a low environmental bearing and the efficient usage of various scarce resources so that R&D can support the world's sustainable development [42]. As mentioned in the earlier sections, carbon has a pivotal role in developing new-generation energy storage devices. Another advantage of carbon over other minerals is that it is one of the biosphere's most abundant and easily available materials. The environmental aspects of carbon electrodes are the following:

1. Green synthesis of various carbon derivatives.
2. Recycling the used carbon electrodes and
3. Applying carbon for various environmental applications.

3.1 Green Synthesis of Carbon Derivatives

3.1.1 Synthesis Methods

Among the various chemical and physical nanoparticle synthesis methods, hydrothermal, solvothermal, microwave-assisted synthesis, electric arc discharge, spray pyrolysis, electrochemical, exfoliation, CVD, etc., are the most commonly used methods. The advantage of these methods is their less complexity, cost-efficient, and their ability to engineer with various properties of the prepared nanomaterials [43, 44].

The hydrothermal/solvothermal method is the most commonly used method for synthesizing various carbon dots due to their easiness and cost-efficiency. Since water is used as the solvent in the hydrothermal method, it is comparatively greener than its solvent counterpart. Another advantage of this method is that nanomaterials' morphology can be easily altered by varying the precursor solutions' reaction temperature, time, and pH [45].

The advantage of microwave-assisted synthesis is that the direct heating of reaction mixtures is possible and takes less time than the hydrothermal method. The lesser reaction time means that compared to the hydrothermal or solvothermal method, the energy expense is less for the microwave-assisted synthesis of carbon materials and other nanomaterials [46]. Even with regular household microwaves, it is possible to develop various nanoparticles, including carbon [47, 48].

The carbon nanotubes, fibers, and fullerenes are commonly synthesized using the electric arc discharge method. When a direct current is applied, the electric arc is produced between two graphite electrodes. The arc produces plasma, producing the heat required to develop carbon dots [49, 50]. Another method to develop various carbon nanotubes is chemical vapor deposition. The CNTs are synthesized using a metallic catalyst on a suitable substrate. The two growth mechanisms involved in synthesizing CNTs using CVD are: a. root-growth mechanism and b. tip-growth mechanisms [51–53].

The CVD can also be used to develop graphene nanosheets [54]. The graphite oxide also has a similar layer structure to graphene, but the oxygen-containing groups decorating the GO will expand the inter-layer distance. By reducing GO, it is possible to develop reduced graphene oxide (r-GO), considered chemically derived graphene [55]. The direct exfoliation of graphene nanosheets (GNS) in the liquid phase is comparatively simple, cost-efficient, and produces quality GNS. Liquid phase exfoliation (LPE) and electrochemical exfoliation (ECE) are popular methods for developing graphene. Using water as the solvent makes it possible to develop GNS by avoiding toxic and expensive solvents [56].

3.1.2 Sources of Carbon

The diverse vegetation can be utilized as the world's chief carbon source. All the common parts of the plants can be utilized for synthesizing various carbon derivatives [57–61]. Any organic source which contains carbohydrates can be used as a sustainable source of carbon instead of the expensive ones such as polyacrylonitrile [62, 63] in the recent past, lignin, cellulose, proteins, carbohydrates, etc., have been used widely to prepare various carbon derivatives by the research community. For example, developing free-standing carbon nanofiber films from bacterial cellulose is possible [64–66]. Biomass is a futuristic carbon source as it can capture CO_2 from the atmosphere and effectively reduce the greenhouse effect [67]. Like all other green plants, the biomass contains chlorophyll, which grows through photosynthesis. For their growth, they use atmospheric CO_2 and convert it into various organic compounds such as glucose [68]. Moreover, biomass-derived carbon is abundant with various functionalities, and the main challenge to developing the carbon material from biomass is to control these functional groups. The production of carbon from various biomass sources can reduce the cost of carbon by a large margin. Still, another difficulty in this approach is the limited control over the developed electrodes' morphology, porosity, and other surface properties [62].

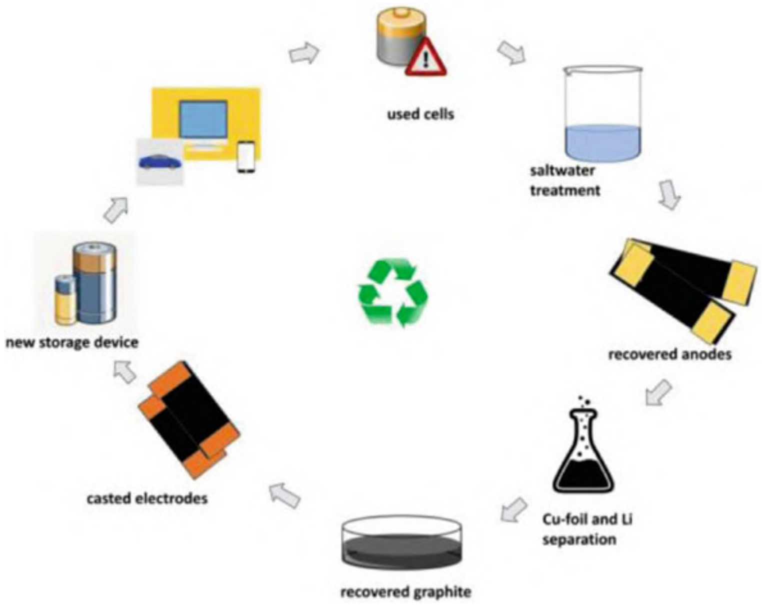
used cells
saltwater treatment
recovered anodes
Cu-foil and Li separation
recovered graphite
casted electrodes
new storage device

Fig. 4 Typical recycling process of carbon derivatives [69]

3.2 *Recycling of Carbon*

The 3R concept (recycle, reduce, and reuse) is a wise method that offers society economic, environmental, and health benefits (Fig. 4). The recovery of graphene and other carbon-derived materials enables the reuse of these materials for other potential applications [70]. The various recycling process of energy storage devices is classified into three.

a. Hydrometallurgical recycling (chemical treatment process) [71]
b. Pyrometallurgical recycling (thermal treatment process) [72], and
c. Direct recycling (Physical and mechanical process) [73].

Even though the recycled carbon materials may not have the shell life and capability as of a newly synthesized one, these can be used for other applications, such as the photocatalytic purification of wastewater [74].

3.3 *Environmental Applications of Carbon*

Carbon-derived materials, such as activated carbon and charcoal, were already used to remove various poisonous gases in the atmosphere. The newly developed nanosized carbons are more efficient than the conventional carbon materials due to their very high surface area, thermal and chemical stability, broad range of pore sizes, availability of various functional groups and reduced mass transfer resistance, etc., [75]. Due to these properties, they can be used to absorb various gaseous pollutants [76, 77], water treatment [78], various catalytic treatments [79], anaerobic digestion [80], etc.

3.3.1 Water Treatment

The contamination of water with various dyes and heavy is an alarming issue in the modern world. They are released into the water sources from various textile [81], automobile [82], and metallurgical industries [83]. Due to the wide availability of carbon allotropes and their diverse properties, they can remove various heavy metals, dyes, and other organic and inorganic impurities, including various bacterial and fungal activities in various water sources [84–90]. The various very high adsorption properties of carbon linked with its very high surface area make it a suitable adsorber of various pollutants. The improved physiochemical properties of activated carbon enhance the elimination and degradation of organic and synthetic dyes for water sources. Experiments using bio-carbon indicate that they can remove various coloring pigments such as methylene blue, levafix red, etc. [91, 92].

3.3.2 Air Purification

The elimination of polluting particles from the atmosphere is called air filtration. The larger dust particles in the air can be easily separated using scrubbers and sedimentation tanks, but these methods are ineffective in filtering out particles less than 10 μm [93]. Carbon fiber filters are commonly used to remove particulate matter with sizes less than 1 μm. along with these particulate matters from the atmosphere, separating various toxic greenhouse gasses, such as the oxides of carbon, nitrogen, sulfur, etc., from the atmosphere is also important [94]. Graphene, especially graphene aerogel, is a good fair filtration material currently available due to its strong filtration, adsorption, and separation properties [95, 96].

3.3.3 Anti-bacterial and Anti-fungal Properties

The fluorescent properties of carbon quantum dots (CQDs) can be effectively used to detect various antibiotics in food and biological samples [97]. The CQDs have very high efficiency in detecting tetracycline-based antibiotics, ampicillin, oxytetracycline hydrochloride, etc. [98]. Further, at a concentration exceeding 250 g/ml, the CQDs exhibit an inhibitory effect on E-coli and Bacillus Subtilis bacterial growths due to the hydrophobicity of CQDs. It is also found that the nanocomposites of CQDs can eliminate various bacteria when illuminated with a UV light source of 470 nm wavelength [88].

The antibacterial properties of graphene and reduced graphene are also well studied in the recent past. The derivatives of graphene, such as the hydrated graphene oxide, polysulfone modified with GO, GO with fold structure on the surface, etc., have been found to have certain anti-bacterial properties. These properties differ from the conventional antibacterial mechanism [99]. Fungal infection is also a threat to human health, similar to that bacterial and viral infections. There is a constant search ongoing for materials that prevent fungal growth. Among the various materials studied throughout, the antifungal properties of the graphite-graphene family are also studied and found to be suitable for this application [100–102].

4 Conclusion

Carbon is one of the most sustainable materials available in solid form. It is a multidimensional material due to its wide range of allotropes and vivid properties. Carbon allotropes' very high cyclic stability attracted the focus of researchers working in the energy conversion and storage field. Since the world is moving towards sustainable development, it is important to know the environmental aspects of carbon and its allotropes. Carbon is one of the most available elements in the earth's biosphere and has been recycled naturally using photosynthesis. Due to the effects of industrialization and unsustainable practices, the carbon content in gaseous form rose exponentially. But reducing gaseous carbon is possible through various means such as the various catalytic reduction of CO_2, developing biomass, etc. [102–104].

The various carbon electrodes provide very high specific surface area, chemical stability, and cyclic stability for various energy storage applications. There is no doubt in the capability of carbon as sustainable electrode material. A wide range of green synthesis methods are available to develop carbon allotropes, and the precursors can also be easily available from the earth's ecosphere [43–53]. Using the 3R method, it is possible to keep the carbon cycle for technological applications under check. The recycled and refurbished carbon electrodes can also be used for secondary applications such as wastewater treatment and air filtration. The various carbon electrodes provide very high specific surface area, chemical stability, and cyclic stability for various energy storage applications. There is no doubt in the capability of carbon as sustainable electrode material. It is concluded that carbon and its allotropes play a vital role in energy storage applications without disturbing the environment.

Acknowledgements The authors sincerely acknowledge Mr. Deepak CP (I5PHY18021) and Mr. Dineesh R (I5PHY18024), integrated MSc physics students, Department of sciences, Amrita School of Physical Science, Amrita Vishwa Vidyapeetham, Coimbatore for their help in drawing the figures.

References

1. Yasoda KY et al (2021) Fabrication of MnS/GO/PANI nanocomposites on a highly conducting graphite electrode for supercapacitor application. Mater Today Chem 19:100394
2. Miller JR, SimonP (2008) Electrochemical capacitors for energy management. Science 321(5889):651–652
3. Iro ZS, Subramani C, Dash SS (2016) A brief review on electrode materials for supercapacitor. Int J Electrochem Sci 11(12):10628–10643
4. Chen X, Paul R, Dai L (2017) Carbon-based supercapacitors for efficient energy storage. Natl Sci Rev 4(3):453–489
5. Jayalakshmi M, Balasubramanian K (2008) Simple capacitors to supercapacitors-an overview. Int J Electrochem Sci 3(11):1196–1217
6. Wang H et al (2010) Ni(OH)$_2$ nanoplates grown on graphene as advanced electrochemical pseudocapacitor materials. J Am Chem Soc 132(21):7472–7477
7. Burke A (2007) R&D considerations for the performance and application of electrochemical capacitors. Electrochim Acta 53(3):1083–1091
8. Najib S, Erdem E (2019) Current progress achieved in novel materials for supercapacitor electrodes: mini review. Nanoscale Adv 1(8):2817–2827
9. Vangari M, Pryor T, Jiang Li (2013) Supercapacitors: Review of Materials. J Energy Eng (Ç) 2:72–79
10. Pomerantseva E et al (2019) Energy storage: The future enabled by nanomaterials. Science 366(6468):eaan8285
11. Lv T et al (2018) Nanocarbon-based materials for flexible all-solid-state supercapacitors. Adv Mater 30(17):1705489
12. Miao L et al (2020) Recent advances in carbon-based supercapacitors. Mater Adv 1(5):945–966
13. Hu Y, Shenderova OA, Brenner DW (2007) Carbon nanostructures: morphologies and properties. J Comput Theor Nanosci 4(2):199–221
14. Falcao EHL, Wudl F (2007) Carbon allotropes: beyond graphite and diamond. J Chem Technol Biotechnol: Int Res Process, Environ Clean Technol 82(6):524–531
15. Hou H et al (2015) Carbon quantum dots and their derivative 3D porous carbon frameworks for sodium-ion b1atteries with ultralong cycle life. Adv Mater 27(47):7861–7866
16. Wang L et al (2015) Carbon quantum dots displaying dual-wavelength photoluminescence and electrochemiluminescence prepared by high-energy ball milling. Carbon 94:472–478
17. Liu R et al (2011) Bottom-up fabrication of photoluminescent graphene quantum dots with uniform morphology. J Am Chem Soc 133(39):15221–15223
18. Semeniuk M et al (2019) Future perspectives and review on organic carbon dots in electronic applications. ACS Nano 13(6):6224–6255
19. Lin L, Zhang S (2012) Creating high yield water soluble luminescent graphene quantum dots via exfoliating and disintegrating carbon nanotubes and graphite flakes. Chem Commun 48(82):10177–10179
20. Yan X, Cui X, Li L-S (2010) Synthesis of large, stable colloidal graphene quantum dots with tunable size. J Am Chem Soc 132(17):5944–5945
21. Tang L et al (2012) Deep ultraviolet photoluminescence of water-soluble self-passivated graphene quantum dots. ACS Nano 6(6):5102–5110
22. Dong Y et al (2012) Blue luminescent graphene quantum dots and graphene oxide prepared by tuning the carbonization degree of citric acid. Carbon 50(12):4738–4743
23. Bottini M et al (2006) Isolation and characterization of fluorescent nanoparticles from pristine and oxidized electric arc-produced single-walled carbon nanotubes. J Phys Chem B 110(2):831–836
24. Shen J et al (2011) Facile preparation and upconversion luminescence of graphene quantum dots. Chem Commun 47(9):2580–2582
25. Dong Y et al (2012) One-step and high yield simultaneous preparation of single-and multi-layer graphene quantum dots from CX-72 carbon black. J Mater Chem 22(18):8764–8766

26. Peng J et al (2012) Graphene quantum dots derived from carbon fibers. Nano Lett 12(2):844–849
27. Jian X et al (2017) Flexible all-solid-state high-performance supercapacitor based on electrochemically synthesized carbon quantum dots/polypyrrole composite electrode. Electrochimica Acta 228:483–493
28. Jian X et al (2017) Carbon quantum dots reinforced polypyrrole nanowire via electrostatic self-assembly strategy for high-performance supercapacitors. Carbon 114:533–543
29. Zhang LL, Zhou R, Zhao XS (2010) Graphene-based materials as supercapacitor electrodes. J Mater Chem 20(29):5983–5992
30. Wang X, Zhi L, Müllen K (2008) Transparent, conductive graphene electrodes for dye-sensitized solar cells. Nano Lett 8(1):323–327
31. Seredych M, Bandosz TJ (2007) Removal of ammonia by graphite oxide via its intercalation and reactive adsorption. Carbon (New York, NY) 45(10):2130–2132
32. Zhang K et al (2010) Graphene/polyaniline nanofiber composites as supercapacitor electrodes. Chem Mater 22(4):1392–1401
33. Shao Y et al (2015) Graphene-based materials for flexible supercapacitors. Chem Soc Rev 44(11):3639–3665
34. Wang G et al (2012) Flexible pillared graphene-paper electrodes for high-performance electrochemical supercapacitors. Small 8(3):452–459
35. Yassine M, Fabris D (2017) Performance of commercially available supercapacitors. Energies 10(9):1340
36. Sevilla M, Mokaya R (2014) Energy storage applications of activated carbons: supercapacitors and hydrogen storage. Energy Environ Sci 7(4):1250–1280
37. Zhi M et al (2013) Nanostructured carbon–metal oxide composite electrodes for supercapacitors: a review. Nanoscale 5(1):72–88
38. Kaur S, Ajayan PM, Kane RS (2006) Design and characterization of three-dimensional carbon nanotube foams. J Phys Chem B 110(42):21377–21380
39. Yang Z et al (2019) Carbon nanotube-and graphene-based nanomaterials and applications in high-voltage supercapacitor: a review. Carbon 141:467–480
40. Nie J et al (2009) Very high-quality single-walled carbon nanotubes grown using a structured and tunable porous Fe/MgO catalyst. J Phys Chem C 113(47):20178–20183
41. Zhang Q et al (2008) Selective synthesis of single/double/multi-walled carbon nanotubes on MgO-supported Fe catalyst. Chin J Catal 29(11):1138–1144
42. Bressi V et al (2021) Graphene quantum dots by eco-friendly green synthesis for electrochemical sensing: recent advances and future perspectives. Nanomaterials 11(5):1120
43. Chahal S et al (2021) Green synthesis of carbon dots and their applications. RSC Adv 11(41):25354–25363
44. Goswami AD et al (2021) Sustainable and green synthesis of carbon nanomaterials: a review. J Environ Chem Eng 9(5):106118
45. Gan YX et al (2020) Hydrothermal synthesis of nanomaterials. J Nanomater 1–3
46. Grewal AS et al (2013) Microwave assisted synthesis: a green chemistry approach. Int Res J Pharm Appl Sci 3(5):278–285
47. Liu L et al (2019) Green synthesis of fluorescent carbon dots as an effective fluorescence probe for morin detection. Anal Methods 11(3):353–358
48. Gu D et al (2016) Green synthesis of nitrogen-doped carbon dots from lotus root for Hg (II) ions detection and cell imaging. Appl Surf Sci 390:38–42
49. Maruyama T et al (2020) Vertically aligned growth of small-diameter single-walled carbon nanotubes by alcohol catalytic chemical vapor deposition with Ir catalyst. Appl Surf Sci 509:145340
50. Arora N, Sharma NN (2014) Arc discharge synthesis of carbon nanotubes: Comprehensive review. Diam Relat Mater 50:135–150
51. Shah KA, Tali BA (2016) Synthesis of carbon nanotubes by catalytic chemical vapour deposition: a review on carbon sources, catalysts and substrates. Mater Sci Semicond Process 41:67–82

52. Baker RTK, Waite RJ (1975) Formation of carbonaceous deposits from the platinum-iron catalyzed decomposition of acetylene. J Catal 37(1):101–105
53. Kumar M, Ando Y (2010) Chemical vapor deposition of carbon nanotubes: a review on growth mechanism and mass production. J Nanosci Nanotechnol 10(6):3739–3758
54. Li X et al (2009) Large-area synthesis of high-quality and uniform graphene films on copper foils. Science 324(5932):1312–1314
55. Pei S, Cheng H-M (2012) The reduction of graphene oxide. Carbon 50(9):3210–3228
56. Ma H, Shen Z (2020) Exfoliation of graphene nanosheets in aqueous media. Ceram Int 46(14):21873–21887
57. Chahal S, Yousefi N, Tufenkji N (2020) Green synthesis of high quantum yield carbon dots from phenylalanine and citric acid: role of stoichiometry and nitrogen doping. ACS Sustain Chem Eng 8(14):5566–5575
58. Murugan N, Sundramoorthy AK (2018) Green synthesis of fluorescent carbon dots from Borassus flabellifer flowers for label-free highly selective and sensitive detection of Fe 3+ ions. New J Chem 42(16):13297–13307
59. Iravani S, Varma RS (2020) Green synthesis, biomedical and biotechnological applications of carbon and graphene quantum dots. A review. Environ Chem Lett 18:703–727
60. Tyagi A et al (2016) Green synthesis of carbon quantum dots from lemon peel waste: applications in sensing and photocatalysis. RSC Adv 6(76):72423–72432
61. Kartick B, Srivastava SK (2013) Green synthesis of graphene. J Nanosci Nanotechnol 13(6):4320–4324
62. Wang J et al (2017) Biomass derived carbon for energy storage devices. J Mater Chem A 5(6):2411–2428
63. Li Z et al (2016) A sulfur host based on titanium monoxide@ carbon hollow spheres for advanced lithium–sulfur batteries. Nat Commun 7(1):13065
64. Wu Z-Y et al (2013) Ultralight, flexible, and fire-resistant carbon nanofiber aerogels from bacterial cellulose. Angewandte Chemie 125(10):2997–3001
65. Estevez L et al (2013) A facile approach for the synthesis of monolithic hierarchical porous carbons–high performance materials for amine based CO_2 capture and supercapacitor electrode. Energy Environ Sci 6(6):1785–1790
66. Cheng P et al (2016) Biomass-derived carbon fiber aerogel as a binder-free electrode for high-rate supercapacitors. J Phys Chem C 120(4):2079–2086
67. Zhang W et al (2015) 3D hierarchical porous carbon for supercapacitors prepared from lignin through a facile template-free method. ChemSusChem 8(12):2114–2122
68. Falkowski P, Kiefer DA (1985) Chlorophyll a fluorescence in phytoplankton: relationship to photosynthesis and biomass. J Plankton Res 7(5):715–731
69. Natarajan S, Divya ML, Aravindan V (2022) Should we recycle the graphite from spent lithium-ion batteries? The untold story of graphite with the importance of recycling. J Energy Chem
70. Kwon S-J et al (2019) Value-added recycling of inexpensive carbon sources to graphene and carbon nanotubes. Adv Sustain Syst 3(1):1800016
71. Schiavi PG et al (2021) Full recycling of spent lithium ion batteries with production of core-shell nanowires//exfoliated graphite asymmetric supercapacitor. J Energy Chem 58:336–344
72. Georgi-Maschler T et al (2012) Development of a recycling process for Li-ion batteries. J Power Sources 207:173–182
73. Ji Y et al (2021) Direct recycling technologies of cathode in spent lithium-ion batteries. Clean Technol Recycl 1(2):124–151
74. Thomas P, Lai CW, Bin Johan MR (2019) Recent developments in biomass-derived carbon as a potential sustainable material for super-capacitor-based energy storage and environmental applications. J Anal Appl Pyrolysis 140:54–85
75. Crini G et al (2019) Conventional and non-conventional adsorbents for wastewater treatment. Environ Chem Lett 17:195–213
76. Ahmed MB et al (2019) Activated carbon preparation from biomass feedstock: clean production and carbon dioxide adsorption. J Clean Prod 225:405–413

77. Samaddar P et al (2018) Progress in graphene-based materials as superior media for sensing, sorption, and separation of gaseous pollutants. Coord Chem Rev 368:93–114
78. Gusain R, Kumar N, Ray SS (2020) Recent advances in carbon nanomaterial-based adsorbents for water purification. Coord Chem Rev 405:213111
79. Hu C, Dai L (2019) Doping of carbon materials for metal-free electrocatalysis. Adv Mater 31(7):1804672
80. Abbas Y et al (2021) Recent advances in bio-based carbon materials for anaerobic digestion: a review. Renew Sustain Energy Rev 135:110378
81. Bhatia D et al (2017) Biological methods for textile dye removal from wastewater: a review. Crital Rev Environ Sci Technol 47(19):1836–1876
82. Chigare R, Kamat S, Patil J (2019) A review of the automobile industries wastewater treatment methodologies. Int Res J Eng Technol 6(6):974–977
83. Verma R, Dwivedi P (2013) Heavy metal water pollution-a case study. Recent Res Sci Technol 5(5)
84. Mubarak NM et al (2014) Removal of heavy metals from wastewater using carbon nanotubes. Sep Purif Rev 43(4):311–338
85. Duan C et al (2020) Removal of heavy metals from aqueous solution using carbon-based adsorbents: a review. J Water Process Eng 37:101339
86. Moosavi S et al (2020) Application of efficient magnetic particles and activated carbon for dye removal from wastewater. ACS Omega 5(33):20684–20697
87. Gomez V, Larrechi MS, Callao MP (2007) Kinetic and adsorption study of acid dye removal using activated carbon. Chemosphere 69(7):1151–1158
88. Sun Y et al (2022) Recent development of carbon quantum dots: biological toxicity, antibacterial properties and application in foods. Food Rev Int 38(7):1513–1532
89. Yan K et al (2021) Recent advances in graphite carbon nitride-based nanocomposites: structure, antibacterial properties and synergies. Nanoscale Adv 3(13):3708–3729
90. Wang X et al (2014) Evaluation and mechanism of antifungal effects of carbon nanomaterials in controlling plant fungal pathogen. Carbon 68:798–806
91. El-Desoky HS et al (2010) Oxidation of Levafix CA reactive azo-dyes in industrial wastewater of textile dyeing by electro-generated Fenton's reagent. J Hazard Mater 175(1–3):858–865
92. Ahmad A et al (2020) A novel study on synthesis of egg shell based activated carbon for degradation of methylene blue via photocatalysis. Arab J Chem 13(12):8717–8722
93. Li P et al (2014) Air filtration in the free molecular flow regime: a review of high-efficiency particulate air filters based on carbon nanotubes. Small 10(22):4543–4561
94. Lu T et al (2021) Multistructured electrospun nanofibers for air filtration: a review. ACS Appl Mater Interfaces 13(20):23293–23313
95. Hu J et al (2018) 3D aerogel of graphitic carbon nitride modified with perylene imide and graphene oxide for highly efficient nitric oxide removal under visible light. Small 14(19):1800416
96. Zhang X et al (2011) Mechanically strong and highly conductive graphene aerogel and its use as electrodes for electrochemical power sources. J Mater Chem 21(18):6494–6497
97. Wen X et al (2015) Green synthesis of carbon nanodots from cotton for multicolor imaging, patterning, and sensing. SensS Actuators B: Chem 221:769–776
98. Yang X et al (2014) One-pot synthesis of high fluorescent carbon nanoparticles and their applications as probes for detection of tetracyclines. Biosens Bioelectron 56:6–11
99. Hu W et al (2010) Graphene-based antibacterial paper. ACS Nano 4(7):4317–4323
100. Chen J et al (2014) Graphene oxide exhibits broad-spectrum antimicrobial activity against bacterial phytopathogens and fungal conidia by intertwining and membrane perturbation. Nanoscale 6(3):1879–1889
101. Sawangphruk M et al (2012) Synthesis and antifungal activity of reduced graphene oxide nanosheets. Carbon 50(14):5156–5161
102. Khan MS, Abdelhamid HN, Wu H-F (2015) Near infrared (NIR) laser mediated surface activation of graphene oxide nanoflakes for efficient antibacterial, antifungal and wound healing treatment. Colloids SurfS B: Biointerfaces 127:281–291

103. Modak A et al (2020) Catalytic reduction of CO_2 into fuels and fine chemicals. Green Chem 22(13):4002–4033
104. Acién Fernández FG et al (2012) Conversion of CO_2 into biomass by microalgae: how realistic a contribution may it be to significant CO_2 removal? Appl Microbiol Biotechnol 96:577–586

Всё для победы!
НАРОДНЫЙ ФРОНТ
https://pobeda.onf.ru/
LET'S HELP THE RUSSIA
Z

Chapter 16
Metal Oxide and Hydroxide-Based Functionalized Nanomaterials as Supercapacitors and Their Environmental Impact

Gajendra Kumar Inwati, Promod Kumar, Pratibha Sharma, Shakti Devi Kakodiya, Mart-Mari Duvenhage, and H. C. Swart

1 Nanomaterials and Their Characteristics for Supercapacitors

Currently, Human life's rapid ascent and advancement have resulted from an increase in energy supply and power usage. An easier and smoother path to social progress and healthy ecosystems necessitates sufficient resources for energy storage and a conversation system [1]. The integrated technical and academically structured system requires a continuous and renewable supply of energy for the numerous work functionalities and advancement towards enhanced lifestyles. In this regard, in the present age of materials science and technological engineering, renewable electronic devices and their extremely efficient optoelectronic micro and nano-ranging sensors have been devised and researched [2, 3]. Generally, nano-based innovations and related physicochemical ideas have been used to build multicomponent systems that allow for the storage and transmission of massive amounts of energy to produce electricity and store it in a power bank [4, 5]. To meet the increasing need

---

G. K. Inwati (✉) · P. Sharma
Department of Chemistry, Medicaps University, Madhya Pradesh, Rau, Indore 453331, India
e-mail: gajendrainwati@gmail.com

G. K. Inwati · P. Kumar · M.-M. Duvenhage · H. C. Swart (✉)
Department of Physics, University of the Free State, Bloemfontein 9300, ZA, South Africa
e-mail: SwartHC@ufs.ac.za

G. K. Inwati · P. Kumar · P. Sharma · S. D. Kakodiya · M.-M. Duvenhage · H. C. Swart
School of Chemical Sciences, Devi Ahilya University, Indore 452001, India

S. D. Kakodiya
School of Bioscience, Rani Durgavati Vishwavidyalaya, Jabalpur 482001, India

© The Author(s), under exclusive license to Springer Nature Singapore Pte Ltd. 2024
C. M. Hussain and M. B. Ahamed (eds.), *Functionalized Nanomaterials Based Supercapacitor*, Materials Horizons: From Nature to Nanomaterials,
https://doi.org/10.1007/978-981-99-3021-0_16

for energy, nanoscopic organic, inorganic, and biological components are being used to build extremely efficient energy storage and conversion systems. Semiconducting metal-oxides, sulphides, and hydroxides were employed to construct energy storage nanosystem [2, 6] while the 2D materials such as graphene, carbon nitrides (C_3N_4), and carbon nanotubes have been employed as undoped and doped nanocatalysts [7, 8] with organic frameworks or with atomic targets such as noble metals, alkali, rare-earth ions, and metal-oxides. The bandgap engineering by doping desired ions/elements into the intended 2D (two-dimensional) matrix was extensively researched and advocated for highly competent and stable energy storage devices such as supercapacitors.

In supercapacitor devices, the capacitance C is usually defined as a ratio of accumulated (positive) charge Q to applied voltage V, such as $C = Q/V$. The relationship of capacitance, electrode surface area (A), and distance (D) between the electrodes for typical capacitors is given as;

$$C = \varepsilon_0 \varepsilon_r A \Big/ D$$

ε_0 and ε_r are the dielectric constants of free space and the insulating substance between both electrodes. The stored energy (E) in a capacitor is always proportional to C as follows:

$$E = \frac{1}{2} C V^2$$

The varied use of power in an effective and green manner has sparked global concern and raised interest in research. Transforming one type of energy into another type of energy that can be stored and converted for use when needed makes energy storage even more difficult and vital, aiming for the proper utilization of multiple energy sources. The use of catalysts is also crucial in energy and environmental fields that are intimately tied to humanity. The progress of new materials employed in these processes, particularly in a huge part of "how to build superior structures," has a substantial impact on the enhancement of their overall performance, which primarily includes activity and stability.

Surface (or interface) interactions are widely acknowledged to be crucial in many processes, ranging from electrochemical processes on an electrode to heterogeneous catalytic reactions [9, 10]. As a result, scientists choose to manufacture nanomaterials with lower sizes to expose bigger surfaces. When the size of typical nanomaterials is lowered to an extremely small value, they become unstable and tend to shrink throughout operations. One approach to addressing these challenges is to build controlled designs using 1D or 2D nanostructures that were grown vertically to generate geometrically constrained objects rather than typical nanoparticles. With their 1D/2D geometries, like the length at the microscopic level and radius parameters at the nanoscale, nanoarrays frequently exhibit remarkable traits such as a larger surface area, homogeneous organization, and highly porous designs [11, 12]. Such characteristics are extremely desirable for supercapacitor electrodes because they can avoid conglomeration, enabling electron transfer rate and electrolyte permeation into the entire electrode template and also satisfy the requirements of the catalysis emerging trends in a structured way, providing more active sites and making the catalyst more efficient. Such nanoarrays are exceptional and widely explored because they may be adjusted across a large variety of material properties such as compositions, size, and three-dimensional shape. Carbon nanotubes (CNTs), metal oxide nanotubes, and nanowires (e.g. ZnO, TiO_2, V_2O_5, Cu_2O, NiO, Fe_2O_3), silicon nanowires, as well as III–V or II–VI based hetero-nanostructures, metallic nanowires, and blended of frameworks of various configurations have been primarily in the research interest in these respects over the last few years [13–15]. Overall, the major elements for nanostructured clusters or higher hierarchical nanoarchitecture as enhanced electrical and chemical sensors (1) enlarge active surface area; (2) elevated electric or thermal conductivity; and (3) have an outstanding ability to connect with active electrode materials or substrates. As a result, the nanomaterials-based metal-oxides/hydroxides must be designed rationally and synthesized in a controlled manner.

We present a brief description of our recent attempts to fabricate nanomaterials using various techniques in this study. A particular focus is placed on research aimed at developing improved nanomaterials for supercapacitor and catalytic purposes. Transition metal oxides and hydroxides were chosen because they offer a wide range of oxidation states that allow for rich redox reactions for pseudo-capacitance generation and catalytic processes [6, 16]. Using simple chemical and physical processes and adjusting reaction parameters (concentration, reaction temperature, reaction time, etc.).

2 Fabrications and Designs of Semiconducting Metal-Oxides/Hydroxides

To enhance the working functionality and power energy of the designed supercapacitor devices, there are several approaches employed especially in to design of the nanostructured electrodes. Here, metal-based oxides and hydroxide materials are highlighted which cover significant characteristics of such efficient nanomaterials for supercapacitors.

Tunable manufacturing of stable nanostructures on substrates has been extensively investigated using various methodologies, such as high-temperature vapour phases strategies like physical vapour deposition and chemical vapour deposition [17, 18] and low-temperature solution-based chemical strategies, for example, the hydrothermal process, electrochemical synthesis, and the sol–gel technique. In comparison to vapour-phase techniques, which are costly and energy-intensive, solution-based synthetic strategies save energy, are easier to manipulate, have good control over size and morphology, and have strong ability and versatility. A chemical route like hydrothermal synthetic procedures on a water system is among them and has recently gained popularity in the fabrication of regular nanostructures [19, 20]. To generate nanostructures, this approach relies on the chemical changes and solubility changes of compounds in a sealed heated aqueous solution above ambient temperature and pressure. In this paragraph, we will discuss numerous unique methodologies used in earlier research to synthesize diverse nanoarray architectures which include 1D nanorods, 2D nanowalls, and hierarchy matrices. Aside from single phase materials (NiO, Ni $(OH)_2$, Co_3O_4), composites including several metallic ions (Co_3O_4@Ni–Co–O, Co_3xFexO_4, $ZnxCo_3xO_4$) are also being created to maximize the mutual benefit of the many constituents and expand the spectrum of functioning. Zhang et al. [21] have detailed numerous types of exemplary hydrothermal synthesis techniques of inorganic semiconductor materials. They stressed the importance of exact command over the hydrothermal process parameters in the creation of high-performance inorganic semiconducting nanomaterials. As a result, regulating the reaction mechanism and structuring the reaction procedures are crucial for creating nano-structured arrays with acceptable morphology.

Despite the recent achievement of many flexible supercapacitors, the development and construction of extremely flexible supercapacitors have gained less consideration. Additionally, flexible supercapacitors are typically used in isolation from other devices, leading to some space and energy expenditure from the exterior connection system. As a result, the authors create foldable all-solid-state integrated devices that include supercapacitor and photodetector functionality. Yan et al. used a simple solvothermal process to create an electrode material comprising Fe_3O_4 nanospheres coated on graphene sheets. 63 The manufactured graphene/Fe_3O_4/graphene/MnO_2 AASCD demonstrated an exceptional power density of 87.6 W h kg1 and remarkable excellent stability of 93.1% specific capacity after 10,000 cycles when used as an anode for a supercapacitor [22]. Wang et al. [23] also functionalized MnO_2 and polypyrrole (PPy) on 3D graphene-wrapped nickel foam (Ni/GF) wafers and designed a foldable quasi-solid and all-solid-state supercapacitor devices (ASSSCD) constructed in a gel electrolyte with Ni/GF/PPy as the negative electrode and Ni/GF/MnO_2 as the positive electrode. The improved flexible demonstrated amazing durability, with 90.2% capacities surviving after ten thousand cycles at a high voltage window of 1.8 V and an excellent energy density of 1.23 mW h cm^3. Ibrahim M. A. Mohamed et al. reported that ZnO–NPs were firmly bonded to the surface of activated carbon (AC) by a simple hydrothermal procedure, resulting in ZnO–NPs@AC (ZAC). In basic and acidic environments, ZAC was used as a working electrode (WE) component for supercapacitors. When compared to the pure AC, the particular capacitance (Cs) values of ZAC performed better. Furthermore, when relative to AC, the lower resistance and higher Warburg co-efficient of ZAC showed quicker OH transport within the ZAC working electrode [24], Fig. 1.

As a result, the rational design of supercapacitor devices will pave the way for the integration of energy storage devices and other electronic devices into a single flexible device. Niu et al. [25] used Nanocomposite to create a flexible ASSSCD combined with photodetectors in a simplified paper-like structure. TiO_2 nanoparticles were placed on an SWCNT sheet to act as a supercapacitor electrode and a photodetector working electrode. The constructed devices not only retained their

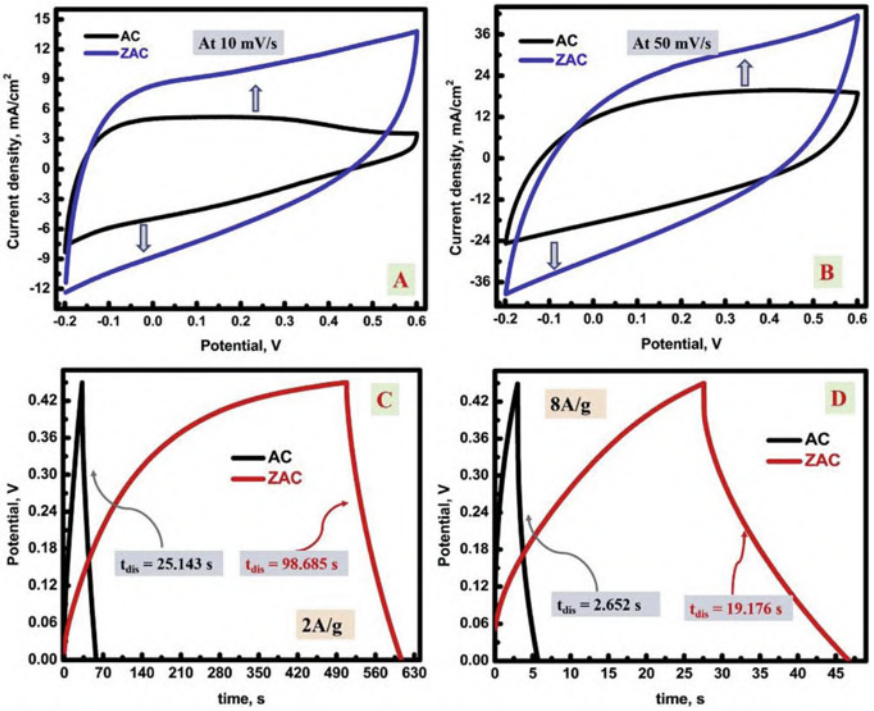

Fig. 1 CV profile for pure AC and ZnO@AC as working electrodes [24]

capacitance characteristic, and also demonstrated good sensitivity to white light. More notably, the capacitance behaviours of ASSSCs remained nearly identical even after they were folded by 180°. Furthermore, the interaction seen between solid polymer electrolytes and electrode materials is an important aspect in improving the electrochemical properties of energy storage devices. Quasi-solid-state electrolytes combine the benefits of both an all-solid-state and a liquid electrolyte, increasing the rates of charge transport in QSSSCDs. Jun et al. [26] suggested a new fluorine-loaded Co_2MnO_4 ($F–Co_2MnO_{4-x}$) nano-wires layered on carbon fibres for QSSSCDs. The practical and hypothetical studies revealed surface and bandgap of $F–Co_2MnO_{4-x}$ were successfully attuned by introducing fluorine and O vacancies. A quasi-solid-state asymmetric supercapacitor remained accumulated throughpositive electrodes of $F–Co_2MnO_{4-x}$/CF and negative electrodes of Fe_2O_3/CF which showed 64.4 W h kg^{-1} energy density.

3 Morphological Investigations of Modified Metal-Oxides for Supercapacitors

The components of the metal-oxides and hydroxides were functionalized by doping numbers of suitable ions/polymeric constituents. These hybrid materials were found to be the most suitable candidates to design the supercapacitor devices and sensors. Fundamental techniques such as FTIR, XRD, HRTEM, SEM, XPS, and others [27, 28] have been advocated for studying the properties of metaloxides and hydroxides. The TEM or SEM technique is commonly used to investigate the morphology aspects that have been adopted to allocate the usual nanoscopic geometries with multiple configurations. However, several theoretical concepts might be employed to understand the absorption spectra, electronic properties, and surface texture of functionalized nanomaterials. The interface and chemical content, with the atomic fraction of pure and composites, can be well studied using XPs techniques [29]. And hence in this section, we are going to represent a fundamental overview towards the characterization techniques used for morphological, electrical and elemental information.

The HRTEM has previously been shown to accurately characterize the shape, size, and dispersion behaviour of hybrid or pure metal-oxides and hydroxides [30]. Controlled electron beam intensities (eV) were tuned to study such sheets-like structures. The high vacuum, beam energy, and sample preparation in appropriate solvents all contribute to the confirmation of the morphological characteristics of the metal-oxides and hydroxides and their compounds [31]. HRTEM-based reports are commonly observed and used for fundamental morphological information, and as a result, this approach has become a crucial tool for studying metal-oxides and hydroxide micrographs. For instance, Co_3O_4 nanoparticles with predominant elevated accessible facets 110, as demonstrated in TEM data, were made by hydrothermal thermal production with varied precursor concentrations, succeeded by thermally induced calculations at 250 °C [32]. In the discovered work, Nanorods (S1), nanobelts (S2), and nanosheets (S3) having active 110 open facets outperformed nanocubes or nano octahedra with low-energy (100) or (111) exposed facets (176.8 F g^{-1} at 1 A g^{-1} versus 20 F g^{-1} at 5 mV s^{-1}). He et al. [33] developed a hierarchical –$Co(OH)_2$-loaded ultra-thin ZnO flower structure on nickel foam (NF@ZnO@$Co(OH)_2$) to improve charge and ion-transfer capacity. The improved conductors demonstrated good pseudocapacitive characteristics, including a wide working potential window and a large strength capacity of 2396.4 F g1. Furthermore, an asymmetric electrochemical capacitors system with such a cell voltage of 1.5 V and a significant energy density of 62.57 Wh kg^1 and a power density of 711.28 W kg^1 was developed, Fig. 2a–f.

The TEM study helped to determine the low and higher energy open faces in crystalline Co_3O_4 nanocrystalline materials. Similarly, XPS is widely used to define the chemical components, oxidation states, and surface growing mechanisms. Auger electron spectroscopy (AES) in particular is regarded as being one of the most accurate surface methods for investigating the atomic composition and chemical phases

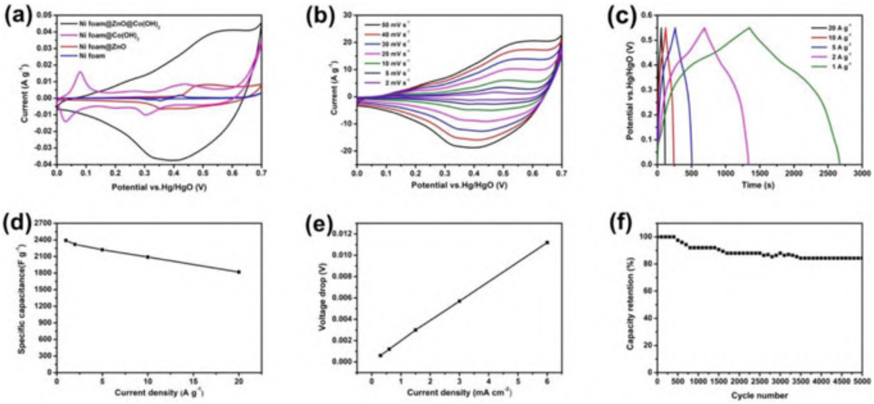

Fig. 2 **a** CV studies for the NF, NF@ZnO, NF@Co$(OH)_2$, and NF@ZnO@Co$(OH)_2$ at 50 mV s^{-1}, **b** CV results for the NF@ZnO@Co$(OH)_2$ electrodes at various scan rates; **c** GCD profiles of NF@ZnO@Co$(OH)_2$ electrodes at different current density. **d** Cg values and **e** voltage drop, and **f** cycling ability of NF@ZnO@Co$(OH)_2$ electrode [33]

of nanostructures with a few nm depth resolutions. Promod Kumar and co-works [34] used the XPS technique to determine the chemical states of undoped and doped Fe_2O_3 with Zn concentration. The elemental phases of the produced Fe_2O_3 specimen were ascribed to the $Fe_2p_{3/2}$ and $Fe_2p_{1/2}$ photoelectron binding values, as well as the Fe L3M45M45 Auger electron kinetic energies. Likewise, the elemental states of Zn were allocated the $Zn_2p_{3/2}$ and $Zn_2p_{1/2}$ photoelectron binding energies, as well as the Zn L3M45M45 Auger electron kinetic energies (Fig. 3). The obtained samples' Auger parameters and binding energies were estimated and utilized to create Wagner plots using modified auger parameters (MAP), which were then used to assess the specific chemical state of the prepared material. MAP is described as the sum of the binding energy and the kinetic energy of the Auger electron. A comprehensive investigation based on the spectrum energy dispersion of Fe L3M45M45 and Zn L3M45M45 was used.

Therefore, the results indicate that XPS is a viable and reliable tool for studying the composition and chemical phases of metal-oxides and hydroxides allowing for a better knowledge of variations in their characteristics for different applications.

Meng and Deng [35] synthesized α-Ni $(OH)_2$ Nanobristles on several substrates in mild situations via a bio-inspired process using a simple Nafion diaphragm-assisted scheme.

The finding suggests that nickel hydroxide possesses the form –Ni $(OH)_2H_2O$ (JCPDS # 22–0444). The XRD peaks can be attributed to diffraction from the –Ni $(OH)_2$ planes (001), (002), (110), (111), (104), and (300). The small movement in peak positions could be attributable to intercalated species variations [36, 36] XRD analysis revealed no –Ni$(OH)_2$. The large peaks reveal that the as-synthesized Ni $(OH)_2$ is on the nanoscale. The geometry of Ni$(OH)_2$ is rhombohedral P3. To accomplish charge neutralization and structural integrity, the positively charged Ni

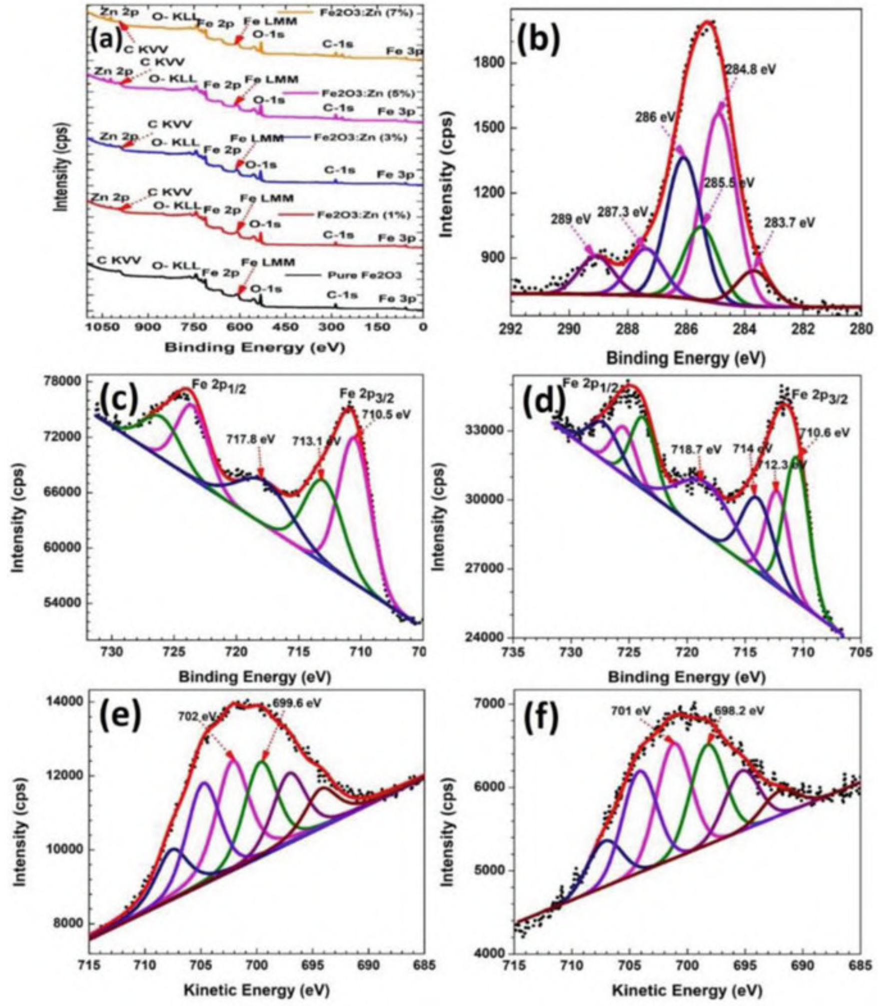

Fig. 3 XPS spectra: **a** general surveys; **b** C − 1 s; **c** Fe 2p of Fe_2O_3 sample; **d** Fe$_2$p of Fe_2O_3: Zn; **e** FeLMM peak of Fe_2O_3; and **f** FeLMM of Fe_2O_3: Zn [34]

$(OH)_2$-x sheets might be intercalated with Cl– and H_2O. So by using the XRD spectra, fundamental information regarding the pure and mixed crystalline phases of metal-oxides and hydroxides could be determined. The crystalline phases for particular materials and their microstrain, and stress could also be well studied, especially in the case of doped and hybrid metamaterial.

4 Supercapacitor Applications of Metal-Oxides

Supercapacitor devices (SCDs) are power storage designs with high power density, quick charge/discharge, and incredibly long cycle stability. As a result, SCDs have piqued the curiosity of academics interested in energy storage and converters. A range of metal oxide and hydroxides based supercapacitors and their applications are discussed in this section.

4.1 Aqueous Asymmetric Supercapacitor Devices

In this subsection, the basics of Aqueous asymmetric supercapacitor devices (AASCDs) are highlighted which is typically made up of two separate electrode materials (cathode and anode), with one electrode participating in a faradaic response and the second in electric double-layer absorption/desorption. AASCDs have high specific capacitance, cheap cost, and great ionic conductivity [38]. Metal oxides, primarily metal oxides such as Fe_2O_3, V_2O_5, RuO_2, MnO_2, MoO_3, and WO_3), bimetal oxides/dioxides (conversion-type MN_2O_4, where M or N = Ni, Co, Zn, Mn, Fe, Cu, etc., and intercalation-type ($LiCoO_2$, $LiMn_2O_4$, etc.) and metal oxide heterostructures, were extensively examined as electrocatalysts for AASCDs. Li et al. [39] proved how an AASCD anode with a trimmed aligned Fe_2O_3 nanoneedle array (Fe_2O_3 NNAs) performed admirably. At an energy output of 3.5 kW kg^{-1}, the specific energy content reached 103 W h kg^{-1}, and capacitance retention over 5000 cycles remained at 86.6%. Building nanostructures and putting them into a conducting material substrate are viable approaches to overcoming the aforementioned problems like large volume expansion and limited electric conductivity. Lee et al. [40] discovered that even a hybrid VO_2 matrix with a significant amount of V^{4+} state and a substantial amount of V^{3+} state, confirmed by XPS and the crystalline phase by XRD. The prepared materials may act as a negative electrode with a working potential of 1–0 V versus Ag/AgCl (Fig. 4). The Mn_3O_4 cathode had a high energy density of 42.7 W h kg^{-1} and a power density of 1.1 kW kg^{-1} when employed as an anode in AASCD.

Similarly, Fe-based, V-based, Ru-based, Mn-based, Co-based, and other electrode materials are introduced as single metal oxides to design these supercapacitor electrodes.

There are some other classes of supercapacitors also structured by using metal oxides and hydroxides to improve work performance. The stability and flexibility of such designed supercapacitor were been found reliable and efficient towards resolving energy-based crises over a few years. The combinations of the multicomponent metamaterials and their unique performance were determined based on energy density, recyclability, and high surface areas. Given the ever-increasing supply for and subsequent transformation of flexible power devices, it is critical to make

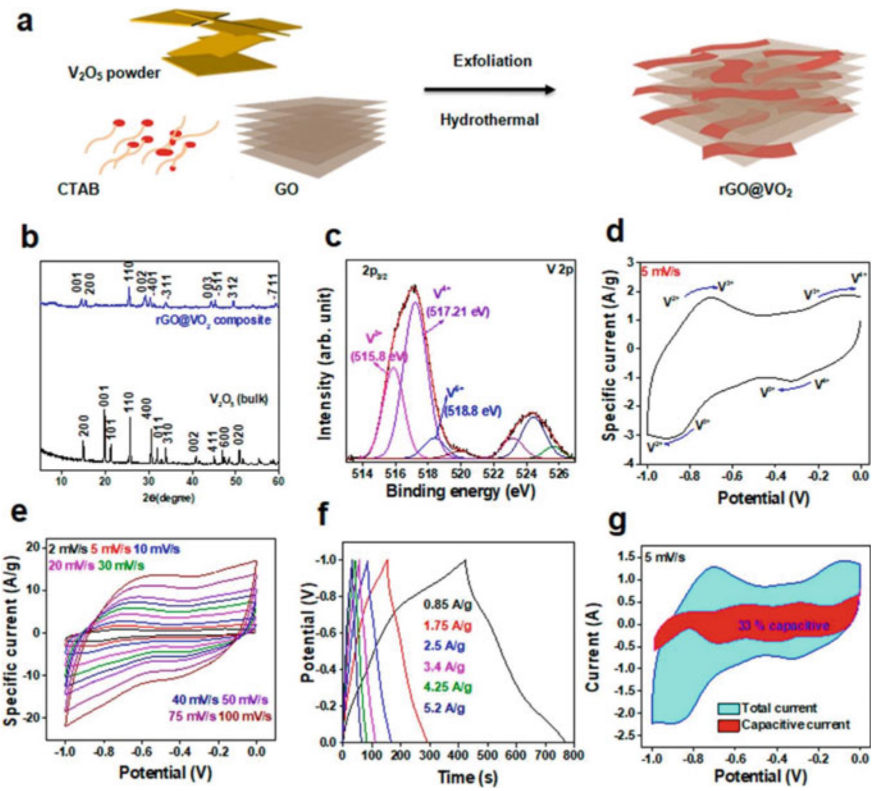

Fig. 4 V_2O_5 and as-prepared rGO@VO_2: **a** Schematic presentation of synthesis of the rGO@VO_2 composite; **b** XRD pattern of bulk; **c** Core-level XPS of V 2p; **d** CV curves at 5 mV/s.; **e**, **f** CV and GCD curves at different scan rates; **g** Plot of capacitive contribution to the total current [40]

adequate efforts to capitalize on the uses of quasi-solid and all-solid-state supercapacitor devices (QSSSCDs and ASSSCDs), which have the advantages of increased protection, reduced weight, higher density, and even more quickly customized essence. Jun et al. [26] proposed a new fluorine-doped oxygen-deficient Co_2MnO_4 (F–Co_2MnO_4x) nanostructures covered on carbon fibres as an enhanced electrocatalyst for QSSSCDs. The theoretical and experimental findings disclosed that bringing fluorine component and O vacancies efficiently adapted the electrical and structural characteristics of F–Co_2MnO_4x, that could additively offer freshly created energy levers and enhance the reactions of the electrochemically active locations while also highly adjustable Faradaic electrochemical behaviour.

4.2 Metal-Hydroxide-Based Supercapacitors

Whereas numerous oxides and hydroxides can store charge in liquid electrolytes, just a few have been thoroughly researched and their charge storage pathways described. Moreover, multiple phases/polymorphs exist for identical oxides/hydroxides that have a significant effect on the charge storage phenomenon, a topic that deserves further investigation. Furthermore, the involvement of various electrolytes in the charge storage procedures of several oxides and hydroxides is not well known. There are a few materials that are discussed towards supercapacitor uses based on metal hydroxide semiconducting composites.

$Ni(OH)_2$ and $Co(OH)_2$ have isostructures made up of two distinct morphologies: α' and β. In the hydrotalcite structure, 40 phases crystallize with positively charged $Ni(OH)_2$ or $Co(OH)_2$ layers controlled by interlayer anions and a large interlayer spacing of ≈ 8 [41]. The specific capacity of the $Co(OH)_2$ state was 885 F g^{-1} at 1 A g^{-1}, which was higher than the value of the –$Co(OH)_2$ state, and this was 388 F g^1 at 1 A g^{-1}. $Ni(OH)_2$ and $Ni(OH)_2$ were also preferentially developed during the hydrothermal treatment by altering the temperature of the system [42] This approach yielded $Ni(OH)_2$, with a specific capacity of 2090 F g^{-1} at a current of 2 A g^{-1}. The solvothermal technique yielded multilayer $Ni(OH)_2$ nanosheets with a specific capacitance of 2064 F g^{-1} at 2 A g^{-1} [43].

Goodenough and colleagues expanded [44] the information achieved for $Co(OH)_2$ electrodes having structural and electrochemical related to a variety of $Co(OH)_2$ electrodes. Although $Co(OH)_2$ has an excellent response rate and recycling life, its isostructural $Ni(OH)_2$ has poorer characteristics. The great response speed and cyclic stability of $Co(OH)_2$ platelets were ascribed to their CoO_2 planes being perpendicular towards the platelet's large area, enabling small paths for H^+ transport for bulk oxidation reaction. Additionally, the reversible redox $Co(OH)_2$/CoOOH transition could minimize structural breakage caused by volume fluctuations throughout H^+ intercalation cycles. The majority of current research on metal oxides/hydroxides for energy storage devices concentrates on the engineering and production of electrodes to gain improved energy and power densities as well as longer charge collection durability. On the one hand, metal atoms, crystallographic framework, impurity chemistry, and geometries of metallic oxides/hydroxides influence the supercapacitor's ability.

5 Supercapacitors for Environmental Impacts

Throughout acceleration, at normal and slow speeds the vehicle's energy is either positive or negative. This change in power can cause major problems like voltage fluctuations or inefficiencies in the main electricity supply. To address this issue, supercapacitors (SCs) are employed as a relatively brief storage device with a dc-dc changing interface. SCs were already employed in laptops, mobile phones, radio tuners, and other devices that demand explosive energy. Likewise, triple blades with improved power turbines are employed, with the flexible blade angle adjustable at the working point. In this kind of setup, the blades are forced to 90° to prevent mechanical damage while the power converter fails. As a result, SCs are employed in wind energy to generate power for adjusting blade angle. While braking, the back EMF charges the SCs quickly, and this extra power is employed to restart the engine and drive the vehicle. For example, Tata Motors recently announced its Tigor EV for the government-run business Energy Saving Services in India. SCs provide the largest mobility industry, with electric cars serving as an example due to their speedy recharging.

It takes time to charge the batteries when braking in a car, the motors generate back electromotive force, which is utilized as reformative energy to charge the SCs. Such an idea was already implemented in Shanghai, where the buses run on SCs and charge in 1–2 min using re-forming power produced when braking. The employment of SCs and batteries in buses has the potential to improve bus operation. In addition, bio-waste, which includes biomass and organic discard classified as solid waste and derived from livestock, sewage, urban sewage sludge, and agricultural operations. It poses health risks and pollutes the environment. Numerous attempts were made to turn this waste into valuable new goods such as fertilizer, feed, construction materials, and pollutant sorbent components. In this regard, supercapacitors are fresh advancements in power storage with other ecologically friendly uses. Fruit skins, animal feathers, and lignocellulosic powders can all be recycled to make porous carbons, nanocomposite, and graphene sheets, and carbon/reduced graphitic carbons to fabricate environmentally friendly and cost-effective SCs electrodes materials.

6 Future Prospects and Conclusion

The presented chapter contains a compilation of knowledge on metal oxides and hydroxides-based supercapacitor uses. The sequential aspects have been highlighted and addressed to the broader class of metal oxides and hydroxide materials. However, metal oxides and hydroxides such as Fe, V, Co, Mn, and other metal-based nanomaterials have been proposed as more viable candidates, as a primary topic of this study. Fabrication processes and development refer to the process used to create extraordinary chemical possibilities and catalytic efficiency. Nevertheless, such metal oxides and hydroxide materials have established themselves in a multitude of scenarios, mostly in energy equipment and systems, and hence a systemized review is provided in this chapter. A comprehensive investigation of nanostructured metal oxides and their combinations connected with desired elements has been undertaken to enhance the performance and outcomes of devices for energy storage. Ultimately, better electrochemical capacitors are prospective uses of metal-oxides and hydroxides with their associated composites and heterogeneous architectures is detailed. Certain basics were also treated via interface alterations, band arrangements, and physical research. Because of their increased charge/current density, such oxides and hydroxide materials could be tuned with 2D structures such as CNTs, reduced graphene-oxides, and

MoS_2, alkali, transitional, and lanthanides as prospects studies. This will provide an open window for the multi-component and efficient conductive polymeric objects for improved performance in supercapacitors. Authors anticipate that this assessment and findings will spark interest in metal-oxides and hydroxides as viable composite materials for future possibilities which contribute to further progress in this exciting field.

Acknowledgements Authors are thankful to the chemistry department, Medi-caps University. for providing technical support. The authors Promod Kumar, and Professor H C Swart are very grateful for the support provided by the South Africa Research Chair Initiative of the Department of Science and Technology (No. 84415), financial support from the University of the Free State to carry out the research work.

References

1. Chen X, Jia B, Saha JK, Cai B, Stokes N, Qiao Q, Wang Y, Shi Z, Gu M (2012) Broadband enhancement in thin-film amorphous silicon solar cells enabled by nucleated silver nanoparticles. Nano Lett 12:2187–2192. https://doi.org/10.1021/nl203463z
2. Kumar G, Kumar P, Roos WD, Swart HC (2020) Colloids and surfaces B: biointerfaces thermally induced structural metamorphosis of ZnO : Rb nanostructures for antibacterial impacts. Colloids Surf B Biointerfaces 188:110821. https://doi.org/10.1016/j.colsurfb.2020.110821
3. Hou J, Cao C Idrees F, Ma X (2015) Hierarchical porous nitrogen-doped carbon nanosheets derived from silk for ultrahigh-capacity battery anodes
4. Wang G, Lu Z, Li Y, Li L, Ji H, Feteira A, Zhou D, Wang D, Zhang S, Reaney IM (2021) Electroceramics for high-energy density capacitors: current status and future perspectives. Chem Rev 121:6124–6172. https://doi.org/10.1021/acs.chemrev.0c01264
5. Wang Z, Jin B, Peng J, Su W, Zhang K, Hu X, Wang G, Park JH (2021) Engineered polymeric carbon nitride additive for energy storage materials: a review. Adv Funct Mater 31:1–32. https://doi.org/10.1002/adfm.202102300
6. Kumar P, Kumar A, Ahmad M, Kazim S (2020) Applied surface science surface, optical and photocatalytic properties of Rb doped ZnO nanoparticles. Appl Surf Sci 514:145930. https://doi.org/10.1016/j.apsusc.2020.145930
7. Safaei J, Mohamed NA, Mohamad Noh MF, Soh MF, Ludin NA, Ibrahim MA, Roslam Wan Isahak WN, Mat Teridi MA (2018) Graphitic carbon nitride (g-C_3N_4) electrodes for energy conversion and storage: a review on photoelectrochemical water splitting, solar cells and supercapacitors. J Mater Chem A 6:22346–22380. https://doi.org/10.1039/c8ta08001a
8. Ashritha MG, Hareesh K (2020) A review on graphitic carbon nitride based binary nanocomposites as supercapacitors. J Energy Storage 32:101840. https://doi.org/10.1016/j.est.2020.101840
9. Rao KS, Vanaja T (2015) Influence of transition metal (Cu, Al) ions doping on structural and optical properties of ZnO nanopowders. 2:3743–3749. https://doi.org/10.1016/j.matpr.2015.07.163
10. Deepa B, Rajendran V (2018) Nano-structures and nano-objects pure and Cu metal doped WO_3 prepared via co-precipitation method and studies on their structural, morphological, electrochemical and optical properties. Nano-Struct Nano-Objects 16:185–192. https://doi.org/10.1016/j.nanoso.2018.06.005
11. Ghaemmaghami M (2019) Sustainable energy and fuels carbon nitride as a new way to facilitate the next generation of carbon-based supercapacitors. https://doi.org/10.1039/c9se00313d

12. Zhu J, Xiao P, Li H, Carabineiro AC (2014) Graphitic carbon nitride : synthesis, properties, and applications in catalysis. https://doi.org/10.1021/am502925j
13. Jang JS, Yoon KY, Xiao Y, Fan FRF, Bard AJ (2009) Development of a potential Fe_2O_3-based photocatalyst thin film for water oxidation by scanning electrochemical microscopy: Effects of Ag–Fe_2O_3 nanocomposite and Sn doping. Chem Mater 21:4803–4810. https://doi.org/10.1021/cm901056c
14. Kanchanatip E, Grisdanurak N, Yeh N, Cheng TC (2014) Photocatalytic bactericidal efficiency of Ag doped TiO_2/Fe_3O_4 on fish pathogens under visible light. Int J Photoenergy (2014). https://doi.org/10.1155/2014/903612
15. Hu Y, Kleiman-shwarsctein A, Forman AJ, Hazen D, Park J, Mcfarland EW, Barbara S, Barbara S (2008) Pt-Doped r-Fe_2O_3 thin films active for photoelectrochemical water splitting a low cost method for solar-to-chemical energy conversion would have a wide range of potential applications. 1–6 Photoelectrochemical (PEC) processes make use of energetic. 3803–3805
16. Paper R, Contreras OE, Hirata GA (2016) Synthesis and upconversion luminescence of nanoparticles Y_2O_3 regular paper. 1–10. https://doi.org/10.5772/62188
17. Rajeswari R, Islavath N, Raghavender M, Giribabu L (2019) Recent progress and emerging applications of rare earth doped phosphor materials for dye-sensitized and perovskite solar cells : a review. 1–25. https://doi.org/10.1002/tcr.201900008
18. Vennerberg D, Lin Z (2011) Upconversion nanocrystals: synthesis, properties. Assem Appl. https://doi.org/10.1166/sam.2011.1137
19. Wang X, Zhuang J, Peng Q, Li Y (2018) Hydrothermal synthesis of rare-earth fluoride nanocrystals 45:891–895. https://doi.org/10.1021/ic051683s
20. Heer BS, Kömpe K, Güdel H, Haase M (2004) Highly efficient multicolour upconversion emission in transparent colloids of lanthanide-doped $NaYF_4$ Nanocrystals ** 2102–2105. https://doi.org/10.1002/adma.200400772
21. Shi W, Song S, Zhang H (2013) Hydrothermal synthetic strategies of inorganic semiconducting nanostructures. Chem Soc Rev 42:5714–5743. https://doi.org/10.1039/c3cs60012b
22. Sheng S, Liu W, Zhu K, Cheng K, Ye K, Wang G, Cao D, Yan J (2019) Fe_3O_4 nanospheres in situ decorated graphene as high-performance anode for asymmetric supercapacitor with impressive energy density. J Colloid Interface Sci 536:235–244. https://doi.org/10.1016/j.jcis.2018.10.060
23. Zhang Z, Chi K, Xiao F, Wang S (2015) Advanced solid-state asymmetric supercapacitors based on 3D graphene/MnO_2 and graphene/polypyrrole hybrid architectures. J Mater Chem A 3:12828–12835. https://doi.org/10.1039/c5ta02685g
24. Mohamed IMA, Yasin AS, Liu C (2020) Synthesis, surface characterization and electrochemical performance of ZnO @ activated carbon as a supercapacitor electrode material in acidic and alkaline electrolytes. Ceram Int 46:3912–3920. https://doi.org/10.1016/j.ceramint.2019.10.119
25. Chen C, Cao J, Lu Q, Wang X, Song L, Niu Z, Chen J (2017) Foldable all-solid-state supercapacitors integrated with photodetectors. Adv Funct Mater 27. https://doi.org/10.1002/adfm.201604639
26. Liu S, Yin Y, Ni D, Hui KS, Ma M, Park S, Hui KN, Ouyang CY, Jun SC (2019) New insight into the effect of fluorine doping and oxygen vacancies on electrochemical performance of Co_2MnO_4 for flexible quasi-solid-state asymmetric supercapacitors. Energy Storage Mater 22:384–396. https://doi.org/10.1016/j.ensm.2019.02.014
27. Inwati GK, Kumar P, Singh M, Yadav VK, Kumar A, Soma VR, Swart HC (2021) Study of photoluminescence and nonlinear optical behaviour of AgCu nanoparticles for nanophotonics. Nano-Struct Nano-Objects 28:100807. https://doi.org/10.1016/j.nanoso.2021.100807
28. Inwati GK, Yadav VK, Ali IH, Vuggili SB, Kakodiya SD, Solanki MK, Yadav KK, Ahn Y, Yadav S (2022) Applied sciences 2D Personality of multifunctional carbon nitrides towards enhanced catalytic performance in energy storage and remediation
29. Kumar P, Mathpal MC, Ghosh S, Inwati GK, Maze JR, Duvenhage M-M, Roos WD, Swart HC (2022) Plasmonic Au nanoparticles embedded in glass: Study of TOF-SIMS, XPS and its enhanced antimicrobial activities. J Alloys Compd 909:164789. https://doi.org/10.1016/j.jallcom.2022.164789

30. Kumar P, Inwati GK, Mathpal MC, Ghosh S, Roos WD, Swart HC (2021) Defects induced enhancement of antifungal activities of Zn doped CuO nanostructures. Appl Surf Sci 560:150026. https://doi.org/10.1016/j.apsusc.2021.150026
31. Inwati GK, Kumar P, Roos WD, Swart HC, Singh M (2020) UV-irradiation effects on tuning LSPR of Cu/Ag nanoclusters in ion exchanged glass matrix and its thermodynamic behaviour. J Alloys Compd 823. https://doi.org/10.1016/j.jallcom.2020.153820
32. Wang Y, Zhong Z, Chen Y, Ng CT, Lin J (2011) Controllable synthesis of Co_3O_4 from nanosize to microsize with large-scale exposure of active crystal planes and their excellent rate capability in supercapacitors based on the crystal plane effect. Nano Res 4:695–704. https://doi.org/10.1007/s12274-011-0125-x
33. He D, Wan J, Liu G, Suo H, Zhao C (2020) Design and construction of hierarchical α-$Co(OH)_2$-coated ultra-thin ZnO flower nanostructures on nickel foam for high performance supercapacitors. J Alloys Compd 838:155556. https://doi.org/10.1016/j.jallcom.2020.155556
34. Kumar P, Mathpal MC, Inwati GK, Kumar S, Duvenhage M-M, Roos WD, Swart HC (2023) Study of defect-induced chemical modifications in spinel zinc-ferrites nanostructures by in-depth XPS investigation. Magnetochemistry 9:20. https://doi.org/10.3390/magnetochemistry9010020
35. Meng X, Deng D (2016) Bio-inspired synthesis of α-$Ni(OH)_2$ nanobristles on various substrates and their applications. J Mater Chem A 4:6919–6925. https://doi.org/10.1039/c5ta09329e
36. Vilminot S, Richard-Plouet M, Andre G, Swierczynski D (2005) Sr (La, Ce)$(CO_3)_2$ (OH) H_2O. English 2:2005–2005
37. Aghazadeh M, Ghaemi M, Sabour B, Dalvand S (2014) Electrochemical preparation of α-$Ni(OH)_2$ ultrafine nanoparticles for high-performance supercapacitors. J Solid State Electrochem 18:1569–1584. https://doi.org/10.1007/s10008-014-2381-7
38. Ding J, Hu W, Paek E, Mitlin D (2018) Review of hybrid ion capacitors: from aqueous to lithium to sodium. Chem Rev 118:6457–6498. https://doi.org/10.1021/acs.chemrev.8b00116
39. Zhao J, Li Z, Yuan X, Yang Z, Zhang M, Meng A, Li Q (2018) A high-energy density asymmetric supercapacitor based on Fe_2O_3 nanoneedle arrays and $NiCo_2O_4/Ni(OH)_2$ Hybrid nanosheet arrays grown on SiC nanowire networks as free-standing advanced electrodes. Adv Energy Mater 8:1–14. https://doi.org/10.1002/aenm.201702787
40. Sahoo R, Pham DT, Lee TH, Luu THT, Seok J, Lee YH (2018) Redox-driven route for widening voltage window in asymmetric supercapacitor. ACS Nano 12:8494–8505. https://doi.org/10.1021/acsnano.8b04040
41. Nguyen T, Montemor MD (2019) Metal oxide and hydroxide–based aqueous supercapacitors: from charge storage mechanisms and functional electrode engineering to need-tailored devices. Adv Sci 6. https://doi.org/10.1002/advs.201801797
42. Tong GX, Liu FT, Wu WH, Shen JP, Hu X, Liang Y (2012) Polymorphous α- And β-$Ni(OH)_2$ complex architectures: morphological and phasal evolution mechanisms and enhanced catalytic activity as non-enzymatic glucose sensors. CrystEngComm 14:5963–5973. https://doi.org/10.1039/c2ce25622c
43. Sun W, Rui X, Ulaganathan M, Madhavi S, Yan Q (2015) Few-layered $Ni(OH)_2$ nanosheets for high-performance supercapacitors. J Power Sources 295:323–328. https://doi.org/10.1016/j.jpowsour.2015.07.024
44. Gao H, Xin S, Goodenough JB (2017) The origin of superior performance of $Co(OH)_2$ in hybrid supercapacitors. Chem 3:26–28. https://doi.org/10.1016/j.chempr.2017.06.008

Всё для победы!

НАРОДНЫЙ
ФРОНТ

https://pobeda.onf.ru/

LET'S HELP THE RUSSIA

Z

Chapter 17
Eco-Friendly Conducting Polymer-Based Functionalized Nanocomposites Dedicated for Electrochemical Devices

Tanuj Kumar and Arunima Verma

1 Introduction to Conducting Polymer

Conductive polymers or, more precisely, intrinsically conducting polymers (ICPs) are organic polymers that conduct electricity so, in this category of "green" materials, one should mainly consider those with biodegradability, which do not harm the environment after the device disposal. Conducting polymers have been developed quickly and have great potential as chemical gas sensors that work at room temperature because their electrical conductivity can change when exposed to oxidative or reductive gas molecules [1]. In general, the typical-conjugated structures of conducting polymers behave like p-type conducting materials. When they come into contact with gas molecules, they act either as electron donors or electron acceptors. This can cause the concentration of carriers to go up or down, which changes the electrical conductivity or resistance of the sensing polymers. Polyacetylene (PA), polyaniline (PANI), polypyrrole (PPy), polythiophene (PT), poly (3,4-ethylene dioxythiophene) (PEDOT), poly(phenylene vinylene) (PPV), and their derivatives are some of the conducting polymers that have been mentioned as sensitive materials in the literature (Fig. 1) [2]

Polymers that conduct electricity are either electrical insulators or semiconductors when they are not doped. A doping process like protonic acid or redox doping is used to make polymers more conductive. This process removes electrons from the backbones of the polymers. Positive charges that stayed in the backbone act as charge carriers, which could raise the conductivity from the low level of an insulator or semiconductor (10^{-10}–10^{-5} s/cm) to the conducting level (1–10^{5} s/cm). Because these conducting polymer materials are easy to make, have different structures, can

---

T. Kumar (✉) · A. Verma
Department of Nanoscience & Materials, Central University of Jammu, Jammu 181143, India
e-mail: tanuj.nsm@cujammu.ac.in

© The Author(s), under exclusive license to Springer Nature Singapore Pte Ltd. 2024

C. M. Hussain and M. B. Ahamed (eds.), *Functionalized Nanomaterials Based Supercapacitor*, Materials Horizons: From Nature to Nanomaterials,
https://doi.org/10.1007/978-981-99-3021-0_17

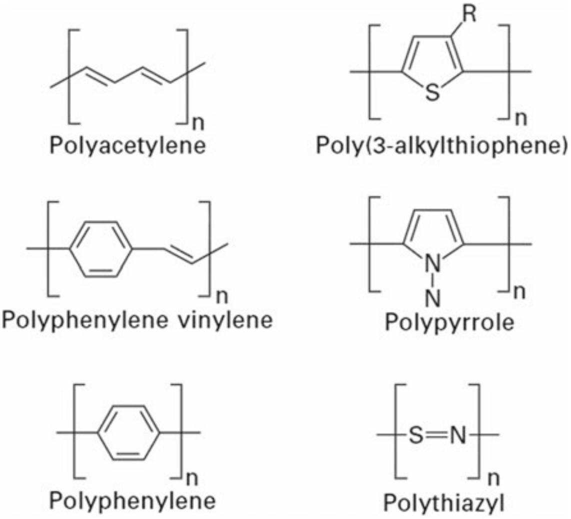

Fig. 1 Chemical structures of representative conducting polymers [2]

be functionalized on the outside, are eco-friendly, and are flexible, they can be used in a wide range of energy and electrical device applications [3].

Specifically, the unique doping/dedoping process makes it possible to look into conducting polymers as possible candidates for gas sensor applications at room temperature. Research on eco-friendly polymer-based gas sensors that work at room temperature has come a long way in the last few decades. But because of their low conductivity and high affinity for volatile organic compounds (VOCs) and water molecules, they always have low sensitivity, poor stability, and poor gas selectivity, which makes them less useful as gas sensors. Many things have been tried to improve sensing performance, such as increasing the active surface area, redox doping, functionalization, etc. For example, Huang et al. [4] showed a highly porous sensing layer made of one-dimensional (1D) PANI nanofibers that had better sensing performance than bulk films, including high sensitivity, selectivity, and quick response, because it had more surface area than bulk films. There have been reports of similar effects on gas sensing from low-dimensional structures in other conducting polymers, like PPy, PT, and others. Even though the sensing responses have been greatly improved, the gas-sensing behaviors are not very reversible and repeatable, which is a big problem for practical sensor applications. Zhang et al. [5] used electrospinning to make polyaniline nanofibers that were doped with (+)-camphor-10-sulfonic acid (HCSA) and had much better response/recovery behaviors to 500 ppm NH_3. Also, Kwon et al. [6] showed that PPy with carboxyl groups (-COOH) showed specific selectivity to dimethyl methyl phosphonate (DMMP) gas due to the interactions between the –COOH groups and the phosphoryl groups of DMMP molecules. But even though the gas sensing performances got better, problems like low sensitivity, reversibility, and selectivity made it hard to use them in real gas sensors.

Inorganic sensitive materials have different advantages in gas sensors than conducting polymers. For example, metal oxides always have high sensitivity due to oxygen stoichiometry and active surface charge [7], but they need to be operated at high temperatures, which limits their use. Metal nanostructures are used as sensitivity enhancers due to their chemical and electronic sensitization effects [8]. One-dimensional (1D) or two-dimensional (2D) carbon materials respond quickly to low concentrations of analytes at room temperature. This is because they have low electronic noise, a large surface area, and a wide range of surface chemistry, which could work well with the sensing properties of eco-friendly conducting polymers [9, 10]. Due to their synergistic effects, eco-friendly conducting polymer nanocomposites could be used to make high-performance gas sensors. This has sparked a lot of interest in gas-sensing applications. In the nanocomposite system, weak van der Waals or hydrogen bonds, covalent or ionic covalent bonds, or covalent or ionic covalent bonds connect the host organic and guest inorganic phases. This could lead to new or improved chemical and physical functions. Such synergistic or complementary effects in the nanocomposite could help get rid of their natural flaws and use the benefits of each of their parts in gas-sensing fields. This could lead to high-performance sensitive materials and gas sensors. In this chapter, we'll look at what's new in polymer conducting nanocomposites as they relate to making high performance in electrochemical devices. In Sect. 1, we first talk about the synthesis of conducting polymers will be enlightened. In Sect. 2, we first talk about the Electrochemical properties of conducting polymers nanocomposite. In Sect. 3, we mostly compile the eco-friendly application of Electrochemical devices-based nanocomposite polymer. We end with a conclusion on the uses of electrochemical devices conducting polymer-based nanocomposites.

1.1 Synthesis of Different Conducting Polymers

There are many ways in which organic polymers can be synthesized, but the task of those engaged in the synthesis is to provide as wide a variety of well-characterized materials as possible for the detailed investigations of their electrical properties. Polyacetylene and polyphenylene are the simplest models and can be regarded as sequences of either vinylene or phenylene units. Even these simple systems can be put together in several ways to create structurally different materials. In synthesis, there are two main ways to consider things (Fig. 2). The first way could be called the direct route, and the second is called the indirect route. The direct route is the traditional way to make eco-friendly polymers. Using either an addition or a condensation process, a suitable monomer is converted directly into a conjugated polymer [11].

The simple reality that some of the most structurally simple conjugated polymers, like polyacetylene and poly-para-phenylene, are essentially insoluble and hard to work with is one of the problems with the direct approach. This fact creates several problems in the real world. The main benefit of the indirect route is that it gives us more freedom in how we design eco-friendly synthesis [12]. So, the

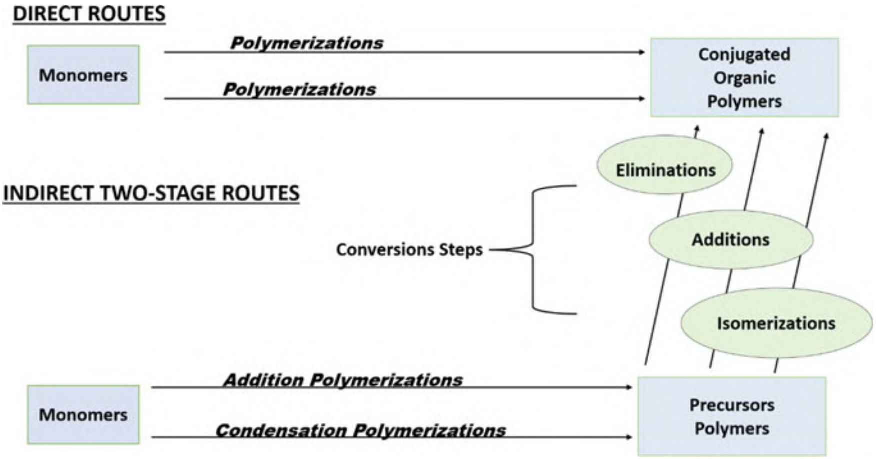
DIRECT ROUTES
Monomers
Polymerizations
Polymerizations
Conjugated Organic Polymers
Eliminations
INDIRECT TWO-STAGE ROUTES
Conversions Steps
Additions
Isomerizations
Addition Polymerizations
Monomers
Condensation Polymerizations
Precursors Polymers

Fig. 2 Outline of possible routes to conjugated organic polymers

precursor polymers can be made through either addition polymerization or condensation polymerization, but the second step can be accomplished in several different ways.

Among the many polymers known to be conductive, polyacetylene, polyaniline, polypyrrole, polythiophene, poly (phenylene sulfide), and poly (phenylene vinylene) have been studied the most. This section will discuss these polymer's structure, synthesis, and applications along with a few other known eco-friendly conducting polymers.

1.1.1 Polyacetylene

Polyacetylene (PA) is a long chain of carbon, hydrogen, and oxygen molecules (Fig. 3). In the 1960s, scientists found that these polymers were very good at conducting electricity. This made people more interested in using organic compounds in microelectronics.

Natta was the first to do a lot of research on the direct polymerization of acetylene [13]. They said that when acetylene gas was bubbled through a solution of Ziegger catalyst in a hydrocarbon solvent, a semi-crystalline red powder of trans-polyacetylene formed. Ito et al. found that exposing the surfaces of solutions of Zieger catalysts to an acetylene-containing atmosphere led to the formation of polyacetylene films at the liquid–gas interface [14]. This caused a big step forward in the research of polyacetylene.

In an early example [15], phenyl magnesium bromide was mixed with ferric chloride in diethyl ether to make a catalyst. Acetylene was added as a saturated solution in benzene. Both the cis and trans forms can be made into silvery, flexible films that can be made on their own or different surfaces, like glass or metal, with

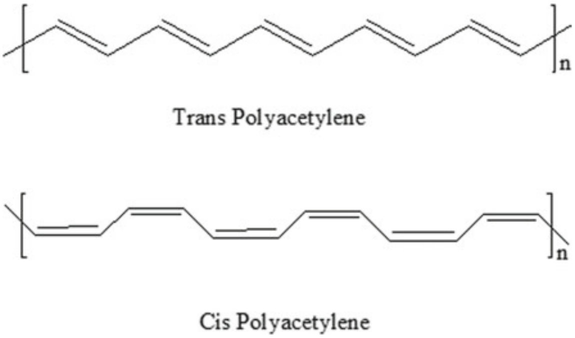

Fig. 3 A segment of cis-and trans-polyacetylene

thicknesses ranging from 10^5 to 0 cm [16]. The trans isomer is the most stable form in terms of thermodynamics. At low temperatures, any cis/trans ratio can be kept, but isomerization from cis-$(CH)_x$ to trans-$(CH)_x$ can be done by heating the film for a few minutes at temperatures above 15°. Studies with X-rays [17] show that $(CH)_x$ films are very crystalline. Because the bonds have changed, tans-$(CH)_x$ is a semiconductor with a 1.5 eV energy gap [18]. Polyacetylene is very different from other covalent semiconductors because it can be doped after it has been made, at room temperature, and with different dopants. After $(CH)_x$ is made using chemical or electrochemical techniques, it can be doped because of its open structure [19], which gives it a large surface area, and its weak interchain binding, which lets the dopant ions move between the polymer chains. Through chemical or electrochemical doping, the electrical conductivity of polyacetylene can be changed in a controlled way over 12 orders of magnitude. Conductivity values of around 10^5 s/cm have already been reported [20, 21]. Controlled electrochemical doping/undoping, and prototype rechargeable batteries have been made with $(CH)_x$ as both the active cathode and anode [22]. Photovoltaic events have been seen in heterojunctions, Schottky barrier junctions [23], and photoelectrochemical junctions [24]. So, even though these and other possible uses will need a lot of work in the future before their true technological value can be determined, the eco-friendly properties look promising.

1.1.2 Poly(p-phenylene Sulfide) (PPS)

Poly(p-phenylene sulfide) (PPS) was the first nonrigid, not fully carbon-backbone-linked polymer that, upon doping, became highly conducting [25]. Figure 4 shows the structure of PPS. PPS has been reported to have a crystal structure by several authors, including Tabor et al. [26] who carried out X-ray research on oriented films. Other authors have also contributed to this research. They proposed an orthorhombic unit cell with the following dimensions: a = 8.67, b = 5.61, and c = 10.26, and it would have space group Pbcn. Both Lovinger et al. and Uemura et al. [27] conducted studies that, in quick succession, provided evidence that confirmed this structure. The conditions under which the sample was prepared were found to affect the structure

Fig. 4 Poly(p-phenylene sulfide)

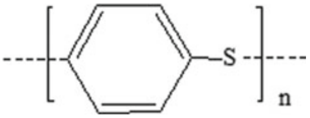

of PPS, as discovered by Jurga [28]. Napolitano et al. [29] presented findings that shed new light on the structure of the PPS. They discovered that PPS samples that were subjected to a variety of thermal and mechanical treatments exhibited a crystal structure that was comparable to that which had been proposed by Tabor et al. [26].

The highest occupied band of a hypothetical perpendicular conformation of poly(p-phenylene) has a bandwidth of only 0.2 eV, and the large IP of 6.3 eV restricts the p-type dopants to strong acceptors like AsF_5. It has been shown that exposing PPS to AsF_5 at room temperature results in significant changes to the backbone structure of the eco-friendly polymer [30]. The dopant seems to predominantly induce the formation of carbon–carbon bonds, which bridge the sulfur linkages to form thiophene rings and lead to polybenzothiophene structure. This chemical modification improves the conductivity of the complex from about 0.01–3 s/cm, and it is estimated that this improvement was brought about by the dopant.

1.1.3 Polypyrrole

Among the conducting polymers that have been discovered to date, those that are based upon polypyrrole (PPy) Fig. 5 have garnered a lot of attention. This is because these polymers have high conductivity, are simple to prepare, have a high degree of flexibility, are stable, and have excellent mechanical properties. Therefore, potential technological applications such as in electronic and electrochromic devices, counter electrodes in electrolytic capacitors, sensors [31], chromatographic stationary phases, lightweight batteries, and membrane separation [32] have attracted a lot of attention over the past few years, and this is currently one of the most active areas of research in polymer science and engineering at present.

The attraction of the polypyrrole systems can be attributed to several distinguishing characteristics. Even if the chemical and thermal stability of these polymers in comparison to (SN)x and (CH)x was the most essential element at the beginning, the simplicity with which they could be made was also enticing. Italian chemists were the first to report that pyrrole monomer can be easily polymerized into a black powder that conducts electricity [33]. This chemistry is simple, as it uses a large number of

Fig. 5 Polypyrrole

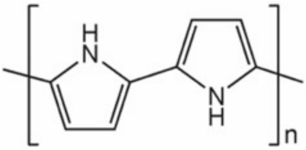

oxidizing agents, and it can be seen taking on the outside of pyrrole down which the monomer has been allowed to flow. This chemistry takes place with a large number of oxidizing agents. The resultant black powder, which conducts electricity, is called pyrrole black. Polymerization can take place both chemically and electrochemically [34]. By using an altered version of the electrochemical method that was initially developed by Dall'Oli et al. [33], Kanazawa et al. [35] and Diaz et al. [36] were the first researchers to produce films of a high enough quality to be useful. PPy is one of the few electronically conducting polymers that can be made by dissolving its precursors in aqueous solutions [37]. Polypyrrole (PPy) and a wide variety of its derivatives can be manufactured through the use of straightforward chemical or electrochemical processes [38, 39]. The process of chemical polymerization is straightforward, and quick, and does not call for the utilization of any specialized equipment. Using oxidative polymerization of the monomer in aqueous or non-aqueous solvents [40] or chemical vapor deposition [39], large quantities of polypyrrole (PPy) powder can be made. Chemical polymerization limits the number of counter ions that can be incorporated into the polymer, limiting the range of conducting polymers that can be made. The chemical polymerization of pyrrole appears to be a general and useful tool for the preparation of conductive composites [41] and dispersed particles in aqueous media [42]. According to research [43], iron (III) chloride is the most effective chemical oxidant, whereas water is the most effective solvent for the chemical polymerization process. Both of these factors are important in achieving the desirable conductivity characteristics. The electrochemical method for producing electroactive or conductive films is extremely flexible and offers an easy method for changing the properties of the films by simply altering the electrolysis conditions (such as electrode potential, current density, solvent, and electrolyte) in a predetermined manner. Electrochemical methods are ideal for making these films. Alternatively, polymer properties can be changed by varying the monomer or electrolyte. Using electrosynthesis, polymer thickness can be easily controlled. Pyrrole is easily electropolymerized in aqueous and non-aqueous solvents because pyrrole monomer is soluble in many solvents. The polymerization reaction is very complicated, and the mechanism of electropolymerization is not yet completely understood. The mechanism that is generally accepted [44] is that in the first step, the neutral monomer is oxidized to a radical cation, which is then followed by aromatization and the oxidation of the dimer. The dimer, on account of its greater conjugation, is more easily oxidized than the monomer under the given experimental conditions; consequently, the dimer is immediately reoxidized to the cation. PPy conductive polymers' electrical conductivity is important for analytical applications. According to the findings of Munstedt and colleagues [45], treating PPy with a solution of NaOH causes the conductivity of all PPys to decrease over time. The films suffered severe embrittlement as a result of the sodium hydroxide treatment as well. Investigations of PPy using scanning electron microscopy (SEM) have shown, among other things, that the surface morphology of the ppy alters when it is treated with either a base or an acid [46]. The electroactive nature or the switching properties of PPy have been utilized as the basis of most proposed eco-friendly applications such as sensors, separation devices, and rechargeable batteries.

1.1.4 Polyaniline (PANI)

Polyaniline (PANI) is one of the most important eco-friendly conducting polymers and has attracted a lot of attention since its electrical conductivity can be controlled, it is stable in the environment [47], and it has interesting redox properties associated with the chain heteroatoms. It has come to everyone's attention that the PANI family of polymers is among the most interesting and unique of all the members of the class of conducting polymers that contain electrons. The electronic properties of many other members of this class, such as polyacetylene, polypyrrole, and polythiophene, are well understood solely based on their conjugated carbon backbones. However, in PANI, a nitrogen heteroatom is incorporated between constituent phenyl (C_6H_6) rings in the backbone. This is in contrast to the electronic properties of many other members of this class. Because of the chemical versatility that the nitrogen heteroatom offers, it is possible to access multiple insulating ground states, each of which can be identified by the oxidation state that it is in. PANI can be found in many different forms, each of which is distinguished by the degree of oxidation it has undergone. The formula that can be used to broadly describe a PANI chain is Fig. 6 [48].

The term "aniline black," which was first used to refer to polyaniline in 1835, was a term that was used for any product that was obtained by the oxidation of aniline. A few years later, Fritzches [48] conducted a preliminary investigation of the products that were obtained through the chemical oxidation of this aromatic amine. After that, Lethe [49] discovered that the final product of anodic oxidation of aniline at a platinum electrode, in a solution of aqueous sulphuric acid, is a dark brown precipitate. These findings have been confirmed by subsequent researchers [50], and similar observations have been made during the oxidation of aqueous hydrochloric acid solutions containing aniline. Bucherer [51] proposed a phenazene-type structure that is more complicated than what is currently understood, which is the opposite of what is the case. A linear octameric structure of the quinoneimine type in the para-position was proposed by Green and co-workers' for the product obtained by the chemical oxidation of aniline. A highly conducting state can be achieved in polyaniline through the straightforward protonation of the imine nitrogen atoms located in the emeraldine base backbone. It is known that polyaniline has a crystalline structure. The number of electrons in the chain structure of the polymer does not change as a result of protonic doping, and the pH of the solution affects the conductivity of the doping [52]. Polyaniline's backbone contains a –NH-group that is chemically flexible; this group is responsible for polyaniline's interesting chemistry and physics [53].

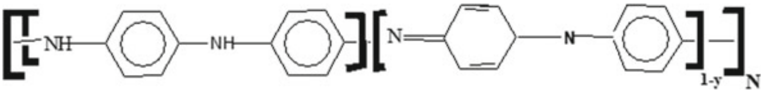

Fig. 6 Three stable forms of PANI are in correspondence to the values y = 0 (leucoemeraldine base, LB), y = 0.5 (emeraldine base, EB), and y = 1 (pernigraniline base, PNB). Where y gives the average oxidation degree

Electrochemical polymerization was used to produce an electrically conducting polyaniline (PANI) that was doped with heteropolyanions (HPA) of a Keggin structure. The cyclic voltammetry experiment revealed that both the polymer itself and the immobilized HPA contained reversible redox systems. Barth et al. [54] conducted studies on the electrocatalytic activity of a PANI electrode that had been modified by HPA in the context of an electroreduction reaction involving bromate. Aniline, hydrochloric acid, sulphuric acid, nitric acid, or perchloric acid, as well as ammonium peroxydisulphate (persulphate), are the typical reagents used in the chemical synthesis of PANI. PANI is the precipitated product of an aqueous solution containing these reagents. Aniline, the monomer, is directly converted into a conjugated polymer through a condensation process in this direct route, which represents the classical approach to the synthesis of polyaniline. An excess of the oxidant and higher ionic strength of the medium lead to materials [55] that are essentially intractable, which is one of the drawbacks of this direct approach. This experimental observation is the source of one of the disadvantages of this direct approach. There have been many different approaches to the synthesis of PANI published in the literature [56].

Four primary factors determine how the reaction will proceed and what kind of product will be produced in the end. These are.

(1) nature of the medium,
(2) concentration of the oxidant,
(3) duration of the reaction, and
(4) temperature of the medium.

Polyaniline is an innovative material because it possesses a symmetrical conjugated structure. This structure has extensive charge delocalization, which is the result of a new type of doping of an organic-polymer salt formation rather than oxidation, which is what happens in the p-doping of all other conducting polymer systems. In addition, polyaniline possesses extensive charge delocalization, PANI is unlike other conducting polymers that have been studied in the past, such as polyacetylene and polypyrrole, because the electronic state of PANI can be controlled through variations in both the number of electrons and the number of protons that are contained within each repeat unit. The redox activity of PANI occurs in an aqueous medium that is pH-dependent. It has been demonstrated that PANI loses its ability to conduct electricity in aqueous media with a pH greater than 4 [57]. On the other hand, the electrochemical behavior of PANI, which was investigated in an aprotic solvent such as propylene carbonate, in the presence of 1 M lithium perchlorate as a supporting electrolyte, demonstrates two purely electronic processes. However, in the presence of a trace amount of the strong base 2,4,6-trimethyl pyridine, these redox processes are rendered moot [58]. Furthermore, the dramatic effect of the conductivity of PANI upon variation of pH (changing pH from 0 to 6 decreases electrical conductivity, by six orders of magnitude) [59] demonstrates that in addition to the dopants (counterions), the presence of protons invariably has a pronounced effect on the conductivity.

In addition to this, the use of polyaniline solution as a redox indicator is being researched [60]. PANI is distinguished from other conducting polymers like polypyrrole and polythiophene by its one-of-a-kind property, which is the imposition of the anion within the polymer through the process of equilibration with an acid solution. The theoretical underpinnings of PANI have been the subject of a great deal of scrutiny [61]

1.1.5 Other Conducting Polymers

- **Poly (Phenylene Vinylene)**

A composite polymer of polyphenylene and polyacetylene is also conductive when doped with AsF_5 [62]. When compared to polyphenylene or polyacetylene, the maximum conductivity levels that could be achieved with poly (phenylene vinylene) were significantly lower, coming in at 3 s/cm. This may not come as a surprise given the low degree of polymerization that was present in the starting polymers. The highest occupied band of poly (phenylene vinylene) has a calculated bandwidth (VEH technique) of approximately 2.8 eV [63].

- **Polydiacetylenes**

In most cases, polydiacetylene is manufactured through a solid-state reaction of a single crystal that contains substituted diacetylenes RCC-CCR [64]. Obtaining a single-crystal polymer with highly one-dimensional electronic properties requires favorable packing conditions, which are dominated by R groups. In 1985, Bloor [65] conducted a study that analyzed the characteristics of PDAs. Since that time, there has been a significant increase in interest in PDAs, and a diverse range of research efforts have led to the discovery of new qualities and insights. PDAs can be structured into a wide variety of different forms, including bulk single-crystals, multilayer films, monolayer films in both the Langmuir and self-assembled [66, 67] forms, vesicles suspended in liquids, and nanocomposite components integrated into inorganic host matrices. Their high nonlinear optical susceptibility [68], ultrafast optical response [69], and strong structural anisotropy imposed by the highly aligned, linear backbones are all properties that are of significant interest. Nevertheless, the chromogenic transitions that PDAs display have received the greatest amount of attention from researchers.

- **Polymethineimine**

The unsubstituted polymethineimine, $(CH = N)_x$, has been synthesized by Wohrle et al. [70], even though a large number of polymers with conjugated carbon–nitrogen backbones already exist. Karpfmen proposed an alternating structure similar to that of trans-PA using ab-initio quantum chemical calculations, and this raises the possibility of soliton excitations occurring along the chain [71]. It is hypothesized that the ionization potential value of polymethineimine will be on the order of 8 eV, which is approximately 3.3 eV greater than the value of polyacetylene.

1.2 Strategies for the Development of Tailor-Made Conducting Polymers

Conducting polymers are prone to chemical instability and poor processibility as a consequence of doping. Various attempts have been made, documented in the scientific literature, to design low-band-gap conducting polymers that maintain both their stability and their ability to be processed. In this part of the article, we will talk about some of the standard methods that have been used up until this point to design conducting polymers with a low band gap. The presence of substitutes is what determines whether or not electropolymerization takes place and whether or not soluble products are produced. Many researchers, such as fluorinated polyacetylenes [72], have looked into the effect that substituents have on the band structure of PA. Highly conductive new aniline copolymers containing butythio substituents have also been successfully prepared with conductivity on the order of 1S/cm [73]. The “push–pull” effect that is induced on the n-electrons of their respective polymers as a result of the substitution of thiophene monomers with appropriate 3-substituents is responsible for the change in the electrical conductivity of the polymer [74]. The electrical conductivity of poly(3-methylthiophene) is therefore one hundred times higher than that of polythiophene. Sometimes, substitution will result in a decrease in the polymer’s conductivity; however, the resulting polymer may have high electronic affinity and may be more stable. For instance, polypyrrole films that have alkyl groups substituted in the 1-position of the monomer units can electrooxidize the anodic potential of polypyrrole by approximately 800 mV. As a direct consequence of this, these films have improved resistance to oxygen. However, 1-alkyl-substituted films have a lower electrical conductivity compared to the parent polypyrrole. This effect can be attributed to the steric constraints that are introduced by the bulky substituents. For instance, the electrical conductivity of polypyrrole is approximately 100 S/cm, but 1-methyl, 1-ethyl, or 1-n-propyl polypyrroles only have conductivities of 10^{-3} s/cm [75]. Therefore, by utilizing substituents, one can enhance the solubility, and bandgaps, and increase the polarizabilities of conducting polymers, in addition to improving other properties of the materials.

The literature reveals that copolymerization is another method that has proven to be very effective in the design of new conducting polymers. Copolymers of fluorine, phenothiazine-quinoline copolymers, and cyclodiborazane-dithifulvene copolymers are some examples of these types of compounds. Aniline and pyrrole copolymers have also been reported [76], and these copolymers exhibit good conductivity and better solubility than the original compounds. It is also possible to design new conducting systems with a low band gap by making use of the ladder polymerization technique. Numerous theoreticians have conducted research into the electronic properties of polyacene, polyacenacene, polyphenanyhrene, polyphenanthrophenanthrene, and polyperinapthalene [77]. The ground state and excited state properties of phenylene oligomers are being investigated with semiempirical methods, and thiophene polymers that have decreased band gap values have been synthesized. Studies have been conducted on a wide variety of other polymers, including poly (aroylene benzimidazoles), polyepoxyloxanes, and ladder polymers with thienylene units, amongst others [78]. Unique new ladder polymer (polyindenoindenes) consisting of a condensed succession of six and five-membered conjugated carbon rings have been synthesized [79]. These polymers are a candidate for new materials with unique electronic properties.

2 Electrochemical Properties of Conducting Polymers

CPs, in comparison to organic polymers typically used, have a high electron affinity and redox activity. The general physical properties of CPs are described in terms of their molecular weight [80], as well as their size and length. The size and length of the CPs are directly related to the CPs. Polymers are insoluble in water because their chemical properties are primarily determined by the polymer chains that make up the polymer, and polymers cannot dissolve in organic solvents. The oxidation of the monomer by oxidizing agents or the application of potential or current through electrodes is the typical method for the preparation of CPs [81]. The first proposed mechanism for the formation of PPy was put forth by Diaz et al. [82] in 1981. This mechanism propagated the polymerization by continually growing chains through the side-to-side coupling of monomeric radical cations into oligomer radicals. In the case of PANI, the electrochemical growth process begins with the formation of oligomers, as illustrated in Fig. 7 [81], and is then followed by nucleation and the expansion of polymer chains. Electrochemistry can be used to dope CPs, which means that the oxidation of CPs can produce a p-doped state and the reduction of CPs can produce an n-doped state. These redox reactions also allow for the conductivity of the CPs to be modulated in the desired manner. Electrochemical preparation methods allow for greater control over the properties of the polymers, including their morphology, conductivity, and thickness [83]. Figure 8 provides an overview of the structural makeup of each of the various CPs. In the early stages of this field, the electrochemistry of CPs was intensively studied by Park's and Shim's groups, who investigated the autocatalytic growth mechanism of PANI and its growth kinetics on the electrode surface [84, 85]. In addition, the degradation mechanisms of electrochemically prepared PANI, PPy, and polythiophene were also investigated [86]. During the past decades, several reports have described CP applications of CPs. Both monomers and CPs can be functionalized with different materials to tailor their properties. The addition of substituents not only improves functions but also improves the chemical and physical properties of the main\polymer chain, including increasing its electrical and mechanical properties. It is possible to make composites of CPs out of highly conductive nanomaterials and catalysts to improve the properties of CPs.

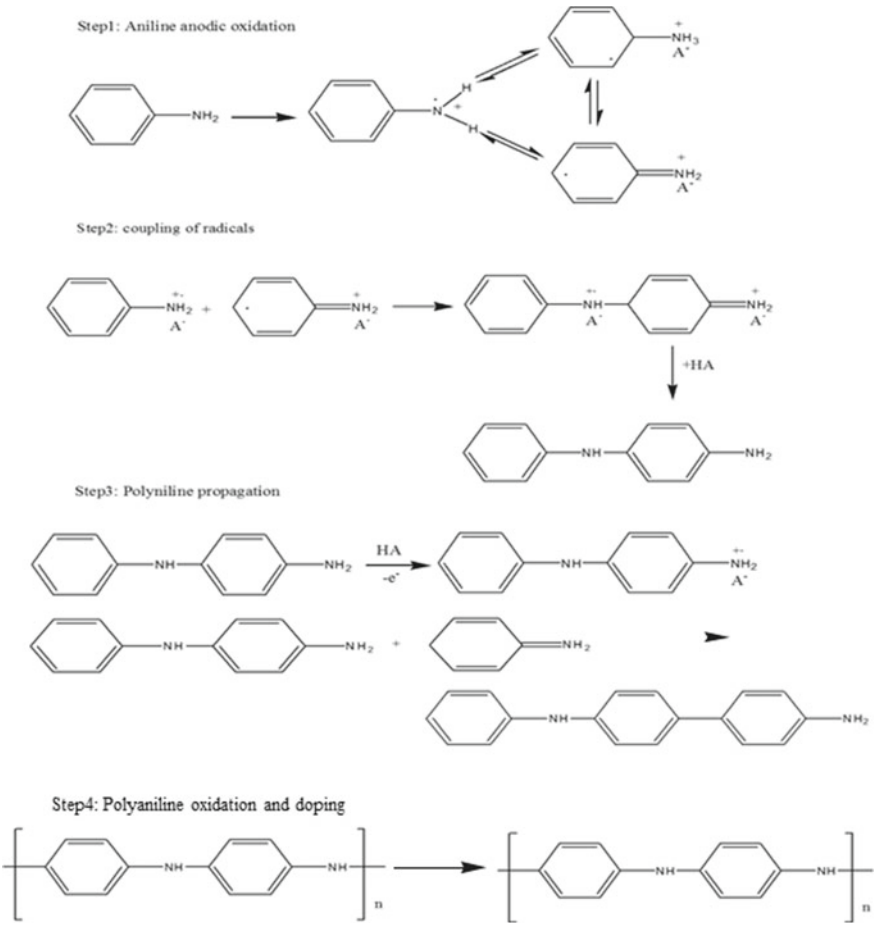
Step1: Aniline anodic oxidation
NH2
N
H
H
NH3
A-
NH2
A-
Step2: coupling of radicals
NH2
A-
NH2
A-
NH
A-
NH2
A-
+HA
NH
NH2
Step3: Polyniline propagation
NH
NH2
HA
-e-
NH
NH2
A-
NH
NH2
NH2
NH
NH2
Step4: Polyaniline oxidation and doping
NH
NH
n
NH
NH
n

Fig. 7 Electrochemical oxidation and doping [81]

2.1 *Composite Materials*

Carbon-based materials, including carbon nanotubes (CNTs), graphene, carbon dots, and porous carbon, are considered to be promising materials in several applications [87]. The rapid development of carbon materials can be attributed to the excellent conductivity, high chemical stability, mechanical strength, and large surface area of carbon materials [88]. All of these properties have the potential to be incorporated into the design of novel types of electrochemical sensors. Using carbon materials alone has a significant drawback, especially when they are used in sensor devices: they lack selectivity for target molecules. This can be a problem when trying to

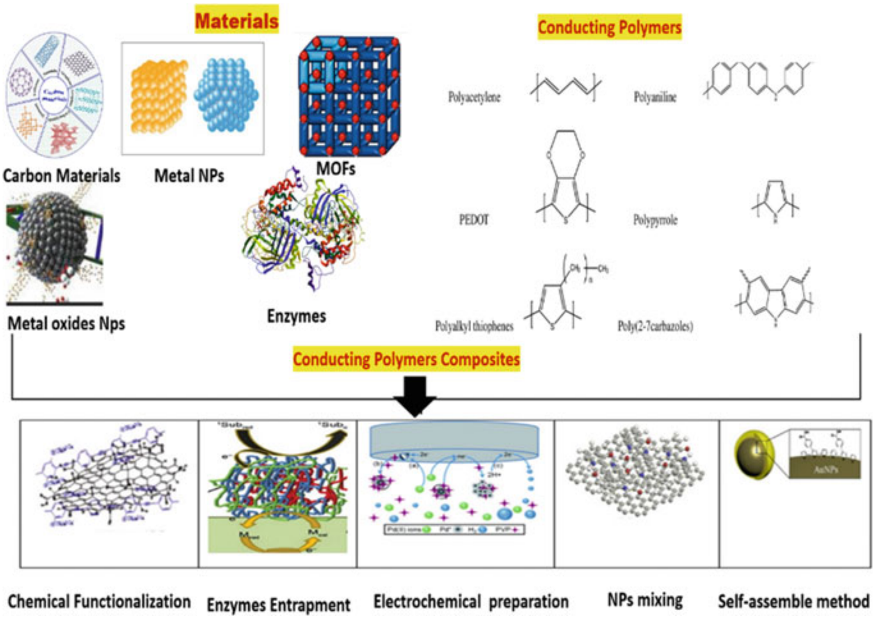
Materials
Carbon Materials
Metal NPs
MOFs
Metal oxides Nps
Enzymes
Conducting Polymers
Polyacetylene
Polyaniline
PEDOT
Polypyrrole
Polyalkyl thiophenes
Poly(2-7carbazoles)
Conducting Polymers Composites
Chemical Functionalization
Enzymes Entrapment
Electrochemical preparation
NPs mixing
Self-assemble method
AuNPs

Fig. 8 Conducting polymers and their composites materials

detect certain types of molecules. For this reason, the formation of carbon composites and their functionalization are essential steps before their use in particular applications. Their use in electrochemical sensors specifically requires selectivity, and making composites with CPs is the most promising way to improve their performance. Carbon materials are used in composites because, depending on the inherent carbon structure of the carbon material, the carbon material can be treated as either an inorganic or an organic reagent. In addition, metal or metal oxide nanoparticles (NPs), such as Au, Pt, Pd, Ni, Cu, TiO_2, MnO_2, ZnO, and Fe_3O_4, are another class of materials [89] that exhibit unique properties in comparison to their bulk counterparts. NPs have found applications in a wide variety of fields, such as biomedical research, optoelectronics, catalysis, sustainable energy, and electrochemical devices. In particular, the utilization of metal/metal oxide NPs as electrode materials results in high performance in comparison to bulk metal electrodes. For instance, AuNPs have been found to have excellent activity and have been utilized as a base material for electrochemical sensing electrodes [90]. Synthesizing NPs has been accomplished via a variety of methods, some of which include dendrimer-mediated assembly, electrochemical deposition, electrochemical synthesis, monolayer formation, and wet chemical synthesis [91]. Metal nanoparticles (NPs) are capable of being functionalized with secondary materials such as carbon materials, enzymes, and CPs. They also have a high level of activity and high biocompatibility on their surface. It has been reported [92] that composite particles can be prepared by combining CPs and metal NPs. Steric hindrance and electrostatic interactions can prevent agglomeration and restacking of metal NPs when composite particles made of CPs and metal NPs are used. In addition, the use of these composites in electrochemical devices has the potential to increase the electron transport rates between the electrolyte and current collectors or electrode materials. In the field of bioanalytical chemistry, biologically active materials, specifically enzymes, DNA, proteins, antibodies, and antigens, have played important roles. Wang's research team conducted a literature review and found that a significant number of biosensor devices involve a variety of enzymatic reactions [93]. For these biomolecules to be useful, they need to be attached to or functionalized with a chemically inert matrix that does not alter the properties of the biomolecules. One promising approach involves using a polymer matrix as the host material for the incorporation of biomolecules.

2.2 Conducting Polymer Nanocomposites

The unique properties originating in CP-carbon nanocomposites make them promising candidates, particularly in electrochemical devices [94]. Several approaches to manufacturing novel CP composites have been published, including template-oriented synthesis, vapor polymerization, chemical functionalization, and in situ composite creation. Electrochemical approaches can alter the shape, thickness, chemical state, and conductivity of CP composites. Figure 8 shows materials and composites. Composites of CPs use CPs as a major component and at least one secondary component [95]. Metal ions, NPs, nanostructures of metal and metal oxides, carbon materials, molecular species (metal phthalocyanines), and physiologically active components (enzymes, proteins, antibodies, and antigens) are included. The purpose of developing a novel composite material is to notice new characteristics [96]. Creating composite materials requires a synergetic approach. The interfacial adhesion between CPs and the secondary component affects CP nanocomposites' characteristics. These composites work well in energy storage, as catalysts, in fuel cells [97, 98], and in biomedicine. Electrochemical trapping, physical adsorption, and affinity or covalent bonding are popular immobilization strategies. Physical adsorption includes electrostatic interactions between CPs and biomolecules because of their functional groups. Hydrophobic and van der Waals forces are also important in physical adsorption, notably of antibodies and proteins [99]. Biosensors utilizing glucose oxidase on PPy investigated adsorption. Adsorption does not require functionalized monomers due to poor biomolecule adsorption pressures, biomolecules may leak from the electrode contact over protracted studies [100]. Entrapment of enzymes by electrochemical means was later proposed to boost biomolecule binding efficiency; glucose oxidase was entrapped in PPy films by an electropolymerization process. This approach resulted in immediate and persistent immobilization, unlike physical adsorption. Enzymes or biomolecules were partially exposed and buried in polymer films, reducing target accessibility. This technique is best for water-soluble monomers and not non-aqueous monomers. Covalently bonding enzymes to CPs was suggested. This method couples carboxylic acids (–COOH) to amines ($-NH_2$) via

NHS/EDC chemistry. The coupling reaction may be done in water, which preserves biomolecules [101]. Due to the covalent attachment of enzymes or proteins to the electrode surface, these sensors have exceptional long-term stability. CPs functionalized with biomolecules have been studied for medication delivery and bioimaging [102].

2.3 Electrochemical Properties of Conducting Polymer Nanocomposites

CP nanocomposites consisting of carbon nano species such as graphene, carbon nanotubes, and carbon nanofibers have been manufactured. The basic properties of the CP chains were improved thanks to the presence of these carbon nano species, which also encouraged the delocalization of charge carriers, which led to an increase in conductivity. It was possible to achieve a wide variety of conductivities, ranging from insulating to metallic [103]. CPs are useful as key substances in light-emitting diodes, transistors, electrochromic devices, actuators, electrochemical capacitors, photovoltaic cells, and sensors [104, 105] thanks to the effective synthesis of eco-friendly CP composites with flexibility, excellent mechanical stability, and conductivity. Improving the electrochemical properties of the CPs is the most important factor in moving forward with developments in this area. As a result, a discussion of the eco-friendly electrochemical applications of CPs and CP composites is presented here in this chapter.

3 Application to Electrochemical Sensors

3.1 Electrochemical Sensors

Electrochemical sensors translate the chemical reactions of the target species occurring on electrodes into observable changes in electrical signals in terms of current, potential, and conductivity. As illustrated by Wang [104], who has made significant contributions to the field of electrochemical sensors and biosensors, these sensors can be divided into voltammetric/amperometric, potentiometric, and impedimetric sensors [106]. Methods based on electrochemistry have extremely low limits of detection and a high level of selectivity, while only requiring a minuscule amount of sample data to obtain the signals. Electrochemical techniques make it possible to measure turbid samples of whole blood, fat globules, red blood cells, and hemoglobin. In contrast, spectrophotometric measurements of these systems typically result in interference effects [107]. Electrochemical devices typically include a set of either two or three electrodes in their construction. A typical three-electrode cell has a working electrode that is made of platinum, gold, and/or carbon; a reference electrode that is typically a silver-silver chloride electrode (Ag/AgCl); and a platinum wire or foil is used as a counter or auxiliary electrode. The working electrode is responsible for conducting electric current within the cell. A voltammetric sensor can perform its function because it is designed to measure current while simultaneously applying a potential to the working electrode with a reference electrode. The electrochemical reaction that takes place at the electrode surface and the interface layer between the electrode and the electrolyte is what causes the response current to be produced. The rate of mass transport of the species to the electrode is what ultimately determines how fast the electrochemical reaction can proceed [108]. Methods that fall under the category of voltammetry include things like linear sweep voltammetry, cyclic voltammetry, hydrodynamic voltammetry, differential pulse voltammetry, square-wave voltammetry, polarography, and stripping voltammetry. These methods offer a broad dynamic range, an extremely low detection limit, and a wide variety of potential applications. Amperometry involves applying a constant potential to the working electrode and measuring the current that flows as a result of this concerning the passage of time. Amperometry is distinct from voltammetry in that it does not involve a potential sweep but rather makes use of a potential step. Voltammetry, on the other hand, does involve a potential sweep. The equation developed by Cottrell describes the current that is produced when a given potential is applied. This current is proportional to the concentration of the electroactive species that are present in the sample. Because the oxidation or reduction potential used for detection is characteristic of the analyte species [109], amperometric sensors have greater sensitivity and selectivity than other types of sensors. When there is no significant flow of current, potentiometric sensors can measure the potential difference between the working electrode and the reference electrode [108]. The measured potential is most commonly utilized in an electrochemical cell to determine ion activity. When performing potentiometric measurements, one can determine the potential difference by applying the Nernst equation. In this equation, Ecell stands for the observed cell potential when there is no current flowing through it. This value is also known as the electromotive force, abbreviated as EMF for short. Ion-selective electrodes (ISE) are currently used quite frequently in potentiometric devices because they allow for the realization of the lowest detection limits [110]. In electrochemical impedance spectroscopy, the impedance of a generic electrical component is calculated by dividing the alternating current potential by the alternating current. This is equivalent to dividing an incremental change in voltage by the change in current that results from the change in voltage. The experimental method involves causing a disturbance in the cell by applying a low-amplitude alternating potential and then observing how the system responds to the disturbance while it is in a steady state. There are two distinct kinds of impedance sensors, and they are distinguished from one another by the presence or absence of certain recognition elements. The first type of this sensor gets its functionality from a change in impedance that is brought about by the binding of targets to receptors (antibodies and nucleic acids) that have been immobilized onto the sensor's surface. The electrode is one type of sensor, while the other type of sensor's response is based on surface alterations that are brought on by the adsorption and desorption of target species as a consequence of development [111]. Within the scope of this review, we will confine our discussion on the construction of eco-friendly electrochemical sensors to CPs and CPs. composites.

3.2 Applications of Polyaniline and Related Nanocomposite Materials as Sensors

PANI has become one of the most promising CP materials for a variety of applications. Composites of the polymer were utilized in the fabrication of numerous devices for various applications, such as batteries, biofuel cells, thermoelectric, and energy storage devices [112]. In addition, a chemical sensor for detecting dissolved oxygen based on a PANI-modified electrode has been reported [113]. The most promising application of these composites was discovered to be in electrochemical applications. Particularly, the fabrication of electrochemical sensors based on PANI and PANI composites has become a popular technique in numerous electroanalytical studies, as they offer high sensitivity and selectivity for the detection of target molecules. Using composites of PANI and $NiCo_2O_4$ nanoparticles to detect glucose was reported. This non-enzymatic glucose sensor demonstrated excellent electrocatalytic glucose analysis performance. The catalytic active sites in $NiCo_2O_4$ with conductive PANI played a synergistic role in the oxidation of glucose and displayed high sensitivity and a reduced detection limit [114]. Electrochemical deposition of poly(3,4ethylenedioxythiophene)-graphene oxide (PEDOT-GO) nanocomposite followed by electrochemical reduction of nanocomposite led to the development of a dopamine sensor with selectivity. As depicted in Fig. 9a, dual polymer sensitivity and very rapid amperometric response are required for glucose detection [115, 116]. As depicted in Fig. 9a, b similar PtNP/PANI hydrogel-based electrode was used to detect human metabolites, and the performance of the sensor probe was exemplary [117]. Recently, a 2,4-dichlorophenoxyacetic acid (2,4-D) herbicide-detecting impedimetric immunosensor based on an AuNP-functionalized PANI and multiwalled carbon nanotube (MWCNT) composite electrode was developed [118]. The sensor probe was manufactured by electropolymerized aniline and 3-aminobenzoic acid in the presence of AuNPs onto an MWCNT-coated screen-printed electrode. To improve the sensitivity of antigen detection, an antibody was covalently attached to the sensor probe. The developed impedimetric sensor displayed a wide linearity range, high stability, and a detection limit of 0.3 ppb 2,4-D. Molybdenum disulfide (MoS_2) is a layered transition metal dichalcogenide with metal Mo layers sandwiched between two sulfur layers and stacked by weak van der Waals interactions. MoS_2 is a nanomaterial that resembles graphene, but its low electronic conductivity is a drawback. MoS_2 was combined with PANI through the facile oxidation of aniline monomers on MoS_2's matrix. This composite material served as an outstanding conductive skeleton with a large electrocatalytic surface area, and it also provided a direct path for electron transfer. The hybrid PANI-MoS_2 material demonstrated superior electrochemical performance compared to pure PANI and MoS_2; consequently, this material was utilized for the electrochemical detection of DNA molecules [119]. Metal electrodes are extremely stable and can be used in a variety of electrochemical applications; however, in biological applications, the metallic surfaces may result in undesirable poisoning effects and nonspecific catalysis. In the production of biosensors, the fouling of electrode surfaces is one of the most significant challenges researchers face. PANI nanofibers were grafted with polyethylene glycol (PEG) to overcome this obstacle [120]. This composite material was conducive and had a large surface area, in addition to exhibiting excellent antifouling activity in single protein solutions and complex human serum samples. The antifouling effect was achieved by making the surface hydrophilic, which prevented interactions with nonspecific proteins in the complex biological samples. This composite was used by the researchers to create an electrochemical biosensor for detecting the breast cancer susceptibility gene BRCA1. In addition, gene sensing is a highly effective method for diagnosing a vast array of diseases, from common viral infections to cardiovascular diseases and cancer. To detect nucleic acids in biological samples, numerous CP composites were developed as an alternative to metal or metal oxide electrode materials. For instance, a new method was developed for the sensitive detection of nucleic acids using a PANI-deposited surface [121]. In this instance, the polymer was deposited by the enzyme-catalyzed formation and template-guided deposition, in which a reporter enzyme catalyzed the deposition of PANI onto the nucleic acid molecules being analyzed by forming an intramolecular complex. After interaction with the nucleic acids, the optical and electrical properties of the newly formed polymers are altered and can be quantified. One of the more recent projects on this topic involves the use of graphene-based PANI arrays for the electrochemical detection of DNA, with a focus on increasing the sensitivity of detection by controlling the substrate's texture [122].

3.3 Poly(o-anisidine) and Its Related Nanocomposite Material Sensor Applications

When compared to other CPs, orthoanisidine polymer is among the best due to its exceptional qualities. Orthoanisidine-based CP composites have been used in the fabrication of semiconductors, thin-film transistors, electrochromic devices, and memory devices. Notwithstanding these uses, polyorthoanisidine-based composite compounds have been employed to create several sensors, including those used for the measurement of neurotransmitters, gases, glucose, and a wide variety of other analytes [123]. For their potential as glucose biosensors, several different compound combinations with orthoanisidine-based polymers have been investigated. Electrochemical synthesis has been used to create polyorthoanisidine films that have been doped with anions like perchlorate and para-toluene sulfonate. Movies were said to

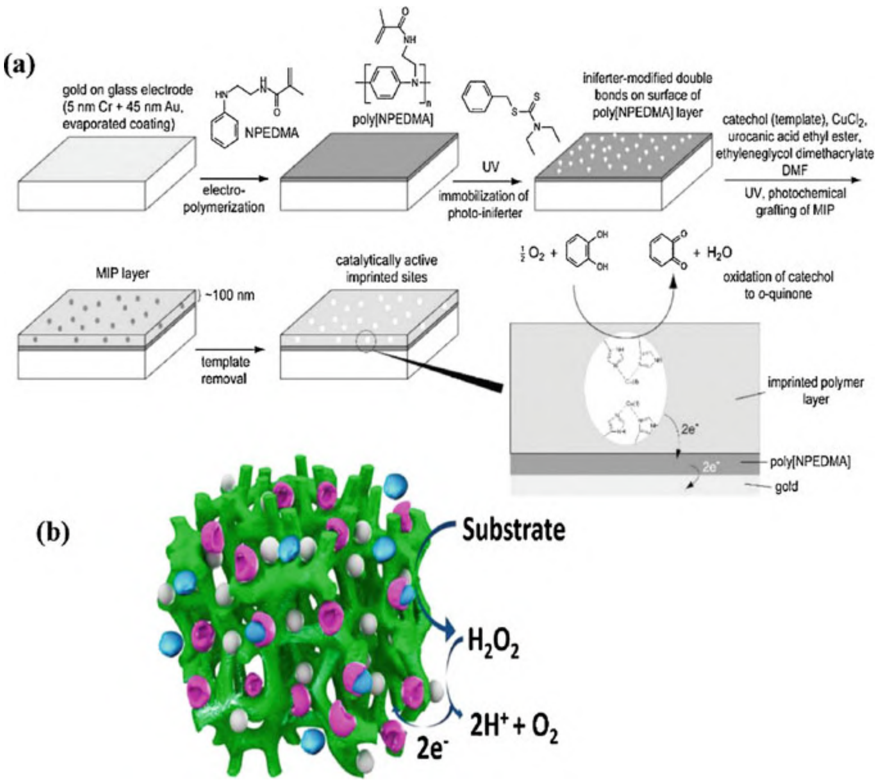
(a)
gold on glass electrode (5 nm Cr + 45 nm Au, evaporated coating)
NPEDMA
electro-polymerization
poly[NPEDMA]
UV
immobilization of photo-iniferter
iniferter-modified double bonds on surface of poly[NPEDMA] layer
catechol (template), CuCl2, urocanic acid ethyl ester, ethyleneglycol dimethacrylate DMF
UV, photochemical grafting of MIP
MIP layer
~100 nm
template removal
catalytically active imprinted sites
½ O2 +
+ H2O
oxidation of catechol to o-quinone
imprinted polymer layer
2e⁻
poly[NPEDMA]
gold
(b)
Substrate
H2O2
2H⁺ + O2
2e⁻

Fig. 9 **a** Schematic of the MIP-conducting polymer hybrid electrode with catechol. Adapted with permission from ref. [113]. Copyright 2009 American chemical society. **b** Schematic of the Pt NPs and enzymes-loaded 3D porous ANI hydrogel hydride electrode. Adapted from Ref [114]

be suitable for use in the immobilization of glucose oxidase protein; found to be a good glucose detection matrix. Reagent transport toward NADH oxidation was also seen in the films [124]. Through a chemical oxidative polymerization process, Sangamithirai et al. created poly(o-anisidine) (PoA)/graphene (GR) nanocomposites. The produced nanocomposites were used to alter glassy carbon electrodes (GCEs), and the GCEs exhibited electrocatalytic activity for the oxidation of NADH Fig. 10. The artificial sensor produced a current response for the detection of NADH, showing great sensitivity, good stability, eco-friendly, and high selectivity. On the other hand, poly(o anisidine)-silver nanocomposites were synthesized and deployed as sensors for the analysis of NADH and dopamine. There was a 6 nM cutoff for NADH and a 52 nM cutoff for DA. High sensitivity, strong stability, outstanding selectivity, and repeatability were all demonstrated by the modified electrodes [125]. Aussawasathien et al. [127] made composite fibers out of poly(o-anisidine) and polystyrene and used them for chemical vapor sensing. A poly(o-anisidine)/silverized multiwalled carbon nanotube (PoAS-Ag/MWCNT) nanocomposite was designed for the sensitive electrochemical detection of 3-methoxy phenol. Adsorption between PoAS and MWCNTs was used in a solution-based procedure to create the PoAS-Ag/MWCNT nanocomposite Fig. 11 Improved electrochemical performance was seen in the presence of 3-methoxyphenol [127], along with increased sensitivity, high dynamic concentration ranges, good stability, and robust fabrication of the electrochemical sensor. In addition, a quick method for determining dopamine (DA) was devised, and a sensor modified with poly(o-anisidine) (PoA) and a silver nanoparticle (AgNP)-based nanocomposite was employed [128]. Electrodeposition of Ag was recently performed on a polyorthoanisidine CP. Please refer to Fig. 12, this nanocomposite was used for the selective detection of paracetamol (PCM), displaying good stability and an electrochemically active region [129]. These same researchers also created a novel functionalized poly(o)-anisidine/GO nanocomposite and used it for the determination of benzaldehyde [130]. Nanocomposite sensors based on poly(o-anisidine) and carbon nanotubes (PoAS/CNT) were used to detect inorganic vapor [131]. Researchers in the sensor field have found that doping them with poly(o-anisidine) (PoA)-tin oxide (SnO_2) nanocomposites is an effective way to achieve a wide range of analytical goals with a variety of techniques. Poly(o-anisidine) and tin oxide were investigated as a humidity sensor combination recently. To make the sensor, o-anisidine was chemically polymerized on-site using SnO_2 nanoparticles. When used to quantify humidity, the PoA-SnO_2 nanocomposite sensor demonstrated superior humidity detecting features to pure PoA, such as high sensitivity, rapid response, fast recovery, and strong repeatability [132]. Khan et al. [133] created a sensor using a poly-o-anisidine Sn(IV) tungstate composite. The detection of Hg (II) ions was demonstrated to be both selective and sensitive using a nanocomposite electrochemical sensor.

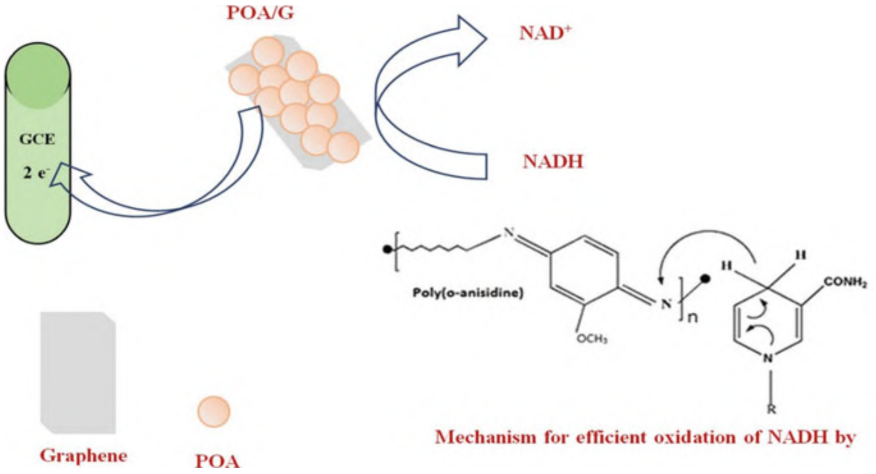

Fig. 10 Intermediate electron transfer on a PoA/GR-modified electrode through NADH oxidation [124]

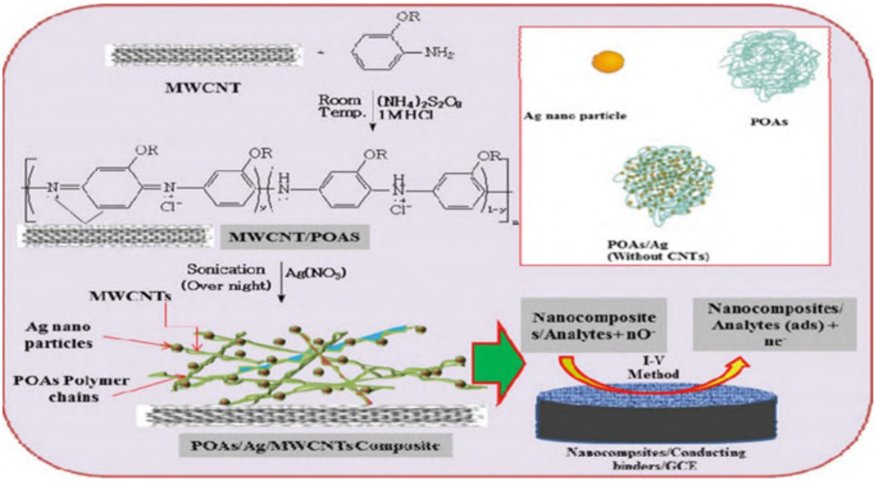
MWCNT
Room Temp.
$(NH_4)_2S_2O_8$ 1MHCl
MWCNT/POAS
Sonication (Over night)
$Ag(NO_3)$
MWCNTs
Ag nano particles
POAs Polymer chains
POAs/Ag/MWCNTs Composite
Ag nano particle
POAs
POAs/Ag (Without CNTs)
Nanocomposites/Analytes+ nO⁻
Nanocomposites/ Analytes (ads) + ne⁻
I-V Method
Nanocompsites/Conducting binders/GCE

Fig. 11 Graphical impersonation of the synthesis of PoAS-Ag/MWCNTs, polymer nanocomposite fabrication onto glassy carbon electrode, and electrochemical sensor applications [127]

3.4 Polypyrrole and Its Related Nanocomposite Material Sensor Applications

One of the most promising CPs, PPy is created by the chemical or electrochemical polymerization of pyrrole. The PPy polymerization process was initially postulated by Diaz et al. [134]. The use of polymer-coated electrodes has been the subject of a plethora of subsequent research. Research into the use of polypyrrole (PPy) and its eco-friendly composites as electrochemical electrode materials, especially for electrochemical biosensor applications, has been conducted. PPy has found application in electrochemical sensing materials due to its advantageous and distinctive chemical, physical, and electronic features. Using a PPy-coated electrode in a flow injection study, Wang et al. [135] presented a novel procedure for electrochemically detecting nucleic acids. A nanocomposite sensor made of AuNP-PPy/Prussian blue was purportedly utilized to detect H_2O_2. Autopolymerization of pyrrole into PPy and simultaneous reduction of AuCl to elemental Au were used to make the composite; the elemental Au was also used to produce Prussian blue, which acted as a catalyst. As a result of the PPy, this H_2O_2 sensor probe was able to detect concentrations as low as 8.3×10^{10} M [136], and it responded quickly and was stable. As a means of sensitive and selective detection of H_2O_2, the electrochemical copolymerization of PPy on mesoporous Pt with a boron-doped diamond electrode was devised. Sensitive, selective, and precise quantification of H_2O_2 was demonstrated by the synergistic actions of MPrPt and PPy copolymer. Mesoporous PtNPs may be to thank for their great sensitivity [137]. To detect glucose, another study used PPy-coated AuNPs that were deposited electrochemically [138]. Electrode conductivity was improved and nanocomposite films were generated by electrolyzing AuNPs onto a PPy layer,

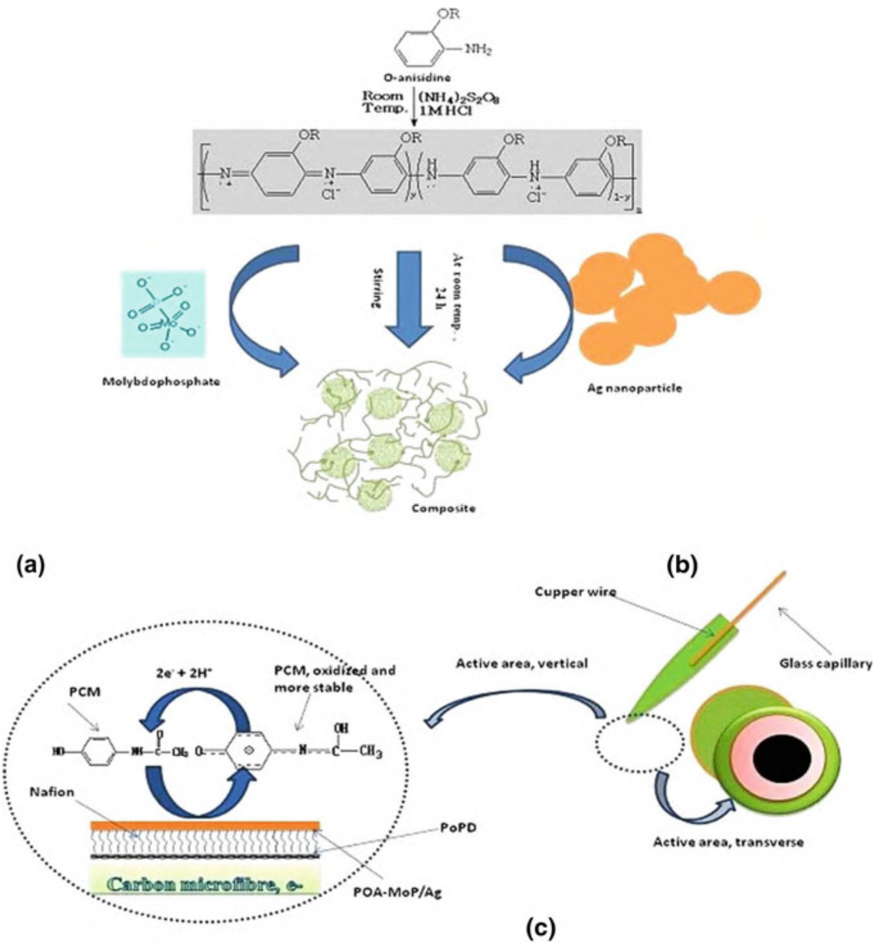
O-anisidine
Room Temp.
(NH4)2S2O8
1M HCl
Stirring
At room temp., 24 h
Molybdophosphate
Ag nanoparticle
Composite
(a)
(b)
Cupper wire
Glass capillary
Active area, vertical
Active area, transverse
PCM
2e⁻ + 2H⁺
PCM, oxidized and more stable
Nafion
PoPD
POA-MoP/Ag
Carbon microfibre, e-
(c)

Fig. 12 Graphical impersonation for the synthesis of PoA-MoP/Ag nanocomposite and modification of carbon fiber microelectrode displaying active sensing area vertical and transverse (**a**)–(**c**) [133]

allowing for their use in a DNA sensor. The capture DNA strand was immobilized on the AuNPs for DNA detection, and the hybridization experiment involved exposing the modified electrode to the target and subsequently the HRP-modified probe strand. The electron transfer to the HRP-labeled probe strand is mediated by the reduction of hydroquinone, and it was during this reaction that a measurable current was produced from the reduction of benzoquinone. The ability to detect DNA quantities below 1 pM was proven in this investigation [139]. Electroanalytical research employing a wide range of analytical goals and methods is increasingly turning to the production of electrochemical biosensors based on graphene-PPy composites. It was recently revealed that adenine and guanine may be detected at the same time using a composite of graphene and overoxidized poly (phenylene pyrrolidone). Together, PPy and GO were electrodeposited using a potential cycling approach, and then GO was electrochemically reduced to make the sensor probe. An oxidized surface of a PPy-graphene (PPyox-gra) composite layer was created by oxidizing the obtained PPy-graphene at +1.8 V. The oxidized form of PPy allows cationic species through while rejecting anionic and neutral species, allowing the sensor probe to function with more selectivity and reducing the likelihood of interference. The PPy ox-grasensor probe could detect concentrations as low as 0.02 and 0.01 M for adenine and guanine, respectively [140]. Utilizing a PPy-GO composite with poly(ionic liquids), Mao et al. created a sensor probe (PILs). Nanosheets of PILs/PPy/GO embedded with sensor probes showed stable and sensitive dopamine detection in the presence of ascorbic acid. The separation of the DA and AA oxidation peaks was greatly aided by the presence of PILs on the sensor probe [141]. By combining AuNPs with graphene and PPy, Tiwari et al. created a genosensor. First, an indium tin oxide (ITO) electrode was coated with GO-AuNP using a one-pot solution preparation technique. Electropolymerization of PPy was then performed on the GO-AuNP layer. The scientists found that the rate at which scans were taken had a significant impact on the morphological alterations in PPy. Using methylene blue (MB) as a redox indicator, this sensor probe was able to detect electrochemical signals with a response time of 60 s and high sensitivity of 1×10^{15} M [142]. Enzyme immobilization on polymer films plays a critical role in the research and development of enzymatic biosensors. Adsorption, trapping, covalent binding, etc., are only a few of the methods that may be used to immobilize enzymes. The covalent attachment between the polymer film and the enzymes makes covalent bonding the most promising of these approaches [143]. The direct electron-transfer process of cytochrome and other proteins, as well as glucose and aptamer and DNA sensors, were all developed using this strategy with great success. Preparation of an enzymatic glucose sensor utilizing PPy nanowires GO_x that is covalently linked to PPyCOOH/PPy composite nanowires. Additionally, to its high sensitivity and broad linear dynamic range, the sensor probe showed not only good sensitivity and low false-positive rates [144]. Here's Yet Another Glucose Monitor designed using a biocompatible chitosan-GO_x complex immobilized on a PPy/Nafion/MWCNT nanocomposite electrode. Within a nanohybrid PPy/Nafion/MWCNT sheet, chitosan-glucose oxidase was encapsulated. The nanohybrid films' large surface area improves GO_x loading on the electrode surface, resulting in great sensitivity and the capacity to detect 5 M glucose [145] in the sensor probe. By using Nafion in the composite, the scientists were able to boost the electrode's stability and improve the MWCNTs' dispersion throughout the material. For xanthine analysis, a new sensor probe based on a ZnO–PPy composite was created. After being immobilized on a ZnO–PPy composite electrode surface, xanthine oxidase demonstrated strong electrocatalytic activity for the oxidation of xanthine [146]. This paper describes the synthesis of a [2,5-[di(2-thienyl)-1H-pyrrole-1-(p-benzoic acid) the DPB monomer to application to the construction of a detection system based on aptamers the kanamycin. Self-assembly of DPB monomers with AuNPs before the electrode surface was prepared for electropolymerization. A molecule that is both apt and aptameric formed a covalent link with the electrode, rendering it immobile connecting the aptamer's –NH_2 groups to the poly—COOH DPB's groups. When kanamycin was bound to the aptamer-immobilized probe, a pair of redox peaks appeared in the sensor response, at around 0.26 and 0.08 V (vs. Ag/AgCl). Selectivity for kanamycin was high, sensor stability was high for up to two months, and the detection limit was 9.4 0.4 nM [147]. Direct electrodeposition of a PPy-gra (PG) nanocomposite was utilized to create a brain microelectrode array, which was then used to monitor dopamine release from pheochromocytoma cells by Wang et al. In the presence of ascorbic acid, the deposited PG composites on the brain microelectrode array showed high dopamine selectivity. Due to its strong negative charge, the electrocatalytic graphene structure, the authors argue, successfully attracts DA cations to the surface of PG nanocomposites while repelling AA anions [148]. According to the amperometric findings, ascorbic acid does not significantly affect dopamine detection. When the PC12 was stimulated with K^+ ions, dopamine was secreted, and the sensor probe was utilized to detect it. This DNA sensor was created by Mndek et al. [149]. who used an MWCNT-PPy composite that had been functionalized with a redox PAMAM dendrimer. DNA has been electrochemically detected using the nanomaterial, proving its efficacy as a molecular transducer. Figure 13 shows that the MWCNT-PPy nanocomposite was created by electropolymerized pyrrole onto MWCNTs and that PAMAM was covalently attached to the nanocomposite through electrooxidation. As a result, ferrocenyl groups were incorporated, and the DNA hybridization was detected using the electrochemical signal from the ferrocene. Detection of the rpoB gene of M. tuberculosis DNA in real-world PCR samples was possible using the sensor probe. A second aptasensor, based on a PPy-PAMAM dendrimer composite, was designed to detect ochratoxin directly (OTA). The Below the 5 ng L–1 OTA detection limit, the aptasensor has a detection limit of 2 ng L–1. Limits are set by European Union laws on the amount of OTA that can be present in food [150]. An aptasensor for the detection of biomarkers of prostate cancer was also developed using a PPy composite. A notable feature of these sensors is their ability to resist fouling. By using a PPy-PEG composite electrode, Jolly et al. created a sensor probe with improved antifouling properties. The sensor probe was made by covalently connecting a molecule of N, N-bis(carboxymethyl)-l-lysine hydrate (ANTA), which is linked to a Cu^{2+} ion complex, to PPy-PEG on a gold electrode surface. It was the PPy and the redox-active copper complex that gave the PPy-PEG-ANTA/Cu^{2+} sensor probe its improved electrochemical characteristics. Using the PPy-PEG adduct as a platform, the Cu^{2+} redox complex immobilized aptamers that had been modified with polyhistidine. Square wave voltammetry was used to observe the shift in copper redox signal upon detection of -methyl acyl-CoA racemase (AMACR; P504S) (SWV). The hybrid materials used to make the sensor probe gave it superior antifouling abilities, and it was able to detect AMACR at Femto molar concentrations (0.15 FM) [151]. This paper describes the development of a biotin-doped PPy dual responsive immune sensor for ultrasensitive detection of numerous tumor markers using a combination of colorimetric identification and an electrochemical response. In comparison to sensor probes with a smooth surface, the PPy immune sensor's nano-rough surface and numerous HRP-labeled and antibody-attached NPs are huge

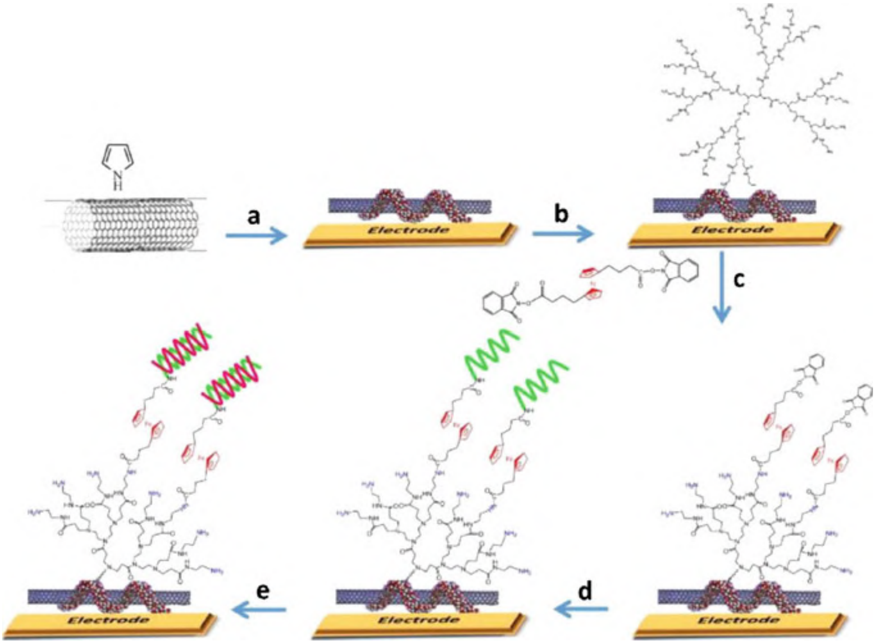

Fig. 13 Schematic representation of DNA biosensor preparation using MWCNTs, PPy, PAMAM G4 dendrimers, and ferrocene. Adapted with permission from Ref. [146]. Copyright 2015 American Chemical Society

benefits. The analytical and clinical performance of the sensor probe were both very strong [152].

3.5 Sensor Applications of Other Conducting Polymers and Their Related Nanocomposite Materials

Despite the widespread use of traditional polymers and their nanocomposites, various other types of electrochemical sensors, including poly(diaminonaphthalene), polypyrrole, polythiophene, polyindole, and polyazulene, have been developed and implemented. In 2009, poly(1,5-polydiaminonaphthalene) and Cibacron blue were utilized in the creation of a composite film that was intended for use in the process of dopamine detection [153]. Shim et al. [154] developed a composite film for acetaminophen and dopamine detection by dispersing blue 4 dye in poly (1,5-DAN). On the surface of an electrode, Mir et al. developed a composite layer in 2015 that consisted of G O mixed with poly (1, 5-polydiaminonaphthalene). At 0.005 M, dopamine was found on this electrode surface, and the increase in response was quite significant [155]. The electrochemical analysis is increasingly supporting the modification of biosensors based on graphene and PPy composites as a method of accomplishing specified analytical purposes. This modification may be accomplished through the use of PPy composites. Recently, researchers have been looking at composites made up of graphene and overoxidized polypyrrole (PPy) to find guanine. Mao et al. [156] alinvention's of an electrochemical sensor probe included the use of poly(ionic liquids), often known as PILs, together with polypyrrole (PPy) cross composite. The regular and specific detection of dopamine was accomplished by using PILs/PPy/GO nanocomposites in electrochemical sensor probes. Tiwari et al. [157] developed an improved biosensor by utilizing graphene materials, AuNP, and PPy in conjunction with one another. This sensor exhibited an extremely high level of sensitivity, measuring one part in 109 M. Shim et al. [158] were responsible for some of the initial investigations done on the potential for terthiophene polymers to enhance sensors. The goal was to create electrochemical sensors and electrocatalytic composite materials that were more effective. To detect DNA hybridization, Shim et al. [159] developed an electrochemical sensor that was based on 5,2:5,2-terthiophene-3-carboxylic acid (TTCA) monomers and was placed on a glassy carbon electrode. Poly(indole-6-carboxylic acid) was another method that was utilized to measure DNA hybridization [160]. Recently, an electrochemical sensor for the detection of H_2O_2 was produced by altering a thiophene acetic acid and azulene copolymer that was coated on the surface of an electrode. In a separate line of investigation, scientists produced a composite layer by combining n-type polybenzimidazobenophenenthroline-poly(ethylene oxide) (BBL-PEO) with p-type polyazulene. This layer was exploited in the study on sensors [161] (Table 1).

In addition to polyindole, polyazulene, and its composites were investigated for a variety of applications alongside one another. At an earlier stage, impedance and in situ Spectro electrochemical methods at platinum electrodes were used to study the electrochemical development and spectroscopic characteristics of polyazulene [450]. Recently, a sensor for the detection of H_2O_2 was fabricated by forming azulene and thiophene acetic acid copolymer on the surface of the electrode [174]. In another study, the donor–acceptor layer was produced by combining n-type poly benzimidazobenophenenthroline-poly(ethylene oxide) (BBLPEO) and p-type polyazulene using a composite material. The electrochemical and spectrochemical research [175] utilized this composite layer as their subject matter. To develop a hydrophobic solid-state electrode for the selective detection of potassium ions, the polyazulene layer was electropolymerized. This created the electrode. Polarization of polyazulene solid contact was implemented as a convenient approach to address the issues of the irreproducible standard potential of solid-state potassium ion-selective electrodes [176]. This was done to address the issue of potassium ion-selective electrodes not being able to reproduce their standard potential. On a platinum substrate, polyazulene and poly(3-[(E)-2-azulene-1yl)vinyl]thiophene were synthesized using electrochemical techniques in a variety of combinations [177]. Using square wave voltammetry, monolayer and bilayer-modified electrodes containing these materials were examined to determine their electrochemical performance as sensing probe materials for the detection of dopamine and 4-nitrophenol. On a carbon nanohorn with a single wall, some of the other polymers, such as poly-ophenylenediamine,

Table 1 Contains a summary of the values for LoD, linear range, and CP detection

Material	Electrochemical sensors	Detection	The linear range	The limit of detection	Refs.
Polyaniline (PANI)	PANI and carbon nanotube (CNT)	Acid penetration	–	–	[162]
	Polyaniline/ZnO	Ammonia gas	–	–	[163]
	PANI/graphene nanocomposite	Hydrazine	0.01 µM–0.01 M	15.38 mM	[164]
	Polyaniline-(acrylonitrile-butadiene-stylenc) composite	Aqueous ammonia	10^{-4}–10^{-5} N	–	[165]
	PAn–PAN/PPO	Phenols	–	–	[166]
	AuNPs-PANABA-(MWCNTs) nanocomposite	2,4-Dichlorophenoxy acetic acid	–	0.0003 ppm	[167]
	AuNPs-PANI	Glucose	0.01–8 mM	0.0007 mM	[168]
	PtNP/PANI hydrogel	Uric acid	0.07–1 mM	0.001 mM	[169]
	AuNPs/PANI/PDA hybrid composite	Ascorbic acid (AA)	1.0×10^{-6}–1.9×10^{-3} M	0.000399 mM	[170]
	Molecularly imprinted poly (aniline-co-metanilic acid)	Progesterone	0.64–5.27 ng mL^{-1}	1.0 pg mL^{-1}	[171]
Poly(o-aniside) (PoAN) Poly(o-anisidine)-silver. nanocomposites		NADH	0.03–900 µM	0.006 µM	[125]
Poly(o-anisidine)-silver nanocomposites		Dopamine	5–270 µM	0.052 µM	[125]
POAS–Ag/MWCNT		3-Methoxyphenol	0.4 nM–40.0 mM	0.36 ± 0.05 nM	[126]
POA-AgNP nanocomposite		Dopamine	10.0–140.0 µM	0.2 µM	[172]
DPOMA/GO		Benzaldehyde	0.1 nM–0.1 mM	0.03 nM	[130]
POA–SnO_2		Humidity	–	–	[173]
F3GA/PDAN		Dopamine	5–100 µM	0.1 ± 0.01 µM	[153]
Poly(1,5-DAN) Blue 4 dye in poly(1,5-DAN)		Acetaminophen and dopamine	–	–	[154]
Poly(1,5-polydiaminonaphthalene)	Poly(1,5-polydiaminonaphthalene)/GO	Dopamine	–	0.005 µM	[155]

(continued)

Table 1 (continued)

Material	Electrochemical sensors	Detection	The linear range	The limit of detection	Refs.
Poly(1,5-polydiaminonaphthalene)	Poly-DAN/GO/AuNP nanohybrid	Dopamine	10 nM–1 µM	5.0 nM (± 0.01)	[155]
Polypyrrole	PPyox/GR	Adenine	0.06–100 µM	0.02 µM	[156]
	PPyox/GR	Guanine	0.04–100 µM	0.01 µM	[156]
	PPy/G	Guanine	–	–	[156]
	PILs/PPy/GO	Dopamine	4–18 µM	73.3 nM	[157]
5,2:5,2-Terthiophene-3-carboxylic	TTCA/GC	DNA	–	–	[159]

were conjugated. The polymer underwent molecular imprinting so that it could uniquely recognize kanamycin molecules, and the electrode was employed for the electrochemical detection of the compound [178]. Similarly, a functional dicarbazole conductive polymer was electrochemically polymerized and described for a variety of eco-friendly applications in electrochemistry [179]

4 Conclusion

Conducting polymers, such as polyaniline, polyorthoanisidine, polyorthotoluidine, and polypyrrole, have recently emerged as crucial new advanced materials for the creation of novel devices and the structure-dependent assessment of distinct characteristics required in developing eco-friendly applications. Analytical devices are known as chemical sensors and convert chemical reactions, into electrical signs. We have provided an overview of the processes involved in the synthesis and functionalization of conducting polymer conjugates, as well as current developments in their application in the production of sensors. According to the research that has been published so far, among the conducting polymers, conjugates of polyaniline, polypyrrole, and polythiophenes display features that indicate they might be useful in the development of future eco-friendly electrochemical applications. In addition, in comparison to the other types of polymer composites, polythiophene composites have shown a level of stability and electrical conductivity that is far higher than the others. In addition to the conventional single polymer systems, many researchers are currently combining two or more polymers with a catalytic eco-friendly nanomaterial to form a highly sensitive conjugated material. This material generates very sensitive signals when it is utilized for any kind of electrochemical sensing application. These nanomaterials, which include several functional groups, have the potential to serve as the most appropriate substrate for the attachment of various recognition components. These findings by a friendly way for a new class of materials, one in which the distinctive qualities of several different materials may be merged to create a single material that possesses several capabilities.

References

1. Rincon ME, Gutierrez-Granados S (2018) Conducting polymers in the fields of energy, environmental remediation, and chemical-chiral sensors. Am Chem Soc
2. Wu W (2019) Stretchable electronics: functional materials, fabrication strategies and applications. Sci Technol Adv Mater 187–224
3. Park SJ, Park CS, Yoon H, Chemo-electrical gas sensors based on conducting polymer hybrids. Polymers (Basel)
4. Jiaxing Huang RBK, Virji S, Weiller BH, Nanostructured polyaniline sensors. Chem A Eur J 10(6):1314–1319. https://doi.org/10.1002/chem.200305211

5. Yuxi Zhang H, Kim JJ, Electrospun polyaniline fibers as highly sensitive room temperature chemiresistive sensors for ammonia and nitrogen dioxide gases. Adv Funct Mater 24(25). https://doi.org/10.1002/adfm.201400185
6. Kwon OS, Park E, Kweon OY, Park SJ, Jang J, Novel flexible chemical gas sensor based on poly(3,4-ethylenedioxythiophene) nanotube membrane. Elsevier 82(4):1338–1343. https://doi.org/10.1016/j.talanta.2010.06.058
7. Logo WO, Guiqin Yang YYO, Zhang M, Dong D, Pan X, Zhou Y, ORCID logo d Su-Ting Han, ORCID logo Zongxiang Xu, TiO2 based sensor with butterfly wing configurations for fast acetone detection at room temperature. J Mater Chem C 36. https://doi.org/10.1039/C9TC03110C
8. Liu Y, Liu J (2013) Core-shell noble-metal@metalorganic-framework nanoparticles with highly selective sensing property. Angew Chem Int Ed Engl 52:3741–3837
9. Zhou Y, Azumi R (2016) Carbon nanotube based transparent conductive films: progress, challenges, and perspectives. Sci Technol Adv Mater 17:493–516
10. Giampiccolo A, Tobaldi DM, Leonardi SG (2018) Sol gel graphene/TiO_2 nanoparticles for the photocatalytic-assisted sensing and abatement of NO2. Appl Catal B-Environ 243:183–194
11. R, AJEAG, MacDiarmid JC (1987) Chaing. Synth Met 18:285
12. MacDiarmid G, Epstien AJ (1989) Chem Soc 88:317
13. Natta G, Mazzanti G, Corradini P (1958) Naz Lincei Cl Sci Fis Mat Nat Rend 2:25
14. Luttinger B, 27:1591
15. AJ, Champetier G, Comptes Rendus 189:1089
16. Shirakawa MH, Ito T, Ikeda S, Chem 179:1565
17. Akaishi KM, Ishikawa K, Shirakawa H, Ikeda S, Phys Ed 18:745
18. Fincher R, Ozaki M, Tanaka M, Peebles D, Lauchlan L, Heeger AJ, Phys Rev B 20:1589
19. Karasz E, Chien JCW, Galkiewicz R, Wnek GE, Heeger AJ, Nature 282:286
20. Suezaki AM, Shirikawa H, Kyotani H, Syn Met D1:28
21. Tsukamoto AT, Kawasaki K (1990) Apl Phys 29
22. Nigrey A, MacDiarmid G, Heeger AJ, Proceedings of the International Conference on Low-Dimensional Conductors, Boulder, Colorado. Mol Cryst Liq Cryst 77
23. Weinberger R, Gau SC, Kiss Z (1981) Appl Phys Lett 38:555; Weinberger BR, Akhtar M, Synth Met 4:187
24. Chen N, Heeger AJ, Kiss Z, MacDiarmid AG, Gau SC, Appl Phys Lett 36:96
25. Chance RR, Shacklette LW, Miller GG, Ivory DM (1980) J Chem Soc Chem Commun 348:348
26. Tabor J, Magre EP, Boon J (1971) Eur Polym 7:1127
27. Uemura A, Isoda S, Tsuji M, Ohara M, Kawaguchi A, Katayama K (1986) 64:66
28. Jurga J (1993) Polymer (Guildf) 34:4203
29. Napolitano R, Pirozzi B (1999) Macromolecules 32:7682
30. Shacklette W, Elsenbaumer RL, Chance RR, Eckhardt H, Frommer JE (1981) J Chem Phys 75:1919
31. Adeloju, Show SJ, Wallace GG (1993) 281:611–620, 621–627
32. Mirmohseni A, Price WE, Wallace GG, Zhao H (1993) Intell Mater Syst Struct 4:43
33. Gardini A (1973) Hetrocyclic Chem 15:67
34. Street GB, Clarke TC, Krounbi M, Kanazawa K, Lee V, Pfluger P, Scott JC, Weiser G (1982) Mol Cryst Liq Cryst 83:253
35. Kanazawa K, Diaz AF, Gill WD, Grant PM, Street GB, Gardini GP (1980) No Titl. Synth Met 1:329
36. Diaz, Kanazawa KK, Gardini GP (1979) Chem Soc Chem Commun 635
37. Simon A, Ricco AJ, Wrighton MS (1982) Am Chem Soc 104:2031
38. Mohhammadi A, Lundstrom I (1987) Synth Met 21:169
39. Warren, Anderson DP (1987) Electrochem Soc 1 134(1):101
40. Armes S (1987) Met 20:365
41. Armes, Vincent B (1987) Chem Soc Chem Commun 287
42. Eisazadeh H (1992) Mater Forum 16:341
43. Bocchi, Gardini GP (1986) No Ti. Chem Soc Chem commun 148

44. Bradner, Shapiro JS (1988) Synth Met 26:69
45. Munstedt H, Naarmann H (1985) Mol Cryst Liq Cryst 118:129
46. Shimidzu T, Ohtani A, Iyoda T, Honda K (1987) J Electroanal Chem 224; Chem 224:123
47. Neoh G, Kang ET, Khor SH, Tan KL (1990) Polym Degrad Stab 27:107
48. Fritsche J (1840) Chem 20:453; 20:453
49. Letheby JH, Chem Sot 15:161
50. Rosenstiehl A (1875) ibid 81:1257
51. Idem (1990) ibid. 42:2931
52. Huang S, Humphrey BD, MacDiarmid AG (1986) Chem Soc Faraday Trans 1,1 82, 2385 (1986); 1(182):2385
53. Zuo F, Angelopoulos M, MacDirmid AG (1987) Phys Rev B 36:3475
54. Barth M, Lapkowski M (1999) Electrochim. Acta 44(12):2117
55. Syed A (1988) Bull Electrochem 4:737
56. Li H (1989) Dong. Synth Met 29:E329
57. Huang S, MacDiarmid AG, Epstein AJ (1987) Chem Sot Chem Commun 1784
58. I&m (1986) ibid 200:127
59. Travers P, Chroboczek J, Devreux F, Genoud F, Nechtschein M, Syed AA, Genies EM, Tsintavis C (1985) Mol Cryst Liq Cryst 121:195
60. Syed A, Dinesan MK, unpublished results
61. Choi CH, Kertesz M (1997) Macromolecules 30:620
62. Wnek GE, Chine JCS, Karasz FE, Lillya CP (1979) Polymer 20:1441
63. Skotheim TA, Hand book of conducting polymers, vol 1. Marcell Dekker, New York, p. 254
64. Baughman RH, Chance RR (1978) Ann N Y Acad Sci 313:705
65. Bloor D (1985) Chance polydiacetylenes: synthesis, structure, and electronic properties
66. Sasaki DY, Carpick RW, Burns AR (2000) J Colloid Interface Sci 229:490
67. Mowery MD, Evans CE (1997) Tetrahedron Lett 38:11
68. Hoofman RJOM, Siebbeles LDA, de Haas MP, Hummel A, Bloor D (1998) J Chem Phys 109:1885
69. Wohrle D (1974) Tetrahedron Lett 1969 (1971), Makrmol Chem 175:1751
70. Rice MJ, Mele EJ (1982) Phys Rev Lett 49:1455
71. Carazzolo G, Valle G (1966) Makromol Chem 90:66
72. Han CC, Hong SP, Yang KF, Bai MY, Lu CH, Huang CS (2001) Macromolecules 34:587
73. Waltman RJ, Bargon J, Diaz AF (1983) J Phys Chem 87:1459
74. Diaz AF, Castillo J, Kanazawa KK, Logan JA, Salmon M, Fajardo O (1982) J Elecrroanal Chem Interfacial Electrochem 133:233
75. Naka K, Umeyama T, Yoshiki C (2003) Macromolecules 33:7467
76. Chen S, Wen TC, Gopalan A (2003) Synth Met 132:133
77. Bozoviv I (1985) Phys Rev B 32:8136
78. Michael F, Anman KO, Scherf U (1999) Macromolecules 32:3159
79. Scherf U, Milier K (1992) Polymer 33:2443
80. Wegner G (1981) Polymers with metal-like conductivity—a review of their synthesis, structure and properties. Angew Chem Int Ed 20:361–381
81. Shim YB, Park SM (1989) Electrochemistry of conductive polymers. VII. Autocatalytic rate constant for polyaniline growth. Synth Metals 29:E169–E174
82. Diaz AF, Castillo JI, Logan JA, Lee WY (1981) Electrochemistry of conducting polypyrrole films. J Electroanal Chem 129:115
83. Yang H, Bard AJ (1992) The application of fast scan cyclic voltammetry. Mechanistic study of the initial stage of electropolymerization of aniline in aqueous solutions. J Electroanal Chem 339:423–449
84. Stilwell DE, Park SM (1988) Electrochemistry of conductive polymers. IV Electrochemical studies on polyaniline degradation—product identification and coulometric studies. J Electrochem Soc 135:2497–2502
85. Stilwell DE, Park SM (1989) Electrochemistry of conductive polymers. V. In situ spectroelectrochemical studies of polyaniline films. J Electrochem Soc 136(2):427–433

86. Park DS, Shim YB, Park SM (1993) Degradation kinetics of polypyrrole films. J Electrochem Soc 140:2749–2752
87. Lee HL, Sofer Z, Mazánek V, Luxa J, Chua CK, Pumera M (2016) Graphitic carbon nitride: effects of various precursors on the structural, morphological and electrochemical sensing properties. Appl Mater Today. https://doi.org/10.1016/j.apmt.20
88. Ghislandi M, Tkalya E, Alekseev A, Koning C, de With G (2015) Electrical conductive behavior of polymer composites prepared with aqueous graphene dispersions. Appl Mater Today 1:88–94
89. Bockris OM, Khan SUM (1993) Surface electrochemistry. Plenum Press, New York
90. Zhu Y, Son JI, Shim YB (2010) Amplification strategy based on gold nanoparticle-decorated carbon nanotubes for neomycin immunosensors. Biosens Bioelectron 26:1002–1008
91. Li C, Jiang B, Chen H, Imura M, Sang L, Malgras V, Bando Y, Ahamad T, Alshehri SM, Tominaka S, Yamauchi Y (2016) Superior electrocatalytic activity of mesoporous Au film templated from diblock copolymer micelles. Nano Res 9:1752–1762
92. Balazs AC, Emrick T, Russell TP (2006) Nanoparticle polymer composites: where two small worlds meet. Science 314:1107–1110
93. Wang J (2007) Electrochemical glucose biosensors. Chem Rev 108:814–825
94. Wang J (2005) Carbon-nanotube based electrochemical biosensors: a review. Electroanalysis 17:7–14
95. Zhao Q, Gan ZH, Zhuang QK (2002) Electrochemical sensors based on carbon nanotubes. Electroanalysis 14:1609–1613
96. Li D, del Rio Castillo AE, Jussila H, Ye G, Ren Z, Bai J, Chen X, Lipsanen H, Sun Z, Bonaccorso F (2016) Black phosphorus polycarbonate polymer composite for pulsed fibre lasers. Appl Mater Today 4:17–23
97. Skotheim TA, Elsenbaumer RL, Reynolds JR (1998) Handbook of conducting polymers. Marcel Dekker, New York
98. Qiao Y, Li CM, Bao SJ, Bao QL (2007) Carbon nanotube/polyaniline composite as anode material for microbial fuel cells. J Power Sources 170:79–84
99. Norde W (1986) Adsorption of proteins from solution at thsolid-liquidid interface. Adv Colloid Interface Sci 25:267–340
100. Evtugyn G (2014) Biochemical components used in biosensor assemblies, biosensors: essentials, vol 84. Springer, Berlin, pp 21–97 (Chapter 2)
101. Bartlett PN, Cooper JM (1993) A review of the immobilization of enzymes in electropolymerized films. J Electroanal Chem 362:1–12
102. Valdés-Ramírez G, Windmiller JR, Claussen JC Martinez AG Kuralay F, Zhou M, Zhou N, Polsky R, Miller PR, Narayan R, Wang J, Multiplexed and switchable release of distinct fluids from microneedle platforms via conducting polymer nanoactuat
103. Cantwell WJ, Morton J (1991) Composites 22:347
104. Wightman RM, Wipf DO (1989). In: Bard AJ (ed) Electroanalytical chemistry. Marcel Dekker, New York, USA, p 267
105. Wang J (2006) Analytical electrochemistry. Wiley, VCH, Hoboken, NJ, USA
106. Zhang XJ, Ju HX, Wang J (2008) Electrochemical sensors, biosensors and their biomedical applications. Elsevier, New York
107. H. Yao, S.H. Jenkins, A.J. Pesce, H.B. Halsall, W.R. Heineman, Clin. Chem. (Washington, DC) 39 (1993) 1432.
108. Kissinger PT, Heineman WR (1996) Laboratory techniques in electroanalytical chemistry. Marcel Dekker Inc., New York, NY, USA
109. Wang J, Musameh M, Lin Y (2003) Solubilization of carbon nanotubes by nafion toward the preparation of amperometric biosensors. J Am Chem Soc 125:2408–2409
110. Bobacka J, Ivaska A, Lewenstam A (2008) Potentiometric ion sensors. Chem Rev 108:329–351
111. Wijayawardhana CA, Halsall HB, Heineman WR. In: Brajter-Toth A, Chambers JQ (eds) Electroanalytical methods of biological materials. Marcel Dekker, New York, pp 329–365

112. Yao Q, Chen L, Zhang W, Liufu S, Chen X (2010) Enhanced thermoelectric performance of single-walled carbon nanotubes/polyaniline hybrid nanocomposites. ACS Nano 4:2445–2451
113. Shim YB, Stillwell DE, Park SM (1991) Electrochemistry of conductive polymers X: the polyaniline-based potentiometric sensor for dissolved oxygen. Electroanalysis 3:31–36
114. Yu Z, Li H, Zhang X, Liu N, Tan W, Zhang X, Zhang L (2016) Facile synthesis of NiCo2O4@Polyaniline core–shell nanocomposite for sensitive determination of glucose. Biosens Bioelectron 75:161–165
115. Lakshmi D, Bossi A, Whitcombe MJ, Chianella I, Fowler SA, Subramanyam S, Piletska EV, Piletsky SA, Electrochemical sensor for catechol and dopamine based on a catalytic molecularly imprinted polymer-conducting polymer hybrid recognition element
116. Zhai D, Liu B, Shi Y, Pan L, Wang Y, Li W, Zhang R, Yu G (2013) Highly sensitive glucose sensor based on Pt nanoparticle/polyaniline hydrogel heterostructures. ACS Nano 7(4):3540–3546
117. Li L, Wang Y, Pan L, Shi Y, Cheng W, Shi Y, Yu G (2015) A nanostructured conductive hydrogels-based biosensor platform for human metabolite detection. Nano Lett 15:1146–1151
118. Fusco G, Gallo F, Tortolini C, Bollella P, Ietto F, Mico AD, D'Annibale A, Antiochia R, Favero G, Mazzei F, AuNPs-functionalized PANABA-MWCNTs nanocomposite-based impedimetric immunosensor for 2,4-dichlorophenoxy acetic acid detection. Biosens
119. Yang T, Meng L, Chen H, Luo S, Li W, Jiao K (2016) Synthesis of thin-layered molybdenum disulfide based polyaniline nanointerfaces for enhanced direct electrochemical DNA detection. ACS Appl Mater Interfaces 3:1500700
120. Hui N, Sun X, Niu S, Luo X (2017) PEGylated polyaniline nanofibers: antifouling and conducting biomaterial for electrochemical DNA sensing. ACS Appl Mater Interfaces 9:2914–2923
121. Gao Z, Rafea S, Lim LH (2007) Detection of nucleic acids using enzyme-catalyzed template-guided deposition of polyaniline. Adv Mater 19:602–606
122. Yang T, Meng L, Zhao J, Wang X, Jiao K (2014) Graphene-based polyaniline arrays for deoxyribonucleic acid electrochemical sensor: effect of nanostructure on sensitivity. ACS Appl Mater Interfaces 6:19050–19056
123. Angaleeswari B, Dura RM, Jeevithaaa AT, Vaishnavia V, Eeveraa T, Berchmansb S, Yegnaraman V (2008) Sens Actuators B 129:558
124. Sangamithirai D, Narayanan V, Muthuraaman B, Stephen A (2015) Mater Sci Eng, C 55:579
125. Sangamithirai D, Munusamy S, Narayanan V, Stephen A (2017) Mater Sci Eng, C 80:425
126. Rahman MM, Khan A, Asiri AM (2015) RSC Adv 5:71370
127. Shimpi NG, Hansora DP, Yadav R, Mishra S (2015) RSC Adv 5:99253
128. Sangamithirai D, Munusamy S, Narayanan V, Stephen A (2016) Surf Interfaces 4:27
129. Khan A, Aslam A, Khan P, Asiri AM (2014) Composites: Part B 58:451
130. Aslam A, Khan P, Khan A, Asiri AM, Rahman MM (2015) J Sol-Gel Sci Technol 77
131. Valentini L, Bavastrellob V, Sturab E, Armentanoa I, Nicolinib C, MKennya J (2004) Chem Phys Lett 383:617
132. Patil D, Patil P, Seo Y, Kyu Y (2010) Sens Actuators, B Chem 148:41
133. Khan AA, Shaheen S, Habiba U (2012) J Adv Res 3:269
134. Letheby H (1862) On the production of a blue substance by the electrolysis of sulphate of aniline. J Chem Soc 15:161–163
135. Wang J, Jiang M, Mukherjee B (1999) Flow detection of nucleic acids at a conducting polymer-modified electrode. Anal Chem 71:4095–4099
136. Lu X, Li Y, Zhang X, Du J, Zhou X, Xue Z, Liu X (2012) A simple and an efficient strategy to synthesize multi-component nanocomposites for biosensor applications. Anal Chim Acta 711:40–45
137. Cui HF, Bai YF, Wu WW, He X, Luong JHT (2016) Modification with mesoporous platinum and poly(pyrrole-3-carboxylic acid)-based copolymer on boron-doped diamond for nonenzymatic sensing of hydrogen peroxide. J Electroanal Chem 766:52–59
138. German N, Ramanavicius A, Ramanaviviene A (2017) Amperometric glucose biosensor based on electrochemically deposited gold nanoparticles covered by polypyrrole. Electroanalysis 29:1267–1277

139. Spain E, Keyes TE, Forster RJ (2013) Polypyrrole–gold nanoparticle composites for highly sensitive, DNA detection. Electrochim Acta 109:102–109
140. Gao YS, Xu JK, Lu LM, Wu LP, Zhang KX, Nie T, Zhu XF, Wu Y, Overoxidized polypyrrole/graphene nanocomposite with good electrochemical performance as novel electrode material for the detection of adenine and guanine. Biosens Bioelectron 62
141. Mao H, Liang J, Zhang H, Pei Q, Liu D, Wu S, Zhang Y, Song XM (2015) Poly(ionic liquids) functionalized polypyrrole/graphene oxide nanosheets for electrochemical sensor to detect dopamine in the presence of ascorbic acid. Biosens Bioelectron 70
142. Tiwari I, Gupta M, Pandey CM, Mishra V (2015) Gold nanoparticle decorated graphene sheet polypyrrole based nanocomposite: its synthesis, characterization and genosensing application. Dalton Trans 44:15557–15566
143. Yon-Hin BFY, Smolander M, Crompton T, Lowe CR, Covalent electropolymerization of glucose oxidase in polypyrrole. Evaluation of methods of pyrrole attachment to glucose oxidase on the performance of electropolymerized glucose sensors. Anal Chem 65
144. Jiang H, Zhang A, Sun Y, Rua X, Ge D, Shi W (2012) Poly(1-(2-carboxyethyl)pyrrole)/polypyrrole composite nanowires for glucose biosensor. Electrochim Acta 70:278–285
145. Shrestha BK, Ahmad R, Mousa HM, Kim IG, Kim JI, Neupane MP, Park CH, Kim CS, High-performance glucose biosensor based on chitosan-glucose oxidase immobilized polypyrrole/Nafion/functionalized multi-walled carbon nanotubes bio-nanohybrid fil
146. Devi R, Thakur M, Pundir CS (2011) Construction and application of an amperometric xanthine biosensor based on zinc oxide nanoparticles–polypyrrole composite film. Biosens Bioelectron 26:3420–3426
147. Zhu Y, Chandra P, Song KM, Ban C, Shim YB (2012) Label-free detection of kanamycin based on the aptamer-functionalized conducting polymer/gold nanocomposite. Biosens Bioelectron 36:29–34
148. Wang L, Xu H, Song Y, Luo J, Wei W, Xu S, Cai X (2015) Highly sensitive detection of quantal dopamine secretion from pheochromocytoma cells using neural microelectrode array electrodeposited with polypyrrole graphene. ACS Appl Mater Interfaces 7
149. Miodek A, Mejri N, Gomgnimbou M, Sola C, Korri-Youssouf H (2015) E-DNA sensor of Mycobacterium tuberculosis based on the electrochemical assembly of nanomaterials (MWCNTs/PPy/PAMAM). Anal Chem 87:9257–9264
150. Mejri-Omrani N, Miodek A, Zribi B, Marrakchi M, Hamdi M, Marty JL, Korri-Youssouf H (2016) Direct detection of OTA by impedimetric aptasensor based on modified polypyrrole-dendrimers. Anal Chim Acta 920:37–46
151. Jolly P, Miodek A, Yang DK, Chen LC, Lloyd MD, Estrela P (2016) Electro-engineered polymeric films for the development of sensitive aptasensors for prostate cancer marker detection. ACS Sens 1:1308–1314
152. Hong W, Lee S, Cho Y (2016) Dual-responsive immunosensor that combines colorimetric recognition and electrochemical response for ultrasensitive detection of cancer biomarkers. Biosens Bioelectron 86:920–992
153. Abdelwahab AA, Lee H, Shim Y (2009) Anal Chim Acta 650:247
154. Chandra P, Son NX, Noh H, Goyal RN, Shim Y (2013) Biosens Bioelectron 39:139
155. Ahmad T, Akhtar MH, Gurudatt NG, Kim J, Soo C, Shim Y (2015) Biosens Bioelectron 68:421
156. Gao Y, Xu J, Lu L, Wu L, Zhang K, Nie T (2014) Biosens Bioelectron 62:261
157. Mao H, Liang J, Zhang H, Pei Q, Liu D, Wu S (2015) Biosens Bioelectron 70:289
158. Hussain KK, Gurudatt NG, Mir TA, Shim Y (2016) Biosens Bioelectron 83:312
159. Lee T, Shim Y (2001) Anal Chem 73:5629
160. Nie G, Zhang Y, Guo Q, Zhang S (2009) Sens Actuators B 139:592
161. Latonen RM, Osterhoim A, Kvarnstro C, Ivaska A (2012)
162. Liu C, Sergeichev I, Akhatov I, Lafdi K (2018) Compos Sci Technol 159:111
163. Mehto A, Mehto VR, Chauhan J, Singh I, Pandey R (2017) J Nanomed
164. Ameen S, Akhtar MS, Shik H (2012) Sens Actuators, B Chem 173:177
165. Koul S, Chandra R, Dhawan SK (2001) Sens Actuators 75:151

166. Xue H, Shen Z (2002) Talanta 57:289
167. Fusco G, Simone AD, Arosio P, Vendruscolo M, Veglia G, Dobsonb CM (2016) Biosens Bioelectron 6:27125
168. Zhai D, Liu B, Shi Y, Pan L, Wang Y, Li W, Zhang R, Yu G (2013) ACS Nano 7:3540
169. Li L, Wang Y, Pan L, Shi Y, Cheng W, Shi Y, Yu G (2014) Nano Lett 15:1146
170. Li F, Yang L, Zhao C, Du Z (2011) Anal Methods 3:1601
171. Leea MHW, O'Hareb D, Guoc HZ, Yangc CH, Linc HY (2016) J Mater Chem B 4:3782
172. Sangamithirai D, Narayanan V, Stephen A, Sangamithirai D, Narayanan V, Stephen A (2017) Electrochemical. MMSE J 9:1
173. Patil D, Patil P, Seo Y, Kyu Y (2010) Sens Actuators B: Chem 148(41):75; Khan AA, Shaheen S, Habiba U (2012) J Adv Res 3:269
174. Lete C, Gadgil B, Kvarnstrom C (2015) The electrochemistry of copolymer films based on azulene and 3 thiophene acetic acid. J Electroanal Chem 742:30–36
175. Latonen RM, Osterholm A, Kvarnstrom C, Ivaska A (2012) Electrochemical and spectrochemical study of polyazulene/BBL-PEO donor-acceptor composite layers. J Phys Chem C 116:23793–23802
176. He N, Gyurcsanyi RE, Lindfors T (2016) Electropolymerized hydrophobic polyazulene as solid state-contacts in potassium-selective electrodes. Analyst 141:2990–2997
177. Lupu S, Lete C, Marin M, Totir N, Balaure PC (2009) Electrochemical sensors based on platinum electrodes modified with hybrid inorganic-organic coatings for determination of 4-nitrophenol and dopamine. Electrochim Acta 54:1932–1938
178. Han S, Li B, Song Z, Pan S, Zhang Z, Yao H, Zhu S, Xu G (2017) A kanamycin sensor based on an electrosynthesized molecularly imprinted poly-o-phenylenediamine film on a single-walled carbon nanohorn modified glassy carbon electrode. Analyst 142:2
179. Diamant Y, Furmanovich E, Landau A, Lellouche JP, Zaban A (2003) Electrochemical polymerization and characterization of a functional dicarbazole conducting polymer. Electrochim Acta 48:507–512

Всё для победы! НАРОДНЫЙ ФРОНТ
https://pobeda.onf.ru/
LET'S HELP THE RUSSIA

Chapter 18
Comparison of Different Functionalized Materials for Supercapacitors: General Overview of the Environmental Awareness

K. S. Rajni, D. Pughal Selvi, and V. Vishnu Narayanan

1 Introduction

Energy storage is one of the main challenges faced in this era. We need eco-friendly, high-energy–density, long-lasting, and cost-efficient energy devices. According to recent intense research reports, the annual greenhouse gas has increased by more than 40% since 1990. A huge downfall in the potential of fossil fuels on earth raises a global energy demand, rising by ~3.6% yearly. With the increasing need to develop next-generation lightweight, flexible, and wearable electronics and optical electronic devices, Supercapacitors act as a solution for this because of their high electrical conductivity, fast charge/discharge rates, and electrochemical stability [1, 2].

Traditional capacitors have comparatively large densities of energy. However, it still has lesser energy density than electrochemical cells (EC) and fuel cells, i.e., a cell can store high energy compared to a capacitor. However, it is still unable to transport it faster, which means it has less power density. However, capacitors hoard comparatively small energy/mass or volume, even so, the electrical energy they hoard shall be suspended faster to make a load of power; hence power density is large for supercapacitors [3, 4]. Supercapacitors have a similar concept to traditional capacitors, but they fuse electrodes of higher aspect areas and slim dielectrics, lowering the space between them. Supercapacitors can gain a relative time rate of energy transfer. Also, they show many merits over EC cells [5] and other cells, like large time rate of energy transfer, small recharging time, with an extended wheel of viability and service [3].

K. S. Rajni (✉) · D. Pughal Selvi · V. Vishnu Narayanan
Amrita School of Physical Sciences, Amrita Vishwa Vidyapeetham, Ettimadai, Coimbatore, Tamilnadu, India
e-mail: ks_rajani@cb.amrita.edu

© The Author(s), under exclusive license to Springer Nature Singapore Pte Ltd. 2024

C. M. Hussain and M. B. Ahamed (eds.), *Functionalized Nanomaterials Based Supercapacitor*, Materials Horizons: From Nature to Nanomaterials,
https://doi.org/10.1007/978-981-99-3021-0_18

1.1 Need for Supercapacitor

In this quickly increasing population, contamination, fossil fuel exhaustion, and the rapid maturation of the universal financial system, it is crucial to have clean, renewable, and orderly energy sources in hands with science and technology for power transformation and repositioning. People have developed a great interest in ultracapacitors due to their advantages, like a long wheel of life and better power density filling the gap between the traditional battery cells and dielectric capacitors; also, they possess the capacity of better energy repositioning and output. Eco-friendliness makes supercapacitors convenient for chemical sciences, whereas the traditional capacitors cannot consummate the requirements of the modern-day as their practicality is bounded only to some execution. The succeeding progeny of EDLC has evolved with the help of transition metal oxide (electrode) that can furnish both favorable power and energy densities [3, 4].

Supercapacitors are grouped into electrochemical double-layer, pseudo-capacitor, and hybrid capacitors. Every class has a unique method to hoard charges like electrostatic, faradaic, and a merge of two of them. The faradaic method uses a redox reaction, including charge transmission connecting electrodes and electrolytes. The electrostatic method doesn't utilize a chemical reaction, but charges are ordered on aspect area by physical methods that do not indulge the forming or splitting of bonds between chemicals [6].

The nature of the electrode materials used for the different types of supercapacitors also varies according to their working principles. These functionalized materials include transition metal oxides, nitrides, sulfides, conducting polymers, carbon, and allotropes. Each of these materials performs well, but each has environmental safety concerns. In this era of sustainable development, the environmental aspects of the electrode material are also important. Hence it is important to know the environmental aspects of various functional materials so that further development in supercapacitors can also be sustainable. This book chapter attempts to improve environmental awareness about various electrode materials utilized in all three types of supercapacitors.

2 Types of Supercapacitors

See Fig. 1.

2.1 Electrochemical Double-Layer Capacitors (EDLCs)

EDLCs usually work by utilizing stable functioning attributes for a good charge–discharge series. Due to their cyclic stableness, EDLCs are suitable for application

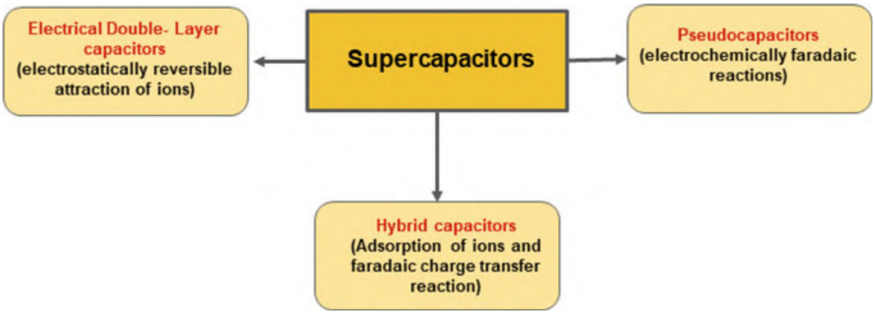
Supercapacitors
Electrical Double- Layer capacitors (electrostatically reversible attraction of ions)
Pseudocapacitors (electrochemically faradaic reactions)
Hybrid capacitors (Adsorption of ions and faradaic charge transfer reaction)

Fig. 1 Classification of supercapacitors

in fields that indulge in places that are not serviceable, like deep inside the sea or hill surroundings. An electrochemical double-layer capacitor (EDLC) merges carbon-based electrodes, a separator, and an electrolyte. They electrostatically hoard charge, and no charge is transferred between the electrolyte and electrode in (Fig. 1) [7]. EDLCs use a charge electrochemical double-layer to hoard energy. On applying current, Charge is collected on the surface of the electrode. Due to an attraction of unlike charges, ions disseminate in the solution of an electrolyte, covering the separator toward the apertures in the electrode with inverse charge, in contrast, electrodes are designed to avert the reclination of the particles [8]. So, a double layer of charge is made in an individual electrode. The charge double-layer is co-joined along with a higher aspect dimension and a lower space between electrodes, making EDLCs gain a large energy density compared to traditional capacitors as charges are not transferred to connecting electrode and electrolyte; also, no synthetic alterations are blended with the electrostatic method. So, hoarding of charge in EDLCs is very much reversible, making them attain higher functioning stableness [9].

2.2 *Pseudo-Capacitors*

Pseudo-capacitors are just opposite to EDLCs, which hoard charge non-faradaic ally, while pseudo-capacitors faradaic ally hoard charge using the charge transfer connecting electrolyte and electrode. This can be attained using absorption on the surface of an electrode, redox reactions, and reversible inclusion of ions (Fig. 1). These Faradaic methods make pseudo capacitors attain higher capacitances and power densities than EDLCs. Conducting polymers and metal oxides are two substances. They are utilized to hoard charge in them and provide good outcomes [10–12]. The electrodes of the pseudo capacitors can be classified into three based on the materials used:

- Transition metal oxides,
- Transition metal nitrides, and
- Conductive polymers.

The performance of conductive polymer-based electrodes is relatively lower than that of their counterparts due to the inferior electrical conductivity. The most commonly used polymer electrodes are polyaniline (PANI), polythiophene (PT), and polypyrrole (PPY), which have long chains with conjugated double bonds. Due to the comparatively good performance of transition metal oxides and nitrides, many studies are ongoing to enhance their performance. Recently there has been a shift in the focus toward carbon-based electrode material by incorporating electroactive transition metal oxide and nitride particles into the carbon matrix [12].

2.3 Hybrid Capacitors

In recent times, ultracapacitors have great energy storage capacity, high power density, cyclic stability, etc. compared to batteries and fuel cells. As a result, hybrid capacitors are developed, which is a combination of both non-faradaic and faradaic materials together (Fig. 1) [13]. The hybrid capacitor is a supercapacitor type that undergoes principles of electrostatic storage and electrochemical, respectively [14]. In hybrid capacitors, the anode part consists of metal oxides or conducting polymers, and the cathode parts consist of carbon-based materials [14, 15].

An asymmetric supercapacitor consists of two electrodes, an anode (positive electrode) made of a polymer or metal oxide material and a cathode (negative electrode) made of a carbon material [16]. Among the different forms of carbon material, activated carbon shows high performance in the form of electrode material because of its large surface area resulting in high capacitance [17]. An increase in capacitance value indirectly increases the energy density. Although commercially available activated carbon is a viable source, it is made using expensive and environmentally unfriendly fossil fuels [17, 18]. The hybrids perform excellent galvanostatic charge/discharge, life-cycle, and specific capacitance. So, it becomes highly imperative to consider a source that is easily available, friendly to the environment, and cost-effective. They can be used in a wide range of applications, such as heavy electric vehicles, power backup, and robotics [19].

Thus, hybrid capacitors intend to make the most use of the comparative merits and weaken the comparative demerits of other supercapacitors to grasp high-functioning attributes. Using one and the other, Faradaic and electrostatic principle to hoard charge, these have attained efficiency and density of power more than EDLC but do not sacrifice in functioning stableness, and affordable cost have bounded the achievement of pseudo-capacitors. Studies focus on three kinds of hybrid capacitors, differentiated using a configuration of electrodes like asymmetric, battery-type, and composite [18, 19].

3 Materials

The more suitable materials for the next-generation supercapacitors are transition metal oxides [20], sulfides [21], hydroxides [22], nitrides [12], conduction polymers such as polypyrrole and polyaniline [23], and carbon materials such as active carbon [24], graphene [25], graphene oxide [26], and carbon nanotubes [27]. These materials have appreciable physical and chemical properties, which can be utilized for energy storage applications.

3.1 Transition Metal Oxides

Metal oxides possess great conductivity and are considered an appropriate electrode for pseudo capacitors [20]. This category's maximum number of studies is based on ruthenium oxide (RuO_2) [28] due to its metal-like conductivity and superior capacitive performance with very high super capacitive performance. The ruthenium oxide's capacitance is attained using the adding and removing or reversible inclusion of protons to its indefinite construct [29]. Another advantage of RuO_2 is the very high overpotential for oxygen evolution and low hydrogen evolution overpotential in acid solution. Thus, the material is mostly utilized as the positive electrode. RuO_2 shows capacitance up to 720 F/g.

Most metal oxides have good electrical conductivity and multiple oxidation states hence, they are preferred as electrode material for pseudo-capacitors [20]. Transition metal oxides have low resistance and show strong faradaic electron transfer reactions, and during the reduction, the free intercalation of protons into the oxide matrix occurs. Pseudo-capacitors with metal oxides electrode have high energy density and cyclic stability compared to carbon-based supercapacitors and conducting polymer-based pseudo-capacitors [20]. Among the transition, metal oxide electrodes such as Iridium (IrO_2) [30], ruthenium (RuO_2) [28, 29], and manganese (MnO_2) [31], as in Fig. 2.

Iridium oxide (IrO_2) has a specific capacitance 293 F/g @ 5 A/g [30]. RuO_2 is preferable due to its wide potential window, multiple oxidation states, low material resistance, etc. [29]. Manganese (MnO_2) has a specific capacitance of 300 F/g @ 1

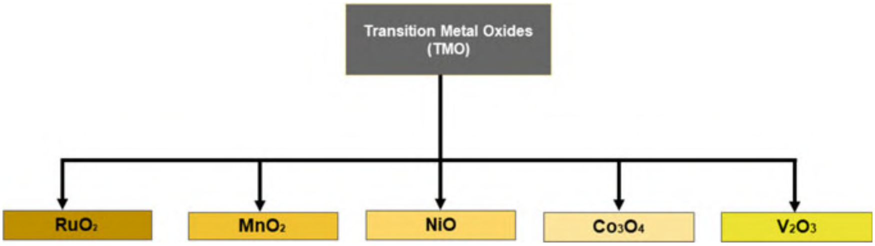

Fig. 2 Commonly used transition metal oxide electrode materials

A/g [31]. Currently, research focuses on ternary and quaternary metal oxides due to their physical and chemical properties, such as multiple oxidation states, high surface area, and high electrical conductivity, which lead to high performance. Due to metals' co-existence and synergistic effects, ternary metal oxides have more reaction sites (higher electrochemical activity) [32]. Nanostructures of transition metal oxide have gained popularity because of their alluring advantages of ease of manufacture, low cost, and environmental friendliness [33].

Transition metal oxides have a wide environmental-related application. They are also used for health care applications such as water purification, air purification, elimination of fungus, bacteria, and viruses, targeted drug delivery, etc. Oxides based on titanium, vanadium, zinc, copper, etc. are the most commonly used material for these applications (Fig. 2). These materials and nanocomposites show high stability, less toxicity, and low cost [34].

3.2 Metal Hydroxides

In recent times, metal hydroxides, due to their layered double hydroxides formation, are capable of multiple oxidation states and active surface regions. Layered Double Hydroxides (LGHs) are fascinating materials that appeal to several sectors, such as nanomedicine for cancer treatment, photocatalytic applications, and electrode materials for energy storage, such as supercapacitors as in Fig. 3 [35]. The researchers discovered it as hydrotalcite in 1842. They are named "hydrotalcite" due to their similarities with talc and a huge amount of water content. In general, two types of hydrotalcite, anionic and cationic clays. The negatively charged ones are at the inner layered region termed cationic clays [36]. These layered structures consist of octahedral sheets in between the tetrahedral sheets. The anionic clays, termed "brucite layers," were positively charged at the inner layered region. Due to their wide range of compositions, adjustable molar ratios of metal cations, and interchanging of anions in inner layers, these structures lead to the unique construction of LDHs. Thus, Layered Double Hydroxides are one of the most promising electrode materials for supercapacitors. Due to high porosity, the nickel–aluminium based LDH composites have a high specific capacitance of 1208 F/g @ 1 A/g, and retention is 80%. Nickel–manganese-based LDH composites have a high specific capacitance of 1268 F/g @ 1 A/g, and retention is 79%. Nickel–cobalt-based LDHs composites have a high specific capacitance of 151.46 F/g @ 2.5 A/g, and retention is 85.6% [37]. Nickel hydroxide ($Ni(OH)_2$) and cobalt hydroxide ($Co–Ni(OH)_2$) have a specific capacitance of 1038 F/g and 1366 F/g @ 1.5 A/g and retention of 96.26% [38].

Fig. 3 Advantages of transition metal hydroxides

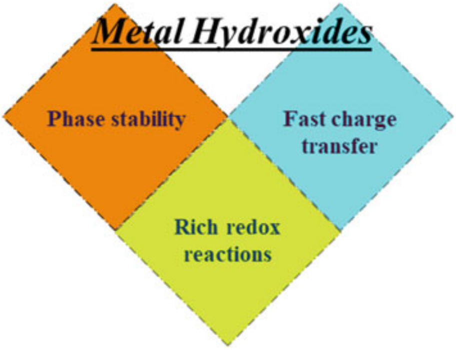

3.3 Metal Sulfides

Sulfide composite materials play a vital role due to their electrical properties. Electronic conductivity is higher than compared to oxide in metal sulfides. Sulfur has a lower electronegativity than oxygen, which avoids splitting the structure in-between layers [38]. Various metal-sulfides such as zinc sulfide [39], iron sulfide [40], nickel sulfide [41], cobalt sulfide [42], copper sulfide [43], manganese sulfide [44], molybdenum sulfide [45], and tin sulfide [46] act as functional materials for supercapacitor applications.

Binary metal sulfides such as $CoMoS_4$, $CuSbS_2$, $ZnCo_2S_4$, $CdIn_2S_4$, $FeMo_4S_6$, $CuCo_2S_4$ [47–49], etc., as shown in Fig. 4 are used for various applications. The metal sulfides are low-cost, low toxicity, and easy to handle. The advantages of metal sulfides are layered structure, exposed active region, and high redox reactions. The disadvantages of metal sulfides are volume expansion. The nickel–aluminum sulfides have a high specific capacitance of 1137 F/g @ 1 A/g, retention is 92.7%, and nickel–cobalt sulfides have a high specific capacitance of 1147 F/g @ 1 A/g and 761 F/g @ 50 A/g [50, 51].

3.4 Conducting Polymers

Conducting polymers have comparatively large capacitance and conduction, lesser ESR, and price than carbon-based electrodes. Specifically, the n- or p-type arrangement of polymer possesses a negative charge or n-type doped, and a positive charge or p-type doped polymer electrode that can conduct can have a higher potential energy and energy density. But they do not have an efficient n-doped polymer substance that can conduct. This averted the capacitors from achieving the goal. Also, the physical strain on large molecules can conduct when the redox reaction bounds the stableness of the pseudo capacitors by several charge–discharge series. This limits the

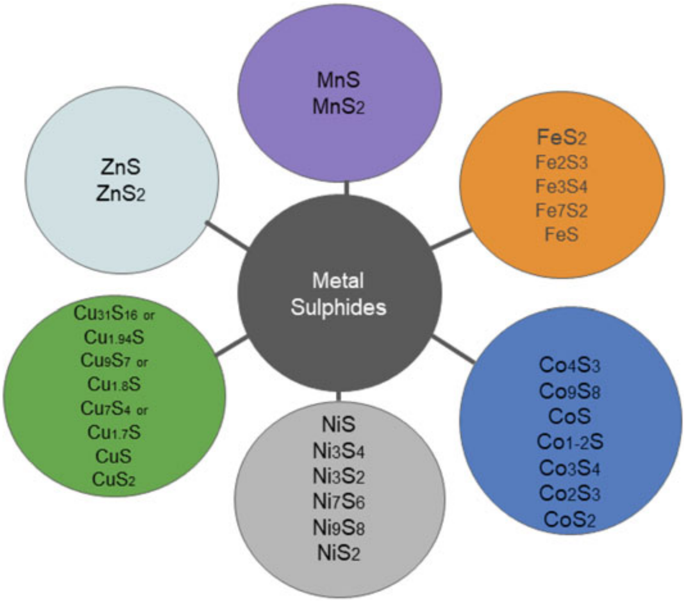
MnS
MnS2
FeS2
Fe2S3
Fe3S4
Fe7S2
FeS
Co4S3
Co9S8
CoS
Co1-2S
Co3S4
Co2S3
CoS2
NiS
Ni3S4
Ni3S2
Ni7S6
Ni9S8
NiS2
Cu31S16 or
Cu1.94S
Cu9S7 or
Cu1.8S
Cu7S4 or
Cu1.7S
CuS
CuS2
ZnS
ZnS2
Metal Sulphides

Fig. 4 List of commonly used primary sulfide electrodes in supercapacitors

functioning stableness and bothers the enhancement of polymers that can conduct in pseudo-capacitors [52, 53].

Polyaniline (PANI) and polypyrene are some frequently used and successful electrode materials, as shown in Fig. 5 [54]. One of their major disadvantages is their poor cyclic stability caused by constant swelling or shrinkage of chains during charge/discharge cycles. Diverse methods of conducting polymer materials enhance the supercapacitor properties of pseudo-capacitive materials. The bulk range of fast redox reaction in conducting polymers improves the capacitive and shows high specific energy. Also, they have low cyclic stability compared to transition metal oxides (TMOs) and carbon-based electrodes supercapacitors [54].

3.5 Carbon-Based Materials

Materials with narrow-band gap properties enhance electrochemical properties and make them ideal for extensive applications with huge demand. Fabricating an electrode material with the expected outcomes, such as energy and capacity, can alter the performance of conventional capacitors and batteries. Carbon-based materials are preferred as electrodes due to their high specific surface area. Among the different

Fig. 5 Commonly used conducting polymers

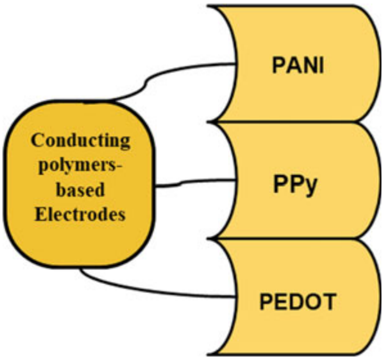
Conducting polymers-based Electrodes
PANI
PPy
PEDOT

types of carbon-based materials, graphene, carbon nanotubes, carbon fibers, and bioactivated carbon are used as electrodes as in Fig. 6 for supercapacitors application due to their cost effectiveness [55–57]

Carbon is obtained via biomass, in which few are used as precursors. Nowadays, novelty research concepts with biodegradable materials play a vital role in electrochemical performance. The progress in applying abundant biomaterials and materials derived from biomass in the field is well established [58]. Though carbon-based materials have high specific capacitance, it is hazardous, causing difficulty breathing and polluting the environment.

Graphene, a single layer of graphite, is a prominent material for the electric double-layer capacitor (EDLC). Graphene's surface area and capacitance value are 26317 $m^2\ g^{-1}$ and 550 F/g. It has higher electrical conductivity than activated carbon [59].

Fig. 6 Various carbon-based electrode materials

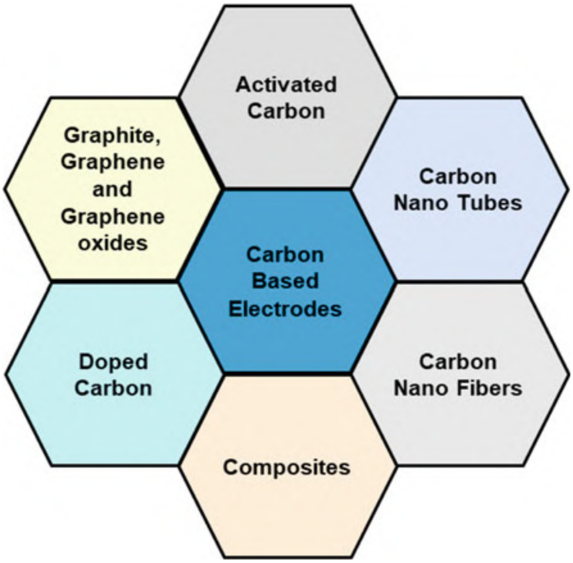
Activated Carbon
Graphite, Graphene and Graphene oxides
Carbon Nano Tubes
Carbon Based Electrodes
Doped Carbon
Carbon Nano Fibers
Composites

Thus, it can be a prominent material for electric double-layer capacitors (EDLC) [60]. This 2D material has a high surface area and can be used as an electrode, resulting in the device's high charge and discharge capability [61]. The quick migration charge carriers into or out of the electrode structures as graphene is in the form of vertically oriented sheets [62].

Carbon nanotubes (CNTs) can be considered a rolled-up sheet of graphene in a tube form and are called single-walled carbon nanotubes (SWNTs). A multi-walled carbon nanotube will be formed if there are several similar graphene tubes around the parental SWNT. The CNTs have very good electrical conductivity, high specific surface areas, good charge transport capability, mesoporous surface structure, and high electrolyte accessibility; hence, the CNT family attracted the scientific community for a wide range of applications, including the development of high-performance electrodes for supercapacitors [63]. The FTO-CNTs can be utilized both as positive and negative electrodes and has a specific capacitance of 542 mF/cm^2 and 410 mF/cm^2 at 10 mV/s, respectively. They also have a specific surface area of 903 mf/cm^2 @1 mA/cm^2 [64]. The theoretical capacitance of CNTs is between 71 and178 F/g, and the surface area is 357 m^2/g [65].

4 Environmental Effects of Various Functionalized Material Electrodes

In the twenty-first century, environmental issues related to various types of pollution are pressing. The various organic and inorganic pollutants released in the biosphere and the various micro-organisms such as bacteria, viruses, and fungi disturb the ecological balance on earth. Environmental remediation is required immediately to fulfill the dream of sustainable development. The success of sustainable development depends on the efficient utilization of various renewable energy sources and their storage. Hence, the development of environmentally friendly materials for sustainable energy conversion and efficient storage is much needed.

Among the various electrode materials used in supercapacitors, transition metal oxides and hydroxides are stable in open atmospheric conditions and are widely used for environmental remediation, the drawback of these materials is their chemical and biological side effects [66, 67]. Various transition metal oxides and hydroxides can be effectively used as absorbents and catalysts to remove organic and inorganic pollutants from the air [67, 68] and water [69, 70]. These can also be utilized effectively to remove contaminated chemicals [69, 70] and biological substances [71]. The transition metal oxides have very good crystalline features with controlled structural properties, and enhanced surface area is highly stable and less toxic when used as a photocatalyst to remove pollutants from water. They can function as semiconductors with wide bandgaps and are cost-effective, nontoxic, and abundant on the earth [72].

The tuneable structural, electrical, optical, physical, and chemical properties of metal sulfides make them suitable for a wide range of environmental as well as energy-related applications, including energy conversion [73], energy storage [74, 75], hydrogen production [76], CO_2 reduction [77], air purification [78], water purification [79] and also for medicinal applications like targeted drug delivery [80]. The chalcogenides are well known for their very high surface area, enhanced surface reactivity, and surface sites and can also be used for sensing applications [81, 82].

The pi electrons are responsible for electrical properties such as electrical conductivity, very high electron affinity, low ionization potential, and low energy optical transitions for the conducting polymers [83]. Due to these properties, conducting polymers are widely used for biosensing devices [83] and in analytical chemistry [84]. The flexibility, lightweight, and enhanced electrical properties make them suitable for flexible and wearable electronic applications [85], energy conversion [86], and storage applications [87, 88]. The environmental applications of conducting polymers include air and water purification [89, 90] and anti-microbial application [91].

The structural and interfacial interactions are the reason behind the carbon nanostructure's unique physical and chemical properties. These unique properties, coupled with the enhanced surface area and wide range of pore sizes, enable the material for many environmental-related applications, including gas adsorption [92], water treatment [93], anaerobic digestion [94], composting [95], soil remediation [96], etc.

5 Conclusion

The sustainable development of modern world economies is strictly oriented around various green energy resources and their efficient utilization. For this, along with highly efficient and sustainable energy conversion devices, energy storage devices with enhanced energy and power factors are also required [97]. The supercapacitors have very high-power conversion efficiency and can be effectively utilized in areas where a huge impulse of energy is required.

Researchers worldwide are in pursuit of developing newer materials and technologies for energy storage applications, especially batteries, and supercapacitors. In this regard, various sustainable materials with different functional groups have been developed worldwide. These materials include transition metal oxides, sulfides, carbon and carbon allotropes, and conducting polymers. Each of these materials has its advantages and disadvantages, which we have discussed in this chapter. Thorough knowledge of various functional groups utilized for supercapacitor applications is one of the primary requirements for advancing energy storage applications without disturbing the stability of the environment [98]. The 3R method [99] must be kept in mind for further developing materials for sustainable energy storage applications.

Acknowledgements The authors sincerely acknowledge Mr. Deepak CP (I5PHY18021) and Mr. Dineesh R (I5PHY18024), integrated M.Sc. Physics students, Department of Sciences, Amrita School of Physical Science, Amrita Vishwa Vidyapeetham, Coimbatore, for their help in drawing the figures.

References

1. Olabi AG et al (2022) Supercapacitors as next generation energy storage devices: properties and applications. Energy 248:123617
2. Wu Q et al (2021) Cyclic stability of supercapacitors: materials, energy storage mechanism, test methods, and device. J Mater Chem A 9(43):24094–24147
3. Sun J, Luo B, Li H (2022) A review on the conventional capacitors, supercapacitors, and emerging hybrid ion capacitors: past, present, and future. Adv Energy Sustain Res 3(6):2100191
4. Jayalakshmi M, Balasubramanian K (2008) Simple capacitors to supercapacitors-an overview. Int J Electrochem Sci 3(11):1196–1217
5. Sharma K, Arora A, Kant Tripathi S (2019) Review of supercapacitors: materials and devices. J Energy Stor 21:801–825
6. Libich J et al (2018) Supercapacitors: properties and applications. J Energy Stor 17:224–227
7. Mei B-A et al (2018) Physical interpretations of Nyquist plots for EDLC electrodes and devices. J Phys Chem C 122(1):194–206
8. Obreja VVN (2008) On the performance of supercapacitors with electrodes based on carbon nanotubes and carbon activated material—A review. Physica E: Low-dimens Syst Nanostruct 40(7):2596–2605
9. Afif A et al (2019) Advanced materials and technologies for hybrid supercapacitors for energy storage–A review. J Energy Stor 25:100852
10. Yao G et al (2021) Nanostructured transition metal vanadates as electrodes for pseudo-supercapacitors: a review. J Nanopart Res 23(2):57
11. An C et al (2019) Metal oxide-based supercapacitors: progress and prospectives. Nanoscale Adv 1(12):4644–4658
12. Yi C-Q et al (2018) Recent advances in pseudocapacitor electrode materials: transition metal oxides and nitrides. Trans Nonferr Metals Soc China 28(10):1980–2001
13. Shaikh NS et al (2022) Sulfur-doped graphene as a rational anode for an ionic liquid based hybrid capacitor with a 3.5 V working window. Energy Fuels 36(5):2799–2810
14. Khomenko V, Raymundo-Pinero E, Béguin F (2006) Optimisation of an asymmetric manganese oxide/activated carbon capacitor working at 2 V in aqueous medium. J Power Sour 153(1):183–190
15. Tang H, Yao J, Zhu Y (2021) Recent developments and future prospects for zinc-ion hybrid capacitors: a review. Adv Energy Mater 11(14):2003994
16. Dubey P et al (2020) Recent advances in biomass derived activated carbon electrodes for hybrid electrochemical capacitor applications: challenges and opportunities. Carbon 170:1–29
17. Kumar R et al (2021) Microwave as a tool for synthesis of carbon-based electrodes for energy storage. ACS Appl Mater Interf 14(18):20306–20325
18. Ratajczak P et al (2019) Carbon electrodes for capacitive technologies. Energy Stor Mater 16:126–145
19. Burke A (2010) Ultracapacitor technologies and application in hybrid and electric vehicles. Int J Energy Res 34(2):133–151
20. Wu Z et al (2016) Transition metal oxides as supercapacitor materials. Nanomater Adv Batter Supercapacitors 317–344
21. Arya D et al (2022) Performance and future directions of transition metal sulfide-based electrode materials towards supercapacitor/supercapattery. Wiley Interdiscip Rev: Energy Environ 11(1):e414
22. Shi F et al (2014) Metal oxide/hydroxide-based materials for supercapacitors. RSC Adv 4(79):41910–41921
23. Snook GA, Kao P, Best AS (2011) Conducting-polymer-based supercapacitor devices and electrodes. J Power Sourc 196(1):1–12
24. Gamby J et al (2001) Studies and characterisations of various activated carbons used for carbon/carbon supercapacitors. J Power Sources 101(1):109–116
25. Lakra R et al (2014) A mini-review: Graphene based composites for supercapacitor application. Inorganic Chem Commun 133:108929

26. Korkmaz S, Afşin Kariper İ (2020) Graphene and graphene oxide based aerogels: synthesis, characteristics and supercapacitor applications. J Energy Stor 27:101038
27. Xia G-T et al (2019) Structural design and electrochemical performance of PANI/CNTs and MnO2/CNTs supercapacitor. Sci Adv Mater 11(8):1079–1086
28. Morag A et al (2020) Nanostructured nickel/ruthenium/ruthenium-oxide supercapacitor displaying exceptional high frequency response. Adv Electron Mater 6(1):1900844
29. Subramani S, Rajiv S (2022) Fabrication of poly (3-methylthiophene)/poly (ethylene oxide)/ruthenium oxide composite electrospun nanofibers for supercapacitor application. J Mater Sci: Mater Electron 33(12):9558–9569
30. Beknalkar SA et al (2021) Construction of IrO_2@ Mn_3O_4 core-shell heterostructured nanocomposites for high performance symmetric supercapacitor device. J Alloy Compd 887:161328
31. Zhang M et al (2020). High performance MnO_2 supercapacitor material prepared by modified electrodeposition method with different electrodeposition voltages. J Energy Stor 29:101363
32. Mayakkannan M et al (2021) Investigations on ternary transition metal ferrite: $NiCoFe_2O_4$ as potential electrode for supercapacitor prepared by microwave irradiation method. J Energy Stor 44:103257
33. Yadav S, Sharma A (2021) Importance and challenges of hydrothermal technique for synthesis of transition metal oxides and composites as supercapacitor electrode materials. J Energy Stor 44:103295
34. Dharmalingam P et al (2022) Synthesis of metal oxides/sulfides-based nanocomposites and their environmental applications: a review. Mater Today Sustain 100232
35. Li X et al (2017) Layered double hydroxides toward high-performance supercapacitors. J Mater Chem A 5(30):15460–15485
36. Sikander U, Sufian S, Salam MA (2017) A review of hydrotalcite based catalysts for hydrogen production systems. Int J Hydrogen Energy 42(31):19851–19868
37. Peng H et al (2019) Crystal structure of nickel manganese-layered double hydroxide@ cobaltosic oxides on nickel foam towards high-performance supercapacitors. Cryst Eng Commun 21(3):470–477
38. Sangeetha Vidhya M, Ravi G, Yuvakkumar R, Velauthapillai D, Thambidurai M, Dangc C, Saravanakumard B (2020) Nickel–cobalt hydroxide: a positive electrode for supercapacitor applications. Royal Soc Chem Adv 33
39. Iqbal MF, Naeem Ashiq M, Zhang M (2021) Design of metals sulfides with carbon materials for supercapacitor applications: a review. Energy Technol 9(4):2000987
40. Tian F et al (2022) Preparation and electrochemical capacitance of different micro morphology zinc sulfide on nickel foam for asymmetric supercapacitor. J Energy Stor 50:104600
41. Wang Y, Xie Y (2020) Electroactive FeS_2-modified MoS_2 nanosheet for high-performance supercapacitor. J Alloy Compd 824:153936
42. Miao Y et al (2020) Hierarchical NiS@ CoS with controllable core-shell structure by two-step strategy for supercapacitor electrodes. Adv Mater Interf 7(3):1901618
43. Zhang Y et al (2020) CoO@ CoS/Ni_3S_2 hierarchical nanostructure arrays for high performance asymmetric supercapacitor. Appl Surf Sci 532:147438
44. Han X et al (2022) Construction of vacancies-enriched CuS/Fe_2O_3 with nano-heterojunctions as negative electrode for flexible solid-state supercapacitor. J Alloys Compd 916:165443
45. Yang M et al (2022) Mn_3O_4/MnS heterostructure for electrode and asymmetric supercapacitor under high charge/discharge current. Electrochimica Acta 424:140630
46. Ghosh K, Pumera M (2021) Free-standing electrochemically coated MoS x based 3D-printed nanocarbon electrode for solid-state supercapacitor application. Nanoscale 13(11):5744–5756
47. Dar MA et al (2022). Supercapacitor and magnetic properties of Fe doped SnS nanoparticles synthesized through solvothermal method. J Energy Stor 52:105034
48. Xu J-M, Wang X-C, Cheng J-P (2020) Supercapacitive performances of ternary $CuCo_2S_4$ sulfides. ACS Omega 5(3):1305–1311
49. Ramasamy K et al (2015) Layered ternary sulfide CuSbS2 nanoplates for flexible solid-state supercapacitors. J Mater Chem A 3(25):13263–13274

50. Wang X et al (2021) Cracked bark-inspired ternary metallic sulfide ($NiCoMnS_4$) nanostructure on carbon cloth for high-performance aqueous asymmetric supercapacitors
51. Li X et al (2015) Two-dimensional, porous nickel–cobalt sulfide for high-performance asymmetric supercapacitors. ACS Appl Mater Interf 7(34):19316–19323
52. Gao Y, Zhao L (2022) Review on recent advances in nanostructured transition-metal-sulfide-based electrode materials for cathode materials of asymmetric supercapacitors. Chem Eng J 430:132745
53. Meng Q et al (2017) Research progress on conducting polymer based supercapacitor electrode materials. Nano Energy 36:268–285
54. Wang K et al (2014) Conducting polymer nanowire arrays for high performance supercapacitors. Small 10(1):14–31
55. Sardana S et al (2021) Conducting polymer hydrogel based electrode materials for supercapacitor applications. J Energy Stor 103510
56. Wang Y et al (2021) Recent progress in carbon-based materials for supercapacitor electrodes: a review. J Mater Sci 56:173–200
57. Kumar S et al (2021) 0D to 3D carbon-based networks combined with pseudocapacitive electrode material for high energy density supercapacitor: a review. Chem Eng J 403:126352
58. Saikia BK et al (2020) A brief review on supercapacitor energy storage devices and utilization of natural carbon resources as their electrode materials. Fuel 282:118796
59. Saini S, Chand P, Joshi A (2021) Biomass derived carbon for supercapacitor applications. J Energy Stor 39:102646
60. Kumar R et al (2022) A review on the current research on microwave processing techniques applied to graphene-based supercapacitor electrodes: an emerging approach beyond conventional heating. J Energy Chem
61. Cossutta M et al (2020) A comparative life cycle assessment of graphene and activated carbon in a supercapacitor application. J Clean Prod 242:118468
62. Fu C et al (2011) Supercapacitor based on graphene and ionic liquid electrolyte. J Solid State Electrochem 15:2581–2585
63. Yang Z et al (2019) Carbon nanotube-and graphene-based nanomaterials and applications in high-voltage supercapacitor: a review. Carbon 141:467–480
64. Zhang Y, Xie E (2021) Functionalized and tip-open carbon nanotubes for high-performance symmetric supercapacitors. Dalton Trans 50(37):12982–12989
65. Lu W, Dai L (2010) Carbon nanotube supercapacitors. Carbon nanotubes. IntechOpen
66. Kalita E, Baruah J (2020) Environmental remediation. In: Colloidal metal oxide nanoparticles. Elsevier, pp 525–576
67. Wang X et al (2022) Hierarchically porous metal hydroxide/metal–organic framework composite nanoarchitectures as broad-spectrum adsorbents for toxic chemical filtration. J Colloid Interf Sci 606:272–285
68. Patil SB et al (2019) Recent advances in non-metals-doped TiO_2 nanostructured photocatalysts for visible-light driven hydrogen production, CO_2 reduction and air purification. Int J Hydrogen Energy 44(26):13022–13039
69. Oyewo OA et al (2020) Metal oxide-cellulose nanocomposites for the removal of toxic metals and dyes from wastewater. Int J Biol Macromol 164:2477–2496
70. Lee SY, Bondietti EA (1983) Removing uranium from drinking water by metal hydroxides and anion-exchange resin. J Am Water Works Ass 75(10):536–540
71. Vega-Jiménez AL et al (2019) In vitro antimicrobial activity evaluation of metal oxide nanoparticles. Nanoemulsions Prop Fabr Appl:1–18
72. Khin MM et al (2012) A review on nanomaterials for environmental remediation. Energy Environ Sci 5(8):8075–8109
73. Le Donne A, Trifiletti V, Binetti S (2019) New earth-abundant thin film solar cells based on chalcogenides. Front Chem 7:297
74. Huang J et al (2019) Molybdenum and tungsten chalcogenides for lithium/sodium-ion batteries: beyond MoS2. J Energy Chem 33:100–124

75. Dahiya Y et al (2022) Modified transition metal chalcogenides for high performance supercapacitors: current trends and emerging opportunities. Coordination Chem Rev 451:214265
76. El Nazer HA, Mohamed YMA (2021) Chalcogenide-based nanomaterials as photocatalysts for water splitting and hydrogen production. In: Chalcogenide-based nanomaterials as photocatalysts. Elsevier, pp 173–183
77. Gao F-Y, Wu Z-Z, Gao M-R (2021) Electrochemical CO_2 reduction on transition-metal chalcogenide catalysts: recent advances and future perspectives. Energy Fuels 35(16):12869–12883
78. Jha RK, Bhat N (2020) Recent progress in chemiresistive gas sensing technology based on molybdenum and tungsten chalcogenide nanostructures. Adv Mater Interf 7(7):1901992
79. Nsude HE et al (2020) Green synthesis of $CuFeS_2$ nanoparticles using mimosa leaves extract for photocatalysis and supercapacitor applications. J Nanopart Res 22:1–13
80. Dirersa WB et al (2022) Surface-engineered $CuFeS_2$/Camptothecin nanoassembly with enhanced chemodynamic therapy via GSH depletion for synergistic photo/chemotherapy of cancer. Mater Today Chem 26:101158
81. Noah NM (2020) Design and synthesis of nanostructured materials for sensor applications. J Nanomater 2020:1–20
82. Seifert G, Köhler T, Tenne R (2002) Stability of metal chalcogenide nanotubes. J Phys Chem B 106(10):2497–2501
83. Gerard M, Chaubey A, Malhotra BD (2002) Application of conducting polymers to biosensors. Biosens Bioelectron 17(5):345–359
84. Bahrani S et al (2022) Conductive polymers in green analytical chemistry. In: Conductive polymers in analytical chemistry. American Chemical Society, pp 1–37
85. Ouyang J (2021) Application of intrinsically conducting polymers in flexible electronics. SmartMat 2(3):263–285
86. Murad AR et al (2020) Conducting polymers for optoelectronic devices and organic solar cells: a review. Polymers 12(11):2627
87. Jia X et al (2019) Tunable conducting polymers: toward sustainable and versatile batteries. ACS Sustain Chem Eng 7(17):14321–14340
88. Han Y, Dai L (2019) Conducting polymers for flexible supercapacitors. Macromol Chem Phys 220(3):1800355
89. Zhang Y et al (2022) Continuous air purification by aqueous interface filtration and absorption. Nature 610(7930):74–80
90. Weidlich C, Mangold K-M, Jüttner K (2001) Conducting polymers as ion-exchangers for water purification. Electrochimica Acta 47(5):741–745
91. Maruthapandi M et al (2022) Antimicrobial activities of conducting polymers and their composites. Macromolecules 2(1):78–99
92. Asgarpour Khansary M, Ali Aroon M, Shirazian S (2020) Physical adsorption of CO_2 in biomass at atmospheric pressure and ambient temperature. Environ Chem Lett 18:1423–1431
93. Lu L et al (2019) A novel TiO_2/biochar composite catalysts for photocatalytic degradation of methyl orange. Chemosphere 222:391–398
94. Masebinu SO et al (2019) A review of biochar properties and their roles in mitigating challenges with anaerobic digestion. Renew Sustain Energy Rev 103:291–307
95. Liu N et al (2017). Role and multi-scale characterization of bamboo biochar during poultry manure aerobic composting. Bioresour Technol 241:190–199
96. Mahmoud E et al (2020) Soil amendment with nanoresidues from water treatment increases P adsorption in saline soils. Environ Chem Lett 18:171–179
97. Fu M et al (2019) Crab shell derived multi-hierarchical carbon materials as a typical recycling of waste for high performance supercapacitors. Carbon 141:748–757
98. Jiang G, Pickering SJ (2016) Recycling supercapacitors based on shredding and mild thermal treatment. Waste Manag 48:465–470
99. Ma C et al (2019). Sustainable recycling of waste polystyrene into hierarchical porous carbon nanosheets with potential applications in supercapacitors. Nanotechnology 31(3):035402

Part V

FNMs Based Supercapacitor for Food and Beverages Applications

Всё для победы!
НАРОДНЫЙ ФРОНТ
https://pobeda.onf.ru/
LET'S HELP THE RUSSIA

Chapter 19
Role of FNMs-Based Supercapacitors in the Food and Beverage Industry

Tanuj Kumar and Arunima Verma

1 Introduction

The goal of nanotechnology is to create and grow organic and inorganic materials with specific chemical, biological, and physical characteristics at the nanoscale [1]. When particles are reduced to this size, the material obtained no longer has the same chemical and physical characteristics as the macroscale components found in the same basic substance. Recent years have seen a flurry of activity in this area of study, with several researchers quickly seeing promising applications in the food and drink industries [2].

According to researchers, food safety is the "scientific regularity" that describes how to acquire, prepare, and store food without exposing people to harmful bacteria conditions such as illnesses [3]. There have been a lot of talks lately about how concerned people are about the quality and safety of their food as well as drinks. Furthermore, establishing high standards in the case of process control is the top priority. Customers have higher and higher standards for food quality. Manufacturers are under pressure to provide foods and drinks that meet the high standards set by consumers, who increasingly look for trust marks and quality labels. Because of the great variety of complicated matrices, food testing labs must identify a broad spectrum of goods (vegetal or animal origins). It poses a significant difficulty for concentration-dependent selectivity and sensitivity. One of the most important and crucial aspects of food safety investigations is the development of analytical methods and tools that can meet today's needs for detecting a wide range of potentially harmful substances in food [4]. Due to the complex matrix of food specimens and the availability of trace levels of dangerous agents, sensitive, high-output, accurate, low-cost, and convenient analytical techniques or apparatuses are introduced in the mainstream

---

T. Kumar (🖂) · A. Verma
Department of Nanosciences and Materials, Central University of Jammu, Jammu 181143, India
e-mail: tanuj.nsm@cujammu.ac.in

© The Author(s), under exclusive license to Springer Nature Singapore Pte Ltd. 2024

C. M. Hussain and M. B. Ahamed (eds.), *Functionalized Nanomaterials Based Supercapacitor*, Materials Horizons: From Nature to Nanomaterials,
https://doi.org/10.1007/978-981-99-3021-0_19

of food safety analysis. There is significant potential for the supercapacitor technique to alter conventional methods of quality control analysis in the food and beverage sector [5].

In the case of quality control analysis, these gadgets may offer a portable, low-cost, and easy-to-use approach. The use of nanomaterials in supercapacitors may significantly boost their growth in the industry [6]. Often in a supercapacitor, nanomaterials have the potential to greatly improve reaction time, sensitivity, and energy storage capacity because of their unrivalled chemical and electrical characteristics, nanoparticles may be used selectively to satisfy the contamination detection criteria in complicated food samples. It should be kept in mind that a solitary nanoparticle is incapable of handling all the demands of a supercapacitor due to the existence of many flaws such as the stacking and curling of graphene, lamellae, the dispersion difficulty, and easy accretion of metal nanoparticles (NPs) in the polymer, the adhesion of carbon nanotubes (CNTs), and the agglomeration of quantum dots (QDs) [7]. Therefore, the nanomaterials have regularly been functionalized or mixed by various inorganic and organic nonfunctional materials/nanomaterials to produce the nanocomposite for practical employment. To create a unique high-level functional material, a nanocomposite with a single nanomaterial type combines the single-component material's property with the cooperative impacts between the nanostructures and the macroscopic qualities of their ordered circumstances. Nanocomposite, widely regarded as one of the most amazing materials, has received much study. Functional nanomaterials, also known as amazing technology [8], may be used to enhance the supercapacitor's ability to identify food and drink.

Despite the technology's fast development, a great deal is understood about nanotechnology. As a result, food scientists and engineers are shifting their attention to improving the security of our food supply, which opens up new avenues for potential innovations new and different varieties of goods (Fig. 1). Public concern over food safety is sparked by the fact that foods including produce, meat, and poultry may be a vector for the spread of human infections, potentially resulting in widespread outbreaks of foodborne illness [9]. Therefore, greater effort must be put into the development of novel antimicrobials in order to guarantee access to nutritious meals. Nanomaterials' inherent antibacterial capabilities provide promising new avenues for developing effective antimicrobial agents for use in the food and beverage sectors. There are two possible approaches to address this problem one, by incorporating nano-antimicrobial agents into the food itself, and two, by enclosing food in antimicrobial packaging. Nanomaterials with unique antibacterial capabilities are increasingly being used in the food and food-related sectors, and this trend is predicted to have far-reaching consequences for the whole food system, from farming and processing to wholesale business.

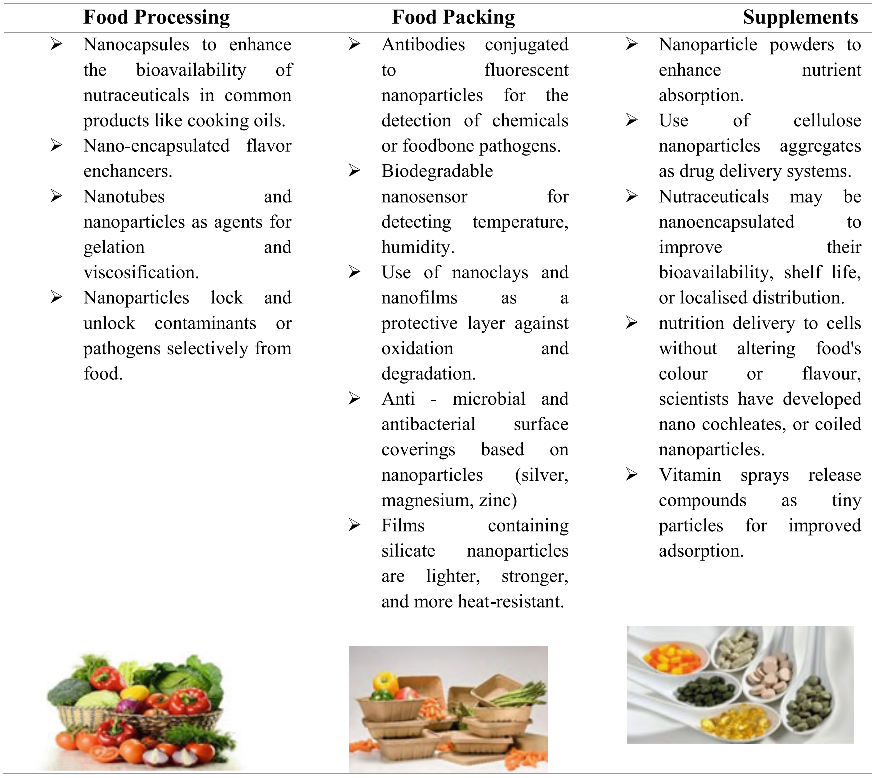

Food Processing	Food Packing	Supplements
➢ Nanocapsules to enhance the bioavailability of nutraceuticals in common products like cooking oils. ➢ Nano-encapsulated flavor enchancers. ➢ Nanotubes and nanoparticles as agents for gelation and viscosification. ➢ Nanoparticles lock and unlock contaminants or pathogens selectively from food.	➢ Antibodies conjugated to fluorescent nanoparticles for the detection of chemicals or foodbone pathogens. ➢ Biodegradable nanosensor for detecting temperature, humidity. ➢ Use of nanoclays and nanofilms as a protective layer against oxidation and degradation. ➢ Anti - microbial and antibacterial surface coverings based on nanoparticles (silver, magnesium, zinc) ➢ Films containing silicate nanoparticles are lighter, stronger, and more heat-resistant.	➢ Nanoparticle powders to enhance nutrient absorption. ➢ Use of cellulose nanoparticles aggregates as drug delivery systems. ➢ Nutraceuticals may be nanoencapsulated to improve their bioavailability, shelf life, or localised distribution. ➢ nutrition delivery to cells without altering food's colour or flavour, scientists have developed nano cochleates, or coiled nanoparticles. ➢ Vitamin sprays release compounds as tiny particles for improved adsorption.

Fig. 1 Examples of nano-food applications

2 Food and Beverage Contamination

The food and beverage sectors are facing a number of issues right now; they are responsible for the elimination of risks associated with several complicated mixes of chemical pollutants [10]. Waste from humans and animals, naturally occurring toxins, disinfection by-products in drinking water, corrosion in plumbing systems, nitrates, sulfates, heavy metals, pesticides, phenolics, pathogens, toxins, packaging and food preparation all contribute to a growing reservoir of chemical pollutions consequence. For a long time, people have been aware that chemical pollution is a major problem because of the serious health effects it may have over time. Many chemicals in particular were implicated in containing cancer-causing agents, whereas other substances may be linked to endocrine-disrupting impacts or accumulated and biomagnified in the food chain [11]. With rising consumer awareness of the need of ensuring the safety of the foods and drinks they eat, the food sciences have developed a wide range of analytical procedures and methods.

2.1 Inorganic Anions and Compounds

Human and animal life are adversely affected by environmental and food pollution, which may have mild to severe long-term effects as well as more immediate and even lethal consequences. Nitrite ions (NO_2^-) are only one example of the many types of inorganic pollutants that may be found in water and food systems and are recognized as major issues in the realm of human health. Methemoglobinemia is a condition caused by nitrite ions binding to hemoglobin and forming potentially cancerous nitrosamines. In the food industry, it is often employed as a preservative in cheeses, unprocessed vegetables, and natural meats [12]. As a result of this study, it was concluded that a concentration of 0.01% is the safest level for use as a preservative in drinking water up to 2.17 mmol L^{-1} The quantitative assessment of (NO_2^-) are in drinking water is especially significant in light of the growing need for precision in environmental conservation and public health measures [13].

The sulphite ions (SO_3^{2-}) pollutants are often utilized as bleaching agents, preservatives, reducing agents, antioxidants and other additives in the food sector. If sulfite levels are too high, it may cause a variety of health problems, including nausea, vomiting, dizziness and even asthma. Although sulphite occurs naturally in foods such as dried fruit, the Food and Drug Administration (FDA) says that it poses a cancer risk when used as a preservative or in the food processing industry, so it must be listed on food labels. The maximum allowable content in food is 10 parts per million ($\leq$10 ppm) [14].

2.2 Heavy Metals

One of our most pressing problems is the widespread presence of heavy metals in our drinking water and food supply. Water purification systems' requirements for metal ion concentrations and foods are important for the protection of both people and the planet [15]. In order to ensure that our drinking water is free of harmful contaminants like cadmium (Cd), lead (Pb), etc., ultralow amounts of these metals must be measured with great precision. Due to their persistence, toxicity and inability to undergo heat decomposition, heavy metals tend to build up in biological systems. Toxins found in water or food have been linked to a wide range of health issues, from birth defects to organ failure.

According to the EPA, drinking polluted water is the leading cause of lead (Pb) and cadmium (Ca) exposure. According to WHO guidelines, 3.0 mg L^{-1} of lead and 10.0 mg L^{-1} of cadmium are permissible in drinking water (WHO). Therefore, determining accurate Pb and Cd levels is a crucial endeavour [16].

2.3 Toxins

Toxins in food, which may originate from microorganisms or plants, can cause serious health problems for humans. Further, mycotoxins are defined as poisons produced by fungi. These poisons are referred to as heterogeneous toxic secondary metabolites of fungal origin because of the great variety of harmful effects they have. There is a wide variety in the chemical structures, toxicological profiles and physicochemical properties of the roughly 400 different mycotoxins that have been identified thus far. Some mycotoxins are embryotoxic, allergic and teratogenic, while others are known to induce genetic disruptions and cancer formation. Mycotoxins may contaminate agricultural products at a number of stages in the food chain, including drying, pre-harvest, storage, transportation and harvest. The potential toxicity of these compounds has prompted several nations to set rigorous standards for the regulation of food and feed, as well as suitable outcomes in the creation of laws to address their potential for pollution [17]. The legal limit for aflatoxin B_1 (AFB_1) in the European Union is between 0.1 and 12 $\mu g\ kg^{-1}$ [18]. Mycotoxin detection is difficult since these molecules may be found in a wide variety of chemicals produced by a single or several fungus species, and their quantities in complex matrices are often rather low. Mycotoxins including ochratoxin OTA and aflatoxins have been found in food samples more often than ever before. Numerous studies have been conducted on these mycotoxins, but more research has to be done on the use of supercapacitors for their detection [19].

3 Functionalized Nanomaterials for Sensing in the Food and Beverage Industry

Nanomaterials have received a great deal of attention in the fields of analytical chemistry and supercapacitors because they have a tremendous amount of surface area for their size and can be made to support unique reaction routes [20]. Besides that, melting temperatures, chemical reactivity, morphology-dependent interatomic bond lengths and optical and electrical characteristics exert a strong influence on nanomaterial usefulness. When the component nanometric elements in their immediate environs interact, they may give the desired functionality [21, 22]. One may examine the electrocatalytic activity of nanomaterials by taking into account supercapacitor data. Exposure to pollutants may activate these materials, opening the door to the development of novel devices with astonishing functions and operations. In addition, they have the potential to enhance mobility and real-time assessment in the event of food use. Supercapacitor techniques based on functional nanomaterials have advanced rapidly in recent years, making this a promising new field of study with the potential to improve and even replace traditional methods of food analysis [23].

Numerous desirable characteristics may be found in carbon-based materials such graphene oxide (GO), graphene and CNTs [24]. They have been presented as excellent materials to be used in supercapacitor detection of specific molecules. In order to develop sensors with the most effective catalytic and supercapacitor properties, gold (Au) has been presented as one of the most promising metals. The usage of Au NPs in the fabrication of various sensors is widespread. Researchers have paid close attention to Au NPs from an electroanalytical perspective because of their superior conductivity, high surface-to-volume ratio and biological compatibility. In addition, supercapacitor performance in nanostructured compounds may be improved by combining metal NPs with carbon-based materials [25, 26]. Taken together, metallic nanocomposites and bimetallic nanostructures may significantly boost sensitivity and selectivity for substance detection in food and beverage matrices. We have compiled, in Table 1, a list of innovative sensors for the detection and determination of various pollutions utilizing nanostructured materials.

3.1 Materials-Based Food and Beverage Supercapacitors

A few examples of such novel and innovative medical technologies and gadgets are deep brain stimulators for Parkinson’s illness, vagal nerve stimulators for epilepsy, electronic aspirin for head or face symptoms and insulin pumps for diabetes. Implantable electronic devices have dramatically improved patient care, but they are not without drawbacks, such as the requirement for surgery and the risk of perioperative problems. Alternatives to implantable electronics can be found in biodegradable technology and the latest bioresorbable devices like single transistors, primary batteries and biosensors, organic field-effect transistors, organic transistors fabricated on bioresorbable substrates and a wide variety of other innovations [37]. Though biodegradable electronics eliminate the need for further surgical procedures, they do have certain drawbacks. For instance, biodegradable batteries have a poor energy density and are limited in size. The digestive system has the potential to be used as an alternative route for the administration of electronics that can influence cellular and organ function without the requirement for implantation, complementing the use of both permanent and biodegradable devices. The National Institutes of Health reports that intake of harmful components like MnO_2, included in some of the edible compounds that have been suggested in the past, may lead to symptoms like stomach discomfort and nausea (NIH) [38]. Humans have evolved to maximize the efficiency with which materials and nutrients move through the digestive system since we have relied on food and digestion for over 200 thousand years. This Communication shows completely functioning and edible supercapacitors that have the ability to operate in the gastrointestinal system by combining existing expertise from the food business, material sciences, device manufacturing and biomedical engineering. For the fabrication of comestible supercapacitors, we opted for the use of electrically conductive and chemically stable carbon (in the form of activated charcoal) and inert metals (edible gold) in addition to other food sources rather than the conventional noninert

Table 1 Some examples of functionalized nanomaterials-based sensors applied in food and beverage analysis

S. No	Sensor type	Nanomaterial used	Techniques used	Analyte	Sample	Linear range	Limit of detection	References
1	GCE	ZnO-AuNPs/ rGO-g-CN	SWV	Sunset yellow	Fruit juice and red wine	5–85 nM	1.34 nM	[27]
2	SPCE	Au NPs-GQD	LSV	Vanillin	–	0.2–40 µM	10 nM	[28]
3	GCE	Fullerene/ MWCNT	DPV	Caffeine	–	10–1000 µM	7.289×10^{-8} M	[29]
4	Au	Nanoporous gold	DPV	Hydrazine/ Sulfite, nitrite	Wine, apple cider, water, and beef	5.0–4000 µM	3.37×10^{-7}, 1.44×10^{-6}, and 9.11×10^{-7} M	[30]
5	GCE	MWCNTs-Au NPs	DPV	Vanillin	Milk powder and ice cream	7.0×10^{-8}–7.5×10^{-5} mol L^{-1}	3.8×10^{-8} mol L^{-1}	[31]
6	SPE	SWCNTs	SWASV	Cd^{2+}, Pb^{2+}	Honey and milk	1–60 µM	0.2 µM, 0.4 µM	[32]
7	GCE	Fluorine-GO	DPV	Caffeic acid	Red wine	0.5–100.0 µM	0.018 µM	[33]
8	CPE	ZnO/G/CTAB	DPV	Bisphenol	Tap water and canned soft drink,	0.5–10 µM	0.06 µM	[34]
9	FTO	PEDOT/ILRGO	DPV	Chlorpyrifos, Malathion/Methyl parathion	Apple juice, aerated drinks	–	0.04 nM, 0.117 nM, 0.108 nM	[35]
10	SPE	PANI-GO	DPV	Pb^{2+}	Peach juice, orange juice, grape juice and mineral water	0.5–10 µM	0,004 µM	[36]

metals (such as iron, magnesium and zinc) and dielectric and semiconducting materials (such as silicon), which can only be taken in very small amounts at the level of micrograms per day [39]. Some edible materials and their potential as supercapacitor components were investigated in this chapter.

In Fig. 2, we have a simplified diagram of a typical supercapacitor's explosive perspective, which includes the packaging, current collectors, electrode materials, electrolyte and separator. As shown in Fig. 2, all of the components are either food-related or dietary-related in nature. In Fig. 2b, we see an opening supercapacitor with activated charcoal serving as the electrode, cheese acting as the segregation layer, and seaweed performing the role of the separator. Activated charcoal (Nature's Way Products, Inc.; Green Bay, WI) from capsules of nutritional supplements was employed as electrode materials (see Fig. 2a, b for an example of these components). The TEM image is shown in Fig. 2c (TEM) activated charcoal micrograph showing individual carbon particles around 100 nm in size. Figure 2d shows that the surface area of the activated charcoal is around 1400 $m^2\ g^{-1}$, which is on par with activated carbon materials utilized in the vast majority of supercapacitors [40]. Edible binders are used to combine active charcoal particles into a continuous film for use as electrodes. Electrodes often employ egg whites, a common binder in the food industry, as a binding agent. Egg whites are utilized as binders in the food processing industry due to the existence of hydrogen bonds and ionic interactions with proteins, which enable the creation of films with high adhesive strength [41, 42]. Inert metals are put to use as current collectors; examples include the thin gold leaf used in artisanal baking and many Eastern cuisines. Pure gold leaves are safe to ingest gold with a purity of more than 23 karats referred to as E175 in the European Union's nomenclature for food production. The four-point probe determined that the sheet resistance of the gold leaf (with a thickness of 3–5 m) was 0.48 sq^{-1}.

Activated charcoal's high electrical conductivity and gold leaves' chemical stability make them ideal components in edible electronics. Their chemical stability makes it possible to consume considerable quantities. For instance, a single dosage of activated charcoal 100 g may induce pulmonary aspiration because the dose is so large [40]. However, less than 1 g of a charcoal is adequate to store enough energy to run a commercial device, thus the worst-case scenario is not even necessary. Adding edible gold leaf to foods is not restricted by any established dose limits. Contrarily, the NIH recommends no more than a daily intake of 0.03, 0.4, and 0.015 g of iron, magnesium, and zinc, respectively, which severely restricts the range of possible uses for these metals in biodegradable and bioresorbable electronics.

The scanning electron microscopy (SEM) picture of the electrode cross-section with a typical thickness of 120 m is shown in Fig. 2e. The separator must allow ions to pass through it yet have a sufficient electrical resistance to prevent current from flowing between the electrodes. This example shows roasted seaweed, a popular snack that is also widely utilized in sushi, with multilayer hydrophilic structures that might function as separators [40]. Cross-sectional SEM picture of roasted seaweed revealing multilayer structure (Fig. 2f). The roasted seaweed was found to have a permittivity of 52 $g^{-1}m^2s^{-1}$.

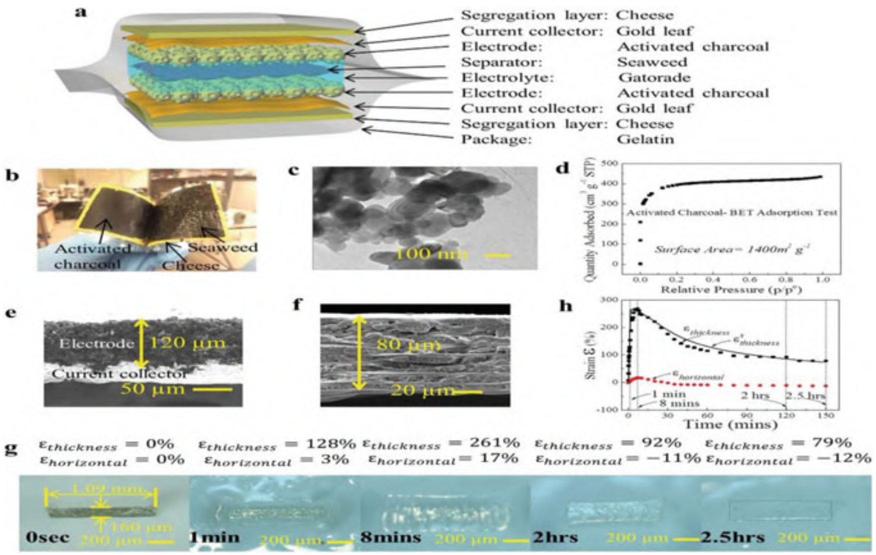
a
Segregation layer: Cheese
Current collector: Gold leaf
Electrode: Activated charcoal
Separator: Seaweed
Electrolyte: Gatorade
Electrode: Activated charcoal
Current collector: Gold leaf
Segregation layer: Cheese
Package: Gelatin
b
Activated charcoal
Seaweed
Cheese
c
100 nm
d
Quantity Adsorbed (cm³ g⁻¹ STP)
Activated Charcoal- BET Adsorption Test
Surface Area= 1400m² g⁻¹
Relative Pressure (p/p°)
e
Electrode
120 µm
Current collector
50 µm
f
80 µm
20 µm
h
Strain ε (%)
ε thickness
ε^s thickness
ε horizontal
1 min
8 mins
2 hrs
2.5 hrs
Time (mins)
g
ε thickness = 0% ε horizontal = 0%
ε thickness = 128% ε horizontal = 3%
ε thickness = 261% ε horizontal = 17%
ε thickness = 92% ε horizontal = −11%
ε thickness = 79% ε horizontal = −12%
1.09 mm
160 µm
0sec 200 µm
1min 200 µm
8mins 200 µm
2hrs 200 µm
2.5hrs 200 µm

Fig. 2 Illustration and study of the edible supercapacitor's constituent ingredients. **a** A structural diagram of an edible supercapacitor displaying the activated charcoal electrode, the seaweed separator, the seaweed separator, the cheese segregation layer, and the gelatin packaging. **c** TEM picture reveals that the average grain size of activated charcoal is around 100 nm. **d** Activated charcoal's surface area is shown to be about 1400 m^2 g^{-1} using the Brunauer–Emmett–Teller (BET) test. **e** Cross-sectional SEM view of the activated charcoal electrode. **f** Photographic slice through a seaweed separator revealing the layered structure. **g** Gelatin dissolution test in artificial gastric fluid. The gelatin becomes indistinguishable from water after 2.5. **h** Strains developed from tests and simulations evolve over time. $\varepsilon_{\text{thickness}}$ is the strain in the thickness direction from experiment, $\varepsilon_{\text{strain}}$ in the thickness direction from simulation, and $\varepsilon_{\text{horizontal}}$ is the strain in the horizontal direction from experiment. Since the horizontal strain is much smaller compared to the strain in the thickness direction, it is disregarded in the simulation.

Aside from the battery, researchers have also looked at the electrolyte and the packaging. The sheets of gelatin (Modernist Pantry, LLC; York, ME) are utilized in the food industry and in numerous medicinal capsules. At 25 °C, as shown in Fig. 1g, a gelatin sheet may be shown being digested in situ while being horizontally constricted in a simulated stomach fluid. Microscopically (Nikon eclipse lv100, 5X objective), after 2.5 h, a gelatin sheet with an initial cross-sectional area of 160 m, 1090 m has shrunk due to the digestion of gelatin and is no longer distinguishable from the simulated gastric fluid. During the process (swelling to shrinkage), the maximum strain in the horizontal direction is only $\varepsilon_{\text{horizontal}}$ 17%, whereas the corresponding strain in the thickness direction is ($\varepsilon_{\text{thickness}}$) 261%. This is due to the limitation in the horizontal direction. This process of quasi-1D restricted digestion may be explained by a theoretical model that incorporates the interplay between mass diffusion, chemical reaction, and massive mechanical deformation. The temporal evolutions of the ($\varepsilon_{\text{horizontal}}\ and\ \varepsilon_{\text{thickness}}$) determined experimentally and numerically demonstrate excellent agreement (Fig. 2h). Crosslinking treatment significantly increases gelatin's stability and stability in humid, acidic, and high-temperature settings, as has been established in several prior investigations [43]. By focusing on surface modification and crosslinking, researchers want to make gelatin dissolving more manageable in our continuing treatment effort.

The electrolyte was a polyelectrolyte drink like Gatorade (Chicago, IL) with a high ionic conductivity (>2 mS cm^{-1}) due to the presence of sodium, potassium, citrate and other stabilizing ingredients. To prevent the extremely hydrophilic gelatin sheet (packaging) and gold leaf (current collector) from coming into direct contact with the gelatin and electrolyte, a segregation layer of cheese slices (Lucerne Foods, Inc.; Pleasanton, CA) was used. The package was then thermally sealed using a controlled-heat impulse sealer. This led to the construction of a supercapacitor made completely of food items such as activated charcoal, egg white, gold leaf, roasted seaweed, Gatorade, cheese and gelatin.

4 Conclusions and Perspectives

Nanotechnology has the potential to enhance the quality of food and drink by reducing pollution and other health risks, but it also poses risks to human health in other contexts. In virtue of the exciting physical and chemical features of nanomaterials, supercapacitors that exploit them have risen in popularity in recent years. Food and drink samples may be analyzed in real time with the use of their features, such as portability, speed, selectivity, and sensitivity. These one-of-a-kind supercapacitors are low-cost and simple to implement, suggesting they may find widespread usage in the food and beverage industry, especially in economically impoverished regions.

In this chapter, we discuss the analyte properties of carbon-based and metal (oxide) based nanomaterials supercapacitors used to ensure the safety of the food and beverage sector. Academics have broadly divided pollutants in the food and drink industry into three categories: organic, toxic and inorganic. Researchers have concentrated on developing derivatives of functional nanomaterials that may serve as conductive electrode sites and catalysts in the food and beverage industries, among other applications. Various investigations have emphasized the synergistic impacts of NPs of noble metals and carbon-based nanomaterials. There is still a significant problem that restricts the use of these analytical tools, and that is the stability and performance of the supercapacitors associated with nanomaterials. As a result, additional research has to be done to address this obstacle before supercapacitors can be mass-produced.

In the future, mechanical action in the process of determining food and beverage may swiftly change the functionalized nanomaterials over the site of the electrode, which can impact the sensitivity, favor life and accuracy of the electrode. Improving the long-term stability of supercapacitors in the context of food analysis necessitates the use of techniques such as optimizing manufacturing, creating adequate isolation fitting and covalent bonding. Because of the rigorous requirements of the specification environment, functionalizing nanomaterials is increasingly important in the context of genuine food samples. Supercapacitors' performance may be improved by the strategic placement of functionalized nanomaterials, which has been shown to increase both their quantity and mechanical properties. It should be noted, however, that its characteristics are constrained by several performance flaws in the control of its directional adjustment. Furthermore, how to precisely characterize the structural property of the functionalized nanomaterials in the process of determining the promoted supercapacitors is a further unresolved challenge. Functionalized nanoparticles provide a challenge for the food and beverage sector because of the necessity to develop and master more sophisticated methods of measurement and combination that can more quickly characterize the trace analyte.

References

1. Vieira Jodar L, Orzari LO, Storti Ortolani T, Assumpção MH, Vicentini FC, Janegitz BC (2019) Electrochemical sensor based on casein and carbon black for bisphenol a detection. Electroanalysis 31(11):2162–2170. https://doi.org/10.1002/elan.201
2. Della Pelle F, Rojas D, Scroccarello A, Del Carlo M, Ferraro G, Di Mattia C, Compagnone D. High-performance carbon black/molybdenum disulfide nanohybrid sensor for cocoa catechins determination using an extraction-free approach. Sens Actuators B
3. Vilian AE, Sivakumar R, Huh YS, Youk JH, Han YK. Palladium supported on an amphiphilic triazine-urea-functionalized porous organic polymer as a highly efficient electrocatalyst for electrochemical sensing of rutin in human plasma, ACS Appl Mater
4. Kumar N, Goyal RN (2018) Silver nanoparticles decorated graphene nanoribbon modified pyrolytic graphite sensor for determination of histamine. Sens Actuators B Chem 268:383–391. https://doi.org/10.1016/j.snb.2018.04.136
5. Zheng W, Xiong Z, Li H, Yu S, Li G, Niu L, Liu W (2018) Electrodeposited Pt@ molecularly imprinted polymer core-shell nanostructure: enhanced sensing platform for sensitive and selective detection of bisphenol A. Sens Actuators B Chem 272:65
6. Herrera-Chacón A, Dinç-Zor Ş, del Valle M (2020) Integrating molecularly imprinted polymer beads in graphite-epoxy electrodes for the voltammetric biosensing of histamine in wines. Talanta 208:120348. https://doi.org/10.1016/j.talanta.2019.120348
7. Teker T, Aslanoglu M (2020) A novel voltammetric sensing platform based on carbon nanotubes-niobium nanoparticles for the determination of chlorogenic acid. Arab J Chem 13(5):5517–5525. https://doi.org/10.1016/j.arabjc.2020.03.029
8. Wu Y, Lei W, Xia M, Wang F, Li C, Zhang C, Zhang Y (2018) Simultaneous electro-chemical sensing of hydroquinone and catechol using nanocomposite based on palygorskite and nitrogen doped graphene. Appl Clay Sci 162:38–45. https://doi.org/10.1016/j.clay.2018.05.026
9. Moraru CI et al (2003) Nanotechnology: a new frontier in food science. Food Technol 57:24–29
10. da Silva W, Ghica ME, Ajayi RF, Iwuoha EI, Brett CM (2019) Impedimetric sensor for tyramine based on gold nanoparticle doped-poly (8-anilino-1-naphthalene sulphonic acid) modified gold electrodes. Talanta 195:604–612. https://doi.org/10.1016/j.talanta.2018.11.054
11. Sha T, Liu J, Sun M, Li L, Bai J, Hu Z, Zhou M (2019) Green and low-cost synthesis of nitrogen-doped graphene-like mesoporous nanosheets from the biomass waste of okara for the amperometric detection of vitamin C in real samples. Talanta 200:300
12. He L, Zou W, Zeng D, Gong F, Wang Q, Xia J, Cao Z (2020) Highly fluorescent dihydropyrimido-diindole derivative as a probe for detecting nitrite in food products and cell-imaging. Dyes Pigments 177:108256. https://doi.org/10.1016/j.dyepig.2020
13. Yue X, Zhou Z, Wu Y, Jie M, Li Y, Guo H, Bai Y (2020) A green carbon dots-based fluorescent sensor for selective and visual detection of nitrite triggered by the nitrite–thiol reaction. New J Chem 44(20):8503–8511. https://doi.org/10.1039/D0NJ01025A

14. Carlos KS, Conrad SM, Handy SM, de Jager LS (2020) Investigation of food products containing garlic or onion for a false positive sulphite response by LC-MS/MS. Food Addit Contam, Part A 37:1–8. https://doi.org/10.1080/19440049.2020.1727965
15. Póti P, Pajor F, Bodnár Á, Bárdos L (2020) Accumulation of some heavy metals (Pd, Cd and Cr) in milk of grazing sheep in north-east Hungary. J Microbiol Biotechnol Food Sci 9(6):389–394
16. Hasan AB, Reza AS, Kabir S, Siddique MAB, Ahsan MA, Akbor MA. Accumulation and distribution of heavy metals in soil and food crops around the ship breaking area in southern Bangladesh and associated health risk assessment. SN Appl Sci 2(2)
17. Zhou Q, Tang D (2020) Recent advances in photoelectrochemical biosensors for analysis of mycotoxins in food. TrAC Trends Anal Chem 124:115814. https://doi.org/10.1016/j.trac.2020.115814
18. Ndagijimana R, Shahbaz U, Sun X (2020) Aflatoxin B1 in food and feed: an overview on prevalence, determination and control tactics. J Artif Intell Res 8:144
19. Schrenk D, Bodin L, Chipman JK, del Mazo J, Grasl-Kraupp B, Nielsen E (2020) Risk assessment of ochratoxin A in food. EFSA J 18(5):e06113. https://doi.org/10.2903/j.efsa.2020.6113
20. Piri S, Piri F, Yaftian MR, Zamani A (2018) Imprinted Azorubine electrochemical sensor based upon composition of MnO2 and 1-naphthylamine on graphite nanopowder. J Iran Chem Soc 15(12):2713–2720. https://doi.org/10.1007/s13738-018-1459-z
21. Hussain CM (2018) Handbook of nanomaterials for industrial applications. Elsevier
22. Hussain CM (2019) Handbook of environmental materials management. Elsevier
23. Raril C, Manjunatha JG, Ravishankar DK, Fattepur S, Siddaraju G, Nanjundaswamy L. Validated electrochemical method for simultaneous resolution of tyrosine, uric acid, and ascorbic acid at polymer modified nano-composite paste electrode. Surf Eng Appl Electrochem
24. Raril C, Manjunatha JG, Nanjundaswamy L, Siddaraju G, Ravishankar DK, Fattepur S, Niranjan E (2018) Surfactant immobilized electrochemical sensor for the detection of indigotine. Anal Bioanal Electrochem 10(11):1479–1490
25. Yang T, Meng L, Zhao J, Wang X, Jiao K (2014) Graphene-based polyaniline arrays for deoxyribonucleic acid electrochemical sensor: effect of nanostructure on sensitivity. ACS Appl Mater Interf 6:19050–19056
26. Yao J, Chen M, Li N, Liu C, Yang M. Experimental and theoretical studies of a novel electrochemical sensor based on molecularly imprinted polymer and B, N, F-CQDs/AgNPs for enhanced specific identification and dual signal amplification in highly selective and ultra-trace bisphenol S determination in plastic products
27. Vilian AE, Kang SM, Oh SY, Oh CW, Umapathi R, Huh YS, Han YK. A simple strategy for the synthesis of flower-like textures of Au-ZnO anchored carbon nanocomposie towards the high-performance electrochemical sensing of sunset yellow. Food Chem
28. Gao J, Yuan Q, Ye C, Guo P, Du S, Lai G, Chee KW (2018) Label-free electrochemical detection of vanillin through low-defect graphene electrodes modified with Au nanoparticles. Materials 11(4):489. https://doi.org/10.3390/ma11040489
29. Tajeu KY, Dongmo LM, Tonle IK (2020) Fullerene/MWCNT/Nafion modified glassy carbon electrode for the electrochemical determination of caffeine. Am J Anal Chem 11(2):114–127
30. Manikandan VS, Liu Z, Chen A (2018) Simultaneous detection of hydrazine, sulfite, and nitrite based on a nanoporous gold microelectrode. J Electroanal Chem 819:524–532. https://doi.org/10.1016/j.jelechem.2018.02.004
31. Koçak ÇC, Karabiberoğlu Ş (2018) Electrochemical vanillin determination on gold nanoparticles modified multiwalled carbon nanotube electrode. J Sci Eng 20(59). https://doi.org/10.21205/deufmd.2018205936
32. Yao Y, Wu H, Ping J (2019) Simultaneous determination of Cd (II) and Pb (II) ions in honey and milk samples using a single-walled carbon nanohorns modified screen-printed electrochemical sensor. Food Chem 274:8–15. https://doi.org/10.1016/j.foodche
33. Manikandan VS, Sidhureddy B, Thiruppathi AR, Chen A (2019) Sensitive electrochemical detection of caffeic acid in wine based on fluorine-doped graphene oxide. Sensors 19(7):1604. https://doi.org/10.3390/s19071604

34. Manasa G, Mascarenhas RJ, Satpati AK, Basavaraja BM, Kumar S (2018) An electro-chemical Bisphenol F sensor based on ZnO/G nano composite and CTAB surface modified carbon paste electrode architecture. Colloids Surf B: Biointerf 170:144–151
35. Rana S, Kaur R, Jain R, Prabhakar N. Ionic liquid assisted growth of poly (3, 4-ethylenedioxythiophene)/reduced graphene oxide based electrode: an improved electro-catalytic performance for the detection of organophosphorus pesticides in beverages, Arab J Chem
36. Wang J, Zhu W, Zhang T, Zhang L, Du T, Zhang W, Wang J (2020) Conductive polyaniline-graphene oxide sorbent for electrochemically assisted solid-phase extraction of lead ions in aqueous food samples. Anal Chim Acta 1100:57–65. https://doi.org/10.1016/j.aca.2019.11.070
37. Yin L, Huang X, Xu H, Zhang Y, Lam J, Cheng J, Rogers JA (2014) Adv Mater 26:3879
38. Kim YJ, Wu W, Chun SE, Whitacre JF, Bettinger CJ (2013) Proc Natl Acad Sci USA 110:20912
39. Li Z, Young D, Xiang K, Carter WC, Chiang YM (2013) Adv Energy Mater 3:290
40. Dorrington CL, Johnson DW, Brant R (2003) Ann Emerg Med 41:370
41. Siegel DG, Church KE, Schmidt GR (1979) J Food Sci 44:1276
42. Gennadios A, Handa A, Froning GW, Weller CL, Hanna MA (1998) J Agric Food Chem 46:1297
43. Digenis GA, Gold TB, Shah VP (1994) J Pharm Sci 83:915

Всё для победы!
НАРОДНЫЙ ФРОНТ
https://pobeda.onf.ru/
LET'S HELP THE RUSSIA

Chapter 20
Polymers Nanocomposite Supercapacitors for Water Treatment and Food Packaging

C. P. Devipriya, B. Sumathi, S. Bamini, and V. Sabari

1 Introduction

"Nanoscience and nanotechnology" deal with the design, fabrication, and characterization, evaluation of properties, and ultimate applications of materials with nanoscale dimensions. Nanoscience and nanotechnology are the most interesting fields for researchers since the past century. A numbers of developments have been made since then in the field of nanotechnology.

Types of Nanoparticles

1. Metal nanoparticles,
2. Non-metal ceramic nanoparticles,
3. Semiconductor nanoparticles, and

C. P. Devipriya · B. Sumathi · V. Sabari (✉)
Research Scholar, PG & Research Department of Physics, Government Thirumagal Mills College, Gudiyattam, Tamilnadu, India
e-mail: vrsabari0306@gmail.com

S. Bamini
Research Department of Mathematics, Marudhar Kesari Jain College for Women, Vaniyambadi, Tamilnadu, India

B. Sumathi
Research Scholar, PG & Research Department of Physics, Government Thirumagal Mills College, Gudiyattam, India

V. Sabari
Research Coordinator, PG & Research Department of Physics, Marudhar Kesari Jain College for Women, Vaniyambadi, India

S. Bamini
Research Coordinator, PG & Research Department of Mathematics, Marudhar Kesari Jain College for Women, Vaniyambadi, India

© The Author(s), under exclusive license to Springer Nature Singapore Pte Ltd. 2024

C. M. Hussain and M. B. Ahamed (eds.), *Functionalized Nanomaterials Based Supercapacitor*, Materials Horizons: From Nature to Nanomaterials,
https://doi.org/10.1007/978-981-99-3021-0_20

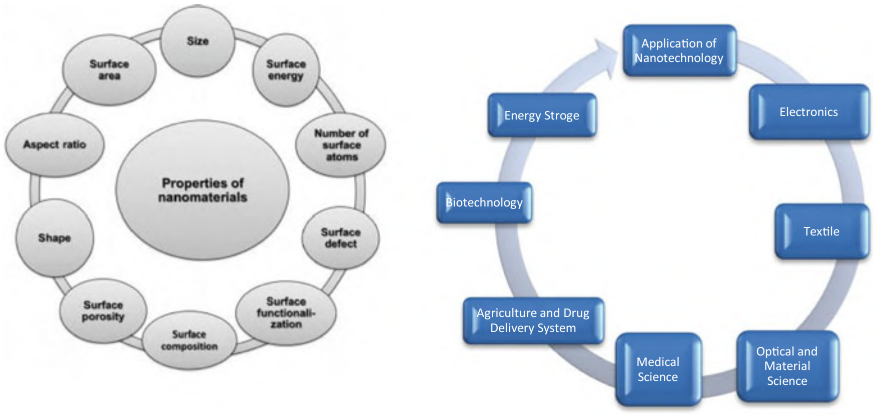
Properties of nanomaterials
Size
Surface energy
Number of surface atoms
Surface defect
Surface functionalization
Surface composition
Surface porosity
Shape
Aspect ratio
Surface area
Application of Nanotechnology
Electronics
Textile
Optical and Material Science
Medical Science
Agriculture and Drug Delivery System
Biotechnology
Energy Stroge

(a) Properties of nanomaterials **(b) Application of Nanotechnology**

Fig. 1 **a** Properties of nanomaterials. **b** Application of nanotechnology

4. Carbon nanoparticles.

Nanotechnology advent the introduction of exciting research areas by exploiting renewable nanomaterials as reinforcements in order to advance materials with innovative properties. Interestingly, nanoscience is a multidisciplinary of chemistry, physics, biology, and materials science that deals with the manipulation and characterization of matter on length scales between the molecular and the micron size [1, 2] (Fig. 1).

1.1 Historical Background of Nanomaterials

The history of nanomaterials is very old, as the existence of a few nanostructured materials has been found in nature itself. Volcanic eruptions, early meteorites, seashells, skeletons, etc. are the creation of nature that generates nanostructured materials. The day fire was discovered, nanoscale smoke particles were formed. However, synthetic nanomaterials were produced much later in laboratories, though the colloidal gold particles had been reported by ***Michael Faraday in 1857***. In the early 1940s, precipitated and fumed silica nanoparticles had begun their industrial manufacture in the United States and Germany as the replacement of ultrafine carbon black for the reinforcement of silicone rubber. Between the 1960s and 1970s, metallic nanopowders for magnetic recording tapes were also developed. Polymer nanocomposites started to develop in the late 1980s in both commercial research organizations and academia laboratories, though the term "***nanocomposite***" had first been coined by ***Theng in 1970***. The reinforcing effect of carbon black filler (individual particles are in nm size) to elastomer was again noticed in the first decade of the twentieth century, though this vulcanizate was never considered as nanocomposite because the size of filler in the matrix is in μm in dimension [3]. The incorporation of layered silicates into polymer matrices has been known for more than half a century. One of the earliest reports described the stable uniform dispersion of ***metallic cobalt particles*** about 100 nm in size in polymer by ***Hess and Parker*** in 1966. However, the actual journey for polymer ***nanocomposites*** started in 1988, when Toyota Company of Japan first used polymer/layered silicate nanocomposite for the production of their novel car models. However, the term "nanocomposite" is universally accepted after Komarneni (1992). The polymeric materials involve at least one of the domains in the size range of 1–100 nm, where the properties are of interest due to the size of the structures, and are typically different from the bulk polymers. In 2021, China has begun to completely ban non-degradable plastic products, especially food packaging materials. Therefore, people are very concerned about the development and application of fully functional food packaging materials.

1.2 Supercapacitor

A supercapacitor (SC), also called ***an ultracapacitor***, is a high-capacity capacitor, with a capacitance value much higher than other capacitors but with lower voltage limits. It bridges the gap between electrolytic capacitors and rechargeable batteries. It typically stores 10 to 100 times more energy per unit volume or mass than electrolytic capacitors, can accept and deliver charge much faster than batteries, and tolerates many more charge and discharge cycles than rechargeable batteries[4].

Supercapacitors are used in applications requiring many rapid charge/discharge cycles, rather than long-term compact energy storage in automobiles, buses, trains, cranes, and elevators, where they are used for regenerative braking, short-term energy storage, or burst-mode power delivery[5]. Smaller units are used as power backup for ***static random-access memory*** (SRAM).

1.3 Composites

Composites are naturally occurring solid materials which result when two or more different constituent materials produced, each having its own significant characteristic (physical or chemical properties) are combined together to create a new substance with superior properties than original materials in a specific finished structure [6, 7].

Properties of Composites

- Stiffness and strength,
- Low coefficient of expansion,

- Resistance against fatigue,
- Ease in manufacturing complex shapes,
- Simple repair of damaged structures, and
- Resistance to corrosion.

1.3.1 Nanocomposites

Nanocomposites are those composites in which one phase has nanoscale morphology like nanoparticles, nanotubes, or lamellar nanostructure. They have multiphase, so are multiphasic materials, at least of the phases should have dimensions in the range of 10–100 nm. Nowadays to overcome the limitation of different engineering materials, nanocomposites have emerged to provide beneficial alternatives.

Advantages of nanocomposites

Nanocomposites are the solid combination of a bulk matrix and nanodimensional phase(s), which differ in properties due to dissimilarities in structure and chemistry.

Properties of nanocomposites

- Mechanical properties (strength, bulk modules, withstands limit, etc.),
- Thermal stability,
- Hinders flame and reduces smoke generations,
- Permeability of gases, water, and solvents is reduced,
- More surface appearance,
- Improved electrical conductivity, and
- Increased chemical resistance.

Among several nanocomposites, polymer-based nanomaterials are the leading materials of current research and development. Characteristics like film-forming ability, activated functionalities, and dimensional variability provide lots of benefits to polymer-based nanocomposites [8].

The potential risk of nanocomposites commonly occurs majorly in areas like

- Risk to health and environment,
- Molecular manufacturing, and
- Societal risks.

1.3.2 Polymer Composites

The term composite materials was first used during the 1960s. Composite materials have been used by the people of earlier civilizations for many centuries. One of the finest examples includes the preparation of bricks for building construction using straw and mud [9].

Polymer composites have been classified into two phases:

1. Polymer or matrix and

2. Binder as the second phase.

Binder includes reinforcing fibers or nanoparticles in a matrix to improve dimensional and thermal stability, stiffness, toughness, and tensile strengths. The fabrication of composites is represented in Fig. 2. Moreover, composites can be classified into three subclasses, including particles, fibers, and structural-based composites, shown in Figure 3 (http://textilelearner.blogspot.my/2012/09/glass-fiber-composites-properties-of.html).

The development of polymer composite materials displays keen interest as they are lightweight, flexible, tougher, and are usually fabricated on large sizes into intricately shaped components for industrial applications by combining large varieties of reinforcements and polymers [10, 11].

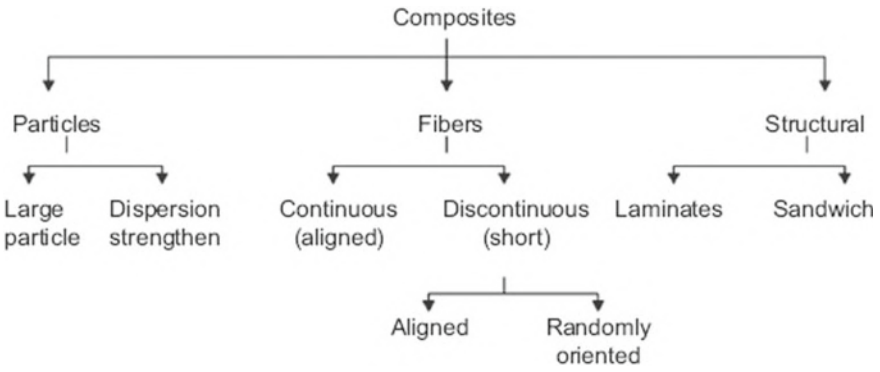
Composites
Particles
Fibers
Structural
Large particle
Dispersion strengthen
Continuous (aligned)
Discontinuous (short)
Laminates
Sandwich
Aligned
Randomly oriented

Fig. 2 Classification of polymer composites

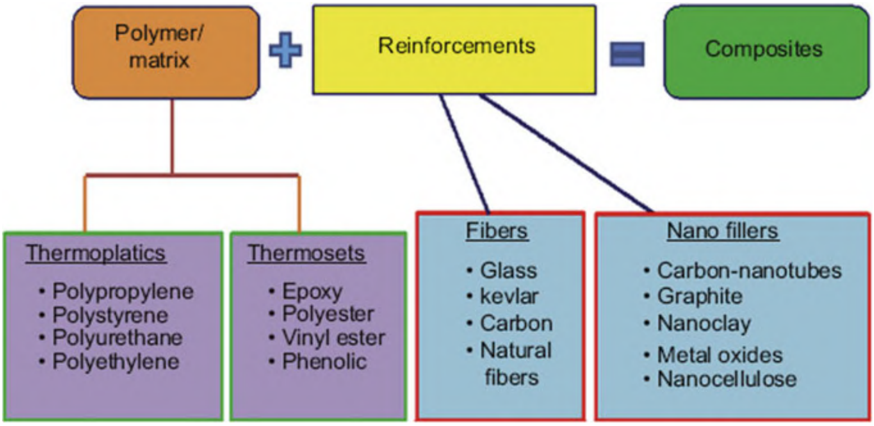
Polymer/ matrix
+
Reinforcements
=
Composites
Thermoplatics
• Polypropylene
• Polystyrene
• Polyurethane
• Polyethylene
Thermosets
• Epoxy
• Polyester
• Vinyl ester
• Phenolic
Fibers
• Glass
• kevlar
• Carbon
• Natural fibers
Nano fillers
• Carbon-nanotubes
• Graphite
• Nanoclay
• Metal oxides
• Nanocellulose

Fig. 3 Scheme of the polymer composites (http://textilelearner.blogspot.my/2012/09/ glass-fiber-composites-properties-of.html)

The structure of nanocomposites usually consists of matrix material containing nano-sized reinforcement components in the form of particles, whiskers, fibers, and nanotubes. Nanocomposites exhibit light weight, good dimensional stability, enhanced heat and flame resistance, as well as barrier properties with far less loading of nanoparticles than conventional composite counterparts [12].

Nanocomposites (NCs) have been used in automotive, packaging, building, and agricultural materials [13]. Various polymeric nanocomposites have been extensively studied, including polyamide, epoxy, polyester, polystyrene, and polypropylene [14]. In recent years, to solve the waste disposal problem of plastic materials, biodegradable polymers have become an important trend [15]. Adding nano-fillers into the biodegradable polymers can increase the mechanical, thermal, dimensional, and barrier properties of the composite films. PBAT (poly(butylene adipate-co-terephthalate)) is a large-scale polymer product used extensively to produce fibers, films, and packaging materials due to its good mechanical and optical properties [3, 16] resistance to creep fracture, and resistance to fatigue and wear. The development of composite PBAT has led to materials with additional functional properties such as antibacterial activity [17, 18]. The high-performance, biodegradable PBS/PBAT composite film exhibited enhancement in tensile strength and elongation at break. This blended composite indicates that good compatibility is achieved between the polymers [19]. PBAT containing SiO_2 film may be a promising novel material for active food packaging applications.

Polymer nanocomposites can be fabricated and processed in ways similar to that of conventional polymer composites, which makes them particularly attractive from a manufacturing point of view. Polymer composites are able to meet diverse design requirements with significant weight savings, as well as high strength-to-weight ratio.

Polymer nanocomposites are composites in which at least one of the phases shows dimensions in the nanometer range ($1\ \text{nm} = 10^{-9}\ \text{m}$). They are reported to be the materials of the twenty-first century in the view of possessing design uniqueness and property combinations that are not found in conventional composites [20]. Nanocomposite materials signify as the most encouraging and promising family of material science to overcome the limitations of microcomposites and monolithics, while posing preparation challenges related to the control of elemental composition and stoichiometry in the nanocluster phase (Fig. 4).

2 Food Packing for Nanomaterials

In everyday life, several ***metallic and nonmetallic materials*** are used in the ***food and pharmaceutical industries***. With numerous practical functionalities and interesting characteristics such as durability, gas barrier properties, and freedom of design, materials like tinplate, aluminum, and high-density polyethylene or polycarbonate are widely encountered in the packaging markets and are highly efficient as food containers. One of the global subjects of interest to scientific researchers, food packaging is expected to be stable under various conditions from its manufacturing to

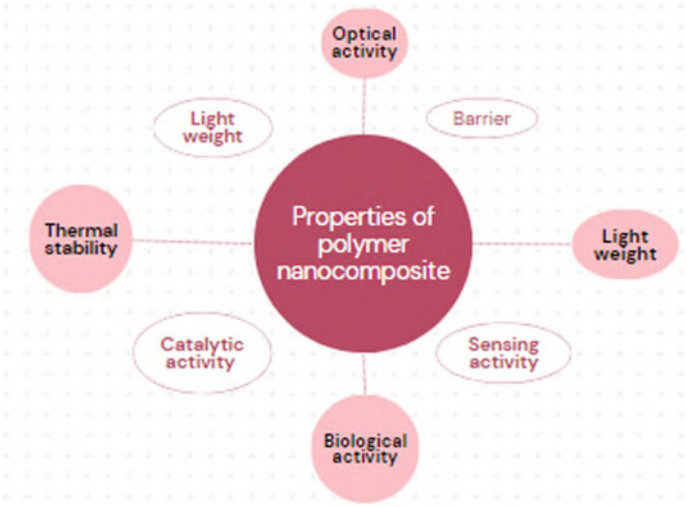
Optical activity
Light weight
Barrier
Thermal stability
Properties of polymer nanocomposite
Light weight
Catalytic activity
Sensing activity
Biological activity

Fig. 4 Properties of polymer nanocomposites

the consumption of food by the consumer, and must offer optimum protection of the packaged product during this process. During the past decades, classical packaging has demonstrated various problems and has created a large gap in the food industry.

Nowadays, the use of plastics in the food markets because such materials are not biodegradable and every piece of plastic ever made is still on this planet [21], thus generating notable waste pollution and impacting the earth's ecosystems. In addition, corrosion phenomena can highly limit the usage of metals like tinplate or aluminum as packaging for food despite offering numerous required properties that provide a safe and long shelf-life of products (heat resistance, full recyclability, durability, and good conductivity) [22] (Figs. 5 and 6).

2.1 Classification of Nano-packaging Systems

Based on researches lab, market applications, and development trends suggest the existing of various categories of nanotechnology applications in the food packaging industry: ***improved packaging, intelligent packaging, and active packaging*** [23, 24].

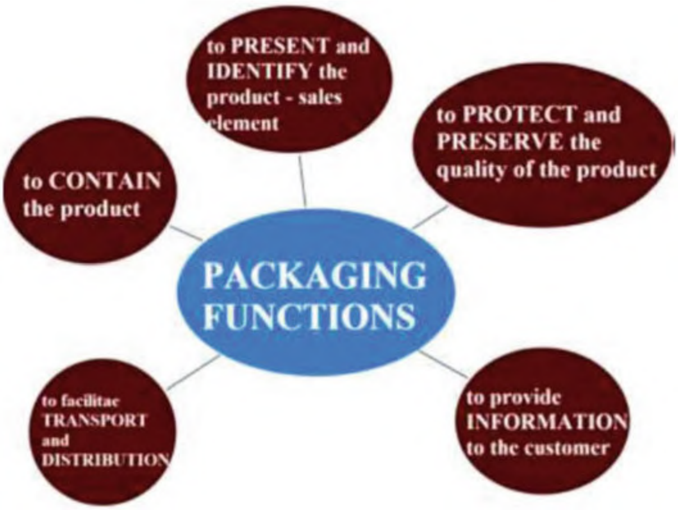
PACKAGING FUNCTIONS
to PRESENT and IDENTIFY the product - sales element
to PROTECT and PRESERVE the quality of the product
to CONTAIN the product
to facilitae TRANSPORT and DISTRIBUTION
to provide INFORMATION to the customer

Fig. 5 Use of nanotechnology packing system

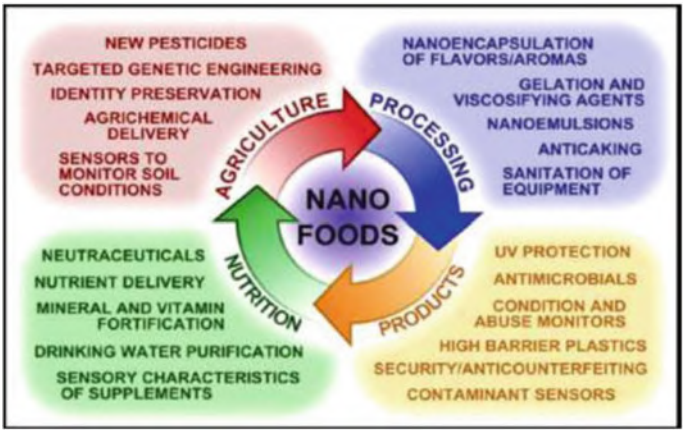
NANO FOODS
AGRICULTURE
PROCESSING
PRODUCTS
NUTRITION
NEW PESTICIDES
TARGETED GENETIC ENGINEERING
IDENTITY PRESERVATION
AGRICHEMICAL DELIVERY
SENSORS TO MONITOR SOIL CONDITIONS
NANOENCAPSULATION OF FLAVORS/AROMAS
GELATION AND VISCOSIFYING AGENTS
NANOEMULSIONS
ANTICAKING
SANITATION OF EQUIPMENT
NEUTRACEUTICALS
NUTRIENT DELIVERY
MINERAL AND VITAMIN FORTIFICATION
DRINKING WATER PURIFICATION
SENSORY CHARACTERISTICS OF SUPPLEMENTS
UV PROTECTION
ANTIMICROBIALS
CONDITION AND ABUSE MONITORS
HIGH BARRIER PLASTICS
SECURITY/ANTICOUNTERFEITING
CONTAMINANT SENSORS

Fig. 6 Nanotechnology application in different food sectors

2.1.1 Improved Packaging

Improved packaging can be achieved using materials for instance clay, silica, cellulose and chitosan, carbon nanotubes, and starch, as these materials provide flexibility, gaseous exchange and maintain temperature and humidity [25]. Improved packaging provides several features, which involve remarkable antimicrobial spectrum and novel properties to the packaging material with ***low cost for food packaging*** [26].

Clay and Silicate Nanoplatelets

Clay is one of the most widely studied materials in the food packaging industry, where different nanocomposites were developed using synthetic polymers to improve food packaging properties [27]. In addition, the combination of silicates and polymers gives preferred properties such as an excellent barrier [28–30].

2.1.2 Smart Packaging (SP) Systems

Smart food packaging is becoming increasingly popular among customers. This is because it can offer communication to consumers as to the status of the product. Due to consumer preference for safe and high-quality food, the market for smart food packaging is growing. Based on renewable natural biopolymers, a variety of packaging materials have already been developed, such as polysaccharides, proteins, and lipids, all of these materials have some limitations, such as they incorporate costly raw ingredients, impair processing difficulties, have poor mechanical and thermal properties or carry negligible electrical conductivity. All these factors show a great need for the development of new packaging materials to address all of these issues in order to provide safer and natural food packaging materials. Among metallic nanoparticles, the most commonly used components are identified as Au, Zn, Cu, Ag, Fe, Sn, and Ti. From those listed, silver nanoparticle (AgNP) is a well-established antimicrobial metal nanoparticle. Silver ions ($Ag^{+)}$, which can dissociate from the AgNPs, have been reported to be non-toxic ingredients to human cells, though they can still have antimicrobial effects at lower concentrations [16, 17].

According to the report of the Food and Drug Administration (FDA), AgNPs are the safe metal nanoparticle; therefore, they have been permitted to be used in all of the food-contact polymer materials in the USA market. The European Union issued a new regulation, EU n. 10/2011 commission 14 January 2011, for food packaging materials where they permitted silver compounds to be applied with the packaging materials. Instead, they considered the banning of some other metallic particles, such as lead (Pb), mercury (Hg), and titanium (Ti) nanoparticles, with the packaging materials. In the preceding studies, the migration of AgNPs from starch-based film and low-density polyethylene film has been described [18, 19]. However, the migration of such NPs to foods was negligible and below the limit of quantification [20]. After viewing all of these characterized features of AgNPs, NPs were chosen to synthesize with nanocellulose and activated carbon to promote good antibacterial, high electrical, and thermally characterized nanocomposite film for smart packaging. For the past few decades, carbon materials have gained tremendous attention to develop biosensor, electrical double-layer capacitors and supercapacitors, and energy storage devices (i.e., batteries) [31–34].

Smart food packaging systems provide enhanced functionality that can be divided into two submarkets:

1. **Active packaging (AP)**, which provides functionality such as gas, microbial, moisture, flavor/odor, temperature, chemical, and radiation controllers.

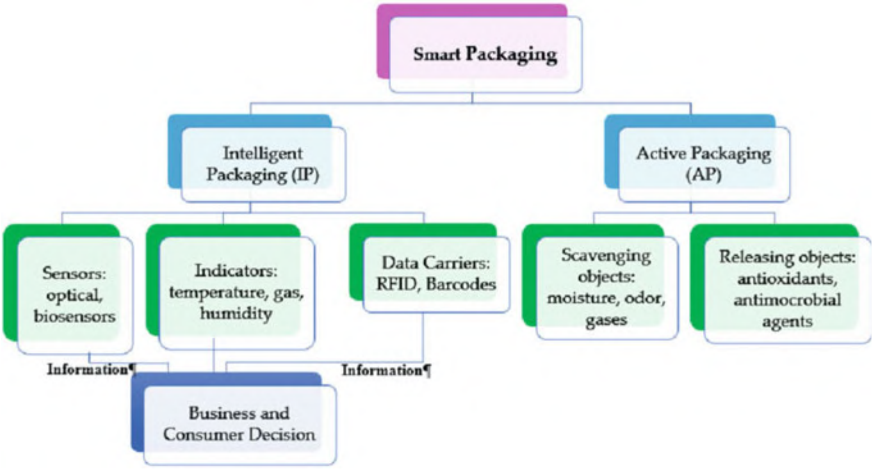
Smart Packaging
Intelligent Packaging (IP)
Active Packaging (AP)
Sensors: optical, biosensors
Indicators: temperature, gas, humidity
Data Carriers: RFID, Barcodes
Scavenging objects: moisture, odor, gases
Releasing objects: antioxidants, antimocrobial agents
Information¶
Information¶
Business and Consumer Decision

Fig. 7 Classification of smart packing

2. **Intelligent packaging (IP)**, which incorporates features that indicate status or communicate food environment changes information such as time, temperature, gas, pH, and freshness indicators [35] (Fig. 7).

Intelligent packaging is also known as intelligent packing one of the solutions offered to reduce food waste, detecting microbic and chemical changes in food, and aims for the monitoring of food products and factors surrounding and affecting it. Moreover, these novel food packaging systems provide the consumer with greater convenience in terms of (quality, distribution, and methods of preparation) [36]. In this packaging system, new and innovative methods and systems are used, such as nanosensors, time and temperature indicators, O_2 sensors, and freshness indicators [27, 37].

Recently, the use of nanotechnology in smart food packaging has been studied and this has been the goal of various food production companies around the world [24]. The application of nanotechnology in intelligent packaging involves different nanosensor systems such as oxygen indicators, time-temperature integrators (TTIs), and freshness and spoilage indicators[24].

2.1.3 Active Packaging

First, a summary of what AP can achieve: it can be used to eliminate an unwanted compound (e.g., ethylene produced by respiring fruits, or oxygen present inside a package), add a requisite compound (e.g., ethanol or carbon dioxide to inhibit microbial growth), prevent microbial growth (e.g., incorporate an antimicrobial (AM) chemical into a film), change a film’s permeability to gases as the temperature changes by several orders of magnitude greater than normal polymeric films, or change the

Table 1 History of nanomaterials, nanotechnology, and polymer nanocomposites

Fact of phenomenon	Associated name	Year
Natural fire and smoke (volcano, forest fire, etc..)	Nature	Millions of years ago
Controlled fire and smoke	Stone age people	~2 million years ago
Preparation of colloidal gold particles	M. Fayman	1857
Magnetic powder	W.E. Hoke	1920
Precipitated and fumed fine silica particles	US and German companies	1940
Nano thinking (there's plenty of room at the bottom)	R. Feyman	1959
Dispersion of metallic cobalt particles in the polymer	P.H. Hess and P.H. Parker	1966
The term "nanocomposites" was first coined	B.K.G. Theng	1970
Nanotechnology word (super thin material processing)	N. Taniguchi	1974
Nylon-6/layered silicate "nanocomposite"	Toyota, Japan	1988
Term "nanocomposite" is used in scientific literature	S. Komameni	1992

physical conditions inside the package (e.g., remove water vapor by absorption or change the temperature of the food).

Active food packaging can be defined as the packaging that changes the conditions of the packed food product for the purpose of increasing the product's validity or improving safety and defined as the type of packaging that is used to give an additional function and a protective barrier against external influences, and it is a phenomenon (that enables interaction, control or influence) that occurs inside the packaging [38]. Active food packaging may involve incorporating antioxidants, antimicrobials, pigments, nutrients, and nanoparticles into food packaging material [39]. Table 1 shows different active packaging types applied in food packaging. Nanomaterials (such as silver nanoparticles) are incorporated in such packaging systems to directly interact with food or the environment, thus, providing enhanced protection against internal and/or external factors [40, 41]. (Tables 2, 3 and 4)

2.2 *Biobased Materials and Their Composites and Food Packing Application*

Biobased materials in this review include biobased polymers, biobased nanomaterials, biobased fibers and their composites (Fig. 8). Biobased polymers can generally be classified into four types: (1) polymers extracted from biomass, such as cellulose, hemicellulose, chitin, (2) synthetic polymers from biomass monomers, such as polylactic acid (PLA) and biopolyethylene (BioPE), (3) polymers produced by microorganisms, such as polyhydroxyalkanoates (PHAs), bacterial cellulose, and (4) biodegradable polymers synthesized from petrochemical mononers, such as

Table 2 A few polymer nanocomposites with different nanomaterials and their potential applications

Types of polymers nanocomposites	Nanomaterials	Main potential application
Polyurethane Polyester Epoxy Polyamide	(i) OMMT (ii) Functionalized CNT (iii) Ag (iv)Fe_3O_4 (v) RGO (vi)CD (vii) POSS (viii) RGO-TiO_2 (ix)CD/ Hydroxyapatite (i) OMMT (ii) MWCNT (iii) RGO/Ag (iv) Fe_3O_4 (v) LDH (vi)CD (i) OMMT (ii) MWCNT (iii) Ag/OMMT (iv) Cellulose nanofiber (v) RGO (vi) PANi/Fe_3O_4 (i) OMMT (ii) Functionalized CNT (iii) Ag (iv) RGO	(i) Packaging, paints, biomaterials, foams, etc. (ii) Stimuli-responsive, flame-retardant, antistatic, electromagnetic-shielding materials, etc. (iii) Antibacterial coating, biomaterials, etc. (iv)Biomaterial, nanocontact smart materials, etc. (v) Catalysts, biomaterials, tough coating, etc. (vi)Catalysts, biomaterials, smart coating, etc. (vii) Flame-retardant materials (viii) Self-healing, self-cleaning smart materials, etc. (ix) Scaffold for bone tissue engineering (i) Packaging, paint, film catalysts, etc. (ii) Fuel cell, coating materials, flame-retardant, etc. (iii) Antibacterial coating, shielding, sterile garments, anti-explosion wear materials, etc. (iv)Biomaterial (v) Catalysts, flame retardant materials, etc. (vi)Photocatalyst, biomaterial, etc. (i) Coating, adhesive, sealant, etc. (ii) Adhesive, flame-retardant, etc. (iii) Antibacterial biomaterial, adhesive, etc., (iv) Implantable scaffold for tissue regeneration, dressing material, etc. (v) Anticorrosive coating, sensor, etc. (vi) Photocatalyst, marine coating, etc. (i) Automobile, packaging (ii) Structural materials, electromagnetic shielding coating, etc., (iii) Antibacterial materials, food packaging, etc., (iv) Supercapacitor, structural materials, etc.,

poly(caprolactone) (PCL), poly(butylene succinate-co-adipate) (PBSA), polybutylene adipate terephthalate (PBAT), poly(glycolic acid) (PGA), polybutylene succinate (PBS), and polypropylene carbonate (PPC). Biobased nano materials include mainly cellulose nanocrystals, cellulose nanofibers, chitin nanocrystals, and other nanomaterials from biomass. Biobased fibers are referred to as natural fibers produced by animals, plants as well as geological processes. As food packaging materials usually need to satisfy several requirements, such as mechanical properties, permeability, and antibacterial properties, the real applications of biobased food packaging materials usually involve their composites. This review presents diverse categories of biobased materials and their composites for their applications in food packaging.

In recent years, the development of novel modified atmospheres and active food packaging has not only increased the shelf life of food, but also its safety and quality. However, the packaging technology must maintain the balance between food protection and other issues, including the costs of energy and materials, heightened social

Table 3 Different active packing types applied in food packing

Types of application	Foods
Oxygen scavengers	Ground coffee, tea, roasted nuts potato chips, chocolate, fat powdered milk, powdered drink, bread, tortillas, pizza, pizza crust, refrigerated fresh pasta, fruit tortes, cakes, cookies, beer, deli meats, smoke and cured meats, fish, cheese
Carbon dioxide absorbers	Ground coffee
Carbon dioxideemitters	Meat, fish
Moistureabsorbers	Dry and dehydrated products, meat, poultry, fish
Ethylene scavengers	Kiwifruit, banana, avocados, persimmons
Ethanol emitters	Bread, cakes, fish
Antimicrobial releasing films	Dry apricots
Antioxidant releasing films	Cereals
Flavor absorbing films	Navel orange juice
Flavor releasing films	Ground coffee,
Color containing films	Surimi
Anti-fogging films	Some fresh fruit and vegetable package
Anti-sticking films	Soft candies, cheese slices
Light absorbers	Pizza, milk
Time-temperature indicators	Microwaveable pancake syrup, refrigerated pasta, deli items

and environmental awareness, and stringent regulations on pollutants and disposal of municipal solid waste [42]. Food packaging plays an important role in preserving food throughout the distribution chain. Biodegradable and compostable polymers have risen as an alternative to conventional plastics. Especially, biodegradable packaging is recommended, as a short-term. Plastic packaging for food where biodegradability is a key advantageous feature, so that it can be discarded with food waste for composting [43].

Based on food packing, biodegradable polymers are classified into three types:

1. Natural polymers found in nature,
2. Polymers derived from renewable resources, and
3. Synthetic polymers derived from fossil resources (Fig. 9).

For biodegradable packaging materials to compete with conventional synthetic polymers, the critical mechanical, thermal, and barrier properties for the intended application must be comparable. The nanocomposite concept shows a motivating way

Table 4 Antimicrobial nanoparticles in different food packing systems

Nanoparticles	Polymer matrix	Tested microorganism
Ag/Chitosan	PLA	Staphylococcus aureus (ATCC6538)
Ag	Agar banana powder	Escherichia coli Lysteria Monocytogenes
TiO_2/Ag/Cu	PVC	Mixed microorganism culture media
ZnO/Ag/Cu	PLA/PEG	Lysteria momocytogenes Saimonella typhimurium
Ag	PE	Escherichia coli
Ag/Cu	Guar Gum	Lysteria momocytogenes Saimonella typhimurium
Ag/TiO_2	PE	Aspergilius flavus
Ag/Cu	Fish skin Gelatin	Lysteria momocytogenes Saimonella enterice sv typhimurium
Ag	Starch PVA	Lysteria inocua, Escherichia coli Aspergilus niger, penicillium, expansum
Ag/TiO_2/SiO_2	LDPE	Escherichia coli
Ag	PHBV3	Lysteria momocytogenes Saimonella typhimurium
SiO_2	PBAT8	Escherichia coli, Staphylococcus aureus
ZnO	LDPE	Bacillus subtilis, Enterobecter aerogenes

for creating new and innovative materials including biodegradable polymers. PLA-based biodegradable nanocomposites have been prepared with improved mechanical, barrier optical, and thermal properties and can be used in the application of food packaging adequately.

Nanocomposites can also be intended to be used as a carrier of antimicrobials, drug delivery, and additives. Recent studies have demonstrated their ability to stabilize the additives and efficiently control their diffusion into the food system. This control can be especially important for the long-term storage of food or for imparting specific desirable characteristics, such as flavor, to a food system. Although there are numerous possibilities existing for packaging in bio-based nanocomposite material, the low level of production, some property limitation, and high costs confine them for a wide range of applications. Therefore, improvements in nanocomposite formulation, production practices, economies of scale, and increasing costs for fossil resources could all be necessary to produce a more favorable economic situation for biodegradable polymers.

Green or eco-friendly materials have been considered next-generation contenders for lightweight, inexpensive, sustainable, environment-friendly, and high-efficiency nanocomposites. Various types of natural and synthetic green polymers and green nanofillers have been employed to form sustainable materials. Green polymeric nanocomposites incarnate exclusive properties of both the sustainable polymer and eco-reinforcement. The eco-friendly nanofiller-reinforced green nanocomposites have found applications in automotive, energy, packaging, and biomedical applications. This review systematically speaks to the concepts and features of eco-polymer,

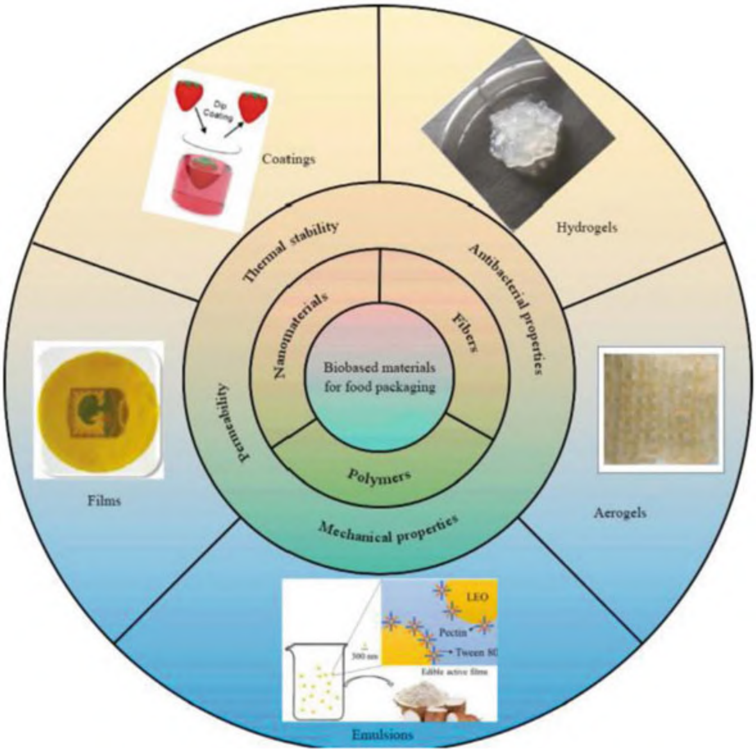
Dip Coating
Coatings
Hydrogels
Thermal stability
Antibacterial properties
Nanomaterials
Fibers
Biobased materials for food packaging
Permeability
Polymers
Mechanical properties
Films
Aerogels
LEO
Pectin
Tween 80
500 nm
Edible active films
Emulsions

Fig. 8 An overview of biobased materials for food packaging. Reproduced with permission [32–35]

eco-nanofillers, and green nanocomposites. In addition to the technical applications, trends, challenges, and future prospects of green nanocomposites have also been discussed.

Both synthetic and natural eco-polymers or eco-friendly polymers and derived materials have been used in industrial fields [44, 45]. Eco-friendly polymers are environmentally friendly, sustainable, and easily degradable. The nanocomposites based on eco-friendly polymers and eco-nanofillers are usually termed green polymeric nanocomposites [46, 47]. The synergistic effect of eco-friendly base materials and green reinforcing nanofillers has resulted in beneficial physical properties, environmental friendliness, and biodegradability of green nanocomposites. The essential features of these nanocomposite materials depend on nanofiller content, processing technique, and matrix/filler interfacial interaction or link. Green polymeric nanocomposites reveal a myriad of remunerations; however, their use in high-performance technical applications is still challenging. Sustainable natural polymer matrices include natural rubber, cellulose, chitin, starch, and polyesters such as polyhydroxyalkanoate. Moreover, a wide range of green synthetic polymers is also available as polycaprolactone, polylactic acid, poly (vinyl alcohol), polyethylene glycol, and many others [48].

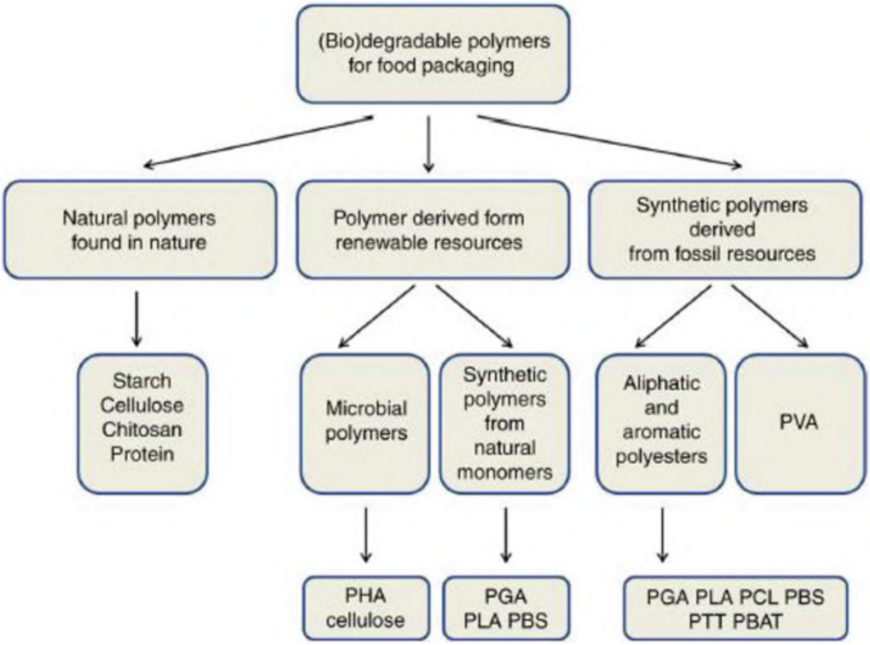
(Bio)degradable polymers for food packaging
Natural polymers found in nature
Polymer derived form renewable resources
Synthetic polymers derived from fossil resources
Starch Cellulose Chitosan Protein
Microbial polymers
Synthetic polymers from natural monomers
Aliphatic and aromatic polyesters
PVA
PHA cellulose
PGA PLA PBS
PGA PLA PCL PBS PTT PBAT

Fig. 9 Classification of biodegradable polymers for food packaging application

Consequently, eco-friendly bio-based polyamide was prepared and plasticized using green plasticizers such as glycerol, soybean oil, and water [49]. The green materials were used for water filtration membrane material. Eco-friendly polycarbonates have also been prepared using limonene and carbon dioxide [50]. The eco-friendly polymers and nanocomposites have offered various engineering applications in energy, transport, and biomedical sectors [51, 52]. Considering the importance of green nanocomposites, this review has been developed focusing on sustainable polymers, nanofillers, and nanocomposites.

Eco-Friendly Polymer Matrices

Due to better biodegradability and sustainability properties, eco-friendly polymer matrices have been employed in advanced materials [53]. The biopolymers such as collagen and chitosan have been used to form hybrids having enhanced morphological and mechanical properties [54]. The development of synthetic polymers, such as polystyrene and poly(vinyl chloride), has caused environmental threats owing to their non-discarding nature [53, 55]. Consequently, eco-friendly resins (bioresins) have been researched as petroleum-based polymer alternatives. Polymers from the categories of proteins and polysaccharides-based biodegradable materials have been used [56–58]. An important class of eco-friendly polymers is polyesters. This class consists of polyhydroxyalkanoate (PHA), polycaprolactone (PCL), polylactic acid (PLA) polyester amide, and other polyester derivatives.

Applications

The biodegradable green composites possess exceptional potential for tissue engineering, bioimplants, and other biomedical applications [59, 60].

The food packaging industry is rapidly growing as a consequence of the development of nanotechnology and changing consumers' preferences for food quality and safety. In today's globalization of markets, active packaging has achieved many advantages with the capability to absorb or release substances for prolonging the food shelf life over the traditional one. Therefore, it is critical to develop multifunctional active packaging materials from biodegradable polymers with active agents to decrease environmental challenges. This book chapter addresses the recent advances in nanocelluloses (NCs)-based nanohybrids with new function features in packaging, focusing on the various synthesis methods of NCs-based nanohybrids, and their reinforcing effects as active agents on food packaging properties. The applications of NCs-based nanohybrids as antioxidants, antimicrobial agents, and UV blocker absorbers for prolonging food shelf-life are also reviewed. Overall, these advantages make the CN-based nanohybrids with versatile properties promising in food and packaging industries,

Nanocomposites (NCs) have been used in automotive, packaging, building, and agricultural materials [43]. Various polymeric nanocomposites have been extensively studied, including polyamide, epoxy, polyester, polystyrene, and polypropylene [61]. In recent years, to solve the waste disposal problem of plastic materials, biodegradable polymers have become an important trend [5].

Polymers are widely used in the packaging industry because of their good performance and relatively low cost;

In recent years both academic and industrial researchers focused their attention on the use of biodegradable materials. To date, synthetic aliphatic polyesters represent one of the most economically competitive biodegradable polymers, being readily susceptible to biological attack [62]. In addition, they have attracted considerable attention as they combine the just mentioned features with interesting physical and chemical properties.

The performance expected from bioplastic materials used in food packaging applications is protecting it from the environment, maintaining of course food quality [63]. Chemical–physical, mechanical, and barrier properties depend on the structure of the polymeric packaging material. In addition, it is important to study the changes in the bioplastics that can occur during the interaction with the food [64].

At present, only polylactic acid (PLA) is commercially used for food contact packaging applications. Poly(butylene succinate) (PBS) and Poly(butylene succinate-co adipate) (PBSA) are two of the main candidate as aliphatic biodegradable polyesters to be used in the food packaging field. In view of a possible application of these two commercial aliphatic polyesters in the food packaging, it is fundamental to evaluate the compatibility of these materials with the food, in terms of loss in food quality properties.

PLA has high mechanical properties, thermal plasticity, fabric ability, and biocompatibility [65, 66]. Over the past decades, the degradation of PLA materials has been studied for practical medical applications such as drug delivery systems, sutures, and surgical implants [67–69]. Polyanhydrides of PLA have been tested for implantations including architecturally fabricated stents that could replace conventional metallic stents [70]. The advantage of polylactide-based biopolymers over conventional metallic or non-biodegradable polymers is to ease of removal by the body system itself and retention of shape over time. PLA-based packaging and containers including bottled water, juice, and yogurt are used in Europe, Japan, and North America for supermarket products [71]. PLA is a biodegradable thermoplastic derived from lactic acid.

Poly(lactide) (PLA) have gained growing attention in the past decade as food packaging materials because they can easily be obtained from renewable resources; their production consumes quantities of carbon dioxide; they can be recycled and composted; and their physical and mechanical properties can be tailored through polymer architecture [72–74]. Although PLA production costs are relatively high over conventional plastics, there are predictions that this will change with time as production volumes and demand both increases [75]. PLA-based packaging materials are currently used for supermarket products in Europe and North America for packaging bottled water, juices, and yogurts (Table 5; Fig. 10). The application of nanocomposites promises to expand the use of edible and biodegradable films [76, 77]. As far as food safety is concerned, nano-structured materials will prevent the incursion of micro-organisms (Table 6).

Table 5 Potential food application of PLA-based packaging material

Type of food	Film properties	Commercial manufacturer	References
Bottled water, bottled juice	Moisture, light, and gas barrier Moisture, light, and gas barrier, inert to migration of flavor	BiotaTM, NobleTM	[74, 75]
Milk, yogurt	Moisture, light, and gas barrier Mechanical strength, barrier of oxygen, carbon dioxide, moisture, and grease	DannonTM	[74, 75]
Cheese, butter/margarine, and mushroom	Moisture, light, and gas barrier Mechanical strength, balanced gas, and moisture barrier; protection against crushing/bruising		[74, 75]

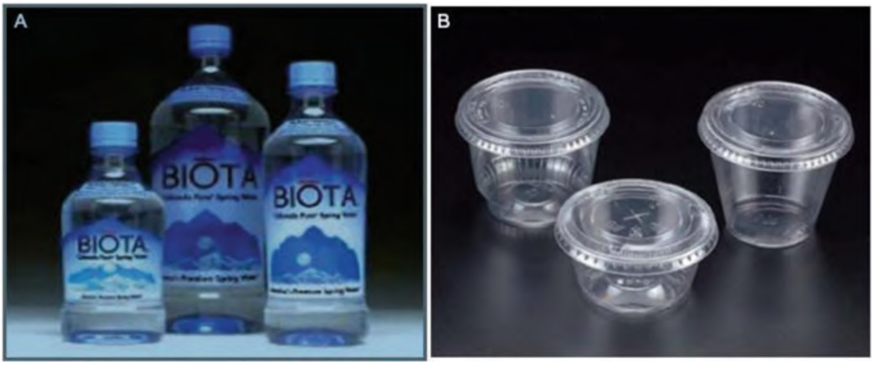

Fig. 10 PLA-based food packaging (Figure provided in color online)

Table 6 Specification and applications of green nanocomposite

Matrix in green nanocomposite	Green nanofiller	Application
Polyvinyl alcohol	Carboxymethyl cellulose	Microelectronic devices
Chitosan	Cellulose nanofiber	Food packaging
Plasticized starch	Hemp cellulose Nanocrystal	Packaging
Potato starch/ glycerol	Colloidal silver	Microelectronic packaging,
Carboxylated acrylonitrile butadiene rubber	Graphene oxide	Sensor packaging
Conjucatedmicroporous polymer	Nanocarbon	Photoluminescence. Light emitting diode, photovoltaic devices
Biopolymer	Ceramic nanoparticles	Capacitors, printed wiring board
Poly(vinylidene fluoride-co-hexafluoro propylene)	Platinum nanoparticle	Nanogenerator
Conducting polymer	Green metal nanoparticle	Thermoelectric generator
Polydimethy is siloxane	ZnS	Light emitting diode
Starch	Nanoclay	Packaging
Cellulose	Sugarcane bagasse nanofiber	Packaging
Polystyrene	Rice straw	Packaging
Biopolymer	Rice straw	Antimicrobial food packaging
Poly(methyl methacrylate)	Hydroxyapatite, multi-walled carbon nanotube	Bone implant
Biopolymer	Silver nanoparticle	Sensor

2.3 *Essentials Oils (EOs) for Active Food Packaging*

EOs are produced by angiospermic plants and have found various usages in different industries [78]. Among all the plant species, only aromatic plants are sources of EOs. Aromatic plants form about 10% of plant species (over 17,000) and are well distributed around the world [79]. EOs are secondary metabolites that could be derived from different plant organs including flowers (jasmine, rose, chamomile, violet, and lavender), buds (clove), leaves (thyme, eucalyptus, salvia, and rosemary), fruits (star anise), twigs (*Luma chequen*), bark (cinnamon), seeds (cardamom), wood (sandal), rhizome, and roots (ginger), all of which have the potential to be applied in food packaging as antimicrobial and antioxidant agents [80–84]. The chemical composition and quality of EOs depend on characteristics of the source plant such as growth conditions, variety, geographical origin, age, season, and condition of the plant when harvested. Extraction method, analysis conditions, and processing chemicals can also affect their properties [85–88]. Their extraction yield is usually very low (about 1%) which makes them valuable rare substances. EOs consist of concentrated lipophilic volatile aroma compounds including terpenes, terpenoids, and phenol-derived aromatic and aliphatic components. The phenolic compounds in EOs can diminish or almost eliminate the presence of microorganisms and minimize lipid oxidation [89]. The natural extracts of EOs are classified as Generally Recognized as Safe (GRAS) by the US Food and Drug Administration (FDA) and received approval for safety and effectiveness [90]. Therefore, in food-related application, they are more suitable alternatives to synthetic antioxidants such as butylated hydroxytoluene (BHT) or butylated hydroxyanisole (BHA) which might have a carcinogenic effect [90]. These oils are substances accountable for the active function of packaging with the flexibility to be settled in a different container or be directly added to the packaging material. In either cases, the release of the oils during transportation and storage leads to increased shelf life. Electrospun-loaded EOs could be the answer to market demands as they allow foods to reach consumers with their original or enhanced organoleptic properties, increased shelf life, and improved safety [91–94]. The packaging materials produced in these systems can contain active ingredients designed for sustained release during storage or transportation to delay food deterioration. Table 7 summarizes the essential oils that have been successfully used in food packaging for improved efficiency (Fig. 11).

3 Water Treatment

In today's world, increasing demand and shortage of clean water sources due to rapid industrialization, population growth, and persistent drought conditions have become critical global issues. As far as the environment is concerned, the reuse and recycling of wastewater is necessary to augment the limited fresh water supply and to meet the growing strain on water resources in the long run. During the past few decades, a variety of practical strategies and solutions have been proposed and applied to develop viable wastewater treatment technologies. As shown in Fig. 12, electrospun materials have been demonstrated as promising candidates for heavy ion adsorbents and photocatalysis of organic pollutants in water treatment, due to their high porosity, interconnectivity, and a large surface-to-volume ratio. Especially benefitting from the interconnectivity, microscale interstitial space, mat characteristics, and nonwoven electrospun nanofiber mats can be used as water filtration membranes for water treatment. Heavy metal ions including Pd, Hg, and Cr are major pollutants not only in the industrial sector, but also in our living environment, which can cause severe

Table 7 Essential oils incorporated in food packaging applications

Essential oil combinations	Properties	Food product	Applied film material
Rosemary	Antimicrobial	Chicken	Cellulose acetate
Cinnamon clove	Antimicrobial	Bakery	Cassava starch
Lemon, thyme, and cinnamon	Antibacterial	NA	Chitosan
Cinnamon, winter savory, and oregano	Antimicrobial	Bologon and ham	Alginate
Bergamot	Antifungal and antibacterial	NA	Chitosan
Garlic, rosemary, and oregano	Antimicrobial	NA	Whey protein isolate (WPI)
Oregano	Antimicrobial	NA	Quince seed mucilage
Oregano	Antimicrobial	Pizza	Cellulosic resin
Oregano	Antimicrobial	Ripened sheep Cheese model	Polypropylene (PP) and polyethylene terephthalate(PET)
Oregano and thyme	Antimicrobial	Fresh ground beef	Soy protein
Oregano	Antimicrobial	Fresh broccoli	Whey protein isolate (WPI)
Mixture of oregano, pimento berry, and lemongrass (mix A) and a mixture of nutmeg, lemongrass, and citric (mix B)	Antioxidant	NA	Methylcellulose (MC) and a blend of polycaprolactone/ alginate(PCL/ALG)
Ginger, turmeric, and plai	Antibacterial and antioxidant	NA	Fish skin gelatin
Satureja hortensis	Antibacterial	Whole beef, muscle	K-carrageenan
Oregano and pimento	Antibacterial and antioxidant	Fish	Milk protein
Clove	Antimicrobial	Sardine patties	Gelatin chitosan
Clove	Antimicrobial	Cheddar cheese	Sunflower protein concentrate
Linalool or methyl chavicol	Antibacterial	Formosa plum	Low-density polyethylene(LDPE)
Oregano and bergamot	Antimicrobial	Tomatoes	Hydroxypropyl methylcellulose and limonene constituent EO
Cinnamon and mustard	Flavoring	Strawberry	Zein
Limonene constitute EO, lemongrass, and oregano		Strawberry	Chitosan
Peppermint, red thyme, chitosan, and lemon			Chitosan

public health problems. Several technologies have been developed for the removal of heavy metal.

ions from water. Compared to other treatment methods, adsorption is simple, economical, and effective. Electrospun nanofiber sorbents possess a large surface area, which facilitates the attachment of target molecules, requiring reduced sorbent amounts, and smaller sample and eluent volumes. Taking lead ions for example, electrospun polystyrene functionalized with dithizone (DZ) as the absorbent can absorb lead (II) at pH 8.5.

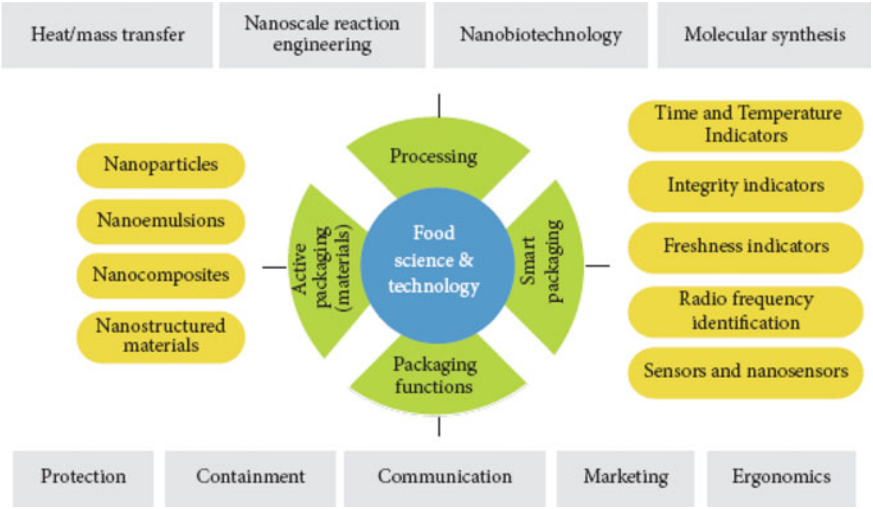
Heat/mass transfer
Nanoscale reaction engineering
Nanobiotechnology
Molecular synthesis
Nanoparticles
Nanoemulsions
Nanocomposites
Nanostructured materials
Processing
Active packaging (materials)
Food science & technology
Smart packaging
Packaging functions
Time and Temperature Indicators
Integrity indicators
Freshness indicators
Radio frequency identification
Sensors and nanosensors
Protection
Containment
Communication
Marketing
Ergonomics

Fig. 11 Application matrix of nanotechnology in food science and technology

Fig. 12 Water treatment from three major types of pollutants through absorption, photocatalysis, or filtration processes

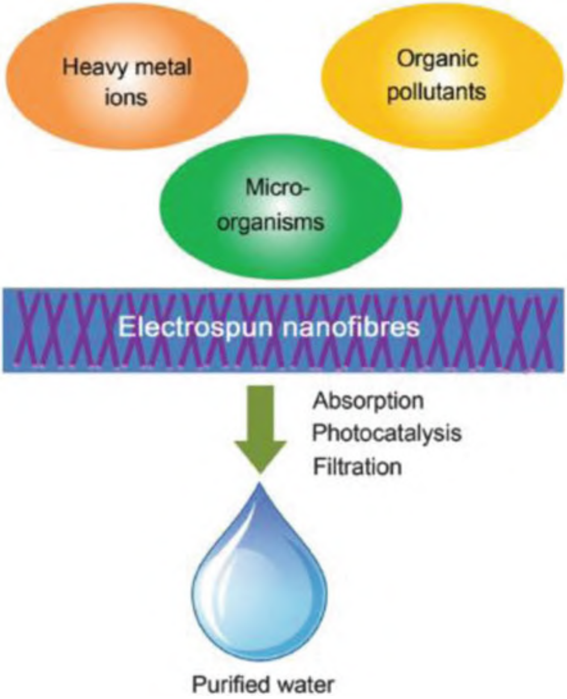
Heavy metal ions
Organic pollutants
Micro-organisms
Electrospun nanofibres
Absorption
Photocatalysis
Filtration
Purified water

Intelligent Indicators

Time and Temperature Indicators (TTI)

TTIs are devices that concatenate the exposure to temperature over time by acquiring the effect of such disclosures and illustrating a change of color (or other physical characteristic). Many devices can be attached to food packages to integrate the TTI. Owing to their simplicity, low cost, efficiency, and affordability, TTIs have been widely used to monitor and translate consumer quality of foodstuffs [70]. A prerequisite for the effective utilization of a control system based on TTI is the kinetic study and modeling of loss ratios of food quality and response [26–30, 36].

Integrity Indicators (InI)

The modified atmosphere package for non-respiring food typically has a low (0–2%) oxygen (O_2) concentration and a high (20–80%) carbon dioxide (CO_2) concentration. Hence, a leak means a considerable increase in O_2 concentration and a decrease in CO_2 concentration. If the package leaks, microbial growth is likely to take place [24, 37–40]. This means that CO_2 may accumulate inside the package.

Freshness Indicators (FI)

FI directly indicates the quality of the food; it is usually in the form of stickers on the food cover. Typically, these indicators focus on the detection of gas composition changes [41]. FI typically under- goes a color change that remains permanent and is easy to read and interpret by consumers. Despite many attempts and several innovative approaches, no quality indicators are in widespread use by the food industry today [95].

Flexible Packaging

Flexible packaging is also an important area that can be explored. The incorporation of graphene into the polymer matrix improves the thermal, mechanical, and barrier properties to a great extent. Further, the antibacterial or antimicrobial activity of graphene-based materials can also be exploited for this purpose. Polylactic acid (PLLA)/graphene nanocomposite is one such example that can be used in bio-based food packaging applications. Many other examples are also available like LLDPE/EVA/graphene, GO nanosheets/poly (vinyl alcohol) nanocomposite. This is also a growing field where many other combinations of polymer and graphene-based materials can be tried.

4 Challenges and Food Active Specific Concerns

There are still some challenges and limitations preceding their large-scale production and extensive application in food industries. Despite the numerous advantages of NCs-based metal oxide nanohybrids in active food packaging, the migration of metal oxide nanoparticles from packaging is considered a major challenge because of their potential toxicity in the human body and the environment. Especially, nanoparticles such as ZnO and TiO_2 have shown to be effective against various bacterial strains and could be a replacement to Ag NPs since the non-ionization of the TiO_2 and the lower toxicity of the ZnO. Active packaging materials display antimicrobial activity which needs direct contact among the metal/metal oxide NPs and the microbial cells, or the release of antimicrobials such as metal ions and reactive oxygen species; nevertheless, the release of these metal ions should be controlled. Therefore, the migration of NCs-metal oxides nano hybrids from packaging into foods has to be determined to guarantee the safety of active packaging. However, the absence of in vivo studies on humans, limited characterizations, and toxicology of NCs-based metal oxides nano hybrids make it riskiness. Current difficulties can be also associated with the dispersion of NCs-based nanohybrids within polymer matrices, the aggregation of NPs, and fabrication techniques. Also, the dispersion of NCs-based nanohybrids within polymer matrices can affect their nucleation movement, compatibility, and UV absorption ability, which may hinder their use in active packaging applications. Consequently, homogenous dispersion and the investigation of the real UV shielding would be perceptive to evaluate the reliability and stability for long-term usage. Regarding biological application, we mainly focused on antimicrobial agents, especially in active food packaging materials. Such new antimicrobial biomaterials could fight human pandemics due to the increased risk of harmful bacteria.

Importance of Food Packaging Systems

Active research on smart food packaging has grown significantly in the past 30 years [95–97]. However, the majority of the work on “responsive materials” has been concentrated in the engineering, chemistry, materials science, and medical fields, with very limited implementation in real food packaging [98–100].

Conclusion

In this book chapter, potential applications of biomaterials-based polymer nanocomposite materials, polymer materials, supercapacitor and their application for food packing, packaging indicator are described.

PLA-based biodegradable nanocomposites have been prepared with improved mechanical, barrier optical, and thermal properties and can be used in the application of food packaging adequately. Nanocomposites can also be intended to be used as a carrier of antimicrobials, drug delivery, and additives. Recent studies have demonstrated their ability to stabilize the additives and efficiently control their diffusion into the food system. This control can be especially important for the long-term storage of food or for imparting specific desirable characteristics, such as flavor, to a food system. Although there are numerous possibilities existing for packaging in bio-based nanocomposite material, the low level of production, some property limitation, and high costs confine them to a wide range of applications.

Hence, we can say undoubtedly that these are the materials for future revolution.

References

1. Kelsall RW, Hamley IW, Geoghegan M (2005) Nanoscale science and technology. Wiley Online Library
2. Mohammad AW, Lau C, Zaharim A, Omar MZ (2012) Elements of nanotechnology education in engineering curriculum worldwide. Proc Soc Behav Sci 60:405e12
3. Noordermeer JWM, Dierkes WK (2015) Carbon black reinforced elastomers. Encyclopedia of polymeric nanomaterials. Springer, New York, pp 1–14
4. Hussain F, Hojjati M, Okamoto M, Gorga RE (2006) Review article: polymer-matrix nanocomposites, processing, manufacturing, and application: an overview. J Compo Mate 40:1511–1575
5. Bordes P, Pollet E, Avérous L (2009) Nano-biocomposites: biodegradable polyester/nanoclay systems. Prog Polym Sci 34:125–155
6. Shin WH, Jeong HM, Kim BG, Kang JK, Choi JW (2012) Nitrogen-doped multiwall carbon nanotubes for lithium storage with extremely high capacity. Nano Lett 12:2283–2288
7. Liu X, Antonietti M (2014) Molten salt activation for synthesis of porous carbon nanostructures and carbon sheets. Carbon 69:460–466
8. .Al-Johani H, Abdel Salam M (2011) Kinetics and thermodynamic study of aniline adsorption by multi-walled carbon nanotubes from aqueous solution. J Colloid Interface Sci 360:760–767
9. Akil H, Omar M, Mazuki A, Safiee S, Ishak ZM, Bakar AA (2011) Kenaf fiber reinforced composites: a review. Mater Des 32(8):4107e21
10. Saba N, Tahir PM, Jawaid M (2014) A review on potentiality of nano filler/natural fiber filled polymer hybrid composites. Polymers 6(8):2247e73
11. Saba N, Paridah M, Jawaid M (2015) Mechanical properties of kenaf fiber reinforced polymer composite: a review. Constr Build Mater 76:87e96
12. Kim HS, Kim HJ (2008) Enhanced hydrolysis resistance of biodegradable polymers and bio-composites. Polym Degrad Stab 93:1544–1553
13. Zeng QH, Yu A, Lu M, Paul DR (2005) Clay-based polymer nanocomposites: research and commercial development. J Nanosci Nanotechnol 5:1574–1592
14. Ray SS, Bousmina M (2006) Polymer nanocomposites and their applications. American Scientific Publishers, New York
15. Komarneni S (1992) Nanocomposites. J Mater Chem 2:1219–1230
16. Morsi MA, Oraby AH, Elshahawy AG et al (2019) Preparation, structural analysis, morphological investigation and electrical properties of gold nanoparticles filled polyvinyl alcohol/carboxymethyl cellulose blend. J Mater Res Technol 8:5996–6010
17. Kumar R, Rai B, Kumar G (2019) A simple approach for the synthesis of cellulose nanofiber reinforced chitosan/PVP bio nanocomposite film for packaging. J Polym Environ 27:2963–2973
18. Tang XZ, Kumar P, Alavi S (2012) Recent advances in biopolymers and biopolymer-based nanocomposites for food packaging materials. Crit Rev Food Sci Nutr 52:426–442
19. Youssef AM (2013) Polymer nanocomposites as a new trend for packaging applications. Polym Plast Technol Eng 52:635–660
20. Sangroniz A, Sangroniz L, Gonzalez A et al (2019) Improving the barrier properties of a biodegradable polyester for packaging applications. Eur Polym J 115:76–85
21. Bideau B, Loranger E, Daneault C (2018) Nanocellulose-polypyrrole-coated paperboard for food packaging application. Prog Org Coatings 123(June):128–133
22. Reis LM, Duarte LF, Souza AG, Garcia EM, Melo JOF, Taroco CG, Taroco HA (2018) Electrochemical corrosion study in tinplate can of green corn. Integr Food Nutr Metab 5(5):1−5
23. Neethirajan S, Jayas DS (2011) Nanotechnology for the food and bioprocessing industries. Food Bioprocess Technol 4(1):39–47
24. Alfadul SM, Elneshwy AA (2010) Use of nanotechnology in food processing, packaging and safety–review. Afr J Food Agric Nutr Dev 10(6)

25. Sharma C, Dhiman R, Rokana N, Panwar H (2017) Nanotechnology: an untapped resource for food packaging. Front Microbiol 8:1735
26. Duncan TV (2011) Applications of nanotechnology in food packaging and food safety: barrier materials, antimicrobials and sensors. J Colloid Interface Sci 363(1):1–24
27. Lagaron JM, Cabedo L, Cava D, Feijoo JL, Gavara R, Gimenez E (2005) Improving packaged food quality and safety. Part 2: Nanocomposites. Food Addit Contam 22(10):994–998
28. Mirzadeh A, Kokabi M (2007) The effect of composition and draw-down ratio on morphology and oxygen permeability of polypropylene nanocomposite blown films. Eur Polymer J 43(9):3757–3765
29. De Azeredo HM (2009) Nanocomposites for food packaging applications. Food Res Int 42(9):1240–1253
30. Adame D, Beall GW (2009) Direct measurement of the constrained polymer region in polyamide/clay nanocomposites and the implications for gas diffusion. Appl Clay Sci 42(3–4):545–552
31. Lu P, Yang Y, Liu R, Liu X, Ma JX, Wu M, Wang SF (2020) Preparation of sugarcane bagasse nanocellulose hydrogel as a colourimetric freshness indicator for intelligent food packaging. Carbohydr Polym 249:116831
32. Zhou W, Fang JW, Tang SW, Wu ZG, Wang XY (2021) 3D-printed nanocellulose-based cushioning–antibacterial dual-function food packaging aerogel. Molecules 26:3543
33. Jung S, Cui YF, Barnes M, Satam C, Zhang SX, Chowdhury RA, Adumbumkulath A, Sahin O, Miller C, Sajadi SM, Sassi LM, Ji Y, Bennett MR, Yu M, Friguglietti J, Merchant FA, Verduzco R, Roy S, Vajtai R, Meredith JC, Youngblood JP, Koratkar N, Rahman MM, Ajayan PM (2020) Multifunctional bio-nanocomposite coatings for perishable fruits. Adv Mater Deerfield Beach Fla 32:e1908291
34. Abral H, Pratama AB, Handayani D, Mahardika M, Ilyas RA (2021) Antimicrobial edible film prepared from bacterial cellulose nanofibers/starch/chitosan for a food packaging alternative. Int J Polym Sci 2021:1–11
35. Marsh K, Bugusu B (2007) Food packaging: roles, materials, and environmental issues. J Food Sci 72(3):R39–R55
36. Lopez-Rubio A, Almenar E, Hernandez-Muñoz P, Lagarón JM, Catalá R, Gavara R (2004) Overview of active polymer-based packaging technologies for food applications. Food Rev Intl 20(4):357–387
37. Majid I, Nayik GA, Dar SM, Nanda V (2018) Novel food packaging technologies: Innovations and future prospective. J Saudi Soc Agric Sci 17(4):454–462
38. Ahvenainen R (ed) (2003) Novel food packaging techniques. Elsevier
39. Sekhon BS (2010) Food nanotechnology–an overview. Nanotechnol Sci Appl
40. Sandhya E, Kooner R, Dixit A (2010) New technologies in food packaging. Food Eng Ingred 35:38–41
41. Morillon V, Debeaufort F, Blond G, Capelle M, Voilley A (2002) Factors affecting the moisture permeability of lipid-based edible films: a review. Crit Rev Food Sci Nutr 42(1):67–89
42. Song JH, Murphy RJ, Narayan R, Davies GBH (2009) Biodegradable and compostable alternatives to conventional plastics. Philos Trans R Soc Lond B Biol Sci 364(1526):2127–2139
43. Calcagno CIW, Mariani CM, Teixeira SR, Mauler RS (2007) The effect of organic modifier of the clay on morphology and crystallization properties of PET nanocomposites. Polym 48:966–974
44. Li XL, Wang J, Wu LL (2015) The influence of curing age and mix proportion on the uniaxial compressive properties of green high-performance fiber-reinforced cementitious composites. Mater Res Innovat 19:S8-624
45. Anita Lett J, Sagadevan S, Joyce Prabhakar J et al (2019) Exploring the binding effect of a seaweed-based gum in the fabrication of hydroxyapatite scaffolds for biomedical applications. Mater Res Innovat 24:75–81
46. Mohanty AK, Vivekanandhan S, Pin JM et al (2018) Composites from renewable and sustainable resources: challenges and innovations. Science 362:536–542

47. Yu L, Petinakis S, Dean K et al (2007) Green polymeric blends and composites from renewable resources. Macromolecul Sympos 249:535–539
48. Mat Desa MSZ, Hassan A, Arsad A et al (2014) Mechanical properties of poly(lactic acid)/ multiwalled carbon nanotubes nanocomposites. Mater Res Innovat 18:S6-14
49. He M, Wang Z, Wang R et al (2016) Preparation of bio-based polyamide elastomer by using green plasticizers. Polymers 8:257
50. Xu Y, Lin L, Xiao M et al (2018) Synthesis and properties of CO_2-based plastics: environmentally-friendly, energy-saving and biomedical polymeric materials. Prog Polym Sci 80:163–182
51. Saba N, Jawaid M, Sultan MTH, et al (2017) Green biocomposites for structural applications. In: Green biocomposites. Springer, Switzerland, pp 1–27
52. Millon LE, Wan WK (2006) The polyvinyl alcohol–bacterial cellulose system as a new nanocomposite for biomedical applications. J Biomed Mater Res B 79:245–253
53. de Souza Machado AA, Kloas W, Zarfl C et al (2018) Microplastics as an emerging threat to terrestrial ecosystems. Global Change Biol 24:1405–1416
54. Kusebauch U, Cadamuro SA, Musiol HJ et al (2007) Photocontrol of the collagen triple helix: synthesis and conformational characterization of bis-cysteinyl collagenous peptides with an azobenzene clamp. Chem A Eur J 13:2966–2973
55. Braun D (2004) Poly (vinyl chloride) on the way from the 19th century to the 21st century. J Polym Sci A: Polym Chem 42:578–586
56. Thakur VK, Thakur MK, Kessler MR (2017) Handbook of composites from renewable materials, biodegradable materials, vol 5. John Wiley & Sons, USA
57. Khulbe KC, Matsuura T (2017) Development of membranes from biobased materials and their applications. In: Handbook of composites from renewable materials, pp 251–281
58. Thakur VK, Thakur MK, Raghavan P et al (2014) Progress in green polymer composites from lignin for multifunctional applications: a review. ACS Sustain Chem Eng 2:1072–1092
59. Nair LS, Laurencin CT (2007) Biodegradable polymers as biomaterials. Prog Polym Sci 32:762–798
60. Ngiam M, Liao S, Patil AJ (2008) Fabrication of mineralized polymeric nanofibrous composites for bone graft materials. Tissue Eng 15:535–546
61. Hussain F, Hojjati M, Okamoto M, Gorga RE (2006) Polymer-matrix nanocomposites, processing, manufacturing, and application: an overview. J Compo Mate 40:1511–1575
62. Nikolic MS, Djonlagic J (2001) Synthesis and characterization of biodegradable poly(butylene succinate-co-butylene adipate)s. Polym Degrad Stab 74:263e70
63. Arvanitoyannis IS (1999) Totally and partially biodegradable polymer blends based on natural synthetic macromolecules: preparation, physical properties, and potential as food packaging materials. J Macromol Sci Rev Macromol Chem Phys C39(2):205e71
64. Scott G (2000) Green polymer. Polym Degrad Stab 68:1e7
65. Fetters LJ, Lohse DJ, Richter D, Witten TA, Zirkel A (1994) Connection between polymer molecular weight, density, chain dimensions, and melt viscoelastic properties. Macromolecules 27:4639–4647
66. Tullo A (2000) Plastic found at the end maize. Chem Eng News 78:13
67. Arshady R (1991) Preparation of biodegradable microspheres and microcapsules: polylactides and related polyesters. J Control Rel 17:1–22
68. Tams J, Joziasse CAP, Bos RRM, Rozema FR, Grijpma DW, Pennings AJ (1995) High-impact poly(L/D-lactide) for fracture fixation: in vitro degradation and animal pilot study. Biomaterials 16:1409–1415
69. Ikada Y, Shikinami Y, Hara Y, Tagawa M, Fukuda E (1996) J Biomed Mater Res 30:553
70. Varshney SK, Hnojewyj O, Zhang J, Rivelli P (2010) Polyanhydride polymers and their uses in biomedical devices. US Patent 7,674,285 B2
71. Jin T, Zhang H (2008) Biodegradable polylactic acid polymer with nisin for use in antimicrobial food packaging. J Food Sci 73(3):M127-134
72. Sinclair RG (1996) The case for polylactic acid as a commodity packaging plastic. J Macromol Sci Part A Pure Appl Chem 33:585–597

73. Haugaard VK, Weber CJ, Danielsen B, Bertelsen G (2002) Quality changes in orange juice packaged in materials based on polylactate. Eur Food Res Technol 214:423–428
74. Auras R, Harte B, Selke S (2004) Effect of water on the oxygen barrier properties of poly (ethylene terephthalate) and polylactide films. J Appl Polym Sci 92:1790–1803
75. Whiteman N (2002) Bio-based materials: a reality in the packaging industry. Packexpo. PMMI, Chicago, IL, pp 37–42
76. Sinha Ray S, Okamoto M (2003) Polymer/layered silicate nanocomposites: a review from preparationto processing. Prog Polym Sci 28:1539–1641
77. Lagarón JM, Cabedo L, Cava D, Feijoo JL, Gavara R, Gimenez E (2005) Improving packaged food quality and safety. Part 2: nanocomposites. Food Addit Contam 22(10):994–998
78. Pavela R (2015) Essential oils for the development of eco-friendly mosquito larvicides: a review. Ind Crops Prod 76:174–187
79. Svoboda K, Greenaway R (2003) Investigation of volatile oil glands of Satureja hortensis L.(summer savory) and phytochemical comparison of different varieties. Int J Aromather 13(4):196–202
80. Wannes WA, Mhamdi B, Sriti J et al (2010) Antioxidant activities of the essential oils and methanol extracts from myrtle (Myrtus communis var. italica L.) leaf, stem and flower. Food Chem Toxicol 48(5):1362–1370
81. Dvaranauskaite A, Venskutonis P, Raynaud C, Talou T, Viskelis P, Sasnauskas A (2009) Variations in the essential oil composition in buds of six blackcurrant (Ribes nigrum L.) cultivars at various development phases. Food Chem 114(2):671–679
82. Hill LE, Gomes C, Taylor TM (2013) Characterization of beta-cyclodextrin inclusion complexes containing essential oils (trans-cinnamaldehyde, eugenol, cinnamon bark, and clove bud extracts) for antimicrobial delivery applications. LWT Food Sci Technol 51(1):86–93
83. Lv J, Huang H, Yu L et al (2012) Phenolic composition and nutraceutical properties of organic and conventional cinnamon and peppermint. Food Chem 132(3):1442–1450
84. Vallverd´u C, Vila R, Tomi F, Carhuapoma M, Casanova J, Cañigueral S (2006) Composition of the essential oil from leaves and twigs of Luma chequen. Flavour Fragr J 21(2):241–243
85. Hussain AI, Anwar F, Hussain Sherazi ST, Przybylski R (2008) Chemical composition, antioxidant and antimicrobial activities of basil (Ocimum basilicum) essential oils depends on seasonal variations. Food Chem 108(3):986–995
86. Khajeh M, Yamini Y, Bahramifar N, Sefidkon F, Reza Pirmoradei M (2005) Comparison of essential oils compositions of Ferula assa-foetida obtained by supercritical carbon dioxide extraction and hydrodistillation methods. Food Chem 91(4):639–644
87. Negi PS (2012) Plant extracts for the control of bacterial growth: efficacy, stability and safety issues for food application. Int J Food Microbiol 156(1):7–17
88. Riahi L, Chograni H, Elferchichi M, Zaouali Y, Zoghlami N, Mliki A (2013) Variations in Tunisian wormwood essential oil profiles and phenolic contents between leaves and flowers and their effects on antioxidant activities. Ind Crops Prod 46:290–296
89. Bakkali F, Averbeck S, Averbeck D, Idaomar M (2008) Biological effects of essential oils—a review. Food Chem Toxicol 46(2):446–475
90. Li K-K, Yin S-W, Yang X-Q, Tang C-H, Wei Z-H (2012) Fabrication and characterization of novel antimicrobial films derived from thymol-loaded zein-sodium caseinate (SC) nanoparticles. J Agric Food Chem 60(46):11592–11600
91. Dainelli D, Gontard N, Spyropoulos D, Zondervan-van den Beuken E, Tobback P (2008) Active and intelligent food packaging: legal aspects and safety concerns. Trends Food Sci Technol 19:S103–S112
92. Ozdemir M, Floros JD (2004) Active food packaging technologies. Crit Rev Food Sci Nutr 44(3):185–193
93. Suppakul P, Sonneveld K, Bigger SW, Miltz J (2008) Efficacy of polyethylene-based antimicrobial films containing principal constituents of basil. LWT Food Sci Technol 41(5):779–788

94. Vermeiren L, Devlieghere F, van Beest M, de Kruijf N, Debevere J (1999) Developments in the active packaging of foods. Trends Food Sci Technol 10(3):77–86
95. Vieira Jodar L, Orzari LO, Storti Ortolani T, Assumpção MH, Vicentini FC, Janegitz BC (2019) Electrochemical sensor based on casein and carbon black for bisphenol a detection. Electroanalysis 31(11):2162–2170. https://doi.org/10.1002/elan.201
96. Della Pelle F, Rojas D, Scroccarello A, Del Carlo M, Ferraro G, Di Mattia C, Compagnone D. High-performance carbon black/molybdenum disulfide nanohybrid sensor for cocoa catechins determination using an extraction-free approach. Sensors Actuators B
97. Vilian AE, Sivakumar R, Huh YS, Youk JH, Han YK. Palladium supported on an amphiphilic triazine-urea-functionalized porous organic polymer as a highly ef- ficient electrocatalyst for electrochemical sensing of rutin in human plasma. ACS Appl Mat
98. Kumar N, Goyal RN (2018) Silver nanoparticles decorated graphene nanoribbon modified pyrolytic graphite sensor for determination of histamine. Sensors Actuators B Chem 268:383–391. https://doi.org/10.1016/j.snb.2018.04.136
99. Zheng W, Xiong Z, Li H, Yu S, Li G, Niu L, Liu W (2018) Electrodeposited Pt@ molecularly imprinted polymer core-shell nanostructure: enhanced sensing platform for sensitive and selective detection of bisphenol A. Sensors Actuators B Chem 272:65
100. Herrera-Chacón A, Dinç-Zor Ş, del Valle M (2020) Integrating molecularly imprinted polymer beads in graphite-epoxy electrodes for the voltammetric biosensing of histamine in wines. Talanta 208:120348. https://doi.org/10.1016/j.talanta.2019.120348

Part VI

FNMs Based Supercapacitor for Health Care Applications

Всё для победы!
НАРОДНЫЙ ФРОНТ
https://pobeda.onf.ru/
LET'S HELP THE RUSSIA

Всё для победы!

НАРОДНЫЙ ФРОНТ

https://pobeda.onf.ru/

LET'S HELP THE RUSSIA

Chapter 21
Functional Polymer Nanocomposites as Supercapacitors for Health Care

Akanksha Verma, Bablu Mordina, Kingsuk Mukhopadhyay, Mayank Dwivedi, and Soma Banerjee

1 Introduction

Initially, the electronic devices were developed mainly for communication devices and later the application areas keep on increasing due to the advancement in the fabrication technology of semiconductors. In recent years, the integration of electronics into the biomedical field for the sake of health monitoring become quite lucrative [1, 2]. This approach helps in analyzing the health condition prior to any complication and also saves medical resources for the large population.

Health monitoring devices consist of sensing unit, data transmission unit and power supply unit [3]. Advancement in materials engineering helped the development of new materials and functional subsystems for application in sensors and components for power supply. The signals are collected from the body by sensing unit as movement, blood pressure, pulse rate, body temperature, etc. which are the essential physical parameters for health monitoring. The signals are then processed and the data is transmitted to the connected smart devices like cell phones and cloud devices. Both the sensing unit and data transmitting unit require a power supply source like battery, supercapacitor, etc. The health monitoring devices stay in close contact with the body or within the body, in the case of implants. Hence, it requires an energy source that does not cause any harm to the body. The device as a whole should possess good stretchability and biocompatibility to provide comfortable contact during the sensing and avoid any adverse effect on health. Moreover, health monitoring devices require only a minute of power for their function. Therefore, energy storage devices

---

A. Verma · S. Banerjee (✉)
Department of Plastic Technology, Harcourt Butler Technical University, Kanpur 208002, India
e-mail: sbanerjeepl@hbtu.ac.in; somabanerjee27@gmail.com

B. Mordina (✉) · K. Mukhopadhyay · M. Dwivedi
Defence Materials and Stores Research and Development Establishment, Nano Science and Coatings Division, G.T. Road, Kanpur 208013, India

© The Author(s), under exclusive license to Springer Nature Singapore Pte Ltd. 2024

C. M. Hussain and M. B. Ahamed (eds.), *Functionalized Nanomaterials Based Supercapacitor*, Materials Horizons: From Nature to Nanomaterials,
https://doi.org/10.1007/978-981-99-3021-0_21

with fast-charging characteristics are required to store the energy generated by the intermittent body motion and also to supply power whenever required.

Lithium-ion batteries are extensively used in electronic devices, which store energy through faradic electrochemical reactions and provide high energy density [4]. They have several disadvantages. They not only possess low cyclic stability, slow charge–discharge cycle but also have the risk of explosion and toxicity. In health monitoring devices, the risk associated with the use of battery cannot be taken lightly. In the place of batteries, supercapacitors can be used as electrochemical energy storage device in health monitoring devices to overcome the limitations and drawbacks of the batteries. Supercapacitors possesse high energy density, high cyclic stability, fast charge–discharge cycle and also they are user-friendly and do not cause any detrimental effect to the health. Supercapacitors also possess the potential to prove themselves as a future generation source for energy storage.

Stretchable supercapacitors are a little ahead of traditional supercapacitors. In the case of traditional supercapacitors, the whole assembly is little bulky consisting of two electrodes separated by a separator and the space is filled with electrolyte. This setup has its own demerits in practical applications like the requirement of proper encapsulation of electrolytes and it is also difficult to integrate the assembly of supercapacitors with other functional systems. Stretchable supercapacitor overcomes these drawbacks faced by traditional supercapacitors. They are made up of stretchable and flexible electrode materials and solid-gel electrolytes so that the whole assembly is flexible and they can be used in any form or shape in the electronic devices. The elastic modulus of assembly is close to the skin, reducing the chances of unnecessary immune responses [5]. They are comfortable to wear and accommodated within the fabric as well. Thus, the stretchable supercapacitor is used in place of a rigid supercapacitor as an energy storage device in health monitoring electronics.

Semiconductors are also used as infrared photodetectors in enzymatic sensors for the measurement of biomarkers in biofluids. Power harvesting for such devices can be done using photoelectric, piezoelectric, triboelectric, and thermoelectric effects in stretchable formats in supercapacitors. The variety of options available for the material selection, power supply unit, mechanism, design, etc. in the fabrication of supercapacitors from the various perspective are shown in Fig. 1.

The nanomaterials used in the fabrication of supercapacitor application purposes can be functionalized to improve their properties. By oxidation of graphene, the electrical conductivity of graphene oxide is improved from 0.005 to 0.14 S/m in aqueous solution at 35 °C [6]. The thermal conductivity [7] and Young's modulus [8, 9] of the monolayer of graphene oxide are also lower than that of graphene (207.6 ± 23.4 GPa). Therefore, nanomaterials can be functionalized specifically for their potential applications in supercapacitors [10], biosensors [11], gas sensors [12], etc.

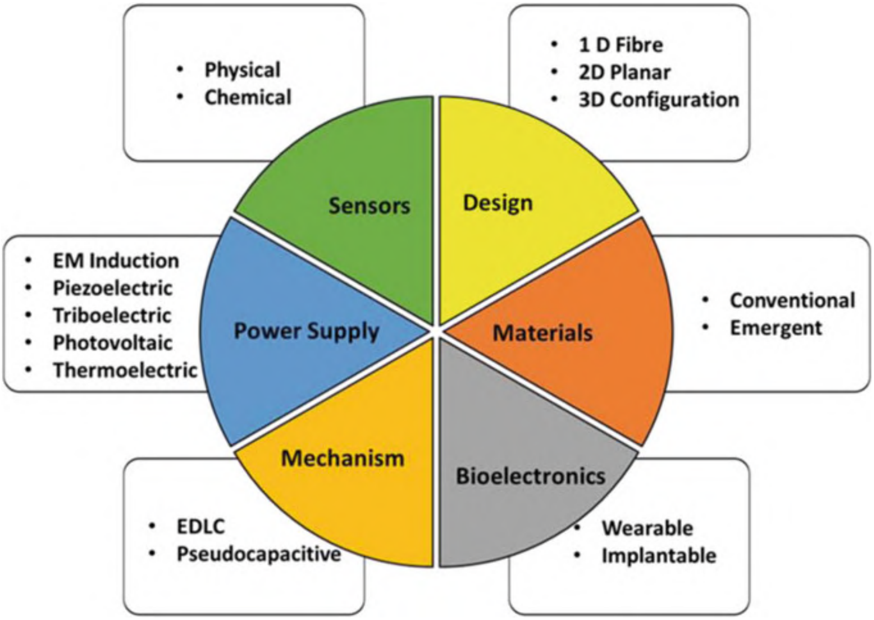
Physical
Chemical
1 D Fibre
2D Planar
3D Configuration
Sensors
Design
EM Induction
Piezoelectric
Triboelectric
Photovoltaic
Thermoelectric
Power Supply
Materials
Conventional
Emergent
Mechanism
Bioelectronics
EDLC
Pseudocapacitive
Wearable
Implantable

Fig. 1 Different basis for variation in the fabrication of flexible supercapacitors

2 Flexible Supercapacitors

The fabricated bioelectronic devices face challenges of human activities, such that they go under bending, stretching, twisting, etc. As such, the supercapacitors powering the wearable and implantable devices should be able to go under various deformations, bearing sudden stretch and release cycles. At the same time, they must possess sufficient energy density and power density without compromising the cycling stability of the device at different mechanical deformations. Such supercapacitors are called flexible or stretchable supercapacitors.

The mechanism involved in the working of flexible supercapacitors is the same as those of traditional supercapacitors. There are largely two types of mechanisms, i.e., electrical double-layer capacitance (EDLC) and pseudo-capacitance. In EDLC, the charge storage takes place at Helmholtz's double layer while in pseudo-capacitance storage of charge takes place through faradic reactions as shown in Fig. 2. The stretchable supercapacitor is basically different from traditional supercapacitor in terms of electrode and electrolyte materials and device design, which provides flexibility to the assembly.

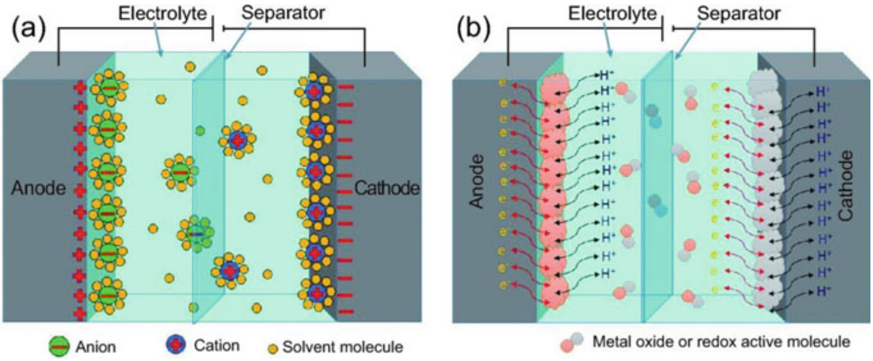

Fig. 2 Schematic representation of **a** EDLC and **b** pseudocapacitive mechanism reprinted with permission from [13]

2.1 Electrode Materials for Supercapacitors

Materials are the key deciding factor of functionality and performance of the supercapacitor. Both electrodes as well as electrolytes should be able to withstand a high amount of strain to comprise the stretchable supercapacitor. By tailoring the material design using polymer nanocomposite and electrolyte, stretchable supercapacitors with high electrochemical performance are fabricated for healthcare applications. The polymers used or the polymeric nanocomposite synthesized should be either intrinsically stretchable or made to be stretchable ensuring good electrochemical performance at high strain and different deformations.

Electrodes are the key components of the supercapacitor which control the performance of the supercapacitor by influencing capacitance, charging-discharging, energy density, power density and electrochemical and mechanical stability. To fabricate a stretchable supercapacitor, the first step is to develop a stretchable electrode using suitable stretchable material and structural design. The suitable electrode materials which are used widely are elastomeric polymers with high in-built stretchability such as polydimethyl siloxane, polyurethane, Ecoflex, etc. Textile, cellulose, carbon fibers like less stretchable materials can be used under different structural work as stretchable materials.

The most suitable current collectors are gold, platinum, and copper due to their high conductivity but under strain, their conductivities are affected. Thus, nanoparticles or nanowires of metals are embedded or deposited into the polymer matrix to build a conductive and stretchable film [14]. Similarly, carbon nanomaterials such as carbon nanotube, graphite, graphene, etc. are used for the current collector in place of bulk material. Activated carbon and carbon-based materials are used as EDLC electrodes and metal oxide and conducting polymer composites as the pseudo-capacitive electrodes in the stretchable supercapacitor as shown in Fig. 3.

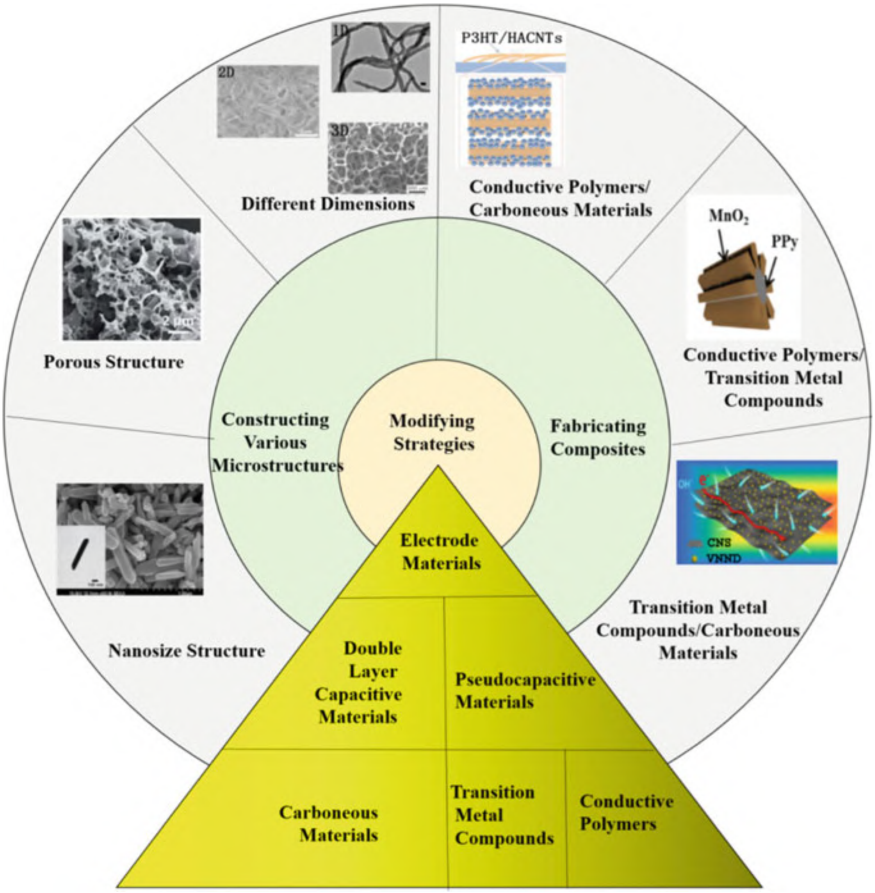
1D
2D
3D
Different Dimensions
P3HT/HACNTs
Conductive Polymers/ Carboneous Materials
MnO$_2$
PPy
Conductive Polymers/ Transition Metal Compounds
Porous Structure
2 μm
Constructing Various Microstructures
Modifying Strategies
Fabricating Composites
CNS
VNND
Transition Metal Compounds/Carboneous Materials
Nanosize Structure
Electrode Materials
Double Layer Capacitive Materials
Pseudocapacitive Materials
Carboneous Materials
Transition Metal Compounds
Conductive Polymers

Fig. 3 Different materials used for the electrode synthesis reprinted with permission from [15]

Although metal oxides or sulphides exhibit good conductivity and capacitance in comparison with carbon-based materials, however, their application in a stretchable supercapacitor is limited. Metals have inherent brittleness and stiffness in them causing degradation and deformation of the system. Hence, they are used in combination with carbon nanocompounds or polymers to increase their flexibility. CNT is added into MoS_2 for the same reason by dip-coating to synthesize a stretchable electrode for supercapacitor [16].

Conducting polymers and their derivatives also provide a good choice as electrode material for flexible supercapacitors. Polymers like polypyrrole are intrinsically flexible materials and able to maintain electrochemical performance under various degrees of strains [17]. Polypyrrole is incorporated with Au/CNT/polyacrylamide hydrogel and used as an electrode for the synthesis of stretchable and self-healing supercapacitors [18]. The fabricated supercapacitor exhibits an energy density up to 123 μWh cm^{-2}, and stretchability up to 800%.

The emergence of various new materials brings about an efficient supercapacitor system with superior performance when compared to the traditional material sources in stretchable supercapacitors [19–21]. The examples of such emergent materials are MXenes, metal–organic frameworks (MOFs), polyoxometalates (POMs) and black phosphorus (BP). The emergent materials have shown efficient charge transfer with better flexibility as electrodes.

MXenes are compounds of transition metals bearing nitrogen or carbon along with them. The usual empirical formula of MXenes is $M_{n+1}X_nT_x$, where M denotes transition metal, X represents either nitrogen or carbon and T stands for surface termination. They have an outstanding ability for fast charging/discharging cycles due to their intrinsic electrical conductivity and active groups on their surface. Hence, they have excellent electrochemical properties bringing the potential benefit for use in supercapacitors [22–24]. They have a porous structure which is preferable for ion transport and their charge storage is pseudo-capacitive in nature [25, 26]. The stacking in MXenes facilitates a multi-layered structure, improving the capacitance of the supercapacitors.

MOFs are compounds made up of metal ions coordinated with organic ligand or molecules to form a porous structure. They have high porosity and tunable framework [27]. MOFs are found to be good electrode materials for supercapacitors. The only limitation of MOFs is their low conductivity causing poor electrochemical properties which can be enhanced by adding conductive materials during the fabrication of electrodes [28]. For example, core–shell ZnO@ZIF-8 on carbon cloth current collector containing polyaniline coating was synthesized and utilized to fabricate a flexible supercapacitor having high areal capacitance [29].

POMs are polyatomic ions consisting of more than one transition metal oxyanions linked together with oxygen atoms creating a cage-like 3-D structure. The transition metals are present at high oxidation states making POMs highly efficient as catalysts for oxidation and hydration. They possess excellent oxidative and reductive abilities which are suitable to use as electrode material in supercapacitors. They are known as electron sponges for their good electronic transfer abilities [28–30]. PMo_{12} was utilized to induce the polymerization of polypyrrole in the presence of reduced graphene oxide (rGO) to develop a flexible electrode [31]. The fabricated supercapacitor showed an areal capacitance of 2.61 mF cm^{-2} at 150 mA cm^{-2} current density, which was much greater than the PPy/rGO electrode prepared in the absence of POM.

Allotropes of phosphorus specifically black phosphorus (BP) is used as an electrode material in combination with conducting polymers and carbon-based materials [32, 33]. BP is a 2D material consisting of phosphorus atoms arranged in a lamellar structure in spaced layers (5.3 Å) having good electrical properties [34]. A BP/CNT hybrid material was developed by chemically joining CNT and BP through a C-P bond. The microfluidic spinning method was utilized to integrate the obtained material into a supercapacitor electrode [35]. The as-prepared supercapacitor showed exceptional stretchability, rate capability, as well as cycling stability.

Apart from the electrode, the electrolyte is another important part of the development of stretchable supercapacitor with good electrochemical performance. An electrolyte should possess high conductivity, high stretchability, electrochemical stability and biocompatibility [36]. Electrolytes used in flexible supercapacitors may be liquid electrolytes and solid-state electrolytes [37, 38]. The liquid electrolytes used can be aqueous based, organic solvent based or ionic liquids. In implantable bioelectronics, physiological fluids like sweat and blood are used as liquid electrolytes [37]. Liquid electrolytes exhibit a risk of leakage in health monitoring devices which brings the advantage of using solid-state electrolyte. There are three types of solid-state electrolytes that are used, gel electrolytes, polyelectrolyte and ceramic electrolytes. Gel electrolyte such as H_3PO_4/PVA is used widely in stretchable supercapacitors due to better ion transportation, high mechanical stretchability and good biocompatibility [39].

The surface functionalization of materials refers to the addition of certain groups to the surface of materials to improve their properties. Various polymers and nanomaterials have inert surfaces limiting their application in industries. Thus, surface modifications are carried out to improve the adhesion, printing and wetting by adding polar and functional groups to the nanoparticles in polymer nanocomposites.

The common mechanism depicts that the first step of surface functionalization is the binding of primary reactive groups to the surface of the particles. The reactive surface is then modified with active agents such as monomers or polymers. The polymers used can either be hydrophobic or hydrophilic according to the desired characteristics for specific requirement. The surface modification of nanoparticles tends to increase the compatibility with the concerned polymer matrix along with enhancement in properties such as their stability, dispersibility and compatibility [40].

3 Bioelectronics Powered by a Supercapacitor

Advancement in materials led to the integration of stretchable supercapacitors into the health-monitoring bioelectronics as an efficient source of energy. Bioelectronics can be wearable or implantable. Among wearables, bioelectronics can be non-touching, skin-touching or skin-conforming wearables. Implantable are also verified on the basis of their intimacy with the body realizing the demand of biocompatibility. Non-touching wearable bioelectronics is integrated with textile or other clothing materials. Although they are in close contact with the body, however, direct touch do not take place and hence for such bioelectronics the requirement of biocompatibility is not much high. In the case of skin-touching bioelectronics, close contact with the skin renders it necessary to take into account compatibility with the skin to avoid any skin problems. Skin-conforming adhered closely to the skin by having a high degree of conformity with the skin. Implantables are integrated inside the body to know about the real-time physiological responses of the body. The highest degree of biocompatibility is needed in implantable bioelectronics due to the risk of immune rejection.

3.1 Wearable

Wearable electronics are the ones that are supposed to be worn on the body either by integrating them into the clothes or on the skin and can be used during physical activities. In this way, they are able to detect physical or chemical signals produced by the body. Functional wearable electronics are of high importance in artificial intelligence [41–44]. The requirement of wearable electronics are mainly mechanical flexibility and stretchability with a robust support substrate. Three types of wearable electronics, non-touching, skin-touching or skin-conforming wearables are mainly categorized according to the compatibility level with the body.

Non-touching wearables

Non-touching wearables are electronics that are integrated with clothes, shoes or any other wearable items. The device can also be directly woven into the textile materials. The substrate apart from clothes can be gloves, wristbands, etc. Apart from weaving, the electrodes or electrolytes can directly be imprinted on the fabric to achieve the same result. Carbon fiber based micro supercapacitor was coupled to a TiO_2 photodetector, to realize a self-powered integrated system [45]. The lightweight and small size are the essential criteria for wearable electronics.

Skin-touching wearable

Skin-touching wearables are the bioelectronics that are in direct contact with the skin. The direct attachment requires high biocompatibility and stretchability in comparison to non-touching wearables to provide a better experience. The bioelectronics in this category, are encapsulated and then attached to the skin like watch bands to monitor the physiological activity of the body. The substrates that are used for the encapsulation require to be soft as well as biocompatible [46, 47] such as silicone-based substrates that are highly biocompatible. For example, silicone-based adhesives can be used to adhere an Ecoflex encapsulated supercapacitor directly to the skin.

A multifunctional wearable electrochromic device was developed and used as an all-transparent stretchable supercapacitor [48]. The fabricated PEDOT:PSS/WO_3 electrode-based supercapacitor was used for an electrochromic wearable patch device which showed stable electrochemical performances even under recurrent stretching-bending cycles. Utilization of PAAm electrolytes improved the stretchability and electrochemical properties and also resolved the leakage problem during the repeated mechanical deformations enabling them to be used as stretchable supercapacitors.

Skin-conforming wearables

Skin-conforming wearables are ultra-thin bioelectronics attached intimately to the epidermis of the body requiring high compatibility and conformation for the safe and comfort use. The device undergoes changes in terms of stretching, compressing, bending, etc. due to the close contact with the epidermis. In this case, the requirement of stretchability and flexibility should be higher to facilitate adaptability in comparison with other wearable electronics.

A supercapacitor was fabricated by using SWCNT/PEDOT hybrid film [49]. The overall thickness of the device was 1 μm and the device showed superior electrochemical performance. The adhesion on epidermal skin can be done by PVC or waterproof eyelash glue having biocompatibility and also stretchability.

3.2 Implantable

Implantable bioelectronic devices have gained a lot of attention and research interest due to the necessity of conformability, flexibility and biocompatibility. The features are of utmost importance in in-vivo monitoring of the health state for biomedical and physiological information in the areas of neural, cardiovascular and ocular monitoring. The device is involved in cardiac pacemaker, automated drug delivery, nerve regulation, sensors, tissue engineering, etc. powered by supercapacitors. Flexible supercapacitor provides a steady flow of energy to the device causing the least adverse effect. In a reported study, a fiber supercapacitor was integrated with an implant device. The electrodes were fabricated with (PEDOT: PSS)/ferritin nanoclusters within the MWCNT sheet. The materials were biocompatible and the areal capacitance and energy density obtained from the supercapacitor were 32.9 mF/cm^2 and 0.82 μWh/cm^2 in a saline solution buffered by phosphate [50].

In powering implantable medical devices, the supercapacitor has two limitations, one is high equivalent series resistance and the other is low breakdown voltage. In a study, to overcome this issue a capacitor in series was combined with the supercapacitor. Although, the way was imperfect however, it was a direct and simple solution to increase the voltage rating [51].

3.3 Sensing Unit

To precisely detect and analyse the signals from the physiological activities of the body, a reliable sensor is needed to be integrated with the bioelectronic system. All the relevant information is perceived by this sensor that is used in health monitoring and further diagnosing the disease and therapeutic uses [52]. Hence, the use of appropriate sensors integrated with the bioelectronic device is essential in assessing

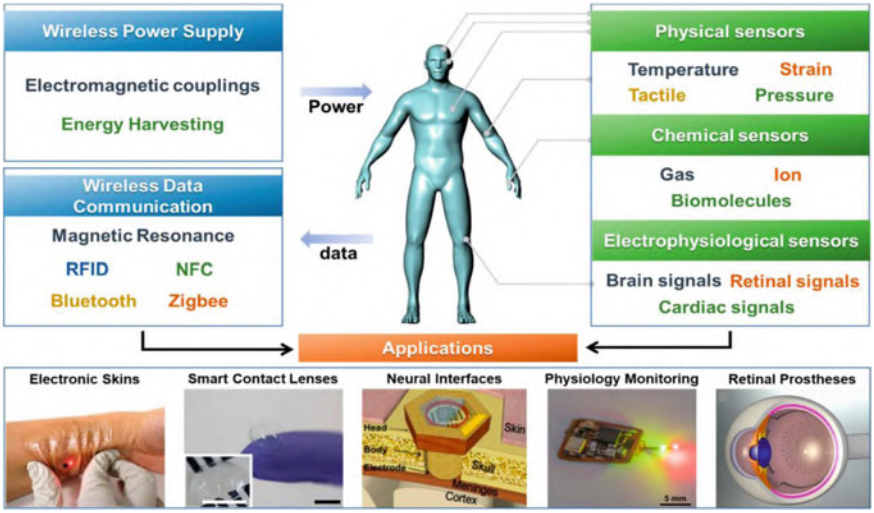
Wireless Power Supply
Electromagnetic couplings
Energy Harvesting
Wireless Data Communication
Magnetic Resonance
RFID
NFC
Bluetooth
Zigbee
Power
data
Physical sensors
Temperature
Strain
Tactile
Pressure
Chemical sensors
Gas
Ion
Biomolecules
Electrophysiological sensors
Brain signals
Retinal signals
Cardiac signals
Applications
Electronic Skins
Smart Contact Lenses
Neural Interfaces
Physiology Monitoring
Retinal Prostheses
Head
Body
Electrode
Skin
Skull
Meninges
Cortex
5 mm

Fig. 4 Components in bioelectronic sensors and their applications reprinted with permission from [63]

the required parameter of the body. The components integrated together to assess the sensor are depicted in Fig. 4 along with the application.

Various physiological reactions can be depicted by various changes in the physical parameters of the body such as temperature, pressure, and local strains [53, 54]. Similarly, blood pressure is detected by measuring the pressure exerted on the blood vessels. Movement causes exertion of pressure on the sensors and this leads to deflection in electrical properties. Such as, a strain sensor is used to detect arterial-pulse and heart-beat [55]. Similar types of investigation have been done by attaching the fabricated devices on the neck to capture carotid artery pulses and heartbeat rate in real time, as well as on the muscles to determine the movements of swallowing, drinking, coughing and breathing [56–58]. Piezoresistive sensor system was developed by integrating a supercapacitor and piezo-resistor to detect the movements [54].

Other than physical sensors, biochemical sensors detect the presence of various chemical molecules along with their concentrations using the electrochemical activity of molecules. For example, the detection of ions and other molecules via perspiration in the human body [59]. For example, the concentration of Na^+, K^+ ions and glucose were detected by analyzing the chemical composition of sweat with sensitivities as high as 0.031, 0.056 $nF\ mm^{-1}$ and 0.5 $\mu A\ \mu m^{-1}$, respectively [60]. This information could be transmitted to a smartphone for subsequent analysis. Apart from small molecules in solutions, several gaseous molecules, such as NO_2, ethanol/acetone [61] and NH_3/HCl [62] were also detected by incorporating sensors with the stretchable supercapacitors.

3.4 Wireless Power Supply

For the continuous functioning of a bioelectronic device, it needs an uninterrupted power supply source. In the case of bioelectronics, bulky nature, incompatibility as well as wired charging limit the application of batteries as energy storage devices. The wireless power supply is an essential requirement for the successful functioning of the device, specifically in the case of implantable bioelectronics.

The wireless power supply takes place through electromagnetic fields among the antennas. Different kinds of electromagnetic radiations are used for the sake of power transfer thus, providing a solution for the power supply of wireless devices. By using inductive electromagnetic coupling between the antennae of the power source and antennae attached to the bioelectronic device, electric current can be induced in the circuit present in the device. This induced current can either be used directly to operate the bioelectronic device [64] or to charge the electrochemical energy storage device which in turn supplies the power to the device. The direct operation will result in the miniaturized form of the system and also prevents any unforeseen conditions like electrolyte leakage or any negative effect on the body. However, this approach is impractical as data transmission may require a large amount of power [65]. Hence, it is practical to integrate an electrochemical storage device such as a supercapacitor with the bioelectronic devices.

When an AC current is passed through the transmitting antenna, it generates a magnetic field. This magnetic field is oscillating due to the alternate cycle in AC current resulting in the induction of electricity in the receiving antennae of the device. The mutual inductance of the pair of antennas can be calculated by the following Eq. (1) [66].

$$M = k\sqrt{L_1 L_2} \tag{1}$$

where, k is the coupling coefficient. It depends on the permittivity and distance between pair of antennas. L_1andL_2 are the inductance of transmitting and receiving antennae, respectively. Inductance of transmitting and receiving antennae should be high and the distance must be shorter for successful inductive coupling. Inductive coupling uses radioactive frequency and is compatible if used on the skin for wearable electronics or inside the body for implants [65, 67].

Ho et al. successfully demonstrated the wireless power transmission process occurring from the antenna fixed at the porcine chest wall to the electronic device implanted in the heart's surface. In their experiment, it is observed that when coupled with 500 mW signals into the tissue, the antenna situated inside the body received about 200 μW signals, at a separation of 4 cm between the transmitting and receiving antennas [68].

Energy harvesting unit

Energy harvesting or energy scavenging are the methods of energy transfer from different sources which are not intended to provide power to the device for its operation. The energy harvesting reduces the burden of power supply from outside of the device such that the design of the device is responsible for powering itself.

For the realization of practical wearable bioelectronic devices, integration of the energy harvesting unit into the system is a better approach as it eliminates the requirement for an external power source [69, 70]. Energy harvesting can be implemented in different ways. One approach is to utilize the energy harvester as a power supply of the bioelectronic device which is connected [71, 72]. Another approach is where the energy harvesting device is to be self-powered sensors that can generate voltage or current as a sensing signal by external stimuli [73, 74].

The introduction of energy harvesters to meet the demand for power supply in bioelectronics gives a viable option for wireless power charging. For the operation of temperature and humidity sensors, Srbinovska and his co-workers utilized photovoltaic cells as a power source [71]. Leonov et al. revealed a wearable electroencephalography (EEG) sensor powered by the harvested energy of the thermoelectric generator integrated into the skin [75]. Recent research is now focusing to use energy harvesters such as nanogenerators for self-powered sensor assembly. A triboelectric nanogenerator was developed which acted as a pressure sensor to measure the produced currents. As a power source, such type of energy harvesters can produce high transient power about 365 V and a current of 65 μA, which is sufficiently higher than what is required for sensor operation. Therefore, these energy harvesters are very suitable for the self-powered sensor application [76].

Piezoelectric energy harvesting device

The muscles present in the body can produce kinetic energy when undergoing muscular movements. These movements can cause mechanical strain on certain structures of electrically polled materials which induces an electric potential. This phenomenon is called piezoelectricity. It was discovered in 1880 by Jacque and Pierre Curie [77] and since then this concept has been utilized extensively. The phenomenon of piezoelectricity is generally exhibited by barium titanate ($BaTiO_3$), zinc oxide (ZnO), lead zirconate titanate (PZT) and polyvinylidenefluoride (PVDF). Each material is unique in terms of its mechanical properties, which provides a wide range of choices to build a piezoelectric energy harvesting device.

Triboelectric energy harvesting

Triboelectric effect produces energy by utilizing frictionally generated charges owing to the collision. This results in the flow of electrons from one object to the other involved in the collision. The transfer of electrons causes potential difference and this phenomenon is called contact electrification. Wang et al. reported on the triboelectric generator in their various research works [78, 79].

The designs of all of these material offer relatively high voltages that can be utilized in power devices and systems which are mainly capacitive in nature and the energy density of such generator is sufficient to power several tiny devices which require as low as few mW power to run. Hence these triboelectric generator technologies are very promising that have the potential to replace current batteries. However, to make use of these triboelectric generators as implantable systems further optimization is essential for lower frequency and amplitude mechanical motions.

Photovoltaic

Photovoltaic devices utilize photon energy from the sunlight to generate electricity which can be used to charge the supercapacitor. The generation of electricity depends upon the intensity of incident rays of sunlight; however, it is not possible to maintain a constant intensity of sunlight at all-time due to changes in weather season and location. Hence, the output of the photovoltaic energy harvesting unit is not reliable and needed to be connected to an energy storage device such as supercapacitor. Ni/NiCoP-based stretchable supercapacitor was coupled with flexible solar cells to design a self-powered energy storage system and applied on a lab coat [80]. The resultant unit was able to power an electronic watch uninterruptedly in the presence or absence of sunlight and has shown the potential for long-term use.

3.5 Self-Powering or Self-Healing

Self-healing materials are a class of smart materials, composed such that they can self-heal the mechanical injury without any external trigger at the ambient conditions [81]. Amongst them, polymers reduce mechanical failure by self-healing wear and tear. Supercapacitors are integrated with such polymers which provide the benefit of long-term reliability, less maintenance and durability. Self-healing polymers can be classified into three types: (i) capsule-based, (ii) vascular-based and (iii) intrinsic self-healing polymers [82]. In capsule-based and vascular-based systems, a polymer matrix contains capsules or vessels filled with monomers and catalyst. On mechanical damage, the monomers and catalysts are released into the polymer matrix and polymerization starts to heal the damage [83]. The process used by the first two methods is time-consuming and can be used one time. Also, the fabrication process is complicated such as enclosing monomers and catalysts and dispersing them into the polymer matrix. On the other hand, molecular interactions such as metal–ligand interaction, π–π stacking and hydrogen bonding are the main factors for healing in the intrinsic type of self-healing polymer [84]. This is mainly governed by the self-healing groups added during the functionalization of polymers [85]. Self-healing polymers are modified in various ways to gain high flexibility and biocompatibility along with physical and chemical properties to incorporate them into bioelectronic devices such as electrochemical sensors, chemiresistors, etc.

CNT/polymer-based material is extensively used in this field due to its unique properties, such as high electronic conductivity, well-established routes of functionalization [86] and low percolation threshold of the CNT-based composites [87].

Self-healing polymers containing CNTs as nanofiller can be used for humidity and touch sensing [88].

4 Design Configuration and Fabrication Techniques

The fabrication technique employed depends on the design configuration of the stretchable electronics. 1D fiber like, 2D planar and 3D architectural design are some novel designs that have been developed so far and they are shown in Fig. 5. The architectural design of the device determines the overall performance that can be realized by employing different fabrication techniques such as spinning, photolithography, templating, deposition approach, etc., some of which are shown in Fig. 6. The aforementioned configurations and their fabrication strategies for biomedical application are discussed further.

1D fiber-like configuration

The basic structure of a fiber-like configuration is two stretchable electrodes arranged parallelly was separated via a solid-state stretchable electrolyte [90]. The arrangement of fiber electrodes in 1D configuration can be simply parallel, twisted or core–shell in a stretchable supercapacitor. The core–shell structure has the advantage of a larger effective surface area for charge storage providing better electrochemical performance [91]. The design can easily be imprinted on the textile by weaving or knitting due to their lightweight and stretchability to integrate wearable electronics with the textile. Another approach is to employ a helical configuration in which fiber

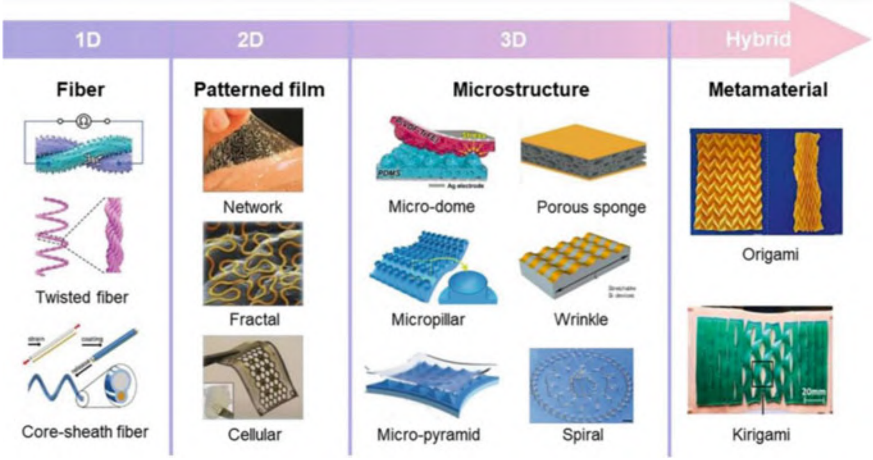
1D
2D
3D
Hybrid
Fiber
Patterned film
Microstructure
Metamaterial
Twisted fiber
Core-sheath fiber
Network
Fractal
Cellular
Micro-dome
Porous sponge
Micropillar
Wrinkle
Micro-pyramid
Spiral
Origami
Kirigami

Fig. 5 Different design configuration for the fabrication of supercapacitor reprinted with permission from [89]

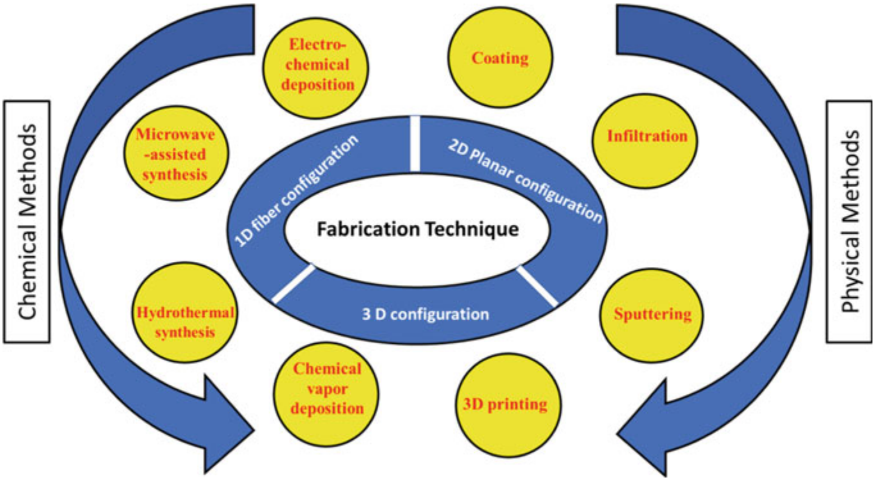
Chemical Methods
Electro-chemical deposition
Coating
Microwave -assisted synthesis
Infiltration
1D fiber configuration
2D Planar configuration
Fabrication Technique
3 D configuration
Hydrothermal synthesis
Sputtering
Chemical vapor deposition
3D printing
Physical Methods

Fig. 6 Fabrication techniques for architectural designing of supercapacitors

electrodes are wrapped around the stretchable substrates providing good stretchability to the whole assembly. Gao's group reported the fabrication of composite fibers based supercapacitor utilizing PPy-decorated with rGO and MWCNTs. Spring-like fibers were coated with the help of polyurethane (PU) matrix to assure self-healability and stretchability. The fabricated stretchable supercapacitor exhibited a capacitance retention of 82.4% after 100% stretching as well as 54.2% capacitance retention after the third healing [92].

The stretchable supercapacitor can be fabricated by following one of the two ways: (i) stretchable fiber electrodes coated by conductive materials (ii) spinning of conductive fiber electrodes from the stretchable materials. Other supporting methods, such as pre-straining, helix winding, and self-twisting, generally result in fiber electrodes with improved electrochemical performances, functionalities and stretchability [93]. The coating methods adopted are dip coating [94], hydrothermal synthesis [95], electrochemical deposition [96], etc.

2D planar configuration

In 2D planar configuration, a sandwich type of design is prominent in supercapacitors where two thin film electrodes are separated by solid-state electrolyte as shown in Fig. 7. The electrodes involved can either be stretchable or in the case of non-stretchable material, buckled/wavy design strategy can be adopted [21, 97, 98]. An omni-healable and highly stretchable supercapacitor was designed by making a sandwich structure of hydrogel electrodes and electrolytes. The fabricated sandwich-type supercapacitor showed a stretchability of up to 800%. [18]. The sandwich-type design can be easily fabricated but major the limitation lies in the difficulty of system miniaturization. To overcome this disadvantage, an in-plane interdigitated design is

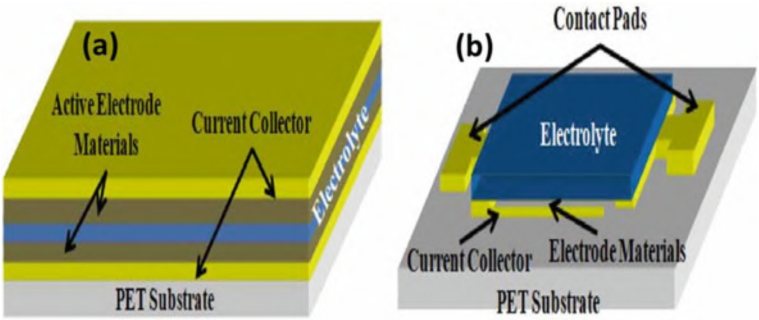

Fig. 7 **a** The sandwich structure of SCs. **b** the in-plane inter-digitated configuration of SCs reprinted with permission from [103]

adopted [99], which allows the miniaturized size of the system by bringing ion transport to a shorter distance favouring the smaller size of the energy storage device. The rigid material used in the fabrication of interdigitated electrodes creates cracks while stretching. Thus, such materials are designed into wavy structures and then lodged into supercapacitors to tolerate large amount of strain. MWCNT/PANI hybrid electrode was utilized to fabricate a fully stretchable microsupercapacitor. Due to the wavy shape of the electrodes, the fabricated device exhibited an areal-specific capacitance as high as 44.13 mF cm^{-2} under 5–40% stretching [100]. The energy density for this sandwich design is relatively low. Therefore, numbers of supercapacitors are connected in arrays in the form of a serpentine bridge-island connection.

Stretchable microsupercapacitor arrays were prepared using SWCNT electrode and ion-gel electrolyte, which were then integrated into metallic serpentine bridge-island interconnections [101]. The fabricated device was stable upon stretching up to 30% without an obvious reduction in capacitance and was able to power micro LEDs under stretched conditions. However, this design is associated with risk related to the breaking of solid metallic interconnects during large deformation. An alternate method was developed which utilized liquid metal to connect the individual supercapacitors and has exhibited a fluidic nature of the liquid metal [102].

Sputtering and spray coating are used for thin films such as coating of the gold current collector. CVD is utilized for developing electrodes with high specific surface area. Layer-by-layer coating allows multiple layers of permeable compact films increasing the power density of the device. The interdigitated pattern with high resolution in 2D designs can be realized by nanofabrication techniques such as etching, photolithography [104] and laser writing [105]. There are many other fabrication techniques that were performed in recent years such as laser direct writing and microfluidic wet-etching technique. In recent studies, microfluidic wet-etching technique was used for the fabrication of in-plane supercapacitors [106]. A thin film of MnO_2 nanofiber was initially deposited by electrospinning technique, which was subsequently transferred onto the gel electrolyte followed by sputtering with an ITO layer. The microfluidic etching method was utilized to fabricate the interdigitated patterns in preformed microfluidic channels. The approach was simpler which makes it more economically viable than other conventional etching methods for electrode patterning.

3D configuration

3D configuration in stretchable supercapacitor can tolerate strain from all 3 directions giving rise to functional advantages over the 1D and 2D configurations. Important designs for 3D configuration are kirigami-inspired [107] and 3D sponge structures [108]. Kirigami-based design is developed from the influence of the kirigami art of paper folding. The paper-sized supercapacitors are cut and arranged into 3D structures. Hence, the designed device is stretchable in all 3 directions [109, 110]. 3D honeycomb, pyramid pop-up, and living-hinge-like structures were designed using stretchable MnO_2 nanowire electrodes to fabricate the kirigami-inspired stretchable supercapacitors [111].

The fabricated honeycomb-like supercapacitor exhibited superior performance. Specific capacitance of 227.2 $mFcm^{-2}$ and stretchability of 500% were achieved. 98% capacitance was retained after 1000 stretching–releasing cycles at 400% tensile strain.

In another study, an origami-type stretchable supercapacitor was fabricated by a unique patterning approach containing a packed series connection [112]. The fabricated origami structure based supercapacitor exhibited both enhanced energy and power density as well as the supercapacitor was capable of accommodating constant deformation from −60% compression to 30% stretching. Similar strategies can be adopted, to design stretchable commercial electronics, such as watch straps [113] and integrated strain sensors [111] using nonactive elastic substrates.

Sponge structure is basically highly porous substrates that can withstand compressions in a 3-dimensional array. This intrinsic compressibility provides its potential use in compressive supercapacitor [26]. As compression is the exact opposite of stretching with negative strains and hence compressible supercapacitors are considered as a separate class of stretchable supercapacitors.

In a recent report, an all-solid-state supercapacitor based on PANI and SWCNTs sponge electrodes with very high compression tolerance has been developed. The electrical performance of the fabricated supercapacitors remained unaltered even when the device was compressed by −60% strain. Similarly, textile-based supercapacitors with 3D configuration have attracted significant attention, due to their stretchability and high porosity [114]. In a pioneering work, a tricot wavy structure with a repeating *zig-zag* pattern has been developed using interwoven inelastic and elastic hybrid yarns [115]. The fabricated design exhibited excellent stretchability as much as 200% and good mechanical stability under the dynamic strain condition. The developed stretchable supercapacitor coated with MWCNTs exhibited sevenfold enhancement in conductivity with a value of 33,000 S cm^{-1} even under 130% strain deformation.

Kirigami-based supercapacitors are designed in a way to facilitate the omnidirectional stretchability. The design is a segmental collection of various planar supercapacitors, such that different electrical connections can be established in one patch. The design can be fabricated by using various methods such as laser-assisted graphitic conversion, template method, etc. In a previous report, a kirigami-inspired highly stretchable supercapacitor was fabricated via graphitic conversion assisted by laser cutting [110]. Then fabricated assembly could tolerate more than 200% elongation. For textile supercapacitors, laser welding, ultrasonic welding and adhesive bonding are utilized. This helps in removing bulky stitched seams as well as improves the flexibility of the bioelectronic device [116]. However, still, the large-scale industrial production of the textile-based stretchable supercapacitor is very challenging and it needs dedicated and continuous research efforts in this field.

5 Conclusions

Heath monitoring devices need very low power for their functioning. The most important requirements of energy storage devices for healthcare device application are their biocompatibility and stretchability. Moreover, they should be fast charging and capable of storing energy generated by intermittent body motion with no harmful effect on the body. In this respect, supercapacitors have come up as promising energy storage devices as compared to the Li-ion batteries because of various functional disadvantages and compatibility issues associated with the batteries such as slow charge–discharge cycles, low cyclic stability, risk of explosion, toxicity and health hazards. However, the miniaturization of energy storage devices is still a critical issue where dedicated research efforts should be directed in order to realize the full potential of supercapacitor devices as an effective power source for healthcare devices.

Acknowledgements Authors are thankful to Vice-Chancellor, Harcourt Butler Technical University for providing the required literature and administrative support for writing this chapter.

References

1. Haghi M, Thurow K, Stoll R (2017) Wearable devices in medical internet of things: scientific research and commercially available devices. Healthc Inform Res 23:4–15. https://doi.org/10.4258/hir.2017.23.1.4
2. Xu S, Jayaraman A, Rogers JA (2019) Skin sensors are the future of health care. Nature 571:319–321. https://doi.org/10.1038/d41586-019-02143-0
3. Khan Y, Ostfeld AE, Lochner CM, Pierre A, Arias AC (2016) Monitoring of vital signs with flexible and wearable medical devices. Adv Mater 28:4373–4395. https://doi.org/10.1002/adma.201504366
4. Nayak PK, Erickson EM, Schipper F, Penki TR, Munichandraiah N, Adelhelm P, Sclar H, Amalraj F, Markovsky B, Aurbach D (2018) Review on challenges and recent advances in the electrochemical performance of high capacity Li- and Mn-rich cathode materials for Li-ion batteries. Adv Energy Mater 8:1702397. https://doi.org/10.1002/aenm.201702397

5. Kim J-K, Shin YJ, Ha LJ, Kim D-H, Kim D-H (2019) Unraveling the mechanobiology of the immune system. Adv Healthc Mater 1801332. https://doi.org/10.1002/adhm.201801332
6. Moradi O, Gupta VK, Agarwal S, Tyagi I, Asif M, Makhlouf ASH, Sadegh H, Shahryari-ghoshekandi R (2015) Retracted: characteristics and electrical conductivity of graphene and graphene oxide for adsorption of cationic dyes from liquids: Kinetic and thermodynamic study. J Ind Eng Chem 28:294–301. https://doi.org/10.1016/j.jiec.2015.03.005
7. Schwamb T, Burg BR, Schirmer NC, Poulikakos D (2009) An electrical method for the measurement of the thermal and electrical conductivity of reduced graphene oxide nanostructures. Nanotechnology 20:405704. https://doi.org/10.1088/0957-4484/20/40/405704
8. Lee C, Wei X, Kysar JW, Hone J (2008) Measurement of the elastic properties and intrinsic strength of monolayer graphene. Science (1979)321:385–388. https://doi.org/10.1126/science.1157996
9. Lu G, Ocola LE, Chen J (2009) Reduced graphene oxide for room-temperature gas sensors. Nanotechnology 20:445502. https://doi.org/10.1088/0957-4484/20/44/445502
10. Pendashteh A, Mousavi MF, Rahmanifar MS (2013) Fabrication of anchored copper oxide nanoparticles on graphene oxide nanosheets via an electrostatic coprecipitation and its application as supercapacitor. Electrochim Acta 88:347–357. https://doi.org/10.1016/j.electacta.2012.10.088
11. Ge S, Yan M, Lu J, Zhang M, Yu F, Yu J, Song X, Yu S (2012) Electrochemical biosensor based on graphene oxide–Au nanoclusters composites for l-cysteine analysis. Biosens Bioelectron 31:49–54. https://doi.org/10.1016/j.bios.2011.09.038
12. Toda K, Furue R, Hayami S (2015) Recent progress in applications of graphene oxide for gas sensing: a review. Anal Chim Acta 878:43–53. https://doi.org/10.1016/j.aca.2015.02.002
13. Chen X, Paul R, Dai L (2017) Carbon-based supercapacitors for efficient energy storage. Natl Sci Rev 4:453–489. https://doi.org/10.1093/nsr/nwx009
14. Tybrandt K, Khodagholy D, Dielacher B, Stauffer F, Renz AF, Buzsáki G, Vörös J (2018) High-density stretchable electrode grids for chronic neural recording. Adv Mater 30:1706520. https://doi.org/10.1002/adma.201706520
15. Wang Y, Wu X, Han Y, Li T (2021) Flexible supercapacitor: overview and outlooks. J Energy Storage 42:103053. https://doi.org/10.1016/j.est.2021.103053
16. Lv T, Yao Y, Li N, Chen T (2016) Highly stretchable supercapacitors based on aligned carbon nanotube/molybdenum disulfide composites. Angew Chem Int Ed 55:9191–9195. https://doi.org/10.1002/anie.201603356
17. Huang Y, Hu H, Huang Y, Zhu M, Meng W, Liu C, Pei Z, Hao C, Wang Z, Zhi C (2015) From industrially weavable and knittable highly conductive yarns to large wearable energy storage textiles. ACS Nano 9:4766–4775. https://doi.org/10.1021/acsnano.5b00860
18. Chen C, Qin H, Cong H, Yu S (2019) A highly stretchable and real-time healable supercapacitor. Adv Mater 31:1900573. https://doi.org/10.1002/adma.201900573
19. Dubal DP, Chodankar NR, Kim D-H, Gomez-Romero P (2018) Towards flexible solid-state supercapacitors for smart and wearable electronics. Chem Soc Rev 47:2065–2129. https://doi.org/10.1039/C7CS00505A
20. Zhao C, Liu Y, Beirne S, Razal J, Chen J (2018) Recent development of fabricating flexible micro-supercapacitors for wearable devices. Adv Mater Technol 3:1800028. https://doi.org/10.1002/admt.201800028
21. An T, Cheng W (2018) Recent progress in stretchable supercapacitors. J Mater Chem A Mater 6:15478–15494. https://doi.org/10.1039/C8TA03988G
22. Zhao K, Wang H, Zhu C, Lin S, Xu Z, Zhang X (2019) Free-standing MXene film modified by amorphous FeOOH quantum dots for high-performance asymmetric supercapacitor. Electrochim Acta 308:1–8. https://doi.org/10.1016/j.electacta.2019.03.225
23. Guo M, Liu C, Zhang Z, Zhou J, Tang Y, Luo S (2018) Flexible $Ti_3C_2T_x$@Al electrodes with ultrahigh areal capacitance: in situ regulation of interlayer conductivity and spacing. Adv Funct Mater 28:1803196. https://doi.org/10.1002/adfm.201803196
24. Liao H, Guo X, Wan P, Yu G (2019) Conductive mxene nanocomposite organohydrogel for flexible, healable, low-temperature tolerant strain sensors. Adv Funct Mater 29:1904507. https://doi.org/10.1002/adfm.201904507

25. Zhou J, Yu J, Shi L, Wang Z, Liu H, Yang B, Li C, Zhu C, Xu J (2018) A conductive and highly deformable all-pseudocapacitive composite paper as supercapacitor electrode with improved areal and volumetric capacitance. Small 14:1803786. https://doi.org/10.1002/smll.201803786
26. Yue Y, Liu N, Ma Y, Wang S, Liu W, Luo C, Zhang H, Cheng F, Rao J, Hu X, Su J, Gao Y (2018) Highly self-healable 3D microsupercapacitor with mxene–graphene composite aerogel. ACS Nano 12:4224–4232. https://doi.org/10.1021/acsnano.7b07528
27. Wang H-N, Zhang M, Zhang A-M, Shen F-C, Wang X-K, Sun S-N, Chen Y-J, Lan Y-Q (2018) Polyoxometalate-based metal-organic frameworks with conductive polypyrrole for supercapacitors. ACS Appl Mater Interfaces 10:32265–32270. https://doi.org/10.1021/acsami.8b12194
28. Zhao W, Peng J, Wang W, Jin B, Chen T, Liu S, Zhao Q, Huang W (2019) Interlayer hydrogen-bonded metal porphyrin frameworks/mxene hybrid film with high capacitance for flexible all-solid-state supercapacitors. Small 15:1901351. https://doi.org/10.1002/smll.201901351
29. Cao X-M, Han Z-B (2019) Hollow core–shell ZnO@ZIF-8 on carbon cloth for flexible supercapacitors with ultrahigh areal capacitance. Chem Commun 55:1746–1749. https://doi.org/10.1039/C8CC09847F
30. Wu H, Zhang W, Kandambeth S, Shekhah O, Eddaoudi M, Alshareef HN (2019) Conductive metal-organic frameworks selectively grown on laser-scribed graphene for electrochemical microsupercapacitors. Adv Energy Mater 9:1900482. https://doi.org/10.1002/aenm.201900482
31. Chen Y, Han M, Tang Y, Bao J, Li S, Lan Y, Dai Z (2015) Polypyrrole–polyoxometalate/reduced graphene oxide ternary nanohybrids for flexible, all-solid-state supercapacitors. Chem Commun 51:12377–12380. https://doi.org/10.1039/C5CC02717A
32. Fu X-Y, Chen Z-D, Zhang Y-L, Han D-D, Ma J-N, Wang W, Zhang Z-R, Xia H, Sun H-B (2019) Direct laser writing of flexible planar supercapacitors based on GO and black phosphorus quantum dot nanocomposites. Nanoscale 11:9133–9140. https://doi.org/10.1039/C9NR02530H
33. Luo S, Zhao J, Zou J, He Z, Xu C, Liu F, Huang Y, Dong L, Wang L, Zhang H (2018) Self-standing polypyrrole/black phosphorus laminated film: promising electrode for flexible supercapacitor with enhanced capacitance and cycling stability. ACS Appl Mater Interfaces 10:3538–3548. https://doi.org/10.1021/acsami.7b15458
34. Yang B, Hao C, Wen F, Wang B, Mu C, Xiang J, Li L, Xu B, Zhao Z, Liu Z, Tian Y (2017) Flexible black-phosphorus nanoflake/carbon nanotube composite paper for high-performance all-solid-state supercapacitors. ACS Appl Mater Interfaces 9:44478–44484. https://doi.org/10.1021/acsami.7b13572
35. Wu X, Xu Y, Hu Y, Wu G, Cheng H, Yu Q, Zhang K, Chen W, Chen S (2018) Microfluidic-spinning construction of black-phosphorus-hybrid microfibres for non-woven fabrics toward a high energy density flexible supercapacitor. Nat Commun 9:4573. https://doi.org/10.1038/s41467-018-06914-7
36. Zhang L, DeArmond D, Alvarez NT, Malik R, Oslin N, McConnell C, Adusei PK, Hsieh Y, Shanov V (2017) Flexible micro-supercapacitor based on graphene with 3D structure. Small 13:1603114. https://doi.org/10.1002/smll.201603114
37. Lv J, Jeerapan I, Tehrani F, Yin L, Silva-Lopez CA, Jang J-H, Joshuia D, Shah R, Liang Y, Xie L, Soto F, Chen C, Karshalev E, Kong C, Yang Z, Wang J (2018) Sweat-based wearable energy harvesting-storage hybrid textile devices. Energy Environ Sci 11:3431–3442. https://doi.org/10.1039/C8EE02792G
38. Mosa IM, Pattammattel A, Kadimisetty K, Pande P, El-Kady MF, Bishop GW, Novak M, Kaner RB, Basu AK, Kumar C, v., Rusling JF, (2017) Ultrathin graphene-protein supercapacitors for miniaturized bioelectronics. Adv Energy Mater 7:1700358. https://doi.org/10.1002/aenm.201700358
39. Lu Z, Foroughi J, Wang C, Long H, Wallace GG (2018) Superelastic hybrid CNT/graphene fibers for wearable energy storage. Adv Energy Mater 8:1702047. https://doi.org/10.1002/aenm.201702047

40. Wichaita W, Kim Y-G, Tangboriboonrat P, Thérien-Aubin H (2020) Polymer-functionalized polymer nanoparticles and their behaviour in suspensions. Polym Chem 11:2119–2128. https://doi.org/10.1039/C9PY01558B
41. Zeng W, Shu L, Li Q, Chen S, Wang F, Tao X-M (2014) Fiber-based wearable electronics: a review of materials, fabrication, devices, and applications. Adv Mater 26:5310–5336. https://doi.org/10.1002/adma.201400633
42. Zheng B, Huang T, Kou L, Zhao X, Gopalsamy K, Gao C (2014) Graphene fiber-based asymmetric micro-supercapacitors. J Mater Chem A 2:9736–9743. https://doi.org/10.1039/C4TA01868K
43. Son D, Lee J, Qiao S, Ghaffari R, Kim J, Lee JE, Song C, Kim SJ, Lee DJ, Jun SW, Yang S, Park M, Shin J, Do K, Lee M, Kang K, Hwang CS, Lu N, Hyeon T, Kim D-H (2014) Multifunctional wearable devices for diagnosis and therapy of movement disorders. Nat Nanotechnol 9:397–404. https://doi.org/10.1038/nnano.2014.38
44. Sun H, You X, Deng J, Chen X, Yang Z, Chen P, Fang X, Peng H (2014) A twisted wire-shaped dual-function energy device for photoelectric conversion and electrochemical storage. Angew Chem 126:6782–6786. https://doi.org/10.1002/ange.201403168
45. Yu D, Goh K, Zhang Q, Wei L, Wang H, Jiang W, Chen Y (2014) Controlled functionalization of carbonaceous fibers for asymmetric solid-state micro-supercapacitors with high volumetric energy density. Adv Mater 26:6790–6797. https://doi.org/10.1002/adma.201403061
46. Kim H, Yoon J, Lee G, Paik S, Choi G, Kim D, Kim B-M, Zi G, Ha JS (2016) Encapsulated, high-performance, stretchable array of stacked planar micro-supercapacitors as waterproof wearable energy storage devices. ACS Appl Mater Interfaces 8:16016–16025. https://doi.org/10.1021/acsami.6b03504
47. Song W, Zhu J, Gan B, Zhao S, Wang H, Li C, Wang J (2018) Flexible, stretchable, and transparent planar microsupercapacitors based on 3D porous laser-induced graphene. Small 14:1702249. https://doi.org/10.1002/smll.201702249
48. Yun TG, Park M, Kim D-H, Kim D, Cheong JY, Bae JG, Han SM, Kim I-D (2019) All-transparent stretchable electrochromic supercapacitor wearable patch device. ACS Nano 13:3141–3150. https://doi.org/10.1021/acsnano.8b08560
49. Luan P, Zhang N, Zhou W, Niu Z, Zhang Q, Cai L, Zhang X, Yang F, Fan Q, Zhou W, Xiao Z, Gu X, Chen H, Li K, Xiao S, Wang Y, Liu H, Xie S (2016) Epidermal Supercapacitor with High Performance. Adv Funct Mater 26:8178–8184. https://doi.org/10.1002/adfm.201603480
50. Sim HJ, Choi C, Lee DY, Kim H, Yun J-H, Kim JM, Kang TM, Ovalle R, Baughman RH, Kee CW, Kim SJ (2018) Biomolecule based fiber supercapacitor for implantable device. Nano Energy 47:385–392. https://doi.org/10.1016/j.nanoen.2018.03.011
51. Meng C, Gall OZ, Irazoqui PP (2013) A flexible super-capacitive solid-state power supply for miniature implantable medical devices. Biomed Microdevices 15:973–983. https://doi.org/10.1007/s10544-013-9789-1
52. Cao X, Halder A, Tang Y, Hou C, Wang H, Duus JØ, Chi Q (2018) Engineering two-dimensional layered nanomaterials for wearable biomedical sensors and power devices. Mater Chem Front 2:1944–1986. https://doi.org/10.1039/C8QM00356D
53. Chen Y, Xu B, Gong J, Wen J, Hua T, Kan C-W, Deng J (2019) Design of high-performance wearable energy and sensor electronics from fiber materials. ACS Appl Mater Interfaces 11:2120–2129. https://doi.org/10.1021/acsami.8b16167
54. Chun S, Son W, Lee G, Kim SH, Park JW, Kim SJ, Pang C, Choi C (2019) Single-layer graphene-based transparent and flexible multifunctional electronics for self-charging power and touch-sensing systems. ACS Appl Mater Interfaces 11:9301–9308. https://doi.org/10.1021/acsami.8b20143
55. Yun J, Song C, Lee H, Park H, Jeong YR, Kim JW, Jin SW, Oh SY, Sun L, Zi G, Ha JS (2018) Stretchable array of high-performance micro-supercapacitors charged with solar cells for wireless powering of an integrated strain sensor. Nano Energy 49:644–654. https://doi.org/10.1016/j.nanoen.2018.05.017

56. Li L, Fu C, Lou Z, Chen S, Han W, Jiang K, Chen D, Shen G (2017) Flexible planar concentric circular micro-supercapacitor arrays for wearable gas sensing application. Nano Energy 41:261–268. https://doi.org/10.1016/j.nanoen.2017.08.060
57. Hwang B-U, Lee J-H, Trung TQ, Roh E, Kim D-I, Kim S-W, Lee N-E (2015) Transparent stretchable self-powered patchable sensor platform with ultrasensitive recognition of human activities. ACS Nano 9:8801–8810. https://doi.org/10.1021/acsnano.5b01835
58. Liang X, Long G, Fu C, Pang M, Xi Y, Li J, Han W, Wei G, Ji Y (2018) High performance all-solid-state flexible supercapacitor for wearable storage device application. Chem Eng J 345:186–195. https://doi.org/10.1016/j.cej.2018.03.104
59. Gao W, Emaminejad S, Nyein HYY, Challa S, Chen K, Peck A, Fahad HM, Ota H, Shiraki H, Kiriya D, Lien D-H, Brooks GA, Davis RW, Javey A (2016) Fully integrated wearable sensor arrays for multiplexed in situ perspiration analysis. Nature 529:509–514. https://doi.org/10.1038/nature16521
60. Lu Y, Jiang K, Chen D, Shen G (2019) Wearable sweat monitoring system with integrated micro-supercapacitors. Nano Energy 58:624–632. https://doi.org/10.1016/j.nanoen.2019.01.084
61. Lin Y, Chen J, Tavakoli MM, Gao Y, Zhu Y, Zhang D, Kam M, He Z, Fan Z (2019) Printable fabrication of a fully integrated and self-powered sensor system on plastic substrates. Adv Mater 31:1804285. https://doi.org/10.1002/adma.201804285
62. Guo R, Chen J, Yang B, Liu L, Su L, Shen B, Yan X (2017) In-plane micro-supercapacitors for an integrated device on one piece of paper. Adv Funct Mater 27:1702394. https://doi.org/10.1002/adfm.201702394
63. Park Y-G, Lee S, Park J-U (2019) Recent progress in wireless sensors for wearable electronics. Sensors 19:4353. https://doi.org/10.3390/s19204353
64. Karalis A, Joannopoulos JD, Soljačić M (2008) Efficient wireless non-radiative mid-range energy transfer. Ann Phys (N Y) 323:34–48. https://doi.org/10.1016/j.aop.2007.04.017
65. Bocan K, Sejdić E (2016) Adaptive transcutaneous power transfer to implantable devices: a state of the art review. Sensors 16:393. https://doi.org/10.3390/s16030393
66. Ng DC, Bai S, Yang J, Tran N, Skafidas E (2009) Wireless technologies for closed-loop retinal prostheses. J Neural Eng 6:065004. https://doi.org/10.1088/1741-2560/6/6/065004
67. Xue N, Lee J-B, Foland S, Chang SP (2011) Biocompatible polymeric wireless pressure sensor for intraocular pressure sensing application. In: 2011 IEEE sensors proceedings. IEEE, pp 1748–1751
68. Ho JS, Yeh AJ, Neofytou E, Kim S, Tanabe Y, Patlolla B, Beygui RE, Poon ASY (2014) Wireless power transfer to deep-tissue microimplants. Proc Natl Acad Sci 111:7974–7979. https://doi.org/10.1073/pnas.1403002111
69. Jeong CK, Lee J, Han S, Ryu J, Hwang G-T, Park DY, Park JH, Lee SS, Byun M, Ko SH, Lee KJ (2015) A hyper-stretchable elastic-composite energy harvester. Adv Mater 27:2866–2875. https://doi.org/10.1002/adma.201500367
70. Lee S, Hinchet R, Lee Y, Yang Y, Lin Z-H, Ardila G, Montès L, Mouis M, Wang ZL (2014) Ultrathin nanogenerators as self-powered/active skin sensors for tracking eye ball motion. Adv Funct Mater 24:1163–1168. https://doi.org/10.1002/adfm.201301971
71. Srbinovska M, Gavrovski C, Dimcev V, Krkoleva A, Borozan V (2015) Environmental parameters monitoring in precision agriculture using wireless sensor networks. J Clean Prod 88:297–307. https://doi.org/10.1016/j.jclepro.2014.04.036
72. Tran TV, Chung W-Y (2016) High-efficient energy harvester with flexible solar panel for a wearable sensor device. IEEE Sens J 16:9021–9028. https://doi.org/10.1109/JSEN.2016.2616114
73. Rao J, Chen Z, Zhao D, Yin Y, Wang X, Yi F (2019) Recent progress in self-powered skin sensors. Sensors 19:2763. https://doi.org/10.3390/s19122763
74. Wen Z, Yang Y, Sun N, Li G, Liu Y, Chen C, Shi J, Xie L, Jiang H, Bao D, Zhuo Q, Sun X (2018) A wrinkled PEDOT:PSS film based stretchable and transparent triboelectric nanogenerator for wearable energy harvesters and active motion sensors. Adv Funct Mater 28:1803684. https://doi.org/10.1002/adfm.201803684

75. Vladimir L, Bert G, Van HC, Tom T, Firat YR, Vullers RuudJ, M., Fiorini Paolo, (2008) Wearable self-powered wireless devices with thermoelectric energy scavengers. 2nd European conference & exhibition on integration issues of miniaturized systems—MOMS, MOEMS. ICS and Electronic Components. Barcelona, Spain, pp 1–8
76. Qiu H-J, Song W-Z, Wang X-X, Zhang J, Fan Z, Yu M, Ramakrishna S, Long Y-Z (2019) A calibration-free self-powered sensor for vital sign monitoring and finger tap communication based on wearable triboelectric nanogenerator. Nano Energy 58:536–542. https://doi.org/10.1016/j.nanoen.2019.01.069
77. Curie, J. & Curie, P. (1880). Development by pressure of polar electricity in hemihedral crystals with inclined faces. Bull. Soc. Miner. Fr. 3, 90–93
78. Zhu G, Chen J, Zhang T, Jing Q, Wang ZL (2014) Radial-arrayed rotary electrification for high performance triboelectric generator. Nat Commun 5:3426. https://doi.org/10.1038/ncomms4426
79. Wang S, Mu X, Yang Y, Sun C, Gu AY, Wang ZL (2015) Flow-driven triboelectric generator for directly powering a wireless sensor node. Adv Mater 27:240–248. https://doi.org/10.1002/adma.201403944
80. Sun P, Qiu M, Li M, Mai W, Cui G, Tong Y (2019) Stretchable Ni@NiCoP textile for wearable energy storage clothes. Nano Energy 55:506–515. https://doi.org/10.1016/j.nanoen.2018.10.067
81. Hager MD, Greil P, Leyens C, van der Zwaag S, Schubert US (2010) Self-healing materials. Adv Mater 22:5424–5430. https://doi.org/10.1002/adma.201003036
82. White SR, Sottos NR, Geubelle PH, Moore JS, Kessler MR, Sriram SR, Brown EN, Viswanathan S (2001) Autonomic healing of polymer composites. Nature 409:794–797. https://doi.org/10.1038/35057232
83. Blaiszik BJ, Kramer SLB, Olugebefola SC, Moore JS, Sottos NR, White SR (2010) Self-healing polymers and composites. Annu Rev Mater Res 40:179–211. https://doi.org/10.1146/annurev-matsci-070909-104532
84. Roy N, Bruchmann B, Lehn J-M (2015) Dynamers: dynamic polymers as self-healing materials. Chem Soc Rev 44:3786–3807. https://doi.org/10.1039/C5CS00194C
85. le Neindre M, Nicolaÿ R (2014) Polythiol copolymers with precise architectures: a platform for functional materials. Polym Chem 5:4601. https://doi.org/10.1039/C4PY00293H
86. Spitalsky Z, Tasis D, Papagelis K, Galiotis C (2010) Carbon nanotube–polymer composites: chemistry, processing, mechanical and electrical properties. Prog Polym Sci 35:357–401. https://doi.org/10.1016/j.progpolymsci.2009.09.003
87. Sandler JKW, Kirk JE, Kinloch IA, Shaffer MSP, Windle AH (2003) Ultra-low electrical percolation threshold in carbon-nanotube-epoxy composites. Polymer (Guildf) 44:5893–5899. https://doi.org/10.1016/S0032-3861(03)00539-1
88. Guo K, Zhang D-L, Zhang X-M, Zhang J, Ding L-S, Li B-J, Zhang S (2015) Conductive elastomers with autonomic self-healing properties. Angew Chem Int Ed 54:12127–12133. https://doi.org/10.1002/anie.201505790
89. Niu Y, Liu H, He R, Li Z, Ren H, Gao B, Guo H, Genin GM, Xu F (2020) The new generation of soft and wearable electronics for health monitoring in varying environment: From normal to extreme conditions. Mater Today 41:219–242. https://doi.org/10.1016/j.mattod.2020.10.004
90. Guo FM, Xu RQ, Cui X, Zhang L, Wang KL, Yao YW, Wei JQ (2016) High performance of stretchable carbon nanotube–polypyrrole fiber supercapacitors under dynamic deformation and temperature variation. J Mater Chem A Mater 4:9311–9318. https://doi.org/10.1039/C6TA02437H
91. Zhang Z, Wang L, Li Y, Wang Y, Zhang J, Guan G, Pan Z, Zheng G, Peng H (2017) Nitrogen-doped core-sheath carbon nanotube array for highly stretchable supercapacitor. Adv Energy Mater 7:1601814. https://doi.org/10.1002/aenm.201601814
92. Wang S, Liu N, Su J, Li L, Long F, Zou Z, Jiang X, Gao Y (2017) Highly stretchable and self-healable supercapacitor with reduced graphene oxide based fiber springs. ACS Nano 11:2066–2074. https://doi.org/10.1021/acsnano.6b08262

93. Wen L, Li F, Cheng H-M (2016) Carbon nanotubes and graphene for flexible electrochemical energy storage: from materials to devices. Adv Mater 28:4306–4337. https://doi.org/10.1002/adma.201504225
94. Kim SJ, Kang M-A, Jeon I, Ji S, Song W, Myung S, Lee SS, Lim J, An K-S (2017) Fabrication of high-performance flexible photodetectors based on Zn-doped MoS_2/graphene hybrid fibers. J Mater Chem C Mater 5:12354–12359. https://doi.org/10.1039/C7TC04274D
95. Xu W, Dai S, Liu G, Xi Y, Hu C, Wang X (2016) CuO nanoflowers growing on carbon fiber fabric for flexible high-performance supercapacitors. Electrochim Acta 203:1–8. https://doi.org/10.1016/j.electacta.2016.03.170
96. Sun G, Zhang X, Lin R, Yang J, Zhang H, Chen P (2015) Hybrid fibers made of molybdenum disulfide, reduced graphene oxide, and multi-walled carbon nanotubes for solid-state, flexible, asymmetric supercapacitors. Angew Chem 127:4734–4739. https://doi.org/10.1002/ange.201411533
97. Cao C, Chu Y, Zhou Y, Zhang C, Qu S (2018) Recent advances in stretchable supercapacitors enabled by low-dimensional nanomaterials. Small 14:1803976. https://doi.org/10.1002/smll.201803976
98. Xie Y, Liu Y, Zhao Y, Tsang YH, Lau SP, Huang H, Chai Y (2014) Stretchable all-solid-state supercapacitor with wavy shaped polyaniline/graphene electrode. J Mater Chem A 2:9142–9149. https://doi.org/10.1039/C4TA00734D
99. Ferris A, Bourrier D, Garbarino S, Guay D, Pech D (2019) 3D interdigitated microsupercapacitors with record areal cell capacitance. Small 15:1901224. https://doi.org/10.1002/smll.201901224
100. Li L, Lou Z, Han W, Chen D, Jiang K, Shen G (2017) Highly stretchable micro-supercapacitor arrays with hybrid MWCNT/PANI electrodes. Adv Mater Technol 2:1600282. https://doi.org/10.1002/admt.201600282
101. Kim D, Shin G, Kang YJ, Kim W, Ha JS (2013) Fabrication of a stretchable solid-state micro-supercapacitor array. ACS Nano 7:7975–7982. https://doi.org/10.1021/nn403068d
102. Yun J, Lim Y, Lee H, Lee G, Park H, Hong SY, Jin SW, Lee YH, Lee S-S, Ha JS (2017) A patterned graphene/ZnO UV sensor driven by integrated asymmetric micro-supercapacitors on a liquid metal patterned foldable paper. Adv Funct Mater 27:1700135. https://doi.org/10.1002/adfm.201700135
103. Rani S, Kumar N, Sharma Y (2021) Recent progress and future perspectives for the development of micro-supercapacitors for portable/wearable electronics applications. J Phys Energy 3:032017. https://doi.org/10.1088/2515-7655/ac01c0
104. Wu Z-S, Parvez K, Feng X, Müllen K (2014) Photolithographic fabrication of high-performance all-solid-state graphene-based planar micro-supercapacitors with different interdigital fingers. J Mater Chem A Mater 2:8288. https://doi.org/10.1039/c4ta00958d
105. Lamberti A, Clerici F, Fontana M, Scaltrito L (2016) A highly stretchable supercapacitor using laser-induced graphene electrodes onto elastomeric substrate. Adv Energy Mater 6:1600050. https://doi.org/10.1002/aenm.201600050
106. Xue M, Xie Z, Zhang L, Ma X, Wu X, Guo Y, Song W, Li Z, Cao T (2011) Microfluidic etching for fabrication of flexible and all-solid-state micro supercapacitor based on MnO_2 nanoparticles. Nanoscale 3:2703. https://doi.org/10.1039/c0nr00990c
107. Maeng J, Kim Y-J, Meng C, Irazoqui PP (2016) Three-dimensional microcavity array electrodes for high-capacitance all-solid-state flexible microsupercapacitors. ACS Appl Mater Interfaces 8:13458–13465. https://doi.org/10.1021/acsami.6b03559
108. Olszowska K, Pang J, Wrobel PS, Zhao L, Ta HQ, Liu Z, Trzebicka B, Bachmatiuk A, Rummeli MH (2017) Three-dimensional nanostructured graphene: synthesis and energy, environmental and biomedical applications. Synth Met 234:53–85. https://doi.org/10.1016/j.synthmet.2017.10.014
109. Jiao S, Zhou A, Wu M, Hu H (2019) Kirigami patterning of mxene/bacterial cellulose composite paper for all-solid-state stretchable micro-supercapacitor arrays. Adv Sci 6:1900529. https://doi.org/10.1002/advs.201900529

110. Xu R, Zverev A, Hung A, Shen C, Irie L, Ding G, Whitmeyer M, Ren L, Griffin B, Melcher J, Zheng L, Zang X, Sanghadasa M, Lin L (2018) Kirigami-inspired, highly stretchable micro-supercapacitor patches fabricated by laser conversion and cutting. Microsyst Nanoeng 4:36. https://doi.org/10.1038/s41378-018-0036-z
111. Lv Z, Luo Y, Tang Y, Wei J, Zhu Z, Zhou X, Li W, Zeng Y, Zhang W, Zhang Y, Qi D, Pan S, Loh XJ, Chen X (2018) Editable supercapacitors with customizable stretchability based on mechanically strengthened ultralong MnO_2 nanowire composite. Adv Mater 30:1704531. https://doi.org/10.1002/adma.201704531
112. Nam I, Kim G-P, Park S, Han JW, Yi J (2014) All-solid-state, origami-type foldable supercapacitor chips with integrated series circuit analogues. Energy Environ Sci 7:1095. https://doi.org/10.1039/c3ee43175d
113. He S, Cao J, Xie S, Deng J, Gao Q, Qiu L, Zhang J, Wang L, Hu Y, Peng H (2016) Stretchable supercapacitor based on a cellular structure. J Mater Chem A Mater 4:10124–10129. https://doi.org/10.1039/C6TA03762C
114. Yu X, Su X, Yan K, Hu H, Peng M, Cai X, Zou D (2016) Stretchable, conductive, and stable PEDOT-modified textiles through a novel in situ polymerization process for stretchable supercapacitors. Adv Mater Technol 1:1600009. https://doi.org/10.1002/admt.201600009
115. Lee Y-H, Kim Y, Lee T-I, Lee I, Shin J, Lee HS, Kim T-S, Choi JW (2015) Anomalous stretchable conductivity using an engineered tricot weave. ACS Nano 9:12214–12223. https://doi.org/10.1021/acsnano.5b05465
116. Huang Q, Wang D, Zheng Z (2016) Textile-based electrochemical energy storage devices. Adv Energy Mater 6:1600783. https://doi.org/10.1002/aenm.201600783

Part VII
FNMs Based Supercapacitor for Emerging Industrial Applications

Всё для победы!
НАРОДНЫЙ ФРОНТ
https://pobeda.onf.ru/
LET'S HELP THE RUSSIA

Chapter 22
Functionalized Graphene and its Derivatives for Industrial Energy Storage

V. Shanmugapriya, S. Arunpandiyan, G. Hariharan, and A. Arivarasan

1 Introduction

Renovation is required in the future energy supply and production policies of several nations due to the continuously increasing demand for energy and the ongoing depletion of conventional sources that are still usable [1, 2]. The development of effective, clean, and renewable energy sources along with suitable storage and energy conversion technologies becomes a top priority for scientists and researchers around the world [1, 3]. Alternative renewable energy sources, like wind and solar energies have been used for great effects. But unlike wind energy, which cannot always be collected, solar energy can be captured when it is exposed to the sun [4, 5]. These non-conventional energy sources must be integrated with suitable energy storage techniques in order to produce a seamless power supply. The numerous uses of these renewable energy types in daily applications are restricted as a result of inconsistency in the delivery of electricity and a number of other restrictions. However, a significant cause of worry is still the large-scale storage of the generated electrical energy. Electrochemical devices including supercapacitors, batteries, and fuel cells simply provide electrical energy [6, 7]. Among these electrochemical energy storage devices, supercapacitors make up the most important next class of energy storage devices, when compared to the several energy storage modes. Supercapacitors offer a greater energy density than regular dielectric capacitors and a far higher power density than batteries [8, 9].

Due to their high power density (>1000 times that of batteries), non-toxicity, low cost reduced heating, wide operating temperature range, long cycle life (>100,000 cycles), low maintenance requirements, mobility, and other factors, supercapacitors

---

V. Shanmugapriya · S. Arunpandiyan · G. Hariharan · A. Arivarasan (✉)
Multifunctional Materials Laboratory, Department of Physics, International Research Centre, Kalasalingam Academy of Research and Education, Krishnankoil, Tamilnadu 626126, India
e-mail: arivarasan.nanotech@gmail.com

© The Author(s), under exclusive license to Springer Nature Singapore Pte Ltd. 2024

C. M. Hussain and M. B. Ahamed (eds.), *Functionalized Nanomaterials Based Supercapacitor*, Materials Horizons: From Nature to Nanomaterials,
https://doi.org/10.1007/978-981-99-3021-0_22

(SCs), often referred to as ultracapacitors or electrochemical capacitors, are preferable to batteries [8-10]. The electric double layers (EDL) that are produced between the electrolyte and electrode's active material as a result of charge separation, are known to hold the charge in supercapacitors without faking out. Through extremely reversible faradic interactions with the electrolyte, certain materials, including polymers and metal oxides, are known to store charge [11-13]. Supercapacitors are widely utilized in consumer electronics, load cranes, forklifts, and electric automobiles, among other industrial equipment. Additionally, supercapacitors are included in systems for managing power, industrial energy, and electronic memory backups [13, 14]. Supercapacitor device integration in Airbus A380 aircraft has demonstrated their safe and reliable performance, and it is anticipated that this will expand their market in the near future [15, 16].

The most crucial component of supercapacitor devices, which determines the effectiveness of the device, is the appropriate conducting electrode material. It offers the proficient electrolyte–electrode interface and is outfitted with an adept transfer path for the electrons [13]. A perfect electrode should also have a hierarchical pore size distribution, high electrical conductivity, chemical, mechanical, thermal stabilities, and a large specific surface area [17]. The best and most common type of material used for EDL capacitive electrodes is carbon derivatives. Due to their advantageous electrical, mechanical, and structural characteristics, several carbon-based materials, including graphene-based materials, such as sheet-like graphene, graphite, fullerenes, and carbon nanotubes received extensive studies as supercapacitive electrode materials [8]. With the reinforcement of its distinctive physical features, graphene typically comprises a single layer of sp^2 hybridized atoms of carbon connected in a hexagonal lattice. However, the restricted specific capacitance that results from pure graphene's poor charge storage ability due to merely surface interaction with the electrolyte severely limits its practical applicability. Additionally, due to its extremely poor out-of-plane conductivity and tendency to aggregate, graphene has been subject to chemical changes to improve its overall electrochemical performances [18, 19].

2 Brief History of Graphene

Graphene, is the hexagonal arrangement of carbon atoms in 2-dimensional lattices and it is well known for its lightweight, stronger and very thin nature. Also, it reveals the best heat and electrical conductivities, than other types of materials. Graphene has a longer history and it have been established in the nineteenth century itself. In 1859, Benjamin Collins Brodie, an english scientist discovered that the thermally reduced graphite oxide possessed a layered structure. Later on, various attempts are made on the layered structure of graphite oxides. P.R. Wallace explains about detailed electronic structure of the graphite oxides and linear dispersion relation in 1947. Finally, Boehm and colleagues discovered the single graphene sheets by TEM in 1962. Actually, the term graphene was first used to describe carbon nanotubes and single-layer graphite in earlier days.

Graphene is made up of a continuously connected honeycomb lattice with two sub-lattices that include C-C σ-bonds. The parent of all graphitic form is graphene as seen in Fig. 1 [20, 21]. Additionally, each C atom in the lattice has a π-orbital, which is primarily in charge of supplying delocalized electrons to the carbon network [22, 23]. The architectural design and the number of layers of the individual graphene sheets are the only factors that affect the electronic properties of graphene materials. Few-layered graphene has an electronic structure and set of characteristics that are very different from those of bulk graphite [20, 24]. The number of stacked layers and the arrangement of the interlayer have an impact on the chemical, electronic, and physical characteristics of graphene at such a thin thickness. One-layered graphene sheet exhibits zero-bandgap semiconductor behavior [18, 25, 26]. Numerous computational methods on halogenation and hydrogenation of graphene have been used to examine the possibilities of engineering the band structure in order to gain insight into the phenomenon of increasing the band gap in the case of graphene sheets [24, 27]. The double-layered graphene electrons exhibit parabolic energy dispersion, and the substance also qualifies as a semiconductor with a zero-bandgap. However, by creating some asymmetry between the bilayers, double-layered graphene's adjustable bandgap can be changed easily [28]. According to these findings, bi-layer graphene has the potential to be an innovative new material with many potential uses in the future.

3 Methods for the Synthesis of Graphene

The invention of single-layer graphene was discovered in 2004 and it received much interest thereafter. As a result, a significant amount of work had been done on the synthesis of graphene using multiple bottom-up and top-down techniques [29-32]. For the usage of graphene for energy storage, notably in supercapacitor and battery applications, it must be readily available in the required form. Numerous fascinating techniques had been reported for the synthesis of few-layer and mono-layer graphene, they can be grouped as follows and were depicted in Fig. 2.

3.1 Mechanical Exfoliation

The discovery of graphene in 2004 was made possible by mechanically separating mono-layer graphene sheets from the densely bound layered assembly known as graphite [33]. This method involved using Scotch tape to micromechanically cleaves well-oriented pyrolytic graphite or natural graphite flakes. Due to its excellent structural homogeneity, electronic quality, lack of any crystal flaws, and demonstration of extremely high carrier mobility, it was the first approach used to create graphene and was ideal for basic research purposes [34]. Although this method makes it simple and reliable to prepare graphene, it had a poor yield.

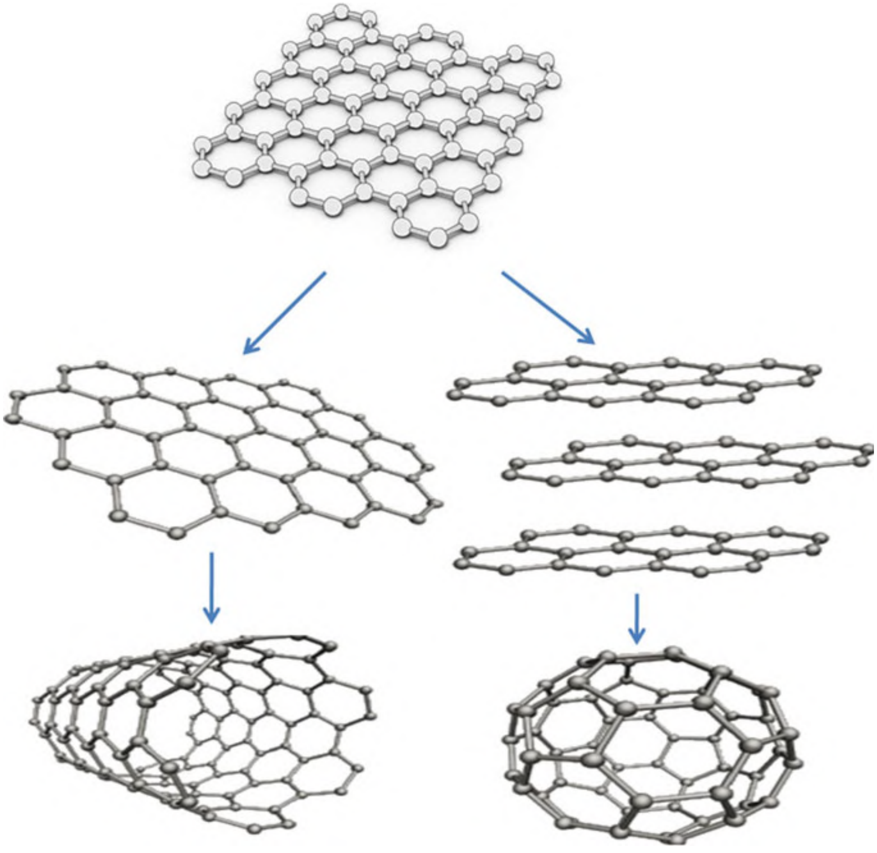

Fig. 1 Parent of all graphitic forms is graphene

The idea of anodic bonding was related to yet another method of mechanical exfoliation. This method was based on the bonding of bulk graphite with borosilicate glass at a specified temperature followed by passing voltage. The graphene sheet then rested on the substrate after being peeled away in one or more layers [35]. Graphene sheets with different thicknesses were created through mechanical exfoliation. Some techniques for making graphene rely on ordered pyrolytic graphite and natural graphite specimens [36].

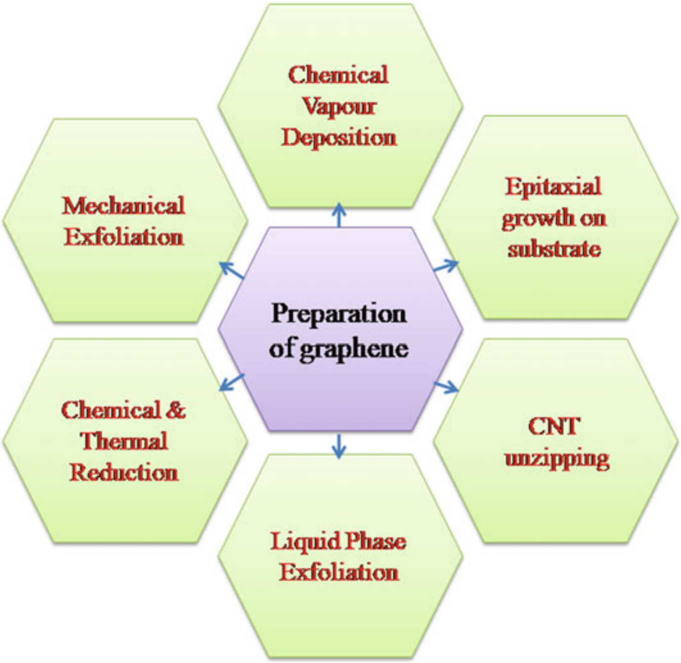
Chemical Vapour Deposition
Epitaxial growth on substrate
Mechanical Exfoliation
Preparation of graphene
Chemical & Thermal Reduction
CNT unzipping
Liquid Phase Exfoliation

Fig. 2 Pictorial representation of different routes to synthesize graphene

3.2 Ultrasonic Cleavage

Ultrasonic cleavage was a word used to describe a process that was conceptually related to the mechanical cleavage approach. The graphene precursors were typically suspended in an aqueous or organic solvent using this method, and then ultrasonic agitation was used as an energy source to cleave the precursors [37]. This concept was born primarily as a result of the discovery that carbon nanotubes can be successfully exfoliated using organic solvents like N-methyl pyrrolidone [38]. The successful completion of the correct synthesis of graphene using ultrasonic cleavage heavily depends on the appropriate selection of solvents along with suitable surfactants coupled with the proper duration of sonication, amplitude, and frequency [39].

3.3 Chemical Vapor Deposition (CVD)

The CVD method, which produced the multi- or single-layered graphene, enabled the large-scale synthesis of graphene [40]. In this type, a suitable metal surface was heated up in order to synthesize graphene sheets on a big scale. A typical chemical vapor deposition procedure entailed dissolving carbon in a metal substrate and then cooling down the substrate to get the carbon to precipitate on it. In a typical procedure, a nickel substrate was placed in a chemical vapor deposition chamber with diluted hydrocarbon gas under vacuum at a temperature of around 1000 °C [41]. Other metal substrates with varying carbon solubilities and catalytic effects, such as cobalt and ruthenium, were also employed as a substrate for chemical vapor deposition in addition to nickel, copper, and platinum [42].

3.4 Chemical Vapor Deposition via Plasma Induction

Plasma induction-enabled CVD provided a different method for the production of graphene at lower temperatures. Some reports reported the synthesis of multi- and single-layered graphene using a methane–hydrogen combination in conjunction with chemical vapor deposition on a variety of substrates. Due to its extremely quick rate of deposition and relatively moderate growth temperature of 500–600 °C, this approach was favored [43].

3.5 Chemical Exfoliation

Additionally, graphene was synthesized chemically by exfoliating graphitic materials. Various steps involved in this process including chemical oxidation, ion intercalation, reduction, and exfoliation of the various graphene derivatives, such as graphite oxide, natural graphite flakes, expandable graphite made of graphite fluoride, additional compounds that used carbon nanotubes, and graphite intercalation [44]. Particularly, the commercial output of graphene produced from graphite was significant. Another important method to produce graphene was reduction through a chemical reaction, in addition to reduction through heat treatment. The first step of this process was the preparation of rGO through the widening of the interlayer gap of the graphite oxide produced by Hummers' method. One well-known example of a chemical exfoliation approach was the multi-layered graphite oxide converted into mono-layer graphene oxide using ultrasonic synthesis [35].

3.6 Thermal Reduction

The most important and simplest method used to produce graphene was thermal reduction. In this process, the single-layer graphene was produced by oxidation through the thermal expansion of the graphene sheets and enough pressure at the time of thermal heat treatment [45]. Importantly, the pressure between the layers was raised, when the rate of breakdown of the oxide and hydroxyl sites exceeded the rate of diffusion of the gases that were produced [46].

3.7 Unrolled Carbon Nanotube

Carbon nanotubes were unrolled in a process that was interesting for producing graphene sheets. The multi-walled carbon nanotubes that were negatively charged were actually electrostatically attracted to ammonia-solvated lithium cations [47]. Both lithium and ammonia were intercalated into multiwalled carbon nanotubes at the same time, and the interlayer distance of these nanotubes rises from 3.35 to 6.62 Å. In some other processes, multi-walled carbon nanotubes were sliced longitudinally and exposed to a powerful oxidizing agent such as potassium permanganate to produce graphene sheets [48]. This method's main benefit was it may be used in a room-temperature environment.

3.8 Graphene from Different Graphite Derivatives

Graphite intercalated compounds, natural graphite, and/or expandable graphites were all classified as a particular type of graphite and were frequently utilized as the precursors to produce monolayer graphene sheets. This process produced extremely pure graphene sheets [49]. Even though the grade of the obtained graphene was quite high, the concentration of the obtained suspension was less. According to the surface energy and solvent cohesive energy of the graphene, several solvents were used to create a homogenous colloidal suspension of graphene. In an N-methyl-2-pyrrolidone solvent, intercalated graphite was mixed with a potassium-based chemical to create a homogenous colloidal suspension of graphene sheets.

4 Basic Aspects of Graphene Functionalization

The chemical functionalization of graphene was used in many applications through non-covalent or covalent bonding. Due to its hydrophobic nature, graphene was rarely dispersed in both polar and nonpolar liquids. The primary goals of graphene functionalization were to increase its dispersion and add necessary chemical and physical features, including greater conductivity or favorable molecular interactions [50].

The covalent functionalization of graphene was primarily accomplished by the creation of a covalent link with either the sp^2 C=C structure of the basal plane graphene or with the native organic molecules' functional groups on the oxidized graphene surface. Various reports were available, which discussed the addition of free radicals to the graphene C=C structure, including nitrophenyls, diazonium salts, hydroxylated aryl groups, and benzoyl peroxide. In addition to these, it was reported that the functionalization of graphene with dienophiles (such as phenyl/alkyl azides, tetraphenylporphyrin (TPP), arynes, azomethine ylide, and nitrenes) improved the dispersion of graphene and used in various applications.

The primary driving reasons behind graphene or GO noncovalent functionalization were π–π interactions, hydrogen bonds, ionic interactions, and van der Waals forces. The functionalization of pyrenebutyrate, 1-pyrenecarboxylic acid (PCA), pyrenebutanoic acid succinimidyl ester, polyaniline (PANI), sulfonated polyaniline (SPANI), and DNA was reported to stabilize graphene in an aqueous solution. Perylenediimide, pyrene, pyrene-butanoic acid succinimidyl ester (PYR-NHS), and sodium lignosulphonate (SLS) were all used to stabilize chemically reduced exfoliated graphite oxides (EGO).

5 Graphene Derivatives

Graphane, graphene oxide, hydrogenated graphene, fluoro-graphene, graphene/metal oxides, graphene/nanocomposites, graphene/polymers, and graphene-nanoribbons are various graphene derivatives that were synthesized through experimental and theoretical investigations [49-51]. The surface functionalization of graphene improved the material's electronic, electrochemical, and structural properties. A detailed description of the many carbon compounds generated from graphene, which focused on their unique characteristics and potential uses for energy storage (Supercapacitor and battery applications) was given as follows.

5.1 Graphene Oxide

In particular, single-layered graphite oxide, also known as graphene oxide (GO), was frequently employed as a reduction precursor for the preparation of graphene. Chemists paid a lot of attention to GO, since it was a substantial oxide-functionalized graphene derivative, as illustrated in Fig. 3 [52]. Commercially, GO can be produced by the chemical oxidation process of natural graphite, followed by its exfoliation. GO was mostly produced using the synthesis method outlined by Offeman and Hummers. The Staudenmaier process, often known as the Hummers' method, was the starting point of this method [53]. In addition to this approach, the Brodie method was occasionally used, which involved the oxidation of graphite while it was fuming in nitric acid and potassium chlorate [54]. This process' fundamental stage was the oxidization of graphite in concentrated sulfuric acid using sodium nitrate and potassium permanganate. The surplus potassium permanganate was then removed by reducing it with hydrogen peroxide to water-soluble manganese (II) sulfate, followed by washing it with methanol [53, 55]. The long-range π-π conjugation interaction that

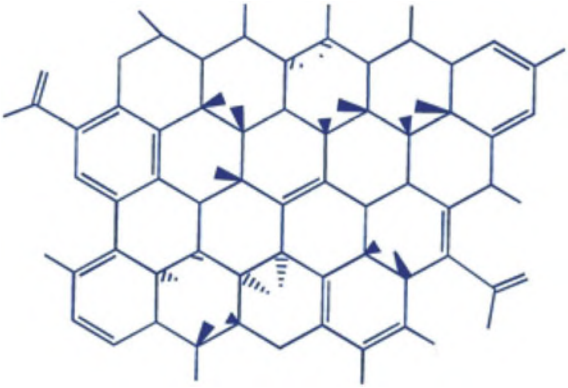

Fig. 3 Graphene oxide structure [57]

was present on the graphite surface was broken up by the oxidation reaction. Finally, sp^2 graphitic domains were formed with sp^3 hybridized domains surroundings, which were irregularly ordered. The resultant product contains additional functional groups with oxygen, such as carbonyls (–C=O), epoxides, ketone, hydroxyls (–OH), phenol, and quinine. Due to the presence of these intervening functional groups containing oxygen, the interlayer forces were significantly reduced, which lead to the very hydrophilic nature. Direct atomic oxygen oxidation of free-standing graphene in an ultrahigh vacuum was another method for producing GO. Other methods were exposure of the material to ozone or molecular oxygen, performing a photochemical reaction with ultraviolet light and oxygen, and controlled electrochemical oxidation in the nitric acid medium under potentiostatic conditions [51, 56].

5.2 Fluorographene

Fluorographene was the fluorinated graphene with the stoichiometric formula CF, which was another key structural derivative of graphene in addition to graphane and graphene oxide. The research on the interaction of fluorine with graphite was started in 1934 [58]. By fluorinating the bulk graphite at a very high temperature, fluorographene, a monolayer of graphite fluoride, was created. Graphite fluoride was regarded as an excellent precursor for the preparation of single-layer graphene fluoride, since it displayed a weak contact between the interlayers. Exfoliation and fluorination approaches were the two main groups of numerous fluorographene production techniques. Photochemical/electrochemical synthesis, hydrothermal fluorination, plasma fluorination, and direct gas fluorination were the principal methods used for the preparation of fluorinate graphene sheets [59]. Different techniques, including sonochemical exfoliation, Hummer's exfoliation, and thermal treatment exfoliation, were used for the exfoliation process. The fluorographene was a promising 2-D material with easy of synthesis and remarkable characteristics. The hexagonal structure of fluorographene was reasonably organized with significant insulation qualities. Additionally, fluorographene possessed up to 400 °C thermal stability and it is chemically inert. Additionally, due to its Young's modulus and its ability to significantly withstand elastic deformations, fluorographene revealed exceptional stiffness and mechanical strength [60].

5.3 Graphane

Actually, graphane was a graphene derivative with incomplete hydrogenation. The total energy calculations from basic principles indicated that it possessed the chemical stoichiometric formula of C-H [61]. Each carbon atom in graphane was sp^3 hybridized, and on the opposite sides of the carbon network, one hydrogen atom was joined to each carbon atom. The structure of this arrangement was comparable to that of the hydrogenated (111) diamond sheet. Two possible configurations of graphene were depicted schematically in Fig. 4, one of which was shaped like a boat with the hydrogen atoms alternated in pairs, and the other one was formed like a chair with the hydrogen atoms alternated on both sides of the carbon atom layer. In comparison to the C–C bond in graphene, the C–C bond in graphane possessed considerably longer sp^3 hybridization. Similar to other hydrocarbons, including polyethylene, benzene, and cyclohexane, graphane possessed a stable structure and binding energy also [62].

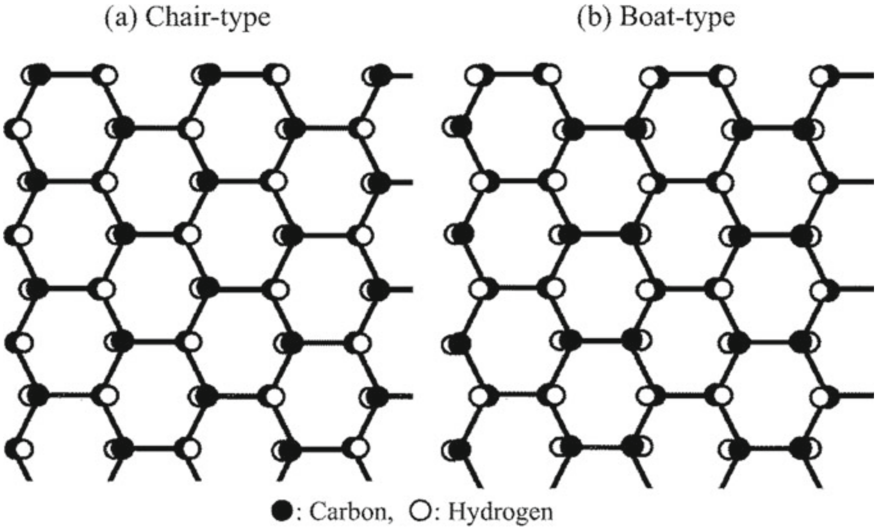

Fig. 4 Types of graphene structure. **a** Chair. **b** Boat [62]

5.4 Graphane Nanoribbons

As the resemblance of graphene, graphane was also separated into graphane nanoribbons, which were 1-D hydrocarbons. Graphane nanoribbons were easily prepared by the graphane nanoribbons are hydrogenated in a hydrogen plasma medium [63]. Also, it can be prepared by unzipping the hydrogenated carbon nanotubes [64]. Compared to graphene nanoribbons, graphane nanoribbons displayed entirely different characteristics [65]. The edge states vanish when sp^3 hybridized carbon atoms were present, because of the delocalized π-electrons.

5.5 Graphene-Carbon Nanocomposites

The combination of two different carbon derivatives with distinct properties enhanced the overall properties of the composites. Various synthesis approaches, such as chemical and physical methods, were used to prepare the various types of graphene/carbon NCs with the combination of nanostructured carbons and graphene. It gives improved conductivity with superior surface area [66, 67]. The self-aggregation of individual sheets, which resulted in the production of graphite, was the primary flaw of single-layer graphene sheets. To overcome these drawbacks, other carbon materials such as porous carbon spheres, carbon nanotubes, carbon black, and activated carbon spheres were incorporated in between the layers of graphene. Even though this process was very simple and efficient, further process was required to decrease the production cost.

5.6 Transition Metal Oxides (TMO)/Graphene Nanocomposites

TMO/Graphene nanocomposites attracted huge attention in energy storage devices. Generally, TMO were used as the materials of the electrode in energy storage applications, since, they possessed rich electrochemical behavior, were eco-friendly and were low cost. But their applications were limited by their higher resistivity and higher agglomeration rate. These serious issues of transition metal oxides were overcome by the preparation of TMO/graphene nanocomposites. TMO/Graphene nanocomposites exhibited the advantages of transition metal oxides (such as superior, redox rate and capacitance), and graphene (including superior active surface area and conductivity).

5.7 Graphene-Polymer Nanocomposites

Research interest in graphene- polymer nanocomposites was increased in modern days because of their unique characteristics, such as yield strength, toughness, optical response, electrical and thermal conductivities, and so on. Conventionally, graphene–polymer nanocomposites were prepared by the addition of a smaller amount of graphene with a polymer matrix. Since graphene has superior characteristics, including superior mechanical strength, high electrical and thermal conductivities, thermal stability, etc., the characteristics of the polymer were greatly enhanced by the addition of graphene. Various types of polymers, such as epoxy, PMMA, HDPE, polystyrene, and nylon were used as the matrices for the fabrication of polymer–graphene nanocomposites [68-71]. The most important applications of polymer–graphene nanocomposites were, (a) in lithium-ion batteries, (b) in electrocatalytic processes, (c) in solar cells, and (d) in thermoelectrics. Various analytical characterization techniques were used to analyze the chemical and physical properties of the graphene nanocomposites. Some of the most important and suitable characterization techniques were high-resolution transmission electron microscopy, atomic force microscopy, X-ray diffraction analysis, optical microscopy, scanning electron microscopy, Raman spectroscopy, etc.,

5.8 Modified Graphene Nanostructures

When utilized as supercapacitor electrodes, graphene modified with functional groups comprising boron (B), sulfur (S), nitrogen (N), silicon (Si), and oxygen (O) has demonstrated enhanced performance. rGOs, for instance, displayed a specific capacitance of 264 Fg^{-1}. An electrochemically reduced graphene-based electrode demonstrated outstanding durability in an aqueous electrolyte, with over 1000 cycles of cycling and a capacitance of 165 Fg^{-1}. In aqueous and IL electrolytes, partially reduced GO possesses capacitances of 348 and 158 Fg^{-1}, respectively. EDLC and pseudocapacitance have synergistic effects that contribute to improved performance in modified graphene. In order to create rGO with a high surface area (1520 m^2g^{-1}) and high electrical conductivity (1738 Sm^{-1}), By eliminating the need for extra binders, carbon black, and current collectors, these materials might be employed directly as electrodes, potentially increasing the energy density of the devices. The 95% capacitance retention for more than 1000 cycles even when bent indicates remarkable mechanical flexibility. The material’s linked network topology and the gel electrolyte are credited with giving it great mechanical flexibility.

Although the inclusion of functional groups on the surface increased the materials' capacities, making these materials requires precise control and sophisticated synthesis procedures, which can raise the cost of production. Due to the surface groups, this can also result in low loading, limiting their usefulness. Furthermore, it is currently difficult to manage the kind, density, and order of graphene surface functional groups.

5.9 Graphene/Transition Metal Nitrides (or Sulfide) Nanocomposites

Due to their superior electrical conductivity, extraordinary electrochemical characteristics, and high specific capacitance, transition metal sulfides (NiS, CoS_2, MoS_2, $CoMoS_4$, MnS, CuS, etc.) and transition metal nitrides (Mo_3N_2, VN, TiN, etc.) are also attractive materials for application in supercapacitors. These materials are similar to TMO (or hydroxides) nanocomposites. However, pure transitional metal nitride or metal sulfide electrodes have low cycleability due to irreversible oxidation processes [72, 73]. Therefore, using conductive carbon, such as graphene, metal nitrides or metal sulfides together can stop the oxidation reaction and increase the cycleability of these materials [74, 75].

6 Characterization of Graphene

Superior thermal conductivity (3000 W/mK), high mobility (15,000 cm^2/Vs), and excellent specific surface area (2600 m^2/g), exceptionally low permeability are only a few of the remarkable attributes of graphene. Large-area polycrystalline graphene has topological flaws, which are regarded to be significant in adjusting the mechanical and physical characteristics of graphene [76-78]. Therefore, characterizing graphene is crucial to comprehending its properties. The graphene sample layer quantity affects both its overall electronic characteristics and purity. To gather structural and morphological information about the generated graphene, many spectroscopic and microscopic techniques are used in graphene characterizations. Determining the purity and flaws of graphene is also a part of the characterization procedure. The purity of graphene is greatly influenced by the synthesis procedures and/or processing settings. The most popular methods for counting the layers of graphene are HR-TEM and AFM. However, Raman spectroscopy is frequently used to identify different crystal structures and bonding information in order to characterize the purity of graphene and count its layers. Additionally, the fundamental techniques for determining the chemical purity of graphene and finding functional groups connected to the material are XPS and Raman spectroscopy.

6.1 X-Ray Diffraction (XRD)

For the characterization of exfoliated and intercalated nanocomposites, XRD is a crucial analytical tool. For instance, GO's interlayer or d-spacing basal plane can be precisely measured using XRD, as can the intercalation of any species in the GO lattice's gallery. While the interlayer spacing of graphite is 3.35, the functionalization of graphite with oxygen-containing groups during conversion to GO causes an increase in the basal plane spacing. A lot of sp^2 carbon compounds have been structurally characterized using X-ray diffraction (XRD). Graphite and graphene exhibit distinctive peaks in their XRD patterns, which can be utilized to distinguish between their structural differences. For instance, in graphite oxide, the sharp peak at $2 = 26.3°$ shifts to 14.1°–14.9°. However, once the GO sheets exfoliate into single sheets, the XRD peaks vanish. [79-82]

A very helpful tool for validating the reduction of GO to graphene and determining phase is the application of X-ray diffraction (XRD). Naturally, given the scant data obtained, it is not as effective as the other methods (AFM, Raman spectroscopy, FT-IR). As a result, other techniques like XPS, Raman, and FT-IR are always used in conjunction with their application to provide more details about the catalyst structure.

6.2 Scanning Electron Microscopy (SEM)

Graphene produced using various ways has a variety of flaws, depending on the method. The remarkable mobility of graphene as well as its other mechanical and physical properties are adversely affected by defects. In light of this, it is crucial to define these flaws using SEM or other cutting-edge imaging methods. SEM is a sophisticated microscopy tool used to characterize materials with micro- and nanostructures. SEM has the high power to provide a 2D analysis of important sample features, but it can also offer details and a variety of qualitative data on a number of physical characteristics, including materials' size, roughness, morphology, surface consistency, and chemical composition. The SEM can be used to define certain nanoscale characteristics of graphene, such as wrinkles, grain morphologies, and folding lines [83, 84].

6.3 High-Resolution Transmission Electron Microscopy (HR-TEM)

A highly effective method for characterizing the structure of graphene is HR-TEM. It is a special tool for describing graphene's atomic structures and interactions. It has been used to examine graphene flakes in a fraction of a micron and to disclose the tiny chemical structure of graphene oxide. It is a TEM with extremely high resolution and cutting-edge imaging characteristics that outperform traditional TEM. In order to characterize graphene-based catalysts, HR-TEM can be used to count the layers of the material. This directly impacts the surface area of the catalyst and significantly affects its catalytic activity. HR-TEM can also be used to gauge a graphene sample's thickness. Thus, the number of layers may be determined [85-88].

Exfoliated graphene sheets show a significant propensity to irreversibly agglomerate or even restack, returning to multilayer structures like graphite as a result of strong interactions and van der Waals forces. Therefore, functionalization is necessary to promote dispersion in aqueous and organic solutions and to decrease hydrophobicity. Graphene is given covalent functionalization by the addition of molecules that causes the sp^2 carbon atoms of the network to rehybridize into an sp^3 configuration, causing modifications to the graphene's inherent chemical and physical properties.

6.4 Atomic Force Microscopy (AFM)

One of the most effective microscopy methods for analyzing samples at the nanoscale is atomic force microscopy (AFM). SPM, or scanning probe microscopy, includes AFM (SPM) with a resolution of the order of nanometer-sized fractions. AFM, for instance, offers 3D views of the number of layers and graphene film's thickness. The most reliable, highest-resolution AFM imaging is available today. In order to confirm the thickness of graphene films, an AFM can be used. Graphene fillings typically have different morphologies (e.g., distorted, crumpled, and folded sheets). AFM can be used to analyze the form, size, composition, aggregation, and absorption/dispersion of nanomaterials, just like SEM and TEM. In AFM research, a variety of scanning modes are used, including dynamic mode, static mode (noncontact mode), tapping mode and contact mode.

Single-layered sheets of reduced graphene oxides (rGO) are produced via the chemical reduction of graphene oxide (GO). The rGO are adaptable for a variety of applications because they have electrical and mechanical properties that are comparable to those of graphene. Reduced graphene oxide has been produced by a variety of methods [52, 78]. Sulfonic acid-grafted GO, or S-reduced graphene oxide, was easily created as an efficient catalyst for the self-assembly of Pt/S-rGO electrocatalysts. AFM performed a thorough analysis of the morphologies of the graphene oxide and S-reduced graphene oxide. The graphene oxide and S-reduced graphene oxide are made up of discrete and evenly spaced graphene oxide sheets. Additionally, the GO sheets have the typical properties of a fully exfoliated graphene oxide sheet, including 0.8 nm thickness.

6.5 Raman Spectroscopy

A common nondestructive method for characterizing nanocrystalline, amorphous, and crystalline carbons is Raman spectroscopy. It is a high-resolution instrument for analyzing the lattice structure, electrical, phonon, and optical characteristics of graphite and 3D diamond, 2D graphene, 1D carbon nanotubes, and 0d fullerenes carbon-based materials. Due to its sensitivity to the vibration of C–C bonds, Raman spectroscopy provides a potent and trustworthy method for the characterization of graphene family materials [52, 78, 80, 89, 90]. The density of flaws in graphene can be determined and measured using this extremely sensitive approach. Numerous other forms of carbon can be produced as byproducts of the diverse processes used to create graphene, including mechanical exfoliation, CVD, and chemical exfoliation.

7 Graphene and Its Derivatives for Industrial Energy Storage

7.1 Supercapacitor

Supercapacitor, also known as ultracapacitor, plays a major role in modern industries and the schematic illustration of the various components of a supercapacitor is depicted in Fig. 5. Generally, a supercapacitor consists of four different components, such as (i) anode, (ii) cathode, (iii) separator and, (iv) an electrolyte. The electrodes (anode and cathode) play a major role in charge separation and/or redox reactions during the electrochemical reactions. Similarly, the role of electrolytes is also very significant, which were used as the charge transport medium. Finally, the separator was used to limit the ion transport between the electrodes. Supercapacitor was classified into three different categories, such as electric double layer capacitors (EDLC), pseudocapacitors (PCs), and hybrid capacitors (HCs) are based on the charge storage mechanism. In EDLCs, charges were stored through a non-faradaic process, such as the charges were separated through the applied electric field and created the electric double layers within the device. Whereas, pseudocapacity was created by the extremely reversible faradaic reactions that occurred at the electrodes and electrolyte interfaces. The term "EDLC" referred to the capacitance produced by the potential-dependent charge storage within the two diametrically opposed charged layers formed at the electrolyte-electrode interface [91]. Helmholtz was mostly recognized for developing the best-practice EDLC model, hence double layers made up of separated charges were also known as Helmholtz double layers. [92]. The term "EDLC" was created to describe the supercapacitors that resulted from Becker's 1957 proposal of the first electricity storage and delivery device. The specific capacitance produced by the EDLC was represented as

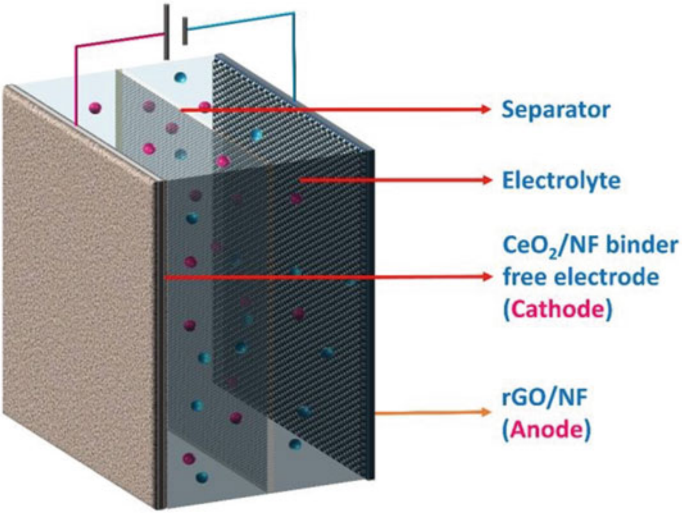

Fig. 5 Schematic representation of a supercapacitor. Reprinted with permission from The Royal Society of Chemistry 2021 and Ref. [94]

$$C = \left(\frac{\varepsilon_r \varepsilon_0}{d}\right)A \tag{1}$$

where A was the specific surface area of the electrode, which was accessible to the electrolyte ions, ε_r relative permittivity, ε_0—permittivity of vacuum, and d—effective thickness of the EDLC. Pseudocapacitance was produced from the charge storage process by the highly reversible faradaic interactions between the electrolyte and electrode active material. Redox-active electrode materials being reduced caused by the lowering of the oxidation state, together with the intercalation/adsorption of electrolytic cations from the electrode surfaces, can be used to explain how such charge storage works [92, 93]. The pseudocapacitance was the derivative of accumulated charges with regard to the voltage change. Since EDLC stored energy using an electrostatic non-faradic method, their electrodes possessed higher power density, far longer cycle life, and lower resistance than those of pseudocapacitors.

7.1.1 Application of Modified Graphene as Electrode Materials for Supercapacitors

Materials made from graphene and/or its derivatives typically hold the advantages like high electrical conductivity, enormous surface area, etc. In general, either non-covalent bonding or covalent interactions lead to graphene alterations. The former was often accomplished using a few methods, such as atom doping or interaction with the remaining functional groups on graphene that were created or destroyed along with the material's unsaturated structure. The surface area, storage capacity, stability,

Fig. 6 Different methods of graphene modification

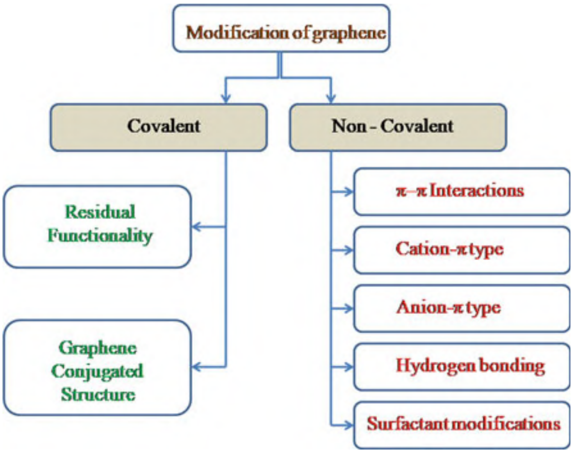

mechanical characteristics, electrical conductivity, handling, and processing capabilities, as well as solving production-related issues were rectified by the chemically modified graphene. A significant cause of worry was the graphene aggregates that form during the reduction process are reversible. The secondary van der Waals forces were activated by accumulation. Graphene must be modified in order to withstand these potent van der Waals forces. As a result of various chemical processes used to modify graphene, distinct interactions between the graphene sheets were depicted schematically in Fig. 6.

- ***Covalent Modification of Graphene***

The existing oxygen linkages, also known as "oxygenated functional groups" or "π–π networks," were often responsible for the attachment of various functional groups through covalent bonds on the graphene surfaces. Additionally, the surface functional characteristics of graphene were modified by the presence of hydroxyl/epoxy functional groups above the surface and carboxylic acid groups at the edges of graphene oxide and graphene. Since stronger bonds were formed between the modifier and the graphene when it undergoes covalent modification, the performance of supercapacitors was improved and this method of modification of graphene was favorable in most of the applications.

- ***Direct Atom Doping Modifications of the Graphene Lattice***

Doping was a popular technique used to change the electronic characteristics of semiconductors. In order to transform carbon compounds into n- or p-type materials, nitrogen or boron atoms, respectively was utilized. At a high annealing temperature of 1200 °C in ammonia, graphene was electronically doped. Due to the changes in electrical structure and surface energy, nitrogen and boron doping created a significant impact on the ability of graphene to store charges. The increased electrical conductivity and wettability by N-doping improved the microporous graphene-specific capacity [95]. Since, N-doping improved and revealed higher charge storage capacity, according to the calculations using density functional theory. Numerous wearable supercapacitors were made by using N-doped graphene based on these theoretical projections. N-doped graphene-based supercapacitor devices were tested in both organic and KOH electrolytes and showed significantly greater capacitance than the device composed of pure graphene. Other small compounds, such as poly (ethylene imine), was investigated as a complementary and stable dopant in addition to nitrogen and boron. Theoretical investigations suggested that doping was used to modify the graphene's band structure.

- ***Covalent Attachment with Organic Functionalities***

Successful preparation of graphene-based nanocomposites was based on the synthesis of scattered graphene sheets in organic solvents. In order to achieve improved dispersion, covalent modification of graphene with the introduction of diverse organic functional groups was the primary strategy. The most important organic species to react with sp^2 hybridized carbon atoms on graphene were fullerene dienophiles and organic free radicals. The successful chemical modification resulted in the insertion surface of redox-active sites and also improved the conductivity of graphene. It was well known that the functional groups formed on the surface gave more pseudocapacitance to the graphene [95, 96]. The hydrophilic functional groups' increased the wettability toward electrolytes possessed a major impact on the properties of EDLC as well. The specific capacitance of the supercapacitor was dramatically increased by additional functional groups found on the surface of graphene.

- ***Modification via the Free Radical Addition***

Graphite, fullerene, and carbon nanotubes were already undergone functionalization by the addition of free radicals and this was successfully used in graphene also, which resulted in bandgap promotion and solubility change. Thermal and photochemical treatments were used to functionalize the graphene using the free radical addition method. Along with the other organic free radicals listed below, aryl diazonium salts were the most often used adducts.

– **Aryl Diazonium Salts**

Aryl diazonium salts, such as diazonium tetrafluoroborate, were synthesized via the free radical method. It was frequently used to incorporate the aryl group through a created covalent bond on the graphene carbon network made up of sp^2 hybridized carbon atoms. Due to its ionic nature, diazonium salt undergoes a polar reaction in an acidic environment, which leads to the creation of an aryl cation. On the other hand, when a neutral condition was upheld, as indicated in Fig. 7, a free radical step was taken place.

These two methods cause N_2 gas to escape from the diazonium salts. In this process, graphene donated an electron to the diazonium salt to form a radical aryl molecule. Further, the functionalization reaction proceeded by a free radical

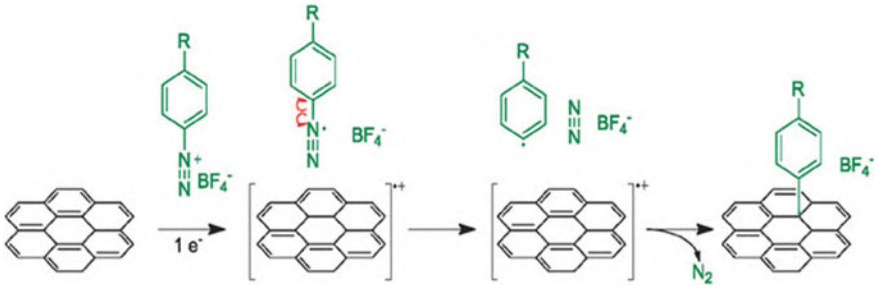

Fig. 7 Mechanism of the addition of free radicals for phenyl compounds to graphene. Reprinted with permission from The Royal Society of Chemistry 2013 and Ref. [97]

mechanism. The aryldiazonium salts utilization for surface modification through the incorporation of various functional molecules on the surface of graphene was a potential solution to weaken the van der Waals forces. But compared to pure graphene, aryl diazonium salts functionalized graphene showed improved electrochemical characteristics with high specific capacitance values. The functionalized graphene produced with aryl diazonium salts showed significant improvements in terms of super capacitive performance, as demonstrated in Fig. 8.

– Peroxides

Peroxides were potentially used to incorporate the aryl group into the sp^2 hybridized network of carbon atoms. Only a few types of peroxides, such as those containing two or more nitro groups in the phenyl ring, were present. These peroxides were useful because they work as radical initiators when exposed to light, which released two molecules of CO_2 and created two radical species of phenyl Fig. 9.

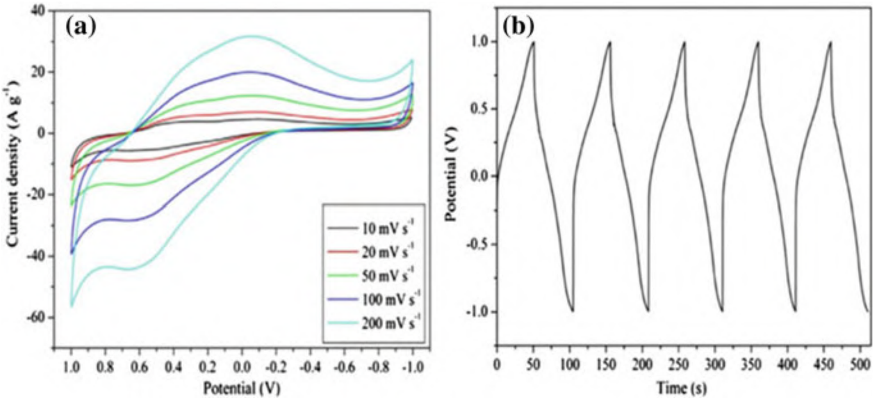

Fig. 8 **a** CV and **b** GCD of ADS-G based supercapacitors. With permission from Elsevier Ltd., reprinted from Ref. [108] in 2012

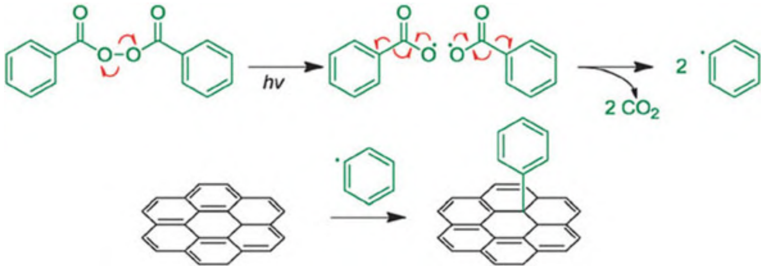

Fig. 9 Mechanism of adding the phenyl moiety by a free radical mechanism on the graphene structure (bottom) and the generation of the phenyl radical from benzoyl peroxide (top). Reprinted with permission from The Royal Society of Chemistry 2013 and Ref. [97]

- **Bergman Cyclization**

Bergman cyclization occurred with the development of a ring with six members. The precursor contains the enediyne group undergone cyclotrimerization after high-temperature thermal treatment using the radical process. 1, 4-Benzenediyl bi-radical types were produced as the result of cyclization. The carbon atoms in graphene were reacted with these extremely reactive bi-radical species, which formed covalent bonds. Both hydrogen bonds and polymerization were the potential outcomes for the radical's other end.

- **Nucleophilic addition**

The cyclopropanation of fullerene was the chemical process that raised the Bingel reaction. In this method, the diethyl malonate group was halogenated, and a base, such as sodium hydride's 1, 8-diazabicyclo or undec-7-ene, was used to carry out the reaction. An in-situ combination of a base and tetrahalomethane produced the halide-malonate. The base produced an enolate by the removal of a proton from the halide-malonate, which then nucleophilically engaged a C=C bond in the graphene framework. A subsequent nucleophilic substitution occurred on the resultant carbanion.

- **Kolbe electro-synthesis**

The electrolysis of carboxylate ions during the Kolbe reaction resulted in the formation of radical species during the subsequent decarboxylation stage (Fig. 10). The radical species was made up only of an alkyl chain.

- ***Non-Covalent Modification of Graphene***

Due to the minimal impact on the graphene's inherent structure, the non-covalent modification strategy for graphene appeared more adaptable and advantageous. Numerous interactions, including nonpolar gas–π interactions, H–π interactions, cation–π interactions, π–π interaction, π–cation–π interaction, anion–π interactions, hydrogen bonds, and coordination bonds, were involved in non-covalent

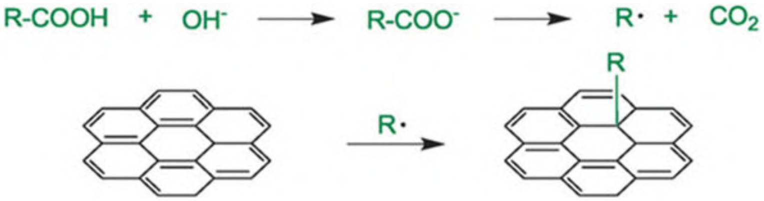

Fig. 10 Free radical addition of radical species onto graphene (bottom) and Kolbe reaction toward the formation of radical species (top). Reprinted with permission from The Royal Society of Chemistry 2013 and Ref. [97],

methods of modification. Compared to covalent interactions, non-covalent changes were far weaker. Multiple non-covalent contacts can, nevertheless, always result in more stability. They were also frequently reversible and simple to acquire throughout the entire surface of graphene. When manufactured graphene needed a high electrical conductivity as well as a high surface area, these non-covalent production techniques were important [98, 99].

On the other hand, a different method for non-covalently altered graphene-based electrodes reduced the issue by using Van der Waals interactions to bind redox-active components to the graphitic framework. Since this method has no impact on the uniform sp^2 carbon network, it also has no negative effects on the double-layer capacitance for the electrodes of graphene-based supercapacitors. By lowering the quantity of chemicals needed and the number of synthesis steps, non-covalent modification also contributed to the simplification of material synthesis methods. The group π–π interaction was the primary interaction when using the non-covalent modification approach. The majority of "π–π" interactions have taken place between two sizable aromatic rings that were non-polar and have overlapped p-orbitals. Additionally, the modification via the "π–π stacking" technique aided in maintaining the conjugation of the graphene layers, and preserved the graphene's electronic properties, which seems to be a major benefit. The reduced graphene oxide electrodes showed better performances, when they were functionalized with hydrophobic Bu-hydroquinone, and revealed 94% of its initial capacitance retention after eight hundred cycles [100]. An expanded p-electron system in polyaromatic hydrocarbon quinone derivatives, such as anthraquinone, makes them more hydrophobic than benzoquinone/hydroquinone and can strengthen non-covalent interactions. The supercapacitor's performance of several polyaromatic-quinones-based materials was tested and it showed 95% of initial capacitance retention after ten thousand cycles. Similarly, sulfanilic acid azocromotrop based non-covalently functionalized graphene oxide revealed the supercapacitor performance of 366 Fg^{-1} specific capacitance value as shown in Fig. 11.

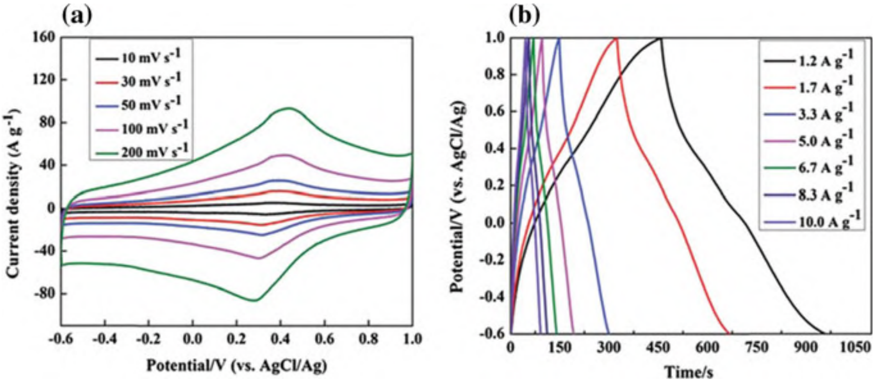

Fig. 11 **a** CV curve and **b** GCD of the modified rGO. Reprinted with permission from The Royal Society of Chemistry 2015, and Ref. [101]

In addition to these, there were other significant interactions in order to change the graphene properties and they were explained below.

- ***H–π Interaction***

Complexes with this type of interaction were of great interest, one of the hydrogen bond interactions was the H–π interaction. The degree of polarizability that the availability of π-electrons possessed a substantial impact on the geometry and makeup of the H–π interaction. According to the total number of electrons involved in the interaction, the amount of the dispersion energy tends to be proportional. The stabilization of the multidentate H–π complexes was caused by a significant contribution from the dispersion energy for bigger π -systems, such as those that were present in larger complexes with multiple hydrogen bonds.

- ***Cation–π Interaction***

It was a unique instance of a π–π interaction, where the counter molecule was a metal cation and the developed interaction was dominated by both induction and electrostatic energy. An accurate assessment of the energy of interaction was necessary for a successful interaction between the negative electron cloud and positive organic cation, which in turn necessitates taking the polarizability of the π-system into account. When transition metal complexes and π complexes were taken into account in place of alkali cations, the nature and characteristics of the numerous interactions in cation–π interactions were changed.

- ***Hydrogen bonding***

The energy storage materials possessed a lot of hydrogen bonds. The bond energy of the hydrogen bond is of 3–7 kcal mol^{-1} was insufficiently strong. Because of the formation of hydrogen bonds between groups containing leftover oxygen from hydroxyl groups and graphene sheets, the material's tensile strength and Young's modulus were improved. For instance, established hydrogen bonding interactions significantly increased Young's modulus of polymeric composites with graphene that contains different poly (acrylonitrile), epoxy, polyaniline, and hydrophilic polymer compounds.

- ***Anion–π Interaction***

Compared to lone pair-π, H–π, and cation–π interactions, anion–π, and π–π interactions were relatively new. Anion–π interactions received a lot of attention recently and have been thoroughly explored as electrode materials. Anion–π system interaction energies were comparable to cation–π system interaction energies. The anion–π complexes' overall energy was largely made up of the dispersion energies. A significant increase in the exchange-repulsion energy was another way to recognize anion–π-type interactions.

- ***Coordination bonds***

Numerous studies were reported on the oxygen-arbitrated coordination bonds, which were particularly common for transition metals. It was demonstrated that controlled alterations made to the macroscopic graphene–metal interface with the aid of oxygen intercalation considerably improved the interaction between graphene and metal.

7.2 Battery

As a crucial component in numerous energy-efficient applications, batteries are enthralling the market. They are heavily enhancing our job efficiency as they are implemented into many aerospace, electrical, textile, automotive, stationary markets, and electric vehicles. The issues with renewable energy sources are being resolved by electrochemical energy storage systems, such as batteries with substantial specific energy densities. Batteries are thought to be promising to give with all energy storage facility for our daily job due to their small structure and size. Due to their high energy density, extended cycle life, safety, and environmental friendliness, lithium-ion batteries are the most often used power sources for electrochemical energy storage types [102, 103]. Due to their unique characteristics, other electrochemical energy storage technologies such as lithium-sulfur, sodium-ion, and lithium-air batteries have also gained increased interest. Although each of these battery types has its own benefits and drawbacks, there is still an opportunity for improvement. Graphene derivatives are particularly appealing as a material for batteries, and they can be used in a variety of battery applications.

7.2.1 Lithium-Sulfur Batteries

Li electrode-based modern generation batteries are well known for their excellent energy density and much-promised safety. Due to their low energy densities, the batteries currently on the market do not meet the requirements for long-term storage.

A new type of lithium-based battery known as “lithium-sulfur” (Li-S) batteries has evolved to solve this issue, attracting interest due to its lighter weight, higher energy density, and increased safety. Lithium-sulfur batteries are the ones that are produced when the heavy anodes of LIBs are swapped out with lighter sulfur. Sulfur exhibits considerable potential to function as an efficient replacement for the traditional electrodes utilized in the LIBs due to their enormous theoretical capacity. Sulfur also has other benefits, such as affordability, environmental friendliness, and natural availability, which make it particularly tempting as an electrode material for second-generation LIBs used in everyday life [102-104]. However, sulfur has a very low electrical conductivity, which is thought to be the cause of the electrode’s poor electrochemical performance and low contact, resulting in a low capacity and quickly depleting electrode. By incorporating highly conductive substrates like graphene and derivatives of graphene, it is possible to boost the electrical conductivity of the sulfur electrode and overcome these limitations. Different sulfur-graphene hybrids have been developed and researched in Li-S batteries in modern days. The use of fluorographene has recently been expanded as an intriguing electrode separator for use in lithium-sulfur batteries, preventing the migration of polysulfides toward the lithium anode. However, their performance was lower than that of the carbon-sulfur hybrids, showing that improvements must be made to the sulfur/graphene and graphene derivatives interface in order to improve performance in the case of Li-S batteries [105, 106].

7.2.2 Lithium-Ion Batteries

The first lithium-ion batteries (LIBs), utilized for commercial applications, were created 28 years ago by Sony Co. in Japan. These commercial batteries use laminar stacked-type compounds because the anode is made of graphite and the cathode is built of lithium cobalt oxide. Lithium ions move through a liquid lithium-ion electrolyte that is situated in between the electrodes as the charge–discharge process continues. Figure 12 provides an illustration of how such batteries’ mechanism functions. Ions are ejected from the negatively charged anode and injected into the positively charged cathode during the discharge process. Through polymeric separator and electrolyte, ions play a major role in the current flow between the negative and positive electrodes. Due to its unique structural, mechanical, and chemical capabilities, graphene and its derivatives are used in a variety of LIB applications as anode and cathode materials. Given that a single Li-ion can interact with six carbon atoms, graphite is expected to have a theoretical capacity of 372 $\mathrm{mAhg^{-1}}$. Due to its exceptional reversibility for the Li ions and extremely long cycling life, this is the anode material that LIBs use the most. On the other hand, graphite remained the most widely utilized anode material in the industry for a very long time. Graphene has the potential to hold lithium ions on both of its sides, theoretically doubling the capacity of conventional carbon compounds. According to theoretical calculations, graphene can have a maximum capacity of 740 $\mathrm{mAhg^{-1}}$ under the double-layer adsorption hypothesis [106, 107].

Fig. 12 Ion intercalation mechanism of a lithium battery. Reprinted with permission from nature publication and Ref. [100],

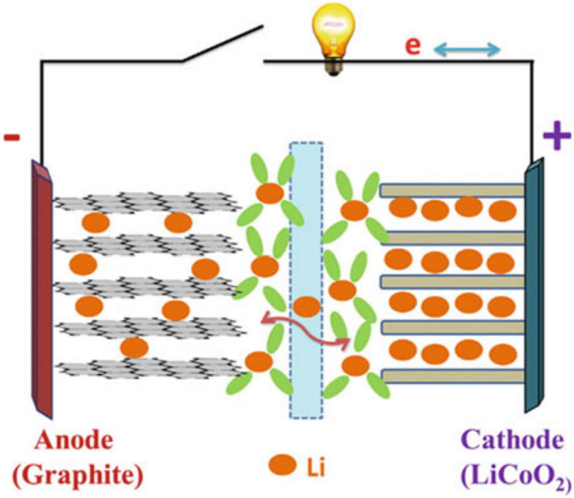

However, creating an appropriate electrode material remains difficult in order to reach the realistic values that would make LIBs viable in electric vehicles. However, because of its electrochemical activity, conductive properties and elastic nature, graphene has been able to successfully address a number of problems, including volume expansion, low conductivity, rate capability, and the rapid fading of capacity. The electrochemical performance of graphene derivatives and enhancement of the electron transportability and is still conceivable, according to experimental and theoretical studies to date. Graphene derivatives: The second option for LIBs is graphene oxide, which is a soft material. Graphene oxide is less mechanically robust than pure graphene, but it is nonetheless regarded as having good strength and has application potential in the fabrication of composite materials. Because graphene's many electronic characteristics can be regulated, LIBs can use it effectively. In order to create new useful materials, chemical modification of graphene has become increasingly popular recently. One of the unique and intriguing functionalized materials is hydrogenated graphene, which has a structure similar to graphene with a high hydrogen concentration. This material is ideal for LIBs fields because almost all of the carbon atoms are in the sp^3 hybridized form. The capacity of the hydrogenated graphene produced by gamma-ray synthesis for use in LIBs is good, measuring at 680 $mAhg^{-1}$ (see Fig. 13).

On the other hand, because it is not associated with the conjugated electrons, fluorographene exhibits much more diverse features than graphene. When compared to pure [108] graphene, fluorographene has a significantly higher theoretical specific capacity for Li of 865 $mAhg^{-1}$. Additionally, this substance is used as a cathode material in secondary and primary LIB batteries, which improves the battery cells' ability to store energy and discharge it. For use as an anode material in LIBs, graphyne/graphdiyne are extremely intriguing options due to their alluring electrical and structural features. For the purpose of examining their possible uses in lithium storage,

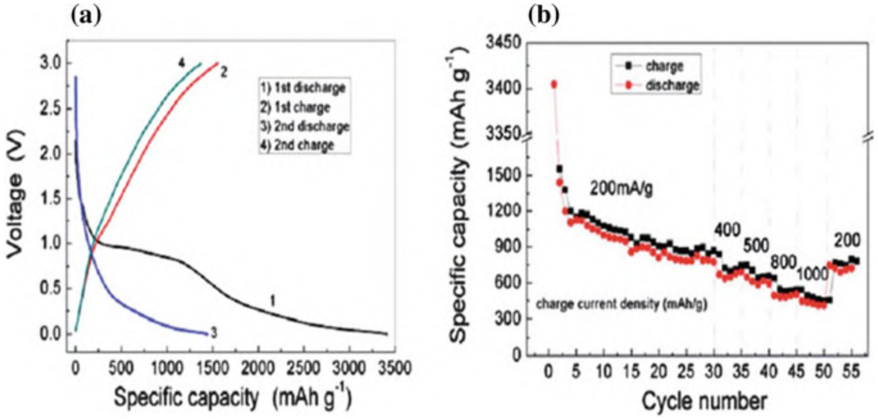

Fig. 13 **a** GCD and **b** cyclic stability of graphene. Reprinted with permission from nature publication and Ref. [108],

the 2-D carbon allotropes graphdiyne and graphyne were investigated using first-principles calculations. The maximum amount of Li that can be stored in graphene is more than the maximum amount that can be stored in graphite. The gap between two subsequent graphyne layers is slightly affected by the intercalation of Li, and this is quite advantageous for the charging procedures. The high Li storage capacity and rapid mobility of graphene make it a potential material for anode uses in batteries.

In addition to this, graphene nanoribbons are emerging as a strong contender for LIBs. Additionally, it has been claimed that the lithium storage capacity and diffusion coefficient are up to two orders greater than those of the graphene nanosheet.

7.2.3 Sodium-Ion Batteries

LIBs have been a popular rechargeable energy source in the past few decades. However, the increasing demand for LIBs on a wide scale raises worries about the high price and insufficient lithium supply on Earth. As a result, sodium-ion batteries (SIBs), which use cheap, readily available sodium from the alkaline earth metal family, have recently attracted more interest as a less expensive alternative to LIBs. SIBs were first suggested as a LIB substitute long ago, but because of their poor performance, they were long forgotten and never used in real-world applications. Although sodium is more readily available than lithium, it does not perform as well in terms of redox potential and ionic radius. The low cost and higher availability of SIBs, however, make them the most viable replacements for LIBs in cases of widespread application. Additionally, as demonstrated, the chemical and physical properties of sodium are extremely similar to those of lithium [95, 102, 103]. Through an aqueous or nonaqueous medium, sodium ions are transferred between the anode and cathode electrodes. Graphene and its numerous derivatives, in addition to sodium, have a great deal of significance in the design of SIBs since they have superior rate capability, higher specific capacity, and longer cycle lives than bare graphene. In comparison to other materials, graphene and its derivatives have, to present, demonstrated increased energy density and gravimetric capacity. Graphene and its numerous derivatives appear to be an effective material for SIBs, as demonstrated by earlier investigations that deemed them to be the best anode material for usage in LIBs.

7.2.4 Other Battery Technologies

A lot of interest has been paid to battery technologies like sodium-sulfur (Na-S) and sodium-air (Na-air) batteries as prospective successors to current battery technologies. Due to its low cost and a number of other unique qualities, such as its high theoretical energy density, low cost, and minimal environmental impact, Na-air has received more attention recently. However, the Na-air battery has issues with its low power density, limited cyclability, and significant overpotential. Additionally, Na-air batteries require ultra-pure oxygen to be stored in a tank in order to produce oxygen, which raises the cost of the overall setup and adds to the inconvenience.

Na-S batteries, on the other hand, provide a number of benefits, including a high theoretical energy density (760 $\mathrm{Whkg^{-1}}$), high efficiency, a long lifespan, and cheap material cost. With all of these benefits, the Na-S is positioned for success in storage applications like load-leveling and smooth power supply. The cell must be operating at a high temperature to provide a large quantity of current flow, which presents safety-related difficulties due to the weaker sodium-ion conductivity. For the Li-S battery, graphene has been predicted to operate as an encasing carbon matrix and a conductive agent; however, no such actions have been discovered for the Na-S battery [102].

8 Conclusion and Future Work

Composites of graphene have taken on a significant role in the nanotechnology field as a result of the increasing need for a sustainable future. The world's water crisis can be resolved with graphene, the strongest, thinnest substance (just an atom thick). Membranes that can segregate salt molecules from water molecules can be created using the tiny pores of graphene films. This could transform desalination technology and lower the cost of running businesses in places like the Middle East. Graphene's distinctive hexagonal shape and the sp2 hybridized bonds that hold it together give it outstanding thermal and electrical conductivity. Supercapacitors can be made with graphene. It can replace silicon in transistors and be utilized to create ultra-thin, flexible touch panels. The scotch tape method was used to separate the first-ever graphene from graphite. Later, researchers created a variety of additional techniques for producing graphene. The bottom-up approach and top-down approach are the two main approaches. Top-notch, expandable graphene is produced using the top-down approach, but there are drawbacks like low yield. The bottom-up strategy creates a large surface area, and nearly flawless graphene, but because processes like epitaxial growth require well-developed operational facilities, it is more expensive than the top-down method. The review study details numerous indirect techniques for synthesizing secondary substrates into graphene and its derivatives. In addition, the review paper explains the numerous top-down and bottom-up methods for synthesizing graphene and its precursor, graphene oxide (GO). It has also been considered to use straw fermentation as a green method of synthesizing graphene. More recently, with the development of green chemistry and environmentally friendly, sustainable methods, graphene was produced using biomolecules as a substrate. The bottom-up method was found to be more effective for producing nanomaterials based on graphene (GBNs). The GBNs' low weight makes them an extremely helpful element in the medication delivery system. Because of a phenomenon known as the "barrier effect," graphene composites offer more corrosion resistance than traditional coatings. GNPs, or graphene nanoparticles, are utilized as adsorbents in the purification of water and in the detection of contaminants. Additionally, graphene has become a superior option for nanofillers in polymer matrices due to its characteristics such as excellent mechanical strength, tensile strength, and thermal degradation temperatures. Researchers have discovered that graphene sheets can withstand twice as much damage as Kevlar, the material that is typically used in bulletproof armor. Due to graphene's small weight, wearing bulletproof jackets will be more comfortable. It has been noted that graphene materials have greatly increased in commercial significance. The potential for using graphene in the future is enormous, paving the way for the development of engineering and technology. The time is quickly approaching when graphene will be utilized in our daily activities.

References

1. Akram U, Khalid M, Shafiq S (2018) Optimal sizing of a wind/solar/battery hybrid grid-connected microgrid system. IET Renew Power Gener 12:72–80. https://doi.org/10.1049/iet-rpg.2017.0010
2. Yang Z, Zhang J, Kintner-Meyer MCW, Lu X, Choi D, Lemmon JP, Liu J (2011) Electrochemical energy storage for green grid. Chem Rev 111:3577–3613. https://doi.org/10.1021/cr100290v
3. Goodwin S, Walsh DA (2017) Closed bipolar electrodes for spatial separation of H_2 and O_2 evolution during water electrolysis and the development of high-voltage fuel cells. ACS Appl Mater Interfaces 9:23654–23661. https://doi.org/10.1021/acsami.7b04226
4. Selvakumar B, Shanmugapriya V, Amudha K, Periasamy P (2022) Enhanced thermophysical properties and productive yield of pyramid solar still combined with shallow solar pond by incorporating ZnO/Al_2O_3 nanocomposites. In: Lecture notes in electrical engineering, springer science and business media Deutschland GmbH, pp 1121–1135. https://doi.org/10.1007/978-981-19-1111-8_86
5. Shanmugapriya V, Mohanapandian K, Periasamy P, Senthilkannan K, Amudha K, Selvakumar B (2021) Enhanced properties of Zn^{2+} substituted Cr_2O_3 nanoparticles in escalating the

distillate yield of acrylic pyramid solar still. Mater Today Proc 1579–1589. https://doi.org/10.1016/j.matpr.2021.07.352

6. Dubal DP, Ayyad O, Ruiz V, Gómez-Romero P (2015) Hybrid energy storage: the merging of battery and supercapacitor chemistries. Chem Soc Rev 44:1777–1790. https://doi.org/10.1039/c4cs00266k
7. Choi HS, Park CR (2014) Theoretical guidelines to designing high performance energy storage device based on hybridization of lithium-ion battery and supercapacitor. J Power Sources 259:1–14. https://doi.org/10.1016/j.jpowsour.2014.02.001
8. Shanmugapriya V, Arunpandiyan S, Hariharan G, Bharathi S, Selvakumar B, Arivarasan A (2022) Enhanced supercapacitor performance of Zno/SnO_2:rgo nanocomposites under redox additive electrolyte. J Alloys Compd 167994. https://doi.org/10.1016/j.jallcom.2022.167994
9. Shanmugapriya V, Arunpandiyan S, Hariharan G, Bharathi S, Selvakumar B, Arivarasan A (2022) Enhanced electrochemical performance of mixed metal oxide (Bi2O3/ZnO) loaded multiwalled carbon nanotube for high-performance asymmetric supercapacitors. J Energy Storage 55. https://doi.org/10.1016/j.est.2022.105739
10. Hariharan G, Arunpandiyan S, Shanmugapriya V, Bharathi S, Babu M, Selvakumar B, Arivarasan A (2023) Role of various redox additive electrolytes on the electrochemical performances of mixed metal oxide loaded multiwalled carbon nanotube based supercapacitors. J Energy Storage 57. https://doi.org/10.1016/j.est.2022.106178
11. Gote GH, Pathak M, More MA, Late DJ, Rout CS (2019) Development of pristine and Au-decorated Bi_2O_3/Bi_2WO_6 nanocomposites for supercapacitor electrodes. RSC Adv 9:32573–32580. https://doi.org/10.1039/c9ra06112f
12. Huang Y, Quan L, Liu T, Chen Q, Cai D, Zhan H (2018) Construction of MOF-derived hollow Ni-Zn-Co-S nanosword arrays as binder-free electrodes for asymmetric supercapacitors with high energy density. Nanoscale 10:14171–14181. https://doi.org/10.1039/c8nr03919d
13. Li L, Zhang X, Zhang Z, Zhang M, Cong L, Pan Y, Lin S (2016) A bismuth oxide nanosheet-coated electrospun carbon nanofiber film: a free-standing negative electrode for flexible asymmetric supercapacitors. J Mater Chem A Mater 4:16635–16644. https://doi.org/10.1039/c6ta06755g
14. Qiu Y, Fan H, Chang X, Dang H, Luo Q, Cheng Z (2018) Novel ultrathin Bi_2O_3 nanowires for supercapacitor electrode materials with high performance. Appl Surf Sci 434:16–20. https://doi.org/10.1016/j.apsusc.2017.10.171
15. Isacfranklin M, Deepika C, Ravi G, Yuvakkumar R, Velauthapillai D, Saravanakumar B (2020) Nickel, bismuth, and cobalt vanadium oxides for supercapacitor applications. Ceram Int 46:28206–28210. https://doi.org/10.1016/j.ceramint.2020.07.320
16. Subagio A, al Hakim Y, Ristiawan MW, Kholil MA (2019) Priyono, Structural and morphological properties of MnO_2/MWCNT composite grown using the hydrothermal method for supercapacitor application. Int J Electrochem Sci 14:9936–9947. https://doi.org/10.20964/2019.10.52
17. Veeralakshmi S, Kalaiselvam S, Murugan R, Pandurangan P, Nehru S, Sakthinathan S, Chiu TW (2020) An approach to develop high performance supercapacitor using Bi_2O_3 based binary and ternary nanocomposites. J Mater Sci Mater Electron 31:22417–22426. https://doi.org/10.1007/s10854-020-04743-3
18. Randviir EP, Brownson DAC, Banks CE (2014) A decade of graphene research: production, applications and outlook. Mater Today 17:426–432. https://doi.org/10.1016/j.mattod.2014.06.001
19. Chen H, Li C, Qu L (2018) Solution electrochemical approach to functionalized graphene: history, progress and challenges. Carbon NY 140:41–56. https://doi.org/10.1016/j.carbon.2018.08.027
20. Pimenta MA, Geracitano LA, Fagan SB (2019) History and national initiatives of carbon nanotube and graphene research in Brazil. Braz J Phys 49:288–300. https://doi.org/10.1007/s13538-018-0618-0
21. Ruoff RS (2012) Personal perspectives on graphene: New graphene-related materials on the horizon. MRS Bull 37:1314–1318. https://doi.org/10.1557/mrs.2012.278

22. Paillet M, Parret R, Sauvajol JL, Colomban P (2018) Graphene and related 2D materials: an overview of the Raman studies. J Raman Spectrosc 49:8–12. https://doi.org/10.1002/jrs.5295
23. Wang JN, Zhang YL, Liu Y, Zheng W, Lee LP, Sun HB (2015) Recent developments in superhydrophobic graphene and graphene-related materials: from preparation to potential applications. Nanoscale 7:7101–7114. https://doi.org/10.1039/c5nr00719d
24. Dreyer DR, Ruoff RS, Bielawski CW (2010) From conception to realization: an historial account of graphene and some perspectives for its future. Angewandte Chemie Int Ed 49:9336–9344. https://doi.org/10.1002/anie.201003024
25. Ferrari AC, Bonaccorso F, Fal'ko V, Novoselov KS, Roche S, Bøggild P, Borini S, Koppens FHL, Palermo V, Pugno N, Garrido JA, Sordan R, Bianco A, Ballerini L, Prato M, Lidorikis E, Kivioja J, Marinelli C, Ryhänen T, Morpurgo A, Coleman JN, Nicolosi V, Colombo L, Fert A, Garcia-Hernandez M, Bachtold A, Schneider GF, Guinea F, Dekker C, Barbone M, Sun Z, Galiotis C, Grigorenko AN, Konstantatos G, Kis A, Katsnelson M, Vandersypen L, Loiseau A, Morandi V, Neumaier D, Treossi E, Pellegrini V, Polini M, Tredicucci A, Williams GM, Hee Hong B, Ahn JH, Min Kim J, Zirath H, van Wees BJ, van der Zant H, Occhipinti L, di Matteo A, Kinloch IA, Seyller T, Quesnel E, Feng X, Teo K, Rupesinghe N, Hakonen P, Neil SRT, Tannock Q, Löfwander T, Kinaret J (2015) Science and technology roadmap for graphene, related two-dimensional crystals, and hybrid systems. Nanoscale 7:4598–4810. https://doi.org/10.1039/c4nr01600a
26. Bonaccorso F, Colombo L, Yu G, Stoller M, Tozzini V, Ferrari AC, Ruoff RS, Pellegrini V (1979) Graphene, related two-dimensional crystals, and hybrid systems for energy conversion and storage. Science 347. https://doi.org/10.1126/science.1246501
27. Lv PH, Wang GF, Wan Y, Liu J, Liu Q, cheng Ma F (2011) Bibliometric trend analysis on global graphene research. Scientometrics 88:399–419. https://doi.org/10.1007/s11192-011-0386-x
28. McCombe BD (2011) A history of narrow gap semiconductors and systems: from graphite to graphene. AIP Conf Proc 9–13. https://doi.org/10.1063/1.3671685
29. Dikin DA, Stankovich S, Zimney EJ, Piner RD, Dommett GHB, Evmenenko G, Nguyen ST, Ruoff RS (2007) Preparation and characterization of graphene oxide paper. Nature 448:457–460. https://doi.org/10.1038/nature06016
30. Radadiya T (2021) Graphene preparation method. www.ijcrt.org
31. Wang Y (2019) Research progress in preparation of graphene. IOP Conf Ser Mater Sci Eng. https://doi.org/10.1088/1757-899X/677/2/022121
32. Cao C, Sun Y, Filleter T (2014) Characterizing mechanical behavior of atomically thin films: a review. J Mater Res 29:338–347. https://doi.org/10.1557/jmr.2013.339
33. Moon J-Y, Kim M, Kim S-I, Xu S, Choi J-H, Whang D, Watanabe K, Taniguchi T, Seop Park D, Seo J, Ho Cho S, Son S-K, Lee J-H (2020) Layer-engineered large-area exfoliation of graphene. http://advances.sciencemag.org/
34. Sinclair RC, Suter JL, Coveney PV (2019) Micromechanical exfoliation of graphene on the atomistic scale. Phys Chem Chem Phys 21:5716–5722. https://doi.org/10.1039/c8cp07796g
35. Danial WH, Norhisham NA, Ahmad Noorden AF, Abdul Majid Z, Matsumura K, Iqbal A (2021) A short review on electrochemical exfoliation of graphene and graphene quantum dots. Carbon Lett 31:371–388. https://doi.org/10.1007/s42823-020-00212-3
36. Yi M, Shen Z (2015) A review on mechanical exfoliation for the scalable production of graphene. J Mater Chem A Mater 3:11700–11715. https://doi.org/10.1039/c5ta00252d
37. Silva LI, Mirabella DA, Pablo Tomba J, Riccardi CC (2020) Optimizing graphene production in ultrasonic devices. Ultrasonics 100. https://doi.org/10.1016/j.ultras.2019.105989
38. Aksoy C, Anakli D (2019) Synthesis of graphene oxide through ultrasonic assisted electrochemical exfoliation. Open Chem 17:581–586. https://doi.org/10.1515/chem-2019-0062
39. Łoś S, Duclaux L, Alvarez L, Hawełek Ł, Duber S, Kempiński W (2013) Cleavage and size reduction of graphite crystal using ultrasound radiation. Carbon NY 55:53–61. https://doi.org/10.1016/j.carbon.2012.12.005

40. Saeed M, Alshammari Y, Majeed SA, Al-Nasrallah E (2020) Chemical vapour deposition of graphene—synthesis, characterisation, and applications: a review. Molecules 25. https://doi.org/10.3390/molecules25173856
41. Al-Hilfi SH, Derby B, Martin PA, Whitehead JC (2020) Chemical vapour deposition of graphene on copper-nickel alloys: the simulation of a thermodynamic and kinetic approach. Nanoscale 12:15283–15294. https://doi.org/10.1039/d0nr00302f
42. Zhang Y, Zhang L, Zhou C (2013) Review of chemical vapor deposition of graphene and related applications. Acc Chem Res 46:2329–2339. https://doi.org/10.1021/ar300203n
43. Sun L, Yuan G, Gao L, Yang J, Chhowalla M, Gharahcheshmeh MH, Gleason KK, Choi YS, Hong BH, Liu Z (2021) Chemical vapour deposition. Nat Rev Meth Primers 1. https://doi.org/10.1038/s43586-020-00005-y
44. Parvez K, Yang S, Feng X, Müllen K (2015) Exfoliation of graphene via wet chemical routes. Synth Met 210:123–132. https://doi.org/10.1016/j.synthmet.2015.07.014
45. Sengupta I, Chakraborty S, Talukdar M, Pal SK, Chakraborty S (2018) Thermal reduction of graphene oxide: how temperature influences purity. J Mater Res 33:4113–4122. https://doi.org/10.1557/jmr.2018.338
46. Le GTT, Manyam J, Opaprakasit P, Chanlek N, Grisdanurak N, Sreearunothai P (2018) Divergent mechanisms for thermal reduction of graphene oxide and their highly different ion affinities. Diam Relat Mater 89:246–256. https://doi.org/10.1016/j.diamond.2018.09.006
47. Liu Q, Fujigaya T, Nakashima N (2012) Graphene unrolled from "cup-stacked" carbon nanotubes. Carbon NY 50:5421–5428. https://doi.org/10.1016/j.carbon.2012.07.028
48. Hartmann RR, Kono J, Portnoi ME (2014) Terahertz science and technology of carbon nanomaterials. Nanotechnology 25. https://doi.org/10.1088/0957-4484/25/32/322001
49. Tahriri M, del Monico M, Moghanian A, Tavakkoli Yaraki M, Torres R, Yadegari A, Tayebi L (2019) Graphene and its derivatives: Opportunities and challenges in dentistry. Mater Sci Eng C 102:171–185. https://doi.org/10.1016/j.msec.2019.04.051
50. Dasari BL, Nouri JM, Brabazon D, Naher S (2017) Graphene and derivatives—synthesis techniques, properties and their energy applications. Energy 140:766–778. https://doi.org/10.1016/j.energy.2017.08.048
51. Lee XJ, Hiew BYZ, Lai KC, Lee LY, Gan S, Thangalazhy-Gopakumar S, Rigby S (2019) Review on graphene and its derivatives: synthesis methods and potential industrial implementation. J Taiwan Inst Chem Eng 98:163–180. https://doi.org/10.1016/j.jtice.2018.10.028
52. Yu W, Sisi L, Haiyan Y, Jie L (2020) Progress in the functional modification of graphene/graphene oxide: a review. RSC Adv 10:15328–15345. https://doi.org/10.1039/d0ra01068e
53. Zhu Y, Murali S, Cai W, Li X, Suk JW, Potts JR, Ruoff RS (2010) Graphene and graphene oxide: synthesis, properties, and applications. Adv Mater 22:3906–3924. https://doi.org/10.1002/adma.201001068
54. Kumar R, Kumar M, Kumar A, Singh R, Kashyap R, Rani S, Kumar D (2019) Science direct surface modification of graphene oxide using esterification. www.sciencedirect.com
55. Shamaila S, Sajjad AKL, Iqbal A (2016) Modifications in development of graphene oxide synthetic routes. Chem Eng J 294:458–477. https://doi.org/10.1016/j.cej.2016.02.109
56. Li J, Zheng H, Liu L, Meng F, Cui Y, Wang F (2021) Modification of graphene and graphene oxide and their applications in anticorrosive coatings. J Coat Technol Res 18:311–331. https://doi.org/10.1007/s11998-020-00435-z
57. Bai RG, Muthoosamy K, Manickam S, Hilal-Alnaqbi A (2019) Graphene-based 3D scaffolds in tissue engineering: fabrication, applications, and future scope in liver tissue engineering. Int J Nanomed 14:5753–5783. https://doi.org/10.2147/IJN.S192779
58. Sun C, Feng Y, Li Y, Qin C, Zhang Q, Feng W (2014) Solvothermally exfoliated fluorographene for high-performance lithium primary batteries. Nanoscale 6:2634–2641. https://doi.org/10.1039/c3nr04609e
59. Chronopoulos DD, Bakandritsos A, Pykal M, Zbořil R, Otyepka M (2017) Chemistry, properties, and applications of fluorographene. Appl Mater Today 9:60–70. https://doi.org/10.1016/j.apmt.2017.05.004

60. Nair RR, Ren W, Jalil R, Riaz I, Kravets VG, Britnell L, Blake P, Schedin F, Mayorov AS, Yuan S, Katsnelson MI, Cheng HM, Strupinski W, Bulusheva LG, Okotrub AV, Grigorieva IV, Grigorenko AN, Novoselov KS, Geim AK (2010) Fluorographene: a two-dimensional counterpart of Teflon. Small 6:2877–2884. https://doi.org/10.1002/smll.201001555
61. Sahin H, Singh S, Peeters FM, Sahin H, Leenaerts O, Singh SK (2015) GRAPHANE: from synthesis to applications electronic properties of nanostructured 2D materials view project theoretical and computational modelling of 2D materials and their nanostructures view project graphane: from synthesis to applications. https://www.researchgate.net/publication/272752455
62. Inagaki M, Kang F (2014) Graphene derivatives: graphane, fluorographene, graphene oxide, graphyne and graphdiyne. J Mater Chem A Mater. 2:13193–13206. https://doi.org/10.1039/c4ta01183j
63. Johnson AP, Gangadharappa HV, Pramod K (2020) Graphene nanoribbons: a promising nanomaterial for biomedical applications. J Control Release 325:141–162. https://doi.org/10.1016/j.jconrel.2020.06.034
64. Dutta S, Pati SK (2010) Novel properties of graphene nanoribbons: a review. J Mater Chem 20:8207–8223. https://doi.org/10.1039/c0jm00261e
65. Celis A, Nair MN, Taleb-Ibrahimi A, Conrad EH, Berger C, de Heer WA, Tejeda A (2016) Graphene nanoribbons: fabrication, properties and devices. J Phys D Appl Phys 49. https://doi.org/10.1088/0022-3727/49/14/143001
66. Singh NP, Gupta VK, Singh AP (2019) Graphene and carbon nanotube reinforced epoxy nanocomposites: a review. Polymer (Guildf) 180. https://doi.org/10.1016/j.polymer.2019.121724
67. Madni A, Noreen S, Maqbool I, Rehman F, Batool A, Kashif PM, Rehman M, Tahir N, Khan MI (2018) Graphene-based nanocomposites: synthesis and their theranostic applications. J Drug Target 26:858–883. https://doi.org/10.1080/1061186X.2018.1437920
68. Sun X, Huang C, Wang L, Liang L, Cheng Y, Fei W, Li Y (2021) Recent progress in graphene/polymer nanocomposites. Adv Mater 33. https://doi.org/10.1002/adma.202001105
69. Potts JR, Dreyer DR, Bielawski CW, Ruoff RS (2011) Graphene-based polymer nanocomposites. Polymer (Guildf) 52:5–25. https://doi.org/10.1016/j.polymer.2010.11.042
70. Kim H, Abdala AA, MacOsko CW (2010) Graphene/polymer nanocomposites. Macromolecules 43:6515–6530. https://doi.org/10.1021/ma100572e
71. Shi G (2012) Gelation of graphene oxide, pp 52–63. https://doi.org/10.1039/9781849736794-00052
72. Shi J, Jiang B, Li C, Yan F, Wang D, Yang C, Wan J (2020) Review of transition metal nitrides and transition metal nitrides/carbon nanocomposites for supercapacitor electrodes. Mater Chem Phys 245. https://doi.org/10.1016/j.matchemphys.2019.122533
73. Shih CC, Lin YC, Gao M, Wu M, Hsieh HC, Wu NL, Chen WC (2019) A rapid and green method for the fabrication of conductive hydrogels and their applications in stretchable supercapacitors. J Power Sources 426:205–215. https://doi.org/10.1016/j.jpowsour.2019.04.030
74. Wang C, Sun P, Qu G, Yin J, Xu X (2018) Nickel/cobalt based materials for supercapacitors. Chin Chem Lett 29:1731–1740. https://doi.org/10.1016/j.cclet.2018.12.005
75. Akbari A, Divband B, Dehghan P, Moradi AH (2021) Application of nanocomposites based on graphene and metal materials in measurement of nitrate/nitrite in food samples. Biointerface Res Appl Chem 11:12769–12783. https://doi.org/10.33263/BRIAC115.1276912783
76. Dehghanzad B, Razavi Aghjeh MK, Rafeie O, Tavakoli A, Jameie Oskooie AA (2016) Synthesis and characterization of graphene and functionalized graphene via chemical and thermal treatment methods. RSC Adv 6:3578–3585. https://doi.org/10.1039/c5ra19954a
77. Dong LX, Chen Q (2010) Properties, synthesis, and characterization of graphene. Front Mater Sci China 4:45–51. https://doi.org/10.1007/s11706-010-0014-3
78. Zhang Z, Schniepp HC, Adamson DH (2019) Characterization of graphene oxide: variations in reported approaches. Carbon NY 154:510–521. https://doi.org/10.1016/j.carbon.2019.07.103

79. Huh SH (2014) X-ray diffraction of multi-layer graphenes: instant measurement and determination of the number of layers. Carbon N Y. 78:617–621. https://doi.org/10.1016/j.carbon.2014.07.034
80. Johra FT, Lee JW, Jung WG (2014) Facile and safe graphene preparation on solution based platform. J Ind Eng Chem 20:2883–2887. https://doi.org/10.1016/j.jiec.2013.11.022
81. Elzatahry A, Abdullah AM, Salaheldin TA, Elzatahry AA, Salah El-Din TA, Al-Enizi AM, Maarouf AA, Galal A, Hassan HK, El-Ads EH, Al-Theyab SS, Al-Ghamdi AA (2012) Nanocomposite graphene-based material for fuel cell applications corrosion atlas phase I at Qatar view project nano-perovskites based electrodes for sensor applications view project. Nanocompos Graphene-Based Mater Fuel Cell Appl. www.electrochemsci.org
82. Ghadiri M, Kang AK, Gorji NE (2020) XRD characterization of graphene-contacted perovskite solar cells: moisture degradation and dark-resting recovery. Superlattices Microstruct 146. https://doi.org/10.1016/j.spmi.2020.106677
83. Wilson NR, Pandey PA, Beanland R, Young RJ, Kinloch IA, Gong L, Liu Z, Suenaga K, Rourke JP, York SJ, Sloan J (2009) Graphene oxide: structural analysis and application as a highly transparent support for electron microscopy. ACS Nano 3:2547–2556. https://doi.org/10.1021/nn900694t
84. Lee J, Zheng X, Roberts RC, Feng PXL (2015) Scanning electron microscopy characterization of structural features in suspended and non-suspended graphene by customized CVD growth. Diam Relat Mater 54:64–73. https://doi.org/10.1016/j.diamond.2014.11.012
85. Dave SH, Gong C, Robertson AW, Warner JH, Grossman JC (2016) Chemistry and structure of graphene oxide via direct imaging. ACS Nano 10:7515–7522. https://doi.org/10.1021/acsnano.6b02391
86. Shalaby A, Shalaby A, Markov P, Staneva A (2015) Structural analysis of reduced graphene oxide by transmission electron microscopy. https://www.researchgate.net/publication/274383728
87. Pelaez-Fernandez M, Bermejo A, Benito AM, Maser WK, Arenal R (2021) Detailed thermal reduction analyses of graphene oxide via in-situ TEM/EELS studies. Carbon N Y. 178:477–487. https://doi.org/10.1016/j.carbon.2021.03.018
88. Meyer JC (2014) Transmission electron microscopy (TEM) of graphene. In: Graphene: properties, preparation, characterisation and devices. Elsevier Ltd, pp 101–123. https://doi.org/10.1533/9780857099334.2.101
89. Lee AY, Yang K, Anh ND, Park C, Lee SM, Lee TG, Jeong MS (2021) Raman study of D* band in graphene oxide and its correlation with reduction. Appl Surf Sci 536. https://doi.org/10.1016/j.apsusc.2020.147990
90. Díez-Betriu X, Álvarez-García S, Botas C, Álvarez P, Sánchez-Marcos J, Prieto C, Menéndez R, de Andrés A (2013) Raman spectroscopy for the study of reduction mechanisms and optimization of conductivity in graphene oxide thin films. J Mater Chem C Mater 1:6905–6912. https://doi.org/10.1039/c3tc31124d
91. Şahin ME, Blaabjerg F, Sangwongwanich A (2022) A comprehensive review on supercapacitor applications and developments. Energies (Basel) 15. https://doi.org/10.3390/en15030674
92. Shukla AK, Banerjee A, Ravikumar MK, Jalajakshi A (2012) Electrochemical capacitors: technical challenges and prognosis for future markets. Electrochim Acta 84:165–173. https://doi.org/10.1016/j.electacta.2012.03.059
93. Sunil Joshi P (2019) Supercapacitor: basics and overview. https://www.researchgate.net/publication/337917546
94. Arunpandiyan S, Raja A, Vinoth S, Pandikumar A, Arivarasan A (2021) Hierarchical porous CeO_2 micro rice-supported Ni foam binder-free electrode and its enhanced pseudocapacitor performance by a redox additive electrolyte. New J Chem 45:12808–12817. https://doi.org/10.1039/d1nj01877a
95. Verma D, Goh KL (2019) Functionalized graphene-based nanocomposites for energy applications. In: Functionalized graphene nanocomposites and their derivatives: synthesis, processing and applications. Elsevier, pp 219–243. https://doi.org/10.1016/B978-0-12-814548-7.00011-8

96. Ke Q, Wang J (2016) Graphene-based materials for supercapacitor electrodes—a review. J Materiom 2:37–54. https://doi.org/10.1016/j.jmat.2016.01.001
97. Kiang Chua C, Pumera M (2013) Covalent chemistry on graphene. Chem Soc Rev 42:3222–3233. https://doi.org/10.1039/c2cs35474h
98. Hu K, Kulkarni DD, Choi I, Tsukruk VV (2014) Graphene-polymer nanocomposites for structural and functional applications. Prog Polym Sci 39:1934–1972. https://doi.org/10.1016/j.progpolymsci.2014.03.001
99. Tale B, Nemade KR, Tekade PV (2021) Graphene based nano-composites for efficient energy conversion and storage in solar cells and supercapacitors : a review. Polym Plast Technol Mater 60:784–797. https://doi.org/10.1080/25740881.2020.1851378
100. Tiwari SK (nd) Hybrid carbon nanomaterials : synthesis and application view project. https://www.researchgate.net/publication/336995271
101. Jana M, Saha S, Khanra P, Samanta P, Koo H, Murmu NC, Kuila T (2015) Non-covalent functionalization of reduced graphene oxide using sulfanilic acid azocromotrop and its application as a supercapacitor electrode material. J Mater Chem A Mater 3:7323–7331. https://doi.org/10.1039/c4ta07009g
102. Nandhinilakshmi M, Vanitha D, Nallamuthu N, Sundaramahalingam K, Saranya P (2022) Investigation on conductivity and optical properties for blend electrolytes based on iota-carrageenan and acacia gum with ethylene glycol. J Mater Sci Mater Electron 33:21172–21188. https://doi.org/10.1007/s10854-022-08925-z
103. Chitra R, Sathya P, Selvasekarapandian S, Meyvel S (2020) Synthesis and characterization of iota-carrageenan biopolymer electrolyte with lithium perchlorate and succinonitrile (plasticizer). Polym Bull 77:1555–1579. https://doi.org/10.1007/s00289-019-02822-y
104. Shukur MF, Ithnin R, Kadir MFZ (2014) Electrical characterization of corn starch-LiOAc electrolytes and application in electrochemical double layer capacitor. Electrochim Acta 136:204–216. https://doi.org/10.1016/j.electacta.2014.05.075
105. Shetty SK, Ismayil G Shetty (2020) Enhancement of electrical and optical properties of sodium bromide doped carboxymethyl cellulose biopolymer electrolyte films. J Macromol Sci Part B Phys 59:235–247. https://doi.org/10.1080/00222348.2020.1711585
106. Nandhinilakshmi M, Vanitha D, Nallamuthu N, Anandha Jothi M, Sundaramahalingam K (2022) Structural, electrical behavior of sodium ion-conducting corn starch–PVP-based solid polymer electrolytes. Polym Bull. https://doi.org/10.1007/s00289-022-04230-1
107. Omotoso MA, Adeyefa OS, Animashaun EA, Osibanjo OO (2015) Biogradable starch film from cassava, corn, potato and yam 7. www.iiste.org
108. Chen W, Zhu Z, Li S, Chen C, Yan L (2012) Efficient preparation of highly hydrogenated graphene and its application as a high-performance anode material for lithium ion batteries. Nanoscale 4:2124–2129. https://doi.org/10.1039/c2nr00034b

Всё для победы!

НАРОДНЫЙ
ФРОНТ

https://pobeda.onf.ru/

LET'S HELP THE RUSSIA

Chapter 23
Functionalized Carbon and Its Derivatives Dedicated to Supercapacitors in Industrial Applications

Ajay Singh and Sunil Sambyal

1 Introduction

Rapid industrialization in all sectors of day-to-day life has drastically escalated the demand for clean, safe, and sustainable energy worldwide, which encouraged researchers to resolve this triggering problem by developing efficient cost-effective novel energy materials utilized for production and storage systems. The depletion of conventional fossil fuel resources and excessive usage has raised many serious environmental pollution issues such as the emission of greenhouse gases, volatile organic compounds (VOCs), ozone layer depletion, and non-biodegradable petro byproducts. Earlier, natural renewable energy sources like water, sun and wind have been tapped to generate electricity via hydroelectricity, solar energy and wind power plants. Recently, many research activities are initiated in the area of energy-generating technologies like fuel/solar cells and energy storage technologies such as lithium-ion batteries (LIBs) and supercapacitors.

Supercapacitors (SCs), also called ultra-capacitors/electrochemical capacitors are considered promising power storage electronic devices owing to their high power density, quick charging/discharging rate, high efficiency (above 99%), cycling stability, eco-friendly and easy construction from easily available materials [1]. The specific capacitance (C), energy density (E) and maximum power density of a supercapacitor are given as $C = \frac{Q}{V}$, $E = \frac{CV}{2}$, and $P_{\max} = \frac{V^2}{4R}$, where '$Q$' is the charge stored on the electrode per unit mass, 'V' is the operating voltage window and 'R' is the equivalent series resistance of all the components in the device.

A. Singh (✉)
Department of Physics, GGM Science College, (Constituent College of Cluster University of Jammu), Canal Road, Jammu, UT of J&K 180002, India
e-mail: ajay.dadwal1234@gmail.com

S. Sambyal
School of Applied Sciences, Shri Venkateshwara University, Gajraula, U.P. 244236, India

© The Author(s), under exclusive license to Springer Nature Singapore Pte Ltd. 2024

C. M. Hussain and M. B. Ahamed (eds.), *Functionalized Nanomaterials Based Supercapacitor*, Materials Horizons: From Nature to Nanomaterials,
https://doi.org/10.1007/978-981-99-3021-0_23

The electrochemical performance of SCs such as specific capacitance, power density, energy density and cycling stability are based on the electrode material used. Ideal electrode materials should possess high specific surface area, controlled porosity, high electronic conductivity, desirable electroactive sites, high thermal and chemical stability, and low costs. Based on the operating mechanism of electrochemical double-layer capacitance (EDLC), the various carbon allotropes widely utilized as electrode material in supercapacitors are fullerenes, carbon nanotubes, graphene, carbon nanofiber, carbon aerogels and porous carbon [2–5].

The two operating mechanisms by which energy is stored in the supercapacitors are: (i) Electro chemical double—layer capacitance (EDLC) and (ii) Pseudo-capacitance. In EDLC, the specific capacitance is given as $C = \frac{\varepsilon_r \varepsilon_0 A}{d}$, where '$\varepsilon_r$' and '$\varepsilon_0$' is the relative permittivity of the medium and that of vacuum, 'A' is the specific surface area of the electrode and 'd' is the effective thickness of the electrical double layer. In EDLC, the accumulation of electrons at the electrode is non-Faradaic process. In the case of pseudo-capacitance, the capacitance is calculated as $C = \frac{n \times F}{M \times V}$, where '$n$' is the mean number of the electrons transferred in the redox reaction, 'F' is the Faraday constant, 'M' is the molar mass of the metal oxide and 'V' is the operating voltage window. In pseudo-capacitance, the accumulation of electrons at the electrode is a Faradaic process.

Due to the high cost of RuO_2 and the electrochemical instabilities of most transition-metal compounds (represented by manganese oxide) in aqueous electrolytes, the application of pseudocapacitors in commercial devices has been hampered [6]. Therefore, most commercially available SCs are EDLCs assembled using porous carbon electrodes and organic electrolytes composed of tetraethyl ammonium tetrafluoroborate solute and acetonitrile or propylene carbonate solvents [7]. A hybrid supercapacitor can be simultaneously both EDLC and pseudo-capacitance. A hybrid supercapacitor can be a symmetric composite hybrid and asymmetric hybrids, which utilizes both Faradaic and non-Faradaic processes to store charge, have higher energy/power densities and good cycling stability. The symmetric supercapacitor has identical materials of the same capacitances at both electrodes (positive and negative) [8]. Inexpensive transition metal oxides have been used for the construction of symmetric supercapacitors [9]. Asymmetric supercapacitors (ASCs) have two different electrode materials with well-separated potential windows. The asymmetric device exhibited higher areal capacitance and energy density (380 mF cm^{-2} and 19.1 Wh Kg^{-1}) than that of the symmetric device (194 mF cm^{-2} and 4.5 Wh Kg^{-1}).

Various carbon materials such as activated carbon, graphene, carbon nanotubes and carbon aerogel are used as electrode materials for supercapacitor applications. However, the energy densities of SCs as low as 5–8 Wh Kg^{-1} (= 250 Wh Kg^{-1} for lithium-ion batteries, and = 40 Wh Kg^{-1} for lithium-acid battery) [10] and the capital cost per watt-hour of SC is much higher than lithium-ion batteries and lead-acid battery [11]. The high capital cost of SC is mainly ascribed to the high cost of porous carbon electrode active materials. Porous carbons used for SC applications have high prices ranging from 30 to 50 \$ Kg^{-1} [12]. The high cost of porous carbon increases the cost of SC devices and the levelized cost of energy storage devices

(LCES). The porous architecture of porous carbon electrodes decides the capacitance and energy of an EDLC-type SC. To enhance the capacitance of EDLC-type SC, the development of high surface area porous carbon is required. The pores in porous materials are classified into macropore (>50 nm), mesopore (2–50 nm) and micropore (<2 nm) [13]. Macropores of porous carbon act as reservoirs of electrolyte ions, mesopores act as the diffusion channels for electrolyte ions and micropores play the roles for ion storage. The structural parameters of porous carbon such as SSA, pore-size distribution, surface functionalities and tap density can be controlled by synthetic parameters. Using porous carbon as electrode material in supercapacitor possess various advantages such as high surface area, surface functionalities and chemical stability [14]. Doping of heteroatoms into carbon enhances the electronic conductivity and surface faradic reactions which improves the capacitance. For example, nitrogen-doped carbon nanocages prepared by in situ MgO template method [15] showed increased capacitance from 11.8 to 17.4 μF cm^{-2} at a current density of 1 A g^{-1} in 6.0 M KOH. By using the thermal treatment of core–shell structured ZIF-8@ZIF-67 crystals [16], highly porous nitrogen-doped carbon (NC) as the cores and highly graphitic carbon (GC) have been prepared which shows high specific capacitance of 270 Fg^{-1} at a current density of 2 A g^{-1} in 1.0 M H_2SO_4. Feng and Zhang et al. investigated graphene-coupled 2D porous carbons which exhibit enhanced capacitance due to long-distance conductivity as compared to porous carbon without graphene as a template [17]. This concept can be easily spreader to design new 2D and 3D composites [18] for energy storage and conversion. Due to redox reactions of electroactive species, pseudocapacitors show higher specific capacitance as compared to EDLCs. The robust redox reactions exhibited by pyridinic-N and pyrrolic-N, the N-doped ordered mesoporous few-layer carbon (OMFLC-N) show capacitance of 855 Fg^{-1} and an ultrahigh energy density of 41 Wh Kg^{-1} [19]. It has been observed that the accessible micropores of carbon materials determine the specific capacitance and rate capability depends on meso- and macropores. An anomalous capacitance with a pore size below 1 nm is observed in porous carbon and the electrochemical performances of porous carbon electrodes depend upon both specific area and pore structure [20]. The other factors which impact the performance of capacitance are specific surface area, pore size distribution, surface heteroatoms (or functional groups), and structural defects [21–25].

This chapter explores the physical and chemical synthesis methods and characterization of activated carbon and graphene-based porous carbon doped with different organic and inorganic dopants for energy storage supercapacitors. The future perspective of the work will also be discussed for enhancing the performance of supercapacitor storage capacity. This book chapter elaborates on the importance of the problem with brief historical, global scenarios with past, present and future perspectives with proposed solutions/advantages/ disadvantages for energy storage device supercapacitor application.

2 Synthesis Strategies of Porous Carbon

Porous carbon is the most significant electrode active material and is manufactured at an industrial scale by the carbonization-activation method. However, this method of production of commercial porous carbon for supercapacitors suffers from various disadvantages such as corrosion of equipment, high production cost and emission of byproduct pollutants. In addition to the traditional carbonization-activation method, the novel strategies developed in recent years for the production of porous carbon materials are: emerging activation methods, template methods and self-template methods.

2.1 Carbonization-Activation Technique

Porous carbons obtained by this procedure are called activated carbon and are used in SC applications as electrode material. Carbonization is done by pyrolysis, which produces nonporous carbonaceous materials having low oxygen and hydrogen contents which are further activated by physical or chemical methods.

2.1.1 Carbonization

It is a physiochemical procedure that involves several reactions simultaneously like deoxygenation, dehydrogenation, crosslinking, hydrogen transfer, condensation and isomerization [26]. Many novel carbonization techniques have been developed to replace pyrolysis which is performed in an inert atmosphere are hydrothermal carbonization [27], dehydrogenation/deoxygenation enabled by high concentrated H_2SO_4 [28], microwave-assisted carbonization [26] and dehalogenation of halogenated organic polymers [29]. These techniques result in the production of carbonization materials having different structures and chemical compositions. Microwave-assisted carbonization technique has various advantages which include: (i) instantaneous on and off of heating; (ii) minimizing heating duration; (iii) facilitating volumetric heating; (iv) minimizing reactor size. Despite various novel carbonization techniques available, pyrolysis is extensively used. In pyrolysis, at low temperature, disordered carbon having defects are produced, while at high temperature, partially ordered carbons having defective graphene layers are produced [30]. In low-temperature pyrolysis, the following reaction occurs: (i) at temperature <150 °C, loss of absorbed water takes place, (ii) at temperature <250 °C, dehydration of carbohydrate unit takes place, (iii) at temperature <400 °C, aromatization and scission reaction takes place. The major drawback of low-temperature pyrolysis is that the obtained carbonized carbon has high oxygen content as compared to high-temperature pyrolysis because the deoxygenation reaction occurs around 400–600 °C. A quasi-percolation model to describe the evolution of the structure of carbon during pyrolysis was proposed by Kercher and Nagle [31]. In this model, at temperature >600 °C, graphene sheets grow substantially, however, very little growth of large turbostratic crystallites occurs. At temperature ~900 °C, impinging of graphene layers on each other occurs.

2.1.2 Physical Activation

This procedure is carried out in an oxidizing atmosphere in high-temperature furnace (600–1200 °C) filled with inert gases. The activation agent used in this procedure is steam or CO_2. During the physical activation process, the pores in porous carbon are formed by oxidation reactions (Eqs. (1) and (2)) in the oxidizing atmosphere [32].

$$C + H_2O \rightarrow CO + H_2 \tag{1}$$

$$C + CO_2 \rightarrow 2CO \tag{2}$$

By physical activation, a more accurate and narrow pore size distribution is obtained which results in the reduction of microdomain size in the activated carbon [33]. The characteristics of physical activation are high activation temperature, relatively low yields, small pore size, long activation duration, low tap density and low specific surface area (SSA). Owing to their low corrosion towards the reactor, physical activation is widely used for industrial production as compared to chemical activation. Sahin and Saka [34] investigated corn shells for the production of activated carbons by physical activation by pretreating with $ZnCl_2$ and HCl followed by CO_2 and H_2O as activation agents. SSA and pore volume of activated carbon obtained using this procedure are 0.927 $cm^3\ g^{-1}$ and 1779 $m^2\ g^{-1}$.

2.1.3 Traditional Chemical Activation

The characteristics of chemical activation are low-temperature process, high carbon yields, and high mesopores ratios [35, 36]. For chemical activation, potassium hydroxide (KOH) [37, 38], sodium hydroxide (NaOH) [39, 40], zinc chloride ($ZnCl_2$) [41], phosphoric acid (H_3PO_4) [42, 43], sodium carbonate (Na_2CO_3) [44] and potassium carbonate (K_2CO_3) [44, 45] are employed as activation agents. Out of these activation agents, KOH is the most powerful followed by NaOH. Porous carbons having SSAs ranging from 500 to 3600 $m^2\ g^{-1}$ [46, 47] can be produced by this method. The activated carbon produced by using NaOH, KOH, and a mixture of them exhibits SSAs of 2260, 1702 and 2747 $m^2\ g^{-1}$, and pore volumes of 1.31, 0.74 and 1.40 $cm^3\ g^{-1}$, respectively. Research reports showed that the most developed pore structure, pore size distribution, and specific capacitance of 194.6 F g^{-1} at 0.5 A g^{-1} measured by galvanostatic charge–discharge (GCD) in H_2SO_4 was obtained by a mixture of NaOH and KOH. Zhang et al. employing one-step carbonization of

K_2CO_3 containing chitosan obtained a 3D porous carbon foam (PCF) with high SSA about 1030 m^2 g^{-1}, mesopores centered at 0.66 nm, and specific capacitance of 246.5 F g^{-1} at 0.5 A g^{-1} [48]. Fuertes et al. employed carbonization and activation in one step by using a mixture of polypyrrole (PPy) and KOH and obtained porous carbon exhibiting SSA of 3000–3500 m^2 g^{-1}, a pore volume up to 2.6 cm^3 g^{-1}, and micropore of 1 nm at 600 °C [49]. Zhang et al. obtained porous carbon by carbonizing lignin and KOH, which exhibits an SSA of 907 m^2 g^{-1}, a pore-size distribution ranging from 0.6 to 40 nm, and a high specific capacitance of 165.0 F g^{-1} at 0.05 A g^{-1} in H_2SO_4 electrolyte [50].

Chemical activation is not employed for the preparation of porous carbon in industrial production owing to its excessive consumption of KOH as an activation agent which is highly corrosive at high temperatures and chemical activation produces contaminants that are highly alkaline and polluting.

2.1.4 New Chemical Activation Methods

Based on different activation mechanisms, the new chemical agents can be grouped into three categories: molten salt, decomposable salt and oxidation salt.

(i) **Molten Salt Etching**

In this method, molten chemical agents such as $CuCl_2$ [51], $NiCl_2$ [52, 53], NaCl [54–56], KCl [56] and $FeCl_3$ [57–59] react with carbon to produce porous structure at high temperature. For example, $CuCl_2$ shows less destructive on the structure of biomass precursor comparison to KOH and $ZnCl_2$, which crushed the carbon precursors during the activation process. The reaction mechanism of $CuCl_2$ is described below [51]:

$$3CuCl_2 + C + 2H_2O \rightarrow Cu + 2CuCl + CO_2 + 4HCl \tag{3}$$

$$4CuCl + C + 2H_2O \rightarrow 4Cu + CO_2 + 4HCl \tag{4}$$

In the above reaction mechanism, carbon is oxidized by Cu^{2+} ions and the role of Cl^{-1} needs to be confirmed. Moreover, the outlet gases released need to be purified for green synthesis.

Wang et al. [54] used a KCl/NaCl mixture of molten salt for the pore formation mechanism through thermogravimetric techniques. In this process, they observed that at low temperature, O_2 act as an etching agent while at high temperature above 800 °C, Cl^{-1} acts as an etching agent and results in micro- and mesopores formation. Through this technique, porous carbon having an SSA of 1588 m^2 g^{-1} and a specific capacitance of 407 F g^{-1} at 1 A g^{-1} is obtained. Chen et al. [56] showed that the SSA of porous carbon obtained using KCl/NaCl mixture molten salt is higher than that obtained using KCl or NaCl separately. A mixture of $ZnCl_2$/KCl molten salt produced porous carbon having SSAs up to 3155 m^2 g^{-1} [58]. The reaction mechanism of $FeCl_3$

as an activation agent has been described below [57]:

$$FeCl_3 + 2H_2O \rightarrow FeOOH + 3HCl \tag{5}$$

$$2FeOOH \rightarrow Fe_2O_3 + H_2O \tag{6}$$

$$6Fe_2O_3 \rightarrow 4Fe_3O_4 + CO_2 \tag{7}$$

$$2Fe_2O_3 + 3C \rightarrow 4Fe + 3CO_2 \tag{8}$$

$$Fe_3O_4 + 2C \rightarrow 3Fe + 2CO_2 \tag{9}$$

$$Fe_3O_4 + 4C \rightarrow 3Fe + 4CO \tag{10}$$

In the above mechanism, the microporous of porous carbon is developed by the synergistic effect of Fe^{3+} and Cl^{-1}. The disadvantage of using molten salt is its high cost which put obstacles for its practical production.

(ii) **Decomposable Salt Etching**

Salts that are decomposable produce various gases which further etch carbon to form pores. The various decomposable salts are: zinc acetate [60], $Zn(NO_3)_2$ [61], $NaNO_3$ [62], calcium acetate [63], sodium acetate, $MgCO_3$ [64], sodium chloroacetate [65], K_3PO_4 [66] and NaH_2PO_4 [67]. The porous carbon synthesized using zinc acetate produces SSA two times more than carbon nanofibers (CNFs) without zinc acetate. Li et al. [60] synthesized porous carbon by using decomposable salt $NaNO_3$ having an SSA of 2872.2 $cm^2\ g^{-1}$. Antonietti et al. [68] investigated oxygen-containing anion salts and their abilities for pore formation and the mechanism is as follows:

$$OH^- : C + 2OH^- \rightarrow CO + H_2 \uparrow + O^{2-} \tag{11}$$

$$CO_3^{2-} : C + CO_3^{2-} \rightarrow 2CO + O^{2-} \tag{12}$$

$$NO_3^- : 5C + 4NO_3^- \rightarrow 5CO_2 + 2N_2 \uparrow + O_2 \uparrow \tag{13}$$

$$PO_4^{3-} : a{:}\ 2C + PO_4^{3-} \rightarrow 2CO + PO_2^{3-} \tag{14}$$

$$b{:}\ C + 2PO_2^{3-} \rightarrow CO + 2P \uparrow + 3O^{2-} \tag{15}$$

$$SO_4^{2-} : a{:}\ C + SO_4^{2-} \rightarrow CO + SO_3^{2-} \tag{16}$$

$$\mathrm{b{:}\ 2C + SO_3^{2-} \rightarrow 2CO + S\uparrow + O^{2-}} \tag{17}$$

$$\mathrm{ClO_3^-:\ 3C + 2ClO_3^- \rightarrow 2CO_2 + 2Cl^-} \tag{18}$$

On the basis of the above mechanism, various oxygen-containing salts have the potential to be utilized as activation agents.

(iii) **Oxidative Salt Etching**

Various oxidative activation agents like HNO_3 [19, 69, 70], $KMnO_4$ [71, 72], KNO_3 [73, 74] and $Mn(NO_3)_2$ are utilized to produce porous carbon. Wang et al. [71] used HNO_3, $KMnO_4$ and H_2O_2 to produce carbon cloth at room temperature with enhanced SSA from 5.3 to 61.2 $m^2\ g^{-1}$. Yang et al. [69] used 69% HNO_3 to fabricate single-wall carbon nanohorns (SWNHs) having an SSA up to 1464 $m^2\ g^{-1}$. In order to generate more macropores and mesopores, $KMnO_4$ is used as an activation agent. The reaction mechanism is as follows:

$$\mathrm{2KMnO_4 \rightarrow K_2MnO_4 + MnO_2 + O_2} \tag{19}$$

$$\mathrm{K_2MnO_4 + C \rightarrow K_2CO_3 + MnO} \tag{20}$$

$$\mathrm{2MnO_2 + C \rightarrow 2MnO + CO_2} \tag{21}$$

The porous carbon produced using $KMnO_4$ activation agent have SSA up to 1199 $m^2\ g^{-1}$, pore volume of 11.7 $cm^3\ g^{-1}$ and capacitance of 242.0 F g^{-1} at 1 A g^{-1} and 145.0 F g^{-1} at 10 A g^{-1}. Wang et al. [74] explode carbon into slices by putting inner stress using KNO_3 and later produces porous carbon nanosheets (PCNSc) after activation by KOH which exhibits SSA up to 2788 $m^2\ g^{-1}$, and capacitance of 226.9 F g^{-1} at 1 A g^{-1} and 154.3 F g^{-1} at 50 A g^{-1}. Ammonium persulfate ($(NH_4)_2S_2O_8$) is another activation agent, which produces carbon nanosheets having SSA of 1122 $m^2\ g^{-1}$, capacitances of 227.0 F g^{-1} at 0.5 A g^{-1} and 176.2 F g^{-1} at 20 A g^{-1}. The reaction mechanism is as follows:

$$\mathrm{2(NH_4)_2S_2O_8 \rightarrow (NH_4)_2S_2O_7 + O_2} \tag{22}$$

$$\mathrm{(NH_4)_2S_2O_7 \rightarrow 2NH_3 + 2SO_3 + H_2O} \tag{23}$$

2.2 Template Methods

To produce a well-defined pore structure of porous carbon, a template synthesis technique is applied.

2.2.1 Hard Templates

SiO_2 [75–77], MgO [78, 79], ZnO [80–82], Al_2O_3 [83, 84], TiO_2 [85], as well as zeolite [86, 87], are used as a hard template. Silica is the mostly used template for the synthesis of mesoporous carbon. The main steps in this methodology are: (i) synthesis of required hard template, (ii) carbon source is used for the impregnation, (iii) pyrolysis at high temperature is done and (iv) acid or alkali solution is used for template etching. Liang et al. [75] employed 12 nm SiO_2 nanoparticles (silica colloid), ordered mesoporous silica (SBA-15), and montmorillonite (MMT) as templates to produce three types of mesoporous carbon catalysts having SSA up to 572, 387 and 134 $m^2\ g^{-1}$. Zhao et al. [84] employed a template based on porous anodic aluminum oxide (AAO) membrane to produce mesoporous carbon nanosheets having porous size distribution in the range of 50–200 nm. Fan et al. [87] investigated MgO nanoparticles and $Mg(OH)_2$ nanosheets to form MgO templates which are used for the production of new porous carbon. Hu et al. [88] investigated a 3D flower-shaped MgO template and produced porous carbon doped with nitrogen using cellulose, acetate, and urea having SSA of 937 $m^2\ g^{-1}$, and capacitance of 333 $F\ g^{-1}$ at 1 $A\ g^{-1}$. Bu et al. [89] used a MgO template to produce high-density porous carbon named CCNC (collapsed carbon nanocage). The obtained CCNC shows an SSA of 1788 $m^2\ g^{-1}$, a pore volume of 0.79 $cm^3\ g^{-1}$, a high volumetric energy/power density of 73 Wh L^{-1}, and 67 kW L^{-1}.

The porous carbon produced using the hard-template method has uniform and controlled pores size. The disadvantage of this method is that it is time consuming, costly and tedious. The removal of inorganic templates by acid or alkali etching restricts their practical utility [90].

2.2.2 Soft Templates

In this method, organic molecules having functional groups are used [91, 92], which provides strong interaction force [93, 94] or electrostatic interactions [95, 96]. The key factors for successful soft template methods are: (i) the ability to form nanostructures, (ii) the formation of micro- or mesopores, and (iii) before the carbon skeleton maintaining the soft template porogens. Based on these factors, various soft templates such as polystyrene-*b*-poly(4-vinylpyridine) (PS-P4VP) [97], the poly (ethylene oxide)-*b*-poly (propylene oxide)-*b*-poly (-ethylene oxide) (PEO-PPO-PEO) (F127 [98–100], F108 [101]and P123 [100, 102]) and some surfactants have been synthesized.

Liang et al. [103] used a self-assembly technique to develop cubic mesoporous carbon, which exhibits an SSA of 637 $m^2\ g^{-1}$, a pore volume of 0.32 $cm^3\ g^{-1}$ and a specific capacitance of 159 $F\ g^{-1}$ at 10 $mV\ s^{-1}$ by employing triblock copolymer EO106-PO70-EO106 (F127) and the phenol–formaldehyde resol. Pang et al. [98] produce carbon nanospheres having a pore size of 37 nm, a small particle size of 128 nm, an SSA of 635 $m^2\ g^{-1}$ and a high N doping ratio of 6.8% by employing F127 as a soft template and the organic molecule 1,3,5-trimethylbenzene.

2.3 Self-template Methods

By carbonizing the self-templated materials directly porous carbon materials can be fabricated. This strategy uses self-generated porogens for the formation of porous carbon material. Ethylenediamine tetra acetates (EDTA)-based salts [104, 105], glycolates [106] MOFs [107] and their derivatives [108] and biomass-based organic salts [109] are used as self-template material.

2.3.1 Organic Salts as Carbon Sources

Organic salts such as potassium and sodium citrate salts are used to produce interconnected porous carbon nanosheets (IPCNs) by carbonization having SSA up to 1736 $m^2\ g^{-1}$, and thickness of 20–50 nm. IPCN with a capacitance of 200 $F\ g^{-1}$ at 5 $mV\ s^{-1}$ is produced using potassium and sodium citrate at a ratio of 2:8. Mesoporous carbon with N-doping having SSAs of 1190–1350 $m^2\ g^{-1}$ is produced using zinc and calcium citrates with melamine [110]. By direct pyrolysis of sodium gluconate, a hierarchical microporous/mesoporous carbon nanosheet having an SSA of 1890 $m^2\ g^{-1}$, a capacitance of 140 $F\ g^{-1}$ at 150 $A\ g^{-1}$ is produced [111]. Xu et al. [105] employed pyrolysis of EDTA disodium magnesium salt to produce nitrogen-doped porous carbon having SSA 1811 $m^2\ g^{-1}$, pore volume 1.16 $cm^3\ g^{-1}$ and specific capacitances of 281 $F\ g^{-1}$ at 0.05 $A\ g^{-1}$and 196 $F\ g^{-1}$ at 20 $A\ g^{-1}$. Interconnected porous carbon nanosheets (PCNS) are produced using potassium citrate at 850 °C, which exhibits an SSA of 2220 $m^2\ g^{-1}$, and thickness of less than 80 nm [112].

2.3.2 MOF Derivatives as Carbon Sources

Metal–organic frameworks (MOFs) contain metal components which are used as self-template during the pyrolysis process. Chen et al. [113] employed electrospinning of PAN/ZIF-8 composite to produce hollow particle based N-doped CNFs (HPCNFs-N), which exhibits SSA of 417.9 $m^2\ g^{-1}$ and specific capacitances of 307.2 and 193.4 $F\ g^{-1}$ at 1 and 50 $A\ g^{-1}$. By pyrolysis of K-MOF nanorods, PCNs can be produced at 200, 450, and 800 °C [114], which exhibits an SSA of 1678 $m^2\ g^{-1}$. Wang et al. [115] employed MOF-5 derived porous carbon film as "mortar" and graphene nanosheets as “brick” to produce porous carbon (C-GMOF), which exhibits low SSA ~979 m^2 g^{-1}, capacitances of 345 F g^{-1} at 2 mV s^{-1} and 201 F g^{-1} at 2 V s^{-1}. Salunkhe et al. [116] used nanoporous carbon and cobalt oxide material to assemble SC, which possesses an SSA of 350 m^2 g^{-1} and capacitance of 101 F g^{-1} at 2 A g^{-1}.

3 Factors Influencing Supercapacitance Based on Porous Carbon

The various factors which determine the electrochemical performance and hence improve the specific capacitance and energy density of supercapacitors based on porous carbon are specific surface area, surface heteroatoms, electrode structure, structure defects and pore structure.

3.1 Specific Surface Area

Theoretically, the capacitance is linearly related to the specific surface area by the relation $C = \frac{\varepsilon_r \varepsilon_0 A}{d}$, however, experimentally no linear relation has been obtained [117–119]. In the case of porous carbon, most of the BET surface area is utilized by adsorption/desorption of probe gas like N_2, CO_2 or Ar, and due to the sieving effect of pores towards ions, only a fraction of ion-inaccessible to the surface [120]. Because of the mismatch between ionic size and pore size, some pore channels cannot absorb ions to form EDL. Since large specific surface area results in more ion adsorption sites and hence improves the specific capacitance. But, excessive surface area induces more microspores which decrease the capacitance of porous carbon. Therefore, to yield a super capacitance value, a balance between surface area and pore structure needs to be maintained.

3.2 Surface Heteroatoms

The electrochemical properties of porous carbon can be affected by the substitution of surface heteroatoms like nitrogen (N), sulfur (S), oxygen (O), boron (B) and fluorine (F). This surface heteroatom influences the conductivity and chemical heterogeneity of porous carbon [110]. Oxygen doping can be achieved by O_2 functional groups like hydroxyl, carboxyl and carbonyl through the process of pyrolysis of oxygen-containing groups ($KOH/NaOH/HNO_3/H_2O_2$). In 1 mol/L H_2SO_4 electrolyte, oxygen-doped carbon shows enhanced capacitance (264 F-g^{-1}) than pristine carbon (30 F-g^{-1}). These oxygen functional groups enhance the capacitance of SCs

[121, 122]. Nitrogen doping provides extra electroactive sites in carbonaceous materials which improve surface polarity, electrical conductivity, wettability and results in the creation of defects. In N-doped carbon, nitrogen atom exists in various forms like pyrrolic-N, pyridinic-N, pyridinic-N-oxide and quaternary-N. Porous carbon doped with 21.7 at.% nitrogen forms electrochemically active nitrogen species exhibits enhanced superior energy density (36.8 Wh Kg^{-1} at 2 kW kg^{-1}) and power density (38 kW kg^{-1} at 25.7 Wh kg^{-1}) [123]. However, carbon derived from cocoon silk doped with 6.05 wt.% nitrogen form electroactive pyrrolic-N, and pyridinic-N and shows a high capacitance of 392 F g^{-1} at 1 A g^{-1} [124]. Heteroatoms of doped carbon are extensively studied and showed excellent capacitance performance [125]. For instance, N (Nitrogen) and F (fluorine) co-doped porous carbon show enhanced capacitance of 291 F g^{-1} at 0.5 A g^{-1} than obtained without F doped (238 F g^{-1}) [126]. Porous carbon co-doped with N and B exhibits enhanced specific capacitance of 268 F-g^{-1} [127]. Similarly, porous carbon co-doped with P and N atoms shows a capacitance of 317 F-g^{-1} (482 F-cm^{-3}) at 1 A g^{-1} in 1 mol/L H_2SO_4 electrolyte [128].

3.3 Electrode Structure

The electrochemical performance of SCs is influenced by the design of the electrode structure. In electrode material, the microstructural exchange between ionic diffusion and electronic transport takes place. The pores or channels present in the electrode material are responsible for ionic diffusion and effective electronic transport is promoted by the connectivity of the carbon network. Recently, graphene has been used in place of Ketjen black (KB), thereby, reducing the volume expansion (from 27 to 11%) of electrodes during the charge/discharge processes of SCs [129, 130] and enhancing the electrochemical performances of activated carbon by supporting carbon particles. The capacitance performance obtained from graphene (173 F g^{-1}) is much better than that obtained from KB (153 F g^{-1}) [131]. The graphene-cellular paper (GCP) as electrode material shows excellent specific capacitance (81 mF.cm^{-2}) and outstanding mechanical flexibility because graphene act as a binder replacing conventional PTFE/PVDF and it constitutes a novel 3D interwoven structure of graphene nanosheets and cellulose fibers [132]. Additionally, the activated carbon intercalates graphene nanosheets and enhances the effective ion-accessible surface area and promotes ionic diffusion. Therefore, an electrode made of binder-free reduced graphene oxide and activated carbon shows a high specific capacitance of 278 F g^{-1} at 1 mV s^{-1}.

3.4 Structural Defects

To enhance the capacitance performance of carbonaceous substances, structural defects such as vacancies, edge-, basal- and surface defects are employed as electrochemically active sites for ion adsorption. Earlier reports show that edge-surfaces of carbon materials possess abundant electrochemically active sites resulting in generating high capacitance than basal-surfaces [133–135]. A single-layer graphene edge exhibits a faster electron transfer rate, enhanced electrochemical activity and shows fourfold higher capacitance as compared to basal-surfaces [136]. Methods such as heteroatom insertion, and activation followed by removal treatment have been employed to insert defects on the surface of carbonaceous materials to produce defective carbons [137, 138]. Defective carbon can be produced by adopting a two-step activation procedure. HNO_3 activation results in the inclusion of nitrogen atoms in the carbon obtained from lotus leaves followed by KOH activation which removes nitrogen atoms and results in the production of some defects and pores [137]. In graphite and expanded graphite, structural defects are created in the carbon layers by ball-milling for 100 h which results in the reduction of crystallite size from 15.4 to 11.3 nm and hence producing numerous in-plane defects [139]. Earlier studies show that defects in carbon graphitic layer generate large values of capacitance and improve their capacitive performance [140].

3.5 Pore Structure

Another important factor that impacts the charge transfer/ion transport and decides the rate performance, and capacitance of porous carbons are pore size, pore size distribution and pore shape. It has been observed from the previous reports that if the pore size is less, it will not contribute to EDL capacitance. Smaller pore size (<1 nm) in microporous carbon yields higher capacitance in various electrolytes having large solvated ions. It has been observed that the formation of effective EDL in porous carbon occurs at pore size 0.7 nm in aqueous electrolytes and 0.8 nm in organic electrolytes [141]. Thus, more research is focused on investigating sub-nanometer porous carbon. In exfoliated graphene (EG)-mediated graphene oxide (GO) film (EGM-GO), when the pore size matches the size of electrolyte ions, maximum pore usage takes place for optimizing volumetric capacitance [142]. Theoretical and experimental computations confirmed that in sub-nanometer pores, an ions desolvation effect improved the capacitance [143, 144], however, it has been observed that as the pore size decreased from 1 nm to 0.65 nm, the desolvation effect increased [145]. Various pores shape exists in porous carbon such as endohedral shape like slit, spherical and cylindrical pores as well as exohedral pores like pores between carbon nanoparticles like CNTs and carbon onions [146]. Huang et al. [147] proposed an electric double-cylinder capacitance (EDCC) model by considering endohedral pore curvatures (cylindrical-shaped mesopores) and the EDCC capacitance is given by

$$C = \frac{2\pi \varepsilon_r \varepsilon_0 L}{\ln(b/a)} \tag{24}$$

And when normalized with area A is given as

$$C/A = \frac{\varepsilon_r \varepsilon_0}{b \ln(b/(b-d))} \tag{25}$$

where 'L' represents the pore length, 'b' and 'a' denotes radii of outer and inner cylinders, and 'd' is the distance between the center of counter ions and the pore walls.

An electric wire-in-cylinder capacitance (EWCC) model is considered for micropores by assuming their cylindrical shape and the capacitance is given by

$$C/A = \frac{\varepsilon_r \varepsilon_0}{b \ln(b/(a_0))} \tag{26}$$

where 'b' is the radius of the micropore and 'a_0' represents the radius of the inner cylinder formed by counter ions.

A sandwich model for slit-shaped pores is given by Feng et al. [148] and the capacitance is expressed as

$$C/A = \frac{\varepsilon_r \varepsilon_0}{(b - a_0)} \tag{27}$$

where b is half of the slit-shaped pore width and a_0 is the ion radius of counter ions.

The outer surface of carbon onion and 1D CNT arrays forms an exohedral capacitance and exohedral electric double-sphere capacitors (xEDSCs) and its capacitance is given as

$$C = \frac{4\pi \varepsilon_r \varepsilon_0 ab}{b - a} \tag{28}$$

$$C/A = \frac{\varepsilon_r \varepsilon_0 (a + b)}{(ad)} \tag{29}$$

$$C/A = \frac{\varepsilon_r \varepsilon_0}{a \ \ln\left[\frac{(a+b)}{a}\right]} \tag{30}$$

where a: radius of the inner sphere/cylinder charge layer; b: outer sphere/cylindrical charge layer and d: effective double-layer thickness.

Thus, the above-mentioned parameters play important roles in their energy density and specific capacitance.

4 Advantage of Pure/Porous Carbon as Compared to Other Earlier Materials Used in Supercapacitor Electrodes Fabrication

Carbon possesses features that make it a good candidate for use as a fuel cell electrode. Carbon is appealing as a spongy substrate because of its decent chemical resistance and electrical conductivity as well as its cheap intrinsic cost. The fuel or oxidant gas disseminates to the electrolyte electrode contact through the porous electrode. In an ideal situation, a three-phase contact between gas, electrolyte and electrode is formed, Homogeneity, regulated typical pore size, extremely fine pore spectra, mechanical robustness below strongly eroding chemical assault, excellent permeability for both reactants and products, and superior electrical conductivity are all desirable characteristics of porous carbon. It is critical that the manufacturing method produces isotropic porous carbon with repeatable characteristics. On the electrochemical recital of oxygen, air and hydrogen electrodes, data on penetrability, pore size dispersal and BET surface area are provided. The corporal characteristics of porous carbon are linked, thus optimizing one attribute may result in unintended changes in others.

4.1 Supercapacitor Carbon Electrodes

In thin film supercapacitors, electrodes consist of a layer of active material that varies from a few nm to several mm thick [149]. Carbon-based substances are commonly employed as electrodes in electric double layer supercapacitors because it meets electrode criteria while having a low specific capacitance. Activated carbon, carbon nanotubes, templated carbon, carbon onions, graphene and carbide-derived carbon were among the carbon materials employed [150–156]. Because these carbon compounds have a large surface area, they can generate a lot of specific energy and power. They are less expensive than supplementary substances, but their preparation technique may be advanced. The shape of the electrode solid is important since it controls the interface and, as a result, the electrochemical act. The energy-storing capacity of nanoporous carbon electrodes can be enhanced by coordinating the average pore size with the basic ion diameter [151]. Redox electrolytes, ionic liquids and the inclusion of redox-active materials, like heteroatom doping or metal oxides are some more techniques to boost the energy storage capacity of supercapacitors [157–159].

4.2 Activated Carbon

It has a great specific surface area, a complicated permeable structure, high electrochemical stability, strong electrical conductivity and is relatively cheap. The downsides include weak mechanical qualities and the requirement for metal current collectors. Carbonization followed by activation (physical, chemical, or a mixture of both) produce activated carbon (fibers) having a large surface area and high capacitance [160, 161]. Doping activated carbon with carbon nanotubes, graphene oxide, polypyrrole or silver nanowires can improve the electrical conductivity of thin film electrodes [162–165]. An increase of 39% in specific capacitance is achieved in an activated carbon electrode doped with 500 nm silver nanowires produced via the ultrasonic spray coating method [165]. In a similar study, activated carbon doped with silver nanowires and NiO–Co_3O_4 nanocomposites (produced via a hydrothermal method), shows a specific capacitance of 707 F g^{-1} with 93% of the capacitance remaining even after 5000 cycles [166]. In a 1 M H_2SO_4 electrolyte, activated carbon fiber electrodes with tin oxynitride nanorod arrays showed capacitance of 673 F g^{-1} at 1.0 applied current/gram and a cycling stability of 99% at 5.0 applied current/gram for 2000 cycles [167]. Thin film electrodes having activated carbon doped with MnO_2 and silver nanowires showed improved conductivity, specific capacitance of 1021 F g^{-1}, which is 325% higher as compared to undoped activated carbon [168]. Recent research described a simple approach for fabricating porous carbon/silicon carbide composites directly from bamboo waste raw material. In this approach, hybrid electrodes are created by mixing semiconductors to offset the problem of porous carbon's low electrical conductivity. At a current density of 1.0 applied current/gram, the HPC/SiC composite had a specific capacitance of 234 F/g [169].

4.3 Carbon Nanotubes

Carbon nanotubes have a large surface area, a distinct core structure, a low-slung density, good electrical conductivity, mechanical qualities and chemical/thermal resilience. Carbon nanotubes are prepared by breaking down particular hydrocarbons and manipulating them into nanostructures. The operating speed of micro-supercapacitors is influenced by the aspect ratio of carbon nanotube electrodes, with an increase in aspect ratio from 0.2 to 7.0 resulting in a non-linear drop in the relaxation time constant from 85.0 to around 0.5 ms [170]. Vacuum filtering with ensuing stamping and electrodeposition of cobalt-hydroxide nanoflakes created single-walled carbon nanotube thin films with outstanding structural stability. These thin film supercapacitor electrodes have a specific capacitance of 314 F g^{-1} [171]. Carbon nanotubes doped into nickel hydroxide thin film electrodes, the doped electrode showed a capacity of 430.0 mAh/g, which remained at 75% after 1000 cycles [172]. Photolithography and vacuum filtering were used to create carbon nanotube-MXene composites for on-chip micro-supercapacitor which exhibit areal capacitance of 61.0

mF/cm^2 at a current density of 0.5 milliampere/cm^2 [173]. The double-layer capacitance of fully stretchable micro-supercapacitors was made using oxidized carbon nanotubes and polyvinyl-alcohol electrodes, which exhibit a capacitance of 20 mF/cm^2 at 0.1 mA/cm^2 [174]. The electrode planar design was used to create ultrathin highly-aligned carbon-nanotubes sheet supercapacitors. With 50 layers and a total thickness of only 300 nm, these devices had an energy density of 10.5 milli Watt hour/cm^3 and a power density of 19.0 W/cm^3 [175].

4.4 Graphene

Graphene is a planar-sheet of sp^2 bonded carbon atoms organized in a honeycomb crystal-lattice that is one atom copious. It possesses exceptional thermal and chemical stability, as well as great electrical, mechanical and morphological qualities. A hydrothermal process can be used to make graphene. The electrochemical performance of quasi-solid-state micro-supercapacitors can be prepared using a cellular graphene layer and polyvinyl alcohol or H_3PO_4 [176]. Graphene fiber electrodes, which were created by electrochemical exfoliation of graphite foil tinny strips had a capacitance of around 248.0 milli Farad/cm^2 at about 2.0 milli Ampere/cm^2 [177]. Chemical vapor deposition is also used to create graphene structures for flexible micro-supercapacitors with outstanding cycle stability and capacitance of 1.5 milli Farad/cm^2 at a scan rate of 10.0 V/sec [178]. Micro-supercapacitors made using laser-irradiated graphene have an ultra-long cycle life with 100% preservation of the original capacitance even after 1,00,000 cycles [179]. Flexible supercapacitors contain electrodes made of graphene-coated copper foil with ruthenium-oxide produced by cathodic-electroplating, with a capacitance of 1561.0 F g^{-1} at a scan rate of 5.0 milli Volt/sec and a high energy density of roughly 13.0-W h/kg at a power density of about 21 kW/kg [180]. To boost the capacitance of graphene, it is doped with fluorine, and amalgamated is created by combining it with nanoscale carbide-derived-carbon, which has a large specific surface area and a graded pore structure. At a scan rate of 5.0 milli Volt/sec, the specific-capacitance of this compound in the aqueous electrolyte is 321.0 F/g [181]. Two-dimensional hierarchically organized dual-meso-porous polypyrrole or graphene nanosheets with a high surface area of 112.0 m^2/g and capacitance of 376.0 F g^{-1} at 1 milli Volt/sec is used to create planar integrated-systems of micro-supercapacitors [182].

4.5 Onion-Like Carbon

Carbon nano-onions, or onion-like carbon, have high stability and low density. As a result, they are ideal electrode materials for high-capacity supercapacitors. Carbon onions provide fast charge and discharge rates, allowing for easy ion accessibility and rapid electrical conduction [183]. Laser-assisted combustion, underwater-arc-discharge, flame pyrolysis and vacuum annealing can all be used to make onion-like carbon [184–187]. Nanostructured carbon-onions with a diameter of 6.0–7.0 nm are used to make micro-supercapacitors with an electrophoretic deposition process generating a layer of several micrometers [188]. Specific-capacitance of onion-like carbon adorned with platinum nanoparticles is increased by four times [189]. In another work, carbon-onion grafted manually with 1.0-nitro-pyrene resulted in a twofold increase in electrode capacity to 38.0 milli Ah/g with primary capacity remaining extremely high even after 4,000 cycles [190].

4.6 Carbide-Derived Carbon

Carbon-derived carbon from carbide powders such as metal carbides, carbo-nitrides or oxy-carbides by a chlorination process at a convinced temperature and time is explored recently [191–194]. Calcium-carbide inorganic salt reaction, hydrothermal leaching and carbide thermal breakdown are some of the various techniques to make CDC [195–197]. The aperture dimensions of these materials may be tailored to bout the solvated ion size in the electrolyte, resulting in increased capacitance [156, 198, 199]. CDC also has excellent chemical resistance and electrical conductivity. CDC is appropriate for EDLC electrodes with outstanding capacitance because of its enough surface area of up to 1800 m^2 g^{-1} and limited pore size dispersion [200]. Combining carbide-derived carbon with metal oxides, noble metals, and conducting polymers can boost energy density [201]. Polymer-derived ceramic materials such as poly-organo-siles-quioxane particles are employed as precursor materials for carbide-derived carbon and are produced using a MicroJet reactor technology on a large scale [202]. The generated CDC shows a pore capacity of 1.3–2.1 cm^3/g and a specific surface area of 2014.0–2114.0 m^2 g^{-1}. In 1 M tetra-ethyl-ammonium tetra-fluoroborate in aceto-nitrile, the material's specific capacitance is 116.0 F g^{-1} at 5.0 milli ampere/gram and 80.0 F g^{-1} at 100.0 milli ampere/gram [202]. Another study investigated the electrochemical behavior and performance of micro meter thick TiC-carbide-derived carbon diluted in either acetonitrile or propylene carbonate in 1-ethyl-3-methylimidazolium tetra fluoroborate ($EMIMBF_4$) for micro-supercapacitor applications. In 2 M $EMIBF_4$/acetonitrile, it demonstrated a typical-capacitive-signature of 169.0 F/cm^3 and an energy density of 90.0 Wh/cm^2 [203]. In supercapacitor setups with a typical organic electrolyte, the effect of nitrogen doping on CDC was investigated. The results revealed that a nitrogen content of 1 to 7 mass percent did not have a significant impact on energy-storing-capacity, but it did have a bigger impact on rate handling capability [204]. carbide-derived carbon-titanium oxide composites with the ranked structure are created by utilizing a solvothermal technique. This composite material exhibited a specific-capacitance of 173.0 F g^{-1} and remarkable cycle stability [201].

5 Parameters Required for Improving the Efficiency of Porous Carbon-Based Electrode

Porous carbons are utilized as role material to examine the impact of pore structure on electrochemical performance, as pore structure is a significant aspect in creating porous materials as EDLC electrodes. An essential characteristic relating to the pore structure of a carbon electrode is the size of electrolytes, including anions and cations [205, 206]. Three different types of electrolytes such as aqueous electrolyte, non-aqueous electrolyte and ionic liquid electrolyte are investigated. Due to the thermal breakdown of water, the aqueous electrolyte had a low working voltage of 1.23 V, but the non-aqueous electrolyte had a higher voltage of roughly 2.7 V [207, 208]. They might be employed for large potential windows bigger than 3.0 V in ionic liquid electrolytes. For aqueous electrolytes and organic electrolytes, Raymundo et al. [141] suggested pore diameters of roughly 0.7–0.8 nm in aqueous and organic electrolytes. The effect of carbon tunnels on capacitive performance is investigated in C/C composite cryogels with mesoporous structures. The larger micropore size distribution and carbon tunnels of C/C composites increase charge propagation inside the pore structure increasing the number of cotton fibers added to the C/C composites which further improved the capacitance. These findings show that the appropriate pore structure and amount of carbon tunnels or macropores may be critical in achieving high capacitance [209, 210]. However, the carbon fibers in the dispersed phase of C/C composite cryogels displayed moderate microporosity without mesoporous capabilities due to the lack of activation to improve the porous qualities like activated carbon fibers. They may obstruct rapid charge propagation, leading to lower capacitance and electrostatics. Carbon fibers reduced the total specific surface area of C/C composites (C/C_0 with cotton fibers had 1230 m^2/g) and obstructed the matrix phase's true capacitance value (the carbon cryogels). The capacitive performance of templated carbon xerogels (TCXs) (making macropores) would allow for high specific capacitance with fast charge propagation at a high discharge rate The influence of macropores on electrochemical performance has been studied using TCXs with a regulated surface area [210]. TCXs containing sponge-like carbon xerogels (TCX1V20, TCX2V20 and TCX3V20) are investigated which shows improved electrochemically for the various RF formulations. At the same time, TCXs highlighted the importance of macropores, micropores and mesopores for EDLCs. Yang et al. investigated the electrical and ionic resistance of carbon aerogels at various pore sizes [211]. The pore size was discovered to be the most important component in determining the EDLC electrode's electrochemical performance. Carbon aerogels with a high pore size have low ionic resistance, while carbon aerogels with a small pore size and a dense structure have low electronic resistance [212]. The capacitances of the ordered mesoporous carbon are greater than those of the disordered mesoporous carbon. The length of the straight channels worked as ion highways, resulting in good capacitance and rate performance [210]. The mass transfer resistance might be reduced by reducing particle size and increasing the mono-dispersity of carbon spheres, hence improving overall EDLC performance [213]. The capacitance was determined not only by the surface area, but also by the pore size distribution [214]. The influence of electrolyte type on capacitance was investigated by Zeller et al. [215]. The pore structure of porous carbon materials is also determined by the kind of electrolyte utilized. An aqueous electrolyte's capacitance is solely determined by the overall surface area. Due to the good wettability of the organic electrolyte, Fang et al. changed the surface of activated carbon with oleate producing better capacitance [216]. The surface capacitance was measured using the $(C_2H_5)_4NBF_4/AN$ electrolyte and several microporous carbons by Centeno's team [217–219]. For the organic electrolyte $(C_2H_5)_4NBF_4/AN$, the surface capacitance became constant at about 0.094 ± 0.011 F/m^2.

6 Conclusion

Owing to their excellent thermal and electrochemical stability, cheap-cost, strong electrical-conductivity, regulated absorbency and adequate lively sites, carbon-based materials are the most popular electrode materials for electric double layer supercapacitors. Micro supercapacitors are available in two major configurations: stacking and in-plane inter-digitated, with a tertiary form, the fiber-molded design, also being shown. The structural design of the electrode has an important effect on supercapacitor performance, and carbon electrode materials with a regulated pore-structure, sufficient specific-surface-area, and enough surface handy groups are required to produce high capacitance. Carbon nanotubes, activated-carbon, graphene, onion-like carbon, and carbide-derived-carbon are all typical carbon materials utilized in micro-supercapacitors. Increased specific-capacitance, hybrid-electrodes, doping of activated carbon, fluorine drugging of graphene, laser irradiation of graphene, embellishment of onion-like carbon with Pt, carbon nanotube composites with MXene, and graphene composites with carbide-derived-carbon are all examples of recent research on these carbon electrode materials.

References

1. Kurzweil P, Hildebrand A, Weiß M (2014) Accelerated life testing of double- layer capacitors: reliability and safety under excess voltage and temperature. Chem Electro Chem 2(1):150–159
2. Pandolfo AG, Hollenkamp AF (2006) Carbon properties and their role in Supercapacitors. J Power Sources 157(1):11–27
3. Li X et al (2013) Large-area flexible core-shell graphene/porous carbon woven fabric films for fiber supercapacitor electrodes. Adv Funct Mater, 1–7
4. Liu J et al (2014) High-performance flexible asymmetric supercapacitors based on a new graphene foam/carbon nanotube hybrid film. Energy Environ Sci 7(11):3709–3719
5. Ran F, Yang X, Shao L (2018) Recent progress in carbon-based Nano architectures for advanced supercapacitors. Adv Compos Hybrid Mater 1(1):32–55
6. Miller JR, Simon P (2008) Electrochemical capacitors for energy management. Science 321(5889):651–652

7. Zhang S, Pan N (2014) Supercapacitors performance evaluation. Adv Energy Mater 5(6):1401401
8. Mohamed SG et al (2014) High-performance lithium-ion battery and symmetric supercapacitors based on $FeCo_2O_4$ nanoflakes electrodes. ACS Appl Mater Interfaces 6(24):22701–22708
9. Yu Z et al (2015) Supercapacitor electrode materials: nanostructures from 0 to 3 dimensions. Energy Environ Sci 8(3):702–730
10. Miller JR, Burke A (2008) Electrochemical capacitors: challenges and opportunities for real-world applications. Electrochem Soc Interface 17(1):53–57
11. Dunn B, Kamath H, Tarascon J-M (2011) Electrical energy storage for the grid: a battery of choices. Science 334(6058):928–935
12. Fic K et al (2018) Sustainable materials for electrochemical capacitors. Mater Today 21(4):437–454
13. Sing KSW et al (1985) Reporting physisorption data for gas/solid systems with special reference to the determination of surface area and porosity. Pure Appl Chem 57:603–619
14. Frackowiak E, Béguin F (2001) Carbon materials for the electrochemical storage of energy in capacitors. Carbon 39(6):937–950
15. Zhao J et al (2015) Hydrophilic hierarchical nitrogen-doped carbon nanocages for ultrahigh Super capacitive performance. Adv Mater 27(23):3541–3545
16. Tang J et al (2015) Thermal conversion of core–shell metal-organic frameworks: a new method for selectively functionalized nanoporous hybrid carbon. J Am Chem Soc 137(4):1572–1580
17. Zhuang X et al (2014) Graphene coupled Schiff-base porous polymers: towards nitrogen-enriched porous carbon nanosheets with ultrahigh electrochemical capacity. Adv Mater 26(19):3081–3086
18. Yang X et al (2015) Nitrogen-enriched hierarchically porous carbon materials fabricated by Graphene Aerogel templated schiff-base chemistry for high performance electrochemical capacitors. Polym Chem 6(7):1088–1095
19. Lin T et al (2015) Nitrogen-doped mesoporous carbon of extraordinary capacitance for Electrochemical Energy Storage. Science 350(6267):1508–1513
20. Chmiola J et al (2006) Anomalous increase in carbon capacitance at pore sizes less than nanometer Science 313(5794):1760–1763
21. Largeot C et al (2008) Relation between the ion size and pore size for an electric double-layer capacitor. J Am Chem Soc 130(9):2730–2731
22. Jiang L, Sheng L, Fan Z (2017) Biomass-derived carbon materials with structural diversities and their applications in Energy Storage. Sci China Mater 61(2):133–158
23. Li Z et al (2020) Quantitative assessment of basal-, edge- and defect-surfaces of carbonaceous materials and their influence on electric double-layer capacitance. J Power Sources 457:228022
24. Lyu L et al (2019) Recent development of biomass-derived carbons and composites as electrode materials for supercapacitors. Mater Chem Front 3(12):2543–2570
25. Wang T et al (2020) Recent advances in fluorine-doped/fluorinated carbon-based materials for supercapacitors. Energy Storage Mater 30:367–384
26. Alslaibi TM et al (2013) A review: production of activated carbon from agricultural byproducts via conventional and microwave heating. J Chem Technol Biotechnol 88(7):1183–1190
27. Chaiwat W et al (2008) Examination of degree of cross-linking for cellulose precursors pretreated with acid/hot water at low temperature. Ind Eng Chem Res 47(16):5948–5956
28. Damodar D et al (2019) Near-room-temperature synthesis of sulfonated carbon nanoplates and their catalytic application. ACS Sustain Chem Eng 7(15):12707–12717
29. Zhang G et al (2016) Unconventional carbon: alkaline dehalogenation of polymers yields N-doped carbon electrode for high-performance capacitive energy storage. Adv Func Mater 26(19):3340–3348
30. Han S-W et al (2014) Effect of pyrolysis temperature on carbon obtained from green tea biomass for superior lithium ion battery anodes. Chem Eng J 254:597–604
31. Kercher AK, Nagle DC (2003) Microstructural evolution during charcoal carbonization by X-ray diffraction analysis. Carbon 41(1):15–27

32. Navarro RM, Peña MA, Fierro JL (2007) Hydrogen production reactions from carbon feed stocks: fossil fuels and biomass. Chem Rev 107(10):3952–3991
33. Kim D-W et al (2017) Structural elucidation of physical and chemical activation mechanisms based on the microdomain structure model. Carbon 114:98–105
34. Şahin Ö, Saka C (2013) Preparation and characterization of activated carbon from Acorn Shell by physical activation with H_2O–CO_2 in two-step pre-treatment. Bioresour Technol 136:163–168
35. Contreras MS et al (2010) A comparison of physical activation of carbon xerogels with carbon dioxide with chemical activation using hydroxides. Carbon 48(11):3157–3168
36. Prauchner MJ, Rodríguez-Reinoso F (2012) Chemical versus physical activation of coconut shell: a comparative study. Microporous Mesoporous Mater 152:163–171
37. Lin G et al (2018) Koh activation of biomass-derived nitrogen-doped carbons for supercapacitor and electrocatalytic oxygen reduction. Electrochim Acta 261:49–57
38. Zou K et al (2018) Hierarchically porous nitrogen-doped carbon derived from the activation of agriculture waste by potassium hydroxide and urea for high-performance supercapacitors. J Power Sources 378:579–588
39. Islam MA et al (2017) Mesoporous activated coconut shell-derived hydrochar prepared via hydrothermal carbonization-naoh activation for methylene blue adsorption. J Environ Manage 203:237–244
40. Lillo-Ródenas MA et al (2001) Preparation of activated carbons from Spanish anthracite. Carbon 39(5):751–759
41. Sayğılı H, Güzel F (2016) High surface area mesoporous activated carbon from tomato processing solid waste by zinc chloride activation: process optimization, characterization and dyes adsorption. J Clean Prod 113:995–1004
42. Reddy KS, Al Shoaibi A, Srinivasakannan C (2012) A comparison of microstructure and adsorption characteristics of activated carbons by CO_2 and H_3PO_4 activation from date palm pits. New Carbon Mater 27(5):344–351
43. Prahas D et al (2008) Activated carbon from jackfruit peel waste by H_3PO_4 chemical activation: pore structure and surface chemistry characterization. Chem Eng J 140(1–3):32–42
44. Yin H et al (2014) Harvesting capacitive carbon by carbonization of waste biomass in molten salts. Environ Sci Technol 48(14):8101–8108
45. Zhang F et al (2017) Multiscale pore network boosts capacitance of carbon electrodes for ultrafast charging. Nano Lett 17(5):3097–3104
46. Kang D et al (2015) ‘egg-box’-assisted fabrication of porous carbon with small mesopores for high-rate electric double layer capacitors. ACS Nano 9(11):11225–11233
47. Fan X et al (2014) A layered-nanospace-confinement strategy for the synthesis of two-dimensional porous carbon nanosheets for high-rate performance supercapacitors. Adv Energy Mater 5(7):1401761
48. Zhang F et al (2016) Hierarchically porous carbon foams for electric double layer capacitors. Nano Res 9(10):2875–2888
49. Sevilla M, Valle-Vigón P, Fuertes AB (2011) N-doped polypyrrole-based porous carbons for CO_2 capture. Adv Funct Mater 21(14):2781–2787
50. Zhang W et al (2015) 3 D hierarchical porous carbon for supercapacitors prepared from lignin through a facile template-free method. Chem Sus Chem 8(12):2114–2122
51. Tian YX et al (2019) Hierarchical porous carbon prepared through sustainable $CuCl_2$ activation of rice husk for high-performance supercapacitors. Chem Sel 4(8):2314–2319
52. Yu M et al (2017) Boosting the energy density of carbon-based aqueous supercapacitors by optimizing the surface charge. Angew Chem Int Ed 56(20):5454–5459
53. Han Y et al (2018) Enhancing the capacitive storage performance of carbon fiber textile by surface and structural modulation for advanced flexible asymmetric supercapacitors. Adv Func Mater 29(7):1806329
54. Wang C et al (2018) A green and scalable route to yield porous carbon sheets from biomass for supercapacitors with high capacity. J Mater Chem A 6(3):1244–1254

55. Chen Y et al (2017) Self-assembly of 3D neat porous carbon aerogels with NaCl as template and flux for sodiumion batteries. J Power Sources 359:529–538
56. Chen Y et al (2018) Synthesis of porous nitrogen and sulfur co-doped carbon beehive in a high-melting-point molten salt medium for improved catalytic activity toward oxygen reduction reaction. Int J Hydrogen Energy 43(10):5124–5132
57. Xu Z et al (2020) Understanding reactions and pore-forming mechanisms between waste cotton woven and $FeCl_3$ during the synthesis of magnetic activated carbon. Chemosphere 241:125120
58. Li J et al (2019) Molten salt synthesis of hierarchical porous n-doped carbon submicrospheres for multifunctional applications: high performance supercapacitor, dye removal and CO_2 capture. Carbon 141:739–747
59. Zhu H et al (2012) Integrated synthesis of Poly(*O*-phenylenediamine)-derived carbon materials for high performance supercapacitors. Adv Mater 24(48):6524–6529
60. Yun SI et al (2019) Facile preparation and capacitive properties of low-cost carbon nanofibers with zno derived from lignin and pitch as supercapacitor electrodes. Carbon 149:637–645
61. Lv Y et al (2012) A self-template synthesis of hierarchical porous carbon foams based on banana peel for supercapacitor electrodes. J Power Sources 209:152–157
62. Li J et al (2018) Cross-coupled macro-mesoporous carbon network toward record high energy-power density supercapacitor at 4 V. Adv Func Mater 28(51):1806153
63. Zhang G et al (2018) High-performance cathode based on self-templated 3D porous micro-crystalline carbon with improved anion adsorption and intercalation. Adv Func Mater 29(2):1806722
64. Wan L et al (2019) Facile synthesis of nitrogen self-doped hierarchical porous carbon derived from pine pollen via mgco3 activation for high-performance supercapacitors. J Power Sources 438:227013
65. Liu T et al (2017) Revitalizing carbon supercapacitor electrodes with hierarchical porous structures. J Mater Chem A 5(34):17705–17733
66. Chen J et al (2018) N/P co-doped hierarchical porous carbon materials for superior performance supercapacitors. Electrochim Acta 271:49–57
67. Yi J et al (2017) Lignocellulose-derived porous phosphorus-doped carbon as advanced electrode for Supercapacitors. J Power Sources 351:130–137
68. Liu X, Giordano C, Antonietti M (2013) A facile molten-salt route to graphene synthesis. Small 10(1):193–200
69. Yang C-M et al (2005) Highly ultra-microporous single-walled carbon nanohorns assemblies. Adv Mater 17(7):866–870
70. Hwang H et al (2019) High-density graphene/single-walled carbon nanohorns composite supercapacitor electrode with high volumetric capacitance. Appl Surf Sci 489:708–716
71. Wang G et al (2014) Solid-state supercapacitor based on activated carbon cloths exhibits excellent rate capability. Adv Mater 26(17):2676–2682
72. Qiu D et al (2019) Preparation of oxygen-enriched hierarchically porous carbon by $KMnO_4$ one-pot oxidation and activation: mechanism and capacitive energy storage. Electrochim Acta 294:398–405
73. Li Y et al (2019) KNO_3-mediated synthesis of high-surface-area polyacrylonitrile-based carbon material for exceptional supercapacitors. Carbon 152:120–127
74. Wang D et al (2019) Gunpowder chemistry-assisted exfoliation approach for the synthesis of porous carbon nanosheets for high-performance ionic liquid based supercapacitors. J Energy Storage 24:100764
75. Liang H-W et al (2013) Mesoporous metal–nitrogen-doped carbon electrocatalysts for highly efficient oxygen reduction reaction. J Am Chem Soc 135(43):16002–16005
76. Schmidt-Winkel P et al (1998) Microcellular siliceous foams with uniformly sized cells and windows. J Am Chem Soc 121(1):254–255
77. Schacht S et al (1996) Oil-water interface templating of mesoporous macroscale structures. Science 273(5276):768–771

78. Xie K et al (2011) Carbon nanocages as supercapacitor electrode materials. Adv Mater 24(3):347–352
79. Zhu C et al (2018) Nitrogen-doped porous carbon as-mediated by a facile solution combustion synthesis for supercapacitor and oxygen reduction electrocatalyst. Chem Eng J 350:278–289
80. Mecklenburg M et al (2012) Aerographite: ultra lightweight, flexible nanowall, carbon microtube material with outstanding mechanical performance. Adv Mater 24(26):3486–3490
81. Wang C, O'Connell MJ, Chan CK (2015) Facile one-pot synthesis of highly porous carbon foams for high-performance supercapacitors using template-free direct pyrolysis. ACS Appl Mater Interfaces 7(16):8952–8960
82. He S et al (2019) High rate-performance supercapacitor based on nitrogen-doped hollow hexagonal carbon nanoprism arrays with ultrathin wall thickness in situ fabricated on carbon cloth. J Power Sources 434:226701
83. Liang Y et al (2010) Direct access to metal or metal oxide nanocrystals integrated with one-dimensional nanoporous carbons for electrochemical energy storage. J Am Chem Soc 132(42):15030–15037
84. Fang Y et al (2013) Two-dimensional mesoporous carbon nanosheets and their derived graphene nanosheets: synthesis and efficient lithium ion storage. J Am Chem Soc 135(4):1524–1530
85. de Almeida Filho C, Zarbin AJG (2006) Hollow porous carbon microspheres obtained by the pyrolysis of TiO_2/poly (furfuryl alcohol) composite precursors Carbon (14):2869–2876
86. Kyotani T et al (1997) Formation of new type of porous carbon by carbonization in Zeolite nanochannels. Chem Mater 9(2):609–615
87. Kyotani T, Ma Z, Tomita A (2003) Template synthesis of novel porous carbons using various types of zeolites. Carbon 41(7):1451–1459
88. Fan Z et al (2012) Template-directed synthesis of pillared-porous carbon nanosheet architectures: high-performance electrode materials for Supercapacitors. Adv Energy Mater 2(4):419–424
89. Chen W et al (2019) Controlling synthesis of nitrogen-doped hierarchical porous graphene-like carbon with coral flower structure for high-performance supercapacitors. Ionics 25(11):5429–5443
90. Bu Y et al (2017) Compressing carbon nanocages by capillarity for optimizing porous structures toward ultrahigh-volumetric-performance supercapacitors. Adv Mater 29(24):1700470
91. Liu J et al (2015) Molecular-based design and emerging applications of nanoporous carbon spheres. Nat Mater 14(8):763–774
92. Chu W-C et al (2017) Tailored design of bicontinuous gyroid mesoporous carbon and nitrogen-doped carbon from poly(ethylene oxide-*b*-caprolactone) diblock copolymers. Chem Eur J 23(55):13734–13741
93. Wu H et al (2013) Stable li-ion battery anodes by in-situ polymerization of conducting hydrogel to conformally coat silicon nanoparticles. Nat Commun 4(1)
94. Zhao Y, Jiang L (2009) Hollow micro/nanomaterials with multilevel interior structures. Adv Mater 21(36):3621–3638
95. Zhang F et al (2006) An aqueous cooperative assembly route to synthesize ordered mesoporous carbons with controlled structures and morphology. Chem Mater 18(22):5279–5288
96. Zhao D et al (1998) Non-ionic Triblock and star diblock copolymer and oligomeric surfactant syntheses of highly ordered, hydrothermally stable, mesoporous silica structures. J Am Chem Soc 120(24):6024–6036
97. Wei J et al (2012) A controllable synthesis of rich nitrogen-doped ordered mesoporous carbon for CO_2 capture and supercapacitors. Adv Func Mater 23(18):2322–2328
98. Liang C et al (2004) Synthesis of a large-scale highly ordered porous carbon film by self-assembly of Block Copolymers. Angew Chem Int Ed 43(43):5785–5789
99. Peng L et al (2019) Versatile Nano emulsion assembly approach to synthesize functional mesoporous carbon nanospheres with tunable pore sizes and architectures. J Am Chem Soc 141(17):7073–7080

100. Hasegawa G et al (2016) Hierarchically porous carbon monoliths comprising ordered mesoporous nanorod assemblies for high-voltage aqueous supercapacitors. Chem Mater 28(11):3944–3950
101. Wang J-G et al (2018) One-pot synthesis of nitrogen-doped ordered mesoporous carbon spheres for high-rate and long-cycle life supercapacitors. Carbon 127:85–92
102. Meng Y et al (2006) A family of highly ordered mesoporous polymer resin and carbon structures from organic−organic self-assembly. Chem Mater 18(18):4447–4464
103. Zhou X, Yu L, Lou XW (2016) Nanowire-templated formation of SnO_2/carbon nanotubes with enhanced lithium storage properties. Nanoscale 8(15):8384–8389
104. Liang Y, Fu R, Wu D (2013) Reactive template-induced self-assembly to ordered mesoporous polymeric and carbonaceous materials. ACS Nano 7(2):1748–1754
105. Yang B et al (2019) 3D nitrogen-doped framework carbon for high-performance potassium ion hybrid capacitor. Energy Storage Materials 23:522–529
106. Xu B et al (2013) Facile synthesis of nitrogen-doped porous carbon for supercapacitors. Journal of Materials Chemistry A 1(14):4565
107. Li W et al (2011) A self-template strategy for the synthesis of mesoporous carbon nanofibers as advanced supercapacitor electrodes. Adv Energy Mater 1(3):382–386
108. Pachfule P et al (2016) Fabrication of carbon nanorods and graphene nanoribbons from a metal–organic framework. Nat Chem 8(7):718–724
109. Liang Z et al (2017) Pristine metal-organic frameworks and their composites for energy storage and conversion. Adv Mater 30(37):1702891
110. Abioye AM, Ani FN (2015) Recent development in the production of activated carbon electrodes from agricultural waste biomass for supercapacitors: a review. Renew Sustain Energy Rev 52:1282–1293
111. Ferrero GA et al (2016) Efficient metal-free N-doped mesoporous carbon catalysts for Orr by a template-free approach. Carbon 106:179–187
112. Fuertes AB, Sevilla M (2015) Hierarchical microporous/mesoporous carbon nanosheets for high-performance supercapacitors. ACS Appl Mater Interfaces 7(7):4344–4353
113. Sevilla M, Fuertes AB (2014) Direct synthesis of highly porous interconnected carbon nanosheets and their application as high-performance supercapacitors. ACS Nano 8(5):5069–5078
114. Chen L-F et al (2017) Designed formation of hollow particle-based nitrogen-doped carbon nanofibers for high-performance supercapacitors. Energy Environ Sci 10(8):1777–1783
115. Jayaramulu K et al (2018) Ultrathin hierarchical porous carbon nanosheets for high-performance supercapacitors and redox electrolyte energy storage. Adv Mater 30(15):1705789
116. Salunkhe RR et al (2015) Asymmetric supercapacitors using 3D nanoporous carbon and cobalt oxide electrodes synthesized from a single metal–organic framework. ACS Nano 9(6):6288–6296
117. Du W et al (2019) Designing synthesis of porous biomass carbon from wheat straw and the functionalizing application in flexible, all-solid-state supercapacitors. J Alloy Compd 797:1031–1040
118. Endo M et al (2001) Capacitance and pore-size distribution in aqueous and nonaqueous electrolytes using various activated carbon electrodes. J Electrochem Soc 148(8)
119. Long C et al (2015) Porous layer-stacking carbon derived from in-built template in biomass for high volumetric performance supercapacitors. Nano Energy 12:141–151
120. Eliad L et al (2001) Ion sieving effects in the electrical double layer of porous carbon electrodes: estimating effective ion size in electrolytic solutions. J Phys Chem B 105(29):6880–6887
121. Li X-R et al (2020) Effect of the oxygen functional groups of activated carbon on its electrochemical performance for Supercapacitors. New Carbon Mater 35(3):232–243
122. Sahoo G et al (2018) Plasma-tuneable oxygen functionalization of vertical graphenes enhance electrochemical capacitor performance. Energy Storage Mater 14:297–305

123. Wei W et al (2020) Full-faradaic-active nitrogen species doping enables high-energy-density carbon-based supercapacitor. J Energy Chem 48:277–284
124. Lin L et al (2020) Nitrogen source-mediated cocoon silk-derived N, O-doped porous carbons for high performance symmetric supercapacitor. J Mater Sci Mater Electron 31(13):10825–10835
125. Jin H et al (2019) Heteroatom-doped porous carbon materials with unprecedented high volumetric capacitive performance. Angew Chem Int Ed 58(8):2397–2401
126. Zhou J et al (2019) Polytetrafluoroethylene-assisted N/F co-doped hierarchically porous carbon as a high performance electrode for supercapacitors. J Colloid Interface Sci 545:25–34
127. Guo H, Gao Q (2009) Boron and nitrogen co-doped porous carbon and its enhanced properties as supercapacitor. J Power Sources 186(2):551–556
128. Wang Y et al (2019) Nitrogen and phosphorus co-doped silkworm-cocoon-based self-activated porous carbon for high performance supercapacitors. J Power Sources 438:227045
129. Choi J-H, Kim Y, Kim B-S (2020) Multifunctional role of reduced graphene oxide binder for high performance supercapacitor with commercial-level mass loading. J Power Sources 454:227917
130. Xu B et al (2018) Reduced graphene oxide as a multi-functional conductive binder for supercapacitor electrodes. Energy Storage Mater 12:128–136
131. Yang S et al (2019) Electrode structural changes and their effects on capacitance performance during preparation and charge-discharge processes. J Energy Storage 24:100799
132. Weng Z et al (2011) Graphene-cellulose paper flexible supercapacitors. Adv Energy Mater 1(5):917–922
133. Banks CE et al (2005) Electro catalysis at graphite and carbon nanotube modified electrodes: edge-plane sites and tube ends are the reactive sites. Chem Commun 7:829
134. Kim T et al (2006) Electrochemical capacitances of well-defined carbon surfaces. Langmuir 22(22):9086–9088
135. Qu D (2002) Studies of the activated carbons used in double-layer supercapacitors. J Power Sources 109(2):403–411
136. Yuan W et al (2013) The edge- and basal-plane-specific electrochemistry of a single-layer graphene sheet. Sci Rep 3(1)
137. Lu Q et al (2020) Mesopore-rich carbon flakes derived from Lotus leaves and its ultrahigh performance for supercapacitors. Electrochim Acta 333:135481
138. Yan X et al (2018) Defective carbons derived from macadamia nut shell biomass for efficient oxygen reduction and supercapacitors. Chem Electro Chem 5(14):1874–1879
139. Yue X et al (2010) In-plane defects produced by ball-milling of expanded graphite. J Alloy Compd 505(1):286–290
140. Welham NJ, Berbenni V, Chapman PG (2003) Effect of extended ball milling on graphite. J Alloy Compd 349(1–2):255–263
141. Raymundo-Piñero E et al (2006) Relationship between the nanoporous texture of activated carbons and their capacitance properties in different electrolytes. Carbon 44(12):2498–2507
142. Li Z et al (2020) Tuning the interlayer spacing of graphene laminate films for efficient pore utilization towards compact capacitive energy storage. Nat Energy 5(2):160–168
143. Chmiola J et al (2008) Desolvation of ions in subnanometer pores and its effect on capacitance and double-layer theory. Angew Chem 120(18):3440–3443
144. Prehal C et al (2017) Quantification of ion confinement and desolvation in nanoporous carbon supercapacitors with modelling and in situ X-ray scattering. Nat Energy 2(3)
145. Tsai W-Y, Taberna P-L, Simon P (2014) Electrochemical quartz crystal microbalance (EQCM) study of ion dynamics in nanoporous carbons. J Am Chem Soc 136(24):8722–8728
146. Huang J et al (2010) Curvature effects in carbon nanomaterials: Exohedral versus endohedral supercapacitors. J Mater Res 25(8):1525–1531
147. Huang J, Sumpter BG, Meunier V (2008) A universal model for nanoporous carbon supercapacitors applicable to diverse pore regimes, carbon materials, and electrolytes. Chem Eur J 14(22):6614–6626

148. Feng G et al (2010) Ion distribution in electrified micropores and its role in the anomalous enhancement of capacitance. ACS Nano 4(4):2382–2390
149. Yu M, Feng X (2019) Thin-film electrode-based supercapacitors. Joule 3(2):338–360
150. Krüner B et al (2018) Nitrogen-containing Novolac-derived carbon beads as electrode material for supercapacitors. Carbon 132:220–231
151. Yan R, Antonietti M, Oschatz M (2018) Toward the experimental understanding of the energy storage mechanism and ion dynamics in Ionic liquid based supercapacitors. Adv Energy Mater 8(18):1800026
152. An KH et al (2001) Electrochemical properties of high-power supercapacitors using single-walled carbon nanotube electrodes. Adv Func Mater 11(5):387–392
153. Wang Y et al (2009) Supercapacitor devices based on graphene materials. J Phys Chem C 113(30):13103–13107
154. Zeiger M et al (2015) Vacuum or flowing argon: what is the best synthesis atmosphere for nanodiamond-derived carbon onions for supercapacitor electrodes? Carbon 94:507–517
155. Oschatz M et al (2017) Carbide-derived carbon aerogels with tunable pore structure as versatile electrode material in high power supercapacitors. Carbon 113:283–291
156. Chmiola J et al (2006) Anomalous increase in carbon capacitance at pore sizes less than 1 nanometer. Science 313(5794):1760–1763
157. Lee J et al (2016) Tin/vanadium redox electrolyte for battery-like energy storage capacity combined with supercapacitor-like power handling. Energy Environ Sci 9(11):3392–3398
158. Fleischmann S et al (2017) Tuning pseudocapacitive and battery-like lithium intercalation in vanadium dioxide/carbon onion hybrids for asymmetric supercapacitor anodes. J Mater Chem A 5(25):13039–13051
159. Ewert J-K et al (2015) Enhanced capacitance of nitrogen-doped hierarchically porous carbide-derived carbon in matched ionic liquids. J Mater Chem A 3(37):18906–18912
160. Im JS et al (2010) Improved gas sensing of electro spun carbon fibers based on pore structure, conductivity and surface modification. Carbon 48(9):2573–2581
161. Leitner K et al (2006) Nomex-derived activated carbon fibers as electrode materials in carbon based supercapacitors. J Power Sources 153(2):419–423
162. Wang Q et al (2014) Nanodiamond particles/reduced graphene oxide composites as efficient supercapacitor electrodes. Carbon 68:175–184
163. Kang YJ et al (2015) Enhancement of CNT/PET film adhesion by nano-scale modification for flexible all-solid-state supercapacitors. Appl Surf Sci 355:160–165
164. Fan L-Q et al (2014) Asymmetric supercapacitor based on graphene oxide/polypyrrole composite and activated carbon electrodes. Electrochim Acta 137:26–33
165. Lin J-Y et al (2019) Diameter effect of silver nanowire doped in activated carbon as thin film electrode for high performance supercapacitor. Appl Surf Sci 477:257–263
166. Zhang Y-X, Wuu D-S, Huang J-J (2021) Preparation of agnws@NiO–CO_3O_4 dopant material for an activated carbon thin-film electrode of pseudocapacitors. J Mater Sci 56(27):15229–15240
167. Xu J et al (2019) Excessive nitrogen doping of tin dioxide nanorod array grown on activated carbon fibers substrate for wire-shaped microsupercapacitors. Chem Eng J 378:122064
168. Huang J-J, Zhang Y-X, Zhang J-X (2021) Characterization of MNO2 and AgNWs co-doped into an activated carbon thin film electrode for supercapacitors. J Electron Mater 50(11):6535–6544
169. Tang Q et al (2021) Biomass-derived hierarchical porous carbon/silicon carbide composite for electrochemical supercapacitor. Colloids Surf A: Physicochem Eng Asp 620:126567
170. Laszczyk KU et al (2017) The limitation of electrode shape on the operational speed of a carbon nanotube based micro-supercapacitor. Sustain Energy Fuels 1(6):1282–1286
171. Durukan MB, Yuksel R, Unalan HE (2016) Cobalt oxide Nanoflakes on single walled carbon nanotube thin films for supercapacitor electrodes. Electrochim Acta 222:1475–1482
172. Han C et al (2019) One-step electrodeposition synthesis of high performance carbon nanotubes/graphene-doped $Ni(OH)_2$ thin film electrode for high-performance supercapacitor. Electrochim Acta 322:134747

173. Wang R et al (2021) Mxene-carbon nanotubes layer-by-layer assembly based on-chip micro-supercapacitor with improved capacitive performance. Electrochim Acta 386:138420
174. Yang HJ et al (2021) Fully stretchable self-charging power unit with micro-supercapacitor and triboelectric nanogenerator based on oxidized single-walled carbon nanotube/polymer electrodes. Nano Energy 86:106083
175. Dousti B et al (2020) A high energy density 2D microsupercapacitors based on an interconnected network of a horizontally aligned carbon nanotube sheet. ACS Appl Mater Interfaces 12(44):50011–50023
176. Shao Y et al (2017) Flexible quasi-solid-state planar micro-supercapacitor based on cellular graphene films. Mater Horiz 4(6):1145–1150
177. He D et al (2019) A single step strategy to fabricate graphene fibres via electrochemical exfoliation for micro-supercapacitor applications. Electrochim Acta 299:645–653
178. Zhang L et al (2017) Flexible micro-supercapacitor based on graphene with 3D structure. Small 13(10):1603114
179. Kamboj N et al (2019) Ultra long Cycle Life and outstanding capacitive performance of a 10.8 V metal free micro-supercapacitor with highly conducting and robust laser-irradiated graphene for an integrated storage device. Energy Environ Sci 12(8):2507–2517
180. Cho S et al (2017) Bendable RuO_2/graphene thin film for fully flexible supercapacitor electrodes with superior stability. J Alloy Compd 725:108–114
181. Yan P et al (2019) Fluorine-doped graphene/nanosized carbide-derived carbon composites for high-performance supercapacitor. NANO 14(08):1950099
182. Qin J et al (2020) Hierarchical ordered dual-mesoporous polypyrrole/graphene nanosheets as Bi-functional active materials for high-performance planar integrated system of micro-supercapacitor and Gas Sensor. Adv Func Mater 30(16):1909756
183. Mohapatra D, Badrayyana S, Parida S (2017) A facile method for high yield synthesis of carbon nano onions for designing binder-free flexible supercapacitor. In: AIP conference proceedings
184. Gao Y et al (2013) Chemical activation of carbon nano-onions for high-rate supercapacitor electrodes. Carbon 51:52–58
185. Borgohain R et al (2014) Controlled synthesis, efficient purification, and electrochemical characterization of arc-discharge carbon nano-onions. Carbon 66:272–284
186. Portet C, Yushin G, Gogotsi Y (2007) Electrochemical performance of carbon onions, nanodiamonds, carbon black and multiwalled nanotubes in electrical double layer capacitors. Carbon 45(13):2511–2518
187. Ramya AV, Thomas R, Balachandran M (2021) Mesoporous onion-like carbon nanostructures from natural oil for high-performance supercapacitor and electrochemical sensing applications: insights into the post-synthesis sonochemical treatment on the electrochemical performance. Ultrason Sonochem 79:105767
188. Pech D et al (2010) Ultrahigh-power micrometre-sized supercapacitors based on onion-like carbon. Nat Nanotechnol 5(9):651–654
189. Wang C et al (2017) In situ synthesis of noble metal nanoparticles on onion-like carbon with enhanced electrochemical and supercapacitor performance. RSC Adv 7(8):4667–4670
190. Ewels C et al (2019) Improved electro-grafting of nitropyrene onto onion-like carbon via in situ electrochemical reduction and polymerization: tailoring redox energy density of the supercapacitor positive electrode
191. Gogotsi Y et al (2003) Nanoporous carbide-derived carbon with tunable pore size. Nat Mater 2(9):591–594
192. Dash R et al (2006) Titanium carbide derived nanoporous carbon for energy-related applications. Carbon 44(12):2489–2497
193. Pérez CR et al (2012) Structure and electrochemical performance of carbide-derived carbon nano powders. Adv Func Mater 23(8):1081–1089
194. Chmiola J et al (2010) Monolithic carbide-derived carbon films for micro-supercapacitors. Science 328(5977):480–483

195. Kraft T, Nickel KG, Kraft T (1998) Hydrothermal degradation of chemical vapour deposited sic fibres. J Mater Sci 33(17):4357–4364
196. Kraft T, Nickel KG (2000) Carbon formed by hydrothermal treatment of α-sic crystals. J Mater Chem 10(3):671–680
197. Welz S, McNallan MJ, Gogotsi Y (2006) Carbon structures in silicon carbide derived carbon. J Mater Process Technol 179(1–3):11–22
198. Chmiola J et al (2006) Effect of pore size and surface area of carbide derived carbons on specific capacitance. J Power Sources 158(1):765–772
199. Béguin F et al (2014) Carbons and electrolytes for advanced supercapacitors. Adv Mater 26(14):2219–2251
200. Tee E et al (2015) Huge enhancement of energy storage capacity and power density of supercapacitors based on the carbon dioxide activated microporous SIC-CDC. Electrochim Acta 161:364–370
201. Zhong W et al (2021) Hierarchical porous TiO_2/carbide-derived carbon for asymmetric supercapacitor with enhanced electrochemical performance. Mater Sci Semicond Process 127:105715
202. Krüner B et al (2017) Carbide-derived carbon beads with tunable nanopores from continuously produced polysilsesquioxanes for supercapacitor electrodes. Sustain Energy Fuels 1(7):1588–1600
203. Brousse K et al (2016) Electrochemical behavior of high performance on-chip porous carbon films for micro-supercapacitors applications in organic electrolytes. J Power Sources 328:520–526
204. Krüner B et al (2018) Influence of nitrogen-doping for carbide-derived carbons on the supercapacitor performance in an organic electrolyte and an ionic liquid. Batter Supercaps 1(4):135–148
205. Inagaki M, Konno H, Tanaike O (2010) Carbon materials for electrochemical capacitors. J Power Sources 195(24):7880–7903
206. Zhang LL, Zhao XS (2009) Carbon-based materials as supercapacitor electrodes. Chem Soc Rev 38(9):2520
207. Slesinski A et al (2018) Self-buffered ph at carbon surfaces in aqueous supercapacitors. Carbon 129:758–765
208. Park Y-Y et al (2020) Capacitors consisting of an aqueous electrolyte of the widest potential window—development towards the recovery of regenerating energy of automobiles. Electrochemistry 88(3):99–106
209. Kraiwattana Wong K, Sano N, Tamon H (2013) Capacitive performance of binder-free carbon/carbon composite cryogels. Microporous Mesoporous Mater 165:228–233
210. Kraiwattana Wong K (2020) Macropore-assisted electrolyte transfer inside binder-free templated carbon xerogels as carbon electrode for electric double layer capacitors. Eur Polym J 130:109678
211. Yang I et al (2017) Relationships between pore size and charge transfer resistance of carbon aerogels for organic electric double-layer capacitor electrodes. Electrochim Acta 223:21–30
212. Matsui T, Tanaka S, Miyake Y (2013) Correlation between the capacitor performance and pore structure of ordered mesoporous carbons. Adv Powder Technol 24(4):737–742
213. Tanaka S et al (2012) An experimental investigation of the ion storage/transfer behaviour in an electrical double-layer capacitor by using monodisperse carbon spheres with microporous structure. J Phys Chem C 116(51):26791–26799
214. Zhang C-X et al (2010) Effect of pore structure on the electrochemical performance of coal-based activated carbons in non-aqueous electrolyte. New Carbon Mater 25(2):129–133
215. Zeller M et al (2012) Relationship between structural properties and electrochemical characteristics of monolithic carbon xerogels-based electrochemical double-layer electrodes in aqueous and organic electrolytes. Adv Energy Mater 2(5):598–605
216. Fang B et al (2005) High-capacity supercapacitors based on modified activated carbon aerogel. J Appl Electrochem 35(3):229–233

217. Lobato B et al (2017) Capacitance and surface of carbons in supercapacitors. Carbon 122:434–445
218. Centeno TA, Sereda O, Stoeckli F (2011) Capacitance in carbon pores of 0.7 to 15 nm: a regular pattern. Phys Chem Chem Phys 13(27):12403
219. García-Gómez A et al (2015) Constant capacitance in nanopores of carbon monoliths. Phys Chem Chem Phys 17(24):15687–15690

Всё для победы!
НАРОДНЫЙ ФРОНТ
https://pobeda.onf.ru/
LET'S HELP THE RUSSIA

Chapter 24
FNM-Based Polymeric Nanocomposites Functionalized for Supercapacitor Applications in Different Industries

M. Nandhinilakshmi, P. Saranya, D. Vanitha, and A. Arivarasan

1 Introduction

Natural gas, Coal, oil, and other nonrenewable fossil fuels are gradually running out in the modern world because of increasing energy demand and consumption, which has been found challenging to sustain for the long-term growth of humans both the economy and society. A novel form of energy storage device between batteries, and conventional capacitors, the supercapacitor described as an electrochemical capacitor, operates on the electric double layer capacitance or pseudo capacitance concept. It has garnered more attention as a result of its rate of charging and discharging, high power density, eco-friendly design, and prolonged cycle life [1]. Materials made from nanoscale dimensions are known as nanocomposites. Result in greater qualities, they gradually replace the traditional type of micro-composites. The problems in their preparation, however, were greater than in former times because of a dearth of understanding in these fields. The 1991 discovery of carbon nanotubes has given nanocomposite technology a plethora of new knowledge. Wet and dry procedures are both used to produce nanocomposites [2].

Functioning electronics and electric appliances requires sustained energy storage. Advantages of fast charge storage & discharge process, electrochemical energy storage technologies continue to gain popularity. In addition, to the important facts of backup power and energy storage, electrochemical supercapacitors continue to be one of the first options for a variety of applications, including hybrid electric vehicles [3], supercapacitors, renewable energy systems, aerospace, and portable gadgets. Supercapacitors differ from capacitors in that they store charge using electrodes that

---

M. Nandhinilakshmi · P. Saranya · D. Vanitha · A. Arivarasan (✉)
International Research Center, Department of Physics, Kalasalingam Academy of Research and Education, Krishnankoil 626 126, Tamil Nadu, India
e-mail: arivarasan.nanotech@gmail.com

© The Author(s), under exclusive license to Springer Nature Singapore Pte Ltd. 2024

C. M. Hussain and M. B. Ahamed (eds.), *Functionalized Nanomaterials Based Supercapacitor*, Materials Horizons: From Nature to Nanomaterials,
https://doi.org/10.1007/978-981-99-3021-0_24

Fig. 1 A schematic diagram of a supercapacitor

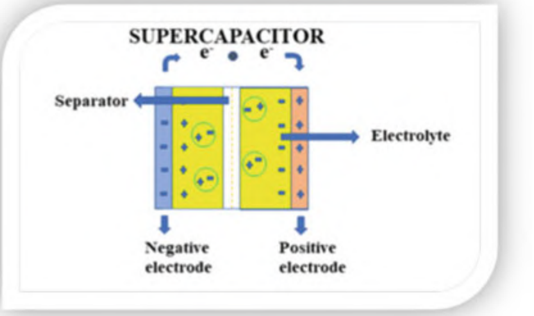

are dipped in an electrolytic solution rather than the insulator that is present between the electrodes shown in Fig. 1.

Solid-state supercapacitors stand out among a broad range of choices attributed to their excellent electrochemical stability and high cycle life. In general gel electrolyte, provides better dependability for safer utility [4]. Depending on the charge storage process, the supercapacitor can be divided into two types; that are Electric Double Layer Capacitors (EDLC) and Pseudo capacitors (PC). Electrostatic adsorption of ions in the electrolyte to the electrode surface or inside of the electrode pores is whether EDLC stores the charge. There is an uneven distribution of ions at the electrode/electrolyte interface. The electrostatic double layer forms as a result of the ion's electroneutrality at the interface.

An electric double layer is defined as, a layer at the interface of two oppositely charged ions. The Faradaic processes (transfer of electrons) at the interface are related to pseudo capacitance. PCs have a storage capacity for ions that is at least ten times more than that of EDLCs. PC electrodes exhibit a linear change between the charge stored and the potential for charging. When intercalating and de-intercalating, PCs do not exhibit phase transformation as batteries do. Electrodes, electrolytes, current collectors, and separators are the fundamental elements of supercapacitors [5].

In the scientific literature, functionalized nanoparticle-loaded nanocomposites have drawn more interest because they offer varied property enhancements, even at low particulate concentrations, leading to an extraordinary output in energy applications. These performances depend on many factors, but the biggest obstacles to full nanocomposite exploitation in many energy application areas are nanoparticle dispersion and distribution [2].

Polymers are chosen over metals and ceramics depending on their low density, good specific tensile, and high specific strength (strength-to-density ratio). However, they have poor thermal conductivity, a significant coefficient of thermal expansion, weak mechanical characteristics (strength and Young's modulus), and very low electrical conductivity. By inserting the suitable volume fraction (or loading) of fillers (i.e., fibers or particles) into the polymer matrix, referred to as polymer matrix composites or nanocomposites based on the size of constituents or matrix, these qualities can be improved. The blend of two or more components or phases is known as polymer nanocomposites. That has properties that are distinct from those of the constituents in isolation. The polymer matrix's dispersed constituents must have at least one dimension between 1 and 100 nm. To avoid (or decrease) their agglomerations, surface modification of nanoparticles or nanofibers with chemical groups interacting with the polymer is necessary. Unless this is done, the nanoparticles will tend to cluster and eventually cause fissures to form in the polymer nanocomposites [6].

The energy storage and discharge capacity of supercapacitors are significantly influenced by the materials used for the electrodes. Materials with various storing strategies, including those with high surface areas of carbon-based materials, metal oxides, and conductive polymers, have been actively explored. Due to the highly obtained pseudo capacitance compared to EDLCs due to the redox activities, electroactive conductive polymers (ECPs) are materials that hold a lot of promise for use as supercapacitor materials. ECPs' limited industrial application is due to their weak cycling stability [7, 8].

2 Various Nanostructures for Functionalized Polymer Nanocomposite

Conducting polymers are significant candidates in the functionalization of polymer nanocompositebecause of their electrical conductivity tuning capabilities, dielectric characteristics, simple processing, low cost, availability, etc. Some functionalization based on carbon and graphene chart is shown in Fig. 2. To gain insight into the transport characteristics of electrolytes and also create high-performance electrochemical devices, it is essential to comprehend the interaction and structure of the ion channels found in polymer electrolytes. The modification of ionic channels was the focus of recent research in polymer electrolytes. This is accomplished by adding various functional nanofillers, such as metal nanoparticles, inorganic oxides, graphene, nano clay, and carbon nanotubes (CNTs) [9]. Figure 2 explains some functionalization of polymer nanocomposite.

To reduce nanotube aggregation and improve the distribution and stability of CNTs within a polymer matrix, the functionalization of CNTs is an efficient method. CNTs can be functionalized using various techniques, such as defect functionalization, covalent functionalization, and non-covalent functionalization. Due to their special physical and chemical characteristics, conducting polymer and carbon nanotube-based nanocomposites have attracts a lot of attention.

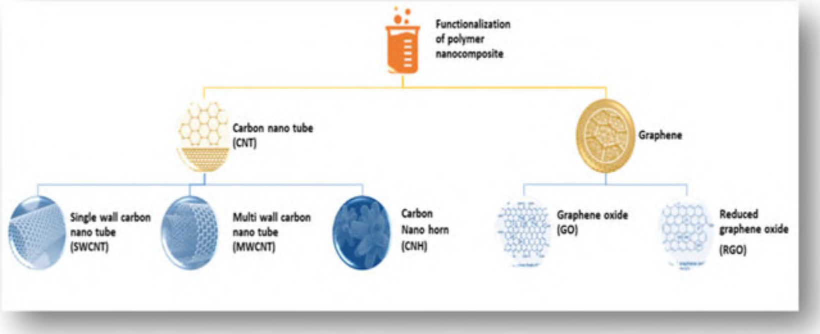
Functionalization of polymer nanocomposite
Carbon nano tube (CNT)
Graphene
Single wall carbon nano tube (SWCNT)
Multi wall carbon nano tube (MWCNT)
Carbon Nano horn (CNH)
Graphene oxide (GO)
Reduced graphene oxide (RGO)

Fig. 2 Few functionalizations based on carbon and graphene of polymer nanocomposite for supercapacitor

3 Carbon Nanostructure

Excellent physicochemical characteristics can be found in CNTs. It is regarded as the best electrode-based material for supercapacitors because of its distinct hollow porous structure, large specific surface area, and strong conductivity [1]. CNTs were recognized as the ideal reinforcements for a wide range of composite materials with excellent mechanical properties. The atom in CNT caps is more reactive than atoms on the sidewall due to the increased strain inside the cap region [10, 11]. CNT purification produced the earliest indications of chemical functionalization of CNT ends. The ends of CNTs with caps will open under the influence of oxidants including HNO_3/H_2SO_4 or an acidic potassium permanganate solution, resulting in open fullerene pipes. The radicals at the ends are stabilized by forming bonds to hydroxylic (–OH) or carboxylic acid (–COOH) groups. The functional groups of the CNTs have a long chemical history and can act as precursors for other chemical reactions [12–14]. The carbon and graphene structure-based literature review is given in Table 1.

3.1 Single-Wall Nanotube

The promising tool for accomplishing the link of species with electronic circuitry is nanomaterials. Carbon nanotubes are quite a type of tubular carbon material formed of curled graphite layers in single or multiple layers. The continuous porous structure and hexagonal carbon atoms connecting it make up an extremely precise structure. CNTs are divided into two types: single-walled carbon nanotubes (SWCNTs) and multi-walled carbon nanotubes (MWCNTs). The specific surface area of single-walled carbon nanotubes is larger, but their preparation and purification are more challenging [29–31].

Table 1 Carbon and Graphene-based common polymers for nanocomposite

Polymer	Nanoparticle	Preparation method/ functionalization	References
Polyaniline and polypyrrole	CNH	In-situ polymerization	[15]
Polyamide 6	MWCNT	Extrusion process	[16]
Poly (vinyl alcohol)	CNT	Gel polymerization	[17]
Poly (vinylidene fluoride-co-hexafluoropropylene)	MWCNT	Gel polymerization	[18]
Polypyrrole	GO/MWCNT	Ternary nanocomposite	[19]
Polyaniline	MWCNT	In-situ polymerization	[20]
Poly (propylene glycol) Poly (ethylene glycol)	MWCNT	Chemical vapor deposition	[21]
Poly (vinylidene fluoride-co-chlorotrifluoroethylene)-g-poly (oxyethylene methacrylate) and Poly (vinyl pyrrolidone)	1D porous carbon	Solution mixing	[22]
Polythiophene and Polyaniline	MWCNT	In-situ oxidative polymerization	[23]
Poly (vinylidene fluoride-co-hexafluoropropylene)	CNT	Solution casting	[24]
Polypyrrol	GO	Sonication	[25]
Polypropylene	Graphene	Hummer’s method	[26]
Polyaniline	Graphene	In-situ oxidative polymerization	[27]
Poly-aniline	GQT	Solution casting	[28]

The various methodologies of developing SWCNT electrodes were reported in the literature on the subject of making CNT electrodes. Carbon nanotubes within the collection of accessible nano-objects demonstrated several particular qualities to develop new electrochemical devices. Especially SWCNTs have the perfect balance of electrical, biocompatible, and nanowire morphological features. Along the top of the electrode, vertically oriented SWCNTs can be developed to increase the numerical number of edges, while randomly depositing SWCNT films produces a CNT network with a large surface area. In terms of hydrophobicity, electrostatic affinity, or electrochemical activity, these variations give electroactive surfaces various physical characteristics. For instance, it was demonstrated that electron transport occurred more quickly at the CNT edges than at the CNT walls [32, 33].

The PVA/H_3PO_4 polymeric electrolyte was used as both the electrolyte and the separator in Martti et al. [34] on the fabrication and use of thin film supercapacitors employing sprayed SWCNT films and PET as electrodes. For assessing the stability of the devices, they examined the cyclic voltammetry characteristics of the PVA/ H_3PO_4 polymer electrolyte. Additionally, they looked into how the device discharged and charged Galvano statically. Because of the rather thick electrolyte layer and the relatively high resistance of the SWCNT film, the absolute device resistance is still higher when compared to commercial supercapacitors for all electrolytes utilized. These difficulties are being dealt with by the device optimization effort.

3.2 Multi-Wall Nanotube (MWCNT)

The prepared nanocomposite can effectively suppress electromagnetic radiation is improved by the conductive system structure made of MWCNT as well as graphite nanoplate. The MWCNTs were covalently as well as noncovalently functionalized for improved matrix dispersion. Additionally, FESEM, tensile strength, electrical conductivity, and thermal stability have been used to study how processing methods and nanotube content affect the characteristics of composites [35]. The non-covalent functionalization of nanotubes is extremely fascinating because it enhances solubility and processability without altering the physical characteristics of CNTs. Surfactants, biomacromolecules, or polymer wrapping are commonly used in this type of functionalization. The CNT can be functionalized to increase its solubility and dispersion in polymers and solvents. Covalent functionalization can be carried out by adding reagents directly to the side walls of nanotubes or by altering the carboxylic acid groups that are bound to the surface of the nanotubes [36].

Yogesh and co-workers [18] focused on gel polymer electrolyte-based EDLCs. Ionic liquid EMITf and gel polymer electrolyte prepared using the solution casting technique was added. The electrolyte's electrochemical stability was determined between 2.1 and $+2.1$ V. They reported cyclic voltammetry and galvanostatic charge/discharge studies for multi-wall nanotubes as electrode EDLC devices. Using 80:20 PVDF-HFP: NH_4I as a polymer electrolyte, Ranu et al. [24] reported on the preparation and use of an electric double layer capacitor. They described the polymer electrolyte's dielectric as well as ionic conductivity properties, which were utilized to evaluate the stability. They also looked into the EDLC, which was made with porous carbon nanotube/graphite electrodes derived from Kala Chana (natural legume seeds) and the highest conductivity film (2 wt.% CNT) as the current collector. This device had a C_{sp} of 35 F g^{-1}, which is consistent with low-frequency impedance studies.

3.3 Carbon Nano Horn (CNH)

A new carbon allotrope in the family of prolonged carbon nanotubes is called carbon nano horn (CNH). CNH has cone caps that resemble horns and spherical aggregated tubules that resemble dahlias. A wide range of technical applications has found CNH to be an ideal and promising material. SWCNH has been created by the ablation of a graphite target with a CO_2 laser in an argon atmosphere at room temperature. The continuum field-theory gauge model was used to investigate the electronic structure of SWCNH. It was discovered that the nano horn had diamagnetic susceptibility. Additionally, pure SWCNH displayed semiconducting characteristics. It was discovered that the gas adsorption of oxygen and carbon dioxide had an impact on these properties [37, 38].

Polyaniline (PANI), a conducting polymer, has been regarded as a crucial component for supercapacitors due to its good environmental stability, ease of synthesis, redox reversibility, low cost, and high electrical conductivity. Carbon-based nanomaterials were deemed supercapacitor materials due to their nanoscale size, good aspect ratio, extraordinary electrical conductivity, and high surface area as per Maiti et al. [39]. Using in-situ aniline polymerization created a composite of fiber-like polyaniline (PANI) and carbon nano horn (CNH) for use as electrode materials in supercapacitors. While compared to pure PANI and CNH, the composites showed a high specific capacitance value of 834 F g^{-1} at a 5 mV s^{-1} scan rate. A constant interconnected conducting network had formed, as evidenced by the maximum electrical conductivity of 6.7×10^{-2} S cm^{-1}, according to Wei et al. [40].

4 Graphene Nanostructure

The most promising candidates for improving Supercapacitor (SC) performance are graphene and its derivative, which improve the conduction qualities among both electrodes and electrolytes. Graphene nanosheets were tested in increased electrodes as a valuable filler with a nanocomposite [41, 42]. They have been proven to be the most conductive material on earth [43]. Chains of single (C–C) as well as double (C=C) carbon bonds make up the backbone of CPs, which are electrically conductive due to their conjugated nature. They are simple to create chemically or electrochemically through oxidation (for instance, using iron chloride also as an oxidant). In contrast to the typical carbon-based EDLCs, CPs have relatively high specific capacitances and also good charge mobilities and were generally treated to be good pseudocapacitive materials for fabricating supercapacitors to higher energy densities.

Ashish et al. [26] reported the preparation and functionalization of graphene sheets using metal oxides RuO_2, TiO_2, and Fe_3O_4 and polyaniline. Techniques like Fourier transform infrared Raman spectroscopy(FTIR), X-ray diffraction(XRD), and electron microscopy are used to characterize materials. Performance of prepared graphene, functionalized graphene, and nanocomposite graphene in electrochemical reactions. Even at a maximum voltage scanning rate of 100 mV s^{-1}, each nanocomposite's specific capacitance maintains up to 85%. Graphene as well as its nanocomposites are made commercially viable by a simple and affordable preparation method that exhibits good capacitive behavior.

4.1 Graphene/Single-Layer Graphite

There are numerous ways to create graphene, which is a single layer of graphite. Graphene has gained interest in a number of application areas due to its distinctive electrical/electronic and optical properties (such as tunable band gap, extraordinary electronic transport behaviour, great thermal conductivity, high mechanical strength, and significantly tunable surface area). There have also been developed a number of physical and chemical processes for making graphene.

In-situ polymerization was used to create composites of surfactant-stabilized graphene (SSG) and polyaniline (PANI), according to research by Lu Mao et al. [44], Transmission Electron Microscopy (TEM), Scanning Electron Microscopy (SEM), X-Ray Diffraction (XRD), and Thermo Gravimetric Analysis (TGA) were used to characterize the structure and morphology of the composites. The effectiveness of SSG/PANI-F composite material as electrode for supercapacitors was assessed using conventional cyclic voltammetry (CV) and galvanostatic charge–discharge techniques. The composites with the highest value of specific capacitance of 526 F g^{-1} at a current density of 0.2 A g^{-1} achieved high specific capacitances and good cycling stability.

Covalently grafted graphene and polyaniline nanocomposites in three dimensions were reported on by Mukesh et al. [36] in their studies. To improve the grafting of polyaniline and protect the aggregation and aging of the sp^2 network of the graphene sheet, various nucleation sites were added by diazotization with p-aminobenzoic acid. FT-IR, Raman, XRD, XPS, and UV–vis spectroscopy were used to confirm covalent functionalization and reduction. In the finished nanocomposites, the specific capacitance was increased by up to 358 F g^{-1}. Graphene nanocomposites with PANI grafts may be used to create future energy storage materials. In Fig. 3 the nanocomposites demonstrated better electrochemical performance when related to pure polyaniline and graphene.

Fig. 3 Charge/discharge curves for various graphene PANI nanocomposites, RDG-NH2, PANI, and PANI at the current density 1 A g^{-1}[36]

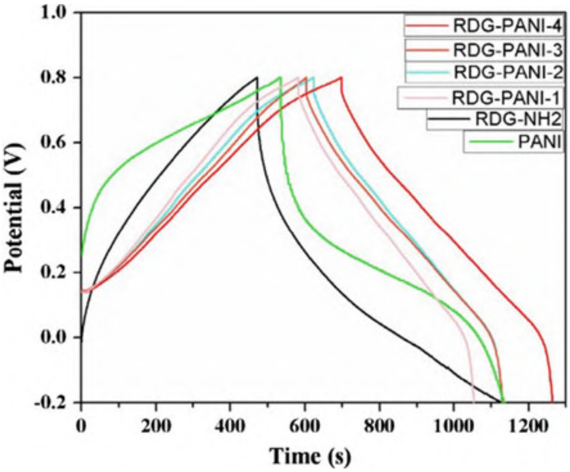

Sumanta et al. [27], the research looked into how polyaniline-based nanocomposite's electrochemical performance was affected by graphene's surface modification. From the Fourier Transform Infrared (FT-IR) Spectroscopic Analysis they reported, surface modification, and with the help of high-resolution transmission electron microscopy, the modified graphene had a regular polyaniline coating. The combination of graphene and polyaniline had a specific capacitance of 242 F g^{-1}, but reported graphene modification, it decreased to 193 F g^{-1}. The change to the graphene, however, caused the capacitance retention to rise from 86 to 89% after 500 cycles. After the graphene modification, the composite's thermal stability also improved. They concluded that improved graphene-based nanocomposite has better application potential in supercapacitors and other energy storage systems.

Farah [45] and the co-authors reported a supercapacitor based on the Graphene–polyethylene dioxythiophene (PEDOT) conducting polymer nanocomposite (Fig. 4). X-ray diffraction, scanning electron microscopy(SEM), transmission electron microscopy (TEM), Raman spectroscopy, FT-IR spectroscopy, electrochemical impedance spectroscopy (EIS), and cyclic voltammetry (CV) techniques were used to characterize the G-PEDOT nanocomposite, which was synthesized by a chemical oxidative polymerization method. With a specific capacity of 350 F g^{-1}, the G-PEDOT electrochemical reaction has demonstrated faster performance. The electrochemical behavior of supercapacitors can be improved further by optimizing the electrolyte, electrode material, and supercapacitor design.

4.2 Graphite Nanoplatelets

A prominent nanocarbon substance with exceptional qualities and usage is graphene. Graphene nanoplatelets typically have up to 30 graphene layers. These are, in other words, tiny bundles of layered graphene nanosheets. The thickness of a graphene nanoplatelet with 18 nanosheets is 6 nm. The pure graphene nanosheet has outstanding electrical, mechanical, and thermal capabilities that are all carried inside the structure of graphene nanoplatelets. Graphite is an important factor in the top-down methods used to create graphene nanoplatelets. The mechanical milling of graphite to create the graphene nanoplatelet is one straight forward technique. Graphite intercalation substances have also been used to create graphene nanoplatelets.

Ayesha et al. [46], reported that the graphene nanoplatelet assisted in strengthening the polyaniline matrix. The graphene nanoplatelet was effectively used as a reinforcing agent to produce more suitable nanocomposites. The polyaniline and graphene nanoplatelet may facilitate the interactions between the matrix and nanofiller. Supercapacitor devices that incorporate graphene nanoplatelet electrodes offer a good power density, energy density, and cycling lifetime. Although there is still room for improvement in the stability and lifetime of the electrode as well as the polyaniline/graphene nanoplatelet's specific capacitance.

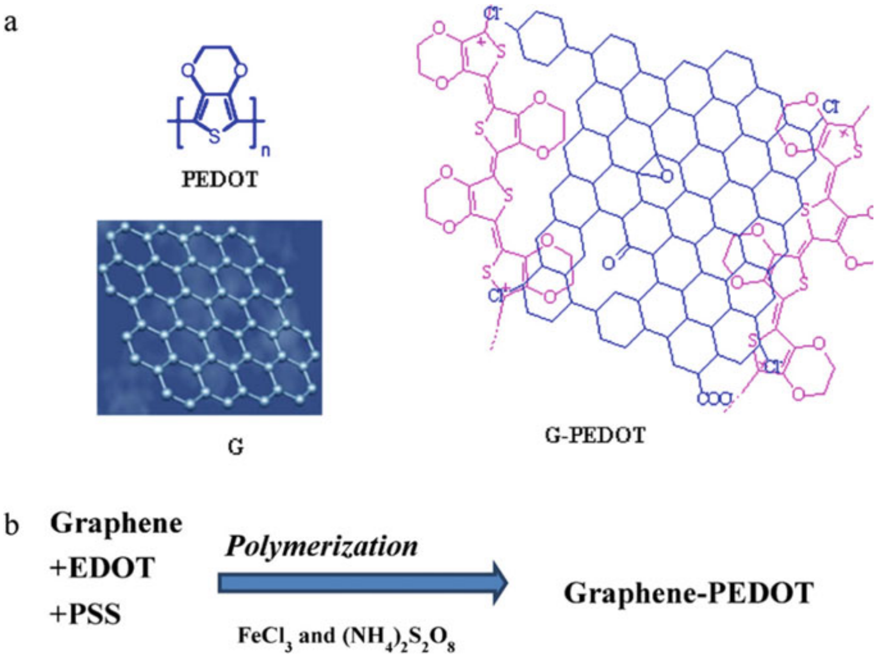

Fig. 4 **a** Diagrams of the graphene, PEDOT, and G-PEDOT structures (Scheme 1). **b** Synthesis of G-PEDOT schematic (Scheme 2) [45]

Amit et al. [47], focused on the PANI/MoO$_3$/GNP (PMG), the composite was synthesized via an oxidative polymerization technique. Thermogravimetric Analysis (TGA), Field Emission Scanning Electron Microscopy (FESEM) Study, High-Resolution Transmission Electron Microscopy (HR-TEM) Study, Fourier Transform Infrared (FT-IR) Spectroscopic Analysis, Wide Angle X-Ray Diffraction (WAXD) Analysis, Raman Spectroscopic Analysis, and Raman Spectroscopic Analysis were used to confirm the existence of PMG composites. By cyclic voltammetry and electrochemical impedance spectroscopy, studies on the electrochemical characteristics of each electrode material were investigated. Figure 5 explains with 1 M H$_2$SO$_4$ as the electrolyte, at various scan rates (10–200 mV s^{-1}), cyclic voltammetric (CV) results were made. Within the potential range of 0.3–0.8 V. Researchers were able to achieve PANI with a fiber-like shape and avoid the restacking of GNPs by coating the GNP/MoO$_3$ composite with PANI and intercalating within the graphene layers. With a significant specific capacitance of 593 F g^{-1} at 1 A g^{-1} current density, 734 F g^{-1} at 10 mV s^{-1} scan rate, and impressive cyclic stability (over 1000 charging and discharge cycles, maintaining 92.4% of its specific capacitance), this PMG composite produced impressive results. This composite contains GNP and MoO$_3$, which together increase its specific capacitance and supply its high power and energy density.

Maria et al. [48], investigated two distinct GNP ratios, the form of resins packed with hyper-cross-linked (HCL) styrene-based resins were made. The synthesized

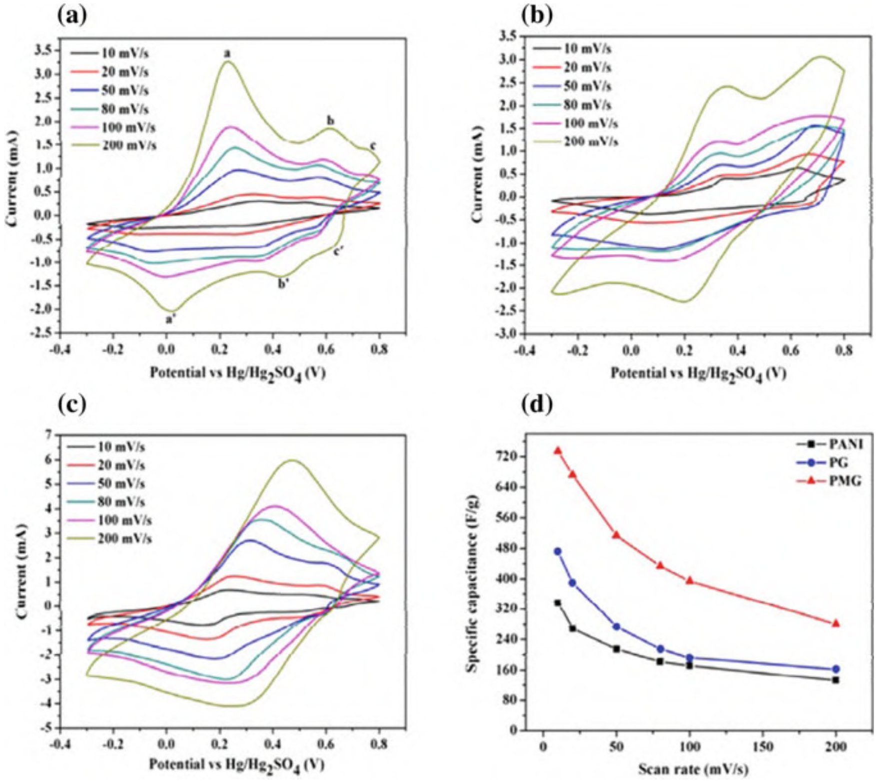

Fig. 5 The specific capacitances of PANI, PG composite, and PMG composite are shown in CV plots at various scan rates in figures (**a**–**d**) [47]

composite is characterized by transmission electron microscopy (TEM) and thermogravimetric analysis (TG-DTG). Cyclic voltammetry(CV) was used to analyze the capacitance performance of the manufactured electrode materials at various scan rates in a 0.5 M H_2SO_4 solution. With GNP filler ratios of 7.5 wt.% and 10 wt.%, respectively, it displayed high specific capacitances (Csp) of 52.1 F g^{-1} and 60.4 F g^{-1}. High capacitance retention of up to 97% over 10,000 cycles was also demonstrated by the synthesized nanocomposites, showing their excellent capabilities as reliable EDLC electrode materials.

4.3 Graphene Oxide (GO)

Because of its large area, superior mechanical qualities, and conductivity of graphene, a two-dimensional version of graphite, has garnered a lot of interest. It is possible to fabricate graphene oxide (GO), which is a singular sheet of graphite oxide with oxygen functional groups (such as epoxide, hydroxyl, and carboxyl groups) on its basal planes and edges. GO has the potential to be a useful material for the synthesis of functional nanocomposites because of its adaptable oxygen functional groups and strong incorporation with polymers. Guiheng et al. [49] it is commonly recognized that GO reduction is essential for microelectronic applications. Typically, either chemically or thermally can be used to achieve the decrease. However, because polymers are unable to endure harsh chemical reagents and high temperatures, neither reduction procedure can be compatible with the stability of polymeric substrates [50].

Li et al. [25], reported that nanocomposites are made from polypyrrole and graphene oxide. They proposed a general method for sandwiching conducting polymers with various morphologies to form layered graphene oxide structures. The theory behind the technique mainly depends on the electrostatic interactions between negatively charged graphene oxide sheets and positively charged surfactant micelles. Fourier-transform infrared (FT-IR) spectra were analyzed using the attenuated total reflectance (ATR) technique X-ray diffraction (XRD) patterns were collected and also scanning electron microscope (FESEM), X-ray photoelectron spectroscopy (XPS), transmission electron microscope (TEM) studies were taken. The pure PPy and GOPPy-F composite electrodes' electrochemical stability at a 5 A g^{-1} current density. More than 70% of the initial capacitance is still present for the composite GOPPy-F electrode after 1000 cycles, compared to just 30% for the pure PPy-F electrode. This shows that the composite material has substantially higher cycle ability than the pure polymer electrode.

Guiheng [49], was prepared via situ polymerization with the support of supercritical carbon dioxide (SC CO_2), and a graphene oxide (GO)/polyaniline (PANI) nanocomposite was synthesized. Scanning electron microscopy (SEM), transmission electron microscopy (TEM), X-ray diffraction (XRD), FT-IR, Raman, and UV–vis spectrophotometry were used to analyze the morphology and chemical composition of the synthesized samples. An aniline concentration of 0.1 M in a GO/PANI nanocomposite results in high specific capacitance (425 F g^{-1}) at a current density of 0.2 A g^{-1}. Due to the synergistic interaction of the small nanosized PANI nanoparticles and the GO with a high specific surface area, the electrochemical capacitance and cycle stability are outstanding. In this investigation, an easy method for covering uniformly-sized carbon materials with conducting polymer nanoparticle nanocomposites is introduced. These nanocomposites have interesting uses in energy storage devices.

Muhammad [19] and the co-authors focused on the multi-walled carbon nanotubes, Graphene oxide, and polypyrrole were combined to synthesize a potentio static ternary nanocomposite in a single step for supercapacitors. Electrochemical analysis, field emission scanning electron microscopy (FESEM), Fourier transforms infrared (FT-IR), and Raman spectroscopy was used to analyze the PPy/GO/MWCNT nanocomposite. For further investigation, the electrodes' capacitive performance was taken by CV measurements. In order to characterize the materials prior to putting the device together, the electrochemical performance of the manufactured electrodes was evaluated using a three-electrode system CV test with a range of 0.5–0.5 V and a scan rate of 50 mV s^{-1} shown in Fig. 6. The PPy/GO, PPy/MWCNT, and PPy/GO/MWCNT CV curves exhibit good capacity behavior with a roughly rectangular shape and no apparent redox peak. High conductivity and high surface area are achieved by the PPy/GO/MWCNT nanocomposite with well-crumpled nanosheets, which enhances the nanocomposite's capacitive performance. High specific capacitance (358.69 F g^{-1}), low R_{ct} (0.87), high specific energy (40.45 Wh kg^{-1}), and great cycling stability (88.69% retention after 2000 cycles) were all characteristics of the PPy/GO/MWCNT nanocomposite. As a result, the PPy/GO/MWCNT ternary nanocomposite is a great choice to be used in next-generation supercapacitors.

According to DayongGui et al. [51], polyaniline and graphene oxide-based nanocomposites were made from aniline (ANI), graphene oxide (GO), and ammonium per sulphate (APS) with the mass ratios (mANI:mGO) of 1000:1, 100:1, and 10:1, respectively, in ice water. Electrochemical characteristics of the composite were observed by impedance spectroscope, galvanostatic charge/discharge, and cyclic voltammetry, respectively. The surface topography and crystal structure of the composites were characterized through Fourier transform infrared spectrum (FT-IR), X-ray diffraction (XRD), and scanning electron microscopy (SEM). The composite electrode materials have improved cyclic voltammetry performance in comparison to pure PANI-based electrode materials. The special surface chemistry of the PG1000:1 composite is responsible for its improved super capacitive performance, which reached 355.2 F g^{-1} at 0.5 A g^{-1}. After 1,000 cycles of charge/discharge, the PG1000:1 composite maintained 285.8 F g^{-1}, showing good cycling stability. The authors are convinced that this composite will produce devices for supercapacitors or other power source systems that are promising.

4.4 Reduced Graphene Oxide

Sulfonated polyaniline (SPANI) was prepared by Parthasarathi et al. [52], as well as functionalized reduced graphene oxide (rGO) (SPANI/G-1) was made using aniline-initiated polymerization. Infrared Fourier transform, Raman, X-ray photoelectron, and thermogravimetric analysis all supported the success of SPANI's surface modification of graphene. An asymmetric supercapacitor device prepared by chemically reduced GO (rGO) as the negative electrode but also SPANI/G-1 as the positive electrode. At a current density of 1 A g^{-1} in a three-electrode system, SPANI/G-1 1107 F g^{-1} had the highest specific capacitance. The lower oxygen content in SPANI/G-1, which enhances the chemical interaction between graphene and SPANI chains, maybe the cause of the higher sp^2 carbon on the graphene sheets. Two electrode asymmetric supercapacitor (SPANI/G-1/rGO) devices were designed by using SPANI/G-1 as the positive electrode and rGO as the negative electrode. The device displayed a specific capacitance of 157 F g^{-1} at a current density of 1.5 A g^{-1}. The suggested device results in cycling stability of retention in C of 94% after 5,000 charge–discharge cycles. Furthermore, the as-prepared asymmetric supercapacitor's energy density and power density maximum up to 31.4 Wh kg^{-1} as well as 14,764

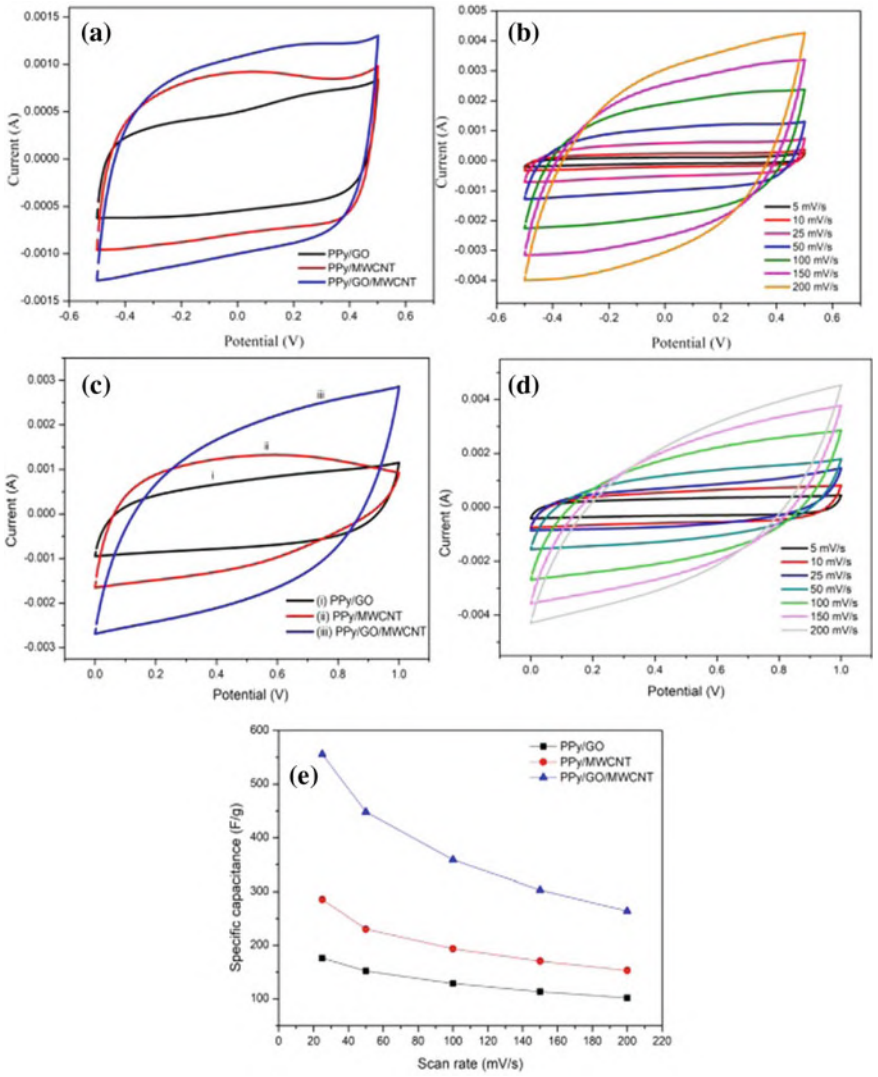

Fig. 6 system with three electrodes **a** At 50 mV s^{-1}, the PPy/GO, PPy/MWCNT, and PPy/GO/MWCNT CV curves are shown. **b** PPy/GO/MWCNT CV curves at various scan rates (5–200 mV s^{-1}) complete cell arrangement **c** In 1 M Na_2SO_4, the CV curves of I PPy/GO, (ii) PPy/MWCNT, and (iii) PPy/GO/MWCNT. **d** PPy/GO/MWCNT CV curves at various scan rates (5–200 mV s^{-1}). **e** Particular capacitance values for PPy/GO, PPy/MWCNT, and PPy/GO/MWCNT nanocomposites at various scan rates [19]

W kg^{-1}, respectively, demonstrating its viability as a new class of high-power edible energy storage device.

Zhisen [53], and their co-author's research based on nitrogen-doped 3D reduced graphene oxide/polyaniline composite as the active material N-3D-rGO/PANI composites were made by a standard in-situ chemical polymer technique. The structure, morphology, and electrochemical properties of the composites are characterized using X-ray diffraction, Fourier transforms infrared spectroscopy, X-ray photoelectron spectroscopy, Brunauer–Emmett–Teller analysis, transmission electron microscopy, scanning electron microscopy, charge–discharge test, cyclic voltammetry, and electrochemical impedance spectroscopy. The supercapacitor had a 282 F g^{-1} specific capacitance at 1 A g^{-1} and a 64.5% retention rate as the current density varied from 1 to 8 A g^{-1}. This outstanding performance is a result of the nitrogen-doped macroporous graphene and β-MnO_2 structures. The cyclic voltammetry performance is given in Fig. 7.

Ramesh et al. [54], reported synthesis and characterization of hybrid nanocomposite of cellulose fiber and multi-walled carbon nanotube (MWCNT), reduced graphene oxide (rGO), Cobalt oxide (Co_3O_4), and tin oxide (SnO_2). By using the

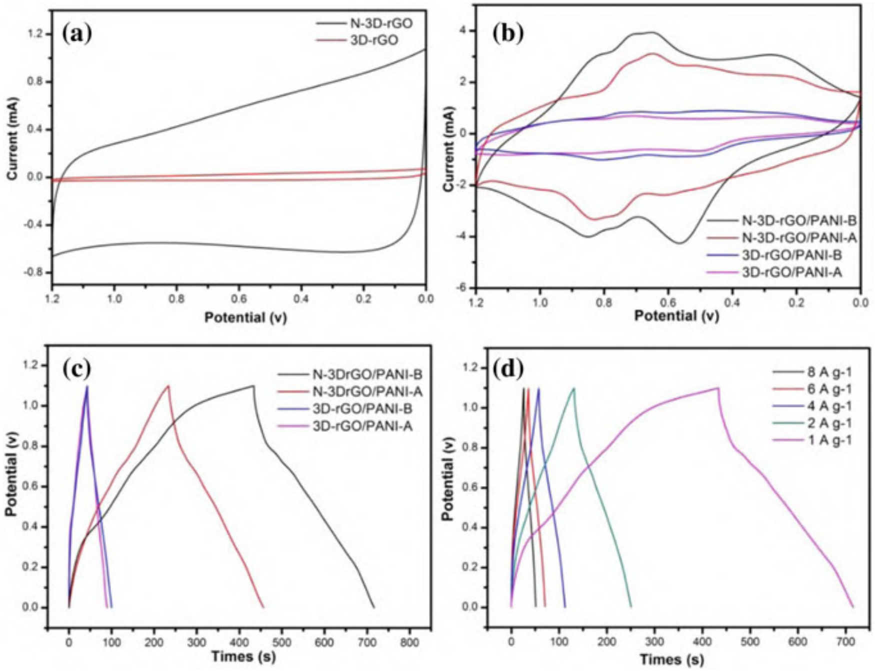

Fig. 7 At a scan rate of 100 mV s^{-1}, the CV curve shows N-3D-rGO, 3D-rGO (**a**), as well as various PANI composites, shown (**b**). Different PANI composites' galvanostatic charge–discharge curves at a current density of 1 A g^{-1} (**c**). At different current densities, the galvanostatic charge–discharge curves of N-3D-rGO and PANI-B (**d**) [53]

hydrothermal method the nanocomposite was prepared. The nanocomposites characterized by scanning electron microscope (SEM), transmission electron microscope (TEM), Fourier transform infrared spectroscopy (FT-IR), X-ray diffraction (XRD) and Raman spectroscopy, Energy dispersive X-ray spectroscopy (EDX). The electrode is made by the nanocomposite. Cyclic voltammetry (CV) showed good cyclic stability with 88% capacitance retention after 1,000 cycles and a capacitance of 215 F g^{-1} and 181 F g^{-1} at a current density of 0.2 A g^{-1} and 0.4 A g^{-1}, respectively.

Zafer et al. [55], reported ternary reduced graphene oxide (rGO), gold nanoparticles (Au NPs), and polyaniline (PANI) nanocomposite prepared with a low-cost, two-step, and green approach. Graphene oxide (GO) was reduced and stabilized by the plant Cetraria Islandica L. Ach lichen extract. The Reduced Graphene oxide nanosheets were uniformly coated with interconnected Au and PANI ultrafine film by polymerization of aniline monomer by using $HAuCl_4$ as an oxidizing agent. The prepared composite was characterized by using Fourier transform infrared spectroscopy (FT-IR), scanning electron microscope (SEM), and X-ray diffraction (XRD). The electrochemical performance was observed by cyclic voltammetry (CV). In two-electrode symmetrical composition, the specific capacitance of rGO-Au and PANI nanocomposite was achieved at a current density of 1 A g^{-1} as 212.8 F g^{-1}. After 5000 consecutive cycles at a current density of 2 A g^{-1}, the ternary rGO-Au and PANI nanocomposite maintained 86.9% of its initial specific capacitance.

5 Functionalization Based on Metal Oxides as Fillers

Generally, polymers are used for a variety of static and anti-static discharging applications, and inherently conductive polymers, don't contain any metals but conduct electricity when chemically altered with dopants. The two main types of conductive polymers [56]. High specific capacitance as well as low resistance, through metal oxides, provides an additional option for the materials used to make the electrodes for supercapacitors. Make highly powerful and energy-efficient supercapacitors. The most widely used metal oxides are copper oxide, iridium oxide, nickel oxide, ruthenium dioxide, manganese oxide, and ruthenium dioxide. They are a practical substitute due to their lower production costs and use of a milder electrolyte [57].

The method of synthesis and ease of production, of various conducting polymers, are the subject of major research for supercapacitor electrodes. Compared to carbon-based electrodes, conducting polymers have high capacitance, conductivity, and equivalent series resistance. The n/p type composition, which consists of one negatively charged (n-doped) and another one positively charged (p-doped) electrode, offers high energy, though the potential of pseudo-capacitors has been constrained by less amount of n-doped conducting polymer electrode materials. Oxidation is used to store and release the charge in conducting polymers through the reduction process. Ions are transferred to the backbone of the polymer if oxidation, also known as doping, takes place [58–61].

Ease of production and low cost of various conducting polymers have been the subject of extensive research as supercapacitor electrode materials. One of the polythiophene family's members, PEDOT, has gained recognition as a strong candidate for pseudo-capacitor electrodes because of its quick electrochemical kinetics and superior intrinsic conductivity [62] compared to other conducting polymers(CPs) [18]. The hydrothermal method was used by Rajesh et al. [63] to demonstrate the in-situ polymerization of Poly(3,4 ethylene dioxythiophene) (PEDOT) on a flexible 3D carbon fiber cloth (CFC). Because of the greater susceptible surface area, high conductivity, good porosity, chemical stability, flexibility, lightweight, and cost-effectiveness, CFC was selected as a substrate for this study. In order to increase the electrode–electrolyte interface and improve ion diffusion, a homogeneous distribution of the growing PEDOT on the surface of the CFC can be very advantageous. This can give a good specific capacitance of 203 F g^{-1} (5 mV s^{-1}) and result in low R_{ct} (0.2 Ω) and R_s (0.6 Ω) values compared to bare CFC. The almost perfect triangular shapes of the galvanostatic charge/discharge curves, coupled with a slight voltage drop (IR drop) at the start of the discharging curve, indicate low internal resistance and good electrochemical reversibility. The capacitance of PEDOT/CFC also held well (about 86% after 12,000 cycles), demonstrating the material's strong electrochemical stability.

Through combining CPs (TMO/CP-based fibers), the pseudocapacitive properties of fiber composites can be improved. In the comparison between TMO- and CP-based fibers individually, TMOs and CPs can co-operate to give outstanding electrochemical behavior of the fiber composites by contributing a greater specific capacitance and superior electrical conductivity. They both have quick/reversible redox reactions and high specific energies, which explains this. Microfibers made of poly(vinyl alcohol), graphene oxide, and manganese oxide (PVA-GO-MnO_2) were used by Mohd et al. [64] as a template for PEDOT deposition. Due to GO's increased surface area, which also prevents MnO_2 NP aggregation, compared to PVA-MnO_2/PEDOT (107.22 F g^{-1}), the homogenous distribution of PEDOT on the PVA-GO-MnO_2 microfibres showed a significantly higher specific capacitance (144.6 F g^{-1}). The PVA-GO-MnO_2/PEDOT micro composite's potential window can be raised to 1.8 V while maintaining an appropriate rate capability (91.18% capacitance maintained after 1,000 cycles).

Resulting in value theoretical specific capacity (1370 F g^{-1}), good environmental compatibility [65], high operating potential, and cost-effectiveness [66–69], MnO_2 has emerged as a superior faradaic material that can be used in place of RuO_2. Yang et al. [70] used MnO_2 to hybridize with PAN/pitch-based CNFs that were boron-enriched through one-step electrospinning and carbonization. This research showed that MnO_2 and Boron both offer more electrochemically active redox reaction sites and low-resistance mechanisms for electron transport. The resulting nanocomposite (Fig. 8) produced a high specific capacitance of 208 F g^{-1} and a maximum specific energy of 25.66 Wh kg^{-1} while having a specific surface area of 718 m^2 g^{-1}.

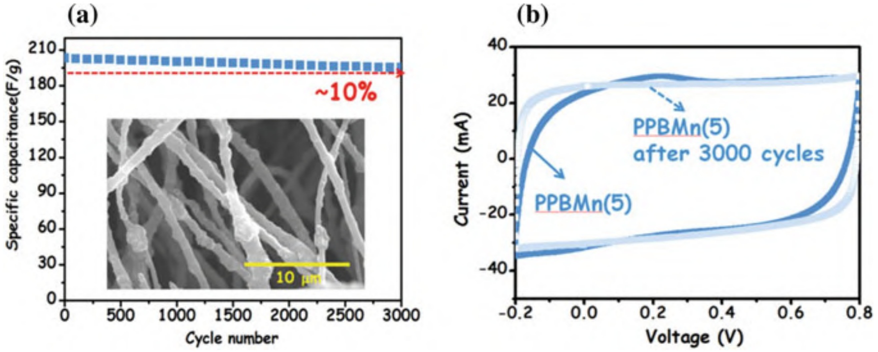

Fig. 8 **a** The variation in specific capacitance of PPBMn(5) about 3000 cycles at a constant current density of 1 mA cm^{-2} through 6 M KOH aqueous electrolyte; **b** CV characterized at 25 mV s^{-1} obtained in both devices upon running for 3000 cycles [70]

6 Nanoparticles as Fillers in Polymer Electrolytes

Besides interacting with mobile ions, metal oxide nanoparticles can significantly improve the ionic conductivity of solid polymer electrolytes and mechanical strength. Perhaps it is a good idea to disperse nanofillers like ZnO, Al_2O_3, SiO_2, and TiO_2. This inclusion offers a wide electrochemical window, good mechanical strength, and high ionic conductivity within the range of 10^{-3} to 10^{-2} S cm^{-1}. The crystallization kinetics of polymer chains are typically slowed down and the degree of crystallinity is decreased when nanoparticles are added to the polymer salt system. Ion transport in the composites is enhanced as a result of this decrease in crystallinity. The polymer dipole orientation is also impacted by the addition of fillers in the polymer electrolyte. Due to the surface charge on the ceramic filler, this altered orientation encourages flexible segmental chain motion as well as ion pair dissociation [71, 72].

Mee et al. [73], reported the solid polymer electrolyte (SPE) based on fumed silica nanoparticles as nanofillers, hydroxylethyl cellulose (HEC) as the host polymer, magnesium trifluoromethanesulfonate salt, and 1-ethyl-3-methylimidazolium trifluoromethanesulfonate ionic liquid was prepared and functionalized. SPE is characterized, and it is concluded that the SPE doped with 2 wt.% of fumed silica nanoparticles achieves the greatest ionic conductivity (2.7×10^{-4} S cm^{-1}) at room temperature as well as a significant reduction in crystallinity at peak $2\theta = 20^\circ$ by 53.4%. However, the nanoparticles' increased ability to adsorb ions onto the polymer backbone was facilitated by their high dielectric permittivity (9.0×10^4) and low activation energy (0.213 eV). As a result, EDLCs that perform well predominate. Higher conducting sample-based EDLC is the best-performing cell because it can maintain 71.3% of the capacitance of its beginning capacitances over 1,600 cycles at a current density of 0.4 A g^{-1}. This result was shown in Fig. 9.

The relation between ionic conductivity and the surface area of the SPE is inverse. The improvement of ionic conductivity of the composite polymer electrolyte system

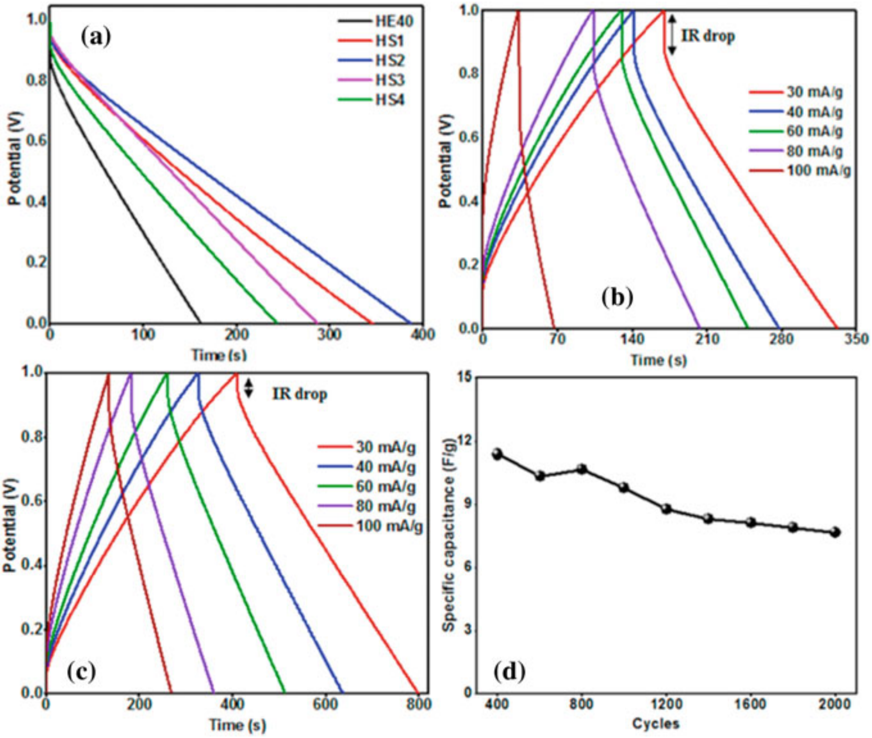

Fig. 9 **a** EDLC cell discharge curves at a current density of 30 mA g^{-1} with and without the inclusion of fumed silica nanoparticles. **b** Curves of HE40's galvanostatic charge–discharge at various current densities Galvanostatic charge–discharge shape of HS2 at various current densities are shown in figure (**c**). (**d**) The HS2-based EDLC's specific capacitance over 1600 cycles at 0.4 A g^{-1} of current density [73]

is largely due to several factors, including high salt ion concentration, large surface area by the porous structure of the system, and amorphous nature of the polymer, Lewis's acid–base interaction among ceramic fillers, as well as the presence of a space charge region at the interfaces. Mukta et al. [74] reported the SPE synthesis using ZnO as a nanofiller, tetraethylammonium tetrafluoroborate (TEABF4) as a salt, ethylene carbonate (EC) and propylene carbonate (PC) as plasticizers, and PVDF-HFP as the polymer. By incorporating 12 wt.% of ZnO nanoparticles in the complex, a maximum ionic conductivity value of 6.3×10^{-3} S cm^{-1} was attained. Ionic transference number and activation energy are calculated to be 0.84 and 0.074 eV, respectively. This demonstrates that ionic conduction is dominant. The current research demonstrates a wide window at 3.3 V, which is adequate for the electrolyte system to function as a separator in EDLCs.

7 Applications of Polymer Nanocomposites in Different Fields

The Nanocomposite application was explained in Fig. 10 chart format. Although "supercapacitors" are currently the most well-known name for electrochemical capacitors (ECs), other names for them include "ultracapacitors" and "power capacitors." NEC, the first company to initiate a product in 1971 [75] under the name Supercapacitor TM, came up with the term "supercapacitor." Since 1957, when Becker [76] used carbon flooded with the use of a sulfuric acid electrolyte for charge storage first at the interface of these two materials, supercapacitors have been under development. However, SOHIO [77] was the company that first introduced this technology to the market in 1969. Supercapacitors' real breakthrough came in the 1990s when government initiatives in the US provided funding for this technology's development so that it could be incorporated into hybrid cars to provide the required energy for acceleration [78, 79].

Today, industrial and commercial supercapacitors are available in many nations (including Japan, Russia, and the United States), and the most of capacitors are

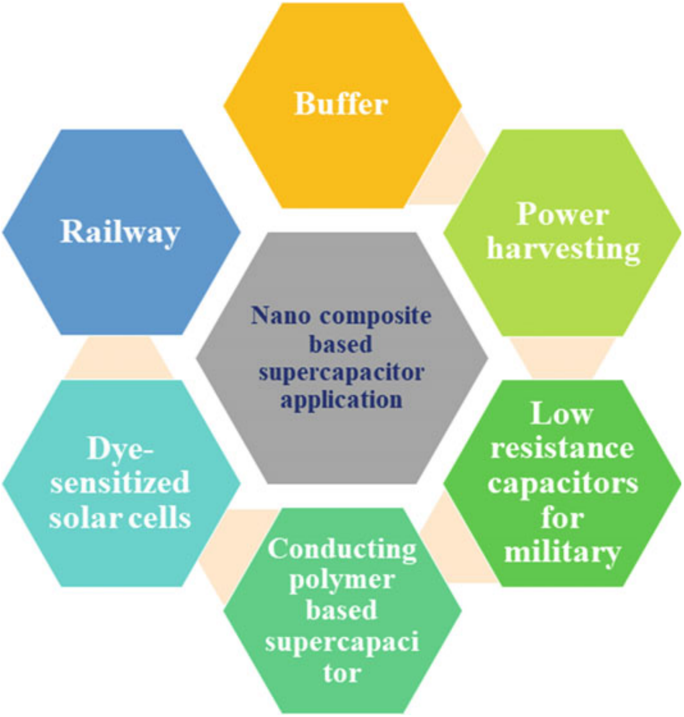
Buffer
Railway
Power harvesting
Nano composite based supercapacitor application
Dye-sensitized solar cells
Low resistance capacitors for military
Conducting polymer based supercapaci tor

Fig. 10 Nano composite based supercapacitor applications

EDLC. Supercapacitors have been the subject of extensive research by US companies, Los Alamos National Laboratory (Los Alamos, NM), Eaton (Cleveland, OH), Evans Capacitor Company (East Providence, RI), and Maxwell Technologies (San Diego, CA). Common electrochemical supercapacitors are produced by industrial and commercial firms like Maxwell Technologies and Panasonic (Osaka, Japan) and used symmetric activated carbon electrode materials also and acetonitrile electrolytes. China is testing a novel electric bus design called the CapabusTM. It uses large onboard EDLC, which are quickly recharged whenever the bus is at a bus stop (under “electric umbrellas”) and are charged up in the terminus, to operate without powerlines. At the beginning of 2005, Shanghai hosted some prototype testing. Bus with a diesel-electric battery drive system and EDLC was tested by VAG (the public transportation provider in Nuremberg, Germany) in 2001 and 2002. A light-rail vehicle (LRV) that uses EDLC to store braking energy has been in use by Mannheim Stadtbahn (Mannheim, Germany) since 2003 [80, 81].

7.1 Buffer

When basic or acidic substances are added, a buffer is a component that can resist the pH change. Few amounts of acid or base can be neutralized by it, keeping the solution’s pH level largely stable. Low-power devices like random access memories, microcontrollers, and computer cards receive their power from supercapacitors, which also serve as an emergency shutdown source. For small-energy applications like automated reading technology or industrial electronics event information, they serve as the only power source.

Supercapacitors act as power “buffers” between rechargeable batteries and the grid, reducing the impact of brief power outages and high current peaks. The largest banks of electrolytic capacitors in UPS have been replaced by supercapacitors. With this setup, the cost per cycle is lower, replacement and maintenance expenses are cut, the battery can be made smaller, and the lifespan is increased. In wind turbine pitch systems, supercapacitors give backup power for actuators so that blade pitch can be changed whether the main supply fails.

7.2 Power Harvesting

For energy harvesting systems, supercapacitors are versatile as alternate energy storage devices. Energy is gathered from external or reusable sources, such as mechanical motion, light, and electromagnetic fields, and it was transformed into an energy storage device as electrical energy in energy harvesting systems. For instance, it has been shown that energy gathered from RF fields can be stored in a printed supercapacitor using an RF antenna as the proper rectifier circuit. Then, an application-specific integrated circuit is powered for more than 10 h using the harvested energy.

Low wind conditions need not call for a system with a megawatt-range generator. Returning to energy harvesting, the research unearths a novel hybrid circuit that combines a battery and supercapacitor. In order to harvest energy, Worthington proposed a novel circuit in 2010 that manages to combine the co-existed switched harvesting technique and a direct connection to a load capacitor. This made it possible for the capacitor to function as a reservoir that could be disconnected once it had reached its full charge before discharging to a load. A charge pump-type circuit was used to connect the circuit [82, 83].

7.3 Low-Resistance Capacitors for Military

Supercapacitors can be used in applications that call for short-term, high currents due to their low internal resistance. The earliest applications were (cold diesel engine starting) motor startups for sizable engines in submarines and tanks. Supercapacitors serve as a battery buffer, coping with brief current peaks and lowering cycling. Military radio communications, phased-array radar antennae, avionic displays, laser power sources, backup power for airbag deployment, and GPS-based missiles and projectiles are additional military applications that call for high power density.

Hejira et al. [84] the outcomes of the current work, in which a highly stable asymmetric SC device was created using a GO and PANI nanocomposite with a 1.2 V extended potential window. After 10,000 cycles at 3 A g^{-1}, the device displayed better coulombic efficiency (98.06%), and extremely high electrochemical stability with specific capacitance retention of 118.6%. Additionally, the device demonstrated strong performance and maintained a specific capacitance of 73.94% even at a higher current density (10 A g^{-1}). It has a power density of 2503 W kg^{-1} at 1 A g^{-1} current density, which results in its highest energy density (28.5 Wh kg^{-1}). At 3.2 mA cm^2, it exhibits an aerial capacitance of 57 mF cm^2. At a power density of 10.47 W cm^2, the maximum energy density was 0.92 m Wh cm^2.

7.4 Nano Composite Supercapacitor

The electrolyte system can be affecting the specific capacitance. The SWCNH-based supercapacitor was reported by Yang et al. [85]. The impact of SWCNH's hole-opening on the capacitive characteristics of the supercapacitor was reported. The relationship between SWCHN's nano window size and specific capacitance also was investigated. High capacitance supercapacitors were produced by SWCNH of larger nano window sizes. Thus, by adjusting the nano window size, a single-wall nanocarbon of high ion selectivity has been created. Izadi-Najafabadi et al. [86] created a composite electrode using meso-micro pore single-wall carbon nanotubes

(SWCNT) and SWCNH. The electrode of the supercapacitor reached its maximum power rating of 1 M W kg^{-1}. Due to its monolithic chemical composition as well as mechanical stability, the composite electrode showed a 6.5% decrease in capacitance over 100,000 cycles.

Li et al. [25] and colleagues created the conducting polymer-pillared graphene oxide sheets with exceptional electro-capacitive qualities. Such nanostructured composites take advantage of the special qualities of both graphene oxide and conducting polymers. These are just a few of the benefits of composite materials are; (1) The highly porous graphene oxide dispersed in solution offers a good accessible surface for joining of the conducting polymer; (2) The mechanical strength of the composite stabilizes the polymers during the charge–discharge process can be improved by the three-dimensional layered structure; (3) The graphene oxide nanostructure with conducting polymer pillars decrease the resistance in the electrolyte; and (4) The readily available conducting polymers significantly increase the overall energy storage's pseudo capacitance. This method produced a graphene oxide-polypyrrole composite with excellent electro-capacitive performance and a high specific capacitance of over 500 F g^{-1}.

7.5 Dye-Sensitized Solar Cells

Dye-sensitized solar cells (DSSC) are the focus of a lot of research [80]. Compared to conventional silicon solar cells, it is cheaper, easier to manufacture, and has a higher conversion efficiency. DSSC has thus been taken into consideration as a possible substitute for traditional silicon solar cells. In DSSC, an electron-collecting dye is adsorbed on a nanocrystalline photoelectrode. Platinum and other noble metals are potential electrode materials for DSSC. However, using platinum is expensive. Nanocarbon, carbon nanotubes (CNT), graphene, carbon composite, polyaniline, poly(3,4-ethylene-dioxythiophene) (PEDOT), and polystyrene sulphonate (PSS) are a few examples of functional materials that have been studied to reinstate platinum [87–90]. For use in DSSC applications,

Sushmita et al. [91] prepared counter electrodes decorated with graphene nanoplatelets (GNP) and SWCNH. The photovoltaic conversion efficiency of the SWCNH-loaded DSSC was higher (4.09%) than that of the GNP (3.13%). Investigations of the SWCNH and GNP composite using atomic force microscopy (AFM) were also carried out. SWCNH was found to have a surface roughness of about 158.59 nm, which was greater than GNP (53.23 nm). By using CV measurements, the catalytic characteristics and reaction kinetics of various types of counter electrodes were examined. Redox peaks in two pairs were noticed. The photocurrent density (JSC) and fill factor of the SWCNH-based electrode were improved (FF).

7.6 Railway

In starter systems for fuel railroad locomotives with diesel-electric transmission, supercapacitors can replace batteries. The capacitors store the braking energy from a complete stop and deliver the peak current for the diesel engine's start-up and train acceleration, and guarantee the stability of the catenary voltage. Recovering braking energy can result in energy savings of up to 30%, depending on the driving mode. Supercapacitors were chosen because of their low maintenance requirements and environmentally friendly construction. Sustainable polymers and environmentally friendly nanofillers are premium characteristics of green nanocomposites. High-performance green nanocomposites have been created by incorporating eco-nanofillers into eco-polymers. The choice of eco-nanofiller, green polymer matrices, and green synthesis techniques affect the energy performance of green nanocomposites [92].

Xi et al. [93] by pyrolyzing, freeze-drying, and dissolving bamboo cellulose fibers, a unique cellulosic carbon aerogel has been created. Porous nanoplatelets wrapped interconnected fiber framework with a micro surface area of 910 m^2 g^{-1} and high flexibility of 86% at a compressive stress of 23 kPa were visible in the texture. Activated carbon fiber aerogel displayed impressive specific capacitance (381 F g^{-1}) as well as an intriguing retention rate (90% at 200 mV s^{-1}) as a result of these structural advantages. Further study on flexible supercapacitors is encouraged by the carbon fiber aerogel's highly stable and ultralight multi-porous structure. Additionally, producing eco-friendly porous carbon fiber aerogel from readily available biomass material offers an affordable and sustainable method of using energy storage devices.

Others reported, Zafer et al. [94] here, a two-step, inexpensive, and environmentally friendly method was used to prepare ternary reduced graphene oxide (rGO)—Au nanoparticles (Au NPs) at polyaniline (PANI) nanocomposite. The first step involved using CetrariaIslandica L. Ach lichen extract to reduce and stabilize graphene oxide (GO). In-situ polymerization of aniline monomer using $HAuCl_4$ as an oxidizing agent was followed by uniformly coating the rGO nanosheets with a combination of Au and PANI ultrafine film. With a current density of 1 A g^{-1}, the rGO-Au and PANI nano composite exhibit a high specific capacitance of 212.8 F g^{-1}. Additionally, after 5,000 cycles, the nanocomposite electrodes show 86.9% specific capacitance retention.

Kalaiarasi et al. [95] in this study, graphene oxide was reduced by plant leaves before hydrothermal preparation was used to create ZnO/rGO composites. When the current density was 0.5 A g^{-1}, the synthesized nano composites' specific capacitance reached 180 F g^{-1}. At a current density of 0. 5 A g^{-1}, the average specific had decreased by 20% after 2,400 cycles. The synthesized nanocomposite has good cycle stability. The attained specific capacitance retention is still 80%. Capacitors are acknowledged as commercial energy storage devices, particularly for electrical energy. Various Functionalized polymer nanocomposites have been fulfilled as high-performance supercapacitors.

References

1. ur Rehman S, Bi H (2021) Electrodes for flexible integrated supercapacitors. Flex Supercapacitor Nanoarchitectonics, 1–26. https://doi.org/10.1002/9781119711469.ch1
2. Saleh TA, Shetti NP, Shanbhag MM, Raghava Reddy K, Aminabhavi TM (2020) Recent trends in functionalized nanoparticles loaded polymeric composites: an energy application. Mater Sci Energy Technol 3:515–525. https://doi.org/10.1016/j.mset.2020.05.005
3. Nithya C, Gopukumar S (2015) Sodium ion batteries: a newer electrochemical storage, Wiley Interdiscip. Rev Energy Environ 4:253–278. https://doi.org/10.1002/wene.136
4. Bibi F, Khan MI, Rahim A, Muhammad N, Santos LSS (2021) Flexible supercapacitors based on fiber-shape electrodes. Flex Supercapacitor Nanoarchitectonics, 27–42. https://doi.org/10.1002/9781119711469.ch2
5. Raghav J, Raghav S, Jain P (2021) Graphene-based electrodes for flexible supercapacitors. Flex. Supercapacitor Nanoarchitectonics, 43–57. https://doi.org/10.1002/9781119711469.ch3
6. Goyal RK (2017) Nanomaterials and Nanocomposites. https://doi.org/10.1201/9781315153285
7. Arulepp M, Leis J, Lätt M, Miller F, Rumma K, Lust E, Burke AF (2006) The advanced carbide-derived carbon based supercapacitor. J Power Sources 162:1460–1466. https://doi.org/10.1016/j.jpowsour.2006.08.014
8. Winter M, Brodd RJ (2004) What are batteries, fuel cells, and supercapacitors? Chem Rev 104:4245–4269. https://doi.org/10.1021/cr020730k
9. Choi BG, Hong J, Park YC, Jung DH, Hong WH, Hammond PT, Park H (2011) Innovative polymer nanocomposite electrolytes: nanoscale manipulation of ion channels by functionalized graphenes. ACS Nano 5:5167–5174. https://doi.org/10.1021/nn2013113
10. Shanmugapriya V, Arunpandiyan S, Hariharan G, Bharathi S, Selvakumar B, Arivarasan A (2022) Enhanced supercapacitor performance of Zno/Sno_2:rGO nanocomposites under redox additive electrolyte. J Alloys Compd 935:167994. https://doi.org/10.1016/j.jallcom.2022.167994
11. Shanmugapriya V, Bharathi S, Esakkinaveen D, Arunpandiyan S, Selvakumar B, Sasikala G, Jayavel R, Arivarasan A (2022) Structural, optical, and magnetic properties of Gd doped CdTe quantum dots for magnetic imaging applications. ECS J Solid State Sci Technol 11:013010. https://doi.org/10.1149/2162-8777/ac4bad
12. Hu Y, Shenderova OA, Hu Z, Padgett CW, Brenner DW (2006) Carbon nanostructures for advanced composites. Rep Prog Phys 69:1847–1895. https://doi.org/10.1088/0034-4885/69/6/R05
13. Liu J, Rinzler AG, Dai H, Hafner JH, Kelley Bradley R, Boul PJ, Lu A, Iverson T, Shelimov K, Huffman CB, Rodriguez-Macias F, Shon YS, Lee TR, Colbert DT, Smalley RE (1998) Fullerene pipes. Science 280(5367):1253–1256. https://doi.org/10.1126/science.280.5367.1253
14. Sowers T, Bender M, Raynaud D, Korotkevich YS, Grootes PM, Steig EJ, Morse DL (1998) Solution properties of single-walled carbon nanotubes. Science 282(5386):95–98
15. Chang CC, Imae T (2018) Synergistic performance of composite supercapacitors between carbon nanohorn and conducting polymer. ACS Sustain Chem Eng 6:5162–5172. https://doi.org/10.1021/acssuschemeng.7b04813
16. Sahoo NG, Cheng HKF, Cai J, Li L, Chan SH, Zhao J, Yu S (2009) Improvement of mechanical and thermal properties of carbon nanotube composites through nanotube functionalization and processing methods. Mater Chem Phys 117:313–320. https://doi.org/10.1016/j.matchemphys.2009.06.007
17. Fan LQ, Tu QM, Geng CL, Huang JL, Gu Y, Lin JM, Huang YF, Wu JH (2020) High energy density and low self-discharge of a quasi-solid-state supercapacitor with carbon nanotubes incorporated redox-active ionic liquid-based gel polymer electrolyte. Electrochim Acta 331:135425. https://doi.org/10.1016/j.electacta.2019.135425
18. Kumar Y, Pandey GP, Hashmi SA (2012) Gel polymer electrolyte based electrical double layer capacitors: comparative study with multiwalled carbon nanotubes and activated carbon electrodes. J Phys Chem C 116:26118–26127. https://doi.org/10.1021/jp305128z

19. Mohd Abdah MAA, Mohd Razali NS, Lim PT, Kulandaivalu S, Sulaiman Y (2018) One-step potentiostatic electrodeposition of polypyrrole/graphene oxide/multi-walled carbon nanotubes ternary nanocomposite for supercapacitor. Mater Chem Phys 219:120–128. https://doi.org/10.1016/j.matchemphys.2018.08.018
20. Potphode DD, Sivaraman P, Mishra SP, Patri M (2015) Polyaniline/partially exfoliated multi-walled carbon nanotubes based nanocomposites for supercapacitors. Electrochim Acta 155:402–410. https://doi.org/10.1016/j.electacta.2014.12.126
21. Trigueiro JPC, Borges RS, Lavall RL, Calado HDR, Silva GG (2009) Polymeric nanomaterials as electrolyte and electrodes in supercapacitors. Nano Res 2:733–739. https://doi.org/10.1007/s12274-009-9080-1
22. Lee CS, Ahn SH, Kim DJ, Lee JH, Manthiram A, Kim JH (2020) Flexible, all-solid-state 1.4 V symmetric supercapacitors with high energy density based on comb polymer electrolyte and 1D hierarchical carbon nanotube electrode. J Power Sources 474:228477. https://doi.org/10.1016/j.jpowsour.2020.228477
23. Deshpande MD, Kondawar SB (2016) Transport properties of multi-walled carbon nanotubes based conducting polythiophene/polyaniline nanocomposites. Adv Mater Lett 7:844–850. https://doi.org/10.5185/amlett.2016.6193
24. Ranu R, Chauhan Y, Ratan A, Yadav S, Tomar SK (2020) Multifunctional biogenically synthesized porous multi-walled carbon nanotubes dispersed polymer electrolyte-based supercapacitor. Appl Phys A Mater Sci Process 126:14–16. https://doi.org/10.1007/s00339-020-3384-0
25. Zhang LL, Zhao S, Tian XN, Zhao XS (2010) Layered graphene oxide nanostructures with sandwiched conducting polymers as supercapacitor electrodes. Langmuir 26:17624–17628. https://doi.org/10.1021/la103413s
26. Mishra AK, Ramaprabhu S (2011) Functionalized graphene-based nanocomposites for supercapacitor application. J Phys Chem C 115:14006–14013. https://doi.org/10.1021/jp201673e
27. Sahoo S, Karthikeyan G, Nayak GC, Das CK (2012) Modified graphene/polyaniline nanocomposites for supercapacitor application. Macromol Res 20:415–421. https://doi.org/10.1007/s13233-012-0042-1
28. Arthisree D, Madhuri W (2020) Optically active polymer nanocomposite composed of polyaniline, polyacrylonitrile and green-synthesized graphene quantum dot for supercapacitor application. Int J Hydrogen Energy 45:9317–9327. https://doi.org/10.1016/j.ijhydene.2020.01.179
29. Lu W (2007) Carbon nanotube supercapacitors, 563–591
30. Niu C, Sichel EK, Hoch R, Moy D, Tennent H (2012) High power electrochemical capacitors based on carbon nanotube electrodes electrodes, 1480. https://doi.org/10.1063/1.118568
31. Yang C (2006) Study of alkaline nanocomposite polymer electrolytes based on PVA–ZrO_2–KOH 131:256–262. https://doi.org/10.1016/j.mseb.2006.04.036
32. Banks CE, Compton RG (2006) New electrodes for old: from carbon nanotubes to edge plane pyrolytic graphite. Analyst 131:15–21. https://doi.org/10.1039/b512688f
33. Pumera M (2009) The electrochemistry of carbon nanotubes: fundamentals and applications. Chem–A Eur J 15:4970–4978. https://doi.org/10.1002/chem.200900421
34. Kaempgen M, Chan CK, Ma J, Cui Y, Gruner G (2009) Printable thin film supercapacitors using single-walled carbon nanotubes. Nano Lett 9:1872–1876. https://doi.org/10.1021/nl8038579
35. Sahoo NG, Rana S, Cho JW, Li L, Chan SH (2010) Polymer nanocomposites based on functionalized carbon nanotubes. Prog Polym Sci 35:837–867. https://doi.org/10.1016/j.progpolymsci.2010.03.002
36. Kumar M, Singh K, Dhawan SK, Tharanikkarasu K, Chung JS, Kong BS, Kim EJ, Hur SH (2013) Synthesis and characterization of covalently-grafted graphene-polyaniline nanocomposites and its use in a supercapacitor. Chem Eng J 231:397–405. https://doi.org/10.1016/j.cej.2013.07.043
37. Urita K, Seki S, Utsumi S, Noguchi D, Kanoh H, Tanaka H, Hattori Y, Ochiai Y, Aoki N, Yudasaka M, Iijima S, Kaneko K (2006) Effects of gas adsorption on the electrical conductivity of single-wall carbon nanohorns. Nano Lett 6:1325–1328. https://doi.org/10.1021/nl060120q

38. Zahab A, Spina L, Poncharal P, Marlière C (2000) Water-vapor effect on the electrical conductivity of a single-walled carbon nanotube mat. Phys Rev B Condens Matter Mater Phys 62:10000–10003. https://doi.org/10.1103/PhysRevB.62.10000
39. Maiti S, Khatua BB (2014) Polyaniline integrated carbon nanohorn: a superior electrode materials for advanced energy storage. Express Polym Lett 8
40. Wei D, Wang H, Hiralal P, Andrew P, Ryhasšnen T, Hayashi Y, Amaratunga GAJ (2010) Template-free electrochemical nanofabrication of polyaniline nanobrush and hybrid polyaniline with carbon nanohorns for supercapacitors. Nanotechnology 21. https://doi.org/10.1088/0957-4484/21/43/435702
41. Moussa M, El-Kady MF, Abdel-Azeim S, Kaner RB, Majewski P, Ma J (2018) Compact, flexible conducting polymer/graphene nanocomposites for supercapacitors of high volumetric energy density. Compos Sci Technol 160:50–59.https://doi.org/10.1016/j.compscitech.2018.02.033
42. Zheng L, Cheng X, Ye P, Shen L, Wang Q, Zhang D, Gu Z, Zhou W, Wu D, Yu Y (2018) Low temperature growth of three-dimensional network of graphene for high-performance supercapacitor electrodes. Mater Lett 218:90–94. https://doi.org/10.1016/j.matlet.2018.01.159
43. Najib S, Erdem E (2019) Current progress achieved in novel materials for supercapacitor electrodes: mini review. Nanoscale Adv 1:2817–2827. https://doi.org/10.1039/c9na00345b
44. Mao L, Zhang K, On Chan HS, Wu J (2012) Surfactant-stabilized graphene/polyaniline nanofiber composites for high performance supercapacitor electrode. J Mater Chem 22:80–85. https://doi.org/10.1039/c1jm12869h
45. Alvi F, Ram MK, Basnayaka PA, Stefanakos E, Goswami Y, Kumar A (2011) Graphene-polyethylenedioxythiophene conducting polymer nanocomposite based supercapacitor. Electrochim Acta 56:9406–9412. https://doi.org/10.1016/j.electacta.2011.08.024
46. Kausar A (2022) Polyaniline/graphene nanoplatelet nanocomposite towards high-end features and applications. Mater Res Innov 26:249–261. https://doi.org/10.1080/14328917.2021.1934281
47. Das AK, Karan SK, Khatua BB (2015) High energy density ternary composite electrode material based on polyaniline (PANI), molybdenum trioxide (MoO_3) and graphene nanoplatelets (GNP) prepared by sono-chemical method and their synergistic contributions in superior supercapacitive performance. Electrochim Acta 180:1–15. https://doi.org/10.1016/j.electacta.2015.08.029
48. Sarno M, Castaldo R, Ponticorvo E, Scarpa D, Cocca M, Ambrogi V, Gentile G (2019) Hypercross-linked polymer loaded with graphite nanoplatelets for supercapacitor application. Chem Eng Trans 73:121–126. https://doi.org/10.3303/CET1973021
49. Xu G, Wang N, Wei J, Lv L, Zhang J, Chen Z, Xu Q (2012) Preparation of graphene oxide/polyaniline nanocomposite with assistance of supercritical carbon dioxide for supercapacitor electrodes. Ind Eng Chem Res 51:14390–14398. https://doi.org/10.1021/ie301734f
50. Longo A, Verucchi R, Aversa L, Tatti R, Ambrosio A, Orabona E, Coscia U, Carotenuto G, Maddalena P (2017) Graphene oxide prepared by graphene nanoplatelets and reduced by laser treatment. Nanotechnology 28. https://doi.org/10.1088/1361-6528/aa6c3c
51. Gui D, Liu C, Chen F, Liu J (2014) Preparation of polyaniline/graphene oxide nanocomposite for the application of supercapacitor. Appl Surf Sci 307:172–177. https://doi.org/10.1016/j.apsusc.2014.04.007
52. Bandyopadhyay P, Kuila T, Balamurugan J, Nguyen TT, Kim NH, Lee JH (2017) Facile synthesis of novel sulfonated polyaniline functionalized graphene using m-aminobenzene sulfonic acid for asymmetric supercapacitor application. Chem Eng J 308:1174–1184. https://doi.org/10.1016/j.cej.2016.10.015
53. Liu Z, Li D, Li Z, Liu Z, Zhang Z (2017) Nitrogen-doped 3D reduced graphene oxide/polyaniline composite as active material for supercapacitor electrodes. Appl Surf Sci 422:339–347. https://doi.org/10.1016/j.apsusc.2017.06.046
54. Ramesh S, Khandelwal S, Rhee KY, Hui D (2018) Synergistic effect of reduced graphene oxide, CNT and metal oxides on cellulose matrix for supercapacitor applications. Compos Part B Eng 138:45–54. https://doi.org/10.1016/j.compositesb.2017.11.024

55. Çıplak Z, Yıldız A, Yıldız N (2020) Green preparation of ternary reduced graphene oxide-au@polyaniline nanocomposite for supercapacitor application. J Energy Storage 32. https://doi.org/10.1016/j.est.2020.101846
56. Manas Chanda SKR (2008) Industrial polymers specialty polymers and their applications, 1st ed. Tylor and Francis Group. https://doi.org/10.1201/9781420080599
57. Iro ZS, Subramani C, Dash SS (2016) A brief review on electrode materials for supercapacitor. Int J Electrochem Sci 11:10628–10643. https://doi.org/10.20964/2016.12.50
58. Banerjee S, Kar KK (2020) Conducting polymers as electrode materials for supercapacitors. Springer Ser Mater Sci 302:333–352. https://doi.org/10.1007/978-3-030-52359-6_13
59. Liu C, Gui D, Liu J (2014) Preparation of MnO_2/graphene nanocomposite for the application of supercapacitor. In: Proceedings of the electronic packaging technology conference, EPTC, pp 177–182. https://doi.org/10.1109/ICEPT.2014.6922631
60. Halper MS, Ellenbogen JC (2006) Ultra-capacitors: a brief overview. MITRE Nanosyst. Gr
61. Sharma P, Bhatti TS (2010) A review on electrochemical double-layer capacitors. Energy Convers Manag 51:2901–2912. https://doi.org/10.1016/j.enconman.2010.06.031
62. Zhang K, Xu J, Zhu X, Lu L, Duan X, Hu D, Dong L, Sun H, Gao Y, Wu Y (2015) Poly(3,4-ethylenedioxythiophene) nanorods grown on graphene oxide sheets as electrochemical sensing platform for rutin. J Electroanal Chem 739:66–72. https://doi.org/10.1016/j.jelechem.2014.12.013
63. Rajesh M, Raj CJ, Manikandan R, Kim BC, Park SY, Yu KH (2017) A high performance PEDOT/PEDOT symmetric supercapacitor by facile in-situ hydrothermal polymerization of PEDOT nanostructures on flexible carbon fibre cloth electrodes. Mater Today Energy 6:96–104. https://doi.org/10.1016/j.mtener.2017.09.003
64. Mohd Abdah MAA, Abdul Rahman N, Sulaiman Y (2018) Enhancement of electrochemical performance based on symmetrical poly-(3,4-ethylenedioxythiophene) coated polyvinyl alcohol/graphene oxide/manganese oxide microfiber for supercapacitor. Electrochim Acta 259:466–473. https://doi.org/10.1016/j.electacta.2017.11.005
65. Qu J, Shi L, He C, Gao F, Li B, Zhou Q, Hu H, Shao G, Wang X, Qiu J (2014) Highly efficient synthesis of graphene/MnO_2 hybrids and their application for ultrafast oxidative decomposition of methylene blue. Carbon N Y 66:485–492. https://doi.org/10.1016/j.carbon.2013.09.025
66. Wei W, Cui X, Chen W, Ivey DG (2011) Manganese oxide-based materials as electrochemical supercapacitor electrodes. Chem Soc Rev 40:1697–1721. https://doi.org/10.1039/c0cs00127a
67. Radhamani AV, Krishna Surendra M, Ramachandra Rao MS (2018) Tailoring the supercapacitance of Mn_2O_3 nanofibers by nanocompositing with spinel-$ZnMn_2O_4$. Mater Des 139:162–171. https://doi.org/10.1016/j.matdes.2017.11.005
68. Liu Y, Liu M, Zheng P, Ge D, Yang L (2019) Controllable hydrogel-thermal synthesis of Mn2O3/CNT aerogels: shape evolution, growth mechanism and electrochemical properties. Mater Des 182:108022. https://doi.org/10.1016/j.matdes.2019.108022
69. Toupin M, Brousse T, Bélanger D (2004) Charge storage mechanism of MnO_2 electrode used in aqueous electrochemical capacitor. Chem Mater 16:3184–3190. https://doi.org/10.1021/cm049649j
70. Yang CM, Kim BH (2019) Incorporation of MnO_2 into boron-enriched electrospun carbon nanofiber for electrochemical supercapacitors. J Alloys Compd 780:428–434. https://doi.org/10.1016/j.jallcom.2018.11.347
71. Mahendrakar S, Anna M, Reddy MJ (2015) Structural, morphological and FTIR of PVDF-HFP and lithium tetrafluoroborate salt as polymer electrolyte membrane in lithium ion batteries. Int J Chem Technol Res 8:319–328
72. MacCallum JR, Vincent CA (1989) Polymer electrolyte reviews. Springer Science & Business Media
73. Chong MY, Numan A, Liew CW, Ng HM, Ramesh K, Ramesh S (2018) Enhancing the performance of green solid-state electric double-layer capacitor incorporated with fumed silica nanoparticles. J Phys Chem Solids 117:194–203. https://doi.org/10.1016/j.jpcs.2018.02.030
74. Tripathi M, Kumar A (2018) Zinc oxide nanofiller-based composite polymer gel electrolyte for application in EDLCs. Ionics (Kiel) 24:3155–3165. https://doi.org/10.1007/s11581-018-2504-8

75. Lu M (2013) Supercapacitors: materials, systems, and applications. Wiley
76. Becker HI (1954) US2800616 low voltage electrolytic capacitor patent
77. Boos DL, Heights G (1970) Electrolytic capactor having carbon pasteelectrodes. US Pat. 3536963 https://patents.google.com/patent/US3536963A/en%0A. https://patentimages.storage.googleapis.com/dd/14/f7/6429b072356a4f/US3536963.pdf
78. Tale B, Nemade KR, Tekade PV (2021) Graphene based nano-composites for efficient energy conversion and storage in Solar cells and supercapacitors: a review. Polym Technol Mater 60:784–797. https://doi.org/10.1080/25740881.2020.1851378
79. Murphy TC, Wright RB (1997) US department of energy electrochemical capacitor. In: Proceedings of the symposium on electrochemical capacitors II, The Electrochemical Society, p 258
80. Narayanan S, Pankajakshan AE, Padmanabhan VT, Joseph A (2022) Conducting polymer nanocomposites for supercapacitorshttps://doi.org/10.1201/9781003174646-2
81. Arasakumari KSM (2021) Effect of anhydrous Gdcl3 doping on the structural, optical and electrical properties of PVP polymer electrolyte films. Res Sq
82. AK MDS, Rajprasad KR, Aravind CV, Wong YW (2016) Cost effective design fabrication of a low voltage vertical axis wind turbine. Int J Control Theory Appl (Serial Publ. 9), 2827–2833
83. Khan MSA, Rajkumar RK, Wan WY, Syed A (2018) Supercapacitor-based hybrid energy harvesting for low-voltage system. Supercapacitors Theor Pract Solut, 1–22. https://doi.org/10.5772/intechopen.71565
84. Gul H, Shah AHA, Bilal S (2019) Achieving ultrahigh cycling stability and extended potential window for supercapacitors through asymmetric combination of conductive polymer nanocomposite and activated carbon. Polymers (Basel) 11. https://doi.org/10.3390/polym11101678
85. Yang CM, Kim YJ, Endo M, Kanoh H, Yudasaka M, Iijima S, Kaneko K (2007) Nanowindow-regulated specific capacitance of supercapacitor electrodes of single-wall carbon nanohorns. J Am Chem Soc 129:20–21. https://doi.org/10.1021/ja065501k
86. Izadi-najafabadi A, Yamada T, Futaba DN, Yudasaka M, Takagi H, Hatori H (2011) High-power supercapacitor electrodes nanotube composite, 811–819
87. Choi KS, Liu F, Choi JS, Seo TS (2010) Fabrication of free-standing multilayered graphene and poly(3,4-ethylenedioxythiophene) composite films with enhanced conductive and mechanical properties. Langmuir 26:12902–12908. https://doi.org/10.1021/la101698j
88. Pringle JM, Armel V, MacFarlane DR (2010) Electrodeposited PEDOT-on-plastic cathodes for dye-sensitized solar cells. Chem Commun 46:5367–5369. https://doi.org/10.1039/c0cc01400a
89. Imoto K, Takahashi K, Yamaguchi T, Komura T, Nakamura JI, Murata K (2003) High-performance carbon counter electrode for dye-sensitized solar cells. Sol Energy Mater Sol Cells 79:459–469. https://doi.org/10.1016/S0927-0248(03)00021-7
90. Wang G, Xing W, Zhuo S (2009) Application of mesoporous carbon to counter electrode for dye-sensitized solar cells. J Power Sources 194:568–573. https://doi.org/10.1016/j.jpowsour.2009.04.056
91. Susmitha K, Kumari MM, Berkmans AJ, Kumar MN, Giribabu L, Manorama SV, Raghavender M (2016) Carbon nanohorns based counter electrodes developed by spray method for dye sensitized solar cells. Sol Energy 133:524–532. https://doi.org/10.1016/j.solener.2016.03.059
92. Kausar A (2021) Green nanocomposites for energy storage. J Compos Sci 5. https://doi.org/10.3390/jcs5080202
93. Yang X, Fei B, Ma J, Liu X, Yang S, Tian G, Jiang Z (2018) Porous nanoplatelets wrapped carbon aerogels by pyrolysis of regenerated bamboo cellulose aerogels as supercapacitor electrodes. Carbohydr Polym 180:385–392. https://doi.org/10.1016/j.carbpol.2017.10.013
94. Çıplak Z, Yıldız A, Yıldız N (2020) Green preparation of ternary reduced graphene oxide-au@polyaniline nanocomposite for supercapacitor application. J Energy Storage 32:101846. https://doi.org/10.1016/j.est.2020.101846
95. Kalaiarasi J, Pragathiswaran C, Subramani P (2021) Green chemistry approach for the functionalization of reduced graphene and ZnO as efficient supercapacitor application. J Mol Struct 1242:130704. https://doi.org/10.1016/j.molstruc.2021.130704

Part VIII
Economics and Commercialization of FNMs Based Supercapacitor

Всё для победы!
НАРОДНЫЙ ФРОНТ
https://pobeda.onf.ru/
LET'S HELP THE RUSSIA

Всё для победы!

НАРОДНЫЙ
ФРОНТ

https://pobeda.onf.ru/

LET'S HELP THE RUSSIA

Chapter 25
Current Trends in the Commercialization of Supercapacitors as Emerging Energy Storing Systems

Aqib Muzaffar, M. Basheer Ahamed, and Chaudhery Mustansar Hussain

1 Introduction

The evolution and rapid development of industrialization in the diverse fields has resulted in the rise of energy requirements to cater to the progress and to meet the growing energy demands [1]. The combination of these two factors has strayed a major dent in the existing energy harvesting and delivering infrastructure, thereby posing severe concerns on the future of both human race and industrialization. Up to twentieth century, most of the energy demands were met by the utilization of fossil fuels. However, the limited energy harvested from these sources has led to the exploration of alternative energy sources, since the beginning of twenty-first century [2]. In recent lines, there has been enormous amount of interest in exploring and development of new energy sources to address the energy challenges. In this context, most of and development has been devoted towards the creation of efficient and low-cost sources, like rechargeable batteries, supercapacitors and fuel calls [3–5]. Particularly, supercapacitors among the mentioned devices are the most promising devices, due to their versatility and overwhelming characteristics [6].

Supercapacitors commonly called electrochemical capacitors formulate one of the most efficient energy-storing devices dedicated to store electrical energy [7]. They are often referred to as the bridging devices between batteries and conventional capacitors to tender advantages like higher power and energy density along with faster charging and discharging kinetics, low cost, long cyclic life, low maintenance and

---

A. Muzaffar · M. B. Ahamed (✉)
Department of Physics, B.S. Abdur Rahman Crescent Institute of Science and Technology, Chennai, Tamil Nadu 600048, India
e-mail: basheerahamed@crescent.education

C. M. Hussain
Department of Chemistry and Environmental Science, New Jersey Institute of Technology, Newark, NJ, USA

© The Author(s), under exclusive license to Springer Nature Singapore Pte Ltd. 2024

C. M. Hussain and M. B. Ahamed (eds.), *Functionalized Nanomaterials Based Supercapacitor*, Materials Horizons: From Nature to Nanomaterials,
https://doi.org/10.1007/978-981-99-3021-0_25

most importantly no environmental pollution [8–12]. Generally, supercapacitors are designed and dedicated for high-power delivery systems, when compared to rechargeable batteries. However, in the last few decades, there has been a gradual expansion in research and development of supercapacitors to surpass the usage of fossil fuels and rechargeable batteries. In this context, various nanostructured materials have been explored to develop next generation supercapacitors [13–15]. The utilization of nanostructured materials for supercapacitors provides better capacitances along with other electrochemical properties than their bulkier counterparts.

The nanostructured materials provide better electrochemical activity with features like better electrochemical kinetics, constrained diffusion paths for ions, higher active surface area along with probation of additional active sites for electrochemical reactions. Supercapacitors apart from these features nowadays require compatibility with the environment to deliver higher performance thereby enhancing their applicability to ensure their place in the commercial market. The commercial aspects associated with any device require parameters like industrial control, miniaturization of devices, power, transportation, etc. Currently, supercapacitors devices occupy a benign marketplace and are mostly used in transportation, defence, medical, communication and hybrid electric vehicles. However, their potential can be extended to many fields thereby understanding the market and designing the devices to suffice the requirements. The extensive exploration of supercapacitors presents unlimited opportunities along with extreme challenges.

This chapter is dedicated to portray supercapacitor insights in terms of historical perspective to understand the developmental phases of supercapacitors along with their commercialization. The opportunities and challenges arising in their development are also discussed.

2 Historical Aspects of Supercapacitors

The history of supercapacitor backs to 1970s and 1980s as an energy-storing option for commercialization using a polarized electrolyte solution. The device was portrayed to perform energy storing activity, intermediate to the conventional capacitors and batteries [16]. Based on charge storing mechanism, supercapacitors are mainly categorized into two main types, viz., electric double layer capacitor (EDLC) and pseudocapacitors. The former stores energy based on the electrostatic means, and the later involves reversible redox reactions of faradaic nature for energy storage. EDLC's rely layer charge storing at the electrode–electrolyte interface while as pseudocapacitors rely more on redox reactions at the interfacial boundary between the electrode and the electrolyte.

Generally, batteries were the main source of energy for the short duration instruments, while as Supercapacitors serve in the applications requiring faster charging/ discharging power kinetics [17]. The applicability of supercapacitors in regenerative braking utilizes the heat power recovery for, the goods and passengers in the hybrid electric vehicles. The high power output delivered by the supercapacitors marks their potent candidature for next generation energy storing devices. However, supercapacitors suffer from comparatively low energy storing capacity as that of batteries thereby utilizing per unit mass of the active material or by utilization of active area in the material. Supercapacitors and batteries both are dependent on electrochemical reactions for energy storage. Thus, for the devices using electrochemical principle of energy storage, the energy storing perspective has led to extensive growth in the research and development of new materials tendering heavy to extreme capacity for energy storage along with relatively smaller recharging speeds for both batteries and supercapacitors [18]. The differentiating factor between supercapacitors and batteries, however, is the electrochemical reactions responsible for charge storage. In batteries (Li-ion battery), the addition of Li-ion causes redox reactions in the materials of the bulk electrodes where in the process kinetics are relatively slower due to ionic diffusion However, in supercapacitors, (EDLC), the ionic adsorption (from electrolyte onto the electrode) is responsible for energy storage. In supercapacitors, the variations in potential in terms of response are more rapid than power thereby leading to faster charging/discharging activity [19]. The batteries can be differentiated from supercapacitors on the basis of potentio-static and galvanostatic methods [20].

These characterization methods are used to depict double-layer capacitances based on the constant current time-dependence against a linear potential variation to yield rectangular-shaped plots [21]. On the other hand, in pseudocapacitors, the behaviour is depicted from reversible reactions occurring at the surfaces of the respectable electrodes enabling higher charge storage [22]. This type of pseudo or false capacitance dictates the energy storage encompassing capacitive behaviour. The key performance parameter evaluation from the supercapacitor is illustrated in Fig. 1.

The commercialized research regarding supercapacitors finds its presence in historical perspectives in countries like the USA, Russia, Japan, France, South Korea and other European countries. The prominent commercial brands for supercapacitors include Maxwell from the USA, Tokin, NEC and Panasonic from Japan, Econd from Russia, etc. The properties of EDLC were estimated early in 1879 by Von Helmholtz thereby proposing the concept of double layer.

However, the concept of a double layer has been applied for energy storage in the last few decades [23]. The applicability of supercapacitors as energy-storing devices was proposed by Becker in 1957 due to their specific energy being in close proximity to the standard batteries. The first patent for a double-layer capacitor was proposed by the oil Corporation Sohio in 1968 using carbonaceous materials with high specific surface areas. Later NEC started to produce supercapacitor systems for electric vehicles starting in 1979. Panasonic also started to develop supercapacitors using activated carbon as the active material for the electrodes immersed in an organic electrolyte around the same time. Since then supercapacitor market has seen continuous growth in terms of industrialization on a higher scale with the introduction of new supercapacitor devices. Supercapacitor industrialization on a massive scale began in the 1980s; Generation-1980NEC is manufacturer with the introduction of supercapacitor products from Panasonic and Mitsubishi in 1987. Later in 1990, Econd and ELIT also introduced their supercapacitors dedicated to

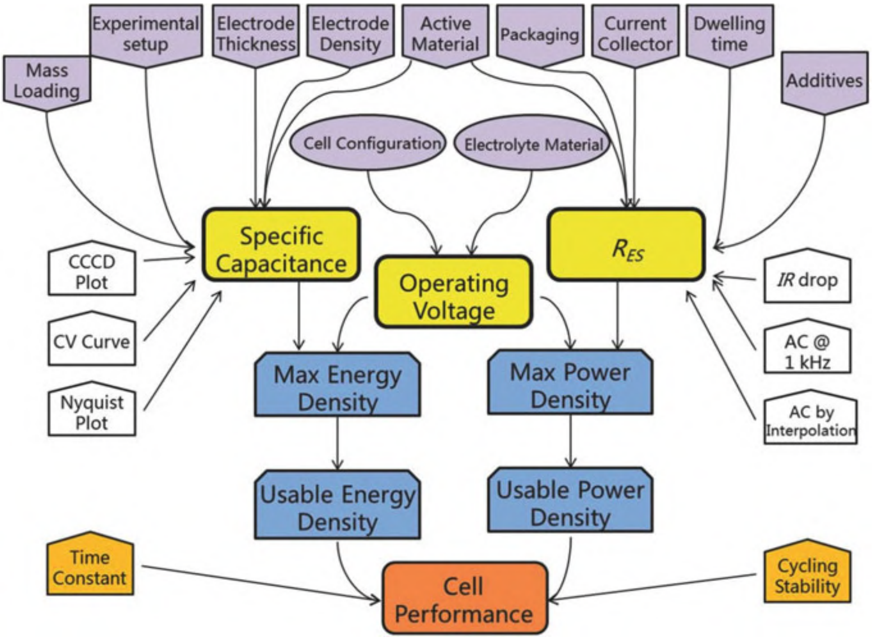
Mass Loading
Experimental setup
Electrode Thickness
Electrode Density
Active Material
Packaging
Current Collector
Dwelling time
Additives
Cell Configuration
Electrolyte Material
Specific Capacitance
Operating Voltage
R_{ES}
CCCD Plot
CV Curve
Nyquist Plot
IR drop
AC @ 1 kHz
AC by Interpolation
Max Energy Density
Max Power Density
Usable Energy Density
Usable Power Density
Time Constant
Cell Performance
Cycling Stability

Fig. 1 Schematic diagram of key performance parameters, test methods, major affecting factors for the assessment of supercapacitors [17]

high power delivery. Currently, in commercial markets, the companies like NEC, Panasonic, Maxwell, EPCOS and NESS are extensively active in the exploration and development of supercapacitors.

Currently, products from Japan, Russia and USA occupy the entire supercapacitor market with supercapacitors from each country tendering their unique features in terms of power delivery, capacitance, energy cost and so on. Supercapacitors due to their unique blend of characteristics have attracted global attention since their introduction to the commercial market. The rise in the expansion of global demand has found a new bright spot in the field of chemical power. As per a report from Bosch, during 2007–2022, the research and development regarding commercialization has major investment from China with a global market estimation of \$16 × 107 up to 2015. As per the report, the supercapacitor market is expected to exceed the \$95 × 109 mark by the end of 2023. The annual growth for the market is expected to rise by 40%. Considering these figures, the supercapacitor market is growing globally at a brisk pace. The breakthrough in terms of material advancements along with device fabrication has improved supercapacitor performance to a significant extent thereby yielding new-generation supercapacitors for industrialization on a high scale. Furthermore, supercapacitor products have become well established with the scope for applicability rising continuously. Supercapacitors have been extensively used in the medical field, defence, transportation and communication, etc. [24, 25].

Supercapacitor in the last few decades has evolved as special energy-storing devices ranging from small-power to large-scale power applications. In addition to that the combination of supercapacitors with batteries and fuel cells as hybrid devices has also been explored tendering a unique set of advantages. In general, supercapacitors present brilliant performance advantages leading to their extensive research portrayed towards a variety of applications with exceptional potential for electronic industries and markets. Thus, supercapacitors in future have been portrayed to exhibit limitless opportunities as next-generation energy-storing devices.

3 Fundamentals of Energy Storage

The electrical energy can be stored directly without the incorporation of transformation steps in devices like capacitors and inductances. Both of these devices are widely used in electronic devices to electricals ranging from electric motors with glued large capacitors to power plants using large transformers [26]. These devices are also found in mobile phones and microelectronics as inductances and capacitances in the miniaturized form [27]. The principle behind energy-storing devices live supercapacitors seems not suitable for large-scale energy storage due to amount of energy stored in them. For instance, an inductance stores energy upto 216 kWh at a maximum current of 5700 A with a self-inductance of 48 Hy at the optimum weight of 276 tonnes as installed at CERN, Geneva in hydrogen bubble chambers. For large-scale energy storing projects (5000–10,000 M Wh), as per the analysts, it is estimated to include large coils of huge diameter thereby engulfing higher magnetic fields requiring underground or remote installations. Similarly, disappointing results have been attained from similar considerations for capacitances [28]. However, both capacitances and inductances for energy storage attract great interest despite fundamentally being capable of storing and delivering energy at rapid and high rates. Thus, there exists substantial and growth in terms of interest for applicability. Although considering inductances, very limited scope is at the stake but for capacitors huge progress has been made beyond conventional dielectric capacitor [29].

The energy (electrical) can be stored as electric U in a capacitor as capacitance C as

$$C = \frac{Q}{U} \tag{1}$$

wherein the stored energy W and the power at constantly varying E (ΔE) as at constant voltage (V) is given by expression:

$$W = \frac{1}{2}C(\Delta E)^2 = \frac{1}{2}C(U)^2 \tag{2}$$

and

$$P = \frac{W}{t} \tag{3}$$

$$\Rightarrow P = \frac{(\Delta E)^2}{\mathrm{ESR}} = \frac{(U)^2}{\mathrm{ESR}} \tag{4}$$

wherein $\Delta E = U$ is the difference of electric potential between the capacitor plates (electrodes), in a capacitor, t is the duration and ESR denotes the equivalent series resistance of the device [30]. ESR comprises the sum of all ohmic components within the capacitor device sandwiched between the current collectors. The resistance incorporates resistances from electrodes, electrolyte ions, current collectors, electrode mass, etc. The value of ESR for supercapacitors ranges from milli-Ohms to few Ohms varying from material to material.

The energy W and power P follows common relation with time. During charging, the supercapacitor undergoes decreasing current thereby leading to decline in power. As per Eq. (4), the changes are spontaneous. However, relation between the voltage, power and ESR is uncertain wherein power is equivalent to the product of current and voltage, where current (I = U/ESR) follows relation with voltage and ESR (internal). Thus Eq. (4) stays valid up to certain time during discharging. The maximum value of energy for supercapacitor is considered at the beginning of discharge, wherein the resulting power designates the maximums power.

The capacitance C of capacitor depends on the area A of the plates/electrodes and the dielectric constant ε_r of the material sandwiched between the plates as determined by the relation:

$$C = \frac{\varepsilon_0 \varepsilon_r}{d} \ A \tag{5}$$

(ε_0 = dielectric constant of medium).

The capacitance and energy storage follow a direct correlation however by enhancement in operating potential can cause relatively large impact on both energy as well as the capacitance.

Initially the supercapacitors (EDL) were developed with an aim to increase electrode surface areas which could be envisaged to the formulation of electrolytic capacitor later termed as the double-layer capacitor [31].

To attain larger values of capacitance, large size electrodes must be considered. This principle however does not hold true for supercapacitors. For supercapacitors, it is the material properties which determine its electrochemical capacitance irrespective of being used in bulk or large size. Also the interfacial interaction between the electrode and electrolyte to greater extent determines the value for specific capacitance along with the active material utilizations. In supercapacitors, the charge is generally stored at the interfaces of the electrode and electrolyte [32].

The charge storage in supercapacitors is accompanied by localized gathering of electrons from the conduction band occupying an electronically conducting phase followed by the simultaneous gathering of counterbalancing ions in the ion-conducting phase. Finally, the energy storage in the supercapacitor follows dependence on the potential difference existing between the electrodes, which in turn are dependent on the change difference between the electrodes. The capacitance outcome for supercapacitors stays substantial due to device conductance in the form of electronically conducting electrodes and ionically conducting electrolytes, combined to attain feasible charge movement during device charging/discharging.

Apart from porous carbonaceous materials, the addition of metal oxides when explored for supercapacitors displayed surface-confined redox reactions; that is the formation of oxide or hydroxide layer on the electrode surfaces followed by reaction products. The hydroxide ion in the reaction stands strongly adsorbed onto the metallic surfaces and displays a current response accompanied by varying electrode potential thereby yielding interfacial capacitances termed pseudocapacitance or redox capacitance [33]. Pseudocapacitance generally describes the electrode's response to the current towards the varying potential as depicted in cyclic voltammetry. It is important to highlight here that the redox response observed in the battery system although being analogous stays different to that of pseudocapacitance. In battery electrodes, the charge transfer reaction occurs within itself with accumulation/decumulation taking place at the electrode/electrolyte solution interface, thereby yielding reaction products. The adsorption of ions strengthens the interaction between the adsorbed ions in response to the electrode potential to demonstrate current responses at the specific conditions thereby displaying a capacitive shape in the voltammograms.

The influence of metal oxide properties with values of band gaps along with the relative positions of band edges, in contrast to the electrochemically approachable electrode potential, stays central to capacitive behaviour [34]. The electrochemically attainable sites in the metal oxides stay pivotal to the conduction band thereby, enabling no charge transfer. As a consequence, limited specific capacitance is attained from metal oxides. The utilization of metallic or metal compound surfaces exhibiting larger specific surface area in contact with electrolyte solution, the specific capacitance and in particular pseudocapacitance exceeds 10–100 times than the double layer capacitance in terms of the actual electrode surface can be attained [35]. In supercapacitors, there exist unlimited possibilities to attain maximum parameter output when explored to the fullest potential.

4 Upscale of Supercapacitors for Commercialization

The success of any product in the commercial market stays central to the cost. For any product after the research and development stages, for industrial upscale, the costs are involved in materials, production and the marketing. The lower the costs are, the more output can be generated in terms of productivity. However, the costs are recovered from the scale of the product sales. The success of the product in the commercial market is the main contributor demand for its economic fame. Thus, lowering supercapacitor costs and price becomes a vital step in the domination of the future markets. The pricing of supercapacitors is not proportional to value per farads. However, the supercapacitor cost and pricing depends on the material and production costs. For high-purity carbon-based supercapacitors, the cost is about \$70/kg thereby portraying the competitive potential of supercapacitors in terms of \$ per kW of energy with respect to other energy-storing devices. Currently, there is huge potential for low, cost energy-storing devices. However, it has been only a few years, since supercapacitors are considered as serious devices in the field of energy storage.

For the commercial market, most of the supercapacitors are fabricated from carbonaceous material with a standard device fabricated from them, yielding capacitance of 100 F g^{-1} with a market cost of \$20 per kg [36]. As per trade estimates, the supercapacitor cell prices are expected to decline due to advancements in material technology thereby translating to a cost of about \$0.0082 F g^{-1} with significant performance enhancement with manufacturing efficiency profits. Furthermore, the prices can still be lowered by enhancing the operating potential for the supercapacitors up to 3.5 V. As such, materials like graphene and nanocarbons are nowadays implied in commercial markets to provide higher capacitance. The market for supercapacitors as per estimates contributed to \$470 million in the year 2010, thereafter reaching \$1.2 billion in the year 2015. The demand after that has eventually doubled in the years after and is estimated to reach \$5 billion in 2025 [37].

The market for supercapacitors in the electronic industry for memory protection is estimated at \$1.34 billion per year [38, 39]. The possibilities are further extended to the portable electronic devices market and the power quality market to aid distributed generation [40, 41]. The supercapacitors market has already been extended to hybrid cars to ensure low emission and also in the transportation industry (buses and trucks). The growth of supercapacitors in the commercial market puts traditional capacitors and batteries on the same page in terms of energy storage delivery. The economic feasibility of supercapacitors as mass energy storing devices can be intrigued by enhancing their energy density to higher values to attain faster charging/discharging activity along with low cost. It has already been established that supercapacitors are high power delivery devices capable of fast discharge; however, they suffer from low energy density. Supercapacitors are generally environmentally friendly, lead-free, safe disposal off and restriction of hazardous substances compliant, thereby rising their preference for industrialization.

The most important and costly components for supercapacitors are the electrodes, electrolyte materials and separator material. Most commercial supercapacitors use electrodes composed of bulk carbon with macropores leading to micropores. The energy density enhancements in supercapacitors following the replacement of battery along with time constant for electrolytic solution replacement in supercapacitors stay exohedral. This means that materials in the nanostructure form like allotropes of carbon like graphene and carbon nanotubes have shown great promise. In particular, graphene has shown better results in terms of electrochemical activity, but the commercial aspect of graphene as a supercapacitor remains uncertain. Bigger supercapacitors are portrayed to be used in electric vehicles, power grids, railways, regenerative braking and other applications. The supercapacitors are considered to replace batteries eventually in vehicles for regenerative braking and bus door opening. Furthermore, they are anticipated to replace inverter capacitors also. The transportation sector presents a huge market opportunity, concerned with engine starting, electrical system augmentation, for braking energy regeneration, torque delivery and thrusts of power for idle start/stop processes [42].

For supercapacitors, the designing enhancements, low-cost manufacturing and assembly along with volumetric sales, all together have contributed to the improvements in managing the manufacturing costs over the recent years. The research and development have been anticipated to increase, considering the industrial point of view. The brands in future energy implicate their dominance for power storage while currently, supercapacitors are emerging as a replacement option for fuel in efficient transportation.

Supercapacitors continue to gain applicability in applications requiring storage and delivery of high-energy output with quick time intervals. The projections of supercapacitors continue to emerge as the bright energy-storing devices in markets due to technological evolutions. As per studies, supercapacitor sales in the USA in 2016 were about $400 million [43]. The reported study by Zion Market Research of Sarasota, Florida, had projected to grow from $684.7 million in 2016 to over $2 billion by the end of 2022 at an annual compound growth rate of 20.5%. In another report, by Research and Markets, the compound annual growth rate for supercapacitors is portrayed at 18.6% from 2017 to 2018 thereby achieving the target of $2.44 billion [44]. The different commercially available supercapacitors are listed in Table 1 [2]. The more anticipated estimates from ID Tech Ex suggest the growth of energy storage devices (supercapacitors) in the market to a tenfold value. ID Tech Ex projected expected growth for supercapacitors as per their estimates at 2 billion by the end of 2026 in contrast to $240 million currently. Supercapacitors are expected to earn the $800 million to $1 billion mark considering their potential market opportunity [45]. Their report suggests the limitations towards the exponential or rapid growth of supercapacitors due to features like high cost and lack of industrial exploitation. Supercapacitor manufacturers continue to improve in terms of technological advancements thereby enhancing power handling and overall performance for the supercapacitors.

5 Importance of Supercapacitors in Current Markets

Supercapacitors exhibit advantages that highly overshadow the limitations of different commercially available energy storage devices. As such supercapacitors have gained enormous popularity in terms of academics and commercial markets [46]. Supercapacitors generally are capable of delivering and generating higher power densities when compared with batteries or fuel cells. On the other hand, they display higher energy density when compared to the dielectric capacitors. The Ragone for different energy-storing devices is depicted in Fig. 2, correlating specific power to

Table 1 Different supercapacitors available in commercial market with their characteristics. Reproduced with copyright permission from Ref. [2]. © 2019 Elsevier Ltd. All rights reserved

Manufacturer	Series name	Capacitance (F)	Cell voltage (V)	Specific power (W kg^{-1})	Specific energy (Wh kg^{-1})	Remarks
A PowerCap	A PowerCap	4–2800	2.7	900	$\leq$4.5	–
AVX	BestCap	0.05–0.56	3.6	–	$\leq$0.13	Modules upto 20 V
Asahi Glass	–	1375	2.7	390	4.9	–
Batscap	–	1680	2.7	2050	4.2	–
CapXX	CapXX	0.17–2.1	2.5	$\leq$2.2	–	–
CDE	Ultracapacitor	0.1–1.0	3.6	–	–	–
Cooper	PowerStor	0.22–3000	2.5/2.7	–	–	Modules upto 62 V
ELNA	DYNACAP POWERCAP	0.047–1500	2.5/3.6	–	–	–
Evans	Capattery	0.001–10	5.5…125	–	–	Hybrid Capacitor
FastCAP Systems	EEX	340–460	1.3	$\leq$10.5	–	–
Green Tech	Supercapacitor	2–600	2.7/2.8	–	–	Modules upto 64 V
Illinios	Supercapacitor	0–3800	2.3/2.7	$\leq$8.6	$\leq$6.6	–
Loxus	Ultracapacitor	100–300	2.7	$\leq$8.7	$\leq$6.4	Modules upto 130 V
JSR Micro	Ultimo	1100–3300	3.8	$\leq$20	$\leq$12	Li-Ion capacitor
Korchip	STARCAP	0.02–400	2.5/2.7	$\leq$7.0	$\leq$6.1	–
LS Mtron	Ultracapacitor	100–3400	2.7/2.8	900	4.45	Modules upto 130 V
Maxwell	BoostCap	1–3400	2.2/2.8	–	$\leq$6.0	Modules upto 160 V
Murata	EDLC	0.22–1.0	4.2/5.5	$\leq$27	$\leq$13.1	2 cells in series
NEC Tokin	Supercapacitor	0.047–200	2.7/11	–	–	
NesCap	EDLC, Pseudocapacitor	3–1800 50–5085	2.7	975, 958	$\leq$4.5 $\leq$8.7	Modules upto 125 V
Nichion	EverCAP	1.0–6000	2.5/2.7	–	–	–
NCC, ECC	DLCCAP	350–2300	2.5	–	–	–
Panasonic	GoldCap	0.1–1200	2.3/2.5	514	2.3	Modules upto 15 V

(continued)

Table 1 (continued)

Manufacturer	Series name	Capacitance (F)	Cell voltage (V)	Specific power (W kg^{-1})	Specific energy (Wh kg^{-1})	Remarks
Power Sys (PC)	–	1350	2.7	650	4.9	–
Samwha	GreenCap, ESD-SCAP	3–7500	2.5/2.7	≤7.6	≤7.0	–
Skeleton	SkelCap	250–4500	2.85	≤14.1	≤10.1	Modules upto 350 V
Taiyo Yuden	PAS capacitor LIC capacitor	0.5–20 0.5–27	2.5/3 3.8	–	–	Pseudocapacitor Li-ion capacitor
VinaTech	Hy-Cap	1–500	2.3/3.0	≤8.7	≤6.3	–
Vishay	ENYCAP	4–15	1.4	–	–	Modules upto 8.4 V
WIMA	SuperCap	100–3000	2.5	–	–	Modules upto 28 V
YEC	Kapton Capacitor	0.5–400	2.7	–	–	–
Yunasko	Ultracapacitor	480–1700	2.7	–	–	Modules upto 48 V

the specific energy [21]. From the plot, it is evident that supercapacitors are the intermediate energy storing and conversion devices to the normal capacitors and batteries in terms of both energy and power delivery factors. In addition to that, supercapacitors exhibit features like longer cyclic life in contrast to batteries due to smaller chemical phase changes in the electrodes while undergoing charging/discharging [47, 48]. Supercapacitors also feature environment friendliness along with a variety of materials capable of exploration. Thus, supercapacitors are versatile and attractive devices, considering high-powered energy storage and hence portrayed to play a major role and energy storing technology [49].

Additionally, supercapacitor provides flexible, lightweight and portable energy downing option, thereby portraying their significance in portable and more miniaturized electronic devices and wearable electronics further strengthening their role in the upcoming year. In commercial terms, huge efforts have been dedicated for improving the performance characteristics of supercapacitor components for their commercial viability. An immense amount of progress has been made in terms of supercapacitor material design and material development, which symbolize two key applicability areas for supercapacitors, viz., electrode and electrolyte material. Considering electrode materials for supercapacitors, the impetus has been on the development of high-capacitive materials including carbonaceous materials, metal oxides and polymeric composites. On the other hand, considering the electrolytes, the most important criterion requiring enhancement is the widening of the potential window. Supercapacitors

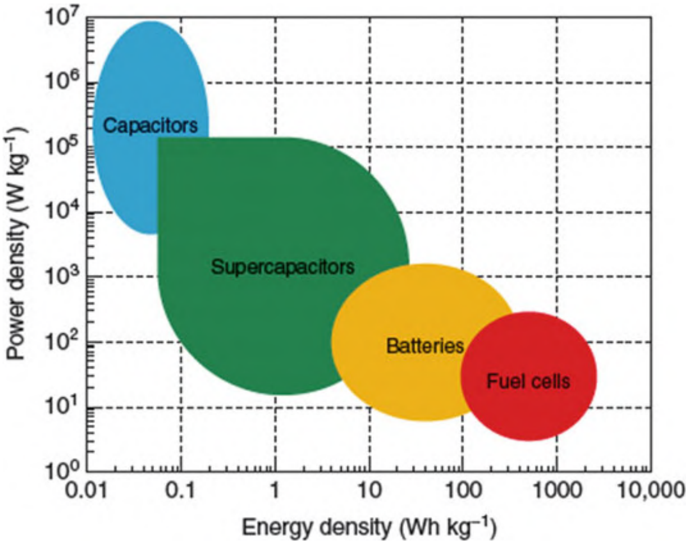

Fig. 2 Ragone plot for different energy storing devices. Reproduced with copyright permission from Ref. [21]

hence are portrayed to hold an important and strategic position in the next-generation energy storage and delivery devices using electrochemical conversion and storage principle.

6 Applicability of Supercapacitors in Marked and Economy

Supercapacitors were produced to provide a backup power supply in electronics as their main application. Contrary to that, supercapacitors exhibited a tendency to discharge large amounts of power within seconds, hence making them ideal for providing uninterrupted and instant power supply during surges in energy or shutdown. In comparison, batteries are considered to be non-ideal for this type of application due to the involvement of more expenses in addition to temperature escalations beyond control [50, 51].

The longer cyclic life and high power delivery characteristics of supercapacitors marks their applicability for both military and consumer applications. In particular, Coleman's portless and cordless screwdrivers powered by supercapacitors are feasible commercially for home usage. The screwdriver exhibits quick charging, taking only one minute and thirty seconds for a full charge [52]. For military applications, supercapacitors are used as power delivery devices for electronics in armed vehicles, in black boxes in fighter aircraft and helicopters [53].

In transportation, supercapacitors find their applicability for energy recovery. by hybrid electric vehicles. In public transportation, the primary challenge erupts in the form of energy harvesting from regenerative means. In particular, energy harvesting from regenerative braking due to frequent stops in public transportation can be reused while accelerating the vehicle. Supercapacitors exhibit the remark tendency to store instantaneous energy while braking and discharge at the time of requirement to enhance fuel efficiency.

The rapid growth of flexible energy-storing devices is growing enormously these days for their potential applicability in portable electronics. In this regard, the new addition to supercapacitors in the form of flexible energy storage devices holds an essential position. Flexible supercapacitors provide advantages like lightweight, a high degree of flexibility along with reduced interfacial resistance when compared with normal supercapacitors. In particular, solid-state flexible supercapacitors composed of flexible and solid-state electrodes and electrolytes are manufactured along with solid-state separators and flexible packaging material [54]. The manufacturing process of these energy-storing devices is relatively low and involves simplistic processing. These flexible supercapacitors are currently used in wearable electronic devices including LEDs and smart watches [53].

7 Summary and Commercial Perspective of Supercapacitors

Currently, supercapacitors are available in the market in the form of modules or cells. The potential window for supercapacitors commercially lies in the range of 0–3 V [55]. Supercapacitors available in the market can reach up to the values of 1000–10,000 Farads [56]. The packaging design for such supercapacitors is depicted in Fig. 3. To attain maximum capacitance values, the supercapacitor dimensions are altered [57, 58].

The technical aspects of a commercial supercapacitor capable of functioning at 25 °C are accomplished by the use of an organic electrolyte. The aspects of such commercial supercapacitor cells are elaborated on in Table 2 [55]. For Commercial supercapacitor cells listed in Table 2, the electrochemical parameters can be varied depending on the organic electrolytes and the manufacturing agency. It is noteworthy to mention here that higher outcomes in terms of energy and power can be attained based on the maximum operating potential. From a manufacturing perspective, the energy and power parameters can vary based on the weight and cell volume.

The application of aqueous electrolytes in supercapacitors for commercial market tenders maximum operating potential of up to 2 V. Due to low operating potential the capacitance value for these supercapacitors is generally low. The comparison of a commercial supercapacitor using organic and aqueous electrolytes is provided in Table 3 [55]. The results commend the ideology lower potential enabled lower output. However, significant improvement in terms of capacitance can be achieved

Fig. 3 Commercial Packaging sketch for supercapacitor cells available (cylindrical and prismatic packaging modules). Adapted with courtesy from Ref. [55]

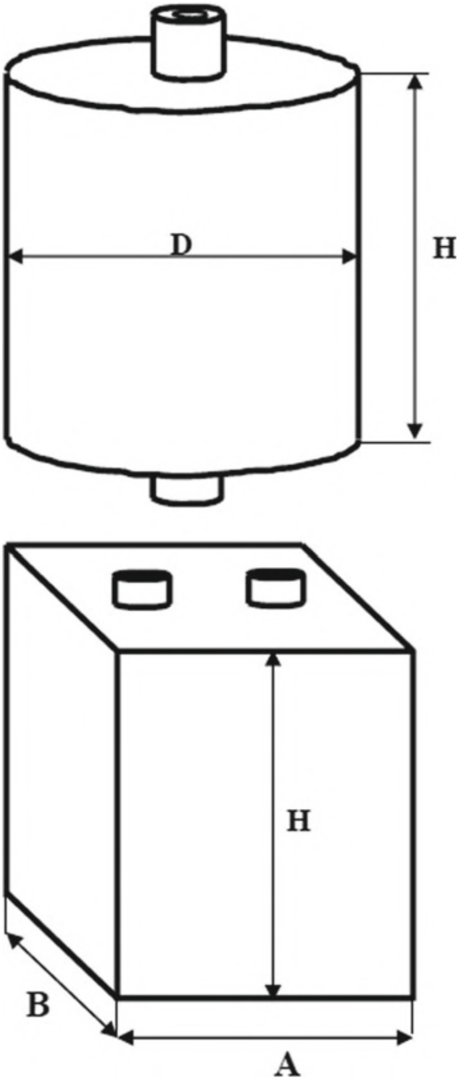

using an aqueous electrolyte instead of an organic one, involving higher weight or volume than that using an organic electrolyte in the cells.

The promising results obtained while using aqueous electrolytes are portrayed in Table 4. However, the supercapacitors enlisted, manufactured by ESMA are yet to be viable commercially. For aqueous electrolytes, higher specific capacitance values can be attained based on the higher weight or volume of electrolytes [55].

The supercapacitor devices employing higher weight or volume of aqueous electrolytes, manufactured by ESMA are enlisted in Table 5 [55]. These supercapacitors relatively display higher specific energy when compared to those mentioned in

Table 2 Properties of commercial supercapacitors using organic electrolyte technology. Adapted with courtesy from Ref. [55]

Technical specifications	NESSCAP Cell-type ESHSP 500C002R7	EPCOS Cell-type B49410B-2506Q0000
Rated capacitance (F)-tolerance (%)	5000 −10%, +20%	5000 −10%, +30%
Rated voltage, V_g (V)	2.7	2.5
Maximum internal resistance (mΩ)	0.35 (0.4)	(0.2) 0.35
Maximum leakage current (mA)	22	No specification
Surge voltage (V)	2.85	2.8
Maximum stored energy at V_g (Joule)	18,225 (5.06 Wh)	15,625 (4.34 Wh)
Specific energy (Wh kg^{-1}) at V_g	5.69:7.10	4.10:4.70
Specific power (kW kg^{-1})	5.12:6.39*	2.00:2.3**
Weight (g)	890	1050
Volume (mL)	713	930
Operating temperature range (°C)	−40 … +60	−30 … +70
Cyclic life (cycles)	500,000	500,000

* The cell load is equal with its internal resistance
** The cell load is higher than its internal resistance

Table 1 using organic electrolytes. The manufacturing alterations and optimizations can yield lower weight or volume of electrolyte for functionality. Consequently, the specific power for these devices is significantly low when compared with those using organic electrolytes. However, the supercapacitor systems using aqueous electrolytes can enable significantly high capacitance values in contrast to organic electrolytes [59].

The concept of making use of accessible energy generated using regenerative processes and designated power systems capable of operating at the potential in the range of 2–5 are required. Supercapacitors are delivering energy during regenerative braking in trains and public transportation. The supercapacitors dedicated to this purpose are connected together following a series connection in a module of the cells to maintain balance within the module [60]. It is also necessary to maintain cell voltage within specific frame rates during the operation. The properties of supercapacitor modules dedicated to high energy are listed in Table 5 [55]. The listed modules depict a trend, wherein the decline in both specific power and energy is observed while following a series cell connection into a module. The supercapacitors from the manufacturing companies like EPCOS and NESSCAP follow a desired pattern at lower rated voltages. While at voltages listed in the table, the supercapacitor modules tend to portray higher values for energy as well as power, thereby promising their applicability in renewable energy or power quality applications. The

Table 3 Comparison of supercapacitor cells characteristics using organic and aqueous electrolyte technology for commercial market. Adapted with courtesy from Ref. [55]

Technical specifications	Maxwell technologies Cell-type BCAP3000P270	ESMA Cell-type (aqueous electrolyte)
Rated capacitance (F)	3000	3200
Rated voltage, V_g (V)	2.7	1.5
Maximum internal resistance (mΩ)	0.24 (0.29)	0.6 (0.9)
Maximum leakage current (mA)	5.2	5
Surge voltage (V)	No Specifications	1.6
Maximum stored energy at V_g (Joule)	10,935 (3.04 Wh)	3600 (1 Wh)
Specific energy (Wh kg^{-1}) at V_g	5.52:6.4	2.94:5.12
Specific power (kW kg^{-1})	5.12:6.39*	2.64:4.61*
Weight (g)	550	340
Volume (mL)	475	195
Operating temperature range (°C)	−40 … +65	−50 … +50
Cyclic life (cycles)	100,000	>300,000

* The supercapacitor load is equal with its internal resistance

energy output in such modules is proportional to the number of cells used in series with values of capacitance reaching up to values of 45,000–80,000 F with higher energy storage attainable.

8 Challenges and Future Opportunities

Supercapacitors find their applicability in transportation, military, electronics, industry and communication fields due to their excellent electrochemical properties. However, supercapacitors also suffer from some hard comings. The challenges for supercapacitors are categorized in terms of technical terms, consistency along with industrial standards for commercialization.

Table 4 Aqueous electrolyte-based cells with higher capacitance values instead of using organic electrolytic cells. Adapted with courtesy from Ref. [55]

Technical specifications	ESMA Cell-type EC501	ESMA Cell-type EC404
Rated capacitance (F)	6000	14,000
Rated voltage, V_g (V)	1.5	1.6
Maximum internal resistance (mΩ)	0.3 (0.5)	0.4 (0.6)
Maximum leakage current (mA)	10	10
Surge voltage (V)	1.6	1.75
Maximum stored energy at V_g (Joule)	6750 (1.87 Wh)	17,920 (4.98 Wh)
Specific energy (Wh kg^{-1}) at V_g	2.67:4.80	5.53:9.05
Specific power (kW kg^{-1})	2.57:4.80*	2.00:3.27*
Weight (g)	700	900
Volume (mL)	389	550
Operating temperature range (°C)	−50 … +50	−50 … +50
Cyclic life (cycles)	>300,000	100,000

* The supercapacitor load is equal with its internal resistance

The energy densities of supercapacitors are relatively low when compared to their counter electrochemical devices. In terms of energy density, currently supercapacitors deliver energy <20 Wh kg^{-1} commercially in comparison to the batteries delivering 30–200 Wh kg^{-1} of energy density. Therefore for commercial supercapacitors as well, the improving factor still remains of energy density as the main challenging aspect requiring a lot of research focus [61, 62]. The consequent improvements in manufacturing processes along with technological advances stay an effective and efficient approach to attain desired results thereby improving the storage capacity of commercial supercapacitors. For long-term results, it is essential to develop new electrode and electrolyte materials to attain higher electrochemical performance. It is essential to develop compact devices capable of storing the higher amounts of energy in contrast to bulkier devices. Already an effective approach for enhancing the electrode surface area to provide more electrochemically active sites along with increasing the operating potential of electrolytes has featured a lot of research development. Currently, most of research and innovation are focused on the development of novel electrode and electrolyte materials to meet the challenges.

The other challenge in the development of supercapacitors arises in terms of establishing a standard model. For instance, the supercapacitor model developed for a certain application may be ideal but for other applications, the model may lack feasibility. The supercapacitor standard model developed by manufacturers may be ideal for commercial applications, however, when the same model features in military

Table 5 Supercapacitors with high capacitance output using aqueous electrolytes. Adapted with courtesy from Ref. [55]

Technical specifications	ESMA Cell-type EC303	ESMA Cell-type EC353
Rated capacitance (F)	45,000	80,000
Rated voltage, V_g (V)	1.6	1.7
Maximum internal resistance (mΩ)	0.2 (0.3)	0.5 (1.0)
Maximum leakage current (mA)	30	No specification
Surge voltage (V)	1.75	1.75
Maximum stored energy at V_g (Joule)	57,600 (16 Wh)	115,600 (32 Wh)
Specific energy (Wh kg^{-1}) at V_g	6.15:9.51	13.33:19.02
Specific power (kW kg^{-1})	1.23:1.90*	0.58:0.80*
Weight (g)	2600	2400
Volume (mL)	1682	1682
Operating temperature range (°C)	−50 … +50	−50 … +50
Cyclic life (cycles)	100,000	>10,000

* The supercapacitor load is equal with its internal resistance

applications (requiring power supply) or in aircraft/spacecrafts or satellites, many potential risks are observed, which cannot be neglected. Thus designing reliability stays an important challenge while dedicating supercapacitors for suitable applications, considering, the impact on load nature, external environmental fluctuations to ensure device stability [63]. The commercialization on huge-scale for supercapacitors is mainly limited due to low-rated voltages (up to 2.7). This means for practical usage, a lot of series connections are required to attain the desired storage. The enhancement of rated voltage for supercapacitors in applications will provide better response. Supercapacitors require high current while charging/discharging during their functionality in a system. At lower rated voltage, the overcharging of supercapacitor becomes a serious issue which alters the life of the supercapacitors. Therefore, it is essential to establish consistent voltage in supercapacitors irrespective of being connected in series or not.

Generally, supercapacitors have shorter development time at fast speeds when it comes to industrialization. The development of supercapacitors under healthy industrial standards along with market supervision stays essential to develop practical standards for the industry to meet global energy storage standards. As such establishment of technical standard models like classification models, electrical performance model, safety testing, specification description methods, charging/discharging parameters and requirements, production requirements, transportation of devices and disposal becomes important to establish device market. However standardization of these models for industrial upscale is necessary to promote and ensure the healthy development of supercapacitor industries.

9 Conclusion

Supercapacitors are one of the most researched and explored devices using electrochemical principle of energy storage and conversions to store and deliver energy. Supercapacitors find an important place in establishment of next generation devices based on utilization of electrochemical energy. This chapter has presented and attempt to elaborate commercial aspects of supercapacitors in accordance with current market trends.

References

1. Muzaffar A, Ahamed MB, Deshmukh K, Thirumalai J (2019) A review on recent advances in hybrid supercapacitors: design, fabrication and applications. Renew Sustain Energy Rev 101:123–145
2. Afif A, Rahman SM, Azad AT, Zaini J, Islan MA, Azad AK (2019) Advanced materials and technologies for hybrid supercapacitors for energy storage–a review. J Energy Storage 25:100852
3. Chakraborty S, Mary NL (2022) An overview on supercapacitors and its applications. J Electrochem Soc
4. Muzaffar A, Ahamed MB (2019) Iron molybdate and manganese dioxide microrods as a hybrid structure for high-performance supercapacitor applications. Ceram Int 45(3):4009–4015
5. Muzaffar A, Muthusamy K, Basheer Ahamed M (2019) Ferrous nitrate–nickel oxide ($Fe(NO_3)_2$–NiO) nanospheres incorporated with carbon black and polyvinylidenefluoride for supercapacitor applications. J Electrochem Energy Convers Storage 16(3)
6. Muzaffar A, Basheer Ahamed M, Deshmukh K (2019) Hydrothermal synthesis of $ZnWO_4$–MnO_2 nanopowder doped with carbon black nanoparticles for high-performance supercapacitor applications. J Mater Sci Mater Electron 30(24):21250–21258
7. Huang S, Zhu X, Sarkar S, Zhao Y (2019) Challenges and opportunities for supercapacitors. APL Mater 7(10):100901
8. Armand M, Tarascon JM (2008) Building better batteries. Nature 451(7179):652–657
9. Etacheri V, Marom R, Elazari R, Salitra G, Aurbach D (2011) Energy Environ Sci 4(9):3243–3262
10. Manthiram A (2011) Materials challenges and opportunities of lithium ion batteries. J Phys Chem Lett 2(3):176–184
11. Vlad A, Singh N, Rolland J, Melinte S, Ajayan PM, Gohy JF (2014) Hybrid supercapacitor-battery materials for fast electrochemical charge storage. Sci Rep 4(1):4315
12. Muzaffar A, Ahamed MB, Deshmukh K (2021) Conducting polymer electrolytes for flexible supercapacitors. Flex Supercapacitor Nanoarchitectonics, 233–262
13. Muzaffar A, Basheer Ahamed M, Deshmukh K (2021) Nature-Inspired electrodes for flexible supercapacitors. Flex Supercapacitor Nanoarchitectonics, 549–573
14. Pandolfo T, Ruiz V, Sivakkumar S, Nerkar J (2013) General properties of electrochemical capacitors. Supercapacitors Mater Syst Appl, 69–109

15. Zhang Z, Mu S, Zhang B, Tao L, Huang S, Huang Y, Gao F, Zhao Y (2016) A novel synthesis of carbon nanotubes directly from an indecomposable solid carbon source for electrochemical applications. J Mater Chem A 4(6):2137–2146
16. Boicea VA (2014) Energy storage technologies: the past and the present. Proc IEEE 102(11):1777–1794
17. Karthikeyan S, Narenthiran B, Sivanantham A, Bhatlu LD, Maridurai T (2021) Supercapacitor: evolution and review. Mater Today Proc 46:3984–3988
18. Miller JR, Simon P (2008) Electrochemical capacitors for energy management. Science 321(5889):651–652
19. Holze R (2015) In: Béguin F, Frąckowiak E (eds) Supercapacitors–materials, systems, and applications. Springer, Heidelberg, 2009. (ISBN: 978-0-387-76423-8) 106.95€
20. Simon P, Gogotsi Y (2013) Capacitive energy storage in nanostructured carbon–electrolyte systems. Acc Chem Res 46(5):1094–1103
21. Kim BK, Sy S, Yu A, Zhang J (2015) Electrochemical supercapacitors for energy storage and conversion. In: Handbook of clean energy systems, pp 1–25
22. Conway BE (1991) Transition from "supercapacitor" to "battery" behavior in electrochemical energy storage. J Electrochem Soc 138(6):1539
23. Augustyn V, Simon P, Dunn B (2014) Energy Environ Sci 7(5):1597–1614
24. Dusastre V, Martiradonna L (2017) Materials for sustainable energy. Nat Mater 16(1):15–15
25. Blay V, Galian RE, Muresan LM, Pankratov D, Pinyou P, Zampardi G (2020) Research frontiers in energy-related materials and applications for 2020–2030. Adv Sustain Syst 4(2):1900145
26. Shen PK, Wang CY, Sun X, Zhang J (2018) Electrochemical energy: advanced materials and technologies. CRC Press
27. Mastragostino M, Soavi F, Arbizzani C (2002) Electrochemical supercapacitors. In: Advances in lithium-ion batteries, pp 481–505
28. Yaseen M, Khattak MAK, Humayun M, Usman M, Shah SS, Bibi S, Hasnain BSU, Ahmad SM, Khan A, Shah N, Tahir AA (2021) A review of supercapacitors: materials design, modification, and applications. Energies 14(22):7779
29. Wang G, Zhang L, Zhang J (2012) A review of electrode materials for electrochemical supercapacitors. Chem Soc Rev 41(2):797–828
30. Forouzandeh P, Kumaravel V, Pillai SC (2020) Electrode materials for supercapacitors: a review of recent advances. Catalysts 10(9):969
31. Conway BE, Pell WG (2003) Double-layer and pseudocapacitance types of electrochemical capacitors and their applications to the development of hybrid devices. J Solid State Electrochem 7:637–644
32. Young MJ, Holder AM, George SM, Musgrave CB (2015) Charge storage in cation incorporated α-MnO_2. Chem Mater 27(4):1172–1180
33. Chen Y, Zhou C, Liu G, Kang C, Ma L, Liu Q (2021) Hydroxide ion dependent α-MnO_2 enhanced via oxygen vacancies as the negative electrode for high-performance supercapacitors. J Mater Chem A 9(5):2872–2887
34. Dubal DP, Wu YP, Holze R (2016) Supercapacitors: from the Leyden jar to electric busses. ChemTexts 2:1–19
35. Olabi AG, Abbas Q, Al Makky A, Abdelkareem MA (2022) Supercapacitors as next generation energy storage devices: properties and applications. Energy 248:123617
36. Storage GE (2013) US department of energy, Washington, DC, USA
37. Lux Research, Inc. News & Events, Market for Supercapacitors; Lux Research, Inc.: Boston, MA, USA. http://www.luxresearchinc.com/news-and-events/press-releases/read/market-supercapacitorsgrow-128-836-million-2018. Accessed 11 May 2016
38. Gidwani M, Bhagwani A, Rohra N (2014) Supercapacitors: the near future of batteries. Int J Eng Inven 4(5):22–27
39. BCC Research (2011) Technology developments & global markets, supercapacitors: EGY068A; BCC Research: Wellesley, MA, USA
40. U.S. Securities & Exchange Commission. File # 001-15477; U.S. Securities & Exchange Commission: Washington, DC, USA. https://www.sec.gov/Archives/edgar/data/319815/00003198151600009z. Accessed 21 Feb 2017

41. Tecate Group. What Is an Ultracapacitor; Tecate Group: San Diego, CA, USA. https://www.tecategroup.com/app_notes/0_Tecate_Group_What%20is%20an%20ultracapacitor.pdf. Accessed 3 Dec 2015
42. Todd R, Wu D, dos Santos Girio JA, Poucand M, Forsyth AJ (2010 Feb) Supercapacitor-based energy management for future aircraft systems. In: 2010 twenty-fifth annual IEEE applied power electronics conference and exposition (APEC), pp 1306–1312. IEEE
43. Zogbi DM (2016) The global supercapacitor market is facing unique challenges in 2016, TTI, Inc. http://www.ttieurope.com/object/mezogbi-20161003.html. Accessed 20 Jul 2017
44. Chin S (2017) Supercapacitor market projected to grow from $684.7 million in 2016 to Over $2 billion by 2022
45. Gonzalez F (2017) Supercapacitor technologies and markets 2016–2026. IDTechEx. http://www.idtechex.com/research/reports/supercapacitor-technologies-and-markets-2016-2026-000486.asp. Accessed 21 Jul 2017
46. Cheng BH, Tian K, Zeng RJ, Jiang H (2017) Preparation of high performance supercapacitor materials by fast pyrolysis of corn gluten meal waste. Sustain Energy Fuels 1(4):891–898
47. Yu A, Davies A, Chen Z (2011) Electrochemical supercapacitors. Electrochem Technol Energy Storage Convers 1:317–382
48. Chen W, Rakhi RB, Hu L, Xie X, Cui Y, Alshareef HN (2011) High-performance nanostructured supercapacitors on a sponge. Nano Lett 11(12):5165–5172
49. Goodenough JB (2007) Basic research needs for electrical energy storage. https://www.osti.gov/servlets/purl/935429
50. Yu A, Chabot V, Zhang J (2013) Electrochemical supercapacitors for energy storage and delivery: fundamentals and applications. Taylor & Francis, p 383
51. Münchgesang W, Meisner P, Yushin G (2014 Jun) Supercapacitors specialities-technology review. In: AIP conference proceedings, vol 1597, no 1. American Institute of Physics, pp 196–203
52. Chun HW, You IK (2014) Market and technology trends in supercapacitor. Electron Telecommun Trends 29(5):186–194
53. Ozoemena KI, Chen S (eds) (2016) Nanomaterials in advanced batteries and supercapacitors. Springer, Switzerland, p 423
54. Chen X, Paul R, Dai L (2017) Carbon-based supercapacitors for efficient energy storage. Natl Sci Rev 4(3):453–489
55. Obreja VVN (2007) On the performance of commercial supercapacitors as storage devices for renewable electrical energy sources. Surge 5:5
56. https://www.tdk-electronics.tdk.com/
57. https://maxwell.com/products/ultracapacitors/downloads/
58. Han C, Huang AQ, Li D, Mamath H, Ingram M, Atcitty S (2006 Mar) Modeling and design of a transmission ultracapacitor (TUCAP) integrating modular voltage source converter with ultracapacitor energy storage. In: Twenty-first annual IEEE Applied Power Electronics Conference And Exposition. APEC'06. IEEE, 7-pp
59. Klementov AD, Litvinenko SV, Stepanov AB, Varakin IN (2001 Dec) Internal losses and features of asymmetric capacitor operation. In: The 11th international seminar on double layer capacitors
60. Linzen D, Buller S, Karden E, De Doncker RW (2005) Analysis and evaluation of charge-balancing circuits on performance, reliability, and lifetime of supercapacitor systems. IEEE Trans Ind Appl 41(5):1135–1141
61. Zhao Y, Ran W, He J, Song Y, Zhang C, Xiong DB, Gao F, Wu J, Xia Y (2015) Oxygen-rich hierarchical porous carbon derived from artemia cyst shells with superior electrochemical performance. ACS Appl Mater Interfaces 7(2):1132–1139
62. Zhao Y, Zhang Z, Ren Y, Ran W, Chen X, Wu J, Gao F (2015) Vapor deposition polymerization of aniline on 3D hierarchical porous carbon with enhanced cycling stability as supercapacitor electrode. J Power Sources 286:1–9
63. Laheäär A, Przygocki P, Abbas Q, Béguin F (2015) Appropriate methods for evaluating the efficiency and capacitive behavior of different types of supercapacitors. Electrochem Commun 60:21–25

Part IX

Future of Functionalized Nanomaterials Based Supercapacitor

Всё для победы!
НАРОДНЫЙ
ФРОНТ
https://pobeda.onf.ru/
LET'S HELP THE RUSSIA

Chapter 26
Future of Nanotechnology and Functionalized Nanomaterials

D. A. Nayana, Nithya S. George, S. Nandakumar, Arun Aravind, and P. K. Manoj

1 Introduction

Nanotechnology results in a huge impact on day-to-day life of human beings. As described from past decades, ‘nanotechnology’ is the branch of science in which the material’s length scale is limited to 1–100 nm. It is time to elaborate this definition more widely to incorporate many developments in the field of nanotechnology. As per Richard Jones, today industries are based on incremental and evolutionary nanotechnology, which involves improving the properties of materials by controlling their nanoscale structure, the production of nanoscale devices with interesting behaviour, including solid-state lasers, quantum dots and sensors respectively [5]. New approaches were needed to tackle the challenges and limitations of future nanotechnology. Nowadays, nanomaterials have a huge impact on various fields of research and engineering.

As per the survey conducted by Royal Society and Royal Academy of Engineering, the concerns and fears regarding nanotechnology were pointed out, which suggests the toxicity of evolving particles. It is always necessary to find efficient solutions to the existing problems involving human health and environmental friendliness [6]. The functionalized nanomaterials, which are currently being developed with a keen scientific eye and scientific patience, are the smart materials of the future material science field. Suitable surface functionalization and modification of nanoparticles

---

D. A. Nayana · P. K. Manoj (✉)
Department of Physics, TKM College of Arts and Science, Kollam, Kerala 691005, India
e-mail: pkmanoj@gmail.com

N. S. George · S. Nandakumar · A. Aravind (✉)
Centre for Advanced Functional Materials (CAFM), Department of Physics, Bishop Moore College (Research Centre affiliated to University of Kerala), Mavelikara, Kerala 690110, India
e-mail: arun@bishopmoorecollege.org

© The Author(s), under exclusive license to Springer Nature Singapore Pte Ltd. 2024

C. M. Hussain and M. B. Ahamed (eds.), *Functionalized Nanomaterials Based Supercapacitor*, Materials Horizons: From Nature to Nanomaterials,
https://doi.org/10.1007/978-981-99-3021-0_26

will enhance their interaction with the rest of the environment [7]. Surface characteristics such as corrosivity, hydrophobicity, hydrophilicity and conductivity of nanoparticles can be modified by surface functionalization. The current impact of multifunctional nanoparticles is notable because in biomedical applications, they enhance the cellular targeted drug delivery [8]. Here we are dealing with the significance of using FNM, various synthesis strategies associated with it, discussing about some highly interesting FNM materials and the recent updates of FNM in various fields.

2 Need for Functionalized Nanomaterials

The development of nanotechnology is increasing with new approaches and maximising the value proposition. The material properties were enhanced by tailoring the nanomaterials structural characteristics [9]. Functionalized nanomaterials are materials developed by considering the faults and limitations of bare nanomaterials with applications including wastewater treatment, biomedical application, water purification, nanobiotechnology, bioenergy and other industrial applications. The functionalized properties of the nanomaterials were investigated in a variety of applications. In functionalization of nanomaterials, various organic molecules and polymers were attached to the surface by different synthesis methods which enhanced the properties of the materials. It will result in making environmentally friendly materials with increased surface-active sites, higher stability, a reduced bandgap and improved reactivity. The main step is to choose the proper linkage material for developing functionalized nanomaterials. Now we are dealing with different synthesis methods employed in functionalization which is discussed below.

3 Methods for Functionalizing Nanomaterials

Surface properties can be modified or enhanced by tailoring the nanoparticle during the synthesis step. Nanoparticles can be functionalized by using various sources in the synthesis technique, such as polymers, dendrimers, biomolecules, surfactants and other inorganic molecules. Hydrophobicity can be developed by treating nanoparticles with hydrophobic molecules such as oleic acid, dodecanethiol, oleylamine, dodecanethiol, triphenylphosphine and tetraoctylammonium bromide during synthesis. Similarly, hydrophilicity can be incorporated by the use of polyethylene glycol, mercaptosuccinic acid, mercaptoacetic acid, mercaptoundecanoic acid. etc. as we have seen in previous reports [10]. These types of surface modifications take time through various synthesis strategies which are depicted in the flowchart (Fig. 1). It includes the use of chemisorption and physisorption methods including (say) the attachment of a thiol group on the surface of nanoparticles and the milling

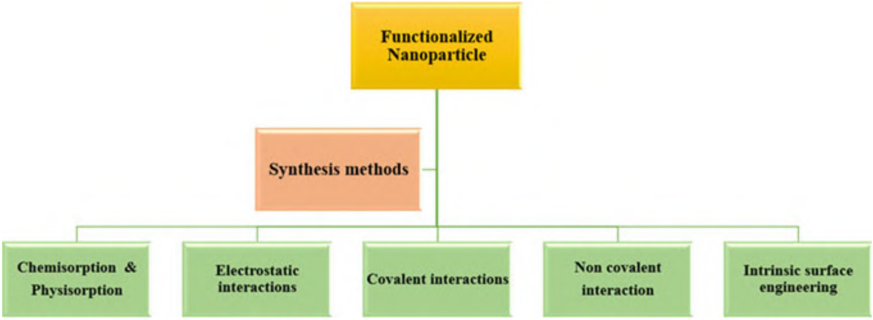
Functionalized Nanoparticle
Synthesis methods
Chemisorption & Physisorption
Electrostatic interactions
Covalent interactions
Non covalent interaction
Intrinsic surface engineering

Fig. 1 Different synthesis strategies employed in functionalization of nanoparticles

method respectively. The electrostatic interaction involves the attraction of negatively charged nanoparticles and positively charged small molecules and vice versa. Covalent interaction is done using the interaction of functional groups of nanoparticles and attaching molecules. Another synthesis strategy involving the non-covalent interaction or the supramolecular affinity is related to the receptor-ligand system and the weak interaction between the molecule and the nanoparticle. Surface engineering is also used, where the incorporation of heteroatoms is accomplished either by defect engineering.

3.1 Covalent Functionalization

Molecular functionalization involves the covalent and non-covalent functionalization of nanoparticles. Covalent functionalization entails using covalent bonds to attach chemical species to nanoparticles. It is widely used in connecting with biomolecules, polymers and organic/inorganic molecules to attain better properties. Different chemical variants attached by means of covalent bonds with the nanomaterials resulted in covalent functionalization. It is well explored because of its wide applicability in various fields such as agriculture, industrial, environmental, biomedical application, catalysis and cosmetics enhancing the basic properties of metal oxide nanoparticles, two-dimensional (2D) derivatives of nanoparticle including Graphene Oxide (GO), layered Transition Metal Dichalcogenides (TMDs), boron nitrides and Carbon Nanotubes (CNTs). The attachment of chemical species like biomolecules, polymers and organic/inorganic molecules to the surface of nanoparticles helps with better adsorption and other viable properties. Most commonly, the covalent functionalization using heterobifunctional cross-linker molecules for the functionalization of proteins, peptides, oligonucleotides and nanoparticles is based on [11],

1. Organofunctional alkoxysilanes
2. Glutaraldehyde (GA)
3. N-hydroxysuccinimide (NHS)
4. 1-ethyl-3-(3-dimethylaminopropyl) carbodiimide (EDC)

Treccani et al. briefly explained the covalent functionalization by silanization, GA, NHS and EDC protocols [12]. Nanoparticles involving 2D derivatives of layered hydroxides, and carbon-based materials such as GO, oxidised CNTs, metal oxides, hydroxyl functionalized boron nitride nanosheets and TMDs can be engineered or modified using the above-mentioned protocols. The incorporation of various groups such as –COOH, –OH and –NH_2 groups on nanomaterials can enhance their dispersibility, effectiveness and can tune the nanomaterial's structure and properties. Table 1 denotes various FNMs with functionalization methods and applications.

Table 1 Various FNMs with functionalization method and applications

FNM	Functionalization method	Specific functional groups	Application/ FNM properties	Ref
Hexagonal Boron Nitride	Covalent chemical functionalization	Alkoxy groups and hydrolytic de functionalization	Enhanced mechanical properties, efficient polymer reinforcement	[13]
GO nanosheets	Salinization protocol	3-Aminopropyltrimethoxysilane (APTMS) coated graphene by oxo-vanadium Schiff base	Efficient catalytic reactivity for oxidation of various alcohols	[14]
SWCNT & MWCNT	Covalent functionalization	Functionalization using heteroarene Iodonium salts and substituted arene	Incorporated many functional groups—electron rich and electron poor arenes, esters and heteroarenes	[15]
MoS_2 & Ag- MoS_2 nanocomposite	Covalent functionalization	Organic functional group decorated TMD using thiol reagents as ligands (mercaptopropionic acid, 1-thioglycerol and L-cysteine)	High density of nucleation sites due to -COOH groups	[16]
Fe_3O_4 and $NaYF_4$: Yb, Er	Covalent coupling method	Carboxyl-functionalized magnetic Fe_3O_4, amino functionalized-silica coated $NaYF_4$: Yb, Er	Biolabeling and fluorescent imaging of cancer cells—Magnetic luminescent multifunctional nanoparticles	[7]

3.2 Noncovalent Functionalization

In non-covalent functionalization, there exist attractive and repulsive forces between the molecules. Foreign material gets adsorbed on the surface of the nanomaterial by chemisorption or physisorption mechanisms. It is mostly preferred for the surface modification in carbon-based materials. The molecules used for the non-covalent functionalization of carbon-related materials enhance the dispersion of nanomaterials in various polymer-based compounds [17]. Functionalization of mesoporous materials with suitable ligands confers desirable properties for the nanostructures including high surface area and rapid reaction kinetics which will act as effective adsorbents for capturing contaminants from wastewater and in other applications too [18].

The following are the main steps in polymer coatings of nanoparticles:

1. The surface of nanoparticle has been functionalized by using a suitable molecule which serves as the instigator for rest of the interfacially controlled polymerization.
2. The synthesis of such polymer material is followed by surface anchoring.

An example for polymer wrapping is shown in Fig. 3. The proposed method has its benefits of managing the surface density of that desired polymer synthesised and the length of polymer chains [20]. Figures 2 and 4 depict the surface functionalization of Iron oxide nanoparticles. Magnetic Fe_3O_4 nanoparticles are an effective adsorbent for various toxic metals from aqueous media. But the functionalization of these materials is challenging since the iron surfaces bound with the complex groups will result in chemical inertness. To solve this, several research projects were reported. The problem can be eliminated by a two-step non-covalent functionalization of nanomaterials [18].

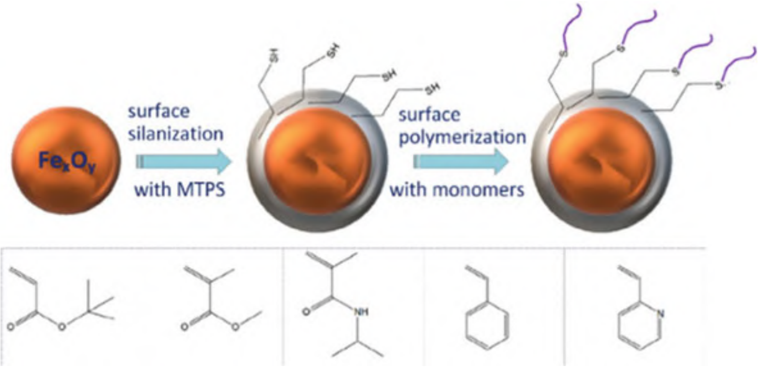

Fig. 2 Surface functionalization of Iron Oxide nanoparticles. Reproduced with permission from [19]. Copyright 2021, Elsevier

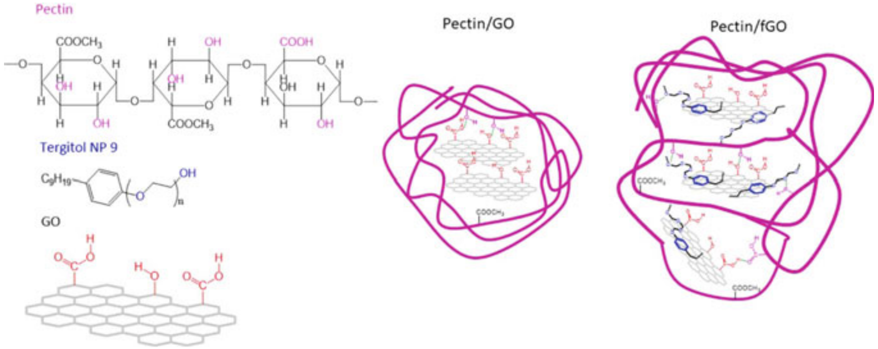
Pectin
COOCH₃
OH
COOH
COOCH₃
Tergitol NP 9
C₉H₁₉
OH
GO
Pectin/GO
Pectin/fGO
COOCH₃

Fig. 3 Diagram showing the chemical structure of pectin, tergitol nanoparticles, schematic representation of GO and interaction between pectin/GO and pectin/GOf* nanocomposites (*pectin funtionalised GO). Reproduced with permission from [17]. Copyright 2017, Elsevier

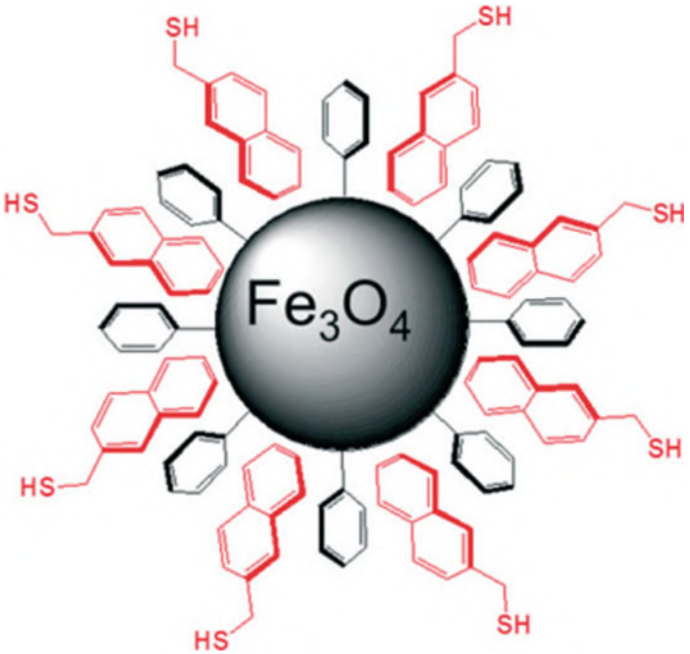

Fig. 4 Schematic diagram of non-covalently functionalized Fe_3O_4 nanoparticles. The phenyl ligand shell (in black) helps non-covalent interaction with the thiol bearing layer. Reproduced with permission from Ref. [18]. Copyright 2015, Royal Society of Chemistry

3.3 Intrinsic Surface Engineering

Surface functionalization or 'intrinsic surface engineering' emerged as a new advanced application in smart materials. The eccentric potential of smart materials emerged primarily as a result of surface functionalization, which changes existing pristine material properties or develops new ones. The methods include surface ligand bonding, incorporation, defect engineering and patching, an effective method to tune the intrinsic physical properties of functionalized nanomaterials (Fig. 5).

Several research works focused on the functionalization of nanomaterial surfaces by various structures including polymers (example in Fig. 6), silica, hybrid structures and inorganic nanoparticles [19]. Bond formation with surface ligands will overcome the mechanical deformations and overall morphological changes. The ligands attaching to the surface of nanoparticles will form a capping layer that separates the material from the surrounding environment and will control the nucleation and growth during the synthesis of nanostructures. Thus, ligands can effectively influence the optical and electronic properties of nanomaterials.

The ability to engineer the surface patches in nanostructures holds great importance. When the material surface is heated above the glass transition temperatures, the polymer patches will melt which has huge potential in many applications in various fields of optics and catalysis.

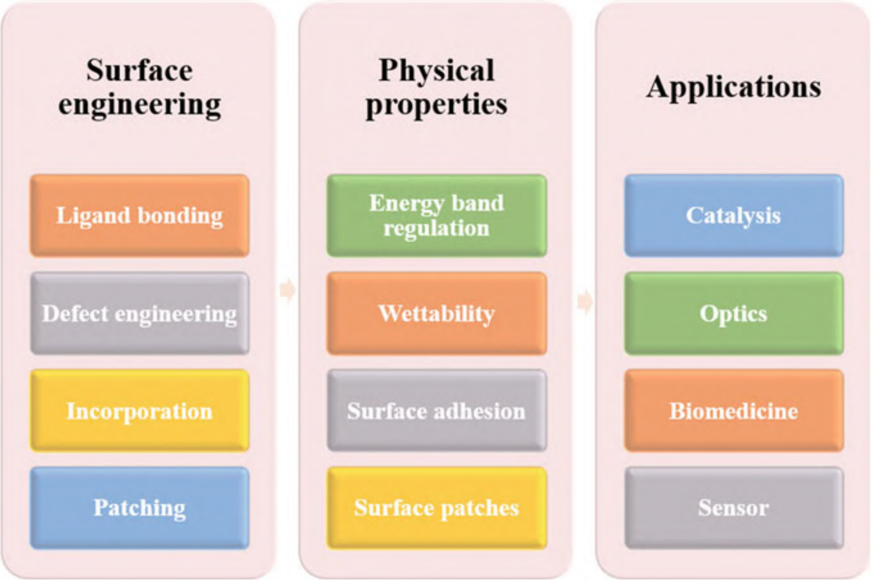
Surface engineering
Ligand bonding
Defect engineering
Incorporation
Patching
Physical properties
Energy band regulation
Wettability
Surface adhesion
Surface patches
Applications
Catalysis
Optics
Biomedicine
Sensor

Fig. 5 Surface engineering strategies for developing functional nanomaterials with specific physical properties and applications

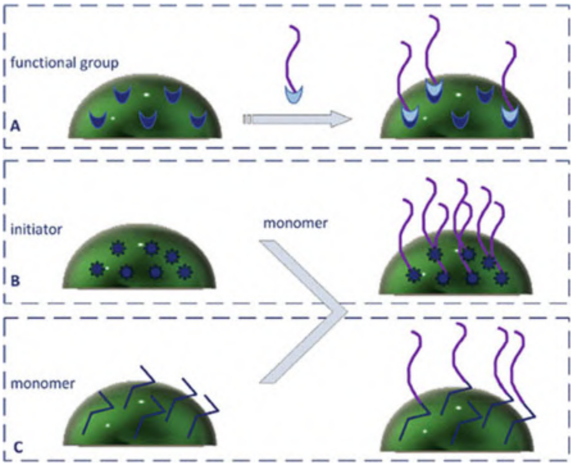

Fig. 6 Surface modification of the nanoparticles by polymers using **A** grafting to, **B** grafting from and **C** grafting through techniques. Reproduced with permission from Ref. [19]. Copyright 2021, Elsevier

4 Functionalization of Different Nanomaterials

Modifying nanomaterials with various groups resulted in developing material with enhanced properties such as high affinity, adsorption capacity, easy dispersibility and fast response in various techniques. The materials having unique properties like as carbon-based materials, magnetic and 2D layered materials, functionalized by covalent or non-covalent functionalization methods for acquiring desired properties for several applications. To reduce the limitation of nanomaterials such as in magnetic materials, the material get modifies with silica, alumina which are that much resultant in huge experimental conditions. Thus, the easy and effective functionalization ability of nanomaterials spreads their application in much more areas. Let's look into some of the most widely used FNMs.

4.1 Functionalization of Carbon-Based Nanomaterials

In the field of nanotechnology, the functionalization of nanoparticles has opened up a lot of possibilities. Carbon-based nanoparticles are functionalized in order to be used in various fields of nanotechnology, such as electronics, composites and biomedicine, opening up numerous future possibilities (Table 2). Some impressive examples include the use of functionalized carbon nanotube in biomedicine, functionalizing graphene oxide for use as cement reinforcement, and non-covalently functionalizing graphene for use as an adhesive with improved thermal conductivity. The highly emerging fields of nanotechnology and engineering are constantly revolutionising many established ones in a vast area, including energy generation, conversion and storage, electronic packaging, catalysis, sensors, drug delivery, additives and in biomedical applications.

Table 2 Functionalization of CNT-based nanomaterials and its analysis

FNM	Application/analysis	Reference
Carbon materials—GO, CNT, AC, carbon fibers	Electronic devices	[21]
CNT Functionalization	Removal of aqueous heavy metal	[22]
CNT Functionalization and Graphene	Adsorption of heavy metal from water	[23]
CNT Functionalization	Interfacial characteristic study	[24]
SWCNT	Optical property analysis	[25]

4.1.1 Functionalized Carbon Nanotubes (CNT)

The need for functionalization of CNT is to enhance the low dispersion and solubility of the material in various solvents due to the chemical nature of CNT. In order to overcome this, we can functionalize the CNT to improvise its chemical properties. Functionalization can be achieved by covalent or non-covalent functionalization which is discussed above. There are several studies under way where the mechanism of functionalization of CNT is done through different functional group additions such as amidation, bromination, fluorination, chlorination, hydrogenation and electrophilic addition (Fig. 7). Thus, functionalized CNTs can be used in various applications including wastewater treatment, dye degradation from aqueous media, medical treatment and in drug delivery.

4.1.2 Functionalized GO, rGO and Graphene

Due to its distinct structural features and versatility in various applications, graphene and its derivatives are attractive among the other carbonaceous compounds. GO and reduced Graphene Oxide (rGO) improvise the functionalization ability and thus widen the applications. GO is the oxidised form of graphene with a honeycomb structure having enormous oxygen-rich functional groups. On the other hand, rGO is the reduced form of GO having some oxygen functional groups and defect structures [27].

The functionalization of graphene is achieved either by covalent or non-covalent methods with respect to their interactions with the ligands and sp^2 lattice. In covalent functionalization, there is formation of covalent bonds between graphene and various functional groups, on other side, π electron delocalization of graphene nanosheets remains consistent in non-covalent functionalization. Chemical functionalization of graphene can be done by other synthesis strategies including spin coating, filtration and the layer-by-layer approach. A schematic diagram of chemical treatment for functionalize GO is shown in Fig. 8. On the other hand, GO is used as the triggering source for the synthesis of functionalized graphene. Graphene's layered structure and large surface area attract the material most in wastewater treatment. These chemically

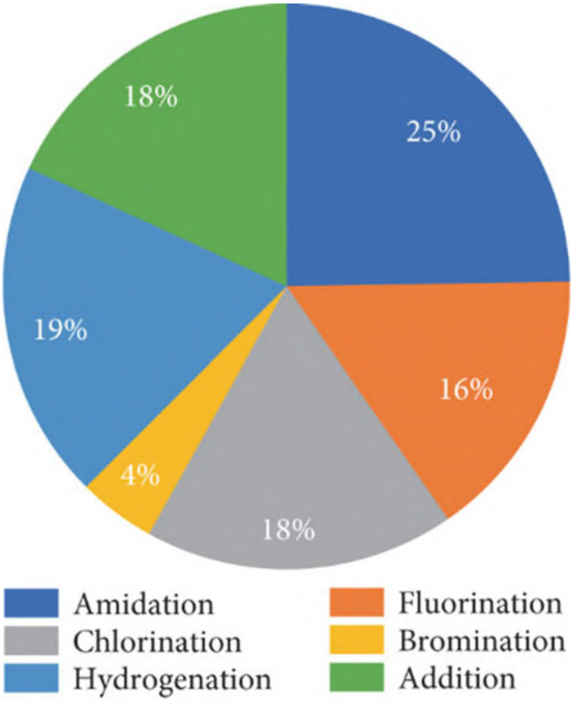

Fig. 7 New strategies for functionalization of CNTs. Reproduced with permission from [26]. Copyright 2021, Hindawi

modified graphenes have been studied widely in energy storage applications, sensors, dye degradation and insulation materials [28].

4.2 *Functionalized 2D TMDs*

The curious investigation on 2D nanomaterials increased very rapidly after the discovery of graphene. The ultra-thin layered property exhibits unique features which are different from their bulk counterparts. Among various 2D materials, transition metal dichalcogenides get considerable attraction. Layered TMDs are attracted to various areas including catalysis, electronics, energy storage and sensing due to the impressive physical and chemical properties shown by them. Because of their electronic configuration (d electrons) and the coordination of transition metal atoms, 2D TMDs are widely used in a variety of applications [29].

Although the TMD characteristics are theoretically excellent, it is found that its excellence can be improved by chemical functionalization (Fig. 9). The property enhancement of these materials is carried out by surface functionalization with various organic and inorganic nanomaterials by covalent and non-covalent interactions. This functionalization may change the fermi level of these 2D materials. 2D WS_2 nanosheets modified with poly (acrylic acid) show high solubility in common

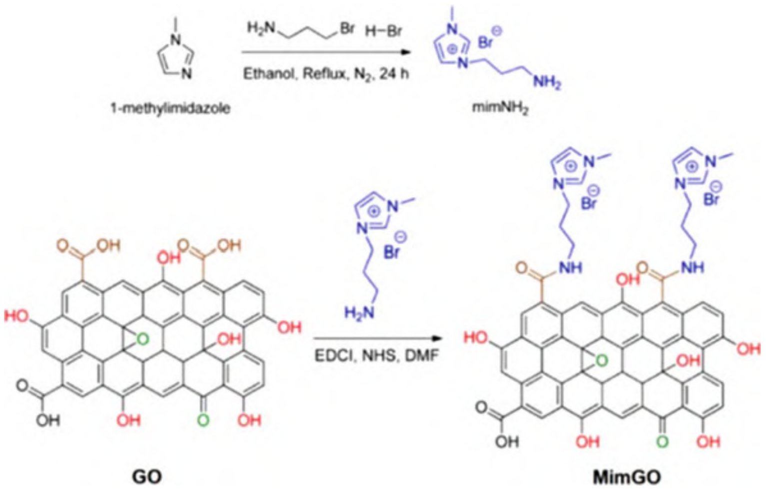

Fig. 8 A schematic diagram of the chemical method used for functionalize GO with amino-methylimidazole IL, Reproduced with permission from Ref. [28]. Copyright 2020, IOP Science

solvents and good stability, thus it can be conserved at room temperature [30]. The photoluminescence effect of 2D MoS_2 is enhanced when it is modified with bis (trifluoromethane)sulfonamide [31]. These enhanced features of the functionalized 2D TMDs have great opportunities to grow up in future applications (Table 3) [32].

4.3 Functionalized Magnetic Nanoparticles

The use of magnetic nanoparticles (MNPs) in large-scale industrial and environmental applications is growing because it can be used for easy functionalization, effective adsorption of pathogens, fast recovery and curing. It has wide applications in drug delivery, ferrofluids, magnetic storage systems, targeting and magnetic resonance imaging (MRI) (Fig. 10).

When reduced to nanoscale dimensions, they provide a large surface area for maximum dissolution of particles. The toxic nature of MNPs arises because of their high chemical reactivity and surface area, which generate highly reactive oxygen species. The biocompatibility of the material is determined by its size, hydrophilicity and surface charge. The properties of the coating molecules such as mass and charge also affect the biocompatibility [38]. Functionalization of these materials attaches various functional groups to provide biologically active sites for specific applications. For the effective targeted delivery and interaction, MNPs are better functionalized with suitable molecules such as bioproteins, carbohydrates and antibodies. Surface

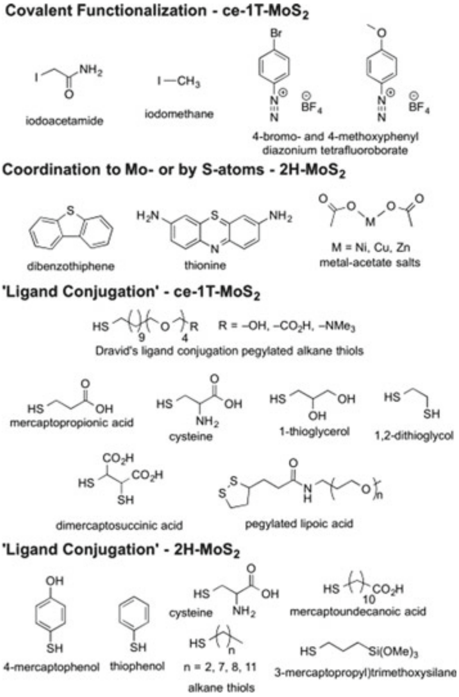
Covalent Functionalization - ce-1T-MoS$_2$
iodoacetamide
iodomethane
4-bromo- and 4-methoxyphenyl diazonium tetrafluoroborate
Coordination to Mo- or by S-atoms - 2H-MoS$_2$
dibenzothiphene
thionine
M = Ni, Cu, Zn
metal-acetate salts
'Ligand Conjugation' - ce-1T-MoS$_2$
R = –OH, –CO$_2$H, –NMe$_3$
Dravid's ligand conjugation pegylated alkane thiols
mercaptopropionic acid
cysteine
1-thioglycerol
1,2-dithioglycol
dimercaptosuccinic acid
pegylated lipoic acid
'Ligand Conjugation' - 2H-MoS$_2$
4-mercaptophenol
thiophenol
cysteine
mercaptoundecanoic acid
n = 2, 7, 8, 11
alkane thiols
3-mercaptopropyl)trimethoxysilane

Fig. 9 Functionalization of TMDs using various organic/inorganic compounds. Reproduced with permission from Ref. [29]. Copyright 2016, WILEY–VCH

Table 3 Applications and enhanced performance of some 2D TMDs functionalized with various materials

FNM	Functionalizing element	Results (after functionalization)/Application	References
MoS_2	Iodine	Metallic to semiconducting phase transition	[33]
WS_2	Ag	Enhanced gas sensing performance	[34]
WS_2	Bovine serum albumin	Signal capturing from tumour inserted site-cancer therapy	[35]
MoS_2	Zinc porphyrin	Increased photocatalytic hydrogen evolution rate	[36]
MoS_2/TiO_2 nanocomposite	Carbon coated along with glucose addition	Enhanced electrochemical performance—LIBs	[37]

engineering of MNPs by organic compounds can be performed by main steps which includes.

- Organic vapour condensation
- Polymer coating
- Surfactant adsorption

Fig. 10 Various applications of functionalized MNPs [20]

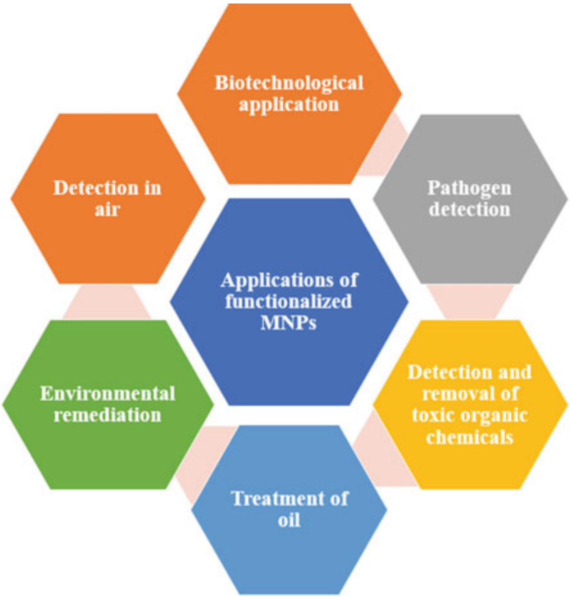
Biotechnological application
Detection in air
Pathogen detection
Applications of functionalized MNPs
Environmental remediation
Detection and removal of toxic organic chemicals
Treatment of oil

- Direct salinization

The high reactivity of spinel ferrite structures over many functional groups results in multiple combinations. Hydrophilic functional compounds can be made by ligand exchange, silica coating or polymer coating of which the main steps for polymer coating are discussed in the previous section. Ligand exchange approaches replace the hydrophobic ligands with hydrophilic molecules without altering the rest of the core structure (Fig. 11) [38].

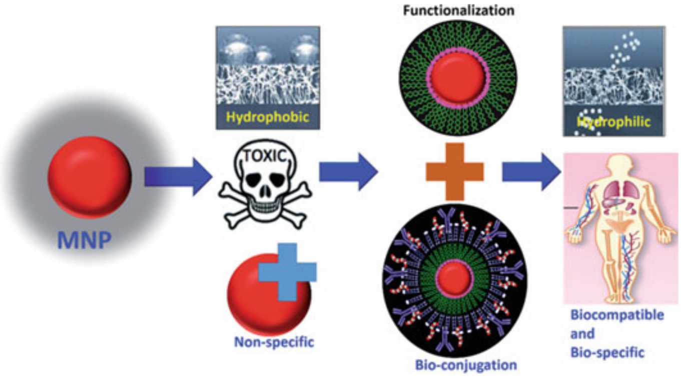
Functionalization
Hydrophobic
Hydrophilic
MNP
TOXIC
Non-specific
Bio-conjugation
Biocompatible and Bio-specific

Fig. 11 Functionalization of Magnetic nanoparticles in biological application. Reproduced with permission from Ref. [38]. Copyright 2016, RSC Advances

Silica coating, on the other hand, provides enhanced chemical stability to the magnetic part. In various methods involving silica coating, silica shells with the desired thickness were obtained with the addition of tetraethyl orthosilicate (TEOS) to the nanoparticle medium and the coating could be done by a dense liquid coating approach. Alternatively, various organ silanes groups such as -SH and -NH groups can be used to functionalize silica coating.

5 Recent Updates and Use of FNM in Various Fields

Environmental engineering, chemical process engineering and petroleum engineering are some of the most challenging areas in material science and engineering today. The main interest is that nanotechnology, nanomaterials and FNM are helping modern research to advance quickly. The major and most important aim as well as the main requirement for modern human civilization is sustainability, whether it is in the fields of environment, energy, society or economy. The key problems that need to be tackled are the environmental catastrophes, climate change and the scarcity of fossil fuel supplies. This field of study is on the bleeding edge thanks to nanoengineering and nanovision.

5.1 Industrial Application

Nanotechnology proffers industrial processes that are both economical and environmentally beneficial since it has the capability to control each atom's uniqueness. Significant research has been conducted to develop functionalized nanomaterials for a wide range of industrial applications due to their excellent technological and industrial characteristics. For the manufacture of stretchy, flexible, and photonic devices in the electronics sector using these functionalized nanomaterials such as semiconductors, noble metals, metal oxides and alloys. Over the past five years, the industrial as well as electronic sectors have significantly increased their usage of nanomaterials. About 900 enterprises around world have centred their efforts on developing cutting edge nanomaterials and nanodevices. Miniature three-dimensional electronic devices with embedded logic circuits enabling wide applications, including wearable electronic gadgets and display devices, have a significant impact on the evolution of our contemporary technology. Next generation flexible and speedier electronic storage systems, which can go beyond micro-processing consisting of millions of small transistors, can contribute to the arrival of new electronic devices. Mobility, toughness, flexibility, compactness and ease of structural integration are the other characteristics of nanodevices.

5.2 *In Human Healthcare—Nanomedicine*

In order to know the impact of using nanomaterials in medical treatment, studies were going on in biomaterials, biosensors, tissue fabrication. It helps with fast drug delivery, improved tissue healing, the detection of cancerous cells and antibacterial performance. Furthermore, efforts and researchers will be made to address safety concerns. Standardized reference materials for nanotoxicity measurements were initiated by international laboratory groups but the nanocomplex structures are great challenges which would lead to more futuristic aspects [39].

The emergence of various diseases paved the way for developing proper target dosages for curing the diseases and maintaining human health [40]. Biomedical applications need complete biocompatibility and biodegradability to overcome adverse reactions of the immune system [27]. Proper sensing of biomolecules and their detection are important to sustain the life cycle. Thus, the design of biosensors is critical. Biosensors are developed for plant disease detection by functionalization [41]. In biomedical applications, surface functionalization with biomolecules provides selectivity, high compatibility, stealth properties, targeted delivery and internalization ability. The ability to activate the molecular oxygen into reactive oxygen species on light irradiation makes graphene and fullerenes an efficient source for cancer treatment. The surface chemical properties of various carbon-based materials and 2D structures get modified by suitable functional materials along with surface engineering in order to reduce toxicity, increase water solubility and have other characteristic features.

Drug encapsulation is becoming a reality for systematic and precise targeted drug delivery. Poly ethylene glycol (PEG) nanoparticles were used for treating tumour cells (Fig. 12) [40]. These polymeric groups have impressive biocompatibility and a non-crystalline nature, possessing unique physical and chemical properties. Also, there exists growing perspectives on therapeutics and in diagnostic application over various diseases such as cancer by using functionalized 2D TMDs [32]. The enhanced biomedical applications employ low toxicity, high stability for these materials as compared to other nanomaterials (Fig. 13).

5.3 *Environmental*

Water, the most needed resource for mankind, poses serious contamination on a large scale. Decolorization due to dyes and organic contaminants is needed to be eliminated for the sake of environmental protection since the consumption of these by the ecosystem causes severe side effects [42]. In addition to its potential to increase energy efficiency, nanotechnology has vast range of applications in detection and removal of environmental pollutants. Through quick, inexpensive detection and treatment of water contaminants, nanotechnology may be able to help address the need for accessible, clean drinking water. Amino functionalized magnetic nanoparticles

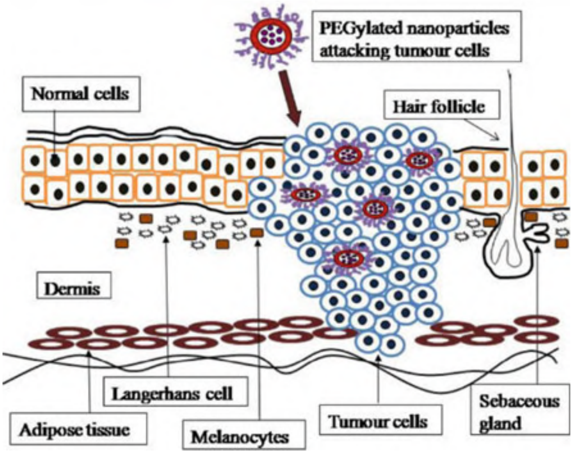
PEGylated nanoparticles attacking tumour cells
Normal cells
Hair follicle
Dermis
Langerhans cell
Adipose tissue
Melanocytes
Tumour cells
Sebaceous gland

Fig. 12 PEGylated nanoparticles used for skin tumour treatment. Reproduced with permission from [40]. Copyright 2019, Elsevier

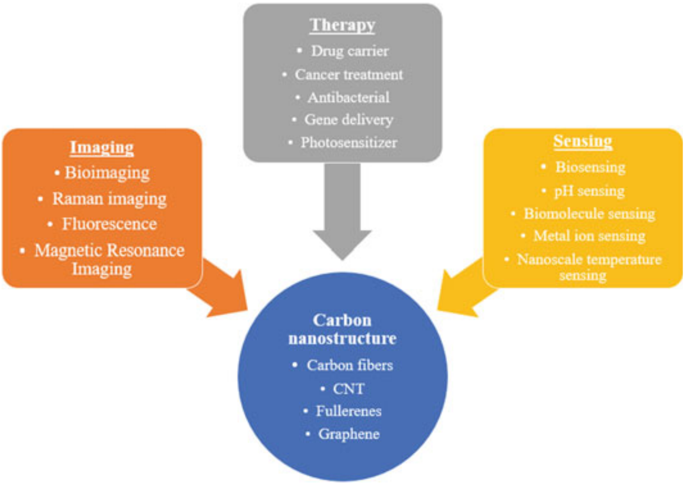
Therapy
• Drug carrier
• Cancer treatment
• Antibacterial
• Gene delivery
• Photosensitizer
Imaging
• Bioimaging
• Raman imaging
• Fluorescence
• Magnetic Resonance Imaging
Sensing
• Biosensing
• pH sensing
• Biomolecule sensing
• Metal ion sensing
• Nanoscale temperature sensing
Carbon nanostructure
• Carbon fibers
• CNT
• Fullerenes
• Graphene

Fig. 13 Applications of various carbon nanostructures in biomedical application

were employed for wastewater treatment. The organic and inorganic coatings on the surfaces of nanoparticles not only stabilize the material and eliminate the agglomeration but also used for easy functionalization with –COOH, –NH_2 and –SH groups [43]. An example of functionalization of GO modified gold electrode is shown in Fig. 14. The strong metal chelating ability and high surface area enable the amino groups to adsorb various heavy metal ions from the aqueous medium.

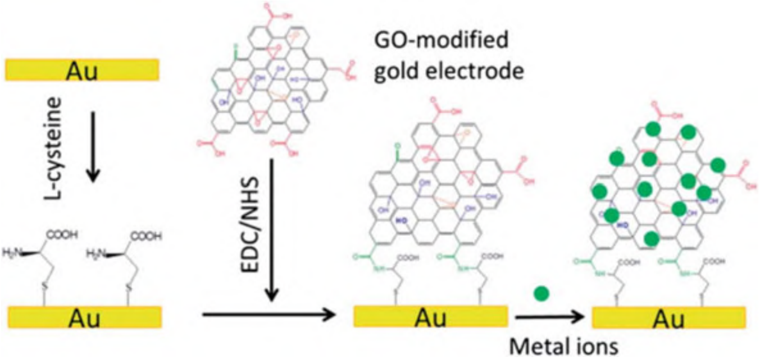

Fig. 14 Modification of gold electrode with L-cysteine functionalization, EDC/NHS coupling of GO. The active oxygenated sites of GO result in capturing and complexation of metal ions. Reproduced with permission from [44]. Copyright 2014, RSC Advances

5.4 Inorganic and Heavy Metal Ion Removal

Identification and evaluation of inorganic and heavy metal ions in aqueous bodies are crucial for human health. Several techniques are employed for the effective removal of these contaminants including membrane filtration, chemical precipitation, ion exchange, flotation and most importantly adsorption. Nanomaterial-based adsorbents are used due to their potential for functionalization and the large surface area attributes increased active sites for heavy adsorption of ions (Table 4). In order to enhance the efficiency, the nanomaterial gets functionalized using various materials including polymers, metal organic frameworks, oligomers, etc. in order to enhance the adsorption capacity. These polymer compounds serve as heavy metal ion binders. Pb^{2+} and Hg^{2+} which are harmful pollutants causing acute damage to the nervous system can be monitored using CNTs with 1,3,6,8-pyrenetetrasulphonic acid sodium (PyTS-CNTs). Doping acrylamide (AM) with titanium oxide (TiO_2–AM) exhibits efficient removal of Cd^{2+} with 50% efficiency in 30 min due to the presence of empty sites on the nanocomposite. Also, treating with sulfuric acid and nitric acid results in the addition of –COOH and –OH functional groups in CNT.

5.5 Sensing Toxic Gases and Other Organic Compounds

Nanomaterial-based sensors are normally conducting or semiconducting and the electrical characteristics may change when they are exposed to some toxic gases. Gas sensing materials that have been extensively explored are CNTs, metal oxide-based semiconductors, conducting polymers and 2D materials for the detection of SO_2, CO, NH_3 and others. PANI/Au/Nafion composite material investigated for NO_2 gas sensing exhibits a high sensitivity of around 2 mA/ppm [49].

Table 4 Heavy metal ion removal application of various FNM

FNM	LOD/Optimized adsorption condition	Heavy metal ions	Reference
CeO_2/AM/CNT	Modified with sulfuric and nitric acid 25 °C, pH 3–7.4	Cr^{4+}	[45]
Mn (TPA)/SWCNT	0.10–14.0 μM, LOD 38 nM	Pb^{2+}	[46]
GO modified Au	Minimum detection limit: Pb (0.4), Cu (1.2) and Hg (0.8) ppb	Hg^{2+}, Cu^{2+}, Pb^{2+}	[44]
Au-chitosan composite	Calibration range $1*10^{-9}$ to 0.1 μM, LOD 0.8 fM	Hg^{2+}	[47]
Phosphonic acid functionalized CNT	Cr concentration 0.01 to 10 ppb, LOD 0.01 ppb	Cr^{4+}	[48]

The π electron transfer from PANI to the adsorbed gas after NO_2 exposure reduces the resistance. Layer-by-layer TiO_2/rGO nanocomposite assembly attributes include fast response, efficient selectivity, reversibility and proper detection of SO_2 gas. Volatile organic compounds (VOCs) including toluene, methanol, acetone, formaldehyde, cyclohexane, n-butanol and so on, get released from oil refineries, vehicle exhaust and transportation. The presence of VOCs is much higher indoors than outdoors and can be readily detected for further adsorption. CuO–Fe_2O_3 nano-cubes have excellent electrochemical capability, high sensitivity and selectivity, long-term stability and a wide concentration range when exposed to ethanol [50].

5.6 Electrochemical

Energy has come to be seen as a defining aspect of civilization and economic growth, and increasing energy use has negative environmental effects. As per the international Energy Outlook in 2017, there was 28% increment in energy demand which is reported from 2015 to 2040. Energy-based research now examines all aspects, including energy generation, harvesting, conserving, converting and storing, in an effort to find more environmentally responsible and sustainable energy sources. All recent advancements in the energy sector have depended heavily on nanomaterials, which have unique characteristics. Li-ion batteries, Zn-air batteries, Na-ion batteries, supercapacitors and fuel cells are a few examples of nanomaterials used for energy storage. Functionalized graphene-based nanocomposite is employed for supercapacitor energy storage applications. The use of functionalized graphene enhances the overall specific capacitance and also provides active sites for modification of metal oxide nanostructures (RuO_2, TiO_2 and Fe_3O_4) and conducting polymers. PANI-coated functionalized graphene and a nanocomposite of metal oxide and functionalized graphene were developed for investigating the supercapacitor device application [51]. The presence of graphene in the metal oxide-based system and PANI-coated functionalized graphene prevents the agglomeration of nanomaterials, which helps in attaining high capacitance. Functionalized DWCNT and GO nanosheets in energy storage applications are interestingly noted widely. The use of $–NH_2$ and –COOH–modified DWCNT improved the electrode quality because the presence of these functional groups results in easy CNT interaction based on the opposite charges [52].

The key element in an electrochemical energy-based systems is the catalyst. Functionalized nanomaterials also enable the creation of catalysts. Materials with high sensitivity, efficiency, optimum electrochemical surface area and energy are the necessary electrochemical characteristics.

5.7 Optoelectronics

Electrical transformers and nanoelectrodes are only two examples of how the industry has benefited from nanotechnology. Electrical transformers are among the most commonly seen components of electricity production and the distribution network since they are the source of energy supply interruptions. They are actually static devices that are internally constructed from a range of materials, including metals and polymers. To protect the interior components of dry-cast transformers, polymeric resin is added; for oil-immersed transformers, insulating fluids with thermal and dielectric properties are added. Recently, nanofluids have been proposed as an alternative. With insulating nanofluids, the most recent transformer's cooling capacity was enhanced. Taha-Tijerina et al. [53] referred to a dielectric mineral oil-based nanodiamond fluid which is used as a transformer insulating fluid. They found that thermal fluids containing nanodiamonds boosted heat conductivity by 70% when compared to normal mineral oil. Li et al. [53] first presented natural ester-based insulating fluids with Fe_3O_4 nanoparticles. The physical, chemical, electrical and ageing properties of the dielectric mineral insulating oil were examined. The lighting impulse breakdown voltage of natural ester nanofluids was found to be improved by the addition of magnetic Fe_3O_4 nanoparticles.

6 Challenges and Future Perspectives

Future nanotechnology discoveries possess both positive and negative impacts. On the one hand, the industry would develop world widely, driven, among other things, by technological advances, increased government assistance, more private investment and increasing consumer needs for smaller gadgets. The environmental hazards, human health, along with safety issues posed by nanotechnology and issues with commercialization, could, however, put limit the market growth. Numerous scientific advances have recently been made in research programmes involving nanomaterials and nanotechnology used to increase the reliability and efficiency of common materials.

Nanotechnology deals with great challenges in plant disease management by decreasing the chemical impacts and enhancing the fast detection of diseases in plants [41]. In terms of cost and reproducibility, the industrial scale-up of graphene-based nanomaterials presents significant challenges. Therefore, new approaches are needed for the efficient design and development of new strategies for increasing the large-scale production and quality of these materials [16]. Various application possibilities of MNPs are still under study, involving the detection and removal of harmful materials and pathogens with high precision and reliability in the future. The main challenges in the case of polymeric nanoparticles are their toxic degradation when the materials associated with them become toxic. But they are widely used in biomedicine, tissue engineering and pharmaceuticals. Thus, polymeric nanoparticles and nanocomposites will have a huge impact on biomedical applications in the future.

The development of multifunctional materials leads to the construction and maintenance of lighter, safer, more intelligent, and more efficient ships, planes and hybrid vehicles. Additionally, nanotechnology provides several ways to enhance the transportation system.

Polymer-based nanocomposites for structural components, high-power density batteries, thermoelectric materials, reduced rolling resistance tyres, high-efficiency, cost effective sensors and electronics, thin-film based solar panels, fuel additives, and efficient catalytic converters for cleaner exhaust and longer range are few examples of nano-engineered materials used in automotive products. The bio-functional magnetic nanomaterials enable the detection and capture of various pathogens at very low concentrations, which is not achieved with conventional methods. Nano-engineering holds great promise for enhancing the performance, resiliency and longevity of highway and transportation infrastructure components while lowering their life cycle costs.

7 Conclusion

The accessibility and vast differences in the properties of various carbon-based materials, 2D TMDs and magnetic materials enable new technological applications. This chapter thus focused on the methods of developing various functionalized nanomaterials, emphasized some of the most relevant nanomaterials functionalized with various inorganic/ organic molecules and also the recent use of FNM in some specific application fields. Even though the surface properties get enhanced upon reducing the bulk to nanoscale dimension, their performance could further increase by various functionalization approaches which leads to incorporating additional functionalities to the existing ones. The ligand conjugation has a key role in covalent functionalization while the interfaces are clean in case of non-covalent functionalization. Thus, these strategies have their own merits and demerits. In addition, the synergetic effects that arise after the interaction between some nanomaterials and functionalizing material are still under research studies and need to be fully utilized with full potential to broaden the application. Reviewing various FNM, there are a lot of concerns with respect to health and environmental hazards. Thu it is crucial and challenging to develop facile and environmentally friendly FNM.

References

1. Cheng Y, Shen PK, Jiang SP (Dec.2014) NiO nanoparticles supported on polyethylenimine functionalized CNTs as efficient electrocatalysts for supercapacitor and oxygen evolution reaction. Int J Hydrogen Energy 39(35):20662–20670. https://doi.org/10.1016/j.ijhydene.2014.06.156
2. Hussain CM (2020) Handbook of Functionalized Nanomaterials for Industrial Applications. Elsevier, 2020. [Online]. Available: https://www.elsevier.com/books-and-journals
3. Sahoo SK, Hota G (2020) Functionalization of graphene oxide with metal oxide nanomaterials: synthesis and applications for the removal of inorganic, toxic, environmental pollutants from water. in *Handbook of Functionalized Nanomaterials for Industrial Applications*, Elsevier, 2020, pp. 299–326. doi: https://doi.org/10.1016/B978-0-12-816787-8.00012-0
4. Chaudhary S, Sharma P, Chauhan P, Kumar R, Umar A (Sep.2019) Functionalized nanomaterials: a new avenue for mitigating environmental problems. Int J Environ Sci Technol 16(9):5331–5358. https://doi.org/10.1007/s13762-019-02253-2
5. Makvandi P, Iftekhar S, Pizzetti F, Zarepour A, and Nazarzadeh E (2021) Functionalization of polymers and nanomaterials for water treatment , food packaging , textile and biomedical applications : a review. pp. 583–611
6. Ramsden JJ (2014) The Future of Nanotechnology. in *Applied Nanotechnology*, vol. 29, no. 1, Elsevier, 2014, pp. 185–193. doi: https://doi.org/10.1016/B978-1-4557-3189-3.00016-6
7. Mi S, Zhang C, Gao J, Wu H, Wang X, Wu M, Xu Y (2010) Doped nanostructures. Nanoscale 2(7):1057. doi: https://doi.org/10.1039/c005273f
8. Liu and Speranza (Nov.2019) “Functionalization of carbon nanomaterials for biomedical applications. C-J. Carbon Res. 5(4):72. https://doi.org/10.3390/c5040072
9. Song J-H, Min S-H, Kim S-G, Cho Y, Ahn S-H (Jan.2022) Multi-functionalization strategies using nanomaterials: a review and case study in sensing applications. Int J Precis Eng Manuf Technol 9(1):323–347. https://doi.org/10.1007/s40684-021-00356-1
10. Sperling RA, Parak WJ (2010) Surface modification, functionalization and bioconjugation of colloidal inorganic nanoparticles. Philos. Trans. R. Soc. A Math. Phys. Eng. Sci. 368(1915):1333–1383. doi: https://doi.org/10.1098/rsta.2009.0273
11. Yilmaz E, Soylak M (2020) Functionalized nanomaterials for sample preparation methods. In Handbook of Nanomaterials in Analytical Chemistry, Elsevier, 2020, pp. 375–413. doi: https://doi.org/10.1016/B978-0-12-816699-4.00015-3
12. Treccani L, Yvonne Klein T, Meder F, Pardun K, Rezwan K (2013) Functionalized ceramics for biomedical, biotechnological and environmental applications. Acta Biomater. 9(7):7115–7150. doi: https://doi.org/10.1016/j.actbio.2013.03.036
13. Sainsbury T et al (Nov.2012) Oxygen Radical Functionalization of Boron Nitride Nanosheets. J Am Chem Soc 134(45):18758–18771. https://doi.org/10.1021/ja3080665
14. Mungse HP, Verma S, Kumar N, Sain B, Khatri OP (2012) Grafting of oxo-vanadium Schiff base on graphene nanosheets and its catalytic activity for the oxidation of alcohols. J Mater Chem 22(12):5427. https://doi.org/10.1039/c2jm15644j

15. He M, Swager TM (2016) Covalent functionalization of carbon nanomaterials with iodonium salts. Chem Mater 28(23):8542–8549. https://doi.org/10.1021/acs.chemmater.6b03078
16. YY, Li Zhou YH, He B (2014) Facile approach to surface functionalized MoS2 nanosheets. 4:32570–32578. doi: https://doi.org/10.1039/c4ra04682j
17. Pandele AM, Andronescu C, Vasile E, Radu IC, Stanescu P, Iovu H (Dec.2017) Non-covalent functionalization of GO for improved mechanical performances of pectin composite films. Compos Part A Appl Sci Manuf 103:188–195. https://doi.org/10.1016/j.compositesa.2017.10.005
18. Nell KM et al (2016) Non-covalent functionalization of high-surface area nanomaterials: a new class of sorbent materials. Environ Sci Nano 3(1):138–145. https://doi.org/10.1039/C5EN00170F
19. Wieszczycka K, Staszak K, Woźniak-Budych MJ, Litowczenko J, Maciejewska BM, Jurga S (Jun.2021) Surface functionalization – The way for advanced applications of smart materials. Coord Chem Rev 436:213846. https://doi.org/10.1016/j.ccr.2021.213846
20. Samui AB (2021) Functionalized nanomaterials for environmental applications. In: Functionalized Nanomaterials Based Devices for Environmental Applications, Elsevier, 2021, pp. 303–328. doi: https://doi.org/10.1016/B978-0-12-822245-4.00014-3
21. Kamran U, Heo Y, Lee JW, Park S (2019) Functionalized carbon materials for electronic devices: a review. Micromachines 10(4):234. https://doi.org/10.3390/mi10040234
22. Verma B, Balomajumder C (2020) "Environmental Technology & Innovation Surface modification of one-dimensional Carbon Nanotubes : A review for the management of heavy metals in wastewater," vol. 17
23. Xu J et al (Mar.2018) A review of functionalized carbon nanotubes and graphene for heavy metal adsorption from water: preparation, application, and mechanism. Chemosphere 195:351–364. https://doi.org/10.1016/j.chemosphere.2017.12.061
24. Chen J, Liu B, Gao X, Xu D (2018) A review of the interfacial characteristics of polymer nanocomposites containing carbon nanotubes. RSC Adv 8(49):28048–28085. https://doi.org/10.1039/C8RA04205E
25. Janas D (2020) Perfectly imperfect: a review of chemical tools for exciton engineering in single-walled carbon nanotubes. Mater Horizons 7(11):2860–2881. https://doi.org/10.1039/D0MH00845A
26. Salah LS, Ouslimani N, Bousba D, Huynen I, Danlée Y, Aksas H (Sep.2021) Carbon nanotubes (CNTs) from synthesis to functionalized (CNTs) using conventional and new chemical approaches. J Nanomater 2021:1–31. https://doi.org/10.1155/2021/4972770
27. Wu H, Huang Q, Tan Y (2019) Carbon nanomaterials for biomedical applications. Carbon Nanomater. Model. Des. Appl. pp. 255–293. doi: https://doi.org/10.1201/9781351123587-7
28. Fraga TJM, Da Motta Sobrinho MA, Carvalho MN, Ghislandi MG (2020) State of the art: synthesis and characterization of functionalized graphene nanomaterials. Nano Express 1(2). doi: https://doi.org/10.1088/2632-959X/abb921
29. Chen X, Mcdonald AR (2016) Functionalization of two-dimensional transition-metal dichalcogenides. pp. 1–9. doi: https://doi.org/10.1002/adma.201505345
30. Chen Y, Tan C, Zhang H, Wang L (2015) Two-dimensional graphene analogues for biomedical applications. Chem Soc Rev 44(9):2681–2701. https://doi.org/10.1039/C4CS00300D
31. M. Amani et al. (2015) Near-unity photoluminescence quantum yield in MoS2," Science (80-) 350(6264):1065–1068. doi: https://doi.org/10.1126/science.aad2114
32. Azadmanjiri J, Kumar P, Srivastava VK, Sofer Z (Apr.2020) Surface Functionalization of 2D Transition Metal Oxides and Dichalcogenides via Covalent and Non-covalent Bonding for Sustainable Energy and Biomedical Applications. ACS Appl. Nano Mater. 3(4):3116–3143. https://doi.org/10.1021/acsanm.0c00120
33. Hirsch A, Hauke F (Apr.2018) Post-graphene 2D chemistry: the emerging field of molybdenum disulfide and black phosphorus functionalization. Angew Chemie Int Ed 57(16):4338–4354. https://doi.org/10.1002/anie.201708211
34. Ko KY et al (Oct.2016) Improvement of gas-sensing performance of large-area tungsten disulfide nanosheets by surface functionalization. ACS Nano 10(10):9287–9296. https://doi.org/10.1021/acsnano.6b03631

35. Yong Y et al (2014) WS 2 nanosheet as a new photosensitizer carrier for combined photodynamic and photothermal therapy of cancer cells. Nanoscale 6(17):10394–10403. https://doi.org/10.1039/C4NR02453B
36. Haque F, Daeneke T, Kalantar-zadeh K, Ou JZ (2018) Two-dimensional transition metal oxide and chalcogenide-based photocatalysts. Nano-Micro Lett 10(2):23. https://doi.org/10.1007/s40820-017-0176-y
37. Chen B, Meng Y, Sha J, Zhong C, Hu W, Zhao N (2018) Preparation of MoS_2/TiO_2 based nanocomposites for photocatalysis and rechargeable batteries: progress, challenges, and perspective. Nanoscale 10(1):34–68. https://doi.org/10.1039/C7NR07366F
38. Bohara RA, Thorat ND, Pawar SH (2016) Role of functionalization: strategies to explore potential nano-bio applications of magnetic nanoparticles. RSC Adv 6(50):43989–44012. https://doi.org/10.1039/C6RA02129H
39. Hulla J, Sahu S, Hayes A (2015) Nanotechnology. Hum Exp Toxicol 34(12):1318–1321. https://doi.org/10.1177/0960327115603588
40. Sur S, Rathore A, Dave V, Reddy KR, Chouhan RS, Sadhu V (2019) Recent developments in functionalized polymer nanoparticles for efficient drug delivery system. Nano-Struct Nano-Objects 20:100397. https://doi.org/10.1016/j.nanoso.2019.100397
41. Elmer W, White JC (2018) The future of nanotechnology in plant pathology. Annu Rev Phytopathol 56:111–133. https://doi.org/10.1146/annurev-phyto-080417-050108
42. Opoku F, Govender PP (2021) Prospective of functionalized nanomaterials in environmental science: A nanotechnological approach. In: Functionalized Nanomaterials Based Devices for Environmental Applications, Elsevier, pp. 13–60. doi: https://doi.org/10.1016/B978-0-12-822245-4.00002-7.
43. You J, Wang L, Zhao Y, Bao W (2021) A review of amino-functionalized magnetic nanoparticles for water treatment: features and prospects. J Clean Prod 281:124668. https://doi.org/10.1016/j.jclepro.2020.124668
44. Gong X, Bi Y, Zhao Y, Liu G, Teoh WY (2014) Graphene oxide-based electrochemical sensor: a platform for ultrasensitive detection of heavy metal ions. RSC Adv 4(47):24653–24657. https://doi.org/10.1039/C4RA02247E
45. Di Z-C, Ding J, Peng X-J, Li Y-H, Luan Z-K, Liang J (2006) Chromium adsorption by aligned carbon nanotubes supported ceria nanoparticles. Chemosphere 62(5):861–865. https://doi.org/10.1016/j.chemosphere.2004.06.044
46. Cai F et al (2017) Selective binding of Pb2+ with manganese-terephthalic acid MOF/SWCNTs: Theoretical modeling, experimental study and electroanalytical application. Biosens Bioelectron 98(July):310–316. https://doi.org/10.1016/j.bios.2017.07.007
47. Aneesh PK, Nambiar SR, Rao TP, Ajayaghosh A (2014) Electrochemical synthesis of a gold atomic cluster–chitosan nanocomposite film modified gold electrode for ultra-trace determination of mercury. Phys Chem Chem Phys 16(18):8529. https://doi.org/10.1039/c4cp00063c
48. Deep A, Sharma AL, Tuteja SK, Paul AK (2014) Phosphinic acid functionalized carbon nanotubes for sensitive and selective sensing of chromium (VI). 278:559–565
49. W.-B. Jing-ShanDo, “Amperometric nitrogen dioxide gas sensor: preparation of PAn/Au/SPE and sensing behaviour.” pp. 101–107, 2001. doi: https://doi.org/10.1016/S0925-4005(00)00607-9.
50. Rahman MM, Asiri AM (2015) Fabrication of highly sensitive ethanol sensor based on doped nanostructure materials using tiny chips. RSC Adv 5(78):63252–63263. https://doi.org/10.1039/C5RA08224B
51. Mishra AK, Ramaprabhu S (2011) Functionalized graphene-based nanocomposites for supercapacitor application. pp. 14006–14013
52. Borges RS, Ribeiro H, Lavall RL, Silva GG (2012) Temperature stable supercapacitors based on ionic liquid and mixed functionalized carbon nanomaterials. doi: https://doi.org/10.1007/s10008-012-1785-5
53. Li J, Liao R, Yang L (2012) Investigation of natural ester based liquid dielectrics and nanofluids. In: 2012 International Conference on High Voltage Engineering and Application, 56(2):16–21. doi: https://doi.org/10.1109/ICHVE.2012.6357155

Всё для победы!
НАРОДНЫЙ
ФРОНТ
https://pobeda.onf.ru/
LET'S HELP THE RUSSIA

Chapter 27
FNM-Based Supercapacitor in Futuristic Application

Soumya Jha and R. Prasanth

1 Introduction

Energy systems are evolving into systems with variable power consumption at every level, from consumer electronics to electrical grids. Indeed, because they perform increasingly diverse duties with varying power needs, contemporary electronic devices, from smartphones to sensors, have varied power demands [1]. The necessity for high-power energy storage is evident as variable renewable energy sources are included into electrical systems. Numerous alternative technologies have emerged to alleviate severe concerns about the energy problem. Energy harvesting from renewable resources has been the main objective of the research community in recent years of energy scarcity. The main objective of the technology is to reduce greenhouse gas pollution caused by the usage of non-renewable energy resources. Additionally, experts are working to develop ways to store this energy as electricity. One of the main concerns in the globalized era is the need for effective energy storage and sustainable energy options [2–8].

Energy storage technologies like batteries, fuel cells, and other energy-storing technologies can be used to meet the need [9, 10]. One such equipment used to store energy is called a supercapacitor. Electrochemical conversions are the basis of unconventional energy storage systems including batteries, fuel cells, and supercapacitors. They offer suitable energy and power densities that are designed for low to high power ensuing uses. They are storage devices that stand between batteries and the typical spectrum of capacitors, thus forming connecting link between secondary ion batteries and conventional capacitors. Energy storage mechanism of supercapacitors is based on the accumulation of charge or reversible redox reactions [11–13].

S. Jha · R. Prasanth (✉)
Madanjeet School of Green Energy Technology, Pondicherry Central University, Pondicherry, India
e-mail: prasanth.get@pondiuni.edu.in

© The Author(s), under exclusive license to Springer Nature Singapore Pte Ltd. 2024

C. M. Hussain and M. B. Ahamed (eds.), *Functionalized Nanomaterials Based Supercapacitor*, Materials Horizons: From Nature to Nanomaterials,
https://doi.org/10.1007/978-981-99-3021-0_27

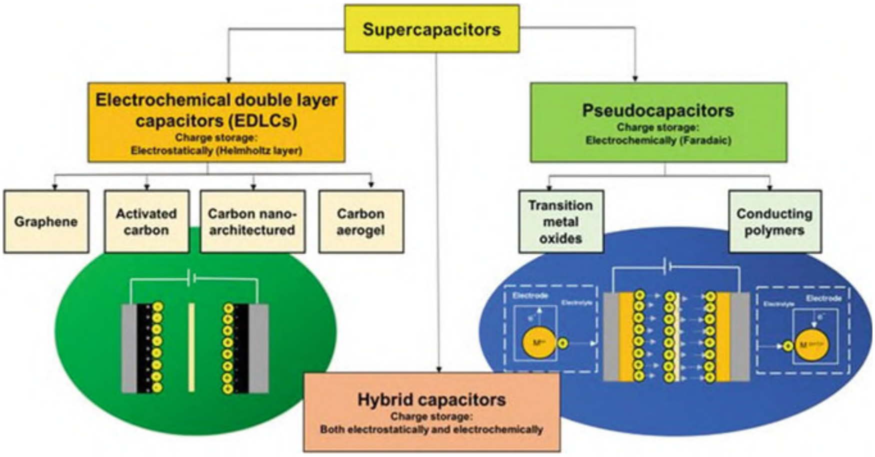
Supercapacitors
Electrochemical double layer capacitors (EDLCs)
Charge storage:
Electrostatically (Helmholtz layer)
Pseudocapacitors
Charge storage:
Electrochemically (Faradaic)
Graphene
Activated carbon
Carbon nano-architectured
Carbon aerogel
Transition metal oxides
Conducting polymers
Electrode
Electrolyte
Electrolyte
Electrode
Hybrid capacitors
Charge storage:
Both electrostatically and electrochemically

Fig. 1 Schematic diagram and classifications of supercapacitors. Reproduced with permission from Ref. [14]. Copyright © 2020 Elsevier

According to the storage criterion, supercapacitors can be divided into three main categories: EDLC, pseudo capacitor, and hybrid supercapacitor. Figure 1 represents the schematic diagram and classifications of supercapacitors [14].

In comparison to secondary ion batteries, supercapacitors are continuously creating energy-producing gadgets that are built for high power supply [15]. Over the past few decades, there has been a steady rise in scientific research about the potential applications of diverse functionalized nanostructured materials in supercapacitors. Compared to their bulk counterparts, these nanostructured materials typically exhibit improved capacitance behavior. Better chemical kinetics, chemical activity, shorter ionic diffusion channel lengths, greater surface area, and an abundance of active sites for electrochemical reactions are all advantages of functionalized nanostructured materials [16, 17]. It is one of the hotspots of multidisciplinary research and involves materials, energy, chemistry, electrical devices, and other disciplines. It can be used in a variety of industries, including industrial control, power, transportation, intelligent instruments, consumer electronics, national defence, communications, medical equipment like defibrillators and pulsed lasers, as well as new energy vehicles, thanks to its excellent performance and environmental friendliness [18–21].

Based on the state of research at the time, the prospects, difficulties, and development patterns of supercapacitors are outlined in this chapter. Section 1 provides information about introduction of functionalized nanomaterials for futuristic application. Next Sect. 2 provides brief summary of principle and mechanism of energy storage in supercapacitors. Next, in Sect. 3 a detailed summary of role of functionalized nanomaterial for energy storage applications is provided. Section 4 describes the current application of supercapacitors whereas Sect. 5 describes future development and application based on supercapacitors. A general summary of this chapter and the prospects for the current research scenario in FNM-based supercapacitor for futuristic application are provided in Sect. 6.

2 Brief of Supercapacitors

At least not in the near future, the entire human population of the planet must run on something other than renewable energy sources. Expanding pollution compels us to consider various methods for managing energy utilization. Figure 2 depicts the proportion of renewable energy sources compared to other energy sources in 2020 [22, 23]. Renewable energy should supply all of the world's energy needs for a sustainable world, but it requires a long-term strategy. Hence, it is essential to continuously boost the share of renewable energy sources in global energy production. Subsequently, due to its non-dispatchable behavior, energy from renewable sources must be stored and used as needed.

The crucial aspect of utilizing renewable energy sources is energy storage and accumulation. One of the options to store energy from renewable energy sources now is to use batteries or special hydropower facilities. Other experimental options include superconducting magnetic energy storage systems (SMES), which keep energy in a magnetic field produced by the current flowing through a superconducting coil that has been cryogenically cooled to a reduced temperature than its superconducting critical temperature. Supercapacitors might be a replacement for traditional batteries [24–31]. This section discusses a succinct overview of supercapacitors, their types, operation principles, and most recent advancements.

Supercapacitors, often called electrochemically or ultracapacitors, use thin electrolytic dielectrics and high-surface-area electrode materials to produce capacitances

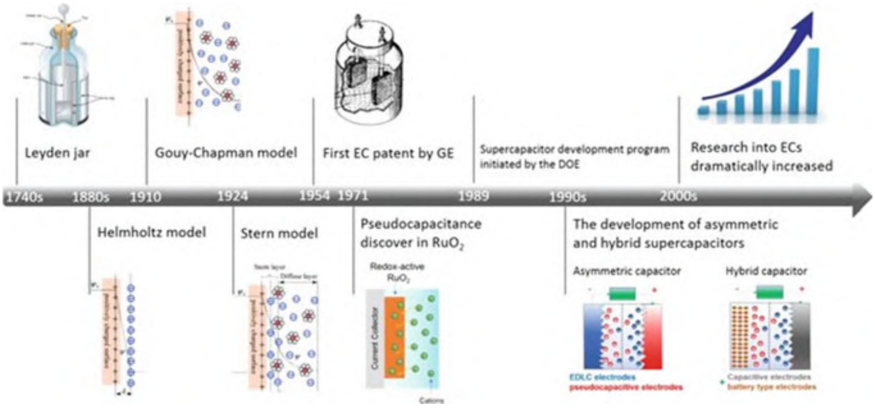
Leyden jar
Gouy-Chapman model
First EC patent by GE
Supercapacitor development program initiated by the DOE
Research into ECs dramatically increased
1740s
1880s
1910
1924
1954
1971
1989
1990s
2000s
Helmholtz model
Stern model
Pseudocapacitance discover in RuO_2
The development of asymmetric and hybrid supercapacitors
Stern layer
Diffuse layer
Redox-active RuO_2
Current Collector
Cations
Asymmetric capacitor
Hybrid capacitor
EDLC electrodes
pseudocapacitive electrodes
Capacitive electrodes
battery type electrodes

Fig. 2 **a** Total generation of renewable energy along with other types of energy sources throughout 2009–2022 in India [22]. **b** Estimated renewable energy share of global final energy consumption [23]

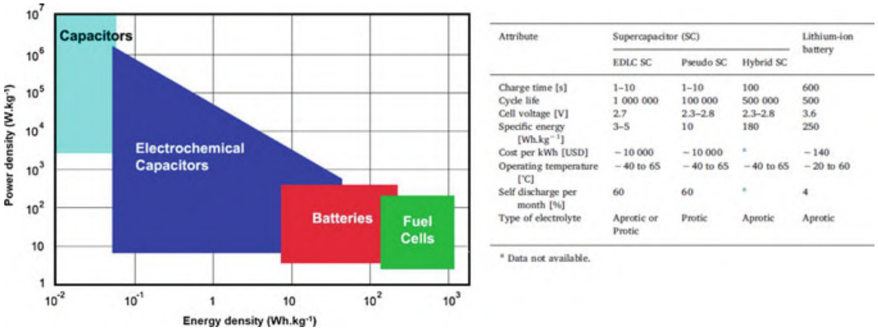

Attribute	Supercapacitor (SC)			Lithium-ion battery
	EDLC SC	Pseudo SC	Hybrid SC	
Charge time [s]	1–10	1–10	100	600
Cycle life	1 000 000	100 000	500 000	500
Cell voltage [V]	2.7	2.3–2.8	2.3–2.8	3.6
Specific energy [$Wh.kg^{-1}$]	3–5	10	180	250
Cost per kWh [USD]	−10 000	−10 000	*	−140
Operating temperature [°C]	−40 to 65	−40 to 65	−40 to 65	−20 to 60
Self discharge per month [%]	60	60	*	4
Type of electrolyte	Aprotic or Protic	Protic	Aprotic	Aprotic

* Data not available.

(a) (b)

Fig. 3 Technical development of supercapacitors throughout years Reprinted with permission from ref. [34] Copyright © 2018, American Chemical Society

that are several orders of magnitude greater than those of conventional capacitors. By accomplishing this, supercapacitors can preserve conventional capacitors' typical high-power density while achieving higher energy densities. In the 1950s, supercapacitor research and development began. General Electric (GE) and Standard Oil of Ohio (SOHIO) undertook the first trials during the 1950s and 1970s. The capacity of these earliest electrochemical supercapacitors was roughly 1F. SOHIO patented supercapacitors of this kind in 1971. In 1982, Panasonic introduced the first commercially available supercapacitor, the "Gold Cap," which had a high equivalent series resistance (ESR). The Pinnacle Research Institute (PRI) created the first electric double-layer capacitor (EDLC) supercapacitor in 1982 for military applications. Supercapacitors became industrialized in the 1980s with the Generation-1980 NEC/Tokin and 1987 Panasonic and Mitsubishi Products. Econd and ELIT introduced electrochemical capacitors or high-power start-up power applications in the 1990s. Companies like NEC, Panasonic, EPCOS, Maxwell, and NESS are currently heavily involved in studying supercapacitors. Currently, the supercapacitor market is nearly entirely dominated by goods from the United States, Japan, and Russia. Figure 3 shows the advancement of supercapacitors in several nations [32–34].

2.1 Supercapacitor Against Other Energy Storage Devices

Energy storage alternatives come in a wide variety of forms, and new ones are constantly being developed as this technology becomes a crucial part of the global energy systems of the future. Energy storage in the industry is becoming more and more necessary. As a result, various solutions become available as the demands get more particular and innovations utilizing cutting-edge materials and technologies are created. Energy storage is booming in the industry, even though the need to decrease imbalances between energy demand and production while utilizing energy produced during peak periods for later use is not new. Electrochemical energy storage systems are among the most appealing because of their many benefits, including high efficiency, affordable price, adaptable capacities, etc. Rechargeable battery chemistries that are technologically mature and well-developed have resulted in their extensive application in various industries, such as electric/hybrid electric vehicles, smartphones, medical equipment, computers, and small to large-scale energy storage applications. But rechargeable batteries have many drawbacks, including lower power densities, shortened cycle lifetimes, longer charging times, problems with thermal management, and environmental safety. Researchers worldwide have recently become more interested in supercapacitors (SCs), which are considered promising alternatives for electrical energy storage and are closely related to and can complement rechargeable batteries. SC technology has advanced in recent years and has demonstrated enormous potential for use as a possible energy storage system at a commercial scale. Supercapacitors are environmentally benign, have unusually long cycle lives compared to traditional rechargeable batteries, and have quick charge/discharge periods. Figure 4 illustrates the demand for supercapacitors and other electrochemical storage devices [24, 25].

2.2 *Supercapacitor Categories and Operation Principle*

As shown in Fig. 1, these devices are divided into three categories based on the energy storage mechanism of supercapacitors. It should be noted that the supercapacitors are under the domain of wet electrolytic capacitors, which use a liquid electrolyte consisting of ions (charged complexes) to facilitate charge transmission. The first category comprises Electric Double Layer Capacitors, often called EDLC Supercapacitors. The surface energy that is electrostatically stored at the interface of the capacitor electrodes is potential-dependent, which results in double-layer capacitance. The size of the electrodes' surface area and the Helmholtz layer's thickness are crucial factors in achieving an extraordinarily high capacity. EDLC supercapacitors have high cycle stability across millions of cycles and durability. Because of its sizeable specific surface area, activated carbon (AC) is frequently employed as an electrode material for EDLC supercapacitors. Liquid electrolyte is used in EDLC supercapacitors. The majority of these electrolytes contain dissolved ions like lithium hexafluoroacetate ($LiAsF_6$) or tetraethylammonium tetrafluoroborate ($TEABF_4$) in aprotic solvents like propylene carbonate (PC), dimethyl carbonate (DME), diethyl carbonate (DEC), or ethylene carbonate (EC) [36–41].

The pseudo-supercapacitors, also known as faradaic supercapacitors, fall under the second category. Electrode materials that perform redox reactions and intermediate electron transfer are characterized as pseudocapacitance. By manner of operation, they resemble batteries more than capacitors [42]. The pseudocapacitance develops at the electrode surfaces, where faradaic reactions initiate, and throughout processes that require the transfer of energy across a double layer, much like when a battery is being charged or discharged [43]. However, capacitance grows because

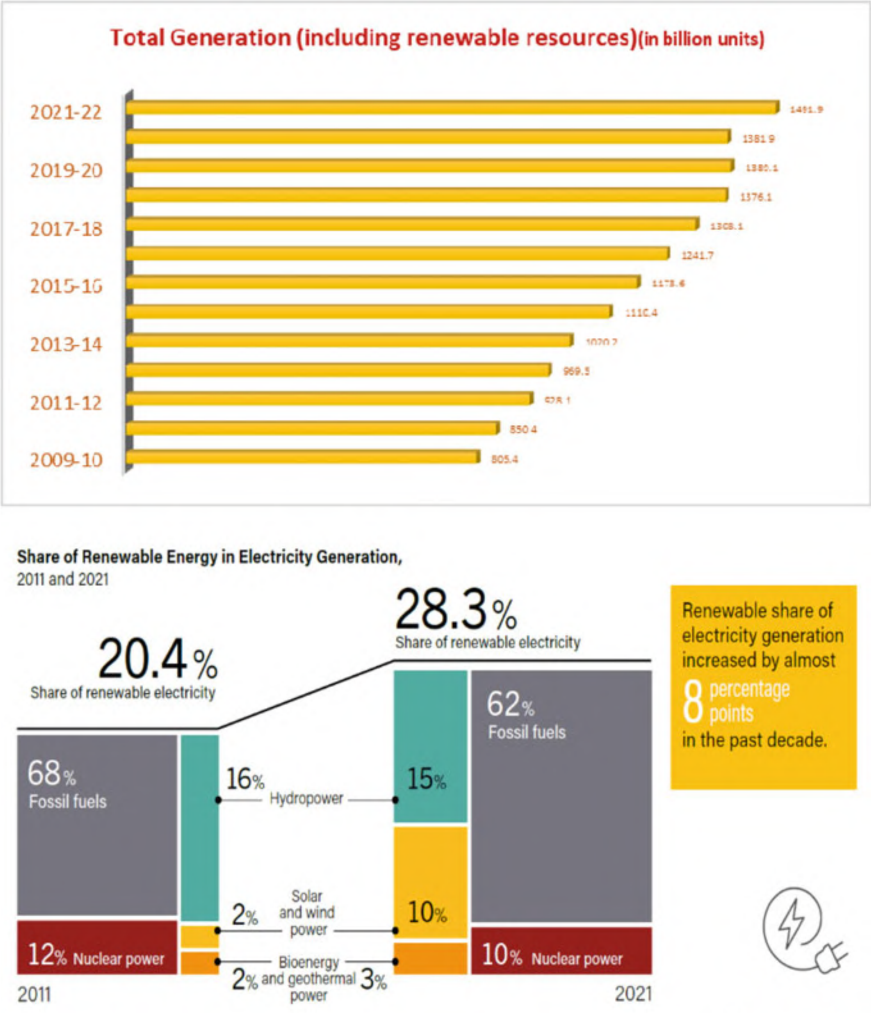

REN21 Renewable 2021 Global status report

Fig. 4 **a** Ragone plot of various electrochemical devices [25]. **b** Comparison between supercapacitors & batteries. Reproduced with permission from Ref. [24] Copyright © 2018 Elsevier

of a unique relationship between the amount of energy accepted (q) and the change in potential (V), such that the derivative d(Δ q)/d(Δ V) or dq/dV is equivalent to the capacitance C. Redox reactions occur resulting from the bonds in the compounds and transfer of energy between the electrolyte and electrode happen during charge and discharge. The "dielectric" layer does not contain energy; the energy of molecular bonding does [44–46]. The difference between an EDLC and a pseudocapacitor is that a pseudocapacitor involves quick and reversible redox reactions that occur at the interface between the active material on the electrode and the electrolyte. In contrast to the electrostatic storage principle, the electrodes in these systems are strained and deteriorate more quickly while charging and discharging. It is related to raising the internal resistance of supercapacitors and conducting polymers like polyaniline (PANI), carbon-based hetero-atoms, other transition metal oxides, nanoporous carbons with electrosorbed hydrogen, and metal oxides such as ruthenium oxides, vanadium nitride, and manganese oxide exhibit pseudocapacitance [47–49].

The final and third kinds of supercapacitors are referred to as hybrid supercapacitors. To increase energy density to between 20 and 30 W h Kg^{-1}, the concept of a hybrid supercapacitor was developed [50]. These efforts were explicitly focused on improving the energy density requirements for EDLCs by using either superior electrode and electrolyte materials or by designing hybrid supercapacitors. Different redox and EDLC materials, such as graphene or graphite, metal oxides, conducting polymers, and activated carbon, are coupled to create hybrid supercapacitors [50–53]. The coupling strategy was proposed to overcome the energy density factor of conventional EDLCs and pseudocapacitors by employing hybrid systems made up of electrodes that resemble both capacitor (nonfaradaic) and battery (faradaic) electrodes [21]. In comparison to traditional capacitors, EDLC, and pseudocapacitors, hybrid supercapacitors have a greater working potential and produce capacitance that is two to three times higher. The storage concepts for hybrid supercapacitors combine the EDLC and pseudocapacitor storage principles. The pseudocapacitor lacks the limiting property of both EDLC and pseudocapacitor. When these two components are combined, the constraints of the individual components are obscured, which has the benefit of supplying a greater capacitance [54]. Hybrid supercapacitors can be symmetric or asymmetric depending on how the assembly is set up. When two separate electrodes of different materials are combined to form a hybrid supercapacitor, it exhibits better electrochemical behavior than the individual ones. The cycle stability and affordability of hybrid systems are maintained, which are the constraining factors in the success of the pseudocapacitor. Compared to the symmetrical EDLC, the hybrid type has greater rated voltages and expanded values of specific capacitance, which correspond to higher specific energies [55, 56].

Electrolytes play an essential role in supercapacitors. Aprotic and protic electrolytes are the two kinds of electrolytes utilized which has unique advantages and restrictions. Protic solvents based on the water offer greater conductivity, safety, and environmental friendliness. Sulfuric acid (H_2SO_4), potassium hydroxide (KOH), and sodium hydroxide (NaOH) electrolyte is the most commonly used protic electrolyte. Aprotic electrolytes are used instead of water-soluble electrolytes, the working voltage window is expanded, increasing the energy density. Lithium salts such as lithium perchlorate ($LiClO_4$), lithium hexafluorophosphate ($LiPF_6$), and lithium tetrafluoroborate ($LiBF_4$) mixed in a variety of solvents like diethyl carbonate (DEC), dimethyl carbonate (DMC), and ethylene carbonate (EC) are among the most popular aprotic electrolytes [57–61].

3 Role of Functionalized Nanomaterials for Supercapacitors

In order to tackle the challenge of storing energy by having high energy density as well as power density, inventing new materials hold the key to significant advancements in energy conversion and storage. Nanomaterials, in particular, provide unique features or combinations of characteristics as electrodes and electrolytes in a broad range of energy storage devices such as supercapacitors. Nanostructured materials have sparked a lot of attention because of the remarkable mechanical, electrical, and optical properties that are given by confining the dimensions of such materials, as well as the interaction of bulk and surface features with the overall behavior [62]. Comparing nanomaterials to traditional battery and supercapacitor materials, they offer significantly better ionic transport and electrical conductivity. They also make it possible for all intercalation sites in the particle volume to be occupied, which results in high specific capacities and rapid ion diffusion. These characteristics enable nanomaterial-based electrodes to withstand high currents, providing a viable method for storing high-energy and high-power density storage [38]. Numerous factors contribute to effectiveness of nanoparticle in energy storage applications. In order to leverage several charge storage methods, such as pseudocapacitance, diffusion-limited intercalation processes, and surface-based ion adsorption, nanostructuring is becoming increasingly crucial for controlling the electrochemical performance. However, there are still a lot of difficulties with their application in energy storage technologies, and there are very few commercial products that incorporate nanoparticles. Due to high surface area of nanomaterials, which leads to parasitic interactions with the electrolyte, notably during the initial cycle, known as the first cycle irreversibility, and their tendency to aggregate, limitation of nanomaterials in energy storage devices. Therefore, future initiatives seek to create controlled geometric designs via adaptive nanomaterial assembly.

The materials utilized for the electrodes have a significant impact on the capacitance and charge storage of supercapacitors. Therefore, the most crucial approach to overcoming these difficulties is to use FNMs with high capacitance and increased performance to boost existing electrode materials. Integrating new elements or functional groups in nanomaterial to create functionalized nanomaterials (FNMs) is one way to tackle all shortcoming faced while using conventional nanomaterials. Functional nanomaterials are enhanced nanomaterials with nanometer-scale internal or exterior dimensions. Compared to other materials, FNMs have better physical, chemical, and mechanical properties. FNMs are thought to be attractive materials for supercapacitor electrode material because they offer specialized surface areas for tailored molecule attachment. Numerous functionalized nanomaterials have been investigated for use as supercapacitor electrodes which include carbon based, polymer based, metal based, and composite FNM. These types of functionalized nanomaterials are intended to enhance the charge storage properties of supercapacitors.

Carbon-based FNMs can be functionalized with the use of components like polymers, hydroxyl and carboxyl groups, and elements like fluorine and nitrogen. Graphene and its variants, as well as carbon nanotubes (CNT), are the most prevalent functionalized carbon nanomaterials. CNT is one of the astonishing carbon nanomaterials whose sides of the nanotube are constructed of hexagonally shaped particles [63]. Functionalization of CNT is usually done by either forming covalent bond between the defect groups on molecules on the conjugated side walls of the CNTs and the functional groups or adsorption of a specific type of functional molecule in a CNT results in chemical interaction [64]. Similar to CNT, graphene exhibits variety of remarkable properties, including good optical transmittance, excellent electronic transport properties, a large specific surface area, superior mechanical stiffness and flexibility, a high 3D aspect ratio, and exceptional thermal response, because of their exceptional microscale crystallinity. Despite having such excellent properties graphene have tendency to get agglomerated while stacking. Self-assembly, spin coating, and filtration are examples of solvent-assisted techniques that can be used to chemically restructure graphene. An extensively grown graphene derivative is graphene oxide (GO), which has been chemically functionalized [65–70].

In order to create units of intermediate specific energy, functionalized conducting polymers are supposed to close the gap between batteries and the current carbon-based supercapacitors. Because of their high charge density and affordable cost, functionalized conducting polymers are usually intriguing. The broadest range of specific capacitance is displayed by polyaniline, which is made into functionalized conducting polymer by doping, adding additional composite materials like activated carbon material, etc. Similarly, functionalization of polypyrrole is thought to improve charge storage qualities because polyimide matrix protects the polypyrrole from oxidative degradation and it is cathodically electroactive. Also, most of functionalized polythiophene-based derivatives are stable in air and moisture and are either p-doped or undoped. Thiophene-based functionalized conjugated polymers hold an unrivaled position among the abundant conjugated polymers and that is continually growing because of their exceptional optical and conductive characteristics [71–78].

Functionalized metal-based supercapacitor electrode material is known for good electrochemical activity and electrical conductivity. Transitional metal-based FNMs are widely exploited in energy conversion and storage systems because of their reasonable affordability, flexible valence states and morphologies, and high capacitance [79]. Theoretically, the low resistance and suitable specific capacitance of the new generation materials utilized to make supercapacitor electrodes include transition metal oxides, hydroxides, dichalcogens, and metal oxide heterostructures [80]. For having functionalized transition metal-based electrode material the first strategy involves increasing the number of active sites on the surfaces of nanomaterials, where electrochemical reactions take place. The second strategy is to develop novel features in nanostructured materials that distinguish them from their bulk material counterparts, i.e., by exposing more atoms on the surface of nanostructured materials, thus optimizing surface-volume ratio [81–85].

Composite FNMs have been used to achieve performance beyond the capabilities of each material, particularly in terms of energy density and durability. Composites are usually combination of one base material, e.g., carboneous material with other components [86]. Combining these different nanoscale capacitive materials with their unique advantages demands for meticulous fabrication procedures. The morphology and interfacial qualities of the constituent components as well as the choice of constituent components affect the features of the composites. When designing and producing nanocomposite electroactive materials for supercapacitors, many factors must be taken into account, such as the choice of material, synthesis methods, fabrication process parameters, interfacial properties, electrical conductivity, nanocrystallite size, and surface area [87].

Although number of research studies have been done on FNM-based supercapacitor electrode material, the wide application of these materials is still limited because research related to synthesizing and developing FNMs are still in infancy. A thorough understanding of the mechanism can serve as an excellent guide for developing next-generation materials that will boost the energy density of SC material systems. Instead of being restricted to lab-scale research, the goal of SC development by using FNM-based electrode material is going forward for actual commercial applications. It is necessary to underline the concomitant vital concerns of large-scale production via a simple synthesis approach, cost-effectiveness, and environmental friendliness. An effective way for achieving the screening of novel, high-performance capacitive-type electrode materials would be to develop and apply new machine-learning algorithms in material design.

4 Current Perspective and Challenges Using FNM-Based Supercapacitors

Supercapacitors are presently commercially accessible. Their capacity to combine better energy density with long-term stability is suitable for applications that need unhindered energy for smooth functioning, such as hybrid electric vehicles. However, their need for more power proficiency restricts their use for many commercial purposes. Using functional nanostructured materials has already improved the tool available for demonstrating the power efficiency of faradaic electrodes. The microstructural alterations that occur while cycling negotiate the impact of nanostructure based on the electrolyte. However, no commercially available device currently uses the core–shell design with FNM-based supercapacitor electrode material. The primary focus for developing supercapacitors is to create a new generation of functional nanomaterials with high cell voltage, electrode capacitance, and an environmentally sustainable and affordable nature. The development of inexpensive materials is made possible in large part by the use of aqueous electrolytes. Recent research is being done on solid-state electrolytes that simultaneously serve as separators. Cell component optimization is an essential aspect of developing functional supercapacitors. Developing an electrolyte that can function well at low temperatures and a low oxidation resistance provided by current collectors in an aqueous medium is required. The output current and voltage can be controlled with such a setup. The functionalization of nanomaterials by incorporating a wide variety of dopants, functional groups, and complexes has been created utilizing various methods, including hydrothermal treatment and straightforward heat treatment of given base nanomaterial with dopant-containing complexes, which results in the formation of functionalized nanomaterial complexes in an inert atmosphere. However, sometimes it is observed due to certain dopants in a particular set of base nanomaterials, e.g., heat treatment techniques in the presence of nitrogen in carbon nanomaterials to decrease in surface area and, vice versa, a method to increase surface area mainly causes a reduction in nitrogen content. More advancements in synthesizing FNM-based supercapacitors are needed immediately to provide the conditions necessary for better-performing devices. This section addresses the present scenario, market analysis of FNM-based supercapacitors, and its challenges.

4.1 Recent Development in the Supercapacitor Market

Supercapacitors have undergone significant development in the last few decades, from specialized energy storage devices with small capacities to large-scale power storage, from distinct energy storage to blended energy storage with batteries or fuel cells. They have demonstrated many different advantages. Due to their excellent performance advantages, supercapacitors have received much attention in research, are used widely, and have enormous promise in the consumer electronics sector. The Global Supercapacitors Market was estimated to be worth USD 549.1 million in 2021, and it is anticipated to grow to be worth USD 1,114.60 million by 2027, at a CAGR of 13.19% [88]. Figure 5 illustrates the current trend analysis of the global supercapacitor market. Supercapacitors offer greater flexibility than conventional batteries, which replace standard electric car batteries with their rapid charging and temperature stability properties. Supercapacitor charging and discharging also aids in the maintenance of peak loads and backup power, which are critical for battery-powered industrial applications such as video doorbells, smoke alarms, smart meters, and medical applications. Supercapacitors have become increasingly in demand in recent years because of their need for communication systems in telecommunications and space. At its Vikram Sarabhai Space Center (VSSC), the Indian Space Research Organization (ISRO) developed the technology for synthesizing supercapacitors (2.5 V) with variable capacitance values, including 5 F, 120 F, 350 F, and 500 F, to meet a variety of societal and space-related applications. Additionally, several market vendors have noticed a rise in revenue in the electric vehicle sector, driving the expansion of supercapacitors in the automotive sector. The digital transformation in the industry also influences the electrical sector with the COVID-19 outbreak. Governments, utilities, and manufacturers are embracing digital technologies more and more. This can be seen in the rise in the purchase of smart meters,

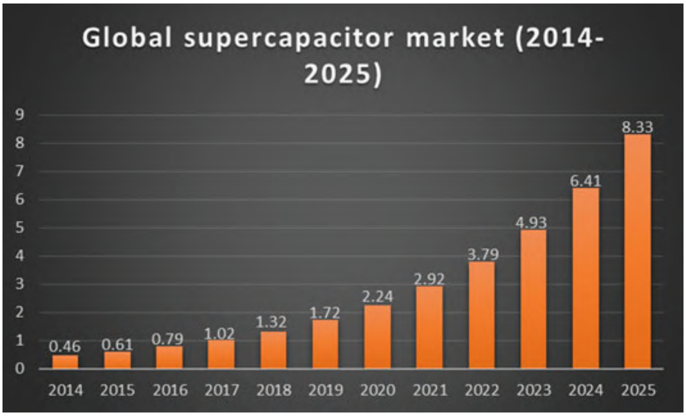

Fig. 5 Global supercapacitor market analysis from 2014 to 2025

digital substations, smart EV charging infrastructure, software solutions like artificial intelligence, digital twins, dynamic line rating, and blockchain technology. New prospects in the supercapacitor industry are anticipated due to such investments.

4.2 Present Scenario of FNM-Based Supercapacitors

The effectiveness of supercapacitors is constantly improving, which causes an increase in their applications. Rechargeable batteries have dominated the energy storage industry for the past two decades. The energy storage industry needs to optimize performance and save costs. Using functionalized nanomaterial for supercapacitor electrode material is one method to solve the issue. This scenario drives current efforts in FNM research for energy applications for future energy. One of the main reasons for selecting FNM-based supercapacitor electrode material is that the dopants or complexes used to functionalize nanomaterials are generally cheaper, abundant, and environmentally friendly. In addition, thanks to FNM's various bonding states and allotropes, a family of new nanomaterials can be derived. This section discusses the application of supercapacitors in the current environment.

4.2.1 Automobiles and Transport Application

Electric Vehicle (EV) producers employ new methods to improve their vehicles' functionality and driving range. Energy storage systems for multi-tasking operations like ignition, start-up, security, transmission, and lighting are well-known needs for the automobile sector. The electric or hybrid vehicles need a high current for a brief period during charging, causing a power pulse that is quickly produced by employing

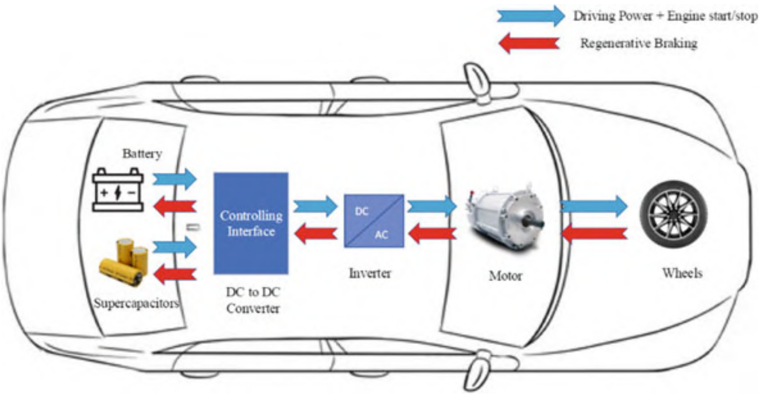

Fig. 6 Power management in EVs [89]

an FNM-based supercapacitor. Examples of such vehicles are those made by Toyota and Mazda. For power bursts, beginning and stopping fuel-saving arrangements that allow for faster preliminary acceleration, Toyota's Yaris Hybrid-R and PSA Peugeot Citron use supercapacitors, respectively. A simplified design of SCs integrated with batteries to power an EV's drive train is shown in Fig. 6. The central control system instructs the motor to provide the necessary torque and speed when the accelerator pedal is pressed [89]. The motor switches to generating mode, and the power flow is reversed to charge the battery and supercapacitors when braking.

It is already widely known that supercapacitors are used in regenerative braking. By halting the automobile while retaining its braking energy, this is accomplished. This was observed when a one-ton hybrid supercapacitors assembly was installed in a tram in Switzerland. Maxwell designed a similar type of assembly that was used on trams in Paris and Belgium. It combined a high cycle rate with the installation of 48 supercapacitors in each vehicle. The FNM-based supercapacitors can supply this energy for the diesel engine's ignition and for accelerating by capturing the braking power. This recuperation has the potential to save up to 30% of energy. Initially, the effective consideration of the use of a supercapacitor with public transportation was the motivating characteristic. The application of a process to increase energy efficiency in vehicles like trucks and buses to prevent the loss of heat energy at a stop while the engine is running. The idea behind supercapacitors is to convert this energy into electrical energy and use it to drive acceleration support requirements. Reducing CO_2 emissions and fuel use promotes eco-saving [90, 91].

4.2.2 Public Sector Applications

Ubiquitous applications include products with simple operations. The cordless screwdriver is powered solely by supercapacitors developed by Coleman Company Inc. and lasts less time than the one powered by a rechargeable battery. The downside of using the supercapacitor model is that the runtime is half that of the battery model, but it has the advantage of 90-s charging and charge retention. Additionally, Maxwell Technologies (a producer of supercapacitors) and Celadon have developed items, including supercapacitor-powered remote controllers [92]. The remote control was initially powered by two AAA batteries and operated with a quick charging function provided by a supercapacitor. In 2010, three Japanese firms 2010's Nippon-Chemi-Con, collaborated to produce eco-friendly street lighting in Japan by combining solar energy with supercapacitors as energy storage devices [93]. The assembly included LED bulbs and solar panels to capture solar energy throughout the day and store it in supercapacitors for later use (charging); supercapacitors help discharge and escort the LED illumination at night. As a result, clean energy systems are more durable and have longer lifetimes than existing energy systems.

FNM-based supercapacitors are employed in renewable and sustainable energy sources because they act as stabilizers in solar and wind energy-based power line systems. Due to their quick reaction time to erratic weather fluctuations, FNM supercapacitors provide wind turbines with brief energy bursts [94]. Such supercapacitors, which can adjust blade orientation and protect a wind turbine from strong winds, are used to handle power outages. FNM-based supercapacitors also benefit from their high cycle count, energy compatibility with power density, and absence of maintenance [95].

4.2.3 Medical and Industrial Applications

Supercapacitors can be used in high-voltage pulse delivery applications in the medical industry. As a result, they are fed into defibrillators, which administer up to 500 J energy push to shock the heart back to regular operation. Patients who have experienced mental trauma are treated using similar techniques. Novel use of supercapacitors is the ventilator backup together with dental technology, etc. JSR Micro created a hybrid supercapacitor for medical imaging equipment for backup power supply [96].

This industry has the broadest range of uses for hybrid supercapacitors, from industrial electronics like automated meter reading (AMR) to emergency backup power sources to prevent catastrophic failures until power is restored. FastCAP developed supercapacitor-powered drills as a result of the stability of supercapacitors. Additionally, there are industrial applications involving the cooperation of batteries and hybrid supercapacitors. The partnership limits the energy benefits from both energy storage device types and may be helpful in many power-related applications [97].

4.2.4 Defense and Military Applications

An intriguing field for FNM-based supercapacitor applications is instruments that rely on batteries, such as navigational, sensing, and communication devices. With the

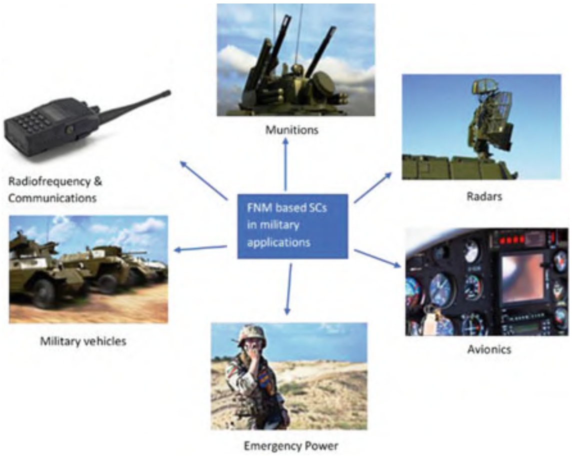

Fig. 7 SCs used for various defences applications [98]

proper FNM-based supercapacitor assembly, the radar system, electromagnetic pulse weapons, torpedoes, etc., may all be operated. Tecate Group has produced numerous supercapacitor systems for use in military applications. Phased array radar antennas, avionics display devices, airbag exploitation power, GPS, and missiles are examples of applications requiring high specific power, which FNM-based supercapacitors can fulfill. Figure 7 illustrates SCs used for various defence applications [98].

4.3 Challenges for FNM-Based Supercapacitors

Because of their exceptional qualities, supercapacitors are widely employed in the automotive, industrial, military, consumer electronics, and other sectors. These technologies do, however, have significant drawbacks. The four major aspects primarily characterize the current issues that need to be solved are illustrated in Fig. 8.

4.3.1 Technical Problem

The energy densities of supercapacitors are low. The energy densities of supercapacitors ($<$20 W h Kg^{-1}) and batteries (30–200 W h Kg^{-1}) now differ somewhat, and how to close this gap remains a research priority and challenge in the field of supercapacitors. Supercapacitor storage capacity can be increased by upgrading manufacturing processes and technologies. However, finding new electrolytes and electrode-active materials with improved electrochemical performance will be challenging and time-consuming in the long run. Low energy density supercapacitors make for bulkier, less compact devices. Supercapacitors' energy densities can be increased by expanding the operation voltage window, increasing the electrochemically active surface area

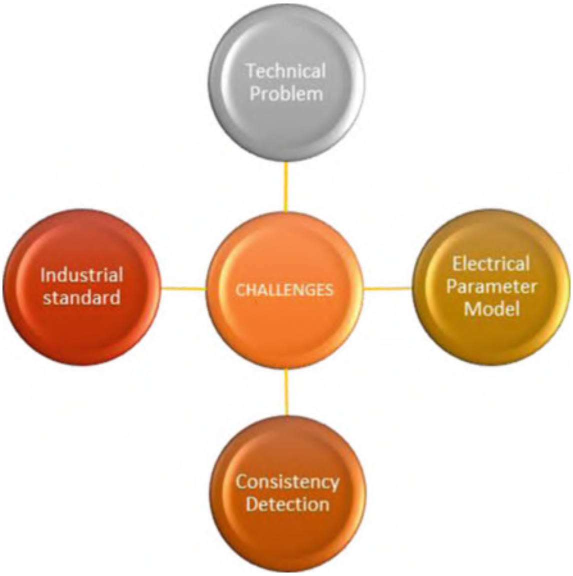

Fig. 8 Four primary challenges faced by supercapacitors

of electrode materials in double-layer capacitors, or doing both. More research is being done to create novel materials with high surface areas and use suitable organic electrolytes that can withstand a wider voltage window [99].

4.3.2 Establishment of Electrical Parameter Model

The supercapacitor model may be comparable to the ideal model in some circumstances. Still, in military applications, particularly in satellite and spacecraft power supply applications, several nonideal factors may provide concerns that must be taken into consideration. Due to its restricted energy, resonance induced by periodic signal, filter, and energy storage capacitor has a stable solution. Due to their tremendous energy, supercapacitors have the capacity for immediate throughput and enormous power. It is crucial to have a trustworthy design to analyze the effects of load nature, load fluctuation or the external environment, and unintentional disturbance on the system's stability [6].

4.3.3 Consistency Detection

Because a supercapacitor's rated voltage is so low (less than 2.7 V), numerous series connections are necessary for use in real-world scenarios. It is crucial to know whether the voltages on each capacitor in series are stable since applications frequently require high current charging and discharging and overcharging hurts the lifespan of capacitors [6].

4.3.4 Industrial Standard

Supercapacitors have hit the market and developed themselves in a short period with high speed. There are various levels of enterprises in the supercapacitor sector. Since supercapacitors are a novel kind of energy storage, their healthy development is inextricably linked to market and industry regulation, which strives to create workable regional, national, and even global standards. For supercapacitors, a set of technical standards should be established, including terms, a classification model naming method, an electrical performance test method, technical safety requirements, general specifications, electrode material requirements, electrolyte requirements, charger requirements, production requirements, transportation requirements, recovery requirements, and destruction requirements. It is an essential tool for fostering the healthy growth of the industry.

5 Future Development of FNM-Based Supercapacitor

Being one of the most popular options to enhance industrial operations, energy storage systems have started to play a crucial role in recent years. These tools boost the productivity of industrial systems while improving the energy effectiveness, dependability, and adaptability of electrical systems. These gadgets improve electrical systems' energy efficiency, reliability, and adaptability while increasing the productivity of industrial systems. Supercapacitors (SCs), which reduce the gap between batteries and traditional capacitors, have a better trend than their rivals due to their high technology readiness level (TRL), TRL8, and auspicious track record. SCs have a high power density but low specific energy [100].

As previously mentioned, SCs concentrate on applications requiring charge–discharge cycle periods between a few seconds and several minutes. Numerous study publications have been published as a result of this. In recent years, research and development initiatives have been created to enhance the performance of industrial processes and electrical systems. These studies seek to develop new ESS industrial products based on SCs. The numerous research on SCs demonstrates the existing need for this technology, which is growing annually and inspiring high hopes for the future. Figure 9 depicts the classification of SC-related scientific publications over the past ten years based on their applications.

In this section, we primarily concentrated on recent efforts to produce electrode materials, characterize functionalized nanomaterials, and analyze and investigate their applicability in the field of energy storage as supercapacitors. Here, we've outlined the cutting-edge methods for using FNMs that improve their use in the field of supercapacitors for future applications. Based on the state of research at the time, supercapacitors' potential, difficulties, and development patterns are enumerated. Figure 10 illustrates the futuristic approach development trend of supercapacitors which is discussed and elaborated in this section.

Fig. 9 Classification of SCs related to scientific publication over past decade based on their applications

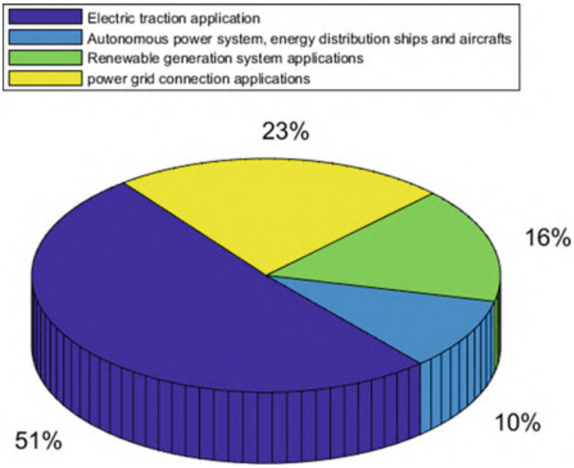

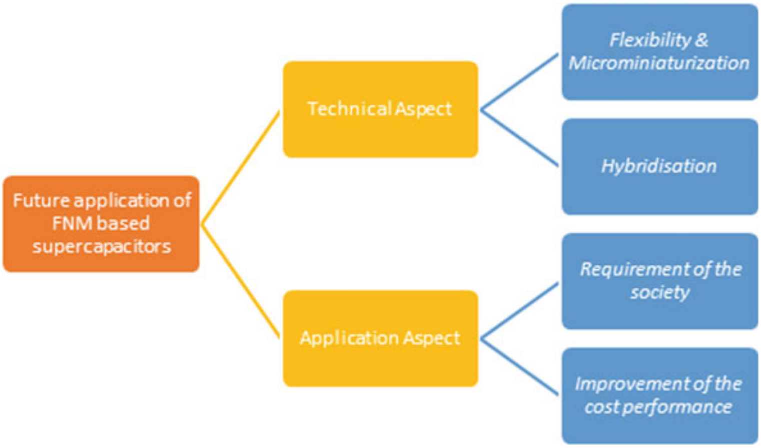
Future application of FNM based supercapacitors
Technical Aspect
Application Aspect
Flexibility & Microminiaturization
Hybridisation
Requirement of the society
Improvement of the cost performance

Fig. 10 Futuristic approach development trend of supercapacitors

5.1 Technical Aspects

5.1.1 Flexibility and Microminiaturization

The development of flexible, compact energy storage systems with strong electrochemical capabilities is crucial. Researchers are increasingly interested in flexible energy storage systems due to the rapid growth of portable electronics and the idea of wearable electronics. The electrode's rigidity severely constrains the geometry of typical FNM-based supercapacitors, and the electrode's preparation with the metal collector and bonding agent further lowers the supercapacitor's electrochemical performance. The next generation of flexible storage devices will be developed to pair a flexible FNM-based supercapacitor with a portable electronic device [101–103]. Numerous reports have been made on flexible supercapacitors with various macromorphologies and microstructures. Positive and negative electrodes, diaphragms, electrolytes, fluid collectors, and packaging shells in flexible supercapacitors are flexible in contrast to traditional nonflexible supercapacitors, which allows for flexible supercapacitors to be assembled in thin, light, and intelligent designs of any shape and size, increasing their potential for use in flexible and wearable fields. From a practical research perspective, finding appropriate flexible electrodes is essential to producing flexible supercapacitors. These can be achievable by the intelligent use of functional nanomaterials, which can be used as electrode material for flexible supercapacitors. Therefore, the fabrication of high-performance flexible electrodes is a study area of interest. Up to this point, a vast and intricate system has been researched on flexible electrodes and supercapacitors. The constructed flexible electrodes and flexible supercapacitors exhibit physical morphology and functional features that are dynamic and diverse. Flexible electrodes can be made by growing the active material ex situ or in situ on a flexible substrate, such as conducting polyethylene terephthalate (PET), carbon cloth, and so on [103]. Since no polymeric binders are necessary for the deposition of active material on the flexible substrate in the case of in situ growth, the electrodes exhibit improved electrochemical performance in addition to being flexible. When designing device structures, it's essential to eliminate electrolyte leakage, simplify the encapsulation process, increase the utilization rate of electrode materials, and provide good compatibility between gel electrolytes and electrode materials [104]. Future research will focus on developing flexible electrodes with straightforward processes, solid electrochemical performance, and flexibility to integrate active ingredients, flexible substrates, and electrolytes. It is essential to design functionalized nanolevel electrode materials to provide additional electrochemical active sites or to compound the materials to reduce the electrode size without reducing its energy density. This can be accomplished by using nanostructures specially designed with the help of functionalization to give an excess of redox reaction sites and increased surface area. Meanwhile, its downsizing is also aided by developing flexible all-solid SC. Ultrahigh power delivery, excellent rate capabilities, and high-frequency response are all desirable qualities of micro-supercapacitors. It is believed that using capacitors in wearable, microelectronic, and other goods may be expanded by developing flexible and micro-capacitors [105–107].

5.1.2 Hybridization

Building hybrid batteries and supercapacitors is an excellent solution to the issue of the low energy density of supercapacitors is to use supercapacitors, which are systems where one electrode stores charge using a battery-type Faradaic process while the other does it using a capacitive mechanism. Lithium/sodium/potassium/magnesium ion hybrid battery-supercapacitors are one type of hybrid battery-supercapacitor device that inherits the high power (0.1–30 kW kg^{-1}) of supercapacitors and the high energy density (5–200 W h Kg^{-1}) of secondary batteries [108]. Additionally, these devices benefit from steady extended cycle performance and affordable prices. Due to its potential use in future electric vehicles, smart electric grids, and even miniaturized electronic/optoelectronic devices, among other things, the battery-supercapacitor hybrid device (BSH), which is typically built with a high-capacity battery-type electrode and a high-rate capacitive electrode, has attracted enormous attention. With the appropriate design, BSH will offer unique benefits like high performance, affordability, safety, and environmental friendliness [109]. The development of an attractive BSH device with a broader cell voltage and more capacity is made possible by swapping out one of a symmetric SC's capacitive electrodes for a battery electrode (thus higher energy density). BSHs could have high power densities comparable to traditional SCs with the right battery electrode architecture design. The findings of laborious research demonstrate that the two-dimensional or nanoscale approach of the battery-type electrode materials may effectively reduce the electrolyte ion transport retardation. Because of this, it still needs to be improved to match the anode and cathode materials properly to perform as hybrid supercapacitors. The voltage window and the electrolyte selection, in addition to the compatibility of the anode and cathode materials, play a significant role in the performance of the hybrid battery-supercapacitors [110].

An optimal power source in broader applications is anticipated to be dense. Supercapacitors can effectively compete with secondary batteries in this circumstance and may even prove to be a superior replacement. Supercapacitors can compete favorably with secondary batteries in such a situation and might even be an acceptable replacement for them as energy storage devices.

5.2 Application Aspect

5.2.1 Requirement of the Society

The application features of supercapacitors are crucial for addressing social requirements and advancing industrial growth. High-capacity portable supplies are becoming increasingly important as the electronic sector develops quickly. On the one hand, environmental preservation and energy use are topics in which people worldwide are becoming more and more interested. The world population is actively looking for solutions, and they are enthusiastic for more and more renewable energy to be employed. The invention of supercapacitors, on the other hand, is a result of the pressing demand for high-capacity, portable backup power to be available for all types of electronic equipment due to the rise of the electronics industry. These societal demands help the supercapacitor sector develop quickly to some extent, and the market opportunity is enormous.

The United States Department of Energy and USABC coordinated national laboratories and businesses (such as Maxwell, GE, etc.) to work together on the development of dual-layer supercapacitors made of carbon materials starting in 1992. The original objective is to achieve a supercapacitor with a 5 W h Kg^{-1} energy density and a 1 kW kg^{-1} power density. This objective has essentially been met. The SAFT firm led the European Community in formulating the supercapacitor research strategy for electric vehicles in 1996. The goal is to meet the specifications of the electrochemical cell and fuel cell electric vehicles by achieving specific energies of 6 W h Kg^{-1}, special powers of 1500 Wkg^{-1}, and cycle lives of more than 100,000 cycles. According to the data sources, supercapacitors will be perfect for hybrid vehicles whenever their specific energy hits 20 W h Kg^{-1}. The current research level must be enhanced to meet the needs of social growth. In addition, new energy vehicles, rail transit, intelligent meters, wind turbines, power grid equipment, heavy port machinery, national defense military industry, and other fields are widely used. The application field for supercapacitors will keep growing as cooperation and communication between upstream and downstream businesses improves.

5.2.2 Improvement of the Cost Performance

The first and most important factor to take into account for every industry to survive is improving product performance and lowering production costs. The study in this area primarily focuses on enhancing the supercapacitor's technology, as well as the manufacturing process and technology. This includes finding stable and efficient electrode and electrolyte materials to improve performance while lowering costs. To realize the goal of complementary performance and low overall price, one must (1) find new minimal crude ingredients, such as natural mineral resources; (2) look for the combination of low-price and high-price raw materials; and (3) improve the production process (such as by streamlining the process) and the production equipment. Consequently, this will also serve as the primary focus and strategic objective of the product's further development; (4) Pay attention to cost concerns when applying new electrode materials, such as carbon fiber graphene, and the potential for industrialization of the materials; (6) The research of group modules should pay more focus on the overall life span characteristics and capacitors and the management system to improve reliability and security. Research on matching existing electrode materials, such as matching of existing electrode materials with the electrolyte, is another critical area [5].

6 Conclusion

Functional nanomaterial-based supercapacitors have demonstrated considerable promise in many sectors and fields as a new kind of environmentally friendly and effective energy storage device. FNM-based supercapacitor development will have countless opportunities thanks to the enormous potential market. These suitable energy storage technologies do, however, nonetheless have issues. While improving energy density, lowering prices, and expanding the range of applications for supercapacitors are vital goals, future research will continue to be focused on the electrode materials that now limit the performance and price of supercapacitors. Exploration of the FNM-based supercapacitor research area is still in its infancy, and the future development of novel, cutting-edge materials for these uses is quite promising.

References

1. Raghavendra KVG, Vinoth R, Zeb K, Gopi CVM, Sambasivam S, Kummara MR, Obaidat IM, Kim HJ (2020) An intuitive review of supercapacitors with recent progress and novel device applications. J Energy Storage 31:101652
2. Tarascon JM, Armand M (2001) Issues and challenges facing rechargeable lithium batteries. Nature 414(6861):359–367
3. Zhang X, Zhu G, Wang M, Li J, Lu T, Pan L (2017) Covalent-organic-frameworks derived N-doped porous carbon materials as anode for superior long-life cycling lithium and sodium ion batteries. Carbon 116:686–694
4. Manthiram A (2011) Materials challenges and opportunities of lithium ion batteries. J Phys Chem Lett 2(3):176–184
5. Huang S, Zhu X, Sarkar S, Zhao Y (2019) Challenges and opportunities for supercapacitors. APL Mater 7(10):100901
6. Tie D, Huang S, Wang J, Ma J, Zhang J, Zhao Y (2019) Hybrid energy storage devices: Advanced electrode materials and matching principles. Energy Storage Mater 21:22–40
7. Wang M, Zhao Y, Zhang X, Qi R, Shi S, Li Z, Wang Q, Zhao Y (2018) Interface-rich core-shell ammonium nickel cobalt phosphate for high-performance aqueous hybrid energy storage device without a depressed power density. Electrochim Acta 272:184–191
8. Wang M, Jin F, Zhang X, Wang J, Huang S, Zhang X, Mu S, Zhao Y, Zhao Y (2017) Multi-hierarchical structure of hybridized phosphates anchored on reduced graphene oxide for high power hybrid energy storage devices. ACS Sustain Chem & Eng 5(7):5679–5685
9. Zhang LL, Zhao XS (2009) Carbon-based materials as supercapacitor electrodes. Chem Soc Rev 38(9):2520–2531
10. Burke AF (2007) Batteries and ultracapacitors for electric, hybrid, and fuel cell vehicles. Proc IEEE 95(4):806–820
11. Balducci A, Dugas R, Taberna PL, Simon P, Plee D, Mastragostino M, Passerini S (2007) High temperature carbon–carbon supercapacitor using ionic liquid as electrolyte. J Power Sources 165(2):922–927
12. Largeot C, Portet C, Chmiola J, Taberna PL, Gogotsi Y, Simon P (2008) Relation between the ion size and pore size for an electric double-layer capacitor. J Am Chem Soc 130(9):2730–2731
13. Kandalkar SG, Dhawale DS, Kim CK, Lokhande CD (2010) Chemical synthesis of cobalt oxide thin film electrode for supercapacitor application. Synth Met 160(11–12):1299–1302
14. Abdah MAAM, Azman NHN, Kulandaivalu S, Sulaiman Y (2020) Review of the use of transition-metal-oxide and conducting polymer-based fibres for high-performance supercapacitors. Mater Des 186:108199
15. Burke A, Zhao H (2015) Applications of supercapacitors in electric and hybrid vehicles. University of California, Davis, Institute of Transportation Studies
16. Ealia SAM, Saravanakumar MP (2017) A review on the classification, characterisation, synthesis of nanoparticles and their application. In: IOP conference series: Materials science and engineering, vol. 263, No. 3. IOP Publishing, p 032019
17. Jeevanandam J, Barhoum A, Chan YS, Dufresne A, Danquah MK (2018) Review on nanoparticles and nanostructured materials: History, sources, toxicity and regulations. Beilstein J Nanotechnol 9(1):1050–1074

18. Zhao J, Burke AF (2021) Review on supercapacitors: Technologies and performance evaluation. J Energy Chem 59:276–291
19. Zhao J, Gao Y, Burke AF (2017) Performance testing of supercapacitors: Important issues and uncertainties. J Power Sources 363:327–340
20. Burke A, Miller M (2011) The power capability of ultracapacitors and lithium batteries for electric and hybrid vehicle applications. J Power Sources 196(1):514–522
21. Lu M (2013) Supercapacitors: Materials, systems, and applications. John Wiley & Sons
22. “Power Sector at a Glance ALL INDIA | Government of India | Ministry of Power” Powermin.gov.in, 2020, powermin.gov.in/en/content/power-sector-glance-all-india
23. Webpage footer for REN21. “REN21”. 13 June 2019, www.ren21.net/reports/global-status-report/
24. Libich J, Máca J, Vondrák J, Čech O, Sedlaříková M (2018) Supercapacitors: Properties and applications. J Energy Storage 17:224–227
25. Goodenough JB, Abruna HD, Buchanan MV (2007) Basic research needs for electrical energy storage. In: Report of the basic energy sciences workshop for electrical energy storage, vol. 186
26. Nègre L, Daffos B, Taberna PL, Simon P (2015) Solvent-free electrolytes for electrical double layer capacitors. J Electrochem Soc 162(5):A5037
27. Zhang J, Wu H, Wang J, Shi J, Shi Z (2015) Pre-lithiation design and lithium ion intercalation plateaus utilization of mesocarbon microbeads anode for lithium-ion capacitors. Electrochim Acta 182:156–164
28. Zhang SS (2017) Eliminating pre-lithiation step for making high energy density hybrid Li-ion capacitor. J Power Sources 343:322–328
29. Conway BE, Pell WG (2003) Double-layer and pseudocapacitance types of electrochemical capacitors and their applications to the development of hybrid devices. J Solid State Electrochem 7(9):637–644
30. Miller JR, Simon P (2008) The Chalkboard: Fundamentals of electrochemical capacitor design and operation. Electrochem Soc Interface 17(1):31
31. Naoi K, Morita M (2008) Advanced polymers as active materials and electrolytes for electrochemical capacitors and hybrid capacitor systems. Electrochem Soc Interface 17(1):44
32. Boicea VA (2014) Energy storage technologies: The past and the present. Proc IEEE 102(11):1777–1794
33. Ngô C, Priem T, Martinet S (2022) Supercapacitors: From material to cell. In: Li-ion batteries, EDP Sciences, pp 145–198
34. Yang W, Ni M, Ren X, Tian Y, Li N, Su Y, Zhang X (2015) Graphene in supercapacitor applications. Curr Opin Colloid Interface Sci 20(5–6):416–428
35. Becker HI, General Electric Co (1957) Low voltage electrolytic capacitor. U.S. Patent 2,800,616
36. Chen H, Cong TN, Yang W, Tan C, Li Y, Ding Y (2009) Progress in electrical energy storage system: A critical review. Prog Nat Sci 19(3):291–312
37. Liu HK (2013) An overview—Functional nanomaterials for lithium rechargeable batteries, supercapacitors, hydrogen storage, and fuel cells. Mater Res Bull 48(12):4968–4973
38. Arico AS, Bruce P, Scrosati B, Tarascon JM, Van Schalkwijk W (2005) Nanostructured materials for advanced energy conversion and storage devices. Nat Mater 4(5):366–377
39. Guidi G, Undeland TM, Hori Y (2008) An interface converter with reduced volt-ampere ratings for battery-supercapacitor mixed systems. IEEJ Trans Ind Appl 128(4):418–423
40. Barrade P, Pittet S, Rufer A (2000) Series connection of supercapacitors, with an active device for equalizing the voltages. PCIM2000 Power conversion and intelligent motion, Nürnberg, Germany
41. Pandolfo T, Ruiz V, Sivakkumar S, Nerkar J (2013) General properties of electrochemical capacitors. Supercapacitors: Mater, Syst, Appl: 69–109
42. Zhao Y, Zheng MB, Cao JM, Ke XF, Liu JS, Chen YP, Tao J (2008) Easy synthesis of ordered meso/macroporous carbon monolith for use as electrode in electrochemical capacitors. Mater Lett 62(3):548–551

43. Huang CW, Teng H (2008) Influence of carbon nanotube grafting on the impedance behavior of activated carbon capacitors. J Electrochem Soc 155(10):A739
44. Balducci A, Bardi U, Caporali S, Mastragostino M, Soavi F (2004) Ionic liquids for hybrid supercapacitors. Electrochem Commun 6(6):566–570
45. Fang Y, Liu J, Yu DJ, Wicksted JP, Kalkan K, Topal CO, Flanders BN, Wu J, Li J (2010) Self-supported supercapacitor membranes: Polypyrrole-coated carbon nanotube networks enabled by pulsed electrodeposition. J Power Sources 195(2):674–679
46. Banerjee S, Sharma YC (2013) Equilibrium and kinetic studies for removal of malachite green from aqueous solution by a low cost activated carbon. J Ind Eng Chem 19(4):1099–1105
47. Boehm HP (2002) Surface oxides on carbon and their analysis: a critical assessment. Carbon 40(2):145–149
48. Frackowiak E, Beguin F (2001) Carbon materials for the electrochemical storage of energy in capacitors. Carbon 39(6):937–950
49. Cottineau T, Toupin M, Delahaye T, Brousse T, Bélanger D (2006) Nanostructured transition metal oxides for aqueous hybrid electrochemical supercapacitors. Appl Phys A 82(4):599–606
50. Wang Q, Yong FN, Xiao ZH, Chen XY, Zhang ZJ (2016) Simply incorporating an efficient redox additive into KOH electrolyte for largely improving electrochemical performances. J Electroanal Chem 770:62–72
51. Duffy NW, Baldsing W, Pandolfo AG (2008) The nickel–carbon asymmetric supercapacitor—Performance, energy density and electrode mass ratios. Electrochim Acta 54(2):535–539
52. Machida K, Suematsu S, Ishimoto S, Tamamitsu K (2008) High-voltage asymmetric electrochemical capacitor based on polyfluorene nanocomposite and activated carbon. J Electrochem Soc 155(12):A970
53. Wang Q, Nie YF, Chen XY, Xiao ZH, Zhang ZJ (2016) Controllable synthesis of 2D amorphous carbon and partially graphitic carbon materials: Large improvement of electrochemical performance by the redox additive of sulfanilic acid azochromotrop in KOH electrolyte. Electrochim Acta 200:247–258
54. Mastragostino M, Arbizzani C, Soavi F (2002) Conducting polymers as electrode materials in supercapacitors. Solid State Ionics 148(3–4):493–498
55. Wang YG, Yu L, Xia YY (2006) Electrochemical capacitance performance of hybrid supercapacitors based on $Ni(OH)_2$/carbon nanotube composites and activated carbon. J Electrochem Soc 153(4):A743
56. Amatucci GG, Badway F, Du Pasquier A, Zheng T (2001) An asymmetric hybrid nonaqueous energy storage cell. J Electrochem Soc 148(8):A930
57. Zhang Y, Feng H, Wu X, Wang L, Zhang A, Xia T, Dong H, Li X, Zhang L (2009) Progress of electrochemical capacitor electrode materials: A review. Int J Hydrogen Energy 34(11):4889–4899
58. Yu G, Xie X, Pan L, Bao Z, Cui Y (2013) Hybrid nanostructured materials for high-performance electrochemical capacitors. Nano Energy 2(2):213–234
59. Lin YP, Wu NL (2011) Characterization of $MnFe_2O_4$/$LiMn_2O_4$ aqueous asymmetric supercapacitor. J Power Sources 196(2):851–854
60. Arbizzani C, Mastragostino M, Meneghello L (1995) Characterization by impedance spectroscopy of a polymer-based supercapacitor. Electrochim Acta 40(13–14):2223–2228
61. Dai J, Fu K, Palanisamy R, Gong A, Pastel G, Kornfeld R, Zhu H, Sanghadasa M, Bekyarova E, Hu L (2017) A solid state energy storage device with supercapacitor–battery hybrid design. J Mater Chem A 5(29):15266–15272
62. Park SJ, Son YR, Heo YJ (2018) Prospective synthesis approaches to emerging materials for supercapacitor. In: Emerging materials for energy conversion and storage, Elsevier, pp 185–208
63. Li Z, Wang L, Li Y, Feng Y, Feng W (2019) Carbon-based functional nanomaterials: Preparation, properties and applications. Compos Sci Technol 179:10–40
64. Iijima S, Ichihashi T (1993) Single-shell carbon nanotubes of 1-nm diameter. Nature 363(6430):603–605

65. Novoselov KS, Geim AK, Morozov SV, Jiang D, Katsnelson MI, Grigorieva I, Dubonos S, Firsov A (2005) Two-dimensional gas of massless Dirac fermions in graphene. Nature 438(7065):197–200
66. Geim AK (2009) Graphene: Status and prospects. Science 324(5934):1530–1534
67. Tasis D, Tagmatarchis N, Bianco A, Prato M (2006) Chemistry of carbon nanotubes. Chem Rev 106(3):1105–1136
68. Karousis N, Tagmatarchis N, Tasis D (2010) Current progress on the chemical modification of carbon nanotubes. Chem Rev 110(9):5366–5397
69. Khabashesku VN, Pulikkathara MX (2006) Chemical modification of carbon nanotubes. Mendeleev Commun 16(2):61–66
70. Yan Y, Miao J, Yang Z, Xiao FX, Yang HB, Liu B, Yang Y (2015) Carbon nanotube catalysts: Recent advances in synthesis, characterization and applications. Chem Soc Rev 44(10):3295–3346
71. Zhang C, Hu J, Cong J, Zhao Y, Shen W, Toyoda H, Nagatsu M, Meng Y (2011) Pulsed plasma-polymerized alkaline anion-exchange membranes for potential application in direct alcohol fuel cells. J Power Sources 196(13):5386–5393
72. Lota K, Khomenko V, Frackowiak E (2004) Capacitance properties of poly (3, 4-ethylenedioxythiophene)/carbon nanotubes composites. J Phys Chem Solids 65(2–3):295–301
73. Suematsu S, Oura Y, Tsujimoto H, Kanno H, Naoi K (2000) Conducting polymer films of cross-linked structure and their QCM analysis. Electrochim Acta 45(22–23):3813–3821
74. Villers D, Jobin D, Soucy C, Cossement D, Chahine R, Breau L, Bélanger D (2003) The influence of the range of electroactivity and capacitance of conducting polymers on the performance of carbon conducting polymer hybrid supercapacitor. J Electrochem Soc 150(6):A747
75. Hashmi SA, Upadhyaya HM (2002) Polypyrrole and poly (3-methyl thiophene)-based solid state redox supercapacitors using ion conducting polymer electrolyte. Solid State Ionics 152:883–889
76. Vol'fkovich YM, Serdyuk TM (2002) Electrochemical capacitors. Russ J Electrochem 9(38):935–959
77. Mastragostino M, Arbizzani C, Meneghello L, Paraventi R (1996) Electronically conducting polymers and activated carbon: Electrode materials in supercapacitor technology. Adv Mater 8(4):331–334
78. Snook GA, Kao P, Best AS (2011) Conducting-polymer-based supercapacitor devices and electrodes. J Power Sources 196(1):1–12
79. Sun L, Wang X, Wang Y, Xiao D, Cai W, Jing Y, Wang Y, Hu F, Zhang Q (2019) In-situ functionalization of metal electrodes for advanced asymmetric supercapacitors. Front Chem 7:512
80. An C, Zhang Y, Guo H, Wang Y (2019) Metal oxide-based supercapacitors: progress and prospectives. Nanoscale Adv 1(12):4644–4658
81. Yu Z, Tetard L, Zhai L, Thomas J (2015) Supercapacitor electrode materials: Nanostructures from 0 to 3 dimensions. Energy Environ Sci 8(3):702–730
82. Lu X, Wang C, Favier F, Pinna N (2017) Electrospun nanomaterials for supercapacitor electrodes: Designed architectures and electrochemical performance. Adv Energy Mater 7(2):1601301
83. Xu Y, Wang X, An C, Wang Y, Jiao L, Yuan H (2014) Facile synthesis route of porous $MnCo_2O_4$ and $CoMn_2O_4$ nanowires and their excellent electrochemical properties in supercapacitors. J Mater Chem A 2(39):16480–16488
84. Gao H, Li Y, Zhao H, Xiang J, Cao Y (2018) A general fabrication approach on spinel MCo_2O_4 (M=Co, Mn, Fe, Mg and Zn) submicron prisms as advanced positive materials for supercapacitor. Electrochim Acta 262:241–251
85. Raj S, Kar P, Roy P (2018) Facile synthesis of flower-like morphology Cu 0.27 Co 2.73 O 4 for a high-performance supercapattery with extraordinary cycling stability. Chem Commun 54(87):12400–12403

86. Yang D (2012) Application of nanocomposites for supercapacitors: Characteristics and properties. Nanocomposites-New Trends Dev: 299–328
87. Singh NB, Agarwal S (2016) Nanocomposites: An overview. Emerg Mater Res 5(1):5–43
88. MarketsandMarkets (n.d.) Supercapacitor Market Size & Share | Industry Report, 2022–2027. [online] Available at: https://www.marketsandmarkets.com/Market-Reports/supercapacitor-market-37140453.html
89. Subasinghage K, Gunawardane K, Padmawansa N, Kularatna N, Moradian M (2022) Modern supercapacitors technologies and their applicability in mature electrical engineering applications. Energies 15(20):7752
90. Park DW, Cañas NA, Schwan M, Milow B, Ratke L, Friedrich KA (2016) A dual mesopore C-aerogel electrode for a high energy density supercapacitor. Curr Appl Phys 16(6):658–664
91. Bian W, Zhu S, Qi M, Xiao L, Liu Z, Zhan J (2017) Electrostatic-driven solid phase microextraction coupled with surface enhanced Raman spectroscopy for rapid analysis of pentachlorophenol. Anal Methods 9(3):459–464
92. Cameron CG (2017) Electrochemical capacitors. In: Springer handbook of electrochemical energy, Springer, Berlin, Heidelberg, pp 563–589
93. Borodin O, Ren X, Vatamanu J, von Wald Cresce A, Knap J, Xu K (2017) Modeling insight into battery electrolyte electrochemical stability and interfacial structure. Acc Chem Res 50(12):2886–2894
94. Dennison CR, Beidaghi M, Hatzell KB, Campos JW, Gogotsi Y, Kumbur EC (2014) Effects of flow cell design on charge percolation and storage in the carbon slurry electrodes of electrochemical flow capacitors. J Power Sources 247:489–496
95. Münchgesang W, Meisner P, Yushin G (2014) Supercapacitors specialities-Technology review. In: AIP conference proceedings, vol. 1597, No. 1. American Institute of Physics, pp 196–203
96. Kumar SKN, Renuga P, SVC, V.C. (2012) Optimal VAR planning using facts. Int J Power Energy Syst 32(2):49–56
97. FastCap. Introducing FastCAP's ulysses power systems for drilling applications2013http://www.fastcapsystems.com/products
98. Tecate group. Backup power for military applications batteries optional! (⟨http://www.tecategroup.com/ultracapacitorssupercapacitors/militaryapplications.php//)
99. Zhao Y, Ran W, He J, Song Y, Zhang C, Xiong DB, Gao F, Wu J, Xia Y (2015) Oxygen-rich hierarchical porous carbon derived from artemia cyst shells with superior electrochemical performance. ACS Appl Mater Interfaces 7(2):1132–1139
100. Patel KK, Singhal T, Pandey V, Sumangala TP, Sreekanth MS (2021) Evolution and recent developments of high performance electrode material for supercapacitors: A review. J Energy Storage 44:103366
101. Xu Q, Wei C, Fan L, Rao W, Xu W, Liang H, Xu J (2018) Polypyrrole/titania-coated cotton fabrics for flexible supercapacitor electrodes. Appl Surf Sci 460:84–91
102. He Y, Chen W, Li X, Zhang Z, Fu J, Zhao C, Xie E (2013) Freestanding three-dimensional graphene/MnO_2 composite networks as ultralight and flexible supercapacitor electrodes. ACS Nano 7(1):174–182
103. Dong L, Xu C, Li Y, Huang ZH, Kang F, Yang QH, Zhao X (2016) Flexible electrodes and supercapacitors for wearable energy storage: a review by category. J Mater Chem A 4(13):4659–4685
104. Dubal DP, Chodankar NR, Kim DH, Gomez-Romero P (2018) Towards flexible solid-state supercapacitors for smart and wearable electronics. Chem Soc Rev 47(6):2065–2129
105. Zeng W, Shu L, Li Q, Chen S, Wang F, Tao XM (2014) Fiber-based wearable electronics: A review of materials, fabrication, devices, and applications. Adv Mater 26(31):5310–5336
106. Chee WK, Lim HN, Zainal Z, Huang NM, Harrison I, Andou Y (2016) Flexible graphene-based supercapacitors: a review. J Phys Chem C 120(8):4153–4172
107. Ma H, He J, Xiong DB, Wu J, Li Q, Dravid V, Zhao Y (2016) Nickel cobalt hydroxide@reduced graphene oxide hybrid nanolayers for high performance asymmetric supercapacitors with remarkable cycling stability. ACS Appl Mater Interfaces 8(3):1992–2000

108. Chen Z, Xiong DB, Zhang X, Ma H, Xia M, Zhao Y (2016) Construction of a novel hierarchical structured NH_4-Co-Ni phosphate toward an ultrastable aqueous hybrid capacitor. Nanoscale 8(12):6636–6645
109. Wang F, Wang X, Chang Z, Wu X, Liu X, Fu L, Zhu Y, Wu Y, Huang W (2015) A quasi-solid-state sodium-ion capacitor with high energy density. Adv Mater 27(43):6962–6968
110. Fan L, Lin K, Wang J, Ma R, Lu B (2018) A nonaqueous potassium-based battery–supercapacitor hybrid device. Adv Mater 30(20):1800804